DE GRUYTER

Karl-Heinz Neeb

THE RADIOCHEMISTRY OF NUCLEAR POWER PLANTS WITH LIGHT WATER REACTORS

PART 1

Karl-Heinz Neeb

The Radiochemistry of Nuclear Power Plants with Light Water Reactors

Karl-Heinz Neeb

The Radiochemistry of Nuclear Power Plants with Light Water Reactors

With a preface written by Günter Marx

Walter de Gruyter · Berlin · New York 1997

Dr. Karl-Heinz Neeb

Up until his retirement, Dr. Neeb was head of the department for radioactivity and environmental studies at the Siemens AG nuclear research station in Erlangen, Germany.

This book contains 164 figures and 60 tables.

Library of Congress Cataloging-in-Publication Data

Neeb, Karl-Heinz.
The radiochemistry of nuclear power plants with light water reactors / Karl-Heinz Neeb : with a preface written by Günter Marx.
p. cm.
Includes bibliographical references (p.) and index.
ISBN 3-11-013242-7 (alk. paper)
1. Radiochemistry – Industrial applications. 2. Light water reactors – Materials. 3. Nuclear power plants. I. Title.
TK9350.N44 1997
621.48'34 – dc21 97-31125
CIP

Die Deutsche Bibliothek – Cataloging-in-Publication Data

Neeb, Karl-Heinz:
The radiochemistry of nuclear power plants with light water reactors / Karl-Heinz Neeb. With a preface written by Günter Marx. – Berlin ; New York : de Gruyter, 1997
ISBN 3-11-013242-7

© Copyright 1997 by Walter de Gruyter & Co., D-10785 Berlin

All rights reserved, including those of translation into foreign languages. No part of this book may be reproduced or transmitted in any form or by any means, electronic or mechanical, including photocopy, recording or any information storage and retrieval system, without permission in writing from the publisher.

Printed in Germany

Disk conversion and printing: Arthur Collignon GmbH, Berlin, Germany
Binding: Lüderitz & Bauer GbmH, Berlin, Germany
Cover design: Hansbernd Lindemann, Berlin, Germany

Preface

Nuclear power has experienced a breakthrough in those areas of the world which are expanding drastically in their economic capacity. South-east Asia is the first in line, together with Japan, and even China is building up advanced technology in this field. In the USA the overwhelming majority of nuclear power plants are still in operation, approximately 100 blocks. In Europe, France with 75% of its electricity output being nuclear is the leader in the field, followed by the United Kingdom. However, in all these countries, one point of interest is central, namely, the safety issue. The aforementioned appliers of nuclear power have always been aware of this problem, even before the Tschernobyl accident in the former Soviet Union.

Quite a number of monographs have been written on reactor physics, the various reactor types with their structural advantages and disadvantages, on safeguard models, the probability of hypothetical disastrous events and the handling of radioactive waste. One topic, however, has been slightly neglected with respect to its importance in the field of safety problems. This is radiochemistry.

This gap has now been closed by Karl-Heinz Neeb's book: Radiochemistry of Nuclear Power Plants with Light Water Reactors.

The book has been divided into three main sections: reactor design, radiochemistry during normal operation of the plant and radiochemistry under the conditions of reactor accidents. All three sections are outlined in detail with numerous subtitles, reflecting the author's wide knowledge and experience in this field gained during his long, successful, professional career. The impressive reference list of the various topics demonstrate the perfect overview he had in this important field of nuclear science. A great part of the literature was only available to the author due to his professional status. This book is unique in its kind and should not be missed by anybody working in the amazing field of reactor chemistry.

It will also be very useful to academics at universities and research centres in their aim to supply future generations with the necessary scientific background to cope with the problems yet to be confronted in this highly technological field.

Karl-Heinz Neeb tragically passed away just after having completed this book, leaving his work as a kind of memorial to the scientific community. He is remembered as a distinguished personality and for his valuable contribution to nuclear science.

Günter Marx
Free University of Berlin
Radiochemical Division

Table of Contents

Introduction 1

Part A
Design of light water reactor nuclear power plants

1 The Pressurized Water Reactor (PWR) 5
1.1 Design of Western PWR plants 7
1.1.1 The primary circuit 7
1.1.2 The reactor core 13
1.1.3 The auxiliary and ancillary systems 23
1.1.4 Safety and emergency installations 27
1.2 VVER design 31
1.3 PWR coolant chemistry 33

References Chapter 1 42

2 The Boiling Water Reactor (BWR) 43
2.1 Design of Western BWR plants 44
2.1.1 The primary system 44
2.1.2 The reactor core 47
2.1.3 The auxiliary and ancillary systems 50
2.1.4 Safety and emergency installations 51
2.2 RBMK design 51
2.3 BWR coolant chemistry 54

References Chapter 2 57

Part B
Radiochemistry during normal operation of the plant

3 Radionuclides in the reactor core 59
3.1 Radionuclides in fresh nuclear fuels 60
3.2 Radionuclides in irradiated nuclear fuels 66
3.2.1 Fission product generation and fuel structure 66
3.2.2 Determination of the burnup of nuclear fuel 91

3.2.3 Chemical state and behavior of the fission products in the fuel . . 93
3.2.3.1 General aspects 93
3.2.3.2 Fission product noble gases 106
3.2.3.3 Halogens and alkali elements 111
3.2.3.4 Polyvalent fission product elements 122
3.2.3.5 Uranium activation products 124
3.2.3.6 Tritium 125
3.2.3.7 Carbon-14 131
3.2.4 Radionuclides in the fuel pellet – cladding gap 133
3.2.5 Radionuclides in the fuel rod cladding 137
3.2.6 Radionuclides in reactor core components and structural materials 144
3.2.7 Determination of the neutron fluence in reactor core materials . . 151
3.2.7.1 General aspects 151
3.2.7.2 Cobalt monitor 153
3.2.7.3 Iron – manganese monitor 154
3.2.7.4 Nickel – cobalt monitor 155
3.2.7.5 Niobium monitor 156
3.2.7.6 Fission monitors 158

References Chapter 3 159

4 Radionuclides in the coolants of light water reactors during normal operation 163
4.1 General remarks 163
4.2 Activation products of the coolant, its additives and impurities . . 164
4.2.1 ^{16}N, ^{13}N 164
4.2.2 ^{18}F 167
4.2.3 ^{3}H 168
4.2.4 ^{14}C 172
4.2.5 ^{32}P and ^{35}S 174

References Section 4.2 176

4.3 Fission products and activation products from the fuel 177
4.3.1 Transport of radionuclides from the fuel to the coolant 177
4.3.1.1 Release of fission products to the coolant during steady-state operation 183
4.3.1.2 Release from defective fuel rods during reactor transients 197
4.3.1.3 Identification of failed fuel rods 207
4.3.2 Reactions and behavior in the reactor coolant 210
4.3.2.1 PWR primary coolant 210
4.3.2.1.1 Fission product noble gases 210
4.3.2.1.2 Iodine isotopes 215
4.3.2.1.3 Cesium isotopes 221
4.3.2.1.4 Other fission products and activation products from the fuel . . . 222
4.3.3 PWR water – steam circuit 227

4.3.4 BWR reactor water 229
4.3.4.1 Fission product noble gases 229
4.3.4.2 Iodine isotopes 229
4.3.4.3 Other fission products and activation products from the fuel . . . 237

References Section 4.3 238

4.4 Activated corrosion products and contamination buildup 241
4.4.1 General aspects 241

References Section 4.4.1 251

4.4.2 Analytical methods applied in contamination buildup studies . . . 252

References Section 4.4.2 263

4.4.3 Contamination buildup in pressurized water reactors 264
4.4.3.1 General aspects 264
4.4.3.2 The sources of the radionuclides 266
4.4.3.3 The behavior of the corrosion product radionuclides in the primary coolant 286
4.4.3.4 The deposition of radionuclides on the surfaces of the primary circuit 302
4.4.3.5 Possible countermeasures against contamination buildup 312
4.4.3.6 Modelling PWR contamination buildup 325
4.4.3.7 Contamination by other radionuclides 330

References Section 4.4.3 333

4.4.4 Contamination buildup in boiling water reactors 339
4.4.4.1 General aspects 339
4.4.4.2 The sources of the radionuclides 341
4.4.4.3 The behavior of the corrosion product radionuclides in the BWR reactor water 350
4.4.4.4 The deposition of radionuclides on the surfaces 356
4.4.4.5 Possible countermeasures against BWR contamination buildup . . 364
4.4.4.6 Modelling BWR contamination buildup 372

References Section 4.4.4 373

4.5 Decontamination in nuclear power plants 376
4.5.1 General aspects 376
4.5.2 Decontamination procedures 380
4.5.2.1 Non-chemical decontamination procedures 381
4.5.2.2 Chemical decontamination procedures 382
4.5.2.3 Electrochemical decontamination procedures 387
4.5.3 Decontamination applications 390
4.5.4 Recontamination of decontaminated surfaces 399

4.5.5 Treatment of radioactive decontamination waste 402
4.5.6 Decontamination within the scope of decommissioning of nuclear power plants 405
References Section 4.5 411

Part C
Radiochemistry under the conditions of reactor accidents

5 General remarks 415
References Chapter 5 418

6 Design basis accidents 419
6.1 General aspects 419
6.2 Specific accident sequences in design basis accidents 421
6.2.1 Break in a main coolant pipe 421
6.2.1.1 The release of fission products from failed fuel rods to the primary circuit 425
6.2.1.2 The behavior of the fission products in the containment 438
6.2.1.3 Investigation of radionuclide behavior in integral experiments . . 447
6.2.1.4 Release of fission products from the containment 452
6.2.1.5 Retention of fission products from containment air under accident conditions 453
6.2.2 Break of a transducer line 458
6.2.3 Steam generator tube rupture accidents 464
6.2.4 Fuel storage and handling accidents 471
6.2.5 Accidents in the auxiliary building 472
References Chapter 6 473

7 Severe reactor accidents 477
7.1 General aspects 477
References Section 7.1 484

7.2 Postulated accident sequences 485
7.2.1 Pressurized water reactors 485
7.2.2 Boiling water reactors 494
References Section 7.2 495

7.3 Chemistry and behavior of radionuclides in the different stages of a severe accident 495
7.3.1 The release of radionuclides from the overheated reactor core . . . 495
7.3.1.1 Fission products from the fuel 496
7.3.1.1.1 General aspects 496
7.3.1.1.2 Out-of-pile experimental programs 501

7.3.1.1.3 In-pile experimental programs 516
7.3.1.1.4 Conclusions regarding fission product release behavior in an actual severe accident 521
7.3.1.2 Radionuclides from core components and structural materials . . 525
7.3.1.3 Radionuclides from the core melt – concrete interaction 532
References Section 7.3.1 538

7.3.2 Chemical reactions and behavior of the radionuclides in the primary system 540
7.3.2.1 General aspects 540
7.3.2.2 Low-volatility substances 544
7.3.2.3 Volatile fission products 550
7.3.2.3.1 Cesium 552
7.3.2.3.2 Iodine 556
7.3.2.3.3 Tellurium 571
7.3.2.4 Radionuclide retention in BWR pressure suppression pools 573
References Section 7.3.2 578

7.3.3 Chemical reactions and behavior of the radionuclides within the containment 582
7.3.3.1 General aspects 582
7.3.3.2 Aerosols 586
7.3.3.3 Tellurium 591
7.3.3.4 Iodine 591
7.3.3.4.1 Iodine chemical species entering the containment 591
7.3.3.4.2 Basic iodine chemistry in aqueous solution and iodine volatility . 594
7.3.3.4.3 Influence of solution partners on iodine chemistry in the sump water 610
7.3.3.4.4 Effects of ionizing radiation on iodine chemistry in the containment 615
7.3.3.4.5 Formation and behavior of organoiodine compounds 625
7.3.3.4.6 Further reactions of iodine in the containment atmosphere 637
7.3.3.4.7 Reactions of iodine with structural surfaces in the containment . . 641
7.3.3.4.8 Large-scale containment experiments 646
7.3.3.4.9 Evaluation of overall iodine behavior in the containment 651
References Section 7.3.3 658

7.3.4 Release of radionuclides from the containment to adjacent areas 664
7.3.4.1 Penetration through operational leaks in the containment steel shell 665
7.3.4.2 Release of radionuclides in the event of a failure of containment isolation 667
7.3.4.3 Late overpressure failure of the containment steel shell 667
7.3.4.4 Controlled depressurization of the containment 672
References Section 7.3.4 677

7.3.5 Integral experiments dealing with severe core damage 678
References Section 7.3.5 683

7.4 Fission product behavior in actual severe reactor accidents 684
7.4.1 General remarks 684
7.4.2 TMI-2 687
7.4.3 Chernobyl-4 700
References Section 7.4 708

Subject Index 711

Introduction

In the past few decades nuclear energy has acquired increasing economic importance, particularly for the production of electricity. By the end of 1994 there were 432 nuclear power plants, with an electrical capacity of about 340 GW, in operation worldwide, with an additional 48 plants with about 39 GW electrical capacity under construction. The cumulative operation time of nuclear power reactors reached about 7230 operation years at the end of 1994 and in the year 1994 alone the total electricity production of such plants was about 2130 TWh, a value corresponding to approximately 17% of the global electricity production. The nuclear share of electricity generation shows large differences throughout the world, reaching values of up to 75% in some countries (e. g., France, Belgium). The greatest contribution by far to the production of nuclear energy is delivered by the so-called light water reactors, in which water of natural isotopic composition serves both as neutron moderator and as coolant. Other reactor types (heavy water-cooled, gas-cooled, liquid metal-cooled) are also operated for power generation, but contribute far less to the total of nuclear energy production. In addition to its economic benefits, nuclear power plays an important role in environmental protection, since by its use the emission of pollutants to the atmosphere, above all of CO_2, has been significantly reduced; on the other hand, with the exception of one severe reactor accident (which will be treated in this book) the environmental risk of nuclear power generation has been and remains negligible.

Despite this favorable record, the further development of nuclear power is greatly handicapped in many countries because of public concern over the radioactive products arising in the course of plant operation and the consequences of their possible release to the environment. Energy generation from the neutron-induced fission of heavy atoms is inevitably accompanied by the formation of radioactive nuclides. This is, first of all, the direct consequence of nuclear fission, which leads initially to fission products that are unstable due to an excess of neutrons in the newly formed nuclei. These products are transformed by a sequence of β^- decays (mainly with associated γ emission) to stable end products. Moreover, neutron capture in the heavy atoms of the fuel results in the buildup of nuclei which are heavier than those of the starting element (uranium, plutonium) and which mostly decay – in part, with very long halflives – by α emission. Finally, from elements present in structural and cladding materials, as well as in the coolant, its additives and impurities, additional radionuclides are formed, induced by neutron capture reactions which take place in the intense neutron field inside the reactor pressure vessel.

As a consequence of these nuclear reactions, the reactor of a nuclear power plant contains a very large radioactivity inventory consisting of radioisotopes of different chemical elements, from the lightest ones through the fission product

elements in the middle range of the Periodic System of Elements to the transuranium elements. This radioactivity inventory represents a potential hazard to the plant employees as well as to the environment and has to be safely confined under all conditions, both during normal operation and, in particular, during and after reactor accidents. In order to attain this goal, the required confinement and retention systems have to be designed and operated in accordance with the properties and behavior of the radionuclides in question. As an important prerequisite for the design and operation of these systems, this behavior under all relevant conditions has to be known.

Radioactivity is a property of matter and, therefore, it is inseparably tied to matter. The consequence of this trivial fact, which nevertheless is very often overlooked, is that radioactivity can only behave in a manner that corresponds to the chemical properties of the radionuclides in question. For this reason, knowledge of the chemical reactions that may occur under the prevailing conditions, as well as of the properties of the species formed, is of great importance for assessing the behavior of radionuclides. Individual measurements are often not sufficient for drawing generally valid conclusions about this behavior under given conditions; rather, one has to have an understanding of why the radionuclides behave as they do and not otherwise. Therefore, one has to know the course of the essential chemical reactions, the nature of their reaction products and the dependence of their yields on different parameters which, in many cases, will be highly influenced by the ambient conditions.

Radiochemistry is a branch of chemistry, but in this context it exhibits various characteristics that make it a somewhat autonomous discipline. To be sure, the radionuclides obey the same chemical laws as their inactive isotopes do; there are, however, additional aspects that have to be considered. The mechanisms in the formation of the radionuclides have to be taken into account, as well as the chemical effects of ionizing radiation and of possible chemical reactions of highly excited atoms ("hot atom chemistry"). The properties of ionizing radiation and the techniques to be applied for their measurement are additional aspects specific to radiochemistry. Generally speaking, one can define radiochemistry as an independent branch situated between inorganic chemistry, physical and analytical chemistry and nuclear physics.

Another characteristic feature of the radiochemistry in nuclear power plants is that of very large differences in the concentrations of substances, which may significantly affect the behavior of the radionuclides. As an example, fission product element concentrations in the aqueous solutions to be considered both during reactor normal operation and in design basis accidents, usually are on the trace level, i. e. at 10^{-9} M and lower, although this often corresponds to a high level of radioactivity. At such low mass concentrations, many elements often display an unusual behavior. Thus, chemical reactions that have reaction rates dependent on a trace element concentration greater than first order are unlikely to proceed at very low chemical concentrations, because of the law of mass action. Other interactions, for example with surfaces or with impurities present at higher concentration levels, may have a greater significance than normal chemical reactions. By contrast, in the sump water solutions which are formed in the course of a severe reactor acci-

dent, element concentrations are to be expected that are normal for macrochemistry. In addition, nuclear power plant radiochemistry has to deal with different states of matter, from the solid state of nuclear fuel to the liquid phases of the coolants to the gas-phase reactions in the containment atmosphere. Numerous transitions between these different states as a consequence of chemical reactions and of physical parameters have to be taken into consideration.

In the following chapters, radiochemistry is understood as including the whole area of radioactivity behavior with special emphasis on the chemical reactions radionuclides are subjected to in different areas of the nuclear power plant. The text will concentrate on commercially operated light water reactors, i. e. pressurized and boiling water reactors which as mentioned above currently represent the greatest fraction by far of the world's nuclear power capacity. Part A of the treatise will be devoted to a short description of the design of the different types of plants in current operation; potential new developments, which will be based on the plans being worked on by various manufacturers, will not be considered in this context. The plant descriptions are not intended to present a detailed picture; they will focus mainly on those aspects of the plants that are relevant for radionuclide chemistry and behavior. In Part B, radiochemistry in the primary systems of the plant during normal operation state will be discussed, whereas Part C will address accident conditions, which are different in essential ways, as regards radionuclide chemistry, from normal operating conditions.

Since the early days of nuclear technology, a large number of investigations, both theoretical and experimental, have been devoted to radionuclide behavior in nuclear power plants. In consequence, this behavior is quite well understood and it can be said that there are no fundamental questions that still remain open; nonetheless, there are certain details that deserve further attention to enable researchers to obtain a reliable basis for theoretical modelling and numerical calculation. The results of the investigations that have been carried out have been presented in various types of publications, such as scientific periodicals, conference proceedings and reports published by different institutions. Because of this very wide field, a complete overview of all relevant findings would be very difficult to achieve and will not be undertaken in this work; nonetheless, the author feels he has included all the results that are of importance for a basic understanding of radionuclide chemistry. Furthermore, since radiochemistry and nuclear power technology are continually developing areas, a treatise covering such a wide range of topics cannot be expected to be fully up-to-date. Finally, it is not the author's intention nor does it lie within his capability, to deliver a model of radionuclide behavior under the different condititons prevailing in a plant, but it is hoped that the treatise will provide an incentive for further work in this field.

The book does not exclusively address experts working in the various fields of radiochemistry in nuclear power plants. On the contrary, it is intended to provide an overview of the topics dealt with for the operators of nuclear power plants, for people working in design and development and in safety-related areas, as well as for those working in licensing and supervision. The author's intention has been to contribute to a better understanding of the long-underestimated importance of radiochemisty issues for the safe operation of nuclear power plants. In addition, it

is hoped it will be of interest to radiochemists working in other fields as well and will make them more familiar with this highly complex and exciting field of radiochemistry.

The basis of the author's knowledge, beyond his education, is his decades-long professional involvement in nuclear power plant radiochemistry. While he has acquired considerable experience of his own over the years, he has learned even more from his discussions with a large number of colleagues from his own company, as well as from nuclear power plants and from research institutions in many countries throughout the world. The author is greatly indebted to all of these colleagues, although it is not possible for him to express his thanks here to each of them individually. Nonetheless, he would like to name a few of them because of the particular role they have played for him over the years: Dipl.Ing. A. Bleier, Dr. F. Funke, Dr. G.-U. Greger, Dipl.Phys. G. Hecht, Dr. S. Hellmann, Dipl.Phys. R. Hoffmann, Dipl.Ing. J. Martin, Dr. W. Morell, Dr. R. Riess, Dr. H. Wille and, finally, the late Dr. E. Schuster for important discussions in the various fields of radiochemistry; Dipl.Phys. R. Holzer for valuable contributions in the field of nuclear fuels; Dipl.Ing. Kh. Orth and Dr. H. Fabian for critical remarks concerning the principles of plant design and reactor safety; further, he would like to express his thanks to the Power Generation Group (KWU) of Siemens AG and to many of the colleagues there for valuable technical support, in particular to Dr. M. Hillerbrandt, Mr. G. Hofmann and Mrs. I. Zeume. Prof. G. Marx of the Free University of Berlin has reviewed the whole manuscript and has contributed from his wide experience in general inorganic chemistry and radiochemistry. Finally, the author would like to thank Mr. P. Germain for his efforts in transforming the author's English into an understandable one and to Dr. R. Weber, Dr. R. Schulze and Dr. M. Noyer-Weidner of deGruyter publishers for their support in the publication of this work.

Part A
Design of light water reactor nuclear power plants

As was emphasized in the introduction to this treatise, the behavior of radionuclides (with the exception of the fission product noble gases) is generally governed by their chemical nature. However, the progress of chemical reactions, as well as the nature and the relative yields of their products, are strongly influenced by the prevailing ambient conditions. In the current context this means temperature, chemical parameters (e. g. concentrations, pH value, radiation field, redox potential), materials confining the reaction system and present within it, and other parameters. The description and evaluation of the chemistry of the radionuclides in the nuclear power plant, therefore, requires a thorough knowledge of the entire system "light water reactor" under all the modes of operation to be considered.

For this reason, the discussion of radiochemical questions in nuclear power plants shall be introduced by a short description of the two currently commercially operating types of light water reactors, namely the Pressurized Water Reactor (PWR) and the Boiling Water Reactor (BWR). This chapter does not aim at a complete and detailed presentation of the design of such plants; on the contrary, only the topics that are of significance for understanding the chemistry of radionuclides will be addressed. In this context, the primary circuit and its components will be described, as well as the reactor core with the fuel and the fuel assemblies, the relevant auxiliary and ancillary systems and, finally, the safety and emergency installations. In doing so, the design of the Siemens/KWU-type light water reactor plants will provide the basis for the discussion; the designs applied by other manufacturers will only be treated insofar as there are deviations in design that are relevant for the behavior of the radionuclides. In general, the plant descriptions will be restricted to the designs currently in commercial operation; the future developments planned by almost all manufacturers (e. g. the European Pressurized Reactor EPR, which was developed by Nuclear Power International NPI, a joint subsidiary of Framatome and Siemens/KWU) and the impact of the details of their design on radionuclide behavior will not be discussed in this context.

1. The Pressurized Water Reactor (PWR)

In most of the nuclear power plants in operation today, the heat generating unit is a pressurized water reactor; 246 plants totalling about 227 GW electrical power were in operation by the end of 1994, a further 39 plants with about 39 GWe were

under construction at that time. In this plant design, the heat generated by nuclear fission in the reactor nuclear fuel is removed by the primary coolant which is circulated in the closed primary circuit. Here the pressure is high enough to keep the primary coolant in the liquid state at operating temperatures. In the secondary circuit (or water–steam circuit) steam is generated and then directed to the turbine. The circuits are separated from each other by the steam generators; as a result of this separation, the water–steam circuit and the turbine normally (i. e. in the absence of steam generator tube leakages) are free of radioactivity.

Originally, the pressurized water reactor was designed for nuclear ship propulsion by the US Navy. From this principle, Westinghouse started in the 1950's to develop civilian electricity generating units, with the first one being the Shippingport 1 plant, a 90 MWe PWR which started operation in 1957. All the PWR designs in the Western world were developed from this original design, although in the course of these developments different manufacturers introduced their own technical solutions. Nonetheless, with regard to the generation and the behavior of the radionuclides, the various designs do not show basic differences from each other,

Table 1.1. Konvoi PWR characteristic data
(By courtesy of Siemens/KWU)

Reactor core thermal power	3765 MW
Gross electrical capacity	1369 MW*)
Net electrical capacity	1285 MW*)
Net plant efficiency	34.1%*)
Number of parallel loops	4
Primary circuit volume (incl. pressurizer)	437 m^3
Total coolant mass flow	18800 kg/s
Coolant pressure (RPV exit)	15.8 MPa
RPV inlet temperature	291 °C
RPV outlet temperature	326 °C
Core heat transfer area	6036 m^2
Average linear heat rating	207 W/cm
Fuel average heat rating	36.4 kW/kg
Number of fuel assemblies	193
Number of fuel rods per assembly	300
Number of control rod guide tubes per assembly	24
Number of spacer grids per assembly	9
Number of control rod assemblies in core	61
Number of steam generators	4
Heat rating per SG	945.5 MW
Heat exchange area per SG	5400 m^2
Number of heating tubes per SG	4118
Coolant flow rate per SG	4700 kg/s
Number of main coolant pumps	4
Power consumption per pump (hot conditions)	5.45 MW

*) site-specific data for Kernkraftwerk Isar-2 (KKI-2)

with the common aim being to confine the radionuclides safely and to keep occupational radiation exposures as well as radionuclide emissions to the environment at a very low, acceptable level.

The first commercial light water PWR manufactured by Siemens, the Kernkraftwerk Obrigheim (KWO) with an original rated electrical output of 300 MW (now 350 MW), was commissioned in 1968. It had a design quite similar to that of the Westinghouse plants built at the same time. The plants constructed by Siemens/KWU over the following years have been characterized by increasing size, two-loop KWO plant, three- and four-loop plants of intermediate rating (in the range 600 to 800 MWe) and larger four-loop plants. In 1974, the 1200 MWe plant Biblis A started operation and the further development has culminated preliminarily in the three so-called Konvoi plants with a rated gross electrical output of 1350 to 1400 MW, which were built according to a virtually identical design. Essentially, the following plant description will concentrate on these Konvoi plants; some characteristic features of this design are summarized in Table 1.1. In case there are major deviations from the former Siemens plants (which are currently all in successful operation) as well as from the plant designs of other manufacturers, which are of relevance for radionuclide behavior, this will be indicated in the relevant sections.

1.1 Design of Western PWR plants

1.1.1 The primary circuit

The primary circuit of a four-loop PWR essentially consists of the reactor pressure vessel, four steam generators and four main coolant pumps, the pressurizer and, finally, the main coolant lines which interconnect the individual components and through which the hot primary coolant is transported from the reactor pressure vessel to the steam generators (hot leg) and then back to the reactor pressure vessel (cold leg). An isometric drawing of such a primary circuit is shown in Fig. 1.1. The arrangement of the different components inside the reactor building can be seen in Fig. 1.2. Summary descriptions of the primary circuit components have been given by different authors, e. g. by Meyer (1991).

The central part of the primary circuit is the reactor pressure vessel (RPV), designed for a pressure of 17.5 MPa and an operational temperature of 350 °C. The inner diameter of the cylindrical shell of the component (see Fig. 1.3.) is about 5.00 m, the wall thickness is 0.25 m; at a clear height of about 11.60 m, the total weight of the component is about 500 Mg. The base material of the RPV is the low-alloy fine-grained structural steel 20MnMoNi 55 (for a short overview of the materials used in light water reactors see Debray, 1991); in order to preclude corrosion, all surfaces that come into contact with the coolant have a weld-deposited austenitic overlay. The reactor pressure vessel is fabricated from seamless forgings and consists mainly of the closure head, the shell flange with 8 main coolant noz-

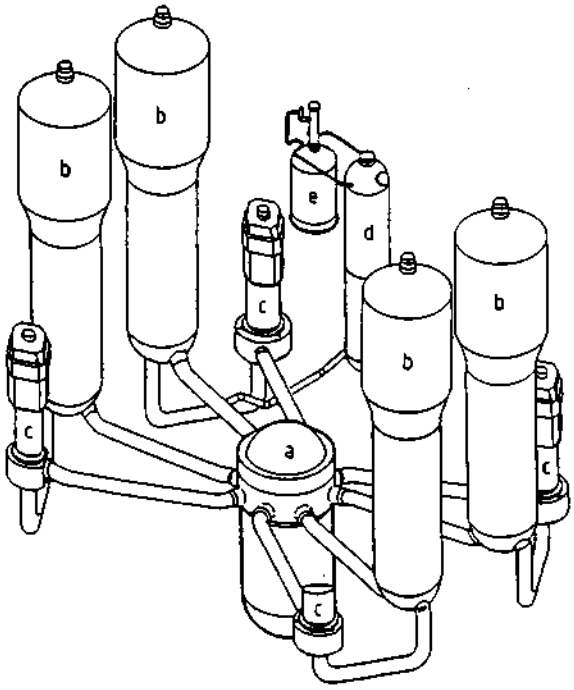

Figure 1.1. Four-loop primary coolant system of a 1300 MWe pressurized water reactor
a) Reactor pressure vessel; b) Steam generator; c) Reactor coolant pump; d) Pressurizer; e) Pressurizer relief tank
(Meyer, 1991)

zles, 2 cylindrical shells, and the bottom dome plate. By this design, welds are minimized, thus reducing sites of possible fatigue. Below the coolant nozzles, the vesssel body has no further openings or connections; this means that in the event of a break in a connected pipe, the reactor core can always be flooded with water by the emergency core cooling and residual heat removal systems.

The closure head of the reactor pressure vessel accomodates the control rod drive mechanism nozzles, the in-core instrumentation nozzles, the RPV water level control nozzles and the venting nozzle. The RPV body and closure head are joined together by means of studs and nuts. During refuelling, the RPV closure head is removed, together with the platform, closure head insulation, control drive mechanisms and the seal rings.

The core structure supporting the reactor core is located inside the reactor pressure vessel. The lower core support structure mainly serves to support the weight of the fuel assemblies, align and position the assemblies, absorb the impact of the control rods in the event of a reactor trip, and channel the flow of coolant in the reactor pressure vessel. It comprises the lower core support with flow distribution plate, the core barrel and the core shroud with core formers, and it defines the geometry of the reactor core. It remains in the reactor pressure vessel during refu-

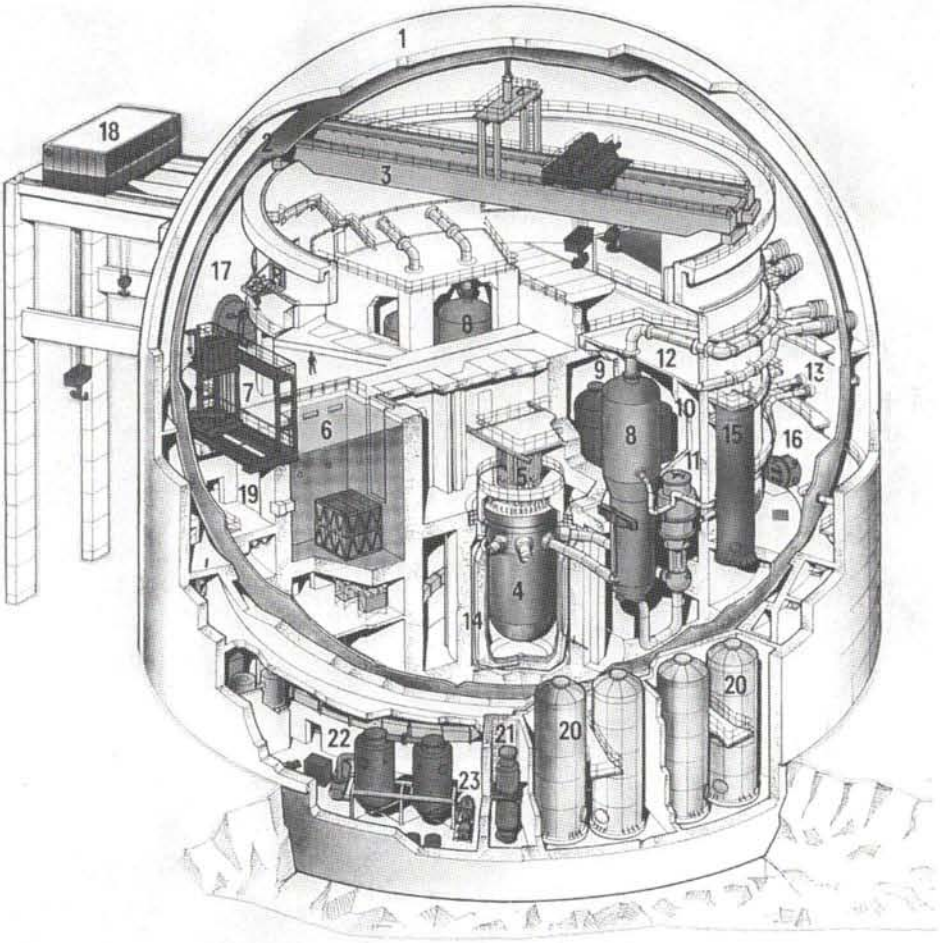

Figure 1.2. PWR reactor building
1) Concrete containment; 2) Containment steel shell; 3) Polar crane; 4) Reactor pressure vessel; 5) Control rod drive mechanism; 6) Spent fuel pool; 7) Refuelling machine; 8) Steam generator; 9) Pressurizer; 10) Pressurizer relief tank; 11) Main coolant pump; 12) Main steam line; 13) Feedwater line; 14) Concrete shield; 15) Accumulator; 16) Personnel lock; 17) Materials lock; 18) Lifting gantry; 19) Fresh fuel assembly storage; 20) Borated water storage tank; 21) Residual heat cooler; 22) Component cooler; 23) Safety injection pump
(By courtesy of Siemens/KWU)

elling, but can be lifted out of the RPV for inspection purposes. The flow skirt attached to the bottom of the reactor pressure vessel, together with the flow distribution plate, assures uniform wetting of the reactor core with coolant. The core shroud surrounds the polygonal reactor core; it is dimensioned to accommodate the expansion of the fuel assemblies. A defined bypass coolant flow provides cooling of the reflector area between the core shroud and the core barrel. The irradia-

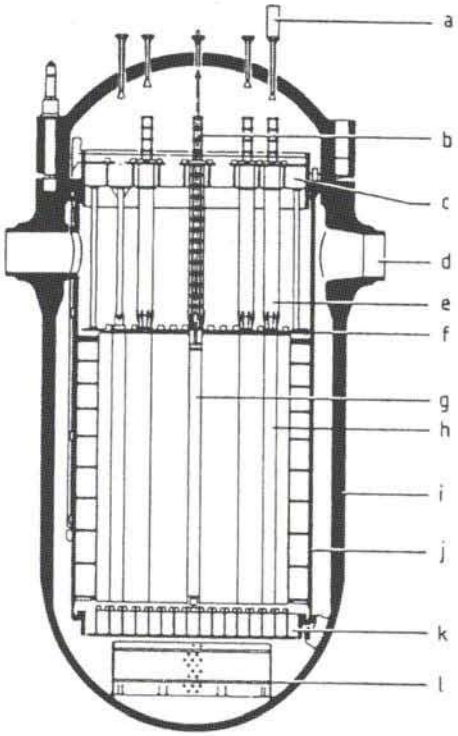

Figure 1.3. Reactor pressure vessel and internals
a) Control rod drive mechanism; b) Control rod guide assembly; c) Upper core support; d) Coolant inlet nozzle; e) Support column; f) Upper core plate; g) Fuel assembly; h) Core shroud; i) Pressure vessel; j) Core barrel; k) Lower core support; l) Flow skirt (Meyer, 1991)

tion channels accommodating the irradiation specimens for fracture mechanics surveillance of the reactor pressure vessel wall are located on the outside wall of the core barrel.

The upper core support structure is located in the nozzle section of the core barrel. It forms the upper closure of the reactor core, houses the control rod guide assemblies and consists of the upper core support with top plate, nozzles and grid plate. During refuelling, the upper core support structure is removed as one unit from the flooded reactor pressure vessel together with the disengaged control rod drive rods and is stored in a designated setdown area in the reactor well. The grid plate serves to align the fuel assemblies and the control rod assemblies and transfers the loads caused by coolant flow to the bolted support columns. The top plate separates the nozzle plenum of the core barrel from the dome plenum in the RPV closure head. The guide tubes for the in-core instrumentation probes are firmly attached to the support columns.

The heat generated by nuclear fission in the fuel is removed by the primary coolant, which has a pressure of about 16 MPa and is completely in the liquid

state. Coming from the main coolant pumps, the coolant flows axially downwards in the outer zone of the reactor pressure vessel (downcomer) and then passes the reactor core in an upward direction to the outlet nozzles. In the main coolant pipes it is then transported to the steam generators. At the entrance to the reactor core, the coolant temperature is about 290 °C, at the exit it is about 325 °C. The recirculation time of the coolant in the primary circuit amounts to about 20 seconds, with about 1 second being required for passage of the reactor core. The main coolant pipes show an inner diameter of 750 mm and a wall thickness (in the linear sections) of 52 mm; they are fabricated from the same base material as the reactor pressure vessel, and they are completely plated with an austenitic weld overlay.

In the four steam generators, the heat generated in the reactor core is delivered to the secondary-side steam generator water, there producing saturated steam (see Fig. 1.4.). The steam generators are equipped with vertical U-shaped heating tubes, made of an optimized Incoloy 800 alloy (32% Ni, 20% Cr) and showing the highest stability against intergranular and transgranular corrosion. Each of the four steam generators contains 4118 U-shaped tubes, providing a heat exchange area of about 5400 m^2. The hemispherical channel head at the bottom is divided into an inlet and an outlet section and is welded to the tubesheet above. The channel head is connected to the reactor coolant system piping by means of inlet and outlet nozzles. The pressure-retaining shell in the secondary-side region encloses the tube bundle mounted on the tubesheet. Upwards, the shell increases in diameter to the steam dome which houses moisture separators and steam dryers to minimize the terminal wetness of the steam. The structural parts of the steam generator as well as the tube sheet are fabricated from the same steel as the reactor pressure vessel, and are also provided with an austenitic weld overlay. The whole component has a maximum outer diameter of 4.81 m, a total height of 21.32 m and a total mass of about 420 Mg.

In the pressurized water reactors designed by Westinghouse, Framatome and other manufacturers, the steam generator tubes are made from Inconel 600, an alloy with high Ni content (about 72%). In newer plants this material has been replaced by Inconel 690, an alloy showing higher stability against selective corrosion attack.

The reactor coolant enters the inlet channel (hot leg) of the steam generator, flows through the heat exchanger tubes where it delivers its heat to the secondary-side steam generator water, and leaves the steam generator through the outlet channel (cold leg). The secondary-side feedwater enters through a nozzle in the steam dome and is distributed uniformly by the feedwater sparger ring to the downcomer between the tube bundle shroud and the steam generator outer shell. The feedwater mixes with the recirculation flow and enters the tube bundle after reversing direction above the tube sheet; when passing the tube bundle a fraction of the rising water evaporates. In the upper part of the steam generator the steam–water mixture is separated in the moisture separator, and residual water droplets are then removed in the steam dryers. The water extracted in the moisture separator flows down again with the feedwater. The main steam leaves the steam generator through the main steam outlet at a temperature of 285 °C, a pressure of 6.9 MPa and a residual moisture content of 0.25% at the maximum (in reality, residual moisture

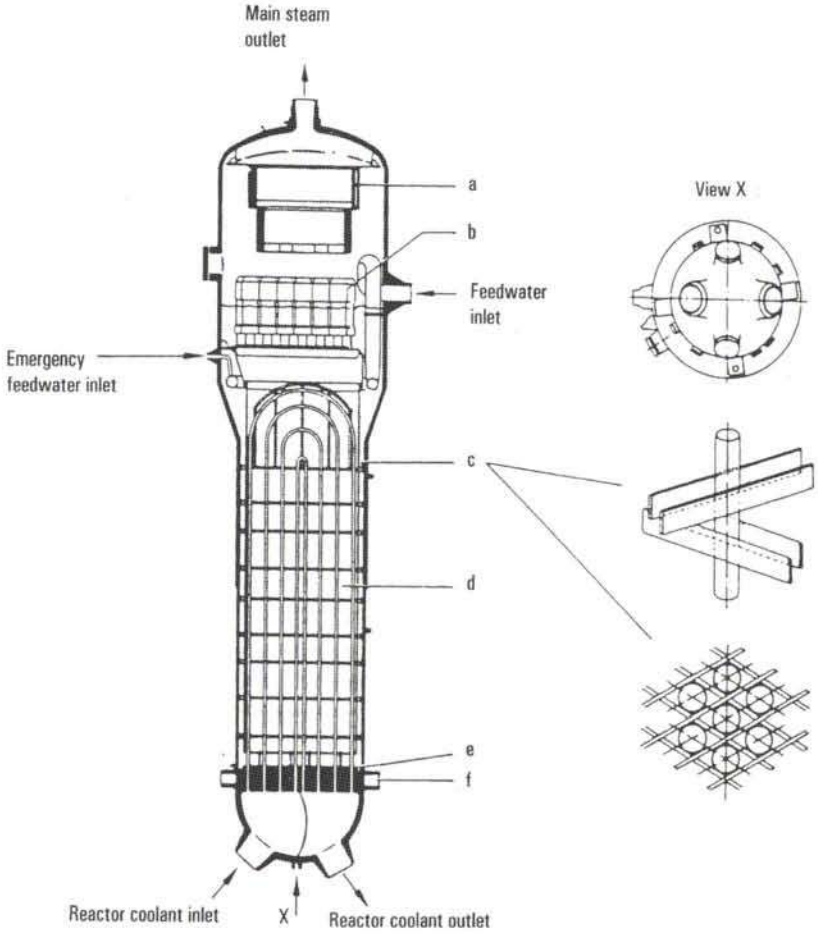

Figure 1.4. Steam generator
a) Steam dryer; b) Moisture separator; c) Tube spacer grids; d) Heating tube bundle; e) Tube sheet; f) Support
(Meyer, 1991)

is lower than this design value by at least a factor of 10). After having passed the high-pressure part of the turbine, the condensate formed here is separated and directed back to the feedwater storage tank; the remaining steam is overheated, then directed to the low-pressure part of the turbine and finally completely condensed in the main condenser.

In the U tube natural-convection steam generator, a recirculation number of about 4 (at rated power) is obtained, i. e. the recirculating mass flow is about four times greater than the feedwater (and the main steam) flow rate. In order to preclude an increase in the concentration of non-volatile inactive and (in the event of steam generator tube leakages) radioactive impurities, a fraction of the steam

generator water is continuously purified in the blowdown demineralizer system, which contains an electromagnetic filter, a mechanical filter and a mixed-bed ion exchanger filter unit.

Unlike the other PWR manufacturers, the pressurized water reactors designed by Babcock and Wilcox (B&W) are equipped with straight-tube, once-through steam generators, in which the supplied feedwater is completely evaporated. The steam leaving the steam generator is somewhat overheated, thus resulting in a higher plant efficiency. Inconel 600 is used as the steam generator tube material.

In each of the primary circuits (two to four, according to the size and design of the plant), one main coolant pump forcing the circulation of the coolant is placed between the steam generator and the reactor pressure vessel. The coolant pressure inside the primary circuit is stabilized by the pressurizer by heating or cooling as needed.

The primary system is shielded from the service compartments by concrete walls; this means that these compartments are accessible during reactor operation in spite of the intense γ radiation of ^{16}N produced in the coolant from ^{16}O by reaction with fast neutrons.

1.1.2 The reactor core

At full-load operation, the core of a Konvoi-type reactor produces a thermal power of about 3800 MW. With one ^{235}U fission contributing about 200 MeV, the total fission rate in the UO_2 mass of about 103 Mg is on the order of 10^{20} fissions per second. Each fission generates two fission products, with the majority of the total being radioactive in the first stage of life; because of their short recoil range, the bulk of the fission products is retained in the fuel matrix. Only a small fraction of them will reach the inner surface of the fuel rod cladding (see Section 3.2.). This means that the overwhelming fraction of the total radioactivity inventory of the nuclear power plant is confined in the fuel rods of the reactor core. The activation products of the core structural materials and of the coolant which are produced by neutrons escaping from the fuel and being thermalized in the surrounding coolant, form only a minor contribution to the total activity inventory. In order to characterize the environment in which nuclear fission takes place during reactor operation, manufacturing and properties of the ceramic fuel matrix as well as of the fuel assemblies used in light water reactors will be shortly described; most of the data given here are generally valid for both PWR and BWR fuels.

The starting material for the fabrication of UO_2 standard fuel is enriched UF_6, which is supplied by the enrichment plant in pressure cylinders (the preceding steps of fabrication starting from uranium ore have been described, among others, by Peehs, 1996). From this material, the UO_2 compound is made either by a wet or by a dry process. Among the wet processes, the ADU (ammonium diuranate) process is mainly used, in which UF_6 gas is hydrolyzed in aqueous ammonia solution to form ammonium diuranate. Besides ADU, the AUC (ammonium uranyl carbonate) process is applied in which UF_6 is hydrolyzed in an aqueous solution

by simultaneous addition of ammonia gas and carbon dioxide, resulting in the precipitation of ammonium uranyl carbonate. In both processes, the precipitates are filtered off and decomposed in a fluidized bed to form UO_2 by addition of hydrogen as a reaction gas. In recent years, the dry production methods have gained in importance; here, in the first step UF_6 gas is hydrolyzed by superheated steam to UO_2F_2, followed by a second step in which UO_2F_2 is reduced to UO_2 by a steam–hydrogen gas flow (integrated dry reduction, IDR process). Recycling of uranium oxide scrap originating from the fabrication line is performed by dissolution in nitric acid and precipitation of the ammonium uranyl carbonate by ammonia and carbon dioxide as described above. A more detailed description of these processes has been given, e. g., by Stoll (1991 a) and by Peehs (1996).

In fuel fabrication, a number of parameters has to be observed which are of significance for fuel behavior during reactor operation, such as pellet density, open porosity, pore size, and grain size. In order to meet the requirements, several measures are applied. For proper adjustment of pellet density in the case of highly sinter-active powder ex AUC, up to 15% of U_3O_8 is added to the powder. The open porosity, which is an important parameter for the extent of fission gas release from the pellet during operation in the reactor, can be reduced by addition of Al_2O_3 or of aluminum stearate to the powder, with the latter compound simultaneously supporting the compaction of the powder to pellets; as a consequence of these additives, the final fuel matrix may contain up to 0.1% Al. The powder is then pressed and the resulting pellets are sintered, typically for about 2.5 hours at 1730 °C. Higher temperatures and longer stay times in sintering result in a reduction of the open porosity and an increase in grain size and pellet density. The final pellets are ground to exact dimensions and to obtain a smooth surface.

In order to compensate for excess reactivity in the initial phase of operation of fresh fuel batches, burnable poisons can be added to the fuel, i. e. elements having isotopes with high neutron absorption cross sections. The favorite material for this purpose is Gd_2O_3; the gadolinium isotopes ^{155}Gd and ^{157}Gd, which have cross sections on the order of $6.1 \cdot 10^{-20}$ cm^2 and $2.5 \cdot 10^{-19}$ cm^2, respectively, are very efficient neutron poisons in the first phase of operation and, consequently, they are consumed almost completely by the end of the first fuel cycle. Moreover, Gd_2O_3 is thermodynamically very stable and highly compatible with UO_2. In pellet manufacturing, Gd_2O_3 in amounts up to 15% of the final fuel mass is homogenized with UO_2 powder; this mixture is then pressed and sintered to pellets as described above.

Plutonium-containing fuels, so-called mixed-oxide (MOX) fuels, can be fabricated by two processes (Stoll, 1991 b). In the OKOM process (optimized co-milling) PuO_2 is milled together intimately with UO_2 powder, whereas in the AUPuC process (ammonium uranyl plutonyl carbonate) a mixed ammonium uranyl plutonyl carbonate is prepared by co-precipitation. In both processes, master mixtures with high plutonium contents, on the order of 30 to 40%, are fabricated in the first stage; these are subsequently diluted with UO_2 (natural isotopic composition or depleted in ^{235}U) to a fuel containing up to 7% total Pu or up to 5% fissile Pu (i. e. Pu isotopes 239 and 241). The following fabrication steps up to the final pellet are identical with those used in UO_2 pellet production. The mixed-oxide fuel fabricated

as described shows at least a two-phase structure consisting of UO_2-PuO_2 particles from the master mixture embedded in a UO_2 matrix; this material can be readily and completely dissolved in nitric acid for reprocessing purposes (Würtz, 1987).

The dimensions of the cylindrical pellets in all three of the fuel compositions described above depend on the specific fuel assembly design. In Siemens/KWU designs with 14x14, 15x15 and 16x16 arrays, they have a diameter of 9.11 mm and a length of 11 mm; in the 18x18 array employed in the Konvoi plants, pellets with a diameter of 8.05 mm and a length of 10 mm are used. The pellet density is about 10.4 g/cm^3 with the exception of $UO_2-Gd_2O_3$ pellets, where it is somewhat lower, depending on the Gd_2O_3 content. On their plane faces, the pellets show a dishing amounting in total to about 2% of the pellet volume. This is intended to compensate for the volume increase during irradiation which is caused by the fission gas-induced swelling of the material, and to minimize the pellet stack elongation due to thermal expansion (mainly at the hot pellet center).

The impurity levels in the UO_2 material are quite low; the maximum allowable concentration limits are mainly defined to minimize parasitic neutron absorption and to preclude a potential adverse effect on fuel and cladding integrity. Fluorine and chlorine as potential initiators of Zircaloy corrosion, therefore, are restricted to maximum concentrations of 10 and 15 ppm, respectively. On the other hand, inert impurities such as iron, silicon, calcium are allowed to be present in concentrations of up to 100 ppm. In practice, the impurity concentrations present in the UO_2 material are considerably lower than the limiting values. The stoichiometry of the oxide fuel is of special importance because the optimum thermal conductivity of the ceramic pellet is attained at its exact stoichiometric composition; as will be demonstrated later on, deviation from stoichiometric composition may also affect fission product behavior. Therefore, the specification for UO_2 fuels is an O:U ratio of 2.000 ± 0.01, and for mixed-oxide fuels an O:M ratio (M designates heavy metal atoms) of 2.00 ± 0.02. In $UO_2-Gd_2O_3$ fuels one has to take tervalent gadolinium into account; as a result, the specification for the O:M ratio is usually $(2.000+0.008 \cdot \text{weight\% } Gd_2O_3) \pm 0.015$.

The very severe conditions the nuclear fuel is subjected to during its stay in the operating reactor core call for a careful quality control during fabrication; an essential part of these measures is the surveillance of the chemical composition of the materials in the different stages of the manufacturing process. Different analytical methods are available which show sufficiently high sensitivity, accuracy and reliability to satisfy the requirements. Chlorine and fluorine impurity contents usually are determined using ion-selective electrodes, either with or without preceding isolation of the trace constituents from the matrix by pyrohydrolysis. Metallic impurities are determined by atomic absorption spectrometry after dissolution of the material. As for the main constituents, uranium can be determined volumetrically by using the dichromate method, plutonium (in the presence of an excess of uranium) by potentiometric titration following oxidation by Ag_2O_2, and gadolinium by X-ray fluorescence spectrometry. The O:M ratios of the oxides (i. e. the stoichiometry of the material) can be assessed by thermogravimetric measurement. Finally, the isotopic composition in particular of mixed-oxide fuels is measured by

Table 1.2. Zircaloy alloy constituents [%]
(By courtesy of Siemens/KWU)

	Zircaloy-2	Zircaloy-4
Tin	1.20 to 1.70	1.20 to 1.70
Iron	0.07 to 0.20	0.18 to 0.24
Chromium	0.05 to 0.15	0.07 to 0.13
Nickel	0.03 to 0.08	–
Oxygen	0.07 to 0.15	0.10 to 0.16

mass spectrometry. The quality of performance of these and other required analytical methods has to be re-evaluated at regular intervals by appropriate calibrations.

The UO_2 fuel pellets consist of grains having a size of 5 to 8 μm, which is increased to 8 – 10 μm upon addition of Al_2O_3. In mixed-oxide fuels, the UO_2 matrix shows a grain size of 6 to 8 μm, whereas the particles of the plutonium master mixture are on the order of 4 to 6 μm, with a part of them forming agglomerates with sizes on the order of 20 to 30 μm. The diameters of the pores in the fuel pellets typically show a logarithmic normal distribution with a maximum in the range of 2 to 3 μm; depending on the manufacturing procedure applied, bimodal distributions are also observed.

To fabricate the fuel rod, the pellets are inserted into the cladding tube which is made of Zircaloy-4, a zirconium alloy (its composition is shown in Table 1.2.). Zircaloy (Zry) is a good compromise with regard to low parasitic neutron absorption, on the one hand, and good mechanical properties under reactor operation conditions, on the other. Zry-4 shows high stability against corrosion under PWR operation conditions, due to the outer oxide layer formed on the metal; in order to further improve the corrosion stability, so-called duplex claddings have been introduced in which the base material is coated by an optimized outer layer (low-tin Zircaloy). Only a few older PWR plants still have stainless steel claddings.

The design of light water reactor fuel rods, as well as their operational behavior, has been described in detail by Wunderlich et al. (1990); therefore, only short remarks will be made in what follows. As can be seen from Fig. 1.5., the pellet stack occupies only a part of the total fuel rod length (active length). In the Siemens/KWU design it leaves space for the upper and lower plena which accommodate the fission gases released from the pellets during operation; other fuel rod designs show an upper plenum only. The pellet stack is kept in position by a steel supporting tube at the lower end and by a steel spring at the top end; sometimes, an Al_2O_3 insulation pellet is placed at the lower end of the pellet stack. The fuel rod is sealed gas-tight by the top and the bottom end plugs. The free space of the fuel rod (plena as well as gap) is pressurized during fabrication with helium at a pressure of about 2.5 MPa at ambient temperature. On the one hand, this is to enhance thermal conductivity; on the other it stabilizes the cladding during reactor operation at a coolant pressure of about 16 MPa.

The dimensions of the fuel rods differ according to the plant and the design of the fuel assembly. In the 1300 MWe plants the total length of the fuel rod amounts

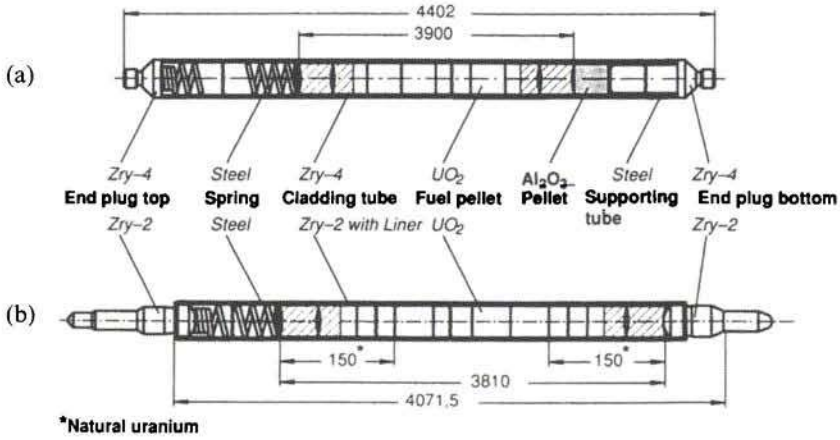

Figure 1.5. PWR and BWR fuel rod data
(a: PWR 18x18–24, FA-type; b: BWR 9–9Q, FA-type)
(By courtesy of Siemens/KWU)

to 4.40 m and the active length (i. e. the length of the fuel pellet stack) to 3.90 m; in the other plants the fuel rod length varies between 2.91 m (KWO) and 3.31 m (Gemeinschaftskernkraftwerk Neckar, GKN-1) with a corresponding active length between 2.75 m and 2.98 m. The fuel rod diameters are also determined by the type of fuel assembly used. In the 14×14, 15×15 and 16×16 arrays used in the KWU plants prior to the Konvoi type, the fuel rod has an outer diameter of 10.75 mm with a cladding wall thickness of 0.725 mm. In the 18×18 array used in the Konvoi plants the corresponding dimensions are 9.5 and 0.64 mm, respectively. This 18×18 design results in a lower linear heat rating of the fuel rod, which leads to a lower thermal burden to the fuel pellet and to the cladding material. The typical data of an 18×18 array fuel rod are summarized in Table 1.3.

Usually, uranium fuel assemblies consist of fuel rods with identical ^{235}U enrichment. In mixed-oxide fuel assemblies, however, fuel rods containing different plutonium contents are frequently combined in order to achieve a homogeneous power distribution over the whole assembly; an example of such an arrangement is shown in Fig. 1.6. The Mox fuel assemblies are designed to be fully compatible with the dimensions of uranium fuel assemblies; thus, both types can be freely interchanged in refuelling the reactor core.

Both the materials used in the fuel rods and their fabrication are characterized by a high operational integrity; most of the PWR fuel assemblies designed and fabricated by Siemens/KWU have achieved a burnup of 35 to 40 MWd/kg HM (heavy metal), a significant fraction reached a burnup in excess of 40 MWd/kg HM. The statistical annual failure rate for Siemens/KWU fuel assemblies is currently $1 \cdot 10^{-5}$, i. e. out of 100,000 rods, on the average one will experience a failure. Post-irradiation examinations have shown that these operational failures are in the main not due to design or fabrication; the most common cause of damage in recent

Table 1.3. Siemens/KWU fuel rod fabrication data
(Examples for fuel rods without gadolinium)
(By courtesy of Siemens/KWU)

		Siemens 18 × 18 (PWR, Konvoi)	Siemens 9 × 9Q (BWR, KKK)
Active length	mm	3900	3810
^{235}U enrichment [1]	%	3.45 [2]	2.5–3.5 [3]
Natural uranium ends	mm	–	2x150
Cladding outside diameter	mm	9.5	11.0
Cladding wall thickness	mm	0.64	0.665
Layer thickness of Zr liner	mm	–	0.095
Pellet diameter	mm	8.05	9.5
Pellet length	mm	10	11.5
Pellet density	g/cm^3	10.4	10.55
Diametrical clearance between pellet and cladding	mm	0.17	0.17
Dishing volume	% [4]	2.2	1.0
Helium fill pressure	bar	22.5	6.5

1) in reload fuel assemblies (FA)
2) valid for all fuel rods (FR) without Gd
3) FA contains several different FR types
4) related to pellet volume

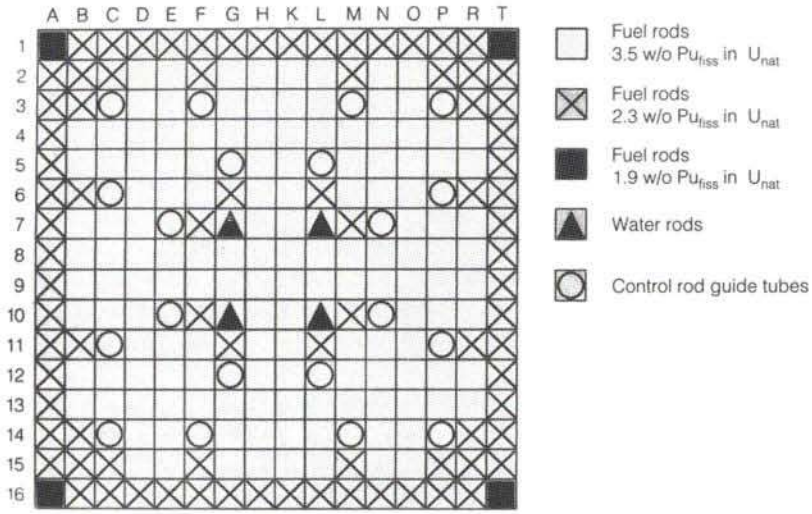

Figure 1.6. Mixed-oxide fuel assembly 16x16–20 array containing different Pu contents; cross-sectional view
(By courtesy of Siemens/KWU)

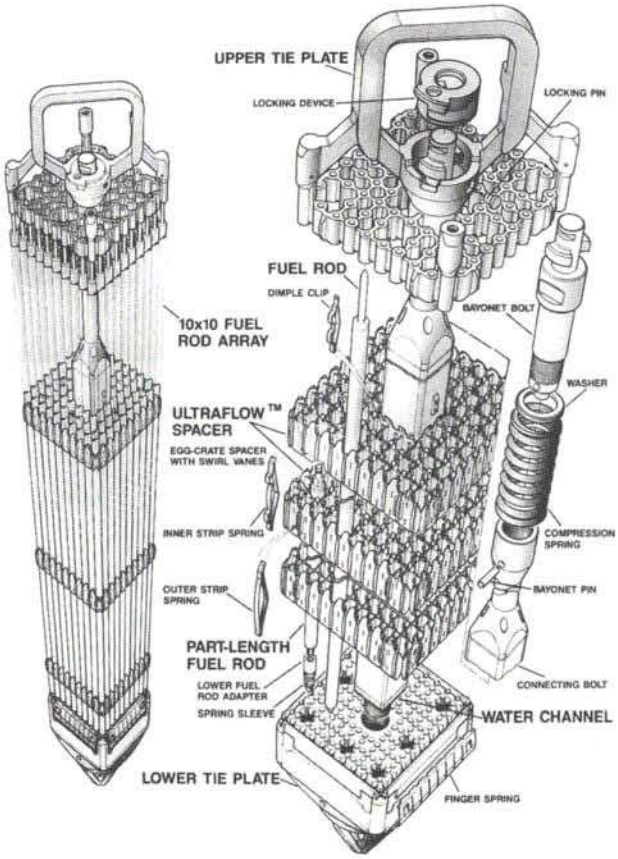

Figure 1.7. PWR fuel assembly Siemens FOCUS 18–24
(By courtesy of Siemens/KWU)

years has been fretting of the cladding caused by metallic debris carried with the coolant. By using specially designed lower end pieces, virtually all of the potentially dangerous debris can now be prevented from entering the fuel assembly; by this means, this type of failure has been significantly reduced. The failure rate does not depend on the type of fuel, i. e. PWR and BWR standard uranium fuel rods as well as mixed-oxide fuel rods show no significant differences in failure rates.

The fuel rods are joined to the fuel assembly by the fuel assembly structure (see Fig. 1.7.), which connects the fuel assembly top and bottom end pieces. In an 18×18 array, 300 fuel rods are fixed in position by the spacer grids, with nine of them being distributed over the length of the bundle. In earlier designs the material of the spacer grids was Ni-coated Inconel X 713; for reasons of neutron economy and in order to minimize the amount of material forming long-lived radionuclides in the neutron field, Zircaloy-4 is now commonly used. Only the very small spacer

springs fixing the fuel rods in position and, in some designs, the top and bottom end spacers which are exposed to a relatively low neutron flux are still made of Inconel X 713. The 24 positions in the fuel assembly lattice not occupied by fuel rods are equipped with guide tubes connecting the top and bottom end pieces of the fuel assembly. They are open at the upper end for the insertion of control rods. In the reactor core, only a part of the available positions are occupied by control rods; the KKI-2 core design, for example, has 61 control rod assemblies which are distributed throughout the core, with 24 rod fingers each. The neutron absorbing material in these control rods is an Ag-In-Cd alloy with 80% Ag, 15% In and 5% Cd encapsulated in an austenitic steel cladding. In other core designs, the control rod equipment is divided into two groups, so-called black assemblies made up of rods consisting of an Ag-In-Cd alloy in the lower section and of B_4C in the upper part, and so-called grey assemblies containing absorber rods made of Ag-In-Cd alloy and steel rods. When the fuel assemblies are placed in the reactor core in the conventional manner (i. e. those assemblies having the highest enrichment of fissile isotopes in the outer zones, see below), then burnable poison rods (e. g. borosilicate glass) can be inserted into free control rod positions in order to guarantee a sufficiently negative temperature coefficient of reactivity; in particular, such rods were frequently applied in the past in core initial charges. When $UO_2-Gd_2O_3$ fuels are used, these burnable poison rods are no longer employed.

Inside the reactor pressure vessel, the reactor core is fixed in position by the core internal structure consisting of the core shroud and an upper and lower core grid plate (see Fig. 1.3.). In a 1300 MWe plant the reactor core itself consists of 193 fuel assemblies arranged in a geometrical pattern inside the reactor pressure vessel; as an example, a core scheme also containing mixed-oxide fuel assemblies is shown in Fig. 1.8.

For the first loading of a new reactor core, the individual fuel assemblies are arranged in different zones according to their ^{235}U enrichment, e. g. 3.5%, 2.8%, 2.1%. In refuelling, the fuel assemblies which have reached their design burnup, typically amounting to about one third or one fourth of the reactor core per operating cycle, are replaced by fresh ones having a ^{235}U enrichment of up to 4% or by mixed-oxide fuel assemblies. The fresh fuel assemblies, as well as the partially spent ones from the preceding cycles, are positioned in the reactor core in accordance with an optimum exploitation of the fuel. To this end, detailed core loading schemes are calculated for each refuelling procedure. In former years, the fresh assemblies were usually placed in the outer regions of the reactor core. In order to improve neutron economy, the outer positions now are in most cases occupied by partially spent assemblies while the fresh ones are distributed throughout the reactor core. Such a low-leakage core loading including both uranium and mixed-oxide fuel assemblies is exemplarily shown in Fig. 1.8. By such a low-leakage loading a saving of approximately 0.2% uranium enrichment or of several fresh assemblies per fuel cycle can be achieved, due to the minimization of neutron losses at the core periphery. In addition, by this type of loading the neutron fluence at the reactor pressure vessel wall is reduced, thus preserving the wall material ductility.

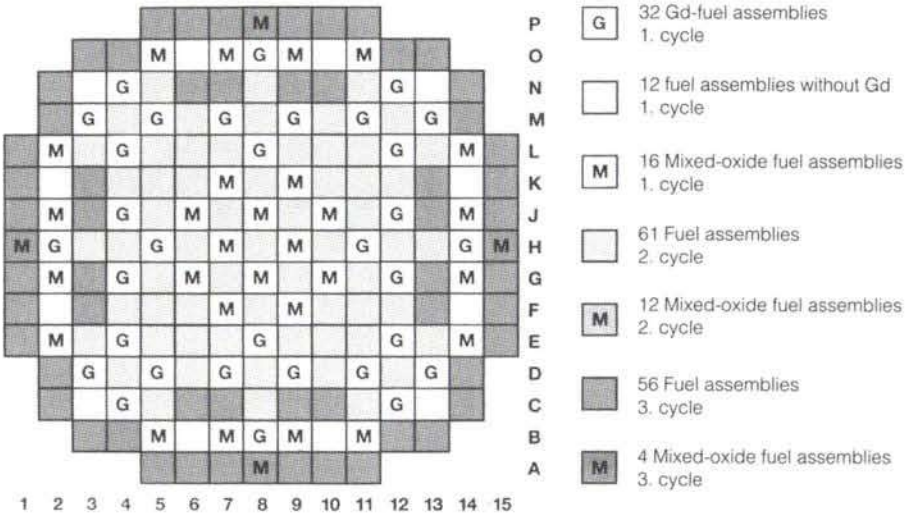

Figure 1.8. PWR reactor core; cross-sectional view
(By courtesy of Siemens/KWU)

During operation at rated power, the temperature in the fuel pellet shows a steep decrease from the center to the surface, with the specific values depending on the linear heat rating of the fuel rod (see Fig. 1.9.). This steep thermal gradient places a high load on the ceramic material, which the pellet has to withstand. In practice, cracks form in the pellets leading to comparatively large-volume fragments by which the stability of the pellet stack is not affected. In the pellet – cladding gap the temperature drops by an additional 100 K, in the cladding by additional 40 K, thus reaching values of about 350 °C at the fuel rod surface. The average linear heat rating of the fuel rods amounts to about 200 W/cm in 1300 MWe plants with a 16x16 array, whereas in an 18x18 array the larger number of fuel rods with smaller diameters results in a lower heat rating of around 170 W/cm and correspondingly lower fuel and cladding temperatures. The temperatures given in Fig. 1.9. apply to a fuel rod with a linear heat rating of 250 W/cm.

In order to provide a base neutron level to ensure that the neutron measurement detectors are operational and responding to core multiplication neutrons, primary and secondary neutron source rods are applied. The primary neutron sources usually contain spontaneously fissioning ^{252}Cf, which provides neutrons during the initial core loading and the first reactor startup. The secondary neutron sources consist of an antimony–beryllium mixture which must be activated by neutron irradiation during reactor operation; the high-energy γ quants of the ^{124}Sb formed during the first fuel cycle induce a (γ, n) reaction in the ^{9}Be nucleus, thus providing neutrons for startup operations in the subsequent fuel cycles.

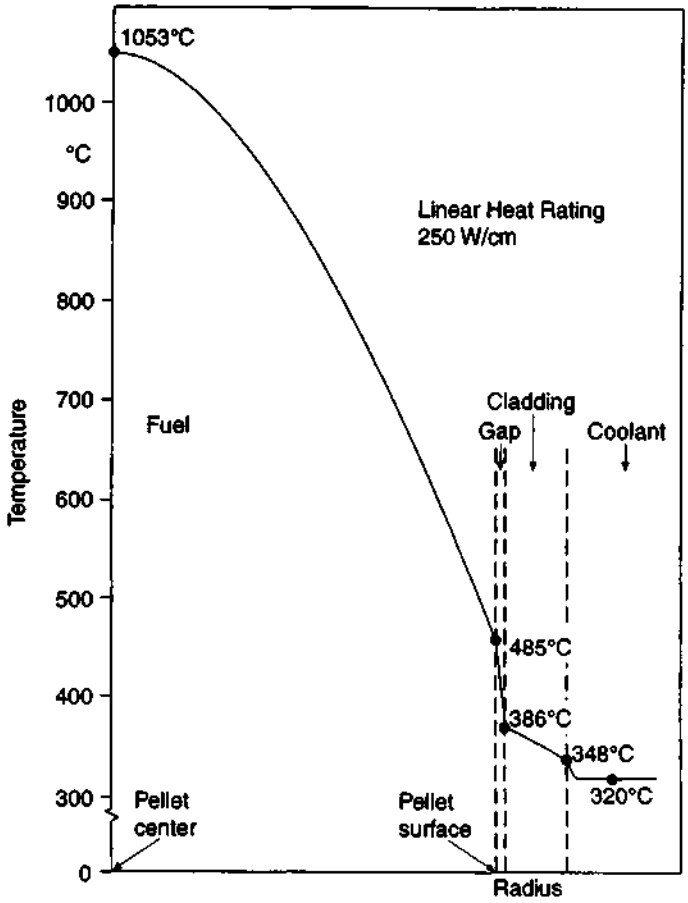

Figure 1.9. Typical radial temperature profile in a PWR fuel rod
(By courtesy of Siemens/KWU)

The spent fuel assemblies which are discharged in the course of refuelling are stored in the spent fuel pool which, in KWU designed plants, is located inside the containment (see Fig. 1.2.), whereas in the plants of other manufacturers it is located in a separate building. In most cases the storage racks in the 1300 MWe plants are capable of holding 768 fuel assemblies, i. e. 9 refuelling charges plus one full core load. The storage racks are made of boron steel (> 1.6% B); this ensures subcriticality even for fresh fuel assemblies with up to 4% ^{235}U enrichment or the equivalent mixed-oxide fuel. The pool water is cooled by a recirculation cooling system; by passing a fraction of it to a mixed-bed ion exchanger bed the concentrations of radionuclides are kept low, even when failed fuel rods are present in the stored assemblies. The storage time of the spent fuel assemblies in the pool is a minimum of 6 months; during this time, a great part of the shorter-lived radionuclides (in particular ^{131}I) will have decayed. In reality, the intermediate

storage time until transport of the spent assemblies to a reprocessing plant or to an away-from-reactor storage site depends on various parameters and can be considerably longer.

1.1.3 The auxiliary and ancillary systems

In the operation of nuclear power plants a number of additional systems are needed to support the regular functioning of the main systems. These systems, which are mainly located in the reactor auxiliary building, essentially have to fulfil the following functions:

- control of the coolant inventory and coolant treatment
- removal of residual heat from the reactor coolant system
- prevention of escape of radionuclides to the environment.

A schematic survey of the nuclear auxiliary systems in a Siemens 1300 MWe plant is given in Fig. 1.10.; in the following, these systems will be shortly described

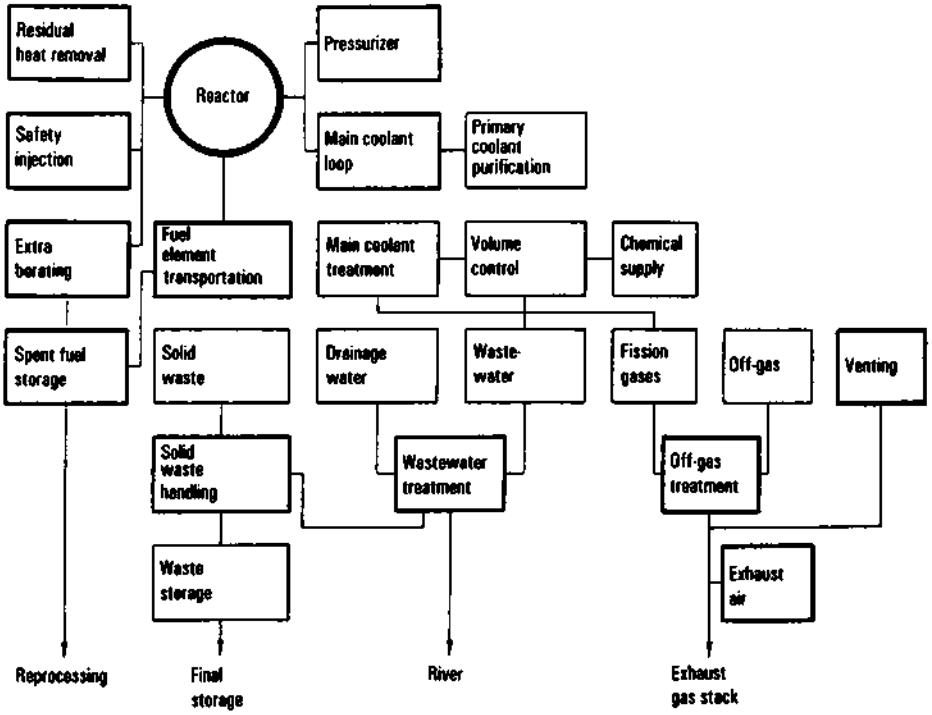

Figure 1.10. PWR nuclear auxiliary systems; schematic overview (Kausz, 1991)

as far as they are of significance for the behavior of the radionuclides (for a more detailed overview see, e. g., Kausz, 1991).

The central constituent of the nuclear auxiliary systems is the volume control system which is the interface between the high-temperature, high-pressure reactor coolant system and the low-pressure parts of the auxiliary system. The variations in density and volume of the primary coolant caused by changes in temperature occurring during heatup, cooldown or load changes of the plant are compensated for by the volume control system if the pressurizer cannot keep the resulting level fluctuations within certain given limits. In addition, the volume control system continuously supplies other auxiliary systems with a defined coolant mass flow, thus rendering it possible to establish an optimum coolant quality with regard to reactor load control (boric acid concentration) and corrosion behavior of the primary system materials (coolant chemistry in general).

The boric acid and demineralized water control system is necessary to adjust the boron concentration in the reactor coolant system. To increase boron concentration in the coolant, boric acid solution is injected through the volume control system; to reduce boron concentration, an adequate volume of coolant is replaced by demineralized water. This system (as well as the other systems discussed here) is a purely operational system and is not required for control of a design basis accident; the extra borating system fulfils the necessary safety functions. However, to guarantee continued supply to the volume control system during emergency power operation, the pumps and motor-operated valves of the system are connected to the emergency power supply system.

The chemical control system serves to adjust the coolant chemical values (oxygen concentration, pH) to the specified levels by supplying hydrazine to the coolant for oxygen-scavenging before heatup and $^{7}LiOH$ to maintain the pH level. The dilute solutions which are required for this purpose are prepared in the chemical mixing tank and fed to the high-pressure charging pump discharge side of the volume control system by means of a chemical metering pump. The H_2 concentration in the coolant, which is required for recombination of the oxidizing species produced by radiolytic reactions in the primary coolant, is controlled by a special H_2 injection installation; in older plants, H_2 was fed into the coolant via the volume control tank.

The specified coolant purity is controlled by the coolant purification system. A continuous coolant flow amounting to about 10% of the primary coolant volume per hour is extracted from the volume control system and passed to the coolant purification system, routed through mixed-bed ion exchanger filters with a connected resin trap and then returned to the volume control system upstream of the volume control surge tank. In the case of high concentrations of fission products in the coolant, e. g. during the shutdown spiking, the coolant flow through the purification system can be doubled, i. e. to about 20% of the primary coolant volume per hour. The main task of the ion exchanger beds is removal of the fission products and activated corrosion products present in the coolant. Two parallel filters are installed which are charged with identical quantities of ion exchanger resin and the same proportion of cation to anion resins. They are operated al-

ternately to perform different functions, one as the main purification filter while the other filter is on standby and can be used to remove lithium and cesium, if necessary, i. e. in the case of a lithium concentration in the coolant in excess of 2.2 ppm or of high cesium radioisotope concentrations. When the main purification filter is exhausted (usually after about one fuel cycle of operation, either due to a decrease in ion removal efficiency or to an increase in flow resistance beyond the specified values), it is replaced by the lithium removal filter. Prior to operation, the ion exchangers have to be saturated with borate and lithium ions to their equilibrium level. The resin traps downstream of the mixed-bed filters are designed to retain any abrased resin material released from the filter during operation; the mesh of the traps is so fine that impurities of colloidal size are removed from the purified coolant. The spent resins of the filters are flushed out and transported hydraulically by the resin flush pump to one of the spent resin tanks for interim storage. From there, they can be flushed into a shipping drum via the resin transfer station or to the resin metering vessel in the radioactive concentrates processing system.

If required, a bypass flow of the primary coolant can also be passed through the coolant degasification system to remove gaseous fission products and other dissolved gases from the coolant. The primary coolant is extracted from the volume control system, passed through the purification system and is then admitted to the degasifier column at a temperature of approximately 50 °C. The subatmospheric pressure required for evaporation at this temperature is maintained by the degasifier vacuum pump. The coolant rises into the degasifier column head and trickles down through a stack of bubble trays into the column sump. A small fraction of the coolant is evaporated in the downstream evaporator; this vapor passes in counterflow to the coolant trickling down from the column head, thus stripping the gases. The vapor is liquified in the condenser and returned to the column head. The gases released are further dehumidified in the gas cooler and extracted to the gaseous waste processing system by means of the degasifier vacuum pump. At the same time, inert gas from the gaseous waste processing system is added to the gas flow in such a quantity as to reliably prevent the formation of explosive hydrogen concentrations. The degasified coolant in the column sump is extracted by means of the degasifier extraction pump and injected back into the volume control system downstream of the volume control surge tank.

The gases released from the primary coolant in the degasification system mainly contain the fission product noble gases which, with the sole exception of ^{85}Kr, are comparatively short-lived nuclides. In order to prevent release to the environment, therefore, it is sufficient to store them for a certain time until these isotopes have decayed. In most of the US PWR plants as well as in the plants built by Framatome, gas decay tanks are used for this purpose. In the plants designed and built by Siemens/KWU, decay lines are employed which are equipped with a series of charcoal beds in which the noble gases are delayed relative to the carrier gas flow by a dynamic adsorption–desorption equilibrium. Under normal operation conditions, delay times on the order of 60 hours for the krypton isotopes and 60 days for the xenon isotopes are obtained, which are sufficiently long for nearly complete

decay of all the radioisotopes (with the exception of ^{85}Kr) before release to the environment. The fission gas delay process will be treated in more detail in Section 4.3.3.1.1.

During startup and control processes, coolant is pumped, after passing the coolant purification system, into the coolant storage system for interim storage. In the coolant treatment system, it is separated by evaporation into demineralized water and boric acid concentrate containing about 7000 ppm B. The distillate then is directed to the coolant storage system, while the boric acid concentrate is transferred to the boric acid and demineralized water control system, from where it can be fed into the primary system via the volume control system, when required.

Waste waters from the reactor system, from peripheral units such as the laboratories, as well as from cleaning actions, laundry and sumps etc. are purified and decontaminated in the liquid waste processing system. The main operation here is evaporation of the liquids; depending on the chemical composition of the waste solutions as well as on their radionuclide concentrations, other techniques can also be applied such as chemical precipitation, separation by precoat filtering and adsorption by ion exchangers. The purified water is then stored in the control tanks to be analyzed for residual radioactivity; if the results show that the radionuclide concentrations are clearly below the licensed values, the water is mixed with the non-radioactive service water and released to the receiving water flow, e. g. to a river. In case the results of the control measurements exceed the licensed values, the water is fed back to the liquid waste processing system and treated a second time. The concentrates from the liquid waste processing system are forwarded to the radioactive concentrates processing system for interim storage and, if necessary, preconditioning, and from there passed on for further conditioning. The extent of conditioning performed at the site is quite different in different plants; often external conditioning is used.

Primary coolant samples for analysis can be taken at various locations by means of the nuclear sampling system. Downstream of the sample line coolers, the liquid is depressurized and transported over the lines to the sampling points; the most important one of these sampling stations is located in the chemical laboratory. This provides convenient access, but it results in a considerable length of the line from the primary circuit to the sampling station.

Following plant shutdown, the core decay heat as well as the heat stored in the primary coolant and in the primary system components are carried off by the residual heat removal system. In the course of a normal shutdown this is done via the steam generators and the main condenser, bypassing the turbine. Below a coolant temperature of approximately 120 °C and a primary circuit pressure of less than 3.5 MPa, the residual heat removal system directly carries off the heat to the component cooling system.

The ventilation systems of the controlled areas that potentially contain airborne radioactivity play an important role in preventing uncontrolled dissemination of radioactive substances within the plant as well as to the environment. For this purpose, their main functions are to maintain directional air flow, to reduce air-

borne radioactivity in the compartment air, either by air recirculation via filters or by exchange, and to retain radioactive substances by air filtration before discharge to the vent stack. In order to achieve these goals, different ventilation systems are installed, the design and operation of which provide a subatmospheric pressure gradient between the various groups of compartments in the containment, thus rendering possible free access to large areas of the containment even during reactor operation. The central part of the ventilation systems is represented by the containment interior subatmospheric pressure system, which extracts the exhaust air from the different compartment groups in the containment. The large equipment compartments in the containment (which are not accessible during reactor operation) are equipped with an air recirculation system whose main task is to remove the heat dissipated from the components to the compartment atmosphere. The annulus air extraction system is a standby system which is not used during normal operation, but is designed to maintain a subatmospheric pressure in the annulus if there is a loss-of-coolant accident within the containment. Additional ventilation systems serve the reactor auxiliary building and the radioactive waste processing building.

In order to remove radioactive substances potentially present in the air flow, most of the ventilation systems are equipped with filter units consisting of high-efficiency particulate filters (HEPA filters, class S) and iodine adsorbers (activated charcoal, KI impregnated). These filters are monitored, either continuously or at regular intervals; the filter efficiency of the iodine adsorbers is determined by taking charcoal samples from the filter beds at regular intervals and analyzing them in the laboratory (see Section 6.2.1.5.).

The vent air from the controlled area, amounting to about 200,000 m^3/h is continuously monitored for radioactive substances. To this end, bypass flows are extracted and passed through radioactivity monitoring lines. After radioactivity measurement, these air flows converge again and then are passed to the vent stack.

1.1.4 Safety and emergency installations

In the event of an accident, the appropriate design of systems and installations has to ensure that radioactive substances will not be released to the environment to an extent beyond tolerable limits. To this end, a series of so-called design basis accidents (see Chapter 6) have been defined, covering conceivable failures of different installations and their possible consequences. In the licensing procedures for a nuclear power plant it has to be demonstrated that in the event of an accident the safety and emergency installations of the plant will be able to keep the reactor core in a safely cooled state and to prevent significant release of radionuclides to the environment.

It has to be emphasized that in a light water PWR a dramatic power excursion of the reactor core is not possible due to physical reasons. This inherent safety is based on three effects that all act in the same direction. Temperature increase in the primary coolant means a dilution of the moderator density, thus reducing the concentration of thermal neutrons and, consequently, decreasing the ^{235}U fission

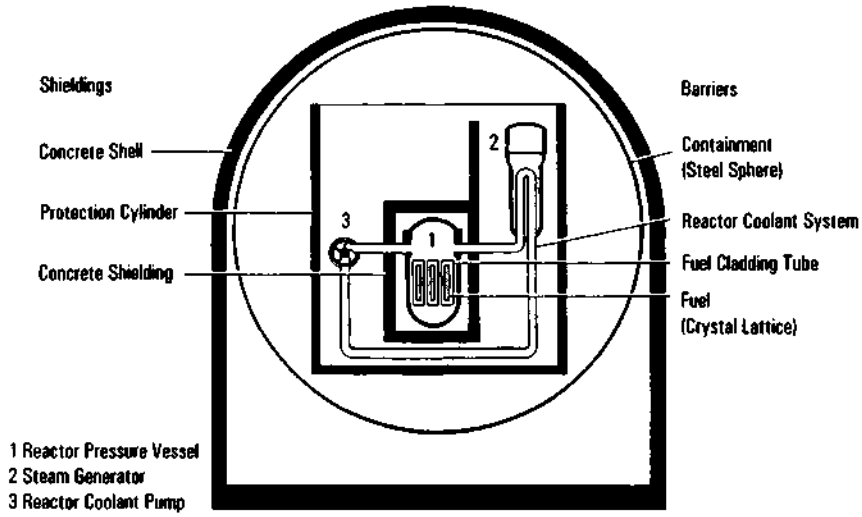

Figure 1.11. Passive safety barriers in a PWR plant (schematic view)
(By courtesy of Siemens/KWU)

rate. In the event of a loss-of-coolant accident, the depressurization of the coolant leads to a steam void formation and, consequently, to a loss of moderator effectiveness, resulting in a sudden interruption of the nuclear chain reaction, even should the safety-grade shutdown system fail to operate. Finally, the neutron capture rate of ^{238}U increases with increasing coolant temperature, the consequence of which is a corresponding reduction in the ^{235}U fission rate. As a result of these effects, the power level of a light water PWR cannot increase dramatically, i. e. the reactor cannot run out of control. All the problems potentially arising in a light water reactor accident are exclusively due to an insufficient removal of the decay heat from the core.

As can be seen from the schematic diagram in Fig. 1.11., four independent, passive barriers prevent the release of fission products from the fuel to the environment in the case of accident:

- the crystal structure of the ceramic fuel pellets
- the gas-tight sealed cladding of the fuel rod
- the primary circuit, which is designed to bear high pressure
- the high-integrity steel shell of the reactor containment.

Thus, fission products which might succeed in overcoming the first of these barriers will be retained by the following ones, resulting in a long-lasting transport pathway during the course of which chemical effects will come to play an important role (see Sections 6 and 7).

In order to retain the fission products within the first barrier, it is important to prevent overheating of the reactor fuel. As a first, passive means of ensuring a sufficiently high heat removal from the reactor core in case the main coolant pumps

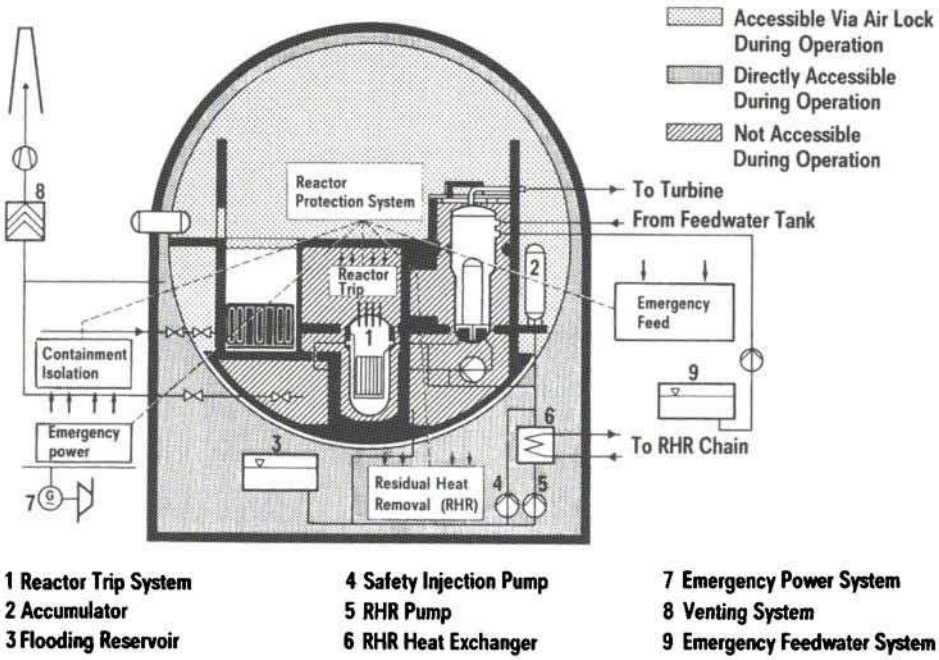

Figure 1.12. Engineered safety features of a Siemens 1300 MWe PWR (By courtesy of Siemens/KWU)

are not operable, the heat transfer surfaces in the primary circuit are arranged in such a manner that the heat source is at a low elevation with the heat sink above. Thus, if coolant is heated by the residual decay heat of the reactor plus the heat stored during operation in the components and structures, its density will decrease and it will rise into the steam generator tubes where it will deliver its heat to the secondary-side water circuit. As a consequence of cooling down, the density of the primary coolant increases and it travels downward into the reactor pressure vessel where the heat removal cycle begins again (natural circulation).

In the event of significant losses of coolant from the primary circuit, the actively working emergency core cooling systems, which are designed to act in a redundant manner, will start operation. In the 1300 MWe PWR plants designed and built by Siemens/KWU, the whole system consists of four independent and redundant lines, with each of them being connected to one of the four primary circuit loops; detailed descriptions of these systems have been given on several occasions, e. g. by Rysy (1986). As can be seen from the schematic view in Fig. 1.12., each line contains the following components:

- a high pressure safety injection pump
- a residual heat removal pump
- a residual heat removal heat exchanger
- two accumulators containing borated water
- a flooding reservoir containing borated water.

The capacity of each of the four lines is dimensioned in such a manner that operation of two of them is sufficient to prevent overheating of the reactor core.

In each of the four primary loops, two safety injection lines are installed, with one of them feeding the emergency coolant (boric acid solution, 2200 ppm B) into the "hot" side and the other feeding it into the "cold" side of the main coolant pipes. This means that in the event of a loss-of-coolant accident, the emergency coolant reaches the reactor core both from the top and the bottom side. This design of both hot- and cold-leg injection is different from the PWR plants of other manufacturers, where only a cold-leg injection line is installed. In principle, in a PWR with only cold-leg injection of the emergency coolant, the hot leg of the broken loop may provide a path for radionuclides to escape from failed fuel rods in the core to the containment atmosphere. Simultaneous injection of the emergency coolant into both the hot and cold legs decreases the temperature of the fuel cladding and thus the probability that it might fail. It also provides a form of retention for non-gaseous fission products between the core and the containment atmosphere.

The high pressure safety injection system is designed to control small- and medium-sized leaks in the primary system by feeding coolant from the flooding reservoir into the reactor pressure vessel. In the accumulators, borated water is stored under nitrogen pressure; if, in the event of a large break, the pressure inside the reactor pressure vessel drops below 2.6 MPa, valves will be automatically opened by the accumulator pressure to feed the water reservoir of the accumulators into the reactor pressure vessel. Following accumulator operation, the low-pressure injection system starts transporting water from the flooding reservoir to the reactor pressure vessel by the action of the residual heat removal pumps. When the flooding reservoir is exhausted, the residual heat removal pumps switch over to the sump which has been formed in the meantime in the lower part of the reactor building; by circulating the sump water inventory via the residual heat removal heat exchangers, the reactor core can be safely cooled for longer periods of time.

The PWR plants designed by Framatome, Westinghouse and others are additionally equipped with a containment spray system for reducing the temperature and pressure inside the containment in the event of a loss-of-coolant accident; because of the lower capacity of the low-pressure safety injection systems (compared with the Siemens/KWU plants), heat removal from the reactor core in these plants in the case of a cold-leg break cannot be performed without water evaporation by boiling. In most designs the spray system is initiated automatically when the pressure in the containment exceeds a preset value and is therefore effective almost from the onset of the accident; nonetheless, the actuation of the spray may be initiated by the operator or delayed, in order to cover all possible situations. The spray solution is taken from the refuelling water storage tank and is fed to the spray nozzles which are located on ring headers attached to the steel containment liner in the upper part of the containment, thus providing maximum coverage of the free gas volume as well as washdown of the containment walls. After about half an hour of operation, the spray pumps switch over to the containment sump, making feasible long-term operation of the spray system. Another beneficial effect

of the spray system is removal of airborne radionuclides from the containment atmosphere; in order to plate out iodine, alkaline substances are usually added to the spray water (boric acid–NaOH, $Na_2S_2O_3$ or others).

Some of the Westinghouse PWR plants are equipped with an ice-condenser system; this is a large quantity of ice (about 1000 Mg) which is stored in perforated metal baskets and which would act as a low-temperature, passive heat sink to condense the steam produced in a loss-of-coolant accident and, thus, to absorb the energy released to the containment atmosphere. Condensation of steam on the ice surfaces also results in a certain degree of washout of airborne radionuclides.

In the Konvoi-type plants, the containment is formed by a large spherical steel shell with a diameter of 56 m and a wall thickness of about 38 mm. This steel shell is designed to withstand an inner overpressure of 0.53 MPa at a temperature of 145 °C; it shows a leak rate of 0.25% of its volume per day at the maximum (in reality, the leak rate is considerably lower). It is virtually gas-tight and capable of retaining radionuclides which are released from the primary circuit to the containment almost completely. The containments of other manufacturers have a cylindrical shape; they are made of prestressed concrete and are provided with an inner steel liner.

The upper hemisphere of the steel shell is surrounded by a shielding made of reinforced concrete with a wall thickness of about 2 m. This shielding protects the nuclear part of the plant against any external impact (e. g. gas explosion, military aircraft crash); it also significantly reduces the likelihood that radionuclides will escape to the environment. The interspace between the steel shell and the secondary containment is held at sub-atmospheric pressure, so that any radionuclides penetrating the steel shell via leaks in the event of a loss-of-coolant accident would be transported by the annulus air extraction system to the standby filters and retained here, thus preventing release to the environment.

1.2 VVER design

The design of Soviet pressurized water reactors is significantly different from that of Western PWRs, with regard both to main components and systems layout, as well as to the safety and emergency installations. The design and the other technical aspects of the VVERs have undergone a long period of evolution, starting from the first commercial plant, Novovoronezh-1, designated VVER-210, which was commissioned in 1963 and shut down in 1986. Roughly, two types of plants can now be distinguished, the VVER-440 and the VVER-1000, with a gross electrical capacity of 440 and 1000 MW, respectively (corresponding to a rated core thermal power of 1375 and 3000 MW).

The VVER-440 reactors are always built in modules of two units which are housed in one single reactor building. Each reactor has six loops, isolation valves in each loop, and horizontal steam generators arranged around the reactor pressure vessel; each reactor supplies two 220 MW turbines. The reactor pressure vessel has

an inside diameter of 3.56 m, a total height of 11.8 m and a wall thickness in the cylindrical part of 0.14 m. It is made of a low-alloy steel; in the older model V230 it has no clad, whereas in the newer model V213 all the surfaces in contact with the coolant are provided with a stainless steel clad. Although no significant corrosion or other problems have been reported with the use of ammonia–potassium water chemistry control in the older plants, the primary circuit surfaces of the Loviisa Unit 1 and of the subsequent plants were provided with a stainless steel clad in order to simplify maintenance of the correct water chemistry. The primary coolant pressure is 12.4 MPa, corresponding to a coolant core inlet temperature of 268 °C and a core outlet temperature of 301 °C.

Each of the steam generators of the VVER-440 plants is equipped with 5536 heating tubes, which gives a total heat exchange surface of 2510 m^2. The tubes are fabricated of the stainless steel Cr18N9T, the shell and the tube sheet of a low-alloy carbon steel.

The reactor core contains 349 hexagonal fuel assemblies, each of them consisting of 129 fuel rods with a diameter of 9.1 mm and a length of 3.21 m; the fuel rods are kept in position by 15 honeycomb-type spacer grids which are fixed on a central channel. Seventy-three of the fuel assemblies contain movable control assemblies with boron steel as an effective material; in the V213 fuel assemblies, six of the fuel rods are replaced by fixed burnable poison rods.

The total uranium mass in the reactor core amounts to 42 Mg, with the ^{235}U enrichment ranging between 2.4 and 3.6%; a central hole in the fuel pellets is designed to reduce the temperature in the center of the fuel. The fuel rod cladding material is Zr-2.5%Nb. The active length of the fuel pellet stack is 2.42 m, the average linear heat rating is 127 W/cm. The reactor core is designed for an average fuel burnup of 28.6 MWd/kg U, with a maximum burnup of 42 MWd/kg U; usually, one third of the fuel assemblies are changed per year.

The reactor building for each pair of VVER-440 units is served by a common auxiliary building which houses waste handling systems (ion exchange filters, evaporators) as well as liquid and dry waste storage facilities. The primary system cleanup system for each V230 unit includes 9 vertical ion exchange resin tanks which are located in one of the corners of the steam generator accident localization compartment.

Release of fission products in the event of an accident is prevented in the older VVER-440 model V230 by a local area compartmentalization. This is a sealed set of interconnected compartments which surround selected primary system components including the inlet and outlet piping, steam generators, pumps, isolation valves and the lower part of the reactor pressure vessel; the total accident localization volume is about 10,000 m^3. The design basis accident is defined as a pipe rupture with an effective 10 cm diameter. The accident localization system is designed to retain an overpressure of 0.1 MPa; in case the pressure in the compartments rises beyond this value, valves will open to discharge steam and air directly to the atmosphere through openings in the outer walls of the steam generator compartment. The V230-type plant is equipped with makeup coolant pumps that provide a limited capability for emergency core cooling, but they do not possess an emergency core cooling system with the capability of Western power reactors.

The plants at Loviisa, Finland, though they are also of the V230 type, are equipped with a concrete containment surrounding the primary system. In addition, they are provided with an ice condenser pressure suppression system.

The newer VVER-440 model 213 differs from the 230 in that it has an emergency core cooling system with limited capacity and a bubbler/condenser tower which is connected with the accident localization compartments of each unit to mitigate the effects of severe accidents. This tower has a rectangular cross section and contains 12 levels of suppression pool trays (in total about 1960 trays). The tower also houses four large receiver volumes referred to as gas holders or air traps.

In the early 1970's, the Soviets designed and began to construct a four-loop 1000 MWe PWR, designated VVER-1000. The pressure vessel of this reactor type has an inner diameter of 4.07 m, a total height of 10.88 m and a wall thickness in the cylindrical part of 0.19 m. The coolant pressure in the primary circuit at the exit of the reactor is 15.7 MPa, the coolant temperature at the outlet of the reactor core is 322 °C and at its inlet is 289 °C. The reactor core contains 151 fuel assemblies of a hexagonal configuration, with each assembly consisting of 317 fuel rods. The fuel rods have an outer diameter of 9.1 mm and an active length of 3.50 m. The fuel pellets are UO_2 with a ^{235}U enrichment of 3.3 and 4.4%; the fuel rod cladding is a Zr–Nb alloy. The reactor core is designed for an average burnup of about 40 MWd/kg U. The steam generators of the VVER-1000 plants have 15,648 heating tubes each, resulting in a heat transfer surface of about 5040 m^2. The tubes are made of the stainless steel Cr18N9T, the shell and other parts are of a low-alloy carbon steel.

The VVER-1000 primary circuit is surrounded by a containment. The accident mitigation systems include a containment spray system and an emergency core cooling system consisting of a high-pressure boric acid injection system, accumulators, and a low-pressure cooling system. The plants currently under construction are further upgraded, in particular as concerns the safety and emergency installations (e. g. Prozenko et el., 1990).

1.3 PWR coolant chemistry

The PWR primary coolant acts as a transport medium for the heat from the reactor core to the steam generators and, simultaneously, as a carrier for dissolved boric acid; for the latter reason, its basic composition has to satisfy the requirements of reactivity control of the reactor core. Given this fundamental fact, appropriate chemistry conditions have to ensure that the impact of the primary coolant will not endanger the long-term integrity of the primary system structural materials. That means that, as a matter of principle, any kind of corrosion during plant operation and shutdown has to be precluded or, at least, kept well below the specified limits. This applies to general corrosion resulting in the release of metal atoms from the materials to the coolant as well as to selective corrosion mechanisms (e. g. intergranular corrosion) and to oxidation of the surfaces of metals. Moreover, the

transport of corrosion products in the primary circuit has to be minimized in order not to affect adversely the heat flux from the fuel rods to the coolant by deposits which, in addition, may lead to an accelerated corrosion of the Zircaloy cladding material. In extreme cases, heavy deposits on the fuel rods may result in an inhomogeneous axial core power density distribution, presumably due to a reversible adsorption of borate ions onto the deposited corrosion product oxides. Finally, the extent of contamination buildup is supposed to be influenced by the coolant chemistry conditions; this topic will be treated in more detail in Section 4.4.2.

In order to meet these requirements, the specified concentrations of additives and impurities in the primary coolant have to be adjusted according to the materials used in the primary circuit. In KWU-type PWRs these materials are

- Zirconium alloys (Zircaloy-4) as fuel rod cladding;
- Ni-Cr-Fe alloys (Incoloy 800) in the steam generator tubes;
- Austenitic Cr-Ni steels in components and piping of the primary system;
- Special alloys (e. g. Cr alloys) in smaller surface areas for special purposes (e. g. wear-resistant positions).

Deviations in the composition of the materials applied in primary circuits (such as the use of Inconel 600 or 690 in Westinghouse or Framatome designed plants) may influence the optimum coolant chemistry parameters.

To fulfil the chemistry requirements, the primary coolant has to be treated by the addition of chemicals. The concentrations of the additives needed have been given in specifications elaborated by specialists in detailed discussions and which are continuously re-evaluated based on the current state of knowledge. Table 1.4. shows an overview of the primary coolant specifications established by various vendors and institutions for plant normal operation periods (Mathur and Narasimhan, 1992). From these data, it can be seen that there is a worldwide consensus on the use of LiOH or KOH as a pH control reagent. Different vendors or organizations may recommend minor changes in some of these specifications as, for example, KWU not specifying fluoride, but fundamentally the plant specifications are virtually identical. During startup and shutdown phases, deviations from these specified data are allowed for a limited period of time.

A special problem during steady-state operation is adjustment of the optimum coolant pH. In general, it is acknowledged that a higher coolant pH level results in reduced metal atom release rates and a minimized danger of selective corrosion forms. Likewise, it was reported (e. g., Neeb et al., 1972; Bergmann and Roesmer, 1984) that during operation at low pH levels (i. e. without addition of an alkalizing agent to the primary coolant), the corrosion product deposits arising on the fuel rod surfaces are significantly larger than at a higher pH coolant chemistry, an effect that is supposed to influence contamination buildup in the primary circuit (see Section 4.4.3.). However, selecting the coolant pH optimum with regard to plant contamination buildup is a complex task. For some time, a pH of 6.9 was recommended since this value corresponds to the zero temperature coefficient of magnetite solubility. Later on, nickel ferrite was assumed to be the most important corrosion product compound, resulting in the recommendation of pH 7.4 as the

Table 1.4. Coolant specifications for PWR power operation (according to Mathur and Narasimhan, 1992; by courtesy of IAEA)

Parameter	EPRI (US)	Westinghouse (US)	VGB (FRG)	Siemens/KWU (FRG)	J-PWR (Japan)	EdF (France)	WWER 440/ 1000 (SU)	WWER 440 (Finland)
LiOH	0.2–2.2*	0.7–2.2*	0.2–2.2*	0.2–2*	0.2–2.2* 0.45–2.2**	0.6–2.2*		
KOH	–	–	–				2–16.5°)	2–22°)
Ammonia	–	–	–				>5	>5
Hydrogen	2.2–4.5	2.2–4.4	1–4	2–4	2.2–3.15	2.2–4.4	2.7–4.5	2.2–4.5
Oxygen	<0.01	<0.005	<0.005	0.005	<0.005	<0.1	<0.01	<0.01
Chloride	<0.15	<0.15	<0.2	<0.2	<0.05	<0.15	<0.1	<0.1
Fluoride	<0.15	<0.15	–	–	<0.1	<0.15	<0.05	<0.1
Conductivity (25 °C)	*	*	–	<30		1–40	4–80*	–
pH (25 °C)	*	4.2–10.5*		5–8.5	4.2–10.5	5.4–10.5	>6	>6
Dissolved iron	–	–	–	(<0.05)	–	–	–	–
Total iron	–	–	(<0.01)		–	–	<0.2	
Sulphate	0.1	–	–	–	–	–	–	
Silica	–	<0.2	–	(<0.5)	–	<0.2	–	–
Suspended solids	0.35	<1	–	(<0.1)	<0.5	<1	–	–
Aluminum	–	<0.05	–	–	–	<0.1	–	–
Calcium	–	<0.05	–	–	–	<0.1	–	–
Magnesium	–	<0.05	–	–	–	<0.1	–	–

( ) = normal operating value
– = not applicable/specified
* = depending on Li and B concentration
** = depending on Li and B concentration, new treatment
° = calculated taking into account K + Na + Li

Concentrations in mg/kg (ppm)
Conductivities in μS/cm

optimum value. Since the neutral point of water at 300 °C is at pH 5.6, these values of coolant pH are clearly in the alkaline region. However, the possibility of raising the pH values in the primary coolant is limited by two facts: fuel assembly corrosion and primary water stress corrosion cracking (PWSCC), which are assumed to be accelerated by higher lithium concentrations.

As was mentioned above, boric acid as chemical shim substance is dissolved in the primary coolant at a concentration according to the current reactivity state of the reactor core. Reactivity control is also provided by the neutron absorbing control rods (see Section 1.1.2.). This neutron absorbing duty is shared between the control rods and dissolved boric acid in such a way as to provide the most economical split. Typically, the control rods take care of short-term reactivity changes and the slower long-term reactivity control is provided by varying the concentration of boric acid in the reactor coolant. During the course of an operating period (fuel cycle), the boron concentration in the primary coolant decreases steadily from about 1000 mg B/l (natural boron isotopic composition) at the beginning of an equilibrium cycle (at the beginning of operation with the first core load, the boron concentration is about 2000 mg B/l) to a few mg/l at the end of the cycle. In order to rule out unintentional criticality, it is adjusted to about 2200 mg B/l during shutdown of the plant. Hence, for chemistry considerations the concentration of boric acid in the primary coolant is a given condition at any time of the operating period.

The boric acid in the primary coolant shows partial dissociation. This results in a pH in the acid range which is undesirable because of the unfavorable impact on metal release rates and selective corrosion. Thus, for compensation of the pH, an alkalizing substance has to be added. Out of the number of water-soluble caustics, LiOH is mostly used since ^{7}Li is produced in any case by an (n, α) reaction from ^{10}B and, therefore, analysis of the concentration of the alkalizing agent present in the coolant can be performed by one single measurement. On the other hand, in order to minimize ^{3}H production in the primary coolant, isotopically pure ^{7}Li has to be used (see Section 4.2.3.).

In practice, different approaches are taken to achieve an optimum coolant pH, the principles of which are shown in Fig. 1.13., where lithium concentrations in the primary coolant are presented as a function of the concentration of boric acid over a fuel cycle (Riess, 1989). Since operation at a low pH (area A) cannot be recommended, some plants operate at the highest possible safe lithium concentration, in area D bounding area C, until a pH of nearly 7.4 (at operational temperature) is reached. This pH is then kept constant by decreasing the lithium concentration according to the current boric acid concentration. This mode of operation has been widely adopted by PWR operators and is called "modified" Li/B chemistry. The reason for the upper limit on ^{7}Li concentration of 2.2 mg/kg coolant, as stated in the specifications, is the risk of accelerated corrosion of the Zircaloy fuel rod cladding material as a result of the increase in concentration of LiOH in the corrosion product deposits caused by nucleate boiling, in particular in fuel rod regions with high heat ratings. This recommended concentration of a maximum of 2.2 mg Li/kg, however, is not sufficient to reach a pH of 7.2 to 7.4 (at

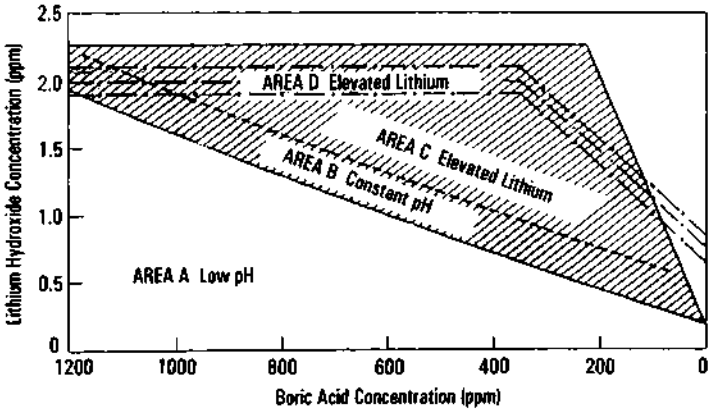

Figure 1.13. Various lithium – boron modes of operation (Riess, 1989)

operational temperature) at the beginning of a fuel cycle at high boric acid concentration.

Another possible approach is to keep the coolant pH constant over the whole length of the fuel cycle (Area B in Fig. 1.13.). In the so-called "coordinated" Li/B coolant chemistry introduced by Roesmer (1983), the starting lithium concentration of 2 ppm is continuously reduced, resulting in a pH of about 6.9 over the whole cycle. A third approach, which has been used experimentally, is to start with a high lithium concentration in excess of 2.2 ppm (e. g. 3.5 ppm in the Swedish Ringhals plants). This kind of treatment is called "elevated" Li/B chemistry. However, because of the risks involved in the application of higher lithium concentrations, this kind of treatment has been widely abandoned.

The dilemma in using boric acid as a soluble neutron poison is caused by the fact that the effective isotope ^{10}B (thermal neutron cross section $3.8 \cdot 10^{-21}$ cm^2) represents only a fraction of 19.78 at% in the natural boron isotope mixture. The most abundant isotope ^{11}B, with a fraction of about 80% and a thermal neutron cross section of $5 \cdot 10^{-27}$ cm^2, is only a ballast substance from the perspective of neutron physics but it is, of course, chemically effective. On the other hand, of the number of chemical elements showing high neutron absorption cross sections, boron is the only one that fulfils all the requirements to be made of a chemical shim substance. These are, in particular, the capability of forming salt compounds of simple composition which are stable in water at 300 °C and under intense ionizing radiation; the ability not to produce insoluble compounds and deposits on the primary circuit surfaces; the ability not to increase materials corrosion as compared to pure high-temperature water; and, finally, the capability of permitting removal of impurities and radionuclides from the primary coolant without changing the concentration of the chemical neutron poison. All the other elements which show sufficiently large neutron absorption cross sections (such as Cd, In, the rare earth elements, Hf, W) violate at least one of these essential requirements.

In principle, the use of commercially available ^{10}B-enriched boric acid would result in a significant reduction in the concentration of boric acid in the coolant which is needed for reactivity control. The possibilities and limitations of this have been analyzed, among others, by Battaglia et al. (1989), who came to the conclusion that the optimum choice depends highly on plant-specific parameters. A 1300 MWe plant has a total boric acid inventory of about 55 Mg which is distributed over the primary coolant, diverse tanks, the spent fuel pool and other systems; per year the losses in US plants which have to be replaced are on the order of 500 kg, with 200 kg of this being consumed by neutron capture. These figures give an idea of the economic side of the question. On the other hand, by the use of enriched boric acid a constant pH water regime would be possible over a longer period of the fuel cycle; if it is true that this would result in a reduction of primary circuit dose rates, one could calculate an economic saving from this effect. Bergmann (1989) performed calculations in this area, but based them exclusively on the impact of the out-of-core cobalt inventories (materials of the primary system, the auxiliary systems etc.), since these are postulated by the author to be the main source of occupational radiation exposures. This assumption contradicts that of other investigators, according to which the out-of-core cobalt inventories play only a minor role in primary circuit contamination buildup; until now, there have been no calculations of the benefits of high pH chemistry in case the main ^{60}Co sources are the materials located inside the reactor pressure vessel (see Section 4.4.3.). Thus, it seems questionable whether the aspect of man-rem reduction is of relevance for the economic justification of the application of enriched boric acid. Further, it seems that the use of enriched boric acid will bring advantages in the future when measures in the direction of better fuel exploitation, e. g. by longer fuel cycles (which would require a higher initial enrichment of the fuel), will be introduced.

In the very intense radiation field inside the reactor core, the H_2O molecule is decomposed by radiolytic reactions, which are induced by γ rays and by recoil protons formed by the action of fast neutrons. The main primary products of these reactions are the radicals $H\cdot$, e_{aq}^-, $OH\cdot$, and $HO_2\cdot$ and the molecules H_2 and H_2O_2. A general assessment of the radiation chemistry of water at elevated temperatures by Buxton (1989) showed that the presently available data on G values (which in most cases were measured at ambient or slightly elevated temperatures) can be extrapolated to reactor operating temperatures. The yields of e_{aq}^- and $OH\cdot$ increase smoothly with temperature, whilst those of H_2 and H_2O_2 appear to be only relatively slightly changed. These studies indicate that spur reactions and track reactions become less significant with increasing temperature, partly due to the fact that some of the spur reactions are slower than diffusion-controlled so that diffusive escape from spurs and tracks becomes more probable. Likewise, the distributions of the primary radiolytic products within the spurs and tracks may be broadened as a result of the decrease in the density of the water. From these and other investigations (e. g. Kent and Sims, 1992) it has been concluded that the G values of irradiated water at elevated temperatures are reasonably well known, at least for low-LET radiation. However, the question is still unresolved as to how the

radiolysis products interact with circulating corrosion products and whether such reactions have any impact on deposition or dissolution processes.

For chemistry purposes, the primary circuit of a PWR can be considered as a closed system in which the products of chemical reactions reach an equilibrium state. In order to prevent accelerated Zircaloy corrosion which is of particular concern with regard to high fuel burnup goals, the O_2 equilibrium concentration in the coolant has to be kept below a certain level, which usually is specified to be 0.01 ppm. This can be achieved by addition of hydrogen to the primary coolant in such amounts that the concentration ratio of hydrogen to oxygen amounts to about 240 at a minimum. Under such conditions, the oxidizing primary radicals formed by radiation-induced reactions will be scavenged and no radiolysis products will be detectable under steady-state operating conditions with the exception of H_2 and the $OH\cdot$ radical. The lower limit of H_2 concentration ensuring suppression of O_2 formation amounts to about 1 mg/kg coolant. On the other hand, an upper limit of concentration of 4 mg H_2/kg should not be exceeded because of the danger of an enlarged hydrogen uptake into the fuel cladding Zircaloy and the resulting hazard of embrittlement of the material, potentially leading to long-term failures. In the case of oxygen ingress into the system, the bulk of it can be effectively removed by addition of hydrazine to the primary coolant; this is done routinely after an opening of the primary circuit (e. g. in the course of refuelling), prior to the start of nuclear operation.

Ionic impurities dissolved in the coolant may affect the system H_2O/H_2 by interfering with the recombination mechanisms of the primary radiolysis products; such impurities are, for example, Cl^- and Fe^{3+}, which can be readily oxidized or reduced. Their presence may lead to an impairment of the equilibrium state resulting in an increase in the concentrations of all radiolysis products, including O_2. For this reason, it is necessary that the concentrations of such impurities be kept as low as feasible.

Agreement of the current coolant data with the specified values has to be monitored at regular intervals by coolant analyses. In spite of the usually long sampling lines (including coolers and pressure reduction valves), representative samples of dissolved, non-volatile species are obtained without difficulties. Sampling of dissolved gases (e. g. H_2, fission product noble gases) requires special equipment. With regard to suspended corrosion products, representative sampling is endangered by deposition and resuspension effects in the sampling line; therefore, appropriate flushing of the line prior to sampling is necessary (e. g. a flushing volume equal to the tenfold volume of the sampling line). Whenever possible, on-line monitoring of the essential data is strived for; for example, chemistry measuring systems have been reported which are able to monitor continuously pH_T and redox potential at primary coolant operating temperature and pressure. Surveillance of radionuclide concentrations in the primary coolant is routinely performed by taking samples and analyzing them in the radiochemical laboratory, either by direct γ spectrometry or by applying appropriate radiochemical separations prior to activity measurement. In this area, too, attempts have been made to monitor the dominant γ emitters (noble gases, iodine, cesium) by on-line γ spectrometry using collimated high-resolution detectors. However, this technique is often complicated by an interfering

background radiation originating from the contamination layers which are deposited on the sampling line inner surfaces. Until now, no fully satisfying solution for this problem has been reported.

To ensure that the chemistry specifications of the primary coolant are maintained the addition of chemicals is necessary. This is usually performed via the chemical control system. This system is part of the nuclear auxiliary systems just as are the primary coolant purification systems described in Section 1.1.3. In order to maintain the specified H_2 concentration in the primary coolant, either an adequate H_2 partial pressure is established in the volume control system or H_2 is directly injected into the high-pressure system (newer Siemens/KWU plants).

In the VVER plants a somewhat different kind of chemistry control of the primary coolant is employed. The operational experiences made in these plants have been summarized by, among others, Martynova and Paschewitch (1986) and by Dragunov et al. (1992). Depending on the boric acid concentration, which decreases steadily from about 2000 mgB/kg coolant to virtually zero over the course of a fuel cycle, a constant pH of 7.1 to 7.3 (at 265 °C) is maintained by using KOH at a concentration decreasing from 12 to 2 mg K/kg coolant over the course of a fuel cycle; this concentration is controlled either by addition of KOH or by removal of K^+ ions via ion exchange. In order to preclude radiolytic O_2 generation, ammonia is added to the primary coolant, which is decomposed in the core radiation field to form H_2; the NH_3 concentrations are kept within the range 3 to 20 mg/kg, with 0.5 mg NH_3 yielding about 1 ml H_2 (STP). In some VVER-440 plants a modified chemistry control has been employed by adding hydrazine to the primary coolant (Pashevich et al., 1992). Besides maintaining reducing conditions in the primary coolant, the nitrogen compounds are claimed to influence favorably the formation of protective layers on the surfaces of the materials, the transport and deposition of corrosion products and, as a consequence, the contamination buildup in the primary circuit. No problems were reported concerning compatibility of this primary coolant chemistry with the materials applied, which are in the early VVER-440 plants mostly low-alloy steels without a stainless steel clad. According to loop and in-pile experiments, addition of hydrazine influences favorably the corrosion behavior (Kysela et al., 1989); however, this compound is decomposed under primary circuit operating conditions by two different mechanisms: Thermal decomposition is catalyzed by nickel traces in the coolant, showing N_2H_4 halflives between 2 and 60 minutes, depending on the nickel concentration; in addition, the N_2H_4 concentrations are also reduced by radiation-induced decomposition.

As a potential disadvantage of $KOH-NH_3$ chemistry, the production of additional radionuclides in the primary coolant has to be mentioned. Thus, by an (n,p) reaction with ^{14}N considerable amounts of ^{14}C are generated. Several radionuclides are produced by neutron capture in the different potassium isotopes, the most important of them being ^{42}K (halflife 12.5 hours), which is a β^- emitter with an associated γ energy of 1.5 MeV. During operation at rated power with a potassium concentration in the primary coolant of about 10 ppm, a ^{42}K steady-state activity concentration on the order of 10 to 50 GBq/Mg is produced. Due to its short halflife, this radionuclide does not pose any problems in refuelling operations; likewise, because of its high solubility in water it does not form deposits on the

surfaces of the primary circuit. Impurities which are frequently present in KOH may be the source of additional radionuclides; here, traces of sodium have to be mentioned, resulting in the production of the β^-, γ emitter ^{24}Na (halflife 15.0 hours). However, as yet there is no detailed information on dose rates and the radionuclide releases caused by these isotopes.

In pressurized water reactors the steam generator separates the primary coolant from the secondary-side steam generator water, thus protecting the secondary side against contamination by radionuclides. However, in the rare event of a steam generator tube leak, radionuclides will reach the secondary side; therefore, besides its main goal of minimizing corrosion and wastage, the chemistry control applied here is also of interest with regard to radionuclide behavior. In order to minimize materials corrosion, in U-tube steam generators the feedwater is chemically treated, so that the pH of the steam generator water is kept alkaline. In Siemens/KWU designed plants it is general practice to inject only N_2H_4 into the main condensate. Hydrazine has two functions here: scavenging of oxygen to secure reducing conditions in the steam generator water and generation of ammonia by thermal decomposition. The injection rate of hydrazine is determined by the ammonia concentration to be achieved in the final feedwater. The NH_3 concentration should correspond to a pH level of >9.8 (at 25 °C) which requires the absence of copper alloys in the water–steam circuit as well as it requires the use of high-integrity condenser materials. This type of secondary-side treatment is called high-AVT (All Volatile Treatment). As an alternative to high-AVT, the low-AVT mode can be used with a pH level in the feedwater of 9.0 to 9.5.

In the 1970's, phosphate treatment was used in addition to low-AVT chemistry. The aim of the phosphate treatment was to preclude formation of aggressive solutions, in particular in the corrosion product deposits covering the tube sheet after longer-term operation of the plant and which are also in contact with the heat transfer tubes. In particular, this danger may occur when salt compounds are introduced via condenser leaks and are concentrated and hydrolyzed in the pores of the steam generator deposits. Using a molar ratio $Na:PO_4$ of less than 2.6, the generation of solutions of lower pH can be precluded even locally due to the buffer effect of this mixture. On the other hand, sodium phosphate concentrations exceeding the specified values of 2 to 6 mg PO_4/kg water may result in a wastage of the heating tubes, endangering their long-term integrity. This might happen in pores of the corrosion product deposits where a concentration buildup of the salts will take place. In order to rule out this hazard, most PWR steam generators are currently operated using AVT chemistry.

In the operation of once-through steam generators, only volatile chemical additives to the secondary-side water can be used. Non-volatile chemicals would be highly concentrated during complete evaporation of the feedwater in this steam generator design, thus leading to very aggressive residual solutions.

In the VVER plants the steam generator water has to fulfil various purity requirements such as low conductivity and low dissolved oxygen, with the pH being 7 or somewhat less. As far as it is known, no additives are used in order to control steam generator water and main steam chemistry.

References Chapter 1

Battaglia, J. A., Waters, R. M., von Hollen, J. M., Lamatia, L. A., Bergmann, C. A., Ditomasso, S. M.: Enriched boric acid for PWR application. Cost evaluation study for twin-unit PWR. Report EPRI NP-6458 (1989)

Bergmann, C. A.: Evaluation of selected parameters on exposure rates in Westinghouse designed nuclear plants. Proc. 5. BNES Conf. Water Chemistry of Nuclear Reactor Systems, Bournemouth, UK, 1989, Vol. 1, p. 9–16

Bergmann, C. A., Roesmer, J.: Coolant chemistry effects on radioactivity at two pressurized water reactor plants. Report EPRI NP-3463 (1984)

Buxton, G. V.: Assessment of the radiation chemistry of water at elevated temperatures. Proc. 5. BNES Conf. Water Chemistry of Nuclear Reactor Systems, Bournemouth, UK, 1989, Vol. 1, p. 123–129

Debray, W.: Materials for light-water reactors. in Ullmann's Encyclopedia of Industrial Chemistry, Volume A17 Nuclear Technology, p. 657–662 (1991)

Dragunov, Yu.G., Markov, Yu.V., Rybalchenko, I. L., Ryazantsev, I. L., Chabak, A. F.: Water chemistry in Soviet nuclear power plants. Report IAEA-TECDOC-667 Coolant Technology of Water Cooled Reactors. Volume 1: Chemistry of Primary Coolant in Water Cooled Reactors. 1992, p. 108–110

Kausz, I. A.: Safety and operating systems and process equipment for light-water reactors. in Ullmann's Encyclopedia of Industrial Chemistry, Volume A17 Nuclear Technology, p. 650–657 (1991)

Kent, M. C., Sims, H. E.: The yield of γ-radiolysis products from water at temperatures up to 300 °C. Proc. 6. BNES Conf. Water Chemistry of Nuclear Reactor Systems, Bournemouth, UK, 1992, Vol. 2, p. 153–158

Kysela, J., Jindrich, K., George, G., Kelm, H., Nebel, D., Schlenkrich, H., Herold, C., Schönherr, M.: Influence of hydrazine and higher pH on the corrosion product layer of austentitic steel. Proc. 5. BNES Conf. Water Chemistry of Nuclear Reactor Systems, Bournemouth, UK, 1989, Vol. 1, p. 97–104

Martynova, O. I., Paschewitch, W. I.: Chemie im Primärkreislauf von Druckwasserreaktoren unter besonderer Berücksichtigung der Alkalisierung mit Kaliumhydroxid (Betriebserfahrungen mit der WWER-440-Baureihe). VGB Kraftwerkstechnik 66, 54–58 (1986)

Mathur, P. K., Narasimhan, S. V.: Chemistry of primary coolant in water cooled nuclear reactors. Report IAEA-TECDOC-667 Coolant Technology of Water Cooled Reactors. Volume 1: Chemistry of Primary Coolant in Water Cooled Reactors. 1992, p. 9–29

Meyer, P.-J.: Pressurized-water reactors. in Ullmann's Encyclopedia of Industrial Chemistry, Volume A17 Nuclear Technology, p. 624–638 (1991)

Neeb, K. H., Grämer, G., Riess, R.: Untersuchung von Ablagerungen auf Brennelementen der ersten Wechselmenge KWO. Proc. Reaktortagung Deutsches Atomforum, Hamburg 1972, pp. 225–228

Pashevich, V. I., Khitrov, Yu.A., Belyayev, M. V., Nemirov, N. V., Grushanin, A. I., Kukharev, N. D.: Hydrazine regime for WWER-440 and WWER-1000 primary circuits. Report IAEA-TECDOC-667 Coolant Technology of Water Cooled Reactors. Volume 1: Chemistry of Primary Coolant in Water Cooled Reactors. 1992, p. 110–114

Peehs, M., Walter, S., Walter, T.: Uranium, uranium alloys and uranium compounds. in Ullmann's Encyclopedia of Industrial Chemistry, to be published (1996)

Prozenko, A. N., Stekolnikov, V. V., Fyodorov, V. G., Vosnesenski, V. A., Ivanov, V. A.: Die Entwicklung von wassermoderierten-wassergekühlten Reaktoranlagen (VVER) in der UdSSR. Atomwirtschaft 35, 129–133 (1990)

Riess, R.: Optimization of water chemistry in PWRs. Nuclear Europe VIII, (3–4), 19–20 (1989)

Roesmer, J.: Minimizing core deposits and radiation fields by coordinated Li/B chemistry. Proc. 3. BNES Conf. Water Chemistry of Nuclear Reactor Systems, Bournemouth 1983, Vol. 1, pp. 29–36

Rysy, W.: Sicherheitstechnische Auslegung von Druckwasserreaktor-Kraftwerken. in Bohn, T. (editor): Handbuchreihe Energie, Band 10, Kernkraftwerke, p. 2–59, Verlag TÜV Rheinland, Köln, 1986

Stoll, W. (a): Fuel assemblies for light-water reactors. in Ullmann's Encyclopedia of Industrial Chemistry, Volume A17 Nuclear Technology, p. 732–738 (1991)

Stoll, W. (b): Fuel assemblies made from reprocessed plutonium. in Ullmann's Encyclopedia of Industrial Chemistry, Volume A17 Nuclear Technology, p. 744–749 (1991)

Wunderlich, F., Eberle, R., Gärtner, M., Gross, H.: Brennstäbe von Leichtwasserreaktoren. Auslegung und Betriebsverhalten. KTG-Seminar Band 5, Verlag TÜV Rheinland, Köln, 1990

Würtz, R.: Löslichkeit bestrahlter Mox-Brennelemente bei der Wiederaufarbeitung. Atomwirtschaft 32, 190–192 (1987)

2. The Boiling Water Reactor (BWR)

By the end of 1994, 92 BWR nuclear power plants with a total electrical capacity of about 79 GWe were in operation in the Western countries and Japan; an additional 5 plants with about 5.6 GWe were under construction at this time. Within the borders of the former Soviet Union a particular type of BWR had been built, the so-called RBMK reactor; 16 plants of this type with about 17 GWe were operating by the middle of 1993. The characteristic feature of the BWR design – in contrast to the closed, one-phase PWR design – is heat removal from the reactor core by boiling water, i. e. by a mixture of water and steam. As a consequence of this difference in design, the behavior of many radionuclides in the BWR primary system during plant operation differs considerably from that in the primary circuit of a pressurized water reactor.

The development of boiling water reactor power plants proceeded largely in parallel to that of the PWR plants. Following small-scale experimental reactors, the first commercial BWR power plant, Dresden-1 with 210 MWe, started operation in 1960. All the BWRs of Western design have been derived from this early General Electric (GE) plant, although in the course of further development a number of modifications were introduced. The first BWR plants were of so-called indirect design, using a heat exchanger between a closed water–steam primary system and the turbine circuit. With increasing experience, this principle was abandoned in favor of a direct design, in which the steam produced in the reactor pressure vessel is directly conducted to the turbine. While in smaller plants natural convection of the coolant is sufficient to remove the heat from the reactor core, in larger plants a forced convection by pumps is required.

Unlike the BWRs of Western design, in which boiling water is both moderator and coolant, the RBMK reactors use graphite as a moderator while the heat is removed from the reactor core by boiling water in separate cooling channels. Be-

cause of these pronounced differences and because of the worldwide attention the Chernobyl accident has drawn to this reactor type, it will also be shortly described in Section 2.2.

2.1 Design of Western BWR plants

2.1.1 The primary system

The basic layout of the nuclear part of various designs for BWR plants shows greater differences than for PWR plants, in particular with respect to the relative arrangement of the components in the containment. The KWU 69 design shows a pear-shaped containment; the KWU design 72 employed in the 1300 MWe plants Gundremmingen B and C plants is schematically shown in Fig. 2.1. In spite of these fundamental differences in plant design, it can be said that those features which are relevant for radionculide behavior are quite similar for all the BWR plants of Western design. Thus, the following short plant description will concentrate on the KWU 72 design; more detailed descriptions of this design have been given by different authors. e. g. by Mattern (1986) and by Hollinger (1991). A short summary of the technical data of the KWU 72 design is given in Table 2.1; significant differences potentially affecting radionuclide behavior which are to be found in the other plant designs will be discussed in the relevant sections.

The central part of the plant is the reactor pressure vessel housing the reactor core with its components as well as the water–steam separators and the steam dryers (see Fig. 2.2.). The dimensions of this component (inner diameter 6.62 m, height 22.35 m, total weight 785 Mg) exceed the dimensions of a PWR reactor pressure vessel considerably. The reactor pressure vessel is made from the high-alloy steel 22NiMoCr37 with an austenitic weld overlay on the inner surface. In its cylindrical section, the wall thickness of the vessel is 16.3 cm plus a weld overlay of 0.8 cm.

The control rod drive mechanisms are installed in the lower part of the reactor pressure vessel, so that the control rods are inserted from the bottom into the reactor core. There are different reasons for this layout, among others the fact that the moderator water shows a higher density in the lower part of the core which is counteracted by the partly inserted control rods, thus resulting in a better homogenity of load distribution in the core axial direction. Movement of control rods during normal operation periods is performed by electrical or hydraulic drive mechanisms; in order to initiate a reactor trip, the control rods are forced into the core by a pressurized water drive mechanism. The load control by the control assemblies which are inserted more or less into the reactor core, depending on the demand, is supplemented by a load control which is effected by the speed of the main coolant pumps. A reduction of speed results in a longer residence time of the coolant in the reactor core and, as a consequence, in an increase of the void fraction in the water–steam mixture. As a result, neutron moderation is reduced and

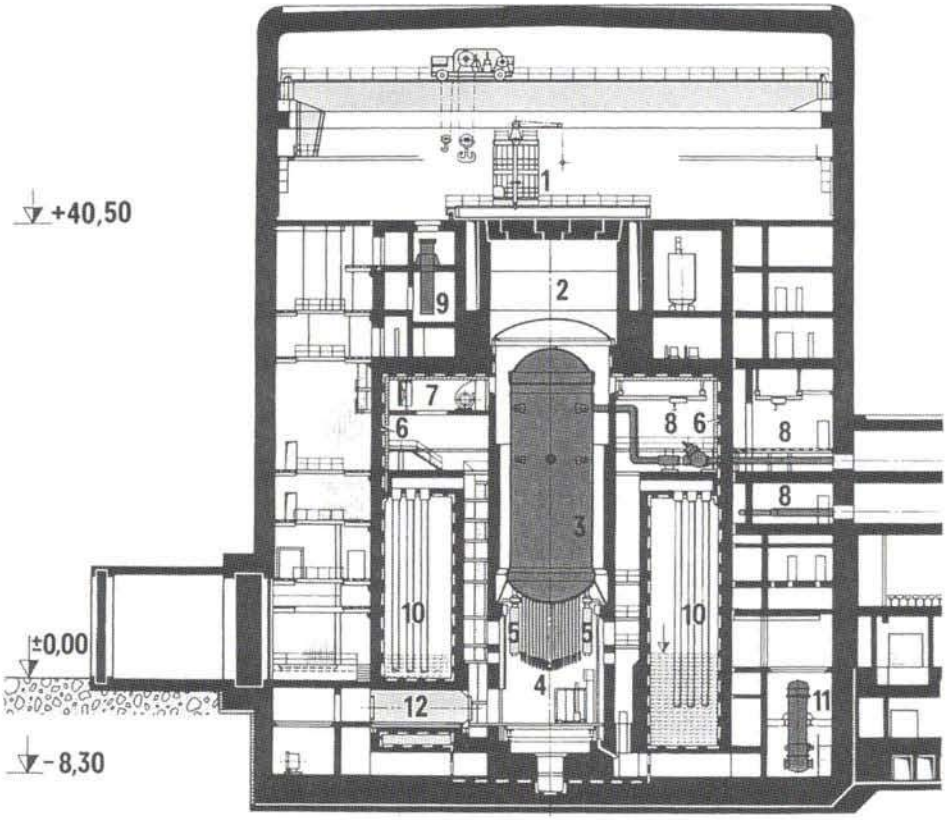

Figure 2.1. BWR 1300 MWe, reactor building
1) Refuelling machine; 2) Reactor wet well; 3) Reactor pressure vessel; 4) Control rod drive mechanisms; 5) Main coolant pumps; 6) Containment; 7) Air recirculation system; 8) Pipe floors; 9) Fuel pool cooling heat exchanger; 10) Pressure suppression pool; 11) Residual heat removal cooler; 12) Lock
(By courtesy of Siemens/KWU)

the fission rate and load decrease (negative void coefficient). Increase in speed leads to a reduction of the void fraction and, consequently, to an increase in power of the reactor core.

Pumps force the recirculation of the coolant. Originally, an external recirculation line system was installed which, for larger plants, was then supported by internal jet pumps. In the KWU 69 and 72 designs, external recirculation was replaced by internal axial pumps operating inside the reactor pressure vessel. The KWU 72 reactor is equipped with 8 internal axial pumps; at rated speed, each of these pumps has a recirculation capacity of about 8700 m^3/h.

The upper part of the reactor pressure vessel houses the water–steam separation facilities. In the moisture separator, the bulk of the water is removed from the steam flow by centrifugal forces down to a residual moisture content of $<10\%$.

Table 2.1. Technical data of a 1300 MWe BWR nuclear power plant (KWU series 72; by courtesy of Siemens/KWU)

Reactor core thermal power	3840 MW
Gross electrical capacity	1310 MW
Net electrical capacity	1249 MW
Net plant efficiency	32.5%
RPV outlet pressure	7.06 MPa
RPV outlet steam temperature	286 °C
Core coolant mass flow	14300 kg/s
RPV outlet steam flow rate	2076 kg/s
RPV outlet steam moisture	0.2% per weight
Feed water temperature	215 °C
Core heat transfer area	6968 m^2
Fuel average heat rating	26.5 kW/kg U
Average enrichment first core load	1.93% ^{235}U
Average enrichment reload batches	2.75% ^{235}U
Number of fuel assemblies in core	784
Number of fuel rods per assembly	62
Fuel assembly total weight (incl. shroud)	315 kg
Total U mass in core	139 Mg
Number of recirculation pumps	8
Mass flow rate per pump	8731 m^3/h
Power consumption per pump	1.03 MW
Number of control rod assemblies	193

The residual moisture then is reduced in the steam dryers to a maximum moisture content of <0.1%; in reality, this moisture content (consisting of very fine water droplets) in the main steam is lower than the specified value by more than one order of magnitude. At the exit of the reactor pressure vessel, the steam temperature is about 286 °C; the corresponding pressure amounts to 7.1 MPa.

The steam produced in the reactor pressure vessel is directed to the high-pressure part of the turbine; downstream, the condensate formed on the high-pressure turbine is separated and directed to the heater drains. The residual steam powers the low-pressure part of the turbine and, finally, is completely condensed in the main condenser. The main condensate is purified in the condensate demineralizers where corrosion products and ionic impurities are retained. The feedwater then is recycled via preheaters to the reactor pressure vessel. In older BWR plants, all the condensates are purified in the condensate polishing system; in the newer, forward-pumped plants only the main condensate is purified there, while the heater drains are directly pumped to the feedwater tank. In some of the BWR plants the feedwater tank is equipped with an electromagnetic filter for removal of suspended corrosion products (mainly iron oxides).

In order to keep the impurity levels in the reactor water low, a continuous flow of the water is passed to the reactor water cleanup system, which in most of the plants is equipped with precoat filters with powdered ion exchange resins.

The nuclear installations of the plant are surrounded by a containment whose design differs according to the type of the plant. The two Gundremmingen BWR

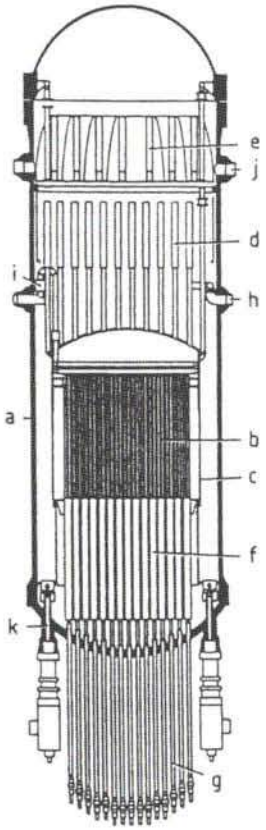

Figure 2.2. Boiling water reactor pressure vessel with internals
a) Reactor pressure vessel; b) Reactor core; c) Core shroud; d) Steam separator assembly; e) Steam dryer assembly; f) Control rod; g) Control rod drive; h) Feedwater nozzle; i) Core spray supply header; j) Main steam nozzle; k) Recirculation pump
(Hollinger, 1991)

plants have a cylindrical containment made of prestressed concrete provided with a steel liner. To preclude a pressure increase in the case of a pipe break inside the containment, which has the potential of endangering the integrity of the containment, condensation chambers are installed containing a water-filled pressure suppression pool in which the steam escaping from the primary system is condensed.

2.1.2 The reactor core

In boiling water reactors as in pressurized water reactors, ^{235}U-enriched UO_2 fuels as well as mixed-oxide fuels are used. Fabrication of the fuel material and the fuel pellets is virtually identical for both reactor types (see Section 1.1.2.). However,

depending on the design of the fuel assemblies in BWR cores, the dimensions of the fuel pellets show a somewhat broader variability than does PWR fuel. Whereas in the older German BWR plants a pellet diameter of 10.44 or 9.5 mm and a pellet length of 12.5 or 11.5 mm are used, the fuel pellets of the Gundremmingen B and C plants with 9×9 fuel rod assemblies show the same dimensions as PWR fuel pellets in 16×16 assemblies, i. e. a diameter of 9.11 mm and a length of 11 mm. Pellet density and dishing volume correspond to that of the PWR fuel pellets; likewise, Gd_2O_3-containing fuel pellets are used as burnable poison to compensate for excess reactivity.

The cladding of the BWR fuel rods consists of Zircaloy-2 (Zry-2), a zirconium alloy whose composition was given in Table 1.2. As with PWR fuel rods, the rod diameter is related to the fuel assembly design. In the older 8×8 array, the outer rod diameter is 12.3 mm, with a cladding wall thickness of 0.74 mm; the corresponding values for the newer 9×9 array are 10.75 and 0.65 mm, respectively. Currently, there are different designs of 9×9 assemblies; typical data for a KWU 9×9Q assembly fuel rod are given in Table 1.3. More detailed information on the design and the characteristic data of BWR fuel rods have been published by Wunderlich et al. (1990).

Currently, most of the BWR fuel assemblies fabricated by Siemens/KWU are operated up to a burnup level of 30 to 35 MWd/kg heavy metal (HM), with a significant fraction of them even being operated up to burnup levels in excess of 35 MWd/kg HM. The failure rates of BWR fuel rods during operation are as low as those of PWR fuel rods (see Section 1.1.2.). BWR fuel rod defects are due almost exclusively to isolated cases of pellet – clad interaction (PCI) occurring during local power increases (ramps) beyond the preceding steady-state level. In order to rule out this type of failure, the inner cladding surface in newer designs for Siemens/KWU BWR fuel rods is coated with a liner consisting of pure zirconium. This measure reduces local stress peaking at the inner surface of the cladding, as well as chemical interaction of the Zircaloy material with fission products. However, this zirconium liner material is somewhat sensitive to water vapor which enters the fuel rod following a rod failure caused by some other defect mechanism. Addition of minor amounts of iron to the liner material enhances its stability considerably.

The reactor core of the KWU 72 BWR design has a thermal output of 3840 MW and contains 784 fuel assemblies. In the 8×8 array which was predominantly used in the initial phases, each assembly is composed of 62 fuel rods, with the remaining two positions being occupied by hollow rods that water flows through, so-called water rods; the aim of the water rods is to improve neutron thermalization in the central region of the bundle. Usually, the first core load of the reactor shows a fuel enrichment of, on the average, 1.93% ^{235}U, the reload batches 2.75%. For most reloads, the fuel assembly design was modified to a 9×9 array, which means 80 fuel rods and one water rod per assembly. In this design, the outer diameter of the rod is 10.75 mm, with all other dimensions being identical to those of the 8×8 array (see Fig. 1.5.). The newer 9×9Q fuel assembly design shows a square-shaped water channel in the center instead of the water rods previously used (see Fig. 2.3.). Such ATRIUM designs with a 10×10 fuel rod array have also been developed by

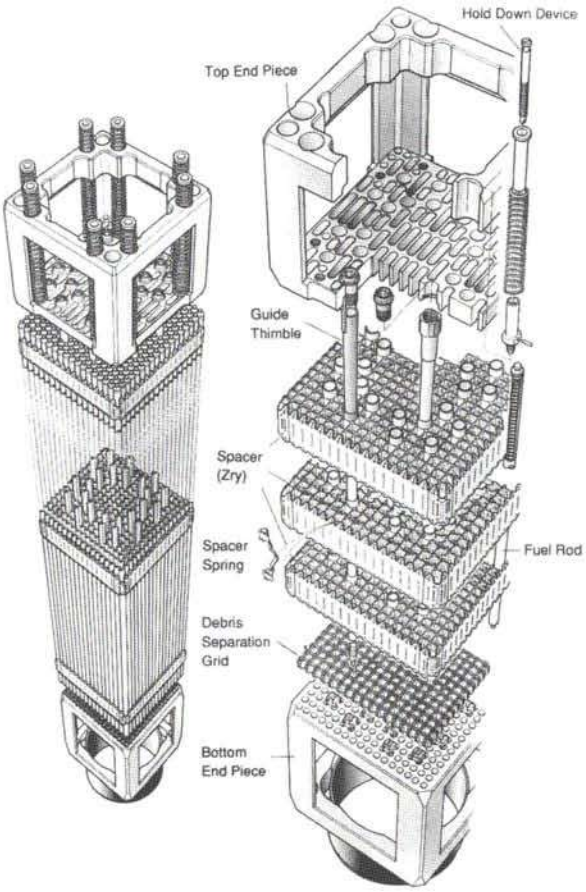

Figure 2.3. BWR fuel assembly Siemens ATRIUM 9x9
(By courtesy of Siemens/KWU)

Siemens/KWU, showing a reduced outer diameter (10.05 mm) and correspondingly smaller pellet diameters. The internal square-shaped water channel used in these designs provides increased and more uniform neutron moderation and leads to a more even power distribution across the fuel assembly. This allows for a more homogeneous distribution of ^{235}U enrichment in the fuel rods, leading to improved fuel utilization. ATRIUM 9 fuel assemblies have been in use since 1986; the first lead fuel assemblies of ATRIUM 10 design were inserted in 1992. The BWR fuel bundle is encased in a fuel assembly channel made of Zircaloy-4 which is re-usable and can be removed for performing inspection or repair work at the assembly. The total uranium weight in the reactor core amounts to approximately 139 Mg.

Control of reactor load in a BWR cannot be performed by a soluble poison such as boric acid, as is used in PWRs, because of the volatility or entrainment of such substances with the steam which, under operating conditions, would result in

the formation of deposits on the turbine. For this reason, cross-shaped control assemblies are used, with the four blades being inserted between four fuel bundles. As a neutron-absorbing material, boron carbide B_4C is loaded into the blades. The reactor core of a 1300 MWe BWR contains 139 control assemblies which are inserted into the reactor core from the bottom. To facilitate movement of the control assembly, the rod tips are equipped with rolls which in former times were made of the high-cobalt alloy Stellite; currently, in order to reduce ^{60}Co buildup, a wear-resistant cobalt-free alloy is used in many plants.

2.1.3 The auxiliary and ancillary systems

Like PWRs, boiling water reactors also need peripheral systems in support of regular operation of the plant, with some of them being of significance for the concentration of radionuclides in the reactor water and their behavior in the reactor primary system. These systems have been described by, among others, Kausz (1991); therefore they will only be described very shortly in what follows. The reactor water cleanup system is designed to limit the concentration of corrosion products (non-radioactive as well as radioactive ones) and fission products, as well as of other impurities, in the reactor water. To this end, reactor water is extracted from the reactor pressure vessel (between 0.5 and 2% of the feedwater throughput), cooled down, depressurized and passed through an ion exchanger bed; in most cases, powdered resins are used for this purpose; otherwise, deep-bed ion exchangers are employed. In the KWU 72 plant design, the capacity of the reactor water cleanup system amounts to about 64 Mg/h. Two parallel lines are installed; when the resins of one bed are exhausted, operation is switched to the second line while the spent resins are flushed to the resin storage tank and replaced by a fresh batch.

Gases dissolved in the reactor water (mainly hydrogen, oxygen and fission product noble gases) are stripped from the boiling water and are transported with the steam to the turbine and then to the condenser. In the main condenser, they are extracted from the condensate by a steam jet and are transported to a recombiner where, on a palladium catalyst, H_2 and O_2 are recombined to form H_2O again. Following H_2O condensation, the residual permanent gases are dried and passed over to the gas delay line where the bulk of the radioactive krypton and xenon isotopes decay due to an adsorption–desorption process on the charcoal surfaces. The gases, which now contain only traces of ^{85}Kr, are then released from the plant through the stack.

The radioactive liquids produced during plant operation, such as leak water, laundry water etc., are collected and processed in a manner similar to that described in Section 1.1.3. by distillation, ion exchange and other appropriate techniques. The concentrates obtained from these procedures are evaporated to dryness by techniques identical to those used in PWR plants; finally, these low-level wastes are passed to an intermediate storage until transport to the final repository.

2.1.4 Safety and emergency installations

In off-normal situations, a reactor trip is initiated by rapid insertion (velocity about 2 m/s) of all control rods into the reactor core. In addition, sodium borate solution can be injected into the reactor pressure vessel, thus ensuring subcriticality of the core even in case the control rods fail to operate. In order to deal with the consequences of a loss-of-coolant accident, BWR plants are equipped with an emergency core cooling system similar to that in PWR plants, consisting of high-pressure and low-pressure injection systems and recirculation systems. By the action of these systems, sufficient removal of the decay heat is guaranteed so that no serious overheating of the fuel rods can occur.

In the event of a loss-of-coolant accident the hydrogen that can be produced in the reactor core by a Zircaloy – water reaction as well as by radiolytic H_2O decomposition will be released to the containment. In order to prevent a hydrogen – air reaction which may endanger the integrity of the containment, containment air is extracted in the course of such an accident and forced to a catalytic recombiner where H_2 is oxidized to form H_2O once again.

The steam which in a loss-of-coolant accident is released from the primary system may lead to a pressure increase inside the containment and to a pressure difference between the drywell and the condensation chamber. As a consequence, a steam–air mixture is transported to the pressure suppression pool where the steam is condensed. Simultaneously, fission products which might be carried with the steam are retained in the water volume of the pool, thus efficiently reducing airborne radioactivity.

2.2 RBMK design

The RBMK reactors are graphite-moderated boiling water reactors which have been exclusively erected within the borders of the former Soviet Union. The Chernobyl-4 reactor, which experienced the by far most severe accident in the history of commercial nuclear power plants (see Section 7.4.3.), belonged to this design. The characteristic difference of this design from the BWR designs described above is that it uses graphite as a moderator. Most of the RBMK reactors have a rated electrical power of 1000 MW, but some 1500 MW plants have also been put into operation. A summary description of the RBMK plants has been given by, among others, Kotthoff (1991); therefore, only some short remarks on the design of the newer, second-generation plants will be made here.

Some technical data of this reactor type are summarized in Table 2.2. As can be seen from Fig. 2.4., the 1000 MW plants have a cylindrical reactor core of about 7 m in height and about 12 m in diameter. The moderator block is made of graphite bricks which are penetrated by about 1700 vertical cooling channels into which the fuel assemblies are inserted. For transport of the heat generated in the fuel, water

Table 2.2. Characteristics of the RBMK-1000 type reactors

Parameters	RBMK-1000
Thermal power (MW)	3200
Gross electrical power(MWe)	1000
Number of turbines	2x500 MW
Efficiency (%)	30.4
Core height (m)	7.0
Core diameter (m)	11.8
Number of fuel channels	1661
Core loading U (Mg)	192
Fuel	UO_2
Enrichment (% ^{235}U)	1.8
Average burnup (MWd/kg U)	18.1
Fuel can material	Zirconium alloy
Water flow through the reactor (Mg/h)	37,500
Steam flow to turbine (Mg/h)	5400
Turbine steam inlet pressure (MPa)	6.5
Turbine steam inlet temperature (°C)	280

enters the individual cooling channels from the bottom at 270 °C and is heated to 284 °C at a pressure of about 7 MPa, thus forming a mixture of steam and liquid water; two separate cooling circuits are installed, with each of them serving one half of the core. The steam–water mixture from the cooling channels is directed by pipes to a steam collector in which the two phases are separated from each other; from there, the steam passes a steam dryer and is then directed to the turbine. The cooling channels are enclosed by pressure tubes consisting of a zirconium alloy so that during plant operation water has no contact with the graphite moderator.

The fuel assemblies in the reactor core represent a total core fuel mass of about 190 Mg of slightly enriched uranium (about 1.8% ^{235}U). The fuel is designed to reach a maximum burnup of about 18 MWd/kg U; unlike the other light water reactor designs, refuelling in the RBMK reactors is performed during operation of the plant. Each day 3 to 4 fuel assemblies have to be removed by the unloading machine to be replaced by fresh ones; the spent assemblies are stored in a spent fuel pool. Besides the cooling channels, the moderator block has an additional 150 penetrations which contain the control rods the reactor load is controlled by.

A reactor core of such a large volume has the disadvantage that load and load distribution in the reactor are difficult to control. Another problem of this reactor type is the positive void coefficient of reactivity which may occur under certain circumstances. With increasing concentration of steam bubbles in the coolant, the absorption of neutrons in the coolant decreases while moderation of the fast neutrons by the graphite moderator remains unchanged. For this reason, an increase in reactor power is not limited by inherent physical properties of the reactor core and, therefore, the reactor load has to be controlled by extensive active measures, i. e. by complicated instrumentation.

In order to protect the graphite moderator, which has an operating temperature of 500 to 700 °C, against corrosive attack by air, the reactor core is surrounded by a steel liner in which an inert atmosphere under slight overpressure is maintained.

The RBMK-1000 plants are equipped with safety systems which are designed to cope with loss-of-coolant and station blackout accidents. These are, in particular, an emergency core cooling system, an emergency feedwater system, a system for condensation chamber cooling and the emergency power supply. The emer-

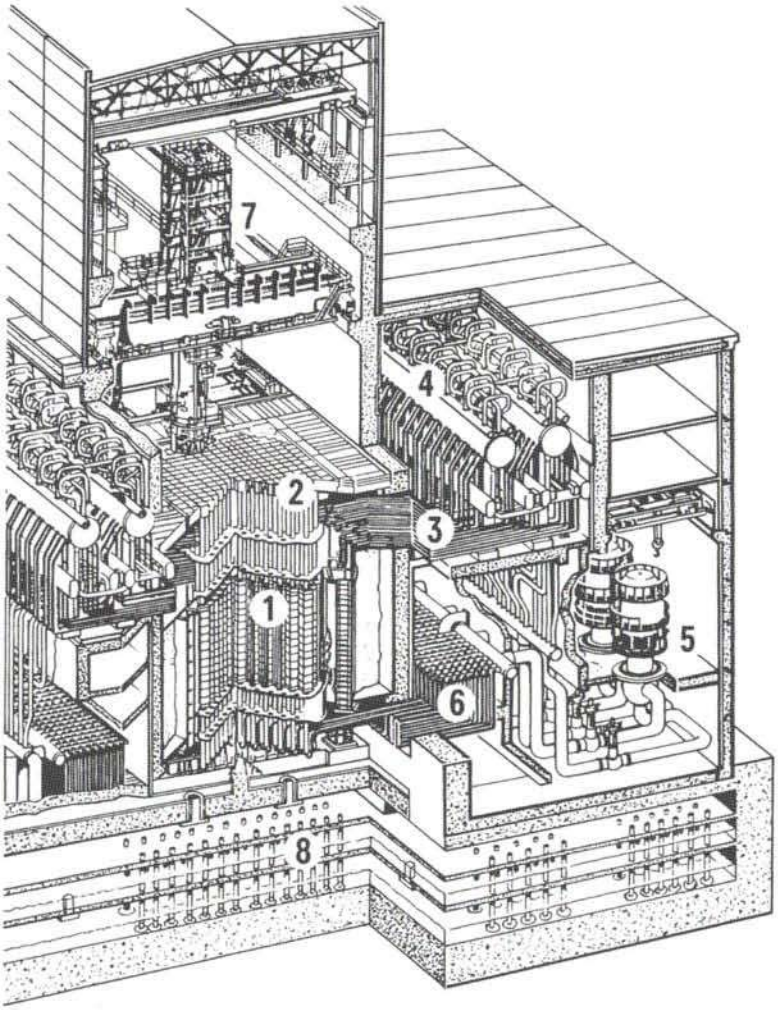

Figure 2.4. RBMK-1000; schematic view
1) Reactor core; 2) Upper cover plate; 3) Water–steam lines; 4) Water–steam separator; 5) Main coolant pumps; 6) Feedwater lines; 7) Refuelling machine; 8) Condensation chambers
(Bild der Wissenschaft 7/86)

gency cooling systems have a 3 × 50% design, but they are not completely separated from each other. The newer RBMK-1000 reactors are equipped with concrete pressure chambers enclosing a part of the reactor coolant circuit (accident localization system); below the reactor, water-filled condensation chambers are installed into which steam escaping in the course of a loss-of-coolant accident is directed. However, there is no pressure-resistant containment confining the whole reactor system; the reactor building is a normal industry building, it is not gas-tight and is not designed to withstand any pressure increase.

In most cases, two RBMK reactors are equipped with a common auxiliary building which is located between the reactor buildings. Parallel to this complex, the turbine building for the two reactors is located.

As a consequence of the Chernobyl accident (see Section 7.4.3.), the RBMK-type reactors have been improved to reduce their sensitivity to the core steam void fraction and to increase the effectiveness of safety provisions. Besides improvements in the shutdown systems, increase in the ^{235}U enrichment of the fuel and installation of a greater number of fixed absorber rods in the reactor core are the most important measures for increasing reactor safety.

2.3 BWR coolant chemistry

Normally, BWR reactor water is not treated by the addition of chemicals. The relevant specifications require high purity of the reactor water and the feedwater as is shown in Table 2.3. (Riess, 1991). This high purity guarantees a minimum corrosion of the materials of the circuits.

During operation, impurities are inevitably introduced into the reactor water, though all necessary measures are taken to minimize the ingress of foreign substances. Impurities that are introduced by the feedwater into the reactor water are

Table 2.3. BWR coolant specifications in continuous operation (Riess, 1991)

Feedwater	
Cation conductivity (25 °C)*	< 0.08 μS/cm
Total iron	< 0.01 mg/kg
Total copper	< 0.002 mg/kg
Oxygen	0.01 – 0.2 mg/kg
Reactor water	
Cation conductivity (25 °C)*	< 1 μS/cm
Chloride	< 0.1 mg/kg
Silica	< 4 mg/kg

* Direct and continuous measurement at the sampling point

mainly iron, nickel and chromium traces, as well as copper and zinc traces in older plants having brass-tubed condensers. Chloride (which may induce selective corrosion of the circuit materials) and other impurities affecting water conductivity may be introduced by the inleaking of cooling water to the condenser hotwell via leaking condenser tubes. These substances are at least in part removed by the ion exchangers of the condensate polishing system. The silica concentration is specified as a maximum to avoid formation of deposits on the heat exchanger surfaces of the core and to minimize impurity concentrations in the steam which in turn could lead to deposits on the turbine blades. Another source of impurities are core oxide layers and surface deposits from which activated corrosion products are released to the reactor water. Finally, if failed fuel rods are present in the core, fission products from the fuel are introduced into the reactor water. In order to limit the resulting impurity concentrations, part of the reactor water (between 0.5 and 2% of the feedwater throughput) is fed to the purification system, which is equipped with ion exchangers. This purification, however, mainly affects the concentration of dissolved species, since suspended solids are predominantly deposited onto the surfaces of the primary system.

Other impurities are generated in the reactor water itself by the radiation-induced decomposition of H_2O which occurs inside the reactor pressure vessel mainly in the liquid phase. Water radiolysis is primarily caused by the action of recoil protons (generated by the collision of fast neutrons with hydrogen atoms) and of gamma rays. For a BWR standard plant with a power density of $50\,W/cm^3$, the core average total neutron dose rate is estimated to be $1.5 \cdot 10^7$ Gy/h and the total gamma dose rate to be $2.1 \cdot 10^6$ Gy/h; the total dose rate in the core region is nearly proportional to the power density of the reactor core. The most important final products of these reactions are H_2 and O_2. In contrast with the situation in PWRs, the intense boiling in the BWR core results in a stripping of the radiolytically generated gases from the water phase, so that radiation-induced recombination of the primary radiolysis products is largely suppressed. The gases are partitioned between the water and the steam phases; as a consequence, the oxygen concentration in the water usually amounts to about 0.2 mg/kg, in the steam at the reactor pressure vessel outlet to about 20 mg/kg. Considerable amounts of H_2 and O_2 are transported by the steam to the condenser where they are extracted from the water phase and recombined in a catalytic recombiner to form H_2O again. By this measure, the oxygen content in the reactor water is limited in order to avoid selective corrosion of the materials as well as buildup of deleterious oxide layers on the Zircaloy fuel rod surfaces. Since in the past in some US plants selective corrosion occurred which was attributed to oxygen impurities, the attempt has been made to reduce them further by the addition of hydrogen to the reactor water (hydrogen water chemistry, HWC). This mode of operation also affects the behavior of certain radionuclides; this will be discussed in more detail in the relevant sections. Another important radiolysis product is H_2O_2, which is a stronger oxidant than O_2 and which shows a concentration in the reactor water which is quite similar to that of O_2. Due to the catalytic decomposition of H_2O_2 in the sampling lines, the measured concentrations usually are considerably lower than the concentration inside the reactor pressure vessel (Rooth et al., 1989).

The only stable radiolysis products discharged from the reactor pressure vessel through the steam and off-gas system are H_2 and O_2. Under normal BWR coolant chemistry conditions, the rate of total gas production is 19.3 ml/s · MW_{th}, with a ratio of $H_2 : O_2$ near 2.1. In the presence of excess H_2, the production of O_2 can be suppressed through reactions reducing the concentrations of $OH\cdot$, H_2O_2 and O_2. Several ionic impurities which are radical scavengers also show significant effects on water radiolysis by reacting with radiolysis products. For example, the reaction rate constants for the Cu^+/Cu^{2+} ions are comparable to those of most of the free radical reactions involved in radiolysis. Thus, if the impurity levels are high enough (e. g. > 10 ppb), the scavenging effect would significantly interrupt the radiolytic reactions. Model calculations performed by Ruiz et al. (1989) have aimed at the evaluation of the impact of H_2 addition as well as of ionic trace impurities on the radiolytic O_2 production, including the various parts of the BWR primary system as well as the main steam. In order to analyze the relative significance of different parameters, Ibe et al. (1989) compared the results of model calculations with measurements performed at a BWR plant. Bubble sizes in the fuel channels of the reactor core were identified as an important parameter. When the bubble diameter is small and, therefore, the contact areas are large, gaseous species are readily released to the vapor, resulting in higher concentrations in the vapor than with a larger bubble size. Oxygen is a bit more easily suppressed when the bubble size is large; in this case, the injected hydrogen stays for a longer period in the liquid phase, thus leading to a higher efficiency of oxygen reduction. A change in the axial power distribution in the reactor core can cause minor variations in the radiolytic environment.

Experience has shown that oxygen reduction in BWR reactor water by hydrogen addition varies in efficiency from plant to plant. These variations can be attributed to plant design and operational parameters such as the power density in the reactor core, the dose rate in the downcomer or the shroud wall thickness. Impurities in the reactor water such as nitric acid and copper may also affect the oxygen level. In general, oxygen reduction under HWC conditions is considered to be a mixed process of suppression of radiolysis in the reactor core and enhancement of recombination of hydrogen and oxygen in the downcomer. Since the mechanisms of suppression in the core are believed to be similar in different plants, the variations are assumed to be mainly due to differences in the recombination of H_2 and O_2 in the downcomer region.

In order to achieve a continuous oxygen suppression, a critical hydrogen concentration has to be maintained which is fixed in the range 0.25 to 0.4 ml/kg in the absence of boiling. At lower hydrogen concentrations, radiolysis will result in the production of oxygen and more hydrogen. Adding hydrogen above the critical limit effects little further reduction in oxygen content and serves only as a buffer capacity against oxygen ingress. In boiling coolant, the quantity of hydrogen necessary to quench radiolysis can be calculated by multiplying the critical hydrogen concentration as obtained in non-boiling solutions by the specific stripping ratios of O_2 and H_2 from the aqueous phase (McCracken et al., 1989).

In order to minimize contamination buildup in the plant primary system, addition of zinc to the reactor water has been proposed. Laboratory investigations have

shown that the properties of oxide layers on steel surfaces change, resulting in a reduced uptake of radionuclides, in particular of ^{60}Co, from the water phase; details on this subject will be given in the relevant section on BWR contamination buildup.

In RBMK reactors, oxygen (up to 0.2 mg/kg) is injected into the feedwater circuit downstream from the condensate polishing system in order to prevent corrosive attack on the perlitic steels, and then removed from the water in the deaerator (Dragunov et al., 1992). Attempts have also been made to inject hydrogen as a remedy for intergranular corrosion attack on stainless steels.

References Chapter 2

Dragunov, Yu.G., Markov, Yu.V., Rybalchenko, I. L., Ryazantsev, I. L., Chabak, A. F.: Water chemistry in Soviet nuclear power plants. Report IAEA-TECDOC-667 Coolant Technology of Water Cooled Reactors. Volume 1: Chemistry of Primary Coolant in Water Cooled Reactors. 1992, p. 108–110

Hollinger, H.: Boiling Water Reactors. in Ullmann's Encyclopedia of Industrial Chemistry, Volume A17 Nuclear Technology, p. 638–650 (1991)

Ibe, E., Karasawa, H., Nagase, M., Tagawa, H., Endo, M.: Parameter identification of water radiolysis in BWR primary systems. Proc. 5. BNES Conf. Water Chemistry of Nuclear Reactor Systems, Bournemouth 1989, Vol. 1, p. 105–109

Kausz, I. A.: Safety and operating systems and process equipment for light-water reactors. in Ullmann's Encyclopedia of Industrial Chemistry, Volume A17 Nuclear Technology, p. 650–657 (1991)

Kotthoff, K.: Graphite-moderated, light-water-cooled, pressure-tube reactors. in Ullmann's Encyclopedia of Industrial Chemistry, Volume A17 Nuclear Technology, p. 682–694 (1991)

Mattern, J.: Kernkraftwerke mit Siedewasserreaktor. in Bohn, T. (editor) Handbuchreihe Energie, Band 10, Kernkraftwerke, p. 401–476, Verlag TÜV Rheinland, Köln, 1986

McCracken, D. R., Rasewych, J. B., Shorter, W. R.: Coolant radiolysis and boiling in water-cooled reactors. Proc. 5. BNES Conf. Water Chemistry of Nuclear Reactor Systems. Bournemouth, UK, 1989, Vol. 2., p. 107–113

Riess, R.: Water chemistry of boiling water reactors. in Ullmann's Encyclopedia of Industrial Chemistry, Volume A17 Nuclear Technology, p. 665 (1991)

Rooth, T., Ullberg, M., Karlsson, E., Persson, I.: Hydrogen peroxide in BWRs: An experimental determination of the actual level. Proc. 5. BNES Conf. Water Chemistry of Nuclear Reactor Systems, Bournemouth, UK, 1989, Vol. 2, p. 55–60

Ruiz, C. P., Lin, C. C., Robinson, R., Burns, W. G., Curtis, A. R.: Model calculations of water radiolysis in BWR primary coolant. Proc. 5. BNES Conf. Water Chemistry of Nuclear Reactor Systems, Bournemouth 1989, Vol. 1, p. 131–140

Wunderlich, F., Eberle, R., Gärtner, M., Gross, H.: Brennstäbe von Leichtwasserreaktoren. Auslegung und Betriebsverhalten. KTG Seminar Band 5, Verlag TÜV Rheinland, Köln, 1990

Part B
Radiochemistry during normal operation of the plant

3. Radionuclides in the reactor core

The reactor pressure vessel encloses the region where the largest fraction by far of the total radionuclide inventory of a nuclear power plant is concentrated. All the radionuclides present in the primary system and in the other systems of the plant have been produced here by reactions of neutrons with different substances. For this reason, the reactor core is the starting point for all further considerations with regard to radiochemistry in a nuclear power plant.

Uranium is a naturally occurring radioactive element and, therefore, fresh nuclear fuel also contains radionuclides. Plutonium and reprocessed uranium, on the other hand, are accompanied by isotopes which were generated during the preceding exposure of nuclear fuel in a reactor. All the radionuclides present in fresh nuclear fuel are of minor importance in reactor operation; nonetheless, they have to be taken into consideration in fuel fabrication in order to protect the employees from undue radiation exposure.

In the course of the operation of a nuclear power plant, a very large radionuclide inventory generated by nuclear fission and neutron capture is accumulated in the fuel. Since this inventory normally is hermetically confined in the gas-tight sealed fuel rod claddings, these radionuclides do not appear to a significant extent in other areas of the reactor plant during normal operation; in this phase, their only sign of existence is the radiation they emit, which has to be shielded by appropriate means. Only in the subsequent stage of reprocessing of the spent fuel is the chemical behavior of the fission products and actinides of vital interest. Nevertheless, there are various reasons for the efforts undertaken in nuclear reactor technology to acquire detailed knowledge of the chemical state and the behavior of the radionuclides in the irradiated fuel. One reason is that the chemical composition of the fuel is significantly altered by the accumulation of fission products belonging to chemical elements originally not present in the fuel; moreover, some of the fission products are suspected of being potential initiators of fuel rod cladding deterioration (e. g. initiation of stress corrosion cracking) when they are deposited on the inner surface of the Zircaloy cladding. In the event of fuel rod failures during reactor operation, radionuclides are released from the fuel to the reactor primary coolant, there leading to contamination; knowledge of the mechanisms and the extent of their transport from the defective fuel rod to the coolant is an essential prerequisite for dealing with the consequences of such failures. Even if

these are comparatively rare events (when compared to the total number of fuel rods present in the reactor core), they cannot be ruled out completely. Finally, in the highly improbable case of a severe reactor accident it has to be assumed that considerable fractions of the fission product inventory will be released from the core; the extent as well as the kinetics of this release depend highly on the chemical state of the radionuclides in the irradiated fuel.

In addition to the radionuclides produced in the nuclear fuel, others are generated in the core structural materials such as the fuel rod cladding, spacers, fuel assembly end pieces, control rods, and core support materials. Here, the main production mechanism is neutron activation. A fraction of the radionuclides generated in this manner is also released to the primary coolant during steady-state operation of the plant or to the primary circuit in the course of a severe reactor accident. Therefore, the following discussion will also cover these radionuclides.

3.1 Radionuclides in fresh nuclear fuels

Uranium as the main starting material for nuclear energy production is a naturally radioactive element, composed of the three long-lived isotopes ^{234}U, ^{235}U and ^{238}U. In undisturbed natural deposits, these isotopes appear in a secular decay equilibrium with their daughter products of the 4n+2 and 4n+3 series, which are presented in a simplified version in Figs. 3.1. and 3.2.

In the course of the fabrication of nuclear fuel from naturally occurring uranium, these equilibria are disturbed; in the first steps of ore processing, the bulk of the uranium decay products is separated from the element to be used further on. The following preparation steps, chemical separations as well as the conversion to UF_6 and its volatilization in the gas diffusion or gas centrifuge processes for ^{235}U enrichment, give rise to an additional purification, so that at the end of these processes a uranium compound is obtained which is virtually free of decay products. However, every delay in these processes, such as the time intervals between isotope enrichment and pellet fabrication as well as that between the fabrication of the pellets and their encapsulation into the fuel rods, leads to a new growth of decay products. As can be seen from Figs. 3.1. and 3.2., in the time periods involved, ranging from a few weeks to several months, this growth concerns exclusively the short-lived protactinium and thorium isotopes, which reach their decay equilibria with the starting nuclides within a few days or months, respectively, after the final chemical separation. The buildup of additional ^{234}U, the growth of its daughter nuclide ^{230}Th as well as of ^{231}Pa (in the 4n+3 series) and, subsequently, of their decay products proceeds very slowly. Therefore, their activity concentrations in the final nuclear fuel remain negligibly small.

The isotope enrichment process does not only lead to an increase in the ^{235}U concentration in the fuel, but also in a more than proportional increase in the ^{234}U concentration, as can be seen from Table 3.1., where the mass concentrations of the actinide isotopes in different types of fresh nuclear fuel are compared. As a

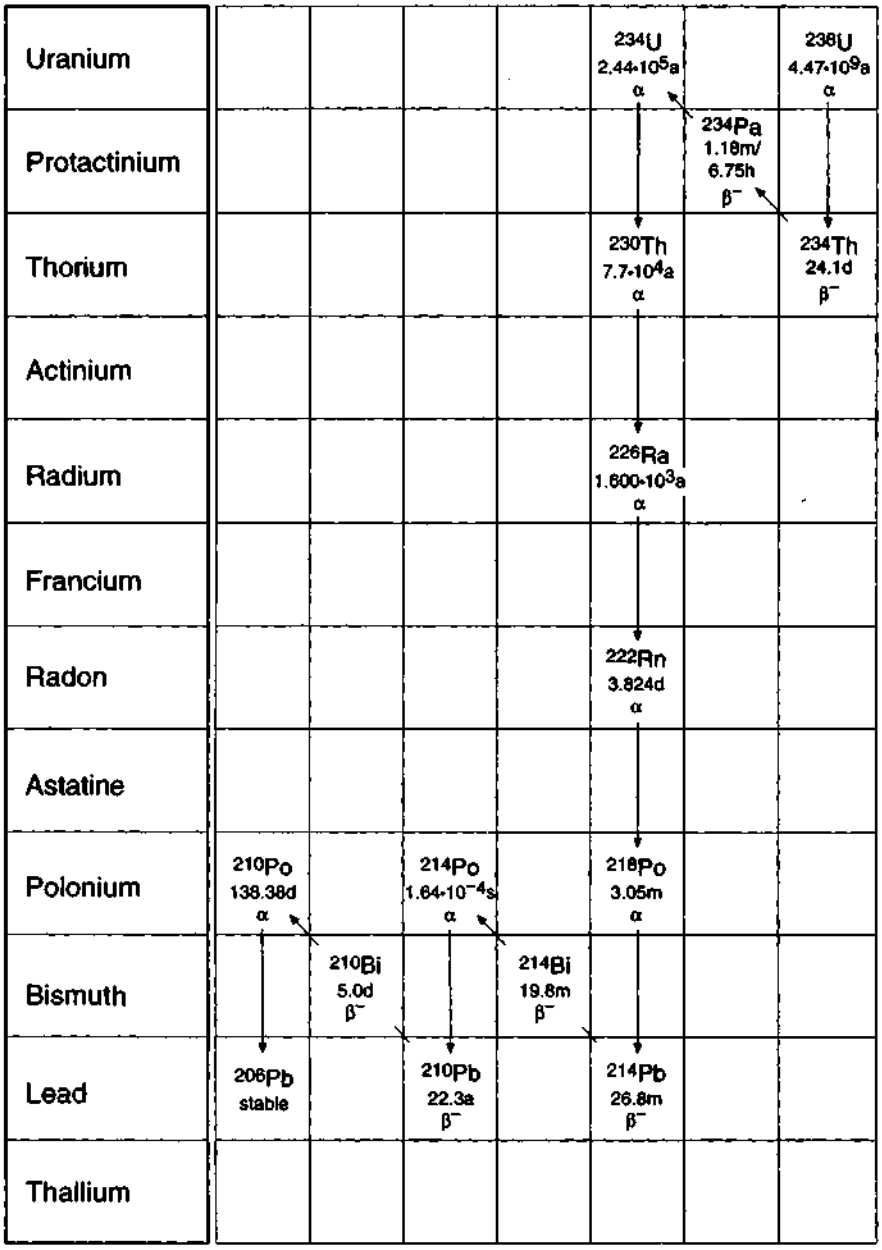

Figure 3.1. ^{238}U decay chain (4n+2 series)

consequence, ^{234}U, which in natural uranium is in a secular decay equilibrium with its parent ^{238}U and, therefore, shows the same decay rate, now becomes the dominant α emitter in the enriched uranium isotope mixture (see Table 3.2.).

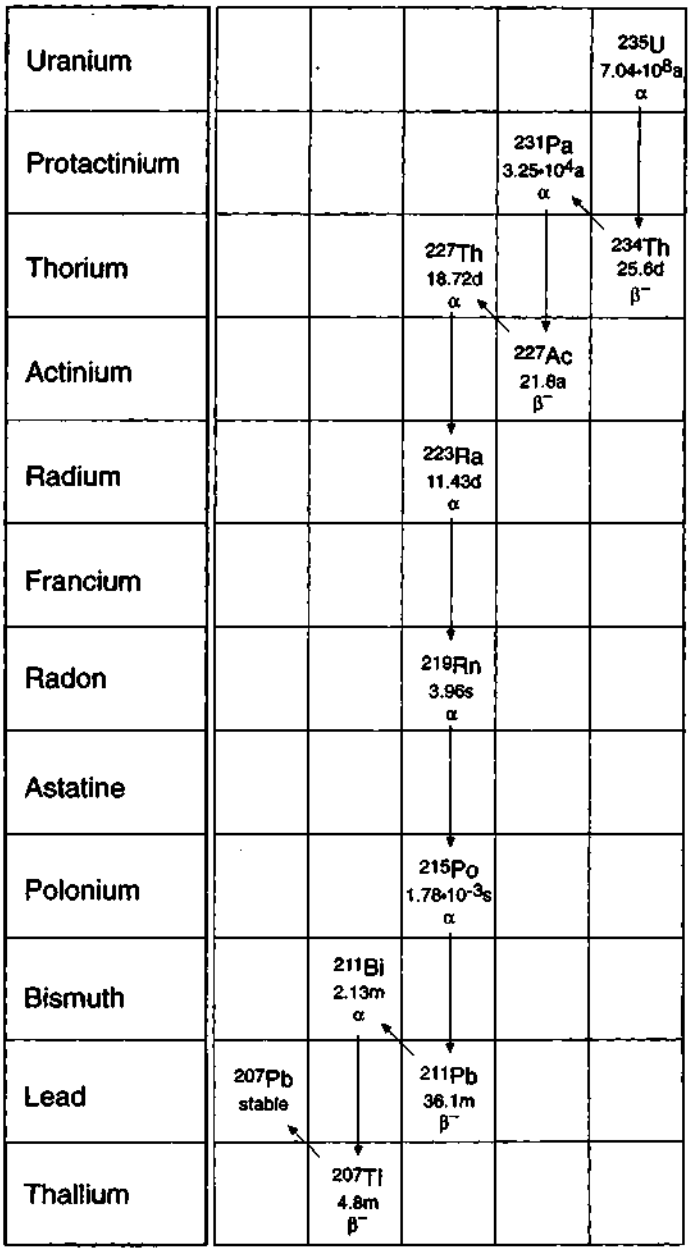

Figure 3.2. ^{235}U decay chain (4n+3 series)

The isotopic composition of the plutonium fraction of mixed-oxide fuels strongly depends on the production history (previous fuel enrichment and irradiation) of the individual plutonium batch supplied from the reprocessing plant. For

Table 3.1. Mass concentrations of actinide isotopes (in g/kg HM) in different types of fresh nuclear fuel
(By courtesy of Siemens/KWU)

	Nat. U	3.5% ^{235}U	3.1% Mox	3.8% repr. U
^{232}U				$1.0 \cdot 10^{-5}$
^{234}U	0.06	0.4	0.05	0.7
^{235}U	7.2	35.0	6.8	38.0
^{236}U				10.0
^{238}U	992.8	965.0	949.0	951.0
^{238}Pu			0.6	
^{239}Pu			27.5	
^{240}Pu			10.7	
^{241}Pu			3.5	
^{242}Pu			2.0	

this reason, the data given in Tables 3.1. and 3.2. are only an example of the composition of a fuel with a 3.1% fissile plutonium (i. e. Pu isotopes 239 plus 241) content. The most important plutonium isotope ^{239}Pu (which decays by α emission to ^{235}U, thus enlarging the 4n+3 series) shows the highest mass fraction but furnishes only a small contribution to the total α activity of the isotope mixture. The dominant activity is due to the β^- emitter ^{241}Pu, which decays to form the α emitter ^{241}Am; one year after a separation of americium from the plutonium material, the proportion of the newly produced ^{241}Am amounts to about 5% of the initial ^{241}Pu activity concentration. That means that in the example given in Table 3.2., one year after americium separation the ^{241}Am decay rate would be on the order of $5 \cdot 10^5$ MBq/kg heavy metal (HM). The ^{241}Am γ component may lead to a complication in fuel manufacturing; for this reason, if the plutonium isotope mixture has been stored for some time, an americium separation is often performed before

Table 3.2. Activity concentrations of actinide isotopes (in MBq/kg HM) in different types of fresh nuclear fuel
(By courtesy of Siemens/KWU)

	Nat. U	3.5% ^{235}U	3.1% Mox	3.8% repr.U
^{232}U				8.0
^{234}U	13	93	11	160
^{235}U	0.58	2.8	0.54	3.0
^{236}U				24
^{238}U	13	12	12	12
^{238}Pu			$3.8 \cdot 10^5$	
^{239}Pu			$6.2 \cdot 10^4$	
^{240}Pu			$9.0 \cdot 10^4$	
^{241}Pu			$1.3 \cdot 10^7$	
^{242}Pu			$2.9 \cdot 10^2$	

starting with mixed-oxide fuel processing. Among the α emitters, ^{238}Pu is the most intense source. The decay products of the α-emitting plutonium isotopes as well as of ^{241}Am are long-lived nuclides, so that their contribution and that of their daughter products to the total activity of the materials used for fuel fabrication is only of minor significance. The only exception is ^{236}Pu, which is mainly generated via ^{237}Np by (n,2n) reaction and β^- decay of the resulting ^{236}Np; this radionuclide decays to ^{232}U, an undesirable nuclide in the use of reprocessed uranium for the fabrication of new fuel (see below).

Due to the high α activity of the plutonium isotope mixture originating from high-burnup LWR fuel, all the steps in mixed-oxide fuel fabrication have to be carried out under the most stringent safety precautions, i. e. inside gas-tight boxes. In modern mixed-oxide processing, the plants are highly automated and remote-controlled equipment is used to protect the employees against γ radiation.

Up to now, reprocessed uranium has only been used for the fabrication of a limited number of test fuel assemblies. For this type of fuel, the uranium fraction from the spent fuel reprocessing process is again subjected to an isotope enrichment procedure to obtain a ^{235}U content which is sufficiently high for reactor operation (3.8% ^{235}U in the example shown in Tables 3.1 and 3.2.). Besides the naturally occurring isotopes ^{234}U, ^{235}U and ^{238}U, this material contains ^{236}U, mainly generated by neutron capture in ^{235}U, and ^{232}U as a decay product of ^{236}Pu. The ^{236}U content of reprocessed uranium strongly depends on the preceding fuel history (fuel burnup, initial fuel enrichment); it ranges between 1 and 3% per weight. ^{236}U is a strong neutron absorber, which reduces the efficiency of the fuel; it does not, however, cause any problems in fuel manufacturing. ^{232}U, on the other hand, as a member of the 4n series, leads via comparatively short-lived decay products (see Fig. 3.3.) to several intense γ emitters, in particular ^{208}Tl which shows γ energies of 2.62 and 0.58 MeV. Due to the short halflives of the intermediate nuclides, the buildup of the γ-emitting radionuclides proceeds comparatively quickly; therefore, fabrication of reprocessed uranium fuel requires shielding of the process lines in order to keep radiation exposure of the employees well below the regulatory limits. The ^{232}U content in the fuel depends both on the fuel burnup and on the decay time (halflife of ^{236}Pu 2.85 years). For a fuel initially enriched in ^{235}U to 2.4%, the ^{232}U proportion will more than double when the burnup increases from 15 to 23 MWd/kg U. The cooling period after irradiation is the second main factor; it becomes particularly significant when associated with high burnup.

Likewise, the enhanced α activity of reprocessed uranium (greater by a factor of 4 to 10 than that of natural uranium) has to be considered in fuel manufacturing. The resulting complications can, in principle, be reduced by optimized fabrication logistics, so that the time elapse between isotope enrichment and insertion of the fuel into the reactor would amount to less than half a year.

According to the generally accepted specifications, the maximum allowable content of residual fission products in the reprocessed uranium amounts to about 10% of the natural uranium β^- activity; as an upper limit for residual γ-emitting fission products $1.1 \cdot 10^5$ MeV·Bq/d·kgU is usually specified. In most cases, the residual fission product activity in reprocessed uranium is below 1000 Bq/g. During the enrichment process of the reprocessed uranium the fission products behave in

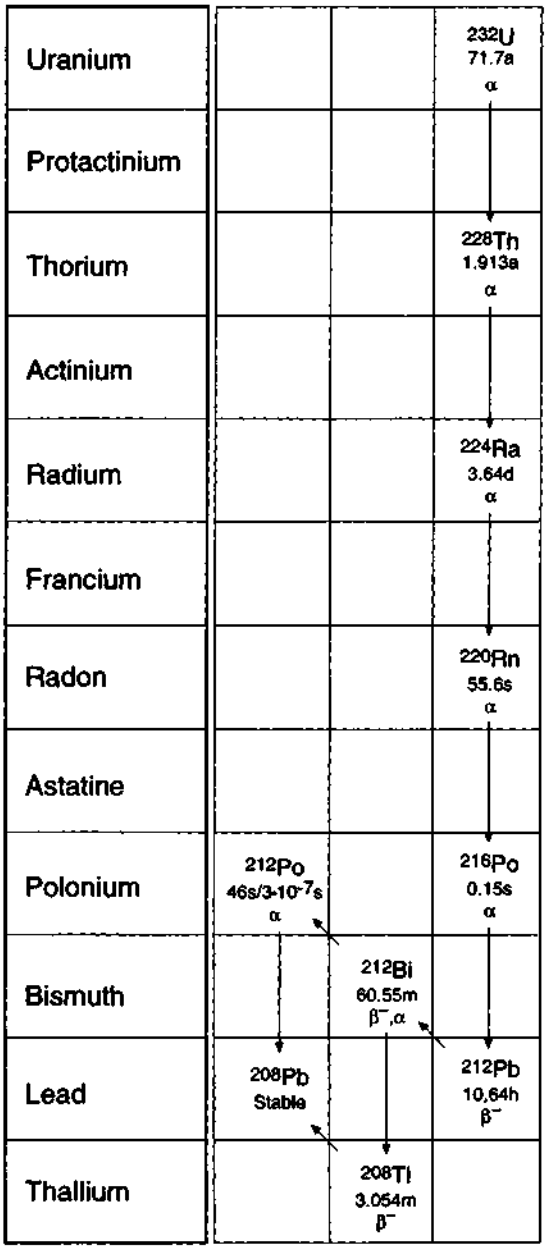

Figure 3.3. ^{232}U decay chain (4n series)

a different manner. ^{99}Tc is the most important fission product with regard to mass concentrations; during fluorination of the uranium fraction, technetium is converted into TcF_6 which has a vapor pressure almost identical to that of UF_6. In

the isotope separation process, TcF_6 preferentially accompanies the lighter uranium fraction, thus leading to a technetium content in the enriched uranium on the order of a few ppm (specification limit 5 ppm). Ruthenium fluoride also shows a vapor pressure similar to that of UF_6, so that virtually no decontamination effect is achieved by the volatilization process. For the other fission products, as well as for the daughter products of ^{232}U, the fluorides are non-volatile and are collected in the residues of the volatilization process.

The transuranium elements such as neptunium, plutonium or americium form hexafluoride compounds at their highest valency state with physical properties close to those of UF_6; but these compounds are not stable when the fluorine partial pressure decreases. Under such conditions they are converted into a lower valency state and remain as a solid product. This means that the main fraction of these impurities can be collected as ash or dust; if there is still a small proportion remaining in the liquid UF_6, it can be removed by a special filter before the container is filled. The specified upper limit for residual transuranium activity in the reprocessed uranium amounts to 2.5 Bq/g U, with ^{238}Pu, ^{239}Pu and ^{237}Np as the guide isotopes.

The chemical process leading from the uranyl nitrate solution to the UF_6 to be delivered to the enrichment process results in a decontamination factor for alpha activity of about 100; beta and gamma activities are reduced to a lower proportion, i. e. by a factor of 2 to 4 (Beck, 1985). From the onset of spent fuel reprocessing, enriched natural uranium has also been contaminated in some instances with traces of ^{236}U, ^{99}Tc, and plutonium isotopes.

3.2 Radionuclides in irradiated nuclear fuels

3.2.1 Fission product generation and fuel structure

Heavy nuclides are unstable; they can be disintegrated not only by α or β decay or, in some cases, by spontaneous fission, but also by neutron-induced fission. The fission cross sections, however, of the various nuclides show great differences. Among the naturally occurring fissile nuclides ^{235}U is the only one that can be used in thermal reactors; in addition, the artificially produced nuclides ^{233}U, ^{239}Pu and ^{241}Pu show fission cross sections and halflives which make them appropriate for use as nuclear fuels. In the currently operating light water reactors, which are exclusively based on uranium as the starting element, only the fissile nuclides ^{235}U, ^{239}Pu and ^{241}Pu are of real interest.

Neutron-induced nuclear fission can be described by the general equation (according to Lieser, 1991)

$$A + n \longrightarrow B + D + \nu \cdot n' + \Delta E$$

Upon neutron capture in the target nucleus A, a highly excited compound nucleus is generated which decays within about 10^{-13} s, forming the two fragments B and D. About 10^{-17} s later, the prompt fission neutrons n' are emitted; in the thermal

^{235}U fission their average number ν amounts to 2.4, in the thermal ^{239}Pu fission the corresponding number is 2.9. The prompt neutrons show a continuous energy spectrum in the range from virtually zero to more than 10 MeV with a peak value at about 0.7 MeV and a median energy of about 1.7 MeV. Simultaneously, prompt γ quants are emitted in the fission reaction, showing an average energy of about 1 MeV.

The energy released in the thermal ^{235}U fission amounts to about 200 MeV, consisting of the following individual contributions

Kinetic energy fission fragments	167 MeV
Kinetic energy prompt neutrons	5 MeV
Energy prompt γ emission	7 MeV
Energy fission product β decay	5 MeV
Energy fission product γ decay	5 MeV
Energy neutrinos	11 MeV

Since the neutrinos escape quantitatively from the reactor, the fission energy which is available for production of utilizable energy amounts to 189 MeV per fission reaction.

In the thermal neutron-induced fission reaction, the heavy nuclides preferentially disintegrate asymmetrically into a lighter and a heavier fragment with a statistical distribution of the fragment masses. This leads in the ^{235}U fission to maxima of formation at mass numbers 95 and 138, with each showing fission yields (isobaric chain yield) of about 7%. As can be seen from the well-known fission product mass distribution curves, between the two maxima a broad and deep minimum exists with fission yields on the order of 10^{-2}%. In the ^{239}Pu fission the maxima of formation are shifted towards the mass numbers 99 and 140, while the basic shapes of the two distribution curves are quite similar. The mass distribution curve of the ^{235}U fission products shows a fine structure near mass number 133 and, to a somewhat lesser extent, also in the region of mass number 95; the ^{239}Pu fission yield curve shows a similar fine structure. The reasons for the fine structure are the preferential formation of fission fragments with the magic neutron numbers 50 and 82 in the nucleus (i. e. saturated neutron shells), as well as the emission of prompt neutrons from fragments which, in addition to having a stable configuration, also have weakly bound neutrons in the nucleus.

The mass distributions in the fission reaction are expressed by the fission yields. Here, three different yields have to be distinguished:

- the independent yield (or fragment yield) describing the formation of one individual fission product nuclide by the primary fission process;
- the cumulative yield, which means the total yield of one individual fission product nuclide as the sum of its independent yield and of its formation by decay of its chain precursors;
- the chain yield (or isobaric yield), which is the cumulative yield of a decay chain.

In general, the independent yield is highest for the first members of an isobaric chain and decreases significantly in the development of the chain; the final mem-

bers of an isobaric decay chain are predominantly produced by the β^- decay of their precursors.

The two fragments formed in the fission process exhibit a total kinetic energy of 167 MeV, which is distributed between the two fragments corresponding to the reciprocal ratio of their masses. This kinetic energy effects a movement of the fragments in opposite directions in the fuel matrix; after a recoil length of about 10 μm in this matrix, they reach their rest position normally inside a UO_2 crystallite after about 10^{-9} seconds. Some 95% of the kinetic energy of the fission fragment is transformed into electronic stopping power, with a minor portion causing lattice defects, e. g. through displacement cascades. Usually, the spur of a fission fragment is considered to be a cylindrical tube having a diameter of 10 nm and a length of about 6 μm. Thus, the high-speed movement of the fragments through the UO_2 lattice results in a short-term intense ionization of the fragments (average atomic charge number +20) as well as of the lattice atoms; near the starting point of the spur, very high local temperatures on the order of 3000 °C are reached within a diameter of about 10 nm. The knocking out of atoms from their regular lattice positions results in the formation of lattice defects. In addition, other direct effects of the fission fragments are to be observed, with the most important ones being radiation-induced creep and fission-induced densification of the UO_2 matrix, as well as redissolution of small fission gas bubbles.

The primary fission fragments are unstable due to an excess of neutrons in the nucleus compared to the neutron-to-proton ratios in stable medium-weight atoms. In order, therefore, to reach a stable nucleus configuration, neutrons have to be converted into protons by emission of β^- particles. Because of the negligibly small mass of the emitted electron, the mass of the remaining nucleus is virtually unchanged, but its electrical charge increases by one unit; this means that the transformations of the nuclei mainly occur in an isobaric chain until the stable final product of the chain has been formed. In most cases, the β^- decay reactions do not lead directly to the ground state of the daughter nucleus but to an intermediate excited state; thus the β^- decay is usually accompanied by associated γ emission. Examples of such isobaric decay chains are shown in Fig. 3.4. At the most, the isobaric chains have about 7 members, with the average being 3 to 5.

In general, the halflives of the individual chain members increase from the primary product to the final product of the chain (there are, however, numerous exceptions from this rule). In chains with odd mass numbers there is a continuous increase in halflife; in chains with even mass numbers, on the other hand, the members show shorter and longer halflives alternately, but with an increasing tendency. In many cases there are branched β^- decays, leading to the formation of isomeric states which subsequently decay to the ground state by internal transition with γ or X-ray emission and a shorter or longer halflife.

However, there are deviations from this isobaric chain behavior, the most important ones will be shortly mentioned.

In some cases the fission product nucleus decays by neutron emission. Examples of such delayed neutron emitters are the iodine isotopes 137, 138, 139 with halflives of 24, 6, and 2.7 seconds, respectively, and the bromine isotopes 87, 88, 89, 90 with halflives of 55, 16, 4.5, and 1.6 seconds, respectively. As a consequence of the

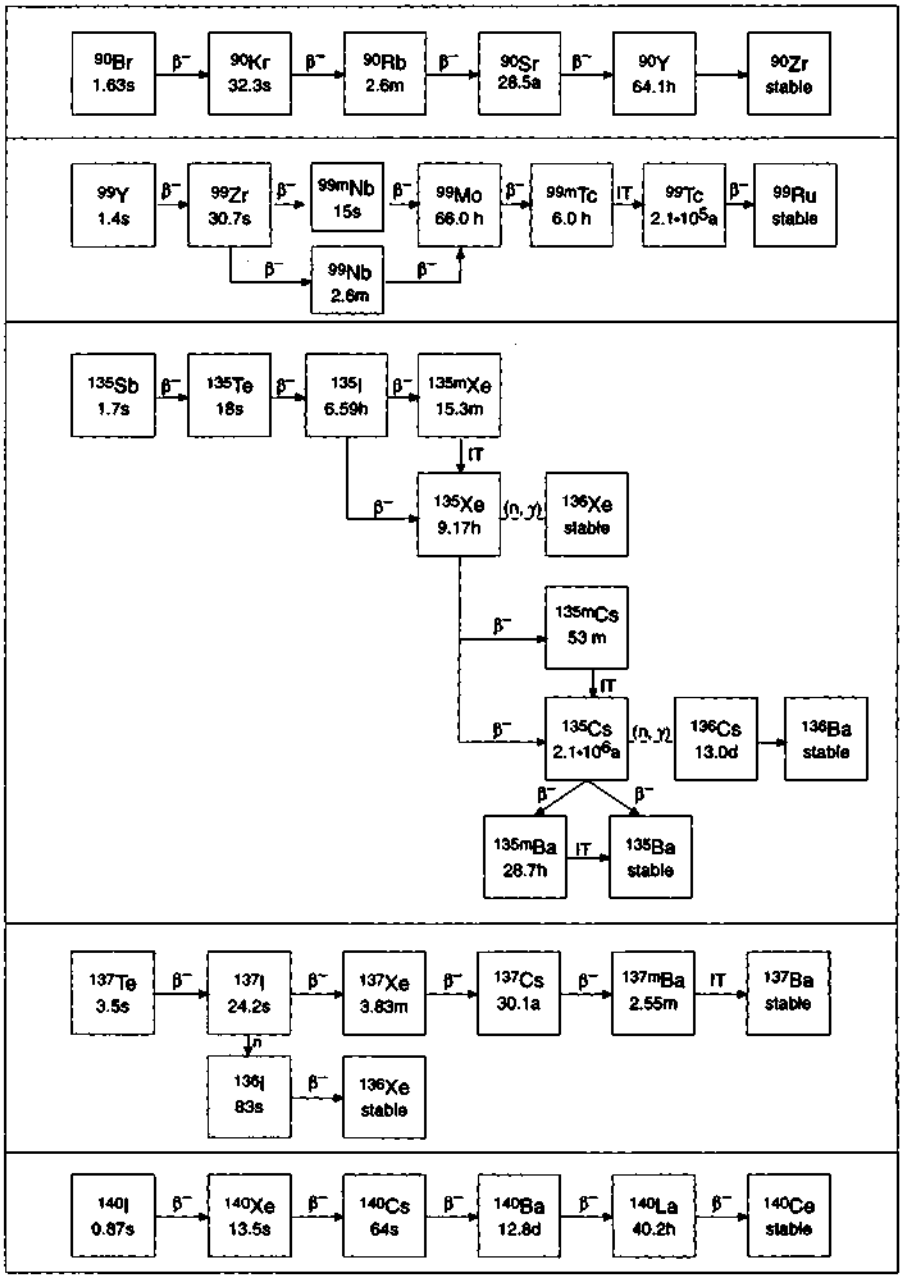

Figure 3.4. Fission product decay chains (schematic)

neutron emission, the relevant nucleus leaves its original isobaric chain and joins the one with a mass number one unit lower. The delayed neutrons account for about 0.75% of the total neutron production in the fission reaction; their energies are in the range 250 to 620 keV. About two-thirds of the delayed neutrons originate from the lighter fission product nuclides, the remainder from the heavier products. Delayed neutrons play an important role in reactor core reactivity control; in heavy-water reactors with separate fuel channels they are taken advantage of for quasi-continuous detection of failed fuel assemblies.

Fission product nuclides may also be transformed by neutron capture; the probability of an n,γ reaction increases with increasing halflife and with increasing neutron absorption cross section of the relevant nuclide. Therefore, in some cases the n,γ reaction competes with the β^- decay and is the limiting parameter for the concentration of the relevant radionuclide in the fuel. The most important example of such a neutron capture conversion is ^{135}Xe with a physical halflife of 9.17 hours and a reactor neutron absorption cross section σ of $6.25 \cdot 10^{-18}\,cm^2$; at a neutron flux, φ, of relevant energy distribution in the fuel at full-power operation of the plant of $5 \cdot 10^{13}\,cm^{-2} \cdot s^{-1}$, its effective halflife is reduced according to

$$\lambda_{eff} = \lambda + \sigma \cdot \phi \quad (\lambda \text{ decay constant})$$

from the 9.17 h mentioned above to about 0.58 h. At a constant supply rate from its precursor ^{135}I, the ^{135}Xe concentration in the fuel is comparatively low at reactor full-power operation; following a significant reduction in reactor load, e. g. in the course of a shutdown, the ^{135}Xe concentration in the fuel increases strongly because of the continuing production by ^{135}I decay (halflife 6.59 h) and lower or almost zero consumption by neutron capture. In practice, reactor operation is affected by this enhancement in ^{135}Xe concentration in the fuel, leading to an increase in the parasitic neutron absorption cross section (xenon poisoning) and, possibly, to problems in reactor startup at low excess reactivity of the fuel, e. g. towards the end of a fuel cycle.

Another secondary effect is the production of radionuclides which themselves are not fission products but which are generated by neutron capture in long-lived or stable fission product nuclides. Examples of the products of such reactions are ^{134}Cs and ^{136}Cs, which are separated from the true members of the isobaric chains by the stable nuclides ^{134}Xe and ^{136}Xe, and which are formed by neutron capture in the fission products ^{133}Cs and ^{135}Cs, respectively. Because of the two-fold neutron-induced nuclear reaction which is necessary for their production, their concentration in the irradiated fuel depends approximately on the square of the local neutron fluence.

Symmetric fission, in which the ^{235}U or ^{239}Pu nuclei disintegrate into two products of equal mass number, has a low probability. For this reason, their products do not play a significant role in the radionuclide composition of irradiated fuel.

In 0.2 to 0.3% of all fissions a third, light fragment beside the two medium-weight products is generated. The light product of ternary fissions with the greatest significance in reactor radiochemistry is tritium ^3H, the yields of which are approximately

- in thermal ^{235}U fission $9 \cdot 10^{-3}\%$
- in thermal ^{239}Pu fission $2 \cdot 10^{-2}\%$
- in thermal ^{241}Pu fission $3 \cdot 10^{-2}\%$.

Investigations performed by Bleier et al. (1984) yielded ^{3}H concentrations in the fuel which were systematically higher than those calculated using the KORIGEN code. The reasons for these differences are not exactly known; beyond possible uncertainties in the code basic data, contributions by other light element impurities such as boron or lithium in the fuel or ^{3}He in the fuel rod fill gas cannot be ruled out. The fission ^{3}H fragment shows a normal-distribution energy spectrum with a most probable energy of about 7 MeV, which results in a recoil length of about 10 μm in the UO_2 lattice before the fragment reaches its rest position (Ray, 1968).

Ternary fissions resulting in the formation of three fragments with approximately equal masses are very seldom, with a probability of about $10^{-6}\%$.

During its stay in the operating reactor core, the nuclear fuel changes its properties, in particular its chemical composition, its radionuclide inventory, and its pellet structure. Some important aspects of UO_2 behavior during reactor operation have been summarized in the review paper of Assmann and Stehle (1982). In Tables 3.3. and 3.4., the element concentrations of the fission products generated in the irradiated fuel are given for different burnup values, both for an enriched uranium fuel and a mixed-oxide fuel. These data were calculated using the KORIGEN code; their accuracy is assumed to be better than 10%. The by far greatest contributions to the element concentrations are delivered by the stable final products or very long-lived intermediate nuclides of the isobaric chains; those isotopes which are mainly responsible for the radioactivity inventory of the fuel generally represent only a small fraction of the total element mass. In total, the mass concentration of fission products in the fuel increases nearly linearily with increasing fuel burnup, reaching about 5.4% at a burnup of 52 MWd/kg HM (heavy metal) in an enriched uranium fuel and about 5.2% in a mixed-oxide fuel at the same burnup; each of the burnup steps chosen in Tables 3.3. and 3.4. corresponds approximately to one additional operating cycle of the fuel. Because of their greater number of stable isotopes, the elements with even proton numbers are generally present in higher concentrations than those with odd proton numbers. The fission product element with the highest mass concentration in the fuel is xenon, followed by the sum of the rare earth elements, the sum of the light platinum elements, and zirconium; however, as concerns chemistry in the fuel, these elements are of minor relevance due to their rather inert character. Molybdenum, on the other hand, which is also present in the fuel in comparatively high concentrations, is of great significance in fuel chemistry; its ability to change between different valency states effects a protection of the existing chemical states of various other fission product elements, in particular that of iodine, against the influence of slightly hyperstoichiometric fuel composition. Furthermore, the cesium-to-iodine atomic ratio in the fuel is of particular interest as regards the release and transport behavior of iodine during a reactor accident; this aspect will be treated in more detail in Chapters 6 and 7.

Table 3.3. Fission product element concentrations (g/kg HM) in irradiated LWR uranium fuel (initial enrichment 4.0% ^{235}U)
(By courtesy of Siemens/KWU)

Element	Fuel burnup (MWd/kg HM)				
	13.0	26.0	39.0	52.0	65.0
Bromine	0.0093	0.018	0.026	0.034	0.041
Krypton	0.16	0.31	0.43	0.54	0.64
Rubidium	0.16	0.29	0.41	0.51	0.60
Strontium	0.47	0.82	1.11	1.36	1.57
Yttrium	0.24	0.42	0.58	0.71	0.82
Zirconium	1.56	2.97	4.27	5.48	6.62
Niobium	0.045	0.044	0.042	0.040	0.038
Molybdenum	1.23	2.57	3.89	5.18	6.46
Technetium	0.33	0.64	0.91	1.14	1.33
Ruthenium	0.84	1.76	2.76	3.85	5.00
Rhodium	0.17	0.35	0.50	0.60	0.66
Palladium	0.23	0.68	1.34	2.18	3.18
Silver	0.015	0.042	0.073	0.11	0.14
Cadmium	0.011	0.037	0.080	0.15	0.23
Indium	0.0007	0.0013	0.0016	0.0017	0.0018
Tin	0.014	0.032	0.054	0.079	0.11
Antimony	0.0058	0.013	0.020	0.027	0.034
Tellurium	0.16	0.34	0.53	0.74	0.96
Iodine	0.080	0.17	0.27	0.37	0.47
Xenon	2.02	4.07	6.16	8.28	10.4
Cesium	1.14	2.27	3.34	4.36	5.32
Barium	0.56	1.10	1.66	2.26	2.89
Lanthanum	0.51	0.99	1.45	1.90	2.32
Cerium	1.30	2.34	3.28	4.19	5.07
Praseodymium	0.43	0.87	1.30	1.71	2.11
Neodymium	1.38	2.89	4.42	5.93	7.41
Promethium	0.13	0.18	0.19	0.19	0.17
Samarium	0.23	0.51	0.81	1.10	1.36
Europium	0.036	0.10	0.19	0.27	0.34
Gadolinium	0.0094	0.037	0.10	0.22	0.40
Totals	13.5	26.9	40.3	53.6	66.8

When comparing the data for the two different types of fuel, uranium fuel and mixed-oxide fuel, one can see the main differences in the region of the lighter platinum elements ruthenium, rhodium and palladium where the higher fission yields in the ^{239}Pu fission lead to higher concentrations of these elements in the irradiated mixed-oxide fuel.

There are, however, some deviations from the linear relationship between the element concentrations of fission products, on the one hand, and fuel burnup on the other, partly resulting in a greater than proportional buildup, and partly a

Table 3.4. Fission product element concentrations (g/kg HM) in irradiated LWR mixed-oxide fuel (initial Pu content 4.0% Pu_{fiss})
(By courtesy of Siemens/KWU)

Element	Fuel burnup (MWd/kg HM)				
	13.0	26.0	39.0	52.0	65.0
Bromine	0.0078	0.016	0.023	0.030	0.038
Krypton	0.087	0.17	0.26	0.34	0.43
Rubidium	0.076	0.15	0.23	0.30	0.38
Strontium	0.22	0.41	0.60	0.78	0.96
Yttrium	0.11	0.21	0.31	0.40	0.50
Zirconium	1.07	2.10	3.13	4.16	5.19
Niobium	0.036	0.037	0.037	0.036	0.036
Molybdenum	1.16	2.42	3.67	4.92	6.17
Technetium	0.32	0.63	0.91	1.15	1.37
Ruthenium	1.22	2.32	3.40	4.49	5.61
Rhodium	0.30	0.59	0.82	0.98	1.07
Palladium	0.70	1.55	2.49	3.52	4.62
Silver	0.069	0.13	0.17	0.21	0.23
Cadmium	0.040	0.098	0.17	0.27	0.39
Indium	0.0016	0.0026	0.0030	0.0031	0.0030
Tin	0.028	0.056	0.085	0.11	0.14
Antimony	0.012	0.023	0.031	0.039	0.045
Tellurium	0.24	0.47	0.70	0.93	1.16
Iodine	0.14	0.27	0.39	0.51	0.63
Xenon	1.97	3.94	5.92	7.92	9.94
Cesium	1.25	2.49	3.68	4.80	5.85
Barium	0.48	0.96	1.48	2.04	2.64
Lanthanum	0.44	0.88	1.31	1.74	2.16
Cerium	1.09	2.02	2.90	3.76	4.61
Praseodymium	0.38	0.80	1.21	1.61	2.00
Neodymium	1.15	2.45	3.80	5.17	6.55
Promethium	0.12	0.19	0.21	0.21	0.20
Samarium	0.27	0.56	0.86	1.16	1.43
Europium	0.056	0.14	0.24	0.35	0.45
Gadolinium	0.025	0.063	0.12	0.21	0.35
Totals	13.1	26.2	39.2	52.2	65.3

less than linear buildup. The main reasons for these deviations are the increasing contribution of plutonium fissions having other fission yields and the consumption of stable primary end products of isobaric chains by neutron capture; the extent of the latter effect is also influenced by the shift in the neutron energy spectrum with increasing fuel burnup.

The activity concentrations of selected fission product radionuclides in a uranium standard fuel are shown in Table 3.5. From these data, it becomes evident that during reactor operation the overwhelming fraction of radioactivity is caused

by the great number of short-lived radionuclides (the very short-lived ones are not given in the Table). These radionuclides are already in their activity saturation state after a short period of reactor operation and, thus, show a radioactivity which is virtually constant over time; for this reason, the total activity concentration in the fuel is not sensitive to the fuel burnup, in contrast to the activity concentration of the long-lived fission products.

With regard to the radionuclide composition of irradiated fuel, there are also deviations from the simple relationship between fission product activity concentrations of longer-lived nuclides and fuel burnup. Similarly to the buildup of the mass concentrations, these deviations are due to the increasing contribution of plutonium fissions to radionuclide production as well as to consumption of long-lived radionuclides by neutron capture; in extreme cases, such as with the short-lived

Table 3.5. Fission product activity concentrations (GBq/kg HM; end of irradiation) UO_2 fuel, initial enrichment 4.0% ^{235}U
(By courtesy of Siemens/KWU)

Nuclide	Halflife	Fuel burnup (MWd/kg HM)			
		13.0	26.0	39.0	52.0
^{3}H	12.3 a	6.6	1.4 E+1*)	2.1 E+1	2.8 E+1
^{79}Se	$6.4 \cdot 10^{4}$ a	5.7 E-3	1.1 E-2	1.6 E-2	2.2 E-2
^{82}Br	35.3 h	4.5 E+1	9.0 E+1	1.4 E+2	2.1 E+2
^{83}Br	2.40 h	5.0 E+3	4.5 E+3	4.1 E+3	3.8 E+3
^{85}Kr	10.76 a	1.7 E+2	3.1 E+2	4.2 E+2	5.1 E+2
^{85m}Kr	4.48 h	1.2 E+4	1.0 E+4	9.0 E+3	8.0 E+3
^{87}Kr	76.3 m	2.2 E+4	1.9 E+4	1.7 E+4	1.4 E+4
^{88}Kr	2.84 h	3.2 E+4	2.7 E+4	2.4 E+4	2.0 E+4
^{88}Rb	17.8 m	3.2 E+4	2.8 E+4	2.4 E+4	2.1 E+4
^{89}Rb	15.2 m	4.3 E+4	3.6 E+4	3.1 E+4	2.7 E+4
^{89}Sr	50.5 d	4.4 E+4	3.8 E+4	3.3 E+4	2.8 E+4
^{90}Sr	28.5 a	1.3 E+3	2.4 E+3	3.3 E+3	4.1 E+3
^{91}Sr	9.5 h	5.3 E+4	4.6 E+4	4.1 E+4	3.6 E+4
^{90}Y	64.1 h	1.4 E+3	2.5 E+3	3.5 E+3	4.3 E+3
^{91}Y	58.5 d	5.5 E+4	4.8 E+4	4.3 E+4	3.7 E+4
^{93}Zr	$1.5 \cdot 10^{6}$ a	2.9 E-2	5.6 E-2	7.9 E-2	1.0 E-1
^{95}Zr	64.0 d	6.5 E+4	6.3 E+4	6.0 E+4	5.7 E+4
^{97}Zr	16.8 h	6.3 E+4	6.2 E+4	6.1 E+4	6.0 E+4
^{95}Nb	35.0 d	6.5 E+4	6.3 E+4	6.0 E+4	5.7 E+4
^{97}Nb	74 m	6.4 E+4	6.3 E+4	6.1 E+4	6.1 E+4
^{99}Mo	66.0 h	6.7 E+4	6.6 E+4	6.6 E+4	6.6 E+4
^{101}Mo	14.6 m	5.8 E+4	6.0 E+4	6.1 E+4	6.2 E+4
^{99}Tc	$2.1 \cdot 10^{5}$ a	2.1 E-1	4.0 E-1	5.7 E-1	7.1 E-1
^{99m}Tc	6.0 h	5.8 E+4	5.8 E+4	5.8 E+4	5.8 E+4
^{103}Ru	39.4 d	4.7 E+4	5.4 E+4	6.0 E+4	6.5 E+4
^{105}Ru	4.4 h	2.6 E+4	3.4 E+4	4.0 E+4	4.7 E+4
^{106}Ru	368 d	6.4 E+3	1.4 E+4	2.0 E+4	2.6 E+4

Table 3.5. (contd.)

Nuclide	Halflife	Fuel burnup (MWd/kg HM)			
		13.0	26.0	39.0	52.0
^{105}Rh	35.5 h	2.5 E+4	3.2 E+4	3.8 E+4	4.4 E+4
^{106}Rh	30 s	7.2 E+3	1.5 E+4	2.2 E+4	2.8 E+4
^{109}Pd	13.4 h	4.8 E+3	7.9 E+3	1.1 E+4	1.4 E+4
^{110m}Ag	249.9 d	9.8	4.9 E+1	1.2 E+2	2.2 E+2
^{111}Ag	7.45 d	1.0 E+3	1.5 E+3	1.8 E+3	2.2 E+3
^{125}Sb	2.77 a	1.1 E+2	2.4 E+2	3.7 E+2	5.0 E+2
^{129}Te	69.6 m	9.4 E+3	1.1 E+4	1.2 E+4	1.3 E+4
^{131}Te	25.0 m	3.0 E+4	3.1 E+4	3.2 E+4	3.2 E+4
^{132}Te	76.3 h	4.9 E+4	5.1 E+4	5.1 E+4	5.3 E+4
^{133}Te	12.5 m	4.2 E+4	4.1 E+4	4.1 E+4	4.1 E+4
^{134}Te	41.8 m	6.5 E+4	5.9 E+4	5.4 E+4	5.0 E+4
^{129}I	$1.57 \cdot 10^7$ a	3.8 E-4	8.4 E-4	1.3 E-3	1.9 E-3
^{131}I	8.02 d	3.4 E+4	3.5 E+4	3.6 E+4	3.7 E+4
^{132}I	2.3 h	5.0 E+4	5.1 E+4	5.3 E+4	5.4 E+4
^{133}I	20.8 h	7.4 E+4	7.3 E+4	7.3 E+4	7.3 E+4
^{134}I	52.0 m	8.1 E+4	8.0 E+4	7.8 E+4	7.7 E+4
^{135}I	6.61 h	6.9 E+4	6.8 E+4	6.8 E+4	6.7 E+4
^{133}Xe	5.25 d	7.4 E+4	7.3 E+4	7.3 E+4	7.3 E+4
^{135}Xe	9.10 h	2.1 E+4	1.9 E+4	1.7 E+4	1.6 E+4
^{135m}Xe	15.3 m	1.4 E+4	1.5 E+4	1.5 E+4	1.6 E+4
^{138}Xe	14.1 m	6.4 E+4	6.1 E+4	5.8 E+4	5.6 E+4
^{134}Cs	2.06 a	9.3 E+2	3.4 E+3	7.0 E+3	1.2 E+4
^{136}Cs	13.2 d	7.3 E+2	1.4 E+3	2.2 E+3	3.1 E+3
^{137}Cs	30.17 a	1.6 E+3	3.1 E+3	4.7 E+3	6.1 E+3
^{138}Cs	32.2 m	7.0 E+4	6.7 E+4	6.4 E+4	6.3 E+4
^{139}Ba	83.06 m	6.8 E+4	6.6 E+4	6.4 E+4	6.3 E+4
^{140}Ba	12.75 d	6.7 E+4	6.5 E+4	6.3 E+4	6.1 E+4
^{140}La	40.27 h	6.8 E+4	6.6 E+4	6.5 E+4	6.5 E+4
^{141}La	3.93 h	6.2 E+4	6.0 E+4	5.9 E+4	5.8 E+4
^{141}Ce	32.5 d	6.3 E+4	6.1 E+4	6.0 E+4	5.9 E+4
^{144}Ce	284.8 d	3.3 E+4	4.4 E+4	4.6 E+4	4.5 E+4
^{143}Pr	13.57 d	5.9 E+4	5.6 E+4	5.4 E+4	5.1 E+4
^{147}Nd	10.98 d	2.4 E+4	2.4 E+4	2.4 E+4	2.3 E+4
Totals		6.3 E+6	6.2 E+6	6.1 E+6	6.1 E+6

*) read as $1.4 \cdot 10^1$

krypton and rubidium isotopes, the activity concentration of some radionuclides decreases steadily with increasing fuel burnup. Since the activity concentrations of the fission products in irradiated mixed-oxide fuels show no basic differences, Table 3.5. is limited to uranium fuel only.

In addition to the fission products, actinide nuclides are generated in the nuclear fuel during irradiation. The main starting reaction for the buildup of the transuranium nuclides is neutron capture in the ^{238}U nucleus leading to short-lived ^{239}U

which decays by β^- emission to ^{239}Np; this nuclide, in turn, decays to ^{239}Pu. As can be seen from Fig. 3.5., where a highly simplified version of the buildup and decay reactions is presented, a large number of different nuclides is formed. The principal reactions for buildup of the transplutonium elements from the lighter transuranium elements neptunium and plutonium are again neutron capture and subsequent β^- decay leading to the curium isotopes; the comparatively short half-lives of these isotopes and their large fission cross sections are the main reasons that the yield of higher actinides is negligibly small. In most cases, the lighter transuranium nuclides are α emitters with rather long halflives; some of them show also disintegration by spontaneous fission.

In Tables 3.6. and 3.7., the actinide element concentrations are given as a function of fuel burnup, both for uranium and for mixed-oxide fuel. In both types of fuel, besides uranium, plutonium is the most abundant element, amounting in the uranium fuel at a burnup of 52 MWd/kg HM to about one third of its concentration in a mixed-oxide fuel at the same burnup. Whereas in the mixed-oxide fuel the plutonium content decreases steadily with increasing burnup, in the uranium fuel the initially steep increase declines at burnup values beyond about 40 MWd/kg HM, reaching an almost constant value with continued irradiation. The higher actinides americium and curium show a steady growth with increasing burnup in both types of fuel; americium, curium and the heavier elements are present in the mixed-oxide fuel in significantly higher concentrations than in uranium fuel, whereas neptunium shows higher concentrations in the high-burnup uranium fuel.

In Tables 3.8. and 3.9. the activity concentrations of actinide nuclides both in uranium and in mixed-oxide fuel are shown. The ^{239}Pu activity in the uranium fuel increases during the first fuel cycle and then remains almost constant with only a slight further increase, while the ^{241}Pu activity increases steadily with increasing burnup. In the mixed-oxide fuel the ^{239}Pu concentration decreases steadily with ^{241}Pu remaining virtually constant over the whole irradiation period under consideration. During reactor operation, the fissile nuclides ^{239}Pu and ^{241}Pu produced are partly consumed again by in-situ fission; in a uranium fuel in the burnup range from 40 to 60 MWd/kg U, about 30 to 40% of the power generated is due to plutonium fissions. Among the actinides, the predominant α emitter is ^{242}Cm; therefore, in the case of failed fuel rods in the reactor core it would be quite erroneous to attribute the gross α activity that appears in the primary coolant to plutonium isotopes. In irradiated mixed-oxide fuels the concentrations of the different actinide isotopes depend strongly on the initial isotope composition of the plutonium employed (the data given in Table 3.9. are an example only). In repeatedly recycled plutonium the nuclides ^{238}Pu and ^{244}Cm, in particular, play an increasing role, thus complicating the fabrication of new mixed-oxide fuel because of greater heat production and higher neutron emission (e. g. Wiese, 1993).

Up to high burnup values the axial fission product distribution in the fuel rod corresponds very closely to the time-averaged neutron flux distribution. In PWR fuel, this results in an almost constant activity level in the middle region of the fuel rod, as can be seen from the gross gamma scan shown in Fig. 3.6. The activity minima in this region are the consequence of the neutron shielding effect of the spacer grids, which leads to a local decrease in fission rates. In a high-resolution

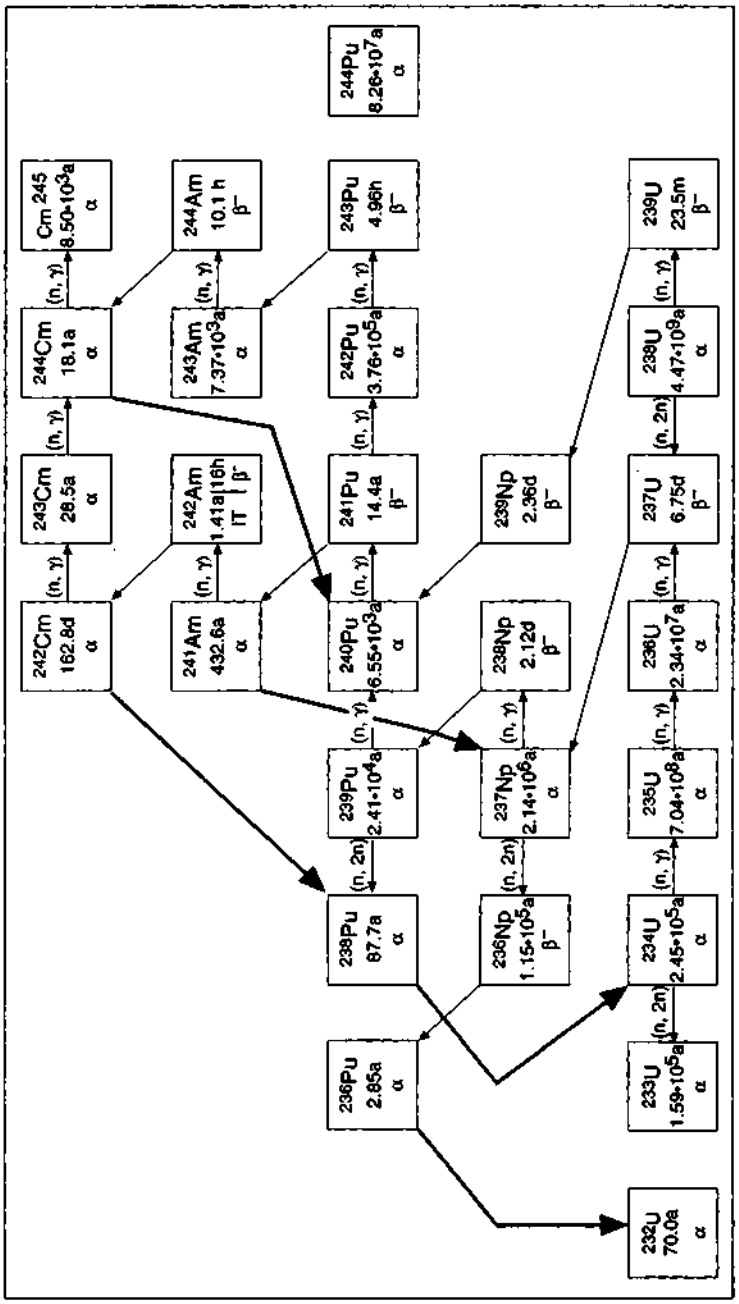

Figure 3.5. Buildup of actinide nuclides in irradiated LWR fuel (schematic)

Table 3.6. Actinide element concentrations (g/kg HM) in irradiated LWR uranium fuel (initial enrichment 4.0% ^{235}U)
(By courtesy of Siemens/KWU)

Element (g/kg HM)	Charge	Fuel burnup (MWd/kg HM)				
		13.0	26.0	39.0	52.0	65.0
Uranium	1.00 E+3	9.82 E+2	9.65E+2	9.49 E+2	9.34 E+2	9.19 E+2
Neptunium	0	1.73 E-1	3.8 E-1	6.3 E-1	8.6 E-1	1.04
Plutonium	0	5.01	8.0	1.01 E+1	1.17 E+1	1.28 E+1
Americium	0	5.3 E-3	4.9 E-2	1.6 E-1	3.3 E-1	5.5 E-1
Curium	0	5.3 E-4	9.8 E-3	5.1 E-2	1.6 E-1	3.7 E-1
Berkelium	0		1.0 E-11	7.7 E-10	1.6 E-8	1.5 E-7
Californium	0		4.1 E-12	4.5 E-10	1.2 E-8	1.4 E-7
Einsteinium	0		1.6 E-16	4.9 E-14	2.7 E-12	5.0 E-11

gamma scan one can observe additional activity minima at the pellet interfaces due to the lower fuel density in these regions, which is caused by the pellet dishings; at high burnup levels, the dishings have largely disappeared as a consequence of fuel swelling. In such fuel rods the pellet interfaces are no longer (or only very weakly) indicated by gamma scan minima. The gamma scans demonstrate that during steady-state operation at linear heat ratings of the fuel rods typical for LWRs there is no measurable axial fission product migration. In BWR fuel rods, the axial gross gamma distribution is asymmetric, which demonstrates the impact of the control rod positions. However, as can be concluded from the distributions of long-lived and short-lived fission products, this effect results from the fission rate distribution in the final fuel cycle rather than from burnup distribution. By an appropriate operational mode of the reactor core, an evenly distributed burnup can be finally obtained.

Table 3.7. Actinide element concentrations (g/kg HM) in irradiated LWR mixed-oxide fuel (initial Pu content 4.0% Pu_{fiss})
(By courtesy of Siemens/KWU)

Element (g/kg HM)	Charge	Fuel burnup (MWd/kg HM)				
		13.0	26.0	39.0	52.0	65.0
Uranium	9.37 E+2	9.29 E+2	9.22 E+2	9.14 E+2	9.05 E+2	8.94 E+2
Neptunium	0	9.35 E-2	1.45 E-1	2.03 E-1	2.74 E-1	3.46 E-1
Plutonium	6.32 E+1	5.61 E+1	4.93 E+1	4.29 E+1	3.75 E+1	3.32 E+1
Americium	0	1.08	1.95	2.64	3.21	3.67
Curium	0	1.2 E-1	4.1 E-1	8.6 E-1	1.51	2.37
Berkelium	0	4.7 E-12	4.6 E-10	7.0 E-9	5.7 E-8	3.2 E-7
Californium	0		1.7 E-10	3.7 E-9	3.9 E-8	2.7 E-7
Einsteinium	0		1.9 E-15	1.1 E-13	2.7 E-12	3.5 E-11

Table 3.8. Actinide activity concentrations (GBq/kg HM; end of irradiation)
UO_2 fuel, initial enrichment 4.0% ^{235}U
(By courtesy of Siemens/KWU)

Nuclide	Halflife	Decay mode	Fuel burnup (MWd/kg HM)				
			Charge	13.0	26.0	39.0	52.0
^{232}U	70.0 a	α	0	4.2 E−5	1.9 E−4	5.3 E−4	1.1 E−3
^{233}U	$1.59 \cdot 10^5$ a	α	0	2.4 E−6	3.4 E−6	3.5 E−6	3.1 E−6
^{234}U	$2.45 \cdot 10^5$ a	α	7.2 E−2	6.1 E−2	5.1 E−2	4.1 E−2	3.3 E−2
^{235}U	$7.04 \cdot 10^8$ a	α	3.2 E−3	2.1 E−3	1.4 E−3	8.3 E−4	4.5 E−4
^{236}U	$2.34 \cdot 10^7$ a	α	0	5.8 E−3	9.6 E−3	1.2 E−2	1.3 E−2
^{237}U	6.75 d	β^-	0	1.6 E+4	2.6 E+4	3.4 E+4	4.0 E+4
^{238}U	$4.47 \cdot 10^9$ a	α	1.2 E−2	1.2 E−2	1.2 E−2	1.2 E−2	1.1 E−2
^{239}U	23.5 m	β^-	0	5.9 E+5	6.6 E+5	7.6 E+5	8.5 E+5
^{236}Np	$1.15 \cdot 10^5$ a	β^-	0	6.8 E−2	2.2 E−1	4.6 E−1	7.3 E−1
^{237}Np	$2.14 \cdot 10^6$ a	α	0	2.7 E−3	8.0 E−3	1.4 E−2	2.0 E−2
^{238}Np	2.12 d	β^-	0	2.1 E+3	7.1 E+3	1.4 E+4	2.3 E+4
^{239}Np	2.36 d	β^-	0	5.9 E+5	6.6 E+5	7.5 E+5	8.5 E+5
^{236}Pu	2.85 a	α	0	2.6 E−3	1.5 E−2	3.8 E−2	7.1 E−2
^{238}Pu	87.7 a	α	0	6.1	3.7 E+1	1.1 E+2	2.1 E+2
^{239}Pu	$2.41 \cdot 10^4$ a	α	0	9.0	1.2 E+1	1.3 E+1	1.3 E+1
^{240}Pu	$6.55 \cdot 10^3$ a	α	0	6.2	1.4 E+1	1.9 E+1	2.3 E+1
^{241}Pu	14.4 a	β^-	0	1.2 E+3	3.8 E+3	5.8 E+3	6.9 E+3
^{242}Pu	$3.76 \cdot 10^5$ a	α	0	3.7 E−3	2.8 E−2	7.7 E−2	1.4 E−1
^{244}Pu	$8.26 \cdot 10^7$ a	α	0	8.9 E−11	1.8 E−9	9.8 E−9	3.0 E−8
^{241}Am	432.6 a	α	0	4.7 E−1	2.9	6.1	8.2
^{242m}Am	141 a	IT	0	1.7 E−3	1.6 E−1	3.7 E−1	5.1 E−1
^{243}Am	$7.37 \cdot 10^3$ a	α	0	1.1 E−2	1.9 E−1	8.0 E−1	1.9
^{242}Cm	162.8 d	α	0	5.1 E+1	6.5 E+2	2.0 E+3	3.5 E+3
^{243}Cm	28.5 a	α	0	6.6 E−3	1.9 E−1	9.7 E−1	2.4
^{244}Cm	18.1 a	α	0	3.1 E−1	1.3 E+1	9.7 E+1	3.7 E+2
^{245}Cm	$8.50 \cdot 10^3$ a	α	0	9.8 E−6	7.7 E−4	8.3 E−3	4.0 E−2

An important feature in characterizing irradiated nuclear fuels is the analysis of the distribution of fission products and activation products in the irradiated fuel rods, as well as in individual fuel pellets. For this reason, some of the analytical techniques developed to this end will be shortly described, each of which meets specific requirements.

Very often, determination of the fission gas fraction released during operation from the fuel pellet to the rod free volume is required. To this end, the fuel rod is punctured inside a hot cell using a special experimental device; the gas inventory of the rod, mainly consisting of helium, is then collected in an evacuated volume and measured by volumetric methods. Analysis of the individual gas composition is usually performed by mass spectrometry.

Axial distribution of fission products in a fuel rod usually is determined by gamma scanning; in this technique, the fuel rod is passed before the slit of a colli-

Table 3.9. Actinide activity concentrations (GBq/kg HM; end of irradiation) mixed–oxide fuel, initial Pu content 4.0% Pu_{fiss}
(By courtesy of Siemens/KWU)

Nuclide	Fuel burnup (MWd/kg HM)				
	Charge	13.0	26.0	39.0	52.0
^{232}U	0	2.0 E−5	8.0 E−5	1.9 E−4	3.6 E−4
^{233}U	0	5.3 E−7	9.3 E−7	1.2 E−6	1.5 E−6
^{234}U	1.1 E−2	1.3 E−2	1.4 E−2	1.5 E−2	1.5 E−2
^{235}U	5.3 E−4	4.4 E−4	3.5 E−4	2.7 E−4	1.9 E−4
^{236}U	0	6.3 E−4	1.2 E−3	1.6 E−3	1.9 E−3
^{237}U	0	4.1 E+3	5.5 E+3	6.9 E+3	9.1 E+3
^{238}U	1.2 E−2	1.2 E−2	1.1 E−2	1.1 E−2	1.1 E−2
^{239}U	0	4.7 E+5	5.0 E+5	5.4 E+5	6.4 E+5
^{236}Np	0	2.7 E−2	6.3 E−2	1.1 E−1	1.9 E−1
^{237}Np	0	1.0 E−3	2.3 E−3	3.7 E−3	5.2 E−3
^{238}Np	0	5.3 E+2	1.3 E+3	2.4 E+3	4.1 E+3
^{239}Np	0	4.6 E+5	5.0 E+5	5.4 E+5	6.4 E+5
^{236}Pu	0	3.5 E−3	8.4 E−3	1.5 E−2	2.5 E−2
^{238}Pu	1.2 E+3	1.1 E+3	9.7 E+2	9.3 E+2	9.2 E+2
^{239}Pu	7.7 E+1	5.9 E+1	4.3 E+1	3.2 E+1	2.5 E+1
^{240}Pu	1.3 E+2	1.4 E+2	1.3 E+2	1.2 E+2	1.0 E+2
^{241}Pu	2.4 E+4	2.9 E+4	3.0 E+4	3.0 E+4	2.7 E+4
^{242}Pu	7.6 E−1	7.4 E−1	7.7 E−1	8.1 E−1	8.5 E−1
^{244}Pu	0	4.6 E−8	9.3 E−8	1.5 E−7	2.3 E−7
^{241}Am	0	3.4 E+1	6.0 E+1	7.1 E+1	7.0 E+1
^{242m}Am	0	1.1	2.8	4.1	4.3
^{243}Am	0	6.0	1.1 E+1	1.5 E+1	2.0 E+1
^{242}Cm	0	3.5 E+3	1.0 E+4	1.6 E+4	2.1 E+4
^{243}Cm	0	6.5 E−1	3.5	8.5	1.5 E+1
^{244}Cm	0	2.6 E+2	9.7 E+2	2.1 E+3	3.9 E+3
^{245}Cm	0	3.3 E−3	2.0 E−2	5.8 E−2	1.2 E−1

mated gamma detector, either in a hot cell or in the spent fuel pool of the reactor plant (provided the required devices can be installed there). By using appropriate detectors, gross gamma scans (representing the total gamma activity) can be obtained as well as nuclide-specific scans (for example, ^{137}Cs distribution). The axial resolution of this technique depends widely on the collimator used; with a large opening of the collimator, the relative burnup of whole fuel assemblies can be determined. When absolute values of the local fission product concentrations or of the fuel assembly burnup are required, a careful calibration of the detection system has to be performed.

For the determination of the fission product distribution over the cross section of a fuel pellet, autoradiography is the simplest method with regard to instrumental needs; this technique, however, requires extensive experience in order to obtain optimum results at the very high radioactivity level of the materials. The distribu-

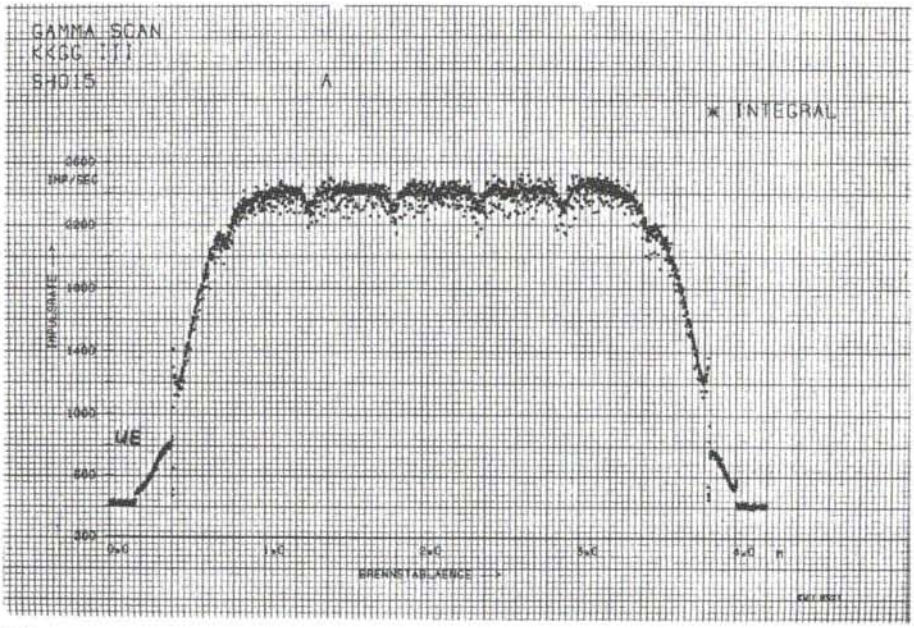

(a)

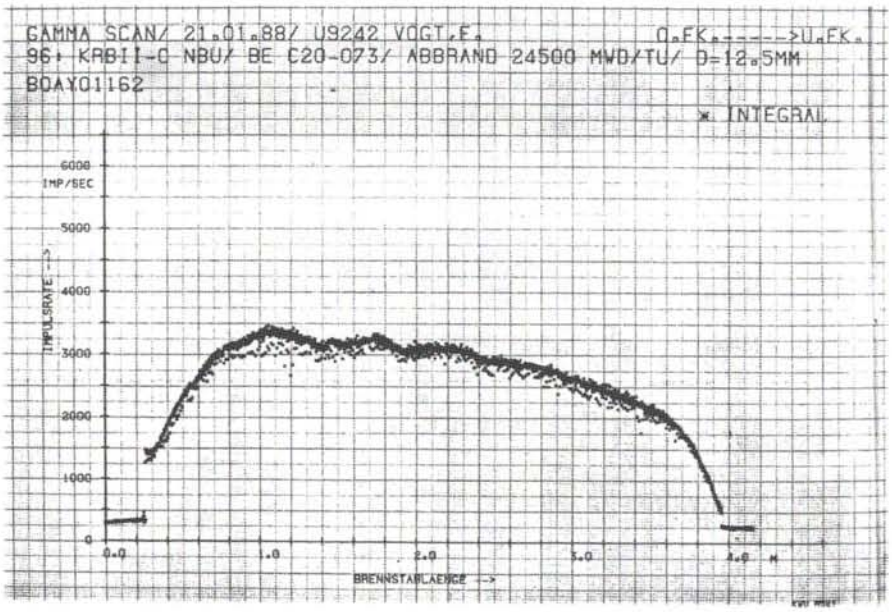

(b)

Figure 3.6. Axial gross gamma scans of high-burnup fuel rods
a) PWR fuel rod; b) BWR fuel rod
(By courtesy of Siemens/KWU)

tion of β^-,γ emitters can be imaged by special X-ray emulsions, while α emitters can be localized even in the presence of a large excess of β^-,γ nuclides by using special polymere foils, with the defects caused by α damaging being developed by caustic etching. A further advantage of this technique is that it can be easily accomodated to different activity levels of the specimen by selection of an appropriate exposure time. Usually, local activity resolutions on the order of a few micrometers can be achieved. Primarily, the results obtained are of a qualitative nature; by optical density measurement after an appropriate calibration of the relationship between radioactivity and density, semi-quantitative results are also possible.

The distribution of γ-emitting fission products across a fuel pellet section can also be determined by micro-gamma scanning. With a carefully designed system, a local resolution on the order of 250 to 500 µm can be achieved (Manzel et al., 1984).

A global analysis of all radionuclides, as well as of non-radioactive constituents, can be performed by taking microsamples from the fuel pellet, e. g. by mechanical drilling or by an ultrasonic technique. By using sophisticated sampling techniques, a local resolution on the order of 300 µm is possible. In order to determine the fission gas contents, the microsamples are dissolved under vacuum in de-aerated nitric acid; the released gases are collected and analyzed by mass spectrometry. Other constituents are determined by an appropriate separation and measurement method; as an example, determination of ^{129}I in such microsamples by neutron activation analysis is described in Section 3.2.3.3.

Determination of the concentrations of the different isotopes of uranium, plutonium and the transplutonium elements plays an important role in the characterization of irradiated nuclear fuels. Radiochemical analysis procedures with subsequent radiation measurement generally cannot deliver the high accuracy required of the results. For this reason, the standard procedure applied for this task is based on an anion exchange separation of uranium and plutonium from the fission products and from each other in nitric acid solution, after addition of ^{233}U and ^{242}Pu spikes to the solution to monitor the separation yields. In the isolated uranium and plutonium fractions the ratios of the concentrations of the individual isotopes to the concentration of the relevant spike nuclide are determined by high-resolution mass spectrometry using thermionic excitation. The high sensitivity of mass spectrometry renders possible the isotope analysis in microgram to milligram samples of irradiated fuel with satisfying reliability and accuracy. Because of its comparatively low mass concentration, ^{238}Pu determination by α spectrometry in an aliquot of the isolated plutonium solution usually offers higher accuracy than mass spectrometry.

In a second aliquot of the same sample, the concentrations of the burnup monitor ^{146}Nd and of the gadolinium isotopes in irradiated $UO_2-Gd_2O_3$ fuel can also be determined. In this procedure, the rare earth elements are first separated from uranium, plutonium and the fission products by anion exchange from hydrochloric acid solution; by addition of known amounts of ^{150}Nd and ^{160}Gd spikes to the sample solution, correction for losses of both rare earth elements during the separation process can be made. In the second step, the neodymium and gadolinium fractions are isolated from the other rare earth elements by cation exchange using

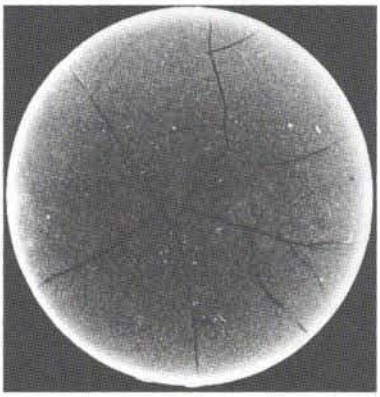

Figure 3.7. Enhanced production of transuranium nuclides at the fuel pellet rim (autoradiographic image)
(By courtesy of Siemens/KWU)

α-hydroxy isobutyric acid as an eluant; finally, the ratios of the concentrations of the isotopes to be determined to that of the added spike isotopes are measured by mass spectrometry.

In recent years, instrumental analysis techniques have gained more and more importance in the determination of fission product distribution in the fuel pellet. X-ray microanalysis and secondary ion microanalysis with local resolution of about 2 μm, Auger electron microanalysis with a local resolution down to 0.1 μm, as well as secondary ion mass spectrometry (e. g. Zwicky et al., 1989) are capable of furnishing informations on almost all chemical elements. By appropriate shielding and encapsulation of the excitation system, highly radioactive and also highly α-active samples can be analyzed without difficulties. These techniques furnish a better local resolution than micro-gamma scanning and microsampling; however, in most cases they are only able to measure the element composition, and do not distinguish between different isotopes. Often, the instrumental microanalytical techniques (such as electron probe microanalysis) give the concentrations of the fission products dissolved in the UO_2 lattice and of those trapped in small bubbles within the grains. Little, if any, of the fission gases and volatile fission products contained on the grain boundaries and in intergranular bubbles contribute to the measured X-ray intensities because in most cases the analyses are made away from the grain boundaries.

The radial distribution of the fission products over the cross section of the fuel pellet is primarily governed by the profile of the thermal neutron flux. However, there are two effects leading to variations in the distribution of some of the fission products. The first one of these effects is the preferential formation of plutonium in the outermost pellet zones due to epithermal neutron capture in the ^{238}U nucleus. This effect is more pronounced in high-burnup fuel than in fuel with a lower burnup. Fig. 3.7. shows an alpha autoradiographic image of a fuel pellet cross section where the enhanced α activity in the outer ring can be seen; it must nonetheless be pointed out that the greatest fraction of this α activity is not due to the

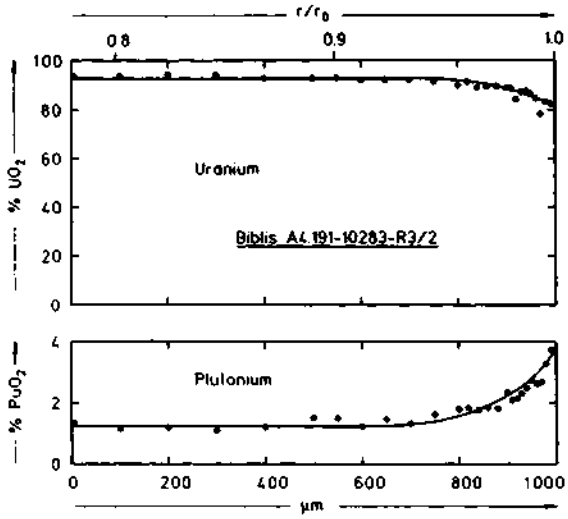

Figure 3.8. Uranium and plutonium concentrations in the surface region of a high-burnup oxide fuel pellet
(Kleykamp, 1990 a)

plutonium isotopes but to the higher actinide isotopes generated, in particular to the curium isotopes.

Detailed studies of the preferential plutonium production in the outer pellet zones were also performed using X-ray microanalysis techniques. As a typical example, the investigation of a high-burnup PWR fuel rod (initial enrichment 3.2% ^{235}U, burnup 55.9 MWd/kg U, time-averaged linear heat rating 210 W/cm) reported by Kleykamp (1990 a) shall be mentioned here. In this material, the average PuO_2 concentration (which represents the difference between total plutonium production and plutonium consumption during fuel operation) amounted to 1.38%; in the outer 100 µm zone this value increased steeply to about 3.8% in the surface region, while in the center of the pellet it only amounted to 1.2% PuO_2 (see Fig. 3.8.). This increase in concentration in the pellet rim zone applies to all plutonium isotopes. The enhanced plutonium concentration in the outer zone of the pellet means higher fission density, resulting in a corresponding increase in the concentrations of the fission products from about a 6% average value to about 14% in the rim zone (see Fig. 3.9.). The almost identical distribution of neodymium, zirconium and cesium indicates that cesium migration in the thermal gradient contributes only insignificantly to the higher level near the pellet surface. Xenon distribution seems to show an opposite behavior to that of the other fission products, since the analytical results indicate that the fuel grains in the outer region are depleted in xenon. However, this region is characterized by a high gas bubble density. It was shown, e. g. by Manzel et al. (1984) and by Manzel and Eberle (1991), that most of the xenon is confined in these bubbles and has not been released to the fuel rod free volume.

The radial distribution of gadolinium, which is added to both PWR and BWR fuels as a burnable poison (see Section 1.1.2.), is also altered during fuel operation

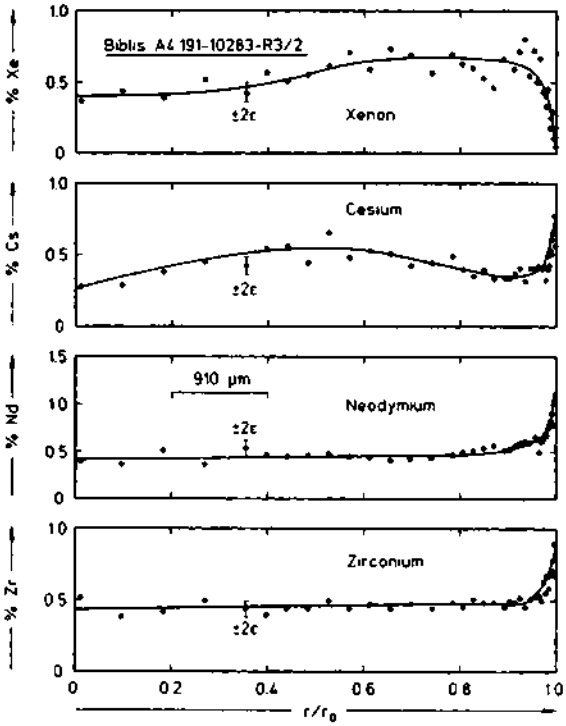

Figure 3.9. Fission product distribution as a function of the relative fuel pellet radius in a LWR high-burnup oxide fuel
(Kleykamp, 1990a)

as a consequence of isotope burnup. Gadolinium consists of several naturally occurring isotopes with markedly different nuclear properties. During fuel operation, the strongly neutron-absorbing isotopes ^{157}Gd (natural isotopic abundancy 15.7%, thermal neutron absorption cross section $2.54 \cdot 10^{-19}\,cm^2$) and ^{155}Gd (20.6%, $6.1 \cdot 10^{-20}\,cm^2$) are preferentially consumed, thus resulting in an increase in the relative concentrations of the weakly neutron-absorbing isotopes ^{158}Gd (24.7%, $2.5 \cdot 10^{-24}\,cm^2$) and ^{156}Gd (20.6%, $1.5 \cdot 10^{-24}\,cm^2$). The nuclear reactions create a pronounced profile of the individual gadolinium isotopes across the spent fuel pellet. In the outer pellet zone, ^{155}Gd and ^{157}Gd decrease to nearly zero concentration after one fuel cycle of irradiation, whereas ^{156}Gd and ^{158}Gd show a corresponding increase; ^{154}Gd and ^{160}Gd distributions are virtually not affected by the neutron irradiation.

The second effect leading to an inhomogeneous fission product distribution, in particular in the radial direction, is migration in the thermal gradient. This effect mainly affects the gaseous and the volatile fission products; its extent depends on several parameters such as the linear heat rating of the relevant fuel rod and, consequently, the temperatures in the pellets during reactor operation, as well as

the stoichiometry of the fuel. Migration in the thermal gradient is a secondary effect and will be treated in more detail in Section 3.2.3.

As was described in Section 1.1.2., fresh mixed-oxide fuels show an inhomogeneous structure with U/Pu oxide master-mix agglomerates embedded in the UO_2 matrix. In the course of reactor operation under steady-state conditions, only little U-Pu interdiffusion is observed up to burnup values of about 40 MWd/kg HM (linear heat ratings around 240 W/cm). However, as a consequence of power transients which reach values near 400 W/cm for about 50 hours (corresponding to a pellet central temperature on the order of 2000 °C), the mixed-oxide agglomerates in the central pellet region are completely dissolved (Goll et al., 1993). Due to their higher concentration of fissile nuclides, these agglomerates show a fission density and a resulting burnup which is considerably higher than that in the bulk of the fuel pellet. In a mixed-oxide fuel with an integral burnup of 38.8 MWd/kg HM, local burnup values in the mixed-oxide phases between 130 and 200 MWd/kg HM have been measured using an electron probe microanalyzer (Walker et al., 1991).

As a consequence of fission recoil, the fission fragments travel in the fuel over a distance of about 10 µm, i. e. a distance comparable to the size of the UO_2 crystallite dimensions. Because of the isotropic distribution of fragment movement, this effect does not lead to variations in the homogeneous distribution of the fission products in UO_2 fuel. In mixed-oxide fuels, however, the recoil effect results in a measurable depletion of the fission product concentrations in the master-mix agglomerates and a corresponding increase in the surrounding UO_2 matrix. Measurements using microanalytical techniques (Walker et al., 1991) have determined excess xenon and cesium concentrations in these matrix zones of about 35%, a value which agrees satisfactorily with recoil calculations (the principles of calculation of recoil release from samples showing dimensions comparable to the fission fragment recoil length were presented e. g. by Wise, 1985). Likewise, fission fragment recoil is the main reason for the buildup of the radionuclide inventory in the fuel pellet – cladding gap (see Section 3.2.4.).

While the bulk of the fission products is more or less homogeneously distributed in the fuel matrix in an atomic-dispersed state, new fission product phases are formed with increasing burnup (i. e. increasing fission product concentration), obviously resulting from an exceeding of the solubility limits of the relevant elements in the oxide matrix. Two such types of phases can be distinguished, a ceramic one and a metallic one. According to Kleykamp et al. (1985), the newly formed ceramic phase crystallizes in the cubic perovskite lattice and consists of oxides of the elements uranium, plutonium, barium, strontium, cesium, zirconium, molybdenum and the rare earth elements (RE), with a general composition $(Ba_{1-x-y}Sr_xCs_y)(U, Pu,RE,Zr,Mo)O_3$, as has been derived from numerous microanalytical investigations. As for the mechanism of formation, it is assumed that the elements strontium, yttrium, zirconium, which in lower concentrations are soluble in the UO_2 lattice, begin to form a particular phase after having reached their solubility limits; rare earth elements appear in this new phase to a significant extent only at very high burnup values of the fuel.

The metallic ε phase is a crystalline compound with a hexagonal lattice consisting of the elements molybdenum (24–43 weight%), technetium (8–16%), ruthe-

nium (27–52%), rhodium (4–10%) and palladium (3–15%), with broad variations in the concentrations of the individual constituents. In LWR fuels, the typical grain sizes of the metallic precipitates are small, on the order of 1 μm; given identical conditions, the amount increases nearly linearily with fuel burnup, starting at about 5 g/kg at 10 MWd/kg U and reaching about 15 g/kg at 40 MWd/kg U. The formation of metallic phases in the fuel is promoted by higher linear heat ratings of the fuel; high palladium concentrations in the metallic inclusions (on the order of 20%) indicate a relatively low fuel temperature. The relative fractions of molybdenum present in the ceramic and the metallic phases are controlled by the oxygen potential of the fuel during irradiation; they may also serve as an indicator of fuel stoichiometry. High molybdenum concentrations in the metallic phases (on the order of 30%) on the other hand imply an average O : M ratio of the fuel close to 2.000; at higher O : M ratios the major fraction of the fission product molybdenum remains in the UO_2 lattice (Kleykamp, 1990 b). Detailed knowledge of the metallic phases was mainly gained by investigations performed in the context of the development of nuclear fuel reprocessing methods, as the ε phase is virtually insoluble in nitric acid under the conditions of fuel dissolution in the process head end. However, in isolating this phase by nitric acid dissolution of the fuel matrix, it has to be taken into consideration that in the course of such an operation fission products which were initially dissolved may be re-precipitated as oxides or oxide hydrates, leading to potentially misleadingly large concentrations of the ε phase (Kleykamp, 1990 b). This oxide fraction consists mainly of ruthenium and molybdenum, but also contains barium, strontium, tellurium, zirconium and tin; usually it represents the bulk of the residues from the fuel (in the particular case mentioned above, 87% of the residue, corresponding to about 0.6% of the dissolved fuel mass).

In principle, mixed-oxide fuel contains the same fission product phases as UO_2 fuel; however, characteristic differences concerning the precipitation behavior can be observed even at low burnup data. This is caused by the different element yields in thermal uranium and plutonium fission, as well as by the less homogeneous distribution of the fissile nuclides in the mixed-oxide fuel matrix due to the fabrication technique applied. In total, in plutonium thermal fission one has to deal with greater proportions of elements forming the metallic ε phase than in uranium thermal fission (see Tables 3.3. and 3.4.). Because of the inhomogeneous plutonium distribution in the mixed-oxide fuel, the fission product concentrations in the master-mixture grains increase more rapidly than in the average fuel volume, reaching the solubility limits earlier, i. e. at a lower average burnup of the total pellet. On the other hand, from test irradiations of UO_2 fuel rods it is known that transients showing high linear heat ratings and high fuel temperatures lead to an accelerated precipitation of metallic phases. These are preferentially formed in the large pores characteristic of mixed-oxide fuel; the sizes of the individual particles usually are in the range of 0.5 to 4 μm. Above a threshold burnup which can be attributed to the solubility limits, the particle concentration increases almost linearily by about 0.2 weight% per 10 MWd/kg HM burnup. This value corresponds approximately to the fission-induced production rate of the stable and long-lived isotopes of the elements Mo, Tc, Ru, Rh, and Pd.

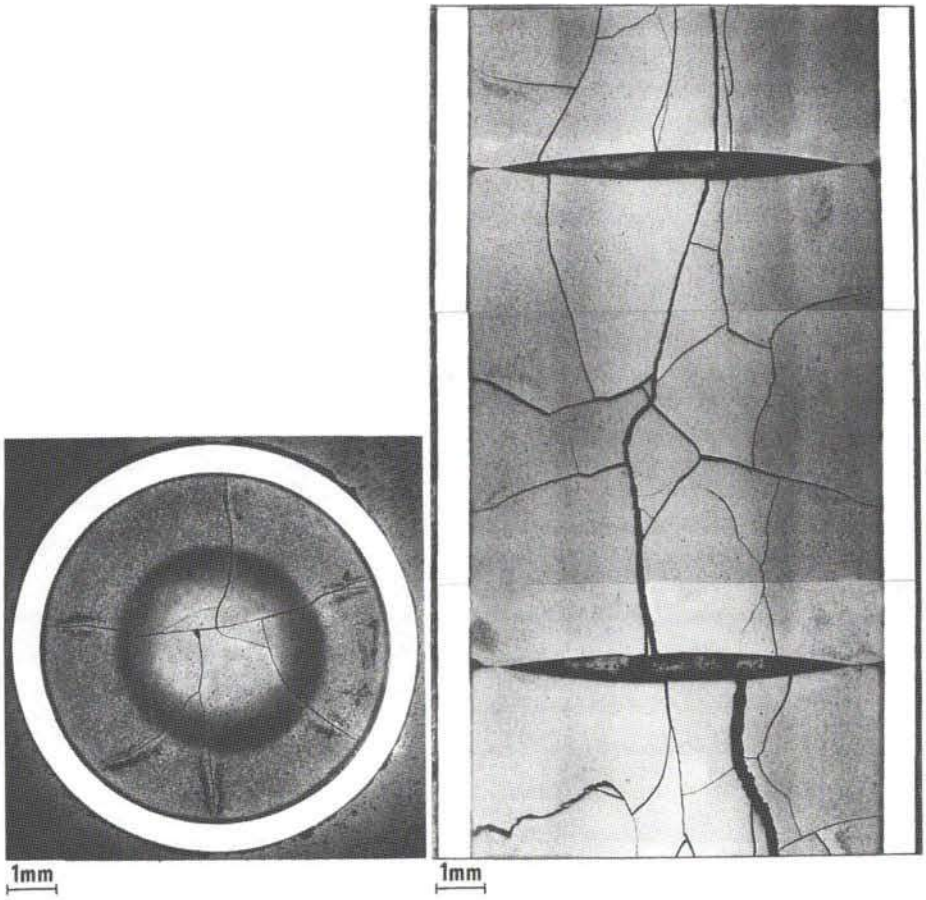

Fig. 3.10 a Fig. 3.10 b

Figure 3.10. Crack formation in irradiated fuel pellets; longitudinal and cross-sectional view (By courtesy of Siemens/KWU)

During reactor operation, the structure of the fuel is significantly altered due to neutron irradiation and thermal load. The most obvious evidence of this is the formation of an irregular network of cracks in the pellets in the radial as well as the axial direction (see Fig. 3.10.) even at low burnup levels. These cracks are formed as a consequence of the steep temperature gradient between the hot pellet center and the cooled cladding. One of the effects of the cracks is a significant increase in the real surface area of the pellet, which facilitates the release of gaseous fission products from the pellet matrix to the gap. In statistical evaluations of a great number of metallographic sections of spent fuel rods which were operated under standard LWR conditions, the specific surface area of the fuel was found to be $210-230\,mm^2/g$ UO_2 (compared to about $50\,mm^2/g$ in fresh fuel pellets), with no significant dependence on fuel burnup; in BWR fuels, the specific surface area is

about 180 mm^2/g UO_2, i. e. somewhat lower than in PWR fuels. In general, with increasing heat ratings the average fuel surface area increases, reaching about 260 mm^2/g UO_2 at 350 W/cm. Mixed-oxide fuels and $UO_2-Gd_2O_3$ fuels show an approximately identical crack development, leading to similar average specific surface areas as in a standard UO_2 fuel.

A high-burnup PWR fuel which was operated at an essentially constant load is characterized by a thin outer zone in which the original grain structure has disappeared and has been replaced by a fine-crystalline structure in which small rod-shaped precipitates are embedded, as well as by a multitude of gas bubbles having diameters between 0.1 and 1.5 μm. In the pores of this rim zone, precipitated particles can be observed using high-resolution electron microscopy. Next to the rim zone, the pellet shows an annular zone with a grain structure quite similar to the original state, which contains a few gas bubbles and precipitated phases in the grains. Another characteristic feature of such a high-burnup fuel is the development of one or more annular zones which are connected with the local release of fission gases. Apparently, these annuli indicate areas of beginning release of fission gases; the conditions necessary for this transformation such as temperature, fission rate and fission gas concentration are reached repeatedly during the residence time of the fuel inside the reactor core. It is assumed that the outer annulus was generated in the course of the final fuel cycle. In the inner annulus, the number of gas bubbles inside the grains decreases strongly, whereas the size and number of the bubbles at the grain boundaries increase markedly. In the pellet center, only isolated gas bubbles are observed inside the grains while large bubbles are present at the grain boundaries and in the channels connecting the grain surfaces, which are typical for the hot central region.

During the first irradiation phase, fuel porosity decreases due to the dissolution of the fine pores; with increasing burnup, the porosity increases again due to the precipitation of fission gas bubbles, and the pore size distribution shifts to somewhat larger pore diameters. The porosity of mixed-oxide fuel is characterized by the large bubbles in the plutonium-containing particles mentioned above, which in the pellet center develop large bubbles at the grain boundaries, partly generating connected channels. At high burnup, the fraction of open porosity originating from fuel fabrication is largely covered by channel formation between the fission gas bubbles. The fraction of open porosity as related to total porosity fluctuates between 1 and 30%.

The size of the oxide grains also changes during reactor exposure of the fuel, mainly caused by the prevailing temperature which shows a radial parabolic distribution from 800–1200 °C in the pellet center to about 450 °C at the pellet rim (see Fig. 1.9.). In the outermost rim zone with a width of 50 to 130 μm (depending on the burnup), fine particles with a grain size of less than 1 μm were formed. An intermediate zone shows grain sizes quite similar to the original shape, whereas in the direction towards the pellet center the grain sizes moderately increase to 8–12 μm. The fuel structure may also be changed by power transients, in particular at high burnup levels and a high final heat rating of the transient. For a UO_2 fuel irradiated to 45 MWd/kg U it was observed after a transient reaching 410 W/cm that the central zone of the pellet was characterized by elongated grains and by a porosity resembling to some extent that known from columnar grain growth. Fur-

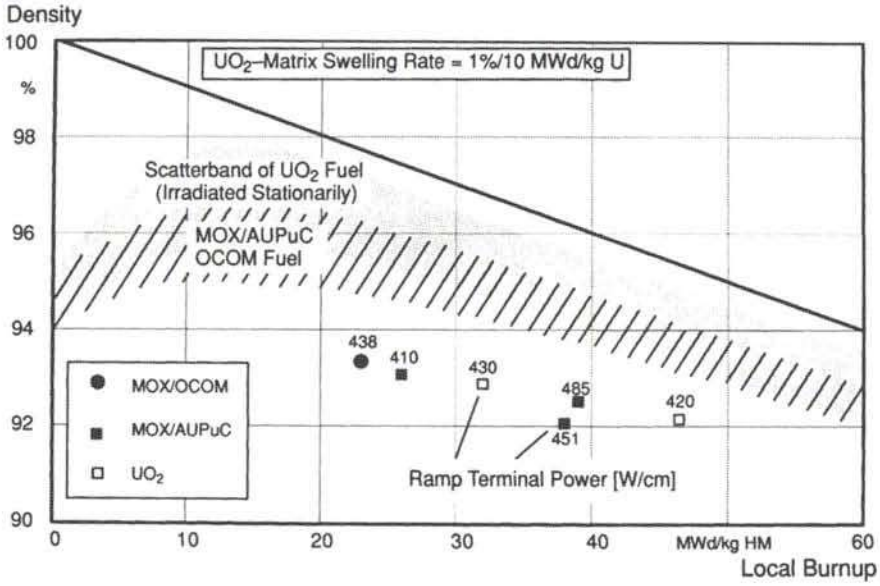

Figure 3.11. Densities of UO_2 and mixed-oxide fuels before and after transient testing as a function of burnup
(Goll et al., 1993; Copyright 1993 by the American Nuclear Society, La Grange Park, Illinois)

ther, large precipitates of the metallic phase containing ruthenium, rhodium, palladium, technetium, molybdenum were observed (Matzke et al., 1989).

The resulting density of the pellet is influenced by different changes in the fuel microstructure. Following an initial increase in density due to the dissolution of fine pores and reaching a maximum at a burnup of about 10 MWd/kg U, the density decreases again with increasing burnup, the reasons for which are the incorporation of fission products into the UO_2 lattice as well as the formation of new, additional phases. The rate of linear swelling of a standard UO_2 fuel amounts to about 1% per 10 MWd/kg U. The density reached during irradiation depends on the initial density of the UO_2 pellet; thus, a scatter band is obtained following irradiation under steady-state conditions (see Figure 3.11.).

The densification data of mixed-oxide fuels shows a tendency to fall near the lower boundary of the scatter band determined for UO_2 fuel (see Fig. 3.11.). This can be understood by taking into account the structure of this fuel type, where about 85% of the fuel volume consists of a UO_2 matrix whose densification is delayed because of its lower specific burnup. At burnup values beyond 20 MWd/kg HM, the swelling of the mixed-oxide agglomerates due to the buildup of porosity and solid fission products compensates for further densification of the UO_2 matrix. At burnup levels of 40 to 50 MWd/kg HM, the mixed-oxide fuel density is similar to that of UO_2 fuel. Fuel transients leading to ramp terminal power values well beyond that of steady-state operation result in virtually identical densities of both UO_2 and mixed-oxide fuels, when burnup is taken into account (Goll et al., 1993).

3.2.2 Determination of the burnup of nuclear fuel

In the preceding section it was shown that most of the important properties of a nuclear fuel are influenced by the burnup the particular fuel has experienced during its stay in the reactor core. For this reason, knowledge of the fuel burnup reached, i. e. of the number of nuclear fissions which occurred in the course of the irradiation (this is equivalent to the number of fissile and fertile atoms consumed) is an essential prerequisite for characterization of the spent fuel. On the other hand, the fuel burnup is an important parameter for the characterization of spent commercial fuels destined for reprocessing work. In reactor technology, usually fuel burnup is expressed in terms of released energy (MWd/kg HM); sometimes, the percentage of fissioned atoms is given. Because of the importance of burnup for all aspects of fission product chemistry, a short overview of the principles involved in reliable determination of nuclear fuel burnup, as well as the limitations encountered, shall be given here.

In principle, two fundamentally different methods can be applied to solve this task. The first one is determination of the residual concentrations of the fissile nuclides after irradiation and calculation of the burnup from the difference between final and initial values. For this purpose, the uranium and plutonium fraction has to be separated from the fission and activation products and from each other (e. g. by extraction chromatography); subsequently, the concentrations of the individual isotopes, in particular of the fissile isotopes, are analyzed by mass spectrometry. Well-established analytical techniques for performing such analyses are available, so that only small error margins are to be expected in the determination of the concentrations of the isotopes under consideration. However, there are two problems that can potentially cause systematic errors. The first one is the well-known question of the accuracy of results which have been obtained as a difference between two numbers, which limits the accuracy at lower burnup values in particular. The second problem is that the fissile nuclides are not only consumed by nuclear fission but by neutron capture as well; in order to avoid systematic errors here, the capture-to-fission ratio valid for the particular irradiation conditions has to be taken into account in the calculation of ^{235}U depletion during irradiation. If one recalls the complicated buildup and decay mechanisms of actinide nuclides during reactor irradiation (see Fig. 3.5.), it is obvious that such correction requires complex calculations. On the other hand, the direct determination of the residual concentration of fissile nuclides is not influenced by errors due to inaccuracies in the fission yields of fission products to be measured nor by migration-induced inhomogenities in the fuel.

The other possibility is determination of the concentration of appropriate fission products in the irradiated fuel. The fundamentally large number of fission products that can be chosen from is reduced by several conditions that have to be satisfied in order to obtain reliable values on the fuel burnup. First, the halflife of the nuclide must be sufficiently long to allow integration over the entire operation period; therefore, its halflife should be longer by at least a factor of about three than the irradiation period of the fuel to preclude an overestimation of the final phase of irradiation. (On the other hand, measurement of short-lived nuclides can

be applied to determine the relative contribution of the final irradiation period to the total burnup). Second, the nuclear data of the nuclide to be measured, such as cumulative fission yield, and, for radioactive burnup monitors, the halflife and decay mode, must be known with sufficient accuracy; further, the neutron capture cross section of the monitor nuclide should be small in order to minimize errors due to a neutron-induced burnup of the nuclide. Third, the monitor nuclide should not show any migration tendency in the fuel during operation to avoid errors caused by inhomogeneous distribution of the relevant nuclide in the fuel, resulting potentially in non-representative sampling. When determination of the integral fuel burnup is required, the fission yields of the monitor nuclide in ^{235}U fission and in ^{239}Pu fission should be as similar as possible; on the other hand, when differentiation between the two types of fissions is required, these yields should show pronounced differences. Finally, the analytical procedure necessary for determination should be comparatively simple to facilitate the work.

It is quite hard to identify a fission product nuclide that fulfils all these requirements ideally. For LWR fuels showing comparatively low operating temperatures, ^{137}Cs has often been applied; its gamma ray at 0.662 MeV is easy to measure, even without chemical separation of the nuclide from the other radionuclides, its halflife of 30 years is long enough even for very long operation and decay periods and its decay scheme is known with a high degree of accuracy. However, in high-burnup fuels migration of this radionuclide in the fuel cannot be ruled out completely.

Because of the lack of other suitable radioactive fission products, attention has been focused on the use of stable fission product nuclides. Extensive research has shown that ^{146}Nd is an optimum burnup monitor; it does not show any migration tendency in the fuel, the fission yield is known with high accuracy, and mass spectrometry determination is not interfered with by other long-lived or stable fission products present in the fuel in significant concentrations. Usually, analysis is performed by separation of the nuclide from the solution of the fuel sample by liquid chromatography using α-hydroxy isobutyric acid as an eluant; the elution behavior of the nuclide from the chromatographic column can be monitored by measuring the γ emission of its radioactive isotope ^{150}Nd. The neodymium yield in the course of the chemical separation procedure can be monitored by addition of a ^{142}Nd spike to the initial solution, since this isotope is not produced in nuclear fission. Using nanogram amounts of the element in mass spectrometry, the concentration of the isotope in the fuel can be determined with an accuracy of 0.1 to 0.5% (Green et al., 1989).

The only disadvantage in the application of this nuclide as a burnup monitor is the fact that non-destructive determination of the fuel burnup is not possible; therefore, to obtain a quick survey of the burnup state of whole fuel rods or fuel assemblies, ^{137}Cs has to be measured. Depending on the question posed, either burnup distribution in the fuel rod can be determined by gamma scanning or an average value can be measured using an appropriate collimator design with a comparatively large opening. When the number of fissions which occurred in the final stage of operation is of interest, a short-lived radionuclide such as $^{140}Ba/^{140}La$ can be measured in the same manner. These measurements can be carried out either in a hot cell or in the spent fuel pool, provided that measures have been taken to install the

collimator – detector unit. When absolute burnup values are required, calibration of the γ detector unit can be done either by calculations taking into account the specific parameters of the measuring system or by subsequent destructive burnup analysis of a sample of the relevant fuel rod.

For safeguards fuel characterization within the framework of the Non-Proliferation Treaty, non-destructive techniques for burnup determination are required, even for fuels with comparatively long decay times. Attempts have been made to select pairs of γ-emitting fission products whose ratio can be used not only to verify the fuel burnup, but also to determine the Pu : U ratio in the fuel as well as the cooling time. It has been reported that the ratios of the radionuclides $^{154}Eu : ^{137}Cs$ and $^{134}Cs : ^{137}Cs$ fulfil these requirements (e. g. Berndt, 1988). The activity concentrations of these radionuclides in the fuel can be determined by a single measurement using a collimated high-resolution γ spectrometer. However, the correlations between the activity concentrations in the fuel and the required data have to be established separately for fuels with different initial ^{235}U enrichment values; likewise, the neutron energy spectrum is of importance. Taking into account these parameters, the results obtained are of satisfactory reliability for verification, in particular for fuels with long cooling periods (up to 20 years).

Using a combination of active and passive neutron interrogation, burnup of PWR and BWR fuel assemblies can be determined with an accuracy of ± 1.2 MWd/kg U and ± 2 MWd/kg U, respectively (Würz, 1991). Measurements of a great number of fuel assemblies performed in the spent fuel pools of LWR plants have shown that the accuracy of the results is not affected by the particular data of the fuel assembly and that it holds as long as ^{244}Cm is the predominant neutron emitter in the fuel.

3.2.3 Chemical state and behavior of the fission products in the fuel

3.2.3.1 General aspects

As was discussed in Section 3.2.1., immediately after the fission reaction the newly formed fission products travel at very high speed through the UO_2 lattice. Since in this phase the fragments are highly ionized atoms (average atomic charge number +20), a well-defined chemical state cannot be attributed to them. After being stopped and reaching its rest position, such an atom re-arranges its electron shell so that the final state is compatible with the conditions prevailing in the fuel. Identification of the chemical state of fission products in irradiated nuclear fuel is a complex task, because of the great number of influencing parameters and of the large differences in the concentration of fission products from that of the matrix substance. Due to these factors, experimental investigations are as difficult as are theoretical calculations. The following sections, therefore, are far from giving a complete picture; mainly those topics will be addressed which are of importance for understanding the succeeding chapters.

An understanding of the principles of fission product chemistry requires at first a description of the chemical system nuclear fuel. In a pure uranium fuel this system in its original state, i. e. prior to irradiation, consists of sintered pellets of stoichiometric $UO_{2.000}$ containing only neglibly small amounts of impurities. The gap between the pellets and the Zircaloy cladding is filled with helium at a starting pressure of about 2 MPa (at ambient temperature), showing very low concentrations of gaseous impurities. The cladding is sealed gas-tight; as a consequence a closed chemical system exists, except in the very seldom case of a cladding failure (see Section 4.3.2.). Nonetheless, this closed system is complicated by the fact that Zircaloy is able to trap oxygen irreversibly by oxide formation, affecting thereby the oxygen partial pressure inside the system. During irradiation, the fuel composition is changed by the buildup of the fission products belonging to different chemical elements; thus, a gross composition of about $(U_{0.95}FP_{0.06}TU_{0.01})O_2$ (where FP means fission product and TU transuranium element) can be assumed to exist at a burnup of 34 MWd/kg HM, when one ignores the chemically inert noble gases as well as the formation of metallic and oxide precipitates within the fuel grains and at the grain boundaries.

Fresh mixed-oxide fuels consist of a UO_2 matrix with a content of 3 to 4% fissile plutonium, with the plutonium concentrated in the master-mixture grains. During irradiation, fission product and transuranium elements are built up in the same manner as in uranium fuel; the newly formed transuranium elements are homogeneously distributed in the fuel matrix with the exception of the preferential plutonium breeding in the outermost zone of the pellet. The plutonium constituent has little effect on the chemical conditions in the fuel; therefore, both types of fuels are quite similar with regard to the chemistry environment of the fission products under the operating conditions of light water reactors.

UO_2 (as well as $(U,Pu)O_2$ for thermal reactors) form a crystal lattice of the calcium fluorite type showing a lattice constant of 0.5468 nm (5.468 Å) at stoichiometric composition. As can be seen from Fig. 3.12., the structure consists of a cubic

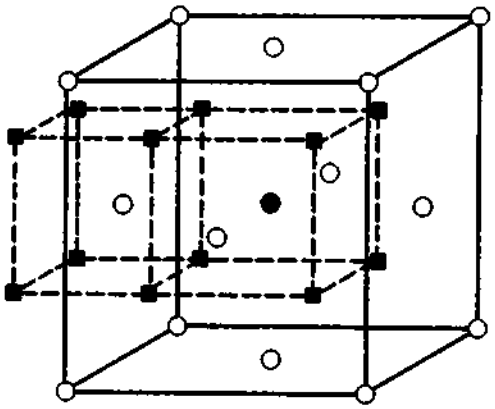

Figure 3.12. UO_2 crystal lattice structure (scheme)
o U atom; ■ O atom; • Vacancy

face-centered lattice (F-type lattice) of uranium atoms incorporating a simple cubic lattice of oxygen atoms (P-type lattice), the edge length of which is half of that of the uranium lattice. The zero position of the oxygen lattice is shifted by one quarter of the volume diagonal of the uranium lattice. Every second cube of oxygen atoms is occupied by an uranium atom in a volume-centering position, whereas the corresponding position in the neighbouring cell is vacant. Such a vacancy can be occupied in a hyperstoichiometric UO_{2+x} by excess oxygen atoms up to the composition U_4O_9 (corresponding to $UO_{2.25}$); within this range, the lattice constant decreases steadily with increasing hyperstoichiometry, whereas the lattice type remains unchanged.

After being stopped, the fission fragments reach their rest positions usually inside a UO_2 crystallite. There, their position might be at one of three different locations:

- at a regular lattice position, either at one which has been made available by the fission of the relevant uranium (or plutonium) atom, or at the lattice vacancy position;
- at an interstitial position or at a defect position within the UO_2 lattice;
- in precipitations inside the crystallites or at the crystallite grain boundaries.

At least in the first two above-mentioned cases, the fission products are present in the fuel in an atomic-dispersed state which does not seem to allow the identification of a definite chemical compound. Usually this is the situation at low fuel burnup with correspondingly low fission product concentrations in the fuel matrix. The chemical state of such finely dispersed fission product atoms cannot be described by the properties of chemical compounds; rather it has to be characterized by atomic properties, the most important of which, under the given circumstances, are the position in the crystal lattice and the valency state.

The number of available lattice positions, i. e. that of fissioned uranium (or plutonium) atoms plus that of the original vacancies, is sufficiently large to incorporate all the fission product atoms generated up to very high burnup values. A first indication of the fact that the original vacancies are also occupied by fission product atoms was obtained by early X-ray analytical observations showing that the lattice constant decreases with increasing burnup (Schmitz et al., 1971; Benedict et al., 1972). The lattice contraction of the CaF_2-type structure was also reported by a number of other investigators, as mentioned in the review paper of Kleykamp (1985). The reason for this lattice contraction is the enhanced mutual attraction due to additional lattice atoms, comparable to the situation in hyperstoichiometric UO_{2+x}. On the other hand, the proportion of the fission products incorporated at interstitial sites in the UO_2 lattice can hardly be quantified; it can be assumed that, due to the high density of fission product fragments and fast neutrons in the material, numerous lattice defects are formed which are only incompletely annealed at the operational temperatures. In any case, an important precondition for the incorporation of foreign atoms into a crystal lattice, either at regular lattice positions or at interstitial positions, is the compatibility of their radii with the lattice dimensions.

For general considerations concerning the chemical state of the fission products in the fuel matrix (in particular of the atomic dispersed ones, but to a certain extent also of those contained in precipitations), one may establish the following postulates:

- The chemical state is characterized by the existing valency state of the relevant fission product atom; chemical compounds with a well-defined chemical composition and an own habitus cannot be defined, with the exception of fuel inclusions.
- For thermodynamic reasons, the existing valency state of the fission product atom must be compatible with the prevailing conditions. This is a consequence of the postulate mentioned earlier that the progress of chemical reactions is controlled by the ambient conditions.
- Chemical compounds which are thermodynamically stable as isolated, pure compounds under the relevant conditions are not necessarily formed in the fuel matrix. There are problems due to kinetic interferences, to the very high UO_2 excess, and to the unfavorable mass ratios of some of the fission product elements under consideration for the formation of compounds that are possible in principle.
- The impact of the high-energy radiation (fast fission fragments and neutrons, as well as α, β and γ radiation) may lead to the formation of unusual valency states, but only for a very limited volume and over a very short time. Global changes in the chemical principles are not assumed to be caused by radiation effects.
- The principle of electro-neutrality has to be obeyed, i. e. the sum of all the positive and negative charges contained in a chemical system (e. g. in a crystallite) has to be zero.

One can expect, therefore, that the fission product atoms in the fuel are in a quasi-equilibrium state with regard to their environment.

With regard to their behavior in the fuel matrix, the fission products can be divided very generally into four groups (see Fig. 3.13., according to Kleykamp, 1985):

- Fission product noble gases and other volatile fission products.
- Fission products dissolved as oxides in the fuel matrix; employing the atomistic aspects discussed above, the term "oxide" should be replaced by "atoms in their adequate oxidized valency state".
- Fission products forming metallic precipitates.
- Fission products forming oxide precipitates.

There are transitions between the different groups which are partly caused by the oxygen potential of the fuel, while the formation and composition of precipitates, in particular, mainly depends on the concentrations of the individual fission product elements in the fuel.

According to the early considerations of Robinson (1958), nuclear fission may be understood as a nuclear chemistry reaction

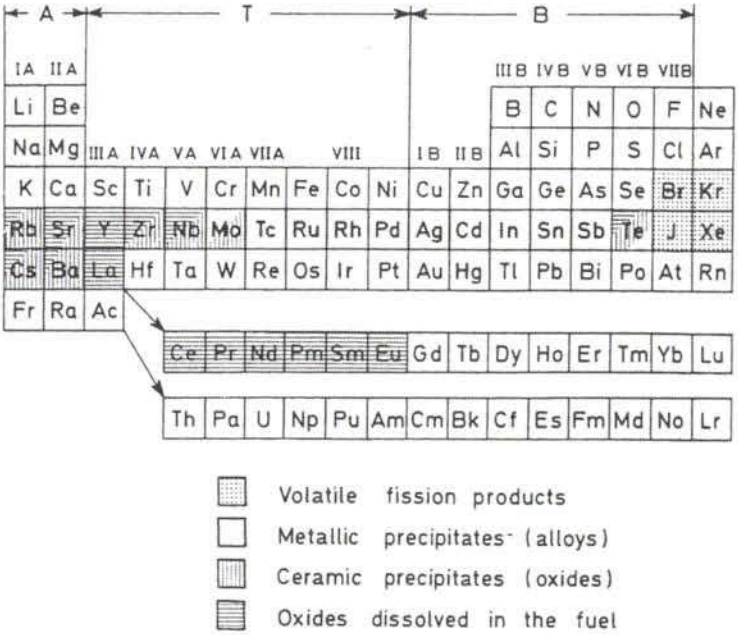

Figure 3.13. Typical properties of fission product elements in oxide fuels (Kleykamp, 1985; with kind permission of Elsevier Science – NL, Sara Burgerhartstraat 25, 1055 KV Amsterdam, The Netherlands)

$$U^{+V} \xrightarrow{n,f} 2\ FP^{+\overline{V}} + (2\,\overline{V} - V)\ e^-$$

where V means the valency state (oxidation state) of the fissile element (e. g. uranium) in the fuel and $\overline{V}$ the average valency state of the fission product mixture represented by the chemistry symbol FP. $\overline{V}$ can be calculated according to

$$\overline{V} = 0.5 \cdot \Sigma\, y_z \cdot V_z$$

where y_z stands for the fission yield and V_z for the valency state of the chemical atom with the proton number z. It has to be pointed out that the definition of the valency state does not necessarily mean the presence of a particular kind or structure of a chemical species. In other words, the symbol Zr(IV) only means that zirconium is present in a tetravalent state in the relevant medium, not necessarily as a zirconium dioxide compound.

The general validity of the electro-neutrality condition requires that in a closed system no net generation or net consumption of free electrons will take place. In the presence of ionizing radiation, free electrons are produced whose concentration is compensated for by unusual atomic valency states; with respect to equilibrium considerations, therefore, this effect can be ignored. As long as the FP in the above formula stands for the most easily oxidizable or reducible species in the system, the equation $(2\,\overline{V} - V) = 0$ is valid. A single crystallite of the UO_2 material can

Table 3.10. Most probable valency states of fission products in irradiated UO_2 fuel (Robinson, 1958; Copyright 1958 by the American Nuclear Society, La Grange Park, Illinois)

Valency state	Elements
−2	(Se), (Te)
−1	(Br), (I)
0	Kr, Xe
+1	Rb, Cs, (Ag)
+2	Sr, Ba, (Cd), (Pd)
+3	Y, Rare earths, (Rh), (As), (Sb), (In)
+4	Zr, (Mo), (Nb), (Te), (Ru), (Ge), (Sn)

be understood as a closed system in the sense of the above-mentioned electro-neutrality requirement. Since the recoil length of the fission fragments is on the same order as the dimensions of the fuel grains (about 10 μm), it can be assumed that a considerable fraction of them will leave the original crystallite. But because of the isotropic distribution of the movement of the fragments in the fuel, an equivalent amount of fission fragments generated in adjacent crystallites can be assumed to enter the given crystallite; therefore, this recoil effect is not expected to change the distribution of the fission product elements in a single crystallite located in the volume of the pellet to an extent that would violate the electro-neutrality condition.

Using simple electrochemical series, the most probable valency states of fission products in UO_2 fuel presented in Table 3.10. can be defined; the setting of an element in brackets means that it is able to exist in different valency states. With increasing burnup, the electrochemical situation in the fuel is assumed to change due to changing concentration ratios of the fission products. These variations are compensated for by changes in the valency states of different fission products (e. g. iodine, ruthenium, molybdenum); thus, redox reactions at the U(IV) matrix atoms are not to be expected.

These electrochemical considerations indicate that the prevailing redox potential of the fuel is of high significance for the chemical state of the fission products. Since determination of this property is an important prerequisite, a short survey of the methods for its determination shall be given. In non-irradiated uranium and mixed-oxide fuels, the redox potential is clearly controlled by the oxygen-to-metal ratio of the material and can be determined either by direct measurement of the metallic constituent, by determination of the non-stoichiometric fraction, or by determination of the redox property by equilibration with $CO-CO_2$ or H_2O-H_2 gas mixtures. In irradiated fuels, the possibilities of determination are more limited, not only because of the high radioactivity of the material, but mainly because of the complex multi-component chemical system of the fuel. Since no definite oxygen-to-metal ratio can be defined, the oxygen potential of the material as the most essential property must be directly measured. This can be done by measuring the electromotoric force of a solid-state galvanic cell, consisting of an yttria-doped thoria crucible which contains the fuel specimen to be measured; in most cases, Fe/FeO

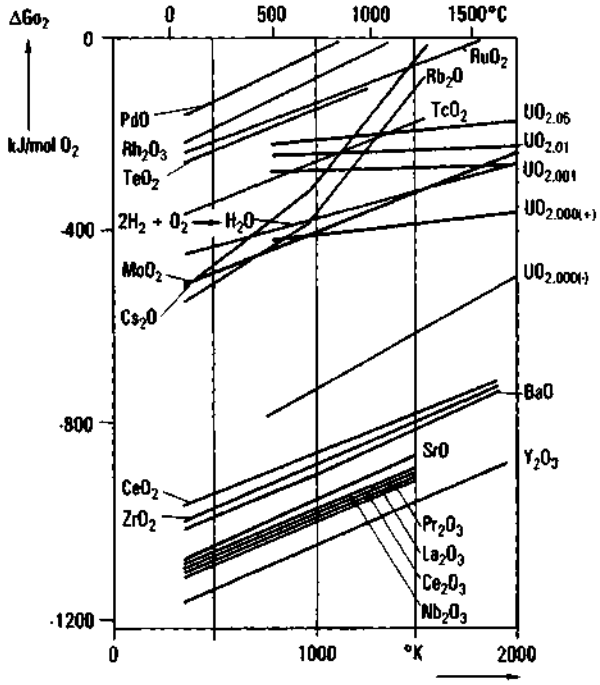

Figure 3.14. Relative partial molar Gibbs free energy of oxygen of the fission product oxides and of UO_2
(according to Assmann and Stehle, 1982)

is used as a reference system. This technique, which has to be carried out at an elevated temperature (about 1000 K) has been employed by various investigators; a miniature cell for the determination of radial oxygen profiles of irradiated fast-breeder oxide fuel has been described by Matzke et al. (1988). Another possible method for determining the stoichiometry of irradiated fuel is measurement of the lattice parameters of the material by X-ray diffractometry. However, in doing so it has to be taken into account that the lattice parameters of the fuel oxides are not only influenced by the stoichiometry of the fuel but, simultaneously, by its fission product content. For this reason, analysis is usually performed in several steps, namely lattice parameter measurement of the fuel sample after irradiation, then equilibration treatment in a $CO-CO_2$ atmosphere to reach a $\Delta G(O_2)$ level corresponding to the stoichiometric composition, and finally a second lattice parameter measurement of the equilibrated specimen. The difference between the two measurements is directly proportional to the change in oxide composition. Finally, the oxygen potential of the irradiated fuel can be derived from the Mo/MoO_2 distribution in metallic or oxide precipitations which can be measured, e. g., by electron microprobe analysis.

A first impression of the chemical state of the fission products in the matrix UO_2 can be obtained by thermodynamic considerations, despite the limitations discussed below. In Fig. 3.14. a simplified presentation of the partial free enthalpies

of formation of fission product oxides and of UO_2 is shown as a function of temperature. Since the oxygen partial pressures of the most stable oxides of Ba, Ce, Zr, Sr, Pr, La, Nb and Y are significantly lower than that of stoichiometric UO_2, it can be assumed that in the fuel the valency states Ba(II), Ce(IV) or Ce(III), Zr(IV), Sr(II), Pr(III), La(III), Nb(III) and Y(III) are stable, which is in general agreement with the data given in Table 3.10. In other words, this means that these elements are present as thermally stable double oxides in the fuel. According to these thermodynamic calculations, the platinum metals Ru, Rh and Pd in contact with stoichiometric UO_2 are stable in the valency state zero, i. e. in the metallic state. At the operating temperature of the fuel, the same applies for the elements Mo, Tc, Cs, Rb, and Te. However, in these cases the distances of their stability ranges from that of $UO_{2.01}$ are small, which means that slightly enhanced oxygen partial pressures, i. e. a slightly hyperstoichiometric composition of the UO_2 matrix, can lead to the presence of these fission products in the valency states +4 (Mo, Tc, Te) or +1 (Cs, Rb).

The thermodynamic calculations using oxygen partial pressures do not give direct evidence of the chemical states of anionic fission products such as iodine, which is of particular interest because of the comparatively high radiotoxicity of its isotope ^{131}I. In general it is assumed that CsI is the most stable iodine compound under these circumstances; this topic will be treated in more detail in Section 3.2.3.3.

A special problem in applying thermodynamic calculations to such systems as irradiated fuel shall be discussed very shortly here; this involves the question of whether conventional thermodynamic laws can be applied to mixed-phases systems showing very different concentration ranges of the individual constituents. Usually, in such calculations it is assumed that both the initial and the final states of a chemical reaction are well-defined compounds about which the relevant data of the basic Gibbs–Helmholtz equation

$$\Delta H = \Delta G - T \cdot \Delta S$$

are exactly known; this usually is the case when pure chemical compounds are under investigation. In multi-component systems with extreme differences in the concentration ranges of the individual constituents and with the possibility of formation of mixed crystals, one has to bear in mind that the partial free enthalpy of formation ΔG itself is a complex value:

$$\Delta G = \Delta G_A + \Delta G_R + \Delta G_B$$

Two of the three constituents on the right side of the equation depend on the initial and the final state of the system, while the free energy of the chemical reaction itself, ΔG_R, can be assumed to be influenced only little by the conditions prevailing in the relevant system. The energy required to make available the reaction partners ΔG_A (e. g. to break down the original crystal lattice by evaporation) and the energy turnover in the formation of the final state ΔG_B (e. g. condensation of the reaction products to a solid compound) depend strongly on the nature of the system. For example, the vaporization energy of a given element from the pure metal or oxide compound usually is quite different from that from the UO_2 mixed crystal. Because

of these uncertainties, which will exist as long as the thermodynamics of multicomponent systems with large differences in the concentrations of the individual constituents are not well-established, one is only able to postulate that the errors introduced by the calculations are not large enough to affect fundamentally the calculated chemical state of fission products having ΔGO_2 values more negative than about 500 kJ/mol (alkaline earths, lanthanides etc); for the other fission products, such as molybdenum, cesium and technetium, the calculated values may be supposed not to have a high degree of reliability.

In an exactly stoichiometric UO_2, the average valency $\overline{V}$ of the fisson products must be 2.000. In reality, the stoichiometry of the fuel material may show a certain range due, e. g., to fabrication processes, in particular in the direction of a slightly hyperstoichiometric composition. The reason for this effect is the capability of the UO_2 lattice to incorporate oxygen atoms very easily into the lattice vacancies. Likewise, in an operationally failed fuel rod UO_2 will be superficially oxidized more or less easily by H_2O. This nominal change in the valency state of uranium atoms from U(IV) in the direction of U(VI) will have consequences for the average valency state of the fission products, leading to a change in the valency states of the most easily oxidizable elements. This effect is well known and has been observed in many experiments, although details of the responsible mechanism are still unknown.

In stoichiometric UO_2 the valency band and the conductivity band show a gap of about 2.3 eV; this material is, therefore, at the boundary between semiconductor and insulator. Normally, the conductivity band of this compound is only weakly occupied, even at the temperatures prevailing in the fuel during reactor operation. The presence of foreign atoms in the lattice may lead to changes in the concentrations of electrons in the valency band and in the conductivity band. An excess of oxygen atoms in hyperstoichiometric UO_2 will result in the formation of holes in the valency band, which means that hyperstoichiometry is equivalent to a p-doping; certain fission product atoms will act in a similar manner. It can be assumed that a local deviation from the nominal value of the concentration of the charge carriers will be spread to the whole crystallite via the conductivity band. The decrease in the electron concentration and the formation of electron holes due to hyperstoichimetric composition can thus lead to the oxidation of an I(-1) fission product atom into its I(0) state, with the responsible mechanism being the release of an electron from its valency band to the conductivity band in order to compensate for the depletion which occurred here. Such an explanation on the basis of atom physics has only been applied in individual cases, e. g. by Catlow (1979) in the treatment of the redox behavior of doped UO_2. A consistent application of these ideas to the system "irradiated UO_2 containing fission products" should be very helpful in explaining the phenomena of the chemical bond of the fission products.

The redox potential of the irradiated fuel material is influenced by the buildup of the fission products. In their review paper, which is strongly influenced by thermodynamic considerations, Assmann and Stehle (1984) stated that the average valency state of the generated fission products is slightly less than the valency state of uranium or plutonium, as a consequence of which the oxygen partial pressure in

the system increases during fuel operation. This applies, in particular, to plutonium fission, which gains more importance with increasing burnup, since the products of plutonium fission show a higher fraction of "noble" elements. According to their calculations, about $5 \cdot 10^{20}$ atoms/cm^3 of excess oxygen atoms are produced by this effect in a standard LWR uranium fuel at a burnup 50 MWd/kg U. However, for two reasons, this production of excess oxygen does not lead to a hyperstoichiometric O : M ratio of the fuel. The first one is the buffering action of molybdenum in the fuel, which is produced with a high fission yield and, consequently, reaches high concentrations. It is partly oxidized from the metallic state to MoO_2 or, from an atomistic point of view, from the valency state Mo(0) to Mo(IV). The second reason is that the Zircaloy cladding acts as an oxygen sink, trapping oxygen irreversibly above 400 °C under oxide formation. As a result, the O : M ratio in high-burnup fuels is stabilized at values between 2.000 and 1.995. However, Kleykamp (1990 a) detected by microprobe analysis of a PWR fuel rod irradiated to 55.9 MWd/kg U, that the oxygen content of the Zircaloy inner surface was increased only in the outermost region from about 0.1 to 0.2%, corresponding to a decrease in the O : M ratio of the fuel of about 10^{-4}; a higher oxygen uptake of the cladding was only observed at linear heat ratings significantly higher than 200 W/cm. This observation leads to the conclusion that oxygen excess in the fuel, even in the presence of Zircaloy cladding, is preferentially consumed by oxidation of the fission product molybdenum. Measurements (Matzke, 1994) of the oxygen potential of a very high-burnup UO_2 fuel (75 MWd/kg U averaged over the cross section of the pellet) using a miniaturized galvanic cell yielded values which were almost identical to that of unirradiated UO_2 fuel or to that of slightly substoichiometric UO_2 containing rare earth fission products. This also applies to the rim zone of the pellet showing local burnup values on the order of 200 MWd/kg U, although the overwhelming fraction of the burnup here is due to plutonium fissions, which usually are assumed to result in an increase in the oxygen potential of the fuel. These results indicate that the fission products (in particular the fission product molybdenum) are the most easily oxidizable species in the fuel.

Most of the thermodynamic data mentioned above are based on investigations carried out with materials of low or medium radioactivity; the question can, therefore, be raised whether the very intense radiation field inside the fuel during reactor operation affects the chemistry conditions. As was mentioned earlier, the highly ionized state of the fission product atom in its fragment phase is of very short duration, due to the rapid re-arrangment of the electron shell. The same applies to the unusual oxidation states of the daughter products of β^- disintegrations. On the other hand, fission fragments, fast neutrons, recoil atoms and α particles cause ionization in their spurs by electron stripping, leading to a higher oxidation state of the relevant atom. Nonetheless, only small areas in the fuel are affected by each of these events and rapid re-arrangement of the electron shells can be assumed. Thus, it seems justified to assume that radiation effects would not require significant changes in the principles of conventional solid-state chemistry which can, therefore, be applied to the system "irradiated fuel" as well. Finally, the high-energy fission fragments may collide with lattice atoms, knocking them from their regular sites in an avalanche-like effect and creating lattice defects that are only

incompletely annealed at the operating temperature of the fuel. No detailed knowledge exists on the potential impact of such a lattice disorder on the chemical state of the fission products and, in particular, on their release kinetics from an overheated fuel matrix. However, the major part of the lattice defects is conserved in the discharged fuel. In this respect the fuel samples investigated in the laboratory are largely identical with the fuel present in the operating reactor core, so that the results of these investigations can be applied to actual operating conditions.

In the discussion of irradiated fuel chemistry, the single crystallite has to be considered as the primary reference system and, here, it has to be taken into account that only at low burnup and at low linear heat ratings can a homogeneous distribution of the fission products be expected; this means that only under such conditions are the integral fission product concentrations calculated using the existing computer codes (e. g. KORIGEN) representative of the single crystallite as well. Deviations from this homogeneous distribution may be caused mainly by the following effects:

- Fission fragments generated in the outermost rim zone of the fuel pellet are transported to the pellet – cladding gap or even implanted into the cladding metal by the action of the recoil energy obtained by the fission process. This depletion in fission product concentration in the fuel is limited to a very thin region only (5–10 μm) and can, therefore, be ignored in bulk fuel chemistry considerations. It is, however, of importance as concerns the chemistry within the gap and will be treated in more detail in Section 3.2.3. In mixed-oxide fuels, the recoil effect results in a fission product depletion in the plutonium-rich master-mix grains and a fission product enrichment in the surrounding UO_2 grains.
- Some fission products migrate in the thermal gradient from the hot central region of the pellet to the cooler rim zone. This effect is of particular interest in fuels exposed to higher linear heat ratings and at higher fuel burnup and mainly involves the fission product noble gases as well as iodine and cesium. The depletion in iodine and cesium concentrations in the central region and their enrichment in the outer zones can lead to a change in the chemical environment and may have implications on the valency states of other fission products.
- At higher fuel burnup, more and more fission product precipitations appear in the fuel matrix, i.e metallic and ceramic inclusions within the fuel grains and fission product compounds at the grain boundaries. These fission products are lacking in the lattice of the fuel grains.

These three effects lead to deviations from the originally homogeneous fission product distribution in the fuel pellet. If one considers the single crystallite as the reference volume in fuel internal chemistry, then these differences have to be taken into account. However, until now this "fuel microchemistry" has not yet been treated in detail.

The second important atomistic feature in the chemistry of irradiated nuclear fuel is the size of the fission product atom, i. e. the question whether or not a given atom is compatible with the dimensions of the UO_2 lattice. Crystal lattices are able to tolerate foreign atoms of deviating size, in particular at trace concentrations;

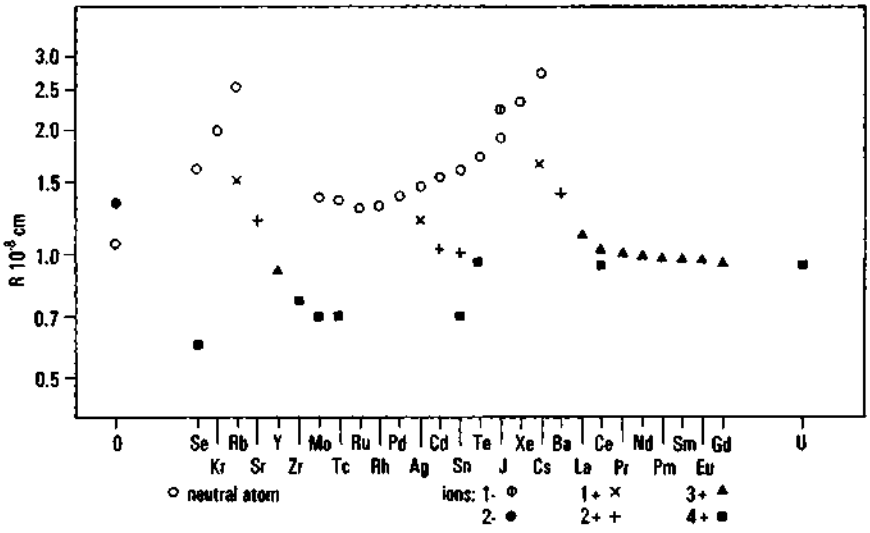

Figure 3.15. Apparent atomic and ionic radii of fission product atoms

according to a general rule, an isomorphic incorporation is possible when the radii of the foreign atoms or ions do not differ from the normal matrix atoms by more than 15–20%. Larger deviations and higher concentrations of such atoms, however, will cause lattice deformation resulting in an energetically unfavorable configuration. UO_2 lattice positions that become available for the uptake of fission products are those of the uranium (and plutonium) atoms consumed by fission, as well as the lattice vacancy positions. From Fig. 3.12. it can be seen that the spaces available at the uranium positions and at the vacancy positions are virtually identical, being in both cases the volume-centering position of an oxygen cube. The radius of such a position has been estimated to be about $1 \cdot 10^{-8}$ cm, but because of the electrostatic attraction between U(+IV) and O(-II) it can be assumed that the space at this position is somewhat larger than the calculated value. For the sake of comparison, Fig. 3.15. shows the atomic and ionic radii of essential fission products (values according to Goldschmidt or Pauling, originally calculated for coordination numbers 12 or 6; the coordination number 8 valid for the relevant positions in the UO_2 lattice requires in principle a correction which, however, can be ignored for the current purpose).

As can be concluded from this figure, the apparent ionic radii of La^{3+}, the tervalent lanthanides and Ce^{4+} are almost identical to that of U^{4+}. The radii of most of the other ions and also of the atoms of the platinum metals are within a range of about ±30% around the calculated value of the lattice vacancy position; thus, one can expect that their incorporation into the lattice will be possible without major difficulties. The same applies for both the neutral atoms and the tetravalent ions of molybdenum and technetium, which means that the question of lattice compatibility will give no preference to one of the two valency states. On the other hand, the atomic radii of the fission product noble gases krypton and xenon are

significantly larger than the available positions; hence, their incorporation into the UO_2 lattice seems quite unfavorable from an energetic point of view. As concerns the alkali elements rubidium and cesium, the radii of their monovalent ions are distinctly smaller than that of the neutral atoms. This would mean that the incorporation of neutral atoms into the lattice is less stable than that of the ions; expressed macrochemically, both elements are assumed to appear as oxides in the fuel and not in an elemental form. Finally, the radii of I° and of I^{-} both are considerably larger than the optimum value, but the difference between the two valency states seems not large enough to be of significance when compared to the other influencing factors, e. g. the redox potential in the fuel.

Fission products having radii significantly different from the optimum value, in particular radii that are too large, can only be incorporated into the lattice when they are present at low concentrations; at higher concentrations, i. e. higher fuel burnup levels, they will be forced at least in part to leave the lattice. At first they will be precipitated on the grain boundaries, where other chemical conditions exist than in the grain itself, although these conditions are incompletely known at this time. From the grain boundaries they can then migrate in the thermal gradient leading to the concentration inhomogenities mentioned above.

These qualitative assumptions are not contradictory to the results of solid-state solubility and phase diagram studies. According to these findings, the rare earth oxides are completely or largely miscible with UO_2, whereas the alkaline earth oxides and zirconium oxide show a limited solubility and MoO_2 is only soluble to a neglibly small extent (Kleykamp, 1985). However, results from studies performed on binary systems are not directly applicable to multi-component fuel – fission product oxide systems. In general, the maximum solubility of the individual fission product species in the fuel matrix will be reduced in the presence of additional constituents.

According to their behavior in annealing experiments which were performed at temperatures between 1450 and 1825 °C using trace-irradiated UO_2 fuel material (in order to prevent formation of compounds between fission products during the tests), Prussin et al. (1988) have grouped the fission products into four categories: Elements with the highest electronegativities, such as tellurium and iodine, exhibited the the highest mobilities in the fuel. A second category consisted of cations with low valency states and low solubility in the fuel (cesium and barium). A third category, which consisted of neutral species with low solubility (xenon, ruthenium, technetium), showed a release behavior quite similar to the second category; apparently, the quite different vapor pressures of these elements did not significantly influence their release characteristics from the UO_2 matrix. Finally, polyvalent elements (neodymium, lanthanum, zirconium, neptunium) were not released at all from the fuel specimens, due to the low mobility of these cations in the fuel and to low thermodynamic activity at the surface.

Summarizing these crystal chemistry considerations one can conclude that the fission products firmly fixed in the fuel are those with higher atomic charges and of dimensions compatible to those of the matrix lattice. Neutral atoms or monovalent fission products, both of which having larger dimensions (e. g. fission product noble gases as well as iodine), are more mobile in the fuel, in particular when they

are present in higher concentrations. This mobility is particularly pronounced at higher temperatures, such as at higher fuel rod heat ratings or, even more extreme, in overheated fuel under accident conditions.

3.2.3.2 Fission product noble gases

The fission product noble gases krypton and xenon are present in the irradiated fuel as neutral atoms and do not undergo any chemical reaction, either with the UO_2 matrix or with other fission products. For this reason, their behavior can be described by means of purely physical principles such as diffusion or migration. The comparatively large amounts of fission gases produced in uranium and plutonium fission (about 15% of the total amount of the fission products) and their mobility in the fuel matrix render, in principle, possible that, as a result of a higher degree of release from the fuel, the internal pressure in the rod would increase markedly. As an example, in a fuel rod containing 1.5 kg UO_2 and showing a burnup of 26 MWd/kg HM, about 6.5 g of noble gases have been produced by nuclear fission, corresponding to a total fission gas volume of about 1100 ml (STP), 90% of which are stable xenon isotopes, with the remainder being stable krypton isotopes and long-lived ^{85}Kr.

Because of the significance of the fission product noble gases for the design of the fuel rods, numerous investigations have been devoted to their behavior in the fuel, resulting in fission gas behavior models which describe reliably the processes occurring under LWR operating conditions. In particular, noble gas diffusion in UO_2 was extensively studied already in the early years of nuclear reactor operation. As can be seen from the review paper of Lawrence (1978), the experimental results of different authors (which were obtained partly by post-irradiation annealing experiments and partly by in-pile experiments) show a broad scatter, indicating that the specific properties of the UO_2 material investigated influence the value of the diffusion coefficient. A basic difficulty in the description of fission gas behavior results from the polycrystalline nature of the UO_2 pellet. Fission gas atoms generated inside a fuel grain will diffuse to the grain boundaries, followed by the growth of channels leading to open surfaces. In order to describe this complex process a mathematical model was developed in which the sintered UO_2 material was treated as an assembly of spheres communicating with the surrounding atmosphere through channels of open porosity (Booth, 1957). This "equivalent sphere model" is the basis of all the fission gas transport models that have been developed since then. To describe the diffusion of fission product noble gases in irradiated UO_2 pellets as well as their release from the pellet during steady-state operation and transients, detailed mechanistic codes have been developed in recent years, such as the FUTURE code and the MITRA code, with the latter dealing with the diffusion and the release of short-lived nuclides. A short description of both codes has been given by Matzke et al. (1989).

A summary description of fission gas behavior under the conditions of light water reactor nuclear power plant operation was given in review papers by Ass-

mann and Stehle (1982; 1984). Because of the rather large atomic radii of krypton and xenon, their solubilities in the UO_2 lattice are comparatively low; this means that already at a low fuel burnup a fraction of these elements is precipitated in the form of gas bubbles inside the UO_2 crystallites as well as at the grain boundaries. The first step in the formation of a gas bubble inside the crystallite is nucleation, for which a heterogeneous mechanism is assumed by most investigators. According to this model, the nuclei develop spontaneously in the track of the fission fragments, with each nucleus containing about 4 fission gas atoms and each fission fragment creating about 5 bubble nuclei. The following bubble growth is a complex dynamic process which depends on a number of physical parameters. The fission gas atoms are distributed between the fuel matrix and the gas bubbles; a redissolution of bubbles due to the action of fission fragments is superimposed upon the mechanisms of nucleation and bubble growth. Small bubbles with a diameter of less than about 2.4 nm can be redissolved by the action of a single fission fragment; their average lifetime is on the order of only one hour; from larger bubbles, gas atoms can be knocked out by a fission fragment. As a consequence of these processes, the bubble population does not show a uniform size; moreover, the size distribution changes with time. During these processes, energetic non-equilibrium states between gas bubble and the surrounding fuel matrix are possible. At high fission rates and low fuel temperatures, a rather narrow bubble size distribution is obtained due to bubble growth and redissolution mechanisms.

The fission gas bubbles produced migrate in the fuel. One possible mechanism is a stochastic migration leading to a combination of bubbles; this mechanism is assumed to be important only at fuel temperatures beyond 1500 °C, which means it can be ignored in LWR fuels. A second mechanism, migration in the thermal gradient, is caused by the evaporation of matrix atoms at the hot rim of the bubble and their recondensation at the colder one, resulting in a movement of the bubble in the direction of higher temperature. This type of migration occurs in particular in the area of high fuel temperatures, i. e. in the central regions of the pellet; on their way the lenticular-shaped bubbles leave behind them columnar fuel grains formed by recrystallization.

Radial fission gas distribution in irradiated fuel pellets from power reactors as determined by X-ray microanalysis is shown in Fig. 3.16. (Kleykamp, 1985). In this diagram, the influence of the linear heat rating, i. e. the fuel temperature, can be clearly seen. While at typical LWR values on the order of 220 W/cm only a moderate migration from the pellet center to the outer regions is observed, higher heat ratings on the order of 430 W/cm result in a pronounced depletion of fission product noble gases in the central region of the pellet. Analyses of microsamples obtained by drilling (Manzel et al., 1984) showed that at fuel centerline temperatures below 1300 °C, fission gas release is confined to the central region of grain growth. At temperatures > 1500 °C, a high fission gas release is observed, starting at the onset of fission gas bubbles precipitated on grain boundaries and reaching fractional release values in the center of the pellet of up to 90%.

In annealing experiments of irradiated UO_2 fuel specimens, the release of fission gases shows a complex behavior, starting with a steep gradient (high release rate) and approaching an almost constant level with low release rates. When the temper-

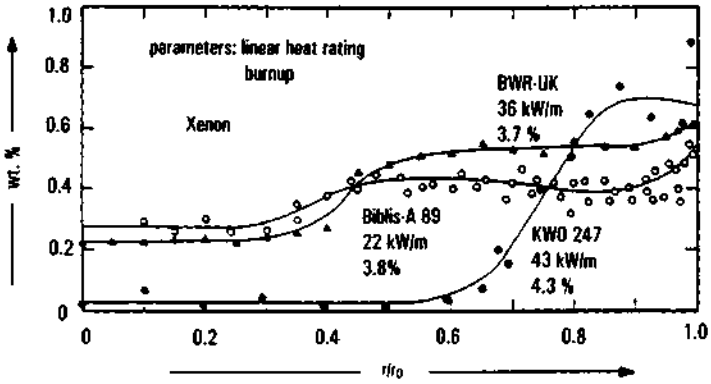

Figure 3.16. Xenon concentration as a function of the relative pellet radius in LWR uranium oxides with a 95% theor. pellet density and different linear heat ratings
(Kleykamp, 1985; with kind permission of Elsevier Science – NL, Sara Burgerhartstraat 25, 1055 KV Amsterdam, The Netherlands)

ature is raised (e. g. from 1400 to 1800 °C), a new steep increase starts leading to a new, higher level which then also remains almost constant. This complex release behavior can be explained by a three-stage mechanism (Matzke et al., 1989): In the first stage, gas already present at grain boundaries is released, escaping through already available tunnels. Subsequently, a rapid restructuring of the grain-face bubbles increases the open porosity and the gas flux from the grains augments the release by raising the pressure in the bubbles and accelerating their interlinkage. Finally, in the third stage, intragranular precipitation becomes predominant and the release rate drops to low values.

The fission gas bubbles present at the grain boundaries can be liberated by mechanical impact. Ruhmann et al. (1987) reported that by impact testing of typical LWR fuel pellets (irradiated to a burnup of 33 MWd/kg U) at ambient temperature with a specific load of about 1000 N·m/g, 6 to 7% of the total ^{85}Kr inventory of the pellet was released. Since these investigations were directed to the study of fission gas release from fuel caused by accidental mechanical impact, the analytical technique used did not aim at a quantitative liberation of the gases present at the grain boundaries. For this reason, the reported values are assumed to represent only a small fraction of the total grain boundary inventory.

In high-burnup fuels, the concentration of fission gases inside the grains decreases steadily from the outer regions of the pellet to the pellet center. Even in fuels with a relatively low central temperature, about 40% of the fission gases are released from the central fuel grains, a fraction of about 15% stays at the grain boundaries, and the remainder is released to the rod plenum. From the cooler outer pellet regions which represent the dominant mass fraction of the whole pellet, only little fission gas is released to the rod plenum, so that in total the fraction of fission gases released from LWR fuel amounts to only 1–2%. Most of this fission gas obviously originates from the center of the pellet according to the local temperature distribution; no significant release from the outer regions of the pellet is

required to explain the measured release data. Migration from the pellet center region to the rod free volume occurs via open grain boundaries and cracks in the outer pellet regions.

The most important parameter controlling fission gas release from the fuel is the linear heat rating of the fuel rod. For a given temperature, the relative noble gas release is favored by increasing burnup at constant fuel density, and by decreasing fuel density for a given burnup. In fuels operated at heat ratings below about 200 W/cm, the fission gas release amounts to less than 1% even at high burnup values. At heat ratings in the range of 200 to 250 W/cm, the extent of release from the pellets depends on the fuel burnup, reaching values of up to 4% at 35 MWd/kg U and of 6 to 10% at burnup values beyond 40 MWd/kg U. In typical LWR fuels with linear heat ratings on the order of 150 to 250 W/cm, the fuelling strategy is also of importance; fuel rods which experienced rather low heat ratings in their first fuel cycle show comparatively low fission gas release even at higher burnup values. In contrast, fuel rods with an initially high heat rating exhibit maximum fission gas release rates in their second cycle, with the release rates decreasing again in subsequent operation. The reason for this behavior is assumed to be a supersaturation of the fuel when the first cycle offers favorable conditions for this effect.

Due to the dependence of fission gas release on the fuel temperature, the advanced fuel assembly configurations (PWR 18 × 18, BWR 9 × 9 arrays) show only low fission gas release to the plenum when operated at correspondingly low heat ratings, as compared to the older 16 × 16 or 8 × 8 assembly configurations.

Experience with fuel rods operated to high burnup levels on the order of 48 to 58 MWd/kg U yielded low fission gas release into the rod free volume which, however, showed a tendency to increase at extended burnup, in spite of the steadily decreasing linear heat generation rate and, consequently, decreasing fuel temperature at high burnup (Manzel and Eberle, 1991). Apparently, the fission gases released stem from the pellet center region. The diameter of this region increases with increasing burnup. From the experimental data, an effective activation energy of diffusion of the noble gases of 50 to 80 kJ/mol was calculated for the temperature range 500 to 850 °C, i. e. lower by a factor of about 6 than that measured at lower-burnup fuels in the high-temperature range above 1000 °C. Furthermore, it was demonstrated that the threshold temperature for a 1% integral fission gas release as a function of the pellet centerline temperature decreases steadily with increasing burnup from about 1300 °C at 10 MWd/kg U to about 700 °C at 50 MWd/kg U.

High-burnup fuel pellets are also depleted in fission gases within the fuel grains at the pellet rim zone. From the investigations it was concluded that the missing fraction was accumulated in gas bubbles in the UO_2 matrix, but that no measurable release from these zones into the free volume of the fuel rod occurred even at high burnup levels.

At the same operating temperature and otherwise comparable conditions, mixed-oxide fuels rods show about the same fission gas release as UO_2 fuel. This can be clearly seen from Fig. 3.17., where fractional fission gas release from the fuel pellets to the rod free volume is shown. The data also demonstrate the effect of rod power in the current or in the preceding fuel cycle (Goll et al., 1993). To be

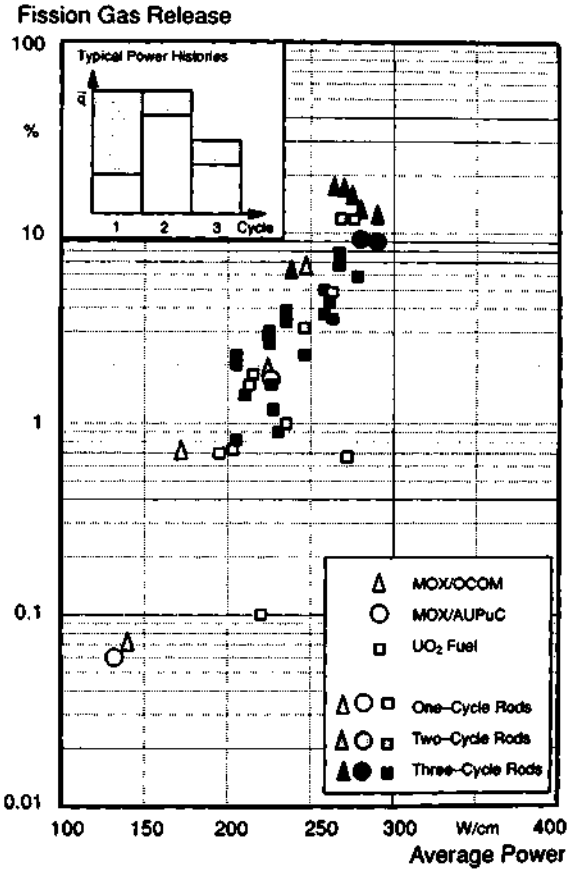

Figure 3.17. Fission gas release of UO_2 and mixed-oxide fuel rods as a function of the average rod power
(Goll et al., 1993; Copyright 1993 by the American Nuclear Society, La Grange Park, Illinois)

sure, the mixed-oxide agglomerates will loose a considerable fraction of the fission gases generated in these grains, partly by fission recoil (in particular from small agglomerate grain sizes), partly by uptake into the pores formed in the agglomerates. The release from the entire mixed-oxide pellet, however, is controlled by migration of the gases in the surrounding UO_2 matrix, which is the reason for the identical fission gas release behavior from both types of fuel pellets.

Transients leading to higher fuel temperatures will result in an enhanced release of fission gases from the pellet to the rod free volume. The degree of release depends on the rod terminal power and increases with higher fuel burnup; following a transient, higher-burnup fuel is largely depleted in fission gases in its central region while the outer regions of the pellet are virtually unaffected. There are no significant differences in transient fission gas release behavior between UO_2 fuels and mixed-oxide fuels (Goll et al., 1993).

The pathway of fission gases from the interior of the fuel pellet to the rod plenum leads through a network of cracks and tunnels which are formed in the course of fuel operation. The comparatively long time needed to cover this distance results in an extensive decay of the shorter-lived isotopes, which means that the gas mixture reaching the plenum is mainly composed of stable krypton and xenon isotopes, of ^{85}Kr and of a fraction of the initial amount of ^{133}Xe. Short-lived isotopes of the fission product noble gases which reach the pellet – cladding gap by fission-induced recoil are superimposed upon this mixture. This isotopic composition is of interest in the event of fuel rod failure when fission products are released from the fuel rod to the primary coolant, a topic that will be treated in more detail in Section 4.3.2.

Diffusion of fission gases in UO_2 is very sensitive to the stoichiometry of the material, increasing considerably even at a slight excess of oxygen. An increase of the diffusion coefficient by about 4 orders of magnitude was observed as the O : U ratio increased from 1.997 to 2.02 (see the review paper by Lawrence, 1978). This effect is of particular importance in operationally failed fuel rods when the UO_2 pellets are superficially oxidized by steam which has ingressed into the free volume of the rod (see Section 4.3.2.).

3.2.3.3 Halogens and alkali elements

From these two main groups of the Periodic System of Elements, only the elements bromine, iodine, rubidium and cesium are produced by nuclear fission to an extent worth mentioning. Iodine and cesium are of particular interest during plant normal operation as well as in accident situations, because of their comparatively high fission yields, their enhanced mobility in the fuel at higher temperatures and the radiotoxicity of some of their isotopes. Both elements are often summarized under the term volatile fission products; their similar properties justify their treatment in the same context, despite pronounced differences in their basic chemical behavior.

In the preceding sections it was pointed out that it is not possible to derive reliable conclusions as to the chemical nature of these two elements in the nuclear fuel exclusively on the basis of theoretical considerations. Specific experimental investigations are required, although care must be taken that the experimental technique chosen not lead to changes in the chemical state of the fission products during the performance of the experiment. This important requirement reduces considerably the number of procedures that are in principle applicable; in general, wet chemical methods are not appropriate because of the difficulties of dissolving UO_2 in non-oxidizing acids (e. g. sulphuric acid–phosphoric acid) which requires a comparatively long-term treatment of the compound at higher temperature, in the course of which a change in the valency state in particular of iodine cannot be ruled out. For this reason, thermochemical methods are widely applied for determining the chemical state of fission products in the fuel; the results of such investigations yield direct information on mobility and release behavior, but they also allow to draw conclusions on the original chemical state of the substances. Thermo-

chemical techniques are of particular interest in reactor safety research, where fission product volatility is the main analytical interest; therefore, this experimental technique will be treated in more detail in Chapters 6 and 7.

In order to obtain answers to the basic questions of thermodynamic stability of the different iodine oxidation states in contact with UO_2, it is adequate to mix very thoroughly the relevant iodine and cesium compounds with UO_2 of different stoichiometric composition and to subject these specimens to a heating process. In such experiments it is very useful to trace the added fission product simulants with radioactive isotopes, since by such a labelling determination of the element behavior can be performed very simply and with great sensitivity, e. g. by micro-γ-scanning of the specimen. The experiments reported by Peehs et al. (1973) and by Garzarolli et al. (1974), in which such mixtures of fission product simulants were heated inside a small capsule in a thermal gradient, showed that upon addition of CsI to stoichiometric UO_2 both elements after a short heating period develop a common concentration maximum in the temperature region of 1000 °C and that this position in the thermal gradient is only insignificantly changed by prolonged heating. Under such circumstances, both elements, which normally show quite different chemical properties, behave in a very similar manner. On the other hand, iodine and cesium exhibit strongly different behaviors in contact with hyperstoichiometric UO_{2+x}: while cesium forms a concentration maximum at about the same temperature as in the experiments with stoichiometric UO_2, iodine migrates very quickly in the thermal gradient and forms a deposition maximum in the region 100° to 200 °C. From these results it can be concluded that in contact with stoichiometric UO_2 iodide I^- is the stable chemical species (in this case as the compound CsI) and that beyond a slightly hyperstoichiometric composition, elemental iodine I° is formed; the exact value at which one iodine chemical state is converted into the other one is unknown, although it is assumed to be in the O : U range 2.01 to 2.02. In both cases cesium is stable in the valency state Cs^+, the reduction to Cs° only being possible in a substoichiometric uranium oxide, quite in agreement with the results of thermodynamic estimates.

Such investigations using fission product simulants in a mixture with fuel material can only yield information on the stability of specific chemical states of the fission product elements in contact with UO_2. They cannot give information on the chemical state and behavior of fission products in actual irradiated fuel, since they do not take into account the original positions of the fission products, their properties inside the fuel grains and their transport from the interior of the UO_2 crystallites to the surfaces. To investigate these questions, experiments were performed using small UO_2 rodlets which had been pre-irradiated in a research reactor for a comparatively short time at low temperature and in which the ^{131}I distribution before and after thermal treatment was analyzed by micro-γ-scanning. The results obtained here (Garzarolli et al., 1974) demonstrated that even at temperatures of about 2250 K at the hot end of the cylinders no iodine migration in the thermal gradient could be detected. This behavior obviously results from the fact that trace concentrations of the fission products are very firmly bound in the UO_2 lattice. Similar results were reported from heating experiments under a vacuum in a tungsten crucible with slightly substoichiometric (O : M 1.98) sol-gel fabricated UO_2

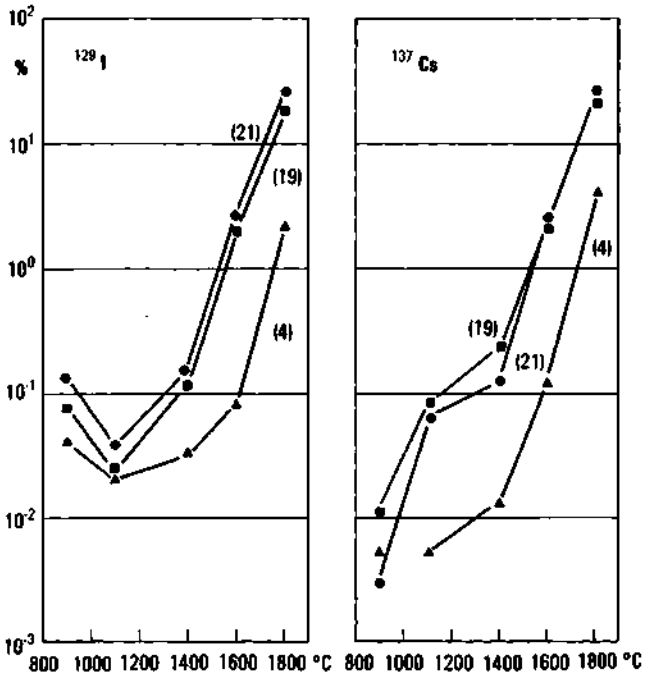

Figure 3.18. Iodine and cesium exhalation from irradiated UO_2 fuel (Sample 4: burnup 11 MWd/kg U; samples 19 and 21: 33 MWd/kg U)
(Peehs et al., 1983; with kind permission of Elsevier Science – NL, Sara Burgerhartstraat 25, 1055 KV Amsterdam, The Netherlands)

spheres of comparatively low burnup (about 10 MWd/kg U), which yielded considerable retention of fission product iodine and cesium even at temperatures as high as 2500 K (Tanke, 1992). Apparently, both the low iodine concentrations and the substoichiometric composition of the fuel matrix act in the same direction of high retention.

The above-mentioned assumption that, due to space problems, higher iodine concentrations cannot be incorporated into the lattice structure of the UO_2 crystallite was experimentally verified by heating small specimens of UO_2 fuel with different irradiation histories in a high-vacuum Knudsen cell (Peehs et al., 1983). In the experimental setup chosen, the dependence of release on temperature and heating time was determined by trapping the volatilized fission products on movable cooled catcher plates. As can be seen from Fig. 3.18., the release of both cesium and iodine from the fuel begins at temperatures of approximately 1100 to 1300 K and the release rates increase with increasing temperature in a logarithmic manner; at 2100 K the largest fraction of the specimen's inventory of both elements was released after a heating time of about 60 seconds. Both elements were released at a significantly faster rate from higher-burnup than from a lower-burnup fuel, indicating that at higher fission product concentrations in the fuel a second release

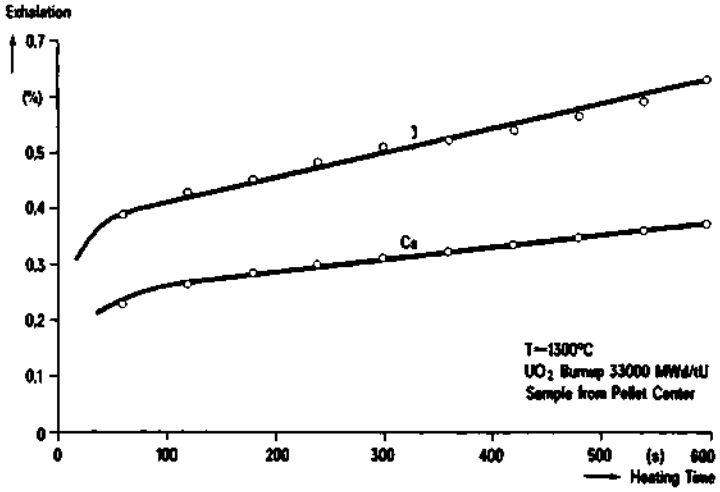

Figure 3.19. Iodine and cesium exhalation from irradiated UO_2 fuel as a function of heating time
(Peehs et al., 1983; with kind permission of Elsevier Science – NL, Sara Burgerhartstraat 25, 1055 KV Amsterdam, The Netherlands)

mechanism acquires more and more importance. The existence of two different release mechanisms can also be seen from the time dependence of release shown in Fig. 3.19., which was measured at a heating temperature of 1570 K. In the first 100 seconds of the heating period, the release shows a very steep gradient which can be attributed to fission product atoms which had already migrated during fuel reactor operation from their lattice positions to the grain boundaries. This hypothesis is supported by experiments in which samples were milled after being heated and then heated again for a second time. In this treatment a new initially steep branch was observed, the gradient of which apparently increased with increasing surface-to-volume ratio of the crushed samples. The deposition of a fraction of the total iodine and cesium inventory at the grain boundaries is quite similar to the formation of fission gas bubbles at these internal surfaces. This behavior confirms the above-mentioned assumption that the UO_2 lattice is capable of incorporating only a limited amount of fission products having atomic radii significantly larger than is compatible with the lattice parameters, with the excess being forced out to the grain boundaries. After about 100 seconds of heating time, the steep gradient is followed by a linear branch which is assumed to result from the release of atoms from the interior of the UO_2 grains. Using an Arrhenius' plot, the activation energy of release can be calculated from the slope of the curve, yielding values of about 330 kJ/mol for both elements. This value is very near to that of the activation energy of krypton and xenon diffusion in UO_2 which, in this temperature range, is reported to be in the range 345 to 375 kJ/mol. This similarity in behavior of elements with very different chemical properties indicates the migration of both iodine and cesium in the UO_2 lattice in the form of neutral atoms and demonstrates that chemical affinities only play at best an inferior role in this process.

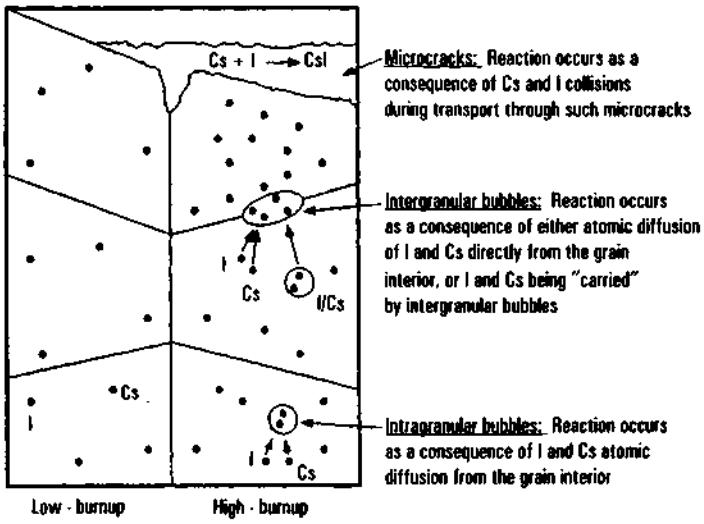

Figure 3.20. Potential reaction sites for Cs and I to form CsI (Cronenberg et al., 1986)

As yet, there is no unanimous opinion on the chemical state of fission product iodine (and cesium) in the irradiated fuel. According to Cronenberg et al. (1986), at low fuel burnup iodine and cesium are present in the fuel in an atomic-dispersed state. At higher burnup (i. e. higher concentrations of both elements) formation of the CsI compound can take place, with the most favorable sites being within the fission gas bubbles, at the bubble/UO_2 matrix interfaces and at grain boundaries or cracks. As is schematically indicated in Fig. 3.20., two basic criteria must be met if CsI formation in the fuel is to occur: (a) a sufficient concentration of reactants must exist at the interaction site; and (b) reaction kinetics must be rapid compared to diffusional release of iodine and cesium from the fuel. It is assumed that CsI formation starts when fission gas microbubbles are formed within the fuel, which usually begins at fuel burnup values of >5 MWd/kg U. Because of the exothermicity of the Cs − I reaction, it is very unlikely to be bimolecular. The formation of stable CsI therefore requires a third body to remove the energy of reaction; for the situation of Cs − I reaction within fission gas microbubbles and open pores, xenon is assumed to serve as the third body. Since the kinetics of CsI formation is very fast, it is predicted that it will occur if the concentration criterion mentioned above is satisfied. Bowsher (1987), however, concluded from the results of different investigators, that iodine is probably present within the fuel matrix predominantly as iodine atoms and molecular iodine with comparatively little formation of cesium iodide.

Theoretical studies performed by Grimes et al. (1992) on the basis of the solution energies of different species in the fuel yielded dependence of the chemical states of both iodine and cesium on the fuel stoichiometry. According to their results, in UO_{2-x} the fission products exist as CsI pairs trapped at neutral trivacan-

cies with iodine being in the -1 state. In stoichiometric UO_2, I_2 pairs are assumed to be more stable than CsI, while upon oxidation of the fuel to UO_{2+x}, formation of molecules becomes unfavorable and iodine atoms are trapped at uranium sites. In total, it is assumed that, despite the increase in stability that cesium and iodine can gain by clustering, CsI will be always insoluble in the fuel lattice.

Iodine volatilization from UO_2 fuel is particularly affected by the stoichiometry of the fuel, indicating a change in its chemical state. In hyperstoichiometric UO_{2+x} iodine mobility in a thermal gradient is strongly enhanced, probably due to the presence of I^o atoms in the fuel. On the other hand, in substoichiometric UO_2 iodine is retained even at high temperatures (Tanke, 1992); these results may also reflect the behavior of small iodine concentrations in low-burnup fuel. Concerning cesium behavior, different studies, including laboratory investigations as well as post-irradiation examinations of real irradiated fuels, indicated that the higher the O : M ratio in particular of mixed-oxide fuels, the higher the cesium fraction remaining on its original position in the fuel (Kleykamp, 1985). It was assumed that the formation of cesium uranates is responsible for this behavior; however, according to the atomistic point of view which was discussed earlier, formation of such specific fission product compounds in the fuel seems questionable. Observations made upon mixed-oxide fuels showed that cesium partial pressure increases with a decreasing O : M ratio, which results in an enhancement of the radial and axial cesium transport into the gap, quite in agreement with the assumption of increasing significance of the Cs^o state. According to Bowsher (1987), the chemical form of fission product cesium in the fuel at higher concentrations (besides that of atomic-dispersed cesium atoms or ions) is for the most part unknown. Out of the number of possible ternary compounds, cesium molybdate Cs_2MoO_4 is assumed to be the only one which could form in typically constituted fuel. Concerning Cs − Cs interactions in the fuel, Grimes et al. (1992) have concluded from theoretical calculations that clustering will occur in UO_{2-x} and UO_2 while in UO_{2+x} isolated cesium ions at uranium vacancies will dominate. Cs_2O is predicted to be insoluble in UO_{2-x} and UO_2, but to show a limited solubility in UO_{2+x}.

Certain conclusions on the chemical states of the fission products in the fuel can be drawn from the analyses of the oxidation states of the species which are released upon heating of the sample, provided that the experiments are performed in an inert atmosphere under strictly controlled conditions in order to preclude any changes of the valency state of the trace amounts; such an effect might be caused by the action of trace impurities present in the experimental system. In the early investigations reported by Castleman et al. (1968), in which low-irradiated uranium metal as well as UO_2 and U_3O_8 were heated in a steam atmosphere, the volatilized iodine species were condensed with the steam and then analytically separated by an extraction procedure. The results showed that the iodine fraction released from uranium metal consisted to an overwhelming degree of I^-, whereas from the oxides predominantly elemental I^o was vaporized, which upon addition of hydrogen to the atmosphere was reduced to I^-. The problem in the interpretation of such results lies in the question of the extent to which secondary reactions occurring during analysis are responsible for the formation of the chemical species detected. As an example of such effects the organoiodine fraction observed in these

experiments can be cited: it was distinctly higher when water distilled in the normal manner was used than with the use of water purified before by distillation over potassium permanganate. It is evident from these findings that very small concentrations of organic substances in the water and in the solutions used in the experiments are sufficient to change the chemical state of the trace amounts of iodine released from the fuel samples. As was pointed out by Eggleton and Atkins (1964), the degree of reagent purity which is required in order to preclude such secondary reactions with fission product iodine released from trace-irradiated uranium fuel amounts to 10^{-10} g/ml and less.

On some occasions the direct release of organoiodine compounds from irradiated nuclear fuel has been reported and from these observations the existence of such compounds in the fuel has been postulated. Taketana and Ikawa (1968) reported that during heating of low-irradiated UO_2 in an inert atmosphere at temperatures below 600 °C a fraction of the radioiodine was volatilized as CH_3I. Tachikawa et al. (1971) obtained after dissolution of low-irradiated uranium metal in concentrated nitric acid, 3 to 4% of the ^{131}I inventory as organoiodine compounds, mainly CH_3I but also small fractions of C_2H_5I. The formation of organoiodine compounds in such dissolution experiments was found to be reduced upon application of dilute nitric acid and addition of non-radioactive iodine carrier. Thus it was concluded that the organoiodine compounds were formed during dissolution of the sample by a reaction between intermediately existing iodine atoms and organic compounds activated by the concentrated nitric acid reagent.

The danger of misleading secondary reactions can be considerably reduced by the use of thermochemical identification reactions in which the volatilized substances are introduced into a thermal gradient tube; since this analytical setup is widely used in reactor safety investigations the technique will be described in more detail in Chapters 6 and 7. A thermal gradient tube has a well-defined temperature gradient along its axis; thus, initially gaseous substances will condense in different zones of the tube according to their vapor pressures. When the thermal gradient tube has been previously calibrated using well-known chemical compounds of the substances of interest, then the chemical nature of the substances introduced can be derived from the resulting activity distribution in the tube. The first experiments of this kind were reported by Castleman and Tang (1967) using irradiated uranium metal which was heated in purified helium to temperatures in the range from 1500 to 2800 K. Under such conditions, iodine volatilized from the sample condensed in the thermal gradient tube in the temperature range 550 K (280 °C), where it did not coincide with any other fission product; this species was interpreted by the authors to be a uranium–iodine compound, but they did not succeed in obtaining any more concrete information. In the presence of air, fission product iodine was deposited at temperatures of around 100 °C, which was explained as resulting from the formation of elemental iodine in a secondary reaction occurring inside the thermal gradient tube. Fission product cesium under both atmospheres condensed at 720 K (450 °C), i. e. far away from the iodine regions.

Such laboratory experiments as discussed above provide valuable information on the basic nature of the fission product radionuclides in the fuel, but they are not able to give direct information on their migration behavior during the long-

term exposure of the fuel in the reactor core. This information can only be obtained by analyses of spent fuel samples, in the course of which the distribution of the fission products in the fuel pellets is determined by isolating microsamples or, in the case of γ-emitting isotopes, by micro-γ-scanning of a pellet section. In fuel samples which have undergone an extended decay time, iodine behavior can only be determined by analyzing the long-lived ^{129}I (halflife $1.57 \cdot 10^7$ years), a radionuclide showing low specific activity and low energies of β^- and γ radiation of 20 and 30 keV, respectively. Because of these unfavorable radiation properties, a direct determination of the ^{129}I activity concentration in the mixture of radionuclides present in irradiated nuclear fuel is not possible. A radiochemical separation has to be employed; based on the volatility of elemental I_2, steam volatilization is an appropriate technique for obtaining an effective separation of ^{129}I from the bulk of the other radionuclides (e. g. Neeb et al., 1976). An additional purification of the iodine fraction can be carried out by liquid–liquid extraction and backextraction, which are well-known conventional analytical methods. In order to avoid or to correct for losses of ^{129}I traces during the volatilization and extraction procedures, known amounts of non-radioactive iodine are added as a carrier, so that the separation yield of the purified specimen can be easily determined.

In principle, this analytical procedure is quite simple to perform, with the initial operations being carried out remote-controlled inside a hot cell; however, in practice it is potentially complicated by an incomplete isotope exchange between the ^{129}I activity from the sample and the added iodine carrier, resulting in differences in the behavior of both species during the analytical operations. Fission product iodine present in the fuel may exchange rapidly with carrier iodide under the conditions of dissolution in hot nitric acid, but in the course of this step a partial oxidation to non-volatile and non-extractable iodic acid may occur, which may be different in extent for ^{129}I and for the carrier iodide added. This difficulty can be overcome by application of oxidation–reduction cycles, by which a complete isotope exchange is obtained. Another potential difficulty was reported by Boukis and Henrich (1991): In the course of development work in the field of nuclear fuel reprocessing they detected ^{129}I chemical species which did not participate in isotope exchange; likewise, they could not be backextracted by aqueous sulfite solution from the organic phase. A more detailed analysis showed that this unusual behavior was caused by the formation of ^{129}I organoiodine compounds during the dissolution step with organic trace impurities present even in high-purity nitric acid. These compounds can be decomposed by heating the sample solution to 105 °C for several hours in the presence of inorganic iodide carrier.

Basically, the ^{129}I content in the purified iodine fraction can be measured by different techniques. Due to the low specific activity of this long-lived radionuclide, direct β^-, γ and X-ray measurement techniques show only a moderate detection capability; better detection limits can be obtained by determination of the ^{129}I mass present in the sample. Here, laser-induced fluorescence spectrometry offers in principle favorable results; however, when this technique is applied, the difficulties associated with the preparation of the I_2 chemical species at very low iodine concentrations have to be taken into consideration. The most sensitive ^{129}I determination technique is neutron activation analysis, which leads to the formation of the

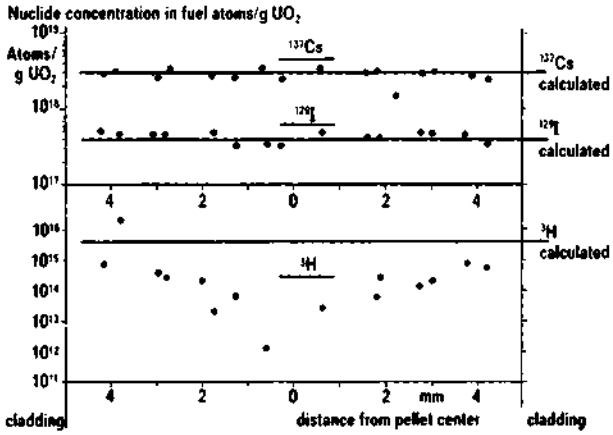

Figure 3.21. Distribution of fission product iodine, cesium and tritium in irradiated LWR fuel pellet
(Neeb et al., 1976; with kind permission from Elsevier Science S.A., P.O. Box 564, 1001 Lausanne, Switzerland)

rather short-lived ^{130}I, which has γ transitions that are easy to measure; by the application of the usual activation conditions in a research reactor, the ^{129}I detection limit is improved by a factor of about 10^5 as compared with direct γ-spectrometry measurement. In order to prepare samples which are suitable for neutron activation in a research reactor, Neeb et al. (1976) precipitated the iodine fraction after separation from the fuel sample as PdI_2; following neutron irradiation, this compound can be easily dissolved in NaOH solution for further purification, if necessary.

The results reported by Neeb et al. (1976) demonstrated that at typical LWR heat ratings in the region of 200 W/cm no migration of iodine and cesium in the thermal gradient of the pellet can be observed (see Fig. 3.21.), i. e. these fission products remain at the positions where they were generated. This behavior applies up to burnup values of at least 35 MWd/kg U. In contrast, tritium shows a very inhomogeneous distribution, caused by migration from the inner hot regions to the pellet rim zone; the behavior of this fission product will be treated in detail in Section 3.2.3.6.

The immobility of iodine and cesium in the fuel, however, only applies when the fuel rod linear heat rating does not exceed a certain threshold value; at higher values, which are distinctly beyond those occurring in LWR fuel during steady-state operation of the reactor, a redistribution of these elements can be observed. Significant transport of iodine and cesium from the pellet center to the rim was observed at heat ratings on the order of 350 to 400 W/cm and is strongly pronounced at 550 W/cm (Peehs et al., 1981), pointing towards the extensive redistribution of these fission products well known from fast breeder reactor fuels, which are usually operated at comparatively high heat ratings. As can be seen from

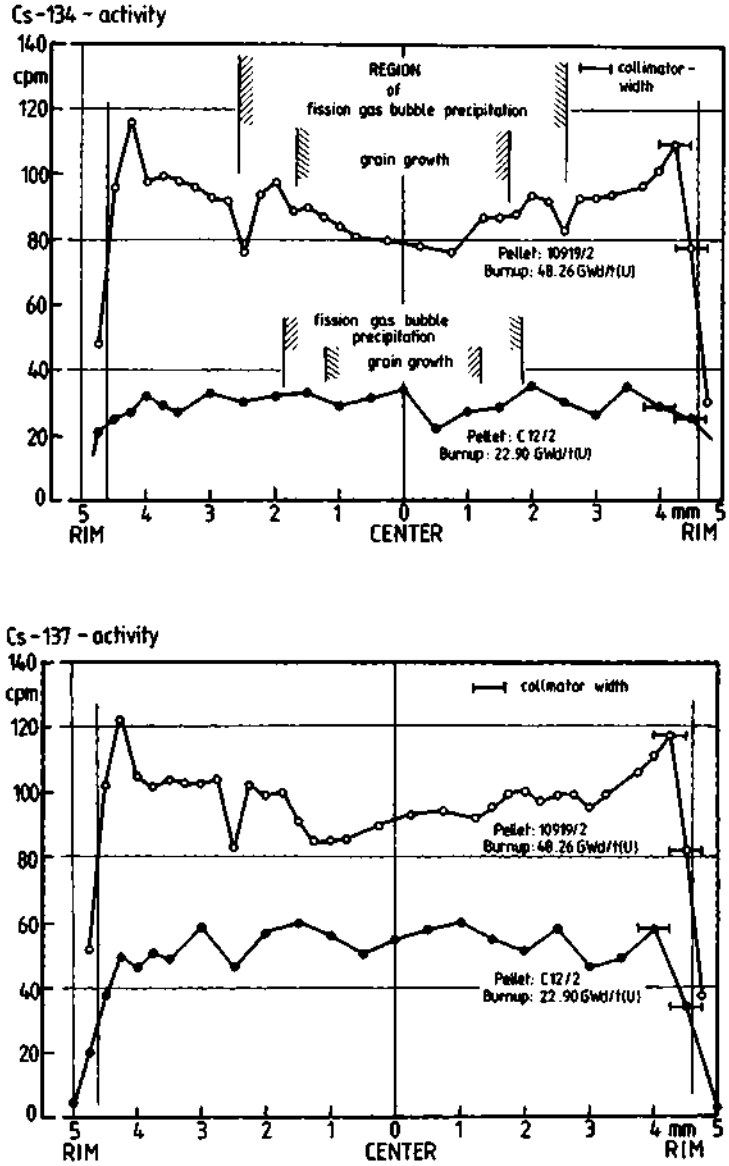

Figure 3.22. ^{134}Cs and ^{137}Cs profiles across fuel pellets after steady-state operation to burnup of 22.9 and 48.3 MWd/kg U
(Manzel et al., 1984; with kind permission of Elsevier Science – NL, Sara Burgerhartstraat 25, 1055 KV Amsterdam, The Netherlands)

Fig. 3.22. (Manzel et al., 1984), the results of micro-γ-scan measurements indicate virtually flat ^{134}Cs and ^{137}Cs distributions over the pellet cross section after a burnup of 23 MWd/kg U at typical LWR conditions (i. e. fuel centerline temper-

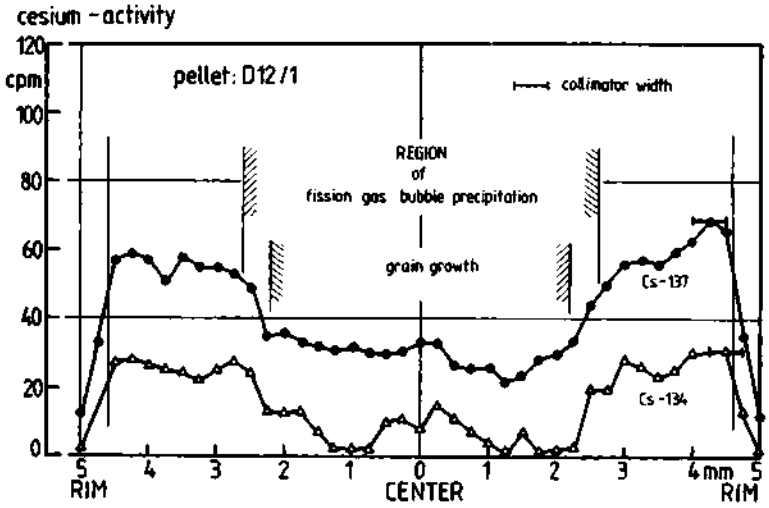

Figure 3.23. Cesium profiles across a fuel pellet after ramping to a terminal power of 404 W/cm
(Manzel et al., 1984; with kind permission of Elsevier Science – NL, Sara Burgerhartstraat 25, 1055 KV Amsterdam, The Netherlands)

atures between 1490 and 1520 K). At higher burnup levels, however, the ^{137}Cs distribution exhibits a clear concentration profile with maxima in the rim zone. These maxima are mainly caused by the enhanced plutonium fissioning in these zones; however, a certain contribution due to cesium migration in the thermal gradient under such conditions cannot be ruled out. ^{134}Cs distribution, on the contrary, shows minima at the outer border of the region of fission gas bubble precipitation; this behavior reflects the production mechanism of ^{134}Cs, which is not a direct fission product but is produced by neutron activation of ^{133}Cs, the decay product of ^{133}Xe. Thus, the ^{134}Cs distribution indicates to a certain degree the migration behavior of fission product xenon in the fuel pellet.

Higher fuel temperatures effect a pronounced transport of cesium from the pellet center to the outer regions. This can be seen from Fig. 3.23., representing measurements performed on a fuel pellet which, after a burnup of about 20 MWd/kg U, was subjected to a power ramp with a terminal power of 404 W/cm (corresponding to a fuel centerline temperature of about 1970 K) for about 48 hours; subsequently, irradiation was continued at the lower, normal power level to a final burnup of about 22 MWd/kg U. The depletion of radioactivity in the central region is particularly pronounced for ^{134}Cs, again reflecting the differences in the production mechanisms for both cesium isotopes.

Redistribution of volatile fission products at elevated fuel temperatures also occurs in the axial direction. As was shown by Sontheimer et al. (1980), this can be a rather fast process; thus, even after short-term power ramps exceeding values of about 400 W/cm, an enrichment of both iodine and cesium at the pellet interfaces can be measured by γ-scanning. Beyond this power level, redistribution is approximately proportional to the height of the ramp, amounting to about 1% of the pellet

inventory at 450 W/cm and to about 3% at 600 W/cm, with each of the ramps lasting for about 50 hours. The extent of redistribution also depends on the fuel density but below 20 MWd/kg U only little on the fuel burnup level. The polyvalent fission products forming stable oxides in the fuel (e. g. cerium, lanthanum) do not show a detectable redistribution in the fuel in the course of power ramps. However, axial movement of ^{137}Cs does not include a detectable transport to the gas plenum of the fuel rod. Only ^{134}Cs was measured here in small amounts, presumably generated by the decay of ^{133}Xe transported from the fuel to the plenum region followed by neutron activation of its decay product ^{133}Cs (Würtz, unpublished).

As was mentioned above, in high-burnup fuels the observed increase in cesium concentration in the outermost zones of the pellet is not predominantly caused by thermal migration, but is the consequence of the enhanced production of plutonium in these zones during fuel operation and the resulting increased fission rates. Mixed-oxide fuels with the plutonium-containing master-mix grains distributed in the UO_2 matrix generally show a similar behavior. From the small mixed-oxide agglomerates, a fraction of the cesium generated (and probably of the fission product iodine, too) is lost to the surrounding UO_2 matrix due to fission recoil. Cesium migration from the plutonium-containing master-mix agglomerates apparently does not play a significant role at normal LWR heat ratings and fuel temperatures (Goll et al., 1993). In general, the two different mechanisms leading to inhomogeneous distribution of volatile fission products, namely differences in fission rates, on the one hand, and migration in the thermal gradient on the other, can be distinguished by comparison of their distribution with that of a polyvalent fission product, e. g. ^{144}Ce, which at LWR typical fuel temperatures does not show any migration in the thermal gradient.

The redistribution of the volatile fission products in the fuel during reactor operation can be described qualitatively by a two-stage mechanism. The first stage is a rather slow and, therefore, rate-controlling matrix diffusion of the atoms in the grains to the grain boundaries, whereas the second step is a comparatively quick transport via the grain boundaries and structural cracks. In mixed-oxide fuel grains containing plutonium, the first stage is assumed to proceed at a higher velocity, with this being the reason for the accelerated redistribution as compared to UO_2 fuels.

The thermally induced redistribution of the tellurium and selenium isotopes shown under certain conditions might be due to the formation of cesium telluride and selenide; both compounds exhibit comparatively high vapor pressures (10^{-4} MPa at 1000 K, 0.1 MPa at 2000 K).

3.2.3.4 Polyvalent fission product elements

As can be seen from the Gibbs partial free energies of formation shown in Fig. 3.14., the alkaline earths, the earth metals and the rare earth elements in contact with UO_2 are stable as oxides. From these data it can be concluded that the fission product isotopes belonging to these elements are present in the fuel in their usual oxidation states or, in macrochemical expression, as double oxides with UO_2.

Usually, such double oxides are highly temperature-resistent and it can be expected that these fission products will show virtually no thermal-induced migration in the fuel matrix. This assumption has been confirmed by numerous measurements that show a distribution dependent on the burnup profile of the fuel. Most of the information in this area has been gained by examining fast breeder reactor fuels (Kleykamp, 1985), i. e. materials which had been irradiated at distinctly higher fuel temperatures than LWR fuels. For this reason, thermal-induced migration of the polyvalent fission products in LWR fuels, with their distinctly lower temperatures during reactor operation, can be ruled out.

For reasons of thermodynamic stability, the isotopes of the light platinum metals ruthenium, rhodium and palladium produced in nuclear fission are expected to be present in the fuel in the metallic state, showing no pronounced migration in the thermal gradient. However, in fuels of a higher burnup level they show a tendency to form metallic precipitates, as has been discussed above in Section 3.2.1. In different fuels the composition of these inclusions may vary considerably, depending on the initial O : M ratio of the fuel, the temperature gradient in the fuel rod and the burnup level. Since the oxygen potential of the Mo/MoO_2 equilibrium is similar to that of slightly substoichiometric mixed-oxide fuel, the molybdenum concentration in the metallic precipitates decreases continuously with increasing burnup because of oxidation of this element due to an increase in the oxygen potential of the fuel. As was discussed above, this increase is due to the fact that the oxygen which is liberated from the oxides of uranium and plutonium as a consequence of their fission cannot be completely consumed by the generated fission products. At low oxygen potentials and high molybdenum fractions the precipitates may become two-phased.

The chemical state of fission product tellurium in the fuel is assumed to be very complex, although the oxygen potential of the Te/TeO_2 equilibrium is markedly higher than that of the LWR oxides (see Fig. 3.14.). According to different observations, tellurium can form metallic phases (e. g. with uranium, palladium or tin, in particular in fast breeder reactor fuel at low oxygen potential), it can be a constituent of multi-component fuel – fission product oxides depending on the local oxygen potential, and it can be dissolved in atomic-dispersed form in the oxide fuel matrix (Kleykamp, 1985).

Although zirconium oxide shows only a limited solubility in the UO_2 matrix, fission product zirconium seems to be homogeneously distributed in the fuel, presumably due to an enhancement in ZrO_2 solubility in the presence of rare earth oxides. That means that, consistent with the results of thermodynamic calculations (see Fig. 3.14.), zirconium is present in the Zr(IV) state. Up to very high linear heat ratings, there is no noticeable zirconium redistribution in the temperature gradient.

Despite the limited solubility of BaO in UO_2 (quite in contrast to SrO, which is highly soluble), barium seems to be homogeneously distributed in the irradiated fuel matrix, presumably as Ba(II) in the UO_2 lattice. Barium can also be incorporated into the perovskite-type "grey phase" which was detected predominantly in high-burnup fast breeder reactor fuels; however, the significance of this phase in irradiated LWR fuels seems to be questionable. The chemical state of fission product barium in the oxide fuel apparently depends strongly on the stoichiometry of

the material. This was demonstrated in heating experiments of slightly substoichiometric UO_2 (O : M 1.98) which showed a higher volatility for barium than for iodine; in these experiments, however, xenon and the volatile fission products cesium and iodine exhibited an unexpectedly high retention (Tanke, 1992). Early heating experiments with irradiated metallic uranium in a helium atmosphere to 1200 °C (Castleman and Tang, 1967) showed almost quantitative barium, cerium and lanthanum vaporization, with their condensation occurring already in the temperature range 1370 to 1470 K. These fission products are probably volatilized from the metallic fuel in their elemental state and then they are quickly oxidized to the corresponding oxides by traces of oxygen present in the helium gas flow. Heating metallic uranium fuel in air results in a negligibly small volatilization of these fission products. On the other hand, fission product molybdenum does not show any volatility when the sample is heated in a helium atmosphere, but considerable vaporization when heated in air; apparently, MoO_3 is the volatile species.

Technetium shows a ΔGO_2 value which is very near that of UO_2; thus, it can be assumed that it is stable in metallic form in contact with stoichiometric UO_2 and as oxide in hyperstoichiometric UO_{2+x}. After dissolution of irradiated fuel in nitric acid, technetium is obtained as TcO_4^-, which in solution is quite stable against U^{4+}. With the exception of the incorporation into the precipitations mentioned above there is no observable redistribution of technetium in the fuel thermal gradient during LWR operation. At rather low fuel temperatures, ruthenium does not show any redistribution in the fuel, quite in agreement with its assumed metallic state. At fuel centerline temperatures above 1750 K, a certain migration of ^{106}Ru was detected (Manzel et al., 1984).

3.2.3.5 Uranium activation products

As was pointed out in Section 3.2.1., the plutonium content in UO_2 fuels increases steadily with increasing burnup in the first irradiation phases, then approaches an almost constant concentration level and decreases again at very high burnup values. The exact development of the plutonium concentrations depends on several parameters such as the neutron energy spectrum and the initial ^{235}U enrichment of the fuel, so that the data given in Tables 3.6. to 3.9. can only be taken as an example. The quasi-steady-state plutonium concentration over a longer period of operation is the result of plutonium buildup on the one hand and plutonium fission on the other. ^{239}Pu is predominantly produced by resonance absorption of epithermal neutrons in ^{238}U and subsequent two-fold β^- decay. Because of the high resonance integral of ^{238}U, the neutron capture preferentially takes place in a rather thin (about 0.3 mm) annular outer zone. As a consequence, the other transuranium isotopes produced from ^{239}Pu by neutron capture and β^- decay are also concentrated in this zone, as can be seen from the autoradiographic image shown in Fig. 3.7. Investigations reported by Kleykamp (1990 a) of a UO_2 fuel irradiated to a burnup of 55 MWd/kg U, using a shielded electron microprobe device, yielded plutonium concentrations in the outer pellet zone of about 3.8% compared to the pellet-averaged value of 1.4%.

The capture of an epithermal neutron by ^{238}U produces $^{239}U^*$ with an excitation energy of 4.806 MeV. The latter nucleus decays to the ground level by γ emission and internal conversion. The $^{238}U(n,\gamma)^{239}U$ reaction can induce rupture of the U−O bond since the recoil energy of the ^{239}U atom can reach 52 eV, while the U-O bond energy is only 7.9 eV (CRC, 1980). The internal conversion radiation, competing with the γ emission, does not influence the recoil of ^{239}U but can induce some local radiolysis, via Auger electrons and low-energy X-rays. On the other hand, the recoil energy of ^{239}Np after β^- decay of ^{239}U should not be sufficient to break the Np−O bond, as it is at most 6.6 eV as compared to the 7.5 eV of the Np−O bond energy. However, as in the case of the $^{238}U(n,\gamma)^{239}U$ reaction, internal conversion can promote local radiolytic processes. Take together, these nuclear effects are not assumed to cause a longer-lasting change in the UO_2 lattice; temporary effects will presumably be annealed after a short time at operating temperature. For this reason, the β^- decays are not expected to induce a displacement of the newly formed atoms nor a change in the chemical compound. The same is true for the effects of the associated γ emissions. Likewise, a significant release of actinide elements into the pellet − cladding gap as a consequence of recoil reactions is not to be expected.

In PWR fuel rods, the axial plutonium distribution is closely correlated to the local burnup, as can be derived from the γ scans of the fuel rods. By contrast, in BWR fuel rod operation the axial shift in the neutron energy spectrum, due to the decrease in moderator density in the upper region of the reactor core, results in axial transuranium element distributions which do not completely coincide with the axial burnup distribution. Besides these inhomogenieties of plutonium distribution in the fuel, which are caused by nuclear effects, a thermal migration of the transuranium elements in the fuel is not to be expected because of the relatively low temperatures prevailing in LWR fuel.

The quite similar chemical properties of uranium and the transuranium elements are the reason for their presence in the irradiated fuel as thermodynamically stable double oxides. According to the redox potential of the fuel matrix, it has to be assumed that neptunium and plutonium will appear in their most stable oxidation state +4. Due to their ionic radii, which are very similar to that of U(IV), both NpO_2 and PuO_2 will form mixed crystals with UO_2. The type and the properties of the crystal lattice remain essentially unchanged; only the dimensions of the elementary cell decrease from 0.5468 nm (5.468 Å) in pure UO_2 to 0.5466 nm (5.466 Å) at 1% plutonium content. This means that neptunium and plutonium will remain at the positions in the irradiated fuel where they were formed; the same behavior is to be expected for the higher transuranium elements as well.

3.2.3.6 Tritium

As was described in Section 3.2.1., tritium is produced in irradiated nuclear fuel as a product of the ternary fission of ^{235}U, ^{239}Pu and ^{241}Pu with the comparatively low fission yield of about 10^{-2}%. In principle, an additional production by neutron capture in light elements present as impurities in the fuel, the fill gas or the cladding

(e. g. boron, lithium, ^3He) may be assumed to occur; however, because of the very low concentrations of these elements, these possible sources are assumed to be insignificant. The low activity concentrations of tritium in the fuel, as well as its low nuclear physics and radiological significance, were probably the reason that only a few authors have looked closely at the behavior of ^3H in the fuel. The observation that a fraction of the ^3H produced in the fuel can be released to the coolant through penetration of intact fuel rod claddings led to more detailed research work concerning its behavior in the fuel during reactor operation. An additional requirement for reliable data on tritium production and behavior had its origin in the development of processes for spent fuel reprocessing and, in particular, in the question of what fraction of the total tritium will be introduced into the process solutions.

In addition, the experimental difficulties involved in the analytical determination of very low concentrations of a pure β^- emitter of low energy in the presence of a large excess of other β^-, γ–active radionuclides have to be mentioned. Since a direct radiation measurement of the ^3H activity in such a mixture is not possible, a sophisticated radiochemical separation has to be performed the details of which will be summarized below. The same problems arise in the determination of the ^{14}C content in irradiated nuclear fuel. On the other hand, both radionuclides show similar chemical and radiation properties so that their determination can be carried out using similar analytical procedures.

Both ^3H and ^{14}C are pure β^- emitters without associated γ transition, with their beta maximum energies amounting to 0.02 and 0.2 MeV, respectively. This means that their determination requires careful separation from virtually all other radionuclides prior to radiation measurement; taking into account that their activity concentrations in irradiated nuclear fuel are small compared to that of the other fission products, only expensive separation procedures will lead to reliable results. Often these procedures are further complicated by the requirement that different chemical forms of the radionuclides have to determined in parallel (e. g. HT–HTO, $^{14}CO_2$–^{14}CO–$^{14}CH_4$). In such cases one additionally has to take care that no change from one chemical state to another occurs during the analytical procedure.

After radiochemical separation, the following radiation measurement techniques can be applied:

- Gas counting of HT as well as of $^{14}CO_2$–^{14}CO–$^{14}CH_4$.
- Liquid scintillation counting of HTO and dissolved ^{14}C compounds.
- β^- counting of solid specimens such as $BaCO_3$ for ^{14}C determination.

Concerning selectivity and detection limits, these three techniques do not exhibit great differences. Therefore, the selection of the counting technique to be applied is usually dictated by pragmatic aspects such as optimum combination with the separation technique applied or the type of counting instrumentation available.

To obtain accurate and reliable results, sampling and radiochemical isolation of both radionuclides from the fuel samples taken at different locations of an irradiated fuel rod can be carried out by using the following procedures (Neeb et al., 1980):

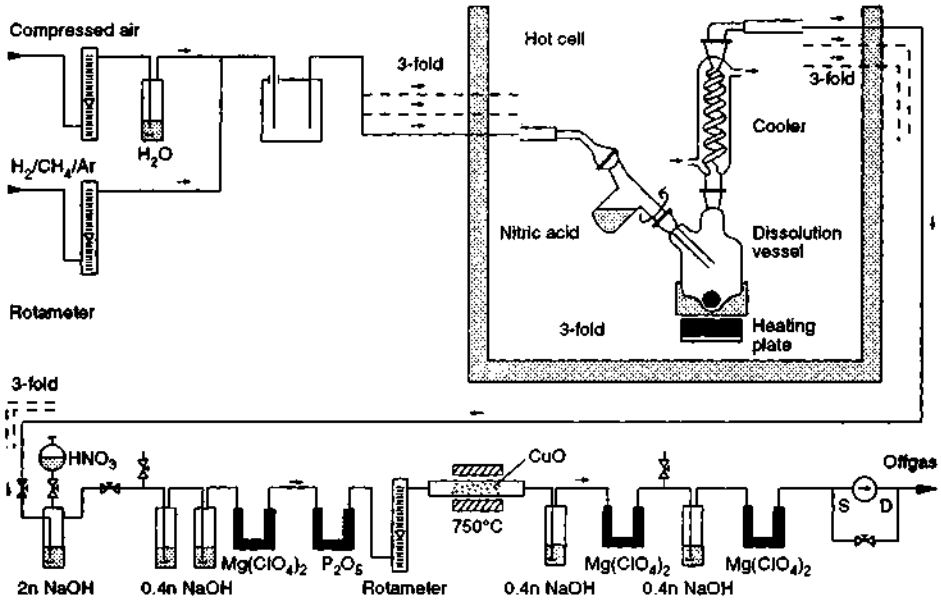

Figure 3.24. ^3H and ^{14}C determination in irradiated nuclear fuel; dissolution device and gas collection system
(Neeb et al., 1980)

For the determination of ^3H and ^{14}C activity concentrations present in the fill gas of the fuel rod, the rod to be investigated is punctured in the evacuated normal fill gas sampling device located inside a hot cell. The fill gas is then extracted from the rod and collected in a Toepler pump. These procedures are well known since they are often applied in the determination of the fission product noble gases released from the fuel pellets to the rod free volume and there they do not pose any problems. In the sampling of HTO, however, there is the danger of significant HTO losses caused by adsorption of H_2O traces on the walls of the sampling lines which, because of the dimensions of the hot cell, inevitably have a considerable length. In order to preclude analytical errors caused by this effect, after evacuation the sampling lines have to be flushed with air containing H_2O, H_2, CO_2, and CH_4 as carriers. These gas volumes are also collected and added to the analytical sample, which for ^3H and ^{14}C determination is transferred to the analytical duct described below.

To determine the ^3H and ^{14}C activity concentrations in the irradiated fuel itself, samples having a mass of a few grams of fuel are taken from previously identified positions that can be correlated to the γ scan of the fuel rod and, thus, to the local fuel burnup. After weighing, the sample is transferred to the dissolution vessel of the analytical duct which is located inside a hot cell (see Fig. 3.24.), 7 N nitric acid is added and after connection of the apparatus to a carrier gas flow consisting of air–Ar–H_2–CH_4, the solution is heated to boiling. After complete dissolution of the sample, the gas absorption duct is disconnected and a fraction of the fuel

solution is distilled in order to obtain a sample for ^3H determination. The distillate is then removed from the hot cell, the non-dissolved cladding material is removed from the sample solution and is stored for further investigation (see Section 3.2.5.).

The sample solution is not analyzed for ^{14}C, as opposed to ^3H, since it can be assumed that the total inventory of this radionuclide in the fuel sample is converted to the volatile compounds CO_2, CO, and CH_4 in the course of the dissolution reaction. This assumption was confirmed by parallel investigations in which ^{14}C was determined by dry ignition of the fuel sample in air; the results obtained by this technique showed good agreement with those obtained after acid dissolution, which led to the conclusion that no ^{14}C compounds are present in irradiated fuel which are stable in boiling nitric acid.

The gas absorption duct (which is also used in the analysis of the fill gas extracted from the fuel rod) consists of vessels containing 0.4 N NaOH solution for the retention of HTO and $^{14}CO_2$, followed by $Mg(ClO_4)_2$ and P_2O_5 absorbers in which even very small residual traces of these compounds are retained. At a CuO catalyst which is kept at 750 °C, HT, ^{14}CO, and $^{14}CH_4$ are oxidized. The resulting compounds HTO and $^{14}CO_2$ are then absorbed in the final absorption vessels containing dilute NaOH solution.

If necessary, further purification of HTO from other radionuclides is carried out by a second distillation. In such slow distillations using a small column, it has to be taken into account that this procedure may lead to a certain isotope fractionation $^1H-^3H$; Baumgärtner et al. (1990) reported a vapor pressure ratio pH_2O : pHTO of 1.04 at 100 °C, of 1.15 at 0 °C, and of 1.4 at −50 °C. Thus, the distillate fraction used for radiation measurement shows a tritium activity concentration which is lower by 2−3% than the average value of the original sample solution, a deviation which, however, usually is within the error margin of the entire analytical procedure; if necessary, the isotope separation effect can be corrected for by using correction factors determined in appropriate tracer experiments. The radiation measurement of the purified HTO sample, the purity of which is checked by γ counting, is performed by liquid scintillation counting using an internal standard and applying the pulse height discrimination technique. ^{14}C is liberated from the absorption solutions as CO_2 by acidification and subsequently precipitated as $BaCO_3$. The precipitate then is subjected to β^- counting, the radiochemical purity of the final specimen is checked by beta absorption measurement.

From investigations performed as just described the results reported by Bleier et al. (1984), which are in good agreement with those published by other authors, shall be reported on in some detail. They showed that after dissolution of the fuel sample in nitric acid, 99.5 to 99.8% of the tritium inventory of the fuel samples is obtained as HTO; from this result one can conclude that in the fuel ^3H is chemically attached to oxygen, probably in the form of OH groups. As a consequence of ternary fission, the ^3H nucleus shows a recoil energy of about 7 MeV; it should be able, therefore, to induce a chemical reaction forming an O-H bond. On the other hand, stoichiometric UO_2 at 1270 K (1000 °C) is in a thermodynamic equilibrium with an H_2-H_2O atmosphere consisting mainly of H_2 (about 90%). This means that the experimental results are apparently not fully consistent with the thermodynamic data. One possible reason for this discrepancy might be oxidation

of ^3H atoms, which might be present in the fuel in an atomic-dispersed state caused by the nitric acid during dissolution; likewise, an isotope exchange of such ^3H atoms with H_2O molecules of the acid solution cannot be ruled out. Another explanation, which is more probable, is that thermodynamic calculations are not adequate for describing correctly the behavior at such very low concentrations. At a fuel burnup of 33 MWd/kg U, the total amount of tritium produced is on the order of 0.06 ppm (related to the fuel weight). Even if one postulates a behavior of ^3H which is identical to that of the residual moisture content in the fuel (which is well below 10 ppm), one would be dealing with very low concentrations, which means that the question of reliable thermodynamic calculations in this context may be considered to be still open.

From Fig. 3.21. one can recognize the migration of ^3H in the radial thermal gradient of the fuel pellet, with the pellet center being virtually free of ^3H whereas towards the outer pellet zones a marked increase in concentration is to be observed. This type of distribution indicates that migration in the thermal gradient is the main parameter dictating ^3H distribution in the fuel pellet. The mechanism may be a kind of "drying" of the hydroxyl groups which were formed by implantation of the fission triton into the oxide material; from other ceramic materials it is known that the removal of residual traces of moisture requires relatively high temperatures, similar to those prevailing in the fuel pellet during operation. The comparatively high residual fraction of ^3H in the fuel (see below), on the other hand, indicates the presence of a ^3H chemical bond in the fuel; neutral tritium atoms are assumed to show a very high mobility that would result in a virtually complete release of tritium from the fuel. These assumptions are consistent with the results of diffusion measurements of ^3H in neutron-irradiated UO_2 (Scargill, 1978), which showed that the diffusion coefficients in the temperature range from 750 to 1250 K (500 to 1000 °C) are lower by four to eight orders of magnitude than those reported for molecular hydrogen in UO_2 single crystals. The activation energy for diffusion of fission product tritium amounts to about 183 kJ/mol and, thus, is much greater than that of H_2 diffusion (about 60 kJ/mol). Diffusion release of ^3H from neutron-irradiated material shows no significant differences between UO_2 single crystals and sintered polycrystalline UO_2.

As is indicated qualitatively in Fig. 3.21., the amount of ^3H measured in irradiated nuclear fuel is considerably below that calculated from burnup and fission yield data. Detailed investigations showed that during fuel operation more than half of the ^3H produced has been released from the fuel pellet and has entered the Zircaloy cladding of the fuel rod. In Table 3.11. (according to Neeb et al., 1980; Bleier et al. 1984), the results of ^3H determinations in different sections of a typical PWR fuel rod operated at a linear heat rating of about 200 W/cm are given, showing that the fuel pellets still contain about 37% (averaged over the total length of the pellet column) of the ^3H amount produced, with the remainder having been released to the fuel pellet – cladding gap and subsequently picked up by the Zircaloy cladding (see Section 3.2.5.). The relative distribution of tritium between fuel and cladding apparently does not depend on local burnup. The tritium concentration in the fuel (and in the cladding) follows the fuel burnup reasonably closely; that means that, in spite of considerable differences in the local heat ratings be-

Table 3.11. ^3H inventory and distribution in a PWR fuel rod (according to Neeb et al., 1980)

Sample No.	Position*) in fuel rod	Local burnup MWd/kg U	^3H in fuel GBq/g UO_2	^3H in cladding GBq/g UO_2	^3H total GBq/g UO_2	% ^3H in fuel
1	219–231	17.9	4.8	–	–	–
2	233–245	18.8	3.8	7.1	10.9	35
3	380–392	26.2	3.6	9.4	13.0	28
4	1048–1060	36.8	9.0	13.8	22.8	39
5	1062–1074	36.8	7.5	13.9	21.4	35
6	1384–1396	35.6	8,7	12.2	20.9	42
7	1398–1410	35.6	9.8	12.7	22.5	44
8	2023–2035	33.5	6.5	11.3	17.8	37
9	2155–2167	34.1	7.5	10.7	18.2	41
10	2183–2195	32.9	7.8	10.1	17.9	44
11	2505–2517	23.6	4.4	10.7	15.0	29
12	2674–2686	13.2	3.1	6.1	9.2	34

*) mm from lower end cap

tween the central region of the rod and the end pellet positions, no axial migration in the pellet stack or in the cladding can be detected. The reasons for the pronounced differences in radial and in axial migration behavior of tritium in the fuel pellets have not yet been clarified.

Comparable analyses of a BWR fuel rod having experienced almost identical heat ratings but a lower burnup (about 20 MWd/kg U), yielded a ^3H fraction still retained in the fuel of about 50% (Bleier et al., 1984). The reasons for the differences in retention between PWR and BWR fuels have not yet been completely clarified. Presumably they are due to a higher density and lower open porosity of the BWR fuel analyzed, the impact of which on H_2O mobility in UO_2 fuels is well known. As for the chemical state of tritium in the fuel there is no difference between the two fuel types, i. e. in analyzing BWR fuel virtually the whole tritium inventory is also detected as HTO after dissolution in nitric acid.

The investigations performed by other authors yielded similar results concerning the fraction of tritium remaining in the fuel. Goode and Cox (1970) reported that a PWR fuel operated at 160 W/cm to a burnup of 34 MWd/kg U still contained about 93% of the ^3H produced. The analyses of Broothaerts et al. (1982) of UO_2–PuO_2 fuel rods operated under PWR conditions (burnup 32 MWd/kg U, linear heat ratings between 150 and 200 W/cm) showed residual ^3H fractions in the fuel of about 40% of the amount produced. Finally, Grossmann and Hegland (1971) reported that in BWR fuel rods after a burnup of 12 MWd/kg U at a linear heat rating of 580 W/cm, about 25% of the ^3H produced was detected in the fuel, but after 21 MWd/kg U at 1030 W/cm only 4%.

From the results of these investigations it can be concluded that the ^3H fraction retained in the fuel decreases with an increasing heat rating of the fuel rod, whereas

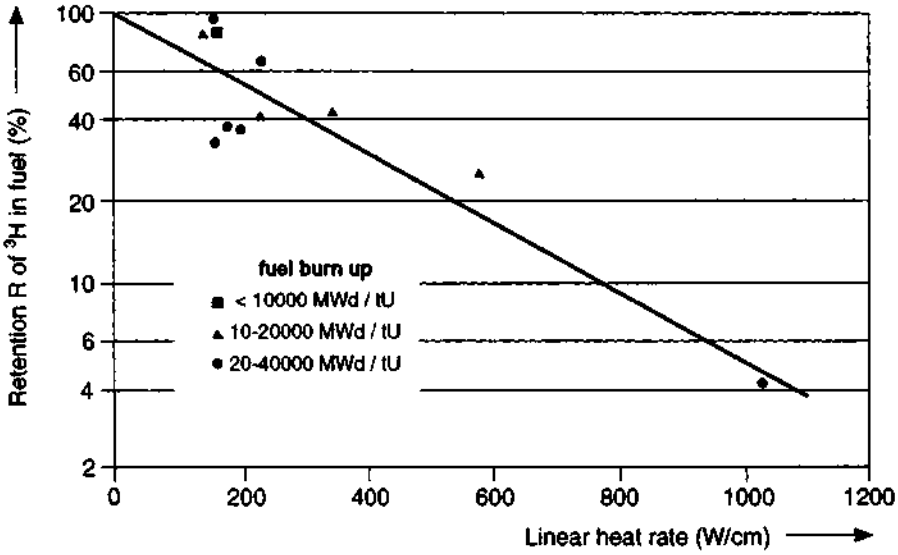

Figure 3.25. ^3H retention in oxide fuel as a function of linear heat rate (Wölfle et al., 1981)

it depends only little (if at all) on fuel burnup. In Fig. 3.25. (from Wölfle et al., 1981) the results of several experimental investigations are summarized as a function of fuel linear heat rating; despite a considerable scatter, the relative distributions of ^3H between fuel and cladding show a clear tendency. These results are consistent with what has been described above on the nature of the chemical bond of tritium in irradiated nuclear fuel. Higher heat ratings mean higher fuel central temperatures and, consequently, a more effective "drying" of the fuel. On the other hand, saturation effects that might influence the behavior of tritium are not likely even at high burnup levels, because of the low ^3H mass concentrations in the fuel; thus, no pronounced effect of fuel burnup on the behavior of tritium is to be expected.

3.2.3.7 Carbon-14

During reactor operation, small amounts of ^{14}C are also formed in nuclear fuels. With regard to the radioactivity balance of the fuel during plant operation, this radionuclide is of no relevance; however, considering its comparatively long halflife of 5736 years and its postulated release behavior from the fuel matrix under storage or accident conditions, it is of definite interest with respect to reprocessing or final disposal of the spent fuel. For these reasons, it is of importance to know the ^{14}C inventories as well as the chemical state of this radionuclide in the fuel.

^{14}C is produced in the nuclear fuel by different nuclear reactions (e. g. Davis, 1977), the most important of which are

- ^{17}O (n,α) ^{14}C: Stoichiometric UO_2 has an oxygen content of 11.8%; the isotopic abundance of ^{17}O in the oxygen amounts to 0.039%. The isotope shows a thermal neutron cross section for the (n,α) reaction of $2.35 \cdot 10^{-25}\,cm^2$ and a resonance neutron cross section of $1.05 \cdot 10^{-25}\,cm^2$.
- ^{14}N (n,p) ^{14}C: This nuclear reaction shows a thermal neutron capture cross section of $1.8 \cdot 10^{-24}\,cm^2$ and a resonance neutron cross section of $8.7 \cdot 10^{-25}\,cm^2$. Usually, the nitrogen content of UO_2 fuel and mixed-oxide fuel is on the order of a few ppm; the ^{14}N abundance in the natural nitrogen isotopic mixture amounts to 99.63%.
- Ternary fission: The ^{14}C fission yields are about $1.7 \cdot 10^{-4}$% for thermal ^{235}U fission and about $1.8 \cdot 10^{-4}$% for thermal ^{239}Pu fission.
- ^{13}C (n,γ) ^{14}C: Due to the large graphite inventories in the cores of high-temperature reactors, this reaction is the main source of ^{14}C production there. In LWR fuels, however, this nuclear reaction is of little significance because of the low carbon content in the fuel (<10 ppm), the low isotopic abundance of ^{13}C of 1.1%, and its small thermal neutron capture cross section of about $1 \cdot 10^{-28}\,cm^2$.

PWR and BWR neutron spectrum averaged cross section data were summarized by Bleier et al. (1987).

Determination of the ^{14}C activity concentration in the irradiated fuel can be performed in a similar manner as ^{3}H determination (see Section 3.2.3.6). An alternative method for determining the ^{14}C contents in spent fuel is combustion of the sample in an oxygen or air atmosphere, followed by absorption of the CO_2 formed in alkaline solution. This method was applied in the analysis of graphite-coated HTGR fuel kernels (Wenzel et al., 1979); however, when using this technique, it is not possible to distinguish between different chemical forms of ^{14}C present in the fuel, since they all are completely oxidized to CO_2 during combustion.

At low nitrogen impurity concentrations in the fuel both the (n,p) reaction and the (n,α) reaction mentioned above are of about equal importance as regards ^{14}C production in the fuel; the data published by Bleier et al. (1987), which are summarized in Fig. 3.26., can be explained by a nitrogen concentration in the fuel in the range of 5 to 10 ppm. It is known from measurements made in fuel fabrication that nitrogen impurity concentrations in BWR and PWR fuels usually are markedly below 10 ppm, frequently below the analytical detection limit of 4 ppm; thus, these data do not contradict the ^{14}C concentrations found in these experiments. Only a few of the results indicating a very high nitrogen content in the range of 20 to 30 ppm cannot be explained. As can be seen from Fig. 3.26., the measured ^{14}C concentrations in the fuel are in good agreement with the local fuel burnup, thus indicating that the ^{14}C produced is completely retained in the fuel matrix and does not migrate to a measurable extent in the axial direction in the fuel rod.

The investigations reported by Bleier et al. (1987), while having the aim of studying ^{14}C behavior under head-end conditions of nuclear fuel reprocessing and, therefore, using analytical techniques not particularly suited for chemical speciation, also yielded information on the chemical state of ^{14}C in the fuel. Upon disso-

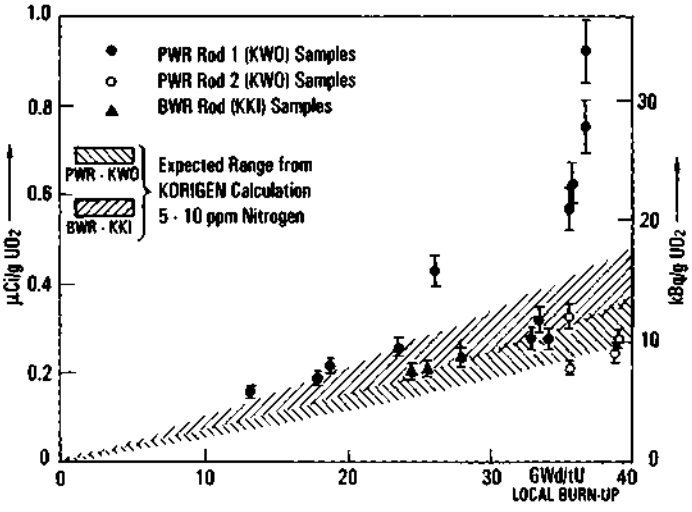

Figure 3.26. ^{14}C activity concentrations in PWR and BWR fuel as a function of local burnup (Bleier et al., 1987)

lution of the fuel specimens in nitric acid, virtually all of the ^{14}C inventory of the fuel is liberated as CO_2, with only a very small fraction in the range of 0.2 to 0.3% appearing as CO and/or CH_4 (these two compounds cannot be distinguished from each other by the analytical technique applied). It seems questionable, however, whether this result means that ^{14}C is chemically bound in the fuel as carbonate; thermodynamically, UO_2 at 1270 K (1000 °C) is in equilibrium with a $CO-CO_2$ mixture with a dominant CO fraction. Therefore, it seems probable that ^{14}C in the fuel exists as a species that cannot be identified in greater detail and which is oxidized by nitric acid to CO_2; besides the possible presence of oxidic carbon species, the presence of very small ^{14}C concentrations in the fuel (<0.1 ppm) in an atomic-dispersed form, which is oxidized by nitric acid during dissolution of the sample, cannot be ruled out.

3.2.4 Radionuclides in the fuel pellet – cladding gap

Besides the fuel, the closed chemical system "fuel rod" includes the fuel pellet – cladding gap and the upper and lower gas plenum, which are filled with helium overpressure (about 2 MPa at ambient temperature) in the course of fuel rod fabrication. During reactor operation, a certain gap inventory of radionuclides is generated which is of interest in the event of an operational fuel rod failure as well as in a loss-of-coolant accident. In typical LWR fuel rods, this gap inventory is mainly formed by fission product recoil from the fuel pellets. According to Wise (1985), one quarter of the fission fragments generated within a recoil length μ from the

surface of the pellet are released by recoil, provided the dimensions of the fuel specimen are large compared with the recoil range of the fission fragments in the fuel. If the fission rate is uniform throughout the specimen (which can be approximately assumed for a LWR fuel pellet), then the ratio of the recoil release rate R to the fission fragment production rate B is

$$R/B = 1/4 \cdot \mu \cdot (S/V)$$

(S = surface area of the specimen, V = volume of the specimen)

The largest fraction of the released fission fragments will enter the Zircaloy cladding of the fuel rod and only a small quantity ε will be stopped within the gas-filled interspace between pellet surface and cladding, forming the recoil-induced gap inventory. Calculation of ε (i. e. of the fraction of fission fragments which have lost their recoil energy almost entirely in the fuel matrix so that they are completely stopped in the gas phase of the gap) is very difficult since it depends on the mass of the fragment and its initial energy as well as on the shape of the gas interspace. Detailed analytical solutions for different geometries etc. have been published by Wise (1985) as well as by Lewis (1987).

In addition, high-energy fission fragments are able to displace uranium atoms from the pellet surface to the pellet – cladding gap. The mechanism of this knock-out effect is assumed to be thermal vaporization due to the extremely high temperatures in the fragment spur; under favorable conditions up to 10^3 uranium atoms can be ejected from the fuel matrix by the action of one single fission fragment. When either a primary fission fragment or an energetic particle created in a collision cascade interacts elastically with a fission product atom, this atom can be knocked out of the fuel matrix. The higher-order collisions occurring in the cascade are the dominant processes in knock-out release; the initial kinetic energy of these processes is sufficiently low (~ 200 eV) for the particles to be stopped within the fuel pellet – cladding gap or within small cracks in the pellet. In general, at least for shorter-lived fission products, the release by knock-out is negligible compared to that by recoil (Lewis, 1987).

In LWR fuel rods operated at normal heat ratings, the second mechanism that can transport radionuclides to the gap, namely diffusion from the fuel matrix in the thermal gradient, is only of importance for the noble gases. In such fuel rods, the gap inventory of the fission product noble gases (including the upper and lower plena) amounts to about 1% of the fuel inventory and consists mainly of stable xenon and krypton isotopes and long-lived ^{85}Kr. Sweep gas experiments have shown that the shorter-lived noble gas isotopes in an intact fuel rod exhibit a release behavior to the gap showing an R : B dependence on $\lambda^{-1/2}$ which, as will be discussed in more detail in Section 4.3.1.1., indicates a diffusion-controlled release from the UO_2 matrix (e. g. Lewis et al., 1990). In standard LWR fuel rods iodine and cesium, which do not show significant migration in the thermal gradient under such conditions, are not expected to be transported to the gap by thermal diffusion. The same applies to the polyvalent fission products (e. g. alkaline earths, rare earths).

Investigations reported by Neeb (1978), in which the inner surface of the cladding of a typical PWR fuel rod was subjected to a selective leaching procedure,

showed gap inventories of the two elements iodine and cesium amounting to 0.3–0.5% of the fuel inventory. Figures on the same order of magnitude were given by Lorenz et al. (1980), based on heating experiments of fuel rod segments at 700 °C in a dry helium atmosphere (so-called gap purge experiments). However, heat ratings beyond 300 W/cm, which in LWR fuel rods will only occur during power transients (ramps), will result in considerably higher gap inventories; in the ORNL gap purge experiments, gap inventories of about 15% for both iodine and cesium were measured in highly rated fuel rods. At such high fuel temperatures, fission product migration in the thermal gradient is the predominant contributor to gap inventory buildup (Collins et al., 1988).

The chemical conditions in the gap are controlled by the oxygen potential, μ_{O_2}, which can be calculated by:

$$\mu_{O_2} = RT \cdot \ln (p_{O_2}/p^{\circ}_{O_2})$$

Besmann and Lindemer (1978) pointed out that the definition of the chemical oxygen potential in the gap of a fuel rod is somewhat problematic. At the outer surface of the fuel pellet it is controlled by the UO_2–fission product mixture; electro-motoric force (emf) measurements at 1023 K yielded μ_{O_2} values between −555 and −450 kJ/mol at fuel burnup data of 11 and 19 MWd/kg U, respectively. On the other hand, at the inner cladding surface the chemical system $Zr-ZrO_2$ dominates, the oxygen potential of which is considerably more negative, being in the range −900 kJ/mol at 1000 K, i. e. roughly comparable to that of the system $U-UO_2$. Assmann and Stehle (1984) claimed that the inner surface of the Zircaloy cladding represents an oxygen sink, where the excess oxygen caused by uranium and plutonium fission is fixed by the formation of an oxide layer at temperatures of around 400 °C. On the other hand, microprobe measurements performed by Kleykamp (1990 a) showed very little cladding oxidation. These chemical conditions are of importance as regards the chemical state of various fission products which are present in the gap. It has to be emphasized that these chemical conditions only apply to intact fuel rods; the appearance of cladding failures will change the conditions significantly, mainly due to the steam entering the gap from the primary coolant and replacing the helium fill gas.

Concerning the chemical state of fission product iodine and cesium in the gap, the ORNL gap purge experiments yielded identical volatilization kinetics for both elements and identical deposition in the thermal gradient tube with a maximum in the temperature range 500° to 350 °C. These results were claimed to indicate the presence of CsI in the pellet – cladding gap, while the presence of elemental iodine and cesium can be ruled out (Collins et al., 1988). The leaching experiments described by Neeb (1978) showed that only about 25% of the fission product iodine and cesium released from the fuel pellets are soluble in organic solvents and in dilute mineral acid, while the bulk of them can only be dissolved by attacking the cladding base material. These experimental results apparently confirm the presence of specific fission product compounds such as CsI and, possibly, traces of I_2 in the gap, i. e. on the Zircaloy surface; on the other hand, they are consistent with the above-mentioned assumption that the majority of the fission fragments are implanted into the Zircaloy base material by the recoil kinetic energy. In limited fuel

rod zones having experienced a transient with comparatively high heat ratings, considerably larger iodine and cesium deposits were detected in the gap (Neeb, 1978). Moreover, the fraction of iodine and cesium which could be dissolved from these zones by organic solvents and by diluted mineral acid was considerably higher, thus indicating that in these areas the recoil-induced transport was superimposed by a thermomigration transport. However, despite the comparatively high fraction of iodine found to be soluble in organic solvents, no significant axial migration of this fission product in the fuel rod gap was observed, an effect which one would expect if elemental iodine with its rather high vapor pressure were present in the gap; as yet, this inconsistency has not been explained.

These results generally agree with the thermodynamic calculations of Besmann and Lindemer (1978), according to which fission product iodine should appear in the gap as a CsI species, which is the thermodynamically most stable iodine compound at oxygen potentials controlled by UO_2 as well as by the Zr-ZrO_2 equilibrium. As for the chemical state of cesium, which is present in an amount greater by about a factor of ten than iodine, the situation is more complex. If the oxygen potential is controlled by UO_2, then Cs_2UO_4 would be the most stable compound besides CsI; in contrast, if the system Zr-ZrO_2 is the dominant one, then elemental Cs would be stable, provided that no cesium zirconate were formed. However, it seems quite questionable whether such well-defined compounds will actually appear in the gap. Iodine and cesium atoms which are incorporated in the superficial oxide layer and form non-stoichiometric compounds are thought to be more probable.

Due to fuel swelling and cladding creep, fuel and cladding at higher burnup levels often come into close contact under the conditions of operating temperature and pressure. Locally, small fuel particles may stick to the cladding material, resulting in fuel residues at the inner cladding surface in post-operational cold conditions. In addition, at the inner cladding surface of fuel rods exhibiting high linear heat ratings (on the order of 300 W/cm) and showing a fission gas release of 10 to 13%, deposits of a different nature are detected. Layers covering narrowly limited areas across from pellet cracks mainly contain uranium, cesium and tellurium; at pellet interfaces these layers show larger dimensions. Likewise, circular-shaped deposits are statistically distributed, predominantly consisting of uranium and cesium.

Besides the fission products mentioned above, small amounts of tritium are also present in a volatile form in the fill gas of the fuel rod. According to Bleier et al. (1984), the amount of tritium present in the rod plena and gap amounts to 10^{-5}–10^{-3}% of the total tritium inventory of the fuel rod, about 80% of which is present as HTO, with the remainder as HT; in this respect, there is no significant difference between PWR and BWR fuel rods. These results are also in reasonable agreement with those reported by Broothaerts et al. (1982). However, the HTO : HT ratio just mentioned does not agree with the calculated H_2O–H_2 ratio which is in thermodynamic equilibrium with UO_2 at 1270 K (10 : 90). The reasons for these discrepancies are not known as yet. If one considers the tritium amounts present in the gas phase, in the fuel and in the cladding and if one assumes that the transport between fuel pellet and cladding occurs exclusively via the gap gas-

eous phase, then one could calculate an average residence time of a tritium atom in the gap of about only 10 hours.

In the analyses reported by Bleier et al. (1984), ^{14}C was not detected in the gas phase of the fuel rod, either as CO_2 or as CO/ CH_4. From this result, one can calculate that the fraction of ^{14}C present in the gap amounts to less than 10^{-5}% of the fuel rod inventory, at the maximum.

3.2.5 Radionuclides in the fuel rod cladding

In light water reactors, Zircaloy is commonly used as the fuel rod cladding material, a zirconium alloy with various metallic constituents. Pressurized water reactors use Zircaloy-4 (Zry-4), while in boiling water reactors Zircaloy-2 (Zry-2) is the preferred cladding material; the compositions of both alloys are shown in Table 1.2. In German PWRs the mass of Zircaloy amounts to about 290 kg/Mg HM (heavy metal), in BWRs to about 320 kg/Mg HM (including the fuel assembly channels).

During reactor operation, the surfaces of the cladding become covered by oxide layers. At the inner surface a thin layer is formed which in high-burnup fuels reaches an oxygen concentration of about 0.2% in the upper 25 µm Zircaloy zone as compared to about 0.1% in the Zircaloy bulk material. This oxygen originates in the oxide fuel; however, as was mentioned in the preceding sections, it does not significantly affect the stoichiometry of the fuel. The inner oxide layer also contains fission products transported there mainly by fission recoil (see Section 3.2.4.). In addition, interaction zones between the cladding oxide and fuel (including fission products) are occasionally observed which are usually locally limited and tightly adherent to the cladding material.

On the outside of the cladding, which is in contact with high-temperature water or steam, the nature and the thickness of the oxide layer on PWR and on BWR rods are markedly different. The PWR rods show a rather homogeneous black oxide layer, the thickness of which depends on the period of exposure as well as on the thermo-hydraulic design of the fuel assembly. The maximum thickness is generally observed in the upper third of the fuel rod length, amounting to about 60 to 100 µm. On BWR rods, normally a very thin oxide layer of a few µm only is observed; in addition, nodular corrosion occasionally occurs with zones reaching a thickness up to 100 µm. Additionally, local oxide layers can be present which are generated by chemical action of the coolant and which are affected by the material properties of Zircaloy-2. At design burnup, these local oxide layers reach a maximum thickness of about 25 µm; by change in the fabrication technology of the material their extent has been significantly reduced. Mixed-oxide fuel rod claddings show the same oxidation effects as those of standard UO_2 fuel rods.

The oxide layers mentioned above are generated by oxidation of the Zircaloy base material by high-temperature water or steam. They must not be confused with the layers formed by deposition of corrosion product oxides originating from the surfaces of the other primary circuit components and structures; these corrosion

product deposits are postulated to be at least partly responsible for contamination buildup in the primary system. The inner fraction of these corrosion product oxide layers adheres very tightly to the cladding material and is usually covered by a loosely-adhering layer. In these oxide deposits radionuclides are formed by neutron activation, mainly ^{60}Co, ^{58}Co, ^{59}Fe, ^{54}Mn, among others. A more detailed description of these processes will be given in Section 4.4.

Since the cladding is in the neutron field during the whole operation period of the fuel assembly (usually for 3 or 4 fuel cycles), considerable amounts of radionuclides are produced in it. The dominant radioactivities stem from the neutron activation products of the zirconium base material, namely ^{95}Zr and its daughter product ^{95}Nb; according to ORIGEN calculations, the ^{95}Zr activity concentration in spent fuel claddings at the time of discharge amounts to about 500 MBq/g (core-averaged value). From the tin content of both Zircaloy-2 and -4, ^{125}Sb is generated by the reaction chain $^{124}Sn\ (n,\gamma)\ ^{125}Sn \xrightarrow{\beta^-} {}^{125}Sb$, with an activity concentration on the order of 5 MBq/g as calculated from the tin content of the Zircaloy material and the neutron fluence. Investigations conducted in the context of spent fuel reprocessing, however, yielded ^{125}Sb activity concentrations greater by a factor of 7 to 20 than the calculated values; potentially, redeposition of fission product ^{125}Sb from the nitric acid solution during leaching of the fuel has been responsible for this discrepancy. Another essential contribution to the cladding total activity is made by ^{60}Co, which is produced by neutron activation of cobalt traces present in the material. The ^{60}Co activity concentration varies according to the trace impurity content of the material, with values between 0.7 and 15 MBq/g Zry being measured (data corrected for decay to the time of discharge).

Zircaloy frequently contains uranium traces which, during reactor operation, give rise to the formation of transuranium isotopes in the cladding. As is known from investigations performed in the context of spent fuel reprocessing, after design irradiation of LWR fuel rods, the cladding contains ^{239}Pu in the range 20 to 100 Bq/g, in addition to 20 to 50 Bq ^{240}Pu/g, 7 to 10 kBq ^{241}Pu/g and 40 to 120 Bq ^{241}Am/g. Depending on their uranium impurity contents, different batches of Zircaloy may show marked differences in their transuranium activity concentrations; however, the values measured in different specimens were in good agreement with those calculated from the actual uranium content and the neutron fluence. Besides the transuranium isotopes, fission products are also formed in the cladding material by nuclear fission of the uranium trace impurities. In addition, in particular at high fuel burnup, transuranium elements become fixed to the inner surface of the cladding where they are present as contamination incorporated into the oxide layer; as has been shown by α autoradiography, these nuclides are not homogeneously distributed but are, rather, concentrated in spots. These spots probably originate from fuel particles adhering to the oxide layer which had not been completely removed from the cladding during dissolution of the fuel.

Fission products are also present in the cladding base material as a result of fission fragment recoil from the fuel. Investigations by Vehlow (1984) of spent PWR claddings using selective electrochemical dissolution techniques showed that ^{137}Cs and various other long-lived radionuclides exhibit a concentration profile with an almost logarithmic slope down to about a depth of 10 μm from the inner

cladding surface. Usually, this profile contains about 80% of the total fission product inventory of the cladding (amounting to about 0.1% of the fuel rod inventory of fission products), while the remainder originates from the uranium impurities present in the Zircaloy base material. Obviously, the concentration profile represents the implantation depth of the fission product fragments caused by the fission recoil. Quite in contrast with the other fission products, the ^{85}Kr concentration profile starts with a value of about zero near the surface, reaches a well-pronounced maximum at a depth of about 2 μm and then decreases again with a logarithmic slope to virtually zero at a depth of 10 μm. This behavior has been attributed to a diffusion of ^{85}Kr in the Zircaloy material which is significantly faster than that of the other fission products, leading to a slow release of implanted atoms from the material to the gas phase during the post-irradiation storage time. This assumption is supported by the observation of measurable ^{85}Kr releases from spent fuel claddings during dry storage.

As was mentioned in the preceding sections, a significant fraction of the tritium produced in the nuclear fuel is transported during reactor operation to the cladding material and deposited there. A reliable evaluation of the magnitude of this fraction is only possible by experimental determination; relevant analyses are complicated, however, by similar difficulties to those for ^{3}H determination in irradiated fuel. According to Bleier et al. (1984), for ^{3}H determination the Zircaloy cladding is dissolved in nitric acid – hydrofluoric acid in a closed dissolution device; subsequently, the acid solution and the different fractions of the gas absorption duct are treated in the same manner as described in Section 3.2.3.6. In such a dissolution process, fine insoluble particles will remain, probably consisting of the original surface oxide layers; they can be isolated from the solution and dissolved by a $KHSO_4$ melt process. An alternative method to acid dissolution is melting of the whole cladding sample with $KHSO_4$; this technique has the advantage that the ^{14}C content of the material can be determined simultaneously by analyzing the volatile compounds in the same manner as described above. In evaluating the results obtained by this melting technique, however, it has to be taken into account that at the high temperatures of the melt the original chemical state of both radionuclides may be changed. After such a treatment, the $^{14}CO : {}^{14}CO_2$ ratio obtained is virtually identical to that what would result from the Boudouard equilibrium, thus giving no information on the original species; comparable reactions concerning the ^{3}H chemical species cannot be ruled out. A similar effect has to be expected in the ^{3}H determination by vacuum hot extraction; at the temperatures of about 1400 K which have to be applied here, HTO originally present is reduced almost quantitatively by the metal to HT. As with the determination of these radionuclides in irradiated fuel, the analytical procedure proposed by Bleier et al. (1984) is expensive in its execution, but it is able to determine reliably ^{3}H and ^{14}C in low concentrations and in the presence of a large excess of other radionuclides, with an analytical error of 5 to 10%.

As can be seen from Table 3.11., in a typical LWR fuel rod about one-half to two-thirds of the ^{3}H produced by ternary fission is released from the fuel to the Zircaloy cladding. The resulting axial ^{3}H profile in the cladding is virtually parallel to the γ-scan data; this means that the relative fraction of total ^{3}H production

transported during operation of the fuel rod to the cladding does not depend on the local fuel burnup and, consequently, also not on the time-averaged local heat rating. Moreover, this profile indicates that during reactor operation no significant axial migration of ^3H in the cladding takes place (Bleier et al., 1984). On the other hand, Broothaerts et al. (1982) reported that in the active zone of the fuel rod the ^3H concentration in the cladding correlates with the axial γ scan, but that it increases in the region of the upper rod plenum to values which, in some cases, exceed the values in the middle region of the fuel rod; in contrast, in the region of the lower Al_2O_3 insulation pellet the ^3H concentration in the cladding was about the same as that in the lowest part of the active zone. These data contradict the results reported by Bleier et al. (1983) showing that the ^3H concentration in the cladding near the insulation pellet is lower by a factor of about 10 than in the central region of the rod, with the concentrations being lower in the middle of the upper plenum region by a factor of 35. The reasons for the differences in the results are still not clear, and cannot be explained by the fact that in one of the cases standard UO_2 fuel rods, in the other one UO_2-PuO_2 fuel rods with a comparatively low linear heat rating had been examined.

The radial ^3H distribution across the cladding wall thickness is quite homogeneous, as was demonstrated by investigations in which thin layers were consecutively removed by mechanical means from the cladding and analyzed for ^3H (Neeb et al., 1980). From these results, a relatively fast ^3H migration in the Zircaloy material in a radial direction can be derived. This behavior seems to be contradictory to the axial ^3H immobility mentioned above. Possible reasons for these differences in ^3H behavior may be the Zircaloy texture, which is different in the axial and radial directions of the cladding, or the temperature gradient in the material, which is considerably larger in the radial than in the axial direction. However, as yet there is no definite explanation.

In the course of the dissolution of irradiated Zircaloy cladding specimens in mineral acids, the ^3H present is liberated almost quantitatively as HT (Goode and Cox, 1970; Neeb et al., 1980), indicating that the chemical form of ^3H in the metal is dissolved hydrogen or ZrH_x. Small fractions of HTO observed in these experiments are probably due to secondary chemical reactions which occur during the dissolution process.

From the experimental results described above, it can be stated that in LWR fuel rods only about one half of the ^3H produced by ternary fission remains in the fuel, with the other half being transported to the cladding material. In principle, this transport can proceed via the direct contact between fuel and cladding which are in close contact during operation. Another possibility is transport via the gas phase of the gap; in this case, however, the rather short average residence time of about 10 hours of ^3H in the gas phase of the gap (see the preceding section) is only difficult to understand. In both transport mechanisms, the ^3H present in the fuel and in the gap gas phase as HTO (or as hydrogen chemically attached to oxygen) has to be reduced to elemental hydrogen, since it appears in the cladding as dissolved hydrogen or as hydride. Basically, such a reduction can be effected by two different mechanisms:

- HTO from the fuel or from the gas phase is reduced by Zircaloy at the interphase oxide–metal and the hydrogen generated is incorporated into the metal.
- In the gap gas phase, HTO is decomposed by radiation-induced reactions, with the ^3H atoms produced passing directly over to the metal.

The probabilities and the rates of both reactions under the prevailing conditions are still not known and, therefore, it is not possible to identify the predominant mechanism.

The comparatively fast incorporation of ^3H into the cladding material has to be compared with its slow release from the Zircaloy cladding to the reactor coolant which, according to calculations based on measurements of the ^3H concentrations in the coolant and its production rates there (see Section 4.2.3.), has been estimated to be less than 1% of the amount produced in the nuclear fuel. In contrast, ^3H release from fuel rods with stainless steel claddings to the coolant is significantly higher; according to the data from older US PWR plants which were summarized by Yario (1982), about 50% of the tritium produced in the nuclear fuel is released through the steel cladding to the coolant under typical PWR operating conditions. This means that tritium release from the fuel is about identical for both cladding materials, but that this radionuclide is not retained by the steel cladding material as is the case with Zircaloy cladding. Since ^3H retention seems to be a specific material property of Zircaloy, the system Zircaloy–hydrogen shall be discussed in somewhat greater detail.

Spent Zircaloy fuel rod claddings usually show a hydrogen content of up to 100 ppm; in claddings having undergone high thermal load the hydrogen concentrations may total 500 ppm. A small fraction of this hydrogen content stems from the Zircaloy fabrication procedure, while the bulk of it is picked up during operation from the hydrogen resulting from Zircaloy oxidation by the reactor coolant. Hydrogen is soluble in Zircaloy up to a temperature-dependent concentration limit amounting to about $5 \cdot 10^{-2}$ ppm at 25 °C and to about 100 ppm at 300 °C. This means that at the reactor operating temperature most of the hydrogen in the Zircaloy is in the dissolved state, while during cooling-down it is precipitated as hydride. These platelet-shaped hydrides mainly appear in the cooler outer zones of the cladding; at lower hydrogen concentrations the composition $ZrH_{1.6}$ is assumed, at very high concentrations a value of ZrH_2 is more probable. Compared with these hydrogen concentrations, the amount of tritium released from the fuel to the cladding is insignificant; at a fuel burnup of 30 MWd/kg U and a release fraction of 50%, the ^3H concentration in the Zircaloy amounts to about 10^{-2} ppm. For this reason, it can be assumed that tritium behaves in a manner largely identical to that of normal hydrogen and that it is also precipitated into the hydride platelets during cooling down. The claim made by Grossmann and Hegland (1971), that ^1H is homogeneously distributed in spent fuel rod claddings whereas ^3H shows an inhomogeneous distribution, i. e. that there is no constant hydrogen isotope ratio in the different zones of the cladding, has not been confirmed up to now.

According to Motz (1962), the H_2 partial pressure over a Zr–1% H_2 alloy amounts to less than 10^{-4} Torr at 400 °C; at the considerably lower H_2 concentra-

tions present in Zircaloy claddings it can be expected to be significantly lower. There is no detailed data on the ^3H partial pressure in Zircaloy, but it can be anticipated that it is virtually identical to that of ^1H. Under heating of the material, ^3H is released in a manner similar to that of ^1H; however, the release kinetics shows remarkable differences depending on the gas phase above the specimen (Wölfle et al., 1981). In a flowing hydrogen atmosphere, tritium release from spent Zircaloy claddings starts at about 550 °C, reaches a rather sharp maximum at temperatures around 950 °C, followed by a fast termination of the release. In contrast, in a helium atmosphere under identical conditions a considerable tailing of the release occurs which is assumed to be due to a lack of recombination (or isotope exchange) partners in a hydrogen-poor environment, thus resulting in a slower decomposition of the ^3H fraction fixed in the hydride precipitates.

Investigations reported by Kearns (1972) on the diffusion coefficient of hydrogen in zirconium and Zircaloy over the temperature range 275° to 700 °C yielded values for the constant D_o of the Arrhenius' equation of $7.16 \cdot 10^{-3}$ cm²/s and an activation energy of 44.5 kJ/mol (all the data are average values for the three main directions of the material, with the specific values showing no pronounced differences).

According to Kunz et al. (1982), tritium diffusion in the Zircaloy matrix is not significantly affected by irradiation, at least at low radiation doses, nor by the concentration of oxygen and tin in the matrix, nor by the hydrogen concentration of the material as far as it does not exceed the solubility limits. Precipitated δ-hydrides, however, act as a sink for tritium, reducing the dissolved ^3H concentration and, therefore, the tritium diffusion current in the Zircaloy α phase. This means that at higher concentrations the effective diffusion coefficient for tritium decreases with increasing hydrogen content of the material. The temperature dependence of tritium diffusion in the Zircaloy α phase can be described by the equation

$$D_\alpha = D_o \cdot \exp(-E_a/R \cdot T)$$

with D_o being the frequency factor ($1.03 \cdot 10^{-3}$ cm²/s) and E_a the activation energy of 42.1 kJ/mol (Greger et al., 1980).

In the preceding sections the discrepancy between the fast tritium uptake into the Zircaloy and the very slow release from the Zircaloy cladding to the coolant was mentioned, the reasons for which have not yet been identified. It has been claimed that the oxide layer present at the outer cladding surface acts as a transport barrier; heating experiments in an inert atmosphere confirmed that ^3H release decreases with increasing thickness of the oxide layer at temperatures around 300 °C (Kunz et al., 1985 a). As an explanation of this difference in behavior from the inner surface oxide, which does not hamper tritium transport, a different composition of both oxide layers might be assumed. However, investigations performed by Bleier et al. (1983) showed that the tritium concentration in the outer oxide layer of PWR claddings is lower by a factor of about 80 than that in the Zircaloy base material and that the ^3H inventory in this oxide layer only amounts to about 10^{-20}% of the tritium inventory in the cladding. Even if a certain loss of ^3H from the oxide during the course of its isolation (selective dissolution of the base material

in HNO_3-HF at 0 °C) is postulated, no indication of a specific barrier effectiveness of the outer oxide layer can be derived from these experimental results.

On the other hand, these leaching experiments (Bleier et al., 1983) showed that the leaching medium is of great importance for ^3H release from spent Zircaloy cladding sections. Using boiling 7 M nitric acid, between 0.04 and 5% of the ^3H inventory was leached within 5 hours, even from cladding sections from which the fuel had been removed before by nitric acid dissolution; more than 90% of the leached tritium appeared as HTO. Leaching with boiling water, NaOH solution or $Ca(OH)_2$ solution resulted in a ^3H release lower by 2 to 4 orders of magnitude. In the initial phase of the nitric acid leaching, a steep increase in the cumulative amount of released ^3H was observed, which follows a $t^{1/2}$ dependence and might be interpreted as a diffusion-controlled mechanism; after 5 to 6 hours leaching time the ^3H release was virtually terminated. Since the release behavior of the other fission products showed an almost identical time behavior, it can be assumed that the nitric acid attack on the cladding surface is the reason for the ^3H release, rather than fission product diffusion in the base material. This assumption is consistent with results of leaching experiments in distilled water and dilute NaOH solution, which showed that the temperature dependence of ^3H release corresponds to an Arrhenius' function with activation energies of 48 kJ/mol for water and of 62 kJ/mol for NaOH solution (Kunz et al., 1985 b). More than 90% of the ^3H released to the solution appeared as HTO. The rates of ^3H release to solutions in the temperature range 20 to 100 °C were higher by about four orders of magnitude than those of release to a dry argon atmosphere at comparable temperatures.

Obviously, the low ^3H release from the cladding to the coolant during reactor operation is mainly due to its very firm bond in the metal, represented by the dissolution enthalpy of 37.4 kJ/mol. In this context, the results reported by Walter et al. (1973) are of interest: they showed that in the coated-particle fuel of high-temperature reactors the tritium released from the fuel is completely retained in the pyrolytic graphite zone; only at temperatures beyond 1700 K is it released from there, showing an activation energy of about 440 kJ/mol. Quite in contrast with this behavior, the ^3H produced in the outer graphite layer by neutron activation of lithium impurities is already released at temperatures of about 800 K. This difference in behavior underlines the importance of the specific properties of the base materials for the retention of ^3H.

Finally, the irradiated Zircaloy claddings contain ^{14}C generated from nitrogen impurities of the material by an (n,p) reaction. According to Bonka (1979), the power-related ^{14}C production amounts to 7.9 GBq/GWe · a · ppm N_2. The data determined by Bleier et al. (1987) are somewhat lower, yielding about 23 kBq/g Zircaloy in a BWR fuel rod at a burnup of 22.4 MWd/kg HM and a nitrogen content of the cladding material of 35 ppm; in a PWR mixed-oxide fuel rod cladding containing 40 ppm N_2 and irradiated to a fuel burnup of 35.7 MWd/kg HM, a ^{14}C concentration of 17 kBq/g Zircaloy was measured. The measurements also indicated that ^{14}C does not migrate in the cladding during reactor operation to a detectable extent.

From the experiments mentioned before, no conclusions can be drawn concerning the chemical state of ^{14}C in the Zircaloy matrix. In order to determine the

activity concentration of this radionuclide, the samples were dissolved by $KHSO_4$ melting; the specific analysis of the gases evolved during the melting procedure yielded about 30% CO_2 and 70% CO, which corresponds roughly to the Boudouard equilibrium at the melting temperature. With regard to the chemical state of the very small mass concentrations of ^{14}C, a solid solution of the traces in the matrix seems to be possible, with a formation of carbide compounds as well. Only a few experiments have been reported (mostly performed in the context of final storage of spent claddings) from which conclusions on the chemical nature of ^{14}C in Zircaloy can be drawn. Release experiments using non-irradiated Zircaloy thermally doped with ^{14}C (Kopp and Münzel, 1990) showed that in an inert atmosphere with extremely low oxygen content at 870 K, less than 1% of the total carbon content of the samples (limit of detection) was volatilized over 400 hours. Apparently, the oxygen of the oxide layer on the Zircaloy material does not contribute to the volatilization of carbon compounds at these temperatures. On the other hand, oxygen and H_2O impurities in the gas phase above the sample have a considerable influence on the release kinetics of ^{14}C. Using spent Zircaloy cladding specimens from a PWR, Smith and Baldwin (1993) observed that at temperatures up to 350 °C about 10% of the ^{14}C inventory appears to be readily available for release; they concluded that this fraction of ^{14}C is present in the crud layer (oxides deposited from the coolant during operation, see Section 4.4.) on the outer surface of the cladding and that this crud is significantly enriched in ^{14}C compared with the Zircaloy base material. The source of this ^{14}C content in the corrosion product oxides, however, is unknown.

3.2.6 Radionuclides in reactor core components and structural materials

In addition to the nuclear fuel rods with the cladding as discussed above, the reactor core also contains structural materials such as spacers, springs, bolts etc., as well as the fuel assembly upper and lower end structures, in which radionuclides are also produced by neutron activation reactions. Quite in contrast with the fuel itself, no generally valid data on the activity inventories of these structural materials can be established. The main reason for this are the differences in composition of the materials used by different manufacturers, in particular as regards impurities such as cobalt (which is the source element of ^{60}Co which is frequently the predominant radionuclide in irradiated structural materials). Another important fact is that the standard codes for activity calculations such as ORIGEN, KORIGEN or ANISN usually are quite accurate for the active zone of the reactor core, whereas in the outer regions (where the fuel assembly end pieces are located) only approximate values can be obtained, due to the steep axial decrease in neutron flux.

The fuel assembly spacer grids are fabricated either of Inconel or of Zircaloy materials, depending on fuel assembly type and manufacturer. While the central grids are located in the region of maximum neutron flux, the upper and the lower

grids are in the region of decreasing flux; for this reason, the activity inventories of the individual grids depend on their position in the fuel assembly. Detailed analyses of the longer-lived radionuclides produced during reactor operation (Robertson et al., 1990) showed that in Inconel spacer grids (Inconel 718 or 625) the nuclides ^{55}Fe and ^{63}Ni, which are activation products of the alloy main constituents, predominate, in addition to ^{60}Co resulting from cobalt impurities. At a fuel burnup of 32.7 MWd/kg U, their activity concentrations in the central grids are on the order of 3 GBq/g each, decreasing to about 1 GBq/g in the bottom and top spacer grids. Compared with these nuclides, ^{59}Ni and ^{54}Mn only play a minor role (all these data relate to the end of irradiation). ^{94}Nb, the (n,γ) activation product of the alloy constituent niobium (nominal value about 4%), shows activity concentrations in the central grids on the order of 4 MBq/g. It is surpassed by far by ^{93m}Nb, which is generated by an (n,n') reaction produced by fast neutrons (threshold energy 0.5 MeV) from stable ^{93}Nb, mainly because of its much shorter halflife (13.6 a vs. $2 \cdot 10^4$ a). The measured $^{93m}Nb : {}^{94}Nb$ activity ratios, on the order of 100, are higher by about three orders of magnitude than those that had been previously calculated. In Zircaloy spacer grids, ^{55}Fe and ^{125}Sb are the main radionuclides, with the latter being produced from the alloy constituent tin (1−2%) by the reaction chain mentioned in the preceding section. After a fuel burnup of 41.8 MWd/kg U, their activity concentrations in the central grids amount to about 0.1 GBq/g each. The other long-lived radionuclides such as ^{60}Co, ^{63}Ni and others show activity concentrations which are lower by two to five orders of magnitude.

Because of the differences in the composition of the various materials, in particular with respect to the impurity elements, the measured activity concentrations are only of limited applicability; more general information can be obtained from the specific activities, i. e. the radionuclide activities related to the masses of their parent elements. These values are fairly independent of the type of material used, at least as far as neutron self-shielding in the relevant structure does not have to be taken into account. When long-lived radionuclides are considered, the specific activities are directly proportional to the time-averaged neutron flux at the relevant position. As an example, the ^{60}Co, ^{55}Fe and ^{63}Ni specific activities of the Inconel spacer grids of a Westinghouse fuel assembly (average burnup 32.7 MWd/kg U) are shown in Fig. 3.27. (according to Robertson et al., 1990). The radionuclide with the by far highest specific activity is ^{60}Co; in the five central grids the specific activities do not show significant differences from each other while the values in the top and bottom grid are distinctly lower.

BWR fuel assemblies are surrounded by a fuel channel made of Zircaloy-2. The radionuclides generated here and their activity concentrations are on the same order of magnitude as in the fuel rod claddings.

The upper and lower end pieces of the fuel assemblies made of stainless steel are in the region of steeply decreasing neutron flux and, therefore, show comparatively low radionuclide inventories. According to investigations reported by Fischer (1987), the most important radionuclide induced in the stainless steel material (Stahl 1.4541) is ^{60}Co, which shows an activity concentration on the order of 500 MBq/g in the upper end piece of a PWR fuel assembly irradiated to a burnup of 32.2 MWd/kg HM (heavy metal) and a corresponding value of about 300

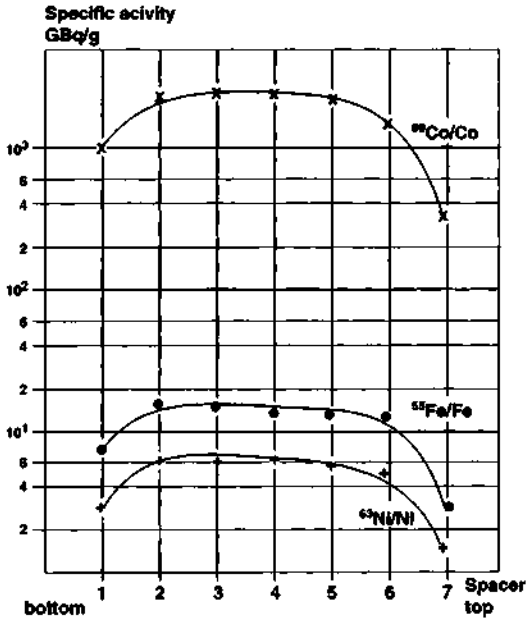

Figure 3.27. Specific activities of activation products in PWR fuel assembly spacer grids (according to Robertson, 1990)

MBq/g in the lower end piece. The axial gradient of activity concentration is more pronounced in the upper end piece than in the lower one. The ^{51}Cr activity concentrations are higher by a factor of about 5 than those of ^{60}Co; however, because of its low γ energy ^{51}Cr is of minor radiological significance. The other long-lived activation products such as ^{55}Fe, ^{63}Ni, ^{59}Ni are present in considerably lower activity concentrations. The activity concentrations of the radionuclides produced by (n,p) threshold reactions (^{54}Mn, ^{58}Co) are quite low due to the low proportion of fast neutrons in these well-thermalized regions. In general, one can say that the thermal neutron flux in the region of the end pieces is lower by two orders of magnitude than in the active zone of the reactor core. Comparable data were reported by Robertson et al. (1990) concerning the ^{60}Co, ^{55}Fe, ^{63}Ni and ^{59}Ni activity concentrations. In the stainless steel material examined by these authors, the ^{93m}Nb activity again was higher by factors of 50 to 100 than the ^{94}Nb activity, thus confirming the results obtained in the analyses of Inconel spacer grids; however, because of the considerably lower niobium content in stainless steel, both radionuclides are present in much lower activity concentrations.

Radionuclides are also produced by neutron activation in the core support structures, the core shroud and, finally, in the wall of the reactor pressure vessel. The relative proportions of the induced radionuclides depend on the particular type of material used (mild steels and stainless steels), while their activity concentrations are much lower than in the core inner materials, due to the much lower neutron flux to which these components are exposed.

Besides the fuel assemblies and the core structures, the reactor core contains additional components. Firstly, the neutron sources required for the startup operation of the reactor have to be mentioned. During the very first startup of the reactor, so-called primary neutron sources are employed containing either spontaneously fissioning nuclides such as ^{252}Cf or (α,n) sources such as ^{241}Am-Be. The main purpose of these sources is to obtain a measurable neutron flux even in the subcritical state of the core, the increase of which can be monitored. During reactor operation, the transuranium nuclides of the neutron sources are consumed by neutron-induced fission, resulting in a corresponding concentration of fission products in the component. After the first fuel cycle, the primary neutron sources are discharged from the reactor core and treated as radioactive waste. In addition to the fission products generated from the transplutonium element, the radionuclide inventory of such a spent primary neutron source consists of the activation products of the stainless steel cladding. The dominant long-lived activation products are ^{55}Fe, ^{59}Fe, ^{58}Co, ^{54}Mn, ^{51}Cr, all of which are generated from the alloy constituents, as well as ^{60}Co, ^{182}Ta and other activation products of impurities present in the alloy.

During startup in the following fuel cycles, as well as after a reactor shutdown in the course of a fuel cycle, so-called secondary neutron sources are used in many plants. Usually, they consist of an antimony–beryllium alloy encapsulated in a stainless steel cladding, in which ^{122}Sb (halflife 2.7 d) and ^{124}Sb (halflife 60.3 d) are generated during reactor operation. The high γ energy of ^{124}Sb of about 1.7 MeV induces the production of photoneutrons in ^{9}Be; its comparatively long halflife ensures the usability of such sources even after a reactor shutdown of several months. Normally, these sources stay in the reactor core for 5 to 7 years before they are discharged and treated as radioactive waste. In a PWR, one rod of the secondary neutron sources contains about 160 g of antimony which gives rise to a ^{124}Sb activity inventory of about $7 \cdot 10^5$ GBq after having reached the saturation level. In addition, activation products of constituents and impurities of the stainless steel cladding, such as ^{60}Co, ^{55}Fe, ^{51}Cr, ^{182}Ta, among others, contribute to the total activity inventory; their activities, however, are lower by far than the ^{124}Sb inventory just mentioned.

The PWR control rods designed for short-term reactivity control of the reactor core contain an Ag-In-Cd alloy in a stainless steel cladding. Depending on the current burnup state of the core, the control rods are inserted more or less deeply into the neutron field; therefore, in order to calculate the radionuclide production one has to assume an average position of the rod over a longer time period. In Table 3.12. results are given on the inventory of long-lived radionuclides in one rod after about 9 years of operation with the lower 50 cm being inserted into the active zone of the reactor core; part 1 means this 50 cm length, part 2 the 50 cm immediately beyond and part 3 the 50 cm beyond that. Each of these sections contains about 250 g silver, 47 g indium and 16 g cadmium. As can be seen, ^{110m}Ag is the predominant radionuclide, followed by indium and cadmium isotopes and by activation products of the stainless steel cladding. Due to the decrease in neutron flux, the sectoral activity inventory decreases rapidly with increasing height.

Table 3.12. Radionuclide inventories of a PWR control rod (activation time 3200 full power days)
(By courtesy of Siemens/KWU)

Radionuclide	Activity(GBq)		
	Part 1	Part 2	Part 3
^{110m}Ag	$7.0 \cdot 10^5$	$8.5 \cdot 10^4$	$3.0 \cdot 10^2$
^{113m}Cd	$2.3 \cdot 10^3$	$2.8 \cdot 10^2$	1.3
^{115m}Cd	$1.2 \cdot 10^3$	$1.5 \cdot 10^2$	0.21
^{114m}In	$3.9 \cdot 10^4$	$4.7 \cdot 10^3$	$1.0 \cdot 10^1$
^{55}Fe	$6.3 \cdot 10^3$	$1.7 \cdot 10^2$	4.2
^{59}Fe	$3.7 \cdot 10^2$	9.7	0.18
^{54}Mn	$1.2 \cdot 10^3$	$3.3 \cdot 10^1$	$3.7 \cdot 10^{-2}$
^{51}Cr	$2.0 \cdot 10^4$	$5.2 \cdot 10^2$	$1.1 \cdot 10^1$
^{63}Ni	$4.0 \cdot 10^2$	$1.1 \cdot 10^1$	0.26
^{58}Co	$3.2 \cdot 10^3$	$8.5 \cdot 10^1$	0.10
^{60}Co	$6.7 \cdot 10^3$	$8.9 \cdot 10^1$	1.4
^{182}Ta	$5.2 \cdot 10^3$	$1.4 \cdot 10^2$	1.0

In order to ensure a sufficiently negative Doppler coefficient of reactivity of a fresh reactor core, burnable neutron poisons are also employed. Either Gd_2O_3 is added to the fuel (see Chapter 1), or special absorber rods containing borosilicate glass with a B_2O_3 content of about 10% are employed, or boron carbide is deposited on the UO_2 pellet surfaces. Besides other radionuclides, tritium is produced in the boron-containing materials during reactor operation according to the nuclear reactions

$^{10}B\ (n,\alpha)\ ^7Li\ (n,n+\alpha)\ ^3H$	σ_1	$3.8 \cdot 10^{-21}\,cm^2$ (thermal)
	σ_2	$8.5 \cdot 10^{-26}\,cm^2$ (E_{th} 2.4 MeV)
$^{10}B\ (n,2\alpha)\ ^3H$	σ	$2.5 \cdot 10^{-26}\,cm^2$ (E_{th} 1.0 MeV)
$^{11}B\ (n,^9Be)\ ^3H$	σ	$1.5 \cdot 10^{-26}\,cm^2$ (E_{th} 10 MeV)

E_{th} refers to the neutron threshold energy for the particular reaction.

The determination of the ^3H activity concentrations in borosilicate glass and in B_4C absorber materials can be carried out in a manner similar to the ^3H determination in irradiated nuclear fuel, with the main difference being the dissolution procedure. According to Bleier et al. (1986) this consists of the following steps:

- Stainless steel cladding: Dissolution in boiling aqua regia.
- Boron glass and B_4C: Melting with NaOH, dissolution of the melt in water.
- Al_2O_3 insulation pellets: Melting with $KHSO_4$, dissolution of the melt in water.

The ^3H fractions present in the water and in the gas absorption duct are then purified as described above and subjected to liquid scintillation counting. The analytical error in this procedure is also on the order of about 6% (standard deviation).

Investigations reported by Bleier et al. (1986) of borosilicate glass absorber rods from a pressurized water reactor which were irradiated for 409 effective full power

days yielded an average ^3H activity concentration per absorber rod (296 g glass) of about 80 GBq. At an electrical gross power of the plant of 660 MW and a total amount of 432 glass absorber rods, a total ^3H production rate of 48 GBq/MWe · a was calculated from these analytical results.

This measured ^3H inventory is higher by about a factor of 5 than the amount calculated from the boron content of the glass, using the well-known neutron cross sections and the neutron fluence. The search for the source of the excess ^3H production resulted in the identification of the reaction

$$^6Li\ (n,\alpha)\ ^3H \qquad \sigma\ 9.4 \cdot 10^{-22}\ cm^2\ (thermal)$$

by which 2 GBq ^3H/ppm Li are produced during the irradiation period mentioned above; this means that a lithium content in the glass of about 30 ppm would be sufficient to explain fully the ^3H inventory measured. Lithium contents in this range are common in borosilicate glasses. This example demonstrates very clearly that under the irradiation conditions of a nuclear power plant, nuclear reactions which are frequently ignored may dominate the radionuclide production.

In BWRs, reactor load is controlled by control rods, the effective constituent of which is boron carbide B_4C encapsulated in stainless steel claddings. In this material, besides the activation products of steel constituents and impurities, considerable ^3H activities are produced as well during reactor operation by the nuclear reactions mentioned above. The investigations likewise reported on by Bleier et al. (1986) of BWR control rods which had been operated for about 3 years, yielded an average ^3H inventory of 32 GBq per rod. When comparing the experimentally determined ^3H activity concentrations with the calculated local boron burnup, the diagram shown in Fig. 3.28. is obtained, which also includes data reported by Eickelpasch et al. (1983). The scatter in the data has various causes: errors in sampling and analysis, but also the differences between ^{10}B burnup (caused by thermal neutrons) and the fast neutron flux in the inner core positions compared to the outer ones. Consistent with this assumption, the ^3H activity concentrations in the outer rods (No. 1, 4, 15) are located in the lower region of the scatter, those from the inner rods in the upper region.

These investigations showed that during operation the ^3H produced is almost quantitatively retained in the borosilicate glass matrix. Similarly, almost complete ^3H retention in boron carbide was observed, confirming the results obtained by Miles et al. (1974) with B_4C pellets from the liquid-metal cooled breeder reactor EBR-II. In the fill gas of the rods only very low ^3H fractions were detected, amounting to $1 \cdot 10^{-2}$% of the inventory in the borosilicate glass rods and to $2 \cdot 10^{-4}$% of the inventory in the boron carbide rods. The tritium fraction detected in the steel cladding material was also very low, $4 \cdot 10^{-3}$% (borosilicate glass) and $6 \cdot 10^{-3}$% (boron carbide) of the inventory. With regard to borosilicate glass, these experimental results contradict earlier claims where significant ^3H release from such burnable poison rods with stainless steel cladding was suspected (Yario, 1980). In the Al_2O_3 pellets which are inserted in the boron glass absorber rods in order to keep the glass column in position in the active zone, the ^3H activity concentration amounted to about 1% of that of the glass itself.

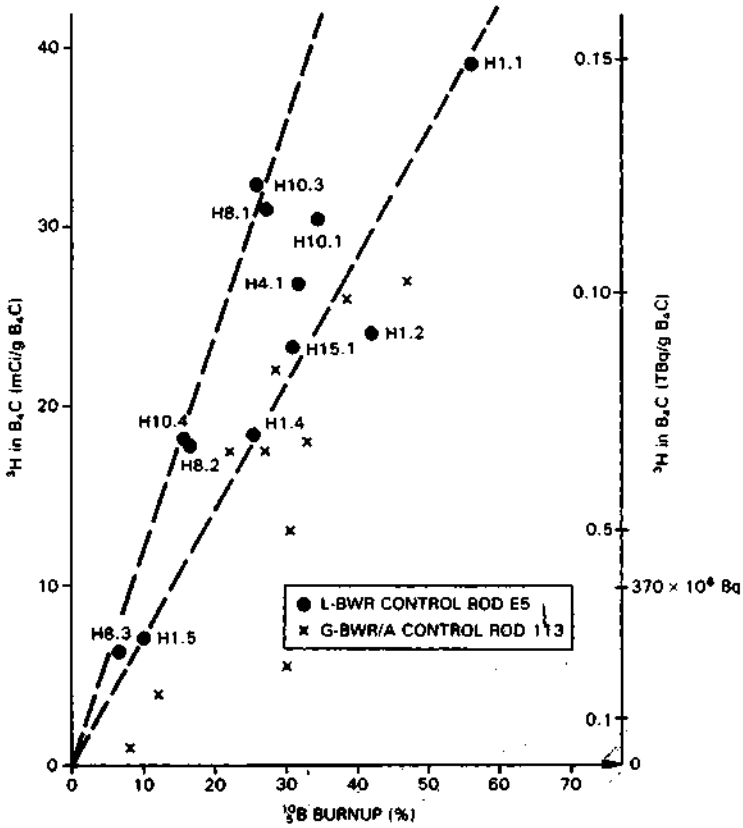

Figure 3.28. ^3H inventories in BWR control rods as a function of local ^{10}B burnup (Bleier et al., 1986; Copyright 1986 by the American Nuclear Society, La Grange Park, Illinois)

The clearly strong fixation of the tritium in the matrix leads to the conclusion that its chemical state is not dissolved atomic or molecular hydrogen, but that it is chemically bound to the base material. In the borosilicate glass a fixation to the oxide groups, potentially as an OH group, seems possible in principle. The recoil energy of the ^3H nucleus obtained as a consequence of the production reaction should be sufficiently high for the formation of such a chemical bond; on the other hand, these groups are assumed to be stable at the operating temperature of about 400 °C. These assumptions are supported by the results of the chemical analyses, in which more than 97% of the ^3H present in the boron glass was obtained as HTO, with only a negligible fraction appearing as HT. It cannot be ruled out, however, that the analytical procedure employed has an influence on the chemical state of the ^3H: in the course of NaOH melting and of dissolving the melt in water, an oxidation of originally present elemental tritium to HTO might occur. In the case of the analytical procedure used for analysis of the cladding material (dissolution in boiling aqua regia) such an effect seems certain: about 50% of the tritium

inventory appeared as HTO, whereas hydrogen dissolved in the steel matrix should be the thermodynamically most stable chemical state.

Post-irradiation heating experiments (Miles et al., 1974) showed that up to temperatures of about 970 K (700 °C) almost no release of ^3H from the B_4C matrix occurs. This strong fixation was attributed to chemical effects, i. e. formation of stable $C-^3H$ and $Li-^3H$ bonds (with the comparatively large excess ^7Li which is formed by the ^{10}B (n,α) reaction). The presence of H_2O or O_2 in the heating atmosphere resulted in a significant decrease of ^3H release rates, resulting probably from retention in the glassy B_2O_3 layer which forms on the surfaces of the B_4C particles.

In the event of a control rod cladding failure, B_4C is slowly decomposed by the reactor coolant and tritium contained in the dissolved fraction is transported to the coolant, thus potentially leading to the erroneous conclusion the ^3H has penetrated through the stainless steel cladding of the control rod. Likewise, during the analytical procedure when the control rod is decladded by dissolving the steel material in aqua regia, there is the danger that irradiated B_4C (which compound is insoluble in this solvent in the non-irradiated state) is partly attacked and the corresponding amount of tritium is released to the solution, where it might be erroneously attributed to the ^3H inventory of the cladding.

3.2.7 Determination of the neutron fluence in reactor core materials

3.2.7.1 General aspects

Some of the radionuclides produced in the materials inside the reactor pressure vessel can be used as monitors of the neutron fluence the components (e. g. the wall of the reactor pressure vessel) are exposed to during reactor operation. The materials located within the neutron field, such as the reactor pressure vessel steels, are subjected to nuclear reactions induced by fast neutrons. This can affect their mechanical properties over the course of the reactor lifetime. This applies, in particular, to the ductility of the materials: as a consequence of neutron irradiation, the ductility is reduced, leading to a shift of the Nil Ductility Transition (NDT) temperature towards higher values.

In general, the (n,γ) reactions induced by thermal neutrons, which lead to an element transmutation via β^- decay, are of no significance, since the resulting concentrations of such transmutation products (e. g. stable ^{55}Mn out of stable ^{54}Fe) are extremely small even after long-term irradiation. In contrast, the physical interactions leading to a change in the positions of the lattice atoms may result in a measurable effect. With regard to thermal and epithermal neutrons, such an effect is primarily caused by the γ recoil that occurs as a direct consequence of the neutron capture; by this recoil, the corresponding atom can be transported from its lattice position to an interstitial position. With fast neutrons, however, the inelastic scattering of neutrons at the lattice atoms is the most important damaging mechanism. The minimum neutron energy needed to remove an Fe atom from its position

in the Fe metal lattice is about 400 eV. The cross section for void formation σ_v, which was introduced by Rossin (1961) as a measure for the damage function in iron metal, is about $10^{-23}\,cm^2$ at a neutron energy of 0.004 MeV and about $3 \cdot 10^{-21}\,cm^2$ for 5 MeV neutrons. This steep increase in σ_v with increasing neutron energy is caused by the fact that in the inelastic scattering of neutrons with energies beyond 0.1 MeV the primary lattice atom receives a high kinetic energy, so that it is able to knock out additional lattice atoms from their original positions in an avalanche-like action. A part of the lattice damage is annealed again at the operating temperatures of the materials; however, the overwhelming fraction causes a permanent change in the properties of the materials. Another possible effect of fast neutrons on the properties of the materials is caused by the (n,α) reactions induced in particular at the copper impurities in the steel. The helium atoms produced by this reaction migrate to the grain boundaries where they form small bubbles which in turn may lead to a reduction in the materials ductility.

In order to determine as early as possible the extent of the change in the properties of the materials to be expected during the lifetime of the reactor pressure vessel, irradiation samples fabricated from the original materials of the pressure vessel wall (base material as well as weld material) are inserted into the reactor pressure vessel at positions where the neutron flux is higher by a factor of 5 to 10 than at the wall itself. By this measure, a time-lapse effect is obtained, so that potential changes can be detected much earlier than they would occur in the wall material. These samples are removed from the reactor pressure vessel at regular intervals, e. g. during refuelling shutdowns, and are subjected to appropriate examinations in the laboratory.

A meaningful assessment of potential changes in the properties of the materials measured in these examinations is only possible when the neutron fluence the sample had been exposed to in the course of reactor irradiation is known. This neutron fluence can be determined by measurement of the radioactivity of specific radionuclides which have been produced by neutron reactions. However, out of the great number of radionuclides produced, only a few can be reasonably applied as fluence monitors, since there are several limitations which have to be taken into account:

- The dependence of the cross section of the monitor reaction on the neutron energy must be exactly known and, moreover, it should be similar to that of the damaging cross section. Interference in the results caused by neutrons of other energy ranges should be small, so that a correction can be made with tolerable accuracy. This also applies to the burnup of the monitor nuclide by neutron capture, i. e. its neutron capture cross section should be small.
- In addition to the cross section, the essential nuclear data of the radionuclide formed, such as halflife and transition probability of the radiation to be measured, have to be known with sufficient accuracy.
- The halflife of the monitor radionuclide must be sufficiently long to render possible the integration of its production rate over the whole period under consideration and to make possible correction calculations for the intermediate decay which occurs, for example, during refuelling shutdowns. Taking into account the time periods to be considered here, only radionuclides with halflives of several years will fulfil this requirement properly.

- The limited space available in the irradiation capsule, as well as the neutron flux gradient over the capsule, require that the activation detectors have small dimensions; ideally, the monitor element is a constituent of the material under investigation, so that no particular detector is required.

Thus, the requirements to be put on a neutron fluence monitor are considerably more stringent than those required for neutron flux monitors whose exposure time is usually only a few hours or days (e.g in neutron activation analysis). Since there is no monitor element that fulfils all these requirements ideally, compromises have to be made. The monitor materials most frequently applied in neutron fluence determinations will be treated in some detail in what follows. The measurements of the activity of the product of the monitor reaction are used to calculate the corresponding neutron fluence, employing appropriate computer codes which also take into account influencing factors such as the dependence of the cross section on the neutron energy according to the prevailing neutron spectrum. In most cases, due to interruptions in the irradiation time (refuelling shutdowns, operation at reduced load), the whole irradiation period has to be subdivided into several homogeneous intervals on the basis of the reactor operation history.

Because of the significance of neutron fluence determinations for reactor safety considerations, standard procedures have been developed and published by the American Society for Testing and Materials (ASTM) as well as by the German DIN Institute.

3.2.7.2 Cobalt monitor

The nuclear reaction $^{59}Co\ (n,\gamma)\ ^{60}Co$ is the most frequently used monitoring reaction for thermal neutrons over longer exposure periods. The only stable cobalt isotope ^{59}Co reacts with thermal neutrons to ^{60m}Co as well as directly to ^{60}Co; since ^{60m}Co decays almost completely (99.74%) to ^{60}Co with a halflife of 10.2 min it can be ignored in the determination of neutron fluence data. Thus, in practice, ^{60}Co can be regarded as the only reaction product. Both γ transitions of ^{60}Co at 1.17 and 1.33 MeV show transition probabilities of 100% each.

In most cases, as a fluence monitor small disks or wires of an Al-Co alloy with 0.1 to 1% Co are used; by such a dilution of the monitor substance, self-shielding and flux depression effects are avoided. In general, since interfering radionuclides produced in the diluting element are small, chemical separations before activity measurement of ^{60}Co are normally not needed. Frequently, the cobalt impurities in stainless steels, which are in the range of 100 to 1000 ppm, can be directly used as a fluence monitor; in such cases, however, the accurate cobalt concentration in the material has to be additionally determined by chemical analysis.

The thermal neutron cross section of ^{59}Co is $3.73 \cdot 10^{-23}\,cm^2$, the newly formed ^{60}Co shows a corresponding value of $2.0 \cdot 10^{-24}\,cm^2$. These comparatively high values result in a burnup of both isotopes in the course of the irradiation, so that the number of ^{60}Co atoms present at the end of irradiation (even when corrected

for radioactive decay during irradiation) is smaller than the number of actually occurring nuclear reactions. The degree of burnup of both isotopes depends on the neutron flux and the irradiation time. When the neutron field at the irradiation position contains a significant fraction of epithermal neutrons, as is the case in light water reactors in the reactor core and its immediate vicinity, then the burnup induced by epithermal neutrons has to be taken into account by appropriate calculations. ^{59}Co is not a pure 1/v absorber; its neutron capture cross section shows resonances in the epithermal region, with the most significant one being at a neutron energy of about 140 eV. This means that the (n,γ) reaction leading to ^{60}Co is not only induced by thermal neutrons but that epithermal neutrons will also deliver a significant contribution, with the value for the resonance integral being $7.0 \cdot 10^{-23}\,cm^2$. In order not to obtain too high values for the thermal neutron fluence, the epithermal activation has to be corrected for in the evaluation of the analytical data. This requires knowledge of the ratio φ_{epi}: φ_{th} at the position of the fluence monitor, which can be experimentally determined by means of the cadmium ratio, i. e. by a simultaneous irradiation of two monitors, one of them shielded by cadmium foil and the other unshielded. In the irradiation capsule of power reactors, however, this technique usually can not be applied because of the limited space there; therefore, in such cases one has to calculate the ratio from the neutron spectra at different positions of the reactor core.

The danger of errors in the experimental determination of the thermal neutron fluence caused by other nuclear reactions is small. ^{60}Co is also produced in stainless steels by (n,p) reaction from ^{60}Ni and by (n,α) reaction from ^{63}Cu, with both reactions being induced by fast neutrons. Since the cross sections of both reactions are very small ($5 \cdot 10^{-28}\,cm^2$ and $4.2 \cdot 10^{-28}\,cm^2$, respectively), no interference is to be expected in light water reactors when monitor materials of the usual purity are used. Due to the 5.28-year halflife of ^{60}Co, details of the irradiation history of this monitor material can only be neglected at gross irradiation periods of up to one year; for longer periods, interruptions in the operation history of the plant, such as shutdowns, load reductions etc., have to be corrected for.

3.2.7.3 Iron–manganese monitor.

Due to its favorable properties, the nuclear reaction ^{54}Fe (n,p) ^{54}Mn is one of the standard reactions for the determination of fast neutron fluences. Since iron is the main constituent of most of the materials to be investigated, this determination can be carried out without the use of a specific fluence monitor. The halflife of ^{54}Mn of 312 days permits the use of this nuclear reaction for irradiation periods of up to about two years, provided that corrections for details of the irradiation history are made. The favorable energy of the ^{54}Mn γ ray of 0.835 MeV (transition probability 100%) frequently allows a direct activity measurement by use of a high-resolution Ge detector; only in the investigation of materials with low iron contents such as Zircaloy, a chemical isolation of the monitor nuclide prior to the activity measurement is recommended. This can be carried out, for example, by precipita-

tion of MnO_2 from sulfuric acid solution. In general, the most important interference is caused by ^{58}Co and its γ ray at 0.81 MeV, in particular in alloys with a higher nickel content. ^{59}Fe produced by an (n,γ) reaction shows activity concentrations usually on the same order of magnitude as ^{54}Mn, which means that no interference in the activity measurement is to be expected. Longer decay times of the monitor material before measurement will shift the activity ratios in both cases in favor of ^{54}Mn.

The effective threshold energy of the reaction amounts to about 3 MeV and, therefore, is somewhat too high for the evaluation of the neutron impact on the materials. Various authors give the cross section for a non-moderated fission neutron spectrum as different values in the range 6.0 to $8.9 \cdot 10^{-26}\,cm^2$, with the scatter probably being caused by differences in the standardization of the actual neutron spectrum to a pure fission spectrum; currently, $7.8 \cdot 10^{-26}\,cm^2$ is regarded as the best value (with an uncertainty of 5%). However, this value only applies for a non-moderated fission neutron spectrum and not for that at the irradiation position; therefore, corrections have to be applied on the basis of the differential cross sections and the particular neutron spectrum at the position in question. For the determination of the fluence of neutrons showing energies beyond 0.1 MeV, a cross section of $5.4 \cdot 10^{-26}\,cm^2$ has been recommended, for neutrons with energies greater than 1 MeV a value of $1.10 \cdot 10^{-25}\,cm^2$. As was mentioned above, these typical cross sections are valid only for the neutron spectrum for which they have been calculated. For other locations inside the reactor pressure vessel, the cross sections have to be re-evaluated on the basis of the relevant neutron spectra.

Competing nuclear reactions leading to an increase or a decrease in the number of ^{54}Mn atoms produced are of little significance and can be ignored. The burnup of ^{54}Fe with a thermal neutron cross section of $2.3 \cdot 10^{-24}\,cm^2$ amounts to 0.2% at a thermal neutron fluence of $10^{21}\,cm^{-2}$; likewise the thermal neutron cross section of ^{54}Mn is less than $1 \cdot 10^{-23}\,cm^2$. The production of ^{54}Mn by an (n,2n) reaction from stable ^{55}Mn with the very low cross section of $2 \cdot 10^{-28}\,cm^2$ does not interfere in samples with an Fe : Mn ratio greater than 1.

3.2.7.4 Nickel–cobalt monitor

Frequently the nuclear reaction ^{58}Ni (n,p) ^{58}Co is used for determination of the fast neutron fluence, but it has two severe drawbacks when compared to the Fe-Mn reaction described above: The rather short halflife of ^{58}Co of 71.3 days limits the application of this reaction to irradiation times of less than 150 days, even when the irradiation history of the sample is taken into account. In addition, the complex nature of the nuclear reaction requires expensive calculations when accurate results are required. On the other hand, the intense γ ray of ^{58}Co at 0.81 MeV (transition probability 99.5%) can be easily measured using a Ge detector, in most cases making chemical separation work unnecessary.

The effective threshold energy of the reaction is about 3 MeV, which means it is very similar to that of the ^{54}Fe (n,p) ^{54}Mn reaction. The total cross section values

for the production of ^{58}Co and ^{58m}Co as given in the literature differ between $7.6 \cdot 10^{-26}$ and $1.2 \cdot 10^{-25}\,cm^2$; this is probably due to differences in the fission neutron spectra used in the different investigations. Currently, a best value of $1.05 \cdot 10^{-25}\,cm^2$ with an uncertainty of about 5% is assumed. From this value a typical cross section of $7.5 \cdot 10^{-26}\,cm^2$ for the determination of neutrons with energies greater than 0.1 MeV and of $1.58 \cdot 10^{-25}\,cm^2$ for neutrons beyond 1 MeV has been calculated.

With fast neutrons, ^{58}Ni reacts to form not only ^{58}Co, but also the short-lived ^{58m}Co which decays completely to ^{58}Co with a halflife of 9.13 h and an associated γ ray of 0.025 MeV energy. The ^{58m}Co production rate amounts to about 27% of the total reaction rate leading to ^{58}Co, with the accurate value depending on the prevailing neutron spectrum. If one assumes a total cross section for the (n,p) reaction of $1.05 \cdot 10^{-25}\,cm^2$, then the specific cross section of the reaction $^{58}Ni(n,p)^{58m}Co$ is $2.8 \cdot 10^{-26}\,cm^2$. Since the thermal neutron cross section of ^{58}Ni is approximately $4.4 \cdot 10^{-24}\,cm^2$, the burnup of this nuclide during irradiation can be ignored. On the other hand, the reaction products ^{58m}Co and ^{58}Co show thermal neutron absorption cross sections of $1.7 \cdot 10^{-19}$ and $1.65 \cdot 10^{-21}\,cm^2$, respectively, resulting in a final ^{58}Co activity considerably lower than would correspond to the number of (n,p) reactions occurring during the exposure. For this reason, the analytical result has to be corrected for the burnup, using a rather complex equation that in turn may lead to additional errors in the result. As a consequence, this reaction is not recommended as a neutron fluence monitor for longer exposure times at a rather high flux of thermal neutrons.

3.2.7.5 Niobium monitor

The nuclear reaction ^{93}Nb (n,n') ^{93m}Nb, first proposed by Hegedüs (1971) as a monitor for fast neutron reactions, is virtually free from the problems and interferences of the reactions mentioned above. Its effective threshold energy of about 0.5 MeV and a comparatively flat excitation function for inelastic neutron scattering are properties which are very similar to those of the neutron damage reactions. The cross section of the reaction in a non-moderated ^{252}Cf fission neutron spectrum was reported by Shani (1980) to be $1.88 \cdot 10^{-24}\,cm^2$. The halflife of ^{93m}Nb is long enough to permit its use as a monitor for long-term irradiations; currently, the best value is assumed to be 16.13 ± 0.14 years. Interfering nuclear reactions such as the production of ^{94}Nb by thermal neutrons and the resulting target burnup are insignificant under prevailing conditions and, therefore, no corrections have to be made to the experimental results.

In addition to these favorable properties there is a severe drawback resulting from the radiation properties of ^{93m}Nb. Since the 30 keV transition of this radionuclide is completely converted, the K_a X-ray of ^{93}Nb at 16.6 keV has to be used in the activity measurements. Another difficulty results from the tantalum impurity content which is often present in niobium metal, since the ^{182}Ta activity produced by an (n,γ) reaction leads to fluorescence excitation of niobium. Therefore, a direct

activity measurement of the niobium foils or wires which are frequently used is not possible. Martin et al. (1977) described a technique by which these difficulties can be avoided. In this analytical procedure, the monitor is dissolved in a nitric acid –hydrofluoric acid mixture and an appropriate aliquot of the solution is soaked onto a filter disk. The dilution of activity which is obtained by this technique reduces the fluorescence radiation to a low level, which no longer interferes with the ^{93m}Nb measurement. The activity measurement can be carried out using an Si(Li) detector with small layer thickness by which X-ray spectra of sufficient resolution are obtained. If ^{93m}Nb standard reference materials (which, for example, can be obtained from the German Physikalisch-Technische Bundesanstalt as a solid specimen showing a 3σ uncertainty of 3%) are not available, other radionuclides such as ^{57}Co and ^{85}Sr with similar X-ray energies can be used for calibration of the measurement system. By this means an accuracy of about 5% can be achieved for the ^{93m}Nb activity measurement; in addition, the uncertainties in the nuclear data of ^{93m}Nb have to be considered in the evaluation of the measured data. Since these uncertainties are comparable to those of the other monitors and because of the favorable nuclear poperties of the niobium monitor, it has gained increasing significance in the determination of the fast neutron fluence, in particular of the reactor pressure vessel.

In special cases, one can take advantage of the fact that most stainless steels contain niobium in the range of 0.2 to 0.8% (depending on the carbon content of the material) as a stabilizer. The other radionuclides produced in the steel sample during irradiation, however, make a chemical isolation of ^{93m}Nb before activity measurement necessary. By ion exchange from hydrofluoric acid and elution of the adsorbed niobium with HF-NH_4Cl solution, a specimen is obtained which is of sufficiently high purity for activity measurement as well as for determination of chemical yield. For this type of neutron fluence determination, small steel samples in the range 10 to 100 mg are sufficient, which can be obtained by scraping or drilling from the inner surface of the reactor pressure vessel (Schweighofer et al., 1983). In this manner, fast neutron fluence determinations can be made directly from the stainless steel plating of the reactor pressure vessel, omitting the usual extrapolation from the location of the irradiation samples to the wall and the possible errors associated with it. As can be seen from Fig. 3.29., the angular neutron fluence distribution along the inner surface of the thermal shield of a PWR can be determined in good agreement with the theoretically calculated values by measurement of the specific ^{93m}Nb and ^{54}Mn activities in small specimens taken from the surface by scraping (Polke, 1993).

Similarly, Baers and Harsanen (1993) have determined the specific ^{93m}Nb activities in reactor pressure vessel steel (containing niobium in the ppm range) and plating (~ 1% Nb). Niobium was isolated from the other radionuclides by ion exchange chromatography and ^{93m}Nb measured by liquid scintillation spectrometry; niobium mass in the samples was determined by inductively-coupled plasma mass spectrometry. In this way, it was possible to rule out interferences caused by other radionuclides. However, the data to be used for the calculation of fast neutron fluence can be impaired by ^{93m}Nb which is formed by β^+ decay of ^{93}Mo which is an (n,γ) product of stable ^{92}Mo. This interference becomes significant when the

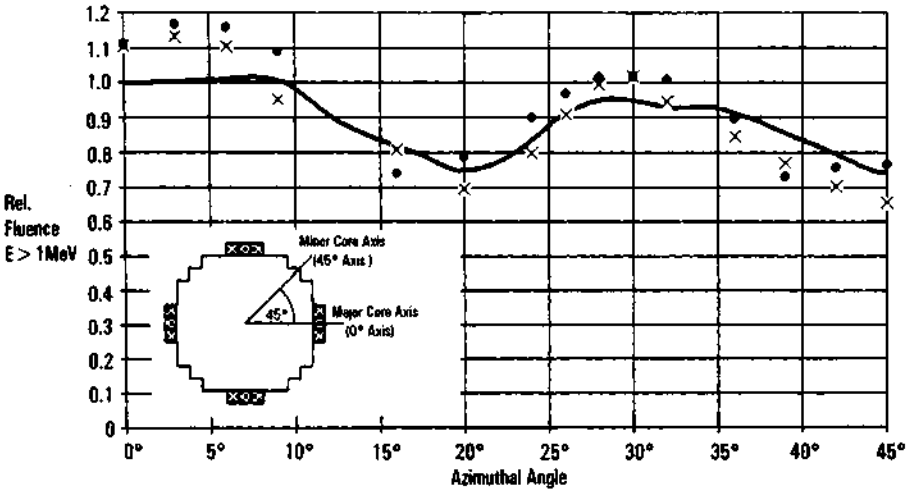

Figure 3.29. Calculated and measured angular neutron fluence distribution along the inner surface of a PWR thermal shield (• niobium monitor; x iron monitor)
(Polke, 1993)

ratio Nb : Mo in the material is below 0.01, which might pertain in the steel base material with its low niobium content; the determinations of the fast neutron fluence in the stainless steel plating are not impaired by this nuclear reaction.

3.2.7.6 Fission monitors

Some actinide isotopes which are fissile by fast neutrons such as ^{232}Th, ^{238}U and ^{237}Np have advantages when used as fast neutron fluence monitors. The effective threshold energies of fission are in the range of 1 to 2 MeV, i. e. sufficiently low for monitoring of the neutron impact on the materials. Moreover, when an appropriate fission product nuclide such as ^{137}Cs is measured, which has a long halflife, well-known nuclear data and easily-to-measure radiation properties, many of the difficulties mentioned above do not arise. From the basic investigations in nuclear physics, the essential data of the nuclear reactions such as the fission cross section and its dependence on the neutron energy are known to a high degree of accuracy.

The essential drawback of the fission monitors is the danger of severe errors in the results due to breeding reactions leading to nuclides which can be fissioned by thermal or epithermal neutrons (e. g. ^{233}U, ^{239}Pu). In order to preclude such interference, the fission monitor has to be wrapped into a cadmium or boron shielding which is sufficiently thick for protection against even high fluxes of thermal and epithermal neutrons. Such a shielding requires additional space in the irradiation capsule, restricting the applicability of the fission monitors despite their other favorable properties. The selection of the fission monitor to be applied is

often dictated by pragmatic considerations. Because of the difficulties of obtaining isotopically pure ^{238}U or ^{237}Np, frequently ^{232}Th is preferred, since thorium is a monisotopic element. In most cases this monitor is inserted into the capsules als ThO_2.

References Section 3

Assmann, H., Stehle, H.: The behaviour of uranium oxide fuels in nuclear reactors. Gmelin Handbook of Inorganic Chemistry, 8th Edition, "Uranium", Suppl. Vol. A 4, p. 1–138 (1982)

Assmann, H., Stehle, H.: Chemie in Reaktorbrennstäben mit oxidischen Kernbrennstoffen. Chemiker-Ztg. **108**, 65–82 (1984)

Baers, B. L., Hasanen, E. K.: Neutron flux estimations based on niobium impurities in reactor pressure vessel steel. Paper presented at the 8. ASTM–EURATOM Symposium on Reactor Dosimetry. Vail, Colorado, USA, 1993

Baumgärtner, F.: Paper presented at the Tagung of the GDCh-Fachgruppe Nuklearchemie, Hamburg 1990

Beck, M.: Conversion of reprocessed uranium. Nuclear Europe V, (5), 32–34 (1985)

Benedict, U., Coquerelle, M., de Bueger, J., Dufour, C.: A study of local composition variations in irradiated oxide fuel by X-ray diffractometry. J. Nucl. Materials **45**, 217–229 (1972/73)

Berndt, R.: Verification of spent PWR fuel data using the ^{154}Eu, ^{134}Cs and ^{137}Cs activities. Kernenergie **31**, 59–63 (1988)

Besmann, T. M., Lindemer, T. B.: Chemical thermodynamics of the system Cs-U-Zr-H-I-O in the light water reactor fuel-cladding gap. Nucl. Technology **40**, 297–305 (1978)

Bleier, A., Beuerle, M., Pezzei, G., Wolfrum, K.: Bestimmung des ^{3}H-Gehaltes und ^{3}H-Auslaugverhaltens von Zircaloy-Hüllen. Abschlußbericht Vertrags-Nr. KfK 220/D2/518426 (1983)

Bleier, A., Kroebel, R., Neeb, K. H., Schneider, E.: Tritium inventories and behaviour in Zircaloy cladding of spent light-water reactor fuel rods. Proc. Internat. Topical Meeting on Fuel Reprocessing and Waste Management, Jackson Hole, Wyoming, USA, 1984, Vol. 1, p. 238–248

Bleier, A., Neeb, K. H., Gelfort, E., Mischke J.: Evaluation of the tritium content in light water reactor control and absorber rods to obtain data for the fuel cycle backend. Nucl. Technology **74**, 152–163 (1986)

Bleier, A., Neeb, K. H., Kroebel, R., Wiese, H. W.: Carbon-14 inventories and behaviour in LWR spent fuel rods during reprocessing. Proc. Internat. Conf. on Nuclear Fuel Reprocessing and Waste Management "Recod 87", Paris 1987, Vol. 3, p. 1089–1094

Bonka, H.: Produktion und Freisetzung von ^{3}H und ^{14}C durch Kernwaffenversuche, Testexplosionen und kerntechnische Anlagen einschl. WA-Anlagen. Wiss. Symposium Inst. f. Strahlenhygiene des Bundesgesundheitsamtes, Berlin 14.–15.11.1979.

Booth, A. H.: A method of calculating fission gas diffusion from UO_2 fuel and its application to the X-2-f loop test. Report AECL CRDC-721 (1957)

Booth, A. H.: A suggested method for calculating the diffusion of radioactive rare gas fission products from UO_2 fuel elements. Report AECL DCI-27 (1957)

Boukis, N., Henrich, E.: Iodine-129 analysis in nuclear fuel solutions. Radiochimica Acta **54**, 103–108 (1991)

Bowsher, B. R.: Fission-product chemistry and aerosol behaviour in the primary circuit of a pressurized water reactor under severe accident conditions. Progress in Nuclear Energy **20**, 199–233 (1987)

Broothaerts, J., Vandersteene, J., De Regge, P., Monsecour, M., Van De Velde, J.: Axial distribution of tritium in Zircaloy-clad fuel rods. European Applied Research Reports **4**, 561–586 (1982)

Castleman, A. W.jr., Tang, I. N.: Vaporization of fission products from irradiated fuels. I. Experimental method and general fission product behavior. Nucl. Sci. Engng. **29**, 159–164 (1967)

Castleman, A. W.jr., Tang, I. N., Munkelwitz, H. R.: The chemical states of fission product iodine emanating into high temperature aqueous environment. J. Inorg. Nucl. Chem. **30**, 5–13 (1968)

Castleman, A. W.jr., Tang, I. N.: Vaporization of fission products from irradiated uranium II. Some observations on the chemical behaviour of fission products iodine and cesium. J. Inorg. Nucl. Chem. **32**, 1057–1064 (1970)

Catlow, C. R. A.: The effects of dopants on the redox properties of oxide fuel. Proc. IAEA Specialists Meeting on Internal Fuel Rod Chemistry, Erlangen, FRG, 1979; IAEA Report IWG FPT/3, p. 127–130 (1979)

Collins, J. L., Osborne, M. F., Lorenz, R. A., Malinauskas, A. P.: Fission product iodine and cesium release behavior under light water reactor accident conditions. Nucl. Technology **81**, 78–94 (1988)

CRC Handbook of Chemistry and Physics, 60th Edition, Ed. R. C. Weast, CRC Press Inc., Boca Raton, Florida 1980

Cronenberg, A. W., Osetek, D. J., Reed, P. R.: Analysis of iodine chemical form for the Severe Fuel Damage Scoping Test and 1–1 Test. Proc. Symposium on Chemical Phenomena Associated with Radioactivity Releases During Severe Nuclear Plant Accidents. Anaheim, Calif., USA, 1986; Report NUREG/CP-0078, p. 6/59–72

Davis, W.jr.: Carbon-14 production in nuclear reactors. Report ORNL/NUREG/TM-12 (1977)

Eggleton, A. E. J., Atkins, D. H. F.: The identification of trace quantities of radioactive iodine compounds by gas-chromatography and effusion methods. Radiochim. Acta, **3**, 151–158 (1964)

Eickelpasch, N., Seepolt, R., Müllauer, J., Spalthoff, W.: Operational experience with and post-irradiation examinations on boiling water reactor control rods. Nucl. Technology **60**, 362–366 (1983)

Fischer, U.: Aktivierung von Endstücken eines DWR-Brennelementes. Atomwirtschaft **32**, 38–41 (1987)

Garzarolli, F., Neeb, K. H., Peehs, M., Steinberg, E., Würtz, R.: Untersuchungen zum Beitrag des Spaltiods auf das Bruchverhalten von Zircaloy-Hüllrohren. Proc. Reaktortagung Dt. Atomforum 1974, p. 408–411

Goll, W., Fuchs, H.-P., Manzel, R., Schlemmer, F. U.: Irradiation behavior of UO_2/PuO_2 fuel in light water reactors. Nucl. Technology **102**, 29–46 (1993)

Goode, J. H., Cox, C. M.: The distribution of fission product tritium in a Zircaloy-clad UO_2 blanket rod from PWR-1. Report ORNL-TM-2994 (1970)

Grimes, R. W., Ball, R. G. J., Catlow, C. R. A.: Site preference and binding of iodine and caesium in uranium dioxide. J. Phys. Chem. Solids **53**, 475–484 (1992)

Green, L. W., Elliot, N. L., Miller, C. F., Leppinen, J. J.: Mass spectrometric determination of burnup of $(U,Pu)O_2$ fuel using nanogram quantities of isotopes. J. Radioanal. Nucl. Chemistry, Articles **131**, 299–309 (1989)

Greger, G., Münzel, H., Kunz, W., Schwierczinski, A.: Diffusion of tritium in Zircaloy-2. J. Nucl. Materials **88**, 15–22 (1980)

Grosmann, L. N., Hegland, J. O.: Tritium distribution in high-power Zircaloy fuel elements. Report GEAP-12205 (1971)

Hegedüs, F.: Détecteur de fluence des neutrons rapides basé sur la reaction ^{93}Nb (n,n') ^{93m}Nb. Report EIR 195 (1971)

Kearns, J. J.: Diffusion coefficient of hydrogen in alpha zirconium, Zircaloy-2 and Zircaloy-4. J. Nucl. Materials **43**, 330–338 (1972)

Kleykamp, H.: The chemical state of the fission products in oxide fuels. J. Nucl. Materials **131**, 221–246 (1985)

Kleykamp, H. (a): Nachuntersuchungen an einem Biblis A-Brennstab nach 5,9% Abbrand. Atomwirtschaft **35**, 256–258 (1990)

Kleykamp, H. (b): Post-irradiation examination and composition of the residues from nitric acid dissolution experiments of high-burnup fuel. J. Nucl. Materials **171**, 181–188 (1990)

Kleykamp, H., Paschoal, J. O., Pejsa, R., Thümmler, F.: Composition and structure of fission product precipitates in irradiated oxide fuels: Correlation with phase studies in the Mo-Ru-Rh-Pd and BaO-UO_2-ZrO_2-MoO_2 systems. J. Nucl. Materials **130**, 426–433 (1985)

Kopp, D., Münzel, H.: Release of volatile carbon-14 containing products from Zircaloy. J. Nucl. Materials **173**, 1–6 (1990)

Kunz, W., Münzel, H., Helfrich, U.: Diffusion of tritium in Zircaloy: Influence of low-irradiation damage, oxygen concentration and formation of δ-hydrides. J. Nucl. Materials **105**, 178–183 (1982)

Kunz, W., Münzel, H., Kunz, U. (a): Tritium release from Zircaloy-2: Dependence on temperature, surface conditions and composition of surrounding medium. J. Nucl. Materials **136**, 6–15 (1985)

Kunz, U., Kunz, W., Münzel, H.(b): Tritium-Abgabe aus Zircaloy an wäßrige Lauglösungen. Zeitschr. Metallkde. **76**, 546–549 (1985)

Lawrence, G. T.: A review of the diffusion coefficient of fission-product rare gases in uranium dioxide. J. Nucl. Materials **71**, 195–218 (1978)

Lewis, B. J.: Fisson product release by recoil and knockout. J. Nucl. Materials **148**, 28–42 (1987)

Lewis, B. J., Hunt, C. E. L., Iglesias, F. C.: Source term of iodine and noble gas fission products in the fuel-to-sheath gap of intact operating nuclear fuel elements. J. Nucl. Materials **172**, 197–205 (1990)

Lieser, K. H.: Einführung in die Kernchemie, Verlag Chemie, Weinheim, 3. Edition, 1991

Lorenz, R. A., Collins, J. L., Malinauskas, A. P., Kirkland, O. L., Towns, R. L.: Fission product release from highly irradiated LWR fuel. Report NUREG/CR-0722 (1980)

Manzel, R., Eberle, R.: Fission gas release at high burnup and the influence of the pellet rim. Proc. International Topical Meeting on LWR Fuel Performance "Fuel for the 90s", Avignon, France, 1991, p. 528–537

Manzel, R., Sontheimer, F., Würtz, R.: The radial distribution of fission gases and other fission products in irradiated PWR fuel. J. Nucl. Materials **126**, 132–143 (1984)

Martin, J. A., Braun, R., Stöckert, H.: Radiochemische Auswertung des Niob-Monitors zur Erfassung der Fluenz schneller Neutronen. I. Bestimmung der ^{93m}Nb-Zerfallsrate. Radiochem. Radioanal. Letters **28**, 59–66 (1977)

Matzke, Hj.: Oxygen potential in the rim region of high burnup UO_2 fuel. J. Nucl. Materials **208**, 18–26 (1994)

Matzke, Hj., Blank, H., Coquerelle, M., Lassmann, K., Ray, I. L. F., Ronchi, C., Walker, C. T.: Oxide fuel transients. J. Nucl. Materials **166**, 165–178 (1989)

Matzke, Hj., Ottaviani, J., Pellotiero, D., Rouault, J.: Oxygen potential of high burnup fast breeder oxide fuel. J. Nucl. Materials **160**, 142–146 (1988)

Miles, C. C., Wexler, S., Ebersole, E. R.: Tritium retention in EBR-II-irradiated boron carbide. Report ANL-8107 (1974)

Motz, J.: Über das System Zirkonium–Wasserstoff. Zeitschr. Metallkd. **53**, 770–774 (1962)

Neeb, K. H.: Zum Verhalten von Spaltprodukten im Kernbrennstoff von Leichtwasserreaktoren. In. F. Baumgärtner (Herausg.), Chemie der Nuklearen Entsorgung, Thiemig-Taschenbücher **65**, 56–88 (1978)

Neeb, K. H., Haas, E., Bleier, A., Würtz, R., Wiencken, R.: ^{3}H- und ^{14}C-Inventare und -Verteilung in abgebrannten LWR-Brennstäben. Abschlußbericht Vertrags-Nr. KfK/PWA 220/D1/465692 (1980)

Neeb, K. H., Karnath, G., Richter, H., Schweighofer, W., Stöckert, H.: Radiochemische Untersuchungen zur Verteilung von ^{129}I und ^{3}H in bestrahltem Kernbrennstoff aus Leistungsreaktoren. J. Radioanal. Chem. **32**, 523–531 (1976)

Peehs, M., Kaspar, G., Neeb, K. H.: Cs and I release source terms from irradiated LWR fuel. J. Nucl. Materials **119**, 284–290 (1983)

Peehs, M., Manzel, R., Schweighofer, W., Haas, W., Haas, E., Würtz, R.: On the behaviour of cesium and iodine in light-water reactor fuel rods. J. Nucl. Materials **97**, 157–164 (1981)

Peehs, M., Neeb, K. H., Steinberg, E.: Untersuchungen zum Verhalten von Spaltiod in Zry-4-Hüllrohren. Proc. Reaktortagung Dt. Atomforum 1973, p. 385–388

Polke, E.: Reactor pressure vessel fluence surveillance by scraping samples from the inner surface of the thermal shield in the nuclear power plant Obrigheim in Germany (KWO) before and after core modifications intended to reduce RPV neutron flux density. Paper presented at the 8. ASTM–EURATOM Symposium on Reactor Dosimetry. Vail, Colorado, USA, 1993

Prussin, S. G., Olander, D. R., Lau, W. K., Hansson, L.: Release of fission products (Xe, I, Te, Cs, Mo and Tc) from polycrystalline UO_2. J. Nucl. Materials **154**, 25–37 (1988)

Ray, J. W.: Tritium in power rectors. Reactor and Fuel-Processing Technology **12**, 19–26 (1968/69)

Robertson, D. E., Thomas, C. W., Wynhoff, N. L., Hetzer, D. C.: Characterization of long-lived activation products in spent fuel assembly hardware and reactor pressure vessel steel. Nucl Engng. and Design **118**, 463–486 (1990)

Robinson, M. T.: On the chemistry of the fission process in reactor fuel containing UF_4 and UO_2. Nucl. Sci. Engng. **4**, 263–269 (1958)

Rossin, A. D.: Radiation damage in steel: Considerations involving the effect of neutron spectra. Nucl. Sci. Engng. **9**, 137–147 (1961)

Ruhmann, H., Peehs, M., Kaspar, G., Löscher, H, Bleier, A., Hofmann, G.: Investigation on the behaviour of nuclear fuel under heavy mechanical impact. Trans. 9. Internat. Conf. on Structural Mechanics in Reactor Technology, Lausanne 1987, p. 311–315

Scargill, D.: Diffusion of fission product tritium in irradiated UO_2. J. Nucl. Materials **74**, 62–67 (1978)

Schmitz, F., Dean, G., Halachmy, M.: Application of lattice constant measurements for stoichiometry determinations in irradiated U-Pu mixed oxide fuels. J. Nucl. Materials **40**, 325–337 (1971)

Schweighofer, W., Richter, H., Koban, J., Freihoff, D., Meyer, W.: Experimentelle Ermittlung der Neutronenfluenz an der Innenwand des Reaktordruckbehälters. Proc. Jahrestagung Kerntechnik Berlin, FRG, 1983, p. 703–706

Shani, G.: The use of the reaction ^{93}Nb (n,n') ^{93m}Nb for fast neutron flux measurement. Nucl. Technology **51**, 83–86 (1980)

Smith, D. H., Baldwin, D. L.: An investigation of thermal release of carbon-14 from PWR Zircaloy spent fuel cladding. J. Nucl. Materials **200**, 128–137 (1993)

Sontheimer, F., Vogl, W., Ruyter, I., Markgraf, J.: Power ramp induced iodine and cesium redistribution in LWR fuel rods. J. Nucl. Materials **88**, 131–137 (1980)

Tachikawa, E., Tamura, N., Furukawa, K., Motojima, K.: Formation of organic iodides on dissolution of irradiated uranium metal in nitric acid. Int. J. Appl. Rad. Isotopes, **22**, 793–798 (1971)

Taketana, K., Ikawa, K.: Detection of methyl iodide upon heating irradiated fuels. J. Nucl. Sci. Technology **5**, 491–497 (1968)

Tanke, R. H. J.: Mass and gamma spectrometric measurements of fission products released from overheated, fresh irradiated, uranium dioxide. J. Nucl. Materials **188**, 262–272 (1992)

Vehlow, G.: Controlled corrosion for measuring the range of fission products in fuel hulls. Proc. ICMC Symposium Toronto 3.–7.6.1984, Vol. III.

Walker, C. T., Coquerelle, M., Goll, W., Manzel, R.: Irradiation behaviour of Mox fuel: Results of an EPMA investigation. Nucl. Engng. and Design **131**, 1–16 (1991)

Walter, K. H., Kienberger, K. H., Lange, G.: Untersuchungen zur Rückhaltung von Tritium in HTR-Brennelementen. J. Nucl. Materials **48**, 287–292 (1973)

Wenzel, U., Herz, D., Schmidt, P.: Determination of ^{14}C in spent HTGR fuel elements. J. Radioanal. Chemistry 53, 7–15 (1979)

Wiese, H.-W.: Investigation of the nuclear inventories of high-exposure PWR mixed-oxide fuels with multiple recycling of self-generated plutonium. Nucl. Technology **102**, 68–80 (1993)

Wise, C.: Recoil release of fission products from nuclear fuel. J. Nucl. Materials **136**, 30–47 (1985)

Wölfle, R., Knieper, J., Stöcklin, G.: Recovery of tritium from Zircaloy-clad UO_2 fuel rods. Radiochim. Acta **29**, 153–157 (1981)

Würz, H.: A simple nondestructive measurement system for spent fuel management. Nucl. Technology **95**, 193–206 (1991)

Yario, W. R.: Tritium inventory and release from core materials. Proc. ANS National Topical Meeting Tritium Technology in Fission, Fusion and Isotopic Applications, Dayton, Ohio, USA, 1980, p. 32–38

Yario, W. R.: Tritium release from stainless steel. In "Evaluation of Stainless Steel Cladding for Use in Current Design LWRs", Report EPRI NP-2642, Section 4 (1982)

Zwicky, H.-U., Aerne, E. T., Bart, G., Petrik, F., Thomi, H. A.: Evaluation of the radial distribution of gadolinium isotopes in nuclear fuel pins by secondary ion mass spectrometry (SIMS). Radiochim. Acta **47**, 9–12 (1989)

4. Radionuclides in the coolants of light water reactors during normal operation

4.1 General remarks

The coolants that come into contact with the nuclear areas of the reactor plants, primarily the PWR primary coolant and the BWR reactor water, are contaminated even during plant normal operation with radionuclides formed by various nuclear reactions. However, the appearance of these radionuclides in the coolants does not cause any difficulties in plant operation since all the relevant circuits are designed for safe operation in the presence of radioactivity.

Depending on the mechanism of their formation, these radionuclides can be divided up into three groups:

- activation products of the coolant, its additives and impurities
- fission products and activation products from the nuclear fuel
- activated corrosion products originating from the materials of the circuits.

The activation products of the coolant, with the sole exception of ^{16}N, are not of substantial importance in plant operation; in some cases, however, they have to be taken into consideration environmentally following release of off-gas or waste water. The fission products and the fuel activation products represent by far the greatest proportion of the radionuclide inventory in the reactor, from the viewpoint of radioactivity as well as from that of radiotoxicity. However, with the exception of severe accidents (which will be treated in Part C), during plant operation they are reliably confined within the fuel rods, so that only the very small amounts released from failed rods to the primary coolant are of interest in this context. Finally, the activated corrosion products are the origin of the buildup of radiation dose rates at the surfaces of the circuits, which potentially complicate the performance of operational procedures, in particular of inspection and repair work.

In the following sections, the production mechanisms of these radionuclides will be discussed, as well as their chemical and transport behavior in the plant during normal operation phases.

4.2 Activation products of the coolant, its additives and impurities

During its circulation in the primary system, each volume element of the coolant is exposed for approximately 10% of the recirculation time (i. e. for about 2 seconds, followed by about 18 seconds residence time outside the reactor core) to the neutron field inside the reactor pressure vessel. During this time interval, a number of nuclear reactions can take place, the most important of which are listed in Table 4.1.

4.2.1 ^{16}N, ^{13}N

Fast neutrons react with the ^{16}O isotope of the H_2O molecule via an (n, p) reaction to ^{16}N, a β^-, γ emitter with a halflife of 7.1 seconds; simultaneously, the recoil protons which are induced by fast neutrons lead to a (p, α) reaction forming ^{13}N, a β^+ nuclide showing a halflife of 9.96 minutes. During reactor operation, ^{16}N is the dominating radionuclide in the coolant. Because of its high activity concentration and its high-energetic γ radiation (5 to 7 MeV), the access to the primary circuit components is restricted during operation and the equipment compartments

Table 4.1. Activation products of water, its additives and impurities

Nuclear reaction	Radionuclide halflife
^{16}O (n, p) ^{16}N	7.13 s
^{16}O (p, α) ^{13}N	9.96 m
^{18}O (p, n) ^{18}F	109.7 m
^{10}B (n, α) ^{7}Li (n, nα) ^{3}H	12.3 a
^{10}B (n, 2α) ^{3}H	12.3 a
^{6}Li (n, α) ^{3}H	12.3 a
^{7}Li (n, nα) ^{3}H	12.3 a
^{14}N (n, p) ^{14}C	5730 a
^{17}O (n, α) ^{14}C	5730 a
^{40}Ar (n, γ) ^{41}Ar	1.83 h
^{35}Cl (n, p) ^{35}S	87.5 d
^{35}Cl (n, α) ^{32}P	14.3 d
^{32}S (n, p) ^{32}P	14.3 d
^{31}P (n, γ) ^{32}P	14.3 d

have to be shielded by concrete walls of an appropriate design. Due to its short halflife, the ^{16}N activity concentration in the coolant follows the neutron flux, i. e. the reactor power, virtually without delay.

When a nitrogen atom freshly produced by a nuclear reaction is broken away from an H_2O molecule, the thermalized nitrogen atom may react with various radicals, ions and molecules in the immediately surrounding area of the aqueous phase. In a high radiation field, such as exists in the core of a light-water cooled reactor, the principal reaction partners will be the products of water radiolysis. In earlier laboratory studies (Schleiffer and Adloff, 1964) the following chemical forms and distribution of ^{16}N produced in pure water were identified:

N_2	NO	NO_2^-	NO_3^-	NH_4^+	NH_2OH
1%	9%	25%	10%	30%	16%

Determination of the chemical forms of short-lived ^{16}N in the primary coolant and reactor water of LWRs is difficult because of the comparatively long time needed to obtain a coolant sample from the primary system under plant operation conditions. Nonetheless, certain information on the state of this radionuclide can be derived from studies concerning the behavior of longer-lived ^{13}N. The recoil energies of the nitrogen nuclides originating from both nuclear transformations are estimated to be about 0.4 MeV, which is several orders of magnitude higher than that required to break a chemical bond (about 3 eV). Therefore, these two radionuclides are expected to behave quite similarly in chemical reactions after they become thermalized (Lin, 1989).

A schematic presentation of chemical reactions and steam transport of nitrogen species in a BWR primary system is shown in Fig. 4.1., demonstrating that the yields of the different products depend on the ambient conditions, i. e. on the redox potential of the aqueous system. Earlier measurements in a BWR with forward-

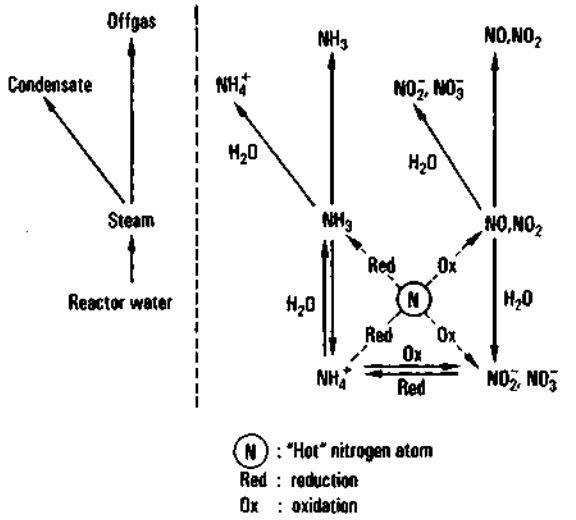

Figure 4.1. Schematic of chemical reactions and steam transport of nitrogen species in BWR primary system
(Lin, 1989; with kind permission from Elsevier Science S.A., P.O. Box 564, 1001 Lausanne, Switzerland)

pumped heater drains, reported by Lin (1983), showed that the bulk of the ^{13}N activity (about 85%) was present in the anionic form in the reactor water, presumably as NO_3^- or NO_2^-, with the remainder in the cationic form, presumably as NH_4^+. Only about 4% of the ^{13}N produced in the coolant was carried with the main steam and most of this amount was isolated in the cationic form from the moisture separator and reheater drains. A small amount of ^{13}N was detected in the condenser off-gas, apparently in a non-condensable gaseous form, i. e. NO or NO_2. Based on these measured ^{13}N anion-to-cation ratios, Lin (1983) predicted that in a reducing reactor water chemistry environment (i. e. under BWR hydrogen water chemistry conditions) the nitrogen activity in the main steam should be higher by about a factor of 5 to 6 than in an oxidizing water environment (i. e. under BWR normal water chemistry conditions). These estimates agreed reasonably well with first measurements performed by Burley et al. (1982) at the Dresden-2 BWR; following injection of hydrogen into the feedwater at a concentration of about 1.5 ppm, the radiation fields at the main steam line increased by about a factor of 5 due to the ^{16}N activity, a result which was confirmed by more detailed plant measurements (Law et al., 1983). On the other hand, in the course of a comparable action at the Swedish BWR Oskarshamn-2, where the oxygen level in the reactor water was reduced to values below 5 ppb as a consequence of hydrogen addition, an increase in the main steam line radiation fields of only 50% was observed (Magdalinski and Ivars, 1982).

A more detailed study of ^{13}N behavior under both BWR normal (NWC) and hydrogen water chemistry (HWC) conditions was performed by Lin (1989), using

ion exchange filters as well as on-line ion chromatography to separate the different chemical forms from each other. Consistently, in the four BWR plants investigated, under NWC conditions more than 98% of the ^{13}N activity in the reactor water appeared in the anionic form, interpreted as $NO_3^- + NO_2^-$, with the remainder being in the cationic form, corresponding to NH_4^+. In contrast with this behavior, under HWC conditions the anionic forms decreased to values between a few percent and about 40%, depending on the particular conditions of the plant (Cu^{2+} traces, among others, in the reactor water can decrease the conversion of ^{13}N anionic to cationic species under HWC conditions), while the cationic form increased to values between 60% and more than 97%. In the NWC steam condensate, about 50% accounted for both the anionic and cationic species; the anionic species NO_2^- and NO_3^- detected here were assumed to be originally transported by the steam as the volatile gases NO and NO_2 and to be formed upon dissolution in the condensate. By contrast, under HWC conditions ^{13}N appeared almost quantitatively in the cationic form, i. e. as NH_4^+, which is probably transported by the steam as NH_3. The experimental data indicated that under NWC conditions, most of the ^{13}N decays away in the coolant and only about 5% of it is transported with the steam phase. On the other hand, under HWC conditions more than 80% of the total ^{13}N production is transported with the steam.

From these results obtained at BWR plants one may conclude that in the reducing environment of the PWR primary coolant both nitrogen isotopes are present in the form of NH_4^+ or of NH_3.

4.2.2 ^{18}F

By the collision of fast neutrons with hydrogen atoms in the coolant H_2O, recoil protons are produced which can react with ^{18}O (isotope abundance in natural oxygen 0.20%) to form ^{18}F. This radionuclide is a β^+ emitter with a halflife of 109.7 minutes. Its activity concentration in the coolant depends directly on the prevailing neutron flux and amounts to about $5 \cdot 10^2$ Bq/ml in a 1300 MWe PWR operating at design power level. In a BWR plant, Lin (1983) determined a ^{18}F production rate of about $2 \cdot 10^8$ atoms/s $\cdot$ MW_{th} (corresponding to $2 \cdot 10^4$ Bq/s $\cdot$ MW_{th}) which is consistent with a theoretically estimated value of about $2.6 \cdot 10^8$ atoms/s $\cdot$ MW_{th}.

Because of the short halflife of ^{18}F and its comparatively low γ energy of 0.511 MeV, this radionuclide is of little importance in reactor operation and, therefore, only limited interest has been shown with respect to its chemical state in the coolant. However, one can suppose that the most probable stable chemical form of fluorine in water is fluoride. According to Lin (1983), the ^{18}F activity was observed exclusively in the anionic state in either the BWR reactor water or the condensate.

Measurements performed by Lin (1983) in forward-pumped BWR plants showed that a large proportion (about 90%) of the total ^{18}F produced in the coolant (core production plus feedwater return) was volatilized with the main steam and that about 80% of the steamborne ^{18}F was condensed in the moisture separa-

tors and returned to the reactor pressure vessel through the forward-pumped feedwater trains. Since the F^- concentration in the reactor water is by far too low to maintain a significant amount of undissociated HF, a complex compound $H_2O \cdot F$ was postulated to explain the appearance of ^{18}F in the steam phase. $H_2O \cdot F$ might be formed as a consequence of the recoil energy of the freshly generated fluorine atom and should be volatile with steam, similar to the corresponding iodide complex (see Section 4.3.4.2.); after condensation in the water phase at lower temperatures it should be reduced to form F^- ions again.

4.2.3 ^3H

The significance of the different potential sources contributing to the ^3H activity concentrations in the reactor primary coolant was already investigated in the early 1970's (e. g. Locante, 1971; Smith and Gilbert, 1971). According to the reports of these authors and to the results of more recent investigations, the following nuclear reactions are the most important sources:

a) ^2H (n, γ) ^3H
The starting nuclide ^2H (deuterium) is present in natural water with an isotope abundance of 0.015%. An additional formation of ^2H during reactor operation by the nuclear reaction ^1H (n, γ) ^2H can be neglected because of the small neutron capture cross section of this reaction. Even if one does not take into account the water exchange which takes place during plant operation, an increase in the natural ^2H concentration of only 0.002 to 0.0035% would occur during one fuel cycle; such an enhancement is too small to influence ^3H production to any measurable extent. The thermal neutron capture cross section for the formation of ^3H from ^2H amounts to about $3.6 \cdot 10^{-28}\,cm^2$ (Maxwell spectrum). In the PWR primary coolant, between 40 and 150 GBq ^3H per fuel cycle are produced by this reaction, depending on the primary coolant volume, the water volume of the active zone in the reactor core and other parameters.

b) ^6Li (n, α) ^3H

c) ^7Li (n, nα) ^3H
'In the majority of operating PWR plants, LiOH is used to compensate for the acidity of boric acid in order to attain an optimum coolant pH; the lithium constituent of this compound consists of isotopically enriched ^7Li (>99.99%) in order to minimize ^3H production. In the primary coolant, the total Li concentration ranges between 0.5 and 2 ppm depending on the current boric acid concentration and on the chemistry regime employed (see Section 1.3).

The nuclear reaction (b) is chiefly induced by thermal neutrons and shows a cross section of $6 \cdot 10^{-22}\,cm^2$ (Maxwell spectrum, T=575 K). Reaction (c) on the other hand is induced by fast neutrons with an effective threshold energy of 2.4 MeV; the cross section averaged over the flux of neutrons with energies beyond this threshold value amounts to $8.5 \cdot 10^{-26}\,cm^2$. Using this data and assuming a lithium concentration of 2 ppm (99.99% ^7Li), which is held constant

over the whole fuel cycle, one can calculate a ^3H production of 100 to 400 GBq from reaction (c) and of 120 to 680 GBq from reaction (b) for one PWR fuel cycle. From these figures it can be calculated that a reduction in ^7Li enrichment from 99.99 to 99.9% would lead to an increase in ^3H production by approximately a factor of 10; in general, such an increase cannot be tolerated.

d) ^{10}B (n, 2α) ^3H

e) ^{10}B (n, α) ^7Li (n, nα) ^3H

f) ^{11}B (n, ^9Be) ^3H

These are neutron-induced nuclear reactions with the boric acid dissolved in the coolant. Another potential source for these reactions are the control rods containing borosilicate glass or boron carbide; the possible contribution of these sources to the coolant ^3H concentration will be discussed below. The nuclear data for these three reactions have been described in more detail in Section 3.2.6. Reaction (d) results in the production of 4000 to 16,000 GBq ^3H during a fuel cycle, taking into account different concentration levels of boric acid in the coolant at the beginning of a cycle (depending on the design and the burnup state of the reactor core), as well as the decreasing concentration in the course of a cycle. When compared with this reaction, the amounts of ^3H produced by the reactions (e) and (f) can be ignored.

g) ^3H permeation from fuel rods and control rods

The generation and the behavior of ^3H in the nuclear fuel as well as in the boron glass and the boron carbide of the absorber rods have been treated in Sections 3.2.3.6. and 3.2.6. However, the database on the amounts of ^3H that penetrate through intact claddings and enter the coolant is not yet very well established, mainly due to the difficulties involved with experimental and calculational approaches. From measurements of the ^3H balance in PWR and BWR coolants performed by Langecker and Graupe (1972) and by Dollé and Bazin (1979), one can conclude that only a small fraction of the ^3H generated inside the Zircaloy-cladded fuel rods is able to penetrate through the intact claddings. The best data available at this time are in the range 0.1 to 1% of the amount of ^3H generated in the fuel.

Significantly larger amounts of ^3H may penetrate through the steel claddings previously used at some PWR and BWR plants. According to the results reported by Yario (1982), which were mainly from US plants, up to 50% of the ^3H produced in the fuel is able to penetrate to the coolant under typical LWR operation conditions. From the experimental results, it can be concluded that the amount of ^3H released from the fuel to the cladding is virtually identical in both Zircaloy and steel claddings, lying in both cases in the range 50 to 60%. In Zircaloy cladding the ^3H is retained very effectively, whereas it penetrates almost completely an intact steel cladding.

As yet, there is no reliable data concerning the question of whether or not ^3H is released into the coolant from defective fuel rods to a greater extent than from intact ones. On the other hand, this question seems to be of little significance for the ^3H balance in the coolant. It is easy to calculate that, even at a low ^3H permeation rate of 0.1% from intact rods, a significantly higher release

from the very limited number of defective rods in the reactor core (ranging from one to a few out of a total number of about 50,000 fuel rods in the core) would not cause any remarkable difference in the final ^3H concentration in the coolant.

The investigations described in Section 3.2.6. demonstrate that tritium is very tightly combined with the boron glass matrix and the boron carbide matrix; therefore, a significant release into the coolant from these materials is not to be expected. At one BWR plant, however, the measured ^3H concentrations seemed to depend on the immersion length of high-burnup control rods; it was, therefore, concluded that there was a significant contribution caused by tritium penetration through the intact steel cladding. Post-irradiation examinations, however, showed the presence of defects in the claddings of these rods and, moreover, a considerable washout of boron carbide, which was probably the source of the increased ^3H concentration in the coolant.

The equilibrium ^3H concentration in the coolant after a longer time of steady-state operation of the plant is controlled by the production rate and the penetration rate, on the one hand, and by the removal rate on the other. For this reason it can vary considerably from plant to plant. In PWR plants, the equilibrium ^3H activity concentration in the primary coolant usually is within the range of 10 to 30 GBq/Mg, in BWR plants it is considerably lower (about two orders of magnitude). In a PWR, the most important source is the ^3H generation from the ^{10}B dissolved in the coolant; in addition, in the case of insufficient LiOH isotopic purity the ^6Li reaction may become important. In BWR plants which contain neither boron nor lithium in the coolant (with the possible exception of inadvertently introduced impurities), neutron capture in deuterium is usually the main ^3H source. Due to the low base level of ^3H activity in the BWR reactor water, the ^3H penetration from fuel and control rods gains a greater significance, the extent of which depends on plant-specific parameters.

Tritium is probably introduced into the reactor coolant water phase as an ionic species from the neutron capture reaction in dissolved boron and as an atomic or molecular species following cladding penetration from fuel rods or control rods. In each case it has to be assumed that ^3H entering the primary coolant will be converted almost immediately to HTO because of the extremely reactive nature of the primary products of H_2O radiolysis. This assumption has been confirmed by numerous analyses of primary coolant in which ^3H was detected almost exclusively in the liquid state, i. e. as HTO species. HTO is not retained by the primary circuit purification systems; therefore, the only effective ^3H removal mechanism from the coolant is with the water which is removed from the primary circuit and is not recycled to it. To be sure, there are small differences in the behavior of HTO as compared to H_2O (e. g. during evaporation), since isotope effects affect the reaction kinetics of these two compounds to a certain extent. In heavy-water cooled reactors where high ^3H concentrations are produced in the D_2O moderator/coolant, purification systems are installed which are based either on an electrolysis process or an isotope exchange between the coolant and D_2 gas; in the resulting gaseous phases $^2H-^3H$ separation is usually performed by cryogenic distillation. The compara-

tively low ^3H equilibrium concentrations in the primary coolant of light-water PWRs, however, do not require such a purification.

The total ^3H production in the coolant can be calculated from the measured ^3H releases from the plant, provided that these measurements are conducted over an extended period of time, e. g. over an entire fuel cycle. From such balance measurements, the power-related ^3H generation rate in the coolant was calculated to be in the range of 11,000 to 17,000 GBq/GWe · a for PWR plants using Zircaloy cladding, and 2000 to 4000 GBq/GWe · a for BWR plants with Zircaloy cladding. The comparatively large differences in ^3H releases which were reported from different PWR plants have not yet been explained; earlier assumptions of higher releases from stainless-steel cladded borosilicate glass rods (e. g. Yario, 1980), which are not consistent with the strong fixation of the ^3H to the glass matrix (see above), have not been confirmed by experimental investigations. In PWR and BWR plants using fuel rod steel claddings one has to expect ^3H production rates in the coolant in the range of 350,000 and of 20,000 to 130,000 GBq/GWe · a, respectively, due to the pronounced tritium penetration from the fuel rods.

In the review given by Luykx and Fraser (1986), the different reactor types show the following characteristic values of ^3H emission via waste water (in TBq/GWe.a):

BWR	4	GCR	14
PWR[1)]	20	AGR	300
PWR[2)]	500	D_2O-PWR	400–900

1) Zircaloy cladding; 2) steel cladding

Besides these typical ranges of ^3H release from the plants, remarkable differences in the ^3H emission and, consequently, in the ^3H power-related production outside the fuel between different reactors of the same type have also been observed, which exceeded considerably the margins one would expect as a consequence of different operating regimes; the reasons for the deviations are still largely unknown.

The total ^3H emission from nuclear plants (including reprocessing plants) in 1984 was on the order of $1 \cdot 10^4$ TBq/a (Luykx and Fraser, 1986); it can be assumed that this value did not significantly change in the following years. These releases from civilian nuclear plants are small compared to the natural ^3H production occurring in the atmosphere, mainly caused by the ^{14}N (n, 3α) ^3H reaction. This naturally induced production rate is estimated to be on the order of $1 \cdot 10^5$ TBq/a, resulting in a global steady-state ^3H inventory on the order of 10^6 to 10^7 TBq, about 90% of which is present in the hydrosphere. In the 1950's and early 1960's, nuclear weapons detonations greatly increased the atmospheric ^3H inventory; this contribution was largely reduced in the following years by radioactive decay and by wet fallout.

According to investigations reported on by Kirchmann et al. (1986), the chemical state of ^3H in waste water is mainly HTO, but a small fraction of it appears as organically bound ^3H. By appropriate experiments it was demonstrated that the organic compounds leached from the resins during reactor operation experience a radiation-induced isotope exchange with ^3H in the strong gamma and neutron field within the reactor core. The T : H ratio measured in such organic compounds is significantly higher than that of the coolant. It is supposed that HT acts as an

intermediate during the course of these reactions. In contrast, the initially assumed tritiation of ion exchange resins in the purification system does not seem to be the main reason for the formation of organo-^3H compounds, since the T : H ratio in the resins was determined to be lower than that of the primary coolant.

Only very small proportions of the total ^3H emission from a PWR plant are released with the exhaust air; this amount varies somewhat from plant to plant and usually amounts to <0.5% of the total emission.

4.2.4 ^{14}C

In the formation of ^{14}C in the coolant of light water reactors, the nuclear reaction

$$^{17}O\ (n, \alpha)\ ^{14}C$$

plays the dominant role. ^{17}O is present in the natural oxygen isotope mixture with an abundance of 0.037%; the neutron cross section of the reaction is $2.4 \cdot 10^{-25}\,cm^2$. In addition, a possible contribution to the ^{14}C production is made by the reaction

$$^{14}N\ (n, p)\ ^{14}C$$

In the natural nitrogen isotope mixture ^{14}N shows an abundance of 99.64%; the cross section of this reaction is about $1.81 \cdot 10^{-24}\,cm^2$. Because of the usually very low levels of dissolved nitrogen impurities in the coolant, the ^{17}O reaction is in most cases the source of about 90% of the total ^{14}C production in the plant outside the nuclear fuel. The (n, γ) reaction with the ^{13}C content of the coolant impurities, as well as release from the ^{14}C inventories in the fuel and the cladding do not contribute to the ^{14}C inventory of the coolant to an extent worth mentioning.

Because of the principal formation from ^{17}O, the production rate of ^{14}C in the coolant depends almost exclusively on the neutron flux, i. e. on the reactor power. Therefore, for a better comparison of the ^{14}C production in different plants it is advisable to express the production rate in relation to the reactor power; this is also justified by the fact that the water volume which is present in the neutron field is approximately proportional to the reactor power. The production rates calculated by different authors (e. g. Bonka et al., 1974; Hayes and Mac Murdo, 1977; Bonka, 1979) differ to a certain extent; assuming low or zero nitrogen concentrations in the coolant, the data given are in the range of 200 GBq/GWe · a for PWRs and of 300 GBq/GWe · a for BWRs. According to Kunz (1985), at a nitrogen concentration in the coolant of approximately 50 ppm (which is higher by far than the usual concentrations) the amount of ^{14}C produced from dissolved ^{14}N would be about equal to that from ^{17}O.

Due to the long halflife of ^{14}C of 5730 years, ^{14}C emissions from LWR nuclear power plants result in a permanent accumulation in the environment. This increase, however, is small compared with the annual natural production of ^{14}C induced by cosmic rays, which amounts to about $1 \cdot 10^6$ GBq/a and which, at least at the moment, is not high enough to compensate for the depletion in the relative natural ^{14}C concentration when compared to pre-industrial times, which is caused by the

massive combustion of fossile fuels (Suess effect). Because of its low β^- energy of 0.16 MeV, ^{14}C exhibits only a moderate radiological relevance which, in addition, depends on its chemical form at release from the plant (CO_2 or CH_4). Nevertheless, detailed knowledge of the behavior of this radionuclide in the reactor coolant is of interest.

Detailed investigations in this field have been performed by various authors, e. g. by Bleier (1981; 1983) concerning PWR plants as well as BWR plants. For the relevant analyses, the coolant samples which were not previously degassed or filtered, were subjected to a three-step analytical procedure:

- Degassing after acidification to pH 1–2 and additional heating to 70–80 °C;
- volume reduction of the solution by evaporation; and,
- wet oxidation of the residue using sulfuric acid – chromic acid and oxygen gas after addition of inactive graphite carrier.

The gases released at each step of the procedure were transported to a combustion duct consisting of NaOH absorption flasks for CO_2, a CuO catalyst heated to 750 °C for oxidation of CO and alkanes to CO_2 and, finally, NaOH absorption flasks once again to trap the newly formed CO_2. From both absorption solutions the collected CO_2 was separately precipitated as $BaCO_3$. After checking the radiochemical purity of the precipitate and, if necessary, repetition of the $BaCO_3$ precipitation step, ^{14}C was measured in a methane flow counter. Since Meacham (1974), within the context of investigations on primary circuit contamination buildup, reported considerable carbon contents in coolant particulate matter, these substances were also included in the analyses by oxidation of filtered particulates from PWR primary coolant at 1200 °C in an oxygen atmosphere under addition of PbO_2, as well as by wet oxidation using sulfuric acid–chromic acid. The CO_2 evolved by this treatment was collected and measured in the way described above. In a similar manner, resins from the primary coolant purification system were also analyzed. In order to complete the ^{14}C balance, samples of the off-gas were taken by passing a part of the stack effluent gas onto a combustion and absorption device similar to that described above. The samples obtained in this manner were processed and measured as described above. From these analyses, the following conclusions concerning ^{14}C behavior in the primary coolant of a light water reactor can be drawn (Bleier, 1981; 1983):

On the basis of the ^{14}C activity concentrations measured in the off-gas, power-related ^{14}C emissions were calculated to amount to 300 to 450 GBq/GWe · a for PWR plants and to about 500 GBq/GWe · a for the only investigated BWR plant. These measured values are higher than the calculated ones mentioned above; since these measurements were conducted over short time periods only, the influence of statistical fluctuations cannot be ruled out. Whereas in the BWR plant (normal water chemistry conditions) more than 95% of the ^{14}C released was in the chemical form of CO_2, in PWR plants about 80% was in the form of CO and/or alkanes (which could not be distinguished from each other by the analytical techniques applied). These differences in the chemical speciation of ^{14}C between PWR and BWR plants are assumed to result from the stronger reducing conditions in the PWR coolant, which are caused by the presence of excess hydrogen.

Similar results on ^{14}C discharges were reported by Kunz (1985) from a long-term surveillance program at two PWR plants and one BWR plant. The resulting power-related release values from the PWR plants amounted to 430 and 350 GBq/GWe · a, and to about 450 GBq/GWe · a for the BWR plant; thus, they are also higher than the above-mentioned calculated rates of production in the coolant. In the PWR plants, a major discharge pathway was the vent flow from the gas decay tanks. The measurements were conducted using continuous sampling of stack gas on a solid CO_2 absorbent, with and without preceding combustion of the hydrocarbons; in this manner, it was possible to distinguish between $^{14}CO_2$ and ^{14}C-bearing hydrocarbons. In addition, grab samples were taken from different locations and the different chemical species were determined by gas chromatographic separation of the hydrocarbons from CO_2 and from each other, followed by internal gas proportionality counting of the ^{14}C content of each species. These measurements showed, consistent with the data mentioned above, that the ^{14}C emissions from PWRs are predominantly hydrocarbons (about 75% CH_4 with decreasing contributions of higher alkanes) and from BWRs mainly CO_2.

According to Bleier (1983), in PWR primary coolant the activity concentration of ^{14}C ranges from 200 to 800 kBq/Mg, 60 to 70% of which is present as dissolved CO_2 or carbonate, 0.1 to 0.5% at the maximum as CO and/or alkanes, and the remaining 30 to 40% attached to particulate matter. Only in one single case were CO/alkane fractions of about 20% observed; occasionally, even higher fractions of ^{14}C attached to particulate matter were measured. Thus, the total ^{14}C inventory in the coolant amounts to only 0.01 – 0.06% of the total production per year, corresponding to an average residence time of ^{14}C in the coolant of only several several hours. The coolant ^{14}C shows a significant enrichment in CO_2 species when compared to the off-gas composition. Since CO_2 as well as carbonate can be assumed to have a significantly lower volatility from a coolant at pH 7 than CO and/or alkanes and, consequently, a slower release to the gas phase, these results seem to be reasonable.

The releases of ^{14}C from the plants with liquid and solid wastes are small, being less than 5% of the gaseous releases (Kunz, 1985).

The ^{14}C amounts detected by Bleier (1983) on the resins of the primary coolant purification system only correspond to 1 – 3% of the annual production; this comparatively low value can be understood when the short residence time of this radionuclide in the primary coolant is taken into account. When the throughput rate of coolant through the purification system is taken into account, a significant decontamination factor of ^{14}C on the ion exchanger resins can be calculated, roughly corresponding to that of CO_2. Consistent with this result, a large fraction of the ^{14}C (about 85%) can be leached from the resins with hydrochloric acid, thus indicating that it is fixed there as a carbonate species (Martin et al., 1993).

4.2.5 ^{32}P and ^{35}S

These two radionuclides are β^- emitters with a negligibly weak associated γ-ray emission. Because of their usually very low activity concentrations in the coolant, they do not have any significance for the operation of the plant. A certain interest

in their behavior emerged as a consequence of discussions that fractions of them could be released to the environment via the waste water, which might cause a certain radiation burden to the public following their enrichment in the food chain.

The production of the two radionuclides is caused by neutron capture in different impurities present in the primary coolant; the main nuclear reactions have been listed in Table 4.1. Taking into account the relevant nuclear data as well as LWR typical concentrations of the relevant impurities in the coolant, it can be shown that phosphorus impurities in the coolant are the main source for ^{32}P, whereas chlorine impurities are mainly responsible for ^{35}S production.

Detailed measurements of the amount and behavior of these two radionuclides in different LWR plants were performed by Stöckert and Trummer (1985). These investigations showed ^{32}P activity concentrations in the primary coolants of six different PWR plants ranging from 4 to 50 MBq/Mg, in the reactor water of two BWR plants from 0.4 to 7 MBq/Mg. It seems reasonable, therefore, to assume that the significantly higher production rate in the PWR coolant is due to phosphorus impurities in the added boric acid. On the other hand, ^{35}S activity concentrations were detected in the range from 0.07 to 2 MBq/Mg in PWRs; about 0.4 MBq/Mg were measured in the reactor water of the only BWR plant investigated.

In order to check the reliability of the calculated results, more detailed investigations were performed at one PWR and one BWR plant. To this end, the concentrations present in the primary coolant and in the reactor water of the chemical elements mainly acting as sources for the two radionuclides were analyzed by ion chromatography. From these results the corresponding steady-state concentrations of ^{32}P and ^{35}S were calculated and compared with the data obtained in the measurements. Whereas there was a reasonable agreement for ^{35}S, when the errors to be expected in analysis and in calculation were taken into account, the ^{32}P data differed to a greater extent; in the PWR primary coolant the experimental result was higher by about a factor of 100 than the calculated result, in the BWR reactor water by a factor of about 10. These differences are too high to be explained by errors in the analytical determinations and in the related calculations. An acceptable explanation is given by the observation that a considerable fraction of the phosphorus impurities in the coolant is not in the dissolved state but is attached to particulate matter and, therefore, is not accessible for ion chromatography analysis. Likewise, the distribution of the ^{32}P activity in the coolant between the dissolved and the suspended fraction was found to vary considerably from plant to plant, with no observable relationship to plant operation parameters. On the other hand, the main source of ^{35}S production, namely chloride impurities, are not able to form insoluble species in the coolant, so that ion chromatography can be expected to give true results as to their concentrations.

The mixed-bed ion exchange resins of the PWR primary coolant purification system show a high retention effectiveness for ^{32}P, with the purification factors being in the range 100 to 3000. In the BWR reactor water cleanup system the purification factors are lower, on the order of 20 to 300. ^{35}S is retained in the purification systems of both PWR and BWR plants to a lower degree, with the purification factors measured being in the range between 6 and just below 100.

In the BWR primary system, the carry-over of both radionuclides from the reactor water to the main steam is very small, less than 0.1%. This figure is on the order of the steam moisture content measured using ^{24}Na, thus indicating that both radionuclides are present in the reactor water in a non-volatile form, presumably phosphate and sulphate, which are exclusively carried by water droplets. The low volatility of both ^{32}P and ^{35}S is also responsible for their high purification factors of about 1000 in the waste water evaporators, resulting in their being almost quantitatively retained in the concentrate, with only traces of them being released to the environment.

References Section 4.2

Bleier, A.: Bildung und Verhalten von ^{14}C und dessen Emissionsüberwachung an Kernkraftwerks-Anlagen. Proc. Jahrestagung Kerntechnik Deutsches Atomforum Düsseldorf 1981, p. 269–272

Bleier, A.: Bildung, Verhalten und Emissionsüberwachung von radioaktivem Kohlenstoff-14 an Leichtwasserreaktoren. Siemens Forsch. u. Entwickl. Berichte **12**, 363–370 (1983)

Bonka. H., Brüssermann, K., Schwarz, G.: Umweltbelastung durch Radiokohlenstoff aus kerntechnischen Anlagen. Proc. Reaktortagung Deutsches Atomforum Berlin 1974, p. 454

Bonka, H.: Produktion und Freisetzung von ^{3}H und ^{14}C durch Kernwaffenversuche, Testexplosionen und kerntechnische Anlagen, einschließlich Wiederaufarbeitungsanlagen. Paper presented at the Wissenschaftliches Symposium des Instituts für Strahlenhygiene des Bundesgesundheitsamtes, Berlin, FRG, 1979

Burley, E. L., Wong, T. L., Law, R. J., Cowan, R. L.: Oxygen suppression in BWR reactor water by hydrogen addition. Trans. Am. Nucl. Soc. **43**, 322–323 (1982)

Dollé, L., Bazin, J.: Wichtige Ergebnisse der Tritiumbilanz in Leichtwasserreaktoren. VGB Kraftwerkstechnik **59**, (2), 171–175 (1979)

Hayes, W. D., Mac Murdo, K. W.: Carbon-14 production by the nuclear industry. Health Physics **32**, 215–219 (1977)

Kirchmann, R., Meurice-Bourdon, M., Fagniart, E., Binet, J., Bonotto, S.: Purification resins in reactor circuit as source for organic tritium. Radiation Protection Dosimetry **16**, 45–48 (1986)

Kunz, C.: Carbon-14 discharge at three light-water reactors. Health Physics **49**, 25–35 (1985)

Langecker, K., Graupe, H.: Tritium in Druckwasserreaktoren. Kernenergie **15**, 165–171 (1972)

Law, R. J., Indig, M. E., Lin, C. C., Cowan, R. L.: Suppression of radiolytic oxygen produced in a BWR by feedwater hydrogen addition. Proc. 3. BNES Conf. Water Chemistry in Nuclear Reactor Systems, Bournemouth, UK, 1983, Vol. 2, p. 23–30

Lin, C. C.: Chemical behaviour and distribution of volatile radionuclides in a BWR system with forward-pumped heater drains. Proc. 3. BNES Conf. Water Chemistry in Nuclear Reactor Systems, Bournemouth, UK, 1983, Vol. 1, p. 103–110

Lin, C. C.: Chemical behaviour and steam transport of nitrogen-13 in BWR primary systems. J. Radioanal. Nuclear Chemistry, Articles **130**, 129–139 (1989)

Locante, J.: Tritium in pressurized water reactors. Trans. Am. Nucl. Soc. **14**, 161–162 (1971)

Luykx, F., Fraser, G.: Tritium release from nuclear power plants and nuclear reprocessing plants. Radiation Protection Dosimetry **16**, (1–2), 31–36 (1986)

Magdalinski, J., Ivars, R.: Oxygen suppression in Oskarshamn-2. Trans. Am. Nucl. Soc. **43**, 323–324 (1982)

Martin, J. E., Cook, S. K., Grahn, K. F.: Relative determination of ^{14}C on spent ion-exchange resins by resin regeneration and sample combustion. Appl. Radiat. Isotopes **44**, 701–705 (1993)

Meacham, S. A.: Sampling and analysis of carbon contained in the primary coolant of pressurized-water reactors. Proc. 7. NBS Material Research Symposium, Oct. 1974, 429–438 (NBS Special Publ. 422, 1976)

Schleiffer, P. J. J., Adloff, J. P.: Formes chimiques de l'azote 16 produit par la réaction $^{16}O(n, p)^{16}N$ dans l'eau. Radiochim. Acta **3**, 145–151 (1964)

Smith, J. M., Gilbert, R. S.: Tritium experience in boiling water reactors. Trans. Am. Nucl. Soc. **14**, 160–161 (1971)

Stöckert, H., Trummer, K. H.: Phosphor-32 und Schwefel-35-Radioaktivität in Leichtwasserreaktoren. VGB-Kraftwerkstechnik **65**, 562–566 (1985)

Yario, W. R.: Tritium inventory and release from core materials. Proc. ANS Topical Meeting Tritium Technology in Fission, Fusion and Isotope Applications, Dayton, Ohio, USA, 1980, p. 32–38

Yario, W. R.:An evaluation of stainless steel cladding for use in current design LWRs. 4. Tritium release from stainless steel. Report EPRI NP-2642 (1982)

4.3 Fission products and activation products from the fuel

4.3.1 Transport of radionuclides from the fuel to the coolant

The intact cladding of the fuel rod represents an absolutely impermeable barrier to any release of radionuclides from the fuel to the coolant, with the sole exception being small fractions of tritium as described in Section 3.2.5. Despite this barrier, the coolants of many plants are contaminated with fission products during individual fuel cycles. This does not cause any problems in plant operation since the nuclear islands (i. e. primary system and auxiliary systems) of the plants are designed to be operated without difficulty even when fission products are present in the coolant up to a certain level. Nevertheless, for various reasons it is of considerable interest to obtain knowledge about the source of the fission products appearing in the coolant, and the mechanisms of their release, as well as to learn about their behavior in the coolant. Among other questions, valuable information on the current state of the reactor core can be derived from the fission product activities measured in the coolant, provided that appropriate knowledge of the mechanisms of transport from a failed fuel rod to the coolant is available. For this reason, considerable effort has been devoted to this subject.

In general, the appearance of fission products in the primary coolant of a light water reactor might have one of two causes:

- Defects in fuel rod claddings.
- Fuel present in the coolant and deposited on in-core surfaces, originating either from fabrication of the fuel assemblies or from larger fuel rod defects in the current or in some preceding fuel cycle.

These two possible sources can be distinguished from each other by a detailed analysis of the activity concentrations of different radionuclides in the coolant and their development over time, in particular by taking into account isotope ratios of specific fission products.

As a whole, the operating behavior of LWR fuel rods containing oxide fuel is excellent: most of the fuel cycles are terminated without any rod failure, and only in isolated fuel cycles are a few failed rods observed. Statistically, the average failure frequency amounts to one failed rod in 10^4 to 10^5 fuel rods operated to their burnup goal. Such cladding failures may have different causes. In the past, hydriding of the Zircaloy material induced by residual traces of moisture in the fuel pellets was one of the principal failure mechanisms, leading to cracks mainly in the regions of high stress in the cladding. Another mechanism, pellet-cladding interaction (PCI), may occur during rod power ramps which start from a low power level, in BWR cores, for example, induced by changes in the positions of the control rods; this failure mechanism can be precluded by using a Zircaloy cladding provided with an inner layer of pure zirconium (see Section 2.1.2.). Cladding corrosion induced by fission products (in particular iodine) deposited on the inner surface during operation has also been suspected as a failure mechanism; however, no clear evidence for this defect type has been detected. Fretting corrosion of the cladding is another potential failure mechanism; vibration of the fuel rods in the spacers, which in former years was one mechanism, has been precluded by construction changes. Fretting failures may also be caused by small particles carried in the coolant (debris) which are trapped in the reactor core; in order to prevent such debris from entering the fuel assembly, special designs of the lower end pieces have been developed. Finally, fuel fabrication flaws (e. g. faulty end cap welds) which occasionally occurred in the early years of commercial reactor operation, were completely ruled out by appropriate quality assurance measures. Thorough studies of all the potential failure mechanisms (which were described in detail e. g. by Garzarolli et al., 1979; Lewis et al., 1993) resulted in a reduction of the former failure rates to the currently very low levels.

The occurrence of fuel rod failures is often characterized by the initial appearance of very small perforations (pinholes). After prolonged operation of a Zircaloy-cladded defective rod, secondary hydride failures may develop, caused by hydrogen which is radiolytically generated from water vapor entering the rod via the primary defect. Such secondary failures may appear at a certain distance away from the primary defect (e. g. 1 m above it). Fretting failures also increase in size with time; often they are located in the lower region of the fuel rod. Thus, the size of the failure as well as its location can differ considerably and it is important to identify these parameters already during the relevant fuel cycle.

In severe cases, fuel rod failures may lead to fuel losses from the rod, with their magnitude depending on the size of the defect and on the question of whether liquid water or only steam has entered the rod. Operational experience has shown that after one year of prolonged operation of a failed rod one has to expect the following fuel losses to the coolant (Assmann and Stehle, 1984; Beslu et al., 1984):

– Pinhole defect	$<10^{-3}$ g
– Defect area 5–10 mm diameter	~1 g
– Fracture 20–50 mm long, 5 mm wide	~10 g
– Broken fuel rod	50 to 200 g and more.

The last-mentioned fuel loss may be caused either by mechanical action of the coolant (erosion) or by chemical leaching of the fuel pellet. Often the UO_2 loss to the coolant depends on the orientation of the defect to the coolant flow, with this being higher when the long axis of the defect is oriented parallel to the coolant flow. Erosion of fuel particles is facilitated by UO_2 oxidation at the grain boundaries (Lewis et al., 1993). Fuel losses of 10 to 15 g U during a 3-year operation period from the area around artificial defects of 1 mm diameter have been reported by Hüttig et al. (1990).

A large fraction of this "tramp" uranium will be deposited on the surfaces of the primary circuit, together with corrosion products. The proportion which is deposited in the neutron field represents an additional source of fission products, while the comparatively small amount which is dissolved or suspended in the coolant does not significantly contribute to fission product generation. Another possible source of fission products is contamination of the outer surface of the fuel rods with uranium traces originating from the fabrication procedures. However, with the fabrication technologies currently employed, the contamination levels of fresh fuel assemblies are very low, on the order of 10^{-7} g UO_2/cm^2 and less (conservative value for fuel rods whose surfaces have not been cleaned by electropolishing) and, therefore, are usually of no significance for the fission product concentration in the coolant. It can be calculated that a homogeneously distributed cladding surface contamination of $1 \cdot 10^{-7}$ g U/cm^2 over the whole core of a 1300 MWe PWR (at a total fuel rod surface of $6 \cdot 10^7 cm^2$, which corresponds to a total amount of a few grams) will yield a ^{131}I source strength of about 10^{11} atoms/s during operation at rated power. With a circulating primary coolant volume of $440 m^3$ and a 10% per hour purification rate, a steady-state ^{131}I activity concentration of about 10 Bq/ml will result, i. e. a value which, even under these conservative assumptions, is far lower than the source strength of one single defective fuel rod.

Experience has shown that removal of fuel contamination from the cladding proceeds very slowly, both when it originates from fabrication as well as from tramp uranium; the predominant fraction stays on the cladding until discharge of the assemblies from the reactor core.

Following the appearance of a cladding defect, the chemical conditions inside the affected fuel rod will change significantly. First of all, the helium fill gas escapes and is replaced by steam. The consequence is oxidation of the pellet surface region leading to an O : U ratio of about 2.1 within a few days; subsequently, further oxidation proceeds at a considerably lower rate, only reaching O : M numbers of about 2.4 after one year. The highest O : M values are obtained in the immediate vicinity of the defect; with increasing distance from the defect position, fuel oxidation is less pronounced. The consequence of the UO_2 oxidation is a decrease in thermal conductivity of the oxide, resulting in an increase of the pellet central temperature; in addition, an increase in the volume and diameter of the pellet occurs.

An increase in the O : M ratio of the oxide from 2.000 to 2.1 in a failed fuel rod with a linear heat rating of 200 W/cm leads to a rise of the pellet central temperature from 700 °C to about 800 °C. The enhanced temperature effects an increase of the diffusion coefficient of the fission product noble gases in the oxide matrix by a factor of about 500 when an activation energy of 238.6 kJ/mol is assumed. In addition, the increase in the O : M ratio itself leads to an increase in the diffusion coefficient of the noble gases, in the case mentioned above (i. e. from 2.000 to 2.1) by a factor of about 40. The combination of both effects, therefore, would theoretically result in an increase of the diffusion rate by about three orders of magnitude. Since the fission product noble gases are transported from the gap of a failed fuel rod to the coolant without significant delay (provided that the size of the defect is not too small), their source strengths to the coolant are virtually identical to their release rates from the fuel. Thus, one can compare the source strengths measured from the activity concentrations in the coolant with the release rates of the noble gases from the fuel of intact rods, with the latter being calculated from the data on gas concentrations in the rod plenum which are determined in post-irradiation examinations, or from the results of sweep gas experiments performed using a specially-designed fuel rod vented during operation by a carrier gas (see, for example, Lewis et al., 1990). As can be seen from Fig. 4.2., the inferred diffusion constants of the noble gases in the fuel of failed rods are higher by a factor of about 100 than in the fuel of intact rods (Schuster et al., 1981). The difference between the estimated data mentioned above and the experimentally obtained data is presumably due to the fact that the mean increase of the O : M ratio averaged over the total length of the fuel rod is considerably smaller than that in the vicinity of the defect. In addition, it seems that the dependence of fission gas release on the linear heat rate is more strongly pronounced in the case of intact rods. Similar results on oxidation-enhanced release of fission gases from UO_2 have been reported by other authors, for example Kurka et al. (1979), Kalfsbeek (1983), Lewis et al. (1993).

Similarly, the mobility of fission product iodine in the oxidized fuel zones of failed rods increases significantly, an effect which is probably due to a change in its chemical state in these zones. As was discussed in Section 3.2.3.3., I^- is stable in contact with $UO_{2.00}$ but it is oxidized to I^o as the stable species in equilibrium with $UO_{2.1}$. As a consequence of this change in the chemical state and the resulting enhanced mobility, the iodine gap inventory in a failed fuel rod is mainly built up by diffusion-controlled release from the pellets instead of recoil release, which is the dominant mechanism in intact fuel rods. The consequence of this change in release mechanism is an increase in the gap iodine inventory to a level which probably depends on the particular parameters of the failure and the extent of fuel oxidation. From measurements of iodine spiking following reactor shutdown (see Section 4.3.1.2.) an increase in the iodine gap inventory from 0.2 to 0.5% of the fuel rod inventory in an intact rod by about a factor of 10 after several days of operation of the failed rod has been calculated; as yet, it is not known whether or not this enhancement factor can be applied to a wider range of defect types and locations.

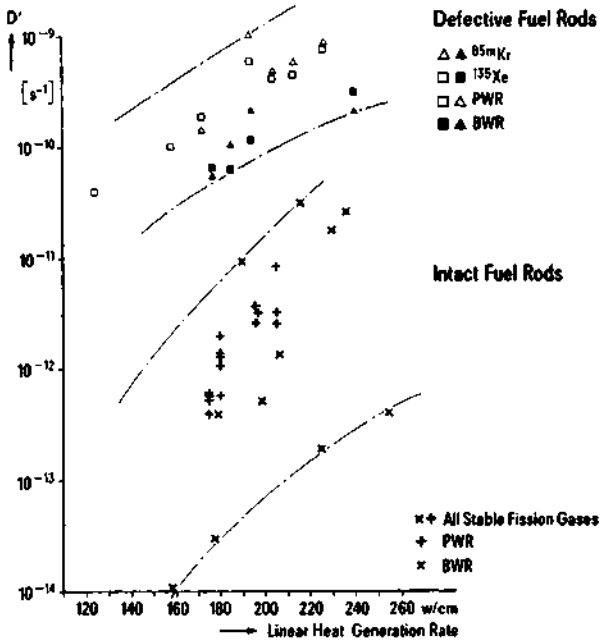

Figure 4.2. Correlation between inferred diffusion constants and linear heat generation rate. Comparison of defective and intact fuel rods
(Schuster et al., 1981; with kind permission from Elsevier Science S.A., P.O. Box 564, 1001 Lausanne, Switzerland)

According to the thermodynamic calculations performed by Besmann and Lindemer (1978), the presence of pure H_2O vapor in the gap does not effect an oxidation of UO_{2+x} to U_4O_9 ($UO_{2.25}$). This oxidation step, which is accompanied by a phase transformation of the uranium oxide, should only be possible in the presence of oxygen in the steam. However, as a consequence of radiolytic reactions the steam in the gap will contain oxygen in any case so that continued oxidation of the UO_{2+x} should be possible. Under such conditions, the CsI assumed to be present as the most stable iodine compound in the gap of an intact fuel rod will become thermodynamically unstable in favor of elemental I_2 and, in contact with zirconium metal, of ZrI_2 or ZrI_3, with the rate of oxidation and its extent depending on the concentration of oxygen present in the steam. These oxidized iodine species have a measurable vapor pressure under the prevailing conditions.

All the observations made up to now do not give any indication of a noticeable difference in the defect behavior between UO_2 fuel, on the one hand, and mixed-oxide fuels on the other. No specific mixed-oxide defect mechanisms have been observed; the release mechanisms of fission products from the failed fuel rods are virtually identical for both types of fuel. It is clear that the low plutonium content in the mixed-oxide fuel does not significantly influence the physico-chemical properties of the fuel material (Goll et al., 1993).

The level of the activity concentration of a specific fission product in the coolant is determined by the strength of the source feeding to the coolant, on the one hand, and by the extent of its removal from the coolant on the other. For "soluble" fission products the main mechanisms of removal are radioactive decay, retention in the purification system and, in BWR reactor water, carry-over with the main steam. Under steady-state conditions, i. e. at an activity concentration level which is constant in time, the rates of supply to the coolant and of removal from the coolant must be identical. For a PWR, therefore, the rate of supply, the so-called source strength or release rate R (in atoms per second), under steady-state conditions can be calculated from the measured activity concentration A in the primary coolant according to

$$R = A \cdot m \cdot (\lambda+\varepsilon) / \lambda$$

where m = circulating primary coolant mass in Mg
λ = radioactive decay constant in s^{-1}
ε = purification constant in s^{-1}.

Of the data needed for the calculation, the decay constant λ of the relevant fission product and the circulating primary coolant mass m are known. The purification constant ε can be calculated from the following formula for the fractional flow rate of coolant to the purification system (degasifier, mixed-bed ion exchanger), taking into account the purification factor F:

$$\varepsilon = m' \cdot (F-1) / m \cdot F$$

where m means the mass of circulating coolant (in Mg) and m' the purification rate (in Mg/h). With a 10% per hour purification rate and a purification factor of 100, the numerical value of ε is about $4 \cdot 10^{-5}\ s^{-1}$. Thus, for example, the effective halflife of ^{131}I activity concentrations in PWR primary coolant is on the order of 6.7 hours, i. e. considerably lower than the physical halflife of this radionuclide of 8.05 days.

In those BWR plants in which all condensates from the turbine cycle are directed to the condensate polishing system, the equations mentioned above can be used with the modification that allowance must be made for the carry-over constant, which describes the loss of some iodine and other non-gaseous fission products from the coolant to the steam phase. The carry-over constant Δ is added to the term $(\lambda + \varepsilon)$, making it $(\lambda + \varepsilon + \Delta)$; Δ is calculated according to

$$\Delta = Q \cdot (\delta-1) / m \cdot \delta$$

with Q = feedwater mass flow in Mg/h
δ = carry-over factor, i. e. concentration in the main steam related to concentration in the aqueous phase

In BWR plants with forward-pumped heater drains, however, a large fraction of the iodine and other non-gaseous fission products carried by the primary steam is directly returned to the reactor water without passing the condensate polishing system. When calculating source strengths from the activity concentrations in the reactor water, the fission product input with the feedwater has to be taken into account as an additional source for the reactor water (Lin, 1983).

The source strength values of fission gas isotopes in BWRs are calculated from their activity concentration in the condenser off-gas flow using the equation

$$R = a \cdot G / \lambda$$

where a = activity concentration in the condenser off-gas in Bq/ml
G = gas flow rate in ml

With regard to long-lived radionuclides that show a low decontamination factor on the purification system (e. g. ^{137}Cs in PWR primary coolant containing LiOH), the purification constant ε also has to include the coolant losses via water exchange or leakages. On the other hand, fission products which form insoluble compounds or can be adsorbed onto non-dissolved corrosion product particulate matter may be removed from the coolant by plate-out onto the primary circuit surfaces. These and other parameters which are liable to affect the activity concentrations of the radionuclides in the primary coolant are the reason why a trustworthy calculation of source strengths can only be made using specific radionuclides such as fission product noble gas isotopes and iodine isotopes.

4.3.1.1 Release of fission products to the coolant during steady-state operation

Because of the usually very small dimensions of the defect areas as compared with the total surface area of the fuel rod and because of the large volume of a fuel pellet as compared with recoil ranges, the fission products have to travel a great distance from the location where they are generated to the coolant. At the first stage of this pathway, the fission product formed inside the pellet moves by recoil, diffusion or migration in the thermal gradient to the outer zone of the pellet and to the gap. There, it has to travel to the location of the defect before being transported to the coolant. Taking into account these different stages, the buildup of the fission product activity concentration A in the coolant (in Bq/ml) can generally be described by the equation (according to Burman, 1986)

$$A = \frac{n \cdot f \cdot Y \cdot V \cdot \lambda \cdot E}{(E+\lambda) \cdot (\beta+\lambda) \cdot Vol}$$

where n = number of failed rods
f = average fission rate in the failed rods (in s^{-1})
Y = average isotopic fission yield
V = escape rate coefficient pellet to gap (in s^{-1})
E = escape rate coefficient gap to coolant (in s^{-1})
λ = isotopic decay constant (in s^{-1})
β = purification constant (in s^{-1})
Vol. = coolant volume (in cm^3)

These transport processes require a certain time during which short-lived radionuclides will decay to a certain extent, so that the fission product mixture entering

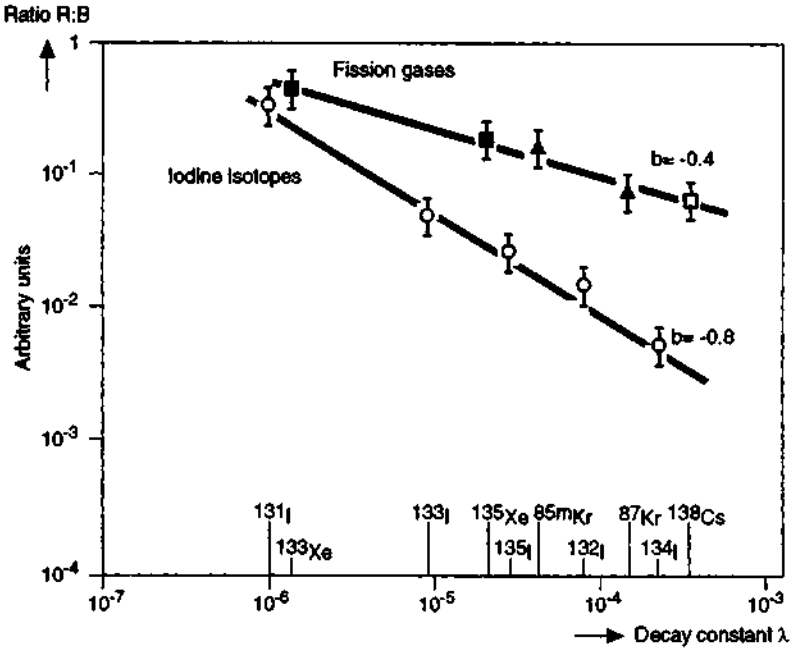

Figure 4.3. R:B ratios of fission products as a function of their decay constants (Neeb, 1971)

the primary coolant is "older" than that which was generated within the fuel pellet. The ratio of the release rate R of a given fission product isotope to its production rate (or birth rate) B in the fuel is a measure of the time needed for transport to the coolant. On the other hand, the nature of the relevant fission product (i. e. its physical and chemical properties) can also be expected to influence the transport time. When, in order to rule out additional complicating effects, one compares the release behavior of two isotopes of the same element that have escaped from a failed fuel rod, the ratio R : B will depend solely on their decay constants λ. For example, Fig. 4.3., which is based on measurements performed at a commercial PWR plant, demonstrates that the isotopes of the fission noble gases krypton and xenon obey a $\lambda^{-1/2}$ relationship with satisfying accuracy. (Besides the noble gases, ^{138}Cs also appears on this straight line, indicating that its transport into the coolant is governed by its precursor ^{138}Xe).

On the other hand, when the fission products are generated by nuclear fission of finely dispersed or dissolved fuel traces in the coolant, they will enter the liquid phase instantaneously by recoil; this mechanism applies to all cases when the dimensions of the fuel particle are comparable to the recoil range of the fission product. Under such conditions, the source strength R is identical to the production rate B and the ratios R : B of different fission product nuclides do not depend on their halflives or decay constants. The same mechanism applies when surface contamination of fuel rods with fuel traces originating from the fabrication

process or from fuel contamination during operation contributes to the fission product levels present in the coolant. However, when small fuel particles are deposited on a solid surface, only about 50% of the fission products generated will enter the coolant by recoil while the remainder will be implanted into the underlying material or the corrosion product layer covering its surface.

As can also be seen from Fig. 4.3., the R : B ratios of the iodine isotopes exhibit a different relationship to the decay constant λ, showing a steeper slope somewhat below 1. This means that the mixture of iodine isotopes which enters the coolant is "older" than that of the noble gases, i. e. more shifted to the longer-lived isotopes. Such an aged mixture indicates an additional delay in the transport of these substances inside the fuel rod, the reason for which might be found in chemical reactions. As will be demonstrated below, taking the release of cesium and other fission products as an example, a continuous transport of fission products from the fuel rod gap to the coolant is only possible when they exist in a volatile state or can be converted to a volatile species (with the exception of large defects with direct contact of liquid coolant to the fuel pellet). As was mentioned in Section 3.2.4., fission product iodine is stable as non-volatile iodide, presumably CsI, in the gap of an intact fuel rod. In different in-pile sweep-gas experiments (e. g. Hastings et al., 1985), using a vented fuel rod through which a carrier gas flow was supplied, no iodine volatility was observed in a pure helium atmosphere in the gap, even at linear heat ratings well beyond those experienced by standard LWR fuel rods; iodine transport was only observed when water and/or steam was allowed to enter the fuel rod. Therefore, steady-state release of fission product iodine from the failed fuel rod to the coolant normally has as a prerequisite the conversion of the non-volatile deposited iodide to a volatile species, and it seems that steam is the essential reaction partner in effecting the conversion.

As a potential reaction mechanism it can be assumed that at the gap temperature of 350° to 400 °C steam reacts with the non-volatile iodides deposited in the gap under hydrolytic generation of HI, presumably supported by a catalytic action of heavy metal oxides such as UO_2, U_3O_8 and ZrO_2, among others. This pyrohydrolysis is a reaction mechanism which is well known from the analytical procedures for the determination of light-halogen impurities (chlorine, fluorine) in oxide materials. The HI formed, as a species which is volatile with steam, then has the possibility of being transported to the coolant via the defect at a rate which is constant over time. According to the thermodynamic calculations mentioned above, there is also the possibility that I^- in the gap of a defective fuel rod is oxidized by radiolytically generated oxygen to I_2, which is also volatile with steam under such conditions. From the investigations performed so far, it is not possible to decide which of these two reactions (or whether perhaps some other one) delivers the main contribution to iodine transport, since after having entered the primary coolant the radioiodine will be instantaneously converted to that chemical state which is stable under coolant chemistry conditions.

During steady-state operation of the reactor and as long as there is no change in the number and type of fuel rod failures, the source strengths of the iodine isotopes and their activity ratios are constant over time. This observation suggests that the amount of fission product iodine deposited in the gap shows an equilib-

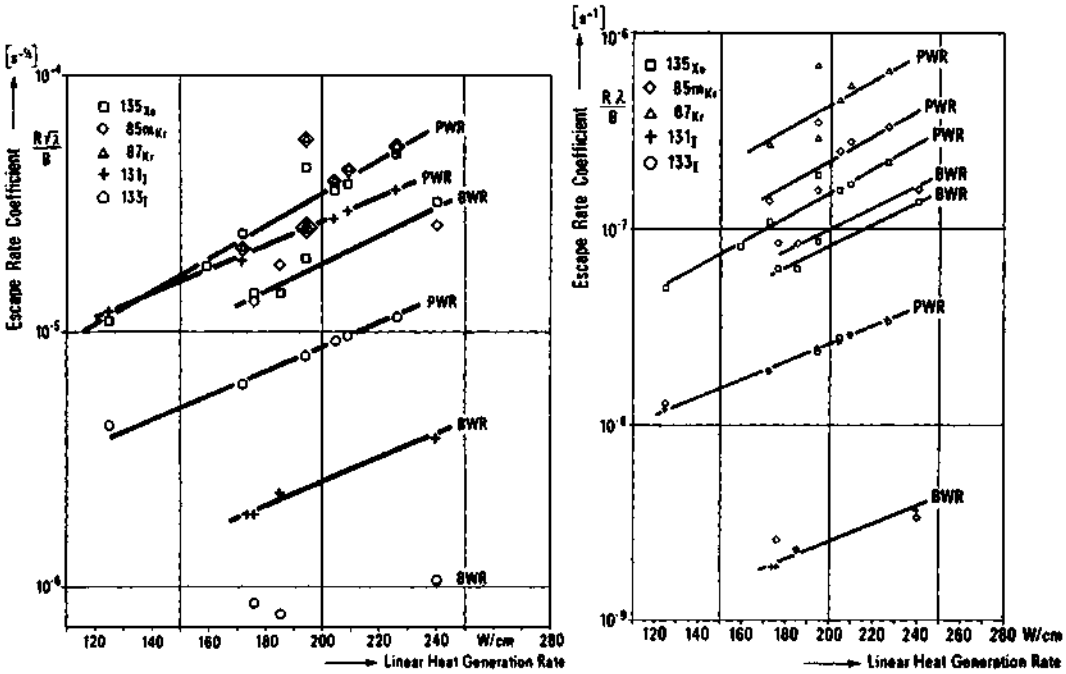

Figure 4.4. Release behavior of iodine and fission gas isotopes according to the diffusion and deposit models
(Schuster et al. 1981; with kind permission from Elsevier Science S.A., P.O. Box 564, 1001 Lausanne, Switzerland)

rium level which is constant over time. This level is determined by the release from the fuel to the gap, on the one hand, and by radioactive decay and transport to the coolant, on the other. The magnitude of the fission product iodine inventory in the gap of a failed rod can be estimated from the iodine releases measured during transients (see Section 4.3.2.2.). From these data and from the source strength data measured under steady-state conditions, it can be calculated that in a PWR core the ^{131}I steady-state release rate is only on the order of 10^{-6} s^{-1} of the gap inventory. This figure indicates a comparatively slow conversion of non-volatile iodides to volatile species by the hydrolysis reactions occurring in the gap during reactor operation and/or a slow transport of the mobilized iodine from its original location to the defect area from where it can reach the coolant.

The differences in behavior between noble gases and iodine isotopes can be clearly seen from Fig. 4.4. (according to Schuster et al., 1981). When the R : B values of the fission product noble gases are corrected for $\lambda^{1/2}$, the isotopes ^{135}Xe, ^{85m}Kr and ^{87}Kr coincide very well and, simultaneously, show a pronounced dependence on the linear heat rating. In contrast, ^{131}I and ^{133}I in this kind of presentation are distinctly separated from each other; however, when their R : B values are corrected for λ, the curves of these two isotopes coincide, too. (More recent investi-

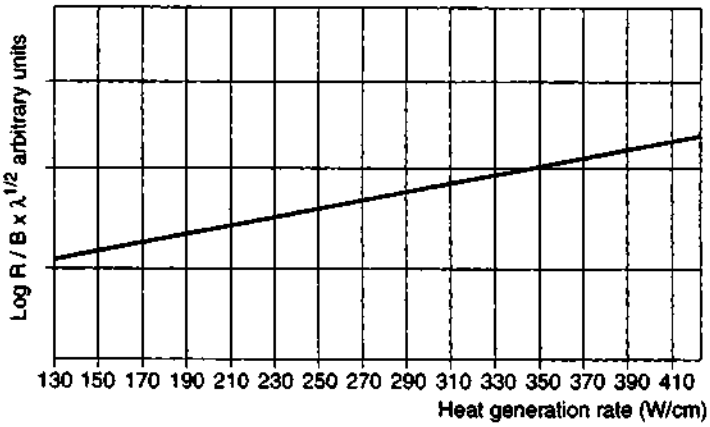

Figure 4.5. Correlation between escape rate coefficient and linear heat generation rate (Schuster et al., 1991)

gations have indicated that the escape rate coefficient for the iodine isotopes is virtually independent of the linear heat rating of the defective fuel rod, contradicting the conclusion implied by the slopes of the iodine curves in Fig. 4.4.). This observation of the differences in dependence on the decay constant between iodine and fission gases can be considered to be an additional confirmation of the existence of iodine deposits in the gap from which fission product iodine has to be mobilized by a chemical reaction. Simultaneously, from Fig. 4.4. one can see a pronounced difference in the escape rate coefficients between PWR and BWR fuel rods, with the PWR values being higher by about a factor of 10. This difference may be due to the fact that in a defective PWR rod (as a consequence of the external coolant pressure which is higher than in a BWR), the H_2O partial pressure is higher, thus accelerating the hydrolysis of iodine compounds which are present in the fuel rod gap.

The escape rate coefficient of the fission product noble gases depends on the linear heat rate of the failed rod. In a logarithmic scale, a straight line dependence of $(R : B) \cdot \lambda^{1/2}$ upon the linear heat rating is obtained with good accuracy (see Fig. 4.5.). This relationship is mainly caused by the accelerated diffusion of the fission products in the fuel at higher temperatures. As an example, the escape rate coefficients of fission product noble gases from a fuel rod showing a linear heat rate of 220 W/cm are higher by a factor of 1.5 to 2 than those from a 170 W/cm rod. In contrast, the iodine escape rate coefficients are not significantly affected by differences in the heat ratings of the fuel rods, thus indicating that the rates of the chemical reactions in the gap are only weakly influenced by the increase in fuel temperature. However, since higher heat ratings mean higher fission rates, the number of iodine atoms escaping from the defective fuel rod (i. e. the source strength) may be influenced to a certain extent. However, Sévéon et al. (1984) reported a clear dependence of the escape rate coeffcients of both the fission product noble gases and the iodine isotopes on the linear heat rating in the region 120

to 350 W/cm from measurements performed on defective fuel rods in a research reactor. Apparently, this dependence is more pronounced for the longer-lived isotopes (^{131}I, ^{133}Xe) than for the shorter-lived ones.

In order to describe the complex mechanism of fission product release from defective fuel rods, several models have been developed, which have been summarized by Lewis et al. (1993). Most of these models are based on physical processes such as diffusion, which means they fully apply for the fission gases only. Chemical holdup in the pellet – cladding gap, which is of relevance for iodine, has been modelled by means of an adsorption isotherm (Beraha et al., 1980). Lewis et al. (1986) reported on a model for describing the steady-state release of noble gases and iodine. In the first stage of this model it is assumed that the release of the fission products from the fuel pellet to the gap is controlled by diffusion. As for the transport of the fission products from the gap to the coolant, two different mechanisms are assumed: In a kinetic model, iodine is postulated to escape from the defective fuel rod following a reaction of wet steam with the non-volatile iodide compounds (presumably CsI) that are deposited on the fuel rod internal surfaces. The observed rate of iodine release into the coolant is assumed to be controlled by a first-order rate process which is proportional to the amount of iodine present in the gap. Transport of the noble gases in the gap is described by a diffusion model. Further, it is assumed that the mobilized iodine diffuses in the gap with a diffusivity which is similar to that of the fission gases; the existence of an equilibrium between the forward and backward (i. e. redeposition of volatile iodine) chemical reactions is also postulated. While the kinetic model covers the whole range of the R : B dependence on the decay constant which was observed in the experiments, the diffusion model can only be applied to those data with an observed dependence near λ^{-1}. A generalized model which includes both the diffusive and the first-order kinetics approach has been developed by Lewis (1990); this model is able to yield the rates of fission product release into the coolant for various defect sizes and locations. Its results are in good agreement for a wide range of defect states with experimental results obtained in an in-reactor program.

With regard to the transport of the noble gases in the gap, Kalfsbeek (1983), in a model intended to be used for determination of the number and size of defects in a BWR core from the concentrations and isotope ratios of noble gases measured in the condenser off-gas, assumed that convective transport in the gap, which is induced by pressure fluctuations of the boiling reactor water, in combination with diffusion, is the mechanism controlling the noble gas transport in the gap. Experiments reported by Sévéon et al. (1984) with defective fuel rods in a research reactor indicated that the noble gas release from the failed rod does not proceed at a constant rate but in bursts with a frequency of about two per hour, accompanied by a parallel decrease of the internal pressure in the rod. From these findings it was concluded that the gases produced by water radiolysis in the pellet – cladding gap were the driving force of the bursts; in the time intervals between the bursts, gases were generated which then initiated the next burst. Such a burst frequency would be too high to be detected in a power reactor with its large primary coolant volume, which responds only slowly to changes in the source strengths; for this reason, the release here appears to proceed steadily.

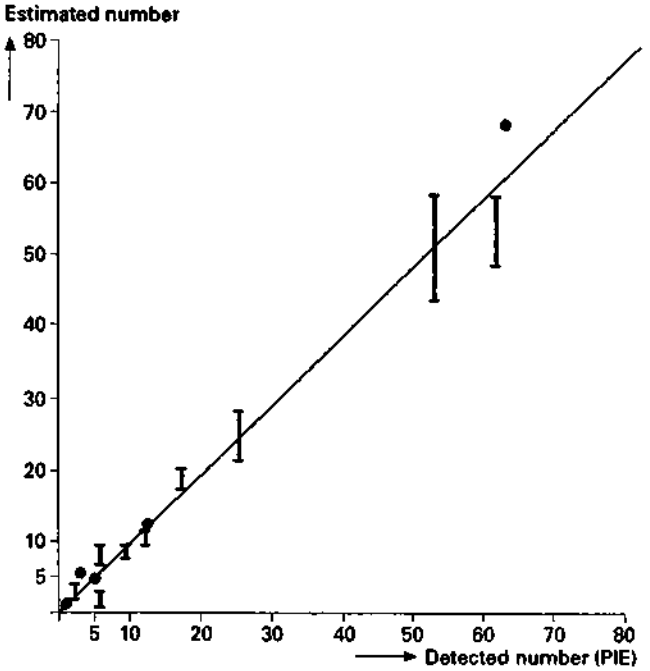

Figure 4.6. Comparison between failed fuel rod estimation and results of refuelling inspections
(By courtesy of Siemens/KWU)

The escape rate coefficients of the iodine and noble gas isotopes identified in one PWR or BWR plant can be directly applied to other plants of the same type, provided that the essential conditions, for example, fuel rod linear heat ratings, are comparable or can be corrected for. By this means it became possible to evaluate the number of failed fuel rods in the core of an operating reactor on the basis of the fission product activity concentrations measured in the coolant; early attempts in this area were reported by Schuster et al. (1977). Although these estimates were based only on empirical data, they permitted a rather trustworthy prediction, as can be seen from Fig. 4.6., where the predicted numbers of failed fuel rods are compared with those detected in the course of post-cycle examinations. These techniques have been considerably improved, on the basis of experimental results as well as of model development and calculations. Because of the great number of parameters influencing the escape of fission products from defective fuel rods, evaluation of the number and type of defects from the measured activity concentration of fission products in the primary coolant is a difficult task which can be performed reliably only by specialists with considerable experience in this field. Attempts were, therefore, undertaken to develop computerized expert systems that could be applied routinely. Lewis et al. (1992) described the development of such a system by means of which information can be obtained on the number of defects and their

average size as well as on the amount of tramp uranium deposited on the in-core surfaces of CANDU reactors. The fission product release model used in this expert system is based on results from in-reactor experiments. The expert system was validated against fuel failure data from operating plants, showing that the number of defective rods can be predicted within a factor of 2.

Such good results are only obtained when all the required data are available and when the operation history of the plant is known in detail. In this context, the fundamental requirement is knowledge of the escape rate coefficient as defined above, by which the standard activity concentration of fission product noble gases and iodine resulting from one defective fuel rod can be calculated. However, in calculating the number of failed fuel rods one has to remember that the escape rate coefficient of the noble gases in particular increases with the linear heat generation rate of the relevant fuel rod, thus reflecting its influence on the diffusion rate of the fission product noble gases (see Fig. 4.5.). Consequently, when the linear heat rating of the defective fuel rods is not known (which is usually the case), the estimates can only be made using a core-averaged linear heat rating. This results in an inherent range of uncertainty.

Besides the number of defective fuel rods present in the reactor core, evaluation of the size of the defects and their development over time is of great interest, since from this information conclusions can be drawn as to the possible defect mechanism. The most important relationship in this context is the dependence of the R : B ratios on the decay constant λ. Relevant experiments in this area have been performed at various institutions. Lewis et al. (1986) reported on in-pile experiments with fuel rods showing different defect sizes (drilled hole, cladding hydriding, machined slits) in a research reactor at the comparatively high linear heat ratings of 480 and 670 W/cm. These experiments yielded release dependences between $\lambda^{-1/2}$ and $\lambda^{-3/2}$, depending on the defect size and on the fission product species, either noble gases or iodine. Since diffusive release from the bulk UO_2 shows a dependence of $\lambda^{-1/2}$, any delay in release from fuel rods with defects of smaller size can be attributed to an additional trapping in the pellet – cladding gap as the fission products migrate toward the defect site. The steeper slope for iodine indicates a greater holdup of this species in the gap which is due to chemical reactions, while the trapping of the noble gases apparently is caused by the slower movement of the gas phase in the gap with smaller defect size. Thus, it is evident that the escape rate coefficient for iodine is more sensitive to changes in the defect size than is that for the noble gases; for a small defect the difference is considerably greater, reflecting greater iodine holdup in the gap. Larger defects usually result in a larger oxidized fuel volume, thus increasing the diffusion rate of iodine from the pellets to the gap; the effective diffusion coefficients reported by Lewis (1986) were similar to the values reported by Schuster et al. (1981) for defective PWR fuel rods, but greater by several orders of magnitude than values for intact elements where the UO_2 fuel was unoxidized. In addition, Lewis et al. (1986) postulated dependence of the fission product iodine mobility in the gap on the defect size. They assumed that for a small-sized defect the small quantity of iodine that is released from the fuel rod originates from a localized area in the immediate vicinity of the defect, where the ratio of liquid-to-steam in the gap atmosphere is comparatively high,

since liquid water or wet steam were considered to be the active reagent in the volatilization of the deposited iodine. Dry steam that is far removed from the defect should be less effective in the mobilization of iodine; thus, the rate constant for release is considerably less than that for decay, yielding a dependence of $\lambda^{-3/2}$. However, the significance of liquid water for the hydrolysis reactions yielding volatile iodine species seems to be questionable. Volatile iodine produced far away from the defect site can be recombined to form non-volatile species once again when it migrates in the gap; such a chromatography-like transport to the defect would also mean that only the deposits in the vicinity of the defect contribute significantly to iodine release to the coolant. This effect also means that the isotope composition of the deposits at a certain distance from the defect position should be older than that in its immediate vicinity, an assumption which is confirmed by the changes in the isotope ratio of iodine released during transients (see Section 4.3.1.2.). For the noble gases, the rate-determining process is assumed to be that of simple diffusion in the gap, thus yielding a total dependence (diffusion from the fuel included) of λ^{-1} (Lewis et al., 1986). With a defect of intermediate size, both iodine and noble gas are observed to exhibit the same dependence, since iodine is now more mobile, with an increased liquid-to-steam ratio in larger regions of the fuel rod (see above). With a large defect, finally, the only rate-determining process for both species is that of diffusion through the fuel matrix. In this case, the escape rate constants for both iodine and noble gases are much greater than the decay constants, yielding a dependence of $\lambda^{-1/2}$.

The results reported by Schuster et al. (1991) demonstrated the applicability of these principles to power reactors by comparing the predictions with the results of the post-cycle examinations of the fuel assemblies. As was mentioned above, as long as the number and size of the defects in the fuel rod claddings remain unchanged, the activity concentrations of the main fission products in the coolant is constant over time. The appearance of new defects in other fuel rods usually will result in an increase in the activity concentrations of noble gas and iodine isotopes in the primary coolant from the former steady-state level to a new, higher one which is reached several days later. From the composition of the fission product mixture entering the coolant, conclusions can be drawn as to the type and development of the defect: Very small defects (pinholes) are in most cases characterized by the fact that a comparatively "old" mixture of fission noble gas isotopes is released, with a corresponding release of iodine isotopes not occurring before an enlargement of the defect size has occurred. The same applies to beginning pellet – clad interaction (PCI) failures, which usually initially lead to tiny cracks in the cladding. Under such conditions, the escape of fission gas isotopes is delayed, resulting in high source strength ratios (e. g. $^{133}Xe : ^{135}Xe$ ratio on the order of 10 to 20); simultaneously, the escape of iodine isotopes from the defect is prevented. It should be emphasized that large PCI failures have not been observed in recent years, due to the general acceptance of specific operational recommendations. Fretting failures in the lower region of fuel rods containing a lower gas plenum are indicated by source strength ratios of the fission gases which are close to the normal values (corresponding to the diffusion mechanism), combined with an enhanced iodine escape and a high source strength ratio of the iodine pair $^{131}I : ^{133}I$ (on the order

of 10). With such defects, fuel rods which only contain an upper gas plenum show iodine source strength ratios that are close to the expected values of radiochemical equilibrium. Baffle jetting generally produces more than one fuel rod failure; in this case, all the fission product activity concentrations in the coolant increase immediately on the appearance of the defects. In such a case, the source strength ratios of fission gas isotopes and iodine isotopes show normal values at the very onset of the defects; however, the ratios soon decrease to values of about two for both $^{133}Xe : ^{135}Xe$ and $^{131}I : ^{133}I$. This behavior is accompanied by an increase in the coolant activity concentrations of the cesium isotopes and a pronounced increase in the ^{239}Np activity concentration, as soon as a direct contact between fuel and liquid coolant occurs. Likewise, as a consequence of the formation of larger-sized secondary defects with a direct contact between liquid coolant and fuel, the above-mentioned source strength ratios of fission gas and iodine isotopes also change to lower values, while ^{239}Np concentration increases moderately over a longer period of time. In contrast with baffle jetting failures, in secondary hydride failures the activity concentrations of noble gases and iodine isotopes remain constant over time, with a tendency to decrease slightly in the long term.

Particular defect types may result in unusual behavior of the activity concentrations of fission products in the coolant. For example, Goncarovs (1993) reported on a steel-cladded PWR reactor core where in the course of a fuel cycle a great number of fuel rods suffered from debris-induced failures near the lower end of the fuel rods. While the ^{131}I activity in the coolant remained virtually constant over the whole fuel cycle, indicating only a few failed rods, the ^{133}Xe activity increased considerably with only little contribution from the shorter-lived fission gas isotopes. Such behavior is a consequence of this defect type in stainless-steel claddings where no secondary hydride failures develop; therefore, with Zircaloy cladding such a fission product behavior is to be expected only during the initial period following the appearance of the primary defects, prior to the formation of secondary hydride failures. A specific model has been developed allowing prediction of the number of defective fuel rods in such cases, which showed satisfying accuracy when compared with the post-cycle examinations.

Another example of unusual failures was reported by Zänker (1989). He described periods of continuously decreasing levels of fuel rod integrity due to debris-induced cladding damage, vibration-induced fretting wear of the cladding, etc., showing a fission product release behavior which might cause difficulties in the assessment of fuel rod performance from the coolant activity data. In such a situation, an increased concentration of a comparatively "old" mixture of fission product isotopes appears in the coolant (e. g. for iodine isotopes characterized by a $\lambda^{-2/3}$ dependence) which, at first sight, may be interpreted as originating from a larger number of very small defects. During such a period, the release of a stored mixture of volatile fission products showing an equilibrium isotopic composition from the gap of the fuel rod represents the predominant release mechanism. In addition, the resulting contact between the fuel pellet and the coolant after the development of such a defect can lead to thermal shocks, resulting in pellet cracking and a sudden release of the stored fission products from bubbles or grain boundaries within the pellet; finally, grain boundary oxidation may also lead to

the release of a stored mixture with a $\lambda^{-2/3}$ dependence. If a singular appearance of such a defect occurs, a spiking will take place which is removed after one or, at most, a couple of days by the action of the coolant purification system; however, when such failures occur repeatedly with a frequency of one or more a day, a continuous increase of the iodine steady-state activity levels in the coolant will result. In order to distinguish such a situation (which might require immediate action from the operators) from the above-mentioned occurrence of a larger number of very small failures, a continuous increase in the ^{239}Np activity level (as well as ruthenium, cerium, etc., activities) is an appropriate indicator, in addition to the enhanced iodine activity level and the $\lambda^{-2/3}$ dependence of the iodine isotope mixture. In such situations, the slope of the long-lived isotopes may be influenced to a certain extent by the recoil release from uranium contamination present in the reactor core from which a very "young" iodine isotope mixture is released to the coolant. However, this effect can be corrected for by using measurements of short-lived isotopes such as ^{134}I, so that interferences are usually small.

As was pointed out above, fission products are released from uranium contamination present on the surfaces of the reactor core by recoil, which means that their R : B ratios do not depend on the decay constant λ; as a consequence, the fission product mixture entering the coolant is characterized by a comparatively high proportion of short-lived isotopes. A a result, this type of source can easily be distinguished from fuel rod failures. In addition, fission product iodine originating from uranium contamination does not show the shutdown spiking that characterizes fuel rod failures (see Section 4.3.1.2.). A more complicated situation exists when both uranium contamination and failed fuel rods are simultaneously present in the reactor core. As was emphasized by Lewis (1987), in such a case there is a superposition of the two release processes, leading to a release curve which is sloped for the longer-lived isotopes, but is independent of the decay constant for the shorter-lived isotopes (see Fig. 4.7. as an example). Since the release of ^{131}I is mainly due to fuel rod failures, its release rate can be used to estimate the number of in-core defects. Similar dependences of the R : B values of the fission product noble gases on the decay constant λ are measured in the off-gas of BWR plants (see Fig. 4.8., according to Lewis, 1988) where the amount of contamination in the reactor core can be determined from the short-lived isotopes, while the longer-lived ones are indicators for fuel rod failures. When the amount of contamination is calculated from the height of the horizontal part of the curve, it has to be noted that this quantity pertains only to the amount of fuel present on surfaces within the neutron field. If it is assumed that the fuel contamination is evenly distributed throughout the entire primary circuit, then the total fuel loss from defective rods can be obtained by multiplying by the appropriate surface area ratio.

According to Hüttig et al. (1990), the amount of uranium released from defective fuel rods and deposited on in-core surfaces can be assessed from the coolant activity levels of various short-lived fission products such as ^{132}I, ^{134}I, ^{138}Cs, calculating their source strengths under the assumption of a direct and instantaneous release to the coolant. Though the releases of these isotopes from failed fuel rods are quite small (due to their short halflives), such data can provide only an upper limit for the uranium contamination if there are simultaneously fuel rod failures in

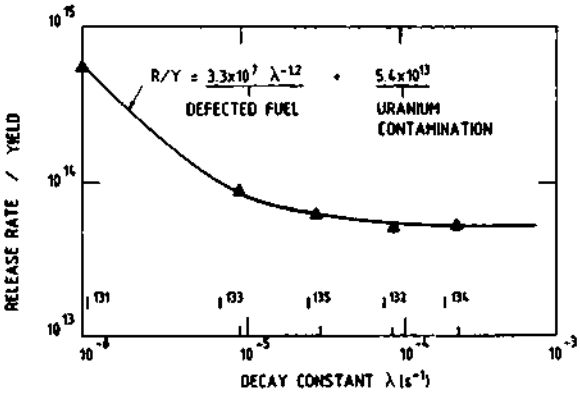

Figure 4.7. R:B ratios of fission product iodine isotopes as a function of the decay constant in the case of the simultaneous presence of fuel rod defects and uranium contamination; PWR primary coolant
(Lewis, 1987; with kind permission of Elsevier Science – NL, Sara Burgerhartstraat 25, 1055 KV Amsterdam, The Netherlands)

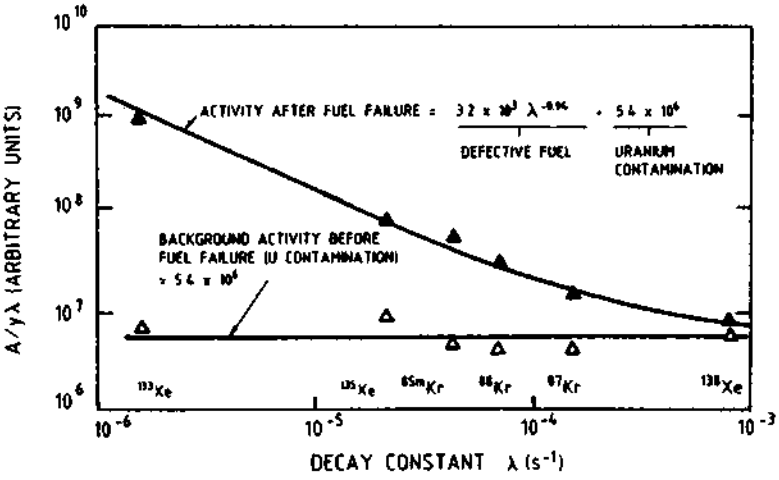

Figure 4.8. R:B ratios of fission product noble gas isotopes as a function of the decay constant in the case of the simultaneous presence of fuel rod defects and uranium contamination; BWR off-gas
(Lewis, 1988; with kind permission of Elsevier Science – NL, Sara Burgerhartstraat 25, 1055 KV Amsterdam, The Netherlands)

the reactor core. In spite of this limitation, realistic conclusions as to the order of magnitude of uranium contamination in the reactor core can be drawn, as has been demonstrated by appropriate post-irradiation examinations.

The other fission product nuclides, such as the isotopes of cesium, the alkaline earths and the rare earth elements, as well as tellurium and the actinides, show an

extremely low vapor pressure under the conditions prevailing in the gap of a failed fuel rod. Consequently, during constant-load operation of the reactor they are released to the coolant only to a very small extent. Despite this, these nuclides are frequently observed in the coolant originating from transport processes which occur during transients (see below). This is in particular true for ^{137}Cs and ^{134}Cs; due to the low decontamination factors of cesium on the ion exchangers of the PWR purification system, residual fractions of the cesium isotopes which were released during a transient will remain in the coolant for a relatively long time.

Among the polyvalent fission product elements, technetium exhibits a somewhat strange release behavior, as can be concluded from the limited database available at this time. As was discussed in Chapter 3, for thermodynamic reasons this element is assumed to exist in the fuel in the metallic state; however, virtually nothing is known about its chemical state in the pellet – cladding gap. On the other hand, ^{99m}Tc analyses in LWR coolants have indicated that its release fraction (related to the fuel rod inventory) is higher by a factor of 10 to 100 than that of the cesium isotopes and that there is a time-constant steady-state release, i. e. that the transport from the failed fuel rod to the coolant is not restricted to spiking transient conditions. Both these observations suggest a gas-phase transport similar to that of iodine isotopes. In PWR primary coolant, the ^{99m}Tc activity usually is distinctly lower than that of ^{137}Cs, whereas in BWR reactor water it is higher; this difference is assumed to be due to the insufficient cesium retention on the PWR purification resins which are saturated with lithium, thus resulting in a cesium accumulation in the PWR coolant. Currently, there is no information as whether or not the differences in PWR and BWR water chemistry affect the transport of fission product technetium from the failed fuel rod to the coolant. It has to be pointed out that ^{99m}Tc can also be produced by neutron activation of molybdenum which is present as a constituent of various primary circuit materials, via decay of ^{99}Mo. Therefore, the appearance of ^{99m}Tc in the coolant is not necessarily caused by fuel rod failures. During a shutdown period, fission product ^{99m}Tc shows a spiking behavior similar to that of iodine and cesium with regard both to its time behavior and to the spiking factor. Differences in the release behavior between PWR and BWR have not been observed, possibly because of the limited experimental data.

The appearance of non-volatile fission products or actinide isotopes in the coolant can indicate the presence of fuel rod defects with a direct contact between the fuel and liquid water. This can occur with large-sized defects, in particular in comparatively cold regions of the fuel rod at the vertical or horizontal periphery of the reactor core. However, any statement in this regard can only be based on radionuclides that are not present in the coolant as a remnant from preceding transients; this means that in a PWR ^{137}Cs or ^{134}Cs are not appropriate indicators for such fuel rod failures. The requirements are in principle fulfilled by ^{239}Np, which is a reliable indicator for defects with fuel-to-water contact, as are ruthenium and cerium isotopes, as well. However, because of the complex behavior of these radionuclides in the coolant (adsorption on suspended corrosion products and deposition on primary circuit surfaces), only qualitative assessments can be made, which means that a quantitative evaluation of the number of fuel rods showing

large-sized defects is not possible on the basis of the measured ^{239}Np activity in the coolant.

According to Beslu et al. (1984), a differentiation between fuel rod failures and fuel contamination should be possible on the basis of the fact that, due to its small particle dimensions, tramp uranium does not show self-shielding against epithermal neutrons, resulting in a faster ^{239}Pu buildup than in the fuel pellet. Because of the considerable differences in the fission yields of the krypton isotopes between uranium fission, on the one hand, and plutonium fission, on the other, their measurement can, in principle, give an indication of the type of source feeding fission products into the coolant. Moreover, calculations have shown that the specific alpha activity in tramp uranium should be higher by a factor of 3 to 4 than in a fuel pellet of the same burnup, at least after an irradiation time of the fuel traces of 2 to 3 MWd/kg U. However, analyses of the activity ratios of ^{134}I and ^{85m}Kr at various plants having different core defect states did not show significant differences. Furthermore, it seems questionable whether the basic idea of the differentiation will hold true under real reactor conditions, since the outermost rim zones of a fuel pellet, which are mainly responsible for fission product release, also do not show a significant self-shielding effect.

With regard to the fission product isotopes of Zr, Nb, Ru, Ce, Pr, La it can be assumed that they are not liberated directly from the fuel of a failed rod but that they are released by leaching of the fuel pellets and that the amount transported to the coolant is equivalent to the amount of fuel released from the defective rod. On the other hand, a direct release is assumed for strontium and barium, with the investigations suggesting a release rate lower by a factor of 10 than that of cesium (Beslu et al., 1984).

With regard to the release of actinides from a failed fuel rod to the coolant, it has to be considered that, with the exception of the small contribution caused by knock-out processes, there is no significant actinide gap inventory because of the comparatively low β^- and γ recoil energies, which are not able to overcome the binding energy of the oxides of these elements, and because of the strong bonding in the fuel matrix which prevents diffusion. As a consequence, there are only two mechanisms for actinide release, namely erosion of the fuel or congruent dissolution of the fuel by liquid coolant. In both cases, the radionuclides transported to the coolant represent the composition of the fuel, explaining why ^{242}Cm is the actinide isotope that shows the dominant α activity concentration in the coolant. On the other hand, from the available data one can conclude that plutonium which is detected in the primary circuit has been predominantly released from the defective fuel rod as plutonium and that only a small fraction of it was generated in the primary circuit by β^- decay of ^{239}Np released from the fuel.

In general, release of actinide isotopes from failed fuel rods and their subsequent behavior in the primary circuit is very similar to that of certain fission products, e. g. of cerium isotopes. For this reason, the γ-emitting cerium isotopes which can easily be measured in the coolant by γ spectrometry, can serve as a suitable indicator for early recognition of higher releases of actinides to the coolant. The release behavior of the actinides from failed mixed-oxide fuel rods to the coolant is almost identical to that from uranium fuel rods. This means that in both cases the U : Pu

ratio of the released material is identical to that present in the fuel, at least to that present in the outermost zones of the fuel pellets. As far as is currently known, there are no significant differences in the solubilities in primary coolant between LWR mixed-oxide and uranium fuels.

Some of the metallic fission products are plated out to a large extent onto the outer surfaces of the fuel rod claddings in the immediate vicinity of the defect; this means that only small fractions of them are transported into the coolant. This is true in particular for tellurium, probably due to an electrochemical reaction on the Zircaloy surface resulting in the formation of the compound SnTe. The rather long-lived ^{132}Te (halflife 76.3 h) decays there under the production and continuous release of its daughter ^{132}I to the coolant; this mechanism is assumed to be the reason for the specific release behavior of this radionuclide, which is markedly different from that of the other iodine isotopes, both during constant load operation and during transients.

On several occasions it has been observed that ^{95}Zr is present in fuel rod deposits in the vicinity of a cladding failure in much higher concentrations (up to a factor of 100) than in the more remote regions of the fuel rod. This inhomogeneous distribution is potentially due to a fast isotope exchange between carrier-free fission product ^{95}Zr escaping from the defect and the constituents of the fuel rod deposits. ^{95}Zr, which is present in the deposits in regions of the fuel rod which are more remote from the defect position, probably does not originate from fission product release, but from neutron activation of the Zircaloy matrix element.

4.3.1.2 Release from defective fuel rods during reactor transients

In the preceding section it was reported that fission product noble gases and fission product iodine escaping from defective fuel rods show source strengths that are constant over time, at least as long as no significant changes in the defect state of the reactor core or of individual failed fuel rods occur. In the course of major variations in reactor load, however, a temporary increase in the activity concentrations of these fission products in the coolant (a so-called spiking) is observed. In particular, this effect occurs during a shutdown of the reactor, which would seem to contradict the dependence of the release rates on the heat rating of the fuel rods, as has been described above. The simplest assumption for explaining this effect would be the appearance of additional fuel rod failures caused by the change in reactor load. But this idea can be ruled out, since, after having again reached the rated load of the reactor, the activity concentrations will once again reach the steady-state values they had attained previously, indicating no change in the number and size of the fuel rod defects. In addition, detailed examinations of fuel rods which had been subjected to relevant experiments in research reactors and which exhibited fission product spiking, showed no significant increase in the number or size of the rod failures (e. g. Lewis et al., 1987). A more detailed exami-

nation of this phenomenon reveals considerable differences in the time behavior of different fission products during the transient which can be interpreted as the consequence of different mechanisms of the spiking effect.

During reduction of reactor load, the activity concentrations of the fission product noble gases in the PWR primary coolant show short-term peaks which correlate directly with regard to time to the variations of reactor load, with the peak values being only moderately higher than the previous steady-state concentrations. The origin of these spikes is assumed to be the formation of cracks in the fuel pellets as a consequence of temperature changes in the ceramic material. As a result, fission product noble gases which had accumulated on the grain boundaries of the fuel pellet can be released without delay to the gap of the rod. Similar effects were observed in heating irradiated fuel pellets in a laboratory furnace and applying short-term temperature changes, as well as in in-reactor sweep gas experiments as a consequence of load changes of the vented test rod. The reason for the enhanced fission product noble gas release from defective fuel rods during a transient, therefore, is the increased release from the pellet due to an enlargement of its effective (open) surface area.

The development of the activity concentrations of the iodine isotopes in the coolant during a reactor transient is quite different from that of the noble gases; in addition, there are marked differences between PWRs and BWRs. Because of the radiological significance of the isotope ^{131}I, the iodine spiking has been thoroughly analyzed by different authors. In the following it will also be treated in detail since some interesting insights concerning fission product behavior in a failed fuel rod can be obtained from this phenomenon. First, a description of the observed behavior will be given, followed by a presentation of the current state of knowledge on the origin and the mechanism of this effect.

Iodine spiking in pressurized water reactors was first analyzed in detail by Neeb (1971) using data obtained by measurment during several reactor shutdowns at the Obrigheim PWR plant. The time-behavior of the activity concentrations of the iodine isotopes in the coolant, which is exemplarily shown in Fig. 4.9., is fully consistent with the results reported by other authors, e. g. by Chubb et al. (1977), from Westinghouse PWR plants.

When in the course of a shutdown of a PWR plant, the reactor load decreases below a level of 40 to 60% of the rated power, a steep increase in the activity concentrations of the iodine isotopes in the primary coolant begins. For ^{131}I, the slope of the curve shows a doubling time of the activity concentration of 10 ± 3 minutes, leading after about 60 minutes to a maximum which is higher by a factor of 50 to 100 than the preceding steady-state level. After having reached its maximum level, the concentration decreases again at a rate corresponding rather well to that calculated from both the purification rate and the physical halflife of the radionuclide, which for ^{131}I at a purification rate of 10% of the primary coolant volume per hour results in an effective halflife in the coolant of about 6.5 hours. Following reduction of the coolant pressure, the decrease of the activity concentration is interrupted by new spikes (depressurization spikes), whose magnitude is usually distinctly lower than that of the initial shutdown spike.

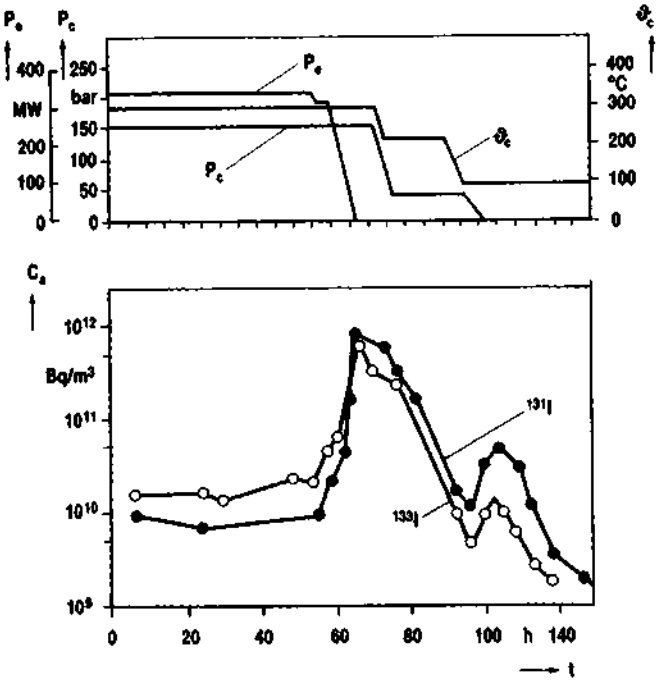

Figure 4.9. Fission product iodine activity concentrations in PWR primary coolant during reactor shutdown (P_e reactor load; P_c coolant pressure; ϑ_c coolant temperature; C_a activity concentration)
(Neeb and Schuster, 1979)

The results reported by Sévéon et al. (1984) from irradiation experiments in a research reactor are consistent with the results of the plant measurements mentioned above. They indicate that the ratio of the steady-state release to the peak value attained during a shutdown depends on the size and the position of the defect, on the heat rating of the failed fuel rod and, finally, on the composition of the gas phase inside the rod. From the experimental results it was also concluded that during the reactor shutdown and the subsequent depressurization of the coolant from 15.5 to 2.7 MPa, only 70% of the fission product iodine inventory originally present in the gap is liberated, presumably because of the incomplete expulsion of the water inventory of the failed fuel rod. A comparison of the magnitude of the release measured in the experiments and the calculated gap inventory resulted in a satisfying agreement, when the limitations mentioned above were taken into account.

By a more detailed analysis of the available experimental data, further effects can also be detected. The increase in activity concentration of the shorter-lived ^{133}I is considerably less pronounced than that of ^{131}I, with the maximum of its activity concentration in the primary coolant during the spike being higher by only a factor of 10 to 30 than the level during the preceding steady-state operation phase. During

constant-load operation, the ratio of activity concentrations $^{131}I : ^{133}I$ in the PWR primary coolant amounts to 0.3 to 0.5, corresponding to a source strength ratio of both isotopes of 3 to 4; in the peak maximum of the spiking phase, however, a ratio of activity concentrations of 1 to 2 is measured from which a source strength ratio of both isotopes of 10 to 15 can be estimated using a simplified calculation method. As for the shorter-lived iodine isotopes, the time behavior of the increase in their activity concentrations in the coolant is similar to that of the two isotopes mentioned above; the altitude of their peak maxima, however, is lower the shorter the halflife of a given isotope is. ^{132}I shows a unique behavior: the increase of its activity concentration in the coolant proceeds almost parallel to that of the other iodine isotopes, whereas it declines more slowly than calculated from purification rate and physical halflife. In addition, during depressurization of the coolant no additional ^{132}I spikes are observed.

Observations in some PWR plants showed that no shutdown spiking occurs when defective fuel rods are present exclusively in regions of low heat ratings, e. g. at the outermost periphery of the reactor core.

When the reactor is started again after the shutdown, a new iodine spiking is observed with a concentration maximum which is usually distinctly lower than that of the shutdown spiking. This startup spike is probably caused by the temperature increase inside the fuel rod and indicates the expulsion of water containing dissolved fission products which remained in the defective fuel rod during the shutdown phase. Because of the radioactive decay of the shorter-lived fission products, the magnitude of this startup spike depends, among other parameters, on the length of the shutdown period. The observation of a so-called critical load range during startup of the reactor at about 165 W/cm, at which the release of short-lived fission products was reported to be higher than at higher heat ratings (Sévéon et al., 1984), is presumably due to this startup spiking.

If a reactor shutdown is followed by a second one after only a few days of plant operation, then the iodine spiking which appears in the course of the second shutdown is distinctly lower than that experienced during the first one. Only after a longer period of operation (more than about 10 days) will the new spike maximum again reach the level of the first one. As was calculated by Schuster et al. (1977), the spikes to be expected as a consequence of load reduction during a load-following operation regime are higher by a factor of only 2 to 3 than the preceding steady-state activity levels. This calculation was confirmed by measurements at a PWR plant during a threefold 100–60–100% load cycle which showed a maximum spike factor of 1.6. However, since the enhancement of iodine release rates during a load-following operation potentially depends on the nature of the cladding defect, this value can only be considered as an example. With small defects (< 100 μm) only a fraction of 10 to 20% of the gap inventory seems to be released during one transient, so that in a load-following operation with a frequency of one load variation per day (day–night cycles), each power reduction will lead to iodine spikes with steadily decreasing height (Leuthrot and Beslu, 1986).

As was discussed above, the maximum iodine activity concentrations attained in the course of a PWR shutdown spiking apparently depend on the type, position and number of defects present in the reactor core. When these parameters are

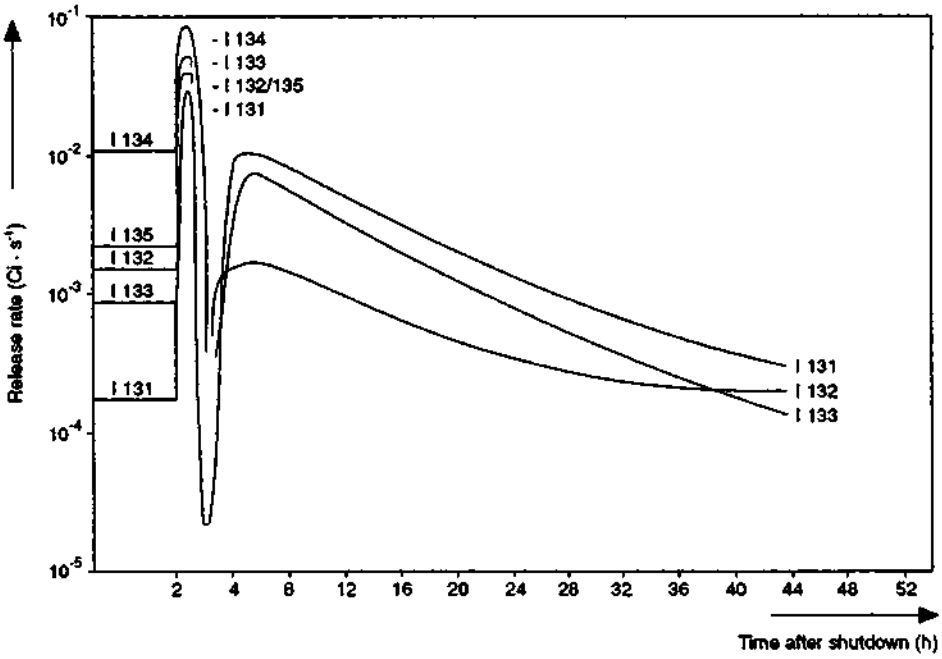

Figure 4.10. Fission product iodine activity concentrations in BWR reactor water during reactor shutdown
(Eickelpasch and Hock, 1974)

essentially unchanged, the spiking levels occurring in subsequent shutdowns are virtually identical. The mode of reduction of the reactor load does not influence significantly the time behavior and the maximum level of the spiking effect; numerous measurements have demonstrated that the spiking provoked by a reactor trip develops in the same manner as that occurring during a planned shutdown.

Boiling water reactors also exhibit an iodine spiking during load reduction; however, the time behavior of the activity concentrations in the reactor water is quite different from that observed in a PWR. As was described in detail by Eickelpasch and Hock (1973), after reactor shutdown initially a decrease in the release rates of all iodine isotopes from the defective fuel rods to the reactor water is observed, followed by an increase which leads to a maximum level with release rates higher by 1 to 2 orders of magnitude than during the preceding constant-load operation phase (see Fig. 4.10.). In this case, too, the enhancement factor for ^{131}I is considerably higher than that for the shorter-lived isotopes (about 20 for ^{133}I and about 5 for ^{132}I). In general, BWR spiking shows increased activity concentrations over a longer period of time than PWR spiking, with both buildup and decrease of the activity concentrations proceeding more slowly. The maximum activity concentrations in the reactor water are usually obtained 5 to 8 hours after reactor shutdown, in extreme cases only after 20 hours. The reduction of the activity concentrations present in the reactor water proceeds very slowly, an effect which

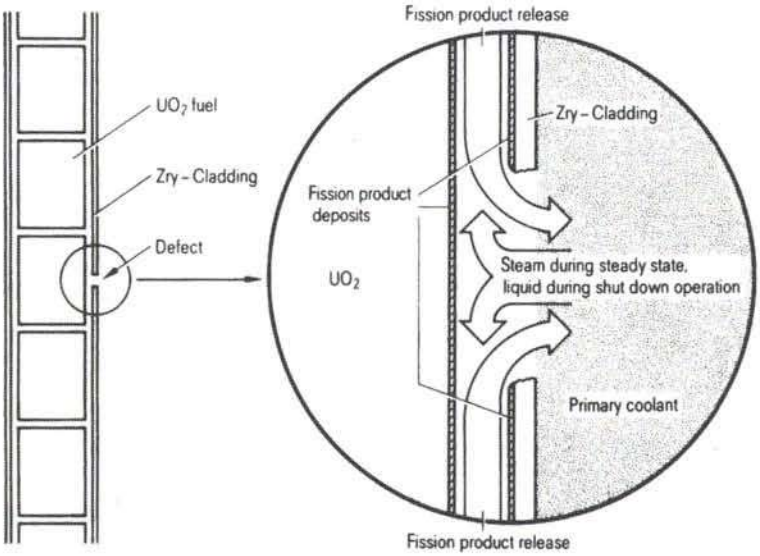

Figure 4.11. Release mechanisms of fission products from a failed fuel rod (Neeb and Schuster, 1979)

can only be explained by a continuing release from the failed fuel rods; the source strength 3 to 4 days after reactor shutdown is often still higher than that during the preceding constant-load operation phase, in spite of the considerably lower fuel temperatures at this time. In a few cases, a spiking immediately following reactor shutdown was observed, the level of which, however, only rarely reached the values of the subsequent concentration maxima.

The activity concentrations of the longer-lived cesium isotopes ^{134}Cs and ^{137}Cs exhibit a spiking behavior during reactor shutdown which is virtually identical to that of the iodine isotopes; this applies to PWRs as well as to BWRs.

In spite of the remarkable differences, in particular in the time behavior, of iodine spiking in PWRs and in BWRs, in both cases the spiking effect can be explained by similar processes. The mechanisms responsible for this effect were analyzed in detail by different authors, for PWRs by Lutz and Chubb (1978) and by Neeb and Schuster (1978; 1979), for BWRs by Eigenwillig and Hock (1976) and by Eickelpasch et al. (1978). The observation which is of the highest importance for the explanation of the release mechanism is the identical behavior of iodine and cesium (and other fission products such as ^{99m}Tc) and the differences from the behavior of the noble gases, indicating a transport of iodine from the defective fuel rod to the coolant via the liquid phase. On the basis of this fact, the following ideas on the mechanism of the enhanced release of fission products during transients have been developed (see Fig. 4.11.):

During reactor operation at full load, coolant which has entered a defective fuel rod is converted to steam because of the higher temperatures in the gap as compared with the coolant (the only exceptions possibly are the colder regions of the

defective fuel rod such as the lower plenum or peripheral rods where water may exist in the liquid state inside a rod even during operation at rated power). For this reason, a continuous transport of fission products from the gap to the coolant is only possible when they exist in a volatile form or when they are converted into such a species by chemical reactions within the gap. In contrast, fission product species showing a very low vapor pressure under the conditions prevailing in the gap can reach the coolant during full power operation only when particular mechanisms such as a direct contact between liquid coolant and the fuel pellet are acting.

In the course of progressive reduction of the reactor load, the temperature of the fuel pellet surfaces and, simultaneously, the temperature in the gap decreases. In the PWR primary circuit, the coolant operating pressure of about 16 MPa is maintained during this phase of shutdown; for this reason, the steam atmosphere in the gap collapses below a definite power level, thus giving way to an ingress of liquid water into the rod. The fission product deposits present in the gap now can be leached by liquid water at a temperature of about 300 °C. Dissolved fission product iodine and other soluble fission products are then transported rather quickly by diffusion via the defect to the coolant, presumably supported during the initial phase by a convective movement of the liquid phase inside the rod. The characteristic doubling time of the activity concentration in the coolant of 10 ± 3 minutes is assumed to result from the progress of the liquid front in the gap as well as from the transport of the dissolved fission products from their original location to the defect position. Because of the long and narrow pathways in the gap, both processes will need some time; which of them is the rate-controlling one for the release to the coolant is not yet known.

The maximum level of the activity concentrations in the coolant is probably reached at the moment when the gap of the failed fuel rod is filled with water and when there is no further movement of the liquid front and no convection within the liquid phase. After this point, additional fission products may reach the leak position and escape to the coolant by diffusion in the liquid phase only, which within the gap is probably a comparatively slow process and does not cause a significant further increase of the activity concentrations in the coolant, which are already high at this moment. Therefore, the activity concentrations in the coolant begin to decrease at a rate which corresponds to that effected by the action of the purification system. Following a reduction in the coolant pressure, however, an additional fraction of the liquid phase can be transported from inside the rod to the coolant by the action of temporary pressure differences, leading to the formation of the secondary depressurization spikes as shown in Fig. 4.9. When the reactor is started up again after the shutdown period, water which still remained in the gap of defective fuel rods, containing dissolved fission products, is transported out to the coolant, forced by the increase in temperature of the fuel pellets.

Basically, BWR spiking can be explained by an identical mechanism. The differences from PWR spiking are due to the fact that in a BWR primary system after reactor shutdown, coolant temperature and coolant pressure decrease in parallel, as a consequence of which the steam atmosphere in the defective fuel rod is maintained for a longer period of time and ingress of liquid water is delayed. For this reason, reduction of reactor load and of fuel temperature at first result in a

decrease of the fission product release rates from the failed fuel rods. Condensation of steam and formation of a liquid water phase inside the defective fuel rod will start later on when the decay heat of the fuel has fallen below a definite value which depends on the degree of subcooling of the reactor water at the position of the defect. With defects in the lower region of the fuel rod, the rather low inlet temperature of the reactor water (possibly mixed with water from the residual heat removal system) together with the higher pressure in this region caused by the geodetic water height will lead to an early onset of the spiking, in some cases even immediately after reactor shutdown. When, on the other hand, the defects are located in the central region of the core, in particular in fuel rods showing higher heat ratings, then the spiking will begin only several hours after reactor shutdown. The onset of condensation of the liquid water in the failed fuel rod therefore depends on the location of the defect, which explains the differences in time behavior of the spiking events observed at different reactors or after different fuel cycles. In general, the gradient of the increase of the activity concentrations in the BWR reactor water is significantly smaller than in a PWR, indicating that the progress of the liquid phase in the fuel rod gap and the convective support of fission product transport to the coolant proceeds more slowly.

The iodine deposits that exist in the gap of a failed fuel rod during constant-load operation are largely depleted during the spiking phase. This can be concluded from the observation mentioned above, that during a second shutdown following a few days' operation of the reactor, an iodine spiking with a comparatively small spiking factor will occur, whose value depends on the length of the operation period between the two shutdowns. Assuming a complete depletion of the iodine deposits in the course of a spiking, their magnitude in a failed fuel rod can be estimated from the amount of iodine activity that is transported to the coolant during this phase. According to calculations based on plant measurements, a standard PWR fuel rod operated with a failure for more than several days contains a ^{131}I inventory in its gap of about 4 to $6 \cdot 10^{18}$ atoms, which means about 3 to 5% of the total ^{131}I inventory in the relevant rod. Thus, this gap inventory is higher by about a factor of 10 than the ^{131}I steady-state gap inventory of an intact rod, which was described above as amounting to 0.3 to 0.5% of the rod inventory. However, the magnitude of the spiking factor might depend on the nature of the defect which means that it seems questionable whether these calculations can be generally applied. As was mentioned above, the reason for this enhanced gap inventory is the higher fuel temperature in a failed fuel rod as well as UO_2 oxidation by steam in the outer zones of the pellet which, within a few days, leads to an O : U ratio of about 2.1. Both effects will result in a considerably increased mobility of fission product iodine in the oxidized zones of the fuel pellet.

A comparison of the ^{131}I gap inventory of a failed fuel rod of about $5 \cdot 10^{18}$ atoms with the steady-state source strength from such a fuel rod of approximately $2 \cdot 10^{12}$ atoms/s shows a low steady-state release coefficient on the order of 10^{-6} s^{-1} (as related to the gap inventory). This means that, without continuing supply from the fuel pellet, the gap inventory would need about 30 days to be emptied by steady-state release. One possible reason for this slow process is the transport through the long and narrow pathways within the gap. In addition, from such a

slow process it can be concluded that fission product iodine is present in the gap of a defective fuel rod as a very stable compound, from which even under the prevailing conditions (350 to 400 °C, steam atmosphere, intense ionizing radiation) iodine is only very slowly liberated in a volatile form. Further, these facts suggest that the presence of a significant fraction of elemental iodine I_2 in the gap can be ruled out, although experimental data on the iodine chemical species present in the gap of defective fuel rods is still lacking.

The mechanisms just discussed do not explain the striking shift of the iodine isotope ratio observed in the course of the spiking. As was mentioned above, the source strength ratio $^{131}I : ^{133}I$ changes from 3 to 4 during constant-load operation to 10 to 15 near the spike maximum; the other, shorter-lived iodine isotopes show a depletion which is even more pronounced. This ageing of the fission product mixture which is released from the failed fuel rod can be basically explained by the following:

The buildup of the gap inventory in a failed fuel rod is caused both by recoil and by migration of the fission products out of the pellet. The recoil mechanism is controlled by the local fission rates over the whole length of the rod, while the migration mechanism depends largely on the degree of UO_2 oxidation and, thus, probably is more strongly pronounced in the neighborhood of the defect than in the more distant regions of the rod. As was discussed in the preceding section, the release of iodine isotopes during the constant-load operation phase originates mainly from the deposits in the gap region near the defect, since from here the volatile iodine species formed will have the possibility of entering the coolant more or less directly, whereas volatile species formed in more distant regions will only move rather slowly in the direction of the defect; their movement is probably delayed by a chromatography-like effect, including consecutive deposition and revolatilization steps. If one postulates identical chemical reaction rates and release rates for both ^{131}I and ^{133}I, then a younger isotope mixture can be expected to be present in the deposits near the defect than in the more remote regions of the rod. From this assumption it can be concluded that the progressive movement of the liquid front in the gap during the spiking phase (as seen from the position of the defect) will reach increasingly older deposits and leach them. A quantitative evaluation of these ideas, however, is still lacking.

Several attempts have been made to establish models to describe iodine spiking. Since the interpretation of the spiking phenomenon on the basis of measurements which were taken from an operating power reactor is often complicated by the largely unknown number and type of the defects present in the reactor core, Lewis et al. (1987) have conducted single-rod experiments on rods with a known defect state (hydride failures) in an in-pile loop. On the basis of these results, a model was developed in which it is assumed that diffusion is the rate-controlling process for the transport of iodine in the liquid-filled gap; convective release is assumed to be of only limited significance because of the long, narrow pathways in the gap. Nonetheless, the diffusion coefficient calculated from the measured escape rates was found to be higher by a factor of about 20 than that predicted from the theory for ionic I^- in water. Besides potential uncertainties in the application of the theory to high temperature and pressure conditions, this discrepancy may indicate the

presence of an additional transport process which may well be convective movement of the liquid in the gap, in particular during the very first stage of the spiking process when the entering coolant contacts hot fuel surfaces. Since the measured escape rate of ^{131}I during shutdown is much greater than the decay rate of this isotope, it is assumed that it is capable of diffusing (or being transported) over the entire length of the fuel rod before significant decay can occur.

In the United States in particular several attempts have been made to establish a generally valid model of the spiking effect, in order to calculate in advance the maximum concentrations of iodine isotopes in the coolant that can be expected during future reactor shutdowns, taking as a basis the number of failed fuel rods in the core estimated from the data obtained during steady-state reactor operation. From the survey given by Bishop (1986), it can be seen that most of these models start from a calculation of the iodine inventories in the fuel based on the power history of the plant. The following step is to calculate the transport of the fission products from the fuel pellet to the gap using a rate constant of 1 to $2 \cdot 10^{-8}\ s^{-1}$, with this figure being based on the assumption of a transport dominated by diffusion. Using another rate constant which can be obtained from the release rates during steady-state operation, the transport from the gap to the coolant is then calculated. Over the duration of the spiking, which is assumed to be on the order of 1 to 2 hours, the rate constants are multiplied by a factor of 200 for the transport from the fuel to the gap and of 250 for the transport from the gap to the coolant; these factors were taken from measured spiking events. The models described, therefore, can be judged to be highly empirical ones, which do not take into consideration the physico-chemical processes occurring during this phase. A comparison of calculated and of measured data of ^{131}I activity concentrations in the coolant during 37 different shutdown procedures showed satisfying agreement in most of the cases; in some of them, however, considerable deviations were noted. Compilations of spiking events in US PWR power plants have also been given by Adams and Sattison (1990) and by Adams and Atwood (1991) as a basis for evaluation of their consequences during steam generator tube rupture accidents (see Section 6.2.3.).

The liquid phase transport during a reactor shutdown from the interior of a failed fuel rod to the coolant results simultaneously in a release of other non-volatile fission products. As mentioned above, the cesium isotopes show a spiking behavior which is quite similar to that of the iodine isotopes; as long as no large-sized defects are present in the core, spiking is the main source of cesium activity in the coolant. After the transient, the bulk of the cesium activity is removed from the coolant by the action of the primary circuit purification system, which initially shows a removal rate similar to that for ^{131}I. Because of the low purification factors for cesium isotopes in the PWR primary coolant (see Section 4.3.2.1.3.), a residual cesium activity level will remain in the coolant for a longer period of time. Other non-volatile radionuclides such as ^{99m}Tc and ^{239}Np exhibit a similar release behavior during reactor shutdown. Usually, ^{239}Np shows very high spiking factors which are comparable with those of the corrosion products, starting from a very low constant-load activity level in the coolant. The ^{239}Np peak activities which

appear in the coolant are very quickly reduced again, indicating that plate-out together with the activated corrosion products or incorporation into them is the main removal mechanism from the coolant for this radionuclide.

4.3.1.3 Identification of failed fuel rods

As was mentioned above, the circuits and systems of a power reactor plant are designed to operate without difficulties even when there is a certain number of failed fuel rods in the reactor core. Nevertheless, it is of importance to keep this number as low as possible, not only to minimize the radioactive emissions from the plant but also to reduce the quantity and the radioactivity inventory of radioactive wastes as well as the radiation exposure to the people engaged in waste processing. Moreover, one has to bear in mind that continued operation of failed fuel rods over a longer period of time may lead to secondary failures with larger sizes (e. g. by hydriding of the Zircaloy cladding), resulting in an increased release of fission products and fuel to the coolant.

The measurement and evaluation of selected fission products present in the coolant during plant operation as described in Section 4.3.1.1. provides information only on the number of defective fuel rods in the reactor core and the nature of the defects, but it is not able to identify the specific fuel assembly containing a defective rod. In reactors with separate fuel channels (e. g. heavy-water reactors), the defective fuel assembly can be identified during plant operation by measurement of delayed neutron emitters in a coolant bypass flow from the individual cooling channels. However, in an LWR plant neither such identification nor removal of failed fuel assemblies from the reactor core are feasible during continued reactor operation. Therefore, one has to identify the fission product emitting fuel assemblies during the refuelling period. Although the length of the shutdown period is usually not determined by the refuelling work itself but by the inservice inspections, one is interested in keeping the time required for identification of failed fuel assemblies as short as possible.

For this reason, several attempts have been undertaken to reduce the amount of this work by conducting preliminary observations during plant operation prior to shutdown. One possible means is the application of flux tilting, i. e. asymmetric insertion of control rods when the gross reactor power is decreased to 70–80% of the rated power level. As a consequence of this control rod movement, the reactor load increases in the other regions of the core not affected by this measure; if there are failed fuel rods in these regions, fission products will be released from the assemblies at an enhanced rate and the activity concentrations in the coolant will increase. In practice, such a procedure only gives one a general idea where failed fuel rods are located, even under the most favorable conditions.

Another way to reduce the work needed for the identification of failed rods is to distinguish during plant operation failed fuel assemblies showing low burnup levels from those showing high burnup levels. In principle, such a differentiation should be possible by comparing the ratio of the source strengths of ^{134}Cs and

^{137}Cs. The activity concentrations in the fuel of ^{137}Cs as a primary fission product, on the one hand, and of ^{134}Cs which is produced by neutron capture in fission product ^{133}Cs, on the other, depend in a different manner on the fuel burnup or on the time-integrated neutron flux. The buildup of ^{137}Cs depends almost linearily on burnup, whereas the ^{134}Cs inventory in the fuel is approximately proportional to the square of the neutron fluence. The possibilities and limitations of conclusions based on the $^{134}Cs : ^{137}Cs$ ratio in the coolant were analyzed in detail by Zänker et al. (1987), with the results showing that their reliability in practice is considerably lower than the basic idea suggests. The observed deviations from the expected values are partly caused by fluctuations in the cesium isotope ratios measured during constant-load operation phases; further, they are due to differences in burnup even in one single fuel assembly. These limitations are also true when the cesium isotope ratios were measured during a spiking following a transient, although it can be assumed that the leaching process occurring in this phase will affect larger areas of the fuel rod gap than the release during steady-state phases, thus yielding a better average. By this procedure, therefore, it is only possible to distinguish failures in freshly loaded fuel assemblies (operating time less than 100 days) from those present in assemblies being operated in their second or third cycle. Despite these limitations, such a differentiation can yield information on failures resulting from manufacturing, since operationally caused failures usually occur only after a longer period of operation. Zänker and Berndt (1988), who analyzed the ratio $^{134}Cs : ^{137}Cs$ in the coolant of a VVER plant during constant-load operation, demonstrated that from these ratios the defects were related to specific refuelling charges, with all of them being in their first operation cycle.

Therefore, an incontestable identification of failed fuel rods or assemblies is only possible by testing the individual assemblies during the refuelling outage, using the so-called sipping technique. This technique is based on the principle that fission products which are still present after the shutdown spiking in the gap of failed rods will be released at a higher rate when the rods are heated to higher than ambient temperatures. The failed fuel assemblies can then be identified by measuring appropriate fission products using a special detection device.

In a BWR reactor core, such a sipping can be performed without discharging the fuel assemblies, i. e. in-situ inside the reactor pressure vessel, due to the breakdown of the water flow by the fuel assembly shrouds, each of which covers one fuel assembly. During the test, a cap is attached onto the assemblies, thus interrupting the water convective flow and resulting in a heating up of the relevant assembly. This in-core sipping technique, initially designed to test the individual assemblies successively, has been considerably improved by development of a sipping hood which covers eight fuel assemblies simultaneously (Krüger et al., 1989). Following disruption of the coolant flow in the covered assemblies, water and gas samples are taken using sampling lines. They are monitored for radioactivity by on-line measurement; in addition, water samples can be collected for a more detailed evaluation. By this technique, an almost 100% detection reliability of the failed assemblies is achieved; the reactor core of a 1300 MWe BWR (748 fuel assemblies) can be completely tested within about 50 hours.

Since the fuel assemblies of the VVER-440 plants are also equipped with a shroud, they can be subjected to an in-core sipping using the above-mentioned improved sipping hood (Knaab et al., 1991). This particular device is equipped with seven test positions allowing seven hexagonal assemblies to be tested in a single hood setting. The application of this technique has resulted in a considerable shortening of the time required as compared to the previously applied sipping test in the spent fuel pool; an entire VVER-440 core can be tested in only 30 hours.

Since the PWR fuel assemblies are not provided with a shroud, an in-core sipping is not possible, because the water cross-flow in the reactor core may cause erroneous results. The individual assemblies have to be discharged from the reactor core and transported to a test facility which is located in the spent fuel assembly pool. In order to obtain a sufficiently high temperature increase, this device is thermally insulated against the pool water. After a residence time of 10 to 20 minutes (depending on the decay heat of the individual assembly) a water sample is taken from the sipping can and analyzed by γ spectrometry. Another possibility is the so-called scanner sipping (e. g. Haag et al., 1986); in this technique, during the heatup phase a continuous side flow of the water from the test device is directed to the front of a germanium detector, which measures the buildup of the fission product activity concentration in the water phase that is caused by a failed fuel rod.

Usually, the fission product nuclides ^{131}I and/or $^{137}Cs-^{134}Cs$ are used as an indicator for fuel rod cladding defects; as they are all γ emitters, their measurement by γ spectrometry poses no difficulties. In particular, with assemblies showing low fission product release, interference can be caused by activated corrosion products which, during the sipping test, are peeled off from the cladding surface and carried away by the water flow, resulting in a strong increase in the Compton background of the γ spectrum. This is particularly true when fuel assemblies with a low burnup and a long decay period are to be examined. In such cases a chemical separation prior to the γ-spectrometric measurement is of advantage; for this purpose Stöckert et al. (1979) employed heterogeneous ion exchange between cesium ions and ammonium molybdato phosphate (AMP), by which a sample free of interfering radionuclides (including antimony isotopes) is obtained in a fast and simple manner. In this technique, the water sample taken from the sipping can is first passed over a membrane filter where all the suspended solids (mainly radioactive corrosion products) are retained. Cesium isotopes are then separated from almost all other radionuclides by adsorption onto a preformed AMP precipitate and they finally undergo γ-spectrometric measurement.

An alternative choice to the wet sipping techniques described above is the so-called dry sipping technique, for which the fuel assembly is placed into a test chamber filled with air; after a short time, the fission product noble gases (in particular ^{85}Kr and/or ^{133}Xe) released from the defective fuel rod during heatup are measured in a gas counter. Reliability and detection limit of this technique are virtually identical to that of the wet sipping procedure.

The techniques described result in the identification of the assemblies containing failed fuel rods; however, the identification of the failed rod itself is not possible. Frequently, in a fuel assembly identified by one of the techniques mentioned above,

only a single fuel rod is defective. In order to increase the usefulness of such fuel assemblies and to keep the amount of radioactive waste and associated costs to a minimum, reconstitution techniques have been developed, so that the upgraded assembly can be reinserted into the reactor core for further operation. In addition to replacement of failed rods in the assembly lattice, techniques have been developed for repairing or replacing the fuel assembly structural components (e. g. damaged spacer grids). In cases where the fuel assembly structure has been irreparably damaged the fuel rods can be transferred to an intact fuel assembly skeleton.

In order to replace failed fuel rods in an assembly lattice, the defective rod has to be identified. Detection of the failed rod in the assembly usually is done by ultrasonic testing, a change in signal intensity indicating the presence of liquid water in the rod. The techniques currently available can be applied to both PWR and BWR assemblies without disassembling the fuel assembly under consideration and without rod withdrawal; their sensitivity does not depend on fuel burnup or other parameters.

4.3.2 Reactions and behavior in the reactor coolant

4.3.2.1 PWR primary coolant

4.3.2.1.1 Fission product noble gases

The fission product noble gas isotopes ^{133}Xe and ^{135}Xe are the predominant radionuclides in the primary coolant of a pressurized water reactor when failed fuel rods are present in the reactor core, in particular when the coolant degasification system is not in operation. Appearance of additional defective fuel rods in the reactor core results in a prompt response of the activity concentrations of the xenon isotopes in the coolant. For this reason, periodic analyses at comparatively short time intervals are required in order to initiate countermeasures in time, e. g. starting operation of the degasification system, whenever necessary.

Besides the release from failed fuel rods, a second source of the appearance of ^{133}Xe and ^{135}Xe in the coolant is the generation by β^- decay of their precursors ^{133}I and ^{135}I, which are released from failed rods. As will be discussed in Section 4.3.2.1.2., a large fraction of these iodine isotopes is accumulated on the ion exchangers of the primary circuit purification system; the xenon atoms newly formed on the resins are not retained and are released to the coolant. The extent of contribution of this source to the total activity concentrations of the two xenon isotopes in the primary coolant depends on the ratio of release from the fuel of the fission product noble gases to that of the fission product iodine isotopes; it is not possible, therefore, to give a generally valid figure. At a given ratio of release from the fuel, the relative contribution of the two xenon isotopes differs considerably because of the different halflives of the four fission products under consideration (xenon and iodine isotopes). The extent of the contribution from the ion exchangers is generally insignificant for ^{135}Xe, while it can amount to a fraction of the total ^{133}Xe input to the coolant that cannot be ignored in the calculation of source terms.

When the plant is operated without degassing the primary coolant, the activity concentrations of the shorter-lived krypton isotopes ^{85m}Kr, ^{87}Kr and ^{88}Kr usually are lower by one to two orders of magnitude than that of ^{133}Xe. The very short-lived heavy fission product isotopes of krypton and xenon showing mass numbers beyond 89 and 137, respectively, are present in the primary coolant in very low activity concentrations only; thus, they do not contribute significantly to the total fission noble gas activity. This is a consequence of the relatively long-lasting transport from the fuel to the coolant, even for noble gases where chemical reactions do not have to be taken into account, resulting in an extensive decay of these short-lived radionuclides during transport.

The long-lived ^{85}Kr, which is usually not detected by γ-spectrometric coolant analysis because of its very low activity concentration and its small γ component, occupies a special position among the fission product noble gases. Due to its long halflife, this isotope does not experience a significant radioactive decay during its stay in the primary coolant and, therefore, is released almost completely with the off-gas to the environment. The level of the ^{85}Kr activity concentration in the PWR primary coolant depends on several factors. It is mainly determined by the burnup of the failed fuel rods since, due to its long halflife, ^{85}Kr will not reach an activity equilibrium in the fuel during its residence time in the reactor core such as is attained by the other noble gas isotopes after a comparatively short irradiation time due to the competition of production and decay. Moreover, also because of its long halflife, the ^{85}Kr activity concentration in the coolant is more strongly affected than that of the other isotopes by water exchange from the primary circuit and by water or gas leakages. For these reasons, the ratio of the activity concentrations $^{133}Xe : {}^{85}Kr$ in the primary coolant can differ considerably, even after a longer time of operation without degassing of the coolant; ratios between 50 and 2000 have been measured in different PWR plants.

As was discussed in Section 4.3.1.1., the fission product noble gas isotopes ^{85m}Kr, ^{87}Kr, ^{88}Kr, ^{133}Xe and ^{135}Xe (besides the fission product iodine isotopes) are valuable indicators for evaluating the number and type of fuel rod failures present in the reactor core.

The behavior of the fission product noble gases in the PWR primary coolant is determined by their solubilities which, according to Henry's law, depend on the partial pressure of the relevant gas in the atmosphere above the liquid. However, because of the closed system "primary circuit" which does not possess an equilibrium gas phase above the liquid coolant, volatilization of the gases from the water phase can only start after depressurization, i. e. when water is routinely extracted from the primary circuit to the volume control tank or after the opening of the system in the course of a refuelling action. When evaluating fission gas release rates from the depressurized coolant, it has to be taken into account that, because of the very small volume concentrations of the fission product noble gases in the coolant, the proportionality constants of Henry's law determined from conventional chemical measurements are not directly applicable. To be sure, the krypton and xenon element concentrations in the coolant are predominantly due to the stable isotopes of these elements, the mass concentrations of which in the fuel, in particular at higher burnup levels, are much higher than those of the radioactive

isotopes. Even when these stable isotopes are taken into account, the noble gas element concentrations in the coolant are very small, resulting in a delayed attainment of the partition equilibrium between liquid and gas phases. The reasons for the deviating behavior often exhibited by such very low concentrations from that of the concentrations normal in chemistry considerations are not clear; besides kinetic effects a hydratization, in particular of the xenon atoms dissolved in water, has been discussed as a possible explanation.

In order to reduce the activity concentrations of the fission product noble gases in the primary coolant, the primary circuit degasification system is operated whenever it is necessary. The effect of degasification on the individual activity concentrations of the different krypton and xenon isotopes is quite different; the ratio of the decay constant of an individual isotope to the purification constant is the parameter that determines the resulting activity concentration. This applies to the degasification system in the same manner to as the coolant purification system (see next section). This means that the activity concentrations of short-lived isotopes are only slightly affected by the action of the degasification system, while the activity concentration of ^{133}Xe in the coolant is efficiently reduced. As a result, the relative isotopic composition of the fission product noble gas mixture in the primary coolant changes during operation of the degasification system and the new equilibrium value is quite different from that prevailing at times when this system is not in operation; the new equilibrium level shows a considerably higher proportion of the shorter-lived isotopes.

The radioactive noble gases liberated from the primary coolant during degasification cannot be released directly to the atmosphere via the stack; in order to keep radionuclide emissions well below the licensed levels of activity release, the bulk of the radioactive noble gases has to be retained within the plant. However, since noble gases are not able to react chemically under current conditions in technical facilities, they cannot be retained by any of the conventional purification and retention techniques. Fortunately, as was described above, all the fission gases of higher significance in nuclear power plant operation are comparatively short-lived, with ^{133}Xe (which has a halflife of 5.25 days) being the longest-lived one; the sole long-lived isotope, ^{85}Kr, is only present in the coolant in very low concentrations and represents no hazard upon release to the environment. This situation is completely different from that in a spent fuel reprocessing plant, where ^{85}Kr is the only fission gas isotope that has not completely decayed in the time span between removal of the fuel from the reactor and head-end dissolution of the material. For this reason, in a nuclear power plant, fission gas can be efficiently retained in an intermediate storage inside the plant for a period long enough to permit decay of the overwhelming fraction of the radioactive fission gases. In a number of light water reactor plants such a delay is achieved by the use of gas decay tanks in which the gases coming from the PWR degasification system (or from the BWR main condenser) are stored for about 60 days, i. e. more than 10 halflives of ^{133}Xe; afterwards, the residual gas inventory of the tank is released to the atmosphere.

In the plants designed and built by Siemens/KWU, a gas delay line is used to achieve the same end. Here, the gas flow from the degasification system, which consists mainly of a carrier gas (nitrogen) containing noble gas concentrations in

the range of several tens to several hundreds ppm per volume (depending on the number of defective fuel rods in the core, the rate of air inleakage to the system, and other plant conditions), is passed over beds of activated charcoal where the noble gases are significantly delayed compared to the carrier gas. The basic factor for this delay is a dynamic adsorption-desorption equilibrium of the gases at the large surface of the charcoal (about 1000 m^2 surface area per g of charcoal). Gas adsorption is effected by van de Waals forces, with the dynamic adsorption coefficient depending on the properties of the particular gas. The amount of gas adsorbed on a given mass of charcoal is nearly proportional to its boiling point (or to its critical temperature); the higher these values, the higher is the amount of gas that can be adsorbed. The adsorption process is a reversible one and is limited by an equilibrium state which is controlled by the prevailing pressure and temperature.

In a flowing gas atmosphere this adsorption–desorption equilibrium results in a delayed transport of the fission product noble gases compared to that of the carrier gas. The mean delay time t_m (i. e. the time span between the entry of a gas volume element into the adsorption bed and the moment at which half of the radioactivity has passed the column exit) can be calculated according to

$$t_m = k \cdot M / Q$$

where M stands for the mass of the charcoal in the bed, Q for the volume flow of the carrier gas and k for the dynamic adsorption coefficient. The delay time increases strongly with decreasing temperature in the charcoal bed and increases almost linearily with increasing gas pressure. The dynamic adsorption coefficient depends on the type of charcoal applied and decreases strongly when the moisture content of the charcoal exceeds values higher than a few percent; for this reason, the gas flow has to be dried before entering the bed to a dew point which is well below the operating temperature of the adsorber bed.

In practice, the gas delay system consists of a number of charcoal beds (6 to 12) in series. In a BWR the system contains about 60 Mg of charcoal; it is operated at about 0.08 MPa and a gas temperature of about 20 °C. The mean delay time for krypton in such a system at a gas mass flow of 28 m^3/h is about 80 hours, increasing to values of about 110 hours at a flow rate of 20 m^3/h. This means that the retention time equals about 25 to 30 halflives of the longest-lived relevant krypton isotope ^{88}Kr (2.84 h), which results in a virtually complete decay on the column. In Fig. 4.12. the delay of krypton in such a system is shown, measured by using ^{85}Kr as a radioindicator. Since this isotope does not decay to a measurable extent during the transport process, the decrease in peak height downstream of the individual beds is due to a broadening of the originally sharp injection peak, caused by the adsorption–desorption mechanisms. In PWR plants, the gas delay system is usually operated at a pressure of 0.7 to 0.8 MPa and a temperature of 10 °C. Due to the favorable influence of these parameters on the dynamic adsorption coefficient k, the dimensions of the system can be kept small, using 3 to 8 Mg of charcoal and resulting in a mean delay time of krypton ranging from 130 to 150 hours. Because of its higher boiling point, xenon shows a delay time on the charcoal beds which is higher by a factor of 13 to 17 than that of krypton, resulting in values in the

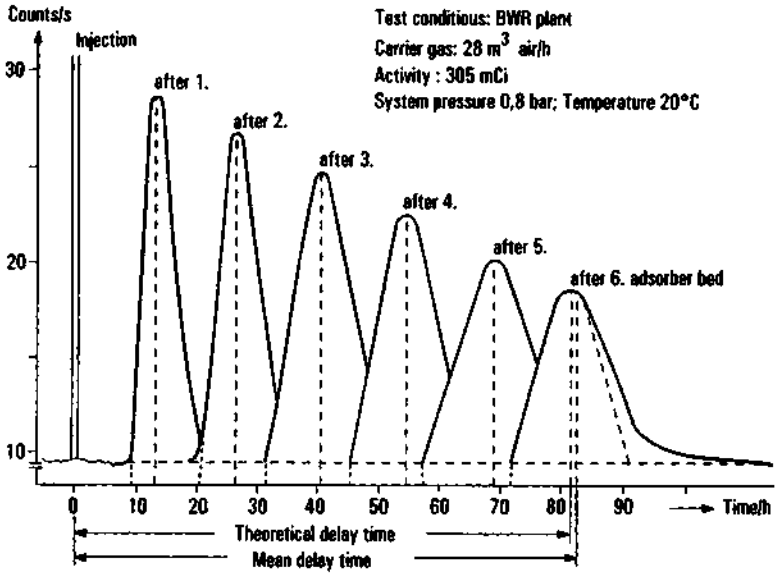

Figure 4.12. Krypton transport in the gas delay line of a BWR plant (^{85}Kr indicator) (By courtesy of Siemens/KWU)

range 40 to 110 days. In the BWR case, the delay time corresponds to about 7.5 halflives of ^{133}Xe; in the PWR case it corresponds to about 13 halflives under the least favorable conditions; this means that only traces of the original xenon activity will penetrate the adsorbers.

Due to the delay times achieved on the charcoal beds, the shorter-lived fission product noble gases are completely retained within the plant. ^{85}Kr is the only one of the radioactive fission gases which passes the delay line and is released completely to the atmosphere, where it contributes to the gobal ^{85}Kr inventory of the atmosphere. As this contribution is very small compared to the remainders of nuclear weapons testing and to the releases from spent fuel reprocessing plants (as far as they are not equipped with a noble gas retention system) it can be ignored.

Testing the retention properties of the delay line can be performed by two different procedures. In functional tests, the test gas (^{85}Kr or ^{133}Xe) is usually added to the carrier gas flow at a given time and the breakthrough time through the columns is measured (see Fig. 4.12.). This method yields accurate results; however, it cannot be applied when the plant is in operation due to the radiation background at the measuring positions. During operation of the degasification system, the delay time is determined by measurement of the activity ratios of different isotopes showing markedly different halflives; for this purpose, gas samples are taken at the entrance and at the exit of the system and measured by γ spectrometry in the laboratory. From the time-dependent change of these isotope ratios the retention time can be calculated, and a beginning deterioration of the essential data of the system can be detected early on. An important precondition for obtaining reliable

results by this method, however, is steady-state operation of the degasification system with constant noble gas concentrations and constant isotopic composition of the noble gas mixture.

4.3.2.1.2 Iodine isotopes

The level of the activity concentrations of the fission product iodine isotopes in the primary coolant depends on the number and the size of the fuel rod failures in the reactor core. The isotopes ^{131}I and ^{133}I are always the main contributors to the total iodine activity, whereas the shorter-lived isotopes ^{132}I, ^{134}I and ^{135}I are only present in comparatively low activity concentrations. As was discussed in Section 4.3.1.1., a comparatively old iodine isotope mixture (compared to that produced by nuclear fision) is released from defective fuel rods to the coolant, due to the delay caused by diffusion in the fuel, intermediate deposition in the fuel rod gap and associated chemical reactions. The source strengths of the individual iodine isotopes are generally the lower the shorter their halflives are. The only exception to this rule is exhibited by ^{132}I, which is the only fission product iodine isotope whose halflife is shorter than that of its precursor (^{132}Te) and whose release behavior, therefore, is largely controlled by the physico-chemical properties of tellurium.

The short-lived iodine isotopes having mass numbers higher than 135 are present in the primary coolant in very low activity concentrations. Among them, only ^{137}I has a certain relevance, because it decays by neutron emission. The measurement of these delayed neutrons (together with those originating from other short-lived fission products) in combination with appropriate control rod positioning (flux tilting) is occasionally used to localize the position of defective fuel rods in the reactor core during plant operation.

Little information is available on the activity concentration of the very long-lived ^{129}I in the primary coolant, mainly due to its extremely low concentration as well as to the difficulties in analyzing low levels of this β^- emitter with only a low-energy associated γ component. While the other iodine isotopes in the primary coolant can be easily measured by γ spectrometry, ^{129}I has to be carefully separated from the other radionuclides prior to activity measurement, in order to preclude analytical errors. Different analytical methods have been developed for this task, such as precipitation as PdI_2 and subsequent neutron activation analysis (similar to the determination in irradiated nuclear fuel, see Section 3.2.3.3.), anion exchange followed by liquid-liquid extraction and liquid scintillation counting (Verrezen and Hurtgen, 1992), distillation followed by extraction and neutron activation analysis of the extraction solution (Martin et al., 1990). In each case, determination of ^{129}I is a time-consuming and expensive procedure and only few analyses of this radionuclide in reactor coolant have been reported. Since its radiological significance in the reactor coolant is small because of its very low concentration, most of these analyses have been performed with regard to the amount of ^{129}I to be expected in the resulting radioactive wastes.

If one assumes a release kinetics of ^{129}I from the failed fuel rod similar to that of ^{131}I, then its source strength should be directly proportional to the burnup of the failed fuel rod, since the fuel inventory of this isotope in the time periods discussed here increases linearily with burnup and does not reach an equilibrium state. On the basis of this assumption, one can calculate that, with a fuel burnup of the failed rod of 20 MWd/kg U and a steady-state ^{131}I activity concentration in the primary coolant of 500 MBq/Mg, the corresponding ^{129}I value will be on the order of only 1 Bq/Mg.

The production of iodine isotopes in the primary coolant from their precursors, which themselves have been released from the defective fuel rod, does not play a significant role compared to the direct release of iodine isotopes from the failed fuel rod. The only exception seems to be ^{132}I with its longer-lived precursor ^{132}Te; a differentiation of both release pathways is possible by using the fact that ^{132}I directly released from the fuel will decay in the coolant with its own halflife of 2.28 hours, whereas ^{132}I present in the coolant in a decay equilibrium with ^{132}Te will decay with the halflife of this radionuclide of 78.0 hours.

The lighter homologue of iodine in the Periodic System of the Elements, namely bromine, is also produced by nuclear fission. Due to the comparatively low fission yields of the relevant bromine isotopes and their short halflives, they are only present in the primary coolant in very low activity concentrations and are of no significance in practice. The only bromine isotope that should be mentioned here, ^{87}Br, is a neutron emitter quite similar to the heavy fission product iodine isotopes.

The chemical state and the behavior of fission product iodine in the PWR primary coolant depend on the prevailing conditions, i. e. on the primary coolant chemistry. As was described in more detail in Section 1.3., this chemical environment is characterized by a boric acid concentration which decreases steadily during the fuel cycle, depending on the reactivity state of the reactor core, from approximately 1000 ppm B at its beginning to near zero at its end. The pH of the coolant is controlled by an LiOH concentration between 0.5 and 2 ppm, and radiation-induced formation of free oxygen is suppressed by the addition of hydrogen gas. In addition, ionizing radiation is a parameter that possibly influences the chemical state of iodine; during operation of a 1300 MWe PWR at rated power, the radiation field at the core periphery amounts to about $1 \cdot 10^8$ Gy/h and in the inner regions of the core to about $2 \cdot 10^8$ Gy/h. In this alkaline and reducing aqueous solution at about 300 °C, only iodide I^- is thermodynamically stable among the iodine chemical species; calculations have shown that the fraction of I_2 and more highly oxidized iodine species should be lower than 10^{-20}. Iodide in the primary coolant is completely present in the ionic dissolved state; small proportions of fission product iodine that are sometimes detected in the filtered corrosion products from the coolant are probably due to adsorption of iodide onto the oxides or the filter material rather than to the occurrence of really insoluble iodine compounds. As a consequence of its high solubility, fission product iodine usually is not incorporated into the oxide contamination layers which are formed on the surfaces of the primary circuit. Deposition of iodine activity is only observed when the primary coolant contains silver traces originating from the wear of silver-containing seals, prob-

ably due to the formation of insoluble AgI; detailed data on the solubility product of this compound under the prevailing conditions have not yet been reported.

The thermodynamic considerations on the stability of I^- in PWR primary coolant were confirmed by laboratory experiments reported by Alm et al. (1979), among others. In these experiments performed in an autoclave with simulated primary coolant containing the comparatively high total iodine concentration of about $7 \cdot 10^{-5}$ M, partitioning of iodine between liquid and gaseous phases was measured in the temperature range 120° to 340 °C. The results showed that the partition coefficient is virtually independent of the chemical form in which the iodine tracer was added, reaching values between 10^5 at 120 °C and pH 6.5 and about 10^2 at 330 °C. These results indicate a rapid transformation of the added iodine chemical species (I_2, IO_3^-, etc) to I^- ions. The measured iodine volatility was attributed to hydrated I^- ions which were assumed to show a hydratation number of about 2 under such conditions, i. e. larger than that of weak electrolytes (e. g. boric acid), but lower than that of strong electrolytes such as NaCl. This interpretation seems questionable, however: besides the postulated volatility of hydrated I^- ions, a droplet carry-over of traces of non-volatile iodide (entrainment) potentially contributed to the measured results. On the other hand, it was concluded from theoretical considerations that formation of iodide – boric acid complexes can, in principle, be responsible for a measurable volatility of iodide from boric acid solutions at elevated temperatures (Turner, 1988).

Investigations of Caruthers and Gritz (1978) using untreated PWR primary coolant at ambient temperature, indicated that 96 to 99.6% of the ^{131}I activity has to be attributed to the iodide species; between 0.3 and 3.8% of the ^{131}I activity was identified as organically bound iodide; and 0.2 to 0.3% belonged to other anionic species such as hypoiodite and iodate. However, these results might possibly have been influenced by the analytical technique applied (ion exchange). In the separation of such low concentrations by ion exchange, there is always the danger that traces of the main constituent iodide are displaced into the other fractions, indicating falsely the presence of other species. Further, a certain oxidation of traces of iodide by air in the time between sampling and execution of the analytical work cannot be ruled out. It should not be overlooked that separation of different iodine oxidation states at these extremely low concentration levels (an activity concentration of $1 \cdot 10^4$ Bq ^{131}I/ ml corresponds to a mass concentration of approximately $3 \cdot 10^{-12}$ g ^{131}I/ ml) may be easily disturbed by secondary effects occurring during the analytical procedure. The experimentally detected iodide fraction, therefore, can be assumed to represent a lower limit rather than the true value. The anomalous behavior of very low iodine concentrations at high temperatures, resulting in the formation of measurable I_2 fractions in an initially pure I^- solution (Daish et al., 1988), probably does not apply to PWR primary coolant conditions because of the presence of an excess of H_2.

It can be assumed that the fraction of organically bound iodine measured in various experiments was the result of secondary reactions occurring in the course of the analytical procedure. Numerous indications give rise to the conclusion that these compounds are not stable in the hot primary coolant under the influence of ionizing radiation. Investigations of the behavior of methyl iodide in alkaline bo-

rate spray solutions showed a complete decomposition to iodide (see Section 6.1.2.); from thermodynamic calculations it was concluded that CH_3I in primary coolant at reactor operating temperature is rapidly destroyed by hydrolysis and has an average lifetime of less than 5 seconds (Postma and Tam, 1978). On the other hand, it was reported from VVER reactors that up to 30% of the iodine activity in the primary coolant was detected in the form of organically bound iodide; this was probably due to the very high concentrations of hydrocarbons in the primary coolant (values as high as 10 mg/Mg were reported) as a consequence of leaking seals. Investigations performed by Habersbergerova (1989) demonstrated that in a neutral borate solution, organoiodides can be produced from iodide and hydrocarbons (such as methane) as a result of radiation chemistry reactions. The first step in this reaction chain is assumed to be the oxidation of I^- by the $OH\cdot$ radical, which runs parallel to the formation of a $CH_3\cdot$ radical that is also a product of an $OH\cdot$ radical reaction. The initial $G(CH_3I)$ values decrease with decreasing iodide and methane concentrations, which explains why at the very low concentration levels of these compounds present in most of the PWR primary coolants, organoiodides may exist, if at all, only in extremely small quantities. With increasing CH_3I concentrations the effective G value decreases, too, and the CH_3I concentration moves towards an equilibrium value, presumably due to the radiolytic decomposition of CH_3I previously produced.

Investigations concerning the chemical state of fission product iodine in the primary coolant of two US PWR plants during constant load operation, as well as in the course of shutdown procedures, were reported by Voillequé (1990). Using the extraction analytical techniques described by Lin (1980 a; see Section 4.3.4.2.), the chemical species I^-, IO_3^-/IO_4^-, I_2, and CH_3I were separated from each other and measured. The results indicated that during constant-load operation I^- is the dominant species, while the concentrations of the other compounds were at or below the detection limits. At the maximum of the shutdown spike, however, a significant increase in the I_2 fraction to up to 20% of the total iodine concentration was observed, together with an increase in the IO_3^- fraction; this relates to ^{131}I as well as to the other isotopes with mass numbers 132, 133, 134 and 135. About 35 to 40 hours after shutdown, a second increase of the I_2 fraction was observed; at one plant this effect was related to the depressurization of the primary circuit, but at the second plant no such correlation could be confirmed. In both cases, the maximum concentration of the I_2 fraction was reduced again very quickly. The reason for this effect has not been explained, the observed behavior over time showed no correlation with operational procedures such as hydrogen removal from the primary coolant or addition of aerated boric acid solution. Therefore, the author concluded that the fission product iodine released from the gap of the failed fuel rods during the transient contains a considerable fraction of I_2.

Elemental I_2 added to borate solutions or simulated VVER primary coolant adjusted to pH 7–9 using KOH is reduced to I^- by gamma and by reactor irradiation, as was demonstrated by Habersbergerova and Bartonicek (1975; 1983). I_2 and IO_3^- are good electron scavengers; they are, therefore, efficiently reduced to iodide. In addition, boric acid, which is simultaneously present in the solution, evidently competes efficiently with iodide for hydroxyl radicals, thus preventing the back-

formation of elemental iodine. This oxidation or reduction is not the result of a direct reaction of the ionizing radiation with the iodine species; on the contrary, it is initiated by the primary radiolysis products of the water. Therefore, competing reactions of the primary radiolysis products with other constituents or impurities of the primary coolant may affect the yields of the different iodine species which, consequently, depend on the particular conditions that exist. According to the data given in Sellers' review (1977), almost all of the dissolved iodine species will be fundamentally affected by the H_2O primary radiolysis products. In general, in the PWR primary coolant during plant operation it has to be assumed that the primary radiolysis products of the water are quantitatively trapped by the excess hydrogen present, thus leaving no possibility for a radiation-induced oxidation of iodide. However, in the absence of excess hydrogen (as, for example, immediately before reactor shutdown), a radiation-induced oxidation of dissolved iodide during the residence time of the primary coolant in the high radiation field of the reactor core cannot be ruled out. Such an oxidation might also take place when hydrogen peroxide is added to the coolant in order to mobilize deposited radioactive corrosion products.

Fission product iodine is removed from the PWR primary coolant very effectively by the action of the primary circuit purification system, usually showing decontamination factors of 100 and more over longer time periods. The measured decontamination factors of the individual iodine isotopes usually show considerable differences, being higher for shorter-lived isotopes than for the longer-lived ones. This effect, however, does not indicate the presence of different chemical states of the different isotopes, but is the consequence of a chromatographic effect of the resin bed, resulting in an extensive decay of the shorter-lived isotopes on the ion exchanger bed; therefore, in the effluent of the resin bed the fraction of the longer-lived ^{131}I shows a relative enrichment when compared to the original isotopic composition of the primary coolant.

Even with identical decontamination factors, the operation of the purification system affects the activity concentrations of the individual iodine isotopes in the primary coolant to a different extent. The purification effect results in an effective halflife T_{eff} of the iodine isotopes in the coolant which is shorter than the halflife of radioactive decay and can be calculated according to

$$T_{eff} = \ln 2 / (\lambda + \varepsilon)$$

where λ is the decay constant and ε the purification constant to be calculated from the purification rate and the purification factor (see Section 4.3.1.). At a purification rate of 10% of the primary coolant volume per hour and a purification factor of 100, an effective halflife of ^{131}I in the primary coolant of 6.7 hours results, as compared with its physical halflife of 8.05 days. In comparison, ^{135}I with a physical halflife of 6.7 hours shows an effective halflife in the coolant of 3.4 hours under such conditions. This means that operation of the purification system will reduce the equilibrium activity concentrations of the longer-lived isotopes in the coolant to a significantly higher degree than that of the shorter-lived ones.

During steady-state operation of the plant, the iodine activity accumulated on the ion exchanger beds is constant over time after having reached decay equilib-

rium; it depends directly on the level of the coolant activity concentration and on the halflife of the individual isotope. This results in a partitioning of the iodine activity present in the primary circuit (i. e. outside the nuclear fuel) which is constant in time and amounts to

– ^{131}I:	3.5% in the coolant	96.5% at the ion exchanger;
– ^{133}I:	25%	75%
– ^{135}I:	52	48%

Despite the high fraction on the ion exchanger in particular for ^{131}I (and for stable ^{127}I and long-lived ^{129}I), there is no danger of a super-saturation of the ion exchange capacity by iodine. It can be easily calculated that, with a steady-state activity concentration of $1 \cdot 10^4$ Bq ^{131}I/ ml in the coolant, a primary coolant volume of 400 Mg and a purification rate of 10% per hour, the ion exchanger in the equilibrium state will contain approximately 10^{20} atoms of ^{131}I, corresponding to about 10^5 GBq. This activity corresponds to only about 25 mg of ^{131}I, i. e. a negligible amount compared to the capacity of the beds; the shorter-lived iodine isotopes are present in significantly smaller amounts. The amounts of the stable isotope ^{127}I and of the long-lived ^{129}I which are accumulated on the ion exchanger in the course of a fuel cycle can be estimated to be on the order of 0.1 to 1 g at a maximum. Nevertheless, the iodine decontamination factor of the purification system is observed to decrease after a certain period of operation, usually after 2 to 3 years. The reason for this effect seems to be an increasing poisoning or passivation of the active groups of the resins by other substances, e. g. by deposited corrosion product oxides.

By the radioactive decay of the iodine isotopes that are accumulated on the ion exchanger beds, radioactive xenon isotopes are produced. These radionuclides are released to the coolant again and are transported back to the primary circuit in periods when the degasification system is not being operated; their contribution to the total xenon activity in the primary coolant was discussed in Section 4.3.2.1.1. When the degasification system is in operation, the xenon isotopes are removed from the purified coolant flow and are transported to the gas delay line.

In order to minimize fission product carry-over to the reactor building atmosphere after removal of the reactor pressure vessel closure head prior to refuelling, the activity concentrations of both fission product noble gases and iodine isotopes, in particular, have to be significantly reduced in advance by purification. The parameter which controls the carry-over of the residual fraction from the primary coolant to the containment atmosphere is the transfer rate, which depends on the prevailing conditions. Laboratory investigations using real PWR primary coolant showed that with a ^{131}I activity concentration of 5.5 kBq/ml, the surface area-related transfer rate amounts to 74 kBq/h · m^2 at 40 °C and to 190 kBq/h · m^2 at 60 °C (without stirring the water phase). In comparison, the ^{133}Xe transfer rate from a coolant having about 35 kBq/ml is on the order of 700 MBq/h · m^2 and of 1 GBq/h · m^2 at 40 and 60 °C, respectively. This large difference between the two elements indicates that oxidation of iodide in the coolant (which in the presence of dissolved oxygen proceeds rather slowly at ambient temperature) is the rate-controlling step in the volatilization of fission product iodine from the primary coolant.

4.3.2.1.3 Cesium isotopes

When failed fuel rods are present in the reactor core, fission product cesium isotopes will also appear in the primary coolant in significant activity concentrations. The high solubility of the cesium compounds deposited in the gap of the fuel rod facilitates the transport to the coolant which, however, is only possible via the liquid phase. This means that under constant-load operating conditions a significant cesium transport will only occur when such fuel rod failures are present in the core that allow a direct contact between fuel and liquid coolant; in addition, the shutdown spiking results in a considerable cesium transport to the coolant with almost all types of fuel rod defects. The comparatively low cesium retention on the primary circuit purification resins which are saturated with LiOH occasionally leads to the buildup of activity concentrations of cesium isotopes in the coolant on the same order of magnitude as that of the iodine isotopes ^{131}I and ^{133}I, even at comparatively low cesium source strengths or those which are not constant over time.

The major cesium isotope in the coolant (like in the fuel) is ^{137}Cs, accompanied by ^{134}Cs, which is produced from the stable fission product ^{133}Cs by neutron capture (thermal neutron cross section $3 \cdot 10^{-23}\,cm^2$); therefore, this radionuclide is of greater significance the higher the burnup level of the failed fuel rod. In addition to these two main isotopes, the very long-lived pure β^- emitter ^{135}Cs appears in the coolant as well as ^{136}Cs produced from it by neutron capture (thermal neutron cross section $8 \cdot 10^{-24}\,cm^2$); their activity concentrations in the coolant also depend on the burnup of the defective fuel rods. Finally, the short-lived ^{138}Cs has to be mentioned; from the dependence of its source strength on the decay constant (see Fig. 4.3.) it can be concluded that this isotope is not released itself from the fuel rod, but that it is generated in the coolant by decay of its precursor ^{138}Xe. Cesium isotopes with mass numbers beyond 138 are usually not detected in the coolant; apparently, because of their short halflives they decay completely on the way from the fuel rod to the coolant.

All the isotopes of the lighter cesium homologue in the Periodic System of the Elements, namely rubidium, which are formed by nuclear fission, show short halflives. Only the longest-lived of them, ^{88}Rb, can be detected in the primary coolant; it is probably generated in the coolant by β^- decay of its precursor ^{88}Kr. Because of the short halflives and the comparatively low fission yields, little significance can be attributed to the rubidium isotopes in the coolant.

It can be assumed that the radioactive cesium isotopes are present in the coolant as Cs^+ ions, but as yet there is no direct experimental proof of this assumption. Very low cesium activities which are occasionally detected in filtered suspended corrosion products are probably attached by occlusion or by adsorption at the surfaces of the solids. Since cesium is not able to form insoluble compounds in the primary coolant, it does not participate noticeably in the contamination buildup on the primary circuit surfaces.

The behavior of the cesium isotopes on the cation exchangers of the primary circuit purification system is complex. A newly inserted ion exchanger bed shows a certain retention efficiency for cesium isotopes which decreases to a purification

factor of about 1 after a short period of operation (i. e. the ^{137}Cs activity concentration in the effluent is virtually the same as in the coolant entering the ion exchanger beds). After a sudden increase of the cesium concentration in the primary coolant, e. g. following a shutdown spiking, the cesium purification factor will rise to figures between 10 and 50, but, when the cesium concentration in the primary coolant has fallen again to the preceding steady-state values, the purification factor decreases again to about 1. This behavior is probably caused by an adsorption-desorption equilibrium on the ion exchanger material with Li^+ and Cs^+ competing for the reactive sites of the resin, with the equilibrium inventory of cesium and lithium on the ion exchanger resins being controlled by their respective concentrations in the coolant. If necessary, an effective removal of cesium isotopes from the primary coolant can be performed by application of an H^+-preconditioned cation exchanger in the same manner as is used in order to remove Li^+ ions from the coolant.

4.3.2.1.4 Other fission products and activation products from the fuel

As was discussed in detail in Chapter 3, the fission product isotopes of the chemical elements of the alkaline earths, the earth metals and the rare earth metals groups as well as the newly formed transuranium elements are very tightly bound to the UO_2 fuel lattice, resulting in a very low vapor pressure and a very low solubility of these elements in water. For these reasons, their transport from failed fuel rods to the coolant is comparatively small and is restricted to fuel failures involving a direct contact between liquid coolant and the fuel matrix. The release mechanism may be a leaching of the fuel pellet or an erosion process; because of the high chemical and mechanical stability of the fuel pellet, these processes proceed very slowly. Besides release from defective fuel rods, the presence of these radionuclides in the coolant may originate from surface contamination of fuel rods by fuel traces resulting from the fabrication process or from tramp uranium which is present in the coolant as a remainder from the preceding operating cycles with severe fuel failures (see Section 4.3.1.1.). In almost all cases, the activity concentrations of these fission and activation products in the PWR primary coolant are lower by 3 to 4 orders of magnitude than those of the iodine and cesium isotopes. This means that the analytical determination of even the γ emitting radionuclides often requires special separation and enrichment procedures.

In evaluating fuel rod failures from the presence of these fission products in the primary coolant, it has to be considered that some of them are also formed by neutron activation of metallic core materials, e. g. $^{95}Zr/^{95}Nb$, $^{99}Mo/^{99m}Tc$, ^{125}Sb. Determining which of these two production mechanisms is responsible for the coolant activity of the isotopes just mentioned is often difficult. In some cases, the shutdown spiking can be used to identify their origin from failed fuel rods; however, in most cases this effect is not unequivocal since the radioactive corrosion products also show such a spiking (see Section 4.4.).

At the PWR primary coolant pH of 7 to 8, the fission product isotopes of the tri- and tetravalent elements show strong hydrolysis, resulting in very low solubilities. This macrochemical behavior is consistent with the observations made in coolant analyses that these radionuclides can be almost quantitatively isolated together with the suspended corrosion products by filtration. However, this behavior does not necessarily indicate the presence of particular oxides or hydroxides of these fission products, since due to their very low element concentrations in the coolant their solubility limits are probably not exceeded. Presumably, these element traces are attached to the corrosion product oxides either by adsorption onto their surfaces or by formation of mixed crystals. A significant fraction of the longer-lived tri- and tetravalent fission products, as well as of the actinides, is incorporated into the contamination layers which cover the primary circuit surfaces. However, because of the usually very low activity concentrations of these radionuclides in the coolant and, consequently, in the contamination layers, their contribution to the contamination dose rates is negligible.

Technetium isotopes in the PWR primary coolant show a behavior which is quite different from that of the other fission products treated in this section. Whereas the short-lived ^{99m}Tc is only of minor radiological relevance, its long-lived isomer ^{99}Tc (halflife $2.1 \cdot 10^5$ a) deserves some attention with respect to safety analyses for the final storage of radioactive wastes. Normally, ^{99}Tc is not analyzed in the reactor coolant because of its very low activity concentration and of its unfavorable radiation properties (β^- 0.3 MeV, negligible γ transition). For this reason, the ^{99}Tc mass is frequently determined rather than its radioactivity; suitable techniques for this task are neutron activation analysis, inductively-coupled mass spectrometry and laser resonance ionization mass spectrometry (see, for example, the comparative evaluation given by Trautmann, 1993). In each case, very expensive analytical procedures are required; therefore, the greatest part of the available information on ^{99}Tc behavior in reactor primary circuits has been derived from measurements of γ-emitting ^{99m}Tc.

There are observations that indicate that in most cases the technetium activity detected in the primary coolant is due to a fission product originating from the fuel rather than to an activation product of the alloy constituent molybdenum. In PWR primary coolant, the ^{99m}Tc activity concentration usually is lower by a factor of about 10 than that of ^{137}Cs, mainly because of the low cesium retention on the primary circuit purification ion exchangers. With a reactor core having one defective fuel rod, the ^{99m}Tc equilibrium activity concentration in the coolant is on the order of 1 Bq/ml; from these data one can calculate the corresponding ^{99}Tc activity concentration, under the assumption of an identical transport behavior from a defective rod with a burnup of 30 MWd/kg U and an identical behavior in the purification system, to be on the order of 10^{-6} to 10^{-7} Bq/ml. The bulk of the ^{99m}Tc activity in the primary coolant is not retained by mechanical filtering (0.1 µm filters), which indicates its presence in an anionic dissolved state, perhaps TcO_4^-. Because of the similarities in behavior between the pertechnetate anion and the iodide anion in normal chemistry, one can conclude from these observations that technetium isotopes are retained on the anion exchanger with good retention effectiveness and that they are not incorporated into the oxide contamination layers on

the primary circuit surfaces. Using simple calculations, one can estimate that after one year of operation with one failed fuel rod present in the reactor core, the ^{99}Tc inventory of the primary circuit purification resins will be on the order of 1 MBq.

Due to their high degree of radiotoxicity, the α-emitting actinide isotopes present in the coolant deserve special attention. During inspection and repair work at the open primary circuit an important question is whether the radiation protection measures to be taken should be dictated by the β, γ emitters of the corrosion product isotopes or by the α-emitting transuranium isotopes. However, because of the usually very low concentrations and of the difficulties in measurement (usually, alpha spectrometry after separation from the bulk of other solids and electrochemical deposition has to be applied), the chemical states of the transuranium isotopes in the coolant are not known in as great detail as those of the γ-emitting fission products. From the well-known chemistry of macroamounts of the transuranium elements one can conclude that immediately after the dissolution of the fuel fractions they may exist in ionic form, i. e. as Np^{4+} and Pu^{4+}, or as Np^{3+} and Pu^{3+} in the presence of hydrogen in the coolant. In a neutral or alkaline solution, these ions will be very quickly hydrolyzed to the corresponding hydroxides, which show very low solubility products in the region 10^{-20} ($Pu(OH)_3$) to 10^{-50} ($Pu(OH)_4$). On the other hand, the mass concentrations of the transuranium elements in the coolant are extremely low; for example, a ^{239}Np activity concentration of 5 Bq/ml as has been measured in PWR coolant corresponds to a mass concentration of this isotope of about $5 \cdot 10^{-16}$ g/ml; if one assumes an identical transport behavior of the long-lived isotope ^{237}Np from the fuel to the coolant and a fuel burnup of the defective assembly of about 30 MWd/kg U, one can calculate a total neptunium concentration in the coolant on the order of 10^{-14} to 10^{-13} g/ml. Similarly, a $^{239+240}Pu$ activity concentration in the coolant of 0.02 Bq/ml can be related to a total plutonium concentration in the coolant on the order of $4 \cdot 10^{-12}$ g/ml. At such low concentration levels, the presence of these two elements in the coolant in a ionic dissolved form (at least temporarily) cannot be ruled out.

The predominant α activity concentration of the actinides in the coolant is usually that of ^{242}Cm; its rather short halflife is responsible for its high specific activity concentrations in fuel and coolant despite its complex production process. Likewise, ^{244}Cm and ^{241}Am usually show higher activity concentrations in the coolant than do the plutonium isotopes. For this reason, the measured gross α activities in the coolant must not be interpreted as being caused by plutonium; in order to determine the plutonium activity concentrations, one has to perform a radiochemical separation procedure followed by α-spectrometric measurement. On the other hand, gross α analyses (in addition to the measurement of γ-emitting cerium isotopes) may be a useful means of following the development of larger fuel rod failures by simple and fast-to-perform measurements.

Experiences with aqueous chemistry and behavior of the transuranium elements obtained in nuclear fuel reprocessing and plutonium processing are only of limited relevance for PWR primary coolants with the extremely low concentrations of these elements in a boric acid–LiOH solution of varying composition. The plutonium polymers which are formed in less acid and neutral solutions and which have been reported to show the highest plate-out potential (e. g. Wilkins and Wisbey,

1984) are not assumed to exist in LWR primary coolant, because of the extremely small mass concentrations of the transuranium elements there. By contrast, it can be assumed that the initially formed neptunium and plutonium ions are rapidly adsorbed onto the surfaces of iron oxide particulate matter and that upon potential redissolution they are incorporated into the contamination layers on the primary circuit surfaces by a mechanism that is quite similar to the incorporation of, for example, cobalt ions. Because of the limited data available, no reliable statements can be made on a possible release of deposited transuranium isotopes from the contamination layers back to the coolant.

Radiochemical analyses of PWR primary coolant show that the major fraction of the neptunium and plutonium traces in the coolant is usually associated with the corrosion product suspended solids and that it can be removed from the coolant by filtering. Only in cases of very low corrosion product concentrations in the coolant were significant proportions of the transuranium elements observed to be present in a dissolved (i. e. non-filtrable) form. As yet, it is not known whether mixed oxide formation between magnetite-type oxides and these elements is responsible for this behavior or whether the actinide traces are adsorbed by van de Waals forces onto the large surface areas of the finely dispersed suspended solids. Under constant-load operation conditions and as long as no additional fuel rod failures occur, the activity ratio Pu : ^{60}Co in the corrosion products remains virtually constant over time, thus indicating a similar behavior of these different elements in the coolant.

Similar Pu : ^{60}Co activity ratios to those in the suspended solids have been measured in the contamination layers which are deposited onto the primary circuit surfaces. From this observation one can conclude that the incorporation of actinide elements into the oxide layers shows a kinetics which is virtually identical to that of cobalt. As will be discussed in greater detail in Section 4.4., on the basis of existing experimental data it is assumed that deposition of cobalt activity into the oxide layer proceeds via dissolved cobalt ions from the coolant, while the cobalt content in the suspended solids only represents a reservoir for the dissolved species. Correspondingly, one may conclude that neptunium and plutonium deposition also proceeds via dissolved ions; experimental proof of this assumption is not yet available. On the other hand, such an incorporation of actinide isotopes into the contamination layers means that during the subsequent fuel cycles the primary circuit is still contaminated with α emitters, even when these cycles are operated without any fuel rod failures. As a general rule, the plutonium content in the contamination layers usually is small and, from the viewpoint of radiological safety, insignificant compared to that of ^{60}Co, which is always present. However, if ^{60}Co production and deposition in the primary circuit could be considerably reduced (see Section 4.4.), this topic would have to be given renewed attention, in particular when severe fuel rod failures are present in the reactor core. In such a case, radiation protection measures for those working on the open primary circuit (e. g. steam generator primary channel head) could potentially be dictated by α emitters.

Only little information is available concerning the behavior of the actinides in the primary circuit purification system. If one assumes a plutonium purification factor identical to that of the cobalt isotopes, one could calculate the approximate level of the plutonium inventory of the ion exchanger beds. Such a calculation for

a 300-day operation with a time-constant coolant $^{239+240}Pu$ activity concentration of about 0.02 Bq/ml and a purification rate of 10% per hour results in an estimated plutonium inventory on the ion exchanger of considerably less than 1 g.

These general considerations were confirmed by measurements performed by Zänker and Nebel (1986) at a VVER-400 PWR plant. According to these investigations, the radionuclides ^{239}Np, ^{103}Ru, ^{141}Ce and ^{144}Ce are present in the coolant almost quantitatively in a non-dissolved form and can be separated by filtering together with the corrosion products. Their behavior in the primary circuit is very similar to that of the corrosion product radionuclides. The comparatively high scatter of the analytical results compared with those of the iodine isotope measurements can be explained by the difficulties associated with obtaining representative samples of suspended solids from the coolant and are probably not caused by temporal variations in the actinide activity concentrations in the coolant. Consequently, it has been concluded that this scatter in the analytical results does not indicate the presence of fuel particles in the coolant. In addition, it has been reported that the oxide layers removed by decontamination from the primary circuit surfaces contained more than 99% of the primary circuit inventory (i. e. outside the reactor core) of ^{239}Np as well as of ^{103}Ru and ^{144}Ce. This high value indicates a comparatively fast exchange of these nuclides between coolant and oxide layer, attaining a rate similar to that of the activated corrosion products. As was mentioned before, this similarity in behavior suggests a deposition mechanism of the transuranium isotopes including as the first step a leaching of these radionuclides from the suspended particles, followed by the incorporation of the newly formed ions into the deposited oxide layers.

Investigations conducted by Beslu et al. (1984) at EdF PWR plants showed that 40 to 65% of the uranium released from defective fuel rods is deposited within the neutron field, with the remainder being deposited on primary circuit surfaces outside the reactor pressure vessel; the primary coolant carries only 10^{-2} to 10^{-3}% of the uranium inventory of the primary circuit outside the fuel rods. These results suggest that the uranium contamination is distributed almost homogeneously over the primary circuit and that only minor fractions of it are in the dissolved state or attached to suspended solids in the coolant. The fission product isotopes of the elements Zr, Nb, Ru, Ce, Pr, and La show a similar behavior; they are deposited rather quickly and almost completely onto the primary circuit surfaces, whereas the fraction carried in the primary coolant (including suspended solids) is on the order of only 10^{-2} to 10^{-3}% of the total primary circuit inventory. Fission product isotopes of the alkaline earth elements show a higher dissolved fraction, amounting for ^{90}Sr to about $1 \cdot 10^{-3}$ at a coolant pH of 7.2 and to about $2 \cdot 10^{-2}$ at a pH of 6.6; the corresponding ^{140}Ba numbers are $1.5 \cdot 10^{-3}$ and $5 \cdot 10^{-2}$, respectively.

The French PROFIP code, which was developed on the basis of these and other measurements, allows the calculation of the distribution of polyvalent fission products and actinides in the primary circuit and of the resulting radiation dose rates for rather simple geometric conditions. According to these calculations, the deposited fractions will be highest in the volume control system, while the main coolant piping will show considerably lower deposited amounts. The dose rates caused by

the deposited fission products are usually only on the order of a few percent of those caused by the activated corrosion products.

James (1988) reported the detection of so-called discrete radioactive particles in a number of US PWR plants, mainly found in contaminations outside the primary circuit and in waste samples. A part of these particles showed a typical fuel composition while others consisted of activated corrosion products, with ^{60}Co being the major radionuclide. In BWR plants, however, no fuel-type particles were detected, thus indicating that they are only stable in the reducing environment of the PWR primary coolant. The appearance of the fuel-type discrete radioactive particles is related to special fuel rod defect types, in particular hydride failures and baffle jetting failures. In the cases documented the size of the fuel particles was usually in the range 5 to 100 μm, with their total activity varying in a broad range between several Bq and 10^5 Bq; the weighted average amounted to 10^4 Bq, and more than 50% of the particles contained less than 10^3 Bq. When compared to the radionuclide composition of the fuel, most of the particles proved to be depleted in soluble fission products such as cesium isotopes, due to leaching by the liquid coolant. The complete absence of iodine isotopes in these fuel particles was explained by the long time interval between the release of the particles from the failed fuel rod and the measurements.

4.3.3 PWR water–steam circuit

Under normal operating conditions, the water–steam circuit (or secondary circuit) of pressurized water nuclear power reactors is completely free of radionuclides. Activated corrosion products and tritium, which have been reported in very low activity concentrations from the water–steam circuits of some high-temperature reactors and which are caused by the neutron field reaching into the steam generator or by ^3H diffusion through intact steam generator heating tubes, do not appear at the PWR secondary side.

In the rare event of a defect in a steam generator heating tube, primary coolant containing radionuclides passes from the primary to the secondary side due to the difference in pressure between two circuits. ^{16}N, which is always present in the primary coolant, probably in form of NH_3 (see Section 4.2.1.), is volatilized from the akaline water of the steam generator almost completely to the steam phase and, therefore, it can be used as an instantaneously acting indicator for more serious heating tube failures. The continuously working ^{16}N detectors which are installed in the main steam line usually are able to detect tube leakages down to several liters per hour. Very small leaks on the order of millilitres per hour, which represent the overwhelming part of tube failures, are detected by collecting samples of the secondary-side steam generator water to be analyzed in the laboratory for primary coolant radionuclides; when fission products are present in the primary coolant, ^{131}I and ^{137}Cs are suitable indicators. The very rare event of a tube rupture is judged to be a design basis accident which requires instantaneous shutdown of

the plant; fission product behavior under such accident conditions will be discussed in Section 6.2.3.

Fission product noble gases entering the water–steam circuit in the event of a tube leak are completely volatilized and transported with the steam to the main condenser where they are extracted and released via the off-gas stack. This release is monitored by a continuously operating detector device located in the condenser off-gas line. Non-volatile fission and activation products which are transported over the leak to the water–steam circuit remain completely in the water phase of the steam generator; by the action of the blowdown purification system their activity concentration is kept at a level which is controlled by the injection rate on the one hand and by the purification rate on the other. Because of the very low vapor pressures of these elements and their chemical compounds (dissolved ions or insoluble oxides/hydroxides), their transport to the steam under the prevailing conditions (270 °C, 7 MPa) is only possible by droplet entrainment. This means that partitioning between liquid and steam phases is proportional to the steam moisture content, which is usually well below 0.1%.

Based on fundamental chemistry considerations one can state that fission product iodine present in the primary coolant as the non-volatile I^- ion will not be converted in the steam generator water to a volatile species. In the U-tube steam generators producing saturated steam, the steam generator water is alkalized by volatile agents or by sodium phosphate according to the operation mode chosen; in addition, the absence of oxygen and other oxidizing substances is ensured. Under such conditions it can be postulated that iodide entering with the primary coolant will continue to exist completely as iodide, which is not volatile and which is transported to the steam exclusively by droplet entrainment, i. e. in the same manner and at the same proportion as the other non-volatile radionuclides. Investigations performed by Neeb et al. (1975) at an operating PWR steam generator which exhibited several small-sized tube leaks fully confirmed these assumptions. The full agreement which was observed between ^{131}I carry-over rates and those of ^{137}Cs (serving as an indicator for non-volatile substances), demonstrated that elemental iodine or other volatile iodine species do not appear under such conditions. These findings contradict various former statements in which the presence of fractions of volatile iodine species in U-tube PWR steam generators was postulated.

In the water–steam circuit, the fission product iodine which is carried by the main steam is distributed between different water and steam flows. A substantial fraction of it is plated out in the cyclone downstream of the high-pressure part of the turbine, and is transported back with the separated condensate to the feedwater storage tank. Similar washdown of iodine occurs at the other locations where condensates are separated from the remaining steam, so that only a small fraction reaches the main condenser. Here as well the major part is plated out to the main condensate water phase and is retained in the ion exchangers of the condensate polishing system; the fraction of iodine which passes over to the condenser off-gas represents only a few percent of the amount originally carried by the main steam.

According to the results reported by Jacob (1978), in a once-through steam generator about 45% of the ^{131}I activity carried by the main steam is separated in the cyclone downstream of the high-pressure part of the turbine together with the

condensed water which amounts to only about 5% of the original steam mass flow; a further 12% of the iodine activity is directed to the water phase of the reheaters, 24% to the main condensate and 19% is transported to the high-pressure feedwater preheaters. Only a fraction of about 1% is transported to the condenser off-gas, more than 97% of it as organically bound iodine. The total secondary-side iodine inventory consists of the circulating fraction plus the fraction which is freshly carried in with the leaking primary coolant; the relative contributions from both mass flows depend significantly on the ratio of the water fractions transported to the condensate cleanup system to the water fractions fed directly back to the feedwater storage tank.

4.3.4 BWR reactor water

4.3.4.1 Fission product noble gases

During reactor operation, the BWR reactor water is continuously and effectively being degassed by the vigorous boiling of the whole water volume inside the reactor pressure vessel. As a consequence, the activity concentrations of the fission product noble gases in the liquid phase are close to zero. The noble gases released from failed fuel rods are rapidly transported by the steam to the condenser off-gas system. Because of the short residence time of the gases in the primary system, their isotopic composition in the condenser off-gas is "younger" than that of a PWR noble gas mixture, i. e. the shorter-lived isotopes are present in a higher proportion. In order to minimize the release of noble gas activity to the atmosphere, the gas flow from the condenser is directed to a delay line consisting of charcoal beds where the noble gases are retained by adsorption-desorption processes, resulting in an almost complete decay of their radioisotopes. A more detailed description of this process was given in Section 4.3.2.1.1.

4.3.4.2 Iodine isotopes

The isotopic composition of fission product iodine present in the BWR reactor water in the case of failed fuel rods in the reactor core is quite similar to that in the PWR primary coolant. Since the iodine purification factor of the reactor water cleanup system is on the order of 100, i. e. virtually identical to that of the PWR primary coolant purification system, this similarity in isotopic composition demonstrates that the release mechanisms of iodine isotopes from the failed fuel rods to the water phase are virtually identical under both PWR and BWR operating conditions. On the other hand, the resulting chemical state of fission product iodine in the BWR reactor water is quite different from that in the PWR primary coolant. The BWR reactor water usually does not contain chemical additives (with the possible exception of a hydrogen addition, see below); as a result of water radioly-

sis, dissolved oxygen in the range 10 to 100 ppb, as well as a corresponding concentration of hydrogen are present. The conditions which are of relevance for the chemical state of the fission products, therefore, can be summarized as: 300 °C, neutral pH, oxidizing, intense ionizing radiation field (about $1 \cdot 10^8$ Gy/h at the center of the core of a 1300 MWe reactor, about $5 \cdot 10^7$ Gy/h at the periphery). This means that from a thermodynamic point of view in the BWR reactor water the existence of oxidized iodine species is favored, quite in contrast with the PWR primary coolant, where I^- is the most stable species.

Styrikovich et al. (1964) pointed out that at very low concentrations in high temperature water I_2 is almost completely hydrolyzed according to

$$I_2 + H_2O \longrightarrow HOI + H^+ + I^-.$$

In addition, the weakly dissociated hypoiodous acid HOI (dissociation constant $4.5 \cdot 10^{-13}$ at 25 °C) is subjected to a disproportionation reaction

$$3\ HOI \longrightarrow 2\ I^- + IO_3^- + 3\ H^+$$

Under the chemical conditions of the BWR reactor water (neutral pH), the last-mentioned disproportionation reaction is not assumed to proceed to a significant extent; it will, therefore, be ignored in this context. Because of its higher significance under reactor accident conditions, it will be treated in more detail in Section 7.3.3.3.2. The comparatively high fraction of IO_3^- measured in BWR reactor water (see below) is believed to be formed by HOI oxidation rather than by HOI disproportionation.

The degree of I_2 hydrolysis increases with increasing temperature and increasing pH of the water phase, as well as with decreasing iodine concentration. This means that in the BWR reactor water during plant operation, fission product iodine primarily exists as I^- and HOI. Experiments at different pH levels and different vapor pressures indicated that HOI is the dominant volatile iodine species under BWR operating conditions. As was shown by Styrikovich and Martynova (1963), the apparent iodine partition coefficient at 3 and 7 MPa saturation pressures shows a minimum at about pH 8 and increases for both lower and higher pH values; this behavior is typical for amphoteric compounds. The magnitude of the HOI partition coefficient and its dependence on the steam saturation pressure is quite similar to that of other amphoteric substances (such as Al_2O_3) and completely different from that of dissociated salt compounds.

In order to preclude any misunderstanding, it has to be pointed out that the term "partition coefficient" here and in the following stands for the volume-related ratio of the concentration of the substance under consideration in the liquid phase to that in the gaseous phase (and not for the reciprocal value, as was often used in former times). This means that a high value of the partition coefficient indicates low volatility of the relevant substance and vice versa. The term "apparent" indicates that the values mentioned are related to non-equilibrium conditions.

The possibility that at very low iodine concentrations (less than about 10^{-5} g/l) other iodine species than I_2 are responsible for iodine volatility has also been discussed by other authors. The investigations of Pelletier and Hemphill (1979), which were mainly related to iodine release from open spent fuel pools and, therefore,

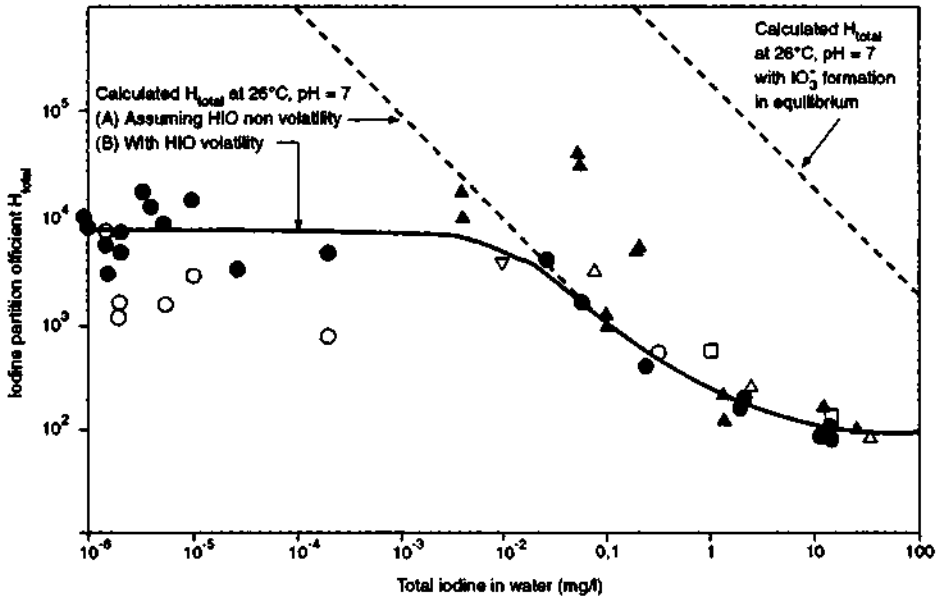

Figure 4.13. Partitioning of iodine between water and gas phase as a function of total iodine concentration
(according to Lin, 1981; with kind permission from Elsevier Science Ltd, The Boulevard, Langford Lane, Kidlington OX5 1GB, UK)

were conducted at temperatures between 25 and 80 °C, showed that with iodine concentrations in the range 10^{-8} to 10^{-11} g/l the partition coefficient is virtually independent of the iodine concentration in the aqueous solution. Lin (1981) demonstrated by his own experiments and by comparison with data published by other authors, that at higher concentrations the iodine partition coefficients which are experimentally determined at pH 7 are in reasonable agreement with calculated partition coefficients (without considering iodate formation). At concentrations below 10^{-5} g/l, however, the partition coefficient clearly no longer depends on the concentration of iodine in the solution and deviates from the calculated data (see Fig. 4.13.). A possible explanation for this behavior is that at higher concentrations I_2 is the main volatile species, with a partition coefficient of about 100 at 21 °C; this behavior is of particular interest under the conditions of severe reactor accidents and, therefore, will be discussed in detail in Chapter 7. Below about 10^{-6} g/l, the partition coefficient, however, remains constant at about 7800 at 21 °C and 1650 at 72 °C, thus indicating that there is at least a second volatile iodine species in the system which exhibits a considerably lower volatility than I_2. It is believed that this species is HOI. On the basis of HOI volatility and its partition coefficient, Lin (1981) has calculated the equilibrium constant and the thermodynamic properties of this compound. Extrapolation of these data to 280 °C yields an HOI partition coefficient of about 10. Taking into account that about 80% of the fission product iodine is present in the boiling reactor water as the non-volatile species I^-

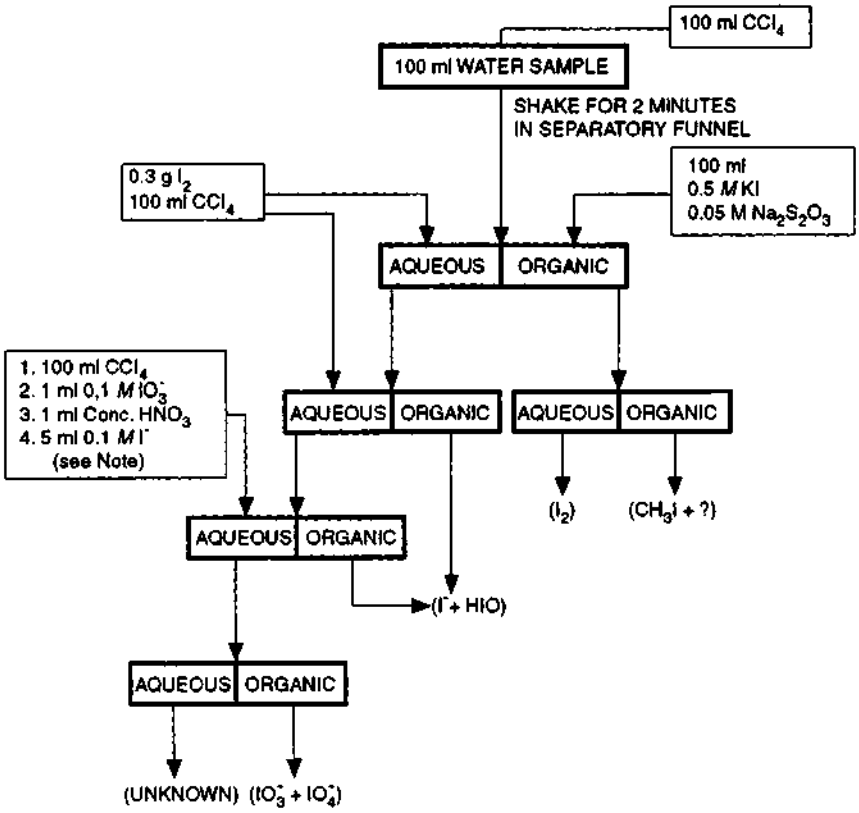

Figure 4.14. Analytical procedure for separation of iodine chemical species by extraction (Lin, 1980 a; with kind permission from Elsevier Science Ltd, The Boulevard, Langford Lane, Kidlington OX5 1GB, UK)

and IO_3^- (see below), iodine carry-over would be about 2%, which agrees well with much of the data measured (Lin, 1992).

As a general remark, it has to be mentioned that analytical identification of the different iodine species, in particular at very low concentrations, poses fundamental difficulties due to possible changes in the original chemical forms during sampling and analysis. The procedure developed by Lin (1980 a), which is frequently used in the speciation of iodine in aqueous solutions, consists of a series of extraction steps (see Fig. 4.14.), during which at first I_2 and organoiodides are simultaneously isolated from the aqueous solution by CCl_4 extraction. Subsequently, both species are separated from each other by backextraction under reducing conditions; during these steps, there is a certain danger that traces of I_2 will react with the organic phase to form organoiodide compounds originally not present in the sample solution. Iodide then is extracted after homogeneous isotope exchange with added inactive I_2. Using a large excess of I_2 carrier, this fast reaction results in a complete conversion of traces of radioactive I^- to extractable I_2; however, any iodide not

exchanged will appear later on as iodate or as an unknown iodine species. On the other hand, systematic investigations reported by Burns et al. (1988) showed that the yield of I_2 extraction into benzene decreases with increasing dilution, falling from about 100% at 10^{-5} M I_2 solution down to 20% at 10^{-8} M I_2 solution. I_2 recovery can be markedly improved by addition of phenol, which results in an extraction of iodophenol. Further, the separation of I_2 from organoiodides by backextraction from the organic phase using an excess of NaOH may lead to simultaneous backextraction of organic iodine compounds which could ionize under such conditions; therefore, backextration of I_2 by equilibration with an aqueous I^- solution is preferred. Similarly, the ion exchange separation technique reported by Caruthers and Gritz (1978) has to be treated with caution; in samples with high excess iodide in particular, breakthrough of minor amounts of this species may falsely seem to indicate the presence of oxidized iodine forms. Finally, iodine analysis in the gaseous phase is mainly performed by sampling onto specific filter packs which consist of different filter materials, with each one of them being selective for one specific iodine species; the efficiency of these filters will be discussed in more detail in Chapters 6 and 7.

In the very intense neutron and gamma field inside the reactor pressure vessel, the H_2O molecule is decomposed by radiation-induced reactions and some of the resulting primary products are capable of oxidizing dissolved iodide ions. Investigations carried out by Lin (1980 b) showed that the product yields in the radiolytic oxidation depend strongly on the iodine concentration in the solution. At higher concentrations, iodide is mainly oxidized to I_2; this reaction is of interest in severe accident chemistry and will be treated in Chapter 7. By contrast, at concentrations below about 10^{-5} M the radiolytic I_2 yield decreases in favor of iodate formation and at concentrations below 10^{-6} M, i. e. in the region of interest in BWR operation, iodate is the dominating iodine species in water in the pH range 2 to 9; at higher pH values, a radiation-induced reduction of all iodine species to iodide takes place. Because of the low yield of the radiation-induced decomposition of iodate, which has a $G(-IO_3^-)$ value of about 0.001 at pH 8, an iodate yield of more than 90% is reached when the solution is exposed to gamma radiation doses of more than 10^3 Gy. Presence of air or of H_2O_2 has little influence on the progress of the reaction and on its product yields. As a possible mechanism of radiation-induced iodate formation, successive oxidation steps are assumed with HOI as the primary intermediate, with the OH· radical being the major oxidizing species (Lin, 1980 b; Ishigure et al., 1985).

These basic results were confirmed by experimental investigations conducted at different US BWR plants (Lin, 1980 a). According to these results, the bulk of fission product iodine in the reactor water during constant-load operation is present as iodide (including HOI which cannot be separately identified by the analytical techniques applied), though the magnitude of this fraction varies between 50 and 85% at different plants. Iodate was measured in amounts between 10 and 48%, whereas elemental iodine was present only in minor amounts (0.1–8%) and organiodide compounds were below the analytical detection limit. However, following reactor shutdown a significant change in the ratio iodide–iodate in the reactor water was observed, resulting in an increase of the iodate fraction to values

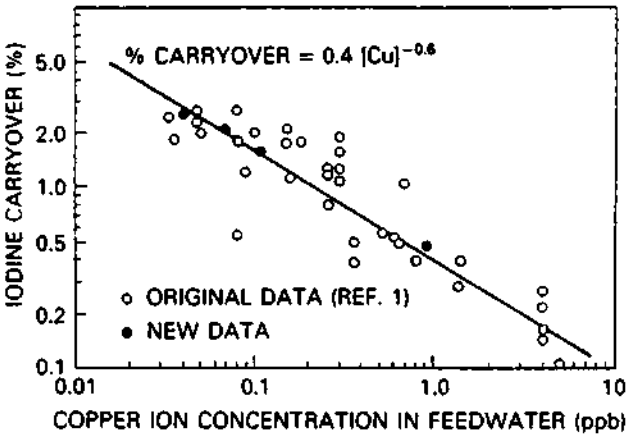

Figure 4.15. Iodine carry-over vs. copper concentration in BWR feedwater
(Lin, 1992; Ref 1 denotes Lin, 1980 a; Copyright 1992 by the American Nuclear Society, La Grange Park, Illinois)

up to 98%. This effect is believed to be a consequence of radiation-induced oxidation: During reactor operation, a significant fraction of the intermediate HOI is removed from the liquid phase by evaporation and, therefore, further oxidation to iodate is limited. After shutdown, the HOI produced remains in the water phase and acts there as the starting compound for iodate formation.

When evaluating these analytical results one has to consider that they represent the iodine oxidation states that are present in the reactor water after sampling, i. e. at ambient temperature, and which may be markedly different from those present at operating temperature. Lindén and Turner (1983) pointed out that at ambient temperature the equilibrium ratio IO_3^-: I^- in water containing 250 ppb oxygen (corresponding to the conditions in some of the BWR plants) is almost completely shifted to the iodate side, whereas in such a solution at operating temperature iodide is the dominant species. As a result, a comparatively small increase in the oxygen concentration in the reactor water at operating temperature may lead to a marked increase in the concentration of the iodate fraction.

The presence of volatile iodine species in the BWR reactor water results in an iodine carry-over to the main steam which is significantly higher than that caused by mechanical droplet transport (entrainment), i. e. higher than the iodine carry-over in the PWR steam generator. Numerous measurements at BWR plants have confirmed this level of carry-over, but also showed that despite comparable reactor water temperatures and pressures, the carry-over fractions can vary between 0.1 and 2%. Lin (1980 a) reported a correlation between iodine carry-over from the reactor water to the main steam and the copper concentration in the feedwater, with the latter depending on the materials present in the turbine and condenser region and on the efficiency of the condensate polishing system (see Fig. 4.15.). This correlation is assumed to be due to Cu^{2+} ions acting as a scavenger for the oxidizing primary products which are generated in H_2O radiolysis. The conse-

quence of this scavenger effect is a decrease in the radiation-induced iodide oxidation and in the resulting production of volatile species; this effect has also been demonstrated in laboratory experiments.

In the past, iodine carry-over rates were observed at some BWR plants which considerably exceeded the range 0.1 to 2% mentioned above; in individual cases they were even higher than 10%. In a detailed investigation, Lindén and Turner (1983) found out that such high values preferentially occurred when the reactor water contained very low dissolved ion concentrations over a longer time period and, simultaneously, an enhanced oxygen concentration. Such conditions favor the oxidation of I^- to volatile HOI, quite in agreement with the results reported by Lin (see above). On the other hand, there are still some effects which cannot be explained by this assumption. One phenomenon is that, in spite of very low copper concentrations in the feedwater of all the BWR plants studied, the iodine carry-over rates showed significant differences from one plant to the other; possibly, Fe^{2+} ions are as effective as Cu^{2+} ions in scavenging radiolytically generated radicals. In addition, Lindén and Turner (1983) reported that upon addition of hydrogen to the reactor water the oxygen concentration decreased significantly while the iodine carry-over was not significantly influenced. Since hydrogen water chemistry (HWC) has gained in importance and this type of BWR chemistry can be assumed to influence the chemical state of fission product iodine in the reactor water, this effect has been studied in greater detail. Apparently, the concentrations of the oxidizing free radicals $OH\cdot$ and $HO_2\cdot$ are decreased by hydrogen addition, thus potentially retarding the oxidation of I^- to IO_3^-. Investigations performed by Lin (1992) at US BWR plants showed that upon addition of H_2 to the reactor water, the I^- fraction increased considerably while the IO_3^- fraction was drastically reduced. The effect of hydrogen addition on iodine carry-over, however, is less clear (see Fig. 4.16.). While in two of the investigated plants the carry-over rates remained essentially unchanged, they increased by a factor of 2 to 3 at the highest H_2 addition rate in the two other reactors. As an explanation for this effect it was claimed that, although the oxidation of I^- to IO_3^- is significantly retarded under HWC conditions, the oxidation potential in the core region is still high enough to oxidize I^- to volatile I_2 and HOI. It seems, therefore, that as the IO_3^- fraction is reduced, more volatile iodine species become available. On the other hand, BWR plants exhibiting low iodine carry-over show a lower IO_3^- fraction under normal water chemistry (NWC) conditions; consequently, iodine carry-over under HWC conditions is practically unchanged. The latter type of reactors happen to be the ones with higher copper concentrations in the reactor water. This confirms the effect of copper traces as efficient radical scavengers, reducing iodine carry-over as well as oxygen supression efficiency under HWC operating conditions.

Lin (1983) also reported on a detailed investigation of the distribution of iodine volatilized from the reactor water in BWR water–steam circuits with forward-pumped heater drains. In this plant design, only the main condensate is directed to the condensate polishing system, whereas the different drains from the turbine are fed directly back to the feedwater tank. Under such plant conditions, about 75% of the iodine carried by the main steam flow is precipitated together with the condensate in the moisture separator downstream from the high-pressure part of

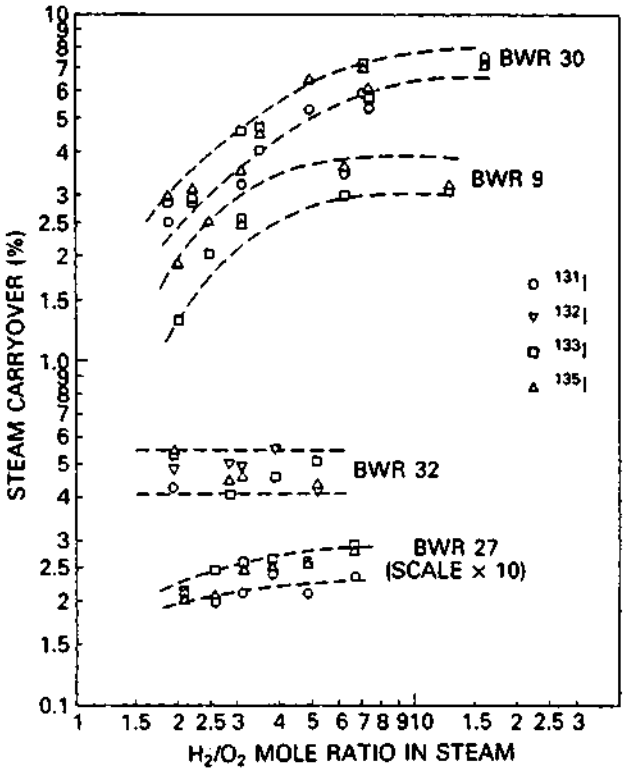

Figure 4.16. Iodine carry-over as a function of H_2/H_2O mole ratio in steam (Lin, 1992; Copyright 1992 by the American Nuclear Society, La Grange Park, Illinois)

the turbine. From the experimental data, an iodine partition coefficient of about 8600 at 180 °C was calculated, which is significantly higher than the value to be expected for HOI; ^{18}F shows an almost identical partition coefficient. This partition coefficient was attributed to an assumed compound $H_2O \cdot I$, which probably is formed after contact of HOI with liquid water.

When evaluating the experimental results it should not be overlooked that steam sampling from a saturated steam flow is generally susceptible to errors which are caused by a non-representative composition of the collected sample. In order to deal with this problem, one has to make provision for isokinetic sampling in order to preclude separation of suspended droplets from the steam phase. Moreover, one has to take into consideration that the walls of the system pipes are always covered by a liquid water film in which radionuclides may be present in higher concentrations than in the steam flow itself. Therefore, when evaluating results of measurements of iodine carry-over it is important to examine closely the experimental techniques which were applied for sampling.

The fraction of iodine that is not condensed in the moisture separator reaches the turbine condenser where at about 33 °C the bulk of it is plated out into the

water phase; more than 80% of this fraction is detected in the chemical forms I^- and/or HOI. In the condenser gas phase, besides HOI and I_2, a significant fraction (about 30%) of the iodine was found to be organically bound (Lin,1983). The composition of the organoiodide represents an iodine isotope mixture that is "older" than the iodine which is present in the reactor water and in the main condensate; from this shift in the isotope ratios it was concluded that the organoiodide is produced by adsorption of iodine onto steel surfaces, followed by reaction with CH_4 which is formed in the corrosion of the steel carbide constituents and, finally, release to the gas phase. In total, these reactions would result in a significant delay in iodine release, thus explaining the measured ageing of the organoiodide isotope mixture.

4.3.4.3 Other fission products and activation products from the fuel

In the case when defective fuel rods are present in the reactor core, the BWR reactor water contains the other fission products and the activation products released from the fuel in concentrations well below those of fission product iodine. This applies as well for fission product cesium, which is retained on the ion exchangers of the reactor water cleanup system with a decontamination factor of about 100. As far as it is known, cesium in the reactor water is present as the Cs^+ ion, whereas large proportions of most of the polyvalent fission products and of the actinides are attached to the corrosion product particles suspended in the water; as yet, there is no detailed knowledge on the chemical state of these elements (i. e., adsorbed to the surfaces or incorporated into the Fe_2O_3 lattice). It was reported that the strontium isotopes as well as ^{239}Np appear in the reactor water in the dissolved cationic state, while ^{99m}Tc was found in the reactor water as a dissolved anionic species, most likely TcO_4^- (Lin and Holloway, 1972). According to James (1988), discrete fuel particles were not detected in the BWR reactor water.

Of the α-emitting nuclides, ^{242}Cm represents more than 95% of the total α activity, with the combined plutonium isotopes 238, 239 and 240 accounting for the remainder. The relative activity proportions of these nuclides in the water as well as those of other "insoluble" fission products such as ^{95}Zr, ^{144}Ce and ^{106}Ru are the same as in the fuel.

The carry-over of these radionuclides from the reactor water to the steam depends on both the steam moisture content and the solubility of the individual elements in the steam. With elements forming strong electrolytes in the reactor water (such as Cs^+), solubility in the steam under BWR operating conditions is very low; this means that cesium carry-over is exclusively controlled by the moisture content of the steam. On the other hand, elements which are present in the water phase in the form of weakly dissociated compounds will show a noticeable solubility in steam even at BWR conditions (i. e. operating pressure in the range 7 MPa), resulting in a carry-over which may be markedly higher than the moisture

content of the steam. As this effect is of particular significance in the volatility of radioactive corrosion products it will be treated in more detail in Section 4.4. Thus, polyvalent fission products and actinides in hot water may show the properties of weak electrolytes and are transferred to the steam to a higher extent than by droplet entrainment alone. However, since their activity concentrations in the reactor water are usually very low the enhanced steam volatility is of little radiological significance.

References Section 4.3

Adams, J. P., Atwood, C. L.: The iodine spiking release rate during a steam generator tube rupture. Nucl. Technology **94**, 361–371 (1991)

Adams, J. P., Sattison, M. B.: Frequency and consequences associated with a steam generator tube rupture event. Nucl. Technology **90**, 168–185 (1990)

Alm, M., Johannsen, K.-H., Dreyer, R.: Untersuchungen zum Verhalten der anorganischen Formen des Radioiods in den Kreisläufen von Druckwasserreaktoren. Isotopenpraxis **15**, 85–89 (1979)

Aßmann, H., Stehle, H.: Chemie in Reaktorbrennstäben mit oxidischen Kernbrennstoffen. Chemiker-Ztg. **108**, 65–82 (1984)

Beraha, R., Beuken, G., Frejaville, G., Leuthrot, C., Musante, Y.: Fuel survey in the light water reactors based on the activity of the fission products. Nucl. Technology **49**, 426–434 (1980)

Beslu, P., Leuthrot, C., Brissaud, A., Harrer, A., Beuken, G.: Solid fission products and actinides release and deposition inside PWR's primary circuits. Proc. 5. Internat. Meeting on Thermal Nuclear Reactor Safety, Karlsruhe 1984, (KfK-3880) p. 1387–1397

Bishop, W. N.: Iodine spiking. Report EPRI NP-4595 (1986)

Besmann, Th.M., Lindemer, T. B.: Chemical thermodynamics of the system Cs-U-Zr-H-I-O in the light-water reactor fuel-cladding gap. Nucl. Technology **40**, 297–305 (1978)

Burman, D. L.: Methods for estimating numbers of failed rods from coolant activity analysis. Proc. Workshop Fuel Integrity Monitoring by Coolant Activity Analysis, Charlotte, N. C., USA, 1986

Burns, W. G., Kent, M. C., Marsh, W. R., Potter, P. E., Sims, H. E.: Radiolytic and surface reactions of dilute iodine solutions. Proc. 2. CSNI Workshop on Iodine Chemistry in Reactor Safety, Toronto, Can., 1988; Report AECL-9923, p. 19–38 (1989)

Caruthers, G. F., Gritz, R. W.: Radioiodine behavior during a postulated steam generator tube rupture accident. Trans. Am. Nucl. Soc. **28**, 653–654 (1978)

Chubb, W., Piplica, E. J., Lutz, R. J.: The iodine spiking phenomenon in pressurized water reactor coolants. Trans. Am. Nucl. Soc. **26**, 517–518 (1977)

Daish, S. R., Beahm, E. C., Shockley, W. E.: Aqueous iodine at low concentrations and high temperatures. Proc. 2. CSNI Workshop on Iodine Chemistry in Reactor Safety, Toronto, Can., 1988; Report AECL-9923, p. 74–95

Eickelpasch, N., Hock, R.: Fission product release after reactor shutdown. IAEA Symposium Vienna 1973, Paper IAEA-SM 178/19 (1974)

Eickelpasch, N., Seepolt, R., Hock, R.: Iodine release mechanism and its verification in plant operation. Trans. Am. Nucl. Soc. **28**, 652–653 (1978)

Eigenwillig, G. G., Hock, R.: Shutdown release of fission products in LWRs. Trans. Am. Nucl. Soc. **23**, 258–259 (1976)

Garzarolli, F., von Jan, R., Stehle, H.: The main causes of fuel element failures in water-cooled power reactors. Atomic Energy Review **17**, (1), 31–128 (1979)

Goll, W., Fuchs, H.-P., Manzel, R., Schlemmer, F. U.: Irradiation behaviour of UO_2/PuO_2 fuel in light water reactors. Nucl. Technology **102**, 29–46 (1993)

Goncarvos, G.: Radiochemical evaluation for debris-induced failures. Nucl. Technology **102**, 323–330 (1993)

Haag, J., Paffrath, G., Ambros, R., Oschmann, W., Schroeder, H. J., Hanstein, W.: Continuous measurements of chemical and radiochemical parameters in nuclear power plants. Proc. 4. BNES Conf. Water Chemistry of Nuclear Reactor Systems, Bournemouth, UK, 1986, Vol. 2, p. 103–109

Habersbergerova, A.: Investigation of the possibility of radiation-induced methyl iodide formation under operating conditions of PWR reactors. Radiat. Phys. Chem. **34**, 781–785 (1989)

Habersbergerova, A., Bartonicek, B.: Radiolysis of iodine in deaerated borate solutions at pH 7–9. Radiochem. Radioanal. Letters **22**, 307–312 (1975)

Habersbergerova, A., Bartonicek, B.: Radiolysis of iodine compounds in model systems of PWR. Radiat. Phys. Chem. **21**, 289–293 (1983)

Hastings, I. J., Hunt, C. E. L., Lipsett, J. J.: Release of short-lived fission products from UO_2 fuel: Effects of operating conditions. J. Nucl. Materials **130**, 407–417 (1985)

Hock, R.: Nachweis von Brennelementschäden. in: Schrüfer, E., Strahlung und Strahlungsmeßtechnik in Kernkraftwerken, Elitera-Verlag Berlin 1974, p. 387 ff.

Hüttig, W., Zänker, H., Forberg, M.: In-core surveillance of defective PWR fuel elements in the case of fuel-to-water contact. J. Nucl. Materials **175**, 147–157 (1990)

Ishigure, K., Shiraishi, H., Okuda, H., Uchida, J., Yoshitani, Y., Fujita, N.: The effect of radiolysis on the chemical forms of iodine species. Proc. Specialists Workshop Iodine Chemistry in Reactor Safety, Harwell, UK, 1985, p. 139–148; Report AERE R 11974 (1986)

Jacob, N. P.: Secondary system fission product transport study at the Oconee Nuclear Station. Trans. Am. Nucl. Soc. **28**, 506–507 (1978)

James, D. W.: Problem assessment of discrete radioactive particles. Report EPRI NP-5969 (1988)

Kalfsbeek, H. W.: The abundance of fission gases in the off gas of a boiling water reactor. Nucl. Technology **62**, 7–21 (1983)

Knaab, H., Stark, R., Sturm, R.: Sipping equipment for leak testing of fuel assemblies in VVER-440 reactors. Kerntechnik **56**, 94–97 (1991)

Krüger, J., Stark, R., Seepolt, R.: Fortschrittliche In-Core-Sipping Technik. Atomwirtschaft **34**, 352–354 (1989)

Kurka, G., Harrer, A., Chenebault, P.: Fission product release from a pressurized water reactor defective fuel rod: Effect of thermal cycling. Nucl. Technology **46**, 571–581 (1979)

Leuthrot, C., Beslu, P.: Release of volatile fission products for commercial PWRs in transient conditions including load follow. Proc. 4. BNES Conf. Water Chemistry of Nuclear Reactor Systems, Bournemouth, UK, 1986, Vol. 2, p. 137–140

Lewis, B. J.: Fission product release from nuclear fuel by recoil and knockout. J. Nucl. Materials **148**, 28–42 (1987)

Lewis, B. J.: Fundamental aspects of defective nuclear fuel behaviour and fission product release. J. Nucl. Materials **160**, 201–217 (1988)

Lewis, B. J.: A generalized model for fission-product transport in the fuel-to-sheath gap of defective fuel elements. J. Nucl. Materials **175**, 218–226 (1990)

Lewis, B. J., Duncan, D. B., Phillips, C. R.: Release of iodine from defective fuel elements following reactor shutdown. Nucl. Technology **77**, 303–312 (1987)

Lewis, B. J., Green, R. J., Che, C. W. T.: A prototype expert system for the monitoring of defected nuclear fuel elements in Canada Deuterium Uranium reactors. Nucl. Technology **98**, 307–321 (1992)

Lewis, B. J., Hunt, C. E. L., Iglesias, F. C.: Source term of iodine and noble gas fission products in the fuel-to-sheath gap of intact operating nuclear fuel elements. J. Nucl. Materials **172**, 197–205 (1990)

Lewis, B. J., MacDonald, R. D., Ivanoff, N. N., Iglesias, F. C.: Fuel performance and fission product release studies for defected fuel elements. Nucl. Technology **103**, 220–244 (1993)

Lewis, B. J., Phillips, C. R., Notley, M. J. F.: A model for the release of radioactive krypton, xenon, and iodine from defective UO_2 fuel elements. Nucl. Technology **73**, 72–83 (1986)

Lin, C. C.: Chemical behavior of radioiodine in BWR systems. J. Inorg. Nucl. Chem. **42**, 1093–1100 (1980 a)

Lin, C. C.: Chemical effects of gamma radiation on iodine in aqueous solutions. J. Inorg. Nucl. Chem. **42**, 1101–1107 (1980 b)

Lin, C. C.: Volatility of iodine in dilute aqueous solutions. J. Inorg. Nucl. Chem. **43**, 3229–3238 (1981)

Lin, C. C.: Chemical behaviour and distribution of volatile radionuclides in a BWR system with forward-pumped heater drains. Proc. 3. BNES Conf. Water Chemistry of Nuclear Reactor Systems, Bournemouth 1983, Vol. 1, p. 103–110

Lin, C. C.: Chemical behavior of radioiodine in boiling water reactor systems. II.: Effects of hydrogen water chemistry. Nucl. Technology **97**, 71–78 (1992)

Lin, C. C., Holloway, J. H.: Behavior of radioactivities in the reactor water without cleanup service. Report GE NEDE-23793 (1972)

Lindén, E., Turner, D. J.: Carry-over of volatile iodine species in some Swedish and American BWRs. Proc. 3. BNES Conf. Water Chemistry of Nuclear Reactor Systems, Bournemouth 1983, Vol. 1, p. 111–119

Lutz, R. J., Chubb, W.: Iodine spiking – Cause and effect. Trans. Am. Nucl. Soc. **28**, 649–650 (1978)

Martin, J. E., Marcinowski, F., Cook, S. K.: Optimization of neutron activation analyses of ^{129}I in low-level radioactive waste samples. Int. J. Appl. Radiat. Isotopes **41**, 727–731 (1990)

Neeb, K. H.: Kühlmittelaktivitäten und ihr zeitlicher Verlauf bei der Abschaltung des KWO. Proc. Reaktortagung Deutsches Atomforum Bonn 1971, p. 461–464

Neeb, K. H., Richter, H., D'Amaddio, E. R., Mayer, R. E.: Verhalten von Spaltiod im Sekundärkreislauf von Druckwasserreaktoren. Proc. Reaktortagung Deutsches Atomforum Nürnberg 1975, p. 611–614

Neeb, K. H., Schuster, E.: Iodine spiking in PWRs: Origin and general behavior. Trans. Am. Nucl. Soc. **28**, 650–651 (1978)

Neeb, K. H., Schuster, E.: Origin and general behaviour of increased release of fission iodine from defective fuel rods upon shutdown of a pressurized water reactor. Siemens Forsch. u. Entwickl. Berichte **8**, 92–97 (1979)

Pelletier, C. A., Hemphill, R. T.: Nuclear power plant related iodine partition coefficients. Report EPRI NP-1271 (1979)

Postma, A. K., Tam, P. S.: Iodine behavior in a PWR cooling system following a postulated steam generator tube rupture accident. Report NUREG-0409 (1978)

Schuster, E., Garzarolli, F., Kersting, A., Neeb, K. H., Stehle, H.: Escape of fission products from defective fuel rods of light water reactors. Nucl. Engng. and Design **64**, 81–85 (1981)

Schuster E., Kersting, A., Neeb, K. H.: Freisetzung von Spaltiod aus defekten Brennstäben im DWR bei Konstantlast und Lastwechseln. Proc. Reaktortagung Deutsches Atomforum Mannheim 1977, p. 817–820

Schuster, E., von Jan, R., Fischer, G.: Evaluation of fuel performance from coolant activity data. Proc. ANS/ENS Internat. Top. Meeting on LWR Fuel Performance (Fuel for the 1990s), Avignon 1991, Vol. 1, p. 285–294

Sellers, R. M.: A review of the radiation chemistry of iodine compounds in aqueous solution. CEGB Report RD/B/N 4009 (1977)

Sévéon, H., Leuthrot, C., Stora, J. P., Chenebault, P., Warlop, R.: Release of fission products by defective pressurized water reactor fuel. Proc. 5. Internat. Meeting on Thermal Nuclear Reactor Safety, Karlsruhe 1984, (KfK 3880) p. 1398–1404

Stöckert, H., Kaspar, G., Fuchs, A., Zegarski, K., Dörr, A.: Ultra-sensitive detection of defective fuel rods (sipping test) with low core burnup and long decay period. Siemens Forsch. u. Entwickl. Berichte **8**, 98–101 (1979)

Styrikovich, N. A., Martynova, O. I.: Contamination of the steam in boiling reactors from solution of water impurities. Atomnaya Energiya **15**, 214–218 (1963)

Styrikovich, N. A., Martynova, O. I., Katkovskaya, K. Ya., Dubrovskii, I. Ya, Smirnova, I. N.: Transfer of iodine from aqueous solutions to saturated vapour. Atomnaya Energiya **17**, 45–49 (1964)

Trautmann, N.: Ultratrace analysis of technetium. Radiochim. Acta **63**, 37–43 (1993)

Turner, D. J.: On the existence of iodide boric acid complexes in saturated steam. Proc. 2. CSNI Workshop on Iodine Chemistry in Reactor Safety, Toronto, Can., 1988; Report AECL-9923, p. 135–150 (1989)

Verrezen, F., Hurtgen, C.: The measurement of technetium-99 and iodine-129 in waste water from pressurized nuclear-power reactors. Int. J. Appl. Radiat. Isotopes **43**, 61–68 (1992)

Voillequé, P. G.: Measurements of radioiodine species in samples of pressurized water reactor coolant. Nucl. Technology **90**, 23–33 (1990)

Wilkins, J. D., Wisbey, S. J.: Contamination of metal surfaces with plutonium from aqueous solutions. Radiochim. Acta **36**, 53–59 (1984)

Zänker, H.: Defective fuel rod detection in operating pressurized water reactors during periods of continuously decreasing fuel rod integrity levels. Nucl. Technology **86**, 239–247 (1989)

Zänker, H., Berndt, T.: Rough localization of defective PWR fuel rods on the basis of the concentration ratio $^{134}Cs/^{137}Cs$ in the primary coolant. J. Radioanal. Nucl. Chem. **122**, 239–244 (1988)

Zänker, H., Berndt, R., Steinkopf, H.: Rough localization of defective PWR fuel rods on the basis of the concentration ratio $^{134}Cs/^{137}Cs$ in the primary coolant. Possibilities and limits. Kernenergie **30**, 193–196 (1987)

Zänker, H., Nebel, D.: On the transport behaviour of ^{239}Np and non-volatile, insoluble fission products in the primary circuits of PWRs. Radiochim. Acta **40**, 165–168 (1986)

4.4 Activated corrosion products and contamination buildup

4.4.1 General aspects

In the course of the operation of pressurized as well as of boiling water reactors, a contamination layer consisting of the oxides of primary circuit materials is formed on all surfaces which are in contact with reactor coolant. In high-temper-

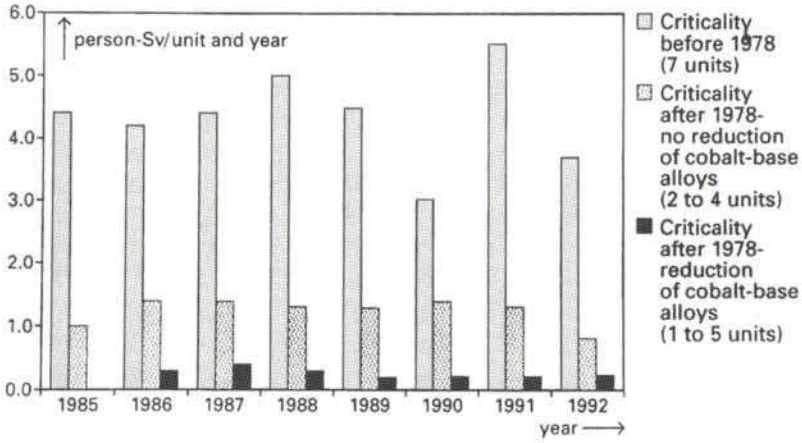

Figure 4.17. Average occupational radiation exposure per unit and year of Siemens PWRs (Marchl and Riess, 1993)

ature zones (i. e. in the primary system) this layer is very thin, but it adheres very tightly to the base material, whereas in low-temperature regions (e. g. in the auxiliary systems or the spent fuel pool) it mainly consists of loosely adhering deposits. The radionuclides which are incorporated into these layers are the origin of substantial radiation dose rates in the area surrounding circuits and systems, potentially rendering work to be performed during operation and inspections difficult and expensive. For this reason, in almost all countries in which nuclear power plants are operated, extensive work has been devoted to the reduction of the occupational radiation doses. These efforts can be roughly divided into three separate groups, the first of which is minimization of the production of disturbing radionuclides and, consequently, of the contamination levels; this topic will be treated in detail in the following sections. The second approach is to reduce personnel radiation burden at a given contamination level, starting with an improved design of the plants, facilitating work as well as access to working areas. Newer plants have been equipped with improved shieldings, training of the staff working in the controlled areas has been intensified, the need for inspection and repair work has been reduced by an optimized selection of the materials and by an improved design of the components and, finally, automated and/or remote-controlled inspection and repair techniques have been introduced whenever feasible. All these topics, which clearly belong to the field of radiation protection, will not be discussed in this context, which is mainly devoted to radiochemistry. As a third possibility, disturbing radionuclide-containing layers can be removed by decontamination, whenever necessary; the procedures applied here will be discussed in Section 4.5.

By a reasonable application of these measures, a drastic reduction in occupational radiation exposure has been achieved. As an example, in Fig. 4.17. and 4.18. the annual cumulative radiation doses are shown for PWR and BWR plants, respectively, which were designed and built by Siemens/KWU (Marchl and Riess,

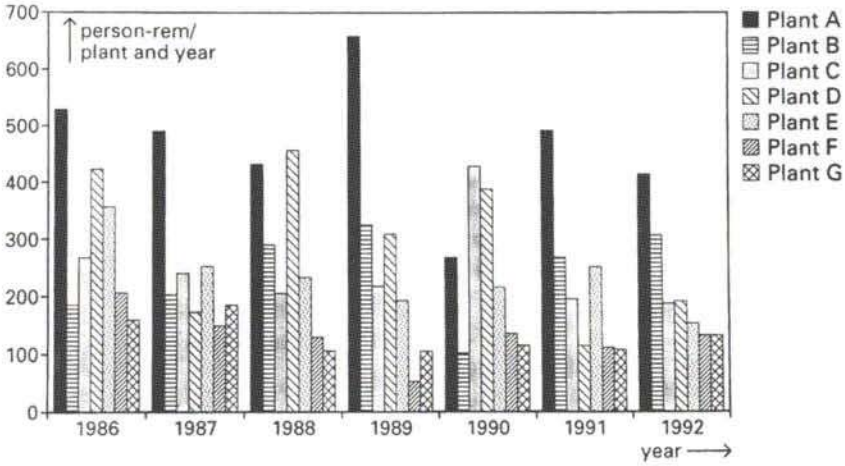

Figure 4.18. Occupational radiation exposures of Siemens BWRs (Reitzner et al., 1993)

1993; Reitzner et al, 1993). Clearly, the cumulative dose levels depend on the year of construction of the particular plant, with the improvements made in design and operation resulting in a substantial decrease of the annual dose values, as has been pointed out before by other authors (e. g. Hecht, 1989). This beneficial development becomes particularly evident for PWR plants commissioned after the year 1985, which are designed with a considerably reduced cobalt inventory in particular in the materials employed inside the reactor pressure vessel. With BWR plants, the benefits of the change in design from the external recirculation lines (plant A) to the internal axial pumps (all other plants listed) are also clearly evident. By contrast, the length of operation of the individual plants (i. e. their age) is not significantly reflected in the radiation dose levels. In most of the plants, the cumulative doses remain virtually constant over the time of operation or they even decline over time (when years of special maintenance such as piping replacement are not considered). This behavior indicates that there are no deterioration effects that adversely influence the operating performance of the plants. A large fraction of the yearly dose exposure values has to be attributed to the refuelling outage periods (about 85% in PWR and about 50% in BWR plants) and is predominantly due to in-service inspection work. Similar observations have been reported from US plants (Wood and Ocken, 1989; Ocken and Wood, 1992), showing that PWR and BWR plants commissioned in the 1980's generally exhibit lower dose exposures and that exposures in older plants have also been declining in recent years.

In light water reactors, the radionuclides are exclusively deposited into the surface oxide layers of the piping, components, etc., while the base materials (with the exception of the materials inside the reactor pressure vessel which are neutron-activated) are free of radioactivity. This fact is a fundamental difference from reactors that operate at higher temperatures (e. g. liquid-metal cooled reactors), where the deposited radionuclides are able to diffuse into the base material to a significant

Table 4.2. Important corrosion product radionuclides in light water reactors

Production reaction	Main source	Reactor type
^{58}Ni (n, p) ^{58}Co ^{59}Co (n, γ) ^{60}Co	Incoloy 800, Inconel 600, 690, etc. Stainless steel, Co alloys	PWR, BWR
^{54}Fe (n, p) ^{54}Mn ^{58}Fe (n, γ) ^{59}Fe ^{50}Cr (n, γ) ^{51}Cr	Incoloy 800 Stainless steel, mild steel Chromium steel	PWR, BWR
^{94}Zr (n, γ) $^{95}Zr \xrightarrow{\beta^-} {}^{95}Nb$	Zircaloy (also fission product)	PWR, BWR
^{109}Ag (n, γ) ^{110m}Ag	Ag-containing seals	PWR
^{63}Cu (n, γ) ^{64}Cu ^{64}Zn (n, γ) ^{65}Zn	Brass condensor tubing	BWR
^{121}Sb (n, γ) ^{122}Sb ^{123}Sb (n, γ) ^{124}Sb	Seals and bearings	PWR

extent. Deposition onto the surfaces of the structural materials in light water reactors essentially occurs with radioisotopes of elements that are able to form water-insoluble compounds or which can become attached to the superficial oxide layers by physico-chemical mechanisms. As a consequence, radionuclides which are easily soluble in water (such as iodine and cesium isotopes) are not deposited onto the surfaces to a noticeable extent and, therefore, do not contribute to the contamination buildup. A possible exception may happen with iodine, when silver is simultaneously present in the primary coolant (e. g. resulting from wear or corrosion of seals), probably due to the formation of insoluble AgI. Polyvalent fission products such as cerium and the rare earth elements as well as actinide isotopes can also be incorporated into the deposits; their extremely low release from the fuel to the coolant (see Section 4.3.), however, means that they are only of significance when severely defective fuel rods with marked fuel losses to the primary circuit are present in the reactor core. Thus, contamination buildup in light water reactors is predominantly caused by activated constituents of the materials employed in the primary circuit. In addition, it has to be pointed out that the deposition behavior of radionuclides from the liquid coolant of light water reactors shows fundamental differences from that from gas flows (such as from the hot inert gases in a gas-cooled reactor) or from that of impurities carried in overheated steam in conventional power plants.

The radionuclides of principal significance in contamination buildup, their origins and their production reactions are summarized in Table 4.2. These radionuclides are all gamma emitters with a comparatively long halflife. In virtually all plants, the radiation dose rates in the area surrounding the circuits and components are predominantly due to ^{60}Co, because of the high energies of its γ quants of 1.17 and 1.33 MeV and the transition probability of both of them of 100%. Besides ^{60}Co, additional activation products of other constituents of austenitic steels and nickel-based alloys, in particular ^{58}Co, have to be mentioned. Only in special cases

will other radionuclides, such as the antimony isotopes, contribute to an appreciable extent to the radiation dose rates on the surfaces of the systems and components.

In addition to the most important γ-emitting activation products listed in Table 4.2., a large number of other radionuclides are produced during plant operation by neutron activation of the in-core materials or of corrosion products temporarily deposited in the neutron field. These radionuclides, however, are of minor radiological importance. In this context, short-lived γ-emitting nuclides such as ^{56}Mn and ^{65}Ni (which, due to their short halflives, do not significantly contribute to the radiation dose levels) have to be mentioned, as well as the longer-lived (n, γ) products ^{55}Fe, ^{59}Ni and ^{63}Ni, since their decay is not accompanied by γ-ray emission. They do not contribute, therefore, to the radiation doses on the outside of the pipes and components, but they have to be considered in waste treatment and waste characterization and, potentially, when work has to be carried out on the open circuit (e. g. in the steam generator primary head). Another potential activation product is ^{57}Co, which has frequently been claimed to be a minor contaminant in the water effluents. Basically, this radionuclide can be generated in light water reactors by the nuclear reactions

$$^{58}\text{Ni (n, np) } ^{57}\text{Co} \qquad \text{and} \qquad ^{58}\text{Ni (n, d) } ^{57}\text{Co}$$

Since both reactions are induced by fast neutrons having energies >10 MeV, the total amount of ^{57}Co released from the materials to the primary coolant of a 1300 MWe PWR was calculated to be only on the order of 10^{11} Bq per year (Siemens/KWU, unpublished). In this calculation, the essential radionuclide sources were assumed to be corrosion product deposits on the fuel rods as well as corrosion and/or wear from in-core materials. This low production rate raises the question of whether the γ rays at 122 and 136 keV occasionally detected in waste water really belong to ^{57}Co or whether they are caused by side-peaks originating from the decay of other radionuclides present in the samples.

From the diagrams presented in the survey paper of Riess (1989), one can clearly see that the development over time of the radiation dose levels shows considerable differences from one PWR plant to the next one (see Fig. 4.19.). Even when identical positions (e. g. steam generator primary channel head) were selected for dose rate measurements, the individual values do not show any systematic structure, indicating that the parameters which control contamination buildup are of a highly complex nature. There is no doubt that the radionuclides are exclusively produced in the neutron field, i. e. inside the reactor pressure vessel, and that they are transported by the coolant from the neutron field to the primary circuit surfaces outside the reactor pressure vessel. The details of activation as well as the mechanisms of transport and deposition, however, are still the subject of discussion. From plant experience it is known that the dose rates at the circuits usually show a continuous increase during the first years of operation, then reach a saturation level which remains more or less constant during further operation. These "equilibrium" dose rates show major differences from one plant to another, the reasons for which are largely unknown. Moreover, as a consequence of frequently unknown parameters the saturation level can be abandoned and a new one, either higher or lower than

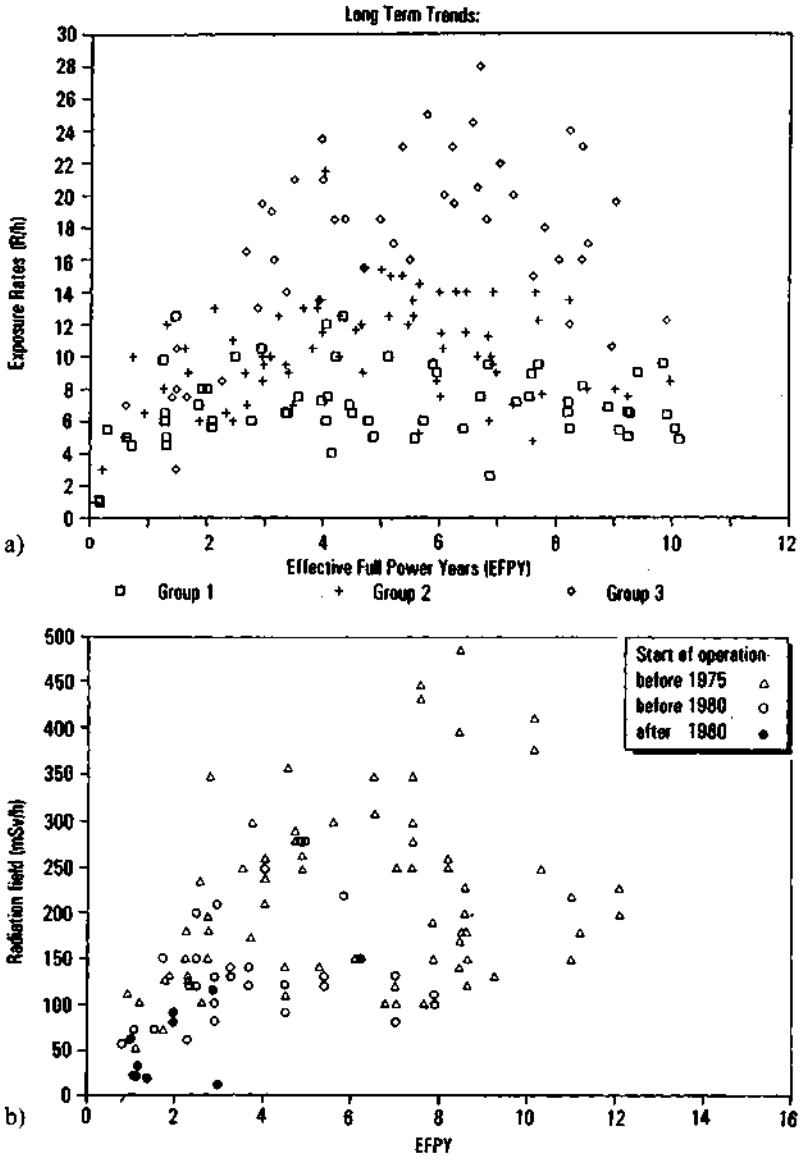

Figure 4.19. Time development of dose rates in the steam generator primary head in PWR plants of two different manufacturers (a – Westinghouse; b – Siemens)
(Riess, 1989)

the preceding one, can be established. In most of the US PWR plants the saturation level typically was reached after 3 effective full power years (EFPYs) of operation, amounting to about 0.1 Gy/h in the PWR steam generator primary channel head (Ocken, 1985), a value higher than typical BWR values which were on the order

of 3 mGy/h at the BWR recirculation piping. However, the time periods needed to reach the saturation level differ considerably from plant to plant. As an example, at the Swedish Ringhals 3 and 4 PWR plants the saturation levels in the primary circuit dose rates were already reached after two years of operation (Gott, 1989). Such time periods indicate that the development of the radiation dose levels is not primarily controlled by the physical halflife of ^{60}Co (5.3. years), since in this case a considerably longer period would be required until the saturation level was reached. It has to be assumed that other parameters are predominant; in particular, one can conclude that contamination buildup is not caused by simple deposition and accumulation of radionuclides on the surfaces, but that deposition and resuspension together result in a complex, dynamic equilibrium situation.

On the basis of a critical evaluation of the dose rate data measured at different Westinghouse-designed PWR plants, Bergmann (1989) concluded that the trends of short-term and long-term exposure rates in plants could be grouped into three broad categories when indexed to the steam generator channel head radiation levels (see Fig. 4.20.). The trends in all three categories were similar in that after 5 to 6 EFPYs, the exposure rates in the channel head leveled off or declined. In most cases, short-term and long-term behavior followed identical patterns, i. e. high dose rates over the short-term resulted in high dose rates over the long-term and analogously for low dose rates. The final contamination level seemed to be a specific feature of the particular plant, as can be seen from the contamination buildup on fresh surfaces which were newly installed in an operating plant. Thus, the replacement of steam generators removes a large percentage of the total corrosion product and activity inventories from the plant, because of the large fraction of the primary circuit surface area represented by the steam generator tubing (about 62% in a typical plant). After replacement, however, the channel head radiation levels generally returned to about the pre-replacement values within 2 to 3 EFPYs (these are results from 5 of 6 Westinghouse plants where steam generators had been replaced).

At BWR plants, the situation with regard to contamination buildup is quite similar insofar as the development of dose rates over time differs considerably from one plant to the other. As an example, dose rate levels at the recirculation lines of a number of plants are shown in Fig. 4.21. (EPRI, 1983): after comparable periods of operation differences by factors of 5 and more can be observed. Saturation levels of the radiation dose rates such as reported from PWR plants cannot be derived from this data.

Often the radiation dose rates resulting from the contamination process reach a level that makes it necessary to take special precautions during inspection and repair work (such as installation of shieldings, use of remote-controlled facilities or even decontamination of the relevant systems before work starts) in order to limit the dose exposure of the staff to a tolerable degree. A meaningful and economic alternative to these time-consuming and costly measures would be the prevention or at least the reduction of contamination buildup. However, as was mentioned above, this buildup is a complex process and it is very difficult to identify the most important parameters for initiating effective countermeasures. A large

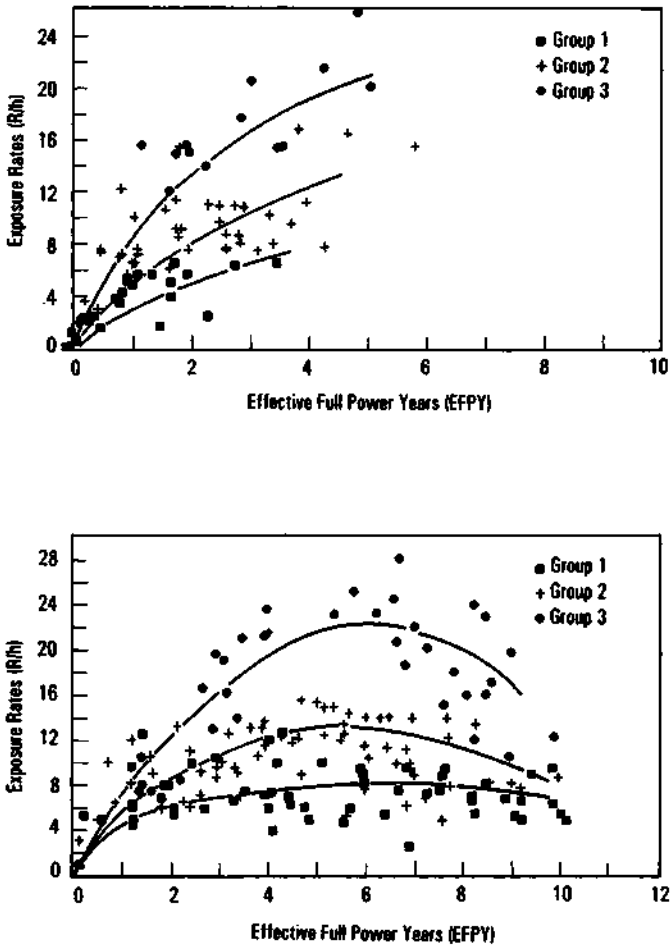

Figure 4.20. Steam generator primary channel head exposure rates, short-term and long-term trends
(Bergmann, 1989; by courtesy of Thomas Telford, London)

number of different parameters have been suspected of influencing this process, such as:

- the mass of elements with high activation cross sections present in the reactor and their location relative to the neutron field;
- the rate of release of metal atoms from the materials inside and outside the reactor pressure vessel;
- the chemistry parameters of the reactor coolant (pH, redox conditions, concentration of trace substances, etc.);
- the concentration, nature and chemical state of the radionuclides carried in the coolant;

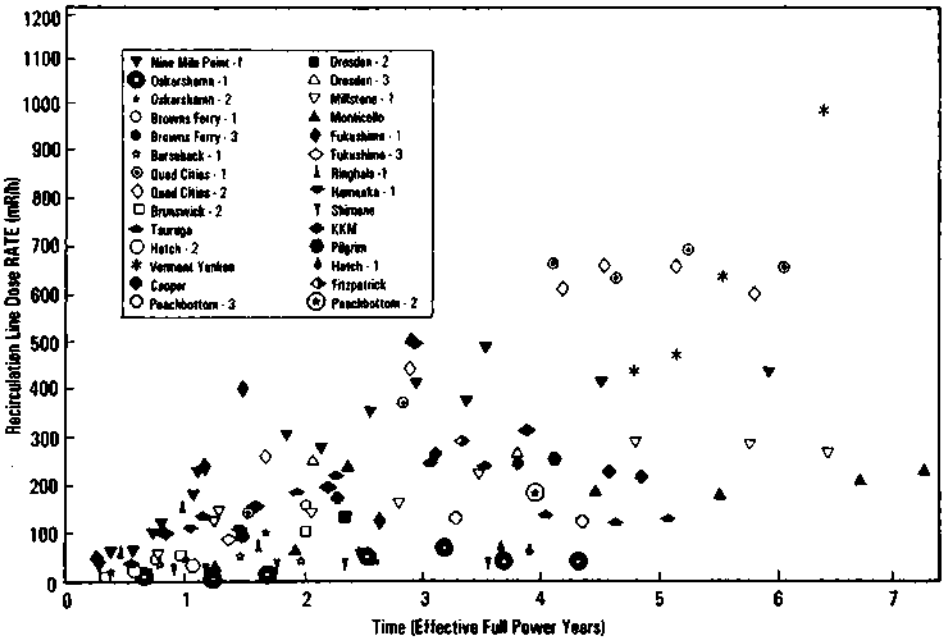

Figure 4.21. Time development of dose rates at BWR recirculation lines (EPRI, 1983)

- the surface roughness of the materials in contact with the reactor coolant: a higher degree of roughness means a greater true surface area and, in addition, offers the possibility of mechanical retention of particles being transported in the coolant;
- the nature of hydrodynamic flow: in a laminar flow the substances transported in the coolant have to move to the walls by Brownian movement, whereas in a turbulent flow they are transported by convection to contact the surfaces of the materials with only a very thin laminar boundary layer to be overcome by diffusion; locally, laminar flow may be converted into turbulent flow, e. g. at bends or valves, resulting in the formation of corrosion product hot-spots immediately downstream from the obstacle;
- the electrochemical potential of the surface (Zeta potential) can act to attract or to repel ions which are dissolved in the coolant;
- the heat flow through surfaces may change the temperature-dependent solubility of corrosion product oxides in their immediate vicinity;
- finally, the mode of operation of the systems may affect contamination buildup positively or negatively; shocks in the system caused by startup or shutdown, as well as changes in coolant pH, oxidation potential and temperature may lead to a redistribution of deposited material.

It cannot be ruled out that all of these parameters are able to influence the buildup of plant contamination, although to a different degree. The principal task,

therefore, is to identify the most important parameters and to develop measures for changing the relevant conditions in the direction of reduced production, transport and/or deposition of undesirable activation products. In order to solve this task, it is not sufficient to conduct laboratory-scale investigations aiming at the clarification of fundamental questions; the evaluation of plant data and analyses, both routine data and the results of special experiments, plays an equally important role. Experiences with operating plants have contributed a great deal to current knowledge in the field of contamination buildup. However, one has to be cautious when comparing data originating from different plants, in order to preclude misinterpretations that might result from incomplete knowledge of the details of specific plant operation as well as from differences in the carrying-out of the measurements (differences in measurement conditions, etc.).

Likewise, when data collected from different sources is to be used as a basis for countermeasures, one has to be extremely careful to avoid erroneous conclusions. As an example: it has often been claimed that corrosion of the Inconel steam generator tubing is the main cobalt source in the PWR primary circuit, that the corrosion of the cobalt-bearing materials inside the neutron field contributes little to the cobalt supply in the BWR reactor water and, finally, that the wear of hard-facing materials employed in valves represents only a small proportion of the cobalt supply to the PWR primary coolant, but is the major cobalt source in BWRs. However, such statements do not suffice to give an indication of the principal source of contamination buildup as long as the activation period and the ^{60}Co production rate from the individual sources is not taken into account. For this reason, it is not possible to conclude what measures should to be taken to reduce the radiation dose rates exclusively from data on the cobalt mass supply to the coolant. Arguments that stainless steel or Inconel with reduced cobalt content will cause higher costs, but that these expenses are more than compensated for by lower radiation exposures to the personnel have to be looked upon with reservations, at least as long as it has not been confirmed that these materials are indeed the main contributors to ^{60}Co production. This difference in the evaluation of cobalt supply rates to the coolant and of ^{60}Co production rates is a typical example of the inadequacy of classical chemistry considerations when they are not complemented by radiochemical evaluations.

In order to reduce contamination buildup by chemical and process engineering means, extensive work has been conducted over the last years. A large number of experiments have been carried out to obtain basic information, both laboratory investigations and measurements in out-of-pile loops and at operating plants. Each type of investigation has its specific advantages and disadvantages. It is certainly true that measurements at operating nuclear plants yield the most representative results; on the other hand, they become quite expensive when, as a prerequisite for their execution, special conditions have to be created in the plant itself or in subsystems of it. Laboratory experiments and loop experiments are essential procedures for understanding the basic nature of transport processes etc., since they provide the opportunity of examining specific aspects (single parameter effects) of reactor operation as well as particular alternative chemical regimes and treatments that have not yet been validated for power reactors. Other advantages of loop

experiments are that samples of circuit components or test specimens can be readily obtained for examination, that the circuit inventory can be clearly defined and controlled and that chemical transients can be introduced without external constraint. However, in order to obtain results which can be applied to real plants, it is important to establish that the behavior of the test loop adequately reflects that of a power reactor.

The interpretation of the results of experiments performed in recent years has yielded contradictory conclusions as to the sources and the mechanisms of contamination buildup. With one exception, the measures taken on the basis of these results have not resulted in a clear success; on the contrary, in some cases a deterioration of the situation has resulted. The question as to the reasons for such consequences emerges and it seems that the failure of many attempts has mainly been due to the fact that only macrochemical aspects (e. g. effect of pH and temperature on the solubility of the corrosion product oxides) have been taken into consideration. In reality, because of the very low mass concentrations of the essential radionuclides and their mother elements in the coolant, severe deviations in behavior from that of macroamounts are to be expected, an effect which is well known in radiochemistry. In particular, in the behavior of ^{60}Co and ^{58}Co trace-chemical mechanisms such as surface adsorption onto oxide particles, co-precipitation together with other elements, as well as ion exchange and isotope exchange with other constituents of the corrosion product oxides can be assumed to play an important role, but in most of the investigations performed up to now these have not been considered.

It has to be pointed out that due to the great interest in this topic, the literature dealing with contamination buildup in light water reactor plants is very extensive; for this reason, only a selection from this literature is given below (in particular of papers published in recent years).

References Section 4.4.1

Bergmann, C. A.: Evaluation of selected parameters on exposure rates in Westinghouse designed nuclear plants. Proc. 5. BNES Conf. Water Chemistry of Nuclear Reactor Systems, Bournemouth, UK, 1989, Vol. 1, p. 9–16

Electric Power Research Institute (EPRI): BWR radiation assessment and control program. Assessment and control of BWR radiation fields. Report EPRI NP-3114 (1983)

Gott, K.: Gamma spectrometry measurements in Ringhals 3 and 4. Proc. 5. BNES Conf. Water Chemistry of Nuclear Reactor Systems, Bournemouth, UK, 1989, Vol. 1, p. 43–47

Hecht, G.: Occupational exposures in LWR plants built by Siemens/KWU including service. Paper presented at the Internat. Workshop on New Developments in Occupational Dose Control and ALARA Implementation at Nuclear Power Plants and Similar Facilities. Brookhaven National Laboratory, Upton, N. Y., 1989

Marchl, T., Riess, R.: Reducing the cobalt inventory in Siemens PWRs. Paper presented at the EPRI Radiation Field Control Seminar, Seattle, Wash., USA, 1993

Ocken, H.: Radiation control to improve nuclear power plant availability. Proc. Internat. Conf. Nuclear Power Plant Aging, Availabilty Factor and Reliability Analysis, San Diego, Calif., 1985, p. 593–600

Ocken, H., Wood, C. J.: Status report on radiation exposure reduction at US nuclear power plants. Proc. 6. BNES Conf. Water Chemistry of Nuclear Reactor Systems, Bournemouth, UK, 1992, Vol. 2, p. 1–8

Reitzner, U., Marchl., T., Riess, R.: Dose rate trends and and chemistry at Siemens-designed BWRs. Paper presented at the EPRI Radiation Field Control Seminar, Seattle, Wash., USA, 1993

Riess, R.: Optimization of water chemistry in PWRs. Nuclear Europe **1989**, (3/4), 19–20

Wood, C. J., Ocken, H.: Recent developments in radiation control technology. Proc. 5. BNES Conf. Water Chemistry of Nuclear Reactor Systems, Bournemouth, UK, 1989, Vol. 1, p. 49–53

4.4.2 Analytical methods applied in contamination buildup studies

Analytical determination of the chemical as well as the radiochemical composition of the different substances that play a role in the production as well as in the transport and deposition of the radionuclides of interest, is a very important tool for the elucidation of the mechanisms leading to contamination buildup. For this reason, a short survey will be given in the following of the available analytical methods with particular emphasis on those that can be used with the coolants and components of the primary systems of nuclear power plants.

The sampling procedure used for the materials to be analyzed is of prime importance, since an analysis cannot yield results better than the sampling procedure. The seemingly simplest task in this context is sampling of the corrosion products and corresponding radionuclides that are transported in the coolant; there are, however, several parameters that have to be focussed on to preclude erroneous results. The analytical samples are taken from the hot and pressurized primary coolant by means of the sampling system which mainly consists of the sample cooler, a pressure-reducing valve and the line which leads to the sampling station. This sampling station is usually located in the laboratory in the nuclear auxiliary building, which results in a considerable pipe length (frequently as long as 100 meters); often additional sampling stations for special purposes are installed near the primary circuit inside the reactor building, which have a considerably shorter pipe length. The sampling lines are usually made of stainless steel; other materials such as Zircaloy have also been proposed in order to reduce the detrimental impact of the pipe materials on the composition of the sample flow. In the sampling stations, the coolant samples are taken at ambient temperature, and there the corrosion products being carried in the coolant are usually separated by filtering (0.45 μm or 0.1 μm filters) into the suspended solids fraction and the dissolved fraction. Concerning the latter fraction, one has to take into account that this material potentially does not only consist of the truly ionic dissolved species, but may also include very finely dispersed colloidal particles; a differentiation between these both species is only possible by using special techniques such as ion chromatography.

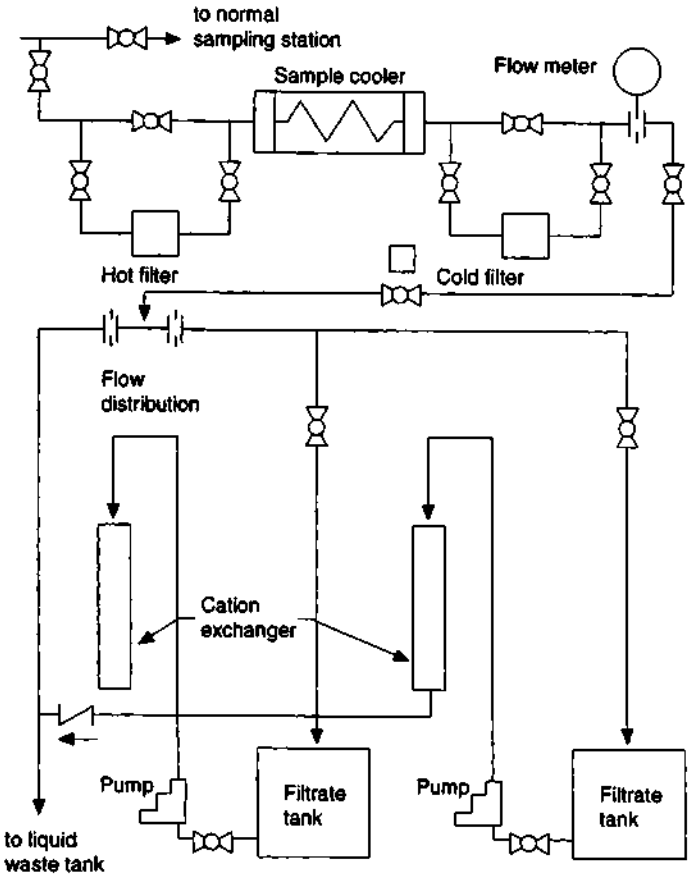

Figure 4.22. Flow scheme of a sampling system for both high-temperature and ambient-temperature sampling of coolant
(Roesmer, 1985)

When analyzing the suspended solids and the dissolved fraction separately, one has to take into consideration that in the course of sampling, due to the cooling-down of the coolant from operating temperature to ambient temperature and the resulting shift in the PWR primary coolant pH from alkaline to slightly acidic (or near neutral) conditions in the cold state, the nature of the corrosion product species may change. In order to overcome this difficulty, high-temperature sampling systems have been developed by various authors; one of the first systems of this kind was described by Wages (1971). As an example, the basic layout of a system which permits sampling of primary coolant at elevated temperatures (170 to 238 °C) as well as at ambient temperature, is shown in Fig. 4.22. (Roesmer, 1985). In this design, the suspended corrosion product particles are isolated from the hot coolant by filtering through a Teflon membrane (0.45 μm pore size); the dissolved corrosion products are collected on ion exchange columns downstream

Table 4.3. Ni : Fe ratios in suspended corrosion products isolated by high-temperature and ambient-temperature sampling
(according to Roesmer, 1985)

	1. Cycle	2. Cycle
High temperature	0.30	0.33
Ambient temperature	0.23	0.11

from the sample cooler. Other authors have used a ceramic or metallic filter matrix with tubings and filter holders manufactured from Zircaloy, in order to preclude contributions of corrosion products from that part of the filter system which is operated at high temperature.

As can be seen from Table 4.3., where results from measurements performed during the first two fuel cycles of a US PWR plant are summarized, differences have been observed in the Ni : Fe ratios of the particulate corrosion products between samples taken at high temperature and those taken at ambient temperature. It can be assumed that high-temperature sampling would deliver information on the nature of the corrosion products which is nearer to the reality in the hot primary coolant of an operating plant than sampling at ambient temperature. However, high-temperature sampling still suffers from problems concerning the long-term behavior of the materials employed and, therefore, such systems have only been installed at a few plants; for routine coolant analysis, the samples are usually taken using the normal ambient-temperature sampling station in the laboratory. The results on corrosion products in the coolant reported on in the following sections were obtained in most cases by sampling at ambient temperature.

For chemical analysis of the usually very low concentrations of corrosion products in the coolant, comparatively large volumes of coolant (up to hundreds of liters) have to be extracted from the primary circuit; for such purposes on-line collection installations are often used. Particulate matter is accumulated from the sample flow by filtering through membrane filters. For the collection of dissolved substances such as Co^{2+} ions, the filtrate from the separation of the particulates is passed over a cation exchanger column; following this preconcentration, the adsorbed substances are eluted and determined by an appropriate analysis method. For example, in order to determine the element concentrations the adsorbed ions are eluted from the resin bed with a dicarboxylic acid, then the metal-ligand complexes are separated from each other using a Dionex resin and, finally, Fe(II), Fe(III), Cu, Ni, Zn, Co, Mn are determined by spectrophotometry after injection of a suitable reagent (Bird et al., 1986). Other customary methods of determination are atomic absorption spectrometry and electrochemical methods. For the continuous determination of the concentrations of γ-emitting radionuclides in a test loop, these substances were collected on a bed of sintered magnetite and their accumulation was monitored by on-line γ spectrometry (Lister, 1986).

The considerable length of the lines from the primary circuit to the sampling station in or near the laboratory can cause difficulties in obtaining representative samples for analysis. Since a fraction of the corrosion products in the coolant is in

the solid suspended form, isokinetic sampling is an essential prerequisite for obtaining samples that contain the same concentration of particles per unit volume as the primary coolant itself. In the sampling line, this concentration may be changed by deposition and resuspension processes, resulting in sudden spikes, in particular following a change in the coolant flow rate. In order to rule out analytical errors that might be caused by such effects, the sampling line has to be flushed and operated for a longer period of time under strictly controlled conditions prior to the collection of the analytical sample.

Not only the concentration of particulate matter in the coolant, but also that of the dissolved corrosion product nuclides can be affected by the sampling procedure. Due to their chemical properties, the behavior of these ions in the sampling line is quite different from that of the dissolved fission products such as iodine and cesium, the concentrations of which are not affected by the sampling procedure to any measurable extent. Investigations performed by Large et al. (1989) in an experimental loop containing a stainless steel test line demonstrated that deposition of dissolved ^{58}Co from the coolant to the tube walls can be described in terms of a first order deposition process and a release process from the tube walls with a very low or zero rate (which could not be determined within the limited experimental period of time). According to the results obtained, the deposition rate constant seems to depend only slightly on the coolant flow rate in the investigated range, suggesting that it is higher at higher flow rates. In the range 300 to 240 °C, the deposition rate constant shows little variation with temperature; at lower temperatures the constant decreases markedly. Obviously, the process of deposition from the coolant onto the surface of a sampling line involves mass transfer through the liquid followed by reaction at the tube surface. The amount of radioactivity retained in the line depends on the material of the line (in a line made of gold it is much lower than in a stainless steel line), thus indicating that reaction with the surface oxide is the mechanism which controls retention of dissolved corrosion product elements, i. e. the same mechanism as in primary circuit contamination buildup (see Section 4.4.3.4.).

Similar experiences were reported by Polley and Andersson (1989) from experiments with the stainless steel sampling line of a PWR plant, which had a length of about 90 and 120 meters between the two primary loops and the sample line cooler, respectively. The results obtained indicated that at the sample line exit the concentrations of dissolved ^{60}Co and ^{54}Mn exhibit a strong inverse dependence on the sample line flow rate, in the range 25 to 125 g/s, showing variations by about a factor of 10 to 20 when the flow rate is varied in both directions within the limits mentioned above. This behavior was quite different from that of the concentrations of the non-dissolved corrosion products, which showed no significant dependence on the steady-state flow rate but, unlike the dissolved species, exhibited pronounced transients of typically 2 hours' duration following a change in the flow rate. Unlike the dissolved corrosion product radionuclides, the concentrations of ^{137}Cs and ^{131}I in the coolant were not affected by changes in the flow rate. In addition, the dissolved ^{54}Mn and ^{60}Co concentrations at the exit of the sampling line decreased by approximately two orders of magnitude as the boron concentration decreased at the end of the fuel cycle from 71 ppm to <1 ppm, indicating that

the extent of deposition of dissolved corrosion product radionuclides in the sampling line also depends on the pH of the flowing solution. From these measurements it has been concluded that the time needed to achieve an equilibrium concentration of the dissolved corrosion products at the sample line exit is very long, on the order of 1 year.

These results suggest that the concentrations of corrosion products measured at the exit of a long stainless steel sampling line potentially do not reflect reliably their entrance concentrations. They may not be generally valid, but only represent a specific design of the sampling system; however, they point to possible sources of errors which cannot be ruled out completely in other designs and which should be carefully investigated for in order to obtain truly representative samples for coolant analysis. In any case, retention of the dissolved species can be decreased by keeping the high-temperature section of the line short, i. e. by placing the sample line cooler as near to the primary circuit as possible. In addition, selection of an optimum material can help to keep retention low; for example, Eley et al. (1992) in their experimental loop have used a PTFE line downstream from the sample cooler.

In order to avoid the difficulties that can arise in obtaining a representative coolant sample, attempts have been made to develop non-invasive, real-time analysis procedures. Unfortunately, the possibilities of such techniques are limited. For example, chemical composition of the corrosion products, as well as radionuclides without appropriate γ emission, are usually not accessible to these procedures. One possible application is the determination of the concentration of particles suspended in the coolant; for this task, optical measuring devices have been developed which are able to operate on-line even at 290 °C, 9 MPa and to count the number of particles with a size down to 1 μm (e. g. Schenker et al., 1992).

Another possibility is monitoring of the activity concentrations of γ-emitting radionuclides in the coolant by on-line γ spectrometry, making sampling unnecessary. Such techniques have been in use for many years already to follow quasi-continuously the activity concentrations of selected fission products such as ^{131}I and ^{137}Cs in the coolant (e. g. Neeb and Hiller, 1974). In order to apply this technique, an appropriate position on a coolant line or on the sampling line has to be selected, which preferentially is located ahead of a sample line cooler, but should be in a compartment with a low radiation dose rate environment. Calibration of the measurement position and device, in order to calculate activity concentrations from the measured radioactivity data, is a somewhat expensive procedure but does not, in principle, pose fundamental problems. The basic difficulty in the practical application of this technique is caused by the buildup of contamination layers on the walls of the analytical line which consist of the same radionuclides as those to be measured, thus rendering the problem much more complicated than in the on-line measurement of fission products. Basically, a differentiation between radionuclides carried in the coolant flow and those deposited on the pipe walls can be made by taking into account the differences in the relative counting efficiencies of the two sources. Such techniques are applied in uranium enrichment plants to distinguish gaseous UF_6 from deposited material. Packer and Armitage (1990) have reported on the development of a device and a corresponding procedure which can

be used to differentiate between the fraction of fission products carried in a steam flow and that deposited on the walls. Their measurement layout consists of two detectors equipped with collimators of different size and somewhat different positioning relative to the pipe; the data obtained from the two detectors are then processed by appropriate calculations. Though a good resolution of both radiation sources has been reported from the experiments, the question is still open as to the acceptable ratio of deposited activity to flowing activity. Since at high contamination levels the deposited corrosion product activity is much higher than the activity concentrations of these radionuclides in the coolant, under such conditions determination of the radionuclides in the coolant will become extremely difficult or even impossible. Several attempts have been undertaken to reduce contamination buildup at the measurement position to a lower level (e. g. by pretreatment of the surfaces or by cyclic decontamination), but until now no satisfying solution has been reported.

The sampling of oxides from the deposits on the primary circuit surfaces may also involve errors. In order to analyze the chemical composition and the concentration of radionuclides in the tightly adhering contamination layers, oxide samples are often isolated by mechanical means such as scraping or brushing. In doing so, care has to be taken to avoid removal of significant amounts of the base material, since this would lead to systematic errors in the results of element and activity concentrations due to dilution of the oxide sample. Chemical dissolution of the base metal using bromine-ethanol solvent, as well as electrochemical techniques using nitric acid as an electrolyte, have also been employed (e. g. Bergmann et al., 1983); in the latter procedure, the base material at the interface to the oxide layer is attacked, resulting in a peeling-off of the oxide, which then is collected by filtering.

Usually, contamination buildup in piping, systems and components is monitored by non-invasive measurement of the dose rates in their surroundings. Such measurements can be rapidly performed and their results are sufficiently accurate for health physics purposes. However, repeated dose rate measurements frequently show fluctuations in the results of up to $\pm$ 50%, which are mainly due to insufficient accuracy in the positioning of the measuring device. Another possible source of error may be caused by differences in the time delay between plant shutdown and dose rate measurement; because of the decay of the shorter-lived radionuclides, the dose rates will decrease even over comparatively short time intervals. This is particularly true for measurements which are to be performed inside the steam generator primary channel head, where deposited ^{58}Co contributes significantly to the total radiation dose rate. Measurements performed on the outside of the components are less affected by ^{58}Co because of the stronger attenuation of its lower-energy γ-ray emissions in the walls (as compared with the longer-lived ^{60}Co). They are, therefore, less sensitive to varying time delays; however, these measurements may be influenced by extraneous radiation fields from other components.

Dose rate measurements yield information about the level of gross γ radiation but without giving details as to the specific contributions of the individual radionuclides. They are, therefore, not able to give useful information on the mechanism of contamination buildup. This disadvantage can be overcome by application of non-invasive γ-spectrometry measurement using a transportable, shielded, high-

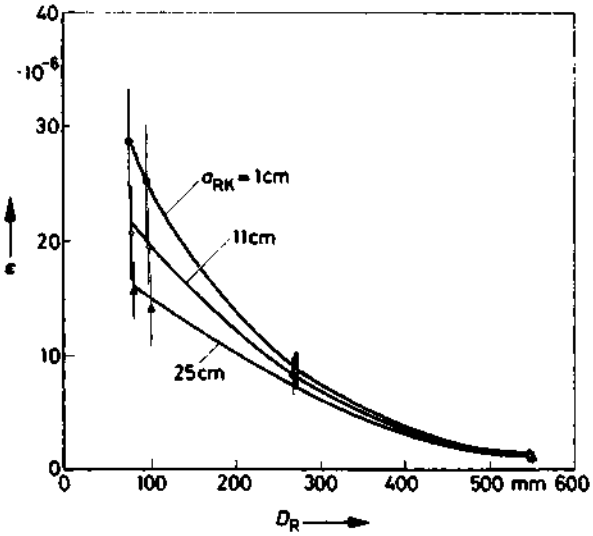

Figure 4.23. Absolute detector efficiency ε as a function of pipe diameter D_R and distance pipe–collimator σ_{RK} (Eγ 136 keV)
(Schuster and Hoffmann, 1983)

resolution germanium detector with appropriate electronics; for carrying out measurements, this device is placed in a well-defined position in front of the piping or component to be investigated. Such an arrangement, which is capable of determining the area-related activities of a number of radionuclides simultaneously was developed and applied, among others, by Schuster and Hoffmann (1983). Their investigations showed that accurate calibration of the device is of predominant importance in the application of this technique; for this reason, there has to be extensive preparatory work in the laboratory, taking into account the influences of different parameters such as pipe diameter, pipe wall thickness, and distance between the detector and the surface of the object. Most of the positions where measurements have to be performed can be considered as an extended radiation source at a comparatively short distance from the detector. The properties of such an object–detector system, with the detector being surrounded by an effective radiation shielding with a hole in front of the detector, is very difficult to describe mathematically because, among other reasons, of the scattering of the entering γ radiation from the collimator walls. Therefore, calibration is usually performed experimentally, e. g. by using pipe sections of different diameter and wall thickness which are coated on their inner surfaces with radionuclides of known activity. In addition to the influence of the wall thickness and of the distance object-to-detector, the calibration factors are different for pipes filled with coolant and empty pipes. In a pipe filled with coolant, the main influencing parameter is attenuation of γ rays from the back wall by the water; on the other hand, the radionuclides carried in the coolant are only of significance when the pipe wall shows a low contamination level. Cumulative detector efficiencies measured by this technique are shown exemplarily in Fig. 4.23., which demonstrates the effects of pipe dia-

Table 4.4. Radionuclide loading of PWR pipe walls
(By courtesy of Siemens/KWU)

Radionuclide	Hot leg (kBq/cm^2) ± 3 σ error margin	Cold leg (kBq/cm^2) ± 3 σ error margin	Hot spot (kBq)
^{54}Mn	16 ± 1.6	13 ± 2.1	$3.9 \cdot 10^4$
^{58}Co	118 ± 3	114 ± 4	$9.9 \cdot 10^4$
^{60}Co	52 ± 1.2	57 ± 1.7	$1.0 \cdot 10^5$
^{59}Fe	5.3 ± 1.6	6.6 ± 2.2	$2.2 \cdot 10^4$
^{95}Zr	3.7 ± 2.6	–	$3.1 \cdot 10^6$
^{95}Nb	16 ± 2.6	8.1 ± 3.3	$3.8 \cdot 10^6$
^{124}Sb	6.1 ± 0.7	2.8 ± 0.6	$6.6 \cdot 10^3$
^{125}Sb	–	–	$7.3 \cdot 10^4$

meter and distance pipe–collimator. After careful calibration of the device, the measured area-related activities (in Bq/cm^2) will show a total uncertainty of less than 20%. By an appropriate shielding of the detector, such measurements can be performed even in compartments showing ambient dose rates of up to 1 mSv/h.

Numerous applications of this technique, in particular at pipings of nuclear power plants, have demonstrated its capability. As an example, results of measurements which were carried out at the hot leg as well as at the cold leg of a PWR main coolant pipe are summarized in Table 4.4. In addition, the radionuclide composition of a hot spot is given, showing a spectrum of radionuclides which is completely different from that of normal contamination layers. Such detailed information cannot be furnished by a simple dose rate measurement; they are nonetheless of considerable importance when countermeasures against contamination buildup are to be evaluated. Similar non-destructive γ-spectrometry measurements were performed by different investigators at different plants; for example, Gott et al. (1986) reported that such measurements were regularly carried out over the course of several years at the Swedish plants Ringhals 3 and 4.

The sampling of material from the corrosion product deposits on the fuel assemblies is best performed in the spent fuel pool using a special device which is attached to the fuel assembly inspection installation. Such sampling devices have been described on several occasions (e. g. Roesmer and Rootham, 1977; Sendelbeck and Schuster, 1984; Bridle et al., 1989). As can be seen from the schematic presentation shown in Fig. 4.24., this installation consists of a revolving device which can brush the deposits off from any area of the outer fuel rods of the assembly. Loosely-adhering deposits can be removed by a nylon brush while tightly-adhering ones have to be isolated using an abrasive tool. The corrosion products which are peeled-off from the surface are then transported by a water flow to a collecting tank and, further on, to a filter unit. The latter is then removed and given to the laboratory for structural, chemical and radiochemical examination. The cleaned surfaces are documented by photography, which makes possible an exact calculation of the surface areas from which the deposits were removed (in order to calculate the area-related corrosion product loadings and, indirectly, the thickness of

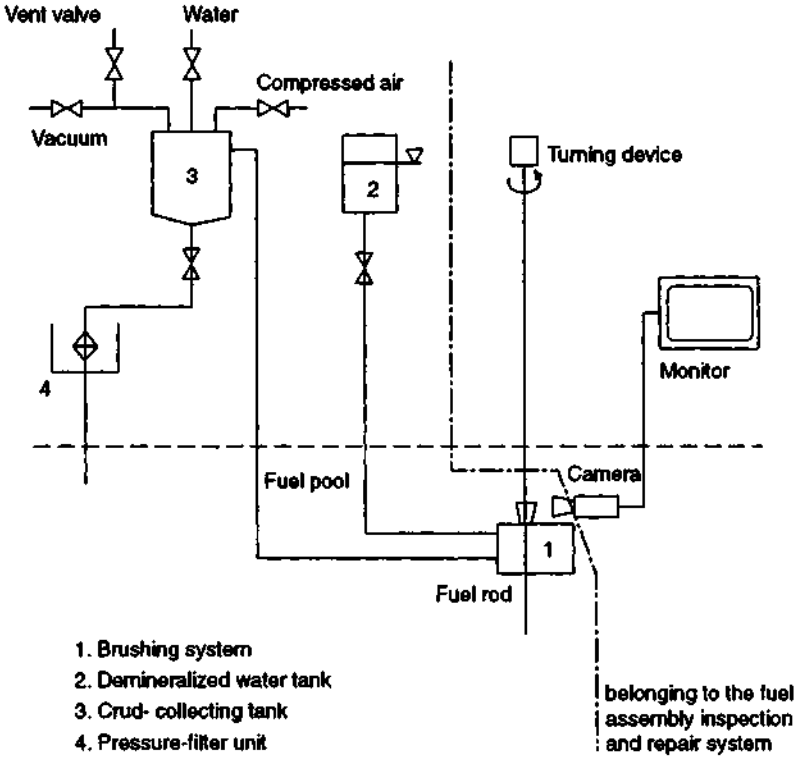

Figure 4.24. Installation for underwater sampling of corrosion products from fuel rod surfaces
(Sendelbeck and Schuster, 1984)

the layers). Alternatively, sampling of the deposits can be performed after transportation of the fuel rod to a hot cell; however, in doing so certain losses of corrosion products during transportation and storage cannot be ruled out, and changes in the composition and structure of the oxide deposits during the period of dry storage are also possible.

When information on the production and transport of the radionuclides in the primary system is requested, it is not sufficient to limit the analyses to those isotopes that are relevant for dose rate buildup such as ^{60}Co, ^{58}Co, and ^{54}Mn. As will be discussed in the following sections, there are two different possible sources of radionuclides in the primary circuit of light water reactors: the materials located permanently in the core region and those located outside the neutron field from which corrosion products are transported to the reactor core and are temporarily deposited there. With regard to the production of radionuclides, the main difference between these two sources is the residence time of the substances in the neutron field, which is equivalent to its activation period; for this reason, determination of the element specific activity, i. e. the activity of a given long-lived radionu-

clide related to the mass of its parent element, deserves particular attention. Provided that the halflife of the radionuclide produced is long enough, and provided that there are no other interfering nuclear reactions, the residence time in the neutron field of the substance in question can be calculated from the specific activity measured and from the thermal neutron flux which is known from the design of the reactor core. Appropriate ratios of activity and mass are $^{60}Co : Co$, $^{55}Fe : Fe$, and $^{63}Ni : Ni$ for longer exposure periods; short-term activation periods can also be calculated using the ratio $^{59}Fe : Fe$. Unfortunately, some of these radionuclides are difficult to measure because of their low-energy radiation; likewise, the chemical determination of element masses which are present in very low concentrations in the samples to be analyzed (such as cobalt) may pose some difficulties. Basically, only isotopic radionuclides should be used for the calculation of activation periods; when using radionuclides produced by threshold reactions (e. g. ^{54}Fe (n, p) ^{54}Mn; ^{58}Ni (n, p) ^{58}Co), interpretation of the results might be complicated by the danger of chemical separation of the parent nuclide from the daughter nuclide as a result of reactions occurring in the coolant.

When calculating activation periods from the measured specific activities, it has to be taken into account that the radionuclides present in the sample may have additionally experienced a decay period during temporary deposition on out-of-core surfaces, perhaps followed by a second activation and decay period. As a consequence, in the determination of the specific activity of a radionuclide only a summary value is obtained, including activation periods as well as decay periods; this complication may lead to erroneous results in calculated residence times, in particular when comparatively short-lived radionuclides are analyzed. Basically, activation periods inside the neutron field and decay periods outside the neutron field could be differentiated by comparing the specific activities of two isotopes with markedly different halflives, for example ^{59}Fe (halflife 45.1 days) and ^{55}Fe (halflife 2.7 years); however, as yet there have been no reports on work showing whether or not this fundamental possibility will be able to yield meaningful results.

A complete procedure for the analysis of corrosion product samples (including determination of the in-core residence periods) is schematically shown in Fig. 4.25. (according to Sendelbeck and Schuster, 1985), giving the volume of work to be performed with normally very small samples in the range of a few milligrams, most of which exhibit rather high radioactivity and dose rate levels. In the determination of the difficult-to-measure radionuclides (i. e. those only emitting low-energy radiation), as well as in the determination of the chemical composition of the corrosion product sample, a chemical treatment of the samples is indispensable. Since the dissolution of PWR primary circuit oxides by acid treatment is quite difficult and time-consuming, a $KHSO_4$ melt is usually applied as a first step. Chemical analysis is usually carried out by trace analysis techniques such as atomic emission or atomic absorption spectrometry, inductively-coupled plasma mass spectrometry, cation chromatography, or electrochemical analysis methods (such as stripping voltammetry). For the determination of very low cobalt element concentrations in small samples, neutron activation in combination with differential γ spectrometry before and after the analytical neutron irradiation has also been applied. The radio-

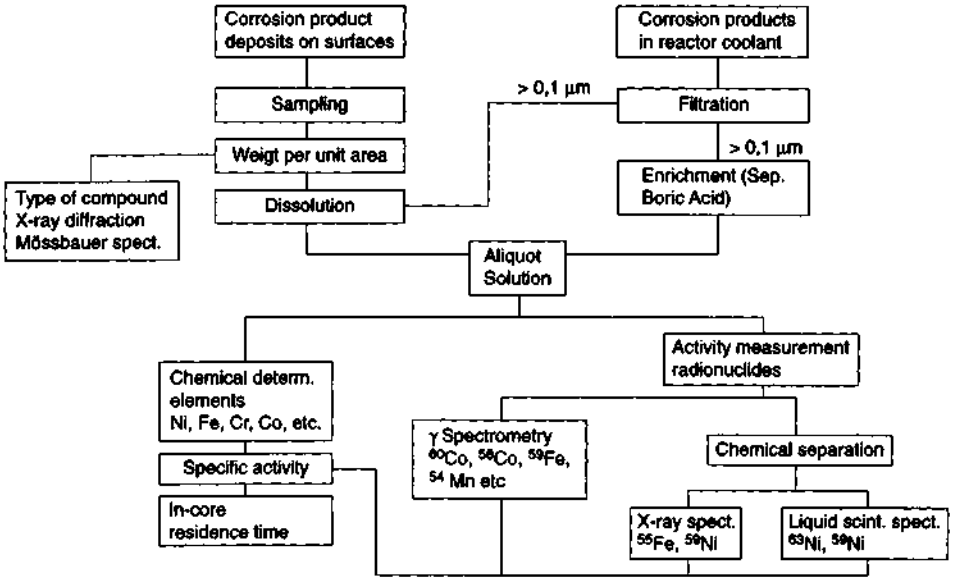

Figure 4.25. Analytical procedure for the complete analysis of light water reactor corrosion products
(Sendelbeck and Schuster, 1985)

activity of electron-capture (EC) nuclides such as ^{55}Fe and ^{59}Ni can be determined either by liquid scintillation counting or by X-ray spectrometry; in each case, these radionuclides have to be isolated prior to measurement from the bulk of the other radionuclides by using appropriate radiochemical separation methods.

Besides the chemical and radiochemical composition, other properties of the collected materials are also often of interest, such as the nature of the chemical compounds present in these substances. For example, the structure of oxide compounds after isolation from the base material or from the coolant is analyzed by X-ray diffractometry or by Mössbauer spectrometry. Other microanalytical techniques can be directly applied to oxide layers deposited on surfaces, e. g. of steam generator tube sections. Examples in this field are Auger electron spectroscopy for the determination of element concentrations in micrometer areas and X-ray induced photoelectron spectroscopy for the determination of the chemical states of the individual elements. In order to obtain depth profiles over the thickness of the oxide layer, these techniques often are combined with an argon sputtering process (e. g. Schuster et al., 1988), which removes nanometer fractions from the surface prior to the next analysis step. By γ spectrometry of the specimen after each sputtering step, the profile of the radionuclides in the oxide layer can also be determined.

The different analytical techniques mentioned above are able to yield answers to specific questions which are of importance for clarification of the individual stages that play an essential role in the process of contamination buildup. There-

fore, well-equipped laboratories and close cooperation between specialists in the relevant fields are an indispensable prerequisite for obtaining reliable and meaningful results.

References Section 4.4.2

Bergmann, C. A., Roesmer, J., Perone, D. W.: Primary side deposits on PWR steam generator tubes. Report EPRI NP-2968 (1983)

Bird, E. J., Bridle, D. A., Amey, M. D. H., Roofthooft, R., de Rauter, K., Philippe, R.: Cobalt measurements on the Doel reactors. Proc. 4. BNES Conf. Water Chemistry of Nuclear Reactor Systems, Bournemouth, UK, 1986, Vol. 1, p. 21–27

Bridle, D. A., Cake, P., Philippe, R.: Underwater sampling and analysis of fuel surface crud. Proc. 5. BNES Conf. Water Chemistry of Nuclear Reactor Systems, Bournemouth, UK, 1989, Vol. 2, p. 165–167

Eley, C. D., Thomas, D. M., Libaert, D. F., Cattell, R. A., Garbett, K., Woolsey, I. S.: Monitoring of soluble species in the NPTEC SPECTRE loop. Proc. 6. BNES Conf. Water Chemistry of Nuclear Reactor Systems, Bournemouth, UK, 1992, Vol. 1, p. 224–226

Gott, K., Andersson, P.-O., Svenson, J.: The build-up of radioactive corrosion products in Ringhals 4 and its relationship to primary system coolant chemistry. Proc. 4. BNES Conf. Water Chemistry of Nuclear Reactor Systems, Bournemouth, UK, 1986, Vol. 1, p. 15–20

Large, N. R., Mead, S., Nichols, J. L., Patel, N. M., Lawson, D., Beckett, N. A.: Studies of problems of corrosion product sampling from PWR primary coolant. Proc. 5. BNES Conf. Water Chemistry of Nuclear Reactor Systems, Bournemouth, UK, 1989, Vol. 1, p. 63–70

Lister, D. H.: Corrosion product release in PWR primary coolants. – Measurements and mechanisms. Proc. 4. BNES Conf. Water Chemistry of Nuclear Reactor Systems, Bournemouth, UK, 1986, Vol. 2, p. 87–98

Neeb, K. H., Hiller, S.: Möglichkeiten und Probleme bei der In-line-Überwachung des Primärkühlmittels von Druckwasserreaktoren. VGB Kraftwerkstechnik **54**, 821–825 (1974)

Packer, T. W., Armitage, B. H.: Application of gamma-ray spectroscopy to the differentiation between mobile and deposited fission products in pipes. Report EUR 13215 EN (1990)

Polley, M. V., Andersson, P.-O.: Study of the integrity of radioisotope sampling from the primary coolant of Ringhals 3 PWR. Proc. 5. BNES Conf. Water Chemistry of Nuclear Reactor Systems. Bournemouth, UK, 1989, Vol. 1, p. 71–76

Roesmer, J.: Zusammensetzung des Kühlmittels eines Druckwasserreaktors nahe der Betriebstemperatur. Proc. VGB-Konferenz "Chemie im Kraftwerk 1985", Essen, Germany, 1985, p. 54–59

Roesmer, J., Rootham, M. W.: Estimation of activity inventories in primary circuits of pressurized water reactors. Proc.1. BNES Conf. Water Chemistry of Nuclear Reactor Systems, Bournemouth, UK, 1977, p. 187–193

Schenker, E., Francioni, W., Degueldre, C.: Online measurement of particles in reactor water of BWRs. Proc. 6. BNES Conf. Water Chemistry of Nuclear Reactor Systems, Bournemouth, UK, 1992, Vol. 1, p. 133–138

Schuster, E., Hoffmann, R.: Charakterisierung innerer Kontaminationsschichten auf Rohrleitungen durch zerstörungsfreie nuklidspezifische Aktivitätsmessungen. Siemens Forsch.- u. Entwickl.-Ber. **12**, 357–362 (1983)

Schuster, E., Neeb, K. H., Ahlfänger, W., Henkelmann, R., Järnström, R. T.: Analysis of primary side oxide layers on the steam generator tubes from PWRs and radiochemical issues on the contamination of primary circuits. J. Nucl. Materials 152, 1–8 (1988)
Sendelbeck, R., Schuster, E.: Entnahme und Untersuchung von Ablagerungen (crud) auf Brennstaboberflächen in Siedewasserreaktoren. Proc. Jahrestagung Kerntechnik 1984, Frankfurt, Germany, p. 575–578
Sendelbeck, R., Schuster, E.: Chemical and radiochemical analytical methods for the investigation of radioactive corrosion products. Paper presented at the Karlsruhe Internat. Conf. on Analytical Chemistry in Nuclear Technology, Karlsruhe, Germany, 1985
Wages, S. R.: Corrosion product sampling from aqueous high temperature dynamic systems. Proc. 32. Internat. Water Conf., Pittsburgh, 1971, p. 91–104

4.4.3 Contamination buildup in pressurized water reactors

4.4.3.1 General aspects

Experience with all operating LWR plants shows that, in general, ^{60}Co is the most important radionuclide in the process of buildup of radiation dose rates in the area surrounding the primary circuit systems and components; other radionuclides originating from corrosion products, such as ^{58}Co, ^{54}Mn and ^{59}Fe play only a secondary role in this process. In particular cases, certain other radionuclides (such as the antimony isotopes), which are not activation products from the main constituents of the primary circuit main materials, may also contribute significantly to the resulting dose rate levels; these radionuclides will be separately addressed in Section 4.4.3.8. The following sections will be exclusively devoted to the corrosion product nuclides originating from stainless steels and similar materials, as well as from special alloys used in the primary circuit.

There is no doubt that the generation of radionuclides from the corrosion product elements can only occur in the neutron field, i. e. inside the reactor pressure vessel (RPV). On the other hand, the radionuclides which cause the radiation fields which potentially complicate work during plant normal operation as well as during inspection and repair work are those deposited on the inner surfaces of the out-of-RPV primary circuit piping and components, regions they are transported to by the primary coolant. This means that contamination buildup in the PWR primary circuit is a complex process. It can be roughly divided up into three stages (see Fig. 4.26.), each of which raises its particular questions:

- the production of the radionuclides and their main sources;
- the transport in the primary coolant of the radionuclides produced;
- the deposition of the radionuclides from the coolant onto the surfaces.

Concerning the generation of the radionuclides, the amount produced is determined by the amount of activable substances present in the neutron field, the abundance of the parent nuclide in the target material, the cross section for the respective nuclear reaction, the neutron flux at the position of the substance and, finally, by its residence time in the neutron field. Short-lived radionuclides will reach their

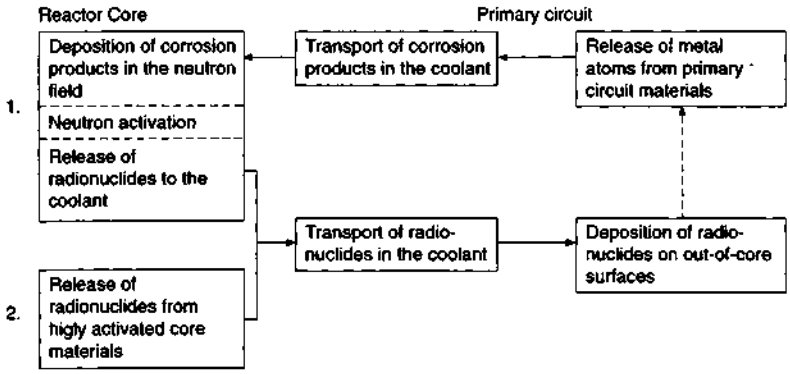

Figure 4.26. Mechanisms of PWR contamination buildup

saturation activity levels after a short residence time, whereas the specific activity of longer-lived radionuclides (which are of greater significance in contamination buildup and resulting radiation dose rates) increases steadily with activation time; therefore, the residence time of the target substances in the neutron field plays a dominant role in the production of the most important radionuclide ^{60}Co. In addition, transport in the coolant and deposition of the radionuclides onto the primary circuit surfaces include several reaction mechanisms, the most important of which can be seen from the schematic flow diagram shown in Fig. 4.27. (according to Rodliffe et al., 1987).

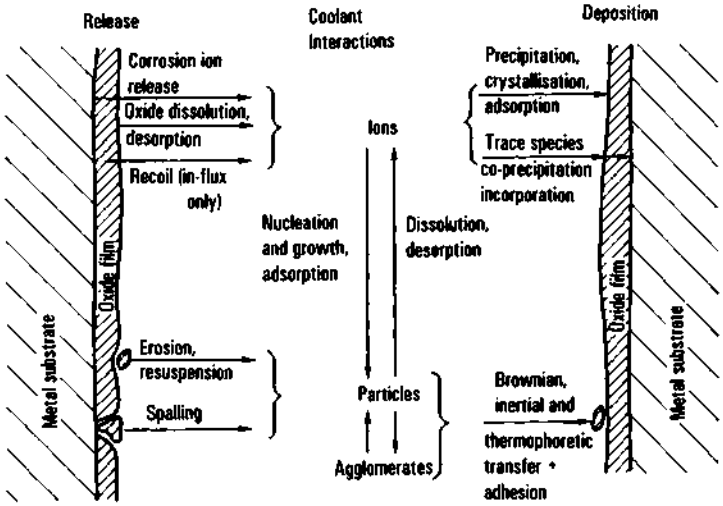

Figure 4.27. PWR corrosion product formation, transport and deposition mechanisms (Rodliffe et al., 1987; by courtesy of IAEA)

Detailed knowledge of the most important reactions in the process of contamination buildup, their progress and their dependence on specific plant parameters is a prerequisite for taking effective countermeasures to minimize accumulation of radionuclides and resulting radiation dose rates. With regard to the first of the above-mentioned stages, reduction of the cobalt content in the primary circuit materials certainly would be helpful, but before initiating this measure one has to know whether, for example, the cobalt impurities in the steam generator tubing material or the cobalt content of the materials located inside the reactor pressure vessel are the main contributor to ^{60}Co production. The production of the radionuclides in the neutron field itself would not result in a contamination of the pipes, systems and components outside the neutron field without their being transported by the coolant. It is, therefore, an important question whether this pathway could be cut off or at least reduced, for example by an optimum adjustment of the primary coolant chemistry, in order to influence the solubility of the corrosion product oxides and its dependence on temperature in a favorable direction. However, when considering such a measure it has to be remembered that out of the several tens of kilograms of corrosion products which are present in a PWR primary circuit after one year of operation, only about 0.1% is transported in the coolant at any point in time (corresponding to a steady-state concentration of several tens of ppbs). This means that primary coolant chemistry has to deal with very low concentrations of the substances of interest in a very large volume of coolant; further, there is a continuous exchange between deposited species and those carried in the coolant. The incorporation of the radionuclides from the coolant into the oxide layers might be influenced by the nature and structure of these layers. A potentially protracted uptake of the radionuclides might result from the introduction of an appropriate structure, which would lead to enhanced transport of the radionuclides out of the primary circuit to the purification system and, further on, to the radioactive waste. These short remarks reveal that there are several possible starting points for promising measures against contamination buildup which are, however, of a quite different nature. The most important question, therefore, is which one of them would prove to be most promising in a commercial facility where not only technical feasibility has to be taken into account, but stringent safety regulations and, last but not least, economic aspects as well.

Because of the great importance of the contamination problem for undisturbed operation of nuclear power plants, as well as for a low radiation exposure of the staff, extensive investigations in this area have been carried out worldwide in many institutions over the years. Their main results, as well as the current state of the art, will be summarized in the following sections.

4.4.3.2 The sources of the radionuclides

Production and transport of corrosion products are the main reasons for contamination buildup in the PWR primary circuit. Basically, in a PWR the generation of radionuclides from elements present in the primary circuit materials can proceed according to two different mechanisms, as is schematically shown in Fig. 4.26.

- Pathway 1: Corrosion products which are released from the primary circuit materials outside the reactor pressure vessel (i. e. primarily originating in the steam generators and the main coolant pipes as well as in the chemical and volume control system) are transported by the primary coolant to the reactor pressure vessel where they are, at least in part, deposited onto heated surfaces, i. e. onto the surfaces of the fuel rods. After a certain residence time there, during which they are exposed to neutron irradiation, they are released again to the coolant and are transported to the primary circuit regions outside the pressure vessel, where they can be deposited onto the surfaces there. A fraction of the deposited radionuclides may be released again from these out-of-RPV surfaces to circulate with the primary coolant and, potentially, to be plated out once again in the reactor core. In contrast, corrosion products which merely pass through the neutron field together with the primary coolant are not activated to a significant extent, because of their short residence time in the neutron field.
- Pathway 2: The second possible source of radionuclides are the materials which are permanently located inside the neutron field. During operation of the plant, they become highly activated; from their surfaces metal atoms are also released to the coolant by corrosion or wear and are transported to the primary circuit where they contribute to contamination buildup.

The main out-of-RPV source of corrosion products is the material of the steam generator tubing (Inconel-600, Inconel-690, Incoloy-800 or, in the VVER plants, stainless steel) which, besides the fuel rod surfaces, represents the predominant fraction of the inner surface of a PWR primary circuit. In addition, the stainless steel surfaces of the components and piping of the primary system as well as of some of the auxiliary systems (such as the chemical and volume control system) may supply corrosion products to the primary coolant. Despite their comparatively small surface areas, the hardfacing surfaces made of cobalt-rich alloys (e. g. Stellite) in valves, pumps etc. are of particular importance, because of the high relative fraction of cobalt which is released from them by corrosion and, in particular, by wear. The corrosion products that are deposited on the surfaces of the reactor core, mainly on the heat transfer surfaces (i. e. on the fuel rod cladding), form there oxide layers of varying thickness. In the early days of Canadian nuclear reactors, the term "crud" was introduced for these deposits, which is still in general use. In the 1950's, experimental irradiations conducted in in-reactor loops demonstrated that operating with a coolant pH below that corresponding to the solubility minimum for magnetite increases deposition of corrosion products on the fuel assemblies, resulting in a pressure drop across the core, whereas operation above the pH of minimum solubility leads to a clean core. To be sure, this experience is with CANDU reactors which had large surface areas of carbon steel in their primary circuits; however, it gave an indication of the importance of coolant chemistry conditions on the production and transport of corrosion products. In modern light water reactors, such thick deposits impairing coolant flow and heat transfer are not observed; here, the predominant negative effect of the oxide deposits in the reactor core is the production of radionuclides in the neutron field. The production

rates there depend on the prevailing neutron flux density; typical values of the neutron flux density averaged over a PWR core are on the order of φ_{therm} $5 \cdot 10^{13}$ and $\varphi_{>1MeV}$ $7 \cdot 10^{13}$ n/cm^2·s.

The reactor core, besides the Zircaloy surfaces which do not contribute significantly to corrosion product release to the coolant, also contains other materials in amounts that differ from plant to plant. Stellite hardfacing platings are often used in alignment pins, in centering bolts, on holddown plates etc.; in the newer KWU plants, these Stellite platings were replaced by hardfacing materials which are free of cobalt. Stainless steel was generally used in the past as control rod guide tube material and Inconel as spacer grid material, but many plants have replaced stainless steel and Inconel for these parts by Zircaloy. In addition, the top and bottom end pieces of the fuel assemblies, as well as the core barrel and the core shroud, are made of stainless steel and, finally, the stainless steel surface cladding of the reactor pressure vessel has to be mentioned as a potential in-core source of corrosion products. The cobalt impurity concentrations present in these stainless steels depend on the origin of the particular material batch; they are generally well below the specification limits of several hundred ppm with low-alloy steels and about 1000 ppm for austenitic steels and nickel-base alloys. Because of the large differences in the neutron flux density to which these different parts are exposed (up to 2 to 3 orders of magnitude), an accurate calculation of the radionuclide production rates in the different components and of the radionuclide release rates from them to the coolant is quite expensive (see Section 3.2.6.). Stainless steel fuel rod claddings which were used in the past in some light water reactors would also represent a significant source of long-lived radionuclides, due to the large surface area in contact with primary coolant.

There is a clear distinction to be made as to the relative importance of both types of potential sources (in-core and out-of-core) for contamination buildup. While the in-core materials generally contribute only a small proportion to the total element input of corrosion products to the coolant (compared to the out-of-core surfaces), they could prove to be the predominant source of radioactive nuclides, due to the high specific activities of their corrosion products, resulting from their long-term exposure to the neutron field. As will be shown in the following, this question has been and still is the subject of debate.

Independent of the location of the most significant source, the corrosion rates (or, more precisely, the metal release rates) of the different materials and, in part, the wear rates of various components are an important parameter for controlling the availability of the radioactive atoms responsible for the contamination process. All the materials employed in the construction of a nuclear power plant and, in particular, of its nuclear systems have to be characterized by high corrosion resistance; further, minimum attack of the materials during operation must be guaranteed by adequate chemical conditioning of the primary coolant. In spite of these measures, a certain degree of corrosion will inevitably occur during operation, which means that the determination of metal release rates under the relevant conditions is one (but not the only) important prerequisite for the evaluation of contamination buildup. For this reason, some short basic remarks on the corrosion process of stainless steels shall be inserted here.

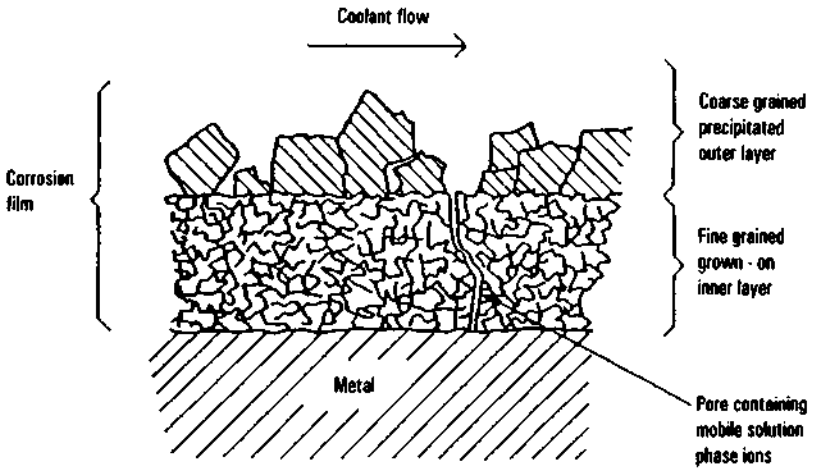

Figure 4.28. Two-layer oxide film on a stainless steel surface (Rodliffe et al., 1987; by courtesy of IAEA)

Fundamental questions with regard to the buildup of corrosion product layers and corrosion release of metal atoms under PWR operating conditions have been addressed, among others, by Robertson (1989). The starting point of all considerations in this field is the fact that the high temperature aqueous corrosion of stainless steels, as well as of nickel and cobalt alloys, produces duplex layers of spinel oxide on the surface of the base material (see Fig. 4.28.). The inner layer grows by access of water through micropores in the oxide to the base metal, whereas the outer layer is formed by solid-state diffusion of metal ions along oxide grain boundaries; the overall corrosion rate is controlled by this diffusion through the inner layer. A part of the outer layer oxide tends to be released to the solution, while the inner layer oxide retains those alloy constituents which diffuse more slowly than the main constituent. Since the growth rates of the oxides are much higher than the diffusion rates of the atoms in the metals at the temperatures in the primary circuit of a light water reactor, no depletion of the underlying alloy will occur during general corrosion and each component of the alloy will pass congruently into the oxide film. The final location of each of the alloying impurities depends on whether or not it diffuses faster than the atoms of the base metal in the newly formed oxide. Impurities that diffuse more quickly will pass through to the outer layer, while more slowly diffusing ones like chromium will remain in the inner layer. The oxides Fe_3O_4, NiO, CoO, like the mixed spinels M_3O_4, are each based on a closely-packed cubic sublattice of oxygen ions in which the metal ions are the faster moving species and, consequently, control the oxidation rates.

A complication which may arise in corrosion is that the prevailing oxidation potential is not always high enough (e. g. in the hydrogen-containing primary coolant) to fully oxidize the more noble components of an alloy such as nickel (and possibly cobalt). In such a case, nickel (or cobalt) can be incorporated in its atomic state into the inner oxide layer (Schuster et al., 1988).

In general, the corrosion rates of stainless steels and related materials pass through a minimum at a slightly alkaline pH of the coolant, where the population of both vacancies and interstitial positions in the oxide lattice is low. The increase in the corrosion rates in more alkaline solutions is ascribed to an increase in the concentration of metal ion vacancies, whereas the rise in acid solutions is caused by an increase in the concentration of metal ion interstitials in the oxide.

On stainless steel surfaces, the outer oxide layer consists of a more or less pure magnetite whereas the inner layer shows a comparatively high chromium content. The chromium constituent in this spinel not only has a low solubility, but it also reduces the solubility of the iron component. The reason for this effect is that chromium raises slightly the stability of iron in the spinel and, as a result, decreases the activity of Fe_3O_4 in the spinel, lowering its solubility. It is usually observed that up to a half of the oxide thickness (depending on the concentration of corrosion products in the water) is released to the water; the outer layer oxide tends to be released while the less soluble inner layer is always retained. This behavior results in a correlation of the release rate to the local corrosion rate and, thus, both show approximately the same time dependence. Since the corrosion rate of the material is controlled by the inner layer, in the majority of the relevant investigations a metal release rate was observed which is virtually independent of the flow rate of the fluid (unless the flow rates enter the region of erosion corrosion).

Because of the high significance of this subject in the context of contamination buildup, experimental investigations of the metal release rates with simulated PWR coolant have been performed by various researchers. However, some of these studies were based on classical analytical techniques, the results of which may be unfavorably affected by deposition and resuspension processes of the freshly formed corrosion products in the experimental system. When such techniques are applied, the impact of these processes on the results of the experiments can only be qualitatively assessed. In studies of corrosion processes, the application of radioindicator methods offers clear advantages, in particular in investigations which are carried out in facilities simultaneously containing non-radioactive metal surfaces which are also subjected to corrosion (for example, investigation of corrosion of steel specimens in a device partly consisting of steel materials). In the extensive investigations of Lister and Davidson (1989), which were partly performed in an in-pile loop, the potential of radioindicator methods was utilized to full advantage. Their results obtained with Inconel 600, Inconel 690, stainless steel SS 304, and Stellite 6 under PWR operating conditions will be shortly described in what follows.

The detailed out-of-pile measurements of metal release rates were conducted using neutron-activated coupons of the different materials to be investigated, which were inserted into a high-temperature loop. At a short distance downstream from the specimens, the released corrosion products were collected on a high-temperature filter (sintered magnetite), and the accumulated radioactivity of the different radionuclides was measured directly by a gamma spectrometry device. After having passed through the filter, the solution was pumped back to the reaction zone; the test coupons were always in contact, therefore, with a medium showing concentrations of corrosion products well below their solubility limits.

There is no doubt that such experiments can only yield reliable results when the conditions they are conducted under are as close to reality as possible. The particu-

lar question in this context is whether or not there are significant differences in the metal release rates of the materials which are caused by their location outside or inside the reactor core, since in the latter case the intense radiation field and its consequences may, in principle, affect the corrosion rates. Basically, such an influence could be caused by one of two different mechanisms:

- the locally enhanced oxygen content of the coolant caused by radiation-induced decomposition of the water may lead to an increase in the corrosion rates. Under BWR operating conditions such effects were actually detected (see Section 4.4.4.), whereas under PWR conditions they are not to be expected because of the excess hydrogen present in the coolant; perhaps, minor effects may occur in pores of comparatively thick oxide layers;
- fast neutrons will affect directly the structure of the materials, and the resulting changes in their lattice structure may lead to increased corrosion. However, it is not to be expected that this effect will result in a significant enhancement of the metal release rates.

In a PWR primary circuit, the in-core and the out-of-core surfaces are wetted by the same coolant; further, the temperature differences over the entire primary circuit amount only to about 35 K; it can, therefore, be assumed that the metal release rates of identical materials are identical over the whole circuit. In full confirmation of this assumption, the comparative investigations of Lister and Davidson (1989) of the corrosion behavior of the materials inside a neutron field (NRX research reactor) and outside of it, when PWR operating conditions were applied, yielded no indication of radiation-induced differences in the metal release rates. As a consequence of these findings, the metal release rates obtained in out-of-pile experiments can be expected to represent the in-pile behavior of these materials with sufficient reliability. As was emphasized above, this conformity is restricted to the corrosion release rates of the elements from the materials and does not give any indication of the rates of supply of radionuclides to the coolant from different locations of the materials.

An important result of these experiments which were conducted for a total of about 3000 hours under different chemistry conditions (see below) was that in most of the cases cobalt release to the solution was favored compared to that of the other constituents of the specimen. A possible explanation for this result is that cobalt is retained in the oxide layers at a lower concentration than it was in the base material. However, this effect typically occurs only when the test solution is not preloaded with cobalt ions, while in the case of a preloaded solution the cobalt retention in the oxide layer is significantly higher. By contrast, chromium release from the specimens was observed to be very small under reducing conditions, due to chromite formation in the inner oxide layer; in the course of transients leading to oxidizing conditions in the test solution, however, an enhanced chromium release was observed.

With the exception of chromium, the time behavior of the metal release rates can be described by a simple exponential function; in the case of cobalt, the time dependence (in g $^{59}Co/cm^2 \cdot h$) is expressed by

$$\text{Release Rate} = K' \cdot (\text{time})^{-m}$$

The values of K' (in $g \cdot cm^{-2} \cdot h^{m-1}$) and m for different materials and different chemistry conditions are summarized in Table 4.5.a.; the individual coolant chemistry conditions

Li:	2.2 mg Li/kg, $pH_{(T)}$ 7.8
Li + B:	1.5 mg Li/kg, 1200 mg B/kg, $pH_{(T)}$ 6.6 ± 0.4
Coord. Li/ B:	2.0 to 0 mg Li/kg, 1100 to 0 mg B/kg, $pH_{(T)}$ 7.5 to 5.7

correspond to different water regimes which are in use in PWR operation (see Section 1.3.). In order to compare the cobalt release rates from different materials, an equivalent penetration rate was defined, which expresses the layer thickness to be removed from the material, to obtain the measured cobalt release. Its time behavior is described by the equation

$$\text{Penetration Rate} = K \cdot (\text{time})^n$$

In Table 4.5.b. the values of the constants obtained from the experiments are given (K in $\mu m \cdot h^{-n}$); by extrapolating these data to an integrated exposure period of 30 years, the cumulative corrosion removal from the materials shown in Table 4.5.c. results.

The oxide layers formed on the surfaces of the coupons used during these experiments consisted of two layers when the experiments were carried out in a solution which was saturated with corrosion products – an inner layer enriched in chromium and an outer layer with higher iron and nickel concentrations. In contrast, in a solution which was virtually free of corrosion products, no outer layer oxide was formed on the test specimens. In both cases, the corrosion rates were almost identical while the metal release rates into a solution free of corrosion products were higher by about the amount of the outer layer. Since the outer layer apparently does not provide a protective effect to the underlying material but rather contributes essentially to the corrosion product inventory in the primary circuit which is accessible to activation, the question arises of whether contamination buildup could be reduced by removal of the outer layer prior to starting nuclear operation of the plant. In theory, this layer could be dissolved by treatment with a decontamination solution such as CAN-DECON (see Section 4.5.2.2.) at 100 °C, without affecting the inner layer since it is rich in chromium, which is not dissolved by this reagent; up to now, no experimental verification of this potential means of reducing contamination buildup has been undertaken.

The investigations of the metal release rates of Inconel 600 and Inconel 690 reported by Beslu et al. (1986) yielded results which were somewhat different from those of Lister and Davidson mentioned above. Their experiments, also using radioindicator techniques, were carried out in the CORELE loop, a so-called zero release loop made almost completely of Zircaloy-4 and titanium. The equivalent penetrations of both Inconel alloys obtained by measuring the cobalt release were lower by a factor of 2 to 8 than the data reported by Lister and Davidson (1989), when normalized to an exposure period of 1000 hours. The measured cobalt release from Inconel 600 was higher by about a factor of 2 than that from Inconel 690, with this difference being largely independent of the experimental conditions applied such as flow rate, temperature and solution pH. Moreover, the cobalt release rates measured by Beslu et al. (1986) did not decrease with time but remained

Table 4.5. Cobalt release from PWR materials
(according to Lister and Davidson, 1989)

a) Release rate as a function of time
Release rate = $K' \cdot (\text{time})^{-m}$

Material	Coolant chemistry					
	Li		Li + B		Coord. Li/B	
	K'	m	K'	m	K'	m
Type 304 SS	$1.36 \cdot 10^{-8}$	0.56	$2.23 \cdot 10^{-9}$	0.55		
Inconel 600	$3.85 \cdot 10^{-10}$	0.31	$5.14 \cdot 10^{-10}$	0.39	$1.34 \cdot 10^{-9}$	0.28
Inconel 690	$1.14 \cdot 10^{-9}$	0.44				
Stellite 6	$3.91 \cdot 10^{-7}$	0.56			$1.08 \cdot 10^{-6}$	0.67

b) Equivalent penetration rate as a function of time
Equivalent penetration = $k \cdot (\text{time})^n$

Material	Coolant chemistry					
	Li		Li + B		Coord. Li/B	
	K	n	K	n	K	n
Type 304SS	$1.95 \cdot 10^{-2}$	0.44	$3.13 \cdot 10^{-3}$	0.45		
Inconel 600	$1.31 \cdot 10^{-3}$	0.69	$1.98 \cdot 10^{-3}$	0.61	$4.36 \cdot 10^{-3}$	0.72
Inconel 690	$4.89 \cdot 10^{-3}$	0.56				
Stellite 6	$1.83 \cdot 10^{-3}$	0.44			$7.63 \cdot 10^{-3}$	0.33

c) Equivalent penetration, integrated value
30 years operation, µm

Material	Coolant chemistry		
	Li	Li + B	Coord. Li/B
Type 304SS	4.7	0.86	
Inconel 600	7.2	4.0	34.8
Inconel 690	5.3		
Stellite 6	0.44		0.41

virtually constant over about 5000 hours of exposure time. The release of the individual constituents of the alloys from the specimens to the test solutions was incongruent, with both alloys increasing in the sequence

$$^{51}Cr \ll {}^{58}Co < {}^{60}Co < {}^{59}Fe < {}^{54}Mn$$

This finding did not agree with the results of Lister and Davidson (1989) either, who measured a preferential cobalt release. Likewise, the observations of these

investigators which suggested higher cobalt release under coordinated Li/B chemistry rather than under other chemistry conditions, were not consistent with the measurements of Beslu et al. (1986). Additional experiments on the corrosion ion release rates from both Inconel alloys under PWR operating conditions were reported by Beslu et al. (1989 b), using a zero concentration of the corrosion products in the experimental solution at the inlet of the test section. These experiments also showed a release of metal atoms from the samples which was almost constant in time up to a test duration of about 6000 hours. Since the thickness of the oxide layers on these test specimens was only around 1 μm (as a consequence of the extremely low concentrations of corrosion products in the test solution), these results do not contradict those reported by Lister and Davidson, who used specimens with thicker oxide layers and, consequently, measured a dependence of the release on t^n with $n < 1$.

A comparative assessment of potentially important cobalt sources in the PWR primary circuit, which was performed on the basis of the results cited above, came to the conclusion that cobalt release from the Inconel steam generator tubing is the main source of cobalt in the primary coolant. In an oxidizing or inert solution, such as in the final period of a fuel cycle when hydrogen has been removed from the primary coolant, the increase in cobalt release from Inconel is more pronounced than that from the other materials included in these investigations. From these considerations it was concluded that reduction of the cobalt content of the Inconel material from 0.05 to 0.01% would result in a decrease in the cobalt concentration in the primary coolant by a factor of about 2.5 during an essential part of the lifetime of the plant. The cobalt content of the stainless steels, in contrast with Inconel, seems to be only of minor significance with regard to the cobalt concentration in the coolant. However, an increase in the release of cobalt from Stellite material to values beyond those obtained in the experiments would mean that this material would be the dominant cobalt source. Since, according to the model used here, the cobalt concentration in the coolant is assumed to contribute directly to the source term of activity transport, it was claimed that a significant reduction in the cobalt concentration in the coolant would result not only in a reduced buildup of contamination levels, but would also effect a reduction in the already existing contamination levels in the primary circuit.

The investigations cited above (like others performed in this field) yielded results on the amounts of corrosion products formed under PWR operating conditions, but not on the amounts of the associated radionuclides. As was emphasized above, "Co source" must not be confused with the term of essential interest "^{60}Co source". Moreover, it has to be pointed out that the conclusions drawn from such evaluations of corrosion rates are only fully valid if the deposition of corrosion products on the fuel rod surfaces and subsequent neutron activation there, i. e. mechanism 1 in Fig. 4.26., were the most important contributor to the production of ^{60}Co carried in the coolant. If this assumption does not apply, as will be discussed below, then these arguments would be of less significance. In order to correlate the two figures "Co supply to the coolant" and "^{60}Co supply to the coolant", the activation period and the neutron flux density to which the different potential sources are exposed also have to be taken into account. Such calculations are comparatively

simple with regard to the radionuclide production in the in-core materials; in this case, the specific activity (e. g. the ratio $^{60}Co : Co$) of the released corrosion products increases steadily with the time of plant operation until the activity saturation level of the individual radionuclide is attained. Of course, the time needed to reach the activity saturation levels depends on the halflife of the particular radionuclide, amounting to several hours to weeks for short-lived radionuclides and to about 20 years of plant operation for ^{60}Co. At any given time, the proportion of radionuclides released from the relevant in-core materials by corrosion (as related to the mass of the relevant element) is governed by the specific activity of the radionuclides at that time.

On the other hand, the amount of radionuclides (in particular of longer-lived ones) produced in the corrosion products that are deposited on the surfaces of the fuel rods depends on the deposited mass of oxides, on their elemental composition, and on their residence time in the neutron field. Because of the great importance of the extent of radionuclide production in such deposits, detailed studies have been carried out to throw light on the mechanisms which control deposition. According to the results obtained, this process may be basically initiated by two different mechanisms: by deposition of solid suspended matter (i. e. non-dissolved corrosion product oxides), on the one hand, and by precipitation of dissolved substances from the coolant on the other.

In the buildup of the corrosion product layers on the fuel rod surfaces, deposition of particulate matter from the coolant may play an essential part (Lister, 1992). This deposition process proceeds in two stages: first, the transport from the bulk of the coolant to the surfaces; second, the attachement of the particle to the surface. For small particles in the size range normally assigned to colloids, the transport is mainly a result of mass transfer effects incorporating Brownian diffusion characteristics of the particles. For particles larger than about 1 μm, inertial effects are assumed to gain increasing importance; however, the details of this process are not yet fully understood, since the existing inertial deposition models were mainly developed for aerosol systems. As a result, they are not able to describe the results of experiments on corrosion product deposition for the system particle –water with a satisfying reliability. Once particles have been transported to the wall, their attachement to the surface is predominantly influenced by chemistry effects. In the case of opposite charges of the particle and the surface, an attractive force supports deposition so that, at small distances, van der Waals forces become effective and the particles will adhere. Sticking of the particles to the surface may be supported by a change in the crystal lattice of the deposited particles under the influence of the hot primary coolant, which is at 300 °C.

The amount of corrosion products deposited in the reactor core by precipitation from the dissolved phase depends on the solubilities of these oxides in the primary coolant and, in particular, on the temperature-dependence of their solubilities. Lower solubility at the higher coolant temperature in the reactor core than at the lower temperature in the steam generator (negative temperature coefficient of solubility) would favor enhanced transport to and precipitation in the core, whereas higher solubility at the higher temperature (positive temperature coefficient) would result in a clean reactor core. From the classical investigations of

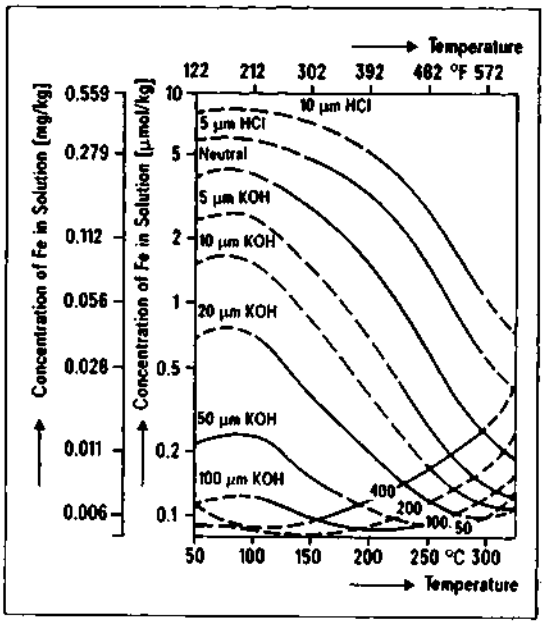

Figure 4.29. Solubility of Fe_3O_4 in aqueous solutions (according to Sweeton et al., 1970)

Sweeton et al. (1970) of magnetite Fe_3O_4 it is known that the solubility of such a corrosion product oxide depends both on the temperature and on the solution pH (see Fig. 4.29.). While at solution temperatures below about 100 °C the solubility of magnetite decreases steadily with increasing pH, at PWR operating temperature (i. e. about 300 °C) the solubility shows a minimum at some pH, with higher solubilities on both lower and higher pH levels. However, at a characteristic pH (in the case of magnetite Fe_3O_4 at pH 6.8) the solubility is virtually independent of the temperature in the range of interest, i. e. 290 to 330 °C. To minimize the transport of corrosion products in the primary circuit, obviously a zero temperature coefficient of solubility should be strived for, and this situation can be achieved by maintaining an appropriate coolant pH. In order to obtain a sound basis for the selection of optimum coolant chemistry conditions, solubility studies of corrosion product oxides have been performed by various researchers. However, the accurate determination of corrosion product solubilities in simulant high-temperature primary coolant is a difficult task since all the influencing parameters typical for a real reactor primary circuit have to be taken into consideration; this is true for experimental approaches as well as for calculations based on thermodynamic data (Thornton, 1992).

While Sweeton et al. (1970) investigated the solubility behavior of Fe_3O_4 and its dependence on temperature and solution pH, Sandler and Kunig (1977) conducted

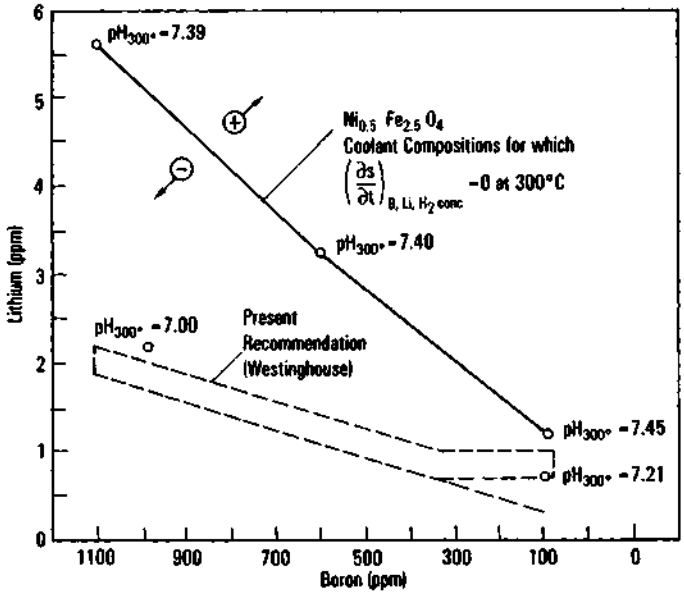

Figure 4.30. Boundary between positive and negative coefficients of solubility for $Ni_{0.5}Fe_{2.5}O_4$ at 300 °C and dissolved hydrogen concentration of 25 cm^3 (STP)/kg H_2O (Thornton 1992; by courtesy of IAEA)

similar experiments with a non-stoichiometric nickel ferrite as an oxide composition more representative of PWR corrosion products. The results of these studies will not be discussed in detail here; as an essential result it shall only be mentioned that they showed a qualitatively similar dependence of the solubility of both compounds on solution chemistry and temperature, with, however, pH and temperature values of the minimum solubility of nickel ferrite being different from those for magnetite. With nickel ferrite, the temperature coefficient of solubility changes from negative to positive with increasing pH at about pH 7; the solubility of nickel from these compounds is generally lower than that corresponding to a congruent dissolution and reaches a minimum near pH 7.4. From the nickel ferrite solubility data, a zero temperature coefficient line was derived which is shown in Fig. 4.30. (according to Thornton, 1992), denoting the required lithium concentration in the primary coolant as a function of the current concentration of boric acid. However, the lithium concentration which is needed for adjustment of an optimum pH is higher than that allowable from the viewpoint of Zircaloy corrosion; for this reason, compromises have to be made in practice in coolant chemistry control (see Section 1.3.).

With regard to the application of the results of these studies to PWR operation, the essential fact is the tendency for a lower coolant pH to favor the deposition of corrosion products in the neutron field, because of their lower solubility at about 330 °C than at 290 °C. This tendency was at least qualitatively confirmed by various investigators who performed experimental examinations on spent PWR fuel

rods. As was reported by Neeb et al. (1972), the fuel assemblies from the first fuel cycle of the German PWR KWO, which during this time had been operated without the addition of an alkalizing agent to the primary coolant, showed corrosion product surface loadings of up to 6 mg/cm^2 in the central region of the core, while in the direction of the periphery the thickness of the deposits decreased significantly. The deposits consisted of a lower tightly-adherent layer and of an upper loosely-adherent layer. While the thickness of the tightly-adhering layer increased only moderately with increasing height from the bottom of the fuel rods to the top, the amount of loosely-adhering material showed a significant increase with height. The chemical composition of these deposits also varied in the vertical direction, with the iron content decreasing and the nickel content increasing with increasing height; in the upper regions of the fuel rods, besides the normal spinel-type oxides NiO was identified by X-ray diffraction analysis. Analogous investigations after the second fuel cycle of this plant, during which the coolant pH had been corrected by addition of LiOH, showed only minor deposits on the fuel rods; moreover, at the fuel rods which were operated during both cycles and were covered after the first one with heavy deposits, the amount of corrosion products was considerably reduced. To be sure, a part of this difference might be explained by the higher corrosion product levels present in the primary system during the first fuel cycle, but there is no question that the change in primary coolant chemistry was the main reason for this reduction in corrosion product loading on the fuel rod surfaces.

Similar results regarding the corrosion product deposits on fuel rods and their dependence on the pH of the primary coolant were obtained by Bergmann and Roesmer (1984) from investigations carried out over several years at the US PWR plants Beaver Valley 1 and Trojan. Whereas Beaver Valley 1 had been operated since commissioning with coordinated Li/B chemistry, the Trojan plant had experienced low lithium chemistry (0.2–0.5 ppm) in its first cycle and was changed to coordinated Li/B chemistry at the beginning of the second cycle. In these investigations, a large number of plant operating parameters was considered, so that the authors were quite sure that the observed differences in the deposited mass of the corrosion products had to be attributed to the differences in coolant chemistry.

In these investigations, it was also found that the fuel rod deposits resulting from the operation at a higher coolant pH were considerably less than those formed during the fuel cycle operated at a lower coolant pH. While corrosion product deposits of 0.5 to 4 mg/cm^2 were measured after the first fuel cycle of the plant operated at low pH, operation with coordinated Li/B chemistry during the second cycle resulted in layers of only 0.3 mg/cm^2 and less. Averaged over all the samples taken from the fuel rods, the difference in the thicknesses of the deposits amounted to a factor of 3 to 6. The nickel concentrations in the deposits from the low-lithium chemistry cycle were significantly higher than in those from coordinated Li/B chemistry; on the other hand, the cobalt concentrations did not show greater differences (these data, however, were somewhat questionable because of the very low concentrations of this element, possibly resulting in a broader analytical scatter). By changing from low-lithium to coordinated Li/B chemistry, as was done in the Trojan plant from the first to the second cycle, the thickness of the deposits in the

Table 4.6. Typical composition of PWR fuel rod deposits
(By courtesy of Siemens/KWU)

Fe_3O_4	84–91%
Cr_2O_3	2–5%
NiO	3–9%
MnO	1–5%
CuO	0.2–1%
CoO	< 0.05%

upper regions of the fuel rods was virtually unaffected. In contrast, the amount of the corrosion products in the middle region of the rods, i. e. in the region of maximum heat ratings, was significantly reduced. This reduction was probably due to a redissolution of deposited corrosion product oxides, an effect which is consistent with the laboratory data on the dependence of the solubilities of these oxides on the coolant temperature in the region of the positive temperature coefficient of solubility at higher pH values. Fuel assemblies which were loaded into the reactor core after the change in coolant conditions to coordinated Li/B chemistry, showed only small amounts of deposits.

The extensive investigations performed by Large and Woodwark (1989) in the DIDO Water Loop (DWL) under PWR operating conditions using different chemistry regimes, have supported the results of the PWR plant investigations mentioned above. In these experiments, during which the DWL was equipped with a fuel rod showing a heat rating quite similar to that of a routine PWR fuel rod, it was shown that at low coolant pH (i. e. pH 6.3) the deposits on the fuel rod were higher by about a factor of 5 to 6 than at a coolant pH of 6.9 or higher. However, on the average, the corrosion product deposits on this experimental rod were significantly less than those observed on commercial fuel rods; the reason for this difference might be that the shorter length of this experimental rod represented only the lower part of a real fuel rod, where even in practice comparatively little corrosion product deposits are observed. A similar dependence of the amount of fuel rod deposits on the coolant pH was observed for heated Zircaloy surfaces outside the neutron field, indicating that the formation of the corrosion product deposits in the reactor core is not significantly influenced by radiation.

Current US experience shows that the magnitudes of the fuel rod deposits vary widely between plants. The fuel rods of newer German PWR plants, which were operated at pH levels around 7, all showed very thin and tightly adherent corrosion product deposits with a typical loading on the order of 2 to $3 \cdot 10^{-2}$ mg/cm^2. As can be seen from Table 4.6., the main constituent of these deposits typically is iron, followed by nickel and chromium; according to X-ray diffraction analyses, substituted spinels are the main component. The dominant radionuclide in these deposits is ^{58}Co, followed by ^{54}Mn and ^{60}Co. From the specific activities of the radionuclides, in particular of ^{59}Ni, an apparent residence time of the deposits in the neutron field of about 1 day was calculated (Siemens/KWU, unpublished).

In the determination of the mass of the deposited corrosion products there is still the question of whether or not the shutdown corrosion product spiking (see

Section 4.4.3.3.) effects the release to the coolant of a major fraction of the deposits which had been present on the fuel rods during reactor operation. If this is the case the question arises of the extent to which the amount of deposits determined after discharge of the fuel assemblies is representative for the amount present on the fuel rod surfaces during plant operation. From balance calculations, however, one can conclude that the amount of corrosion products which is mobilized during the shutdown spiking amounts to less than 25% of the measured deposit loading. Thus, the results obtained in post-irradiation investigations can be assumed to yield data that are representative for the operating phase.

The hydrazine chemistry regime employed in some VVER plants is reported to result in a reduced deposition of corrosion products on the fuel assembly surfaces and, consequently, in less production of radionuclides (Pashevich et al., 1992). Changing from $KOH-NH_3$ chemistry to hydrazine chemistry in an operating plant is claimed to effect a peeling-off of deposited oxides from the core surfaces, with the consequence of temporarily enhanced corrosion product and activity levels in the primary coolant. However, because of the rather limited experience that has been had with this type of water chemistry so far, no detailed informations about its effects on the contamination levels in the primary circuit could be given.

The corrosion products deposited on the fuel rods mainly originate from the materials of the steam generator heating tubes and the primary circuit pipes and components. However, observations of cobalt concentrations in corrosion films on primary circuit surfaces which were markedly higher than those in the underlying base materials (Bergmann et al., 1983) suggested the presence of additional cobalt sources. Potentially significant contributors are the hardfacing materials (Stellites) which are used in valves, pumps etc. in the auxiliary systems, in particular in the chemical and volume control system (CVCS). From these surfaces, cobalt can be released during plant operation by corrosion or by wear and can be transported to the primary circuit. As was mentioned by Heard and Freedman (1983), maintenance work at the valves may be a major source of cobalt input from these parts. According to these investigations, in US PWR plants an average of 10 to 30 g cobalt per year entered the primary coolant in the course of such work; in BWR plants the figure was 30 to 90 g. The wear material consists mainly of small particles of 4 to 40 μm size which remain suspended in the coolant for longer time intervals and which may be deposited together with other corrosion products in the neutron field. Estimates reported by Bergmann (1989) suggested that the high-cobalt alloy containing valves which are located downstream from the charging pump in the CVCS may be significant contributors to the amount of cobalt carried by the primary coolant. Using realistic figures on the operation and maintenance of such valves in a particular plant, it was concluded that about 4 g cobalt per year are released to the coolant by their corrosion, wear and maintenance, corresponding to a fraction of 4 to 7% of the total annual cobalt input. Another potentially significant cobalt source may be the CVCS pipework, in particular the stainless steel surfaces, which are operated at intermediate temperatures (e. g. regenerative heat exchangers), where the release rates are likely to be markedly higher than for the main primary circuit surfaces. Finally, the solutions in the boric acid storage tank may contain cobalt impurity contents which are higher than those in the main

CVCS recirculation flow and, therefore, may represent an additional source of cobalt input. Apparently, these observations are not generally valid; investigations in other plants after a longer period of operation did not show significant cobalt input from the CVCS during steady-state operation (Bridle et al., 1989 a).

As a very important topic in contamination buildup, the question is still open to what extent the data on corrosion product solubilities in the primary coolant are of importance for the behavior of trace amounts of cobalt. It seems to be still questionable whether cobalt ferrites as a well-defined compound with properties similar to the nickel ferrites can exist under PWR primary coolant conditions, whether cobalt atoms can be incorporated into a nickel ferrite lattice or whether traces of cobalt may be deposited onto the surfaces of the reactor core by adsorption on other, already deposited oxides. Such adsorption processes may occur even on the Zircaloy oxide films in the absence of any net deposition of corrosion products. Experimental investigations of the interaction of dissolved cobalt with heated Zircaloy surfaces (Lister et al., 1983) indicated that at low crud levels in the coolant cobalt deposition on surfaces is dominated by processes involving dissolved species, with adsorption/desorption processes being the responsible mechanisms. The extent of cobalt deposition is controlled by the type of oxide present on the Zircaloy surface: thin black films of zirconium oxide will pick up less cobalt from the solution than thick white oxide films, even when the differences in the available surface areas of both types of oxides are taken into account. The deposition process seems to be little affected by the heat flux in the exposed metal. According to Thornton (1992), such adsorption-desorption exchange processes provide a pathway for radioactive species to be transported around the circuit even when the net movement of corrosion products is minimized; this means that under such circumstances the processes of activity transport and of corrosion product transport may be decoupled. They may provide a pathway for target nuclides such as ^{59}Co to be adsorbed onto fuel rod surfaces even in a core which is virtually free of deposited corrosion product particles.

In agreement with these findings, Large and Woodwark (1989) have observed in their experiments in the DWL that the activity inventories and, in particular, the ^{60}Co inventory of the deposited corrosion products, do not depend significantly on the prevailing coolant pH; the same behavior applies to the element-specific activities (see below). A considerable fraction (about 50%) of the ^{60}Co plated out onto the surface of the fuel rod was found to be incorporated into the oxide layer which had developed on the Zircaloy surface, indicating that at least a part of the radioactive and also of the inactive cobalt is deposited onto the surface from the ionic dissolved state. Thus, it can be assumed that by a reversible exchange a fraction of the deposited cobalt will again be released to the coolant. The action of such exchange processes means that the solubilities of the corrosion products and their dependence on temperature and coolant pH alone are not able to give complete insight into the processes controlling the behavior of traces of cobalt on the fuel rod surfaces. Summarizing these important findings, it can be said that the fraction of cobalt which is incorporated from the dissolved state in the coolant into the oxide layers on the surfaces of the fuel rods does not significantly depend on the type of PWR coolant chemistry applied.

In order to select appropriate countermeasures against contamination buildup, an answer has to be derived from the results of the research work performed to the question, which of the two mechanisms shown in Fig. 4.26. is of greater significance. If mechanism 1 – i. e. the activation of corrosion products which are temporarily deposited on the surfaces of the reactor core – is the one that mainly controls production of the most disturbing radionuclides (as was postulated by Metge et al. (1986), among others, based on calculations with the PACTOLE code as well as on measurements performed at EdF plants) it would be reasonable to minimize the cobalt content of the steam generator tubing materials and, in addition, to optimize the chemistry conditions in the primary coolant so that release of corrosion products from Inconel is minimized and the residence time of the corrosion products in the neutron field is as short as possible. If, on the other hand, mechanism 2 – i. e. ^{60}Co release from highly activated in-core materials – is the more important one, then the cobalt inventory inside the reactor pressure vessel should be kept to a minimum and, simultaneously, chemistry conditions should be adjusted to ensure the lowest possible metal release rates from the in-core materials.

Fundamentally, the dominance of one of these two mechanisms can be determined in one of two ways. The first method, which is chemical, is determination of Fe : Co ratios in the corrosion products and comparison of them with those that are typical for the different materials present in the primary circuit. As can be seen from Table 4.7. (Siemens/KWU, unpublished), these ratios show pronounced differences between the steam generator tubing material Incoloy 800 and the materials present inside the reactor pressure vessel (in the latter case, an equivalent value taking into account the relative surface areas of the different materials was used). Considering the specific metal release rates of the materials, an assumed composition of the corrosion products can be calculated; because of the relatively large scatter of the published data on metal release rates, three different sets of values have been used in Table 4.7. This rather simple comparison is assumed to be justified since the corrosion rates are not influenced by the location of the relevant materials, in-core or out-of-core, as was discussed above. The data demonstrate that the corrosion products which are transported in the coolant during steady-state operation show Fe : Co ratios which, in spite of considerable fluctuations, are similar to those of the in-vessel materials and, on the other hand, are significantly different from the steam generator tubing material Incoloy 800. This is true for the solid suspended matter as well as for the so-called dissolved fraction. Comparable Fe : Co ratios were measured at all German PWR plants. As a consequence, the results of the chemical analyses of the corrosion products in the coolant can be judged to be an indicator that mechanism 2 is the more important one for contamination buildup.

The second method for distinguishing between the two mechanisms responsible for contamination buildup is radiochemical and is based on the measured element specific activities of appropriate radionuclides such as ^{60}Co/Co, ^{59}Ni/Ni, and ^{55}Fe/Fe. These ratios can be determined in the corrosion products collected from the fuel rod surfaces as well as in those isolated from the primary coolant (see Fig. 4.25.). From these analytical results and from the neutron flux density known from the design of the reactor core, apparent residence times in the neutron field

Table 4.7. Fe : Co ratios in PWR primary circuit materials and in primary coolant corrosion products
(By courtesy of Siemens/KWU)

	Fe : Co ratio	
	PWR-A	PWR-B
Material SG tubing (Incoloy 800)	3100	2900
Material in-core (stainless steel, Inconel, Co alloy)	600	600
In-core corrosion products		
– case 1*	20	10
– case 2*	150	60
– case 3*	415	365
Corrosion products in primary coolant (steady-state operation)		
– >0.45 μm	16–280 (average 70)	100–530 (average 350)
– <0.45 μm	10–320 (average 110)	60–190 (average 110)

* Corrosion rates assumed
– case 1: Stainless steel, Incoloy: 15 mg/m²·month
Co alloy (incl. wear): 1000 mg/m²·month
– case 2: Stainless steel, Incoloy: 50 mg/m²·month
Co alloy (incl.wear): 500 mg/m²·month
– case 3: Stainless steel, Incoloy: 363 mg Fe/m²·month; 0.8 mg Co/m²·month
Co alloy (corrosion only): 186 mg Co/m²·month

can be calculated. Since non-radioactive metal atoms are simultaneously released to the coolant from all surfaces during plant operation (preferentially from the larger ones located outside the neutron field), a continuous dilution of the element-specific activities has to be expected. This means that the calculated residence times are certainly shorter than the true ones, although to an extent which is still not precisely known. On the other hand, the specific activities of the in-vessel materials and, consequently, of their corrosion products can easily be calculated from the neutron flux density and the effective operation time of the reactor.

As was mentioned above, measurements of $^{59}Ni/Ni$ ratios in fuel rod deposits from German PWR plants revealed apparent residence times of the deposits in the neutron field of only about one day (Riess et al., 1984). According to analyses carried out by Bergmann and Roesmer (1984) at two US PWR plants, the apparent residence times calculated from measurements of the element-specific activities of ^{59}Fe, ^{58}Co, ^{54}Mn and ^{60}Co in fuel rod deposits did not significantly depend on the type of primary coolant chemistry applied. On the other hand, the calculated residence times of the individual radionuclides were found to be different, with the element-specific activity of ^{60}Co (the longest-lived of the analyzed radionuclides) showing the highest values. These results indicate a dynamic process which is char-

acterized by deposition and redissolution of the corrosion products, in which the decay intervals between the individual activation periods have a more pronounced effect with shorter-lived radionuclides. The apparent residence times of corrosion product elements in the neutron field which were calculated by Large and Woodwark (1989) on the basis of specific activities are in the range of 1 to 5 days for $^{60}Co/Co$, and are even shorter for the other, shorter-lived radionuclides.

On the other hand, from numerous analyses of specific activities of the radionuclides in corrosion product samples from the primary coolants of German PWRs, apparent residence times in the neutron field of about 55 days for ^{55}Fe and about 100 days each for ^{59}Ni and ^{60}Co production were calculated, i. e. much longer than the values obtained in the analyses of the fuel rod deposits (Riess et al., 1984). Because of the above-mentioned dilution by non-activated elements, these data represent a lower limit for the residence time of the corrosion product elements in the reactor core. Hence, the results on the element-specific activities are also consistent only with contamination buildup mechanism 2, suggesting that the corrosion products originating from the highly irradiated in-core materials predominate. Among these materials, evidently the most important ones are the Stellite hardfacing materials used in components inside the reactor pressure vessel. In order to minimize the radiation dose rates in the area surrounding the primary circuit, therefore, the most promising way would be to replace these Stellites by wear-resistant materials which are free of cobalt. Precisely this measure was put into effect in the German PWR plants starting with the KKP 2 plant; comparative measurements at several plants over the past few years have clearly confirmed its success (see Section 4.4.3.5.).

The radioactivity of the so-called Discrete Radioactive Particles which were detected in US PWR plants (James, 1988), with the exception of the fraction showing irradiated fuel composition (see Section 4.3.4.3.), consisted mainly of ^{60}Co in the range from 10^3 to 10^5 Bq per particle. They were, therefore, assumed to be wear products from Stellites located inside the reactor pressure vessel.

In particular cases, other in-core materials than the hardfacing materials may also be significant sources for the production of corrosion product radionuclides. Kockx and Olijve (1983) reported very high ^{58}Co and ^{60}Co concentrations in the water of the fuel assembly sipping device during several consecutive sipping actions and, during the same period of time, a marked increase in the radiation dose rates at the primary circuit. A more detailed investigation of this phenomenon yielded the result that the nickel plating of the Inconel spacers of several fuel assembly batches contained cobalt contents as high as 1% (compared to $<0.06\%$ for the grid base material). Similar observations were reported by Weitze et al. (1986). The contribution of the Inconel base material of the fuel assembly spacers to the appearance of ^{60}Co in the primary coolant and in the contamination layers has not yet been clarified. Comparisons made between fuel cycles of KWU-designed plants operated with Inconel spacers in the reactor core and those with Zircaloy spacers did not show significant differences, either in the radiation dose rates at the primary system or in the $^{58}Co : {}^{60}Co$ ratio in the primary coolant (Siemens/KWU, unpublished). On the other hand, Bergmann (1986) reported a certain influence of

the spacer material on the radiation levels, based on calculations using the CORA code.

The most important sources for ^{58}Co activity in the coolant and in the contamination layers have been the fuel assembly spacers made of Inconel-X 718, which are covered by a nickel plating, as well as the control rod guide tubes fabricated of austenitic steel. In order to improve neutron economy in the reactor core, almost all fuel element manufacturers have replaced these materials by Zircaloy structural materials, which has resulted in a significant reduction of the ^{58}Co production. Whereas this radionuclide is of minor importance compared with ^{60}Co with regard to radiation dose rates on the outside of the primary circuit piping and components, it might have considerable significance for the personnel radiation exposure during work at open components (e. g. inside the steam generator channel head).

Summarizing the results cited above, it can be concluded that the buildup of ^{60}Co and ^{58}Co in the PWR primary circuit is predominantly controlled by the release of metal atoms from the materials that are permanently located inside the reactor pressure vessel. The temporary deposition in the reactor core of corrosion products which are released from materials outside the neutron field (e. g. steam generator tubing), on the other hand, can be assumed to be only of minor significance for the production of these radionuclides. Only ^{59}Fe, ^{54}Mn and other radionuclides of less importance in contamination buildup are predominantly formed according to mechanism 1 as shown in Fig. 4.26. The consequence of these findings is that a primary coolant chemistry control that aims primarily at a reduction of the residence time of the corrosion products in the neutron field (e. g. by appropriate adjustment of coolant pH) cannot be expected to have any significant impact on the radiation dose rates at the primary circuit. This conclusion is strongly supported by operational experience with German PWR plants. It must, however, be pointed out that this interpretation concerning the most important ^{60}Co sources in the primary circuit is not accepted by all the researchers working in this field. Based on the solubility data of Fe_3O_4 and $NiFe_2O_4$which were obtained by Sweeton et al. (1970) as well as by Sandler and Kunig (1977), among others, and, in particular, on the dependence of the solubilities on the temperature and pH of the primary coolant, a considerable part of those working in the field still considers the steam generator materials to be the most important source of contamination buildup. However, the design of Westinghouse and Framatom plants is different from that of KWU plants, in particular with reference to the use of high-nickel containing Inconel 600 or Inconel 690 as steam generator tubing material, and it cannot be ruled out completely that this difference might give rise to certain changes in the origin of contamination buildup.

During shutdown of a PWR plant and, somewhat less pronounced, also during its startup, a strong increase in the concentrations of corrosion products and the associated radionuclides in the primary coolant is observed, an effect which will be discussed in more detail in Section 4.4.3.3. This process causes a dissemination of the radionuclides over the entire primary circuit and, as a possible consequence, results in increased radiation dose rates in the area surrounding it. For this reason, the origin of these radionuclides is of interest, with their possible source being the resuspension of activated corrosion products previously deposited either inside or

outside the reactor pressure vessel. Several investigators have tried to identify the original location of these substances. Balance calculations suggested that the amount of mobilized radioactivity is on the same order of magnitude as the total radioactivity deposited during steady-state operation in the primary circuit outside the reactor pressure vessel. From this calculation and from the observation that the activity ratio $^{58}Co : ^{60}Co$ increased drastically during this phase, it was concluded that these corrosion products during steady-state operation had been deposited inside the reactor pressure vessel (Beslu et al., 1982). A direct identification of the location where these radionuclides are deposited during plant steady-state operation is possible by measuring a short-lived radionuclide which would have decayed after a short stay outside the neutron field. Measurements of the short-lived ^{56}Mn (halflife 2.5 h) have shown that its increase in activity concentration during plant shutdown proceeds virtually identically to that of ^{60}Co (Siemens/KWU, unpublished). From this result, one can conclude that the corrosion products mobilized during reactor shutdown originate from inside the neutron field, i. e. inside the reactor pressure vessel, where they are deposited during plant steady-state operation.

4.4.3.3 The behavior of the corrosion product radionuclides in the primary coolant

The corrosion product radionuclides generated inside the reactor pressure vessel are to a certain extent released to the coolant and are transported by it to the other regions of the primary circuit. Such a release of radionuclides to the coolant can proceed by congruent dissolution of the oxide layers covering the surfaces of the core materials, as well as of the corrosion product deposits present on the fuel rod surfaces. Likewise, ion exchange or isotope exchange between radioactive atoms in the oxide layers within the core and inactive atoms dissolved in the coolant might be a possible source of radionuclides in the coolant and, finally, corrosion product particles may be peeled off from the surfaces of the reactor core by the coolant flow. On the other hand, radioactive atoms which have already been incorporated into the contamination layers present on the surfaces of the primary circuit may be released again to the coolant, as is implied by the attainment of a saturation level of contamination after a few years of plant operation. Thus, the concentration of radioactive corrosion product nuclides in the coolant is determined by the rate of release from the various surfaces, on the one hand, and by the rates of deposition onto surfaces and of removal through the primary coolant purification system, on the other.

The radioactive atoms represent only a small fraction of the total mass of the corrosion products carried in the primary coolant which, in turn, is only a small proportion (on the order of 0.1%) of the total corrosion product inventory of the primary circuit. In newer PWR plants, the concentrations of corrosion products carried in the primary coolant during steady-state operation rarely exceed a few

Table 4.8. Activity concentrations of the main corrosion product radionuclides in PWR primary coolant (Bq/m^3) (Average values, undisturbed constant-load operation) (By courtesy of Siemens/KWU)

	Plant A	Plant B
^{60}Co	$3 \cdot 10^6$	$3 \cdot 10^5$
^{58}Co	$2 \cdot 10^6$	$1 \cdot 10^6$
^{54}Mn	$7 \cdot 10^5$	$7 \cdot 10^5$
^{56}Mn	$<3 \cdot 10^5$	$3 \cdot 10^5$
^{59}Fe	$<2 \cdot 10^5$	$2 \cdot 10^5$

tens of micrograms per kilogram of coolant (ppb). Usually, iron is the major component (10 to 30 ppb) with smaller contributions of nickel (< 10 ppb), chromium and manganese (< 2ppb); cobalt which is of particular interest because of its radioisotope ^{60}Co, in most cases is present in the primary coolant in concentrations of 10 to 100 ng/kg (ppt).

As a rule, ^{58}Co is the dominating γ-emitting radionuclide in the coolant, followed by ^{60}Co, ^{59}Fe, ^{54}Mn and the short-lived ^{56}Mn. Typical activity concentrations of the main corrosion product radionuclides from two German PWR plants are summarized in Table 4.8. These data represent average values over four fuel cycles, with the scatter of individual values during undisturbed constant-load operation amounting to less than a factor of 2 to 3. Plant A is equipped with Stellite hardfacing materials in the conventional manner, while in plant B these materials inside the reactor pressure vessel were largely replaced by materials free of cobalt. Both plants started operation at about the same time. Other activation products of the corrosion product elements which appear in the primary coolant, such as ^{55}Fe, ^{59}Ni, ^{63}Ni, do not show any significance for the radiation dose rates resulting from contamination buildup, due to their radiation properties (no or very low-energy γ emission); nonetheless, they deserve a certain attention in the context of the characterization of radioactive wastes. While the ratios of the activity concentrations of the different radionuclides to each other can be significantly different from one PWR plant to the next one, they are almost constant over time in an individual plant over the duration of a fuel cycle (usually with the exception of the initial operation period of the first fuel cycle). Despite the marked differences in the activity concentrations in the primary coolants of different plants, no simple relationships to characteristic features of the plants, during commissioning or during continued operation, have been observed.

The appearance of short-lived radionuclides such as ^{56}Mn in the primary coolant indicates that there is no static equilibrium between radionuclides carried in the coolant and those attached to the surfaces, but a dynamic one in which the supply of radionuclides to the coolant and their removal from it compensate for each other, resulting in steady-state activity concentrations that are virtually constant as long as the operational characteristics of the plant remain constant.

Primary coolant analyses show that a fraction of the corrosion product radionuclides is present in the "dissolved" state, while the remainder appears in the form

of solid suspended particles with particle sizes up to a few micrometers. Differentiation between these two states is usually carried out by filtering the coolant samples via 0.1 or 0.45 μm filters. However, this measure results in a quite arbitrary differentiation, since not all the matter that passes through such filters may be in a truly dissolved state rather than being present as very finely dispersed colloidal matter; on the other hand, a fraction of the dissolved ions is potentially adsorbed onto the filter material from the penetrating liquid phase and retained. Usually, in the samples taken from the primary coolant during plant steady-state operation, the overwhelming part of the corrosion products is present as suspended solids; ^{60}Co, ^{58}Co as well as the other corrosion product radionuclides are predominantly attached to these particles. However, since most of the analyses have been carried out on coolant samples taken at ambient temperature, there are some uncertainties whether or not these findings give a true view of the situation in the hot coolant circulating in the primary circuit. A change in the ratio of dissolved to particulate species as a consequence of cooling down the liquid from operating to ambient temperature, cannot be ruled out completely. Analyses of samples obtained by high-temperature sampling indicated differences in the ratio of both species as compared with ambient-temperature sampling; nonetheless, after high-temperature sampling the bulk of the corrosion products was also observed to be in the particulate state. Thus, sampling at ambient temperature may be burdened with a systematic deviation from the true state which, however, is not expected to affect severely the interpretation of the analytical results. When one takes into account the results of investigations on sampling mentioned in Section 4.4.2., it cannot be ruled out that a fraction of the originally dissolved species is retained in the sampling line. Since after a longer period of operation of the sampling line, an adsorption–desorption equilibrium in the line is established, it can be assumed that this effect does not result in serious errors in the measured element and activity concentrations, at least as far as the longer-lived radionuclides such as ^{60}Co and ^{58}Co are concerned.

To get a closer look at the mechanisms that lead to the partitioning of the corrosion product elements (and their radionuclides) between dissolved and particulate species, it seems advisable to give some short remarks on the general behavior of metal atoms which are released from metallic surfaces to a high-temperature coolant.

In the process of corrosion of the metallic primary circuit materials, first metal ions are released to the coolant which are converted to non-dissolved oxides or hydroxides when the solubility limits of these compounds in the coolant are exceeded. This behavior relates to the bulk of non-radioactive atoms and may also include their radioisotopes. As can be seen from Fig. 4.31., the formation of the suspended solid particles is a process consisting of several intermediate steps, starting from the lowest organisation state of the dissolved ions and leading to the colloidal state and, further on, to the crystalline oxides and hydroxides representing the highest organisation state. In general, the significance of the solid suspended corrosion products in the mechanisms and processes controlling contamination buildup has not yet been completely clarified. In each case, it is evident that a description of their behavior exclusively on the basis of transport phenomena of

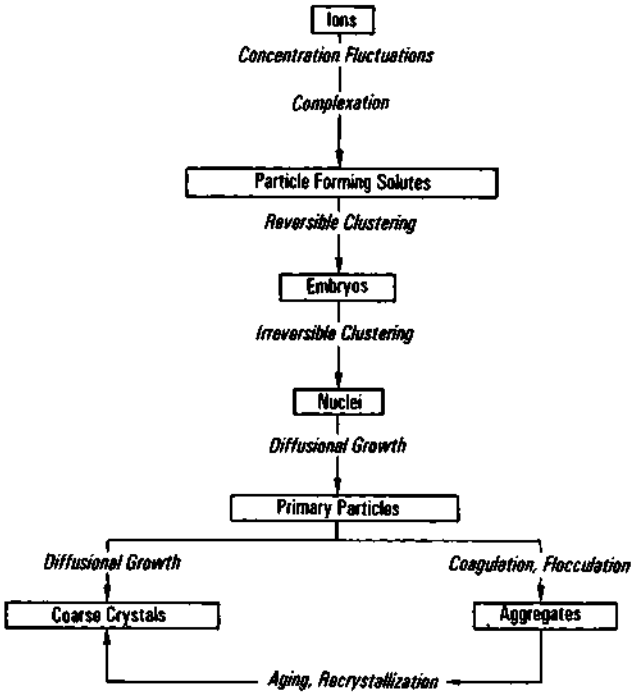

Figure 4.31. Mechanism of formation of corrosion product suspended solids in the PWR primary coolant
(Smith-Magowan, 1984)

inert particles (e. g. using Stokes' law) is incomplete, due to the potentially important effects of electrochemical surface reactions which are not considered in such models.

From the comprehensive paper of Smith-Magowan (1984) in which the results obtained by different researchers were summarized, one can see that the first step in the conversion of ions to solid matter is the formation of colloidal nuclei (see Fig. 4.31.). Colloids are defined as particles where surface forces prevail as compared to mass forces; thus, the upper limit of the colloidal range of size cannot be regarded to be a constant value but depends on the nature of the corrosion products and on the hydrodynamic conditions. In general, particles showing diameters of less than 1 μm are ascribed to the colloidal state. Several investigators reported that the colloidal fraction may amount up to 90% of the total mass of the corrosion products carried in the primary coolant. Such a high fraction would represent a very large colloidal surface which is able to adsorb dissolved Co^{2+} ions (as well as traces of other polyvalent ions) by surface charges, which means that colloids would be able to act as a carrier of ^{60}Co atoms. The potential significance of colloids in contamination transport and buildup was evaluated by different authors (see the review paper of Hüttner and Winkler, 1992); however, there seems as yet

to be no unanimous opinion in this regard. On the other hand, colloidal nuclei are reported to be unstable in the high-temperature primary coolant and, depending on the prevailing conditions, are redissolved to ions or grow by diffusion-controlled addition of further ions or other suspended particles to crystalline compounds. For this reason, colloids frequently are not expected to play a significant part in the contamination buildup process at PWR operating temperature.

Homogeneous nucleation of corrosion product particles in the bulk coolant is not considered to be a significant source of crud particles. Because of their similarity in composition and structure to the ferrite compounds that form the outer layer of corrosion products on piping and steam generator tubing it was concluded that at least a significant fraction of the suspended particles originates in these layers. However, the manner in which such particles are released from the surfaces and how their subsequent careers develop in the coolant under normal operating conditions of a light water reactor are generally unknown (Lister, 1992).

Iron oxides are the main constituent of the suspended corrosion product particles, magnetite (or spinel-type substituted ferrites) in the PWR primary coolant and hematite in the BWR reactor water, i. e. the chemical compound which is formed depends for the most part on the oxidation potential of the coolant. When considering the simultaneous presence of dissolved species and of non-dissolved corrosion product particles in the coolant, it is evident that the relative proportions of both species are determined by their solubilities under the prevailing conditions. For this reason, extensive work has been devoted to this topic in the past years. Out of these studies, the investigations conducted by Sweeton et al. (1970) as well as by Sandler and Kunig (1977) concerning the solubility of Fe_3O_4 and of a non-stoichiometric nickel ferrite in simulated PWR primary coolant have been shortly mentioned in the preceding section; their results on the dependence of oxide solubility on the pH and temperature of the coolant have been employed to develop solubility models which can be used as a basis for calculations of the mechanism of contamination buildup. However, in the past years some questions were raised with regard to the relevance and the applicability of such data. In a critical survey of the frequently used solubility data of the corrosion product oxides, Walker and Thornton (1989) have particularly concentrated on quantifying the uncertainties in the predicted values for pH of minimum solubility and for the zero temperature coefficient of solubility under the chemistry conditions of a PWR primary coolant. According to this study, one main difficulty in applying the solubility models is due to the fact that the original papers have used different correlations for the ionisation constant of water and Henry's law constant for hydrogen when deriving their thermodynamic constants for solubility. This means that the different studies cannot be directly compared, and the derived constants cannot be used with new correlations for the constants without introducing systematic errors.

Another important problem in using iron oxide solubility data which were obtained in laboratory experiments is caused by the fact that such experiments usually are conducted in a closed system under equilibrium conditions, whereas the primary circuit represents a quasi-closed system in which the coolant passes regions of different temperatures in very short time intervals. If reaching the solubility equilibrium is a slow process compared to the flow rate of the coolant (which

usually is true with such oxides), the concentrations of dissolved ions in the solution will be predominantly controlled by kinetic parameters and not by equilibrium conditions. This means that, at least for a certain time, undersaturated or supersaturated solutions can be in contact with suspended particles or with surfaces coated by oxide layers. In addition, there is still a question whether or not the synthetic oxides which are frequently applied in solubility studies are really representative for the corrosion product oxides present in the primary coolant of an operating PWR.

The most important doubts concerning the significance of the solubility data of such corrosion products for the explanation of PWR contamination buildup, however, arise from the question to what extent they are of relevance for the partitioning of cobalt species between the particulate and dissolved states; it has to be remembered that ^{60}Co and ^{58}Co are usually the major sources for the radiation dose rates on the primary circuit surfaces and that the iron and nickel isotopes are of less significance. Current knowledge on the solubility data of cobalt oxides and, consequently, on the upper limit of the concentration of dissolved Co^{2+} which can be present in high-temperature water is still rather scarce. Investigations on the solubility of cobalt ferrite $CoFe_2O_4$, which were reported by Lambert and Joyer (1992), demonstrated that in a solution containing 650 ppm B and 0.7 ppm lithium, the solubility of this compound exhibits a minimum at about 300 °C, resulting in dissolved cobalt concentrations in the solution on the order of 500 ppt. Recent investigations on the solubility of CoO reported by Dinov et al. (1993) yielded the calculated results summarized in Fig. 4.32., showing a pronounced decrease in solubility in the temperature range 100 to 250 °C, down to values of less than 1 μmol Co/kg in pure water at 250 °C. With increasing acidity of the test solution (HF originating from the Teflon coating of the experimental vessel) the solubility increases steadily.

When the above-mentioned data on the very small cobalt concentrations usually found in PWR primary coolant are taken into consideration, such solubilities would mean that cobalt traces in the primary coolant should be present in the ionic dissolved state. However, from the routine analyses of PWR primary coolant it is well known that the overwhelming fraction of cobalt present in the solution can be retained by filtering, together with the particulate corrosion products. This discrepancy raises the question of what mechanism is responsible for the uptake of the cobalt traces into the spinel-type oxides. According to Matijevic (1986), there are three possibilities:

a) Adsorption of cobalt traces onto the surfaces of already existing iron oxides (substituted spinel oxides in PWR coolant, hematite in BWR coolant). The uptake of $^{60}Co^{2+}$ rises with increasing pH and temperature of the coolant, but depends also on the quantity and the properties (such as the specific surface area) of the suspended particles. As can be seen from Fig. 4.33., at low cobalt concentrations and at a pH of the solution above 7 an almost complete adsorption of the dissolved cobalt traces is observed (Tamura et al., 1983). Diffusion of the cobalt traces into the solid particles and formation of a cobalt ferrite could, in principle, take place but would require long periods of time.

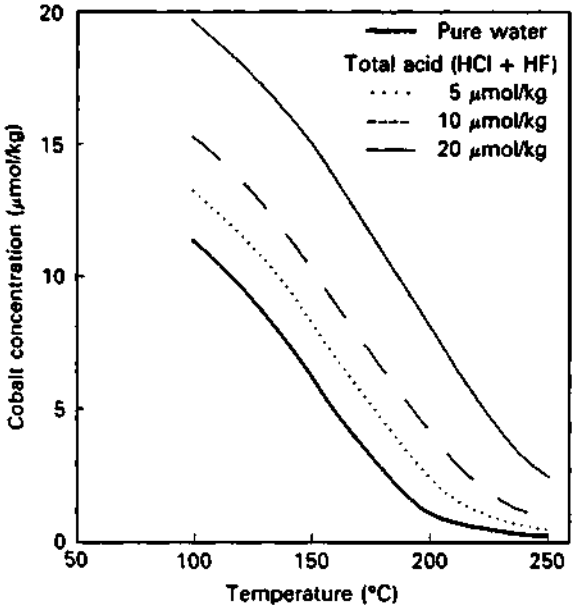

Figure 4.32. Solubility of CoO in high-temperature water; recalculated results with different acidities
(Dinov et al., 1993; Copyright 1993 by the American Nuclear Society, La Grange Park, Illinois)

b) Coprecipitation of Co(II) and Fe (II) hydroxides, e. g. onto the metal surfaces, with subsequent crystallization into ^{60}Co-containing ferrites. In principle, this reaction can take place; under appropriate conditions cobalt is preferentially incorporated into mixed ferrites, leading to a selective enrichment of cobalt in the solid particle compared to the initial composition of the solution.
c) Ion exchange of $^{60}Co^{2+}$ ions for Fe^{2+} ions in the ferrous hydroxide gel with subsequent crystallization into ^{60}Co ferrites. Cobalt ferrite can be obtained from a $Fe(OH)_2$ gel or from gels consisting of mixed $Ni(OH)_2-Fe(OH)_2$ into which Co^{2+} is introduced by diffusion and exchange from an aqueous solution.

Summarizing his investigations, Matijevic (1986) concluded that the incorporation of $^{60}Co^{2+}$ from circulating cooling solutions into the iron oxides is most likely to proceed by uptake of these ions either by ion exchange or by coprecipitation.

A direct experimental detection of the state of cobalt traces in the particulate corrosion products is very difficult to obtain. One practical reason for this difficulty is the cobalt concentration, which is usually far too low for the usual structure analysis methods such as X-ray identification of the prevailing chemical compound; moreover, the similarity of the crystallographic data of cobalt and nickel ferrites to those of Fe_3O_4 complicates the interpretation of the analytical results. However, there are two observations which raise doubts about whether the above-mentioned assumption of cobalt incorporation from the primary coolant into the

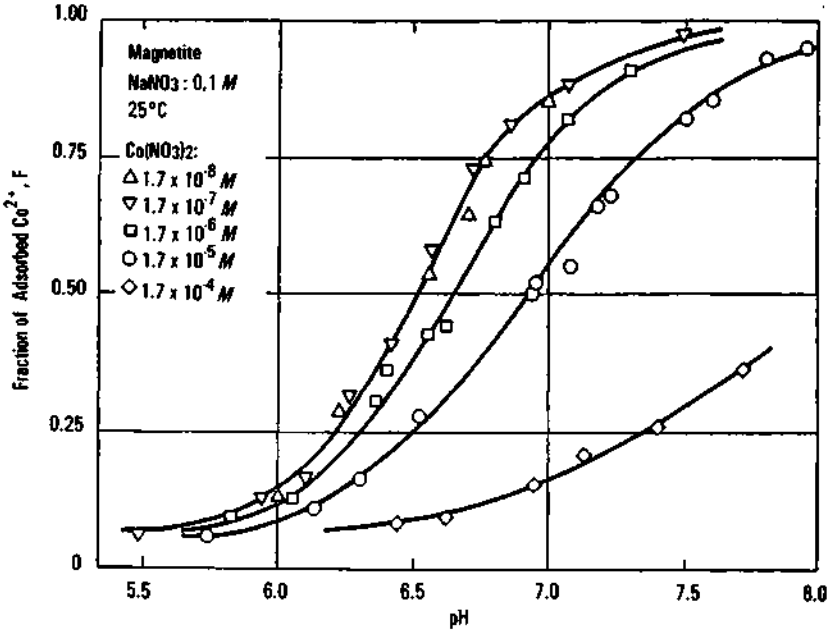

Figure 4.33. The fraction of adsorbed Co^{2+} on 0.2 g of spherical magnetite particles (1μm diameter) (20 ml suspension, 25 °C)
(Tamura et al., 1983; by courtesy of Academic Press, Inc.)

ferrites is correct. The first one is the change in the ratio of particulate to dissolved ^{60}Co species which is observed during a reactor shutdown (see below), which indicates that at least a large fraction of the cobalt radionuclides is only reversibly bound to the ferrite particles carried in the primary coolant. This phenomenon could best be explained by the assumption that the cobalt traces are attached to the surfaces of the particles by adsorption.

Secondly, serious doubts on the presence of cobalt ferrites in the coolant are based on the question of whether or not nickel and/or cobalt ferrites can exist under the conditions prevailing in the PWR primary coolant. According to Smith-Magowan (1984), the formation of these ferrites can only proceed in a solution with a comparatively high oxygen partial pressure. The fundamental question of stability can be answered by thermodynamic considerations using the data which were summarized by Rummery and Macdonald (1975) concerning the redox reactions of Fe, Ni, and Co in aqueous systems at 300° C in the presence of hydrogen and oxygen. Using the equations cited there, the Gibbs free energies ΔG and the related H_2 and O_2 partial pressures can be calculated in the temperature range from 25 to 300 °C. The driving forces of these oxidation and reduction reactions are controlled by the ratio of the H_2 and O_2 partial pressures; they increase with increasing difference between actual pressure and equilibrium pressure. Only when the actual partial pressures are identical with the equilibrium pressures, do the driving forces equal zero and the reaction partners will be in an equilibrium with

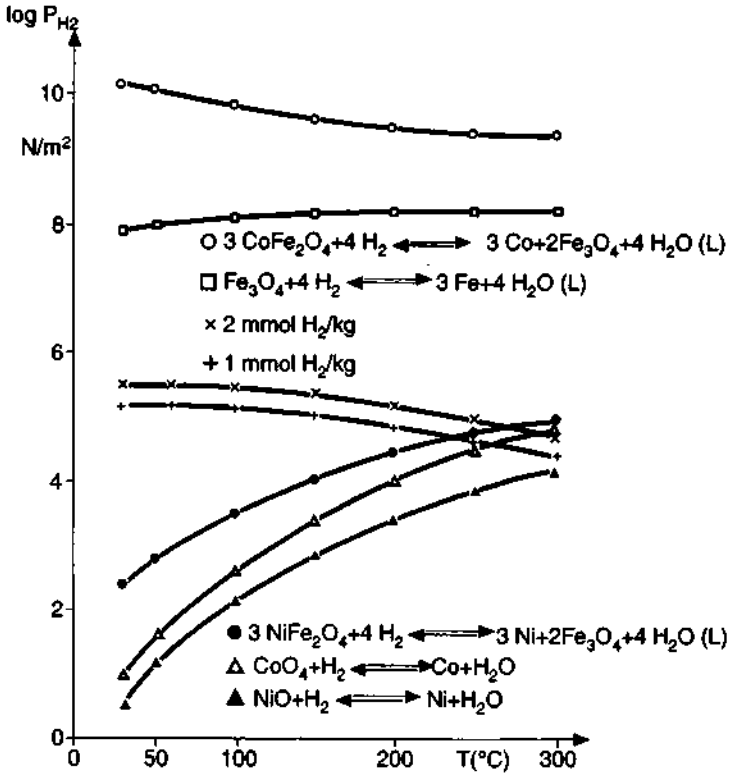

Figure 4.34. Thermodynamic stability of nickel and cobalt ferrites in PWR primary coolant (Schuster et al., 1988; with kind permission of Elsevier Science – NL, Sara Burgerhartstraat 25, 1055 KV Amsterdam, The Netherlands)

their reaction products. In Fig. 4.34. the H_2 equilibrium partial pressures for the reduction of NiO, CoO, Fe_3O_4, $NiFe_2O_4$ and $CoFe_2O_4$ are shown as a function of temperature, together with the upper and lower limits of H_2 concentration in the coolant as stated in the KWU water chemistry guidelines. According to these data, the thermodynamic driving forces for the reduction of NiO, CoO, and $NiFe_2O_4$ should be small in the range of operating temperature, which would mean that the reaction partners should be in an equilibrium with their reaction products. However, because of the large excess of the iron as compared to the nickel and, in particular, to the cobalt concentrations, it seems questionable whether cobalt ferrites can exist in the primary coolant. Therefore, the question still remains open as to whether the ^{58}Co and ^{60}Co transported with the suspended matter is chemically bound as a ferrite or whether it is merely adsorbed onto the surfaces of the particles. At significantly lower temperatures, nickel ferrite is thermodynamically unstable, quite in agreement with the difficulties encountered in the synthesis of nickel ferrite which were described by Smith-Magowan (1984). Chromium spinels are stable under the conditions prevailing in the PWR primary coolant; this corre-

sponds well with the experimental findings that ^{51}Cr in the primary coolant is quantitatively attached to the particulate matter, with the dissolved ^{51}Cr concentration usually being at or below the analytical detection limits.

The relative importance for the contamination process of the ions, colloids and suspended crystalline compounds transported in the coolant is still a subject of discussion; however, there are strong indications that the dissolved cobalt species determine the rate of deposition onto the surfaces of the primary circuit. One reason for this lack of knowledge is the uncertainty as to whether or not the experimental results obtained with samples analyzed at ambient temperature are representative of the situation at operating temperature as well; this relates in particular to the question of whether insoluble suspended matter is also present in the coolant at operating temperature or whether it is formed from dissolved ions during cooling of the sample. Studies including high-temperature sampling and filtering, performed by different researchers, have not yielded clear results. A strong indication for the presence of solid suspended matter in the coolant at operating temperature as well is given by the results of analyses showing different chemical and radiochemical compositions of different grain size fractions of the particles. If the particles had been formed during cooling down of the coolant, a homogeneous composition should be the consequence, due to the similar chemical properties (in particular with respect to the formation of oxides and hydroxides) of the elements under consideration. The cobalt-rich particles described by James (1988) have to be mentioned here, as well as the higher specific activities of the suspended matter as compared to the dissolved substances, a result which was obtained in numerous studies at operating PWR plants. In part these results indicate that the particles probably were not generated by the mechanism shown in Fig. 4.31., but rather by direct peeling-off of oxide particles from the surfaces of the materials.

Some authors have claimed that the suspended corrosion products are of particular relevance for the process of contamination buildup. The most extensive investigation of the behavior of suspended solid corrosion products in PWR primary coolant was carried out by Bridle et al. (1989 b) as well as by Comley et al. (1989), who studied over the course of four years the composition and the behavior of suspended matter in the primary coolant of 5 Belgian PWR plants which had been manufactured by Westinghouse. In these investigations, identical sampling techniques were used in all the plants (isokinetic reduction of the mass flow in the sampling line by insertion of capillary tubes), which means, at least, that the results obtained from the different plants are comparable to each other. Even under plant constant load operating conditions, the populations of the suspended particles varied over a broad range from one plant to another and showed no evident dependence on the operation history of the respective plant. Moreover, in the same plant fluctuations in time of more than a factor of 2 in the particle concentrations were observed without a discernable reason. Particles with diameters above 2 μm showed concentrations in the primary coolant in the range 1 to 30 particles/ml, corresponding to about 1 to 10 ppb; besides these comparatively large particles, there were numerous particles with diameters of less than 1 μm. With regard to the larger-sized particles, the fraction 2 to 5 μm predominated during the first fuel cycles; with increasing age of the plant, the fraction of larger particles with diameters

>8 μm increased significantly. Taking the finer particles into account as well, the bulk of the material belonged to the fraction 0.6 to 1 μm; when calculated on the basis of particle mass, the fractions 0.6 to 1 μm and 10 to 30 μm were the predominant ones, with their proportions increasing with increasing age of the plant. The particles were chemically heterogeneous at all stages; during commissioning of the plant, nickel-based material dominated, but in the course of the first fuel cycle iron-rich particles became predominant. The ^{60}Co specific activities in the particulate matter were variable but tended to increase with time over the first fuel cycles. Autoradiographic examination of individual particles filtered from the primary coolant indicated that less than 1% were significantly radioactive. Hence, the average value of the measured ^{60}Co specific activity of suspended corrosion products does not provide a measure of the extreme variability of the activities of the individual particles and their particular irradiation periods in the neutron field.

In KWU PWR plants, the suspended solids mainly consist of iron, with chromium and nickel as side consituents. According to X-ray structural analyses, they show a spinel lattice; in mineral acids they are difficult to dissolve, thus indicating that chromium is a substituting constituent of the spinel lattice. In contrast with these findings, in the commissioning phase of Westinghouse PWR plants high concentrations of very fine crystalline particles rich in nickel were observed, indicating a rapid initial metal release from the Inconel 600 steam generator tubing material, which is characterized by a high nickel content of about 70% (Bridle et al., 1989 b). When approaching the full-power operation level, the nickel content of the particles in these plants decreased from an initial 80% to about 20%, with a corresponding increase in the iron content. Frequently, zirconium and silicon were observed as impurities in the suspended particles. The existence of the substituted spinel oxides in the primary coolant is mainly stabilized by the dissolved hydrogen in the primary coolant. At H_2 concentrations below 20 ml (STP)/kg, Fe_2O_3 becomes the thermodynamically stable species; as a consequence of the extremely low solubility of this compound, such a conversion can lead to an enhanced formation of deposits on the fuel rod surfaces, where oxidizing conditions may first occur due to the radiolytic O_2 formation.

As yet, no generally valid relationship between the concentration of the suspended solids in the coolant during undisturbed constant-load operation periods and coolant chemistry parameters has been established. In the investigations of Bridle et al. (1989 b) the lowest concentrations of the particulates were observed during the stretch-out phase of a plant, that means in the absence of boric acid and at a coolant pH of about 7.4. On the other hand, high concentrations of suspended solids were detected even at an advanced stage of operation of a plant which started operation with a comparatively low coolant pH. Likewise, the ratio of the dissolved to the non-dissolved fractions of radionuclides can vary from one plant to another and even over time in a single plant. In most cases the reasons for these variations are not fully understood, since a correlation between the current ratio and plant operation or coolant chemistry parameters is not possible. Bridle et al. (1989 b) concluded from the results of their measurements that the non-dissolved fraction increases with increasing operation time of the plant; however, the general validity of this statement seems to be questionable. But there are

also operating conditions under which the dissolved fraction of the corrosion product radionuclides is dominant: for example, this was observed during certain fuel cycles of the Borssele PWR plant, coinciding with enhanced ^{60}Co production as a consequence of the installation of Inconel fuel assembly spacers with a high cobalt content in the nickel plating (Kockx and Olijve, 1983). This divergence from the normal situation, where the overwhelming fraction of the corrosion product radionuclides in the coolant appears in the particulate state, also could not be correlated to any particular coolant chemistry conditions.

Like the fission products, the radionuclides produced in the corrosion products are removed from the primary coolant by the action of the purification system. The deep-bed ion exchange filters normally used in this system affect the dissolved Co^{2+}, Ni^{2+} etc. ions by ion exchange processes and, consequently, the purification factors are similar to those of the dissolved fission product nuclides. Suspended particles of corrosion product oxides can be removed from the coolant purification flow by mechanical filtration. They are also retained on the ion exchanger bed, with mechanical filtration supported by van de Waals adhesive forces being assumed to be the main retention mechanisms; however, the purification factors for the non-dissolved species are comparatively low (compared to that of the dissolved species), on the order of only 5 to 10. As a consequence of the deposition of suspended solids on the resin grains, the retention efficiency of the ion exchanger bed for dissolved species decreases and, after a longer period of operation of the bed, the ion exchanger material is exhausted and has to be replaced by a new charge.

However, the effect of the primary circuit purification system on the concentrations of both dissolved and suspended corrosion products in the coolant is small compared to that of the deposition of these substances onto the surfaces of the primary circuit. Different figures on the deposition velocities of the corrosion products from the primary coolant have been given; Bridle et al. (1989 b) measured deposition halftimes between 50 and 230 minutes, i. e. shorter by a factor of 2 to 7 than the halftime of the concentrations of these substances in the coolant which result from the action of the purification system; even shorter deposition halftimes have been reported by other authors. Thus, in order to improve the relative effectiveness of the purification system on the concentrations of the corrosion product radionuclides present in the coolant, the purification rate would have to be greatly increased, a measure which, however, is limited by technical difficulties associated with the depressurization and cooling-down of such large mass flows. In practice, a significant increase in the purification flow rates would be possible only with high-temperature filtration, e. g. by using an electromagnetic filter (see Section 4.4.3.5.).

The results and conclusions which were reported above are related to the conditions prevailing in the primary circuit during constant-load operation of the plant. In the course of a shutdown of the plant a considerable increase in the concentrations of the corrosion products in the coolant is observed, involving both the radionuclides and the non-radioactive element concentrations, leading to peak values which are higher by 2 to 3 orders of magnitude than the concentrations during the preceding constant-load operation. The magnitude and the duration of this spike can differ considerably from plant to plant and from one shutdown to the next

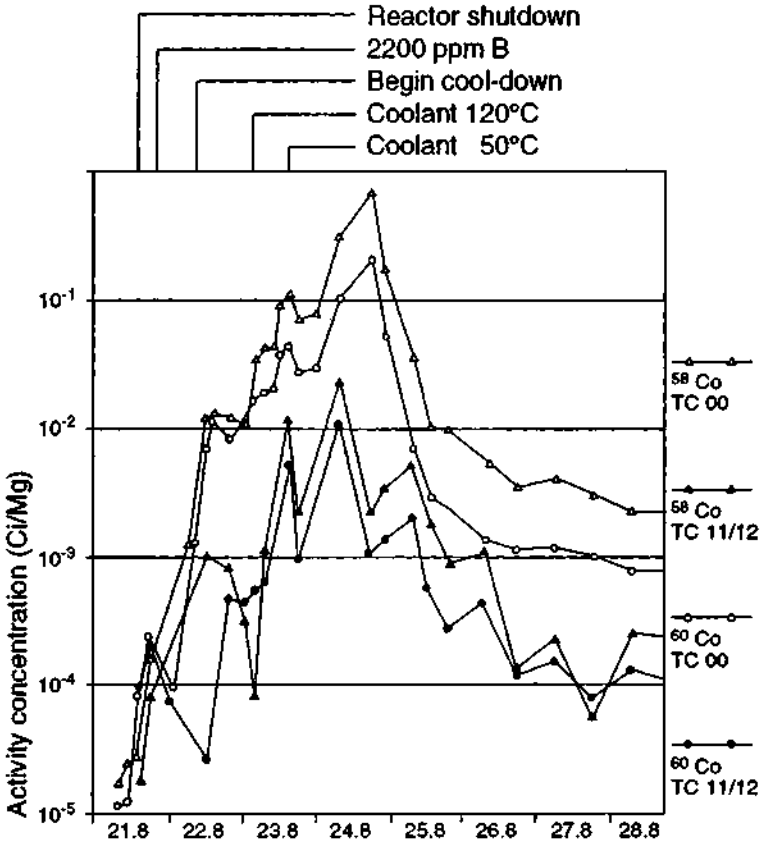

Figure 4.35. Activity concentrations of ^{58}Co and ^{60}Co in PWR primary coolant during plant shutdown
(By courtesy of Siemens/KWU)

one. Obviously, these parameters depend on the mode of shutdown, as different paths during this phase can have different effects on the stability of corrosion product deposits. In Fig. 4.35. such a corrosion product spiking is examplarily shown; in this diagram one can see a series of maxima of corrosion product activity concentrations which can be correlated to specific operating procedures in the plant. In general, the time sequence of the corrosion product spiking is fundamentally different from that of the iodine and cesium isotopes described in Section 4.3.1.2., indicating different mechanisms. Detailed measurements performed by different investigators have shown that the first spiking usually occurs during hydrogen removal from the coolant; in this period, the dissolved and the non-dissolved species behave quite similarly and the specific ^{60}Co activity does not change significantly. A second spiking occurs immediately after reactor shutdown and boration of the coolant; the resulting peaks decrease rapidly, probably due to deposition of the particles. The subsequent reduction of the coolant temperature gives

rise to a drastic increase in the concentration of dissolved corrosion product radionuclides in the coolant. This increase starts when the coolant temperature drops below 130 to 150 °C; simultaneously, a significant increase in the specific ^{58}Co and ^{60}Co activities and in the $^{58}Co : ^{60}Co$ activity ratio can be observed. Some authors (e. g. Beslu et al., 1982) have reported that upon aeration of the coolant the increase in coolant activity is stopped and is followed by a decrease which sometimes corresponded to the circuit purification rate; in other cases, a faster decrease of the activity concentrations was observed.

According to the investigations reported by Comley et al. (1989), such power transients increase the concentrations of particles in the coolant by two to three orders of magnitude. The results of their studies showed that the faster the change of reactor load, the higher the peak values of the particle concentration; they typically involve 10^6 particles per litre, which is equivalent to about 1 g/Mg or several hundred grams of suspended crud in the circulating coolant. Redeposition of the particles mobilized by the transient proceeds comparatively fast and apparent halftimes of the concentrations between 50 and 230 minutes were measured; continued disturbances of the system may prolong the redeposition process. Since the purification halftime typically is on the order of 8 to 16 hours, its impact on particle removal during the spike seems to be small. Particles which were retained in the ion exchanger resin bed during constant-load operation are only loosely held there, so that they can also contribute to transient releases to the coolant. From the comparatively short deposition halftime it can be concluded that the bulk of the mobilized corrosion products is deposited onto the surfaces of the primary circuit, potentially increasing the contamination level, in particular in low-flow regions. The significance of this contribution to the total contamination level cannot be quantified; however, it can be assumed that it is small compared with the level caused by the contamination process during constant-load operation of the plant.

Obviously, the effect of shutdown spiking is caused by a resuspension of corrosion products that had been deposited in the primary circuit during the preceding constant-load operating phase. It is, therefore, of considerable interest to learn from what location these corrosion products are mobilized and distributed over the whole primary circuit, whether from inside the reactor pressure vessel or from the out-of-RPV primary circuit surfaces. Most of the results obtained by different investigators indicate that the mobilized substances originate from the reactor pressure vessel, where they had been deposited during the preceding operation phases. This is demonstrated, firstly, by the spiking behavior of the short-lived ^{56}Mn, which during shutdown shows an increase in activity concentration in the coolant that is virtually identical to that of the longer-lived radionuclides (see Section 4.4.3.2.); secondly, by the enhanced $^{58}Co : ^{60}Co$ activity ratio; and, finally, by the substantial increase in the ^{60}Co element specific activity. According to measurements reported by Anthoni et al. (1989), the ratio ^{60}Co : Co increases from 7 GBq/g to 20 GBq/g at hot shutdown and, further, to 60 to 120 GBq/g in the course of temperature reduction from 286 to 90 °C, reaching about 300 GBq/g during aeration of the coolant at 70 °C. Afterwards, these values decrease again. Similar results were measured at German PWR plants and were confirmed on the whole by the results of the experiments conducted by Bridle et al. (1989 b) at Belgian plants. Thus, the

main source of the shutdown spiking effects are the oxides located during constant load operation inside the reactor pressure vessel, comprising both deposited corrosion products as well as oxide layers which had developed on the surfaces of the materials due to corrosion. Corrosive attack on metallic materials such as the electroplated nickel layer on the Inconel spacer grids has also been suspected as a significant source (Anthoni et al., 1989). The high specific ^{60}Co activity indicates that these substances had a comparatively long residence time in the neutron field and/or that there was less dilution of the activated species by freshly formed, non-radioactive corrosion products, as compared to the situation during constant-load operation. Only in the final stage of shutdown, when the steam generators are drained and the primary coolant level is lowered to the main coolant pipe mid-level, do corrosion products with a reduced specific ^{60}Co activity appear in the coolant, suggesting that they originate from the steam generator region.

It can be assumed that the changes in thermal-hydraulic conditions in the primary circuit which occur during plant shutdown effect a resuspension of loosely deposited corrosion product oxides, but they cannot be the reason for the significant increase in the dissolved fraction, in particular of ^{58}Co and ^{60}Co, which is regularly observed in the course of the shutdown spiking. This effect can only be initiated by chemical reactions, and there are various changes in coolant chemistry conditions occurring during the shutdown period which may potentially affect the state of the corrosion products. Usually, the initial hot alkaline–reducing environment changes to an acidic–oxidizing one in the cold state. However, the change in coolant chemistry conditions depends strongly on the shutdown procedure applied, in particular on the time sequence of the steps hydrogen removal – addition of boric acid – temperature reduction; thus, when hydrogen removal is delayed, cooldown may convert the initial alkaline–reducing environment temporarily to one that is acidic but still reducing.

During the shutdown procedure, boric acid is added to the primary coolant up to a concentration on the order of 2000 ppm to guarantee sub-criticality of the reactor core in the cold state. In addition, the degree of polymerization of boric acid decreases with decreasing temperature of the coolant and its degree of dissociation increases. Both effects result in a shift of the coolant pH to lower values, around 4 to 5. On the other hand, upon hydrogen removal, which is conducted prior to the shutdown, radiolytic H_2O decomposition leads to a buildup of the oxygen concentration in the coolant; the aeration of the primary circuit following temperature reduction represents an additional step in the direction of oxidizing conditions. This change from reducing to oxidizing coolant conditions may lead to an enhanced solubility of the oxides (Rummery and Macdonald, 1975). Mäkelä et al. (1989), using an on-line chemistry system for measuring pH_T and redox potential at primary coolant operating temperature, reported a change of both figures during a reactor shutdown; in parallel to the decrease of the coolant pH to values of about 4, the redox potential increased from about −0.7 V (SHE) to about −0.4 V.

Nonetheless, it seems highly unlikely that these comparatively small changes in pH and redox conditions of the coolant would be able to effect a rapid and extensive dissolution of the corrosion product oxides, which normally are quite resistent

even against mineral acids. These doubts raise the question of whether the increase in the dissolved fraction, in particular of ^{58}Co and ^{60}Co, reflects a true dissolution of the oxides or only a desorption of the cobalt radioisotopes which during constant load operation were attached to the surfaces of the suspended oxide particles merely by adsorption. According to the results shown in Fig. 4.33. concerning the dependence of Co^{2+} adsorption onto magnetite surfaces on the solution pH, one has to expect a strong dependence in particular in the pH range 6 to 7.5, which might be an explanation for the pronounced increase in Co^{2+} dissolved concentrations during cooling down and boration of the coolant. Finally, it cannot be ruled out completely that the steep increase in the dissolved ^{60}Co concentration in the primary coolant during shutdown is in part caused by sampling effects. As was discussed in Section 4.4.2., dissolved radionuclides are retained in the hot sections of the sampling lines, with the extent of retention depending on the boric acid concentration in the coolant, among others. Thus, it seems possible that during shutdown ^{60}Co that was previously adsorbed on the inner surface of the sampling system is dissolved again, contributing to the enhanced concentration of dissolved ^{60}Co species in the sample taken; however, it is generally assumed that this contribution is comparatively small.

Dobrevski and Winkler (1992) have tried to explain the corrosion product shutdown spiking by a hideout–return effect. According to their hypothesis, a dynamic layer of colloidal corrosion products is formed during steady-state operation at the hydrodynamic boundary layer between the coolant flow and the surfaces of the fuel rods. This layer is stabilized by heat flux and electrophoretic forces. Dissolved corrosion product ions are fixed to the charged surface of the colloids. Following reactor shutdown, this layer is assumed to collapse under dispersion of the colloids and ions to the coolant. In the course of reactor startup, the dynamic layer is restored again, resulting in a rapid removal of the startup spiking by a hideout effect. There is, however, no detailed evidence for such effects; in addition, the observed time behavior of the spiking is different from that which would be expected according to this hypothesis.

In the course of the startup of a PWR plant after a shutdown period, a sharp increase in the concentrations of non-radioactive and radioactive corrosion products in the primary coolant is observed, with the details of this spiking also showing considerable variation from plant to plant and, within one plant, between startups. Often the first concentration maximum of the particulate corrosion products can be correlated with the start of operation of the main coolant pumps and, thus, can be explained as a whirling up of previously deposited substances. Spiking of the dissolved radionuclides occurs some hours later when the temperature of the primary coolant has been raised to about 120 °C, i. e. to the same temperature region where the spiking of these radionculide species during plant shutdown is observed. When the coolant temperature passes above 150 °C and removal of boric acid from the primary coolant begins, the concentrations of all radionuclides decrease rapidly to the lower steady-state values. As yet it is not known whether these corrosion products are then deposited inside or outside the neutron field. No clear correlation was observed between the magnitude or the radioactivity inventory of the shutdown spiking and that of the subsequent startup spiking. However,

it has to be assumed that the startup spiking also adversely affects the contamination level of the plant, even when quantitative estimates cannot be given at this time.

4.4.3.4 The deposition of radionuclides on the surfaces of the primary circuit

During the initial hot trial operation period of the plant, prior to the start of nuclear operation, a thin and tightly adherent oxide layer is generated on all primary circuit surfaces wetted by the hot primary coolant; in a PWR, these layers mainly consist of a mixed spinel oxide with iron as the main constituent. In the course of nuclear operation, radionuclides being carried in the coolant are incorporated into these layers. They are the origin of the buildup of radiation dose rates in the areas surrounding the primary circuit piping and components. In light water reactors, these contaminating radionuclides only appear in the surface oxide layer; diffusion into the underlying base material, as is observed to a certain extent e. g. in liquid-metal cooled reactors, does not proceed to any measurable extent, mainly because of the comparatively low temperatures the material is exposed to during plant operation. The presence of traces of ^{60}Co in the base material on the order of 1 Bq/g and less, which was sometimes reported from older plants, was not caused by operational plant contamination, but originated with the formerly employed radiometric control of steel melting, in which this radionuclide was used as a monitor. A production of radionuclides by activation of the base material is only to be expected in areas near the neutron field, i. e. inside the reactor pressure vessel. Delayed neutrons which are emitted by fission products in the coolant are not able to induce a measurable ^{60}Co production in the materials of the primary circuit outside the reactor pressure vessel, because of their very low flux density.

The radionuclides incorporated into the oxide layers, which lead to a radiation field in the surrounding area, are mainly the activated corrosion product nuclides, above all ^{60}Co and ^{58}Co. Out of the fission products present in the primary coolant during plant operation with failed fuel rods in the reactor core, iodine and cesium isotopes are not deposited into the surface oxide layers; this reactor experience is consistent with the general chemical properties of these elements which do not allow the formation of insoluble compounds under the prevailing conditions (with the sole exception of AgI, see Section 4.3.3.1.2.). On the other hand, fission product elements that are able to form insoluble compounds (such as oxides, hydroxides or ferrites) in the primary coolant are incorporated almost quantitatively into the contamination layers (see Section 4.3.3.1.4.). However, because of the usually low concentrations of polyvalent fission products in the primary coolant, only in very rare cases will these radionculides make a measurable contribution to the total contamination level; for this reason, they will not be treated in this context.

When looking for measures to minimize contamination buildup, one of the important questions involves the mechanisms controlling the deposition of the radio-

nulides onto the primary circuit surfaces to form a thin and very tightly adherent layer. At first sight, the most obvious explanation seems to be a deposition of suspended particles from the coolant to the walls, according to the mechanisms discussed above in Section 4.4.3.2. However, all the experience with operating PWR plants demonstrates that this explanation cannot be correct, since the observed increase in the activity burdens on the surfaces of the materials is not accompanied by a corresponding increase in the thickness of these oxide layers, which remains virtually constant from the beginning of plant operation for many operation cycles. On the other hand, the concentration of radionuclides in these surface layers increases steadily during the first fuel cycles, reaching a steady-state value that remains nearly constant during the course of further operation. Occasionally, the equilibrium radionuclide loading of the oxide layers changes to a higher or, in rare cases, to lower value, a behavior that frequently coincides with a change in the steady-state concentration of the corrosion product radionuclides in the primary coolant.

This experience indicates the existence of an exchange equilibrium of cobalt radionuclides between the primary coolant, on the one hand, and the oxide layers on the other. A better understanding of the mechanisms controlling these exchange reactions might make possible a reduction or at least a delay in contamination buildup; if the deposition rates of the radionuclides could be significantly reduced, their removal from the coolant by the action of the primary circuit purification system would gain in importance. For this reason, numerous investigations have been devoted to this topic, including both basic laboratory research and analyses of oxide layers taken from the components of operating PWR plants. In order to give an idea of the current state of knowledge in this area, some of these studies will be exemplarily discussed in what follows.

One of the most extensive studies in this field was carried out by Bergmann et al. (1983), who analyzed steam generator tube sections from a number of Westinghouse PWR plants (all equipped with Inconel-600 tube material), not only by nondestructive γ-spectrometric and autoradiographic analyses, but also by detailed physical and chemical studies of isolated oxide layers (concerning the isolation techniques employed see Section 4.4.2). As a general result of these investigations, it was reported that the linear sections of the tubes in an individual steam generator, reaching from the tube sheet to the U-bend, show a homogeneous distribution of the radionuclides, within a range of $\pm$ 20%; in the U-bend itself, the area-related radioactivity is higher by a factor of about 2 than in the linear sections of the tube, probably due to a geometric effect which is well known from other components (see below). Likewise, different tubes in one steam generator exhibited differences in activity loadings of only $\pm$ 20%. By autoradiographic examination of the surfaces of the tubes, an almost homogeneous distribution of radioactivity was determined; in addition, some radioactivity hot spots of unknown origin were detected, possibly associated with boric acid crystals. However, the activity burdens on steam generator tubes from different PWR plants which experienced operating periods between 0.5 and 9 effective full power years (EFPYs) showed pronounced differences; in spite of these variations, a steady increase in ^{60}Co loading of the surface layers during the first 3 to 4 EFPYs was observed in all the plants investigated.

Table 4.9. Activity loadings of various corrosion product radionuclides on the inner surface of main coolant pipes
(according to Schuster et al., 1989)

Radionuclide	Plant A		Plant B	
	Hot leg Bq/cm^2	Cold leg Bq/cm^2	Hot leg Bq/cm^2	Cold leg Bq/cm^2
^{54}Mn	nd*)	nd	$3.1 \cdot 10^3$	$1.2 \cdot 10^5$
^{58}Co	$4.0 \cdot 10^4$	$5.2 \cdot 10^5$	$4.8 \cdot 10^4$	$1.2 \cdot 10^5$
^{59}Fe	nd	$1.2 \cdot 10^4$	$1.2 \cdot 10^3$	$1.4 \cdot 10^3$
^{60}Co	$1.3 \cdot 10^4$	$1.3 \cdot 10^5$	$4.9 \cdot 10^3$	$1.1 \cdot 10^4$
^{124}Sb	$9.8 \cdot 10^3$	$5.8 \cdot 10^4$	$1.4 \cdot 10^4$	$1.9 \cdot 10^4$

*) nd = not detected

The average thickness of the oxide layers on the primary side surfaces of the steam generator tubes amounted to about 1 µm, with an average apparent density of the oxide removed of about 3.9 g/cm^3, i. e. considerably higher than the densities of the deposits removed from the surfaces of the fuel rods, which amounted to about 1.2 g/cm^3. The oxide layers on the primary circuit surfaces showed numerous cracks which roughly followed the grain structure of the base material, but which were distinctly broader than the grain boundaries of the metal. The oxide particles, which were removed from the tubes using electrochemical techniques, consisted of flakes of irregular shape showing diameters ranging from 30 µm down to a few µm. The chemical composition of the removed oxides differed from that of the base material in so far as chromium and iron were significantly enriched; the ratio Ni : Fe measured in the steam generator oxide layers amounted to about 1.0, which was significantly higher than that of typical deposits from the reactor core, where it was measured to be in the range of 0.5. The cobalt content of the oxide, in particular in the upper zones of the tubes, amounted to about 0.1 to 0.3%, being higher by about a factor of 10 than in the underlying base material. Crystallographic analyses showed that the oxide layers consisted of two different phases, metallic nickel and a mixed spinel showing the general composition $Ni_xFe_y(Co,Mn)_zCr_{3-x-y-z}O_4$; in this formula x, y and z may vary, depending on the axial position, even on the same steam generator tube.

The concentrations of radionuclides in the oxide layers differ considerably from plant to plant; as an example, data from two German PWR plants are given in Table 4.9. Plant A is equipped with Stellite hardfacing materials inside the reactor pressure vessel in the conventional manner, while the reactor core of plant B is virtually free of these materials; both plants started operation at about the same time and the measurements cited were carried out after a few fuel cycles using an on-line γ-spectrometry technique. The data show some differences in deposition behavior, the activity concentrations of the cobalt isotopes being higher in the cold leg of the main coolant pipes than in the hot leg region. According to the measurements reported by Bergmann et al. (1983), the mass-related concentrations of ^{55}Fe,

^{60}Co and ^{54}Mn, in particular in the upper zones of the oxide layers in the steam generator tubes of US PWRs, seem to decrease with increasing operating time; the same is apparently true for the element-specific activities of ^{58}Co and ^{54}Mn, but not for that of ^{60}Co (each related to the mass of the respective parent nuclide). The predominant fraction of the deposited radionuclides, in particular of ^{60}Co, is incorporated into the lower section of the oxide layer, i. e. into the chromium-rich spinel directly covering the base material.

Apparently, the amount of radionuclides (in particular of ^{60}Co) deposited on the primary circuit surfaces and incorporated into the superficial oxide layer depends on different parameters, such as their concentration in the coolant, the pH and redox potential of the coolant, the nature of the surfaces, etc. In the investigations conducted by Large and Woodwark (1989) at the DIDO Water Loop, it was possible to study a wider range of the coolant pH, as well as of the materials for the deposition coupons, than can be studied in a commercial reactor in which the operating conditions usually are restricted within narrow boundaries. According to these results, activity deposition onto the surfaces of the circuit, in particular of ^{60}Co, is higher at low coolant pH than at a higher one; however, this influence of pH on the deposition process is often complicated by radionuclides originating with former operating periods which are redistributed from their original deposition locations to other ones within the primary circuit. The extent of ^{60}Co and ^{58}Co deposition depends strongly on the nature of the base material and was shown to be comparatively low on Zircaloy, higher on Inconel 600 and highest on stainless steels. Whereas activity buildup on Inconel surfaces proceeds approximately linearily with time, the buildup rate on stainless steel surfaces decreases with time. Similar studies reported by Lister et al. (1989) revealed that ^{60}Co buildup on stainless steel surfaces usually satisfies the relationship

$$A_t = K \cdot t^{0.5}$$

where A_t is the deposited activity at time t and K is a coefficient. The results of Large and Woodwark (1989) showed that, in contrast to the cobalt isotopes, deposition of ^{95}Zr is largely independent of the nature of the base material, probably because of the plate-out of non-dissolved suspended particles of highly insoluble zirconium oxide; apparently, the sticking effects which control the deposition of such particles onto the surfaces are quite similar for the various base materials which have been investigated here. From the Swedish Ringhals 3 and 4 PWR plants, a markedly lower deposition of ^{58}Co and ^{60}Co on the Inconel steam generator tubes was reported than on the surfaces of the stainless steel main coolant piping (Gott, 1989). From these results it was concluded that the high pH coolant chemistry applied in these plants did not prevent the production of corrosion products as efficiently as it delayed the buildup of ^{60}Co on the surfaces of the primary system. Sometimes, considerable variations in the area-related activities were observed, in particular in horizontal lines, which were assumed to be due to the deposition of particulate matter from the plant shutdown spiking. According to the investigations performed in the DIDO Water Loop (Large and Woodwark, 1989), the flow rate of the coolant strongly influences the deposition of ^{95}Zr but not that of the cobalt isotopes. This difference in behavior is probably a consequence of

the different mechanisms that control the deposition of suspended solids and of dissolved ions.

According to the results of Large and Woodwark (1989), the chemical composition of the oxide layers which were formed on stainless steel surfaces in the course of the experiments did not show a pronounced dependence on the type of primary coolant chemistry applied. The outer oxide layer (i. e. on the coolant side) exhibited the composition $Fe_{2.4}Ni_{0.6}O_4$, while the inner, very thin layer (about 0.2 µm) varied over the range $Cr_2Fe_{0.75}Ni_{0.25}O_4$ to $CrFe_{1.5}Ni_{0.5}O_4$, depending on the sampling technique applied. Analyses of the oxide layers which were isolated from the surfaces by selective dissolution techniques showed that on stainless steels more than 70% of the total deposited ^{60}Co was incorporated into the inner oxide layer. Since this part of the layer is formed by growing from the base material, this observation is a strong indication that incorporation of cobalt into the oxide proceeds via dissolved ions and not by deposition of suspended particles.

As was mentioned above, the corrosion product radionuclides are incorporated into the superficial oxide layer and it can, therefore, be assumed that the extent of deposition of cobalt isotopes depends, among other parameters, on the pretreatment of the surfaces of the materials. Prefilmed surfaces apparently adsorb more ^{58}Co and ^{60}Co than surfaces which were not prefilmed (Large and Woodwark, 1989). The different prefilming conditions which were applied in these experiments did not significantly influence cobalt deposition onto Inconel surfaces, whereas on steel surfaces a prefilming at higher solution pH resulted in a higher cobalt uptake than prefilming at lower pH. Investigations reported by Pick and Roofthooft (1989) showed considerable differences in the deposition behavior of radionuclides onto the surfaces of coupons of different materials with different surface finishings which were exposed in the hot leg of a PWR steam generator channel head over a whole fuel cycle. Electropolished and electropolished/passivated Inconel 600 coupons showed a four-fold reduction in the levels of ^{58}Co and ^{60}Co compared with "as-received" Inconel. In contrast to the Inconel specimens, activity levels on the "as-received" and on the electropolished stainless steel specimens were similar, i. e. in this case a pretreatment merely by electropolishing of the surface showed no significant beneficial effect. But for the electropolished/passivated (i. e. heated to about 290 °C in air for 150 hours with a small amount of steam continuously injected during the process) stainless steel coupons, a three- to four-fold reduction in the activity levels of ^{58}Co and ^{60}Co, compared to the "as-received" surfaces, was observed.

In order to study fundamental questions concerning the mechanism of deposition of radionuclides onto the oxide surfaces, a part of the coupons emloyed in these experiments was provided with a palladium coating with a thickness of 1.5 to 2.0 µm, which was deposited by electroless plating. Unexpectedly, the total β/γ near-contact dose rates of long-lived radionuclides on these coupons were higher by a factor of 30 to 70 than on the electropolished and electropolished/passivated coupons. A more detailed γ-spectrometric analysis revealed that the ^{58}Co and ^{60}Co levels on the Pd-coated coupons were similar to each other and were higher by a factor of 6 to 8 than that on the passivated Inconel coupons and higher by a factor of 2 than that on the electropolished SS 304 coupons. In marked contrast to these

radionuclides, the levels of ^{51}Cr, ^{113}Sn, ^{110m}Ag and, in particular, of ^{125}Sb on the Pd-coated coupons were approximately three orders of magnitude higher than that on the electropolished/passivated and electropolished coupons. The lack of ^{124}Sb on the Pd-coated coupons suggested that the high uptake of ^{125}Sb was, by analogy with the uptake of ^{113}Sn, a consequence of the preferential sorption of tin isotopes. The short-lived ^{125}Sn decays to ^{125}Sb which would have remained on the coupons to be measured there. The markedly higher uptake of these radionuclides appears to be a specifically enhanced adsorption effect associated with metallic palladium; metallographic investigations of the coupons revealed no evidence of any appreciable deposition or formation of oxide on the surface of the palladium coating. However, other experiments which were performed in a test loop showed contradictory results, with the ^{60}Co deposition onto Pd-plated materials being lower by a factor of about 25 than that onto adjacent stainless steel areas which were pretreated by preoxidation and other passivation techniques (Lister et al., 1989).

Preliminary experiments on coupons which had been plated with a chromium layer and subsequently passivated by hot moist air treatment showed significantly smaller radionuclide deposition when inserted into a PWR steam generator for the duration of a fuel cycle (Asay et al, 1991 b). Other experiments with stainless steel coupons which were exposed over several fuel cycles in the hot as well as in the cold legs of a steam generator channel head showed that chromium-plated coupons exhibited very low levels of activity uptake, as ^{58}Co and ^{60}Co were in all cases lower by more than an order of magnitude than on as-received or on electropolished/passivated coupons. The addition of a passivation step after the chromium-plating treatment had a detrimental effect by increasing the uptake of activity by up to a factor of two (Pick et al., 1992).

In general, the results reported by different authors on the dependence of the deposition rates of corrosion product radionuclides on the nature of the pretreatment of the material surfaces do not show good agreement. Presumably, these discrepancies are due to differences in the details of the performance of the tests (e. g. pretreatment process, deposition testing); they reflect the fact that the essential details of the mechanisms of incorporation of radionuclides from the solution into the superficial oxide layers are not yet fully understood. On the other hand, the possibility cannot be ruled out that the nature of the superficial oxide layer plays only a minor role in the deposition of radionuclides from the solution.

The postulated equilibrium between the radionuclide concentration in the coolant and the area-related radioactivity on the surfaces of the wall materials requires a clear correlation between the concentrations of relevant radionuclides (in particular of ^{60}Co) in the coolant and the radionuclide inventory in the oxide layers, i. e. that higher numbers in the coolant will result, with a certain time delay, in higher activities in the oxide layers and vice versa. As can be seen from Fig. 4.36. (according to Marchl and Riess, 1993 a), a clear relationship exists between the average ^{60}Co activity concentration in the primary coolant over a fuel cycle and the radiation dose rate at the main coolant pipework, even when different plants with different ages and different Stellite surface areas inside the reactor pressure vessel are compared.

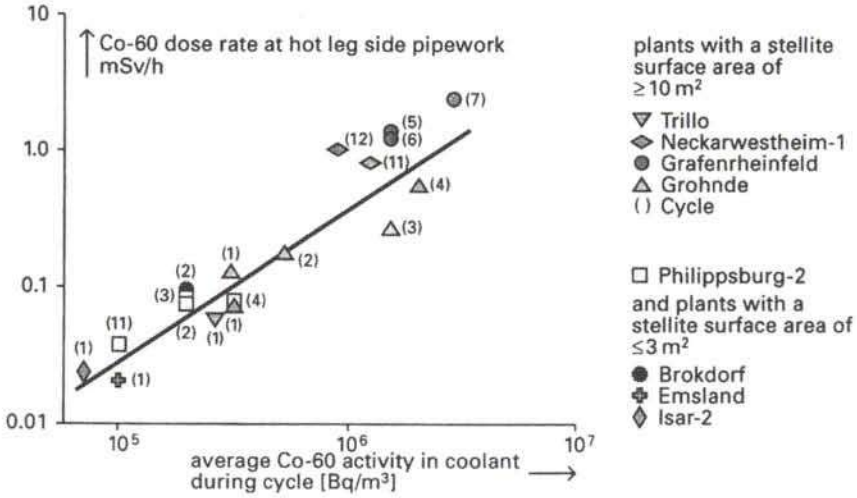

Figure 4.36. Comparison of ^{60}Co coolant activity concentrations and radiation dose rates at the main coolant pipework
(Marchl and Riess, 1993 a)

The experimental studies cited above, as well as other investigations, have yielded valuable results on the progress of contamination buildup; however, they are not able to provide detailed information on the basic mechanism of the contamination process. In this respect, two aspects are of particular interest: first, the question of whether the solid suspended particles transported in the coolant or the dissolved ions are chiefly responsible for the supply of radionuclides to the surface oxide layers and, second, the question as to the chemical state of the ^{60}Co deposited in the surface layer oxides.

Concerning the first question, there is little doubt that deposition of larger suspended corrosion product particles cannot be the predominant mechanism for contamination buildup, since in such a case the thickness of the oxide layer on the surfaces should increase parallel to the activity buildup. Some authors (e. g. Smith-Magowan, 1985; Matijevic, 1986) have assumed that colloidal particles play an essential part in the deposition reactions since they are subjected to electrochemical surface forces which control the surface reactions within a distance of several micrometers. The deposition of colloidal particles on a metal surface depends in a most sensitive way on the electrical charge of the particles and of the substrate. Thus, the most effective uptake would occur in solutions of low ionic strength, when the particles and the surface bear electrostatic potentials which are opposite in sign. Subsequently, under the influence of the hot primary coolant the deposited amorphous particles can be converted to crystalline layers; in the course of this conversion radionuclides would have the possibility of migrating into the oxide layers below. The electrochemical surface forces depend strongly on the pH and temperature of the liquid phase (isoelectric point, zeta potential) and, consequently, it should be possible to minimize the rate and extent of deposition by an appropri-

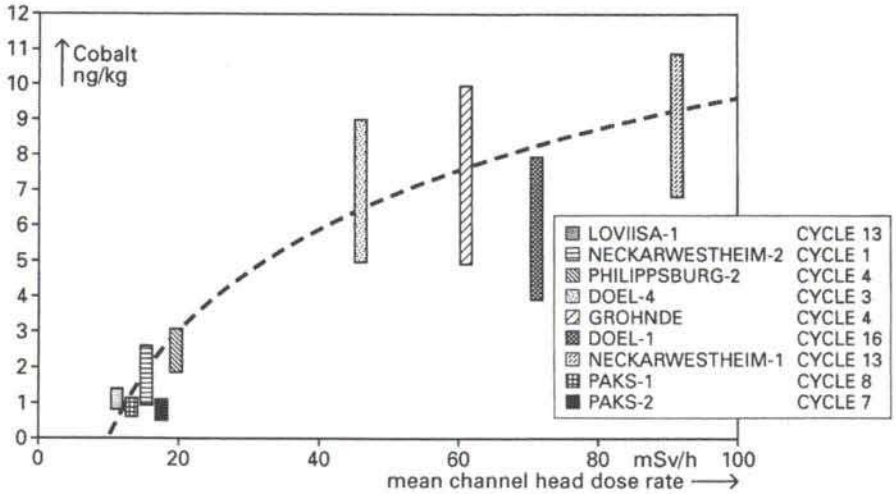

Figure 4.37. Comparison of the concentration of dissolved cobalt in PWR primary coolant with radiation dose rates in the steam generator primary channel head (Bridle and Cake, 1992; by courtesy of Thomas Telford Limited, London)

ate choice of coolant chemistry. Colloidal particles adsorbed onto the surface can be desorbed again by a change in critical parameters of the solution (flow rate, electrolyte content, pH, etc.). However, the hypothesis of colloidal particles as an important contributor to contamination buildup has not been confirmed by observations at operating plants, where different pH chemistry regimes in different plants could not be correlated with significant differences in the radionuclide burdens in the oxide films. Moreover, a deposition of significant amounts of ^{60}Co-bearing colloids should simultaneously result in an increase in the thickness of the oxide layer, quite contrary to all observations. Finally, since the coolant chemistry parameters do not change significantly during plant steady-state operation, resuspension of deposited colloidal particles would only occur to a narrowly limited extent, resulting in a steady growth of the oxide layer thickness during plant lifetime, which is also contrary to all observations.

In contrast, numerous observations from operating PWR plants strongly suggest that dissolved Co^{2+} ions (including $^{60}Co^{2+}$) is the species that enters the deposition process. As an example, the pronounced increase in the activity concentration of dissolved ^{60}Co which occurred as a consequence of high cobalt contents in fuel assembly spacer grids has been mentioned above, the direct result of which was a drastic increase in the primary circuit radiation levels (Kockx and Olijve, 1983). Apparently, the concentration of ^{60}Co in the surface oxide layer is in a dynamic equilibrium with the concentration of dissolved ^{60}Co in the coolant. This can be clearly seen from Fig. 4.37., where different plants with different operation histories, different cobalt inventories and, in addition, differences in coolant chemistry history are compared (Bridle and Cake, 1992). In spite of a considerable scatter in these data, there seems to be no doubt that dissolved $^{60}Co^{2+}$ is the species

whose concentration in the primary coolant controls the extent of ^{60}Co buildup in the oxide layers on the surfaces of the materials.

As for the deposition mechanism, it can be assumed that the first step in the deposition of Co^{2+} ions is adsorption on the surface of the oxide, corresponding to the reactions discussed by Smith-Magowan (1984). Investigations performed by Bosholm et al. (1978, 1981), Hoffmann and Bosholm (1984), Schlenkrich (1985) and others have indicated that this initially reversible fixation of Co^{2+} ions on the magnetite surfaces changes rather quickly into an irreversible one, with the degree of irreversibility depending on pH, temperature and cobalt concentration. At 250 °C, cobalt deposition increases steeply above pH 4 and reaches a maximum at pH 7 to 8, where the irreversibly bound fraction amounts to about 90%; at lower temperatures, deposition is shifted to higher pH values and reaches only a significantly smaller irreversibly bound fraction. Increasing Co^{2+} concentrations in the coolant result in a shift of the deposition maximum to lower pH values and in a decrease of the deposited fraction, but in an increase in the absolute amount of deposited cobalt. The rate of deposition, expressed in terms of a deposition constant, does not significantly depend on the solution pH in the range 5 to 9. In general, deposition starts at a solution pH at which species of the first hydrolysis product of the dissolved metal ions appear, reaching its maximum value at their maximum concentrations. This behavior, apparently, cannot be explained by the formation of the insoluble compound $Co(OH)_2$, since the Co^{2+} concentrations present in the solution are too low to exceed the solubility limits.

As was mentioned above, the major fraction of the deposited ^{60}Co is incorporated into the lower zone of the oxide layer, i. e. into the oxide layer which grows on the surface of the base material; this behavior can be judged to be an additional indication of a deposition process initiated by dissolved ions. On the other hand, the incorporation of cobalt atoms into the crystal lattices of the oxides apparently depends strongly on the existing crystal structure. Crystal field calculations reported by Lister (1992) yielded that normal spinels, such as the chromites, incorporate cobalt into tetrahedral sites with favorable site-preference energies; inverse spinels, such as the ferrites, incorporate cobalt into octahedral sites with less favorable energies. The chromium content of the oxide, therefore, is a highly important parameter, since it controls the corrosion rates by promoting protective films, but also favors incorporation of cobalt within those films. Zn^{2+} shows also a high site-preference energy in spinels, competing therefore with Co^{2+} for the available sites and, potentially, inhibiting cobalt uptake by those films.

Other studies have indicated that nickel, which is incorporated into the superficial oxide layers on Incoloy 800 steam generator tubes, is present there in the form of neutral atoms. Schuster et al. (1988) analyzed contamination layers from different PWR plants using AES and XPS techniques; their results showed, besides an almost homogeneous ^{60}Co distribution over the whole thickness of the oxide layers, that they consist of a Cr-Fe spinel in which, with the exception of the uppermost regions (some nanometers), nickel is exclusively present in its atomic state and not as a chemically bound constituent of a nickel ferrite. The existence of Ni^{o} under the conditions prevailing in the PWR primary circuit can be explained by thermodynamic causes. By analogy, it seems justifiable to assume that cobalt

(whose concentrations in the oxide are by far too low to be detected by the techniques mentioned above) is also present in its atomic state. To be sure, cobalt ferrites are reported to show a higher degree of stability against reduction than nickel ferrites; however, there the question still remains as to the impact of the large differences in concentration between cobalt and iron on the stability of the cobalt compound. Similar observations were reported from VVER reactors using $NH_4OH-KOH$ water chemistry; upon addition of hydrazine, the redox potential of the coolant should be sufficiently negative to keep cobalt traces in the Co^o state (Pashevich, 1992). It can be assumed that Co^o shows a higher mobility in the oxide layer than cobalt that is chemically incorporated into the lattice of the substituted spinels, presumably due to the possibility of oxide grain boundary diffusion. This would explain the observed release of cobalt once incorporated in the oxide back to the coolant without congruent dissolution of the spinel.

Thus, in the system coolant – oxide layer the Co^{2+} ions are subjected to an adsorption–desorption process leading to a cobalt concentration in the oxide layer on the surface of the materials which is controlled by the cobalt input into the coolant. In the case of very low or zero cobalt input, the cobalt concentration in the oxide (and, simultaneously, the ^{60}Co activity concentration) decreases steadily according to a power-law decline (Lister, 1992). As yet it is not known whether the release of chemically bound cobalt from the chromites would be fast enough to explain the observed processes or whether the above-mentioned oxide grain boundary diffusion of Co^o is the rate-controlling process.

Prior to a planned shutdown of a PWR plant, hydrogen is removed from the primary coolant which, as a consequence, becomes slightly oxidizing for a short period of time, changing the environmental conditions of cobalt deposition. Laboratory investigations have shown that from a slightly oxidizing coolant ^{60}Co is adsorbed onto the oxide layers on stainless steel at a higher rate than from a reducing coolant (Allsop et al., 1992). This behavior is assumed to be due to a change in the structure of the oxide layer from the ferrite structure in direction of a chromium-containing hematite structure. However, because of the comparatively short duration of the phase of oxidizing coolant it seems highly questionable whether this effect contributes significantly to contamination buildup.

Frequently, enhanced contamination levels are observed downstream from pipe bends and geometric discontinuities, for example in the region of the beginning of the main coolant piping at the outlet of the steam generator primary channel head; with increasing distance from the bend or from the discontinuity, the contamination levels decrease steadily until they again reach a steady-state value. The cause of this effect is of hydrodynamic nature, the effect itself does not contradict the above-mentioned postulate of the dominating role of dissolved ^{60}Co species in contamination buildup. In straight-line pipe sections, the laminar boundary layer of the coolant flow becomes more and more depleted of radioactive nuclides, due to their deposition onto the surfaces of the walls; thus, the rate of deposition of radionuclides is controlled by the rate of their supply from the bulk of the coolant, with the boundary layer acting as a diffusion barrier. Downstream from a discontinuity, however, the coolant flow becomes more turbulent and the thickness of the laminar boundary layer decreases, resulting in an accelerated supply of radionu-

clides to the boundary layer and in an enhanced contamination level, until the depleted boundary layer is established again.

To summarize the different findings which have been discussed above, it can be stated that the two main features in LWR contamination buildup: (a) time-constant thickness of the oxide layer covering the primary circuit surfaces; and (b) increase in the radionuclide concentration in these layers up to a saturation level that remains virtually constant over longer time periods, can be explained by the following mechanism: $^{60}Co^{2+}$ ions (as well as $^{58}Co^{2+}$ ions) which are carried in the coolant travel through the laminar liquid boundary layer to the surface of the materials at a rate which is diffusion-controlled. There, in the first step, they are adsorbed onto the reactive sites of the oxide and, in an adsorption-desorption equilibrium, a fraction of them might be released again to the liquid. The remainder will move into the lower regions of the oxide layer, to be incorporated there into the oxide in a chemical state which is not yet definitely known. Simultaneously, cobalt atoms already present in the oxide layer are released to the coolant. In the initial stages of plant nuclear operation, only ^{59}Co atoms are released from the oxide layer; with increasing ^{60}Co concentration in the oxide, the re-released ^{60}Co fraction increases until a ^{60}Co deposition–release equilibrium is established which shows identical rates of deposition and release, resulting in an activity concentration (and radiation dose rate) which is constant over time. Suspended oxide particles, including the ^{60}Co attached to them, do not directly participate in the deposition process; they are a potential reservoir from which adsorbed $^{60}Co^{2+}$ can be supplied to the coolant according to an adsorption–desorption equilibrium.

If this description is correct, then minimum cobalt solubility in the coolant would be an important parameter since it reduces the concentration of the cobalt species that are available for incorporation into the oxide surface layer. However, in this context, it has to be emphasized that the chemistry regime which effects minimum concentration of dissolved cobalt in the coolant is not necessarily identical with that of minimum solubility of the bulk of the corrosion products. As yet, there is no detailed information on the conformity (or the lack of conformity) of these two figures and, therefore, on the nature of optimum coolant chemistry.

4.4.3.5 Possible countermeasures against contamination buildup

From the different topics discussed in the preceding sections it can be concluded that there are different possible ways of keeping the buildup of primary circuit contamination low or of reducing already existing contamination levels. Their common aim is to keep the production of radioactive cobalt isotopes low and/or to minimize the transport of the radionuclides produced from the reactor pressure vessel to other regions of the primary circuit and, in addition, to minimize their plate-out on the surfaces there. Because of the importance of low radiation levels for an undisturbed operation and maintenance of the plants, different measures have been attempted with quite varying success.

Table 4.10. Substituted Stellites in the reactor pressure vessel of KKP-2 and Konvoi plants (Rühle and Riess, 1989; by courtesy of Thomas Telford Limited, London)

Component	Amount	Gross Area	Substitute
Alignment pins etc	244	$0.8\,m^2$	Cr_3C_2/CrNi-binder
Grid plate centering bolts	4	$0.08\,m^2$	Fox Antinit Dur 300
Hold down plates upper core support	112	$0.24\,m^2$	Fox Antinit Dur 300
Centering bolts upper core support	4	$0.04\,m^2$	Fox Antinit Dur 300

To evaluate the effectiveness of the individual measures, a ranking of the problems to be dealt with was established by Amey and Johnson (1990), according to which the highest priority is to exclude high-cobalt alloys from the primary circuit and, in particular, from the region of the reactor core; further reduction of the cobalt trace contents present in the materials of the steam generator tubing, the pipe wall steel etc. seems to be of lesser significance. As a second priority, the large quantities of corrosion products generated during commissioning of new plants should be removed from the primary system as completely as possible prior to start of nuclear operation. Pretreatment of the primary circuit surfaces is given third priority. Besides these measures in the design and the operation of the facility, maintaining of optimum chemistry conditions is of great importance; in this regard, they recommend operation at a coolant pH of 6.9 to 7.4. Finally, when all these measured have failed, decontamination of the whole primary circuit or of parts of it has to be envisaged (see Section 4.5.).

When considering the applicability of one or of several of the above-mentioned measures, one has to distinguish between two completely different situations. The first is when a new plant is to be designed and constructed; the second relates to plants which have already been in operation for a shorter or longer period of time. In the first-mentioned case, the most effective way certainly is the proper selection of the materials to be used, in order to reduce the cobalt inventory of the primary circuit as far as possible; in particular, the high-cobalt materials inside the reactor pressure vessel should be dropped in favor of substitute alloys of equal quality. In the second case, on the other hand, replacement of such materials is only rarely feasible (e. g. in the course of a replacement of components), so that other measures have to be taken into account.

Early on, Siemens/KWU started work to replace the Stellite hardfacing materials by new materials of equal or superior quality, which did not contain cobalt either as a main or a side constituent. With regard to their priority, the components to be equipped with the substitute materials were divided into three categories: Group 1 included those components located permanently in the neutron field, Group 2 the components of the primary system located outside the neutron field and, finally, Group 3 the components in the auxiliary systems. There is no doubt that replacement of Stellite materials in the components belonging to group 1 will give the highest effect in dose rate reduction. The new hardfacing materials were first applied in the Philippsburg-2 plant (KKP-2) to replace the Stellites located inside the reactor pressure vessel; in Table 4.10. the replaced Stellites are listed,

Table 4.11. Primary circuit materials and areas
(Schuster et al., 1989; by courtesy of Thomas Telford Limited, London)

Component	Material	Area (m^2)		Co ratio*
		KWG	KKP-2	KWG : KKP-2
Outside RPV				
Steam generators	Incoloy 800	20,512	20,612	1.63
Main coolant pumps	Stellite 6	2.92	1.04	2.81
Inside RPV				
RPV cladding	Austenite	2610	2610	0.99
Hardfacing surfaces	Stellites	1.534	0.054	35.7

* based on areas and cobalt analyses of materials

together with their gross surface areas and their substitute materials. Table 4.11. shows a comparison of the cobalt content in the primary circuit materials between KKP-2 and the Grohnde plant (KWG), which was the last German PWR equipped with the once normal amount of Stellite materials. From these data, cobalt input values for the primary coolant were calculated using two different sets of release rate data; as can be seen from Fig. 4.38., the measures taken in KKP-2 (plant C) have reduced the annual cobalt input to the primary coolant by 46 to 65% (depending on the metal release rates assumed) as compared with the KWG plant (plant B). The saving of ^{60}Co input to the primary coolant is still more pronounced, due to the almost complete removal of the Stellites inside the reactor pressure vessel; this effect becomes particularly evident when the ^{60}Co activity concentrations in the primary coolant are compared (see Table 4.8.), showing a significant reduction of ^{60}Co in the Phillipsburg-2 plant compared with the Grohnde plant (e. g. Jacobi and Rühle, 1987).

In the Konvoi plants following KKP-2, the Stellites located at the main coolant pumps were included in the replacement program; likewise, the materials of the valves were also taken into account, thus removing Stellite almost completely from the primary circuit. The impact of these measures on the activity concentrations of the cobalt radioisotopes in the primary coolant can be clearly seen from Fig. 4.39., showing that on the average the activity concentration of ^{60}Co is reduced by about a factor of 10 (^{58}Co reduction is mainly due to the replacement of the Inconel spacer grids in the fuel assemblies, see below). This decrease in ^{60}Co concentration in the primary coolant is a direct result of the reduction of the cobalt sources and not of an enhanced purification or deposition effectiveness. In particular, the reduction of the ^{60}Co activity concentration is due to a preferential decrease in the non-filtrable "dissolved" fraction (the average difference between both plants is about a factor of 40), which, as was mentioned above, is assumed to be mainly responsible for contamination buildup.

Similarly, the consequences of the replacement of the high-cobalt bearing materials on the ^{60}Co activity levels in the oxide surface layers of the primary circuit

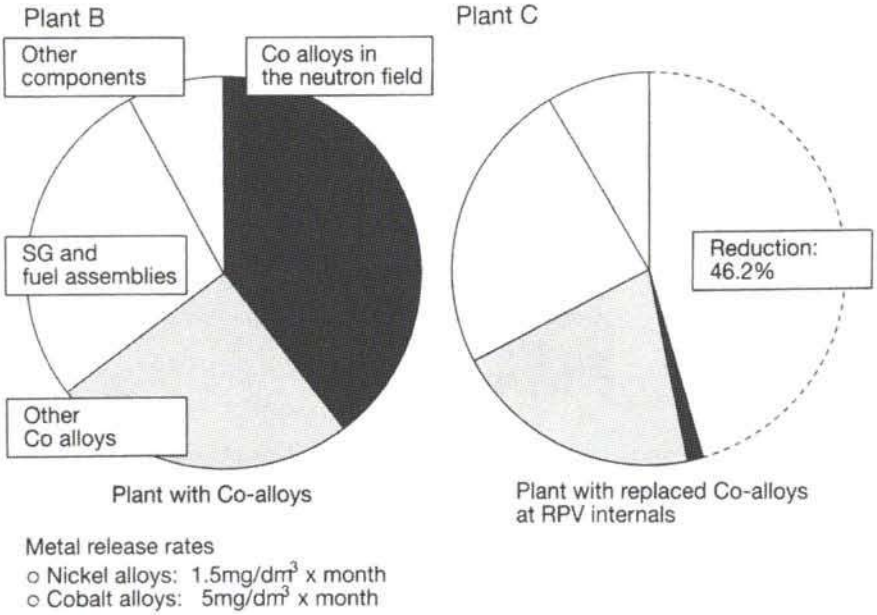

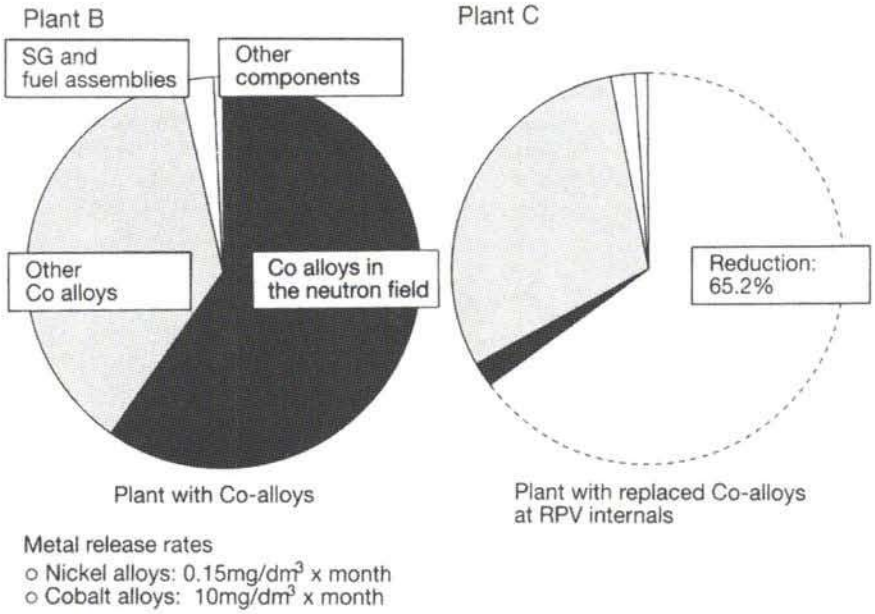

Figure 4.38. Sources and reduction of cobalt input
(Schuster et al., 1989; by courtesy of Thomas Telford Limited, London)

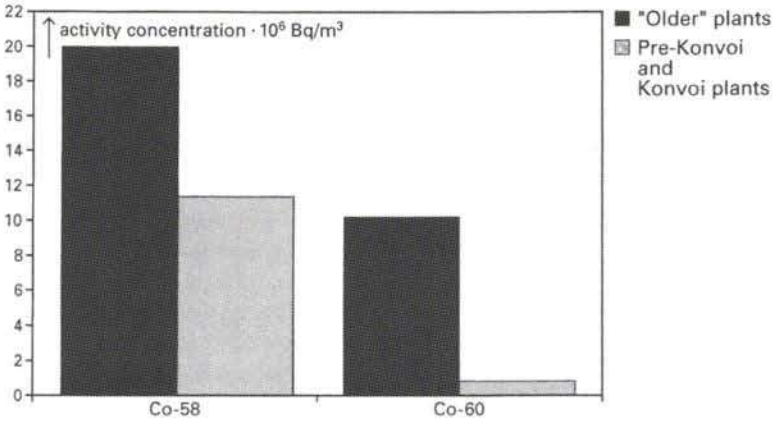

Figure 4.39. Influence of the material concept on the activity concentrations of ^{58}Co and ^{60}Co in the primary coolant of Siemens PWRs
(Marchl and Riess, 1993 b)

(see Table 4.9.) and, in turn, on the radiation dose rates at the main coolant piping are very impressive, as can be seen from Fig. 4.40. When comparing plants B, C, and E (which have all employed the same primary coolant chemistry, the "modified" Li/B chemistry), a significant reduction of the radiation dose rates can be recognized at plants C and E, in which the cobalt replacement program was performed. On the other hand, the development of the dose rates in plants C and E shows almost no difference; given that at plant C only the Stellites inside the reactor pressure vessel were replaced (about 11% of the total Stellite inventory of the primary circuit), whereas in plant E about 84% of the Stellite inventory of the primary circuit was replaced, there is a strong indication that by replacing cobalt

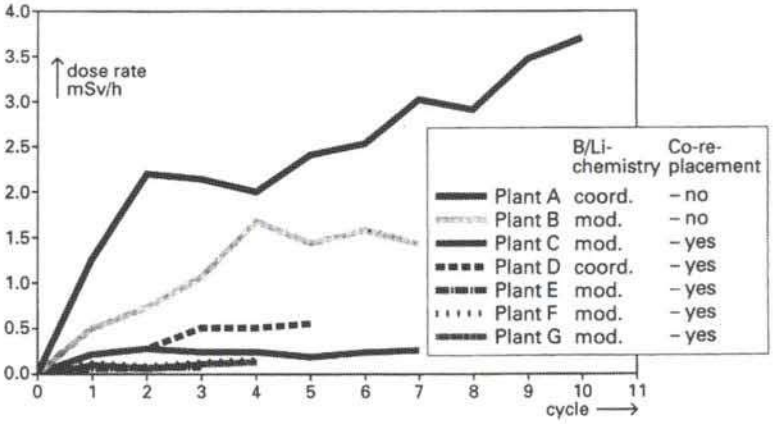

Figure 4.40. Dose rate development at main coolant piping of seven Siemens PWRs
(Marchl and Riess, 1993 b)

alloys in the core internals the main contributors to dose rate buildup have already been removed (Marchl et al., 1992). Since all the plants shown in Fig. 4.40. are equipped with Incoloy-800 steam generator tubing of identical quality, the data clearly demonstrate that corrosion products originating from the steam generator materials play only a small part (if any) in the process of contamination buildup. As for the higher radiation levels measured in plant C during its first fuel cycles, it has to be mentioned that there have been some problems with ^{124}Sb contamination (see Section 4.4.3.7.).

The highly beneficial effect of Stellite replacement in the newer Siemens PWRs was confirmed by a comparative study performed by Garbett (1992). In this study it was emphasized that cobalt impurities in the primary circuit materials are only minor contributors to the radiation fields in the areas surrounding the piping, components and systems.

Direct γ-spectrometry measurements performed on the plant piping and components, as well as radiochemical analyses of samples taken from contamination layers (Schuster et al., 1989), have confirmed that the reduction in the radiation levels is due to a decrease in the ^{60}Co concentration in the oxide layers and not to a reduction of the layer thickness.

The significance for the contamination buildup of replacing the Inconel fuel assembly spacer grids by ones made of Zircaloy (which is quite favorable from the perspective of neutron economy) is judged differently by different authors, as was discussed in Section 4.4.3.2. In the first place, the Inconel spacers are a main source of ^{58}Co and, consequently, replacement will result in a significant reduction in the amount of ^{58}Co which is plated out onto the steam generator tubes (Beslu et al., 1989 b). In their survey studies of a number of Westinghouse-designed plants, Bergmann and Perock (1992) as well as Polley et al. (1994) mentioned that plants with Zircaloy fuel assembly grids showed markedly lower radiation dose rates in the steam generator primary channel head than plants with Inconel grids (all plants investigated operated at $pH_{(300)}$ 6.9 "coordinated" coolant chemistry regimes). According to Garbett (1992), ^{58}Co production showed no particular trend from plant to plant when Stellite was reduced. From this study it was additionally concluded that ^{58}Co contributions to the dose rates were reduced upon replacing Inconel 718 spacer grids by those made of Zircaloy, thus confirming the higher importance of direct activation of nickel for ^{58}Co production, compared to the formation of ^{58}Co by neutron activation of nickel, which is contained in corrosion products deposited in the reactor core. On the other hand, ^{58}Co is only a minor contributor to the total radiation dose rate as compared with ^{60}Co, at least as long as no work has to be done at open components. However, as was also mentioned in Section 4.4.3.2., the cobalt content in the nickel plating of Inconel grids has to be kept low, in order to preclude the input of greater amounts of ^{60}Co into the primary coolant which would result in higher radiation dose rates (see, e. g., Bergmann and Perock, 1992). Most of the Zircaloy spacer grids contain springs made of Inconel X-750. In a 1300 MWe core they have a total surface area of about 60 m^2; the maximum allowable cobalt content in this material was therefore restricted by several manufacturers to 2000 ppm instead of the 10,000 ppm previously accepted.

Reduction of cobalt inventories in the materials outside the reactor pressure vessel is only likely to be effective after measures have been taken to minimize the ^{60}Co production from in-core sources (Thornton, 1992). The most important material to be considered in this context is Inconel or Incoloy, which are used for the steam generator tubes, because of their large surface area. As an example of the efforts undertaken in this field, in the French PWR plants the cobalt content of the materials used in the primary circuit was restricted to a maximum value of 300 ppm (Beslu et al., 1989 a); further improvement is expected by the use of Inconel 690, which has an average cobalt content of 180 ppm. Bergmann and Perock (1992) reported that plants which shifted in steam generator replacement from Inconel 600 tubing material to Inconel 690 with low cobalt impurity content experienced markedly lower radiation dose rates after 2 effective full power years of operation. Replacement of the Stellite surfaces in valves, etc., outside the reactor pressure vessel by hardfacing materials that are free of cobalt is also promising, as well as limitation of the cobalt contents in the surface cladding materials of the primary circuit piping and, in particular, in the materials of the chemical and volume control system.

Basically, the metal release rates of the materials to be employed can be reduced by a preceding appropriate surface treatment. Electropolishing leads to a removal of the surface roughness and of the uppermost surface layer, which frequently is extensively damaged during fabrication. This damaged layer, which consists of fractured grains and which can contain some phase-transformed material, is more sensitive to corrosion than the underlying intact base material. Therefore, such a surface finishing of the main materials (a fine abrasive finish might also be suitable here) prior to the commissioning of the plant will reduce the concentrations of corrosion products in the primary coolant, in particular during the first fuel cycle. A number of authors have reported on such surface treatments, mainly with regard to steam generator tubes (see Thornton, 1992). Passivation of the treated surfaces (e. g. by means of hot, moist air) is reported to have a beneficial effect on the metal release rates to the primary coolant, in particular for stainless steels. The aim of such a passivation treatment is to generate a protective surface layer with minimum porosity, to reduce the corrosion of the underlying metal. It has to be mentioned, however, that the plant results are not sufficiently clear to confirm a beneficial effect of such finishing processes.

It is also assumed that smoothened surfaces keep radionuclide pickup low, partly due to the smaller true surface area, but also due to the removal of reactive surface sites. A pronounced surface roughness as well as imperfections in the uppermost region of the base material are assumed to favor deposition of corrosion products from the coolant; attempts have been made, therefore, to achieve an optimum quality of the surfaces during the manufacturing of the components. Experiments have shown that mechanical polishing does not effect a noticeable reduction of the radiation field buildup, presumably because of the generation of new damages on the surface during polishing. Better results have been obtained by using electropolishing techniques for the pretreatment of the surfaces. Several experiments, in which steam generator manway inserts that had been previously electropolished using a perchloric acid–glacial acetic acid electrolyte, had been

exposed to primary coolant over the length of a fuel cycle, yielded contamination levels which were lower by a factor of 2 to 5 than mechanically polished surfaces (Price et al., 1989). Similar results were reported by Asay et al. (1991 a). Passivation of the electropolished surfaces by treatment in moist hot air yielded an additional factor of 2, while passivation in hot, simulated primary coolant proved to be less effective. Additional tests showed that the beneficial effect of electropolishing plus passivation is more pronounced with Inconel surfaces than with stainless steel surfaces (Asay et al., 1991 b). Based on the results of such experiments, some manufacturers have decided to pretreat the channel head surfaces of new steam generators by electropolishing (e. g. Saurin et al., 1989).

It was also reported that deposition of corrosion products onto the surfaces of the fuel assemblies can be prevented or decreased by a pre-oxidation step, either by autoclaving or by electrochemical anodizing prior to use (Antipov et al., 1992).

Other measures, such as chromium plating of the surfaces of the materials, which in experiments showed a beneficial effect in retarding the incorporation of radionuclides into the oxide layers have also been considered. As yet, however, no technical-scale application has been reported; presumably, there are still technical questions to be solved.

Commissioning of the plant seems to be the most effective time for establishing an optimum coolant chemistry, since during this period corrosion product transport processes and oxide film composition are established which can indirectly affect the subsequent development of radiation fields. Experience from operating plants suggests that dose rate patterns for individual reactors are in fact established early on in their operational history (see Section 4.4.1.). For this reason, a preconditioning process is frequently conducted during the hot functional testing period of the plant, e. g. by using an alkaline primary coolant which is free of oxygen; sometimes, chelate compounds have also been employed to attain this goal. The main aim of this treatment is to minimize the input of cobalt to the primary circuit, since its removal once it has entered the system is difficult and time-consuming. Though positive effects were measured in laboratory and loop experiments, as well as with coupons inserted into operating primary circuits, the plant results are not unequivocal; presumably, the effect of such measures is small when compared to that of other parameters, in particular the presence or absence of Stellite surfaces. Therefore, they are assumed to demonstrate their potential advantages only after the main cobalt sources have been removed from the system.

Another important parameter in controlling the buildup of radiation fields is employment of an optimum primary coolant chemistry throughout plant operation, even when all the facts mentioned above indicate that deposition and activation of corrosion products in the reactor core do not represent the most important contamination mechanism. As was discussed in detail in Section 1.3., the primary aim of coolant chemistry is to keep the corrosion of the materials and, consequently, the release of metal atoms to the coolant as low as possible. With the main source of radioactive atoms being the in-core materials, this requirement particularly concerns the conditions prevailing inside the reactor pressure vessel. A second requirement which is of equal importance is to keep the concentration of

dissolved cobalt in the coolant low, since this is the species which is incorporated into the oxide layers on the primary circuit surfaces.

As can be concluded from Fig. 4.40., "modified" coolant chemistry resulting in a coolant $pH_{(300)}$ in the range 7.1 to 7.4 is best suited to fulfil these requirements (Marchl et al., 1992). The effectiveness of this type of coolant chemistry can be seen on comparing plants A and B, in which no Stellite replacement was performed. The same effect can be seen when comparing plants C and D. Plant C, at which 11% of the Stellite surfaces was replaced, was operated at a coolant pH of 7.4, while plant D applied "coordinated" coolant chemistry resulting in a pH of 6.9; although in plant D the Stellite surfaces had been reduced to a considerably higher degree than in plant C, it exhibited significantly higher dose rates at the main coolant piping. Analyses of the concentrations of dissolved cobalt performed in the primary coolant of plant C using stripping voltammetry and cation chromatography showed very low values, on the order of 2 to 5 ppt (Rühle and Riess, 1989).

However, the optimum value of the coolant pH in the range between 7.1 and 7.4 may depend on plant-specific parameters and, therefore, has to be determined individually for each plant. This can be done using the empirical calculation code OPTIMI in which different parameters influencing the contamination process have been incorporated (Marchl and Greger, 1989).

In the US, several plants have shifted the primary coolant pH towards higher values after several years of operation. As was reported by Bergmann (1989), with these plants the impact of changes in the chemistry regime on the primary circuit dose rates was not clear. In some cases, the radiation levels in the steam generator channel head showed a significant reduction as a result of operation at higher pH, in particular when the facility had undergone a decontamination prior to starting operation at the new pH level; however, in other plants the radiation levels increased slightly when the coolant pH was changed. From these experiences, the author assumed that more than two cycles of "modified" chemistry operation are needed to establish the new trend of the radiation levels. Similar results were obtained at a US PWR plant (Millstone Point Unit 3) which, after operating in its first fuel cycle according to the standard "coordinated" Li/B coolant chemistry control at a constant pH of 6.9, was shifted to "elevated" pH chemistry in the second fuel cycle. For this purpose, the lithium concentration was raised to a maximum level of 3.5 ppm where it was maintained until the boron concentration fell below 600 ppm; then the Li : B ratio was coordinated to maintain a constant pH of 7.4 throughout the rest of the cycle. Radiation field measurements showed an increase by about 10% during the second cycle, which was slightly less than the 25% increase calculated for continued operation with standard pH 6.9 chemistry. On the other hand, since post-cycle fuel examinations yielded Zircaloy oxide layers slightly thicker than experienced with fuel rods of comparable burnup but operated at a coolant pH of 6.9, it was decided to limit the coolant pH for continued operation to a maximum of 7.2 (Bergmann et al., 1989). Based on 2.4 effective full power years of plant operation, Bergmann and Perock (1992) concluded that operation with "modified" coolant chemistry results in about 25% lower component dose rates as compared with "coordinated" coolant chemistry operation. Moreover, these authors reported that operation with an "elevated" coolant pH since the

startup of the plant will lead to radiation levels lower by about a factor of 2 as compared to operation with a "modified" or "coordinated" chemistry regime; if the chemistry regime is changed to "elevated" pH conditions after a certain time of "coordinated" chemistry operation, the resulting decrease in radiation levels will be less pronounced.

In an extensive study, Polley et al. (1994) correlated coolant chemistry data versus radiation field data in 16 Westinghouse PWR plants. From the results it was concluded that operation at a "modified" chemistry regime with 2.2 ppm Li and a $pH_{(300)}$ of 7.4 produces a benefit in radiation levels in the steam generator primary channel head of roughly 15%, compared to a "coordinated" chemistry regime with a $pH_{(300)}$ of 6.9. Operation at a $pH_{(300)}$ 7.2 "modified" chemistry regime is expected to yield a somewhat lower benefit; on the other hand, from the results it was concluded that an "elevated" Li chemistry regime with 3.35 ppm Li and a $pH_{(300)}$ of 7.4 will result in an additional benefit of about 10%. These data apply for plants experiencing a 12-month fuel cycle; for plants operating 18-month cycles, the benefit of adopting "modified" chemistry regimes is expected to be about 25% lower, due to the lower coolant pH during the first months of the cycle.

In the meantime, a number of PWR plants worldwide have shifted the primary coolant pH to values between 7.2 and 7.4. In most of the plants a beneficial effect of elevated pH chemistry on the contamination levels and radiation dose rates has been reported; in other plants, however, after a few fuel cycles the beneficial effects were difficult to detect and less than had been expected.

As was mentioned above, adjusting the coolant pH to the range which is required in "modified" or even in "elevated" pH chemistry by addition of a sufficiently high concentration of LiOH poses some problems in the first months of a fuel cycle. The LiOH concentrations which would be needed are on the order >5 ppm and may adversely affect stress corrosion of Inconel 600, in particular in the U-bends, as well as Zircaloy corrosion; however, according to Roesmer (1989) these effects seem to be of minor significance.

Some authors have claimed that $KOH-NH_3$ primary coolant chemistry as applied in the VVER reactors leads to lower radiation dose rates on the primary system. In the course of their work at the DIDO Water Loop, Large and Woodwark (1989) investigated this type of primary coolant chemistry under conditions which were comparable to those applied in the experiments with LiOH chemistry. Their results showed comparatively low corrosion product concentrations in the coolant, suspended solids as well as dissolved species; the radioactivity buildup on the loop surfaces, however, was on the same order as that experienced with "coordinated" Li/B chemistry. From these findings the authors concluded that the comparatively low radiation dose rates which are reported from VVER plants are not due to the type of coolant chemistry employed, but to the absence of Stellite and Inconel in the primary circuit, i. e. to low cobalt and nickel inventories of the materials in contact with the primary coolant.

Laboratory investigations have shown that, similar to the situation in BWRs (see Section 4.4.4.4.), addition of zinc to the primary coolant is potentially able to reduce the incorporation of ^{60}Co into the surface oxide layers. These results may give an incentive to consider zinc addition as a possible countermeasure against

contamination buildup in PWR primary circuits as well. However, there are still some open questions, in particular concerning possible adverse side effects of this measure (Ocken and Wood, 1992).

Since the radionuclides produced in the reactor core are transported by the reactor coolant to the out-of-core components, where they are the origin of contamination buildup, various institutions have thought of ways to reduce this pathway by appropriate purification of the coolant. However, as was reported in Section 4.4.3.3., the deposition halftimes of the radionuclides in the primary coolant are much shorter than the purification halftimes which can be effected by the normally employed primary coolant purification systems; this means that even with satisfying purification factors of 10 and higher for particulates as well as for dissolved corrosion products, these systems cannot be sufficiently effective in reducing the concentrations of corrosion products and associated radionuclides in the primary coolant. In order to improve its effectiveness, a significant increase in the purification rates has to be strived for which, however, is not feasible when using the conventional purification systems equipped with organic ion exchange resins, which require cooling down of the purification flow to about 80 °C. For this reason, only high-temperature purification techniques can be considered which offer the basic possibility of cleaning up a much higher fraction of the circulating coolant flow. One purification technique which is able to operate efficiently at elevated temperatures is electromagnetic filtration.

Electromagnetic filters (EMFs) are widely used in industrial plants to remove ferromagnetic impurities such as magnetite from water flows. For a number of years, the secondary side feedwater in many nuclear power plants has been purified efficiently by this technique (see, for example, Heitmann, 1977). Several different designs for EMFs have been developed. One of them is a vessel filled with steel balls and surrounded by a magnetic coil. During operation of this facility, ferromagnetic suspended solids from the water phase are attracted to the surface of the balls by magnetic forces; when the pressure drop in the filter becomes too high, the balls can be demagnetized and the loosely adherent particles are flushed from the filter by a water flow. This technique has been widely employed in water flows at temperatures up to about 180 °C. Experiments at LWR primary coolant operating temperature, i. e. at about 300 °C, showed a rather good removal of magnetite particles from the coolant flow (Siemens/KWU, unpublished). Using an in-pile loop in a research reactor, removal efficiencies of 90 to 95% for ^{51}Cr, ^{60}Co and, surprisingly, for ^{95}Zr as well were measured, indicating that non-ferromagnetic compounds are also retained in the filter device, presumably because the trace amounts are attached to ferromagnetic oxide particles (Dollé and Chenouard, 1983). However, experiments have shown that backflushing of the particles which were previously deposited at 300 °C is difficult to perform, because of the formation of a tightly adherent layer on the balls. This means that the whole ball bed would have to be treated as radioactive waste, resulting in unacceptably large waste volumes. Alternatively, a decontamination of the balls could be carried out; however, no attempts in this direction have been undertaken so far.

Emory (1983) has reported on the development of a high-gradient electromagnetic filter with a mesh matrix, showing a retention efficiency of >80% for particu-

late iron (mainly magnetite) and of >90% for ^{60}Co, ^{59}Fe and ^{54}Mn, as demonstrated by experiments in the bypass of a PWR primary circuit (N reactor). These experiments show that more than 90% of the trapped crud can be backwashed from the filter by using a flash method in which a two-phase water–steam flow causes a violent scrubbing action on the surfaces of the filter matrix.

In general, it is highly uncertain whether the removal of solid suspended corrosion products from the coolant will have a significant impact on contamination buildup in the primary circuit. As was discussed in Section 4.4.3.4., all the observations made in the corresponding investigations indicate that it is dissolved cobalt species that are predominantly responsible for this process; therefore, removal of solid suspended matter can be assumed to have only a limited effect. On the other hand, by keeping the concentrations of non-dissolved corrosion products in the primary coolant low, a beneficial effect on contamination and dose rate buildup in the pipes, tanks and components of the low-temperature auxiliary systems can potentially be achieved. As yet, technical-scale electromagnetic filters have not been applied to the primary systems of operating PWR plants, with the reason for this being mainly the problems in incorporating such a large facility into the primary circuit in a manner that all the safety requirements are met.

Some observations made at operating PWR plants have suggested the idea of influencing the primary circuit dose rates by appropriate modalities of the reactor shutdown procedures, e. g. in the course of refuelling, either to achieve minimum corrosion product redistribution during the shutdown spiking or to achieve a certain decontamination of the out-of-core surfaces. In this context, different procedures carried out at PWR plants have been reported; however, when evaluating the results obtained one has to bear in mind that in some of the reported procedures it is not possible to correlate cause and effect properly; therefore, the possibility of pure coincidence cannot always be ruled out.

As was pointed out in Section 4.4.3.3., the corrosion product shutdown spiking usually proceeds in two or more stages, with one of them occurring during addition of boric acid and cooling down to 180–150 °C, which is obviously caused by the decrease in pH. The other stage occurs as the result of the change from reducing to oxidizing coolant conditions after removal of hydrogen from the primary circuit and ingress of air. This increase in the corrosion product concentrations seems to be unavoidable. In order to reduce the amount of radioactivity spread into the make-up water which is needed for flooding, the question arises of whether it would be possible to concentrate these different stages into one stage without disadvantages. It has been reported that maintaining the full hydrogen content in the primary coolant until the coolant temperature has reached 120 °C and, at that point, adding H_2O_2 to obtain an oxygen concentration of 2 to 3 ppm would result in a far-reaching suppression of the corrosion product shutdown spike and, as a consequence, in a considerable reduction of the activity carry-over to the water of the spent fuel pool (Samuel, 1989). Another shutdown procedure proposed for minimizing the amount of mobilized corrosion products is to cool down the circuit quickly when the temperature has fallen below 150 °C and to introduce oxygen into the primary circuit when the temperature is below 100 °C (Beslu, 1992).

However, the question is still open whether or not the corrosion product shutdown spiking contributes significantly to the permanent contamination level of a PWR plant. Observations made at different plants have shown that the spike only gives rise to the deposition of some loosely adherent matter in the steam generator whose radioactivity burden is insignificant when compared with that of the tightly adherent oxide layer (Bishop and Stagg, 1984). Therefore, any efforts made to suppress or to minimize corrosion product spiking do not appear to be a promising way of reducing the radiation dose rates on the primary circuit.

Some in-service decontamination techniques have also been proposed to reduce the amount of deposited radionuclides. According to the results of loop experiments reported by Amey et al. (1989), the amount of cobalt which is deposited in a PWR primary circuit can be reduced by treatment with elevated boric acid concentrations at temperatures around 120 °C. This procedure results in a comparatively high concentration of dissolved cobalt in the coolant (values on the order of 500 ppt were measured) which can be removed by the purification system. This effect is probably due to dissolution or leaching of the outer iron-rich corrosion product layer, which usually contains comparatively high amounts of cobalt. Based on these results, an on-line chemical treatment for cobalt management was proposed for application to established plants as well as in the pre-operational phase during which the parent nuclide ^{59}Co can be removed before activation to ^{60}Co occurred.

In-service decontamination can also be attained by adding a complexing agent to the primary coolant, which is able to enhance the transport of radionuclides to the primary system purification resins; however, in the case of an insufficient stability of the resulting complex compound against thermal or radiolytic decomposition, merely a redistribution of the radionuclides in the primary system may be the consequence. In order to study this situation, Large and Woodwark (1989) have added nitrilotriacetic acid (NTA) to the loop coolant which, according to the results of preceding investigations, is the most stable of the available complexing agents; however, its halflife under primary circuit conditions is reported to be less than 0.5 seconds. The result is that NTA addition initially leads to a drastic increase in the corrosion product concentrations in the coolant, followed by a rapid redeposition on the loop surfaces inside and outside the reactor core, in particular on Inconel surfaces. During subsequent operation with "coordinated" Li/B chemistry (high pH), the concentrations of suspended solids decrease rather quickly, that of dissolved species more slowly; the enhanced deposition on the surfaces remained over a rather long period of time. Such a behavior means that, on the whole, addition of complexing agents to the coolant probably will result in more disadvantages than benefits.

In the early 1970's, some of the Canadian CANDU plants introduced a so-called redox-cycling, i. e. alternating additions of oxygen and hydrogen to the primary coolant during reactor shutdown (LeSurf, 1977). This treatment resulted in the removal of considerable amounts of ^{60}Co from the system and in the limitation of the radiation dose rates of the systems to comparatively low levels, in particular in a plant equipped with Monel steam generator tubing. At about the same time, Westinghouse started to recommend the addition of H_2O_2 to the coolant in the

course of plant shutdowns at a rather early stage during cooling down. This procedure was performed in many US plants with good success in the mobilization of previously deposited radionuclides. On the other hand, the question remained open whether or not such a treatment would merely cause a redistribution of cobalt activity in the primary circuit and an increase in the radiation dose rates at the out-of-core surfaces. A comparative evaluation of the data originating from shutdown phases at different US plants which was performed by Kormuth and Barkich (1983) demonstrated that such suspected adverse side effects did not occur. The rate of reduction in the dissolved ^{58}Co activity in the coolant corresponded approximately to the values calculated from the purification rate and the purification factor; this means that there was no significant deposition of mobilized radionuclides onto the walls. The observation that the ratio $^{58}Co : {}^{60}Co$ in the coolant increased markedly during H_2O_2 addition, whereas it remained virtually constant in the steam generator corrosion product deposits, indicated that the mobilized corrosion products mainly originated from inside the reactor pressure vessel and, consequently, that no significant decontamination of the out-of-core surfaces was achieved. Finally, on-line γ-spectrometry measurements revealed that the composition of the existing deposits was not markedly changed by this procedure, even when the enhanced cobalt concentration in the coolant was in contact with the walls for some time, an effect that may be a consequence of insufficient capacity of the purification system. Clearly, the incorporation of the dissolved cobalt species into the oxide layers on the primary circuit surfaces at such a low temperature proceeds rather slowly.

In total, the efforts undertaken to minimize contamination buildup in the primary circuit have resulted in a pronounced decrease in the radiation levels and of the radiation exposure to the staff. This effect becomes particularly evident when the current values are compared with those recorded in the 1970's. Of the different measures undertaken, reduction of the cobalt inventory inside the reactor pressure vessel, mainly by abandoning the Stellite hardfacing materials, has proved to be by far the most effective. In comparison, the long-term success of the other measures applied or recommended is far less pronounced. It might well be, however, that their effect is hidden by the inevitable fluctuations in the contributions originating from the main ^{60}Co source, i. e. from the in-core materials. It can be expected, therefore, that upon removal of the cobalt sources from the reactor core, the other measures will be an effective means of further reducing the contamination phenomenon. The most promising procedure involves establishing an optimum primary coolant chemistry. According to all information currently available the most effective chemistry in this regard would seem to be the "modified" chemistry regime.

4.4.3.6 Modelling PWR contamination buildup

High radiation dose rates on the primary circuits and components caused by contamination buildup are a severe handicap in plant operation and maintenance. Therefore, several attempts have been made to predict the rate and extent of dose

rate buildup and to identify the most important parameters. To this end, modelling of the generation, transport and deposition of activated corrosion products had already been proposed at an early stage of commercial power plant operation (e. g. Walton and Hesford, 1962; Kushneriuk, 1971). Since the process of contamination buildup is of a very complex nature, the use of computer-based codes is the only feasible means of including all the parameters that might influence dose rate buildup. Most researchers agree that the materials that are in contact with the hot primary coolant (in particular, their cobalt content), on the one hand, and the chemistry conditions in the primary coolant (in particular, coolant pH), on the other, represent the predominant parameters; in addition, the state of the primary circuit surfaces may also play a role, as well as surface pretreatment operations.

Predictions of future radiation dose rates in nuclear power plants are only useful if they are precise. In this respect, the requirements placed on the models describing contamination buildup differ significantly from those in most of the reactor safety codes describing the course of reactor accidents, where it is usually sufficient to demonstrate that the numerically expressed consequences or the probability of a given event are lower than a predetermined number; gaps in the knowledge of reaction mechanisms may be quite legitimately bridged by using the most pessimistic data or assumptions. Such strategems are unlikely to be appropriate in any calculational route for predicting contamination buildup (Harper et al., 1992). It has to be admitted, however, that most of the current models describing contamination buildup are not yet able to meet these high standards. The main reason for this is that the mechanisms they are based on involve considerable uncertainty, which means that the resulting model necessarily reflects these uncertainties. Among these uncertainties are the existing inaccuracies in the numerical values of the release rates of the corrosion products and the deposition rates of the radionuclides as functions of temperature and coolant chemistry; in most cases these data were acquired by laboratory and loop experiments, under conditions that often differ in many respects from those prevailing in a real primary circuit. Another essential item in this context is the nature of the corrosion product species present in the coolant, which is of pre-eminent relevance for contamination buildup. Sometimes, magnetite was assumed to be the most important constituent, while other codes were based on nickel ferrite, thus favoring a higher optimum coolant pH. Moreover, it is unclear to what extent the behavior of the trace amounts of cobalt and ^{60}Co present in the coolant and in the corrosion products is controlled by the solubilities of the above-mentioned main constituents. Last but not least, most of the models are based on the assumption that the buildup of contamination is mainly governed by activation of corrosion products which are temporarily deposited on the fuel assembly surfaces (i. e. pathway 1 in Figure 4.26.), quite in contrast to the results and observations discussed in the preceding sections, which indicate that high-cobalt alloys permanently located in the neutron field are the main ^{60}Co sources. Given these weaknesses, it is not surprising that agreement of code predictions with the experience from reactor operation can sometimes only be obtained by arbitrary adjustment of one or several parameters; such practices raise considerable doubts as to the ability of the codes to predict the behavior of activated corrosion products outside narrowly restricted areas.

Some of the existing codes shall be shortly addressed in the following to give an impression of the nature and amount of data required to describe the process of contamination buildup as completely as possible.

The first attempts to predict radiation fields involved the Canadian heavy-water, pressurized-tube CANDU reactors (Lister, 1976a; 1976b). The model developed included numerical calculations of the deposition and release of corrosion products in the reactor core, and of the deposition of radionuclides and the corresponding radiation buildup in the out-of-core feeders and boilers. With regard to radionuclide deposition, it was assumed that ^{60}Co is incorporated into the growing oxide film, so that the contamination rate is governed by corrosion kinetics. Release of ^{60}Co to the coolant is controlled by solid-state diffusion and, therefore, proceeds very slowly. One result of the calculations which, in spite of the great differences in plant design, is also relevant for light water PWRs is that purification of the primary coolant does not significantly affect the contamination rate, unless the purification halftimes are considerably below around 20 minutes, an effect which can be only achieved by particular cleanup systems such as high-temperature filters.

The French PACTOLE code, which was first described by Beslu et al. (1977) and, from that time, has been continuously developed further (e. g. Beslu et al., 1989 b), is based on theoretical studies as well as on the results of experiments performed in different loops. In this model, the PWR primary circuit is subdivided into successive zones which are characterized by their own geometries and thermal-hydraulic data. The basic feature of the mechanism of the code calculations is the role of oxide solubility, with the main driving force for the corrosion product transport being the gradient of solubility which exists between the local and the equilibrium value. The solubility data are obtained from thermodynamic calculations which are performed taking into account the influence of the water chemistry regime. As the starting mechanism, it was assumed that oxidation of the base metal leads to the formation of adherent oxide as well as to the release of dissolved elements. If the concentration of a given element at a given location in the primary circuit is different from its saturation value, then deposits will either be formed by precipitation or they will be re-dissolved with the constituents released again to the primary coolant. The dissolution and release rates are assumed to be proportional to the difference between the local concentration and the saturation concentration and to the ion transfer from the wall, which is dictated by Brownian diffusion. The theoretical treatment of the dissolution process leads to the result that, if the oxide layer on the surface of the wall is thin, the release rate is proportional to the mass transfer and independent of the oxide thickness and, therefore, of time. On the other hand, if the oxide layer is thick compared to the diffusion length, pore diffusion would be the parameter which governs the kinetics. Only in such a situation can the release law be of the type t^n with $n < 1$. Deposition of the radionuclides on the surfaces is treated as deposition of solid particles depending on particle size, Brownian and turbulent diffusion and inertial effect. Thus, the contribution of dissolved ions to the deposition of radionuclides is not taken into consideration.

Nevertheless, it was reported that the application of the PACTOLE code to different PWR plants yielded results that were in reasonable agreement with the prac-

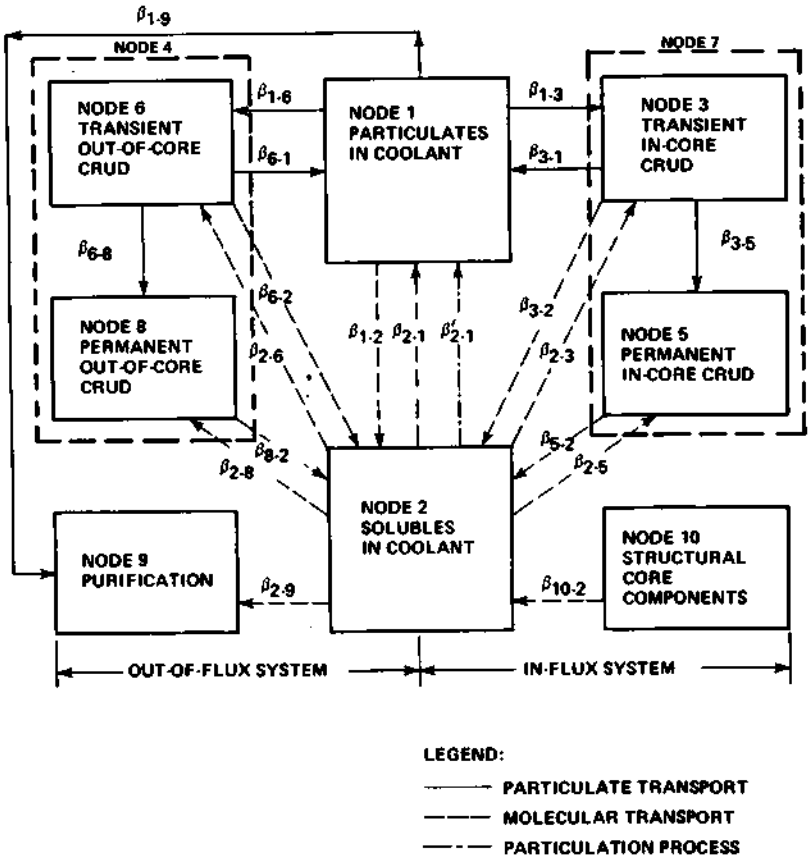

Figure 4.41. Modelling activity transport in the CORA-II code; schematic (Kang and Sejvar, 1985)

tical observations. Because of the differences in the material concepts, however, the code could not be successfully applied to PWR plants of Siemens/KWU design.

The CORA code was developed in the US; it is based on the principal aspects of corrosion product transport in a PWR plant and it permits a time-dependent calculation of the radionuclide activities and concentrations, of the corrosion product masses and the activity concentrations they contain, as well as of the radiation levels at the primary circuit surfaces. As can be seen from Fig. 4.41., where a schematic diagram of the improved code CORA-II is shown (Kang and Sejvar, 1985), this code uses 8 nodes for the activity transport and 2 additional nodes for the mass transport, taking into account the total masses inside and outside the neutron field. In each node the general mass balance is defined according to

$$\text{net buildup rate} = \text{rate of input} - \text{rate of output}.$$

In the transfer of a nuclide from one node to another, a transport is assumed which is proportional to the amount of nuclide present and to the mass transfer coeffi-

cient for the relevant transport path. Therefore, an important prerequisite for the calculations is that the transfer coefficient be known or that it can be determined.

In the CORA code, the corrosion product layers outside the reactor core are rather arbitrarily subdivided into two layers, a transient one and a permanently deposited one. Supply to the transient layer occurs via deposition of suspended particles from the coolant, release from it includes erosion of particles back to the coolant as well as transport into the permanently deposited layer and partial conversion into dissolved species. In a comparable manner, the supply of nuclides to the permanent layer is assumed to result from transfer from the transient layer and the exchange equilibrium with the dissolved species present in the coolant. The deposition coefficients of suspended solids can be calculated on the basis of particle size and flow characteristics. The coefficients of relevance for the permanently deposited layer, including ionic transfer mechanisms between liquid and solid phases, can be derived from theoretical considerations as well as from laboratory studies of corrosion product solubilities. Finally, diffusion rates of nuclides at the interphase layers are needed, from the oxide layer to the coolant as well as in the reverse direction. These data can be obtained in part by theoretical considerations and by measurements at the plants.

The authors have emphasized that there are too many unknown variables to predict discrete activity or radiation levels accurately; therefore, the primary application of the CORA-II model is in the evaluation of relative changes and trends in the levels caused by major changes in the systems or in the operating chemistry conditions.

The CRUDSIM code, which was developed by Westinghouse researchers (Lindsay, 1985), represents the primary circuit as two tanks – hot and cold. Activation of corrosion products takes place in the hot tank and transport between the two tanks is controlled by the behavior of dissolved species, as determined by solubilities according to the results of the Kunig and Sandler studies and the operating history of the plant (coolant chemistry and power levels), which provide the basis for calculating a relative out-of-core activity inventory. The so-called CRUDSIM chemistry factor represents the ratio of the relative activity value for the actual operating chemistry to the relative activity value if the plant would have previously been operated under "coordinated" coolant chemistry conditions. Comparisons of observed dose rates in the steam generator channel head with CRUDSIM-predicted relative activity using the CRUDSIM chemistry factor yielded a satisfying correlation, which showed the importance of an optimum coolant chemistry in particular during the first fuel cycle operation.

The influence of coolant chemistry on radiation buildup can be expected to differ from plant to plant, due to plant specific parameters such as chemical composition and morphology of the surface oxide layers in the system, operating parameters (e. g. temperature), and the structural materials employed. In order to take into account these parameters in the selection of an optimum primary coolant chemistry, the empirical code OPTIMI was developed which uses a so-called "Chemistry Influence Factor" which is calculated from the differences in the concentrations of dissolved iron in the coolant at the primary system hot-leg and cold-leg side (Marchl and Greger, 1989). By comparing the results of the calculated chemis-

try influence factor with actual radiation dose rates in the plant, plant-specific optimum chemistry conditions for control of the radiation fields can be predicted. This code was successfully applied to a number of PWR plants of different suppliers and was further developed to calculate the solubilities of iron, nickel and cobalt from a spinel with the composition $Fe_{2.45}Ni_{0.5}Co_{0.05}O_4$ and of Ni from NiO.

Taking into account that development of a comprehensive model is not feasible given the current state of knowledge, a simple kinetic model ACTRANF has been elaborated by Harper et al. (1992). In this model, the primary circuit is divided into three main sections: the coolant, the in-core surfaces and the out-of-core surfaces. Cobalt is introduced into the system by release from circuit materials, either as ^{59}Co from any point in the circuit or as ^{60}Co from activated materials in the neutron field. Both isotopes are removed from the coolant to the purification system by a first-order process, and are also removed from the circuit when they have been deposited on fuel assemblies that are withdrawn from the reactor in the course of refuelling. ^{59}Co is converted to ^{60}Co by neutron activation when it is deposited on fuel surfaces or when it is contained in the internals of the reactor pressure vessel. Thus, unlike the models described above, ACTRANF considers both possible ^{60}Co sources; the calculations showed that activation of ^{59}Co which is temporarily deposited in the reactor core is only a small contributor when compared with the direct release of ^{60}Co from in-core sources, in particular in plants equipped with Stellites inside the reactor pressure vessel. Distribution of cobalt isotopes around the surfaces of the primary circuit proceeds by exchange of dissolved species with the coolant; deposition and re-release are assumed to be first-order processes. The first applications of the model to operating plants with and without Stellite materials in the primary circuit have yielded encouraging results.

4.4.3.7 Contamination by other radionuclides

As has been discussed above in detail, ^{60}Co and ^{58}Co are usually the radionuclides that determine the radiation dose rates at the primary circuit surfaces. In isolated cases, however, other radionuclides, usually activation products of other primary circuit materials, may also be of significance. Fission products normally do not contribute to a significant extent to contamination buildup.

Järnström (1982) reported that in the first operating cycles of the VVER plants Loviisa 1 and 2 the radionuclides ^{122}Sb, ^{124}Sb and ^{110m}Ag were chiefly responsible for the radiation dose rates at the primary circuit. The most important sources for antimony were identified to be the ammonia solutions added, which contained antimony impurities in the range of 10 to 50 μg/kg; for silver the main source was KOH used for alkalizing the coolant which contained silver impurities in the range of 5 to 10 mg/kg. Both impurity elements, as well as their radioisotopes, were removed with a low efficiency from the primary coolant by the action of the purification system. In the course of plant shutdown, a marked increase in the concentrations of these radionuclides in the primary coolant was observed, which was counteracted by a change in the cooldown procedure: the purification system was

operated at its maximum throughput until complete cooldown of the coolant and one to two weeks prior to shutdown the resins were replaced by a new charge in their H^+ and OH^- forms.

At several other PWR plants, the antimony isotopes ^{122}Sb and ^{124}Sb had a significant impact on the radiation dose rates in the area surrounding the primary circuit. In one plant, the contribution of ^{124}Sb to the total dose rates on the main coolant piping was measured to be on the order of 30 to 50% (Paffrath et al., 1986); in another plant, where the cobalt-bearing hardfacing materials had been replaced by those free of cobalt (KKP-2), in its first fuel cycle the resulting reduction in ^{60}Co dose rates was partly compensated for by the radiation emitted by the antimony isotopes. During constant-load operation of the plant, the activity concentrations of both antimony isotopes in the primary coolant were comparatively low, on the order of 10 MBq/Mg; upon plant shutdown, however, a steep increase occurred, reaching a peak value higher by two to three orders of magnitude than the preceding steady-state operation level. During this period, the ion exchanger resins of the primary circuit purification system exhibited only a low purification factor for antimony isotopes and, simultaneously, an insufficient capacity. This resulted in an early break-through and a subsequent purification factor of about 1. The heating-up of the primary coolant for a new startup then resulted in a rapid decrease in the activity concentrations of the antimony isotopes in the primary coolant, apparently due to deposition of antimony onto the surfaces of the primary circuit. As a consequence of this behavior, the antimony activity could not be effectively removed from the primary circuit by the action of the primary circuit purification system.

The activity ratio $^{122}Sb : ^{124}Sb$ measured during the shutdown spiking indicated an isotope mixture which was freshly released from the neutron field, i. e. showing no significant decay of the shorter-lived ^{122}Sb. From measurements of the element-specific ^{122}Sb and ^{124}Sb activities, the average residence time of antimony in the neutron field was calculated to be about 100 days. When performing such calculations, one has to take into account the strong epithermal neutron activation of ^{121}Sb and of ^{123}Sb. The flux of thermal neutrons in an LWR reactor core is higher by a factor of about 4 than that of the epithermal neutrons; however, the resonance absorption cross sections of both isotopes are by far larger than the thermal neutron cross sections (180 and $120 \cdot 10^{-24} cm^2$ vs. 6 and $4 \cdot 10^{-24} cm^2$). For this reason, meaningful values of residence times of antimony in the reactor core can only be obtained when both types of neutron activation, thermal as well epithermal, are included in the calculations (Bleier, unpublished). Because of the long activation times measured, it was initially assumed that cladding defects in the secondary neutron sources in the reactor core containing an Sb-Be alloy were the main source of the antimony activity (Paffrath et al., 1986); however, post-irradiation inspection of these components confirmed this suspicion only in one single case. Detailed investigation showed that antimony-impregnated graphite bearings (Sb content about 30%) of the main coolant pumps were the main source. From these bearings, antimony is leached by primary coolant during plant operation and is transported to the core region, where it is deposited onto the surfaces. When, in the course of a shutdown of the plant, hydrogen is removed from the primary

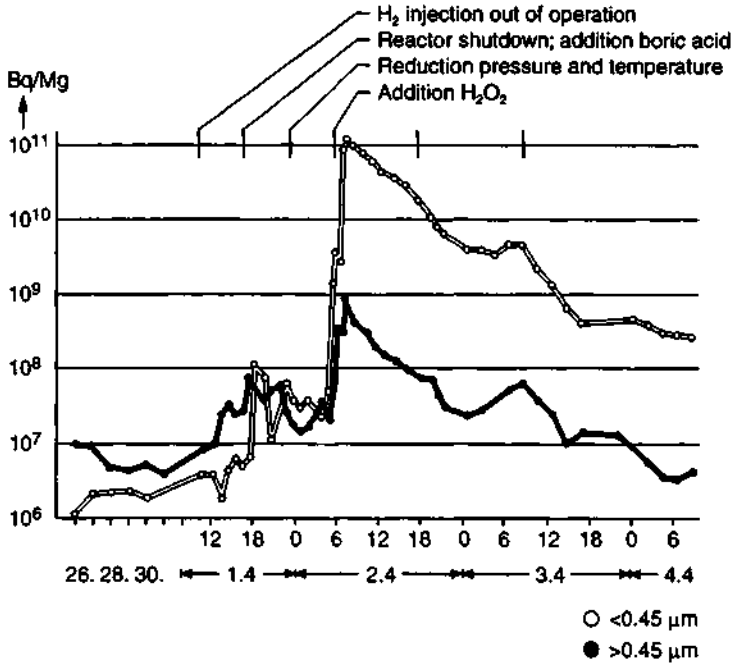

Figure 4.42. ^{124}Sb activity concentrations in PWR primary coolant following H_2O_2 addition during plant shutdown
(Stöckert et al., 1987)

coolant and boric acid dissolved in aerated water is added, the deposited antimony is oxidized to soluble $HSbO_2$. This compound is only weakly dissociated; for that reason, it is not effectively retained by the ion exchanger resins. According to Paffrath et al. (1986), adsorption on the oxide layers on the fuel rod surfaces is the mechanism responsible for antimony plate-out in the reactor core, an effect which has to be attributed to the ion exchanger properties of zirconium oxide.

In response to these findings, the antimony-impregnated graphite bearings were replaced by ones free of antimony. Nevertheless, the difficult task remained of cleaning the antimony-contaminated primary circuits. To this end, it was proposed to reduce the lithium concentration in the primary coolant during the last week before shutdown to values < 1 mg/Mg, as a result of which antimony would be mobilized from the core deposits and transported to the purification system (Paffrath et al., 1986). Another very effective means is oxidation of the Sb(III) present to Sb(V); the resulting compound $HSbO_3$ is easily soluble in water and shows appreciable dissociation, which means that it would be effectively retained by an anion exchanger. In practice, H_2O_2 is added to the antimony-contaminated primary coolant at temperatures < 100 °C, resulting in an immediate and drastic increase, in particular, of the activity concentrations of the dissolved antimony species (see Fig. 4.42.). Within about 40 hours, the ^{124}Sb concentration can be reduced by about three orders of magnitude; the average antimony purification

factor during this period amounts to about 500, which corresponds to an effective halflife of ^{124}Sb in the coolant of about 4 hours (Stöckert et al., 1987). In one such operation at a 1300 MWe plant, about 50 TBq ^{124}Sb together with a total of about 130 grams of antimony were removed from the coolant and transported to the purification system, about 90% of this amount within the first 11 hours. Simultaneously, during this period an improved retention efficiency of the ion exchangers for ^{58}Co and ^{60}Co was observed. In order to preclude a re-elution of the antimony isotopes from the ion exchanger during further operation, it was recommended that this filter afterwards be used in the spent fuel pool purification system where air-saturated water is treated, thus preventing reduction of the adsorbed Sb(V) to eluting Sb(III).

Concerning the ^{110m}Ag activity in the primary coolant of several plants, silver-containing sealings were identified as the main source, from which traces were released to the coolant by corrosion or mechanical wear. Usually, ^{110m}Ag does not significantly contribute to the radiation dose rates at the systems; however, from some VVER plants higher levels were reported, ranging from 1 to 5% of the total activity deposited on the hot-leg surfaces to 8 to 25% on the primary circuit cold-leg surfaces, reaching 50 to 80% on surfaces with temperatures around 60 °C (Burclová et al., 1986). It was observed that such silver (or ^{110m}Ag) deposits are able to adsorb iodine activity, presumably by formation of highly insoluble AgI. In in-pile experiments it was demonstrated that a high coolant flow rate, radiation and a higher oxygen concentration in the coolant will increase the corrosion of silver by several orders of magnitude above the values obtained in out-of-pile experiments. In the primary coolant during steady-state operation, ^{110m}Ag is mainly present in a non-filtrable state (dissolved or very finely dispersed). During plant shutdown, its concentration exhibits a spiking similar to that of the other corrosion products. In this stage it is mainly present in an insoluble form, presumably as AgI; there was, however, no direct evidence for the occurrence of this compound.

References Section 4.4.3

Allsop, H. A., Sawicki, J. A., Godin, M. S. L., Lister, D. H.: The effect of dissolved oxygen in lithiated coolant. Proc. 6. BNES Conf. Water Chemistry of Nuclear Reactor Systems, Bournemouth, UK, 1992, Vol. 1, p. 25–32

Amey, M. D. H., Campion, P., Comley, G. C. W., Symons, W. J., Butter, K. R.: Behaviour of cobalt and other corrosion products in PWR primary circuits and out-of-pile loops. Proc.5. BNES Conf. Water Chemistry of Nuclear Reactor Systems, Bournemouth, UK, 1989, Vol. 1, p. 55–61

Amey, M. D. H., Johnson, P. A. V.: Improved chemistry: Key to reduce occupational radiation exposure in water-cooled reactors. Nucler Europe Worldscan X, 34–36 (1990)

Anthoni, S., Ridoux, P., Chevalier, C.: Evaluation of corrosion products in a pressurized water reactor during shutdown. Proc. 5. BNES Conf. Water Chemistry of Nuclear Reactor Systems. Bournemouth, UK, 1989, Vol. 2, p. 35–39

Antipov, S. A., Dranenko, V. V., Konkov, V. F., Sokolov, I. B., Khaikovskij, A. A.: Influence of fuel clad surface on performance under operational and accident conditions. Report

IAEA TECDOC-667 Coolant Technology of Water Cooled Reactors. Vol. 2, Corrosion in the Primary Coolant Systems of Water Cooled Reactors. Vienna, 1992, p. 65–68

Asay, R. H., Naudin, O., Thiry, M., Lantes, B., Gouillardou, G., Saurin, P., Weber, C. (a): Effect of surface treatments on radiation buildup in steam generators. Vol. 1. Manway seal plate tests in the Chinon B1 PWR. Report EPRI TR-100059, Vol. 1 (1991)

Asay, R. H., Pick, M. E., Roofthooft, R., van Melsen, C. (b): Effect of surface treatments on radiation buildup in steam generators. Vol. 2. Test coupons in the Doel-2 PWR. Report EPRI TR-100059, Vol. 2 (1991)

Bergmann, C. A.: Effects of coolant chemistry and other parameters on exposure rates and doses in Westinghouse-designed nuclear plants. Proc. 4. BNES Conf. Water Chemistry of Nuclear Reactor Systems, Bournemouth, UK, 1986, Vol. 1, p. 7–14

Bergmann, C. A.: Evaluation of selected parameters on exposure rates in Westinghouse designed nuclear plants. Proc. 5. BNES Conf. Water Chemistry of Nuclear Reactor Systems, Bournemouth, UK, 1989, Vol. 1, p. 9–16

Bergmann, C. A., Durkosh, D. E., Lindsay, W. T., Roesmer, J.: The role of coolant chemistry in PWR radiation field buildup. Report EPRI NP-4247 (1985)

Bergmann, C. A., Jacko, R., Roesmer, J., Miller, R., Hudson, M. J. B., Burns, T. F., Wood, C. J.: PWR primary system chemistry: Experience with elevated pH at Millstone Point Unit 3. Proc. 5. BNES Conf. Water Chemistry of Nuclear Reactor Systems, Bournemouth, UK, 1989, Vol. 2, p. 7–12

Bergmann, C. A., Perock, J. D.: Evaluation of factors affecting radiation field trends in Westinghouse-designed plants. Proc. 6. BNES Conf. Water Chemistry of Nuclear Reactor Systems. Bournemouth, UK, 1992, Vol. 2, p. 16–23

Bergmann, C. A., Roesmer, J., Perone, D. W.: Primary side deposits on PWR steam generator tubes. Report EPRI NP-2968 (1983)

Bergmann, C. A., Roesmer, J.: Coolant chemistry effects on radioactivity at two PWR plants. Report EPRI NP-3463 (1984)

Beslu, P.: Observations on recent application of high coolant pH in French PWRs and optimization of chemistry during shutdown. Report IAEA TECDOC-667 Coolant Technology of Water Cooled Reactors. Vol. 3, Activity Transport Mechanisms in Water Cooled Reactors, Vienna 1992, p. 61–65

Beslu, P., Anthoni, S., Brissaud, A., Ridoux, P., Chevalier, C., Saurin, P. (a): Trend of plant radiation fields of French reactors: Analysis and perspectives. Proc. 5. BNES Conf. Water Chemistry of Nuclear Reactor Systems, Bournemouth, UK, 1989, Vol. 2, p. 1–6

Beslu, P., Frejaville, G., Lalet, A.: A computer code PACTOLE to predict activation and transport of corrosion products in a PWR. Proc. 1. BNES Conf. Water Chemistry of Nuclear Reactor Systems, Bournemouth, UK, 1977, p. 195–201

Beslu, P., Frejaville, G., Brissaud, A., Nunge, R., Ridoux, Ph.: Effet du refroidissement et de l'oxygenation au moment des arret des reacteurs a eau pressurisee. Colloque Internat. sur la Chimie de l'Eau et les Problemes lies a la Corrosion des Systems et de Composants des Reacteurs Nucleaires, Vienna, 1982, Paper IAEA-SM-264/5

Beslu, P., Jadot, F., Noe, M., Brissaud, A., Favennec, J., Metge, M.: Elemental release rate measurement of Inconel 600 and Inconel 690 in PWR primary coolant. Proc. 4. BNES Conf. Water Chemistry of Nuclear Reactor Systems, Bournemouth, UK, 1986, Vol. 1, p. 57–61

Beslu, P., Masse, F., Anthoni, S., Brissaud, A., Ridoux, P., Saurin, P., Weber, C. (b): Corrosion ion release from stainless steel and higher nickel alloys under PWR conditions: Experimental and theoretical conditions. Proc. 5. BNES Conf. Water Chemistry of Nuclear Reactor Systems, Bournemouth, UK, 1889, Vol. 1, p. 77–80

Bishop, W. N., Stagg, W. R.: Effects of shutdown/cooldown techniques on radiation fields in PWR primary coolant loops. Report EPRI NP-3461 (1984)

Bosholm, J., Gläsel, H., Junge, O., Reinhard, G.: Zur Abscheidung von Kobaltionen an Austenitoberflächen in Gegenwart verschiedener Anionen. Kernenergie **21**, 84–87 (1978)

Bosholm, J., Hoffmann, H.-J., Schillert, B., Winkelmann, K.: Untersuchungen zur Abscheidung gelöster Metallionen an Oxidoberflächen von Metallen. Kernenergie **24**, 382–385 (1981)

Bridle, D. A., Cake, P.: Elemental and radiochemical measurements carried out on primary coolant at German KWU and other European PWRs. Proc. 6. BNES Conf. Water Chemistry of Nuclear Reactor Systems, Bournemouth, UK, 1992, Vol. 2, p. 324–326

Bridle, D. A., Comley, G. C. W., Butter, K. R., Philippe, R. (a): Significance of the chemical and volume control system in corrosion product transport to PWR coolant. Proc. 5. BNES Conf. Water Chemistry of Nuclear Reactor Systems, Bournemouth, UK, 1989, Vol. 1, p. 31–37

Bridle, D. A., Butter, K. R., Cake, P., Comley, G. C. W., Mitchell, C. R. (b): The nature and behaviour of particulates in PWR primary coolant. Report EPRI NP-6640 (1989)

Burclová, J., Blazek, J., Kapisovsky, V., Bena, J., Duris, J., Kysela, K., Barta, O., Jindrich, K.: Behaviour of silver in the primary circuit of 440 MWe PWR. Proc. 4. BNES Conf. Water Chemistry of Nuclear Reactor Systems, Bournemouth, UK, 1986, Vol. 1, p. 85–86

Comley, G. C. W., Bridle, D. A., Butter, K. R., DeRauter, K., Roofthooft, R.: Nature and behaviour of particulates in PWR coolants. Proc. 5. BNES Conf. Water Chemistry of Nuclear Reactor Systems, Bournemouth, UK, 1989, Vol. 1, p. 297–300

Dinov, K., Matsuura, Ch., Hiroishi, D., Ishigure, K.: Solubility of nickel and cobalt oxides in high-temperature water. Nucl. Sci. Engng. **113**, 207–216 (1993)

Dobrevsky, I., Winkler, R.: A new point of view on the drastic change in coolant activity by power transients in PWRs. Report IAEA TECDOC-667 Coolant Technology of Water Cooled Reactors, Vol. 1, Chemistry of Primary Coolant in Water Cooled Reactors, Vienna 1992, p. 56–58

Dollé, L., Chenouard, J.: How can electromagnetic filtration of corrosion products work with efficiency in electronuclear power plants? Proc. 3. BNES Conf. Water Chemistry of Nuclear Reactor Systems, Bournemouth, UK, 1983, p. 171–179

Emory, B. B.: Development of magnetic filters for the primary coolant circuit of a PWR. Proc. 3. BNES Conf. Water Chemistry of Nuclear Reactor Systems, Bournemouth, UK, 1983, Vol. 1, p. 181–186

Garbett, K.: Overview of the impact of Stellite removal on radiation fields in KWU PWRs. Proc. 6. BNES Conf. Water Chemistry of Nuclear Reactor Systems, Bournemouth, UK, 1992, Vol. 2, p. 31–38

Gott, K.: Gamma spectrometry measurements in Ringhals 3 and 4. Proc. 5. BNES Conf. Water Chemistry of Nuclear Reactor Systems, Bournemouth, UK, 1989, Vol. 1, p. 43–47

Harper, A., Johnson, P. A. V., Amey, M. D. H., Symons, W. J.: Modelling of activity transport and uptake of cobalt by oxide films in PWRs. Proc. 6. BNES Conf. Water Chemistry of Nuclear Reactor Systems, Bournemouth, UK, 1992, Vol. 2, p. 80–85

Heard, D. B., Freedman, R. J.: Cobalt contamination resulting from valve maintenance. Report EPRI NP-3220 (1983)

Heitmann, H. G.: Use of electromagnetic filters in nuclear power plants: Experiments and operating experience. Proc. 1. BNES Conf. Water Chemistry of Nuclear Reactor Systems, Bournemouth, UK, 1977, p. 351–360

Hoffmann, H.-J., Bosholm, J.: Untersuchungen zur Reversibilität der Abscheidung gelöster Kobaltionen an Oxidoberflächen von Metallen. Kernenergie **27**, 160–163 (1984)

Hüttner, F., Winkler, R.: Behaviour of colloidal corrosion products. Report IAEA TECDOC-667 Coolant Technology of Water Cooled Reactors, Vol. 3, Activity Transport Mechanisms in Water Cooled Reactors, Vienna, 1992, p. 70–72

Jacobi, G., Rühle, W.: Erfahrungen im Chemiebereich aus dem ersten Betriebszyklus der Kernkraftwerke Grohnde und Philippsburg 2. VGB Kraftwerkstechnik **67**, 58–63 (1987)

Järnström, R. T.: Corrosion product behaviour in Loviisa NPP primary coolant and measures taken to lower the radiation levels by modified startup and shutdown procedures. IAEA Internat. Symp. Water Chemistry and Corrosion Problems of Nuclear Reactor Systems and Components, Vienna 1982, Paper IAEA-SM-264/8

James, D. W.: Problem assessment of discrete radioactive particles. Report EPRI NP-5969 (1988)

Kang, S., Sejvar, J.: The CORA-II model of PWR corrosion product transport. Report EPRI NP-4246 (1985)

Kockx, J. H., Olijve, J. G.: Incore Co-59 and radiation levels in the Borssele Nuclear Power Station. Proc. 3. BNES Conf. Water Chemistry of Nuclear Reactor Systems, Bournemouth, UK, 1983, Vol. 1, p. 163–169

Kormuth, J. W., Barkich, J. L.: Effects of cold shutdown chemistry on PWR radiation control. Report EPRI NP-3245 (1983)

Kushneriuk, S. A.: Dispersion of radioactivity in a closed coolant system. Nucl. Sci.Engng. **43**, 247–256 (1971)

Lambert, I., Joyer, F.: Solubility of cobalt in primary circuit solutions. Proc. 6. BNES Conf. Water Chemistry of Nuclear Reactor Systems, Bournemouth, UK, 1992, Vol. 1, p. 196–197

Large, N. R., Woodwark, D. R.: Effect of coolant chemistry on PWR radiation transport processes. Report EPRI NP-6657 (1989)

LeSurf, J. E.: Control of radiation exposures at CANDU nuclear power stations. J. British Nucl. Energy Soc. **16** (1), 53–61 (1977)

Lindsay, W. T.jr.: Development of correlating equations for solubility of iron from nickel-cobalt ferrites in high-temperature water. Appendix A in: Bergmann et al., Report EPRI NP-4247 (1985)

Lister, D. H. (a): Predicting radiation fields around reactor components. Report AECL-5522 (1976)

Lister, D. H. (b): The transport of radioactive corrosion products in high-temperature water. II. The activation of isothermal steel surfaces. Nucl. Sci. Engng. **59**, 406–426 (1976)

Lister, D. H.: Activity transport and corrosion processes in PWRs. Proc. 6. BNES Conf. Water Chemistry of Nuclear Reactor Systems, Bournemouth, UK, 1992, Vol. 2, p. 49–60

Lister, D. H., Anderson, P. G., Barry, B. J., Lavoie, R. G.: Deposition of cobalt on surface-treated stainless steel under PWR conditions. Report EPRI NP-6528 (1989)

Lister, D. H., Davidson, R. D.: Corrosion product release in light water reactors. Report EPRI NP-6512 (1989)

Lister, D. H., Kushneriuk, S. A., Campbell, R. H.: The transport of radioactive corrosion products in high-temperature water. – III. The interaction of dissolved cobalt with heated surfaces. Nucl. Sci. Engng. **85**, 221–232 (1983)

Mäkelä, K., Aaltonen, P., Paavola, A.: Corrosion in nuclear power plants moderated by water chemistry. Proc. 5. BNES Conf. Water Chemistry of Nuclear Reactor Systems, Bournemouth, UK, 1989, Vol. 1, p. 39–42

Marchl, T., Greger, G. U.: Optimized coolant chemistry with regard to dose rate reduction: Calculations with the OPTIMI code. Proc. 5. BNES Conf. Water Chemistry of Nuclear Reactor Systems, Bournemouth, UK,1989, Vol. 2, p. 13–18

Marchl, T., Riess, R. (a): Update on dose rates in Siemens-designed PWRs. Paper presented at the EPRI Radiation Field Control Seminar, Seattle, Wash., USA, 1993

Marchl, T., Riess, R. (b): Reducing the cobalt inventory in Siemens PWRs. Paper presented at the EPRI Radiation Field Control Seminar, Seattle, Wash., USA, 1993

Marchl, T., Riess, R., Odar, S.: Possibilities to influence personnel exposures illustrated at recent pressurized water reactors. VGB Kraftwerkstechnik **72**, 561–563 (1992)

Matijevic, E.: Properties of colloidal corrosion products and their effects on nuclear plants. Report EPRI NP-4817 (1986)

Metge, M., Beslu, P., Lalet, A.: Cobalt sources in PWR primary systems. – PACTOLE prediction. Proc. 4. BNES Conf. Water Chemistry of Nuclear Reactor Systems, Bournemouth, UK, 1986, Vol. 1, p. 71–74

Neeb, K. H., Grämer, G., Riess, R.: Untersuchungen von Ablagerungen auf Brennelementen der ersten Wechselmenge KWO. Proc. Reaktortagung Deutsches Atomforum Hamburg 1972, p. 225–228

Ocken, H., Wood, C. J.: Status report on radiation exposure reduction at US nuclear power plants. Proc. 6. BNES Conf. Water Chemistry of Nuclear Reactor Systems. Bournemouth, UK, 1992, Vol. 2, p. 1–8

Paffrath, G., Haag, J., Schroeder, H. J.: Behaviour of antimony in the primary coolant. – Antimony: an essential factor in the aim to reduce doses by chemistry. Proc. 4. BNES Conf. Water Chemistry of Nuclear Reactor Systems, Bournemouth, UK, 1986, Vol. 2, p. 35–42

Pashevich, V. I.: USSR experience in decontamination and water chemistry of VVER type nuclear reactors. Report IAEA TECDOC-667 Coolant Technology of Water Cooled Reactors. Vol. 3, Activity Transport Mechanisms in Water Cooled Reactors. Vienna 1992, p. 155–174

Pashevich, V. I., Khitov, Yu.A., Belyayev, M. V., Nemirov, N. V., Grushanin, A. I., Kukharev, N. D.: Hydrazine regime for VVER-440 and VVER-1000 primary circuits. Report IAEA TECDOC-667 Coolant Technology of Water Cooled Reactors, Vol. 1, Chemistry of Primary Coolant in Water Cooled Reactors, Vienna, 1992, p. 110–114

Pick, M. E., Young, M. A., Roofthooft, R.: Effect of surface treatment on radioactivity deposition on stainless steel coupons exposed in Doel 2. Proc. 6. BNES Conf. Water Chemistry of Nuclear Reactor Systems. Bournemouth, UK, 1992, Vol. 2, p. 74–79

Pick, M. E., Roofthooft, R.: Examination of type 304 stainless steel and Inconel 600 with various surface finishes exposed in Doel 2. Proc. 5. BNES Conf. Water Chemistry of Nuclear Reactor Systems, Bournemouth, UK, 1989, Vol. 1, p. 23–29

Polley, M. V., Garbett, K., Pick, M. E.: A survey of the effect of primary coolant pH on Westinghouse PWR plant radiation fields. Report EPRI TR-104180 (1994)

Price, S. G., Polley, M. V., Brookes, I. R., Pick, M. E.: Corrosion and deposition coupon measurements in the primary circuit of Ringhals 4 PWR. Proc. 5. BNES Conf. Water Chemistry of Nuclear Reactor Systems, Bournemouth, UK, 1989, Vol. 2, p. 29–34

Riess, R.: Current status of PWR primary coolant chemistry. Proc. 4. BNES Conf. Water Chemistry of Nuclear Reactor Systems, Bournemouth, UK, 1986, Vol. 1, p. 1–5

Riess, R., Greger, G. U., Schuster, E.: Water chemistry of PWRs to reduce dose and dose rate during operation and maintenance. Nuclear Europe **9**, 14–17 (1984)

Robertson, J.: Modelling of corrosion and corrosion release in PWR primary circuits. Proc. 5. BNES Conf. Water Chemistry of Nuclear Reactor Systems, Bournemouth, UK, 1989, Vol. 1, p. 81–87

Rodliffe, R. S., Polley, M. V., Thornton, E. W.: Modelling the behaviour of corrosion products in the primary heat transfer circuits of pressurised water reactors. – A review of principles. IAEA Report TECDOC-429 Water Chemistry Relevant to Coolant–Cladding Interaction, Vienna, 1987, p. 105–164

Roesmer, J.: Minimizing core deposits and radiation fields in PWRs by coordinated Li/B chemistry. Proc. 3. BNES Conf. Water Chemistry of Nuclear Reactor Systems, Bournemouth, UK, 1983, Vol. 1, p. 29–36

Roesmer, J.: Recent developments in PWR coolant chemistry. Nuclear Europe **1989**, (3/4), p. 21

Rühle, W., Riess, R.: Overview of activity buildup in the later West German PWRs. Proc. 5. BNES Conf. Water Chemistry of Nuclear Reactor Systems, Bournemouth, UK, 1989, Vol. 1, p. 1–8

Rummery, T. E., Macdonald, D. D.: Prediction of corrosion product stability in high-temperature aqueous systems. J. Nucl. Materials **55**, 23–32 (1975)

Samuel, Th.: Discussion contribution. Proc. 5. BNES Conf. Water Chemistry of Nuclear Reactor Systems, Bournemouth, UK, 1989, Vol. 2, p. 44

Sandler, Y. L., Kunig, R. H.: The solution of nonstoichiometric nickel ferrite in high-temperature aqueous solution. Nucl. Sci. Engng. **64**, 866–874 (1977)

Saurin, P., Weber, C., Brissaud, A., Gouillardou, G.: French experience with electropolishing. Proc. 5. BNES Conf. Water Chemistry of Nuclear Reactor Systems, Bournemouth, UK, 1989, Vol. 2, p. 23–28

Schlenkrich, H.: Untersuchungen zum Aktivitätsaufbau im Primärkreislauf von Druckwasserreaktoren. 7. Untersuchungen zur Korrosionsproduktablagerung auf Stahloberflächen unter Druck-Temperatur-Bedingungen von Primärkreisläufen. Kernenergie **28**, 179–182 (1985)

Schuster, E., Neeb, K. H., Ahlfänger, W., Henkelmann, R., Järnström, R. T.: Analysis of primary side oxide layers on the steam generator tubes from PWRs and radiochemical issues on the contamination of primary circuits. J. Nucl. Materials **152**, 1–8 (1988)

Schuster, E., Sendelbeck, R., Hoffmann, R., Rühle, W., Jacobi, G.: Influence of Co hardfacing materials inside reactor pressure vessels on the ^{60}Co contamination of PWR primary circuits. Proc. 5. BNES Conf. Water Chemistry of Nuclear Reactor Systems, Bournemouth, UK, 1989, Vol. 1, p. 17–21

Smith-Magowan, D.: Evaluation of the application of colloid studies to cobalt-60 deposition in LWRs. Report EPRI NP-3773 (1984)

Smith-Magowan, D.: The impact of colloidal chemistry on radioactivity transport in nuclear power plants. Report EPRI NP-4032 (1985)

Stöckert, H., Emmert, H., Meyer zu Schwabedissen, Ch., Seifert, K.: Entfernung von Antimon aus dem Primärkreis von DWR-Anlagen und Ergebnisse aus der Durchführung beim Kernkraftwerk Phlippsburg-2. VGB Kraftwerkstechnik **67**, 288–290 (1987)

Sweeton, F. H., Baes, C. F.jr., Jenks, G. H.: The solubility of Fe_3O_4 in dilute acid and base solutions of 300 °C. J. Chem. Thermodyn. **2**, 479–500 (1970)

Tamura, H., Matijevic, E., Meites, L.: Adsorption of Co^{2+} ions on spherical magnetite particles. J. Colloid Interfaces Sci. **92**, 303–314 (1983)

Thornton, E. W.: Activity transport mechanisms in water cooled reactors. Report IAEA TECDOC-667 Coolant Technology of Water Cooled Reactors, Vol. 3: Activity Transport Mechanisms in Water Cooled Reactors., Vienna, 1992, p. 9–51

Walker, S. M., Thornton, E. W.: Reanalysis of oxide solubility data. Proc. 5. BNES Conf. Water Chemistry of Nuclear Reactor Systems, Bournemouth, UK, 1989, Vol. 1, p. 89–95

Walton, G. N., Hesford, E.: The migration of activated corrosion products in high-pressure water loops. Proc. Conf. Corrosion of Reactor Materials, Salzburg 1962, Vol. 2, p. 547–556

Weitze, H., Braun, D., Odar, S., Greger, G. U., Walter, K. H., Weber, K. G.: Dose rate buildup investigations and modelling for Goesgen and Neckarwestheim. Proc. 4. BNES Conf. Water Chemistry of Nuclear Reactor Systems, Bournemouth, UK, 1986, Vol. 2, p. 17–21

4.4.4 Contamination buildup in boiling water reactors

4.4.4.1 General aspects

Despite all the design differences between PWRs and BWRs, the phenomenon of contamination buildup shows many similarities or even identical patterns in both types of plants. As in the PWR, ^{60}Co is the most important radionuclide in the BWR determining the resulting radiation dose rates at the components and systems, usually contributing 80 to 90% to the total γ dose rate, followed by ^{54}Mn and ^{58}Co. In many of the BWR plants, the last-mentioned radionuclide is of minor significance because of the lack of larger surfaces of materials with higher nickel contents, and because of the comparatively short halflife of this radionuclide. As in the PWR primary circuit, the contaminating radionuclides are incorporated into the superficial oxide layers which adhere tightly to the materials. Due to the differences in the water chemistry conditions, the upper part of the oxide layers in the BWR circuits and components mainly consists of hematite, while the inner layer (which directly covers the base metal) is an iron-based spinel-type oxide. These contamination layers are present on all surfaces which are wetted by reactor water during operation and, also, during shutdown periods.

In the first generation of BWRs, the release of non-ferrous metals to the feedwater, in particular from the copper-based alloys in the feedwater heater tubes, led to tenacious deposits of metal oxides in the reactor core and resulted in an increase in the core pressure drop and in restrictions of the coolant flow. The replacement of these materials by stainless steel tubes has eliminated these difficulties; the deposits which were observed in the following plant generations are too thin to cause such problems.

Comparable to the situation in the PWR primary circuit, the generation of activated corrosion products in the BWR may proceed in two basically different ways which are similar to those shown in Fig. 4.26. Corrosion products with their corresponding radionuclides are released to the reactor water from materials that are permanently located in the neutron field and, therefore, have undergone long activation periods at a comparatively high neutron flux, with one example being the control rod guide rollers made of Stellite. On the other hand, corrosion products which are generated outside the reactor pressure vessel are introduced by the feedwater into the reactor pressure vessel, where they are deposited on the fuel rod surfaces and are subjected to activation by neutrons. Due to the different designs employed in BWR plants, the corrosion products originating from the out-of-core surfaces may take different paths. In each case, all the surfaces wetted by the liquid reactor water (such as the lines of the reactor water cleanup system and, in a part of the BWR plants, the recirculation lines) will contribute to the corrosion product input into the reactor pressure vessel. In the plants with 100% condensate polishing, only the feedwater preheaters are significant additional sources of corrosion products. In contrast with these plants, in the so-called forward-pumped plants corrosion products originating in the high-pressure part of the turbine as well as in the high-pressure heaters (inactive atoms released due to corrosion as well as corrosion product radionuclides carried by the main steam) are transported with

these condensates directly back to the preheaters. Thus, in the forward-pumped plants about one-third of the circulating medium is not purified by the condensate polishing system. As a consequence of these differences, the relative contribution of the two paths depicted in Fig. 4.26. to the total contamination buildup may depend (at least to some extent) on the specific design of the plant.

As with PWRs, a detailed knowledge of the relative significance of each of the possible sources of radionuclides described above is a basic requirement for taking effective countermeasures against contamination buildup. Unfortunately, the current state of knowledge on the mechanisms of BWR contamination buildup is not yet as complete as in the PWR case (see Section 4.4.3.). In addition, similar to the PWR situation, cobalt transport and deposition in a BWR is a complex chemical reaction which can be affected by many parameters. This is an essential reason for the considerable variation in the radiation dose levels frequently observed between different plants, which often cannot be explained in a simple manner by differences in design and/or operation.

However, there are some features which are quite similar in most of the BWR plants. According to the critical evaluation of the practical experience of contamination buildup at 19 BWR plants conducted by Anstine et al. (1984), the buildup trends of the radiation dose rates from the recirculation lines in 17 of these plants followed a similar pattern; after a steady increase during the first 2.5 to 4 effective full power years (EFPYs) of operation, the dose rates leveled off or even began to decrease slightly. This behavior, which is observed in the great majority of all operating BWR plants, indicates a dynamic equilibrium between deposition of radionuclides from the coolant and release of radionuclides once deposited on the surfaces back to the water phase. Even though similar qualitative trends exist, the equilibrium dose rates in the different plants vary over a broad range from 0.5 to 7 mGy/h (measurements performed at comparable positions). The two above-mentioned plants which did not follow the general trend experienced a rapid dose rate increase after about 4 EFPYs of operation, without any evident correlation with plant operation parameters. Thus, while the dose rates in most BWRs level off or begin to decrease slightly after 3 to 4 EFPYs, there is always the possibility of a rapid radiation buildup in a later phase of plant life. From these comparative evaluations, a generic correlation was developed between the initial (after the first fuel cycle) dose rates and the long-term equilibrium dose rates on the recirculation lines. The majority of the plants experiencing high dose rates after the first fuel cycle showed also high equilibrium dose rates, while those plants with low first cycle dose rates maintained the low dose rates (with the exception of the two plants mentioned above) during further operation. Such a correlation indicates that initial plant parameters may play a significant part in determining the long-term dose rates on the recirculation lines.

Another study (Marble, 1985) showed that the time behavior of the contamination buildup in different BWR plants may exhibit significant differences. Usually, the buildup is a logarithmic or parabolic function of time, possibly indicating that the incorporation of dissolved radioactive cobalt species into the oxide layers on the surfaces of the materials is the responsible mechanism. In individual cases, however, pronounced increases in the radiation levels were observed in the first

fuel cycles which correlated with unusually high corrosion product concentrations in the reactor water and which were normalized again by improving the water chemistry conditions. Additional increases in activity buildup were observed to be caused by severe fuel rod failures and subsequent deposition of fission products, mainly ^{95}Zr and ^{103}Ru, onto the surfaces of the primary system.

A more recent overview of the current state of the art concerning the essential mechanisms and parameters determining contamination buildup in BWR plants was given by Alder (1992) and by Alder et al. (1992). Though the interactions between the materials of the primary system and the chemistry conditions in the coolant which dictate production, transport and deposition of radionuclides are very complex and are not yet fully understood, several ways have been identified of minimizing radiation field buildup. Comparing the situation now with that in the early years of commercial BWR operation, significant progress in reducing dose rates and personnel radiation exposures can be noted. However, the basic problem still exists and needs continued attention.

4.4.4.2 The sources of the radionuclides.

In both PWRs and BWRs, corrosion of the primary circuit materials is an essential factor in the buildup of contamination layers on the surfaces of the pipes and the components. The materials used in BWRs which are in contact with the reactor water and, therefore, are potential sources of radionuclides are mainly stainless steels; wear-resistant hardfacing alloys such as Stellite are also present in most of the plants. Zircaloy as the material of fuel rod claddings, spacers and fuel assembly casks need not be considered in this context, because of the extremely small release of activated constituents from this material. Due to differences in temperature and environment, the mechanisms of the corrosion process and the resulting metal release rates, which contribute to the input of corrosion products into the region of the reactor core, may show differences in different regions of the plant. Thus, corrosion of materials in the water-steam cycle exhibiting H_2O phase transformations and considerable temperature differences will proceed differently than in the recirculation lines and the reactor water cleanup system, which are in contact with liquid water exclusively and show comparatively small variations in operating temperature.

The mass of corrosion products introduced into the BWR recirculating coolant is in most cases dominated by iron, which originates primarily in the uniform corrosion of stainless and carbon steels in the feedwater systems, with a significant or even dominant contribution coming from the surfaces operated at comparatively low temperatures. The corrosion mechanisms and metal release rates of these materials depend strongly on the concentration of dissolved oxygen in the water as well as on the flow characteristics, with another important parameter being the conductivity of the water. Corrosion of reactor components located inside the reactor pressure vessel is usually only of minor significance when the mass fractions of the corrosion products are considered; however, as will be outlined below, it is of

considerable significance as regards release of radionuclides due to the high specific activities induced in these materials by permanent neutron irradiation over the entire operating period of the plant. As was mentioned above, due to the differences in plant design, there are considerable differences to be observed concerning the corrosion product input into the reactor water between the plants with and without (so-called forward-pumped plants) complete recirculation of the high-pressure condensates to the condensate polishing system. In addition to operation at steady-state conditions, changes in reactor load as well as outage periods may have an important impact on the total input of corrosion products.

In addition to the total input of corrosion products, the origin of the different elements is also a matter of concern. In a detailed analysis performed at one BWR plant, it was found that about 99% of the total iron in the reactor water originated from the feedwater system, whereas 35% of the cobalt was released from reactor components (EPRI, 1982; according to Alder et al., 1992). Another potentially significant source of cobalt, other than the cobalt alloys, are the nickel alloys used in the primary system, whose cobalt content is occasionally distinctly higher than that of stainless steel. It has to be emphasized that these data relate to the mass of cobalt released to the reactor water and not to the amount of cobalt radioactivity.

The corrosion of the stainless steel 304SS, as well as of Stellite 6, under BWR conditions was studied in detail by Lister and Davidson (1989) using the same experimental setup as for the corresponding experiments under PWR conditions (see Section 4.4.3.2.). The results of these investigations concerning stainless steel 304SS are shown in Fig. 4.43.a. in the form of equivalent penetrations (see Section 4.4.3.2.) over the experimental period of 2000 hours. Using log-log coordinates, cobalt shows an almost linear increase which can be described by the equation

$$\text{equivalent penetration } (\mu\text{m}) = 1.87 \cdot 10^{-4} \cdot (\text{time})^{0.88}$$

Similar to PWR conditions, cobalt shows a preferential release to the coolant as compared to iron, indicating a comparatively weak cobalt retention in the oxide layers formed on the surfaces of the materials. Furthermore, the results show a chromium release which initially increases more than linearily with time and a somewhat irregular ^{58}Co release behavior which was possibly influenced by errors in the measurement of the very low ^{58}Co activity concentrations present in the experimental solutions. Since the ^{60}Co release rate is almost constant over time, the equivalent penetration under BWR operating conditions is lower than that under PWR conditions for the time period of the experiments; however, when integrated over the 30-year operational life of the plant, the ^{60}Co release under BWR conditions is significantly higher than that under PWR operating conditions.

As for Stellite 6, the results of the investigations under BWR conditions shown in Fig. 4.43.b. demonstrate that at least over a long time period the cobalt release can be approximately described by the equation

$$\text{equivalent penetration } (\mu\text{m}) = 4.2 \cdot 10^{-4} \cdot (\text{time})$$

The release of chromium from the Stellite material initially shows a considerably steeper increase with time, with this finally changing to a slope that is virtually identical with that of the cobalt release. From these results it can be concluded

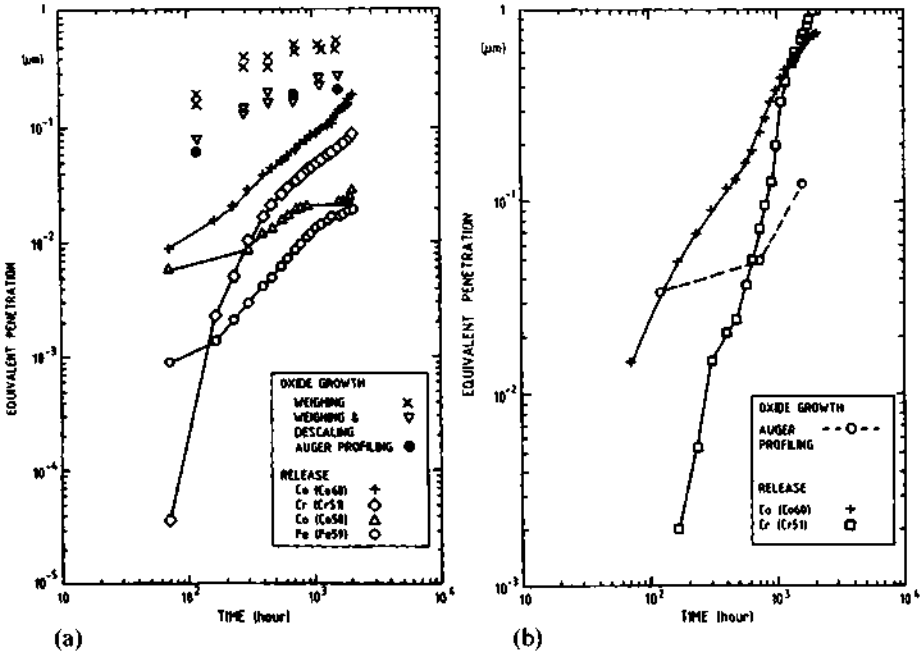

Figure 4.43. Oxide growth and release of corrosion products from materials under BWR operating conditions; a) Stainless steel 304SS; b) Stellite 6
(Lister and Davidson, 1989)

that, in spite of their comparatively small surface areas, the Stellite materials represent the dominant source of supply of cobalt to the reactor water, even when mechanical wear is not taken into account. The steel surfaces outside the reactor pressure vessel apparently are of minor significance for cobalt supply as well as for ^{60}Co production.

According to the investigations of Lister and Davidson (1989), the formation of oxide layers on the stainless steel surfaces is affected by the concentrations of corrosion products present in the test solution. A coolant free of corrosion products results in a surface oxide layer depleted in nickel which is less effective from the perspective of protection against the progress of corrosion. The addition of zinc to the coolant (which will be treated in more detail in Section 4.4.4.5.) has a pronounced effect on the metal release rates, in particular on the release from stainless steels, due to the formation of a thin but very effective protective layer that results in a drastic decrease of the release of metal atoms to the coolant. As an important parameter, addition of zinc to the reactor water has to be carried out during the early stages of the formation of protective layers, since addition at a later time will show little effect. The experimental results suggest that the effect of zinc addition is most pronounced with alloys which form a protective layer containing chromium; however, Inconel 600 and Stellite 6 will also acquire thin and effective protective layers after the addition of zinc.

Whereas in a PWR primary circuit the metal release rates of the materials in the reactor core are virtually unaffected by radiation, under BWR conditions irradiation results in an increase in the metal release rates. This effect is primarily caused by the oxidizing products of water radiolysis; since the primary radiolysis products, as well as H_2O_2, show only a limited lifetime in the reactor water, the materials inside the reactor pressure vessel are far more strongly affected than those located outside the neutron field, resulting in an enhanced release of highly activated corrosion products. Studies performed, among others, by Ishigure et al. (1980) and by Kawaguchi et al. (1981) showed that upon irradiation of the test specimens during the corrosion tests the concentrations of non-dissolved iron and cobalt in the water phase increased significantly, while the concentrations of the dissolved species were only little affected. The irradiation effect can be suppressed by the addition of NH_3 to the test solution; moreover, the differences between irradiated and non-irradiated experiments largely vanished at test temperatures below about 100 °C. These results can be explained by the assumption that the non-dissolved suspended particles measured in the water medium were formed in the water itself from iron ions. This means that primarily Fe^{2+} ions are released from the surface of the metal (for thermodynamic reasons, release of Fe^{3+} ions is not to be expected at temperatures around 250 °C). In the water phase, these ions are immediately oxidized to Fe^{3+} by dissolved oxygen or by radiolytically generated $OH\cdot$ radicals and H_2O_2 molecules; Fe^{3+} in turn, because of its extremely low solubility, is hydrolyzed to insoluble $Fe(OH)_3$ and later on converted to Fe_2O_3. Since oxidation of Fe^{2+} to Fe^{3+} is the rate-controlling step in this reaction chain, an increase in the concentration of oxidizing species in the water phase will favor the formation of suspended matter. The inhibiting effect of NH_3 is assumed to be due to its $OH\cdot$ scavenging effect; in addition, at temperatures below 100 °C, Fe^{2+} is not oxidized by the radiolytically generated species, rather Fe^{3+} is reduced at such a low temperature by radiolytically generated aquated electrons. As regards the behavior of cobalt it can be assumed that Co^{2+} ions are removed from the solution by adsorption onto the surfaces of hematite particles and that, therefore, the non-dissolved cobalt concentration increases with increasing hematite concentration in the water (see Section 4.4.4.3.). Since this adsorption is an endothermal process, it is understandable that the effect of irradiation on the formation of non-dissolved cobalt species is less pronounced at temperatures below 150 °C.

Taking into account that dissolved cobalt species are assumed to be primarily responsible for contamination buildup (see below), it still seems questionable whether the irradiation effect, which results in an enhanced release of metal atoms from the materials, will significantly affect the rate and the magnitude of deposition of radioactive cobalt on the out-of-core surfaces.

As was pointed out at the beginning of this section, the second possible mechanism of radionuclide production and of contamination buildup is neutron activation of corrosion products which are temporarily deposited inside the neutron field, in particular on the claddings of the fuel rods. These corrosion products mainly stem from the turbine cycle of the plant and are introduced into the reactor pressure vessel with the feedwater. In most of the BWR plants, where all the arising condensates are purified in the condensate polishing system (mainly using precoat

Table 4.12. Corrosion product loadings and corrosion product composition on a typical BWR fuel rod
(By courtesy of Siemens/KWU)

Sample No.	Sampling position*)	Area-related mass, mg/cm²	Oxide constituents, %						
			Fe	Co	Ni	Cu	Zn	Cr	Mn
1	750	0.21	41	xx	4.0	1.3	2.8	1.3	1.1
2	1250	0.20	44	0.6	5.1	1.6	2.4	1.7	0.9
3	1750	0.29	52	0.4	4.4	1.8	2.2	1.2	2.2
4	2250	0.21	48	0.2	6.2	1.6	2.0	1.2	1.7
5	3250	0.17	51	0.02	4.1	0.9	2.2	1.4	1.1

*) mm from lower end of the fuel rod
xx) below detection limit

filter techniques), corrosion occurring in the pipes downstream from the condensate polishing system essentially contributes to corrosion product input into the reactor water. In the so-called forward-pumped plants, however, the high-pressure heater drains are directly returned to the feedwater, so that a significant contribution can also come from this region of the turbine cycle. Detailed investigations performed at a number of BWR plants have shown that these corrosion products mainly consist of crystalline hematite (Hermansson et al., 1993).

The thickness of the corrosion product deposits on BWR fuel rods differs markedly from plant to plant, obviously depending on the iron concentration in the feedwater (which usually is below 10 ppb). Values on the order of a few mg/cm² were reported from some plants, whereas others showed layers of only 0.1 to 0.5 mg/cm². The differences in layer thickness to PWRs (up to an order of magnitude) are mainly due to the fact that crud deposition on BWR fuel rods is supported by the boiling effect on the fuel rod surfaces. In the Soviet RBMK reactors, fuel rod deposits on the order of 40 to 60 μm are typical (according to Dragunov et al., 1992).

As an example, the results of the area-related corrosion product loadings and of the chemical composition of the corrosion products collected from different positions of a typical fuel rod from a German BWR using a sampling device as described in Section 4.4.2., are given in Table 4.12. Due to high-purity feedwater, these corrosion product loadings are comparatively low, showing a flat distribution along the axis of the fuel rod with a maximum thickness in the region of highest thermal loading. The investigated fuel rod was located during operation in the center of an assembly; fuel rods located in the outer rows of an assembly usually show somewhat lower corrosion product loadings. The main constituent of the deposits on this fuel rod was iron, with its overwhelming fraction being α-Fe_2O_3, with some contribution of spinel-type oxides. The concentrations of the other constituents show but little variation with increasing height on the fuel rod.

In their survey paper, Anstine et al. (1984) summarized the knowledge gained in the analysis of core deposits from a greater number of BWR plants (mostly US

plants). Such a comparative evaluation is often complicated by a considerable number of possible sampling variables as well as by the dependence of the nature of the deposits on the type of condensate treatment system installed in the particular plant. Despite these differences, the deposits usually consist of two layers, an outer loosely-adherent one and an inner tightly-adherent layer. In sampling, the outer loosely-adherent fraction can be easily removed using a nylon brush, whereas the tenacious inner layer can only be effectively removed by scraping with an abrasive stone. Usually, the outer layer makes up approximately 60% of the total deposits and contains a higher percentage of iron; the inner tightly-adherent layer shows higher levels of the other elements, such as Ni, Co, Cu, Zn and Mn, with each of them amounting to a few percent. In all the investigated plants, the deposits in both fractions were predominantly α-Fe_2O_3, with traces of Fe_3O_4 detected on several occasions.

There are, however, marked differences in the nature of the fuel rod deposits formed in different facilities which can be correlated with the type of the condensate treatment system installed. The use of filter/demineralizer systems (precoat filters) results in lower metal loadings on the fuel rod surfaces (average 0.7 mg/cm^2) when compared to plants with deep bed filters (average 4 to 5 mg/cm^2); by far the highest corrosion product loadings were measured at one plant equipped with forward-pumped heater drains, which showed loadings of about 8.6 mg/cm^2. The lower deposit loadings on the fuel rods in the filter/demineralizer plants are due to the lower corrosion product concentrations in the feedwater which result from the high capability of such a system to remove suspended solids. The fuel rod deposits from the plants equipped with filter/demineralizer systems exhibit marked differences in the chemical composition of the two layers, in particular in the iron content which is about 83% in the brushed fraction and only about 70% in the scraped fraction. The later layer, in turn, showed higher levels of the other elements. The deposits from all the plants with other condensate treatment systems showed iron contents of more than 90%, and the two fractions of the deposits were essentially similar in their chemical composition.

Knowledge about the mechanism of deposition of corrosion products onto the fuel rod surfaces is still limited. The dissimilar elemental concentrations for the brushed and scraped fractions in the filter/demineralizer plants are probably due to the fact that these two fractions were created by different mechanisms. The brushed fraction most likely results from the deposition of suspended particles from the reactor water, while the scraped fraction is assumed to be formed by precipitation of dissolved corrosion product species. The axial distributions of both fractions of the deposits on the fuel rod surfaces usually show differences which also suggest that they were generated by different mechanisms. The brushed fraction shows a characteristic profile, in which the corrosion products deposit preferentially near the bundle inlet and which can be correlated with the fluid shear at the heat transfer surface. This distribution is consistent with the assumption that particle deposition is the predominant mechanism for the buildup of the loosely-adherent deposits, since low fluid shear favors particle deposition. On the other hand, the axial profile of the tenacious fraction is quite different, being relatively constant over the middle region of the bundle and decreasing towards each end.

This profile resembles the exposure profile of the assembly, indicating that the heat flux controls the buildup of the scraped fraction. It is generally assumed that some of the loosely adhering deposits may be converted into the tenacious layer on the surface, but little is known about the processes that might be responsible for such a conversion.

The deposition as well as the adhesion of suspended particles on the fuel rod surfaces are potentially influenced by colloid chemistry effects and may be regarded as a coagulation of the hematite particles suspended in the reactor water. According to a model which was developed by DeHollander (according to Alder et al., 1992), such a deposition is promoted by the heat flux, predominantly by bubble evaporation. It is assumed that corrosion product particles with diameters smaller than about 0.2 μm are transported by the growing bubbles to the surface where they frit together to form a tightly adherent layer; larger particles (about 0.1 to 1 μm) are deposited by whirl processes, sintering together with the fine-grained, tightly-adhering material, which shows good adhesive properties. Since particles with still larger diameters (in the range 1 to 10 μm) adhere less well, their residence time on the fuel rods may be only on the order of several days to weeks; however, they are assumed to effect the largest part of the activity transport from the reactor core to the recirculation loops. In this postulated mechanism, the question remains still open of why the cobalt content in the fuel rod deposits is higher than in the circulating crud, an observation which has been reported by several investigators; such a purely mechanical deposition process should not lead to an enrichment in the cobalt concentration.

The linear dependence of the deposition rate R on the concentration of corrosion products in the reactor water is largely undisputed. On the other hand, there are differences in opinion as to the impact of the heat flux, whether R is directly proportional to the heat flux Q or whether it is proportional to the square of the heat flux. According to Alder et al. (1992), the deposition of corrosion products onto the fuel rod surfaces preferentially occurs in the zone where nucleate boiling begins (about 1 m from the bottom end of the fuel rod) and is expressed in the following equation:

$$R = k \cdot c \cdot Q / L$$

where R = deposition rate
k = constant
Q = heat flux
L = heat of vaporization
c = crud concentration in the reactor water.

Moreover, the deposition rate seems to depend on the particle diameter, showing a maximum in the range 0.5 to 1 μm and decreasing for both smaller and larger values (Kawaguchi et al., 1983). Generally, the deposition rate of the corrosion product particles on the fuel rod surfaces decreases with an increasing flow rate of the water phase.

As was mentioned above, such purely physical crud deposition mechanisms are not able to explain the relative enrichment of cobalt in the layers on the fuel rod surfaces. In Section 4.4.3.2. it was discussed that under PWR conditions dissolved

Table 4.13. Activity concentrations of γ-emitting radionuclides in the deposited corrosion products on a BWR fuel rod
(By courtesy of Siemens/KWU)

Sample No.*	Activity concentrations, GBq/g oxide					
	^{51}Cr	^{54}Mn	^{59}Fe	^{58}Co	^{60}Co	^{65}Zn
1	1.9	0.23	0.22	1.0	0.34	0.55
2	2.1	0.28	0.26	1.2	0.36	0.61
3	0.91	0.15	0.15	0.59	0.17	0.26
4	0.62	0.13	0.11	0.58	0.16	0.24
5	0.46	0.11	0.08	0.44	0.12	0.17

*) sample location see Table 4.12.

Co^{2+} ions from the water phase can be adsorbed onto zirconium oxides present on the surfaces of the fuel rods; according to Alder et al. (1992), similar processes can be expected under BWR operating conditions. Such processes are irreversible and proceed very fast (Kawamura et al., 1984); however, they are only of significance with new fuel assemblies for a comparatively short period of time. From experimental results it can be concluded that the iron oxide deposited on the fuel rod cladding surfaces also provides adsorption and reaction sites for other metal ions; the more iron in the coolant, the more easily traces of cobalt and nickel deposit on the fuel rod surfaces (Lin, 1990). Other experiments have shown that Co^{2+} ions from the water phase are readily picked up by α-Fe_2O_3 under formation of a $CoFe_2O_4$ compound (Nishino et al., 1992). The rate of this conversion largely depends on the temperature and proceeds comparatively fast at BWR operating temperatures. This suggests that the hematite already deposited on the fuel rod surfaces takes up dissolved Co^{2+}, which would then contribute to the enhanced cobalt concentration observed in the fuel rod deposits.

Nickel ions present in the reactor water are initially deposited as NiO onto the fuel rod surfaces. There, NiO reacts with the deposited α-Fe_2O_3 to form $NiFe_2O_4$. When the Ni : Fe ratio is higher than the theoretical value of 0.5, NiO remains precipitated on the surface of the fuel rod; since the dissolution rate of this compound in high-temperature water is higher by a factor of 3 to 10 than that of the spinel oxides, the presence of NiO results in an increase in the concentration of dissolved ^{58}Co in the reactor water (see Section 4.4.4.5.).

The activity concentrations of the main γ-emitting radionuclides in the fuel rod deposits of a German BWR plant are exemplarily shown in Table 4.13. (data corrected to the end of irradiation). Typically, the values are in the range from 0.1 to 2 GBq/g oxide, with ^{51}Cr and ^{58}Co showing the highest values, followed by ^{60}Co. Since the radionuclide composition of the deposits varies greatly from plant to plant, the data given in Table 4.13. cannot be judged to be representative of all BWR fuel rods. In most of the BWR plants investigated by Anstine et al. (1984), ^{60}Co was the predominant radioisotope on the fuel rod surfaces. It was about evenly divided between the brushed and the scraped fraction of the corrosion product deposits.

In order to become activated to an extent which is of significance for contamination buildup, the corrosion products have to stay in the neutron field for a certain period of time (weeks to months). From the measured specific activities given by Anstine et al. (1984), it was calculated that the residence time of cobalt in the neutron field in the loosely-adhering fraction was in most cases on the order of 100 days, whereas in the tightly-adherent fraction it can be considerably longer. However, from the data given in Table 4.13., cobalt residence times in the neutron field of only a few tens of days were calculated, compared to residence times of nickel and iron ranging from 30 to 70 days. Since residence time in the neutron field is an important parameter in ^{60}Co production, a smaller amount of deposits and a shorter residence time would be beneficial. On the other hand, it has also been argued that very long residence times (i. e. two to three years) would be favorable for plant contamination buildup, since under such conditions a considerable fraction of the ^{60}Co produced would be removed from the primary system together with the spent fuel assemblies. The difficulty here is that the reprocessing plants usually specify an upper limit of allowable fuel rod contamination, so that the surfaces of the highly contaminated assemblies would have to be cleaned prior to shipment.

Basically, the amount of iron deposited on the fuel rod surfaces is of minor importance for contamination buildup, since its activation products ^{54}Mn, ^{55}Fe and ^{59}Fe contribute only to a minor degree to the radiation dose rates in the areas surrounding the circuits and systems. Only in plants which show comparatively high crud inventories does the sum of ^{54}Mn and ^{59}Fe activities deposited on the out-of-core surfaces nearly equal that of ^{60}Co. Nonetheless, due to the different radiation properties, their contribution to the environmental dose rate levels is comparatively small. As was mentioned above, however, iron oxides may provide deposition sites for dissolved cobalt species which means that they contribute indirectly to contamination buildup. In order to minimize the concentration of such reactive sites, different attempts have been made to minimize the generation and transport of corrosion products, the overwhelming part of which originates in the feedwater train. From fossile-fired power plants it is known that maintaining a certain oxygen concentration (on the order of 50 ppb) in the feedwater considerably reduces the corrosion of low-alloy steels. Consequently, this technique has been applied in a number of BWR plants, resulting in a decrease in the amount of corrosion products deposited in the reactor core. However, release of cobalt from the materials to the water is not as effectively suppressed by oxygen addition as release of iron (Ishigure, 1987).

With increasing amount of deposits on the fuel rod surfaces, the release of material back to the water phase gains in importance, with the amount of deposited material approaching an equilibrium value after an extended period of time. The deposition and release processes can be described by equations of the general type:

$$dW / dt = k_1 \cdot c - k_2 \cdot W$$

where W means the deposit weight per unit area and c the concentration of particles in the reactor water. As was mentioned above, the deposition rate constant k_1 depends on several parameters, whereas little is known about the release rate

constant k_2 (Asakura et al., 1978). It is assumed that the release of radionuclides from the fuel rod deposits is enhanced in the presence of a thick and loosely attached porous deposit layer. Basically, corrosion product release from the fuel rod surfaces is promoted by different mechanisms such as erosion, spalling and dissolution and occurs mainly in the loosely-adhering outer layer. Thus, the release rate of activity from the reactor core is expected to be much higher in those plants showing high concentrations of corrosion products. The radionuclides can be released from the fuel rod deposits either together with crud particles or in ionic form; as yet it is not definitely known which of these is the dominant release process for contamination buildup. While it is stated below that dissolved cobalt species are mainly responsible for ^{60}Co deposition on the out-of-core surfaces, it has to be taken into account that the species released from the surfaces of the reactor core may undergo changes in state (dissolution as well as precipitation) during their transport in the hot reactor water.

4.4.4.3 The behavior of the corrosion product radionuclides in the BWR reactor water

The pronounced differences in the chemistry conditions of the BWR reactor water and the PWR primary coolant have a profound influence on the chemical state of the corrosion products and of the radionuclides produced from them. The most important parameters in this context are the pH of the water, which in a BWR is virtually neutral, and the O_2 concentration. The latter parameter shows significant differences from one plant to the next and also may vary over time. As a result, the question of the chemical nature of the radionuclides cannot be answered as definitively as for the PWR primary coolant.

As in the PWR primary coolant, a fraction of the corrosion products in the BWR reactor water appears in an ionic dissolved state, with the remainder being in the form of particulate matter; in the oxidizing environment of the BWR coolant, α-Fe_2O_3 hematite is the predominant form of the non-dissolved corrosion products. The solid particles suspended in the reactor water may be further differentiated into colloidal ($< 1\,\mu m$) and inertial ($> 1\,\mu m$) particles, since not only their transport to and from the surfaces but their interactions with surfaces as well are presumably determined by distinctly different mechanisms. Little information is available on the size of the hematite crud particles present in the reactor water. One reason for this lack of knowledge is the difficulty of determining particle diameters reliably. Scanning electron microscopy is often used to measure the sizes of filtered particles, but there is always the danger of particle coagulation during preparation of the sample. Reported measurements showed an average particle diameter of about $5\,\mu m$ (Uchida et al., 1981), but it seems questionable whether these values are generally valid.

Iron is the major constituent of the corrosion products in the feedwater in BWRs, comprising approximately 85% of the metal total. By far the greatest frac-

tion of iron appears as particulate matter, while the other corrosion products are mainly in the dissolved state. Cobalt shows a dissolved fraction of 80 to 95%, but this fraction depends highly on the iron concentration (see below). In a comparative evaluation of US and foreign BWR plants (Anstine et al., 1984), it was demonstrated that most of the plants showed high initial iron concentrations in the feedwater which gradually decreased in the course of plant steady-state operation. BWRs with deep-bed condensate treatment systems show feedwater total iron concentrations approximately a factor of 10 higher than BWRs with filter/demineralizers; these differences are mainly due to the higher effectiveness of precoat filters for the removal of particulates. The cobalt concentrations show a similar trend (12 ppt vs. 8 ppt). The reason for this difference is not understood since the deep-bed ion exchangers show a higher retention efficiency with regard to dissolved species; possibly, analytical difficulties at the very low cobalt concentrations may have contributed to these apparent differences.

The concentrations of the corrosion products in the reactor water are controlled by a number of parameters, including feedwater input, particle deposition and resuspension, precipitation and dissolution, and quality of performance of the reactor water cleanup system. As a consequence, these concentrations vary considerably from plant to plant and also within a plant, frequently without showing a discernible trend. The concentrations of total iron may vary by more than 3 orders of magnitude, primarily as a result of variations in the concentration of insoluble iron species, while that of dissolved iron is relatively constant and typically below 10 ppb. The concentration range for total cobalt in different plants is considerably smaller, and is typically in the range 10 to 200 ppt. In general, even when extreme fluctuations are ignored, there is no consistent trend in the concentrations of the corrosion products in the reactor water.

The partitioning of cobalt between particulate and dissolved species depends directly on the total corrosion product concentration in the reactor water (Lin, 1990). This dependence is apparently due to interactions between dissolved ionic species and crud particles, resulting in an adsorption of the ionic species onto the surfaces of the corrosion product particles suspended in the reactor water. As can be seen from Fig. 4.44., at very low total iron concentrations in the reactor water, ^{60}Co is almost completely present in the dissolved state; with increasing iron content, the dissolved ^{60}Co fraction decreases steadily, reaching values of only a few percent at iron concentrations around 100 ppb. It is assumed that the ^{60}Co traces are at first adsorbed onto the surface of the Fe_2O_3 crud particles and then are converted into a stable mixed oxide of the type $CoFe_2O_4$.

Similar results on the chemical state of the corrosion products in the reactor water were reported from other BWR circuits, e. g. the reactor water of the British Steam Generating Heavy Water Reactor (SGHWR) (Bridle et al., 1986), where the insoluble iron essentially appeared as α-Fe_2O_3, containing minor amounts of Fe_3O_4. In this case, approximately 50% of the ^{60}Co present in the reactor water was attached to the suspended solids, with the remainder being in a ionic dissolved state; similar ratios between the particulate and the dissolved state were obtained for ^{58}Co.

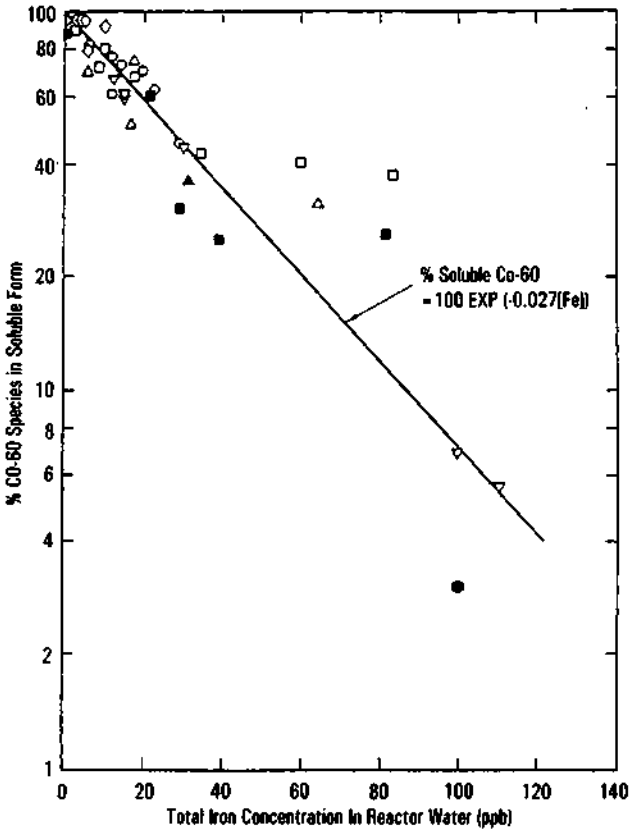

Figure 4.44. Percent dissolved ^{60}Co as a function of total iron concentration in BWR reactor water
(Lin, 1990)

The concentrations of the corrosion product radionuclides in the reactor water depend on the same parameters as those that control the behavior of the total corrosion products and, in addition, on the intensity of neutron activation. As a consequence, the concentrations of radioisotopes may vary considerably from plant to plant and also within a plant. According to the observations reported by Anstine et al. (1984), the concentrations of ^{60}Co and ^{58}Co, the two most prevalent radioisotopes, do vary, but not as greatly as the iron concentrations. In the BWR plants examined in this context, the majority of ^{60}Co and ^{58}Co in the reactor water appeared in the dissolved state. On the average, the concentrations of dissolved ^{60}Co increased for the first 3 to 5 fuel cycles and then leveled off to values on the order of 7 kBq/l, whereas the dissolved ^{58}Co already reached its steady-state level in the same range of concentrations during the first fuel cycle. These differences in the time behavior of both cobalt isotopes probably are to be attributed to their different halflives. The concentrations of particulate ^{60}Co and ^{58}Co, on the other

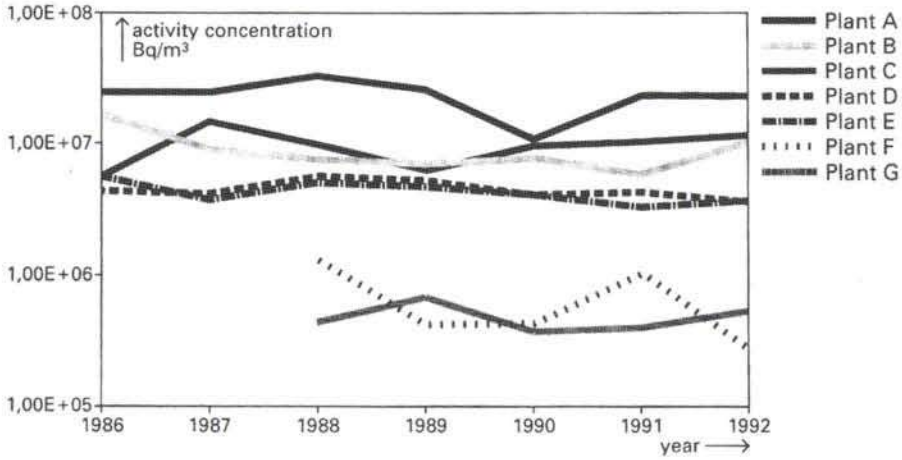

Figure 4.45. Average ^{60}Co activity concentrations in the reactor water of Siemens/KWU BWRs
(Reitzner et al., 1993)

hand, were relatively constant over time, fluctuating around 2 and 1 kBq/l, respectively.

In the German BWR plants at least, the ^{60}Co and ^{58}Co activity concentrations in the reactor water can be correlated to differences in plant design and choice of materials. As can be seen from Fig. 4.45. (according to Reitzner et al., 1993), the ^{60}Co activity concentrations (averaged over the duration of a fuel cycle) in most of the plants were on the order of 10 MBq/m^3 with only small fluctuations over time. The only German BWR plant with external recirculation lines (plant A, the other plants are equipped with internal axial pumps) showed a somewhat higher value, while the plants F and G, in which control rod guide rollers made of Inconel are installed instead of ones made of Stellite, showed ^{60}Co activity concentrations which were lower by about one order of magnitude.

Increasing the pH of the BWR reactor water results in a decrease of the release of atoms from activated in-core materials as well as from oxide layers and, as a consequence, in a reduction of the activity concentrations of ^{58}Co and ^{60}Co appearing in the reactor water. As can be seen from Fig. 4.46., which shows the results of a KOH injection experiment in a German BWR, the concentrations of the dissolved radionuclides reach a minimum at a reactor water pH of 7.5 to 8. One could use, therefore, a pH correction to counteract acidification of the unbuffered reactor water, which might be caused by introduction of CO_2 or of decomposition products of ion exchanger materials. However, when considering pH correction to reduce the buildup of system contamination, one also has to take into account the possible impact of this measure on the cleanup units and the offgas system (Marchl and Reitzner, 1992).

Usually, the concentrations of the other corrosion product radionuclides such as ^{54}Mn, ^{59}Fe and ^{65}Zn in the BWR reactor water are typically below those of ^{60}Co. The high ^{51}Cr concentrations (usually higher by a factor of more than 10

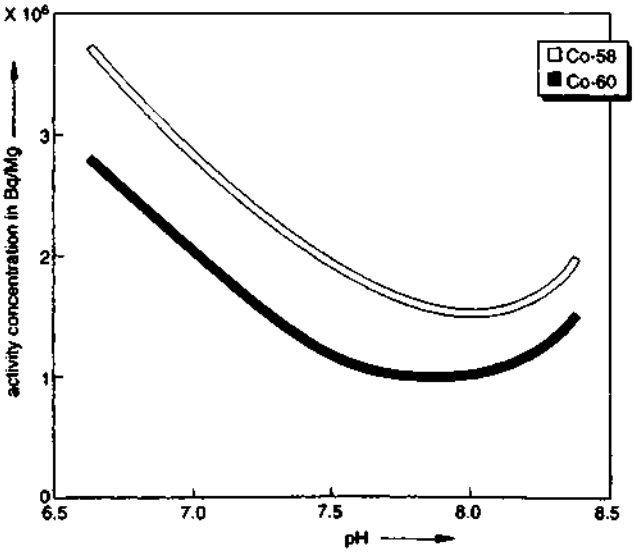

Figure 4.46. ^{58}Co and ^{60}Co (< 0.45 μm) activity concentrations in BWR reactor water as a function of pH
(Marchl and Reitzner, 1992)

than that of ^{60}Co) are primarily due to anionic chromium species. Since ^{51}Cr has a comparatively short halflife and does not exchange readily with the oxide films on the out-of-core surfaces, its concentrations on these surfaces are typically low.

Investigations on the transport behavior of cobalt in BWR systems in which cobalt had been added to the effluents from the condensate treatment system have been described by Palino et al. (1986). The validity of such studies can be adversely affected by cobalt traces which are released from parts of the sampling system containing cobalt alloys (e. g. valves), by which an elevated cobalt content of the feedwater or the reactor water would result; for this reason, for these analyses the authors installed a sampling system completely made of titanium. The results showed that cobalt transport is delayed (compared to the water flow) in the feedwater train by about 6 hours and in the reactor pressure vessel by several days; the reason for this delay seems to be chemisorption at the high-temperature oxide surface layers, leading to a chromatographic effect in the cobalt transport. From balance measurements and calculations it was concluded that the rate of cobalt deposition from the reactor water to the surfaces of the systems is higher by a factor of about 10 than the removal rate via the reactor water cleanup system. Another conclusion which was drawn from the experimental results is that the feedwater system is the main source for the supply of non-radioactive cobalt to the reactor pressure vessel and that the cobalt release from the in-vessel materials seems to be of minor significance. However, it seems questionable whether these findings are generally valid for other BWR plants.

From their comparative investigations, Anstine et al. (1984) concluded that the majority of the corrosion products enter the feedwater by leakage through the

condensate treatment system and, therefore, that the performance of this system controls the corrosion product concentrations in the final feedwater. However, the contribution from this source may be quite different from one plant to another and, in addition, several other factors may affect the corrosion product levels in the feedwater, including corrosion in the feedwater train, corrosion in the balance of the plant, condenser performance, as well as startup, shutdown, and layup practices, and finally the frequency of outages. Several of these factors typically improve with continued operation; for example, it is likely that the corrosion product levels in the feedwater would be high initially and decrease with time. However, because of the large number of influencing parameters, individual plants may deviate from this general trend.

The carry-over of corrosion product radionuclides with the main steam in the direction of the turbine is effected, on the one hand, by droplet entrainment with the residual moisture content of the steam and, on the other, by steam volatility. Usually, droplet carry-over is the most significant transport mechanism; however, the oxides of the primary system metals show a measurable solubility in steam even at BWR operating conditions. At different plants, concentrations of dissolved cobalt on the order of 60 ng/kg were measured in condensed samples of main steam, i. e. significantly higher than could be explained by droplet entrainment (e. g. Hepp et al., 1986). These observations are consistent with the fundamental results on steam volatility of weakly dissociated compounds under BWR operating conditions which were reported by Styrikovich and Martynova (1963). Since only non-dissociated substances are volatile with steam, it has to be assumed that a fraction of the cobalt present as dissolved ions in the reactor water at ambient temperature is converted to non-dissociated oxide, hydroxide or ferrite at the plant operating temperature.

During shutdown of a BWR plant, as well as during startup and during transients, the corrosion product concentrations in the reactor water (as well as the conductivity of the water) show a spiking which, at least with regard to its magnitude, is similar to that familiar from PWR plants (see Section 4.4.3.3.). The peak values of the spiking are quite different from plant to plant and from one transient to another, ranging from tens to thousands of times higher than the level during the preceding steady-state operation. However, in contrast with PWR shutdown spiking, no changes in the state of the cobalt isotopes (particulate vs. dissolved) have been reported. This behavior confirms the significance of the ambient chemistry conditions for the chemical state of the corrosion product radionuclides in the coolant. Since during the shutdown phase the chemistry conditions in the BWR reactor water do not change as drastically as in the PWR primary coolant, the lack of a shift in the chemical states can be understood. The presumed mechanisms responsible for this spiking are the disturbances in core operating conditions (e. g. temperature, pressure, water flow, boiling) which can lead to an increase in the release of loosely deposited corrosion products from the surfaces of the fuel rod claddings. The released high specific activity corrosion product particles may be redistributed to out-of-core surfaces, particularly to low-flow regions, where they are the sources of activity hot spots. The dissolved radionuclides released in the course of the spiking are not assumed to plate out directly onto the surfaces be-

cause of the lower temperatures prevailing during shutdown, but their adsorption onto the oxides which have already accumulated on the surfaces may intensify the activity buildup. An important negative effect of the shutdown spiking is that it leads to a significant contamination of those plant regions which are not in contact with hot liquid reactor water during steady-state operation. During operation, reactor water only contaminates the surfaces of the reactor pressure vessel, the reactor water cleanup loops and, as far as they are present, the external recirculation lines. Quite in contrast with this, during shutdown and during the period of residual heat removal there are a lot of additional pipes, valves and coolers in contact with the reactor water. During this period the reactor water level is lifted up to the steam lines and the feedwater lines, and part of the steam lines are now used as a constituent of the residual heat removal system. Since modern BWR plants (e. g. Gundremmingen B and C plants) are equipped with three residual heat removal systems, each containing a number of valves etc., the radionuclide contamination is spread throughout a large piping system, resulting in large additional areas with potentially high radiation levels. Balance measurements at the Gundremmingen B and C plants have shown that the amount of ^{60}Co released from the surfaces inside the reactor pressure vessel to the reactor water within a 24-hour shutdown period can be of the same magnitude as the release during one year of full power operation (Eickelpasch and Lasch, 1986).

Besides the corrosion products, there are other impurities present in the reactor water, such as silicate and organic compounds. Their possible significance in the process of activity buildup has scarcely been investigated. These substances can form complex compounds with dissolved metal ions or modify the chemical properties of the colloidal matter by adsorption. However, in modern BWR plants the silicon and carbon contents in the reactor water are extremely low, on the order of a few ppb during steady-state operation (Thornton, 1992). They are, therefore, not expected to have any noticeable influence on the contamination levels.

4.4.4.4 The deposition of radionuclides on the surfaces

In the BWR plants, the out-of-RPV surfaces which are subject to contamination during steady-state operation are mainly those wetted by high-temperature reactor water. These are, in the main, the pipes leading to the reactor water cleanup system and the recirculation lines (as far as the plant is equipped with an external recirculation system). In addition to these surfaces, the main steam lines and the turbine, as well as part of the feedwater system, may be contaminated by radionuclides carried with the steam. In the course of a shutdown of the plant, certain regions of the main steam lines and of the feedwater lines are also in contact with low-temperature reactor water containing radionuclides.

As is reported in the review paper of Anstine et al. (1984) in which data from a large number of BWR plants were critically evaluated, the corrosion product films on BWR out-of-core surfaces consist of two different layers: An outer, loosely-adherent layer which is formed by deposition of particles and, partly, by conversion

of the inner spinel layer, and an inner, tightly-adherent layer which is created by corrosion of the underlying base metal. The loosely-adherent layer consists predominantly of α-Fe_2O_3 and comprises approximately one-third of the total metal loading. Its buildup does not show any discernible trend over time, which is not necessarily surprising since it originates primarily with deposition of crud particles and, consequently, should depend on the concentration of particulate corrosion products in the reactor water. This concentration varies considerably with time in a plant and also from plant to plant, so that a time-dependent linear relationship of the buildup of the loosely-adherent deposits cannot be expected. At low flow rate positions, so-called hot spots, enhanced deposition of the loosely-adherent nature may occur.

The inner, tightly-adherent layer consists predominantly of a $NiFe_2O_4$ spinel whose buildup also does not show a discernible trend with time; after 1.5 EFPYs its thickness varies considerably between about 0.2 and 0.9 mg/cm^2 in different BWR plants. The buildup of indigenous films is known to be comparatively rapid during the first few hundred hours of contact with the hot coolant; it gradually decreases with continued exposure. A number of variables such as temperature, concentration of dissolved oxygen, flow rate and corrosion product impurity levels in the reactor water will affect the corrosion rate and the indigenous film buildup, resulting in considerable fluctuations in the buildup rate and the consequent equilibrium thickness in different plants.

Higher concentrations of nickel and cobalt in the lower, tightly-adherent layer are the main difference in the chemical compositions between the layers. The comparatively high cobalt concentrations are assumed to result from incorporation of dissolved cobalt from the coolant into the indigenous film and not to originate in the underlying base metal. As was observed in PWR oxide layers (see Section 4.3.4.4.), the crystalline structure of the tightly-adherent layer is able to incorporate cobalt more readily than the structure of the loosely-adherent layer.

Approximately 85 to 90% of the total amount of ^{60}Co deposited on the out-of-core surfaces is associated with the inner, tightly-adherent layer, with the remainder being incorporated into the outer layer. In contrast, ^{54}Mn and ^{59}Fe, which are almost completely associated with non-dissolved corrosion product particles in the reactor water, are predominantly found in the outer layer. The higher ^{60}Co concentrations in the inner layer are the consequence of higher metal loadings and of higher ^{60}Co : Fe ratios, whereas the ^{60}Co element-specific activity is reported to be virtually identical for the two layers. The ^{60}Co : ^{58}Co ratios are also similar for the two layers; the ^{60}Co : ^{54}Mn ratio, however, is considerably lower for the loosely-adherent layer. The reason for this is that the loosely-adherent layer originates from deposited corrosion product particles, a part of which was resuspended from the fuel rod surfaces. These predominantly iron-containing particles have a comparatively high ^{54}Mn activity concentration; therefore, high ^{54}Mn levels on an out-of-core surface may indicate high deposition of particulate matter from the reactor water.

In all the BWR plants analyzed by Anstine et al. (1984), ^{60}Co was the dominant radionuclide in the contamination layers. It, therefore, determines the dose rates at the outside of the systems. However, the ^{60}Co concentration in the oxide layers

varied considerably from plant to plant, with differences of up to a factor of 20 being reported. Even in the same plant, the ^{60}Co buildup trends and levels on different surfaces (such as reactor water cleanup inlet lines and recirculation lines) may vary considerably. Quite in contrast, the ^{58}Co and ^{54}Mn equilibrium concentrations in the oxide layers, which were reached following the initial increase, were remarkably similar in all the plants investigated.

Apparently, the area-related ^{60}Co activity on any section of the piping is controlled by the metal loading, the cobalt content and the ^{60}Co : Co specific activity. However, no evident correlation was observed between either the metal loading or the cobalt concentration in the oxide layer, on the one hand, and the ^{60}Co loading on the other. This lack of correlation may mean that the thickness of the oxide film is not the controlling parameter. A reasonably good correlation was observed to exist between both the ^{60}Co : Co and ^{60}Co : Fe specific activities and the ^{60}Co loadings. Since these specific activities are primarily determined by the incorporation of dissolved species from the reactor water into the oxides, it appears that long-term ^{60}Co buildup on the surfaces depends on the structural exchange properties of the oxide film, on the one hand, and the dissolved ^{60}Co concentration in the reactor water on the other.

Observations from operating BWR plants suggest that on the surfaces wetted by high-temperature reactor water, one has to expect a deposition mechanism which is similar to that on the surfaces of a PWR primary circuit. The activation products released from the activated in-core materials, as well as from the fuel rod deposits, as dissolved ions are incorporated into the oxide layers on the austenitic out-of-core surfaces directly from the reactor water. The activated crud which is resuspended from the fuel rod surfaces is also partly deposited on the out-of-core surfaces; here, colloid chemistry processes may participate in the deposition process. These corrosion products often show a higher cobalt content than the non-activated corrosion products that are brought in with the feedwater. During the residence time of the particulate corrosion products on the out-of-core surfaces, this excess cobalt content is reduced; therefore, the activated crud can be considered as an additional source of ionic cobalt (Alder et al., 1992).

It seems to be undisputed that ^{60}Co that is attached to crud particles suspended in the reactor water leads to the formation of loosely deposited contamination, particularly in low flow regions. In contrast, from all observations at operating BWR plants one can conclude that it is primarily the concentration of dissolved ^{60}Co ions in the reactor water that determines the deposition rate and the resulting contamination level in the tightly-adhering oxide layer. This assumption is supported by the results of investigations conducted by Bridle et al. (1986) in which the contamination buildup on steel surfaces (SS 304) in a high-temperature loop upstream and downstream from an electromagnetic filter (EMF) was analyzed. The retention of non-dissolved iron (hematite) in the EMF was found to be about 80% and that of ^{60}Co and ^{58}Co which were attached to particles about 70%; despite this retention, the contamination buildup on the surfaces before and after the filter showed no significant differences, at least during the first experimental period. Only after a longer exposure time did the surfaces upstream from the filter exhibit a higher contamination than those downstream from the filter. These results can

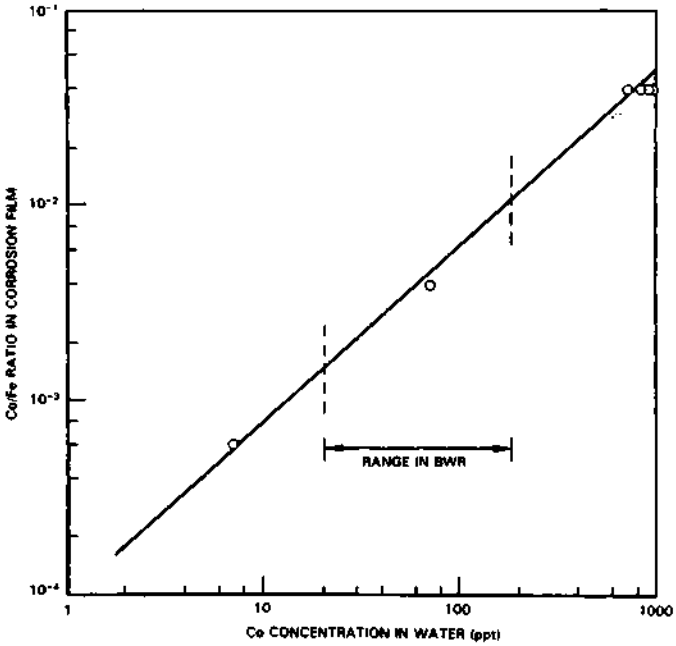

Figure 4.47. Variation of the Co : Fe ratio in oxide films as a function of cobalt concentration in the water phase
(Lin and Smith, 1988)

be understood if one assumes that mainly cobalt that is in the dissolved state in the reactor water is incorporated into the oxide layer and that only after a longer operation period does deposition of particulate matter begin to play a certain role. Moreover, the results showed that the activity buildup was almost identical on pretreated and on as-received surfaces, indicating that the nature of the oxide layers is not of prime importance, at least under the conditions of these experiments. Likewise, the thickness of the oxide film seemed to have little, if any, influence on the amount of ^{60}Co deposited in the equilibrium stage.

The investigations described by Marble (1985) demonstrated that the extent of incorporation of cobalt into magnetite layers is a linear function of the concentration of dissolved cobalt in the aqueous phase and that the incorporation is apparently not affected by possibly competing solution partners such as nickel in its usual concentration range in the reactor water. In these investigations, the total amount of incorporated cobalt was found to be proportional to the thickness of the oxide layer. From the results it was concluded that the uniform, tightly-adherent cobalt contamination on the out-of-core surfaces is caused by ionic ^{60}Co dissolved in the coolant, a conclusion that was confirmed by detailed laboratory investigations performed by Lin and Smith (1988). Their results demonstrated that the Co : Fe ratio in the oxide films on stainless steel directly depends on the concentration of dissolved cobalt in the water phase (see Fig. 4.47.).

This behavior is of particular interest when the cobalt specific activity (i. e. the ratio $^{60}Co : Co$) becomes an important factor. They suggest that, as long as the cobalt concentration in the water is <1 ppb (normal range 20 to 200 ppt), there should be no saturation problem for ^{60}Co deposition in the oxide layer, regardless of the level of the specific activity. However, the problem of saturation would certainly arise if the concentration of other transition metal ions (i. e. Ni^{2+}, Zn^{2+}) in the water phase became distinctly higher (e. g. >5 ppb). Under such circumstances, the divalent ions are expected to compete with each other for the reactive sites in the spinel oxide layers. Based on laboratory investigations it was suggested that the order of incorporation of transition metals into the spinel oxide compound is Ni ~ Co > Zn > Mn > Cu. It is theoretically possible and it was demonstrated experimentally that these transition metal ions are able to retard the ^{60}Co buildup in the oxide film. Concentrations of these metal ions in the reactor water beyond 10 ppb would practically saturate or block the available adsorption sites for ^{60}Co, provided that all the transition metal ions had similar properties with respect to forming a stable mixed oxide with iron in the corrosion film (Lin and Smith, 1988). This effect is the basis for the proposed addition of zinc to the BWR reactor water as a means of reducing contamination levels. In addition, Zn^{2+} ions seem to retard significantly the growth of the corrosion film, resulting in an additional reduction of available adsorption sites for ^{60}Co. However, for both effects to be effective, the concentration of zinc ions in the reactor water has to be continuously maintained above some minimum level; at a lower concentration of zinc in the water phase, ^{60}Co buildup can even be accelerated as a result of zinc ions in the oxide film being released and/or exchanged.

Practical experience shows a certain variability in the relationship between the concentration of dissolved ^{60}Co in the reactor water and the ^{60}Co concentrations in the out-of-core oxide films, indicating that the process of incorporation may be influenced by additional parameters, such as the types and morphologies of the oxides or the specific environment in the plants (Anstine et al., 1984). The characterization of the out-of-core films suggested that their chemical compositions and crystal structures were rather similar throughout all the BWRs investigated. However, detailed SEM examinations showed that two distinctly different types of particles may exist in the inner layers on BWR surfaces. Small (0.1 to 1.0 μm), irregular-shaped particles were observed on pipes removed from three BWRs with relatively high radiation levels, while larger (0.5 to 3 μm) particles with sharp edges and faces were found on pipes from three other BWRs with comparatively low radiation levels. The apparent correlation between radiation level and particle size is consistent with the behavior expected, since the smaller, irregular-shaped particles have considerably higher surface areas and probably a higher percentage of lattice defects in the crystal structure. Both these properties would cause the particles to have higher exchange rates for divalent ions.

In order to improve our basic understanding of the fundamental reactions, the kinetics and the mechanisms of ^{60}Co deposition on stainless steel surfaces under BWR operating conditions were studied in detail in loop experiments by Lin and Smith (1988). The results of these investigations showed that the progress of corrosion on the stainless steel surface is the key controlling process for ^{60}Co deposition

and its incorporation into the corrosion film. The surface of the base metal is covered by a thin epitaxial oxide film which is formed by the reaction of metal atoms from the base metal with oxygen and which presumably consists of an amorphous form of Fe(II) oxide. At the surface of this layer, new crystals of mixed oxides in spinel form are generated, which will force the outer crystals out towards the water phase. During the course of this process, reactions such as dissolution, recrystallization, exchange reactions, and oxidation may take place and it is assumed that while these reactions progress ionic ^{60}Co from the reactor water is incorporated into the oxide layer. As corrosion continues, the older crystals move further outwards towards the water phase; in doing so they may change their composition and morphology. By oxidation of spinel compounds to hematite, cobalt and other spinel-forming divalent ions can be released to the water phase. Finally, the oxide particles will also be released.

This mechanism means that diffusion of ^{60}Co from the water phase into the oxide film may be the first obstacle for ^{60}Co species to be overcome. Larger crystals with higher porosity in the film may facilitate the diffusion process, and vice versa. Thus, the characteristics of the oxide film can be expected to play an important role in ^{60}Co deposition and incorporation on stainless steel surfaces. A thick oxide film with a high density, as is obtained by pretreatment of the surfaces with oxygen-containing water, is therefore assumed to be effective in reducing ^{60}Co deposition since it lowers the diffusion rates of cobalt into the oxide layer and reduces the corrosion rates of the underlying base materials.

Thus, the corrosion rate seems to be the rate-determining process for ^{60}Co deposition onto the stainless steel surfaces when cobalt ions are incorporated into the growing oxide layer. Various authors have described ^{60}Co deposition by either a logarithmic or a parabolic rate law. From the results of their loop experiments, Lin and Smith (1988) derived the equation

$$A = R \cdot c \cdot \ln (k \cdot t+1)$$

where A = ^{60}Co activity on surface
R = deposition rate constant
k = corrosion kinetic constant
c = ^{60}Co concentration in water
t = exposure time.

The constants R and k obviously depend on the type of base material used, with molybdenum-containing stainless steel 316 SS having other values than the normally used 304 SS. To explain these differences, it was assumed that molybdenum ions present in the spinel oxide film are oxidized under normal water chemistry conditions, creating additional vacancies which may act as additional adsorption sites for cobalt and other transition metal ions. Under hydrogen water chemistry conditions, the difference in ^{60}Co buildup rate between these two base materials vanishes, obviously due to the fact that no molybdenum oxidation occurs so that no additional vacancies in the oxide film are formed.

Under hydrogen water chemistry (HWC) conditions, the ^{60}Co deposition was observed to proceed faster than predicted from a logarithmic rate law, suggesting that under such conditions cobalt deposition is not controlled exclusively by the

corrosion rate of the materials. The initial buildup rate is lower because of the lower buildup rate of the corrosion film, but the following long-term buildup rate proved to be higher. Since under HWC conditions the oxide films on the surfaces are comparatively thin, ionic diffusion could be an important factor in ^{60}Co deposition. When the water chemistry conditions in the plant are changed from normal to hydrogen addition, the activity level in the oxide layer may start to increase due to a higher deposition rate. The enhanced deposition is probably due to the fact that, as a consequence of this change in ambient conditions, the oxide morphology undergoes some transformation in order to equilibrate with the new O_2/H_2 environment in the water. During the course of the transition period the surfaces of the oxide particles may become more receptive to ^{60}Co until a new equilibrium is established.

The corrosion rate of stainless steel in BWR reactor water is comparatively high during the first few thousand hours, decreasing thereafter to a considerably lower level. Thus, the majority of the indigenous corrosion film is created during the first months of operation. If the morphology of the oxide particles on the surface of the materials is the prime variable in radiation buildup, then the relative radiation buildup rates might be established in the first fuel cycle. This hypothesis is strongly supported by the frequently observed correlation between the initial buildup rate and the long-term equilibrium dose rates. As was mentioned above, the deposition rate of radionuclides onto the surfaces is assumed to depend on the quality of the oxide layer present; however, as yet no detailed information is available on the structure an optimum layer for a minimum deposition rate should have, which would result in an increased radionuclide removal from the water phase via the reactor water cleanup system.

Apparently, other reactor water chemistry parameters additionally affect the deposition rate of ^{60}Co onto the stainless steel oxide layers. It has been reported that higher conductivity levels of the water (on the order of 0.5 μS/cm) lead to an increase in ^{60}Co buildup. The reason for this effect is probably the formation of an oxide layer with larger particle sizes and greater porosity, which would increase the ^{60}Co diffusion rate inside the layer. Likewise, under hydrogen water chemistry conditions the buildup trend seems to be significantly different from that observed under normal water chemistry conditions: the buildup is slower in the initial phase, but it continues to grow rather than to level off at the end of a 2000-hour test period (Lin and Smith, 1988). Presumably, there are additional parameters that potentially affect the deposition rate, such as electrochemical potential, specific conductivity, corrosion product concentrations, pH and impurity levels. The available data base on the influence of these parameters is extremely limited and, therefore, it is impossible to evaluate their potential effects. Nonetheless, according to the data compiled by Anstine et al. (1984), it would seem that these parameters have only a secondary effect, at best. A higher water pH may increase the surface charge (more negative) and/or the Zeta potential on the surface of the oxide particles in the film, and it may help the positively charged Co^{2+} or $CoOH^{+}$ ions to approach the reaction sites on the surfaces of the oxide particles. On the other hand, a reactor water pH of 7.5 to 8 results in minimum cobalt solubility (see Fig. 4.46.) and should, therefore, reduce cobalt incorporation into the superficial

oxide layers. Higher water pH most likely enhances the ^{60}Co deposition by supporting the adsorption mechanism (see below), whereas at lower water pH the adsorption mechanism may be insignificant compared to the mechanism of direct reaction (Lin and Smith, 1988). In addition, it is entirely possible that the buildup of the dose rates is influenced by other parameters characteristic of the particular plant design and mode of operation which remain rather constant throughout plant life, possibly providing an explanation for plant-specific differences in the radiation dose rates at the primary systems.

Basically, there are three different mechanisms that potentially determine the incorporation of dissolved ^{60}Co into the crystal structure of the indigenous corrosion films (Lin and Smith, 1988). The first one is a direct reaction at the interface between the basal layer of amorphous Fe(II) oxide and the spinel oxide layer. Cobalt ions that have travelled down to this interface by diffusion will be incorporated into the newly formed spinel crystals. It is believed that for a fresh surface or for a surface covered by a non-protective oxide film, the ^{60}Co buildup by this mechanism is faster than by other mechanisms, and the rate of activity buildup is controlled by the rate of corrosion of the base metal which produces the other constituents for this reaction. The second possible mechanism starts with the adsorption of cobalt ions onto the surface of hematite particles; the degree of adsorption increases with increasing pH and is believed to be initiated by an exchange reaction between the cobalt ions and the surface hydroxyl groups of the oxide. At higher temperatures (i. e. BWR reactor water operating temperature), the adsorbed cobalt ions are rather quickly converted to a spinel compound of the type $CoFe_2O_4$. In general, the ^{60}Co deposition by the adsorption mechanism is slow as compared with the direct reaction mechanism mentioned above, as has been demonstrated by measurements of the activity buildup on prefilmed samples. However, the reaction rate of this mechanism may increase significantly if the oxide film becomes more porous and the water chemistry more basic.

Finally, ion exchange or isotope exchange between cobalt ions in the water and cobalt atoms (or metal atoms of similar properties) already incorporated into the spinel oxide is a basic possibility for ^{60}Co incorporation into the oxide layer. However, due to the high thermodynamic stability of the spinel compounds under the conditions prevailing in the BWR reactor water, this reaction is expected to proceed very slowly. By comparison of the $^{60}Co : {}^{58}Co$ activity ratio in the reactor coolant and in the surface film on the out-of-core piping, it was found that the isotope mixture in the surface film is generally 200 to 300 days older (corresponding to about 4 halflives of ^{58}Co), indicating very slow rates of ion exchange. Likewise, the activity buildup on prefilmed surfaces indicates the limited significance of exchange reactions; if the exchange between ^{60}Co ions in the water and either Ni(II) or Fe(II) atoms in the oxide took place at an appreciable rate, the activity buildup would be faster than the empirical rate law predicts; but measurements have shown that in these cases the original rate law remains valid. However, some degree of exchange may be expected as the crystals crack and/or undergo morphology transformations and the divalent atoms in the oxide film become exposed to water and become leachable; this is probably particularly true when the film is exposed to changing water chemistry conditions (Lin and Smith, 1988).

The radionuclides incorporated in the oxide layer are in part released again to the coolant in a manner very similar to the release of corrosion products from corroding stainless steel. The exact mechanism of release is not certain, but it may be a combination of dissolution, diffusion, ion exchange and desorption or spalling of smaller oxide particles. The overall time constants for the ^{60}Co activity release from the inner and the outer layer oxides were empirically determined from a number of reactors to be about $2 \cdot 10^{-4}\ d^{-1}$ and $8.6 \cdot 10^{-3}\ d^{-1}$, respectively (Lin, 1990).

4.4.4.5 Possible countermeasures against BWR contamination buildup

Because of the highly complex mechanisms of the production of corrosion product radionuclides and of contamination buildup, it cannot be expected that a single measure will result in an effective reduction of radiation levels. Rather a whole series of measures is necessary, aiming primarily at a reduction of the production, transport and deposition of ^{60}Co, but in the second in an analogous reduction of the other corrosion product radionuclides. As can be concluded from the results discussed in the preceding sections, the dominant parameters responsible for contamination buildup are the concentration of dissolved ^{60}Co in the reactor water and the readiness of the out-of-core oxide layers to incorporate ^{60}Co from the reactor water. As with the PWR, in the BWR there are two possible main sources of corrosion product radionuclides: the cobalt content of the in-core materials and the cobalt content in the corrosion products that are temporarily deposited on the surfaces of the fuel rods. Since the relative significance of these two mechanisms has not yet been analyzed to the same extent as in the PWR, the different measures taken up now have aimed at reducing both possible sources.

As in the PWR, the most promising countermeasure is the reduction of the cobalt inventory in the primary system, in particular the replacement of the high-cobalt materials which are located inside the neutron field. According to Ocken (1985), in a number of US BWR plants control rod guide rollers made of Inconel-X750/PH13−8 Mo were installed in place of the Stellite materials previously employed; the same material is used in the German Gundremmingen B and C plants. In addition, the cobalt impurity content in stainless steels is now generally limited to values <500 ppm or even lower for materials in the neutron field of the core, and <2000 ppm for other materials, although the effect of such a reduction of the cobalt content for materials outside the neutron field remains questionable. Experience with modern Japanese BWR plants has shown that the consistent employment of low-cobalt materials results in a reduction of the ^{60}Co contribution to the radiation dose rates by a factor of about 4 when compared to older BWRs. As can be seen from Fig. 4.48., the different materials contribute to a different extent to total radiation field buildup, with the Stellite materials in the reactor pressure vessel and the Inconel materials in the reactor core being the most important

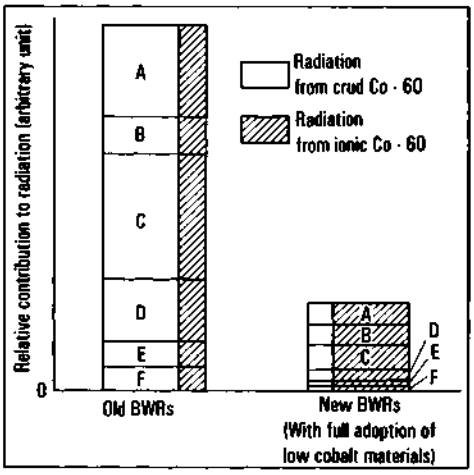

Figure 4.48. Contribution of different materials to ^{60}Co radiation: Comparison of older and modern Japanese BWR plants (A: Stellite in reactor; B: Stainless steel in reactor internals; C: Inconel in reactor core; D: Stainless steel in feedwater heater; E: Stellite of turbine blades; F: Carbon steel, other)
(according to Anonymous, 1990)

sources (Anonymous, 1990). Experience with German BWR plants, which are all operated in accordance with a normal water chemistry (NWC) regime and without zinc addition, have shown that the plants equipped with Inconel control rod guide rollers exhibit distinctly lower radiation dose rates than those with Stellite rollers (Reitzner et al., 1993). In addition, the replacement of Inconel spacers by Zircaloy spacers in the fuel assemblies, a measure which was originally introduced in order to improve neutron economy, results in a significant reduction of ^{58}Co production.

The shift in the relative significance of the different sources also seems to affect the status of ^{60}Co in the reactor water; while in older BWRs about 70% of the ^{60}Co activity is attributable to crud and about 30% to ionic species, in more modern plants this ratio is reversed (Asakura et al., 1989).

Occasionally, changes in the design of the plant effect more a reduction of personnel radiation exposure than of the contamination levels on the surfaces of the piping and components. As an example, the replacement of the external recirculation systems by internal axial pumps has to be mentioned; from Fig. 4.18. the benefits of this measure can be clearly seen (Reitzner et al, 1993).

Besides reduction of the cobalt inventory of the primary systems and minimization of the generation of corrosion products by appropriate coolant chemistry control, prevention or at least reduction of the transport of non-radioactive as well as of radioactive corrosion products is another effective countermeasure, independent of the predominant source of radionuclide production. The reactor water cleanup system in its usual design is not efficient enough for a significant reduction in the concentrations of non-dissolved and dissolved corrosion products in the

reactor water, since the removal rates that can be obtained at reasonable expense are small compared with the deposition rates of the corrosion products onto the surfaces of the circuits. Satisfactory results can only be obtained by using a purification system that can work at a high throughput at the reactor water operating temperature, such as an electromagnetic filter. However, as was mentioned in the preceding section, the experiments reported by Bridle et al. (1986) showed that an EMF has a good retention efficiency for the suspended corrosion products but, as can be expected, is quite ineffective with regard to dissolved cobalt isotopes, which are the main source of contamination buildup. Other types of high-temperature filters have also been proposed such as stainless steel materials with large surface areas. ^{60}Co and other radionuclides are adsorbed by them from the coolant flow; however, no technical-scale results have been reported so far on the impact of such high-temperature filtration devices on plant contamination levels.

Since the bulk of the corrosion products is transported with the feedwater to the reactor pressure vessel, condensate cleanup is a possibly effective means of reducing the production of activation products. Usually, BWR plants are equipped with a condensate polishing system which consists either of powdered-resin precoat filters or of a deep-bed ion exchanger system. Both types of purification system have their specific advantages and disadvantages; powdered resins are excellent particulate filters but are only moderately effective in retaining ionic impurities (70 to 90% efficiency) while deep-bed demineralizers eliminate dissolved ions more efficiently, but retain particles less effectively than filter/demineralizer systems. In order to minimize the impurity contents of the feedwater, the condensate polishing systems were improved in a number of BWR plants, in particular in newer Japanese plants (Nagao et al., 1986; Anonymous, 1990). Prefilters were installed to retain particulate corrosion products prior to the ion exchangers; in addition, several plants were equipped with a dual condensate treatment system, consisting of deep-bed ion exchangers plus powdex filters. Using such a combination, a feedwater conductivity of $<0.1\ \mu S/cm$ and a feedwater corrosion product concentration <1 ppb can be attained, provided that the high-pressure condensates are also recirculated to the main condenser. Without recirculation of the high-pressure condensates (forward-pumped plants), the corrosion product input into the reactor pressure vessel is higher by about a factor of 10. Experience with the German BWR plants has shown that the radiation levels in forward-pumped plants generally are higher than in plants in which all the condensates are directed to the condensate polishing system (Reitzner et al., 1993).

In some plants, however, the attempts made to attain lower radiation levels by reducing the iron crud concentration in the feedwater resulted in an increase in the radiation levels; the radiation dose rates caused by the radioactivity of both ^{58}Co and ^{60}Co increased inversely as the iron crud concentrations decreased. From the investigations performed to throw light on the reasons for this surprising behavior it was concluded that at low iron concentrations (ratio Ni : Fe >0.5), NiO is precipitated onto the surfaces of the fuel rod claddings in addition to nickel ferrite (see Section 4.4.4.2.). Since the dissolution rate of NiO (and probably of CoO as well) under BWR reactor water operating conditions is markedly higher than that of $NiFe_2O_4$, radionuclides are released from such deposits at a higher rate. Several

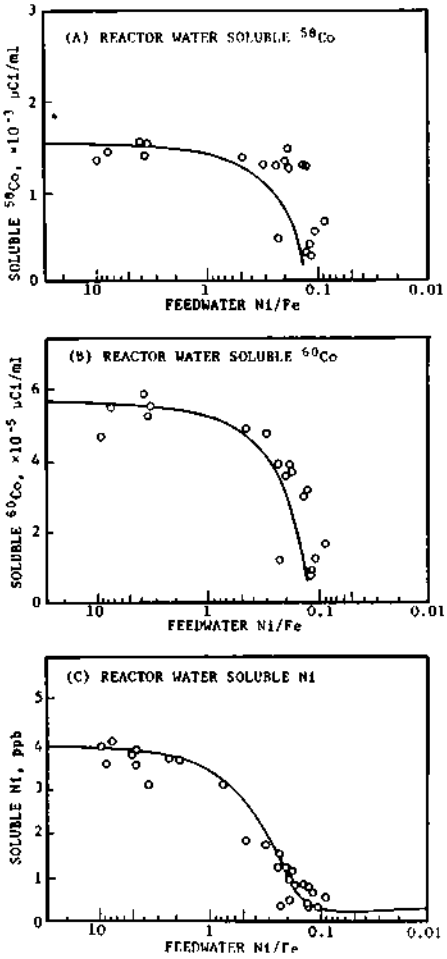

Figure 4.49. Optimum Ni : Fe ratio for reduction of (A) ^{58}Co, (B) ^{60}Co, and (C) nickel in reactor water
(Nagao et al., 1986; by courtesy of Thomas Telford Limited, London)

options have been developed to adjust the Ni : Fe ratio to the required value. If the possibility exists of reducing the nickel concentration (e. g. by improving the efficiency of the condensate polishing system), this is the preferred method. Otherwise, the iron concentration in the feedwater has to be increased to a level high enough to suppress NiO precipitation. As can be seen from Fig. 4.49., the optimum Ni : Fe ratio for stabilization of ionic nickel (and also of ionic cobalt) was determined to be <0.2 (Nagao et al., 1986). For this reason, in the case of extremely low concentrations of corrosion products in the feedwater, iron has to be added to attain a sufficiently high concentration. This can be performed either by bypass operation of the condensate polishing system and/or by iron injection into the

feedwater system; an alternative process is electrolysis using iron electrodes, by which procedure a simultaneous introduction of other impurities into the feedwater is minimized.

As was discussed in Section 4.4.4.3., the corrosion product shutdown spiking gives rise to a dissemination of contamination throughout the plant's systems. For this reason, several attempts have been undertaken to reduce the height of the spiking burst as far as possible. Since the speed of bubble ascent in the reactor water after shutdown is an important parameter in the resuspension of deposited corrosion products from the surfaces of the reactor core, a modified mode of temperature and pressure reduction which minimizes steam production during this period was developed and applied in several BWR plants (Eickelpasch and Lasch, 1986). When using this procedure, a reduction in cobalt mobilization by about a factor of 10 as compared to conventional shutdowns was observed. Similar experience was reported by Otoha et al. (1989); reduction of the cooling rate of the reactor water temperature during shutdown to values of less than 15 K/h resulted in a suppression of the maximum concentration of corrosion product radioactivity in the reactor water by one to two orders of magnitude compared to that of conventional shutdown practices. In addition, in some cases the reactor pressure was kept constant for 3 to 4 hours after having reached a value of about 5 MPa; as a result of this measure, a reduction of the ^{58}Co and ^{60}Co activities deposited on the inner surfaces of the piping of the reactor water cleanup system by about 10% was measured.

Over the entire shutdown period, the reactor water cleanup system has to be operated at its maximum throughput in order to remove as much of the radionuclides as possible from the primary system and to minimize radionuclide redeposition on the out-of-core surfaces.

A possible means of reducing the contamination buildup is the addition of low concentrations of zinc in the range of 10 ppb to the reactor water in order to saturate the reactive sites in the spinel oxide lattice. As was described by Marble (1985), this idea originates with the observation that BWR plants that are equipped with brass-tubed condensers and powdered-resin condensate polishing systems (by which zinc is only incompletely removed from the water flow) generally exhibited lower dose rates at the recirculation lines, for example. Laboratory investigations showed that zinc which is dissolved in the reactor water acts as a corrosion inhibitor in particular for austenitic steels; the oxide layers that develop in the presence of zinc are relatively thin (up to a factor of 5 less than those created in its absence) and should, therefore, have a lower potential for incorporating cobalt atoms. As was described in the preceding section, the zinc atoms occupy vacancies in the magnetite defect structure, resulting in an increased protective effect of the oxide layer. To reach this effect, a continued addition of zinc to the reactor water is required, a single preconditioning not being sufficient. More detailed analyses of oxide layers taken from the recirculation lines and from fuel assembly deposits showed zinc contents varying between less than 1 and 10 to 20%.

Wood et al. (1989) reported on experience with zinc injection passivation at BWR plants in the USA. In most cases, a dilute suspension of zinc oxide is injected into the final feedwater. Although the ZnO dissolution rate is very low at ambient

temperature, it increases greatly upon exposure to the elevated temperature of the final feedwater and the compound is completely dissolved within the first few seconds. The concentration of dissolved zinc in the final feedwater is typically less than 1 ppb. As an alternative to zinc injection by pumps, a passive zinc system was also proposed. This system passes hot feedwater over a bed of pelletized zinc oxide and dissolves zinc directly from the pellets. Laboratory testing of this concept was successful, but a full-scale prototype test has not yet been performed.

When zinc is introduced into the BWR reactor water, one of its primary removal mechanisms is adsorption by the iron-based corrosion products deposited on the fuel rods. It is this incorporation and subsequent release which gives rise to the buildup of an inventory of radioactive ^{65}Zn (see below). It is important, therefore, to minimize the input of iron to the reactor water so that the inventory of ^{65}Zn generated is also minimized. As was mentioned above, the "natural zinc" plants are all equipped with a powdered resin condensate treatment system and, thus, show low iron input to the reactor water. Based on this experience, the goal for iron input in the case of zinc addition is a feedwater total iron concentration of less than 2 ppb.

The changes in the ambient conditions that occur in the course of a shutdown of the plant facilitate the release of zinc from the iron oxide fuel deposits, resulting in a ^{65}Zn spiking similar in magnitude to that of the other corrosion product radionuclides.

In most plants using zinc injection, a concentration of dissolved zinc in the reactor water of 5 to 10 ppb is maintained; experience has shown that concentrations on the order of 2 ppb are not adequate. In one of the plants analyzed, zinc injection also resulted in a decrease in the concentration of dissolved ^{60}Co in the reactor water. Though the mechanism responsible for this effect is not yet understood, such a reduction in the concentration of dissolved ^{60}Co contributes to a reduced radiation buildup on the piping. In sum, the experience gained at a number of operating BWR plants confirmed the expected beneficial effect of zinc addition on radiation buildup. In Fig. 4.50. the measured dose rates at the piping of the recirculation system of different plants are shown, indicating that the radiation levels in plants treated with zinc are significantly lower than those in other plants. This applies as well for replacement piping and for decontaminated piping (Wood et al., 1989).

Nonetheless, the beneficial effect of zinc injection has not been observed at all plants; for example, Asay (1991) has reported upon contrary operational experience at the Monticello BWR plant using hydrogen water chemistry and zinc addition. Because of high dose rates, this plant had been subjected after its fuel cycle No. 13 to a full systems LOMI decontamination (see Section 4.5.2.2.); upon restart, hydrogen and zinc water chemistry were introduced and the rate of contamination buildup was followed over the whole fuel cycle No 14 by γ-spectrometry measurements at different selected locations. Contrary to all expectations, the measurements revealed a recontamination rate that was higher by a factor of about two than that during earlier cycles following a systems decontamination, when normal water chemistry without zinc addition had been used. Besides ^{60}Co, a significant contribution to the dose rates was due to ^{65}Zn. Although the interpretation of the

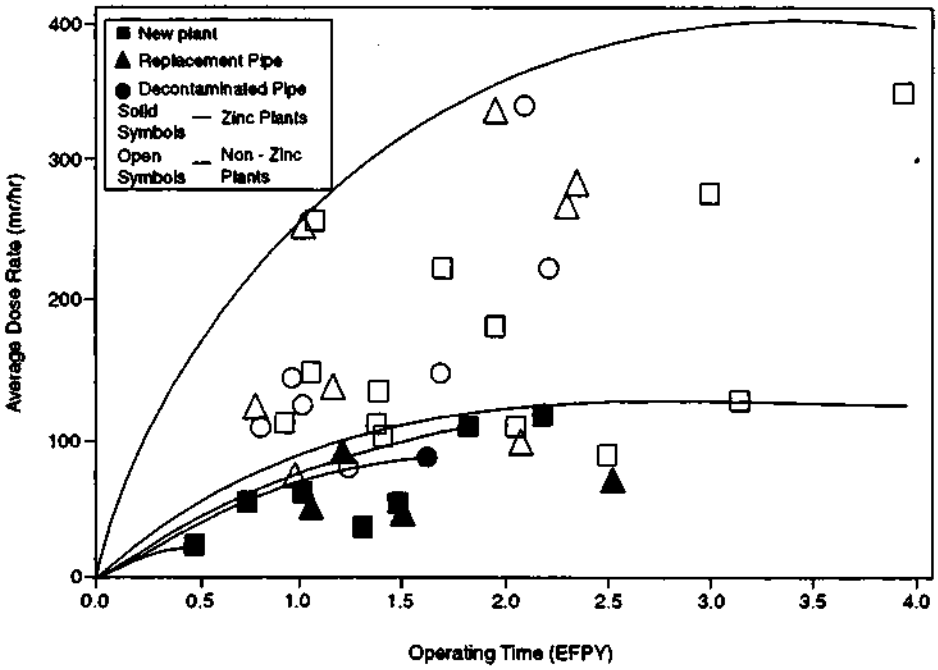

Figure 4.50. Radiation buildup for GE BWR recirculation system piping; Influence of zinc addition
(Marble, 1989; according to Alder, 1992; by courtesy of IAEA)

measured data was complicated by several changes in plant operation which occurred at about the same time, it seems clear that the ^{60}Co deposition rates increased when hydrogen water chemistry was adopted. Zinc injection appeared to reduce the deposition effects of ^{60}Co but had only little effect on the behavior of particulate matter.

Naturally occurring zinc contains approximately 48% ^{64}Zn, which is the parent nuclide of the long-lived γ emitter ^{65}Zn (halflife 244 days), the decay of which is accompanied by a 1.12 MeV γ ray. In order to preclude adverse effects on the radiation dose rates at the circuits and components of a plant, use of a source of zinc depleted in ^{64}Zn would seem to be highly desirable. Using a gas centrifuge process, natural zinc can be subjected to isotope separation to yield a final product which is depleted in ^{64}Zn to varying degrees, depending on the process parameters applied. Since the technique of production of ^{64}Zn-depleted zinc is new, initial costs are expected to be high, but the price is likely to decrease as experience and the market increase.

Addition of hydrogen to the reactor water, originally performed in order to minimize stress corrosion risks to the materials, is also reported to affect the transport behavior of the radionuclides (Magdalinski and Ivars, 1984). Experiments in the Swedish BWR plant Oskarshamn-2 showed a drastic reduction (by about a

factor of 10) of the chromium as well as of the ^{51}Cr concentrations in the reactor water following H_2 addition. However, as was mentioned above, other authors have reported that deposition of the most important radionuclide ^{60}Co on the out-of-core surfaces is not at all or even adversely affected by hydrogen water chemistry.

From the basic investigations on the deposition of radionuclides onto stainless steel oxide films it can be concluded that the type of oxide film which is formed during the initial corrosion process may be an important parameter in the long-term radiation buildup process. This means that an appropriate pretreatment of the surfaces of the primary system under controlled conditions might be an effective countermeasure. It can be performed either prior to nuclear heatup or during nuclear heatup at low reactor power level. In both cases, water near operating temperature and containing a dissolved oxygen content of about 200 ppb is circulated for a number of days in the primary system. Laboratory investigations (e. g. Lin and Smith, 1988) showed a beneficial effect on ^{60}Co deposition; however, long-term experience with the reduction of activity buildup by this measure is still lacking. Prefilming of the piping is also assumed to be a promising procedure for minimizing the corrosion rates. Since a large fraction of the corrosion product input into the reactor water originates from the feedwater train, inhibition of these surfaces by an alkaline prefilming process has been proposed. Investigations of such a treatment at high pH water conditions, carried out during the hot commissioning period of the plant, yielded somewhat smaller amounts of deposited radioactivity on pretreated surfaces, both in the as-received and in the mechanically polished state; the effect seems to be weak, however. On the other hand, polishing of the surfaces prior to plant startup, in particular electropolishing, was reported to suppress corrosion and cobalt deposition to about one third as compared to using a pickled material (Honda et al., 1986). Almost all BWR plants in the US that have replaced the piping of the external recirculation system have specified pretreatment by electropolishing for new piping materials. Relevant experiments showed that the benefits of electropolishing and moist air oxidation are additive (Shaw et al., 1986).

From comparative measurements performed at 10 US BWRs where different chemistry measures and materials pretreatment procedures had been employed, it was concluded that electropolishing and pre-oxidation of the materials, plus subsequent addition of zinc to the reactor water, results in a slower contamination buildup, whereas electropolishing alone did not show any significant effect (Duce, 1990). These findings apply to decontaminated pipework just as for new pipes installed in the course of the replacement of components.

In systems containing low-alloy steels, the progress of corrosion during outage periods may be a serious source of corrosion products. Therefore, appropriate lay-up practices have to be applied during these periods, including the construction phases as well as the annual outages and startup periods. Wet practices in which the systems are filled with oxygen-containing water controlled by hydrazine addition are in use, as well as dry practices in which the system is continuously vented by dry air.

4.4.4.6 Modelling BWR contamination buildup

As with PWRs, several attempts have been made to describe activity and contamination buildup in BWR plants by computerized models. These models are essentially based on materials balances for the iron transport and on materials and activity balances for the cobalt transport. The reaction rates and the reaction orders needed for the calculations in the partly very complex models are in most cases empirical values or even assumptions. The principles of some of the models have been outlined e. g. by Ishigure (1987) and by Alder et al. (1992).

The General Electric model (Lin et al., 1981) is a comprehensive analytical description of the activity transport as well as of the activity buildup. Iron transport and cobalt transport are treated in separate sets of equations of balance. The block diagram of Co/^{60}Co transport is shown in Fig. 4.51. In this model, several interactions are considered to exist between dissolved ions and corrosion product particles, including adsorption of ionic species onto the surfaces of the particles. Moreover, both particulate and dissolved species are assumed to be deposited onto the surfaces of the fuel rods, with corrosion product particles playing an important role in the deposition of the ionic species. The fuel rod deposits are assumed to consist of two layers, loosely-adherent and tenacious ones, and a certain amount

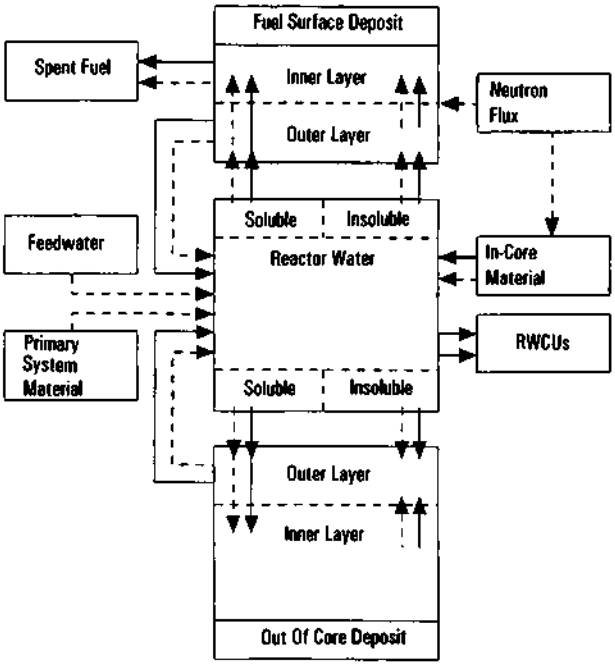

Figure 4.51. Block diagram of the General Electric model for cobalt transport (Continuous lines: ^{60}Co transport; Broken lines: ^{59}Co transport)
(Lin et al., 1981; Copyright 1981 by the American Nuclear Society, La Grange Park, Illinois)

of the former is converted into the latter in the course of plant operation. Radioactive species are released from the in-core materials as well as from the corrosion product deposits on the fuel rod surfaces. Upon release, they are distributed between dissolved and particulate species, essentially following Freundlich adsorption isotherms. Finally, dissolved as well as insoluble radioactive species are assumed to be deposited onto out-of-core surfaces; double oxide layers, inner and outer layers, are formed on the surfaces of the out-of-core base metals. The mechanisms of the deposition and the incorporation of the radionuclides into the out-of-core oxide layers are not included in the model.

In the GE model, differences in the characteristics of the corrosion product particulate material are emphasized in detail; they are considered to arise from the different types of condensate cleanup systems (powdex or deep-bed) employed in the plants and from the option of forward-pumped heater drain systems. The model includes many empirical coefficients obtained through laboratory experiments and, above all, by the aid of a large number of data from measurements at operating BWR plants. For this reason, the model is mainly applicable to plants of GE design (Alder et al., 1992).

In the Toshiba model (Hemmi et al., 1980), the corrosion product species in the reactor water are grouped into four categories: crud, large particles, small particles and ions. Four types of deposited oxide are assumed to be on the surfaces of the fuel rods: tightly-adhering hematite, loosely-adhering large and small particles and tightly-adhering spinels. The out-of-core surfaces are assumed to have a double oxide layer structure, an upper loosely-adhering hematite layer and a lower tenacious spinel layer. In addition, it is assumed that a significant contribution to the dose rates is delivered by radioactive particles which were temporarily sedimented around the bottom of the reactor pressure vessel. In sum, the model postulates rather complex relationships of mass and activity tranport.

To summarize these short remarks on modelling of BWR contamination buildup, it can be stated that all the existing models suffer from the same problems as the corresponding PWR models (see Section 4.4.3.6.), i. e. primarily from the fact that some of the fundamental steps are still insufficiently known. To develop a causative model based on physico-chemical principles, further work is claimed to be necessary to elucidate the mechanisms and the kinetics of the steps involved in activity buildup (Alder et al., 1992). Finally, it is still an open question whether it is possible to reflect the very complex conditions in a real BWR plant satisfactorily by a mathematical model that can be applied in daily work.

References Section 4.4.4

Alder, H. P.: Corrosion products, activity transport and deposition in boiling water reactor recirculation systems. Review of the state of the art, May 1990. Report IAEA-TECDOC-667 Coolant Technology of Water Cooled Reactors. Vol. 3: Activity Transport Mechanisms in Water Cooled Reactors, Vienna, 1992, p. 124–132

Alder, H. P., Buckley, D., Grauer, R., Wiedemann, K. H.: Corrosion products, activity transport and deposition in boiling water reactor recirculation systems. Report IAEA-TEC-

DOC-667 Coolant Technology of Water Cooled Reactors. Volume 3: Activity Transport Mechanisms in Water Cooled Reactors, 1992, p. 98–123

Anonymous: Japanese reduce BWR dose rate to PWR levels. Nucl. Engng. Internat., Febr. 1990, p. 31–33

Anstine, L. D., Zimmer, J. J., Wong, T. L.: BWR corrosion product transport survey. Report EPRI NP-3687 (1984)

Asakura, Y., Kikuchi, K., Uchida, S., Yusa, H.: Deposition of iron oxide on heated surfaces in boiling water. Nucl. Sci. Engng. **67**, 1–7 (1978)

Asakura, Y., Uchida, S., Ohsumi, K., Shindo, T., Aizawa, M., Usui, N., Amano, O., Yoshikawa, S., Otoha, K.: Current operating experience with water chemistry in crud concentration suppressed boiling water reactors. Proc. 5. BNES Conf. Water Chemistry of Nuclear Reactor Systems. Bournemouth, UK, 1989, Vol. 1, p. 115–122

Asay, D.: Radiation-field buildup at the Monticello BWR with hydrogen water chemistry. Report EPRI NP-7520 (1991)

Bridle, D. A., Bird, E. J., Mitchell, C. R.: Cobalt deposition in oxide films on reactor pipework. Report EPRI NP-4499 (1986)

Dragunov, Yu.G., Markov, Yu.V., Rybalchenko, I. L., Ryazantsev, I. L., Chabak, A. F.: Water chemistry in Soviet nuclear power plants. Report IAEA-TECDOC-667 Coolant Technology of Water Cooled Reactors. Volume 1: Chemistry of Primary Coolant in Water Cooled Reactors. 1992, p. 108–110

Duce, S. W.: Effectiveness and safety aspects of selected decontamination methods for LWRs. – "Recontamination experience 1988". Nucl. Engng. and Design **118**, 487–496 (1990)

Eickelpasch, N., Lasch, M.: Investigations on transport and activation of corrosion products in the 2 × 1300 MWe twin boiling water reactors of Gundremmingen. Proc. 4. BNES Conf. Water Chemistry of Nuclear Reactor Systems, Bournemouth, UK, 1986, Vol. 2, p. 55–58

EPRI (Electric Power Research Institute): Proceedings of the BWR Radiation Control and Radwaste Processing Seminar. Report EPRI NP-2417-LD (1982); Chapter 16

Hemmi, Y., Kamata, T., Nakayama, Y., Tani, A., Morikawa, Y., Sato, Y., Nagao, H., Sasaki, S., Sato, Y., Kuba, M., Kakefuda, M.: BWR cobalt transport model. Proc. 2. BNES Conf. Water Chemistry of Nuclear Reactor Systems, Bournemouth, UK, 1980, p. 319–326

Hepp, H., Rühle, W., Bohnsack, G.: Überlegungen zum Aktivitätsaufbau durch Kobalt 60. VGB Kraftwerkstechnik **66**, 268–273 (1986)

Hermansson, H.-P., Persson, G., Reinvall, A.: Corrosion product particles in boiling water reactor condensates. Nucl. Technology **103**, 101–112 (1993)

Honda, T., Ohashi, K., Furutani, Y., Sato, Y., Mochizuki, H.: Suppressing effect of surface treatment on radiation buildup in a BWR. Proc. 4. BNES Conf. Water Chemistry of Nuclear Reactor Systems, Bournemouth, UK, 1986, Vol. 1, p. 139–143

Ishigure, K.: A review of models describing the behaviour of corrosion products in primary heat transfer circuits of BWRs. Report IAEA-TECDOC-429 Reactor Water Chemistry Relevant to Coolant-Cladding Interaction. Annex III, p. 165–214 (1987)

Ishigure, K., Fujita, N., Tamura, T., Oshima, K.: Effect of gamma radiation on the release of corrosion products from carbon steel and stainless steel in high-temperature water. Nucl. Technology **50**, 169–177 (1980)

Kawaguchi, M., Ishigure, K., Fujita, N., Oshima, K.: Effect of radiation on release of corrosion products in high-temperature aqueous systems. Radiat. Phys. Chem. **18**, 733–740 (1981)

Kawaguchi, M., Ishigure, K., Fujita, N., Oshima, K.: Deposition of model crud on boiling Zircaloy surfaces at high temperature. Nucl. Technology **62**, 253–262 (1983)

Kawamura, F., Funabashi, K., Kikuchi, M., Ohsumi, K.: Using titanium oxide for cobalt removal from high-temperature water. Nucl. Technology **65**, 332–339 (1984)

Lin, C. C.: Foreign approaches to controlling radiation-field buildup in BWRs. Report EPRI NP-6942-D (1990)

Lin, C. C., Pao, C. R., Wiley, J. S., DeHollander,W. R.: A mathematical model of corrosion product transport in the boiling water reactor primary system. Nucl. Technology **54**, 253–265 (1981)

Lin, C. C., Smith, F. R.: BWR cobalt deposition studies. Final report. Report EPRI NP-5808 (1988)

Lister, D. H., Davidson, R. D.: Corrosion product release in light water reactors. Report EPRI NP-6512 (1989)

Magdalinski, J., Ivars, R.: Hydrogen water chemistry – A proven method to inhibit intergranular stress corrosion cracking in BWRs. Proc. 5. Internat. Meeting on Thermal Nuclear Reactor Safety, Karlsruhe 1984, Report KfK-3880, p. 248–257

Marble, W. J.: Control of radiation-field buildup in BWRs. Report EPRI NP-4072 (1985)

Marble, W. J.: Control of radiation buildup in BWRs using zinc injection passivation. SVA-Kurs Wasserchemie im Kernkraftwerk, Winterthur, 1989, p. B3.1-B3.12

Marchl, T., Reitzner, U.: Chemistry parameters influencing the dose rate build-up in BWR plants and their investigation with analytical methods. VGB Kraftwerkstechnik **72**, 654–660 (1992)

Nagao, H., Morikawa, Y., Yamazaki, K., Hemmi, Y., Nakayama, Y., Tagaki, K., Yoshikawa, S., Suzuki, Y., Otoha, K.: Corrosion product behaviour in low crud boiling water reactors. Proc. 4. BNES Conf. Water Chemistry of Nuclear Reactor Systems, Bournemouth, UK, 1986, Vol. 2, p. 59–66

Nishino, Y., Nagase, M., Sawa, T., Uchida, S., Ohsumi, K.: Reactions of iron crud with metallic ions under BWR water conditions. Proc. 6. BNES Conf. Water Chemistry of Nuclear Reactor Systems, Bournemouth, UK, 1992, Vol. 1, p. 63–67

Ocken, H.: Radiation control to improve nuclear power plant availability. Proc. Intern. Conf. Nuclear Power Plant Aging, Availability Factor and Reliability Analysis, San Diego, Calif., USA, 1985, p. 593–600

Otoha, K., Yoshikawa, S., Amano, O., Nagao, H.: Data survey on radionuclides during BWR shutdown. Proc. 5. BNES Conf. Water Chemistry of Nuclear Reactor Systems, Bournemouth, UK, 1989, Vol. 1, p. 315–316

Palino, G. F., Hobart, R. L., Wall, P. S., Sawochka, S. G., Gardner, J., Prystupa, M.: Cobalt transport at the Vermont Yankee BWR. Report EPRI NP-4560 (1986)

Reitzner, U., Marchl, T., Riess, R.: Dose rate trends and chemistry at Siemens-designed BWRs. Paper presented at the EPRI Radiation Field Control Seminar, Seattle, Wash., USA, 1993

Shaw, R. A., Ocken, H., Wood, C. J.: Recent progress in LWR radiation field control. Proc. 4. BNES Conf. Water Chemistry of Nuclear Reactor Systems, Bournemouth, UK, 1986, Vol. 1, p. 49–55

Styrikovich, N. A., Martynova, O. I.: Contamination of the steam in boiling reactors from solutions of water impurities. Atomnaya Energiya **15**, 214–218 (1963)

Thornton, E. W.: Activity transport mechanisms in water cooled reactors. Report IAEA-TECDOC-667 Coolant Technology of Water Cooled Reactors. Volume 3: Activity Transport Mechanisms in Water Cooled Reactors. 1992, p. 9–51

Uchida, S., Kitamura, M., Matsushita, Y., Yonezawa, K., Ohsumi, K., Miki, M.: Deposition of cobalt-60 on the stainless steel surface used for the primary cooling system of a boiling water reactor. Nucl. Sci. Engng. **77**, 496–501 (1981)

Wood, C. J., Marble, W. J., Prystuba, M., Hudson, M. J. B., Wilkens, D. L.: Experience with zinc injection passivation at BWR plants in the USA. Proc. 5. BNES Conf. Water Chemistry of Nuclear Reactor Systems, Bournemouth, UK, 1989, Vol. 1, p. 111–114

4.5 Decontamination in nuclear power plants

4.5.1 General aspects

As was discussed in the preceding sections, in many operating nuclear power plants the buildup of contamination results in radiation levels at the systems and components which lead to considerable radiation exposure of workers, in particular during the course of inspection and repair work. In order to meet this situation, permanent or temporary shieldings are frequently installed and, as far as necessary, remote-controlled and automatically operating equipment is employed to reduce, as far as possible, the stay time of people in the radiation field. Nevertheless, there are often operations to be carried out whose preparation and execution make the removal or at least a radical reduction in the radiation sources, i. e. a decontamination of the respective regions, necessary.

In 1977, the US Nuclear Regulatory Commission (NRC) declared reactor coolant system decontamination (as well as steam generator secondary-side chemical cleaning) as Generic Issue A-15. According to this regulation, in the case of high radiation dose rates, decontamination of the reactor coolant system or of parts of it should be considered, provided that such an action could be performed in accordance with the ALARA ("as low as reasonably achievable") principles. These principles state that a decontamination should result in a net dose reduction to the employees during the whole lifetime of the individual plant. This means that the radiation doses received by the workers in the course of a decontamination (including preparatory work and radioactive waste processing) plus that received during subsequent operation of the decontaminated plant have to be lower than what would be received without decontamination. In addition, certain cost–benefit relations have to be taken into account.

In order to meet this fundamental requirement the procedures to be applied in the decontamination of a nuclear power plant have to satisfy a number of conditions. The most important ones will be summarized in the following; it must be kept in mind, however, that in a given situation one or two of them may have greater importance than the others. Further, the following sections will concentrate on the removal of the tightly-adherent contamination layers present in the primary system, whereas removal of loosely-adhering contamination in "cold" systems or from the building walls and surfaces will not be treated.

The fundamental and self-evident requirement is that the practical application of a decontamination process has to show a decontamination effectiveness sufficiently high for the specific purpose; in general, this means that a decontamination factor greater than 10 should be achieved (in some cases, however, reduction of the radiation dose rates by a factor of more than 2 means an appreciable success). Consequently, the decontamination process to be applied has to be chosen to suit the nature of the contaminating matter to be removed. However, in different reactor plants and, moreover, in different regions of a plant the radioactive corrosion product oxides can be of a quite different nature. In systems which during plant

operation are solely in contact with low-temperature contaminated fluid, the majority of the deposits of activated corrosion products is present in the form of loosely-adherent particles or sludge which can, therefore, be removed by flushing, e. g. using a high-pressure water jet. In contrast, the tightly-adherent contamination layers in the PWR primary circuit or in the BWR reactor water systems require more sophisticated procedures for removal. Here, fundamental differences exist between the oxide layers that form in the oxidizing environment of a BWR and those formed in the reducing environment of a PWR. The chemical compositions of the oxides to be removed from the surfaces of the pipes and components may range from almost pure hematite or magnetite to chromium and nickel containing ferrites with a spinel structure; as a consequence, their behavior in contact with a decontamination solvent may show considerable differences.

In order to overcome these problems, extensive research and development work has been carried out in the past years at numerous institutions. As an important result, these investigations have shown that there is no single decontamination technique which is optimally suited for all applications; on the contrary, the procedure to be applied must be selected according to the specific situation. In the choice of both the chemical composition of the decontaminant as well as of the decontamination procedure the nature of the radioactive oxides to be removed has to be taken into consideration. As an essential detail, testing of potential decontamination solutions and processes has to be carried out using specimens which were contaminated during plant operation. Synthetic oxides can only give a first idea of the applicability of a specific decontamination process, because of the differences in their composition and structure from that of a surface layer oxide that has developed during a long-term exposure of the materials to the hot reactor coolant.

In the decontamination of components and systems which are going to continue to be used (which usually is the case in operational decontamination), materials compatibility of the decontamination solution and the process to be applied is of equal importance. Under no conditions may the decontamination process directly or indirectly weaken the primary pressure boundary of the reactor system. In the course of the decontamination procedure, the reactor system or parts of it are exposed to chemical solutions they have no contact with during periods of normal operation; therefore, the fundamental risk of corrosion initiation cannot be ruled out. For this reason, the selection of a suitable procedure is harder to achieve, in particular in cases when the decontamination solution will come in contact with different materials or with differently pretreated materials. The application of a decontamination process not only must not lead to a direct corrosion attack on the material, but possible initiation of a damage which may break out during subsequent operation has to be precluded. Therefore, as an important prerequisite, extensive process qualification work has to be done, considering general corrosion as well as selective corrosion types. In order to evaluate the effects of pretreatment and pre-exposure (such as sensibilization), materials which were exposed to reactor coolant over a longer period of time under plant operation conditions have to be included in the qualification work. In order to rule out any danger to the materials

of the plant, NRC (as well as the safety authorities of other countries) requests that, prior to the application of a decontamination procedure, a safety evaluation of that specific procedure has to be carried out; if in the course of this evaluation unreviewed safety questions arise, then special approval would be required before performance of the process. In Germany, a new decontamination process or the application of a known process to a plant containing materials other than those the process has proven suitable for has to be reviewed by independent experts appointed by the state authorities before it is allowed to be used. For this reason, there has been and still is a pronounced general interest in the development and qualification of standard decontamination processes.

Many plant utilizers initially had strong reservations about the application of such chemical operations in their plants. These were overcome, however, by the careful development work and excellent decontamination results obtained in many plants.

As a third item, technical feasibility of the process has to be considered, as well as the costs of the decontamination and of the installations and the chemicals required. If plant systems (e. g. pumps, heat exchangers) are needed for the procedure, as is sometimes the case in the decontamination of subsystems and full primary systems, then the parameters of the procedure must be tailored to the conditions of these systems. As often only limited space is available in the plant, the extent of additional equipment required must be kept low. The time needed for carrying out the process is also an important parameter, in particular when the decontamination is on the critical path of a plant outage. This implies that the procedure and installations have to be qualified prior to beginning decontamination work; a sufficient number of specialists as well as sufficient time for preparatory work, therefore, is an indispensable requirement. In this preparatory work it has to be remembered that the decontamination will result in the transport of a considerable amount of radioactivity from the treated circuit or component to the decontamination equipment; therefore, health physics considerations have to be taken into account, possibly requiring shieldings and/or remote-controlled facilities.

Finally, the selection of the optimum decontamination process has to take into consideration the available techniques for treatment of the resulting radioactive wastes, which in their chemical composition usually differ considerably from the wastes produced during plant normal operation. According to the procedure chosen, the radionuclides dissolved from the surfaces of the systems are removed continuously from the decontamination solution by ion exchange during the performance of the decontamination process or they are still present in the spent decontamination solution and can be subsequently fixed to ion exchange resins or treated by evaporation. In order to reduce the final volume of the radioactive waste as far as possible (an important requirement with regard to the costs of final disposal of these materials), sophisticated techniques of waste processing have to be developed and applied. The final waste products have to meet the requirements of the particular waste repository, which are quite different in different countries.

Early decontamination reagents usually were based on traditional steel descaling solutions, such as mixtures of mineral acids (e. g. nitric acid–hydrofluoric acid).

Later on, the process solutions contained comparatively high concentrations of organic acids (hard decontamination methods); the processes at that time were based on fixed, preset chemical and application parameters and special procedures for component and system decontamination. Today, most of the processes applied for operational decontamination use extremely low concentrations of chemicals (soft decontamination methods) and are applied in several brief cycles, possibly including variations in the chemical composition of the decontamination solution. In doing so, it became possible to adapt the decontamination process to the conditions and requirements of the system or component to be decontaminated. Several successive short decontamination cycles make better use of the allocated time frame, since an additional cycle can always be added. Important benefits of these new decontamination technologies are improved decontamination factors, shorter time requirements, less radioactive waste and a virtually zero hazard to the materials.

Besides the above-mentioned requirements, selection of the process also has to take into account that decontamination may be needed in different areas of the plant. Most frequently, decontamination of a system or a component or of parts of them is required as preparatory work for inspections or repair. Many applications in this field have been carried out in recent years, involving, for example, internals of main coolant pumps, BWR recirculation pumps and piping, reactor water cleanup systems and regenerative heat exchangers. For these purposes, standard procedures have been developed and qualified by different suppliers. Decontamination of such components (or of the whole reactor system) at the beginning of a plant outage will give increased worker availability (due to lower accumulated doses) and improved ease of working (due to lower radiation fields). These improvements will enable the inspection, maintenance, and repair work to be carried out more quickly, so that the outage time can be minimized.

From the above it can be concluded that a selection of various procedures is needed to cope with all the required decontamination tasks. As an example, in Table 4.14. the chemical, electrochemical and mechanical processes developed and applied by Siemens/KWU are shown, together with the different fields of application and the materials for which they have been qualified (according to Wille and Bertholdt, 1989).

In decontaminating a reactor component, there is always the problem that after a relatively short period of continued plant operation redistribution of radionuclides from the non-decontaminated surfaces of the other circuits and components will result in a recontamination of the cleaned regions. This effect can only be reliably precluded by decontamination of the whole reactor system, possibly with the fuel in place. Such decontamination operations require additional preparatory work as compared with the decontamination of components, due to the large volumes to be treated which require large amounts of decontamination solution, resulting in large amounts of radioactive waste. Further, additional preparatory work is necessary because different materials are exposed simultaneously to the decontamination solution. Since the mid-1960's, a number of reactors have been decontaminated in this way; more details will be given in Section 4.5.3.

Table 4.14. Chemical, electrochemical and mechanical decontamination processes used by Siemens/KWU
(according to Wille and Bertholdt, 1989; by courtesy of Thomas Telford Limited, London)

Process	Materials	Application
MOPAC 88	High-alloyed Cr- and CrNi-Steels, Ni-Alloys	Structural parts, Components Subsystems, Large components, Systems
CORD		
CAN-DEREM		
LOMI		
CAPA	Non-alloyed and low-alloyed steels	Structural parts, Components, Systems
ELPO		
Mechanical processes	Alloyed and Non-alloyed steels Ni alloys	Components, Subsystems Accessible parts

Often the success of a decontamination operation is expressed in terms of a cost–benefit analysis, i. e. a comparison of the expenses incurred during execution of the total procedure to the cumulative dose exposure (man-rems) which can be expected to be saved as a consequence of the reduced radiation levels. The problem with such an analysis, which is mainly in use in the USA, lies in the difficulty in translating radiation dose exposures saved into an equivalent amount of money. The result of such an analysis, therefore, depends highly on the equivalent assumed. On the basis of such cost–benefit analyses, substantial radiation exposure savings to the staff have been calculated, in particular when decontamination was carried out prior to inspection, repair or replacement work. As was shortly mentioned above, the initial concerns of the plant owners with regard to the costs, the potential success and the potential hazards of such an action have been largely dissipated and, at many plants, decontamination of particular systems has become a standard technique. However, as the measures taken for reduction of plant contamination buildup (see Sections 4.4.3. and 4.4.4.) will prove to be more and more successful in the future, the need of operational decontamination in the plants is expected to decrease.

4.5.2 Decontamination procedures

The following sections will concentrate on procedures which are applied for operational decontamination of reactor components, systems and circuits, i. e. decontamination of materials that are going to continue to be used, often for decades; a summary description of the relevant topics has recently been published by IAEA

(1994 a). Decontamination of components which were finally removed from plants in the course of replacement actions or in the context of decommissioning of nuclear power plants will be shortly treated in Section 4.5.6.

4.5.2.1 Non-chemical decontamination procedures

These procedures aim at a mechanical separation of the radioactively contaminated surface layers from the underlying base material. Many of these techniques (such as scrubbing, water jetting, ultrasonic cleaning) are only appropriate for removal of loosely-adhering substances such as are present in those regions of the circuits and components which, during operation, are exclusively in contact with low-temperature water, such as the steel liner of the spent fuel pool. The tightly-adherent contamination layers in the primary systems of both PWRs and BWRs are not significantly attacked by such techniques and require more aggressive procedures. Basically, two different types of mechanical techniques are in use: abrasive blasting and mechanical brushing and machining (IAEA, 1994 a).

Abrasive blasting can be applied either as a dry or as a wet method. The abrasives mostly used in the dry technique are sand or similar minerals, metallic beads or glass beads, which result in an efficient removal of the oxide layers from the metallic surfaces. However, when this technique is used there is always the danger of generation of radioactive dust which has to be countered by installation of a vacuum system around the surface to be treated in order to collect the spent abrasive including the radioactive material. In addition, the entire spent abrasive usually has to be treated as radioactive waste, since separation of the radioactive substances from the sand etc. is a difficult and expensive task. Wet abrasive blasting, i. e. propelling abrasives such as boron oxide or magnetite in a water jet, is a milder action and the problem of airborne contamination is significantly reduced. However, the major disadvantage of this technique is the extra volume of liquid waste produced, although both liquid and abrasive can be recirculated. Finally, dry ice blasting has been developed; in this technique, pelletized carbon dioxide in a gaseous CO_2 jet is directed onto the surface to be decontaminated. The main advantage of this process is that the dry ice sublimes into gaseous CO_2, leaving behind only a small volume of radioactive waste; as yet, however, no plant applications of this technique have been reported.

In mechanical brushing and machining normal metal finishing processes are used, which are applied e. g. for removal of surface oxides or rust. These processes normally generate aerosols and associated radioactive contamination, a problem which has to be met by the use of appropriate installations (e. g. glove boxes).

The decontamination effectiveness of these non-chemical procedures varies greatly depending on the specific technique and installations applied. Usually they are applied for the decontamination of limited and well-defined areas, such as the end regions of the main coolant pipes in steam generator replacement actions. The application of abrasive methods often suffers from the hazard of surface damaging of the materials, so that rapid recontamination of the decontaminated areas during

further operation has to be expected. As a result, these techniques are only used in special cases. They play a certain role in the decontamination of materials to be finally removed from the plant.

4.5.2.2 Chemical decontamination procedures

The chemical composition and the structure of the contamination layer oxides in the primary systems depend highly on the reactor type (PWR, BWR) and also on the operational history of the plant. The optimum decontamination process to be applied, therefore, must be selected and, if necessary, optimized to meet the task in question. In particular, when components and systems are to be decontaminated, different structural materials and, consequently, oxide layers of different composition are involved, resulting in more stringent demands on the decontamination procedures to be applied.

Since the application of mineral acids to dissolve the oxides is usually not considered today because of the hazard to the long-term integrity of the materials and the nature of the radioactive waste generated, most of the chemical decontamination procedures currently applied are based on organic chelating agents. Under favorable conditions, rather pure iron oxides can be dissolved in such solutions at a rate which is sufficiently high for practical application. In particular, this is true for the oxide layers on the surfaces of the structural materials in older BWR plants, which mainly consist of low-alloy steels (chromium content $<13\%$). In such cases, single-step decontamination processes are often of satisfactory efficiency. One of them is the CAPA process developed at the end of the 1970's by Siemens/KWU, which uses an oxalic or citric acid and formic acid solution at temperatures of about 90 °C. When this process was applied for the decontamination of BWR main steam lines, sufficiently high decontamination factors were achieved. The process was thoroughly examined with regard to materials compatibility and was approved for such applications by independent experts. The application of this process to systems with larger volumes, however, is adversely affected by the comparatively high reagent concentrations required, resulting in an increased complexity of the procedure as well as in the processing of the resulting radioactive waste solutions.

The CAN-DECON process developed by AECL and London Nuclear and originally applied to the Canadian CANDU reactors (LeSurf, 1977) uses a citric acid –oxalic acid solution. When the decontamination is carried out at temperatures around 90 °C, only a rather poor process efficiency is achieved; therefore, in most of the applications temperatures around 120 °C have been used, leading to an overpressure in the systems of about 0.3 MPa, resulting in complications in process engineering. Under such conditions, decontamination factors between 10 and 20 were obtained when the process was applied to US BWR plants. From these applications no adverse effects on the base materials have been reported. In the early 1980's tests under aggravated conditions yielded stress corrosion phenomena in sensitized steel SS 304; as a result, the importance of the process decreased markedly for a certain time. It has to be pointed out, however, that the conditions

these tests were performed under were not representative for most decontamination applications.

The decontamination solution of the Citrox process (Pacific Nuclear) shows a similar chemical composition, originally using comparatively high reagent concentrations; besides oxalic acid and ammonium citrate it contains $FeSO_4$ and diethyl thiourea as inhibitors. Sufficiently high decontamination efficiencies at LWR contamination layers in components including pumps, heat exchangers and chemical and volume control systems, however, were only obtained when a pre-oxidation step (see below) was applied.

In the Dilute Chemical Decontamination (DCD) process developed by Westinghouse, a solution of citric acid, oxalic acid, EDTA and an inhibitor is applied, resulting in decontamination factors on the order of 10, as was determined in laboratory studies; higher efficiencies were obtained when a pre-oxidation step was included (Murray et al., 1985). In order to improve the decontamination effectiveness, it was proposed that the spent solution be circulated over a porous DC electrode where dissolved ions are reduced. The Fe^{2+} ion generated in this manner is assumed to attack the contamination layer in a one-electron reaction, thus accelerating the dissolution of the oxides (Murray and Snyder, 1985). However, this process seems not yet to have been applied to operating light water reactor plants.

In the processes described before, oxalic acid is applied as an efficient chelate-forming agent. This compound, however, is suspected to induce intergranular attack in sensitized 304 stainless steel when decontamination is carried out at temperatures around 120 °C. In order to minimize this hazard, investigations were performed on alternative chelating substances showing a comparable decontamination effectiveness. The results have shown that solutions of EDTA or citric acid–EDTA will meet the requirements when applied to BWR contamination oxide layers at temperatures around 120 °C. At 90 °C, where the possibility of intergranular attack is greatly reduced, higher decontamination rates are obtained only when mixtures of oxalic acid, citric acid and EDTA are used. In order to achieve an effective decontamination in a minimum time when using such mixtures, the concentration of ferric ions in the decontamination solution has to be kept low during the entire procedure (Speranzini, 1989). The CAN-DECON process described above was developed further to the CAN-DEREM process in which oxalic acid is replaced by citric acid; reagent concentrations, application times and temperatures of the CAN-DEREM process are similar to those used for the CAN-DECON process.

In the NS-1 process developed by Dow Chemical, organic chelating agents such as ethylenediamine tetra-acetic acid plus organic inhibiting additives were used at temperatures around 125 °C and an associated overpressure in the systems of about 0.4 MPa. From several applications to piping and systems in US BWR plants, decontamination factors between 10 and 100 have been reported; in some cases pre-oxidation steps had to be applied in order to improve the efficiency of the process (Anonymous, 1985).

One of the most frequently reported decontamination processes is the LOMI process (Low Oxidation State Metal Ions), which was originally developed by the British CEGB for removal of corrosion product deposits from the fuel bundles of the Steam Generating Heavy Water Reactor (SGHWR). Since Fe^{3+} always is the

predominant constituent in the contamination oxide layers in BWR systems and since it can, in principle, be reduced to the bivalent state, dilute reductive methods can be regarded as a potential alternative to organic acid attack. The decontamination solvent applied in the LOMI process contains picolinic acid as a chelating agent and vanadium(II) formiate which reduces Fe(III) in the Fe_2O_3 oxide layer via a one-electron reaction, thus creating reactive centers. The oxide layer broken up in this manner is then dissolved by the chelate-forming picolinic acid (Swan et al., 1984). The process was successfully applied over many years in the SGHWR, in spite of the low stability of the V(II) solution, which has to be prepared right before use by electrochemical reduction of a V(III) solution. The solvent has to be protected against oxygen by pretreatment with hydrazine and by flushing of the entire system with an inert gas, an action which has to be continued during the decontamination procedure as well. These requirements are a handicap in the application of the process.

With oxides containing higher chromium contents, the LOMI process proceeds very slowly since vanadous picolinate is not able to reduce Cr(III). If the chromium concentration in the oxide exceeds 15%, the dissolution rates will become unacceptably low. Therefore, in such applications, the Cr(III) must first be oxidized to Cr(VI) by an appropriate preoxidation step (AP and NP steps, see below). In order to save this time-consuming additional step, attempts have been made to replace V(II) by another reducing cation. Only a combination of Cr(II) with nitrilo triacetic acid or with EDTA shows a faster reaction, but it suffers from insufficient thermal stability; thus, it cannot be used in the decontamination of systems and circuits.

In modern LWR plants, the primary circuits are mainly made of austenitic steels or they are provided with an austenitic plating. The oxides formed on these surfaces are rich in chromium and nickel and, hence, are only very slowly attacked by chelating solvents. Some attempts have been undertaken to develop solvents which are able to remove such layers in a single-step procedure. One example of such a procedure is the application of an aqueous solution of Ce(III) nitrate and chromic acid having a pH in the acid range and saturated with ozone before use. It was claimed that this process, in which Ce(III) is oxidized by O_3 to Ce(IV), which in turn oxidizes Cr(III) to Cr(VI), will yield decontamination factors of 20 to 300 even when the process is performed at temperatures below 60 °C (Arvesen, 1988). A technical-scale application of this process, however, has not yet been reported. In contrast, general experience has shown that in order to attain a sufficiently high decontamination efficiency, two-step processes have to be applied, with the first step being an oxidation treatment to convert Cr(III) to Cr(VI), forming reactive starting centers in the oxide layer for the subsequent dissolution of the oxide by a chelating agent. The first and, for an extended period of time, only two-step process was the APAC (Alkaline Permanganate Ammonium Citrate) process (Ayres, 1970) using alkaline permanganate as an oxidizing agent and ammonium citrate as complexing agent. The principles of this process have been the basis for most of the modern processes which have been developed by various institutions. In the original KWU MOPAC process which, like the APAC process, had to be classified among the hard decontamination procedures, a pre-oxidation step was also conducted using an alkaline permanganate solution, whereas a citrate–oxalate solu-

tion served as complexing solvent containing Fe(III) formiate as an inhibitor. In the original version of this process comparatively high concentrations of chemicals were used, which restricted its application to the decontamination of components such as running gears of main coolant pumps, pressurizer heaters etc. The process is conducted at temperatures of about 95 °C, i. e. without the need for maintaining overpressure conditions in the decontamination facility. Initial radiation dose rates of 100 to 200 mSv/h are typically reduced to values of about 0.5 mSv/h; the decontamination success can be significantly increased by a final ultrasonic treatment. Detailed investigations have been performed to determine materials compatibility, showing that even repeated application of this process will not adversely affect the long-term integrity of the components.

In a similar manner, the effectiveness of other processes such as CAN-DECON and LOMI has been improved by introduction of a pre-oxidation step using permanganate solution. Concerning the LOMI process, several pre-oxidation and pretreatment steps were developed such as nitric acid $KMnO_4$ treatment (NP) and alkaline $KMnO_4$ treatment (AP), with the acid reagent being particularly effective with stainless steel oxides, whereas the AP reagent is recommended for the removal of contamination layers from Inconel-600 surfaces. In addition, a final treatment using an oxalic acid–citric acid solvent may be applied to dissolve residual oxides which had not been removed by the original LOMI step. For PWR applications in particular, several of these steps can be combined; usually, the whole process is repeated two or three times to obtain a decontamination factor which is sufficiently high. Of course, such multi-stage processes require a prolonged time to achieve a complete decontamination; in addition, a rather complex facility is required for the execution of the process.

Several modifications of the two-stage decontamination processes have been reported, in particular with regard to the optimum selection of reagents. In one of these processes, a decontamination solution containing citric acid and ascorbic acid is used at 85 °C, resulting in decontamination factors of about 10 when it was applied to specimens of stainless steel 304 which had been removed from the primary circuit of an operating PWR plant; in this process, a pre-oxidation step using permangante in boric acid solution is used (Lambert et al., 1989). The EdF-EMMA process consists of an acid oxidation step with $KMnO_4$ dissolved in sulfuric acid and a reductive step with a mixture of ascorbic acid, citric acid and oxalic acid. Application is performed at 80 °C with simultaneous ultrasonic treatment whenever the industrial conditions permit it (Gregoire et al., 1989). Decontamination of primary loops of VVER reactors was performed using two-step methods with a $KMnO_4$ solution as oxidizing agent and citric acid, EDTA or Trilon B as the complexing solution. When decontaminating removable equipment (e. g. pump shafts), the two-step decontamination is often combined with subsequent treatment with an alkaline $KMnO_4$ solution and, finally, with oxalic acid containing different additives (Pashevich, 1992).

There is an abiding interest in reducing the concentrations of the chemicals in the decontamination solutions, not only to further improve materials compatibility but also to minimize the resulting volume of radioactive waste. To this end, a simple reduction in concentration alone is not sufficient, since such a measure

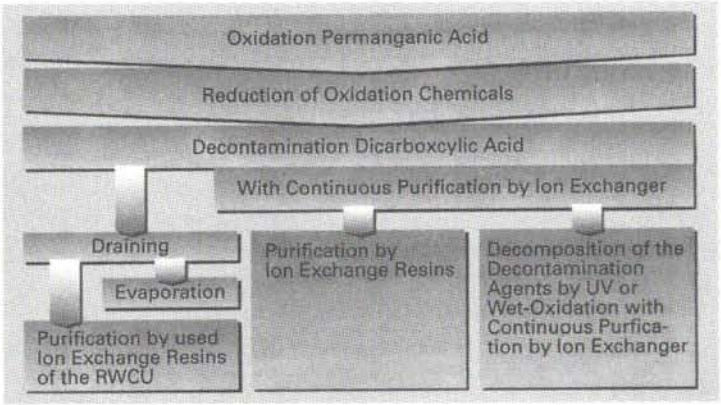

Figure 4.52. Principles of the CORD process
(By courtesy of Siemens/KWU)

would also reduce the decontamination rates and the overall efficiency. A considerable improvement can be obtained by subdividing the decontamination process into several brief cycles in which the surfaces of the materials are repeatedly contacted with fresh solvent. In the so-called regenerative processes the reagents are continuously regenerated during decontamination by being passed over ion exchange resins, which remove dissolved cations from the solution. An additional, highly effective improvement is based on the observation that preoxidation by an $HMnO_4$ solution is considerably more effective than by a $KMnO_4$ solution; as a consequence, lower MnO_4^- concentrations are required (50 ppm of $HMnO_4$ are sufficient to convert Cr(III) present in the spinel layers to the more soluble Cr(VI)). Simultaneously, application of $HMnO_4$ results in a significant reduction of the volume of radioactive waste produced during the decontamination. Due to its comparatively poor stability, the $HMnO_4$ solution has to be freshly prepared prior to each application; this can be performed by ion exchange and does not cause any difficulties. By such means, the amount of chemicals employed in the newer MOPAC 88 process has been decreased by a factor of about 7 compared to the original MOPAC process, without any loss in decontamination effectiveness (Wille and Bertholdt, 1989).

A further development of the MOPAC process led to the KWU CORD process (Chemical–Oxidation–Reduction–Decontamination), a multi-cycle, low-concentration process which proved to be especially suitable for the decontamination of subsystems and full reactor systems (Wille and Sato, 1994). The principles of this process are shown in Fig. 4.52. A CORD decontamination cycle starts with an oxidation step, using a dilute solution of permanganic acid; the excess MnO_4^- is then reduced by addition of a dicarboxylic acid, thereby generating CO_2. By further addition of the dicarboxylic acid up to a concentration of about 0.2%, dissolution of the oxides starts and the metal ions are retained in the solution as complex compounds. The whole process is conducted at about 95 °C; it does not require a fixed number of cycles, but can be repeated according to the final radiation dose

rate levels required. If continuous ion exchange is used (see below), the whole process can be performed with only one filling of the system with liquid.

The spent decontamination solution can be treated in several ways. Non-regeneratively, after termination of a CORD cycle the solution is drained and is treated either by evaporation or by ion exchange using the spent resins of the primary coolant purification system. More efficiently, the solution is continuously purified by ion exchange; the dicarboxylic acid is decomposed either by wet oxidation using permanganic acid or by intensive irradiation by UV light within the decontamination system. In this mode of operation, only comparatively small amounts of cation exchanger resins are needed for the removal of the dissolved radionuclides and corrosion product elements. Moreover, the final radioactive waste is free of chelating agents, which otherwise might cause difficulties with acceptance of the waste packages by the final repositories.

In another effort to further reduce the concentrations of chemicals in the pre-oxidation solution without loss of decontamination efficiency, a dilute mixture of permangante and chromic acid is used in the VS (Very Soft) procedure (Heess et al., 1989; Schenker et al., 1989). In this process, the pre-oxidation step is conducted at 70 °C, followed by a reduction step with oxalic acid solution at 30 to 35 °C. Using a two-cycle operation supported by ultrasonic treatment, decontamination factors on the order of 10 to 50 have been reported when PWR main coolant pumps were treated.

Normally, radiation-induced decomposition does not affect the functioning of the decontamination solutions. Only in the case of decontamination inside the reactor pressure vessel with the fuel still in place, may dilute reagent solutions show some degradation, in particular when decontamination is carried out shortly after reactor shutdown. Likewise, minor constituents of the solution such as corrosion inhibitors may be affected to some extent by radiation-induced degradation. At high radiation levels, the LOMI reagent can be attacked by radiation-induced oxidation of the V^{2+} ion; by addition of formiate to the solution the V^{3+} formed is reduced again so that a high stability of the reagent against radiation is obtained (Sellers, 1983).

4.5.2.3 Electrochemical decontamination procedures

As was described in the preceding section, the chemical decontamination processes result in a chemical dissolution of the oxide contamination layers present on the surfaces of the materials. In contrast, the electrochemical decontamination procedures are based on the anodic dissolution of a thin surface layer of the base material, as a consequence of which the oxide layer is peeled off from the surfaces of the materials. As a prerequisite for successful application, the electrolyte used has to be in electrical contact with the base material. Basically, the oxide layers are electrical insulators, but their porosity is usually large enough to ensure a sufficiently high electrical conductivity. On some occasions, very tight Fe_2O_3 layers have been observed in BWR circuits which rendered the direct application of the

electrochemical decontamination techniques impossible; in such cases, remedial measures can be taken such as a prior cathodic treatment of the oxide layer by which locally active centers in the layer are created, probably by reduction of Fe(III) atoms to Fe(II) atoms.

Compared with the chemical procedures, electrochemical decontamination shows several advantages. Local hot spots controlling the radiation dose levels in their vicinity can be selectively removed within a comparatively short time; in most cases a high decontamination factor is achieved; the surface of the base materials is simualtaneously smoothened during the decontamination process; and the required volume of electrolyte is comparatively small. On the other hand, various disadvantages also have to be mentioned, such as the need to design the cathode electrodes very carefully in order to achieve a uniform removal of the contamination layers from the surfaces, and the comparatively high expense of design and construction of the required facilities, which in many cases can be used for one special application only.

The electrolyte most frequently used is phosphoric acid in various concentrations – in most applications 20% – although in particular cases higher concentrations may be required. The oxide particles removed from the surfaces of the materials remain to a great extent as suspended solids in the electrolyte and can be continuously or semi-continuously removed by filtration, keeping the radioactivity burden of the solution to a tolerably low level. Nonetheless, a fraction of the oxides is dissolved in the electrolyte and this fraction increases with increasing application time of the electrolyte; therefore, several attempts have been made to purify the electrolyte from the dissolved fraction of the corrosion products and radionuclides before re-use (see Section 4.5.5.). According to the extensive investigations performed, the phosphoric acid electrolytes are compatible with the primary circuit materials and do not represent any hazard for their long-term integrity.

Phosphoric acid is, however, a hazardous chemical which requires special precautions for safe handling; moreover, processing of radioactive phosphoric acid waste is a difficult task. For this reason, attempts have been undertaken to introduce alternative electrolytes. For example, in the ELDECON process alkali metal sulphate solutions, mainly Na_2SO_4, are used as the electrolyte (Westerberg and Waltersten, 1989). The process temperature is low and ranges between 20 and 60 °C, depending on the material to be treated; the treatment times are typically on the order of 5 to 15 minutes. During treatment, the polarity of the object and the counter electrode is changed repeatedly; by this means, the process time needed can be reduced by up to a factor of three, the contamination background can be reached more easily, and the effects on the base material are minimized. The metal ions produced during dissolution of the oxide and base metal precipitate as hydroxides, forming a sludge when the electrolyte has settled; trace elements such as cobalt (^{60}Co) precipitate as hydroxides by co-crystallisation. The only exception is chromium which is converted into soluble Cr(VI) during the process; in order to simultaneously precipitate chromium, a reducing agent can be added to the electrolyte solution. The sludge particles are separated from the electrolyte either by sedimentation or by filtration. The alkali metal sulphates are not consumed during the process; electrolyte losses only result from the electrolytic decomposition of water

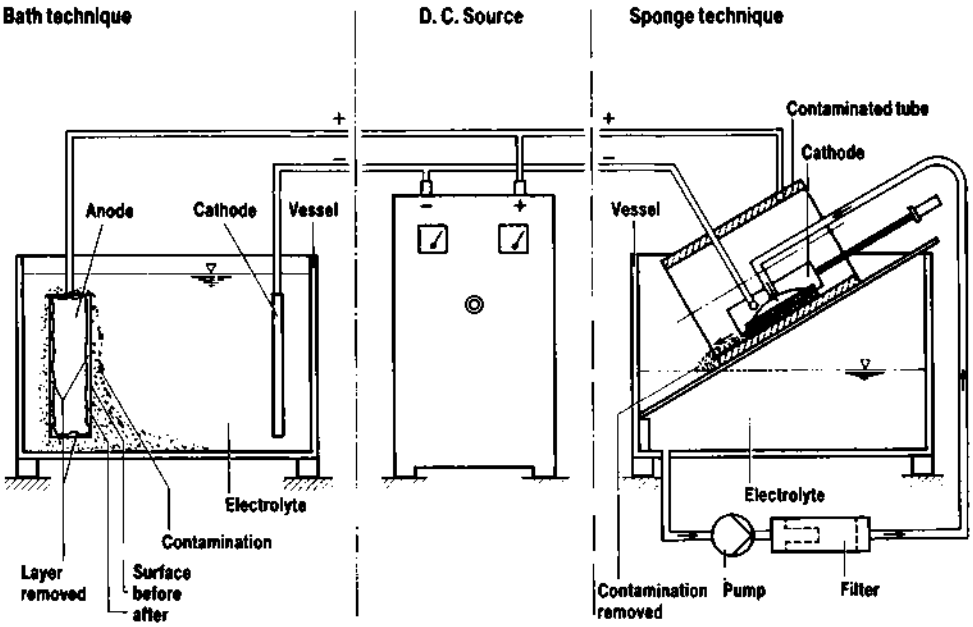

Figure 4.53. Techniques of electrochemical decontamination
(By courtesy of Siemens/KWU)

and from the draining off of settled hydroxide sludges. Other electrolytes proposed are aqueous solutions of oxalic acid or of sulphuric acid (Pashevich, 1992).

Leuchte et al. (1994) have developed two electrolyte systems by which the amount of resulting secondary radioactive waste can be considerably reduced: First, an aqueous system based on KF as a conductive salt and acetylacetone as a precipitating agent and, secondly, an anhydrous system based on glycole as a solvent and KBr as a conductive salt, also using acetylacetone as the precipitating agent. The combination of the anodic dissolution step with the chemical reaction leads to a continuous precipitation of the complex salts, which show low solubility, together with radioactive species such as ^{60}Co. A fraction of the electrolyte flow is deviated to separate the crystalline precipitate and to compensate for the stoichiometric loss of the complexing agent; it is then fed back to the operating cell. The bath performance can thus be maintained for a decontamination period of more than 6 months. This procedure combines high removal rates (more than 1.5 μm/min), short decontamination times, smooth surfaces and, after treatment of the separated salts by incineration to oxides, a comparatively small volume of secondary waste.

In the practical application of electrochemical decontamination procedures, different electrode arrangements are possible, depending on the geometric form of the component to be treated. Two basic possibilities, namely the bath (or immersion) technique and the in-situ technique, are schematically shown in Fig. 4.53. When the bath technique is used, which is mainly applicable for disassembled parts with

not too large dimensions, the part to be decontaminated is brought into a tank containing the electrolyte solution where it is arranged as an anode. The walls of the tank serve as the cathode; if necessary, additional specially-shaped cathodes can be employed. For the in-situ decontamination of the inner surfaces of piping, vessels, etc., the cathode is attached to an adapter (e. g. a sponge) to which the electrolyte is applied and which is moved continuously or stepwise across the surface. This technique can also be used in the decontamination of comparatively narrow pipes such as steam generator tubes; in this context, special facilities have been designed by which electric power and the electrolyte can be provided over distances of more than 10 meters. When decontaminating areas with a high radiation level, remote-controlled facilities can be employed.

4.5.3 Decontamination applications

In the past years a large number of decontaminations have been carried out, most of them in nuclear power plants in the USA, with the fields of application ranging from components which have been removed from the primary circuit to subsystems and to full reactor primary systems. In the following section only a few examples will be cited with special respect to the procedures applied; a more detailed survey of decontamination applications in water-cooled reactors was given by the IAEA (1994 a).

Hard decontamination processes were applied for components removed from the primary system such as pumps etc., but also in the final decontamination of the Dresden-1 BWR, which was finally shut down in 1978. The application of these processes resulted in a highly efficient removal of the radionuclides present in the contamination layers; however, waste processing and disposal proved to be a major difficulty, and concerns about corrosion effects necessitated a large and expensive materials qualification program. For this reason, and because of the highly successful development of soft decontamination processes, it seems unlikely that hard processes will continue to be used on operating plants.

Among the components removed from the primary circuits, main coolant pumps and recirculation pumps play a particular role; in order to save radiation exposure to the employees during the regular inspection of the rotating parts, decontamination is frequently required. Wille and Bertholdt (1989) reported on the carrying out of numerous reactor coolant pump decontaminations using the MOPAC and the MOPAC 88 processes. In a single-cycle procedure, decontamination factors on the order of 50 were obtained, which was increased to more than100 by the employment of two or more cycles. In case radiation levels after such cycles are still too high, the pump can be dismantled and the individual parts such as impeller, running gear house etc. can be decontaminated once more separately; in this manner, decontamination factors of up to 1000 can be reached.

In the execution of decontamination processes, special equipment is required in order to ensure full decontamination success and to save time and expenses, and minimize radiation exposure. Since this equipment, which mostly is used once a

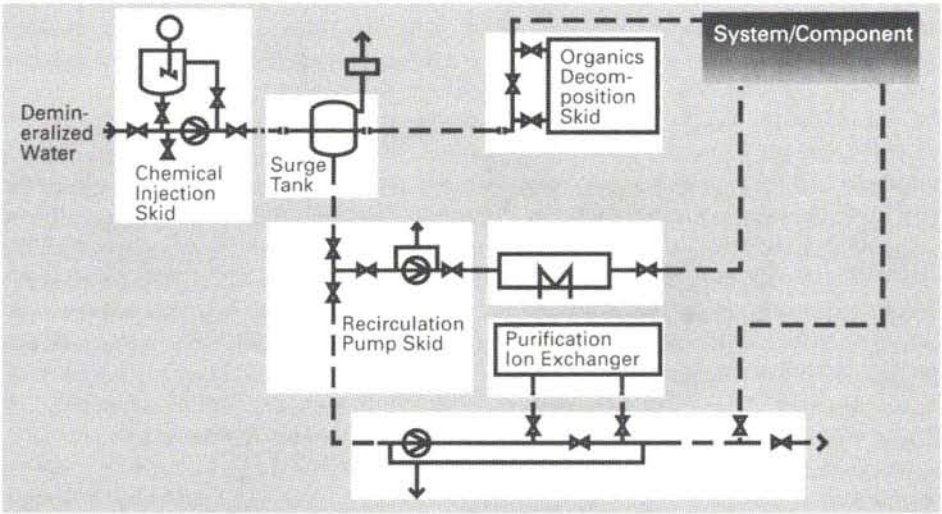

Figure 4.54. AMDA installation for decontamination of sub-systems using the CORD process (By courtesy of Siemens/KWU)

year or less, is often too expensive to be a permanent installation of the reactor plant, mobile decontamination facilities have been developed. An example for such a mobile unit is the Siemens/KWU AMDA facility (Automatic Mobile Decontamination Appliance), the basic setup of which is schematically shown in Fig. 4.54., as it is used for the decontamination of subsystems with the CORD process. In order to ensure optimum performance of a decontamination application, the chemical process and the engineering equipment have to be tailored to a consistent total concept, as was developed with AMDA/CORD technology. AMDA consists of a decontamination vessel equipped with ultrasonic cleaning installations (which is required for the decontamination of removed components); for subsystem decontamination, the assembly of different modules such as a chemical dosing module, recirculation pump and heater, the ion exchanger module, the skid for the decomposition of organic compounds and an auxiliary module are directly connected as an external loop to the respective system or component of the plant. The entire facility can be shipped in a container to a plant where a decontamination has to be carried out. All the operations are performed using a control panel which is positioned a certain distance from the component to be treated, resulting in low radiation exposure to the staff doing the work. The capacity of the AMDA equipment is adequate for the decontamination of components and subsystems such as PWR steam generator primary channel heads or BWR recirculation loops, without the need for using plant systems. In the decontamination of an entire primary circuit, however, the mobile unit has to be supported by plant installations, such as the ion exchanger beds of the primary circuit purification system.

As an example of the decontamination of subsystems, the treatment of a BWR recirculation loop and, in addition, parts of the residual heat removal system and the reactor water cleanup system, by using the CORD process in parallel to the

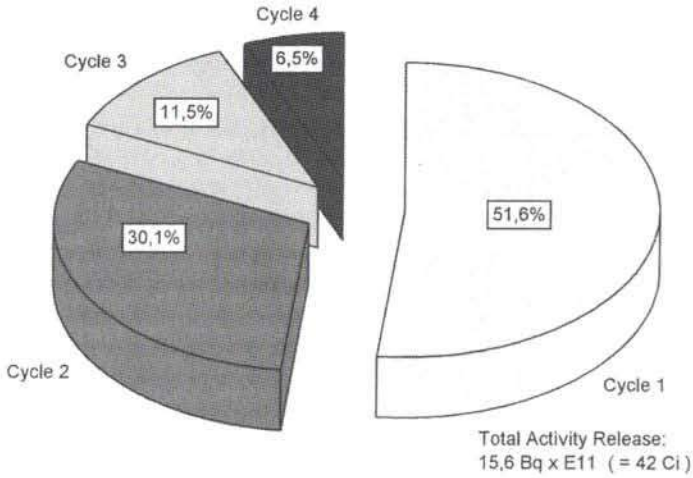

Figure 4.55. Activity release during CORD cycles in the decontamination of a BWR recirculation loop
(Wille and Bertholdt, 1992; by courtesy of Thomas Telford Limited, London)

refuelling operations shall be shortly described (Wille and Bertholdt, 1992). For this purpose, the AMDA facility was used as an external decontamination loop. As can be seen from Fig. 4.55., about 52% of the total release of radionuclides was already removed during the first CORD cycle, with decreasing amounts over the course of the following three cycles. The decontamination factor achieved (averaged over about 15 measuring positions) amounted to 17 after the third and 26 after the fourth cycle. For the accomplishment of the four CORD decontamination cycles, four days were required. In a similar manner, several subsystems at other BWR plants have been decontaminated by the CORD process (Wille and Bertholdt, 1992). As an example, results of decontaminations of BWR reactor water cleanup systems are given in Table 4.15., showing that high activity removal and high decontamination factors can be achieved in a comparatively short time and with a rather low radiation exposure of the people doing the work.

Table 4.15. BWR reactor water cleanup system decontaminations using the CORD process (1990–1993)
(By courtesy of Siemens/KWU)

System volume (m^3)	Time required (hours)	Number of decont. actions	Activity removed (Bq)	Decont. factor component	Pers. dose applied (mSv)
0.7–5	33–96	8	$4 \cdot 10^{10} - 1.4 \cdot 10^{12}$	4.3–53	3.4–50
5–10	22–120	4	$1.8 \cdot 10^{11} - 7.6 \cdot 10^{12}$	11–100	3.7–20
10–20	72–96	4	$3.5 \cdot 10^{11} - 1.6 \cdot 10^{12}$	11–194	10–38.5

In US BWR plants, decontamination of subsystems was most frequently applied to the external recirculation loops of the primary system. (It has to be pointed out that, with one single exception, the German BWR plants are equipped with internal recirculation pumps, so that this problem does not arise here). In most cases, the LOMI process was applied for these operations (as well as for the decontamination of other BWR subsystems) with either a single or double application, generally showing good decontamination factors. In low-flow areas, a second LOMI step was often required to deal with excessive oxide burdens, since in such cases catalytic decomposition of the reagent may occur before it contacts the surface oxides. In general, the application of a pre-oxidation step has yielded only a small further reduction in residual radiation fields in the decontamination of BWR subsystems; only for certain components such as the recirculation pumps, has use of an NP oxidation step proved to be beneficial (Wood and Spalaris, 1989). Concerning the flow path of the decontamination solution, use of the annulus between the shroud surrounding the core and the pressure vessel has proven to be a convenient choice, allowing an effective reagent circulation. A summary description of the carrying out of a BWR recirculation system decontamination (as well as of a PWR steam generator channel head decontamination), including the technical details, was given by Wood and Spalaris (1989).

From the experience gathered during BWR decontaminations it was concluded that the differences in the decontaminating power of different solvents and procedures currently in use are generally less significant than the differences in the nature of the oxide films in various plants. High decontamination factors can be achieved with any of the processes currently in use, but longer application times may be required and an increase in the waste volume may result in some cases (Wood and Spalaris, 1989). For these reasons, the particulars of the process to be applied have to be selected according to the extent of inspection or repair work planned at the specific component and the residual radiation dose rates that can be tolerated.

In PWRs, subsystem decontamination has mainly been applied to steam generator primary channel heads prior to inspection and/or repair of the heating tubes. A pre-oxidation step is required to attack the chromium-containing spinel oxides; among others, the CORD, LOMI and CAN-DECON processes have been used. Frequently, after termination of the chemical decontamination loosely-adhering radioactive particles remain on the walls which may contribute to rapid recontamination upon return to service; for this reason, these particles have to be removed in a final action, e. g. by high-pressure hydrolazing or by repeated water flushing.

When components or systems with larger volumes have to be treated, the large amount of decontamination solvent required can cause considerable expense during handling and waste processing. In order to minimize this volume, spray nozzles were used to inject the solution into the respective subsystems such as BWR recirculation systems or PWR steam generator channel heads (Oliver and LeSurf, 1989). Moreover, this technique has the advantage that continuously fresh solvent is brought into contact with the surfaces of the system, resulting in correspondingly increased decontamination rates and reduced time to reach a preset decontamination factor; in addition, the impact of the solvent droplets onto the walls prevents

the formation of a residual oxide film on the surfaces. When using rotating nozzles in steam generator channel heads, the solvent can be sprayed further up the steam generator tubes than is usually accomplished with a static system, thus reducing radiation shine from the tubes and giving a better reduction factor for the dose rates in the channel head.

When PWR steam generators are to be replaced, the radionuclides deposited on the inner surfaces of the main coolant pipes represent a radiation source which may severely handicap the work; therefore, the end sections at least have to be cleaned before starting the work. Decontamination of the relevant pipe sections by electrochemical techniques is a very effective means of removing the contamination layers and has been repeatedly applied. Mechanical procedures such as glass bead blasting have also proven highly effective in reducing the radiation levels in such limited areas.

In the past years increasing attention has been paid to full reactor system decontamination, if necessary with the fuel in place inside the reactor pressure vessel (e. g. Ferrett and Lister, 1984). This measure is the only means of removing all the significant radiation sources from the primary circuit which otherwise would be the origin of rapid recontamination of the decontaminated component or subsystem surfaces; on the other hand, in the context of decommissioning of a nuclear power plant (see Section 4.5.6.), a prior full-system decontamination will facilitate the work to be done and reduce the radiation exposure of the employees. Since the mid-1960's, a number of reactors experienced such a decontamination, mainly pressure tube reactors such as the Hanford N reactor (860 MWe, LGR), the Steam Generating Heavy Water Reactor (SGHWR) at Winfrith, UK, and several CANDU PHWRs (e. g. Pickering, 540 MWe). In Table 4.16. a summary of full-system decontaminations performed at power reactors is given.

In a number of full coolant system decontaminations of CANDU reactors with the fuel in place, the CAN-DECON process was applied (LeSurf, 1977); in these applications, the chemicals needed for the decontamination solvent were added directly to the heavy water coolant and removed from it after completion of the work by mixed-bed ion exchange. These decontamination operations resulted in an extensive removal of the contamination layers on the pressure tubes as well as of the fuel assembly deposits without any adverse effects on the long-term fuel behavior. Fuel rods with minor defects may be left in place during decontamination, while those showing major defects have to be removed before the procedure; experiments demonstrated that the process of decontamination did not aggravate small defects. The amount of fission products released from failed fuel rods during decontamination was low, with $^{95}Zr/^{95}Nb$ being the main contributor which may at least partly originate from activated fuel rod claddings.

Other full-system decontaminations (e. g. of the Steam Generating Heavy Water Reactor) have been performed using the TURCO reagent or the LOMI process with and without the NP pretreatment step. The results of these operations were satisfactory as regards decontamination factors and materials compatibility at the circuit surfaces, as well as at the fuel assemblies.

Although the results obtained in full-system decontaminations at CANDU plants as well as at the SGHWR reactor proved to be encouraging, there are sufficient

Table 4.16. Summary of reactor full-system decontaminations
(By courtesy of Siemens/KWU)

Reactor	Power (MWe)	Type	Date of decontamination	Decont. process	Remarks
Shippingport	68	PWR	1964	APAC	
Rheinsberg	70	PWR (VVER)	1968...1975 1976...1990	AP/Citrox AP/CE	
Winfrith	100	SGHWR	1971...1979 1980...1990	TURCO LOMI, NP/LOMI	
Gentilly, Pickering, Douglas Point, Bruce	25...800	CANDU	1973...1989	CAN-DECON, AP/CAN-DECON	
Greifswald 1...4	440	PWR (VVER)	1978...1990	AP/CE	without fuel
NovoVoronesh 1,2	210, 365	PWR (VVER)	1981, 1984	AP/CE	decomm.
Dresden 1	200	BWR	1984	NS-1	decomm.
BR-3 Mol	10.5	PWR	1991	CORD	decomm.
VAK Kahl	16	BWR	1992	CORD/UV	decomm.
Oskarshamn-1	462	BWR	1994	CORD/UV	without fuel
Loviisa-2	445	PWR (VVER)	1994	CORD/UV	without fuel
Greifswald-5	440	PWR (VVER)	1994	AP/CE	decomm.

decomm: decontamination prior to decommissioning

differences in design to make independent testing of decontamination processes necessary prior to the execution of a full-system decontamination in light water reactors. A major problem in transferring the experience obtained in pressure-tube reactors to pressure-vessel reactors is due to the latters' larger volumes, which require greater amounts of decontamination solvents and, as a consequence, result in larger waste volumes. Another difficulty to be expected in pressure-vessel reactors is the presence of low-flow regions (dead legs and crud traps), while the pressure-tube configuration permits a higher flow velocity of the decontaminant through the reactor core, potentially resulting in a greater decontamination effectiveness.

Full-system decontaminations require a particularly extensive preparatory work. Compatibility of the materials to the reagents applied in the decontamination solutions is of highest significance when further operation of the plant is planned; not only the materials present in the primary circuit have to be tested for corrosive attack, but those in the components of the nuclear auxiliary systems as well, which will be in contact with the solutions in the course of the decontamination procedure. Due to differences in the materials applied, such a test might only be applicable for the plants of a given manufacturer; occasionally, a special composition of materials present in one individual plant has to be taken into account. Another

important item is the evaluation of the suitability of the plant systems needed for carrying out the procedure. From these and other data such as waste processing and evaluation of the long-term benefit of a full-system decontamination, a project concept for execution of the work has to be developed.

In order to prepare for decontamination of a PWR full reactor coolant system, Aspden and Grant (1991) investigated behavior of materials under the conditions of the LOMI process. Different materials used in Westinghouse four-loop PWRs such as stainless steels (also in the sensitized state), Inconel, Stellite and other special alloys were exposed to three cycles of the LOMI process, with each cycle consisting of four steps (AP–LOMI–AP–LOMI). The materials were subsequently examined to get information on general corrosion, crevice corrosion and stress corrosion. In general, material losses during the exposure to the decontamination solution were on the same order of magnitude as the corrosion rates experienced over the course of a few years of plant normal operation. No stress corrosion cracking was observed; at some material surfaces a roughening of up to 10 μm occurred. According to these results, no severe problems are to be expected in the application of the LOMI process to a full-system decontamination. Currently, in the USA the LOMI and CAN-DEREM processes are given equal prominence in the development of corrosion data necessary for full-system decontamination in PWRs (Wood and Spalaris, 1989).

As can be seen from Table 4.16., several commercial light water PWR and BWR plants have also been subjected to a full-system decontamination, partly with and partly without the fuel in place. Starting with the early Shippingport action, other plants such as Rheinsberg, Novo Voronesh-1 and 2 and Dresden-1, have been successfully cleaned, using different decontamination procedures. The Rheinsberg VVER reactor was repeatedly decontaminated, initially using a modified AP/Citrox process, in later years with the more effective AP/CE process using mixtures of citric acid and EDTA as chelating agents. The experience gained here was extended to the USSR standard 440 MWe VVER plants. Decontamination factors of 2 to 5 have been reported without any deterioration of the materials observed. Likewise, full-system decontaminations with the fuel in place were carried out in the Soviet RBMK reactors using an oxalic acid–hydrogen peroxide reagent with good decontamination effectiveness and only insignificant attack on circuit alloys and fuel claddings.

The CORD process is especially suited for the decontamination of PWR and BWR full primary systems. Detailed investigations (Wille and Bertholdt, 1989) have shown optimum materials compatibility with the solvents to be applied. Calculations showed that using the volume control system of the plant and the connected auxiliary systems, the time required for one decontamination cycle depends on the capacity of the purification system; at a purification rate of 15% of the primary loop volume per hour, 24 hours are required. Heating of the entire loop can be achieved by running the main coolant pumps. As the reagents used for the oxidation step are chemically reduced, no time is lost with ion exchange, and a purification step by ion exchange is required only at the end of the decontamination step. For the decontamination of Siemens PWR primary loops, no external equipment is required while the installed capacities in other PWRs and BWRs are

often not adequate and additional equipment is required in these cases. For large PWRs, 5 to 20 m^3 of ion exchange resins are needed for the collection of the removed corrosion products, i. e. considerably less than the amount needed in other decontamination processes. The extremely low waste generation in the CORD process is due to the decomposition of the reagents after the decontamination step by wet oxidation or photo-reaction (Wille and Bertholdt, 1992).

Using the CORD process, the complete primary circuit of the Belgian BR3 PWR (10.5 MWe) was decontaminated as well as that of the German VAK BWR (16 MWe). Both plants were finally shut down several years ago and decontamination was intended to be an effective means of reducing personnel radiation exposure during the decommissioning work. In the BR3 decontamination, about 24 kg of corrosion products were removed from the primary circuit by application of three CORD cycles, together with about $2 \cdot 10^{12}$ Bq of radioactivity, resulting in an average decontamination factor of >10. Thus, experience from both applications confirmed the initial expectations concerning high decontamination factors and only low waste volumes (ion exchange resins). It also showed that it is possible to perform such a task with only minor modifications in the plant. In both cases, the AMDA mobile facility was used as an external decontamination loop.

If the reactor is to continue in operation after the full-system decontamination, besides materials compatibility the time needed for carrying out the procedure is often of great importance. As Bertholdt and Wille (1994) have reported, the CORD/UV process is able to satisfy the time requirement as well. After 22 years of operation, the Oskarshamn 2 BWR had to be decontaminated in order to permit extensive inspection and repair work in the reactor pressure vessel. For this purpose, all fuel assemblies and the RPV internals were removed from the pressure vessel. Included in the decontamination, besides the reactor pressure vessel, were the control rod drives and instumentation housings, all four recirculation loops (including pumps and valves), the residual heat removal system, the reactor water cleanup system and parts of the feedwater system. The total volume to be decontaminated amounted to about 160 m^3, with a surface area of about 1500 m^2. Decontamination was performed by using the auxiliary systems of the plant; the only external systems required additionally were the UV decomposition skids and a chemical injection skid from the AMDA mobile facility. Four CORD cycles applied in 7 days resulted in the removal of about 30 kg of iron, chromium and nickel from the systems with an activity of $2.3 \cdot 10^{12}$ Bq. This activity represented about 99.5% of the initial corrosion product activity inventory of the plant primary system, about 80% of it was removed during the first decontamination cycle; the main radionuclide was ^{60}Co, which amounted to about 90% of the total activity removed. The average decontamination factor achieved in the recirculation loops was about 30, at the bottom of the reactor pressure vessel a value of about 1000 was measured. Only 2.1 m^3 of ion exchange resins were consumed in the action, mainly due to the extensive decomposition of the organic chelating reagents by means of intense UV radiation.

The Loviisa 2 PWR had been in operation since the beginning of 1981; extensive inspection and repair work had to be done during the outage in 1994. In order to carry out this work with minimum radiation exposure to the staff, the complete

primary circuit had to be decontaminated, including the reactor pressure vessel without fuel and control rod drives but with the RPV internals, 6 coolant loops with one steam generator, one reactor coolant pump and two isolation valves each, as well as the volume control and chemicals injection system and the primary coolant purification system. The total system to be decontaminated had a volume of about 300 m^3 with a surface area (fuel excluded) of about 17,000 m^2. By using four CORD cycles, which took 9 days, about 290 kg iron, chromium and nickel were removed. The decontamination resulted in the removal of about $4 \cdot 10^{13}$ Bq of radionuclides (about 50% of which was during the first CORD cycle), corresponding to about 98.5% of the initial inventory of radioactive corrosion products of the primary circuit; the main radionuclides removed were ^{51}Cr (48%) and ^{60}Co (26%). The decontamination factors achieved ranged from about 15 in the primary system compartments to about 150 measured on the secondary side of the steam generator tube bundles. The amount of cation exchanger resins and anion exchanger resins consumed during the entire action was 8.5 m^3 and 22.5 m^3, respectively. The comparatively large amount of anion resins, which were mainly consumed by residual organic reagent, was due to a tight time schedule; however, as a consequence of the application of the UV decomposition procedure an additional 8 m^3 of resins were saved (Bertholdt and Wille, 1994).

The experience gained in these and other actions has demonstrated that an efficient full-system decontamination is feasible in both PWRs and BWRs, and that it can be performed within an acceptable time and with a reasonable effort.

When performing a full-system decontamination with the fuel in place, problems may arise due to the high burnup and the long residence times usually experienced by the LWR fuel assemblies, which might make the materials more susceptible to chemical attack by the decontamination solution. In order to evaluate possible risks to the materials, O'Boyle et al. (1989) conducted decontamination tests of discharged BWR fuel bundles (burnup about 30 MWd/kg U) using the AP/LOMI and the AP/CAN-DECON processes. This work was performed in a specially designed stainless-steel chamber placed in the spent fuel pool. From a comparative evaluation of the measured effectiveness of the decontamination processes it was shown that the AP/LOMI process removed more than six times as much activity from the fuel assemblies than AP/CAN-DECON did ($3.6 \cdot 10^4$ GBq vs. $5.7 \cdot 10^3$ GBq). The dominating radionuclide removed was ^{55}Fe, accounting for 80–90% of the total activity; the ^{60}Co fraction amounted to 10–20%, while all the other radionuclides yielded only small contributions to the total activity removed. From the spent decontamination solution the radionuclides were adsorbed on ion exchange resins which afterwards were solidified in cement. Besides the fuel bundles, highly irradiated Type 304 SS specimens cut from control blades which had been discharged from a BWR were also subjected to a decontamination. Post-decontamination examination of these materials showed no adverse effects resulting from the AP/LOMI process. However, there was some evidence of intergranular attack of Inconel X-750 springs after decontamination with AP/CAN-DECON. A subsequent feasibility study which was based on the experience obtained during this action, showed no technological impediments to a decontamination of the full reactor primary system with the fuel in place. It is assumed that certain difficulties will arise from the

surprisingly high ^{55}Fe activities, resulting in unexpectedly high costs for the disposal of the decontamination waste.

In the decontamination of a BWR reactor recirculation system with the fuel in place in the reactor core, a three-step Citrox–AP–Citrox process was applied resulting in decontamination factors between 10 and 40 (Oliver and LeSurf, 1989).

4.5.4 Recontamination of decontaminated surfaces

Following a decontamination, redardless of whether by a chemical or an electrochemical procedure, a clean metallic surface without a protective oxide layer remains, which during subsequent operation of the plant is covered again by an oxide layer into which radionuclides are incorporated at a comparatively fast rate. Recontamination occurs when freshly decontaminated surfaces pick up activity, as the surface reestablishes its protective oxide film. When part-system decontamination is performed after several years of plant operation, in the following operation period the reactor coolant will carry comparatively high concentrations of radioactive species, originating from the non-decontaminated surfaces. This is in marked difference to the situation during the original plant commissioning time period when corrosion films were initially developed on these surfaces and when the coolant was still free of radioactivity or contained only low concentrations of long-lived corrosion product radionuclides. Consequently, following a decontamination the newly developing corrosion films incorporate radionuclides at a faster rate, causing a rapidly increasing radiation field in the areas surrounding the component. In most cases, the radiation levels which had been present before the decontamination operation are nearly reached again after only one fuel cycle. As an example, Fig. 4.56. (according to IAEA, 1994 a) shows measured recontamination values at the main coolant pumps of two German PWR plants, indicating that the activity buildup on decontaminated surfaces proceeds at about the same rate as on virgin material and that the activity level attained after a given time is proportional to the ^{60}Co activity concentration in the primary coolant. Observations from US BWR plants showed that surfaces which were exposed to high-temperature water recontaminated to about 95% of their pre-decontamination levels over a two-year period; recontamination rates were particularly high during the first three months following decontamination (LeSurf et al., 1983). However, from Fig. 4.56. it can also be seen that repeated decontamination does not result in faster recontamination rates.

Several authors have reported that recontamination rates are usually less severe when dilute chemical decontamination processes have been applied. The most likely explanation of the high recontamination rates observed after the use of concentrated reagents is that these solutions were corrosive, removing the entire protective film from the surfaces and roughening the underlying base material. Nevertheless, even when applying soft decontamination procedures, the phenomenon of recontamination is a severe handicap for further work. Numerous attempts, therefore, have been made to reduce the rate of recontamination in order to reduce

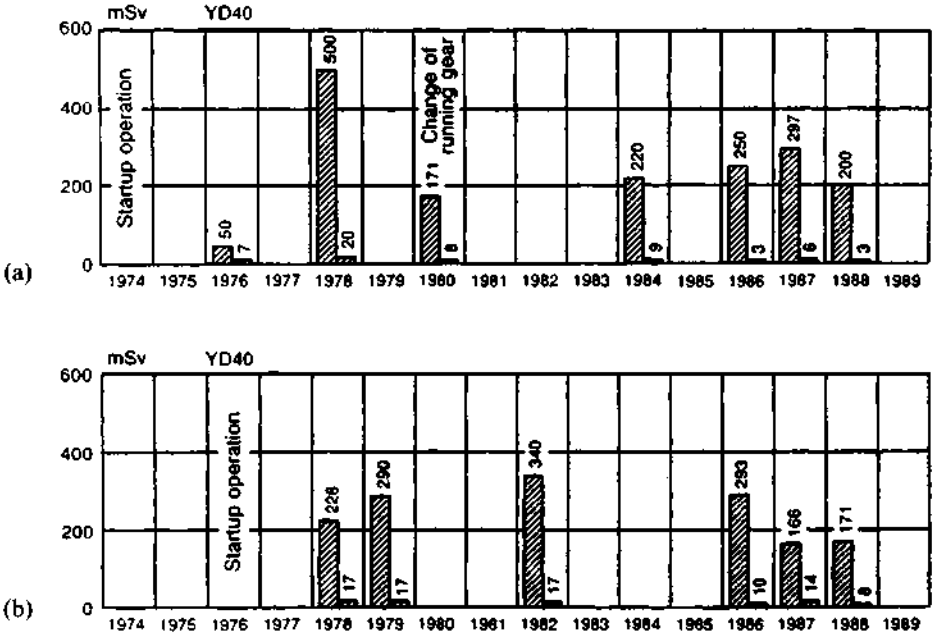

Figure 4.56. Radiation fields on pump YD40 before and after decontamination, showing recontamination over time (a) Biblis A; (b) Biblis B
(IAEA, 1994a; by courtesy of IAEA)

personnel radiation exposure and/or to prevent the need for repeated decontamination operations. One possible way to meet this goal is the complete (or nearly complete) removal of the corrosion product radionuclide inventory present in the primary circuit by full-system decontamination as described in the preceding section; this would prevent recontamination, which is caused by redistribution of the radionuclides still present after a part-system decontamination.

As was mentioned above, recontamination proceeds according to the same mechanisms as radionuclide buildup on virgin surfaces and, therefore, the measures to be taken to decrease the recontamination rates are similar to those reported in Sections 4.4.3.5. and 4.4.4.5. One of these potential measures is an appropriate pretreatment of the surfaces prior to the start of operation. By smoothening of the surface, the true surface area can be reduced due to the preferential removal of the roughness peaks, resulting in a potential decrease in the deposited amounts of oxides and radionuclides. A proven technique for smoothening of the surfaces is electropolishing; as a consequence of the anodic dissolution process, a passivation of the surface occurs which also should favor a slower recontamination. An approximate 50% reduction of the recontamination rates after electropolishing as compared to as-received surfaces has been reported (e. g. Blok, 1984).

Normally, metallic clean surfaces will show a faster recontamination rate than those covered by an oxide layer. Therefore, several attempts have been made to create a suitable oxide layer either by treatment in an air–steam atmosphere or by

treatment with simulated coolant (free of radionuclides), both performed at elevated temperatures. However, practical experience with such passivation procedures did not yield significant improvements in recontamination. The only exception has been observed with surfaces that are in contact with low-temperature water, such as the steel liner of the spent fuel pool. Electropolishing results in a surface from which adsorbed corrosion product particles can be removed more easily (e. g. by a water jet) than from "as-received" surfaces. On the other hand, electropolishing requires the use of 80% phosphoric acid as an electrolyte, which causes more difficulties than the 20% phosphoric acid used in electrochemical decontamination when it has to be purified of radionuclides or when it has to be treated as radioactive waste.

Experiments performed in an SGHWR loop showed that specimens of stainless steel SS 304, Inconel 600 and Zircaloy-4, previously decontaminated with the LOMI or the NP/LOMI processes, recontaminate within a few months to their preceding activity levels (Bridle et al., 1986). Surfaces which had been decontaminated with the LOMI process alone experienced a faster recontamination than those treated with the NP/LOMI process. This difference may be explained by the fact that application of the NP/LOMI process results in a complete removal of the surface oxide layer, leaving behind a surface which shows less tendency to attract suspended corrosion product particles.

According to the survey paper of Ocken (1985), a smoothened (e. g. by electropolishing) surface favors a lower recontamination rate. On the other hand, formation of passivation layers does not result in all cases in a lower uptake of radionuclides; depending on the technique applied for passivation, even a faster and higher incorporation of ^{60}Co into these oxide layers has been observed. The experience made with new parts in the course of replacement operations at BWR and PWR plants has shown that electropolishing and subsequent passivation pretreatment of the surfaces results in recontamination rates which are lower by a factor of 2 to 3 than for untreated surfaces (Asay, 1989). According to this experience, the optimum passivation layers are obtained by pretreament in moist air at about 300 °C. By pretreatment with simulated liquid primary coolant (free of radionuclides) under PWR primary circuit operating conditions, a surface layer rich in chromium is formed which reduces the corrosion rates; in contrast, pretreatment under BWR operating conditions results in an oxide layer depleted in chromium. In order to minimize corrosion, other techniques for stabilizing the oxide layer were proposed such as incorporation of palladium atoms; however, no experimental verification of this idea has been reported. Basically, if the rate of contamination buildup is determined by the incorporation of dissolved cobalt atoms into the oxide layer, then this rate should be reduced by formation of a "perfect" oxide with no or only few lattice defects. As yet, however, no ideas have been developed on how to realize this goal on a technical scale.

Recontamination rates at the recirculation piping of a number of BWR plants have been compared by Duce (1990), in order to get an indication of the impact of different measures. These results show that the concentration of dissolved ^{60}Co in the reactor water is the key parameter controlling the rate and extent of recontamination. When the measured recontamination rates were normalized with re-

gard to the coolant ^{60}Co concentration, the influence of specific pretreatement processes applied to new pipe sections could be identified. Thus, electropolishing plus pre-oxidation showed a clear beneficial effect while electropolishing alone did not reduce significantly the process of recontamination. Addition of zinc to the reactor water has also proven to be an efficient means of reducing recontamination.

In summary, the most promising means of reducing the rate of recontamination of decontaminated surfaces seems to be minimization of the ^{60}Co concentration in the coolant. All the attempts made to reduce recontamination of decontaminated surfaces by appropriate pretreatment did not show a clear beneficial result. When, in the course of a replacement action, new pipes or components are installed, a pretreatment of these surfaces by electropolishing plus pre-oxidation (hot moist air) seems to be effective. However, because of the complex process of ^{60}Co incorporation into the superficial oxide layers it is often difficult to distinguish clearly between incidental correlations and those which are in fact caused by the measures taken.

4.5.5 Treatment of radioactive decontamination waste

The spent decontamination solutions have to be processed in order to yield a final product able to meet the requirements of the applicable state regulations (e. g. the Vorläufige Annahmebedingungen für das Endlager Konrad in the Federal Republic of Germany or the NRC 10CFR Part 61 criteria for shallow land burial in the USA). On the other hand, economic aspects such as the costs of a specific technique of waste processing and the size of the final waste volume obtained by this technique have to be taken into consideration; because of the high costs for intermediate and final waste disposal, a minimum final volume has to be strived for in each case. Due to their chemical composition, which is quite different from the radioactive waste produced during plant normal operation, special pretreatment steps have to be applied in the processing of decontamination wastes.

For a number of decontamination processes, evaporation of the spent solutions in the waste water evaporator of the plant is a practicable method. In order to reduce the amounts of solid chemicals, a simultaneous treatment of the oxidation solution and the complexing solution is advantageous, since the organic chemicals (dicarboxylic acids) are then oxidized to CO_2 by the permanganate present, which is reduced in acid solution to Mn^{2+}, in neutral and alkaline solutions to MnO_2. Oxalic acid and citric acid are only oxidized by permanganate in an acid solution, whereas ascorbic acid and EDTA are also readily decomposed in neutral and alkaline solutions. Since oxidation of the chelating substances by permanganate is an exothermal process, the reaction solutions will heat up automatically with only little external heat supply. As an example, evaporation of the spent solutions from the decontamination of a BWR recirculation loop using the CORD process resulted in a residual amount of only 12 kg of salts and of 6.4 kg of removed corrosion products (Wille and Bertholdt, 1992).

Minimization of the concentrations of chelate-forming chemicals in the final waste volume is an important measure, since in the acceptance criteria of most of the final repositories these values are restricted to comparatively low levels. The reason for these limitations is that chelates may influence the transport behavior of radionuclides in the soil upon unintentional leaching of the waste volumes by ground water, which would change the basis for the calculations conducted in the safety analyses of the repository.

Flocculation of added $FeCl_3$ solution by proper addition of $Ca(OH)_2$ removes the bulk of the radionuclides from the spent decontamination solution; decontamination factors of up to 500 can be achieved by an appropriate performance. While the resulting volume of precipitate is comparatively high, it can be reduced by separation using a centrifuge-decanter system (Gregoire et al., 1989). Several attempts have been made to process spent decontamination solutions by inverse osmosis, but so far these attempts have been unsuccessful, mainly due to rapid plugging of the membranes.

When larger volumes of dilute decontamination solutions are used (e. g. in the decontamination of subsystems and of full systems), removal of the radionuclides from the solution by ion exchange is the most economic way, either continuously during the course of the process or from the final spent solution. The ion exchange resins, which usually contain a considerable activity inventory, are then dried and packed into thick-walled containers which meet the requirements of the final disposal regulations. Alternatively, the spent ion exchange resins can be solidified using an organic binder or they can be incorporated into concrete or bitumen to obtain a product which is ready for safe intermediate or final disposal. Besides the disadvantage of comparatively large volumes of the final products, difficulties in the solidification process may be caused by organic acids that are still attached to the resins. Investigations have shown that these organics (oxalic acid, citric acid etc.) can be decomposed by permanganate oxidation after suspension of the resins in dilute H_2SO_4 solution (Holmberg et al., 1983).

The required volume of ion exchange resins depends strongly on the concentrations of chelate-forming chemicals (dicarboxylic acids) still present in the solution. The most efficient way of minimizing these residual concentrations is oxy-photolytic decomposition, as it is performed in the CORD/UV process (Bertholdt and Wille, 1994), in which the spent decontamination solution is irradiated by an intense UV source. With this technique, the volume of consumed resins is considerably smaller than it is in processes employing chemical decomposition techniques.

Several attempts have been made to reduce the final volume of the spent ion exchange resins prior to packaging. Since such resins have a low density with voids both within the grains and between them, compaction may be a suitable means for volume reduction; this technique, however, suffers from the fact that upon pressure reduction the resins will swell again. As a remedial measure, destruction of the structure of the resin grains can be achieved by heating the material during compaction to temperatures of up to 400 °C. There are also other techniques that lead to a higher volume reduction factor. One is chemical digestion using strong acidic mixtures (wet oxidation). After decomposition of the material the solution is neutralized, but this technique suffers from the high salt concentration in the resulting

solution. Another method is incineration, i. e. high-temperature oxidation. Here, besides normal dry incineration several other high-temperature oxidation processes have been proposed. Pyrohydrolysis of the organic material by high-temperature steam or oxidation by high-temperature pressurized water are possible alternatives resulting in small final waste volumes and very low radionuclide volatilization. As yet such techniques have not, however, been employed on a technical scale.

In order to reduce significantly the waste volumes arising in the decontamination of subsystems and full reactor systems using the LOMI process, an electrochemical technique, ELOMIX, has been developed in which the ion exchanger resins are used as an intermediate waste form and are continuously regenerated by the passage of an electric current (Bradbury et al., 1992). For this purpose, the cation exchanger resin is placed in an electrochemical cell, in which the ion exchanger compartment is separated from the anode and cathode compartments by cation exchange membranes. Upon passage of an electric current, the adsorbed cations (Fe^{2+}, Co^{2+} etc.) are eluted from the resin and migrate to the cathode where they precipitate as particulate metallic deposits which afterwards can be washed down to a vessel where they are finally solidified. Due to its purely inorganic nature and its small volume, this precipitate is especially suited for both intermediate and final storage. Pilot-plant applications in the bypass of the decontamination flow at two US plants yielded satisfying results for the process.

The spent phosphoric acid solutions from electrochemical decontaminations pose special problems in processing. An effective separation of the radionuclides and dissolved corrosion products from the solution can be achieved by neutralization with a $Ca(OH)_2$ suspension, resulting in the precipitation of calcium phosphate; however, this technique results in large volumes of solid material which are difficult to separate from the residual liquid. In consequence, the electrolyte solution is normally kept in use as long as possible by removal of the suspended solids by continuous filtering, keeping the radiation dose rates of the solution at a tolerable level. A fraction of the radionuclides in the solution, however, is in the dissolved state and this fraction increases over the time of use of the electrolyte (including the periods of storage between two applications). Experiments have shown that dissolved radionuclides (e. g. Co^{2+} ions) can be removed very efficiently from a 20% phosphoric acid electrolyte by ion exchange using specially prepared resins. Another possibility is iron oxalate precipitation from phosphoric acid solution by which cobalt isotopes are simultaneously removed via co-precipitation. The purified electrolyte can be re-used while the iron oxalate precipitate can be thermolyzed to yield iron oxide as an acceptable product for final storage. This regeneration procedure has been developed and successfully applied in the context of the dismantling of the Gundremmingen A BWR (Eickelpasch et al., 1994). Electrolytic regeneration of spent phosphoric acid electrolyte has also been reported (Sasaki et al., 1991).

Of course, the operations to be performed in the context of processing of the waste resulting from decontamination operations lead to additional radiation exposure of the employees which has to be included in the man-rem balance required for justification of a decontamination. Usually, processing the waste contributes only to a minor degree to the total radiation exposure to be expected during decon-

tamination and, therefore, does not affect the balance significantly. However, further reduction of the waste volumes will result in increased radiation dose rate levels; consequently, remote-controlled techniques have to be considered. This might be particularly true for spent ion exchange resins with their comparatively high activity inventories.

4.5.6 Decontamination within the scope of decommissioning of nuclear power plants

Like any other industrial plant, nuclear power plants have to be decommissioned when they have reached their lifetime, which is determined either by the lifetime of the main components (such as the reactor pressure vessel) or by the fact that a new type of power plant is able to work more economically. The current assumed lifetime of operation is about 40 years, although individual values depend on the actual condition of a plant and the specific circumstances of its operation. In the decommissioning of nuclear power plants, the most important difference from non-nuclear industrial plants is the presence of large amounts of radioactive substances in the plant which have to be safely removed without hazard to the staff engaged in the work or endangering the environment. There is, therefore, no fundamental difference between the planning and carrying out of decommissioning work for nuclear power plants and of industrial plants in which poisonous or hazardous non-nuclear substances have been processed.

According to an estimate made in 1991 by the OECD Nuclear Energy Agency, by the year 2000 more than 60 nuclear power plants around the world are expected to become candidates for decommissioning. Unlike most other industrial plants, nuclear power plants to be decommissioned are subjected to particularly stringent rules and regulations. In addition, German electricity utilities are required to prove the decommissioning capability of their plants even before these plants are put into operation. This means that in a very early stage relevant studies have to be carried out with regard to the technical procedures to be applied in decommissioning as well as the possibilities for treatment and conditioning of the arising radioactive wastes. Last but not least, evaluation of the expenses associated with plant decommissioning have to be included as well.

To date, well over 650 research reactors have been built or are in the construction or planning phase throughout the world. Out of these, more than 350 have already been shut down and decommissioned to different stages. Considerable experience has been accumulated, so that general conclusions on decommissioning techniques for different types of research reactors can now be drawn (IAEA, 1994 b). Nonetheless, because of the large differences in the design, materials and operating conditions of nuclear power plants as compared to research reactors, the experience gained with research reactors is only of limited applicability for commercial facilities. As to light water reactors, the Shippingport Atomic Power Station, the first PWR plant in the world, was definitively shut down in 1982 and disman-

tled to the state of "green field" in the period 1985 to 1989. As a consequence of the experience gained in this operation and of the considerable efforts undertaken to develop strategies and techniques for the decommissioning of power reactors, a well-established state of the art has been attained.

The technological aspects of decommissioning nuclear facilities in general have been treated in a number of publications such as the documents published within the IAEA Technical Reports Series. Depending on the particular situation, the most appropriate of the available different decommissioning strategies has to be selected; given the scope of this treatise, the different strategies cannot be discussed in detail. The general procedure of decommissioning a nuclear power plant can be shortly summarized as follows:

The first technical action to be undertaken after the decommissioning license has been granted is removal of the spent fuel assemblies from the reactor core to an appropriate storage facility (i. e. the spent fuel pool), followed by their transport from the plant to another, central storage facility or to a reprocessing plant. These are actions which are common in reactor operation and, therefore, do not require any unusual measures. Upon removal of the fuel from the reactor core, the primary coolant and the other operational fluids are taken from the different circuits and processed in the same manner as had been done during the operational period of the plant. So far, decommissioning does not require any work which is markedly different from that already experienced during plant operation.

After termination of this work, the remaining radionuclide inventory of the plant can be divided up into two categories: activated structural materials and surface-contaminated piping and components. Normally, the dominant radionuclide in both types of sources is ^{60}Co; its comparatively short halflife of 5.27 years offers the possibility of reducing the radiation exposure to the personnel engaged in decommissioning work as well as the activity inventories of the resulting radioactive wastes by postponing this work by a time period of 10 to 20 years. Considerably longer waiting times do not result in a corresponding further decrease in the radioactivity inventory, since other longer-lived radionuclides then take over the leading role. During this delay period, the regions of the controlled areas of the plant which contain radioactive substances have to be safely confined, precluding the danger of uncontrolled dissemination of radioactivity inside the controlled areas and of any release of radioactivity to the environment. Over the period of safe confinement all the plant installations needed for the subsequent dismantling work have to be kept operational. When deciding on the decommissioning strategy to be applied, the expenses of a longer period of safe confinement, including surveillance and maintenance, have to be evaluated against the higher costs of an immediate dismantling resulting from the higher radioactivity inventory. In addition, other aspects such as the need of the site for a new power or other industrial plant may dictate the length of the period between plant shutdown and dismantling.

Thus, after a period of several years to decades dismantling work of the plant will begin, aiming at a complete removal of the radioactive materials and, later on, the buildings as well from the site to finally reach the state of a "green field". As a first stage of this work, decontamination of the entire primary circuit is a

proven means of considerably reducing the occupational collective radiation dose which will be associated with the further dismantling of the systems, components and piping. To this end, a decontamination technique has to be selected which, on the one hand, shows appreciable decontamination factors (values of 10 and more are generally required) but, on the other hand, results in a comparatively small amount of final radioactive waste. Some of the modern soft decontamination processes are able to fulfil these requirements. As an example, the full-systems decontamination of the Belgian BR-3 PWR using the CORD process shall be mentioned here (Wille and Bertholdt, 1992; Massaut et al., 1994). As was shortly described in Section 4.5.3., the application of this decontamination step resulted in a pronounced reduction of the radiation dose rates and, as a consequence, in a considerable saving of radiation exposure to the personnel carrying out the dismantling work. In addition, the surfaces of the circuits as well as of the reactor vessel internals were remakably clean, which facilitated the subsequent dismantling operations.

Besides the metallic structures of the circuits and components, nuclear power plants contain huge masses of concrete, a small fraction of which is activated and/or contaminated. In order to keep the resulting waste volumes as small as possible, the fraction which contains radionuclides has to be separated during dismantling from the non-radioactive bulk of the material; the techniques used for this will not be discussed in what follows. Likewise, decontamination of building walls and surfaces will not be treated here.

In the dismantling of the metallic structures and components of the plant, conventional as well as newly developed cutting techniques are applied; besides mechanical techniques, others such as plasma torch and laser cutting techniques are available. By using appropriate installations, uncontrolled dissemination of radioactive particles during this work can be reliably precluded. The subsequent treatment of the dismantled parts depends both on the level and on the state of the radionuclides associated with them.

The reactor pressure vessel and its internals are activated by neutrons during plant operation. This means that the radionuclides associated with these parts cannot be isolated from the bulk of the material which, consequently, has to be treated entirely as radioactive waste. A significant fraction of it belongs to the category of medium-active materials and, therefore, at least a part of the cutting-down and packing actions has to be performed by using remote-controlled working techniques. The remainder of the material can be classified as low-active waste; whenever possible, its volume is reduced, e. g. by compacting.

The surface-contaminated materials which, during plant operation, were located outside the neutron field represent the largest fraction by far of the spent materials; even when a full-systems decontamination has been performed, residual contamination is still associated with these materials. In principle, they also have to be conditioned and finally disposed as radioactive waste. The same applies to components which were removed from the plant during a replacement action (such as PWR steam generator tube bundles or BWR recirculation piping). In order to further reduce the remaining contamination level, hard chemical decontamination methods can be applied, since materials compatibility of the solutions is not re-

quired in this context. Using a decontamination solution consisting of nitric acid, cerium (IV) and ozone (as a Ce(IV)-regenerating agent), steam generator tube bundles were cleaned at room temperature with a decontamination factor of about 4000 (Dubourg, 1994).

Even low residual activities on parts and components (in particular on those which were subjected to an initial full-system decontamination of the plant, see above) cause large expenses when the parts are finally disposed of as low-level radioactive waste. Therefore, attempts have been made to decontaminate the surfaces down to a residual activity level which would render possible the release of the parts from the controlled areas for unrestricted use as non-radioactive materials. Several decontamination techniques are available for this task, such as traditional steel descaling techniques using mineral acids, often supported by an ultrasonic treatment, in particular for components with a complex geometry. Bregani et al. (1994) have reported on the decontamination of a carbon steel line from a BWR (including valves, elbows and T joints) using a solution of formic acid plus hydrofluoric acid, supported by ultrasonic transducers which were directly applied to the external surface of the component. The residual activity levels were well below 0.3 Bq/cm^2, a factor of 4 to 10 lower than on components which were decontaminated without ultrasonic treatment. Soft chemical processes are also able to reach this goal; using the CORD process with increased oxalic acid concentration and simultaneous ultrasonic treatment, PWR components were cleaned down to a very low level of residual activity (Wille, 1994). As another example, using an electrochemical technique a large fraction of the contaminated materials from the Gundremmingen A plant was decontaminated down to a residual level which rendered feasible the subsequent unrestricted use of the materials.

However, when aiming at such low residual activity levels for free release of the materials, a main problem is the accurate and reliable measurement of the very low residual activity concentrations, necessary in order to not exceed the regulatory limits. In Germany, all primary and secondary waste arising from decommissioning measures at inspected and controlled areas in nuclear facilities is considered potentially radioactive and may not be dismissed from the respective areas. Only materials showing a contamination level of < 0.5 Bq/cm^2 (β, γ emitters) or a mass-related activity concentration of < 0.1 Bq/g are allowed to be released for free reuse or for normal disposal. In principle, such low activity levels can be accurately and reliably determined when high-energy γ emitters such as ^{60}Co are concerned; frequently, however, this task is complicated by the complex geometry of the parts to be measured as well as by heterogeneous distribution of the radionuclides on the surfaces. For these reasons, melting of the materials has gained in significance; the current state of the art of this topic has been recently summarized by Pflugrad and Hofman (1993). Melting of low-level radioactive scrap has several advantages: The volume is significantly reduced, a part of the radionuclides is tightly and homogeneously incorporated into the metal ingot and, finally, for some radionuclides an additional decontamination of the metal is achieved. The resulting metal ingots can be dismissed for use in a normal foundry, provided their mass-related activity concentration is < 1 Bq/g; at higher activity levels, they can be recycled for use in

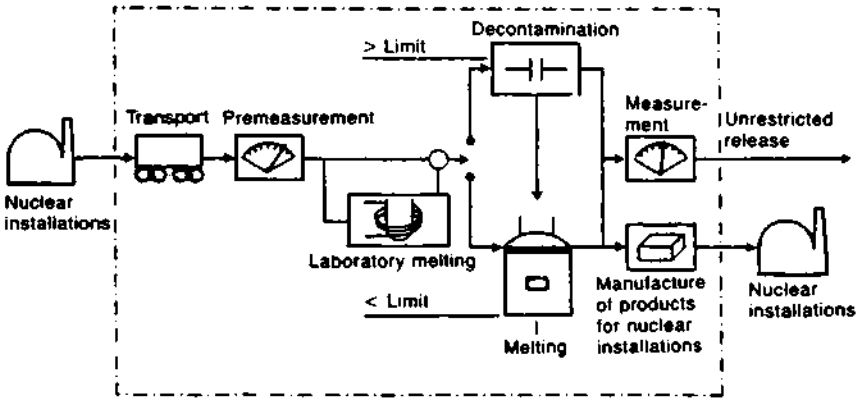

Figure 4.57. Treatment of contaminated metal scrap from nuclear installations (Gräbener et al., 1990; with kind permission from Elsevier Science S.A., P.O. Box 564, 1001 Lausanne, Switzerland)

nuclear facilities (e. g. as shielding walls and doors, as transport or storage containers for radioactive waste) or they can be finally disposed of in a space-saving manner.

The different steps in the process of recycling metallic scrap from nuclear installations can be seen from the schematic diagram shown in Fig. 4.57. (according to Gräbener et al., 1990). The behavior of the radionuclides in the melting process was thoroughly examined prior to the industrial application of this technique, as has been reported on e. g. by Haas et al. (1995). According to these results, which have been completely confirmed in the industrial-scale applications (see Table 4.17.), ^{60}Co is virtually homogeneously incorporated into the metal ingot during the melting of steel, with only very small fractions being transported into the slag; the same behavior applies to the radioisotopes of other alloying elements such as ^{55}Fe, ^{54}Mn, ^{59}Ni, ^{63}Ni (Schuster and Haas, 1990; Feaugas et al., 1994). Strontium isotopes are released to the slag during the melting process (Schuster and Haas,

Table 4.17. Comparison of decontamination factors measured in laboratory and in industrial-scale steel melting
(according to Haas et al., 1995)

Nuclide	Laboratory-scale	Industrial-scale
^{60}Co	~ 1	~ 1
^{63}Ni	~ 1	~ 1
^{90}Sr	10 to 1000	~ 30
^{134}Cs, ^{137}Cs	17 to > 50	> 100
^{235}U, ^{238}U	10 to 230	~ 100
$^{239/240}Pu$	30 to 160	~ 100
^{241}Am	~ 100	~ 100

1990), while ^{137}Cs is almost completely transported to the dust (Feaugas et al., 1994). Consequently, the slag and dust formed in the process have to be monitored with respect to their radionuclide content and, in the case of higher concentrations, they have to be treated as radioactive waste; however, their mass usually accounts for only 5 to 10% of the initial mass of steel. Currently, the melting of steel in specially designed installations (meeting the standards of controlled or inspected areas) is an industrial technique in a number of countries and has proven to be a powerful tool in the efforts to reduce the space required for final disposal of radioactive waste.

Other combinations of radionuclides and materials can also be treated by the melting process. Tritium present in steels originating from D_2O-moderated reactors or gas-cooled high-temperature reactors is completely released as HTO or DTO and can be trapped in appropriate filter devices (Holland et al., 1994). Uranium contamination on steel parts as well as transuranium isotopes can be removed with a high decontamination factor (Gräbener, 1994); however, when measuring the residual α activity, one has to remember that steels are usually preloaded with a natural uranium content on the order of 1 ppm, potentially confusing the decisive activity measurement of parts to be dismissed for unrestricted use. Finally, the melting of aluminium (using addition of salts as cleaning agents) and copper results in decontamination factors of ~10, rendering feasible the recycling of these materials as well (Gräbener, 1994).

In order to make a decision as to the further disposition of the low-level materials to be dismissed from the nuclear plants, or of the molten metal ingots, decisive activity measurements have to be performed. As was mentioned above, measurement of high-energy gamma emitters such as ^{60}Co can be easily and accurately performed, but the low-energy radionuclides such as ^{55}Fe, ^{59}Ni, ^{63}Ni, and transuranium isotopes which are potentially present in the specimens pose serious problems when the measurements have to be conducted so as to ensure a high throughput of the materials. The activity of these low-energy radionuclides can be measured to sufficiently low detection limits, when adequate detectors are used, such as large-area proportional counters for materials of plane or slightly bent geometries and specially-shaped proportional counters for tubes and structural materials (e. g. Hoffmann and Leidenberger, 1991). However, since these radionuclides are of minor radiological relevance, their explicit measurement is not necessary even if their abundance in the contamination layers is comparatively high. Instead, in order to account for the low-energy radionuclides as well, a "fingerprint" method is often applied by which the measured ^{60}Co activity or the total γ activity is corrected for the contributions of the difficult-to-measure nuclides. Since the activity ratios of these isotopes to each other and to ^{60}Co depend on several parameters (type of plant, type of materials used in the plant, operation history of the plant, time interval between shutdown of the plant and dismantling), these ratios have to be first determined experimentally using both γ spectrometry and methods of radiochemical analysis (see for example Schuster and Haas, 1990); during the measurement work the ratios have to be re-determined at regular intervals in order to ensure continuing validity in different regions of the contaminated systems. When

these preconditions have been fulfilled, the activity measurements of the parts to be released can be performed by a total-gamma-activity measurement device, provided that α contamination is negligible (this applies to the structural materials of almost all light water reactors). Such a device can consist of a tunnel or a box whose walls are equipped with large-area liquid or plastic scintillator detectors. Appropriate shielding on the outside of the measuring chamber keeps out interfering background radiation (e. g. Küchler et al., 1994). Calculation of the ^{60}Co equivalent of the specimens from the measured count rates (including the activities of the difficult-to-measure radionuclides using the standard nuclide vectors previously determined) and the calibration data of the arrangement are performed with the help of specially written computer software. With such an installation, decisive release measurements of large-sized specimens can be carried out in short measuring times (about 60 seconds each).

References Section 4.5

Anonymous: Applying the NS-1 solvent to the complete primary system of a BWR. Nucl. Engng. Internat. **1985**, (November), 33–35

Arvesen, J.: Decontamination of pressurized water reactors. European Patent Specification 0 174 317 B.1 (30.11.1988)

Asay, R. H.: Pretreatmant of primary system components using preoxidation. Proc. 5. BNES Conf. Water Chemistry of Nuclear Reactor Systems, Bournemouth, UK, 1989, Vol. 1, p. 313–314

Aspden, R. G., Grand, T. F.: PWR full-reactor coolant system decontamination. Materials evaluation after three cycles of exposure to the LOMI decontamination process. Report EPRI NP-7512-M (1991)

Ayres, J. A.: Decontamination of nuclear reactors and equipment. New York, Roland Press Inc., 1970

Bertholdt, H.-O., Wille, H.: Field experience with full system decontamination at Oskarshamn 1 and Loviisa 2 with the CORD/UV process. Paper presented at the Suppliers Seminar during the European Nuclear Conf. ENC '94, Lyon, France, 1994

Blok, J.: Recontamination and passivation. Paper ANS Executive Conf. Decontamination of Power Reactors: The Costs, Benefits and Consequences. Springfield, Ma., 1984

Bradbury, D., Elder, G. R., Hendawi, A., Waite, M., Wood, C. J.: Decontamination waste volume reduction by the ELOMIX process. Proc. 6. BNES Conf. Water Chemistry of Nuclear Reactor Systems, Bournemouth, UK, 1992, Vol. 2, p. 168–175

Bregani, F., Colafato, R., DellaNotte, A., DeCanditiis, L., Borroni, P., Pinacci, P.: Decontamination of complex components using ultrasounds and flowing chemicals. Proc. CEC 3. Internat. Conf. on Decommissioning of Nuclear Installations, Luxembourg 1994, p. 293–301

Bridle, D. A., Bird, E. J., Mitchell, C. R.: Cobalt deposition in oxide films on reactor pipework. Report EPRI NP-4499 (1986)

Dubourg, M.: In situ hard chemical decontamination of a tube bundle from a removed PWR steam generator. Proc. CEC 3. Internat. Conf. on Decommissioning of Nuclear Installations, Luxembourg 1994, p. 353–364

Duce, S. W.: Effectiveness and safety aspects of selected decontamination methods for LWRs – "Recontamination experience 1988". Nucl. Engng. and Design **118**, 487–496 (1990)

Eickelpasch, N., Steiner, H., Fischer, A.: Pilot dismantling of the KRB A boiling water reactor. Proc. CEC 3. Internat. Conf. on Decommisioning of Nuclear Installations, Luxembourg 1994, p. 40–52

Feaugas, J., Laplante, D., Puechlong, Y., Barbusse, J. R.: Experience with melting beta and gamma contaminated materials. Proc. CEC 3. Internat. Conf. on Decommissioning of Nuclear Installations. Luxembourg 1994, p. 410–421

Ferrett, D. J., Lister, D. H.: Experience with whole system decontamination including fuel. Paper ANS Executive Conf. Decontamination of Power Reactors: The Costs, Benefits and Consequences, Springfield, Mass., 1984

Gräbener, K.-H.: Melting and recycling of contaminated (α, β and γ) aluminium, copper and steel. Proc. CEC 3. Internat. Conf. on Decommissioning of Nuclear Installations, Luxembourg, 1994, p. 433–445

Gräbener, K.-H., von Koch, C., Nickel, W.: Volume reduction, treatment and recycling of radioactive waste. Nucl. Engng. and Design **118**, 115–122 (1990)

Gregoire, M., Noel, D., Roofthooft, R., Wolters, F.: Optimisation and application of EdF-EMMA process in decontamination of primary pumps for pressurized water reactors. Proc. 5. BNES Conf. Water Chemistry of Nuclear Reactor Systems, Bournemouth, UK, 1989, Vol. 2, p. 117–121

Haas, E. W., Gräbener, K.-H., Neudert, N., Hofmann, R.: Labortechnische Entwicklung der Schmelzdekontamination von Eisen- und Nichteisenmetallen. Proc. KONTEC Conf., Hamburg, Germany, 1995, p. 345–366

Heess, W., Schenker, E., Petzold, G., Conrath, A., Diewald, H. P.: Dekontamination von Hauptkühlmittelpumpen mit dem neuen VS-Verfahren. Atomwirtschaft **34**, 83–86 (1989)

Hoffmann, R., Leidenberger, B.: Optimization of measurement techniques for very low level radioactive waste material. Report EUR 13307 EN (1991)

Holland, D., Sappok, M., Seidler, M.: Behaviour and removal of tritium in the industrial-scale melting of steel from nuclear installations. Proc. CEC 3. Internat. Conf. on Decommissioning of Nuclear Installations, Luxembourg, 1994, p. 422–432

Holmberg, K. E., Aittola, J. P., Arvesen, J., Hermansson, H. P.: Pretreatment of organic decontamination waste for solidification in bitumen and concrete. Proc. 3. BNES Conf. Water Chemistry of Nuclear Reactor Systems, Bournemouth, UK, 1983, Vol. 1, p. 353–358

IAEA (International Atomic Energy Agency) (a): Decontamination of water cooled reactors. Technical Reports Series No. 365 (1994)

IAEA (International Atomic Energy Agency) (b): Decommissioning techniques for research reactors. Technical Reports Series No. 373 (1994)

Küchler, L., Auler, I., Günther, H.: Further development and operation of an automatic large-scale activity measurement facility for low-level decommissioning waste. Proc. CEC 3. Internat. Conf. on Decommissioning of Nuclear Installations, Luxembourg 1994, p. 271–281

Lambert, I., Brunet, S., Roy, M., Gerlinger, Ph.: Chemical decontamination process for PWR primary circuits. Proc. 5. BNES Conf. Water Chemistry of Nuclear Reactor Systems, Bournemouth, UK, 1989, Vol. 1, p. 321–322

LeSurf, J. E.: Control of radiation exposures at CANDU nuclear power stations. J. British Nucl. Energy Soc. **16**, (1), 53–61 (1977)

LeSurf, J. E., Smee, J. L., Beaman, T. A.: Recontamination following dilute chemical decontamination. Proc. 3. BNES Conf. Water Chemistry of Nuclear Reactor Systems, Bournemouth, UK, 1983, Vol. 1, p. 213–218

Leuchte, H. W., Stenersen, F., Steringer, A.: Development and optimization of an easy-to-process electrolyte for electrochemical decontamination of stainless steel components. Proc. CEC 3. Internat. Conf. on Decommissioning of Nuclear Installations, Luxembourg 1994, p. 312–324

Massaut, V., Klein, M., Lefebvre, A., Scholl, K., Saumon, P., Roberts, P.: Pilot dismantling of the BR 3 pressurized water reactor. Proc. CEC 3. Internat. Conf. on Decommissioning of Nuclear Installations, Luxembourg 1994, p. 25–39

Murray, A. P., Eckhardt, D. A., Weisberg, S. L.: Dilute chemical decontamination process for PWR and BWR applications. Nucl. Technology **71**, 482–496 (1985)

Murray, A. P., Snyder, T. S.: European Patent Application 8510 1645.1 (15.2.1985)

O'Boyle, D. R., Walschot, F. W., Ocken, H., Wood, C. J.: Recent developments in full-system decontamination. Proc. 5. BNES Conf. Water Chemistry of Nuclear Reactor Systems, Bournemouth, UK, 1989, Vol. 1, p. 159–162

Ocken, H.: Radiation control to improve nuclear power plant availability. Proc. Internat. Conf. Nuclear Power Plant Aging, Availability Factor, and Reliability Analysis, San Diego, Calif., 1985, p. 593–600

Oliver, T. W., LeSurf, J. E.: Recent Pacific Nuclear decontamination experience. Proc. 5. BNES Conf. Water Chemistry of Nuclear Reactor Systems, Bournemouth, UK, 1989, Vol. 1, p. 169–173

Pashevich, V. I.: USSR experience in decontamination and water chemistry of VVER type nuclear reactors. Report IAEA-TECDOC-667 Coolant Technology of Water Cooled Reactors. Vol. 3: Activity Transport Mechanisms in Water Cooled Reactors. Vienna, 1992, p. 155–174

Pflugrad, K., Hofman, D. (editors): Proceedings of the Technical Seminar on Melting and Recycling of Metallic Waste Materials from Decommissioning of Nuclear Installations. Krefeld, Germany, 1993

Riess, R.: German experience including chemical, electropolishing and decontamination for decommissioning. Paper ANS Executive Conf. Decontamination of Power Reactors: The Costs, Benefits and Consequences. Springfield, Ma., 1984

Sasaki, T., Kobayashi, T., Wada, K.: Method and apparatus for regenerating an acid electrolyte that has been used in the decontamination of components with radioactively contaminated surfaces. European Patent Specification 0 141 590 B. 1 (30.1.1991)

Schenker, E., Buckley, D., Alder, H. P., Francioni, W., Heess, W., Conrath, A.: VS decontamination process. Proc. 5. BNES Conf. Water Chemistry of Nuclear Reactor Systems, Bournemouth, UK, 1989, Vol. 2, p. 186–187

Schuster, E., Haas, E. W.: Behaviour of actinides and other radionuclides that are difficult to measure in the melting of contaminated steel. Report EUR 12875 EN (1990)

Sellers, R. M.: The radiation chemistry of nuclear reactor decontaminating reagents. Radiat. Phys. Chem. **21**, 295–305 (1983)

Speranzini, R. A.: Decontamination effectiveness of mixtures of citric acid, oxalic acid and EDTA. Proc. 5. BNES Conf. Water Chemistry of Nuclear Reactor Systems, Bournemuth, UK, 1989, Vol. 1, p. 319–320

Swan, T., Segal, M. G., Comley, G. C. W., McLean, A. N., Remark, J. F.: UK development of decontamination reagents for water systems. Nuclear Europe **IV**, (9), 27–29 (1984)

Westerberg, K., Waltersten, T.: ELDECON – Electrochemical decontamination in low temperature neutral electrolyte. Proc. 5. BNES Conf. Water Chemistry of Nuclear Reactor Systems, Bournemouth, UK, 1989, Vol. 1, p. 191–195

Wille, H.: Assessment of decontamination procedures for VVER-PWRs for waste minimization. Proc. CEC 3. Internat. Conf. on Decommissioning of Nuclear Installations, Luxembourg 1994, p. 365–374

Wille, H., Bertholdt, H. O.: Recent developments in component and system decontamination. Proc. 5. BNES Conf. Water Chemistry of Nuclear Reactor Systems, Bournemouth, UK, 1989, Vol. 1, p. 163–167

Wille, H., Bertholdt, H.-O.: Concept and experience of system decontamination with CORD. Proc. 6. BNES Conf. Water Chemistry of Nuclear Reactor Systems, Bournemouth, UK, 1992, Vol. 2, p. 161–167

Wille, H., Sato, Y.: Field experience of chemical decontamination and waste reduction with the CORD process. Paper presented at the Internat. Conf. Chemistry in Water Reactors – Operating Experience and New Developments. Nice, France, 1994

Wood, C. J., Spalaris, C. N.: Sourcebook for chemical decontamination of nuclear power reactors. Report EPRI NP-6433 (1989)

Part C
Radiochemistry under the conditions of reactor accidents

5. General remarks

In all technical installations, malfunctioning or failure of systems or components may lead to an accident with more or less serious consequences for the plant, the staff and, possibly, the environment as well. This also applies to nuclear power plants. For this reason, from the beginning of nuclear power production extensive measures have been taken to preclude accidents or to reduce the probability and the consequences of an accident to a level well below that of other technical installations or of naturally occurring events. As a consequence of these efforts, nuclear power plants of an adequate design currently show the highest safety level among all types of electricity-generating facilities.

In the operation of nuclear power plants, undisturbed operation resulting in high plant availability is a very important feature. Besides maintaining conditions which ensure undisturbed operation, the modern safety concepts of nuclear power plants aim at a reliable confinement of the radionuclide inventory of the plant under all circumstances, during normal operation as well as under accident conditions. This goal is achieved by a multi-level system of safety measures such as is schematically shown in Fig. 5.1. for the KWU Konvoi design. On the first safety level, i. e. normal operation phases, high quality of all parts of the plant is achieved by extensive quality assurance measures, supported by in-depth training of the plant staff; these measures not only ensure a high degree of plant availability but keep to a minimum the demands made upon the safety installations. On the second safety level, deviations from normal operation conditions are counteracted (e. g. by power reduction), to prevent them from developing into dangerous situations; an important feature in this context are the inherent safety properties of light water reactors. On the third safety level, the safety installations of the plant are designed in such a manner that automatic start and reliable operation are ensured, to mitigate the consequences of any accident. Since these accident analyses are the basis for the design of countermeasures, they are called "design basis accidents". Nonetheless, in spite of these measures, the occurrence of a severe reactor accident cannot, of course, be ruled out with absolute certainty, even though it is extremely improbable. Advanced plant designs, therefore, are equipped with "beyond design basis accident" management measures forming a fourth level of defense, consisting

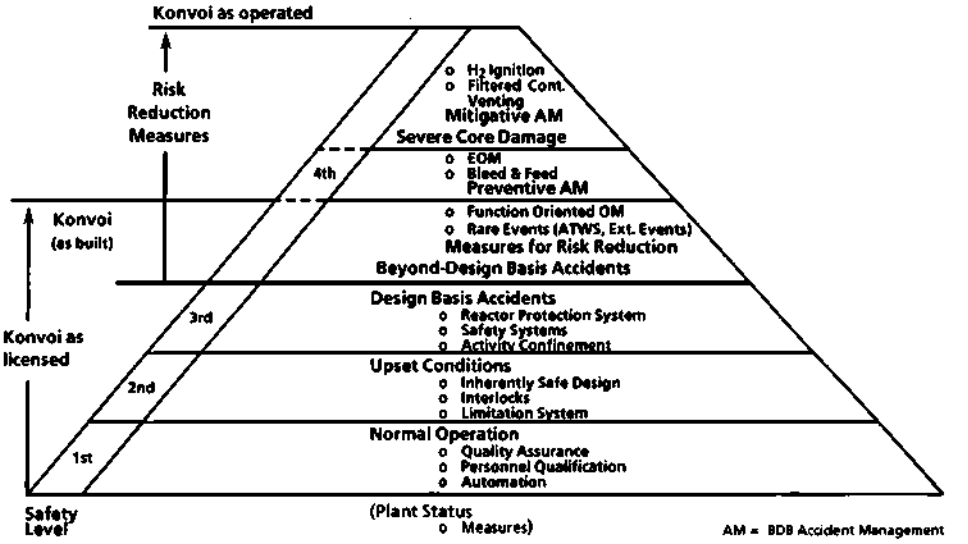

Figure 5.1. Multi level defense-in-depth safety concept (Fabian, 1995)

of measures which are able to prevent core damage and/or to mitigate the consequences of severe core damage.

The most serious consequence of a reactor accident would be the dissemination of radionuclides from the plant to the environment. In this context, the most important figure is the so-called "source term", which is the rate, amount and physico-chemical characteristics associated with the escape of a given radionuclide (in the first place fission product nuclides) from the plant in the event of an accident. The source term depends strongly on the assumed accident sequence and the prevailing conditions, but also on the design of the plant, in particular of its safety installations. Apart from these parameters, the source term is determined by the transport behavior of the radionuclides and, therefore, is greatly influenced by the chemical reactions the fission products undergo under the conditions prevailing during the accident and by the resulting chemical state of these radionuclides. Under the safety design of US and West-European nuclear power plants, only airborne radionuclides, aerosols as well as volatile and gaseous species, have the potential of escaping from the plant and reaching the environment. For this reason, formation of airborne radionuclide species by both physical means and by chemical reactions in the course of an accident deserves particular interest.

During an accident, many of the ambient conditions inside the reactor plant which are of relevance for fission product chemical reactions (such as temperatures, concentrations, redox properties, reaction partners) are fundamentally different from those prevailing during normal operation periods. As a consequence of these changed conditions (which, in addition, may be different for different accident scenarios), a specific behavior of the fission products will result. In order to evalu-

ate the consequences of a reactor accident, this behavior has to be known. In addition, the chemical reactions occurring under such abnormal conditions and the nature and the yields of their products are of great interest from a radiochemistry point of view. For these reasons, the behavior of the radionuclides under accident conditions will be treated in the following in greater detail than these postulated and very unlikely events of design basis accidents and, in particular, of severe accidents would strictly deserve.

Several accidents, including ones developing to severe core damage, have occurred in nuclear reactors, most of them in research and test reactors; one accident with considerable release of radionuclides to the environment occurred in a military plutonium production reactor (Windscale-1). Only two severe accidents have involved light-water cooled power reactors, those at Three Mile Island-2 and Chernobyl-4, with the design of the latter plant being representative of an only comparatively small number of plants and, in addition, not at all for light water reactors of Western design. This small number of events means that the evaluation of radionuclide source terms which might occur as a consequence of a reactor accident cannot be based on real experience alone, though highly valuable information can be obtained from the experience gained by the detailed investigation of these accidents. As an example, the behavior of the fission products in the TMI-2 accident has to be mentioned which, over the years following, strongly influenced reactor accident research and especially source term research in the direction of a more realistic approach. Because of the lack of experience with real reactor accidents, models have to be developed and applied which are based on postulated accident sequences established by systems analyses, on the one hand, and on data on fission product behavior determined by experiments and calculations, on the other. One has to recognize that the models and the corresponding analyses and experiments always describe one specific accident sequence and, therefore, this must be the sequence which covers all the effects the other sequences will involve.

With the sole exception of the noble gases, during reactor normal operation as well as in the course of reactor accidents, all the fission products are subjected to chemical reactions which govern their transport and behavior. These reactions have to be taken into account, therefore, when the release of fission products in anticipated accidents is calculated. However, chemical reactions and physical phenomena to be expected under the conditions of reactor accidents, as well as the resulting products, are only accessible for theoretical calculations in a very global manner. For this reason, experiments are needed at least to validate the theoretical results or, in many cases, to get an idea on the possible reaction mechanisms. The planning and performance of such experiments and the interpretation of the results obtained will pose some problems which have to be taken into consideration before the work is begun.

Experiments on a laboratory scale are best suited for the investigation of basic phenomena. They are intended to provide a fundamental understanding and result in data with a high accuracy and reliability for specific chemical reactions; in the case of doubt, such experiments can be easily repeated in order to rule out errone-

ous results. On the other hand, it is often very difficult to transfer the results obtained with limited volumes under well-defined clean laboratory conditions to the real reactor dimensions, with the main reasons being complicating side reactions, large differences in the volume-to-wall ratio and other parameters. Large-scale experiments, on the other hand, are very expensive and, therefore, they are frequently limited to one single trial. The only meaningful way to obtain reliable data, therefore, consists in conducting measurements to acquire the required basic data in laboratory experiments, evaluating the influence of potentially disturbing effects in a technical-scale experiment and, finally, simulating the whole (or nearly the whole) accident sequence by an integral experiment. Thermohydraulic parameters prevailing during the accident play an important role in the specification of the experiment and, therefore, have to be known as detailed as possible in advance.

Whatever effort might be put into the planning and realization of the experiments, there will be a remainder of uncertainty in the final results which has to be compensated for by a conservative evaluation in a radionuclide behavior and release model. The problem with using a conservative evaluation is, of course, that very often the magnitude of the gap between the conservative assumption and the situation occurring in reality is not known. Conservative models, therefore, should always be accompanied by a best-estimate evaluation which is based on a critical analysis of all known data, including phenomena known from basic physics and chemistry.

When analyzing the behavior of radionuclides in reactor accidents, one has to distinguish between so-called design basis accidents and accidents with further-reaching consequences. The term "design basis accident" is used to describe accident conditions a nuclear power plant has to be designed to withstand according to established deterministic design criteria, so that radionuclide releases do not exceed the limits set down in state regulations; they are an established part of the licensing requirements. Beyond design basis accidents, on the other hand, may result in plant states worse than the above-mentioned accident conditions, including those causing significant degradation of the reactor core. Both types of accident include specific conditions which will influence the chemistry and the behavior of the radionuclides. The design basis accidents and, in particular, chemical reactions and radionuclide behavior occurring in the course of them will be treated in Chapter 6; radionuclide behavior in the course of degrading core accidents will be discussed in Chapter 7.

References Chapter 5

Fabian, H.: Accident management (AM) – Background and implementation in German PWRs and BWRs. Paper presented at the Internat. ENS Topical Meeting Safety of Operating Nuclear Power Plants "ENS TOPSAFE '95", Budapest, Hungary, 1995

6. Design basis accidents

6.1 General aspects

Legal regulations in the different countries require that nuclear power plants, like other nuclear installations, be licensed and allowed to start operation only when appropriate precautions against possible hazards to the environment have been taken. In the Federal Republic of Germany, this general requirement was put in concrete terms in § 28, Sect. 3 of the "Strahlenschutzverordnung" (Radiation Protection Ordinance). Here the maximum radiation exposures to the population in the area surrounding the plant are laid down, which are permissible in the event of a nuclear accident (Störfallplanungswerte). The safety design of the plant has to guarantee that these levels not be exceeded even as the consequence of an accident; compliance with this requirement has to be demonstrated by accident consequence analyses using a methodology which is established by the state safety authorities.

The evaluation of possible radionuclide releases occurring as a consequence of a nuclear accident necessitates a detailed definition of the accident sequence and of the conditions prevailing at different stages of the accident under consideration. The general assumption of a loss-of-coolant accident (LOCA) as it was defined in the early years of nuclear reactor technology in the USA by the USAEC (1974) relates exclusively to one single accident sequence and, due to its incomplete specification, is not sufficiently detailed to permit a well-founded analysis of the behavior of the radionuclides. As a result, the US Nuclear Regulatory Commission (NRC) created the concept of design basis accidents which "are a set of accidents which have been chosen to envelop the anticipated worst credible conditions in what was perceived to be a very conservative manner. Thus these accidents are not representative of expected or realistic conditions but have been judged to bound any credible accident" (Pasedag et al., 1981). Similarly, in the German "Störfall-Leitlinien" (Accident Guidelines) for PWRs, which were issued by the Federal Ministry of the Interior (BMI, 1983), a larger number of possible design basis accidents was defined, eight of which were declared to be radiologically representative, i. e. covering the other accident sequences with regard to the release of radionuclides from the systems and to the environment. These representative accidents comprise the following scenarios, with each of them referring to both the origin of radioactivity and the initiating event:

- Break of a main coolant pipe
- Break of a transducer line containing primary coolant under system pressure
- Break of a main steam pipe downstream from the outer isolation valve with simultaneous damage of steam generator heating tubes
- Long-term failure of the ultimate heat sink during operational leakages of steam generator heating tubes
- Break of a pipe in the off-gas system
- Damage of a fuel assembly during handling in the spent fuel pool (e. g. during refuelling)

- Leakage of a tank containing radioactively contaminated water
- Effects of an earthquake on the reactor auxiliary building.

The basic data to be used in calculating the accident consequences as regards the transport and behavior of the fission products were laid down in the "Störfall-Berechnungsgrundlagen" (Technical Basis for the Assessment of Reactor Accidents), issued by the German RSK/SSK (1983). In other countries where nuclear power plants are operated, comparable regulations have been issued. As concerns the radiation exposure of the public which might result from such a design basis accident, in Germany (in contrast with the other countries) ingestion of radionuclides with the food (including potential enrichment in the food chain) and its radiological consequences also has to be taken into consideration in the calculations.

For BWRs, the radiologically representative design basis accidents have not been defined as precisely as for PWRs. However, the possible events are phenomenologically quite similar (with the exception of the steam generator tube rupture accident, which does not apply for BWRs) and there are no significant differences to be expected in radionuclide behavior. Consequently, equivalent requirements are applied to the design of both PWR and BWR plants. This means that in most cases the radiochemistry principles discussed in what follows will apply mutatis mutandis to boiling water reactors as well. In the event of a loss-of-coolant accident, the BWR pressure suppression pool represents an effective retention system; the behavior of the fission products in this pool will be discussed in Section 7.3.2.4.

With regard to their behavior during a design basis accident, the fission products can be classified into three groups. First, the fission product noble gases have to be mentioned, which are only poorly soluble in water and do not enter into any chemical reactions with other substances. This means that upon release from failed fuel rods they will be almost quantitatively transported from the reactor core and the primary circuit to the containment atmosphere. The second category includes the volatile fission products such as iodine and cesium isotopes; among these elements, fission product iodine shows a highly complex behavior resulting from its potential to form both volatile as well as poorly volatile species, with its partitioning between the different species depending on the prevailing conditions. Finally, as the third category, the other fission products and the activation products originating from the fuel as well as from the structural materials in the reactor core exhibit extremely low vapor pressures at the temperatures inside as well as outside the reactor pressure vessel; they will, therefore, be transported predominantly as aerosols to the sump water phase which is formed in the containment in the course of the accident. Regarding the radiotoxicity of the radionuclides, iodine and cesium isotopes are of greatest importance among those fission products that are released from the reactor core to a significant extent. Iodine particularly is subject to chemical reactions that can influence its transport; therefore, chemical reactions and their products are of considerable interest in the analysis of the behavior of radiologically important fission products.

The main sources of information used as a basis for evaluating fission product behavior are experimental investigations, both in the laboratory and on a technical

scale, measurements at operating nuclear reactors and, finally, theoretical studies using thermodynamic and kinetic calculations. However, the thermodynamic data base for higher temperatures as well as at very small concentrations of a given element, when there is a large excess of other constituents, is generally scanty and calculations using extrapolated data are often questionable. Basically, data obtained from measurements at reactor plants, in particular from off-normal situations, would be most reliable; however, the extremely small number of relevant accidents which have happened until now has provided only a limited amount of data. As has been mentioned above, laboratory experiments are a highly useful tool for obtaining basic data on reaction mechanisms which can subsequently be applied in theoretical calculations. In order to take into account the effects of the dimensions of the actual systems on the progress of the reactions, technical-scale experiments are needed to validate the laboratory and theoretical results; finally, in integral experiments the different stages of a complex accident sequence can be studied. Thus, the data to be used in fission product behavior analyses have to be obtained from all the sources mentioned above, using a meaningful and economic selection and combination.

In the following sections, the current state of knowledge of the behavior of fission products under the conditions prevailing during different design basis accidents will be discussed. The related experimental and theoretical investigations will be described and, as far as possible, conclusions as to the behavior and transport of the radionuclides will be derived from them.

6.2 Specific accident sequences in design basis accidents

6.2.1 Break in a main coolant pipe

Among the postulated loss-of-coolant accidents, different event sequences are assumed depending on the size of the leak through which primary coolant may escape from the primary circuit. In the event of breaks of small pipes up to a diameter of approximately 10 mm, the resulting coolant loss is compensated for by coolant feed from the chemical and volume control system, so that a normal shutdown of the reactor can be carried out. As a consequence of a medium-sized break (which includes the largest pipe diameters directly connected to the main coolant piping), a reactor trip will occur and, as far as is necessary, the high-pressure injection system will start operation, feeding borated water into the reactor pressure vessel. Following such pipe breaks, the reactor core will be kept flooded and sufficiently cooled; as a result, no fuel rod damage will occur. The fraction of coolant which escapes from the leak is released to the containment together with the radionuclides present at that moment in the escaping primary coolant volume. The consequences of small and medium-sized breaks with regard to radionuclide transport will not be discussed in detail in the following, since they are covered by the large break

scenario. The assumed sequences of large-break loss-of-coolant accidents in PWRs of different design currently in operation in Europe have been described by Stephenson et al. (1992), who also gave an assessment of the behavior of fission products and their release from the plant.

This accident scenario, the sudden break of a main coolant pipe, is the only one among the design basis accidents during the course of which a failure of fuel rods in the reactor core is postulated. In this scenario it is assumed that such a pipe, which has a diameter of about 750 mm and serves as the pathway for the 326 °C, 15.8 MPa primary coolant from the reactor pressure vessel to the steam generator and back to the reactor pressure vessel, breaks suddenly in such a manner that the double cross section of the pipe becomes available as a discharge area for the primary coolant (2A break). In most of the accident sequence analyses it is assumed that the break of the main coolant pipe will happen in its cold leg, i. e. in the section leading from the steam generator to the reactor pressure vessel (since this is the most conservative assumption, in particular in plants with only cold-leg injection of the emergency coolant) and that a simultaneous loss of off-site power has to be taken into consideration. This assumption of a sudden break of the main coolant pipe is a highly conservative one; due to the materials used, as well the design and the quality assurance measures employed in the construction of the primary circuit, such a sudden guillotine break can in practice be ruled out. Nevertheless, it is assumed that as a consequence of such a break the primary coolant will be flashed very rapidly out of the primary circuit as a two-phase water–steam mixture in a time interval of about 25 seconds; this blowdown phase covers the period from the moment of the break until the pressure in the primary circuit has reached approximately the same level as that in the atmosphere of the primary containment. About 1 second after the break, the fall in pressure in the reactor coolant system generates signals to initiate a reactor trip as well as the start of the safety injection system and, simultaneously, the isolation of the containment, i. e. the closing of all penetrations through the containment steel shell.

The time period which follows the start of operation of the safety injection systems, during which emergency coolant solution is fed into the reactor pressure vessel, is usually divided into several distinct phases. The refill phase lasts until the rising water level in the reactor pressure vessel reaches the bottom of the active core; the following reflood phase continues until the reactor core is completely recovered by emergency coolant. In plant designs with only cold-leg injection of the emergency coolant, the maximum level of temperature of the fuel rod claddings will typically be attained before the core has filled to mid-core height, which will be the case no later than 300 to 500 seconds after the onset of the accident. In KWU designs, which have both cold- and hot-leg injection of the emergency core coolant, reflooding is complete after 120 seconds, with correspondingly lower maximum temperatures of the fuel rod claddings. After the core has been quenched, the safety injection pumps continue to deliver cold borated water and to further reduce the temperatures of the fuel and cladding. In designs where injection is only into the cold legs, a part of the injected water will bypass the core and the water in the core will continue to boil (in this design, boiling does not occur after a hot-leg break) until one of the pumps has been realigned to inject water into the hot

leg. When a low water level is reached in the refuelling water storage tank, the suction for the emergency core cooling pumps is switched over to the containment sump water which has formed in the meantime. This is the start of the recirculation phase, which may last for a longer period of time; during this phase, the reactor core is in a safely cooled state.

As was described above, following the coolant loss the reactor core will be partly uncovered for a short period of time; for this reason, it has to be assumed in the accident analyses that a number of fuel rods will fail. Whether or not the cladding of any fuel rod will become defective depends on several parameters such as the design of the fuel rod, the properties of the cladding material, the temperature transient and pressure differential the cladding experiences, as well as any phenomena which may affect the embrittlement, strength and thickness of the fuel cladding. For this reason, different numbers of failed fuel rods are postulated in the guidelines in different countries. In the German "Störfall-Berechnungsgrundlagen" it is assumed that during the time the reactor core is uncovered, some of the fuel rods showing the highest heat ratings will reach temperatures that will lead the cladding to burst; it was postulated that 10% of the fuel rods in the reactor core will fail. It has to be strongly emphasized that, according to best-estimate calculations, the rapid refill of the reactor pressure vessel in KWU-type PWRs in which the emergency core cooling systems are designed to feed the coolant to the cold-leg as well as to the hot-leg part of the reactor pressure vessel, will keep the fuel rod temperatures low enough so that no damage to them is to be expected. In other countries, a 100% fuel rod failure is postulated in PWRs provided with only a cold-leg injection of the emergency coolant. Generally, it is assumed that some of the most highly stressed fuel rods will fail during the blowdown phase of the accident; however, the probability of fuel rod failure is higher during the following refill and reflood phases.

Fission products will be released from the failed fuel rods to the reactor pressure vessel. This release can occur in two phases. The first one occurs when the cladding fails (burst release). Independent of the particular temperature which is assumed to effect a cladding failure, it can be assumed that at this moment a fraction of the fuel rod gap inventory of fission product iodine and cesium will be in the gaseous state prior to cladding rupture. This fraction of the fission products (fission product noble gases as well as volatile elements) is released into overheated steam, which carries them to the atmosphere of the primary containment via the break. Along this way, the fission product noble gases will remain in the gaseous phase, but the vapors released in the "dry" phase, such as CsI and CsOH, will condense. These are both hygroscopic compounds which will either form nuclei for condensation droplets or become dissolved in the blowdown aerosol or in the water covering the wet surfaces of the containment. The second release phase will occur later on when the reactor core is recovering and the fuel in the failed rods comes into direct contact with the liquid emergency coolant at or below its boiling temperature, depending on the design of the plant (leaching phase). At this time, there might be a release of non-gaseous fission products into the reflood water which will carry the radionuclides through the break in the main coolant pipe into the containment sump. Fission products which are released during this phase will reach the atmo-

sphere of the primary containment only if they partition from the liquid into the gas phase.

The basic number for calculation of the amount of radionuclides released from the failed fuel rods during both these phases is the fission product inventory in the reactor core, which depends on the time within the fuel cycle at which the accident is assumed to occur. From the point of view of calculating the inventory, the end of an equilibrium fuel cycle, just prior to refuelling, is the most unfavorable moment. However, due to the short time interval until the core is covered again by the emergency coolant (refill and reflood phases), the fuel rod claddings do not reach temperatures exceeding 1000 °C. As a consequence of these comparatively low temperatures, diffusion of fission products from the fuel matrix will not take place to a significant extent. For this reason, only those fission products which during the preceding constant-load operation were present in the fuel pellet – cladding gap will have the potential of escaping from the failed fuel rods to the primary system. Thus, the magnitude of the gap inventory in intact fuel rods is also an essential figure in the evaluation of fission product release during an accident.

In different countries, different assumptions are made as to the amount of radioactivity that will be released from the failed fuel rods and as to the time this release will take place (dry phase or dry and wet phases). In the German "Störfall-Berechnungsgrundlagen" it is postulated that from the failed rods, 10% of their fission product noble gas inventory, 1% of the fission product halogen and alkali metal inventories and 0.01% of the non-volatile fission product inventory will be liberated during the burst phase. From these amounts, 100% of the fission gases, 10% of the halogens and alkali metals and 1% of the other fission products will directly reach the containment atmosphere to be homogeneously distributed there. The remaining 90% of the halogens and alkalis as well as 99% of the other solid fission products released from the failed fuel rods during the dry phase are assumed to be washed down to the reactor pressure vessel by the hot-leg injection emergency coolant and to be subsequently transported directly to the containment sump without becoming airborne. During the following leaching phase, 5% of the halogen and alkali metal inventories and 0.5% of the other fission products are assumed to be released in the dissolved state from the failed fuel rods to the coolant. With regard to the behavior of fission product iodine, a partition equilibrium is assumed to become established between sump water and containment atmosphere within 7 hours, resulting in a volume-related partition coefficient of 10^4.

The overwhelming fraction of the fission products released from the fuel rods to the primary circuit will leave the primary system via the break and enter the containment building regions, but in a different manner. The fission products already present in the primary coolant during the preceding operation phase and which originated from operationally failed fuel rods, will be transported together with the flashing water–steam mixture. However, since their amount is small compared to the assumed releases occurring during the burst phase, and since the spiking phenomenon discussed in Section 4.3.2.2. will contribute to the leaching phase only, these contributions will not be treated in detail. The radionuclides released from the fuel rods during the following burst phase will be transported by an almost pure steam atmosphere; finally, the fission products leached from the

failed fuel rods are dissolved in a liquid phase at a temperature at or well below the boiling point. As was mentioned above, within the containment the fission products are distributed between sump water and atmosphere; since only the latter fraction will have the potential of escaping to the environment, the behavior of the airborne fraction of the radionuclides is of highest interest.

In the course of a loss-of-coolant accident, hydrogen is produced by different reactions. Besides the possible impact of hydrogen–air reactions on the integrity of the containment, basically the presence of H_2 in the steam and later on in the containment atmosphere may influence the chemical state of various fission products, in particular that of iodine. According to the summary paper of Odar (1983), the most important contributions to total hydrogen production are due to the steam–Zircaloy reaction and to the radiation-induced decomposition of water. The steam–Zircaloy reaction starts when the temperature of the fuel rod claddings exceeds 900 °C; because of the short period during which the reactor core is uncovered, even conservative calculations come to the result that only about 0.3% of the Zircaloy inventory of the reactor core will be oxidized by steam, leading to an amount of hydrogen that will cause a volume-related H_2 concentration in the containment free volume of about 0.06% (assuming complete homogenization). While this reaction only proceeds during the burst and refill phases, the radiolytic production is a process which feeds H_2 to the containment atmosphere over a longer period of time. Two different mechanisms have to be distinguished here: core radiolysis affecting the emergency coolant volume present in the reactor pressure vessel, and sump water radiolysis caused by the fission products transported to the containment sump. Using the conservative $G(H_2)$ value of pure water of 0.44 and not considering possible recombination reactions, the amount of H_2 produced by the two mechanisms under the conditions prevailing in a KWU-type 1300 MWe PWR reaches about a 1% concentration in the free volume of the containment 10 days following accident initiation and about 3% after 100 days; in these calculations a homogeneous distribution was assumed and no countermeasures (such as the action of hydrogen recombiners) were taken into account. Other possible reactions producing hydrogen, such as water radiolysis in the spent fuel pool and metal–water reactions on the surfaces of the containment, will only generate small amounts of hydrogen, which means they can be neglected here. In total, the resulting hydrogen concentration in the containment is expected to remain well below the lower ignition limits of hydrogen–air mixtures (4% H_2); likewise, their impact on the chemical behavior of the fission products in the containment can be assumed to be negligibly small, quite in contrast to the situation in a severe reactor accident (see Section 7.).

6.2.1.1 The release of fission products from failed fuel rods to the primary circuit

As was discussed above, the release of fission products from the fuel rods which failed during the burst, refill and reflood phases of the loss-of-coolant design basis accident is limited to their gap inventories; due to the comparatively low maximum

temperatures and the short period when the reactor core is uncovered, no significant diffusion of fission products out of the fuel pellet matrix can occur. In addition, it has to be assumed that only a fraction of this gap inventory will have the possibility of escaping from the failed fuel rod. The fuel pellet – cladding gap in a commercial fuel rod represents a long and very narrow pathway for fission product transport; therefore, among other parameters, the extent of release depends on the geometry of the gap and on the size (and potentially the location) of the defect, which means that it is mainly a question of kinetics. For this reason, theoretical calculations cannot be expected to yield well-founded results on the released fraction of the gap inventory and trustworthy results can only be obtained by appropriate experiments.

From the early years of nuclear reactor technology on a great number of experiments has been carried out in which irradiated fuels have been heated to temperatures well above the operational level in order to learn more about the fission product behavior under such conditions. The most detailed studies in this field were conducted in the framework of the Reactor Safety Program of the Oak Ridge National Laboratory (ORNL), and focused both on conditions that occur in design basis accidents and in core melt scenarios. The principal objectives of these studies have been to determine the quantity of radiologically significant fission products released from defective fuel rods under accident conditions, to identify their chemical and physical forms and to interpret the results for use as an input to computer models of fission product behavior in loss-of-coolant accidents. The conditions these experiments were conducted under, as well as their results, have been described in numerous reports and, as far as they are related to design basis accidents, have been summarized by Lorenz et al. (1980 a; 1981) and, more recently, Collins et al. (1988); release experiments performed at higher temperatures under conditions prevailing in reactor accidents involving severe core damage will be discussed in Section 7.

The experimental setup used in the ORNL experiments conducted under design basis accident conditions is schematically shown in Fig. 6.1. The fuel rod specimens used in the experiments consisted of segments of approximately 30 cm length, encapsulated in Zircaloy claddings and fabricated from normal fuel rods that had been previously employed in commercial PWRs as well as in BWRs to burnup levels on the order of 30 MWd/kg U. These segments were inserted into the furnace which is located inside a hot cell, and were heated to temperatures between 500 and 1300 °C in a flowing helium–steam–hydrogen atmosphere. The fission products volatilized upon failure of the segment cladding were transported by the gas flow from the furnace zone to a thermal gradient tube which covered a temperature range from 850 to 150 °C and in which volatile species were plated out according to their condensation temperatures. In order to retain those fission products which were not condensed in the thermal gradient tube, aerosol filters and charcoal filters kept at room temperature and at liquid nitrogen temperature, respectively, were installed at the end of the analytical duct. After termination of the experiment, the experimental setup was disassembled, the thermal gradient tube was at first scanned by a gamma spectrometry device, then the deposited substances were leached in sections from the tube wall for the determination of radionuclides which

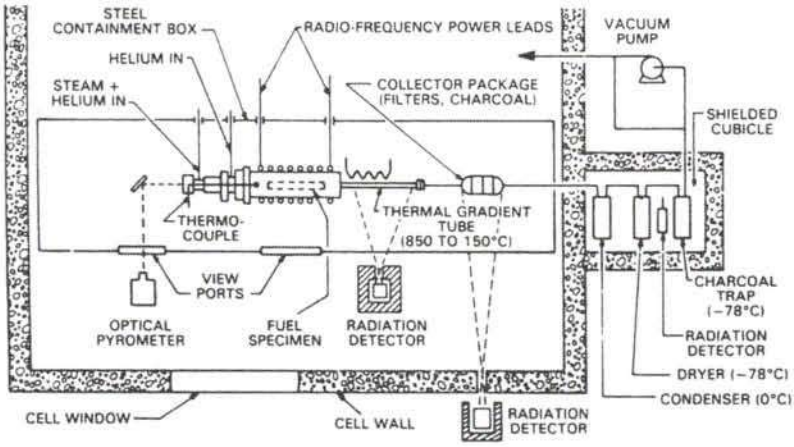

Figure 6.1. ORNL fission product release and collection system
(Collins et al., 1988; Copyright 1988 by the American Nuclear Society, La Grange Park, Illinois)

are not gamma emitters (e. g. ^{129}I, the only iodine radioisotope still present in the long-term cooled fuel material). Finally, the filters were also disassembled and separately subjected to analysis.

Similar release experiments under loss-of-coolant accident conditions have been carried out by Groos and Förthmann (1984 a; 1984 b), also using fuel rod segments which had been irradiated before under PWR conditions to burnup levels of 20 to 40 MWd/kg U; for these experiments, however, a somewhat different experimental procedure was applied. Prior to the heating experiments, the segments were re-irradiated in a research reactor for a short period (on the order of a few weeks) to generate ^{131}I activity again for gamma-spectrometry measurement of iodine behavior, thus avoiding the very time-consuming ^{129}I analysis. The segments were then heated to temperatures of 800 to 1100 °C in a pure steam flow, which was completely condensed after having passed the furnace. By measurement of the individual fractions of the condensates, the amount of total fission product iodine released from the fuel was determined as well as the gaseous fraction which had not been plated out by the condensing steam. In addition, chemical analyses were performed to determine the chemical state of the fission product iodine which had been dissolved in the condensate.

In the ORNL experiments, the fraction of krypton which was released from the failed fuel segments amounted to a few percent of their inventories; it can be assumed that similar numbers also apply for the xenon isotopes, which could not be analyzed in the experiments because of their short halflives. At temperatures exceeding 900 °C, the krypton release did not depend very much on the temperature, indicating that the released fraction originated exclusively from the krypton which had already been present in the gap of the fuel rod before the experiment, and that diffusion of krypton from the fuel matrix did not contribute to the release to any measurable extent.

In contrast, in these experiments iodine and cesium releases showed a pronounced dependence on the temperature. In the lower temperature region, the iodine release was significantly higher than that of cesium; with increasing temperatures, the figures approached each other. According to the experimental results, at postulated maximum fuel temperatures during the accident of 900 to 1000 °C iodine burst release fractions on the order of 0.005 to 0.05% of the fuel rod inventory are to be expected, with the cesium release fractions being somewhat lower. The laboratory heating experiments of Groos and Förthmann (1984 a; 1984 b) yielded iodine release fractions which were slightly lower than the ORNL data at comparable temperatures. The release fractions measured in both series of experiments are considerably lower than the gap inventories of these two elements, which were determined by Lorenz et al. (1980 a) in the course of the ORNL gap purge experiments, in which irradiated fuel rod segments were heated in an atmosphere of purified helium for an extended period of time. This difference is probably the consequence of the long, narrow pathways inside the fuel rod, as a result of which only a fraction of the fission product gap inventory can be transported to the defect position in the comparatively short time periods of tens of minutes used in the experiments (which, however, are distinctly longer than the period the reactor core is assumed to remain uncovered under the conditions of a design basis loss-of-coolant accident). In addition, the magnitude of the release fraction can be assumed to depend significantly on the size of the cladding failure.

The magnitude of the gap inventory of about 0.5% of the fuel rod inventory (see Chapter 3) is representative for fuel rods showing linear heat ratings up to about 220 W/cm; typical average values of commercial light water reactors are slightly to significantly below this limit. However, in the event of a loss-of-coolant accident, the fuel rods with the highest heat ratings will fail first and will therefore be the main contributors to the release of radionuclides from the reactor core. As was discussed in Chapter 3, the gap inventories of highly rated fuel rods are higher than the average values just mentioned, since at the correspondingly higher fuel temperatures within these rods migration of fission products in the thermal gradient of the fuel pellet will significantly contribute to their buildup, whereas at lower heat ratings recoil is the only mechanism of formation of the gap inventory. For this reason, one has to expect gap inventories in the failing fuel rods which are higher than the average values, with their magnitude depending on the heat ratings of the fuel rods showing the highest thermal loadings in the reactor core at the moment of the accident. In the ORNL gap purge experiments, gap inventories of about 15% for iodine and cesium were measured in a BWR fuel rod which during the preceding reactor operation had been exposed to a linear heat rating of about 300 W/cm (Collins et al., 1988). Normally, the maximum values of the linear heat rating in freshly loaded fuel assemblies are higher by a factor of about 2 than the core-averaged value; these values will decrease with increasing burnup. Therefore, when modelling a loss-of-coolant accident it is justified to assume fission product release fractions that are higher than the experimental values obtained for core-average LWR fuel rods.

In order to verify the results of the laboratory heating experiments mentioned above (Groos and Förthmann, 1984 a; 1984 b) the ISOLDE in-pile tests were con-

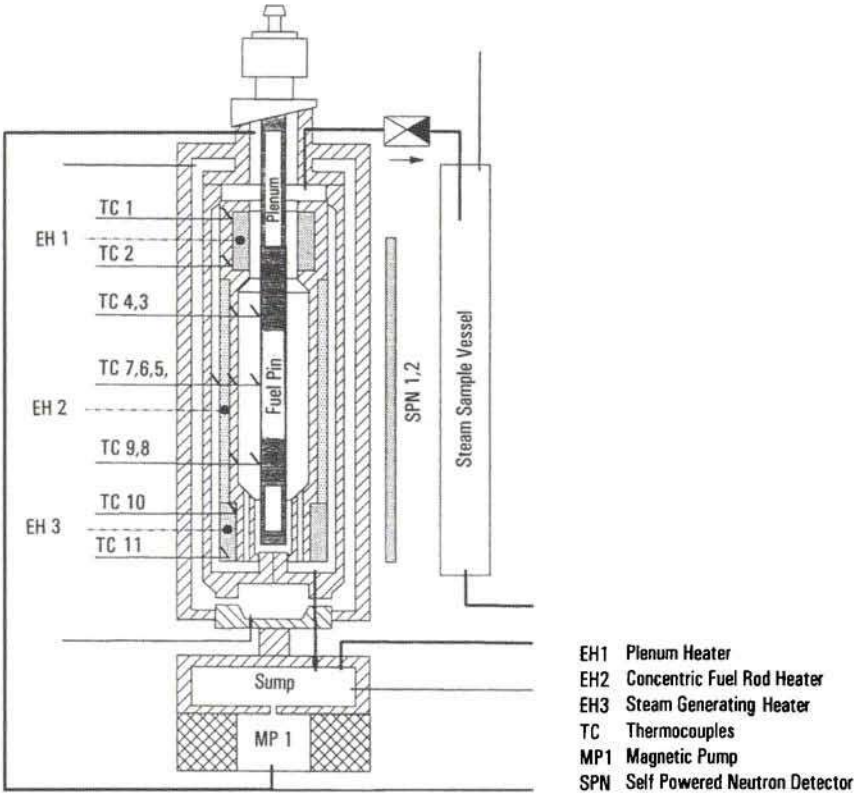

Figure 6.2. ISOLDE irradiation capsule (schem.) (Kühnlein et al., 1993)

ducted (Kühnlein et al., 1993). In these tests fuel rod segments pre-irradiated in a power reactor to burnup levels ranging from about 15 to about 43 MWd/kg U were used, which, in order to generate ^{131}I again for ease of measurement, were re-irradiated in a research reactor to an additional burnup of 1.4 to 2.7 MWd/kg U. Following re-irradiation, the segments were inserted into the irradiation capsule (see Fig. 6.2.) and were damaged at temperatures of about 800 °C by stopping the coolant flow and additional electrical heating. The ^{131}I released from the failed segment then partitioned inside the experimental capsule between the water and vapor phases; both fractions were separately analyzed later on. The results of these tests are shown in Table 6.1., indicating that the iodine release fractions depend on fuel burnup and average heat rating; they also demonstrated that even over the course of several hours at 800 °C no significant diffusion of iodine out of the fuel pellets takes place, i. e. the iodine released originates exclusively from the fuel rod gap inventory. The measured release fractions agree well with that of the laboratory heating experiments mentioned above; on the other hand, they are distinctly smaller than the magnitude of the gap inventories to be expected at the different

Table 6.1. Release of ^{131}I from the fuel rod segments in the ISOLDE test series (according to Kühnlein et al., 1993)

Test No.	IT1	IT4	IT5
Fuel burnup (MWd/kg U)	17	27	45
Heat rating power reactor (W/cm)	155	245	220
Heat rating re-irradiation (W/cm)	180	215	170
Maximum cladding temperature (°C)	756	823	827
^{131}I release (% of inventory)	$2.9 \cdot 10^{-3}$*)	$1.0 \cdot 10^{-2}$	$8.1 \cdot 10^{-2}$

*) no leaching of the capsule

levels of linear heat ratings these segments experienced during pre-irradiation in the power reactor and during re-irradiation.

During heating-up of the fuel rods to temperatures in the range 800 to 1000 °C, it can be assumed that a fraction of the cesium and iodine species deposited in the fuel rod gaps is converted into the gaseous state. Upon failure of the cladding, the overpressurized fill gas will escape and act as a carrier for the fission product noble gases and the gaseous fission products, as well as for small fuel dust particles. The burst release component for both iodine and cesium is the product of two terms, the flux of plenum gas released during rupture of the cladding and the effective concentration of the particular fission product in the gas phase during the rupture period. The former is virtually independent of the position at which the cladding failure occurs; on the other hand, the concentration of fission products in the gas phase depends on the temperature. Thus, in experiments where the whole segment is at a uniform temperature, no influence of the position of the defect is to be expected, whereas in a real fuel rod with its axial temperature gradient the position at which cladding failure occurs will in principle influence the amount released during the burst. However, it can be concluded from the experiments that so little gap inventory is released over the temperature range of interest in a design basis loss-of-coolant accident that the dimensions of the fuel rod will have little influence on the mass of material released during depressurization of the rod. There would be a pronounced dependence on fuel rod length, however, if releases were described as a fraction of the total inventory or as a fraction of the gap inventory. Similarly, the release component caused by diffusion of gaseous fission products in the gap which follows the true burst release, over relatively brief time periods (on the order of 10 minutes at 1200 °C, for example) involves only the fission product material located within a few centimeters of the point of rupture. It can, therefore, be concluded that, because of the short time interval until quenching of the reactor core (in particular in plants with combined hot- and cold-leg injection), only the true burst release will contribute to the fission product transport from the failed fuel rod to the coolant, and that the length of the fuel rod has little effect on the mass of material released, although it has a pronounced influence on the magnitude of the release fractions (Lorenz et al., 1979).

On the basis of the results obtained in the ORNL experiments a model was developed by Lorenz et al. (1978; 1979), describing cesium and iodine release from

fuel rods failing at temperatures of 700 to 1200 °C. In this model, complete release of the gap inventories of the fission product noble gases is assumed, whereas for iodine and cesium the release is assumed to consist of two components: first, the true burst release during which a fraction of cesium and iodine present in the gap in gaseous form is liberated together with the fill gas during the short venting period of the failed rod; second, subsequent diffusion of the remaining gas-phase cesium and iodine species through the gap region and out of the rupture (diffusion release). The equations describing both processes in the temperature ranges 700 to 900 °C and 500 to 1200 °C lead to results which are lower by more than a factor of 10 than the escape data used in WASH-1400. From a very conservatively modelled fuel rod, containing 30% of its cesium inventory in the gap (normal gap inventories for typical LWR fuel rods are around 0.5%), the burst release at 700 °C was calculated to amount to approximately 0.3% of the rod inventory. The following diffusion-controlled release at 700 °C during 10 minutes was lower by a factor of about 10^3; it will reach the same order of magnitude as the true burst release at temperatures around 1000 °C. According to these calculations, the iodine release shows similar figures as cesium release in the temperature region 500 to 700 °C (when related to element masses present in the fuel), whereas in the region 900 to 1200 °C it only amounts to 5–30% of the cesium release.

On the basis of these investigations, in NUREG-0772 (US NRC, 1981) the following fractions of the fuel rod inventories are assumed to be transported during the burst release from the fuel rods to the primary circuit:

	PWR	BWR
Fission product noble gases	3%	6%
Iodine	0.04%	0.08%
Cesium	0.02%	0.04%

The ORNL experiments also showed that during the burst failure at 900 °C approximately 0.02% of the fuel inventory of the rod is transported to the primary circuit as aerosols with diameters between 9 and 200 μm.

When the fuel rod segments were heated in a dry air atmosphere, much higher release fractions were observed (Collins et al., 1988). At 500 and 700 °C test temperatures, the iodine release fractions were considerably larger than those obtained in steam tests conducted at the same temperature; likewise, at 700 °C the cesium release fraction was larger by about a factor of 60 than it was in a steam atmosphere. This increase in release rates was assumed to be caused by an increased porosity of the fuel pellet as a consequence of superficial UO_2 oxidation, as well as of oxidation of iodide originally present in the fuel and in the gap to elemental iodine.

As was reported by Groos and Förthmann (1984 b), higher release fractions are obtained when fuel rods are heated which had been re-irradiated prior to the experiment at heat ratings well in excess of LWR-typical values; under such conditions, the iodine release fraction also depends on the burnup level of the respective

rod. For fuel rod segments which had been operated at linear heat ratings of 200 to 250 W/cm to burnup values of 20 to 44 MWd/kg U and re-irradiated before the experiment at about 400 W/cm, the iodine release fraction proved to be a semi-logarithmic function of the product of total burnup and the linear heat rating during the re-irradiation period. The reason for this enhanced release is an increased gap inventory which is produced by a significant diffusion of iodine out of the fuel matrix at the higher fuel temperatures prevailing during the re-irradiation period. The dependence of the release fraction on the burnup is a consequence of the higher fission product concentrations in the fuel, leading to increased concentrations of iodine (as well as of fission product noble gases and cesium) at the grain boundaries of the fuel pellets at the end of the power reactor irradiation period; from the grain boundaries, a comparatively fast diffusion out of the pellet occurs at the higher temperatures of the research reactor re-irradiation period. Enhanced diffusion of the fission products in the fuel matrix which is caused by a higher concentration of defect positions in the fuel crystallites at higher burnup may also contribute to the observed higher release.

In a reactor accident, the transport behavior of the fission products, in particular that of iodine, after they have been released from the reactor pressure vessel, depends highly on their chemical state. Therefore, in the experiments cited above attempts were made to identify the iodine chemical species escaping from the heating device. In the ORNL experimental setup, the individual sections of the analytical duct were interpreted by the investigators in the following manner: The substances which were plated out on the walls of the thermal gradient tube represent chemical species condensing from the gaseous state; the substances trapped by the aerosol filters were assumed to be transported as aerosols, including iodine which was attached to aerosol particles, either by formation of iodide or by adsorption. Iodine detected at the first charcoal filter (i. e. at ambient temperature) was identified as elemental I_2, though it could not be ruled out that fractions of it consisted of HI or organoiodide compounds. The final charcoal filter kept at −170 °C served as a control filter to ensure complete retention of all the volatilized iodine species in the analytical duct; in the experiments, only fission product noble gases were detected on this filter.

The separation and identification of chemical compounds from the vapor phase by condensation profiles, as occurs in a thermal gradient tube, is based on the fact that the vapor pressure above a deposited species at a given temperature is identical to its saturation pressure, provided that the mass transport from the gaseous phase to the inert wall is sufficiently fast. As can be seen from Fig. 6.3., where deposition profiles of iodine and cesium in a thermal gradient tube (coated with a platinum liner) are shown (the cesium concentration was measured by gamma scanning, iodine by sectional leaching of the tube wall and subsequent neutron activation analysis), above a temperature characteristic for each species, no deposition occurs; below this temperature, condensation starts with a rather sharp edge followed by an exponential decrease for decreasing temperature. Interpretation of condensation profiles is complicated when different gaseous species are simultaneously present in the gas − steam flow or when gaseous compounds react chemically with the wall material of the thermal gradient tube. It is generally acknowledged that only

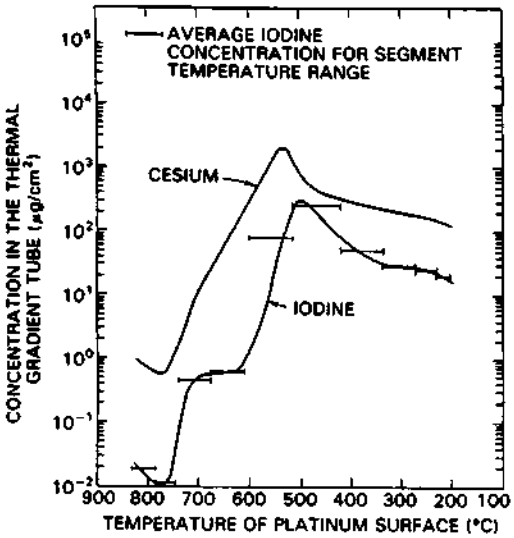

Figure 6.3. Deposition profiles for iodine and cesium in the thermal gradient tube (Collins et al., 1988; Copyright 1988 by the American Nuclear Society, La Grange Park, Illinois)

qualitative conclusions can be drawn from condensation profiles. In practice, the thermal gradient tube has to be calibrated using well-defined chemical compounds; in performing this calibration, the limitations of the method just mentioned have to be taken into account.

In the ORNL experiments, the fission product iodine released from the fuel rod segments at heating temperatures of 500–700 °C and dry air as the ambient atmosphere was deposited almost quantitatively (about 98%) on the charcoal filter, indicating its transport as elemental I_2; the other sections of the analytical duct only showed very small fractions of the iodine released from the fuel specimen. The behavior of cesium under such conditions appeared to be that of a cesium oxide, probably CsO (Collins et al., 1988). In contrast, in a steam–helium–hydrogen atmosphere (hydrogen was generated by the steam–Zircaloy reaction), the iodine released from the fuel specimen was distributed between the thermal gradient tube, the particulate filter and the charcoal trap in varying proportions, depending on the test parameters. Under these experimental conditions, the deposition profiles of both cesium and iodine in the thermal gradient tube were virtually identical (see Fig. 6.3.), indicating the transport of iodine as CsI. This compound appeared to be very stable under the conditions prevailing in the release experiments, showing little tendency to react with the hot quartz, hot zirconia, and hot oxidized and non-oxidized steel surfaces to which it was exposed during the tests. The release and transport behavior of cesium in these tests corresponded to that of CsOH and CsI. CsOH appeared to be very reactive; it was retained by silica at temperatures <950 °C, by zirconia in the temperature range 800 to 1200 °C, and by oxidized stainless steel at temperatures between 600 and 850 °C (Collins et al.,

1988). The two first-mentioned reactions of CsOH are of little significance in a reactor accident, since only small amounts of these materials are present in the primary circuit outside the reactor pressure vessel. The reaction with stainless steel surfaces, however, may lead to significant retention of cesium in the reactor pressure vessel, in particular at the upper core structural materials; there will be a more detailed discussion of these reactions in the context of severe reactor accidents (see Section 7.3.2.).

From these experiments it can be concluded that fission product iodine released from the reactor core during a loss-of-coolant accident is rapidly converted to CsI (or a similar iodide compound) and only a fraction of significantly less than 10% of the iodine released from the fuel rod segments is transported to the containment as elemental I_2 (or HI). This conclusion is supported by the results of the laboratory heating experiments of Groos and Förthmann (1984 a; 1984 b) as well as by that of the ISOLDE tests (Kühnlein et al., 1993), which showed that more than 90% of the fission product iodine released from the fuel rod segments appeared as non-volatile iodide. However, in the ISOLDE tests it was also observed that a considerable fraction of the released iodine was deposited onto the surfaces of the stainless steel experimental capsule.

The mechanism of fission product release from the failed fuel rod segments which was discussed above does not explain the appearance of elemental iodine as a minor fraction in the above-mentioned experiments. For thermodynamic reasons (see Section 3.2.3.), fission product iodine is assumed to be present in the gap of an intact fuel rod quantitatively as an iodide compound; this means that an additional reaction would be required to oxidize iodide to elemental iodine in the course of the burst. Basically, radiolytic oxidation of iodide to I_2 may proceed in the steam atmosphere in the gap after fuel rod failure; however, because of the comparatively low radiation doses at the isolated test segments (compared to the situation in a reactor core) and because of the short duration of the burst phase, it seems unlikely that such an oxidation would effect a measurable iodide oxidation. Another possible explanation is that secondary reactions in the experimental setup resulted in the oxidation of a small iodide fraction. In the context of the ORNL high-temperature release experiments, it was observed that the amount of elemental iodine detected in the analytical duct of the experimental facility was almost independent of the release temperature, i. e. the I_2 fraction decreased with increasing amount of iodine transported from the fuel specimen to the analytical duct (see Section 7.3.1.1.). This behavior supports the assumption of I_2 formation by secondary reactions of original iodide with trace impurities present in the experimental setup. In the Jülich tests the iodine chemical species in the resulting condensates were separated by an extraction technique; in this case as well it cannot be ruled out that the I_2 fractions measured are the misleading results of secondary reactions of foreign substances with the extremely small total iodine concentrations. Thus, when considering the situation in an actual design basis loss-of-coolant accident, the magnitude of the fractions of I_2 detected in the above-mentioned experiments can be assumed to be an upper boundary.

In the actual case of a loss-of-coolant accident in a commercial light water reactor, the fission products released from the reactor core will be transported

through the upper plenum of the reactor pressure vessel and the primary circuit to the break position from where they can escape to the containment. Along this path, a fraction of the fission products (with the exception of the fission product noble gases) will be retained by vapor deposition or by chemical reactions with surfaces, resulting in less volatile compounds. The degree of retention in the primary circuit depends strongly on the residence time of the fission products in the primary circuit, i. e. mainly on the size and location of the break, in the sense that a rather short distance in large-sized pipes will result in low retention, whereas longer pathways through small and medium diameter tubes will lead to a higher deposition; in addition, the temperature of the respective surfaces is an important parameter. In the cold-leg LOCA, the fission product-containing vapor has to pass both the steam generator tubing and the pump suction leg before reaching the break position. In contrast, the pathway from the core to the break in a hot-leg LOCA only consists of a short length in a large-diameter pipe. When calculating the condensation rate of CsI along this path using the method given by Kress (1984; according to Stephenson et al., 1992), it was found that between 70 and 90% of the CsI initially carried by the gas-steam flow is retained in the case of a cold-leg break and that between 15 and 30% of this activity is retained in the event of a hot-leg break. Thus, if this retention is ignored (as is done in most of the accident consequence calculations), the release of iodine to the containment in a cold-leg LOCA would be overestimated by about a factor of 5. On the other hand, fission product compounds can be affected by chemical reactions with other substances present in the primary system, as is the case with CsI; from this compound more volatile iodine species may be formed upon reaction with boric acid or with other reaction partners. So far, there is only little information available on the deposition and resuspension of fission products in the primary circuit under the conditions of a design basis loss-of-coolant accident; in the past, the development of methods to predict the extent of retention of activity in the primary circuit has concentrated on severe reactor accidents (see Section 7.3.2.), which show significant differences in temperatures and fission product concentrations from the design basis accidents.

In PWR plants equipped with both a cold-leg and a hot-leg injection of the emergency coolant, a fraction of the fission products released from the failed fuel rods will be washed down by the downward water flow. Thus, it will be transported back to the water phase inside the reactor pressure vessel and, finally, to the containment sump water. Since the extent of this type of retention of fission products depends strongly on the contact time between the steam flow and the downward flow of the liquid emergency coolant, it is only difficult to quantify. It can be assumed that CsI (and other iodides) will be trapped almost completely in the water phase; for this reason, a 90% retention of the halogens and alkalis and a 99% retention of the so-called solid fission products has been assumed in the German "Störfall-Berechnungsgrundlagen". For the I_2 fraction in the steam flow a similar degree of washout can be expected; experiments performed under conditions similar to those in the relevant LOCA period have yielded I_2 washout fractions of about 92% at 25 °C and about 96% at 85 °C water temperature (Kabat, 1980).

In BWRs, the steam–water mixture escaping from the primary system in a LOCA event is directed to the pressure suppression pool (see Section 2.) where the steam is condensed in the large water volume. Simultaneously, radionuclides carried by the escaping steam are to the most part retained in the water phase; the processes occurring in the pool will be discussed in more detail in Section 7.3.2.4.

During the refill and reflood phases, the reactor core is covered again by emergency coolant (boric acid solution containing approximately 2200 ppm B), which is subsequently circulated by the emergency coolant pumps through a heat sink to remove the decay heat as well as the heat stored in the components and structures. In this recirculation phase, liquid water may penetrate into the failed fuel rods and contact the fuel surface with the consequence that additional fission products may now be transported via the liquid phase to the primary circuit and, subsequently, to the sump water phase formed in the lower regions of the containment. In the "Störfall-Berechnungsgrundlagen" it is postulated that this leaching phase will last for approximately 24 hours.

At the temperature of the emergency coolant, which is 100 °C and less (depending on the capacity of the emergency core cooling systems), only the fission products outside the fuel matrix, i. e. in the fuel rod gap and on the pellet surfaces, are accessible for leaching. Of the laboratory investigations on the leaching of fission products from irradiated fuel, those of Mitchell et al. (1981) were related to the conditions similar to that prevailing in a loss-of-coolant accident. However, these experiments were carried out using fuel grinded to small pieces and not protected by a cladding (burnup of the fuel 23 MWd/kg U). As a leachant, a boric acid solution containing 3000 ppm B and adjusted to pH 8.0 by the addition of NaOH was used at temperatures of 100 °C and 85° C. Since the duration of the experiments was on the order of 280 days, their results are more representative for longer-term post-accident leaching releases than for the accident phase itself. Moreover, the experimental conditions chosen were more closely related to those of an accident involving severe core damage in which the core melt progress has been stopped inside the reactor pressure vessel, as was the case in the TMI-2 accident. In spite of these limitations, part of the results can be used in this context; the other part of the results will be discussed in Chapter 7 in the context of accidents involving severe core damage. In analyzing a loss-of-coolant design basis accident, the results obtained after a short leaching period are of special interest. After some days at 100 and 85 °C, the leached ^{137}Cs fraction amounted to about 0.1% of the fuel inventory of this isotope, the dissolved ^{129}I fraction to 0.2–1%. The leached fractions of the other fission products such as ^{90}Sr and ^{144}Ce were significantly lower, on the order of 10^{-2} to 10^{-3}%; only ^{125}Sb showed a leach fraction of about 0.1%, i. e. on the same order of magnitude as the cesium isotopes. The leach fractions determined for the two different temperatures applied did not show pronounced differences. Because of the rather fine grain size of the material used in these experiments, the results obtained can be judged to be upper limits for the leach fractions to be expected in this stage of a loss-of-coolant design basis accident.

The leaching experiments reported by Johnson et al. (1983; 1984) performed with sections of irradiated fuel rods, as well as with whole fuel rods (linear heat

ratings ranging from 250 to about 500 W/cm) showed that the release of ^{137}Cs and ^{129}I is controlled almost entirely by the access of water to the gap fission product deposits, and that the cesium and iodine species present in the gap are highly soluble in water. At 25 °C leaching temperature, less than 0.5% of the fuel rod inventories of both elements were leached from the low-power rods or rod sections, while from high-power rods 1 to 2% were leached. At 150 °C leaching temperature release of ^{137}Cs from the low-power rods was significantly enhanced relative to the 25 °C tests (^{129}I behavior was not reported), indicating additional release from the fuel pellet grain boundaries; high-power fuel specimens did not show this enhanced release at 150 °C. Groos and Förthmann (1984 a), after termination of their laboratory heating experiments, subjected the segments used to a leaching treatment in water at 25 to 30 °C for approximately 4 hours. Under these conditions, an iodine leach fraction of $5 \cdot 10^{-3}$% was measured, a value which is well below the iodine gap inventory of the segments. At such low temperatures, virtually no convection can be assumed to occur in the liquid phase inside the segment, resulting in a slow transport of dissolved fission products out of the rod. As a result, these leached fractions are probably lower than those which are to be expected in an actual accident situation.

The laboratory leaching experiments of irradiated UO_2 fuel do not completely reflect the situation in the reactor pressure vessel during the leaching phase of an accident, since the radiation doses prevailing in the laboratory investigations (even when high-burnup fuel samples are used) are lower by several orders of magnitude. Oxidizing primary products of H_2O radiolysis can in principle attack the UO_2 pellet by oxidation, potentially leading to an enhanced release of fission products to the emergency coolant. Basic studies at comparatively low radiation dose rates (up to 280 Gy/h) have been conducted in the context of development work for direct final disposal of spent fuels (Sunder et al., 1992). The results showed that, in particular, the radical species generated in water radiolysis are capable of oxidizing UO_2. The reaction mechanism involved apparently consists of two distinct stages: At first, formation of a thin layer of UO_{2+x} with a stoichiometry close to $UO_{2.33}$ occurs, followed by the oxidative dissolution of this surface layer to produce soluble U^{6+} species as well as solid secondary phases (such as hydrated UO_3), with the latter remaining deposited on the pellet surface. A direct relationship of these results to the radiolytic reactions proceeding in the reactor pressure vessel during the leaching phase cannot be established; however, it seems that radiolytic oxidation is a slow process which does not enhance significantly fission product release during the loss-of-coolant accident leaching phase.

As was discussed above, the fuel rods which are expected to fail in the course of the accident are those which, prior to the onset of the accident, have experienced the highest heat ratings and, therefore, show fission product gap inventories that are distinctly higher than in an core-average fuel rod. On the other hand, the data cited above demonstrates that only a comparatively small fraction of the gap inventory of the failed rods is transported out of the cladding during the burst, refill and leaching phases, due to the long, narrow pathways in the gap. The magnitude of the released fraction presumably depends on the size and, perhaps, on the location of the defect as well. It is, therefore, difficult to establish generally valid

figures but, in any case, the magnitude of the released fraction will be markedly lower than the magnitude of the gap inventory. As "gap inventory" in this context, the gap inventory of operationally intact fuel rods is to be understood. The operationally defective fuel rods, with their significantly higher gap inventories, which are potentially present in the reactor core, are also affected by the processes occurring in the course of the accident and will contribute to the amount of radionuclides transported to the primary circuit. However, this contribution to the total radioactivity transport can be neglected, since the number of operationally failed fuel rods is in any case smaller by far than the number of fuel rods postulated to fail during the burst and refill phases of the accident.

The chemical forms of the radionuclides liberated from the fuel rods during the leaching phase of the accident are of importance as regards their behavior later on in the containment sump water. There is no doubt that the cesium isotopes are dissolved as Cs^+ ions in the liquid phase. Iodine isotopes can be assumed to exist initially as I^- ions in the emergency coolant; whether or not in this stage a radiation-induced oxidation to I_2 has to be assumed, cannot be judged on the basis of the currently known data. Subsequently, in the containment sump water, it may be more likely that such a radiation-induced oxidation will occur; however, the radiation levels in this liquid phase are low compared with those arising in a degraded core accident (see Section 7.3.3.3.4.). The alkaline earth elements strontium and barium probably exist in the leaching solution in their divalent ionic state, at least when they are present in very low concentrations. Other fission products such as cerium, lanthanum and others, as well as uranium and plutonium, may be partly present in the ionic state. It can be assumed, however, that the major fraction of them is attached to suspended solid particles present in the sump water in a chemical form which is as yet unknown.

6.2.1.2 The behavior of the fission products in the containment

In the very first stage of the loss-of-coolant accident, the primary coolant discharges through the break into the reactor building as a two-phase water–steam mixture with a steam fraction of about 50% (by mass). The radionuclides in the primary coolant during the preceding phase of normal operation are transported in this two-phase mixture; however, as was already mentioned, the amount of these radionuclides is small compared to that which is postulated to be released during the burst phase. The liquid water phase discharged from the primary circuit will run down into the containment sump and smaller sumps may additionally be formed at various locations in the reactor building; in the following discussions, all the liquid water volumes present in the reactor building will be included under the term "sump water". The steam fraction formed during the discharge of the coolant will expand into the containment free volume and, because of the lower temperatures here, will partly condense, with the condensates running down to join the sump

water. The finer water droplets will remain for a longer period of time in the containment atmosphere. The behavior of this blowdown aerosol will determine the ambient conditions in the containment atmosphere when the fission products are released from the primary circuit. The mechanisms which contribute to aerosol removal (including the blowdown water droplets) from the atmosphere of the containment were treated in detail by Stephenson et al. (1992).

According to experiments performed under appropriate conditions, about 1% of the fission product iodine present in the flashed primary coolant volume is transported with the steam phase, about half of it in form of aerosols (Alm and Dreyer, 1980). This figure agrees well with that reported by Morell et al. (1985) and Hellmann et al. (1991), obtained in flashing experiments from small-diameter pipes (see Section 6.2.2.). In the experiments of Alm and Dreyer (1980), which were carried out in an uncoated steel vessel, only particulate iodide and elemental I_2 were detected in the atmosphere of the vessel. The rate of plate-out of iodine from the atmosphere was found to depend on the specific geometric conditions of the experimental setup. In a comparatively small vessel, deposition halftimes of 8.5 hours for I_2 and of 0.9 hours for aerosol iodide were measured within the first two hours after blowdown; these values increased to 9.9 and 5.7 hours, respectively, during the following 22 hours. From other experiments markedly different values have been reported (e. g. CSE tests, see Section 7.3.3.3.8.). The reasons for these differences are not only due to the dimensions and true surface areas present in the respective experimental facility, but also to various other parameters, such as initial concentrations, turbulences in the atmosphere, rate of water droplet plate-out and of steam condensation.

Following failure of the fuel rods, the fission products released from them will be transported in a superheated dry steam atmosphere containing a certain percentage of hydrogen originating in the steam–Zircaloy reaction. At the end of the refill phase or, in the case of hot-leg injection, with the start of operation of the emergency coolant systems, the superheated steam atmosphere will be replaced by a saturated steam atmosphere. Finally, in the recirculation phase, the fission products are transported out of the primary circuit in their dissolved or suspended forms in liquid water at temperatures at or below the boiling point. According to this sequence, the chemical composition of the sump water developing in the containment will change with time. Initially, its basic composition is that of the primary coolant, but because of the evaporation of about one-half of the original water volume during blowdown, the concentrations of boric acid and lithium hydroxide are higher than in normal primary coolant, whereas the hydrogen content has been lost completely to the containment atmosphere. This means that the pH value of the sump water during this phase will be in the range 6 to 7.3 at 100 °C, depending on the burnup state of the reactor core at the moment of the accident and, as a consequence, the corresponding boric acid concentration in the primary coolant. After the onset of the emergency core cooling systems operation, the pH of the sump water will decrease due to the high boric acid concentration in the coolant solutions and the absence of alkalizing agents, as well as to the dilution by condensing steam. The resulting pH will be in the range of 5 to 6. Moreover, the sump water will contain oxygen from the air-saturated emergency coolant and

from its contact with the containment air. In American and various other plants, the final composition of the sump water is further complicated by the addition of the containment spray system solution which usually is an alkalized borate solution with a pH of about 10, which raises the pH of the sump water to a value of about 8. In British PWRs, the sump water solution in the recirculation phase is buffered by the dissolution of trisodium phosphate which is stored in the lower regions of the containment as a solid compound, so that the final sump water pH in these plants will also be around 8 (at 25 °C). Relevant experiments have demonstrated that the long-term storage of anhydrous sodium triphosphate in open racks in a humid atmosphere results in a caking of the granules although this does not adversely affect their rate of dissolution in simulated sump water (Handy et al., 1989).

The total sump water volume in the containment is approximately 1500 m^3, depending on the design of the safety systems in the particular plant.

The fission products released from the primary circuit into the containment in the course of the accident sequence can be divided into three groups with regard to their behavior. The fission product noble gases will enter the containment atmosphere where they will be distributed homogeneously in a comparatively short time, supported by the convective forces caused by the expansion and subsequent condensation of the steam. Less volatile radionuclides, including CsOH, CsI and other iodides which enter the containment free volume as aerosols, will be partly washed down by the condensing steam, with another part being plated out upon aerosol agglomeration and sedimentation processes. The most complex behavior is exhibited by elemental iodine I_2. This results from its disproportionation in water and from the volatility of certain iodine species. For this reason, iodine will be treated in more detail below; part of these discussions are based on the detailed investigations reported by Bawden et al. (1983) in the context of the safety analyses of the first British PWR. Since only the gaseous phase will have the potential of escaping from the containment, the concentrations of volatile and airborne radionuclides are of particular interest.

The final partitioning of fission product iodine between the sump water and the atmosphere of the containment is determined by the equilibrium partition coefficient; as will be discussed in more detail in Section 7.4.3.1., this figure depends on several parameters, such as iodine concentration and sump water pH and, to a lesser extent, temperature. As can be seen from Fig. 4.13., the iodine partition coefficient increases with decreasing iodine concentration in the solution; this behavior is the consequence of the shift in the I_2 hydrolysis reaction towards a lower I_2 equilibrium fraction at lower total iodine concentration. Below a concentration of about 10^{-5} g/l, however, the partition coefficient remains virtually constant, an effect which has been attributed to the volatility of the hydrolysis product HOI (Lin, 1981). This constant value is about 10^4 at pH 7 and 25 °C; it applies as well for the concentration range to be expected in a loss-of-coolant accident. Concerning the HOI partition coefficient at 100 °C, several measurements yielding quite different values have been reported. The lowest one is 240 given by Lin (1981); Lemire et al. (1981) reported values between 100 and 10^4, while Wren and Sanipelli (1984) measured values between $7 \cdot 10^3$ and $3 \cdot 10^4$. Since the HOI compound was

not directly measured in the gaseous phase, the higher values for its partition coefficient seem to be more realistic.

When calculating the I_2 equilibrium concentration in the containment atmosphere from these data, one has to remember that the partition coefficients usually were determined using pure I_2 solutions. The fission product iodine in the sump water, however, mainly consists of non-volatile iodide with smaller fractions of I_2 on the order of 10% and less. The airborne fraction of I_2, therefore, has to be calculated from the dissolved I_2 concentration only. The excess I^- present in the solution will act to shift the I_2 hydrolysis equilibrium towards a higher I_2 fraction; at the low total iodine concentrations present, however, this effect is not expected to result in a significant decrease in the total iodine partition coefficient.

The time needed until the iodine partitioning equilibrium in the containment is established is a difficult question to answer, mainly because of the complex geometry of the reactor building, with its different compartments and structures; in the German "Störfall-Berechnungsgrundlagen" a halftime of 7 hours is anticipated. The complex structures in the reactor building may delay the emergence of the equilibrium state; on the other hand, the convective movement of the atmosphere can be expected to accelerate this process. In total, a time period dependent upon the halftime mentioned above seems to be a meaningful value.

If one assumes, in accordance with the German "Störfall-Berechnungsgrundlagen", that in the course of the accident 10% of the fuel rods in the reactor core will fail and that roughly 1% of their fission product iodine inventory will be transported to the containment, then the total iodine concentration in the sump water will amount to about $1 \cdot 10^{-5}$ g/l (i. e. about $1 \cdot 10^{-7}$ M). As was mentioned in the preceding section, the results of Lorenz et al. (1980 a; 1981) indicate that the major part of the iodine released is transported as CsI and only a small fraction as I_2. Assuming a ratio of these two species of 9:1 in the sump water, Förthmann et al. (1985) calculated a volume-related partition coefficient of about $5 \cdot 10^4$ for total iodine under containment conditions. This means that, after equilibrium has been established between sump water and containment atmosphere, approximately 0.1% of the total iodine released from the failed fuel rods will be present in the gaseous phase as volatile I_2 (taking into account the volumes of sump water and containment atmosphere), corresponding to some 100 GBq ^{131}I. It was assumed that by this time the fraction of the iodine which was originally transported to the containment atmosphere and was not plated out by the condensing steam fraction had also reached partition equilibrium between the water and gaseous phases. In these calculations it was postulated that no retention of fission product iodine in the reactor pressure vessel and the primary circuit will take place.

This estimation is a very simplified one and does not take into account a possible oxidation of iodide to elemental iodine in the sump water. At the very low iodine concentrations present and at the temperatures under consideration, thermal oxidation caused by dissolved oxygen proceeds rather slowly, as far as it is not catalyzed by UV light or by traces of metals. According to the calculations reported by Burns and Marsh (1986), a fraction of only about 10^{-3} of the original iodide is thermally oxidized in the ten days following the accident. Since the extent of iodide oxidation in the sump water is determined by the redox potential of the liquid

phase and this, in turn, is determined by the oxygen partial pressure in the atmosphere above the solution, one has to expect a minimum partition coefficient at oxygen partial pressures on the order of 10^{-4} to 10^{-2} atm (see Fig. 7.30.). Both the progress and the products of radiation-induced oxidation reactions at the low iodine concentrations present in the sump water are less well known than at the higher concentrations to be expected in a severe core damage accident (see Section 7.3.3.3.4.). Investigations of 3 μM I^- solutions in aerated boric acid solution showed oxidation to IO_3^- and I_2, reaching steady-state levels of 10 and 20%, respectively, after irradiation to about 10 kGy at ambient temperature, with no obvious dependence on the radiation dose rate. With increasing temperature, the IO_3^- and I_2 yields decreased steadily; with decreasing iodine concentration in the solution (10^{-4} to 10^{-6} M) the I_2 yield fell, while the IO_3^- yield increased (Burns et al., 1988). The rate of radiation-induced iodide oxidation under sump water conditions is not yet known reliably; in particular, the influence of the largely unknown impurities dissolved in the sump water is difficult to evaluate. In the containment, the radiation levels are mainly due to the release of noble gases from the reactor core, which are present in the containment atmosphere. Because of the relatively low radiation dose rates in the sump water (caused by volatile and solid radionuclides) and the comparatively high pH of the water, the formation of volatile iodine can be assumed to proceed only slowly. Therefore, its partition rate is also slow, being typically on the order of 10^{-6} s^{-1}. This means that fission product iodine present in the sump water after a design basis loss-of-coolant accident is and remains essentially non-volatile.

Under such conditions, the iodine species which are responsible for volatilization are assumed to be HOI at low concentrations and I_2 at higher concentrations. Iodine volatility and partitioning are strongly influenced by the question of whether or not iodate is formed to a significant extent, either by direct oxidation or by disproportionation of I_2. Since this question cannot be answered in a quantitative manner, Bawden et al. (1983) have given lower and upper limits for the partition coefficient, between $1 \cdot 10^{10}$ if no iodide oxidation occurs and $2 \cdot 10^3$ in the case of rapid iodide oxidation and no iodate formation. These figures are valid for pH 6.1; at pH 7.8 they are higher by about two orders of magnitude. The partition coefficient applied by Förthmann et al. (1985), which was mentioned above, agrees well with these numbers and, therefore, can be judged to be reasonably conservative.

Gaseous iodine which is present in the containment atmosphere has the ability to react with organic materials such as the coatings of the walls to form organoiodide compounds, mainly methyl iodide CH_3I. On the other hand, these compounds can be decomposed again under containment conditions, so that after a certain period of time an equilibrium fraction of organoiodide will be established. Currently, there are no specific data on organoiodide formation and decomposition under the conditions of the design basis accident discussed here; most of the publications in this field are related to severe core damage accidents and, therefore, will be treated in Chapter 7. Bawden et al. (1983) tried to use the data given in some of these publications to derive formation rates that can be applied to the conditions of a loss-of-coolant accident. Their recommendation is to calculate the quantity of

organoiodide present in the containment atmosphere by integration of a formation rate of 0.01% of the total containment iodine inventory per day, up to a maximum of 0.2% of the inventory; after this time, the proportion is assumed to remain constant. As a result, during the first hours to days after the onset of the accident the fraction of organically bound iodine will be very small and can be ignored for short-term evaluations. It has to be pointed out that formation inside the containment is the only production mechanism for organoiodide compounds during the accident; because of their instability at higher temperatures, these compounds will be decomposed rather than generated inside the reactor pressure vessel or the primary circuit during the burst and refill phases (Lorenz et al., 1976).

Stainless steel surfaces which are in contact with I_2 solution (50 μM) at 100 °C effect a slow reduction of I_2, while concrete surfaces, due to the alkaline nature of this material, give rise to I_2 disproportionation. Surfaces which are coated with epoxy phenolic paint are very reactive towards I_2 in solution, especially at elevated temperatures (100 °C), causing reduction of I_2 to I^-, but these surfaces are also able to remove up to 50% of the initial I_2 inventory of the solution (Burns et al., 1988). The results of these laboratory experiments clearly demonstrate that "dirt" effects may have a marked influence on iodine behavior, in particular at such low concentrations.

Containment spray systems are used in some types of PWR plants, resulting not only in a condensation of steam but also in a washout of airborne radioiodine and other fission products from the containment atmosphere. Normally, an alkaline borate spray solution is used, resulting in a shift of the I_2 disproportionation equilibrium to the iodate side and a suppression of revolatilization of iodine previously trapped by the spray droplets. In some cases, solutions containing sodium thiosulphate have been used to decompose volatile organic iodides present in the containment atmosphere, but because of its corrosivity this reagent has been largely abandoned. By the addition of boric acid to the spray solution, subcriticality of the reactor core is guaranteed when, after the injection phase, the sump water is recirculated for removal of decay heat from the core.

The effectiveness of a spray system in removing fission product iodine from the containment atmosphere depends on several parameters, as is known from early investigations, among others those conducted by Row et al. (1969), by Patterson and Humphries (1969) and by Row (1971). Other experiments have demonstrated that spray solutions buffered at pH 9.5 are more effective in iodine removal by a factor of 3 than pure water, probably because acidification of the outer droplet layer is prevented which, in pure water, may be caused by the I_2 hydrolysis and disproportionation reactions (Hyder, 1991). Other parameters controlling iodine removal by sprays are specific for the individual system under consideration (internal geometry, spray rate etc.). Spraying experiments performed in the context of the CSE tests (see Section 7.3.3.3.8.) showed a reduction of the airborne iodine concentration of more than one order of magnitude within a spray time of about 10 minutes; subsequent spray periods were much less effective (Hilliard and Postma, 1981). In the case of airborne particulate iodide, the chemical composition of the spray solution (water, boric acid, alkaline borate solution) does not affect

the removal rate nor the final equilibrium level of iodine remaining in the atmosphere (Alm et al., 1980).

For the rational design of spray systems and for predicting the behavior of existing spray systems under accident conditions, models are required which are able to describe the rate of iodine absorption by the spray droplets. However, modelling of the essential steps of iodine uptake into the spray droplets is quite difficult, even for a single droplet; consequently, the treatment of entire sprays will involve a considerable number of assumptions. Among the different attempts, the model developed by Albert et al. (1987) was the first one that also took into account iodine hydrolysis reactions in the spray solution; it is a quasi-steady-state mass transfer model with the parameters spray drop size, initial concentrations of the gas and liquid phases, temperature, pressure, spray flow rate and others. The results of the model calculations were compared with those measured in the CSE experiments, showing differences of about a factor of 2. The reasons for these differences are in part due to the fact that in the complex, large-scale CSE tests many other removal processes were simultaneously effective, the contributions of which are difficult to separate from the effects of the sprays. On the other hand, several potentially important effects such as enhanced mass transfer during drop formation, non-sphericity of the drops and heat transfer are not considered in the model; as a consequence, a certain degree of uncertainty in the predictions of the model has to be expected. This model was developed further by Weber et al. (1992), in particular with regard to severe core damage accidents (see Section 7.3.3.3.6). Here, improved models of the aqueous chemistry of I_2 and CH_3I were used; likewise, the capability of calculation at any temperature was included. Different iodine species were treated separately, and the behavior of each of them was treated as mass transfer with simultaneous chemical reaction.

The benefits of containment spray systems regarding removal of airborne radionuclides from the atmosphere are not undisputed. Condensing steam in the atmosphere as well as reactions with the walls ensure an effective removal of elemental iodine, whereas organoiodides, as far as they are produced under the prevailing conditions, are decomposed by ionizing radiation. Thus, even without the action of containment spray systems, radioiodine is removed from the containment atmosphere rapidly and effectively by passive reactions.

In the post-LOCA atmosphere, the spray solution is subjected to radiolytic decomposition caused by the intense β^-, γ field in the containment atmosphere, with the main final radiolysis products being H_2 and H_2O_2. In the range of low radiation doses, the $G(H_2)$ value of the alkaline borate solution with a pH of 9 amounts to 0.45, i. e. is virtually identical to that of pure water; it is not affected by the addition of I_2 and does not depend on the ratio liquid-to-gas in the system (Habersbergerova, 1982). At radiation doses above 10^5 Gy in a system consisting of a liquid without any gas phase above it, the $G(H_2)$ value decreases with increasing radiation dose and reaches values of about 0.05 at $5 \cdot 10^5$ Gy. By contrast, in a system containing both gaseous and liquid phases (volume ratio 20) the $G(H_2)$ value remains virtually constant at 0.3 to 0.4 in the range 1 to $12 \cdot 10^5$ Gy. As a reason for this effect it is assumed that in the former case the $OH\cdot$ radicals formed are trapped by the excess H_2 remaining in the solution, whereas in the latter case the H_2 produced

escapes out of the liquid phase, so that further H_2 production can proceed. However, the average spray drop fall time is quite short, probably too short for an appreciable radiolytic buildup of H_2O_2, which is the primary reactant in iodine hydrolysis. Thus, radiation effects on iodine speciation within droplets are not expected to be very pronounced, except in situations where the spray water is recirculated from the sump back to the spray system (Weber et al., 1992).

Elemental iodine trapped in an alkaline spray solution is rapidly hydrolyzed to I^- and IO_3^-. Investigations of Habersbergerova (1982) showed that irradiation of such a solution results in a complete reduction of all inorganic species to I^-. As measured at low irradiation doses, $G(-IO_3^-)$ is identical to $G(I^-)$; it increases linearily with the initial IO_3^- concentration, does not depend on the ratio of the liquid to the gaseous phase and is not influenced by an excess of I^-. At higher irradiation doses, I^- is also the only iodine-containing reaction product; the pH and borate concentration of the solution are not affected by the irradiation. According to these results, the radiation chemistry of iodine in aerated alkaline borate solutions is quite different from that in pure neutral water, where elemental I_2 is the main product. Pulse radiolysis experiments reported by Janovsky (1980) showed that in both media the same intermediates are produced. In the aerated solution, however, H_2O_2 and O_2^- produced radiolytically will completely reduce the I_2^- intermediate to I^-. As these studies were carried out using comparatively high iodine concentrations (10^{-4} and 10^{-3} M), the question still remains of whether or not the assumed reaction mechanisms also apply to the considerably lower iodine concentrations present in the spray solution in a design basis LOCA event.

Methyl iodide dissolved in aerated alkaline borate spray solutions (0.23 M H_3BO_3 – 0.153 M NaOH) is completely decomposed by ionizing radiation. Experiments reported on by Habersbergerova and Sistek (1982), in which solutions containing 10^{-5} to 10^{-3} M CH_3I were exposed at room temperature to γ doses in the range 10^5 to 10^6 Gy (corresponding to those to be expected under accident conditions), resulted in a virtually complete decomposition of CH_3I to iodide as the only iodine-containing radiolysis product, with methyl hydroperoxide CH_3OOH and small amounts of CH_4 being the residues of the organic constituents. The initial yield of I^-increases with increasing CH_3I concentration in the solution, showing $G(I^-)$ values of about 0.5 for a $1 \cdot 10^{-4}$ M solution and of about 3 at $1.5 \cdot 10^{-3}$ M; the yields of CH_3OOH show a similar tendency. CH_3I absorbed from air by NaOH solution is also chemically decomposed by a base-catalyzed hydrolysis reaction to CH_3OH and I^-, but this hydrolysis is much slower than the rate of radiolytic decomposition: In an H_3BO_3–NaOH spray solution containing about 10^{-5} moles CH_3I/l, only 35% of the initial concentration was hydrolyzed by the chemical reaction after 1000 hours at room temperature.

In spray solutions containing thiosulphate, the chemical decomposition of methyl iodide is so fast that it overlaps the effect of gamma radiolysis (Habersbergerova and Bartonicek, 1983). The thiosulphate anion itself is oxidized by ionizing radiation, with the yield of decomposition being highly dependent not only on the solution pH but on the ratio of the volume of spray solution to that of air in the system. Experiments reported on by Habersbergerova (1981) showed that after application of a gamma dose of $3 \cdot 10^6$ Gy to an air-saturated solution of thiosul-

phate, borate and NaOH in the absence of a gaseous phase above it, only 60% of the thiosulphate inventory was decomposed. In contrast, at a ratio of V_{air} to V_{liquid} of 9 and a gamma dose of $1 \cdot 10^6$ Gy, all the thiosulphate was oxidized to sulphate. In the first-mentioned case the $G(-S_2O_3^{2-})$ value amounted to about 0.11, with the main radiolysis products being SO_3^{2-} at lower doses and SO_4^{2-} at higher doses; the oxygen initially dissolved in the solution had been completely consumed at an irradiation dose of about $1 \cdot 10^4$ Gy. With a gas atmosphere above the solution, the average $G(-S_2O_3^{2-})$ value is on the order of 0.6. I_2 added initially to the solution did not show any influence, either on the decomposition of thiosulphate or on the nature and ratios of the products formed.

In addition to this large-break loss-of-coolant accident, Bawden et al. (1983) analyzed fission product iodine behavior during small-break accident sequences with break sizes ranging from $8 \cdot 10^{-5}$ to $9 \cdot 10^{-2}\,m^2$. The leak rates occurring as a consequence of such break areas are fully controlled by the emergency cooling systems, so that the reactor core remains flooded and no damage of fuel rods in the core is to be expected; as a result, radionuclide release from the primary circuit is limited to the amounts present in the primary coolant which are due to operationally failed fuel rods. Radionuclide behavior in the containment (in particular iodine behavior) in the course of such an accident is quite similar to that in a large-break LOCA, with the total amount of radioactivity under consideration being lower by two orders of magnitude or even more. For this reason, such accident sequences shall not be treated here.

From the reactions described above, the concentrations of volatile fission product species, in particular of iodine, which are present in the containment atmosphere can be calculated. When doing so, one has to remember that a real reactor building has a very complex structure which can only be simulated in a highly simplified manner in a mathematical model. First of all, in such models usually a direct contact between the surface of the sump water and the free volume of the containment is assumed, rendering possible an iodine partition equilibrium which can be described by the partition coefficients obtained in the experiments. In reality, however, the equipment compartments are separated from the containment free volume by walls and doors, so that the exchange of matter between the liquid phase and the containment atmosphere is hindered. As a consequence, a delayed establishment of the partition equilibrium has to be expected, as well as significant deposition of substances along the path between the two phases, possibly associated with changes in their chemical states. Since these pathways depend on the location of the pipe break (among other factors), they cannot be modelled in a generally valid manner. The reactions occurring, such as deposition, resuspension, change in chemical species, are of even greater significance in severe core damage accidents and will, therefore, be described in more detail in Chapter 7.

In sum, the reactions that can occur on the way from the sump water to the containment free volume (and vice versa) are assumed to result in a significant reduction of the amount of airborne radionuclides, in particular of volatile iodine species. Ignoring these reactions, therefore, would lead to an overestimation of the amount of volatile radionuclides and, as a consequence, to a conservative assumption regarding a potential release.

6.2.1.3 Investigation of radionuclide behavior in integral experiments

The application of the results on radionuclide behavior obtained in laboratory-scale experiments to a real accident is a difficult question because of the substantial differences in the dimensions of the reaction system and, sometimes, in the prevailing conditions as well. For example, as concerns the release of fission products from the failing overheated fuel rods, there are differences in how the rods heat up: in the laboratory experiments this is brought about by external heating, whereas in the affected reactor core it results from the internal decay heat. The in-reactor ISOLDE experiments mentioned in the preceding section suggested only a minor, if any, impact of these differences on the radionuclide release behavior; however, such an influence cannot be ruled out completely. Another item of potential relevance is the difference in radiation fields which are higher by several orders of magnitude inside the reactor pressure vessel than in the laboratory test facilities. In particular, the chemical state of fission product iodine during its release from the fuel and its transport to the containment may be affected by the magnitude of the radiation field. Finally, the differences in length and temperature gradient of the fuel rod segments heated in laboratory experiments from those of real fuel rods are assumed to be of little influence on the amount of fission products released from the failed rods; however, they will affect the magnitude of the released fraction of the total gap inventory.

Another problem is due to the fact that laboratory experiments are only able to simulate a small section of the whole accident sequence; as a result, a model of radionuclide behavior has to be synthesized from a number of individual pictures. This problem can be overcome by integral experiments which include all (or almost all) the stages of the accident; however, such an integral experiment is very expensive and, for this reason, usually only one or a few tests can be carried out, with the significance of the results depending highly on an optimum planning and preparation. As yet, the only integral test which was specifically designed and operated to study fission product behavior in a design basis accident was the LOFT FP1 experiment at the Idaho National Engineering Laboratory (INEL); in the following, this experiment will be described in somewhat more detail.

The LOFT reactor shown schematically in Fig. 6.4. was a small pressurized water reactor with a thermal rating of 38 MW which consisted of a complete intact primary circuit, including main coolant pump, steam generator and pressurizer, and a second primary circuit (the so-called Broken Loop) in which a break could be simulated by opening a valve. The primary coolant which discharged through the "break" flowed through piping to a blowdown suppression tank which simulated the reactor containment. Prior to the fission product experiments, the reactor had been used in a number of thermohydraulic tests aimed essentially at code validations; these experiments were shortly summarized, e. g., by Brittain and Aksan (1990). In order to analyze fission product transport and distribution in the course of the simulated accident, the reactor was equipped with appropriate measuring and sampling devices, which are shown schematically in Fig. 6.5.; besides directly-counting gamma spectrometers, steam sampling units as well as deposition coupons were installed at different locations in the primary circuit.

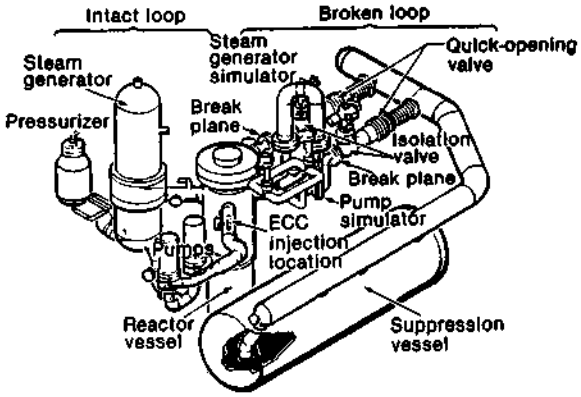

Figure 6.4. LOFT testing reactor; schematic view
(Hicks and Sato, 1990; Copyright OECD, 1991, The OECD/LOFT Project: Achievements and Significant Results, 9th–11th May 1990, Madrid, Spain. Reproduced by permission of the OECD)

The steam sampling systems were designed to collect samples from the dry steam phase of the experiment. They each consisted of a gamma detector, a moisture separator, an iodine species sampler, a flow meter, a steam condenser, and a charcoal absorption trap. The γ spectrometer system, which was operated during the twelve-hour post-transient period, consisted of four detector positions, located at the reactor pressure vessel lower plenum (primary coolant liquid phase), the gas space of the blowdown suppression tank and its liquid space and, finally, in the gas space of the blowdown header. The deposition coupons were installed to measure fission product retention on the upper structures of the reactor core and on the surfaces of the upper plenum at different elevations. In order to protect the fission products plated out there during the burst and refill phases against leaching in the reflood phase, some of the coupons could be isolated and sealed prior to initiation of the reflood phase (protected coupons), while the other coupons remained exposed.

Individual aspects of the test have been described in detail in several OECD reports; the results of the measurements on fission product behavior have been summarized by Schuster (1990). For this experiment, a central fuel module was placed in the reactor core, which consisted of 22 pre-pressurized fuel rods containing uranium dioxide fuel enriched to 6% ^{235}U, which had been designed in such a manner as to fail during the experiment. The burnup of the fuel had been adjusted to 1.4 MWd/kg U (average value) by pre-irradiation at linear heat ratings between 357 and 530 W/cm, i. e. values which were well beyond the heat ratings experienced in average LWR fuel rods. This very low burnup value resulted in fission product concentrations in the fuel which were significantly lower than in normal LWR fuels, with possible implications for their release behavior from the failed rods. In order to overcome this problem, addition of fission product simulants to

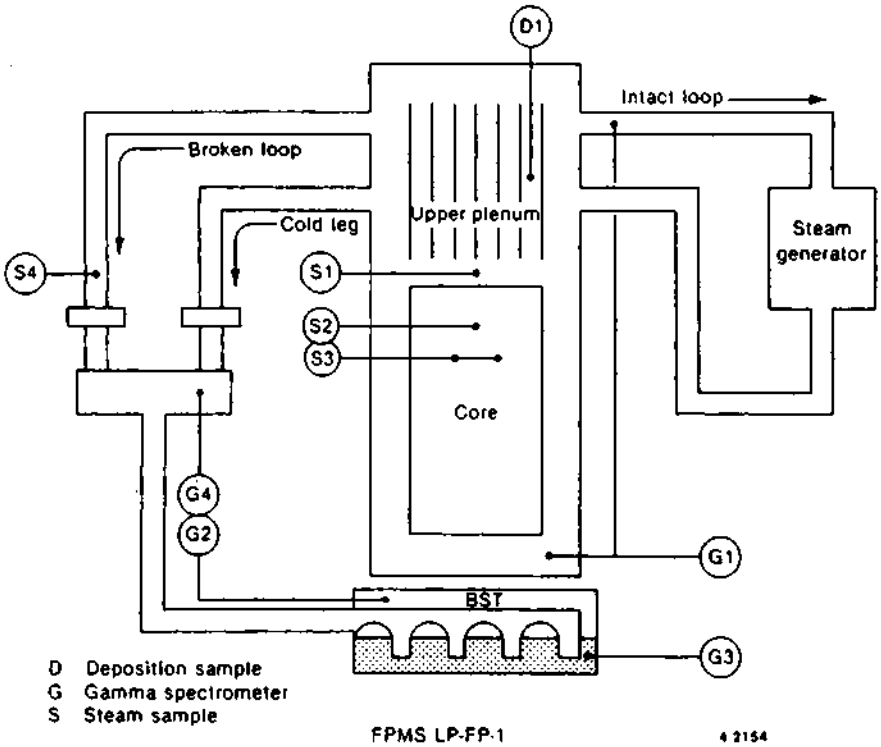

Figure 6.5. LOFT experiment FP 1, fission product sampling and measuring instrumentation (Schuster, 1990; Copyright OECD, 1991, The OECD/LOFT Project: Achievements and Significant Results, 9th–11th May 1990, Madrid, Spain. Reproduced by permission of the OECD)

the fuel was discussed, but was not carried out because of the difficulties associated with a representative doping of the simulant materials. From the data of burnup and heat rating, a Cs : I atom ratio in the fuel of 6.5 and in the gap of 3.0 was calculated using the code ORIGEN 2; using the same methodology, a fission gas release from the fuel during the pre-irradiation period of 1.2% was calculated. The experimental sequence of this fission product release test FP1 corresponded to a large-break loss-of-coolant accident with both cold-leg and hot-leg injection of the emergency coolant, which corresponded to the safety design of KWU-type PWR plants. During execution of the experiment, emergency coolant injection was intentionally delayed in order to ensure ballooning of the cladding and failure of the pre-pressurized rods. As the result of an unplanned water injection into the upper plenum of the reactor pressure vessel right before the scheduled time of fuel rod failure, only 8 out of the 22 designated rods failed. Moreover, in the following phases of the experiment various difficulties in the operation of the measuring and sampling systems occurred, with the consequence that not

all the experimental data intended could be obtained. Nevertheless, the results obtained in this integral experiment have to be judged a valuable supplement to those of the laboratory experiments in which specific phenomena of the accident sequence were studied.

As a consequence of the comparatively high linear heat ratings the fuel rods experienced during their pre-irradiation period, their relative gap inventories of the noble gases, halogens and alkali elements (related to the total rod inventory) were considerably higher than in a commercial LWR fuel rod (see Section 3.2.4.). Quantitative calculations of the gap inventories were difficult to perform because of the lack of experimental data on such high-rated rods. Estimates yielded figures of 10% for iodine (uncertainty range 5 to 20%) and 12% for cesium (uncertainty range 6 to 24%). Because of the local temperature differences along the fuel rod immediately before cladding failure, probably only a fraction of the gap inventories of iodine and cesium isotopes was in the gaseous state. On the other hand, the short time interval between cladding failure and quenching of the reactor core by the injected emergency coolant did not allow for a significant axial migration of the volatile fission products in the gap. For this reason, only a comparatively small fraction of the gap inventories had been expected to escape from the failed rods during the burst phase, amounting to about 20% of the cesium and 12% of the iodine gap inventories.

In spite of the incompleteness of the measured data, caused by the above-mentioned failures of part of the instrumentation, it was shown that during the burst and refill phases (both phases could not be separately evaluated due to difficulties in instrumentation) the release fractions from the failed fuel rods amounted to 1.3% of the ^{133}Xe, 0.8% of the ^{131}I and 0.2% of the ^{137}Cs inventories of the failed rods. For the fission product noble gases, this fraction represented more than 90% of the total amount released over the course of the entire experiment, for iodine about 60% and for cesium about 10%; the remainder of these radionuclides was transported to the coolant during the subsequent leaching phase, which in this experiment was conducted for about 12 hours.

As can be concluded from these results, the fission product release fractions from failed fuel rods measured in the LOFT experiment are significantly higher than the values measured in the laboratory experiments discussed in Section 6.2.1.1., and also considerably higher than those measured in the in-reactor ISOLDE tests. This effect is the result of the comparatively high heat ratings of the fuel rods during pre-irradiation, resulting in the buildup of a gap inventory which is considerably higher than in fuel rods operated under typical LWR conditions. This assumption is supported by the observation that the measured ratios of $^{131}I : {}^{133}I$ in the released iodine fraction were significantly higher than is to be expected from a gap inventory that has been exclusively generated by the recoil mechanism. Apparently, in these fuel rods migration of fission products in the thermal gradient from the fuel pellet to the gap provided a significant contribution to the gap inventory, additionally resulting in a partial depletion of the shorter-lived iodine isotope ^{133}I. Besides the enhanced gap inventory, the increased fragmentation of the fuel pellets resulting from the unplanned water injection onto the already overheated

fuel rods, might also have contributed to the higher release of fission products from the failed fuel rods.

The results reported by Schuster (1990) also include information on the transport behavior of iodine and cesium in the primary circuit. Unfortunately, no detailed statements are possible on the fractions of these elements deposited on the structures of the upper plenum of the pressure vessel and in the sampling lines, because of problems in the analysis of the deposition coupons. The results of measurements of several protected coupons suggested that about 10% of the total iodine released from the reactor core was plated out onto the structures during the burst and refill phases. The gamma spectrometric evaluation of the iodine-selective filters installed at the sampling positions S2 and S4 showed that during the burst and refill phases about 85% of the fission product iodine was transported attached to aerosols; only 7% was detected at the CdI_2 filter section and was interpreted as elemental I_2. The filter section equipped with a silver-impregnated molecular sieve contained about 8% of the iodine transported in this phase. However, it seems questionable whether this fraction can be interpreted to be an organoiodine compound; more probably, it represents aerosol or elemental iodine material which had passed through the preceding filter sections.

The Cs : I atom ratios measured at the different sampling positions were in the range 2.0 to 3.5, roughly corresponding to the ratio of 3.0 which was calculated for the gap inventory of the failed fuel rods. These measured values strongly support the assumption of iodine transport in the primary circuit as CsI species.

From the iodine fractions measured in the liquid and in the gaseous phases of the blowdown suppression tank, an iodine partition coefficient of 77 at a pH of the water phase of 4.8 was calculated. This figure agrees reasonably well with the experimental data obtained, for example, by Richter et al. (1985) at a pH of 5.3 and a water temperature of 100 to 200 °C; however, because of the low pH of the water phase, its applicability in the modelling of iodine behavior in the containment seems questionable. Moreover, the particular geometry of the blowdown suppression tank, in which the volume ratio of the gas to the liquid phase was considerably smaller than in a real reactor containment, presumably influenced the iodine partition coefficient.

During the recirculation phase, which lasted for 12 hours, 0.3% of the iodine inventory and 1.3% of the cesium inventory of the failed fuel rods were dissolved in the coolant. These figures are also within the expected range.

Summarizing the results of this integral reactor experiment, one can conclude that the iodine and cesium release fractions from the failed fuel rods were significantly higher than those measured in the laboratory experiments, an effect which can be explained by the particular mode of pre-irradiation of the LOFT fuel rods. The other measured data agree well with the results derived from the laboratory investigations (with the exception of the iodine partition coefficient measured in the blowdown suppression tank). Incorporation of these data into an accident model as a supplement to the laboratory results, therefore, will lead to reasonably conservative results on the fission product release and transport in a large-break LOCA design basis accident.

6.2.1.4 Release of fission products from the containment

The containment steel shell of the reactor containment normally shows very small leaks originating in the manufacturing and construction processes. For example, in German PWR plants the air leak rates through these leaks are allowed to amount to 0.25% of the containment free volume per day; in practice they are considerably lower. These figures have to be verified by appropriate leak tests which are to be performed in the course of commissioning of the plant as well as at regular intervals during in-service inspections. In the guidelines to be used in accident analyses (e. g. in the German "Störfall-Berechnungsgrundlagen") it is postulated that during a loss-of-coolant design basis accident, airborne radionuclides will be released from the containment to the annuli at a rate that is identical with the maximum allowed leak rate mentioned above.

There is no doubt that the penetration rate of noble gases through small leaks is identical to that of air, but this does not necessarily apply for other substances also. Early investigations at the US Containment Systems Test Facility (CSTF), an 850 m^3 experimental vessel, indicated that addition of steam to the containment air results in a decreasing leak rate because of a plugging of the small natural slits present in the steel shell by condensing water (Witherspoon, 1970). Aerosols present in the leaking atmosphere will also be retained in such small slits, a phenomenon which is well known from non-nuclear technology, as was described in the summary paper of Morewitz (1982). Plugging of slits by aerosols is only to be expected at the higher aerosol concentrations which will appear in the course of severe core damage accidents (see Section 7.4.3.1.); at the much lower aerosol concentrations occurring in a design basis accident, steam condensing in the slits will support aerosol retention. Experiments at the CSTF vessel (Witherspoon and Postma, 1971; Hilliard and Postma, 1981) showed that small concentrations of iodine and cesium are also efficiently retained during passing of the leak flow through narrow slits. Using artificially-made leaks (since the natural leaks in the CSTF vessel had been completely plugged by steam), attenuation factors of 0.076 and 0.011 (airborne mass penetrating leak path divided by airborne mass entering leak point) were measured for iodine and cesium, respectively, during the first 2 hours of the experiment. Gaseous I_2 present in the containment atmosphere will be retained due to chemical reactions in the leak path (see Section 7.4.3.1.).

Due to the broad variety in the characteristics of leak paths potentially present in a real steel shell, generally valid quantitative retention factors are difficult to establish. As yet little attention has been paid to the essential retention mechanisms. In spite of this lack of knowledge, it can be assumed that natural leaks in steel or concrete with their irregular crack shapes will show higher retention factors than artificial leaks with the same air leak rate, because of the larger contact area and the resulting higher significance of inertial effects on particle deposition. In addition, taking into account the plugging effect of steam, it can be expected that the leak rates of airborne iodine and cesium from the containment under loss-of-coolant accident conditions will be lower by a factor of 100 or more than a test leak rate of the containment steel shell measured with air.

6.2.1.5 Retention of fission products from containment air under accident conditions

Following a loss-of-coolant accident, a fraction of the radionuclides released from the primary circuit remains airborne in the containment atmosphere, as was discussed in the preceding sections. In order to reduce the airborne activity concentrations, standby filters are installed in the annulus of the German PWR plants, consisting of aerosol filters and iodine filters. In the German RSK Guidelines a retention efficiency of 99.9% for particulate iodine, of >99.99% for I_2 and of >99% for organoiodides is required under accident conditions. In certain other countries, the specified iodine species as well as the required retention efficiencies differ somewhat from these values.

The radionuclides present in the form of aerosols are very efficiently retained in the particulate filters (so-called HEPA filters); the differences in temperature and humidity of the atmosphere to be filtered under LOCA conditions compared to normal operation conditions do not adversely affect the retention effectiveness of these aerosol filters. Retention of radioiodine poses greater problems, since this radionuclide in principle may appear in the atmosphere in different chemical forms such as iodide aerosol, elemental iodine and organoiodide compounds; this applies to normal operation conditions in the same manner as to the conditions following a LOCA event. Moreover, because of the high radiotoxicity of its isotope ^{131}I, only very low radioiodine concentrations in air can be tolerated. For this reason, airborne iodine has to be retained very efficiently on filters guaranteeing permanent fixation of this comparatively long-lived isotope, both during normal operation of the plant as well as in the case of a design basis accident. Therefore, techniques for trapping the various forms of radioiodine from gas flows have been thoroughly investigated since the early days of nuclear technology. Summary papers on the techniques and problems of iodine filtering from air have been published by several authors, e. g. by Kovach (1982) and by Wilhelm (1982).

Aerosol iodides are also retained by the HEPA filters very efficiently. I_2 and HI present in gaseous form in the atmosphere are to a part trapped on the surfaces of aersosol particles, with the responsible mechanisms being adsorption or chemical reaction. However, early on it was recognized that a fraction of the adsorbed iodide may desorb again from these filters (e. g. Adams and Ackley, 1968), due to reactions of reversibly bound iodine with the flowing air, the water vapor or the impurities present in it. Thus, at higher concentrations of particulate iodine in air a special iodine filter has to be added to the particulate filter.

Traces of elemental I_2 in air are readily adsorbed onto beds of activated charcoal, with physical adsorption and chemisorption being the responsible mechanisms. Because of the strong adsorptive binding, the high porosity, the favorable pore structure and the extremely large inner surface of many charcoals (approximately 800 to 1000 m^2/g, according to BET measurements), the physical process of adsorption itself constitutes an important retention mechanism, even in humid air. Functional groups which are present on the charcoal surface (e. g. phenolic or other alcoholic hydroxyl groups) may react with the iodine to create a chemical

bond. Irreversible adsorption of I_2 can be assumed with only minor reservations in the low and intermediate temperature range as long as the charcoal is loaded with relatively small amounts of iodine. This is true under the conditions usually prevailing during plant normal operation. Substantial temperature increases (to above 120 °C) may lead to the desorption of considerable fractions of the adsorbed radioiodine, unless the desorption processes are suppressed by appropriate impregnation of the charcoal (see below). Organic compounds present in the gas to be purified may also be adsorbed onto the charcoal filter and thus be available for chemical reaction with the iodine already retained; the resulting reaction products may desorb from the charcoal. In the latter case, however, desorption will proceed slowly, at least at comparatively low temperatures. When deep-bed charcoal adsorbers are used desorption may be insignificant because of the radioactive decay of ^{131}I on the filter bed.

The extent and strength of iodine retention on charcoal depends on various parameters, with one of them being the type of charcoal applied, in particular when higher temperatures have to be taken into consideration. Charcoals made from coconut shells generally show the best retention properties, probably due to their comparatively high potassium content which raises the pH, resulting in the conversion of adsorbed iodine species to non-volatile iodide.

Organoiodide compounds are only retained on activated charcoal to a sufficiently high extent when the humidity of the air flow is quite low (below 30% at ambient temperature); at higher humidities, water is preferentially adsorbed, seriously interfering with the adsorption of CH_3I. Moreover, after longer operation of the filter bed, the retention efficiency decreases considerably and the adsorbed CH_3I will desorb again. Early investigations have shown that this problem can be overcome by using impregnated charcoals; here, two different types have been developed. On charcoal impregnated with a solution of stable ^{127}I (e. g. KI or KI + I_2, so-called KI_3), CH_3I is retained by isotopic exchange according to

$$CH_3{}^{131}I + {}^{127}I \text{ (on charcoal)} \longrightarrow CH_3{}^{127}I + {}^{131}I \text{ (on charcoal)}.$$

This reaction consists of several steps starting with the diffusion of $CH_3{}^{131}I$ from the gas flow to the surface of the charcoal grains and from there into the pores, adsorption of $CH_3{}^{131}I$ and isotopic exchange with the KI impregnant, followed by desorption of $CH_3{}^{127}I$ and diffusion of this compound out of the pores and away from the grain surface. Due to the complexity of this process, which generally is an irreversible reaction of (pseudo)-first order, its progress may be influenced by several parameters.

Traces of CH_3I in air can also be retained on charcoal impregnated with organic amines, preferentially triethylendiamine (TEDA), with a chemical reaction between the two substances being the responsible mechanism. The retention effect is assumed to be due to the conversion of CH_3I into a quarternary ammonium salt which is fixed to the charcoal. TEDA-impregnated charcoal is reported to have a larger capacity for CH_3I uptake than KI-impregnated material, but is somewhat sensitive to degradation by an access of CO_2 from the flowing air.

The influence of different parameters on the CH_3I retention efficiency of KI-impregnated charcoal has been thoroughly investigated, e. g. by Deuber and Ger-

lach (1985). According to these studies, the retention efficiency increases linearily with increasing temperature in the range 20 to 80 °C; it is claimed that the direct influence of the temperature is small compared with its indirect influence due to the decrease in relative humidity of the gas flow. However, the direct temperature influence may also contribute to this enhanced retention, since the rates of diffusion as well as of isotope exchange and chemical reactions will increase with increasing temperature. On the other hand, the adsorption strength decreases with increasing temperature, resulting in a certain revolatilization of adsorbed iodine, although this effect will only be of significance at temperatures well beyond those to be expected both in plant normal operation and during the course of a design basis accident (Kovach, 1982). The retention efficiency declines exponentially with increasing relative humidity of the air flow over the range 20 to 100%; therefore, relative humidities in excess of about 70% should be avoided, e. g. by preheating the gas flow ahead of the filter bed. With increasing face velocity of the gas flow, the retention efficiency increases continuously; however, at higher flow rates the increase in retention efficiency declines due to the reduction in residence time of the particular gas volume on the filter matrix. Other parameters such as preconditioning time, injection time and purging time are of little influence on the retention behavior of the charcoal. For CH_3I concentrations in excess of 1 mg/m^3, the retention efficiency will decrease; however, since this value is far higher than the concentrations occurring in reality, this effect is not of relevance for practical purposes.

According to the results of detailed investigations (Wilhelm, 1982), the retention efficiency of activated charcoals does not depend on the iodine concentration in the gas flow; in particular, there is no indication of a decrease in efficiency in the regions of low and extremely low concentrations. Observed deviations from the adsorption curves at very low concentrations may be attributed to the presence of small amounts of difficult-to-retain species. When using charcoal impregnated with KI, loadings in excess of 0.1 mg methyl iodide and 1 mg elemental iodine per gram of charcoal should be avoided. However, these loadings are far higher than will be reached both during normal operation periods of the plant and in the case of a design basis accident, because of the low mass concentrations of airborne iodine. Thus, iodine loading is not the limiting parameter in the operation of an iodine filter.

Organoiodine compounds other than methyl iodide are also efficiently retained by impregnated charcoals. It has, however, been reported that at a BWR plant in the course of a refuelling period an unusually high penetration of iodine activity in the purge air flow through the filter was observed. Detailed investigations (Patzelt, 1983; Deuber et al., 1984) have shown that neither filter leaks nor ageing effects of the filter materials could have caused this effect; therefore, an unknown penetrating iodine compound was assumed to be responsible, but no detailed information on the nature of such a compound could be obtained. Since penetration of iodine through the filter mainly occurred when spent ion exchangers had been handled, the appearance of organoiodine compounds of an unknown composition cannot be ruled out.

According to the detailed investigations of Deuber (1986), KI-impregnated charcoals yield fully satisfying retention results under the conditions prevailing

during design basis accidents. Tests with different types of impregnated charcoal at 130 and 180 °C and relative humidities of 1 to 2% (dew point 30 °C) with a 25 cm charcoal layer (corresponding to a residence time of the air flow on the filter of about 0.5 seconds) exhibited retention efficiencies which were significantly higher than the required values. Comparable data were obtained at 30 °C and 100% relative humidity, which are the most probable conditions in the annulus stand-by filters during a loss-of-coolant accident. Such conditions are considerably less severe than those at which desorption of adsorbed iodine from impregnated charcoals will begin.

Revolatilization of deposited iodine species from the filter can be increased by radiation due to fission product decay in the filter; the radiation mainly originates from fission product noble gases trapped temporarily on the charcoal beds. This effect is reported to be caused primarily by the resulting increase in the filter temperature and only to a lesser degree by radiolytic reactions. In filters exposed during plant normal operation and during design basis accidents this effect, therefore, is not of relevance; only accident filters loaded with very high activities (much higher than those to be expected in the current models of design basis accidents and even of severe accidents) would be affected.

The iodine retention efficiency of impregnated charcoals is adversely affected by weathering and poisoning effects, in particular as a result of temporary or permanent adsorption of impurities present in the flowing air or by the deposition of dust. Ageing of impregnated charcoal is reported to be primarily caused by processes occurring within the charcoal which block the active sites of the material and to a minor degree by changes in the impregnant. Under the combined influence of oxygen and moisture, the retention efficiency can drop sharply, whereas material stored in a dry state and sealed undergoes only minor changes. During use, the sorbent in iodine filters is exposed to a number of pollutants which may reduce the retention efficiency. The effect of this dynamic ageing is much greater than that of static ageing and can in a comparatively short time lead to a sharp decline in retention efficiency, possibly to a level below the required minimum. The extremely large surface of the charcoal favors the adsorption, in particular, of traces of hydrocarbons present in the air, whose sources are mainly the organic paints used to cover the walls and structures of the containment. NO_2 formed in air under the influence of intense radiation fields may also act as a filter poison.

The effect of different pollutants on CH_3I retention on TEDA-impregnated charcoal has been studied by Wren and Moore (1991 a; 1991 b). Among the substances studied, NO_2 and SO_2 showed the strongest degradation effects. The reaction mechanisms of these pollutants, however, exhibit marked differences. NO_2 produces a stronger degradation in dry atmosphere than under humid conditions (about 60% relative humidity), presumably because the adsorbed water provides alternative adsorption sites for NO_2 to those provided by TEDA, leaving the TEDA impregnant able to adsorb CH_3I. In contrast, adsorbed water significantly increases the degradation effect of SO_2 on CH_3I retention (about 70% relative humidity), with the reason for this synergistic reaction probably being the formation of H_2SO_4 on wet charcoal which subsequently reacts readily with the TEDA impregnant.

As has been mentioned above, the retention efficiency of impregnated iodine filters can be affected by different parameters such as filter design, operating conditions, and the quality and current condition of the sorbent. A wide range of impregnated activated charcoals is available and it is essential to demonstrate the efficiency of the material to be used by means of appropriate tests. In principle, three different kinds of tests have to be distinguished: qualification tests of fresh charcoal batches, tests of the retention efficiency of charcoal which has been in operation in a filter for a certain period of time and, finally, in-place testing of an entire filter. The tests have to be carried out under conditions which simulate the most adverse operating conditions for a given iodine filter. In addition, standard tests are needed to compare the retention efficiency of different batches and types of iodine sorbents.

For the batch tests to be conducted in a laboratory device, charcoal samples of about 25 ml volume have to be used. Taking a representative sample from fresh charcoal batches poses no problems, quite in contrast with the sampling of charcoal from an operating filter bed. Usually, pollutants are unevenly distributed in the bed; taking larger samples, however, might endanger the integrity of the filter bed. For this reason, so-called control filters are often installed in a bypass to the operating filter, in which samples are exposed under identical conditions to those of the operating filter (time, number of air changes, atmosphere, temperature etc.) and can then be removed as a whole for testing.

Besides deficiencies in the properties of the charcoal material (which should be discovered by the batch tests described above), the performance of the whole filter can be impaired by leaks, e. g. between the charcoal and the filter housing, or by channels in the charcoal layer. Because of the usually low iodine activity concentrations in the air to be cleaned and the high decontamination factors achieved by the filters (on the order of 10^4), routine iodine measurement downstream from the filter will often give results below the detection limit, yielding a minimum value for the retention efficiency which, however, is sufficient for routine control. In order to obtain more accurate results, in-place tests are conducted in which a measured amount of a test agent is injected into the air flow upsteam from the filter, and the fraction penetrating the filter is measured at its exit. To keep the required amount of test agent as small as possible, sampling and measuring devices of high sensitivity have to be employed.

In virtually all cases, ^{131}I-labeled methyl iodide is applied as a test agent for the quality control of impregnated charcoal materials as well as for in-place filter testing. Usually, this compound is prepared by reaction of $K^{131}I$ of high specific activity with dimethyl sulphate in aqueous solution. Following purification of the reaction product by distillation, it is condensed in an appropriate steel flask. Due to the high volatilty of CH_3I and the high radiotoxocity of ^{131}I, all the reactions have to be carried out in gas-tight boxes with thorough filtering of the off-gas going to the stack. Particular care is needed when comparatively large CH_3I batches are synthesized (10 to 100 MBq) for in-place testing of plant filters; in the transport of the test agent from the laboratory to the plant special containers have to be used in order to prevent losses by leaks, as well as to minimize radiation exposure.

Under extreme filtration conditions (temperature >150 °C), impregnated charcoals suffer from an increasing desorption of radioiodine. For such severe conditions other iodine filter materials have been developed such as silver-containing inorganic sorbents which exhibit a very low desorption of iodine even under extreme conditions, since the adsorbed iodine is bound as the very stable chemical compound AgI. However, such conditions are far more severe than those to be expected in design basis accidents; there is no need, therefore, to replace the impregnated charcoals by these expensive materials.

6.2.2 Break of a transducer line

In this design basis accident scenario it is anticipated that a transducer line with an internal diameter of about 15 mm will break while it contains primary coolant at system temperature and pressure (300 °C, 16 MPa). As to the stages in this type of accident, it is stated in the German "Störfall-Berechnungsgrundlagen" that such a break will result in a flash evaporation of the coolant volume escaping from the leak into the transducer compartment (which is located outside the containment steel shell), in the course of which a significant fraction of it will be instantaneously converted to steam. The magnitude of this fraction is determined by the enthalpy balance of the escape process and amounts to about 50% in this particular case. While it is assumed that the fission product noble gases present in the escaped primary coolant volume will be transported quantitatively to the gas phase, it is postulated in the guidelines that iodine and the other solid radionuclides will not be volatilized, but will be transported to the steam phase in accordance with the steam moisture fraction (droplet entrainment). Taking into account that the remaining liquid fraction contains about double the activity concentration as compared with the original primary coolant, it is stated that the mass-related activity concentration of the steam (steam moisture included) amounts to 10% of that of the escaped, non-evaporated coolant fraction. Moreover, it is postulated that the airborne halogens are present to 10% as gaseous I_2 (in the case of iodine) and to 90% as aerosols. The airborne radionuclides are transported with the steam flow to the annulus air extraction system, where retention by the filters (see Section 6.2.1.5.) can be assumed depending on the filter characteristics. The activity concentrations postulated to be present in the primary coolant at the moment of the accident were defined according to a conservative evaluation of operational experience. In case the accident leads to a shutdown of the reactor, then the associated fission product spiking also has to be taken into account. In this context it has to be assumed that the radiologically most important radionuclides ^{131}I, ^{134}Cs and ^{137}Cs show an exponential increase in their activity concentrations, with a doubling time of 10 minutes up to a peak value that is higher by a factor of 30 than the preceding steady-state value. Finally, it is postulated in the guidelines that the broken line can be isolated from the primary circuit no later than 30 minutes after the accident occurs.

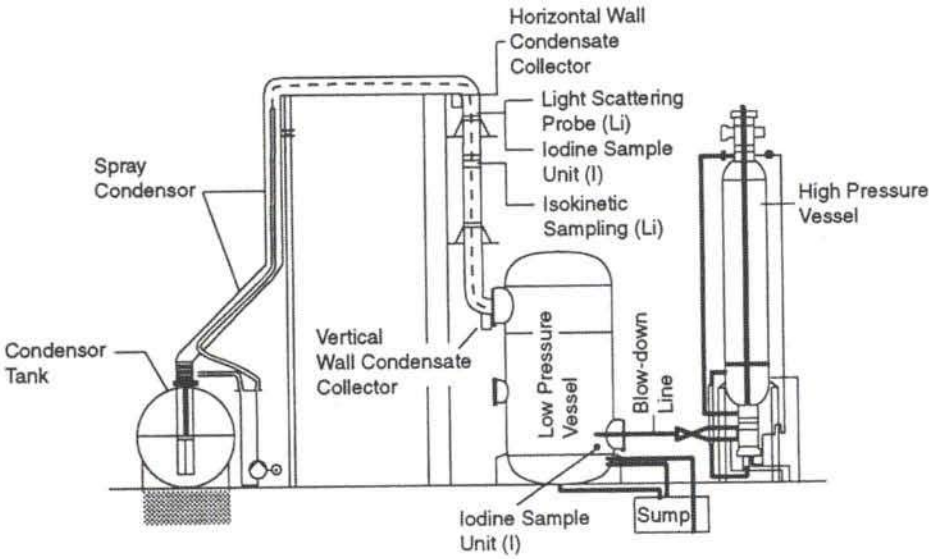

Figure 6.6. Investigation of fission product behavior during flash evaporation of PWR primary coolant
(Hellmann et al., 1991)

To be sure, flash evaporation of water in the course of which about one-half of the solution is evaporated within an extremely short time interval is a rather strange process with regard to the behavior of substances dissolved in the original solution. Similar flashing phenomena would occur in the event of a steam generator tube rupture accident, but under somewhat different conditions; this scenario will be treated in Section 6.2.3. Due to incomplete knowledge of such processes, highly conservative assumptions have been made in the past in some accident consequence analyses. In particular, partitioning of fission product iodine between steam and liquid phases under such conditions is difficult to evaluate; thus, it was occasionally estimated that the fraction of iodine volatilized would be identical to the steam fraction generated. It is obvious that reliable results can only be obtained by appropriate experiments which, because of the complexity of the problem, have to be carried out in a technical-scale apparatus in which all the parameters involved (temperature and pressure differences, flow rate of the medium at the leak, expansion volume) can be reproduced in a realistic manner.

Morell et al. (1985) as well as Hellmann et al. (1991) reported on such technical-scale experiments using an experimental setup which is schematically shown in Fig. 6.6. From a high-pressure vessel, water at 310 °C, 10 MPa and doped with an appropriate tracer is supplied to a 15 mm diameter orifice simulating the break in the transducer line, from where it expands into a 50 m^3 vessel initially kept at ambient temperature (which in the course of the experiment increased to about 100 °C) and pressure; this volume roughly corresponds to that of a transducer compartment. The steam produced in the flash evaporation process is carried off

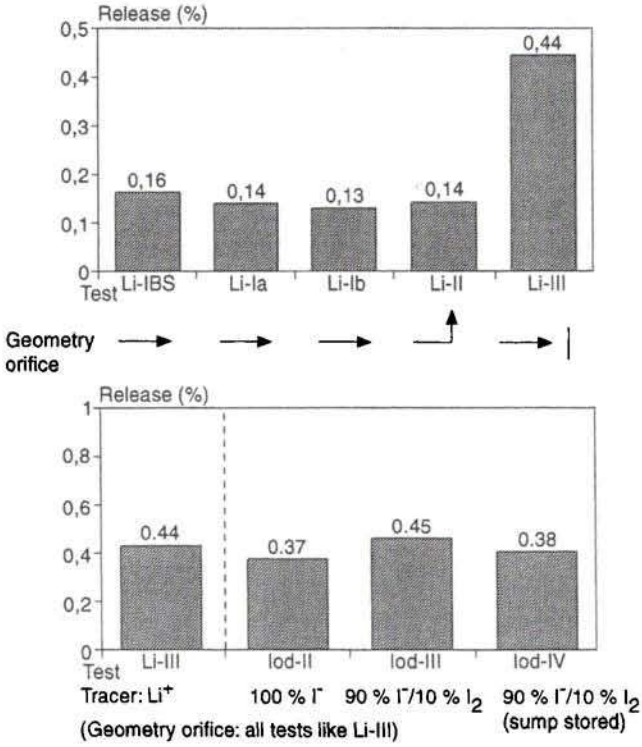

Figure 6.7. Fission product entrainment by steam during primary coolant flash evaporation (Hellmann et al., 1991)

by an exhaust pipe in which isokinetic sampling devices are installed in order to obtain analytical samples from the steam flow, including the finely dispersed liquid droplets carried by it; in addition, collector positions are provided to sample the vertical and horizontal wall condensates, the composition of which may differ from that of the flowing steam. Finally, the entire steam flow is condensed; from the condenser tank additional analytical samples were taken, as well as from the sump generated in the low-pressure vessel, in order to obtain a mass balance of the amount of tracer element added.

In a flash evaporation the liquid is atomized, forming very fine droplets with diameters of less than 20 μm which will be transported in part by the steam flow; these droplets are the carriers of non-volatile radionuclides. In order to determine the extent of entrainment, Li^+ was used as a non-volatile tracer in these experiments. The results of the experiments performed over periods of more than 30 minutes each (in order to obtain information on the initial discharge phase as well as on the steady-state phase) showed an entrainment of liquid with the steam to the condenser tank on the order of 0.2% (related to the total amount of tracer used), independent of the geometrical position of the orifice (in a horizontal or a vertical direction; the arrows shown in Fig. 6.7. indicate schematically the direction

of flow). When an impingement plate was placed a short distance in front of the orifice (the distance was equal to twice the diameter of the orifice) to simulate a wall at close distance, entrainment increased to about 0.4% (see Fig. 6.7., experiment Li-III) and to 0.6% when the wall condensates were included in the balance. A part of the droplets initially entrained was plated out in the pipe, joining the condensate films on the vertical and horizontal walls. When expressed in terms of the "Störfall-Berechnungsgrundlagen", the mass-related tracer concentration of the steam phase (including moisture) amounts to 0.3–0.8% of that of the escaped, non-evaporated coolant fraction.

The behavior of iodine in the flash evaporation process is expected to be more complex. Iodide present in the ionic dissolved state in the primary coolant is a non-volatile species under such conditions and it can be assumed, therefore, to behave in the same manner as other non-volatiles, e. g. the Li^+ tracer. On the other hand, a partial oxidation of I^- by air during the flashing process cannot be ruled out, which would lead to the formation of volatile I_2 and/or HOI, resulting in a transport with the steam which would be higher than with pure droplet entrainment. In the course of the technical-scale tests mentioned above, experiments were also carried out using ^{123}I tracer. Since these measurements yielded results that were virtually identical with those of the Li^+ tracer tests, it can be concluded that no significant amounts of volatile iodine are produced in the flash evaporation process. Even when a fraction of the ^{123}I tracer (up to 10%) was added as I_2 species to the solution to be flashed, no increase in the volatilization rate was observed, indicating a complete hydrolysis and/or reduction of I_2 during its short residence time in the line between the tracer injection station and the orifice (see Fig. 6.7.). Thus, the iodine release of 10%, which was assumed in the "Störfall-Berechnungsgrundlagen" as a basis for the calculations, is too high by a factor of at least 10; the realistic value of less than 1% is valid for all fission products present in the original primary coolant with the sole exception of the fission product noble gases.

It is suspected that, besides I_2 and HOI, hydroiodous acid HI can, in principle, contribute to iodine volatility in a transducer line break. HI is a strong acid which in dilute aqueous solution is highly dissociated. However, according to the equilibria

$$H^+ + I^- \rightleftharpoons HI_{aq} \rightleftharpoons HI_g$$

a small amount of the molecular compound is always present in solutions containing H^+ and I^- ions which, in turn, may result in an equilibrium HI concentration in the gas phase above the solution. Gwyther and Turner (1989) have reported on calculations of the equilibrium constants at temperatures up to 300 °C, which were performed in order to obtain information on iodine transport to the vapor phase during steam generator tube rupture faults. Their results confirm that volatility of HI depends strongly on both the temperature and the pH of the solution. The product of the volume-related partition coefficient and the H^+ concentration was shown to depend exclusively on the temperature, decreasing from about $7 \cdot 10^{10}$ at 25 °C to about $2 \cdot 10^2$ at 300 °C. Thus, at a solution pH of 5 to 7, HI volatility is extremely low and its contribution to iodine carry-over can be neglected, even when one takes into consideration that the non-ideality of behavior of this compound in steam at higher temperatures would potentially result in somewhat higher volatil-

ization rates than the results of thermodynamic calculations would indicate. The results of the calculations, therefore, do not contradict the experimental findings discussed above.

Similar results concerning the behavior of non-volatile substances during flash evaporation after coolant release from a small-diameter pipe have been reported from the Canadian WALE (Water Aerosol Leakage Experiments) program (Fluke et al., 1990 a; 1990 b). The purpose of these WALE test series was to clarify aerosol behavior under flashing conditions over a wider range of variables than the above-mentioned KWU tests and to characterize the resulting aerosols in greater detail. In spite of differences in the experimental setup (e. g. the low-pressure vessel in the WALE tests was 19 m^3, different geometries of the nozzle), the cesium tracer fraction carried with the steam was small, typically less than 1%, i. e. in the same range as in the KWU tests discussed above. Only in particular cases where there was a direct line-of-sight between the nozzle and the vessel vent, were larger carry-over fractions of cesium tracer observed; however, even in these unfavorable cases, the carry-over was less than 3%. By placing an obstruction plate near the vent take-off location, blocking the line-of-sight with the nozzle, the carry-over fraction was significantly reduced. This effect obviously was due to the removal of larger droplets from the steam phase, since the amount of cesium tracer measured in the steam samples (representative of fine particles with diameters less than 2 μm) was about the same, regardless of whether the obstruction plate was in place or not. Differences in the residence time of the steam in the low-pressure vessel (between 70 and 900 seconds) did not result in a significant impact on the steam-borne fraction of the tracer.

More detailed examinations revealed that there were two droplet populations, one having a size of a few to a few tens of micrometers, the other with a droplet size of less than about 2 μm. The release of the fine particles was observed to be maximized when the discharge enthalpy was high and when the impingement plate was at a short distance from the nozzle. This fine aerosol was formed by the flashing process itself and not by any secondary interactions such as splashing; it comprised up to half of the total tracer released through the vent. Separation of the bulk of the water droplets occurs rapidly and apparently very efficiently; observations made in this context suggested that mixing and transport within the vessel occurs very quickly (i. e. on the order of seconds). Such a rapid separation of the liquid and the steam phases cannot be explained by gravitational settling of the aerosols; it is, therefore, assumed that direct impingement upon surfaces in the vessel is the dominant removal mechanism.

From the excellent agreement between the results of the WALE tests and the KWU experiments, as well as from their weak dependence on the different experimental conditions, it can be concluded that the results mentioned above, showing low fission product transport in the flash evaporation process, are generally applicable for different dimensions of the compartments in which the break of a line occurs as well as for a wide range of break conditions, geometries and locations.

The liquid water fraction that escapes from the break during the accident remains on the floor of the transducer compartment as an open shallow pool, from which radionuclides can potentially be released to the atmosphere. This situation of an open pool inside a building is common to several design basis accidents.

Regarding non-volatile radionuclides, transport from the aqueous phase, which is at a temperature well below its boiling point, to the atmosphere can only proceed by the formation of small water droplets caused by an air flow over the surface of the liquid phase. As yet few experimental studies of the radionuclide release rates from a liquid phase under such conditions have been performed. Some information on this question can be extracted from experiments on the release of americium and europium from unperturbated solutions arising in the context of nuclear fuel reprocessing (Moon et al., 1984). From a 5 M hydrochloric or nitric acid solution containing 0.06 M ^{241}Am/l or 0.13 M Eu/l, with a total volume of 25 ml and a free surface area of 27 cm^2, carry-over rates of $3 \cdot 10^{-15}$ g Am/h · cm^2 and of $2 \cdot 10^{-12}$ g Eu/h · cm^2 (averaged over the duration of the experiment) were measured. In spite of a broad scatter of the individual data, a tendency for the initially relatively high release rates to decrease within about 50 hours to a lower steady-state value could be seen; the decrease was more pronounced in hydrochloric acid solutions than in nitric acid solutions. This steady-state value remained constant over a longer period of time for hydrochloric acid solutions, while in nitric acid solutions a new increase occurred when the solution was exposed to daylight. According to the explanations given by the authors, the escape of dissolved gases from the solution is the main transport mechanism for the release of the non-volatile radionuclides. The higher initial release rate from the hydrochloric acid solution is attributed to the higher vapor pressure of dissolved HCl, whereas the subsequent increase in release from the nitric acid solution is assumed to be caused by photolytic decomposition of HNO_3 and the escape of nitrous oxide gases from the solution. These findings suggest that the release of non-volatile radionuclides from an unperturbated solution is mainly the result of a mechanism not to be found in the shallow pools arising in the course of a design basis accident. Therefore, the results of these experiments cannot be directly applied to the release of non-volatile radionuclides from open surfaces in pools and sumps in a light water reactor; nonetheless, they show that the release rates of the non-volatile radionuclides will depend on the extent of formation of micro-bubbles either by the escape of dissolved gases from the liquid or by the velocity of flowing air above the surface. In summary, it can be assumed that the experimental data given above represent upper limits for the release rates of non-volatile radionuclides from unperturbated solutions with a chemical composition typical for light water reactors.

Fission product iodine present in the pool water is assumed to show a more complicated behavior. The iodide species originally present in the primary coolant can be considered as non-volatile and will behave, therefore, in the same manner as, for example, Li^+ and Cs^+; however, it cannot be ruled out that I^- will be in part oxidized by air, forming volatile I_2. Since the compartments in the annuli (and also in the nuclear auxiliary building) are not closed systems, but have a normal air circulation, the principles of calculation of I_2 volatilization using an equilibrium partition coefficient cannot be applied. Assuming an instantaneous iodine partitioning according to the equilibrium values would result in a drastic overestimation of iodine release, since I_2 transport from the liquid to the gas phase is controlled by kinetics. The main characteristic in this context is a boundary layer at the interface between the sump and the gas phase, which is saturated with iodine in accor-

dance with the partition coefficient. This means that the establishment of the I_2 equilibrium in the gas phase moving parallel to the phase boundary applies only to a boundary layer (the thickness of which is determined by the flow characteristics of the gas phase) and not to the whole moving gas phase. Thus, iodine carry-over from the pool water to the atmosphere is controlled by three parameters: the rate of iodide oxidation, the state of the I_2 hydrolysis equilibrium in the liquid phase and the kinetics of I_2 transport from the liquid to the gas phase. The methods to be applied for the theoretical treatment of iodine volatilization under such conditions will be discussed in Section 7.3.4.3.

In their evaluation of possible iodine releases from open pools, Bawden et al. (1983) have distinguished between two conceivable cases: Firstly, an open shallow pool which may evaporate to dryness over a relatively short time period, so that the evaporation rate of the water is greater than the iodine volatilization rate, resulting in iodine concentrating to higher than tracer levels in the remaining water volume. In the second case, a deep pool is assumed from which water evaporation losses are so small that a significant increase in the iodine concentration in the water phase will not result. In both cases, it is assumed that no iodine volatilization occurs as long as reducing conditions are maintained in the water phase. When iodide oxidation cannot be ruled out (which, however, proceeds at a slow rate under such conditions), then in a shallow pool iodine will concentrate to a level where, finally, elemental iodine I_2 is the only species present; the appropriate volume-related partition coefficient for such conditions can be assumed to be 80 at 25 °C. It is admitted that this is a very conservative assumption which may be pessimistic by several orders of magnitude. In a deep pool, no significant increase in the iodine concentration is to be expected; thus, it is claimed that for the tracer levels (oxidation of iodide included) a volume-related partition coefficient of 10^4 is appropriate. In practice, the shallow pool alternative is highly unlikely; after such an accident, all efforts will be made to remove such a water pool from the compartment floor prior to extensive evaporation. For untreated primary coolant an initial organoiodide percentage of $<<0.1\%$ is estimated, and these compounds are assumed to show a volume-related specific partition coefficient of 3 at 25 °C (specific value for CH_3I).

Hellmann et al. (1991), in their experiments mentioned above, also measured the extent of iodine volatilization from the sump remaining in the low-pressure vessel after termination of a flash release test. From these measurements, a volume-related partition coefficient of about $2 \cdot 10^5$ was calculated at a water temperature of 60 to 80 °C, resulting in an iodine volatilization of less than 0.1% within 10 hours under the conditions prevailing in a transducer compartment. Thus, iodine release from the sump formed by the escaped primary coolant can be neglected in the evaluation of the consequences of such an accident.

6.2.3 Steam generator tube rupture accidents

In a pressurized water reactor, the steam generator heating tubes represent the barrier between the radioactivity-containing primary coolant and the secondary-side water–steam circuit, which usually is free of radioactivity. In the event of a

small leak in one of these tubes, primary coolant will be transported at a small rate (several milliliters to several liters per hour) to the steam generator secondary-side water. Fission product noble gases present in this primary coolant volume are immediately transported to the steam phase, whereas iodine, cesium and the other non-volatile radionuclides will remain in the water phase; only a small fraction of them, corresponding to the steam moisture content, will be transported in the direction of the turbine. Due to the action of the blowdown purification system, the radionuclide concentration in the steam generator water is kept low, so that it represents no handicap for plant normal operation (see Section 4.3.3.).

In the event of a sudden rupture of a steam generator heating tube, a primary coolant volume on the order of several Mg/h will escape from the broken tube. Because of the pressure difference between the primary and the secondary side, a flash evaporation of the escaping primary coolant will result during which a fraction of it will be spontaneously vaporized; in this respect, the escape mechanism of the coolant is quite similar to that in the case of a break of a transducer line (see Section 6.2.2.), with the difference, however, that the coolant fraction vaporized from the steam generator tube will be smaller (on the order of 10 to 15%), due to the smaller differences in temperature and pressure between the primary and the secondary side. Another difference is due to the fact that the flashing primary coolant does not enter into a free space, but into the water and steam-containing secondary side of the steam generator; as a result, the subsequent behavior of the radionuclides also depends on the location of the tube break, as is schematically shown in Fig. 6.8. If, in addition, it is assumed that the main condenser is not functional, the secondary side pressure will increase to values greater than the design limits; as a consequence, safety valves will open for a short time and volatile fission products might be released to the atmosphere. Non-volatile fission products mainly remain in the steam generator water, similar to the situation occurring in an operational tube leakage; a small fraction of them is transported to the main steam by droplet carry-over. When no additional faults occur simultaneously, the bulk of the droplets is retained from the main steam in the moisture separator and the steam dryer and only a fraction of 0.25% (conservative value) or $<0.1\%$ (realistic value) is transported via the steam dump system to the condenser. The rupture of a steam generator tube is immediately detected by the ^{16}N monitors; by this signal, a reactor shutdown or a reactor trip is initiated and, subsequently, the primary coolant pressure is reduced in order to decrease the escape rate of the coolant through the tube break. With regard to the secondary side, different procedures can be chosen; in order to preclude an opening of the safety valves with associated emission of steam to the environment, a continued transport of the steam from the steam generator via the turbine to the condenser has to be maintained for as long as possible. Finally, the affected steam generator is isolated from the water – steam flow; according to the German "Störfall-Berechnungsgrundlagen" (RSK, SSK, 1983), this isolation should be completed not later than 30 minutes after initiation of the accident.

Over the years several steam generator tube rupture accidents have occurred (see the compilation of steam generator tube faults in US PWR plants given by Adams and Sattison, 1990), none of which resulted in activity releases to the sur-

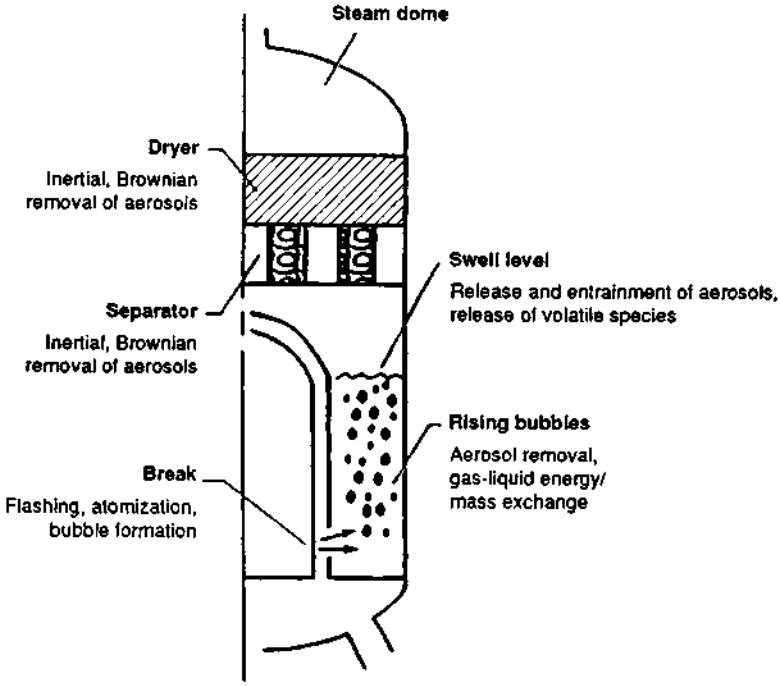

Figure 6.8. Activity transport and retention in a U tube steam generator showing tube rupture
(Kalra, 1990)

roundings exceeding or even reaching the regulatory limits. Due to improvements in materials and design and due to an optimized secondary-side water chemistry control, the risk of such a fault has been greatly decreased.

In the German "Störfall-Berechnungsgrundlagen" it is postulated that the steam generator tube rupture is a consequence of a break of the main steam line downstream from the isolation valve. Due to the increased steam transport, the steam dryers would be flooded 4 seconds after the onset of the accident and a water–steam mixture would be released through the break for 1 second until complete closing of the valve. The escaped mixture is assumed to be completely converted to saturated steam and moisture, with its iodine content consisting of 10% I_2 and 90% aerosol iodide. After closing of the main steam line valve, steam with a moisture content of 0.25% is assumed to be released via the blowdown valve, until the defective steam generator has been isolated.

In calculating the amount of fission products released to the secondary side together with the escaping primary coolant volume, the spiking that occurs as a consequence of the reactor shutdown or reactor trip has to be considered in addition to the preceding fission product steady-state concentrations in the primary coolant. In this context, it is important to take into account the timetable of the two events. As was described in Section 4.3.1.2., the doubling time of the concen-

trations of fission product iodine and cesium in the primary coolant during the first stages of the spiking amounts to about 10 minutes, quite independent of the mode of shutdown, i. e. during a planned shutdown it is virtually the same as that following a reactor trip. This means that in the course of the 30-minute time interval until completion of steam generator isolation, the fission product concentration in the primary coolant increases steadily from the preceding constant-load level to values higher by about a factor of 8, which is reached not earlier than at the moment of steam generator isolation. Thus, the peak activity concentrations occurring in the spike will reach the steam generator secondary side only after the completion of isolation; the radionuclides will be removed from the steam generator water by the blowdown purification system. It is possible that a spiking could occur prior to the tube rupture, so that the iodine (and cesium) concentration in the primary coolant would already be at an enhanced level at the moment of tube rupture. However, the probability of a simultaneous occurrence of these two events (which, in this case, are independent of each other) is extremely small, so that it can be ruled out in the evaluation of the consequences of a tube rupture. In order to get generally valid models of iodine release as enhanced by spiking, this effect has been analyzed in detail (e. g. by Adams and Sattison, 1990; Adams and Atwood, 1991), taking spiking data from a number of US PWRs as a basis.

The size of the droplets formed during flashing of the escaping primary coolant is an important parameter. These droplets are the carriers of non-volatile radionuclides; their transport behavior depends highly on the droplet size, since it is expected that small droplets (submicron size) will penetrate through the secondary-side pathways with much less attenuation than would larger drops. Experiments in which a simulated primary coolant flashed through tube breaks into a secondary-side environment under conditions where 10 to 15% of the primary coolant mass was converted to steam, showed that the type of break (open end vs. slit of equal flow area) does not significantly influence the resulting droplet sizes (Gieseke et al., 1985). For both tube leak configurations, mass median drop sizes in the range 20 to 60 μm were measured; it was estimated that less than 1% of the droplet mass was associated with droplets smaller than 2 μm. These measured droplet diameters are considerably larger than those obtained by calculations (e. g. Postma and Tam, 1978), which yielded values on the order of 2 μm. No significant influence on the droplet sizes of the pressure difference between the primary and secondary system was observed.

Because of its potential to form volatile species, the behavior of fission product iodine is of particular significance in this context. In Section 4.3.3. it was pointed out that both in the primary coolant and in the steam generator secondary-side water iodine is present as non-volatile iodide; the measured carry-over rates to the main steam are identical with those of fission product cesium, indicating that carry-over is exclusively effected by droplet transport (entrainment).

Detailed measurements of iodine partition coefficients from PWR primary coolant at 285 °C and 6.9 MPa (i. e. under secondary-side conditions) were performed in laboratory experiments by Clinton and Simmons (1987), using pure iodide solutions ($6 \cdot 10^{-11}$ mol/l) in boric acid solutions of various pH values between 4 and 9. The results showed a gross iodine partition coefficient that decreases with

increasing boric acid concentration: $4 \cdot 10^5$ in pure water (deaerated); $1.4 \cdot 10^4$ in 0.1 M H_3BO_3; and $4.3 \cdot 10^3$ in 0.2 M H_3BO_3 solution. At a constant boric acid concentration, the partition coefficient was found to be virtually independent of the solution pH. Given this behavior, it is questionable whether iodine volatility is caused by the formation of I_2 or of HI; in each case iodine volatility is small compared to droplet carry-over and, therefore, does not have to be taken into account in calculating iodine release from the steam generator water. For evaluation of iodine volatilization from the secondary-side water, the change in pH that occurs when primary coolant escaping from the ruptured tube mixes with the steam generator water potentially is of importance. Adams and Peterson (1993) calculated the pH that will be reached during the 30-minute transient after tube rupture, taking as a basis the current EPRI water chemistry guidelines for both primary and secondary coolant as well as the thermohydraulic conditions prevailing in different designs of US PWR plants. The results indicate that the pH of the secondary-side water decreases from an initial value of 8 to 9 to a final value of about 6.5, virtually independent of the particular PWR design.

The investigations reported on by Clinton and Simmons (1987) also showed that the presence of dissolved oxygen in the solution results in an iodine partition coefficient lower by a factor of about 10, apparently due to the formation of volatile iodine species. This effect might be of interest in a steam generator tube rupture accident which happens shortly before a planned shutdown of the plant, after hydrogen had been removed from the coolant and/or H_2O_2 had been added to reduce the primary circuit contamination and radiation dose rates. In order to cover such conditions as well, in the US Guidelines a total iodine partition coefficient of $2 \cdot 10^3$ has been specified for tube rupture accidents.

In experimental flash evaporations of very dilute iodide solutions, performed in a laboratory autoclave facility, the formation of small amounts of I_2 was observed (Beahm et al., 1990), with the magnitude of these fractions depending on the solution pH and on the I^- concentration in the solution. In an argon–steam atmosphere at 285 °C and with a 10^{-9} M pure I^- solution, the I_2 fraction amounted to about 2% at pH 5 (25 °C) and decreased to 0.44% at pH 7 and to 0.02% at pH 9; correspondingly, the total iodine partition coefficient increased from $7 \cdot 10^3$ at pH 5 to $4.8 \cdot 10^4$ at pH 9. In an air–steam atmosphere, the I_2 fraction was considerably higher, resulting in a correspondingly lower partition coefficient. In 10^{-4} M iodide solutions under an argon–steam atmosphere, however, the measured I_2 fraction amounted to 0.1% at pH 5 only with an associated partition coefficient on the order of $8 \cdot 10^3$. The mechanisms for the concentration-dependent formation of I_2 are not definitely known; however, there are some indications that surface reactions under the influence of residual amounts of oxygen present in the system may play a role. Even if these O_2 concentrations were very small, they could be on the same order of magnitude as the iodine trace levels. Test results showed that no I_2 was formed when the primary coolant initially contained its normal-operation H_2 content.

These experiments concentrated on iodine behavior under primary coolant conditions and did not take into account the mixing of the flashed primary coolant with the steam generator secondary-side water. Thus, it seeems highly unlikely that

the enhanced I_2 fraction at iodine trace levels will have any consequence for iodine transport behavior under steam generator tube rupture conditions.

In Section 4.3.1.2. it was mentioned that in the course of a shutdown spiking an increasing I_2 fraction in the primary coolant iodine content had been observed, rising to 20% of the total iodine at the spike maximum (Voillequé, 1990). If these I_2 concentrations in the primary coolant were in effect over the whole shutdown period, a gross iodine partition coefficient during flashing in the range 100 to 150 would result, i. e. significantly lower than the value stated in the US Guidelines. However, these values are also related to the pure primary coolant and do not take into account its dilution by the steam generator secondary-side water. Moreover, steam generator isolation will be completed well before the spike maximum is attained; for this reason, the reported I_2 buildup during the spiking does not seem to be of relevance in the analysis of iodine behavior on the steam generator secondary side.

In this accident sequence as well, the question arises as to the significance of undissociated HI as an additional potential volatile iodine species. Calculations taking into account the conditions in the hot primary coolant showed that under the prevailing conditions the equilibrium fraction of HI in the solution is very small and that this compound does not contribute noticeably to iodine volatility under flashing conditions.

As was mentioned above, in such a tube rupture accident two different situations can arise, depending on the location of the tube break, either below or above the level of the steam generator water phase. In each case, fission product noble gases will be immediately and quantitatively transported to the main steam and, finally, reach the condensate gas extraction system. The behavior of the other fission products, however, will be influenced by the location of the break. When the break occurs below the water level, it will be possible for the escaping primary coolant volume to homogenize with the circulating secondary-side water (see Fig. 6.8.); experience has shown that this position is the most probable break location. When, on the other hand, the break occurs above the water level (e. g. in the U-bend of a tube), the atomized primary coolant will be transported directly to the steam dome without intimate contact with the steam generator water; this situation can only occur when the water level has accidentally decreased, e. g. by loss of the feedwater supply. Several attempts have been made to model fission product behavior under these circumstances (Hopenfeld, 1985), including experimental investigations in model facilities. More recently, Kalra (1990) has summarized the results of model calculations and of experimental investigations using a model U-tube steam generator.

If the tube break is submerged, the flashing primary coolant will expand into the boiling water–steam mixture; a fraction of the droplets formed during flashing will be entrained by the rising steam bubbles which continuously exchange mass and energy with the surrounding water volume. As a result of various deposition mechanisms involved, the liquid aerosols in the bubbles will be scrubbed by the steam generator water. When the break location is at least a few meters below the water level, no primary coolant bypassing is assumed to take place; this means that the concentration of non-volatile radionuclides in the droplets reaching the water–

steam separator represents a complete mixing of the escaped primary coolant with the full secondary-side water volume. As long as no flooding of the steam separator and dryer occurs, the steam moisture content is reduced here to the normal operating value, i. e. to 0.25% (conservative value) or < 0.1% (realistic value). When, as a consequence of a simultaneous break of the main steam line, the steam separator and dryer are flooded, they will loose their retention effectiveness and a two-phase water–steam mixture will expand into the main steam line, with the water fraction showing the same radionuclide concentrations as the steam generator water phase.

Volatile fission product iodine, if present at all, would also be completely scrubbed from the rising steam bubbles, so that the vapor iodine concentration in the steam leaving the swell level (see Fig. 6.8.) would be at equilibrium with the secondary-side water. Thus, the iodine partition coefficient at such conditions will determine I_2 release to the steam. Using the data given by Lin (1981), which yield an iodine equilibrium partition coefficient in very dilute solutions of about 10^4, Kalra (1990) has calculated that the bulk of the iodine leaving the system is in the gaseous state, whereas the mass flow rate of non-volatile iodide is small. In these calculations, however, it was not taken into consideration that the above-mentioned partition coefficient data were measured using pure I_2 solutions at pH 7. In contrast, in U-tube steam generators the steam generator water is an alkaline and reducing solution, so that fission product iodide present in the primary coolant volume which enters the secondary side cannot be oxidized to form I_2. Consequently, it can be assumed that the species I_2 does not exist under secondary-side water conditions and that iodine carry-over to the steam phase proceeds exclusively by droplet entrainment, comparable to the situation in a leaking steam generator during plant normal operation phases (see Section 4.3.3.).

Bawden et al. (1983) assumed an iodine vapor separation factor in the faulted steam generator of $3 \cdot 10^4$ (best estimate value) or of $1 \cdot 10^3$ (conservative value). Thus, iodine volatility would be insignificant against 0.1% entrainment if the best estimate value is taken, but it would become comparable when the conservative value is used. Organoiodide compounds are not assumed to significantly increase total iodine volatility.

When the water level in the faulted steam generator secondary side is low and the tube break is not submerged, the flashing primary coolant will not mix with the secondary-side water volume and the droplets formed will be directly transported to the separator-dryer, together with the droplets formed on the boiling water level. Kalra (1990), who investigated this case, assumed that the retention effectiveness of the separator-dryer is one or two orders of magnitude lower than it is under steady-state operation conditions; he further assumed that the retention effectiveness is almost independent of the break height and relatively insensitive as well to the size distribution of the aerosols generated at break flow. In general, the presence of volatile iodine species seems highly questionable, since under the prevailing chemistry conditions I^- transported with the primary coolant to the steam generator secondary side does not have the opportunity to become oxidized; therefore, it should be possible to describe iodine carry-over in the same manner as the carry-over of non-volatile substances, i. e. by entrainment.

6.2.4 Fuel storage and handling accidents

In this accident scenario it is assumed that in the course of handling operations of spent fuel assemblies (e. g. in the spent fuel pool) an irradiated fuel assembly is damaged so that fission products are released to the pool water. In such a case, the fission product noble gases present in the gap of the defected rods are liberated; in addition, water-soluble fission products such as cesium and iodine isotopes will be leached from the gap of the damaged rods. A corrosive attack of the pool water on the fuel matrix resulting in a release of larger amounts of fission products from the failed rods can be ruled out, due to the comparatively low temperature of the pool water (30–45 °C). The radionuclides which become dissolved or suspended in the pool water are removed again by continuous cleanup of the water in the spent fuel pool purification system. As regards the consequences of such an accident, those fission products are of primary interest which can be transported from the pool water to the containment atmosphere, i. e. the fission product noble gases and, potentially, iodine. Considering the possibility of a release of fission products to the environment, it has to be taken into account that in the KWU PWR plants the spent fuel pool is located inside the reactor containment building, whereas in other designs a separate fuel pool building exists.

In the German "Störfall-Berechnungsgrundlagen" it is postulated that in such an incident all the fuel rods of one outer row of the respective assembly are damaged. It is further assumed that 10% of the fission product noble gas inventories of these rods is released to the containment atmosphere. As for the fission product iodine, 5% of the inventory has to be assumed to be transported to the pool water; from there, a fraction of the iodine is assumed to be volatilized, in accordance with a partition coefficient of $1 \cdot 10^5$, which is calculated for a pool water volume of $1500\,m^3$ and an atmosphere volume limited to $20{,}000\,m^3$. Airborne iodine is assumed to be present as 90% I_2 and 10% organically bound iodine.

A release of 5% of the iodine inventory from the damaged fuel rods would only be possible when very high gap inventories are present, which are only generated in fuel rods that have experienced comparatively high heat ratings. Such high values usually occur in freshly loaded fuel assemblies; discharged assemblies, however, which have been in operation for one year or longer, will have experienced considerably lower heat ratings during the last months of their residence time in the reactor core, i. e. during the time period which determines the ^{131}I gap inventories of discharged assemblies. Therefore, a considerably smaller ^{131}I release fraction (e. g. on the order of 0.5% of the rod inventory) would seem to be reasonable; for longer-lived fission products (e. g. ^{137}Cs) the leached fraction may be somewhat higher. In addition, the long, narrow pathways in the gap as well as the low temperature of the pool water can be assumed to effect a complete leaching of the gap inventories within a short time period only with severely damaged or dismantled fuel rods.

Since in the fuel pellet – cladding gap fission product iodine is present as an iodide compound, it will be dissolved in the pool water as I^-ion. This means that a significant transport to the atmosphere can only proceed after oxidation to elemental I_2, induced by the oxygen which is dissolved in the air-saturated pool water;

radiation-induced oxidation is, in principle, also possible. As yet, there is no detailed knowledge on the kinetics of iodide oxidation under the prevailing conditions, which can be characterized by the parameters 2200 ppm boron dissolved as boric acid, 0.2 ppm Li as LiOH, less than 10^{-9} g I/l, O_2 saturated, and water temperature of 30–45 °C. Therefore, no reliable prediction of the iodine partition coefficient to be expected can be made. The iodine partition coefficients ranging from $4 \cdot 10^3$ to $1 \cdot 10^4$ which were reported by Pelletier and Hemphill (1979) are assumed to be conservative, since in these experiments elemental I_2 had been added to the test solutions. Bawden et al. (1983) have recommended relating the iodine partition coefficient exclusively to the fraction of molecular iodine present in the iodine gap inventory. However, this fraction in the gap of an operationally intact rod is not definitely known; given the thermodynamic considerations discussed in Section 3.2.4., it can be assumed to be extremely small. Moreover, since the air above the surface of the pool water moves due to ventilation, equilibrium partition coefficients cannot be directly applied in the calculation of iodine release to the atmosphere of the containment; kinetic effects controlling the transport to the liquid–gas boundary layer have to be taken into account (see Section 7.3.4.3.). Another essential parameter controlling iodine release rates from the water pool is the rate of formation of I_2 by oxidation of initially present I^-. For these reasons, a quite slow release rate can be assumed; in consequence, iodine removal from the water phase by the action of the pool purification system will limit the amount of volatilized iodine to very low levels.

6.2.5 Accidents in the auxiliary building

Out of the number of incidents potentially occurring in the auxiliary building, the scenarios "Leakage of a tank containing radioactive contaminated water" and "Impacts of an earthquake to the reactor auxiliary building" have been selected to be radiologically representative (German "Störfall-Leitlinien", 1983). In both scenarios it is anticipated that the contents of a waste water evaporator tank will run out completely and flow down to the floor of the building. It is assumed that 1% of the water volume will evaporate, with the resulting steam showing a mass-related activity concentration of the halogens and solid fission products amounting to 5% of that of the remaining concentrate. The airborne iodine is assumed to be composed of 50% I_2 and organoiodides each; for long-term considerations, an iodine partition coefficient of 10^5 has to be employed in the calculations.

In both accident scenarios ^{131}I is the most important radionuclide because of its radiotoxicity and its potential volatility; in comparison, the release of other radionuclides from the resulting sump due to droplet or aerosol carry-over can be ignored. The postulated identical release fractions of iodine and non-volatile radionuclides can only be explained by the assumed presence of iodine in the solution as iodide ion. However, such a high droplet entrainment seems to be very unlikely, since even from boiling water surfaces a significantly smaller fraction of droplets (on the order of 0.1% and less) is formed and transported over distances

larger than a few meters; from non-boiling surfaces, this fraction is still significantly smaller (see Section 6.2.2.). The water droplets formed during the flowing out of the liquid from the damaged component or, afterwards, released from the surface of the pools on the floors are subjected to deposition processes on their way to the ventilation system. In the relevant compartment, a large proportion (more than 90%) can be expected to be retained by different deposition mechanisms such as gravity settling and wetting of walls and surfaces. The droplets which enter the ventilation system will mostly evaporate to dryness and the remaining solid particles will be retained in the HEPA filters.

Fission product iodine present in these solutions may be oxidized to some extent upon contact of the solution with air; on the other hand, competing reactions of iodine or iodide with unspecified constituents and impurities present in the solution may favor iodide oxidation, I_2 reduction or the formation of volatile organoiodine species. Detailed experimental investigations in this field have not yet been reported; due to the non-specified composition of such waste waters, it is very difficult to define test solutions similar to those encountered in reality. Therefore, it is not possible to evaluate the validity of the iodine partition coefficient of $1 \cdot 10^5$ postulated in the German "Störfall-Berechnungsgrundlagen" (1983). Bawden et al. (1983) recommended a conservative volume-related partition coefficient of 10^4 for iodine trace levels in a deep pool, i. e. a water pool which does not evaporate to dryness before it has been removed (see Section 6.2.2.). This value is assumed to be true for oxidizing conditions prevailing in the water volume; for reducing conditions, inorganic iodine can be regarded to be non-volatile species.

As was mentioned above, calculation of iodine volatilization under such conditions using equilibrium partition coefficients is somewhat problematic, since the compartments of the auxiliary building do not represent a closed system, but are flowing-air systems. Similar to the situation in the long-term phase of the accident "Break of a transducer line" (see Section 6.2.2.), a correct modelling of iodine release from the water pool would require the application of volatilization rates; however, as yet there are no reliable data verified in experiments specially designed for the conditions prevailing in the compartments of the nuclear auxiliary building.

References Chapter 6

Adams, R. E., Ackley, R. D.: Removal of radioiodine from gases. Nucl. Safety **9**, 373–382 (1968)

Adams, J. P., Atwood, C. L.: The iodine spike release rate during a steam generator tube rupture. Nucl. Technology **94**, 361–371 (1991)

Adams, J. P., Peterson, E. S.: Steam generator secondary pH during a steam generator tube rupture. Nucl. Technology **102**, 304–312 (1993)

Adams, J. P., Sattison, M. B.: Frequency and consequences associated with a steam generator tube rupture event. Nucl. Technology **90**, 168–185 (1990)

Albert, M. F., Watson, J. S., Wichner, R. P.: The absorption of gaseous iodine by water droplets. Nucl. Technology **77**, 161–174 (1987)

Alm, M., Dreyer, R.: Untersuchungen zum Verhalten der anorganischen Formen des Radioiods beim Wärmeträgerverlust eines Druckwasserreaktors. Isotopenpraxis **16**, 20–25 (1980)

Alm, M., Johannsen, K.-H., Runge, K.: Zum Radioiodverhalten in einer Luft-Wasserdampf-Atmosphäre. Kernenergie **24**, 471–477 (1980)

Bawden, R. J., Deane, A. M., Garbett, K., Handy, B. J., Large, N. R.: Chemical data for the calculation of fission product release in design basis faults in PWRs. Report AERE-R-10494, Rev.1 (1983)

Beahm, E. C., Daish, S. R., Shockley, W. E., Hopenfeld, J.: Iodine partitioning in pressurized water reactor steam generator accidents. Nucl. Technology **90**, 16–22 (1990)

Brittain, I., Aksan, S. N.: OECD–LOFT Large Break LOCA experiments: Phenomenology and computer code analysis. Proc. Open Forum The OECD LOFT Project. Achievements and Significant Results. Madrid, Spain, 1990, p. 102–143

Bundesministerium des Inneren (BMI): Leitlinien zur Beurteilung der Auslegung von Kernkraftwerken mit Druckwasserreaktoren gegen Störfälle im Sinne des § 28 Abs. 3 StrlSchV – Störfall-Leitlinien vom 18.10.1983

Burns, W. G., Kent, M. C., Marsh, W. R., Potter, P. E., Sims, H. E.: Radiolytic and surface reactions of dilute iodine solutions. Proc. 2. CSNI Workshop on Iodine Chemistry in Reactor Safety, Toronto, Can., 1988; Report AECL-9923 (1989), p. 19–38

Burns, W. G., Marsh, W. R.: The thermal and radiolytic oxidation of aqueous I^- and the hydrolysis and disproportionation of aqueous I_2. Report AERE-R-10767 (1986)

Clinton, S. D., Simmons, C. M.: Iodine partition coefficient measurements at simulated steam generator conditions. Report NUREG/CR-4817 (1987)

Collins, J. L., Osborne, M. F., Lorenz, R. A., Malinauskas, A. P.: Fission product iodine and cesium release behavior under light water reactor accident conditions. Nucl. Technology **81**, 78–94 (1988)

Deuber, H.: Investigations on the retention of elemental radioiodine by activated carbons at high temperatures. Nucl. Technology **72**, 44–48 (1986)

Deuber, H., Gerlach, K.: Parametric investigations on the retention of methyl iodide by a KI impregnated activated charcoal. Nucl. Safety **26**, 157–169 (1985)

Deuber, H., Gerlach, K., Wilhelm, J. G.: Investigations on the extremely low retention of ^{131}I by an iodine filter of a boiling water reactor. Proc. 18. DOE Nuclear Airborne Waste Management and Air Cleaning Conf., 1984, Paper 2–7

Fluke, R. J., Ogram, G. L., Rogers, L. N., Weaver, K. R. (a): Aerosol behaviour in the Water Aerosol Leakage Experiments. Paper presented at the 2. Internat. Conf. on Containment Design and Operation, Toronto, Ont., Can., 1990

Fluke, R. J., Weaver, K. R., Ogram, G. L., Rogers, L. N., Forrest, C. F. (b): The Water Aerosol Leakage Experiments: Programme description and preliminary results. Paper presented at the 2. Internat. Conf. on Containment Design and Operation, Toronto, Ontario, Can., 1990

Förthmann, R., Groos, E., Neeb, K. H., Morell, W., Richter, F.: Chemie des Spaltiods beim DWR-Auslegungsstörfall. Atomwirtschaft-Atomtechnik **30**, 263–266 (1985)

Gieseke, J. A., Flanigan, L. J., Collier, R. P., Denning, R. S.: Steam generator tube rupture iodine transport mechanisms. Report NUREG/CR-3937 (1985)

Groos, E., Förthmann, R. (a): I-131-Freisetzung aus defekten LWR-Brennstäben bei Temperaturen bis 1100 °C. Paper presented at the Jahrestagung Kerntechnik Deutsches Atomforum 1984

Groos, E., Förthmann, R. (b): Determination of iodine 131 release from defect irradiated fuel rods under simulated LOCA conditions. Proc. 5. Internat. Meeting on Thermal Nuclear Reactor Safety, Karlsruhe 1984, Vol. 3, p. 1377–1386

Gwyther, J. R., Turner, D. J.: Volatility of hydroiodic acid in steam. Proc. 5. BNES Conf. Water Chemistry of Nuclear Reactor Systems, Bournemouth, UK, 1989, Vol. 1, p. 289–294

Habersbergerova, A.: Radiolysis of aerated spray solution containing thiosulphate. I. Radiolytic products. Radiochem. Radioanal. Letters **47**, 157–166 (1981)

Habersbergerova, A.: Radiolysis of inorganic iodine compounds in aerated borate spray solution. Radiat. Phys. Chem. **19**, 403–407 (1982)

Habersbergerova, A., Bartonicek, B.: Radiolysis of iodine compounds in model systems of PWR. Radiat. Phys. Chem. **21**, 289–293 (1983)

Habersbergerova, A., Sistek, I.: Radiolysis of methyl iodide in aerated borate spray solution. Radiat. Phys. Chem. **19**, 409–413 (1982)

Handy, B. J., Murray, A., Longster, M. J.: Ageing characteristics of a PWR sump buffer chemical. Proc. 5. BNES Conf. Water Chemistry of Nuclear Reactor Systems, Bournemouth, UK, 1989, Vol. 2, p. 184–185

Hellmann, S., Bleier, A., Rippel, R., Funcke, J., Morell, W.: Large-scale experiments on iodine release associated with coolant flashing due to ruptured high-pressure tubes. in: Ishigure, K., Saeki, M., Soda, K.,Sugimoto, J. (editors): Proc. 3. CSNI Workshop Iodine Chemistry in Reactor Safety, Tokai-Mura, Japan 1991; Report JAERI–M 92–012 (1992), p. 280–297

Hicks, D., Sato, K.: The contributions of the OECD/LOFT project to nuclear safety. Proc. Open Forum The OECD/LOFT Project. Achievements and Significant Results. Madrid, Spain, 1990, p. 42–47

Hilliard, R. K., Postma, R. K.: Large-scale fission product containment tests. Nucl. Technology **53**, 163–175 (1981)

Hopenfeld, J.: Experience and modeling of radioactivity transport following steam generator tube rupture. Nucl. Safety **26**, 286–300 (1985)

Hyder, M. L.: Measurements of iodine uptake in falling water droplets. Nucl. Technology **94**, 80–86 (1991)

Janovsky, I.: Pulse radiolysis of aqueous borate solutions containing iodide. Radiochem. Radioanal. Letters **44**, 115–124 (1980)

Johnson, L. H., Burns, K. I., Joling, H. H., Moore, C. J.: Leaching of ^{137}Cs, ^{134}Cs, and ^{129}I from irradiated UO_2 fuel. Nucl. Technology **63**, 470–475 (1983)

Johnson, L. H., Stroes-Gascoyne, S., Chen, J. D., Attas, M. E., Sellinger, D. M., Delaney, H. G.: The relationship between fuel element power and the leaching of ^{137}Cs and ^{129}I from irradiated UO_2 fuel. Proc. Am. Nucl. Soc. Meeting on Fission Product Behavior and Source Term Research, Snowbird, Utah, USA, 1984; Report EPRI NP-4113-SR (1985), p. 15/1–12

Kabat, M. J.: Chemical behaviour of radioiodine under loss-of-coolant accident conditions. Paper presented at the 16. DOE Nucl. Air Cleaning Conf., San Diego, 1980,

Kalra, S. P.: On the methodology for assessing steam generator tube rupture safety margins. Nucl. Safety **31**, 187–201 (1990)

Kovach, J. L.: The evaluation and current state of radioiodine control. Nucl. Safety **23**, 44–56 (1982)

Kress, T. S.: Review of the status of validation of the computer codes used in the NRC Accident Source Term Reassessment Study (BMI-2104). Report ORNL/TM-8842 (1984)

Kühnlein, W., Ruyter, I., Schröder, J., Markgraf, J. F. W.: Iod-Freisetzung in den LOCA-Simulations-Experimenten ISOLDE. Proc. Jahrestagung Kerntechnik Deutsches Atomforum, Köln, Germany, 1993, p. 163–166

Lemire, R. J., Paquette, J., Torgerson, D. F., Wren, D. J., Fletcher, J. W.: Assessment of iodine behaviour in reactor containment buildings from a chemical perspective. Report AECL-6812 (1981)

Lin, C. C.: Volatility of iodine in dilute aqueous solutions. J. Inorg. Nucl. Chem. **43**, 3229–3238 (1981)

Lorenz, R. A., Collins, J. L., Malinauskas, A. P.: Modelling fission product release from ruptured LWR fuel rods. Trans. Am. Nucl. Soc. **28**, 505–506 (1978)

Lorenz, R. A., Collins, J. L., Malinauskas, A. P.: Fission product source terms for the light water reactor loss-of-coolant accident. Nucl. Technology **46**, 404–410 (1979)

Lorenz, R. A., Collins, J. L., Malinauskas, A. P., Kirkland, O. L., Towns, R. O. (a): Fission product release from highly irradiated LWR fuel. Report NUREG/CR-0722 (1980)

Lorenz, R. A., Collins, J. L., Malinauskas, A. P., Osborne, M. F., Towns, R. L. (b): Fission product release from highly irradiated LWR fuel heated to 1300–1600 °C in steam. Report NUREG/CR-1386 (1980)

Lorenz, R. A., Collins, J. L., Osborne, M. F., Towns, R. L., Malinauskas, A. P.: Fission product release from BWR fuel under LOCA conditions. Report NUREG/CR-1773 (1981)

Lorenz, R. A., Osborne, M. F., Collins, J. L., Manning, S. R., Malinauskas, A. P.: Behavior of iodine, methyl iodide, cesium oxide, and cesium iodide in steam and argon. Report ORNL/NUREG/TM-25 (1976)

Mitchell, A. D., Goode, J. H., Vaughan, V. C. A.: Leaching of irradiated LWR fuel in a simulated post-accident environment. Report ORNL/TM-7546 (1981)

Moon, H. C., Baumgärtner, F., Kim, J. L.: Generation of Am and Eu aerosols from unperturbated solution surfaces. Radiochim. Acta **35**, 223–226 (1984)

Morell, W., Röbig, G., Kastner, W., Rippel, R., Richter, F., Ahrens-Botzong, R.: Neuere Meßergebnisse zur Freisetzung von Radionukliden beim Auslegungsstörfall "Meßleitungsbruch" an Druckwasserreaktoren. Atomkernenergie-Kerntechnik **46**, 272–274 (1985)

Morewitz, H. A.: Leakage of aerosols from containment buildings. Health Physics **42**, 195–207 (1982)

Odar, S.: Bildung von Wasserstoff im Sicherheitsbehälter von DWR-Kernkraftwerken und seine Überwachung. VGB Kraftwerkstechnik **63**, 162–166 (1983)

Pasedag, W. F., Blond, R. M., Jankowski, M. W.: Regulatory impact of nuclear reactor accident source term assumptions. Report NUREG-0771 (1981)

Patterson, C. S., Humphries, W. T.: Design considerations of reactor containment spray systems. – Part II. Removal of iodine and methyl iodide from air by liquid solutions. Report ORNL-TM-2412 (1969)

Patzelt, A.: Zum Abscheideverhalten von Iod aus der Abluft nuklearer Hilfssysteme bei einem Siedewasserreaktor. VGB Kraftwerkstechnik **63**, 1078–1080 (1983)

Pelletier, C. A., Hemphill, R. T.: Nuclear power plant related iodine partition coefficients. Report EPRI NP-1271 (1979)

Postma, A. K., Tam, P. S.: Iodine behavior in a PWR cooling system following a postulated steam generator tube rupture accident. Report NUREG-0409 (1978)

Reaktorsicherheitskommission, Strahlenschutzkommission (RSK, SSK): Störfall-Berechnungsgrundlagen für die Leitlinien des BMI zur Beurteilung der Auslegung von Kernkraftwerken mit DWR gemäß § 28 Abs. 3 StrlSchV vom 18.10.1983

Richter, F., Fischer, P., Morell, W., Neeb, K. H.: Experimentelle Daten zur Iod-Verteilung unter den Bedingungen hypothetischer Kernschmelz-Unfälle. Proc. Jahrestagung Kerntechnik Deutsches Atomforum 1985, p. 247–250

Row, T. H.: Reactor containment-building spray systems for fission product removal. Nucl. Safety **12**, 516–522 (1971)

Row, T. H., Parsly, L. F., Zittel, H. E.: Design considerations of reactor containment spray systems. – Part I. Report ORNL-TM-2412 (1969)

Schuster, E.: Fission product release and dispersion in LP-FP-1. Proc. Open Forum The OECD LOFT Project: Achievements and Significant Results. Madrid 1990, p. 224–241
Stephenson, W., Dutton, L. M. C., Handy, B. J., Smedley, C.: Realistic methods for calculating the release and consequences of a large LOCA. Report EUR 14179 EN (1992)
Sunder, S., Shoesmith, D. W., Christensen, H., Miller, N. H.: Oxidation of UO_2 fuel by the products of gamma radiolysis of water. J. Nucl. Materials **190**, 78–86 (1992)
USAEC: Assumptions used for evaluating the potential radiological consequences of a loss-of-coolant accident for boiling water reactors. Regulatory Guide 1.3., Revision 2 (1974)
USAEC: Assumptions used for evaluating the potential radiological consequences of a loss-of-coolant accident for pressurized water reactors. Regulatory Guide 1.4., Revision 2 (1974)
US Nuclear Regulatory Commission (NRC): Technical bases for estimating fission product behavior during LWR accidents. Report NUREG-0772 (1981)
Voillequé, P. G.: Measurements of radioiodine species in samples of pressurized water reactor coolant. Nucl. Technology **90**, 23–33 (1990)
Weber, C. F., Beahm, E. C., Kress, T. S.: Models of iodine behavior in reactor containments. Report ORNL/TM-12202 (1992)
Wilhelm, J. G.: Iodine filters in nuclear installations. Report Commission of the European Communities, Contract No. 1175–80–12 L/V (1982)
Witherspoon, M. E.: Leakage rate tests on the CSE containment vessel with heated air and steam-air mixtures. Report BNWL-1475 (1970)
Witherspoon, M. E., Postma, A. K.: Leakage of fission products from artificial leaks in the Containment Systems Experiment. Report BNWL-1582 (1971)
Wren, J. C., Moore, C. J. (a): The effect of wethering on charcoal filter performance. I. The adsorption and desorption behavior of contaminants. Nucl. Technology **94**, 242–250 (1991)
Wren, J. C., Moore, C. J. (b): The effect of wethering on charcoal filter performance. II. The effect of contaminants on the CH_3I removal efficiency of TEDA charcoal. Nucl. Technology **94**, 252–260 (1991)
Wren, D. J., Sanipelli, G.: The volatility of HOI. Proc. ANS Topical Meeting on Fission Product Behavior and Source Term Research. Snowbird, Utah, USA, 1984; Report EPRI NP-4113-SR (1985), p. 42/1–13

7. Severe reactor accidents

7.1 General aspects

The design basis accidents described in Chapter 6, in particular the loss-of-coolant accident, are characterized by the fact that, as a result of the action of the emergency core cooling systems and the residual heat removal systems, the reactor core is stabilized in a safely cooled state and, therefore, no fuel rod damage or additional fission product release beyond that of the transient phase will occur. In the so-called beyond design basis accidents, on the other hand, the assumption is made that the reactor safety systems fail to fulfil the design purposes. This type of accidents can be divided up into three categories with increasing consequences, but decreasing probability (Mayinger and Birkhofer, 1988):

(1) The plant safety systems do not work fully according to their design purposes; nevertheless, the remaining emergency installations prevent a heating-up of the fuel rods to temperatures exceeding those calculated for a design basis loss-of-coolant accident.
(2) Insufficient cooling of the reactor core results in a severe core damage, but cooling can be restored again so that the reactor pressure vessel is not damaged by the molten phase.
(3) Reactor core cooling cannot be restored, so that the core melt penetrates the reactor pressure vessel and falls down to the containment basemat.

The consequences of a category 1 accident do not exceed those of a design basis loss-of-coolant accident (see Section 6.2.1.). In contrast, in the course of accidents belonging to categories 2 and 3, the fuel is damaged by overheating to the point of allowing substantial escape of fission products to the primary circuit and to the containment.

The probability of the occurrence of a severe reactor accident as well as its propagation depend strongly on the general design of the reactor plant. Most of the initiating events for the severe reactor accidents that have occurred up to now do not apply to light water reactors of Western design. This is true, for example, for a moderator fire such as occurred at the Windscale-2 reactor, as well as for an unintended criticality excursion such as occurred at the Chernobyl-4 plant. The only possible initiating event leading to a severe core damage in a light water reactor is insufficient decay heat removal, as happened in the TMI-2 accident. For this reason, all the analyses of accident propagation and of the behavior of the radionuclides have to start from such plant conditions. It has to be pointed out that the probability of a category 3 accident is far lower than that of category 1 and 2 accidents, which, in turn, have a considerably lower probability than design basis accidents. Since our interest is in questions of radionuclide chemistry under conditions to be expected in severe reactor accidents, the question of the probability of such events will not be discussed.

In order to provide criteria for the siting of nuclear reactors, the US Atomic Energy Commission (AEC) in 1962 developed the concept of a maximum credible accident "the consequences of which are not exceeded by any other accident" (The Code of Federal Regulations (CFR), Title 10, Part 100, Reactor Site Criteria). As was specified in the US Regulatory Guides 1.3 and 1.4 (1974), this hypothetical accident involved the release to the containment of all the noble gases present in the reacor core, half of the iodine isotopes, and one percent of the inventories of all the other fission products. The chemical form of the iodine released was assumed to be predominantly elemental I_2 (91%), with 5% in the form of particulate iodide and 4% as organic iodine compounds; the airborne concentration of the solid fission products in the containment was assumed to be subjected to natural plate-out processes. Furthermore, while it was assumed that the reactor containment would be designed to accomodate such an accident without failure, it was also anticipated that it would leak at its maximum allowable leak rate. Based on these assumptions, it was concluded that the high fission product release from the reactor core would result in source terms to the environment, which were quite modest and not large

enough to justify extensive research into possible accident sequences and associated fission product behavior. On the other hand, these assumptions have significantly affected the design of the engineered safety features of reactor plants.

At the beginning of the 1970's, researchers in the United States began to work out a detailed description of possible severe reactor accident sequences in order to quantify their consequences. These investigations resulted in the Reactor Safety Study (1975), widely known by the designationWASH-1400, which is generally regarded as a pioneer study for probabilistic safety analyses not only in the field of nuclear technology. In contrast with the earlier assumptions, this study postulated failure of the reactor containment for certain core melt accident sequences, resulting in extensive radionuclide release to the environment. When the study was completed, there was only scarce information available on accident source terms; thus, the assessments of the consequences of such an accident were quite pessimistic, especially since several physico-chemical processes with the potential of effecting a retention of fission products within the reactor plant were not taken into consideration. The probability of such severe accidents, however, was found to be exceedingly small, much lower than that of other many man-made or natural hazards involving a similar magnitude of consequences. Using the fundamentals of WASH-1400, but taking into account the current state of knowledge, probabilistic safety analyses have been applied to a large number of PWR and BWR plants (US NRC, 1990).

Using the same methodology, but applied to the design of a German 1300 MWe PWR plant, the "Deutsche Risikostudie Kernkraftwerke" (1979) was worked out in the Federal Republic of Germany and updated by phase B of this study (1989). Both studies relate to PWRs; for BWRs similar studies have been worked out, but not in comparable degree of detail.

In the analysis of the consequences of severe reactor accidents, the source term plays a central role. Usually, two different types of source terms are used: the in-containment source term and the source term to the environment. The in-containment source term is defined as the quantity, chemical form and chemical and physical properties of the radioactive fission product species released from the reactor core to the containment. This source term normally is a function of time and involves consideration of fission products released from the reactor core into the containment, as well as removal of fission products by engineered safety features (e. g. pressure suppression pools, spray systems, ice-bed condensers) or by natural removal processes. In a reactor accident, a major concern is that all the engineered safety features might fail to operate. Even the failure of each engineered barrier to function properly, however, does not necessarily mean that a significant amount of radioactivity will escape to the environment. The behavior of fission products, particularly of ones in the volatile and particulate forms, is governed by physical and chemical laws that remain in effect independent of the engineered safety features or the containment building; the results of the reactions occurring in the system, however, might be influenced by these engineered installations. The source term to the environment, on the other hand, describes the amount and type of radioactive materials that could potentially escape to the environment from a reactor which has undergone a severe accident. This term differs from the in-contain-

ment source term by the fraction of radionuclides retained in the containment, either by natural deposition processes or by the action of the engineered safety systems.

From the beginning of the development of nuclear energy, source terms were recognized as the important factor of risk. Because knowledge was insufficient for making accurate and valid estimates of the source terms during the early days, highly conservative assumptions were made, mainly focusing on radioiodine because of its large inventory in the fuel, its high biological activity and its anticipated elemental gaseous form. Former studies, including WASH-1400, assumed massive radionuclide releases to the environment as the consequence of such a severe accident, with the main reason for this assumption being the neglect of important physical and chemical phenomena and their impact on radionuclide behavior. From a scientific point of view, it is highly unsatisfactory that the specific ambient conditions were only incompletely reflected in the evaluation of the effects of chemical reactions. It was only with the TMI-2 core melt accident, where surprisingly small amounts of radioiodine and other fission products escaped to the environment, that it was recognized that a proper consideration of chemistry effects would be an absolute prerequisite for obtaining realistic results on source terms. As an example, an early estimation performed by Levenson and Rahn (1981) showed that a correct assessment of these effects would lead to a drastic reduction in radionuclide releases and, consequently, of the accident consequences as compared to the predictions of WASH-1400. As a result of these findings, an extensive research effort was begun worldwide to obtain more accurate and reliable data on source terms. Evaluating the TMI-2 accident, it is of particular interest to find out whether the observed fission product behavior, especially the phenomenon of the "missing iodine", was caused by circumstances unique to the TMI-2 reactor or whether it reflected a generally valid trend. In order to get a clearer idea of the prevailing effects, several studies on source terms have been initiated, e.g by the American Nuclear Society (1984) and by the American Physical Society (1985). These studies came to the result that physical and chemical phenomena, previously neglected, will lead to the retention of fission products and that this retention is particularly effective the longer the elapsed time before containment failure. On the other hand, they indicated that additional potential radionuclide sources might exist, such as the molten core – concrete interaction in the reactor cavity, which had not been or only incompletely considered in former studies.

When evaluating these phenomena, it has been recognized that from a chemical perspective a severe reactor accident would represent "the scene of a diverse range of highly dynamic chemical environments (see Table 7.1.), with a broad spectrum of chemical species released from the degrading core being available for a multitude of interactions within the plant... As the released materials were being transported within the plant, they could undergo an essentially infinite variety of interactions as they encountered different physicochemical environments and different materials" (Niemczyk, 1986). Some of those interactions would be able to trap volatile radionuclides within the plant, others would result in the formation of more volatile species. Thus, chemical reactions would strongly influence the transport behavior of the radionuclides.

Table 7.1. Ranges of in-plant severe accident environments (according to Niemczyk, 1986)

Feature	Potential range
Temperature	1500 to 2500 °C in vicinity of melting fuel to about 100 °C in the containment or reactor building
Pressure	Up to 16 MPa in the core and coolant system to close to atmospheric in the containment or reactor building
Radiation Field	High levels in vicinity of core and in areas of significant radioactive deposition to relatively low levels elsewhere
Atmosphere	Oxidizing to reducing, depending on location and time Possibly dense with aerosols Very humid, with possibility of operating sprays Possible hydrogen burns in some regions of containment or reactor building

The renewed interest in fission product chemistry under severe accident conditions prompted an evaluation of the then current state of the art of knowledge on fission product behavior, as was documented in NUREG-0772 (Nuclear Regulatory Commission, 1981) and re-evaluated by Silberberg et al. (1986). Likewise, in the 1980's a group of experts was established by the OECD Committee on the Safety of Nuclear Installations (CSNI) with the main function of keeping under observation the most significant areas of source term development. As a result of their work, state-of-the-art reports on highly important topics in this field have been issued (e. g. CSNI, 1987). These reviews of the available knowledge suggested that it is feasible, in spite of a not fully complete experimental data base, to produce more realistic estimates of severe accident source terms than those of WASH-1400, by addressing several phenomena which are able to affect the transport of fission products (e. g. deposition in the reactor coolant system, agglomeration of high density aerosols, effects of the chemical formation of reactive fission product species) which had been ignored in previous analyses. Detailed investigations of these effects led to a considerable increase in knowledge on fission product behavior under extreme conditions, as can be concluded from the summary paper of Malinauskas and Kress (1991), where the current state of the art is compared with the assumptions made in the WASH-1400 calculations.

However, with increasing knowledge it became evident that the progress of chemical reactions in the different regions of the plant as well as the yields of their products depend strongly on a number of parameters such as the type of plant (PWR, BWR) and its specific layout, and on the details of the accident sequence. Thus, when including chemical reactions in the evaluation of radionuclide behavior, extensive calculations are needed which can only be based upon the use of appropriate models and computer codes. Such models and computer codes have been developed on the basis of experimental and theoretical work, involving the fission product release during the fuel melt process, the behavior and transport of fission products and aerosols in the reactor pressure vessel, the behavior and trans-

port in the primary cooling system, the behavior and transport in the containment, as well as the effect of engineered safety features. This information then flows into the calculation of the extent to which the fission products are released from the containment to the environment. The computer codes used for this purpose include both mechanistic and phenomenological models of the essential processes, where available, and approximations of other important natural, physical and chemical processes involved, with particular emphasis on the radiologically significant elements such as iodine and cesium, in the airborne (vapor or particulate) state. The computer codes are recognized as being representative of the current state of the art of knowledge of the various processes involved, although they are not perfect. Therefore, continuing development work in this field is being conducted by various institutions to reduce the uncertainties and conservatism associated with the current estimates of source terms.

For a complete description of the fission product behavior in the course of a severe accident, a combination of different computer codes has to be used, a so-called Source Term Code Package, as is exemplarily shown in Fig. 7.1. (according to Soffer, 1991). Starting from the fission product inventory (calculated using the ORIGEN code), the release from the fuel is calculated with the CORSOR code and the retention and transport in the reactor coolant system with TRAPMELT. Releases from core – concrete interactions are modeled using the VANESA code. Depending on the containment type, NAUA, SPARC (describing aerosol attenuation in pressure suppression pools) or ICEDF (aerosol retention in ice compartments) are used to model the transport and retention of fission product releases from the reactor cooling system and from the core – concrete interaction into the containment, with subsequent release of fission products to the environment consistent with the state of the containment. In parallel, thermal hydaulic behavior is introduced by the MARCH, MERGE and CORCON codes. These codes do not take into consideration chemical reactions occurring in the respective systems; this lack is of particular concern for fission product iodine, with its tendency to change its chemical state depending on the prevailing ambient conditions. For this reason, specific iodine behavior codes were developed, for example IMPAIR-2 and its subsequent versions. These codes describe the chemical reactions occurring under containment conditions and will be treated in somewhat greater detail later on. In recent years, improved code systems have been developed; in Europe, the code set ESTER is being developed, which combines several existing codes for special areas, such as thermohydraulics, aerosol physics and iodine chemistry (e. g. Shepherd et al., 1993).

As a basis for the evaluation of fission product behavior and transport during a severe accident, a definition of possible accident sequences is required, containing all the information on physical and thermohydraulic conditions required for the assessment of the chemical behavior. The basis for the definition of such accident sequences was provided in 1975 by the US Reactor Safety Study mentioned above; it has been continuously improved during the following years. The comparable German study is the "Deutsche Risikostudie Kernkraftwerke, Parts A and B". These studies cover all the possible accident sequences which are of significance as regards the release of radionuclides from the plant to the environment. The details of the scenario that a specific accident sequence follows depend highly on assump-

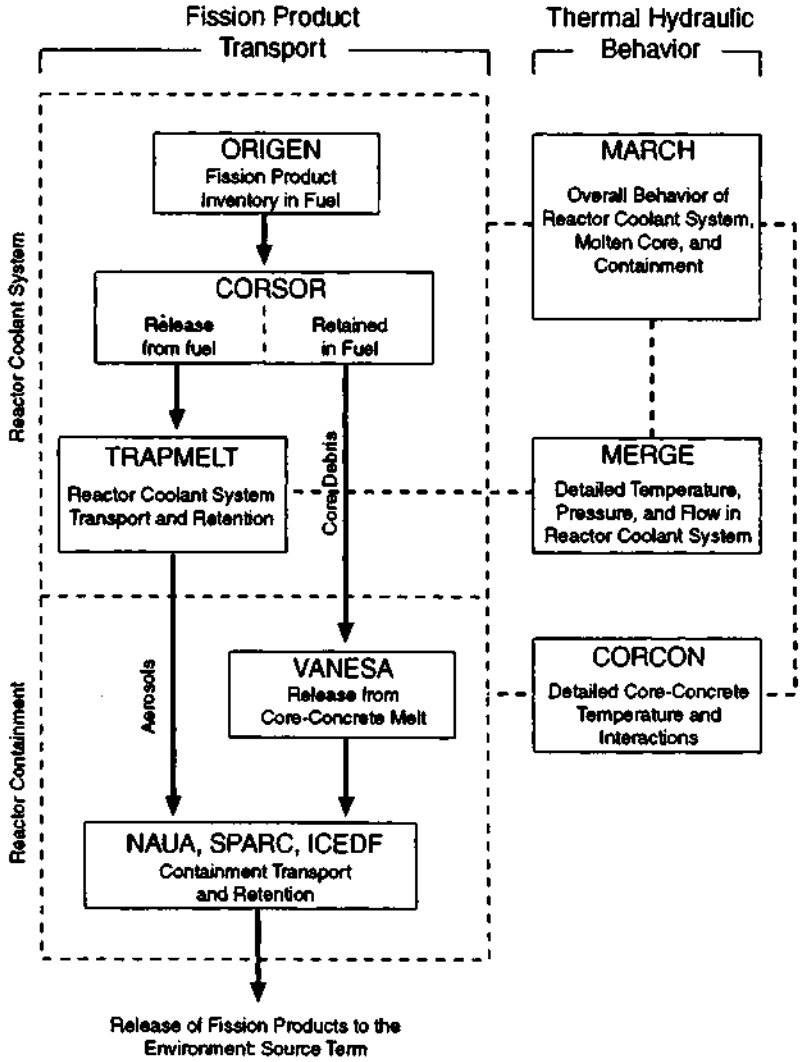

Figure 7.1. Source Term Code Package (Soffer, 1991)

tions made as to the availability of engineered safety features. If a part of these systems is assumed to operate correctly, the accident sequence may be terminated or its consequences greatly ameliorated. Further, although operator actions generally were not taken into account in these considerations, such actions may also terminate the sequence, in particular during sequences which are predicted to be very protracted in time. As a consequence, close cooperation between systems engineers, safety analysts and chemists is essential to identify possible pathways of the fission products in the plant, to evaluate the importance of chemical phenomena

for the magnitude of risk and to prioritize safety issues involving fission product chemistry. Since it is virtually impossible to cover all the conditions which may potentially occur in the course of a severe accident, detailed studies on fission product chemistry have to concentrate on the risk-dominating sequences, since this is the only way to keep the uncertainties due to chemical reactions low enough so that their contribution to total source term uncertainties remains minor.

The transport and release behavior of the fission products depends not only on the nature and the timing of the accident phenomena but also on details of the reactor design. The inclusion of detailed design information, for example, the characteristics of the upper plenum of the reactor pressure vessel, as well as the treatment of some of the engineered safety features (e. g. containment sprays, suppression pools) will not only provide a better foundation for estimating radionuclide release, but also will result in a better understanding of the accident sequence and of the results of radionuclide behavior.

The radionuclides present in the irradiated nuclear fuels are of different importance as regards the environment in the very unlikely case of a severe accident. The factors determining their importance are 1) the total inventory of the radionuclide in the reactor; 2) the physical and chemical properties which control their behavior in the plant and in the environment; and 3) their radiobiological characteristics. Some of these factors are inherent, others depend on features of the accident and plant design. In this context, radioiodine is considered to be of greatest importance; other important nuclides include radioisotopes of cesium, tellurium and, of lesser importance, of some of the alkaline earths and noble metals. The noble gases, though highly volatile, are chemically inert and, thus, are of lower radiological importance in severe accidents.

It has to be pointed out that the aim of the following chapters is a presentation of the chemical reactions which are of importance for understanding the behavior of the radionuclides. The impact of these reactions on accident progression and on the source terms of the radionuclides will only be outlined in a very general manner; in particular, it is not intended to give numbers for source terms which are typical for specific accident sequences.

References Section 7.1

American Nuclear Society (ANS): Report of the Special Committee on Source Terms. 1984

American Physical Society: Radionuclide release from severe accidents at nuclear power plants. Reviews of Modern Physics 57, 3, Part II (1985)

CSNI (Committee on the Safety of Nuclear Installations): Selected source term topics. Report to CSNI by an OECD/NEA Group of Experts. Report CSNI 136 (1987)

Gesellschaft für Reaktorsicherheit (GRS): Deutsche Risikostudie Kernkraftwerke. Eine Untersuchung zu dem durch Störfälle in Kernkraftwerken verursachten Risiko. Verlag TÜV Rheinland, Köln, 1979

Gesellschaft für Reaktorsicherheit (GRS): Deutsche Risikostudie Kernkraftwerke, Phase B. Bericht GRS-72 (1989)

Levenson, M., Rahn, F.: Realistic estimates of the consequences of nuclear accidents. Nucl. Technology **53**, 99–110 (1981)
Malinauskas, A. P., Kress, T. S.: Effects of chemical phenomena on LWR severe accident fission product behavior. Nucl. Safety **32**, 56–64 (1991)
Mayinger, F., Birkhofer, A.: Neuere Entwicklungen in der Sicherheitsforschung und Sicherheitstechnik. Atomwirtschaft **1988**, 426–434
Niemczyk, S. J.: In-plant chemical phenomena potentially important to nuclear reactor severe accidents and their source terms. Proc. ACS–USNRC–IAEA Symposium on Chemical Phenomena Associated with Radioactivity Releases During Severe Nuclear Plant Accidents. Anaheim, Calif. USA, 1986; Report NUREG/CP-0078 (1987), p. 1/21–40
Reactor Safety Study – An assessment of accident risks in US commercial nuclear power plants. Report WASH-1400 (1975)
Shepherd, I., Jones, A., Jacq, F., Schmidt, F.: ESTER: A new approach in modelling severe accidents. Paper presented at the 4. Internat. Conf. on Simulation Methods in Nuclear Engineering. Montreal, Can. 1993
Silberberg, M., Mitchell, J. A., Meyer, R. O., Ryder, C. P.: Reassessment of the technical bases for estimating source terms. Report NUREG-0956 (1986)
Soffer, L.: Iodine chemical form in LWR reactor accidents: Regulatory perspectives in the United States. in: Ishigure, K., Saeki, M., Soda, K., Sugimoto, J. (editors): Proc. 3. CNSI Workshop on Iodine Chemistry in Reactor Safety, Tokai-Mura, Japan, 1991, p. 35–48 (Report JAERI–M 92–012, 1992)
USAEC: Assumptions used for evaluating the potential radiological consequences of a loss-of-coolant accident for boiling water reactors. Regulatory Guide 1.3., Revision 2 (1974)
USAEC: Assumptions used for evaluating the potential radiological consequences of a loss-of-coolant accident for pressurized water reactors. Regulatory Guide 1.4., Revision 2 (1974)
US Nuclear Regulatory Commission (NRC): Technical bases for estimating fission product behavior during LWR accidents. Report NUREG-0772 (1981)
US Nuclear Regulatory Commission (NRC): Severe accident risks: An assessment for five US nuclear power plants. Report NUREG-1150 (1990)

7.2 Postulated accident sequences

7.2.1 Pressurized water reactors

In the different reactor risk studies performed up to now, a number of potential accident sequences have been analyzed in detail. The conditions prevailing in the different stages of such an accident have been described in numerous publications, with regard to KWU-designed plants, for example, by Hassmann et al. (1987). These physical and chemical conditions (such as temperature, pressure, flow characteristics, hydrogen-to-steam ratio) vary widely between the different postulated accident sequences, influencing the release and transport behavior of the fission products. In the following sections only those parameters will be discussed which are of importance for fission product chemistry and behavior.

The different investigated accident sequences can be subdivided into two main categories:

- The low-pressure scenario which is initiated by a large-sized break in the primary circuit, that is an event similar to that of the loss-of-coolant design basis accident described in Section 6.2.1.. In the severe accident scenario it is additionally postulated that, after the action of the accumulators and the borated water storage tanks, the sump water recirculation pumps will fail to operate. Thus, the decay heat cannot be removed from the reactor core with the consequence that the water volume present inside the reactor pressure vessel (RPV) begins to boil off at about atmospheric pressure. The AB sequence of WASH-1400 describes such a large-break scenario. In this low-pressure scenario, the treatment of fission product behavior inside the primary circuit is comparatively simple; the probability of occurrence of such an accident, however, is extremely small.
- The high-pressure scenario, which may result from a small break or a transient such as a loss of feedwater supply or a station black-out with additional failures in the safety functions. In this scenario the coolant escapes from the primary circuit via an orifice which is so small that a pressure of about 16 MPa is maintained inside the primary circuit. Additionally, it is assumed that the leak cannot be closed and that the emergency core cooling systems are not capable of removing the decay heat sufficiently, so that the primary coolant is completely evaporated from the reactor pressure vessel, though at high pressure. The small-break LOCA sequence and the transient sequence (S_2D and TMLB' according to WASH-1400), as well as a steam generator tube rupture, are examples of such high-pressure accident scenarios. The probability that such a high-pressure accident will occur is greater than that a of low-pressure accident; by appropriate means the pressure inside the reactor pressure vessel can be decreased and, thus, the high-pressure sequence can be transformed into a low-pressure one. As is commonly known, the TMI-2 accident was initiated by a small leak, so that it belongs to the high-pressure category.

It has to be pointed out again that such initiating events will only lead to a severe core damage if all the emergency core cooling systems failed to operate. If only a part of them (they are installed on a conservative basis with sufficient overcapacity and redundancy, see Sections 1.1.4. and 2.1.4.) functions, the postulated accident sequence would be terminated before severe core degradation occurred. This is particularly true for plants with extensive accident management systems.

When, in the low-pressure scenario, the water level inside the RPV falls noticeably below the upper edge of the reactor core, the fuel rod regions that are no longer covered with water will start to heat up as a result of the decay heat, which now is only insufficiently removed by steam and water droplets; this heating-up proceeds down the reactor core at approximately the same rate as the water level continues to fall. At cladding temperatures exceeding 1000 °C, an exothermal reaction between Zircaloy and steam will start. Beyond 1200 °C this reaction roughly doubles the thermal rating caused by radioactive decay, provided that sufficient amounts of steam are available for the reaction; the result is an intensification of the heating-up process and, in addition, an excessive production of hydrogen (see below).

In case the emergency core cooling systems are not able to stop further heatup of the reactor core, a severe degradation of the reactor core will be the consequence. The processes occurring in the overheated reactor core cannot be described by a simple meltdown of the individual components; rather, they are characterized by numerous interactions between the different materials present in the reactor core (fuel, Zircaloy cladding, stainless-steel structural materials, control rod materials, etc.) in a steam–hydrogen environment. In most cases, the products of these interactions have lower melting points or ranges than the original materials.

According to the investigations reported on by Hofmann et al. (1989), the chemical reactions among the various core components which result in the formation of liquid phases can be classified into three distinct temperature ranges (see Fig. 7.2.): Above 1200 °C, a liquefaction of portions of the fuel assemblies which are equipped with absorber rod starts as a result of interactions between Zircaloy and stainless steel as well as between Zircaloy and Ag-In-Cd control rod material. This low-temperature melt of the absorber material will run downward and may form coolant channel blockages upon solidification in the lower, still cooler part of the fuel rod bundle. This temperature regime reaches to values above 1400 °C, where the absorber rods and the Inconel spacer grids will be completely molten. The melt formed is able to dissolve the Zircaloy cladding and the UO_2 fuel far below their melting points. The second temperature regime starts at about 1800 °C with the onset of melting of the still unreacted metallic Zircaloy cladding, accelerating the rate of fuel dissolution. The final thermodynamically stable products of these reactions in the core are oxide compounds, with the exception of the silver constituent of the control rods. Even if a metallic eutectic phase is initially formed, the resulting metals will be oxidized later in the course of the core meltdown. However, metallic melts reaching cooler core regions are potentially not subjected to further interactions.

Finally, at about 2600 °C (2900 K) the various oxidized core components and their resulting mixture will be completely liquefied. Depending on the chemical composition and on the oxidation state of the various core materials, the completely molten components and phases will form either a homogeneous metallic or a homogeneous ceramic melt or two immiscible melts in the temperature range 2600 to 2850 °C. Solidification of the ceramic melt begins at about 2400 °C, which is distinctly higher than that of the metallic melt (about 1800 °C); in both cases, the temperature range for complete solidification of the melts can be very wide.

The details of the core melt-down processes depend both on the particular composition of the respective reactor core and on the particular conditions of the accident sequence under consideration. However, as a comparative evaluation of the results from different experiments on core melt progression performed in test reactors and from examination of the damaged core of the TMI-2 reactor (Hobbins et al., 1991) has shown, in spite of considerable differences in the conditions and physical scales, several important phenomena seem to be common to all such events. Eutectic interactions between core materials cause the formation of liquid phases and loss of original core geometry at comparatively low temperatures (about 1500 K). The first liquids to be formed are metallic in nature and consist

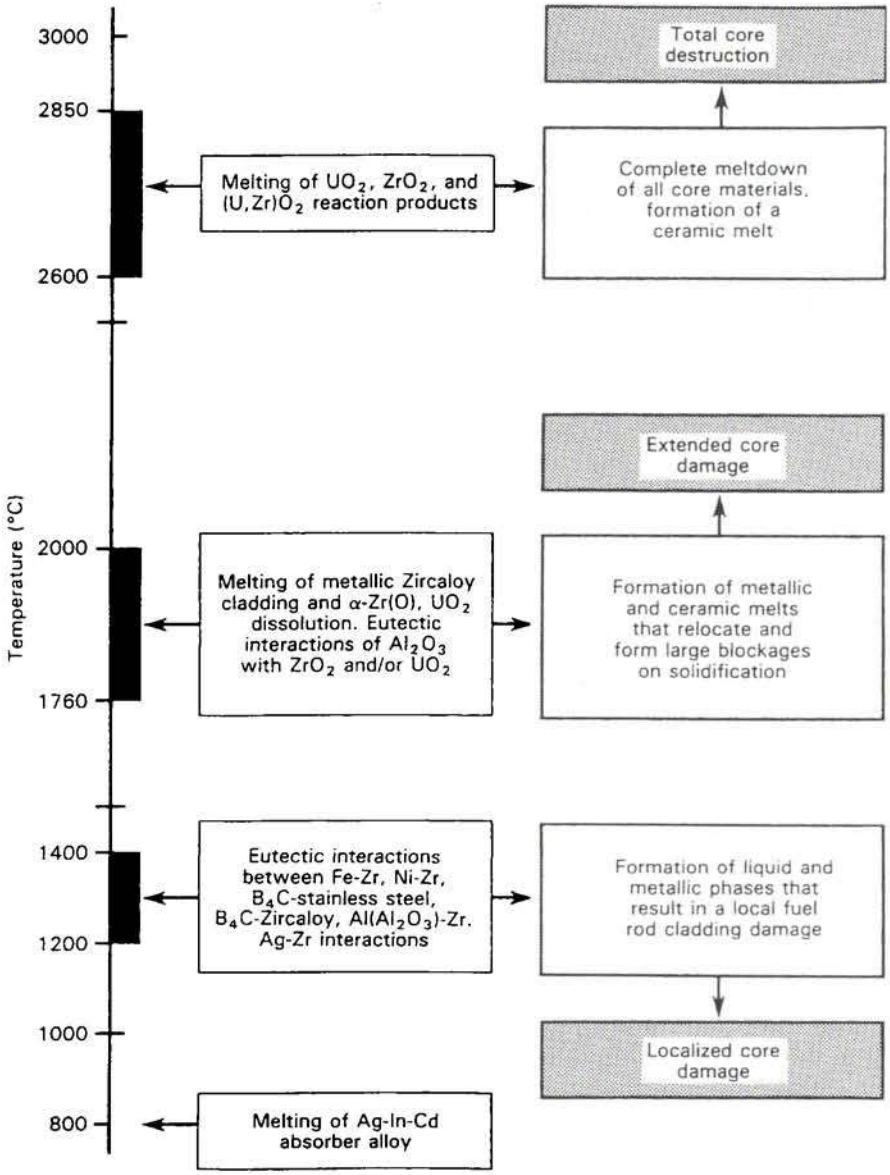

Figure 7.2. Temperature regimes for liquid-phase formation in a severe reactor accident and possible consequences for reactor core damage
(Hofmann et al., 1989; Copyright 1989 by the American Nuclear Society, La Grange Park, Illinois)

mainly of Zircaloy and control material (stainless steel, Ag-In-Cd in PWRs, and B_4C in BWRs), and they relocate to lower elevations in the core, where they may freeze into a crust that forms a partial flow blockage. Eutectic reaction of B_4C with its surrounding stainless steel cladding appears to eliminate the possibility of the reaction of B_4C with steam, CsI and CsOH. At temperatures above 2000 K, fuel liquefaction causes fuel-bearing debris to accumulate in the core above the metallic lower crust. Fuel liquefaction predominantly starts at the fuel grain boundaries, thus promoting the release of volatile fission products, and occurs over a range of space and time within the core, due to axial and radial temperature gradients in the core, the variety of melting points of the different core materials and variations in the access of steam to different core regions. The liquefied material oxidizes in steam as it relocates, and the accumulated melt can incorporate unmelted fuel rod debris. The result is the formation of a molten ceramic pool above the metallic crust. This molten pool can be uncoolable, as was the case in the TMI-2 accident, but failure of the peripheral crust can cause a coherent relocation of core melt to the lower plenum of the reactor and fragmentation of the melt in water to form a coolable debris (as also occurred in the TMI-2 accident).

When the core melt process cannot be stopped by restoration of sufficient cooling, the residual water level in the pressure vessel continues to drop and the solidified melt heats up again to its melting point; the melting process expands in the core from the center to the periphery, and the molten material pours down to still cooler regions. This core slumping represents, therefore, a kind of stop-and-go process. In running down the reactor core, the melt will additionally attack structural materials such as steel, thus forming a four-component mixture U-Zr-Fe-O which separates into an oxide and a metallic fraction. When the residual water level drops below the lower core grid plate, this structure will also fail and the melt together with still solid material will fall down into the residual water volume in the lower plenum of the reactor pressure vessel. During the following approximately 50 minutes, this residual water volume will boil off, leaving behind a two-phase (oxide and metallic) melt which then is able to penetrate the reactor pressure vessel within some 20 minutes.

This process of melting down of the reactor core inside the reactor pressure vessel is associated with an extensive release of the volatile fission products and a partial volatilization of the other fission products, uranium and the actinides (in-vessel release). The volatilized fuel constituents are transported by the steam–hydrogen flow out of the core region, together with volatilized fractions of the core structural materials (stainless steels, Ni alloys).

Failure of the reactor pressure vessel initiates another strong release of radionuclides to the containment atmosphere (ex-vessel release). Such a failure, however, is highly unlikely, since the experience at TMI-2, among others, demonstrated that cooling of the reactor core, even when it is only started at an advanced stage of the accident and at a largely degraded state of the core, is still able to prevent a vessel failure. However, since the aim here is to give as complete a description of events as possible, such effects of very low probability also have to be considered. Details of the failure mode of the reactor pressure vessel are difficult to predict;

however, they are not expected to influence significantly the extent of fission product release from the melt. In the low-pressure sequence a mixture of liquid and solid materials will run down to the concrete basemat; at this time steam explosions can occur as the molten core material falls on the water which may be present in the reactor cavity. In the high-pressure sequence, the molten core mixture is ejected from the leak together with superheated steam which, afterwards, may react with Zircaloy not yet oxidized. In particular in US accident considerations it has been assumed that molten material is released in a jet and fragmentated, leading to a fast quenching and to a dispersion of molten spots onto the walls (so-called direct containment heating).

Upon failure of the reactor pressure vessel, about 160 Mg of oxide melt (fuel, zirconium oxide) and about 70 Mg of metallic melt (Fe, Zr, Cr, Ni) suddenly flow down to the concrete basemat below, where this mixture enters into a high-temperature interaction which progressively decomposes the concrete materials; as a result of the decomposition reactions aerosols as well as gases (CO_2, H_2, CO) are produced. Due to the dilution of the core melt with concrete constituents, the initially high temperature decreases to values below 2000 °C. In what follows, a destruction of the structure of the biological shield may occur, as a consequence of which the sump water volume which is present in the lower regions of the reactor building will flood the molten core – concrete interaction zone. This sump water volume differs according to the design of the plant and the accident sequence assumed and consists of the original primary coolant volume (approximately 400 m^3), the contents of the accumulators (appr. 300 m^3) and, in the low-pressure sequences, potentially the contents of the borated water storage tanks (appr. 1000 m^3). After flooding, about 50% of the core melt decay heat is consumed by water evaporation, leading to a pressure increase in the containment free volume. The remaining fraction of the decay heat continues to react with the concrete basemat material.

During the propagation of the accident sequence, burnable gases are generated in considerable amounts which, in the case of an ignition, may represent a potential hazard for the integrity of the containment, but which can also influence fission product chemistry and behavior. In the early stage of the accident, the most important burnable gas is hydrogen produced by the exothermal Zircaloy–water reaction

$$Zr + 2\ H_2O_{(steam)} \longrightarrow ZrO_2 + 2\ H_2 + \text{heat}$$

between the overheated fuel rod cladding material and the steam. The amount of oxidized metal increases with the square root of time, since the rate-controlling step is diffusion in the solid-state material. The temperature-dependence of the reaction rate follows Arrhenius' law resulting in a considerable acceleration with increasing temperature; beyond 1580 °C (1850 K), a further marked increase in zirconium oxidation occurs due to a phase transformation of the oxide formed. The resulting increase in heat release of the exothermal reaction in turn leads to an additional acceleration of the reaction rate. The gas pressure inside the reactor pressure vessel has only a weak influence on the reaction rate.

Despite considerable knowledge of the basic principles of the zirconium oxidation reaction, all predictions of the amount of hydrogen that will be produced in

the course of a severe reactor accident suffer from several uncertainties. These uncertainties have various causes, in particular the multitude of possible accident sequences for which the essential data such as the temperature distribution in the reactor core, the amount of steam reaching the reaction zone, the size and position of the leak in the primary circuit, the emergency core coolant feed and the behavior of the systems can only be specified within a broad range.

The extent of oxidation of the core materials and, consequently, the rate of H_2 production is largely controlled by steam supply conditions and depends, therefore, on the particular accident sequence. Hydrogen production continues after melt formation and relocation of the core components from the upper part of the core; partial flow-area blockages do not drastically reduce the rates of H_2 production. In case the progress of the melt can be stopped inside the reactor pressure vessel by re-establishing the coolant flow (as it was successfully achieved in the TMI-2 accident), considerable H_2 production has to be expected during the first stages of reflooding. Evaluation of the results of different experiments (e. g. LOFT FP-2, PBF-ST, CORA) showed that the amount of hydrogen produced during the reflooding phase may be greater than during core uncovery (Cronenberg, 1992).

In addition to zirconium oxidation, the chromium content of the stainless steel internals of the reactor pressure vessel can also be oxidized by steam in this phase of the accident, resulting in the production of additional hydrogen. Since the rate of chromium oxidation is lower by a factor of 2 to 3 than that of zirconium under comparable conditions and since the temperatures of the core internals are distinctly lower than that of the fuel rod claddings, the contribution of this reaction to total hydrogen production during this phase of the accident can be neglected.

The hydrogen produced is transported together with the steam to the primary circuit and, finally, to the containment atmosphere. The total amount of hydrogen released to the containment in the course of a low-pressure accident sequence is schematically shown in Fig. 7.3. (GRS, 1989). As an important consequence, reducing conditions prevail along the entire path of fission product transport from the overheated reactor core to the containment, the consequences of which for fission product chemistry will be discussed later on.

During the phase of interaction between the molten core materials and the basemat concrete, additional amounts of hydrogen and carbon monoxide are produced by reactions of concrete water and carbon dioxide with Zircaloy not oxidized in the reactor pressure vessel, as well as with chromium and iron. During this period, steam and carbon dioxide also evolve, increasing the total gas pressure inside the containment. Following the access of sump water to the interaction zone, the steam production in particular increases significantly, additionally contributing to the total gas pressure, but also reducing the relative hydrogen concentration in the containment atmosphere and, simultaneously, the danger of explosive H_2–air reactions. As a consequence of steam production in the containment sump, as well as of the transport of permanent gases to the containment, the pressure in this closed volume will increase, reaching the design pressure of the containment steel shell of 0.6 MPa after about 100 hours (see Fig. 7.4., calculated for a low-pressure accident sequence, according to GRS, 1989). This increase in pressure in turn leads

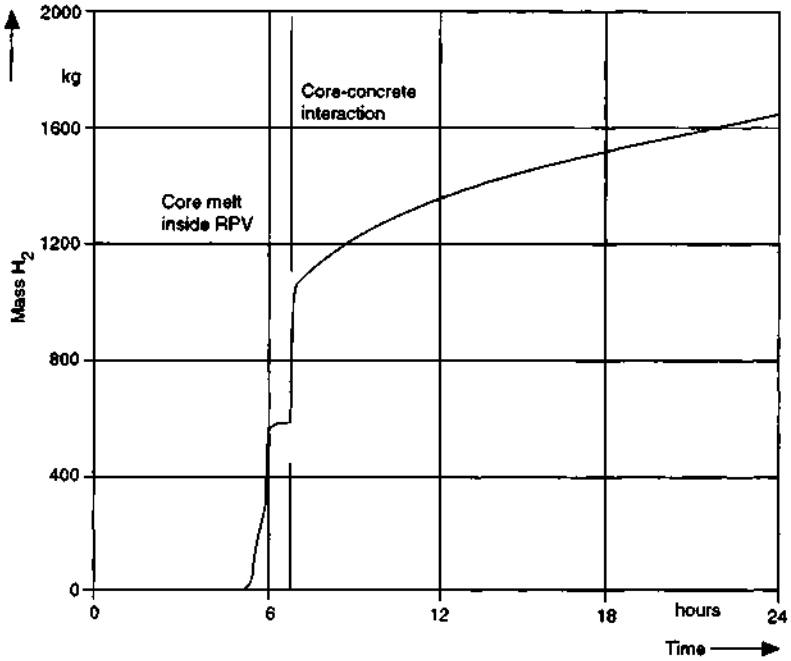

Figure 7.3. Total amount of hydrogen released to the containment; German low-pressure sequence
(GRS, 1989)

to an associated increase in temperature of the sump water and the containment atmosphere to final values on the order of 150 °C, considerably affecting the kinetics of the chemical reactions occurring in the containment. In earlier studies, it was postulated that when its design pressure was exceeded considerably the containment steel shell would fail; in Fig. 7.4. a controlled depressurization was assumed, supported by feeding additional water into the containment. If the molten core – concrete interaction zone is not flooded by sump water, the pressure increase will proceed more slowly, reaching the postulated failure pressure of the containment steel shell only after about 10 days.

Tightness of the containment over a longer period of time is an important factor in the retention of radionuclides in support of natural deposition processes and engineered safety features. To this end, facilities for controlled depressurization of the containment have been installed in many plants (see Section 7.3.4.4.).

In the high-pressure sequence, the progress of the core melt depends strongly on the particular conditions. As an example, the station blackout initiating event shall be described shortly. The highly unlikely event of a total failure of the grid power supply and, simultaneously, of all the emergency diesel generators of the plant results in a failure of the secondary-side feedwater supply, leading to a dryout of the steam generators within about 2 hours; this loss of the heat sink is followed by an increase of the coolant pressure in the primary circuit, leading to the opening

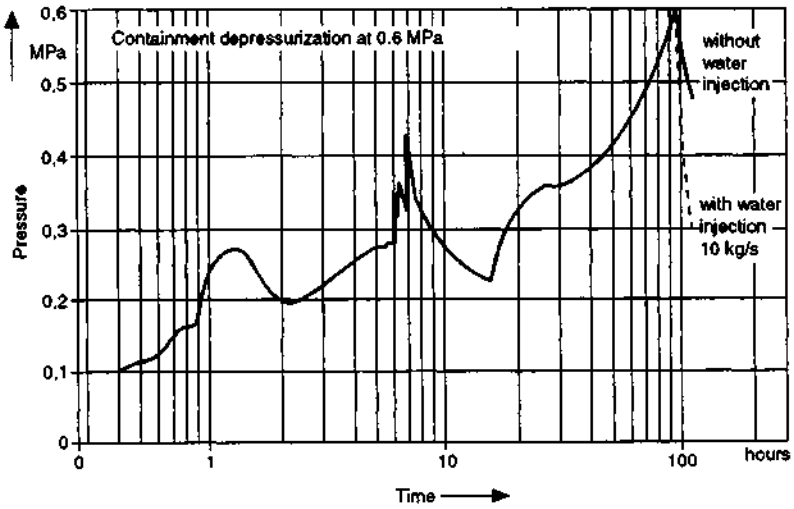

Figure 7.4. Pressure buildup in the containment following severe accident after sump water ingress
(GRS, 1989)

of the safety valves. If these valves fail to close again, contrary to their design behavior, they will form a leak through which primary coolant can escape as overheated steam. As a consequence, the coolant inventory in the primary circuit will decrease and, after about one hour, the water level in the reactor pressure vessel will have reached the core upper edge. After an additional 5 hours, the water level will have dropped to about half of the core height, Zircaloy oxidation by steam will begin, as well as core damage at an inner pressure in the reactor pressure vessel of about 16 MPa; the following core slumping will proceed in a manner similar to that in the low-pressure path. Since the high-pressure failure of the reactor pressure vessel is a somewhat problematic event, the accident management measures to be taken aim at a conversion from the high-pressure to the low-pressure path preferably by a secondary-side bleed-and-feed operation or by a direct primary-side feed-and-bleed operation.

The description of the accident sequences given above is only a very global one; depending on the different scenarios, more or less serious deviations have to be expected in a given case, which have to be taken into account when analyzing fission product transport behavior. However, these deviations mainly affect the possible source terms rather than the chemical reactions occurring in the primary system and in the containment. Since this treatise does not aim at a calculation of source terms, the individual accident sequences will not be described here. Insofar as chemical reactions are affected by special conditions prevailing in a particular accident sequence (e. g. temperature, pressure, residence times), corresponding reference will be made in the respective section.

The progress of a severe accident as described above finally results in the presence of large amounts of fission product radionuclides in the containment, in part

in the sump water or deposited on the surfaces, in part in the containment atmosphere. As long as the steel shell of the containment is absolutely tight (with the exception of small operational leaks), no releases to the environment will occur, i. e. the source term to the environment will be zero. In the safety analyses, however, it is assumed that failures in the containment steel shell will occur, leading to pathways for the fission products to the environment. In the "Deutsche Risikostudie Phase B" (GRS, 1989) five potential failure mechanisms have been investigated with regard to the amount of fission products released; their behavior under such conditions will be treated in Section 7.3.4.

7.2.2 Boiling Water Reactors

Due to the differences in design, in BWR plants other initiating events for severe reactor accidents have to be considered than in PWR plants; the essential aspect common to them is insufficient decay heat removal from the reactor core. Out of the number of possible events, two different accident sequences can be selected which, in a BWR of the KWU series 90, will cover the other sequences as regards their consequences (Fabian and Eyink, 1988). These sequences are:

- a transient, in the course of which all emergency diesel generators fail to start, resulting in a loss of energy supply to the emergency installations;
- a loss-of-coolant accident, initiated by the break of a residual heat removal train and followed by a complete failure of the residual heat removal system.

In both sequences, the reactor core will start to heat up, beginning in the transient sequence at about 20 minutes after accident initiation, and in the loss-of-coolant accident about 1.5 hours after the initiating event. Basically, core heat-up proceeds in a manner which is quite similar to that in a PWR accident; however, because of the larger inventory of Zircaloy in a BWR core (in particular in the fuel assembly channels, see Section 2.1.2.) the energy available in core meltdown can be greater than in the PWR case. The B_4C inventory of the control rods together with stainless steel and Zircaloy will form a eutectic mixture melting at temperatures above 1200 °C. This molten phase runs down to the residual water level; as the accident progresses, the fuel rods are attacked and the molten material falls down to the lower part of the reactor pressure vessel. Later on, the melt may penetrate the reactor pressure vessel via the control rod drive mechanism nozzles, provided that no measures have been taken to re-establish coolant flow. Failure of the reactor pressure vessel is predicted to occur 4.9 hours after accident onset in the transient case and after 6.5 hours in the loss-of-coolant case.

In the event of a transient, there is no direct contact between the reactor pressure vessel and the containment, so that the steam–gas flow escaping from the reactor pressure vessel, as well as the volatile fission products and the aerosols carried by it, are transported through the relief line to the pressure suppression pool. When it passes through the water volume of this pool, the overwhelming fraction of the aerosols is retained (as well as iodide), while a small fraction of elemental iodine can potentially escape from the water phase due to its volatility

(see Section 7.3.2.4.). In the loss-of-coolant accident, on the other hand, steam enters the containment during an early stage of the accident, carrying aerosols and volatiles with it; from there the steam flow is directed through downcomers to the suppression pool. The high concentration of aerosols in the containment drywell during a short period of time leads to the deposition of nearly 25% in this compartment. Most of the aerosols entering the suppression pool are expected to be retained in the water.

After evaporation of the sump water and remelting of the corium, the reactor containment may fail, provided that no countermeasures (containment venting) have been taken. In the event of such a failure, gases as well as aerosols have to pass the reactor building and turbine hall before reaching the environment. Along this way a considerable deposition of the remainder of the radionuclides which had escaped from the pressure suppression pool has to be expected.

References Section 7.2

Cronenberg, A. W.: Hydrogen generation behavior in the LOFT FP-2 and other experiments: Comparative assessment for mitigated severe accident conditions. Nucl. Technology **97**, 97–112 (1992)

Fabian, H.-O., Eyink, J.: Assessment of relevance and consequences of severe accidents in Siemens/KWU BWRs. Proc. IAEA/OECD Internat. Symposium on Severe Accidents in Nuclear Power Plants, Sorrento, Italy, 1988, Vol. 1, p. 295–307

Gesellschaft für Reaktorsicherheit (GRS): Deutsche Risikostudie Kernkraftwerke, Phase B. Bericht GRS-72 (1989)

Hassmann, K., Hosemann, J. P., Peehs, M.: Spaltproduktfreisetzung bei Kernschmelzen; Methodische Bestimmung und experimentelle Absicherung. Verlag TÜV Rheinland Köln, 1987

Hobbins, R. R., Petti, D. A., Osetek, D. J., Hagrman, D. L.: Review of experimental results on light water reactor core melt progression. Nucl. Technology **95**, 287–306 (1991)

Hofmann, P., Hagen, S. J. L., Schanz, G., Skokan, G.: Reactor core materials interactions at very high temperatures. Nucl. Technology **87**, 146–186 (1989)

7.3 Chemistry and behavior of radionuclides in the different stages of a severe accident

7.3.1 The release of radionuclides from the overheated reactor core

The release of fission products and structural materials from the overheated and, finally, molten reactor core represents the initial and, therefore, most important component of the source term. It provides vapor and aerosol sources for radionuclide transport in the reactor primary system and, further on, to the containment.

The quantity, time-dependence and composition of the volatilized substances may significantly influence the further behavior of the radionuclides as well as the progress and the products of chemical reactions occurring in the primary system and in the reactor containment. On the other hand, the volatilization of the fission products from the reactor core is able to affect the further progress of core heatup and degradation, since in the first hour after reactor shutdown the gaseous and volatile fission products contribute approximately 30% of the total decay power of the core.

In the following description of the reactions occurring during this stage of a severe core damage accident, three different topics will be discussed: the release of fission products from the fuel, the release of constituents of the core structural and control rod materials (although these two sources develop almost simultaneously in the reactor pressure vessel so that the volatilized substances can be assumed to enter the gas flow as a mixture) and, finally, volatilization of substances during the molten core – concrete interaction phase. The current state of the art will be discussed with special emphasis on the important chemical phenomena; no attempts will be made to establish numerical values of source terms from the results of these experimental and theoretical efforts.

7.3.1.1 Fission products from the fuel

7.3.1.1.1 General aspects

The failure of the fuel rod claddings and the heating-up of the fuel in the course of the propagation of a severe accident leads to a volatilization of fission products and activation products from the fuel and from the core structural and control rod materials which increases with increasing temperature. At the high temperatures which are reached during such an accident, the release of fission products is no longer restricted to the gap inventories of the failed fuel rods, as it is in the case of a loss-of-coolant design basis accident, but will affect the inventories present within the fuel matrix as well. These inventories are determined by the burnup state of the nuclear fuel. With respect to the behavior of the radionuclides and their physico-chemical reactions during such an accident, the mass concentrations rather than the activity concentrations of the fission products in the fuel are of particular interest; in Tables 3.3. and 3.4., mass concentrations of the most important fission product elements at different burnup states of the fuel are given. In addition, the chemical form of the fission products in the fuel, their spatial distribution within the fuel pellet, both established during reactor normal operation, and their effective mobilities may considerably influence the release behavior at elevated temperatures; these topics have been discussed in Chapter 3.

In general, four different mechanisms can be distinguished in the release of fission products from the overheated reactor core:

- The failure of the fuel rod claddings in the temperature region of 1000 °C (~ 1300 K) is accompanied by the burst release of fission products, the same phenomenon which transports the fission products into the primary circuit in

the event of a loss-of-coolant design basis accident. The release during this phase exclusively concerns the fission products which during plant normal operation have been deposited in the fuel pellet – cladding gap, the so-called gap inventory (see Section 3.2.4.).

- If the fuel temperature remains in this range for a longer period of time, grain boundary diffusion of the fission products present within the fuel matrix and their migration along cracks in the fuel pellet would gain in importance, in particular in high-burnup fuels. This mechanism mainly affects those fission products of which a significant fraction, during reactor operation, is deposited at the grain boundaries, such as the noble gases, but iodine and cesium as well. In addition, UO_2 is oxidized by steam at temperatures above 1100 °C to form hyperstoichiometric UO_{2+x}, potentially influencing the release behavior of various fission products by the change in their chemical environment.
- At temperatures beyond 1350 °C (~ 1600 K), diffusion of the fission products within the UO_2 crystallites to the grain boundaries and from there out of the pellet begins to become a significant parameter. The rate of release at this stage depends, among others, on the fuel burnup and on the fuel pellet morphology (grain size, porosity, cracks), which means that differences in behavior may occur when fuels of different manufacturing parameters and different irradiation histories are considered. In addition, enhanced oxidation of UO_2 by steam may accelerate the release of volatile fission products during this stage; on the other hand, the Zircaloy cladding may act as an oxygen sink and hydrogen source, to a certain extent protecting the fuel against oxidation. The impact of some of these parameters will be discussed in more detail below.
- After melting of the fuel, starting with fuel liquefaction initiated by a UO_2–Zircaloy reaction, diffusion of the fission products in the molten phase becomes the mechanism determining the release rates; in addition, release may be increased by convective movement in the melt. During this phase, the vaporization of elements of lower volatility begins, leading to the production of substantial amounts of aerosols; simultaneously, the remainder of the volatile fission products still present in the fuel matrix is released from the melt. During the subsequent molten core – concrete interaction phase, which starts after penetration of the reactor pressure vessel, the gases produced from concrete decomposition will effect an intense mixing of the melt and, as a result, effect an increased release rate. Moreover, the changed chemistry conditions prevailing in the melt at this stage of the accident (compared to the melt in the in-vessel phase) may lead to variations in the release behavior of specific radionuclides or elements.

However, in the course of an actually occurring severe core damage accident the reactor core will not be at a uniform temperature; at any given moment still-intact fuel rods, liquefied fuel and molten core materials will be present simultaneously within the reactor pressure vessel, though in different regions of the core. Therefore, releases of different elements from the core are not isolated in time but will in fact take place simultaneously in the different regions, with consequences for the potential chemical reactions in the steam–gas phase above the core.

With respect to their release behavior during the process of core degradation, the radionuclides can be roughly divided into two groups: The group of volatile fission products includes the noble gases krypton and xenon, as well as iodine, cesium (and the less important fission product isotopes of bromine and rubidium) and, under certain circumstances, tellurium (see below); all the other fission products, as well as the activation products of the fuel, can be classified into the less volatile group. This behavior of the fission products generally corresponds to the well-known macrochemical properties of the respective elements and of the compounds of these elements that are to be expected under such conditions, such as oxides. There is, however, still the question as to the behavior (in particular the volatilization behavior) of these elements at very high temperatures when they are present in a mixture together with a large surplus of foreign substances (such as uranium and zirconium oxides), with such conditions possibly resulting in the formation of compounds with specific properties. Quantitative predictions based on the principle of minimum energy are possible when modern thermochemical codes are used such as ChemSage, which is based on the earlier SOLGASMIX code and which takes into account a large number of chemical species in the different phases of matter, and which is also applicable to thermochemical calculations in complex systems involving phases that exhibit non-ideal mixing properties (Eriksson and Hack, 1990). Basic research in recent years has furnished a broad data base with regard to the thermochemistry of fission products in irradiated fuel (see, for example, the review paper of Cordfunke and Konings, 1993). At temperatures beyond 1400 K, kinetic limitations generally are not assumed to play a significant role, which means that calculations of fission product chemical states in the overheated fuel using thermodynamic methods are not believed to be adversely affected by non-equilibria situations. The calculation of the amounts of substances evaporating from mixed-phase specimens according to Raoult's law (the effective vapor pressure of each constituent is proportional to its concentration in the mixture), which was frequently applied in former years, can yield trustworthy results only for those mixtures of substances in which no chemical interactions between the different constituents take place. In applying Raoult's law to a mixed-phase substance, however, the release could be under- or overestimated to a considerable extent (Wichner and Spence, 1985).

When evaluating the volatilization behavior of fission products it has to be taken into account that, in particular in high-burnup fuels, fission product condensed phases may have been formed within the fuel (as a result of interactions of fission product elements either with each other or with the fuel main constituents) which may affect their vapor pressures. In addition, the chemical states of the fission products in the fuel can be changed as the core heats up and finally melts during the course of a severe accident. Important factors in this regard are reactions of selected fission products with the Zircaloy cladding material, the constituents of the control rod materials, the constituents of stainless-steel, etc. Finally, the composition of the steam–hydrogen mixture in the core affects the volatilization behavior, since the ratio of steam (an oxidant) to hydrogen (a reductant) determines the effective oxidation potential in the core, which in turn can influence

considerably the chemical form of elements released as well as the rate and degree of Zircaloy oxidation.

In addition to theoretical calculations, appropriate experiments have to be carried out taking into account the highly complex situation in the reactor core during a meltdown accident, not only to make available basic data to be used in the calculations, but also to validate the results of prior code calculations. As an important aspect in the preparation of such experiments, the question arises of whether to use real irradiated fuel samples or non-irradiated UO_2 specimens containing artificially prepared fission product simulants. When using true spent fuel samples, there is no doubt about the correct chemical form of their fission product inventories. However, such experiments are very expensive and time-consuming because of the extensive radiation protection measures which have to be taken. These difficulties do not arise when fission product simulants are applied, even when they have been labelled with radioactive tracers for ease of measurement. Nonetheless, the use of such simulant specimens in vaporization experiments is not undisputed since there are considerable differences in their composition as compared to irradiated fuel, which may have a potential influence on the results. While in irradiated fuels the fission products are incorporated into the fuel grains or are located at the grain boundaries, in simulant samples they are more or less present in a mechanical mixture with the fuel matrix. Thus, even when they have been intimately mixed with finely powdered UO_2, the first step in the vaporization process, which is the release from the fuel matrix grains, is lacking when simulant mixtures are applied; as a result, differences in the vaporization kinetics may occur. As a remedial measure, the doped specimens can be subjected to a sintering process prior to the experiment, which effects a mutual diffusion of fuel and simulant material; however, such a pretreatment step is only possible with low-volatility fission product simulants, since volatile elements are already vaporized to some extent during this procedure. Moreover, even after such a pretreatment the question continues to be whether the simulant contains the correct chemical form of the fission product element. In general, experiments have yielded significant differences only in the release behavior of the volatile fission products from the two types of experimental materials, whereas fission products with very low vapor pressures are not noticeably affected by the difference between using actual irradiated fuel and a simulated one.

Because of the great interest in the processes of vaporization of fission products from overheated nuclear fuels, corresponding experimental investigations were performed in the early years of commercial nuclear power generation, but they were mainly carried out using small fuel specimens. As an example, the ORNL in-pile melting experiments shall be mentioned (Browning et al., 1964), in which small UO_2 specimens encapsulated in stainless-steel claddings were heated in a loop of a research reactor in a flowing helium atmosphere to temperatures beyond their melting point. The results demonstrated the complete volatilization of noble gases, iodine, cesium and tellurium from the fuel matrix, as well as a high degree of release of the other fission products which, however, were mainly retained in the cooler regions of the in-pile experimental device.

Since the transport behavior of the volatilized fission products is largely determined by their chemical state, attempts were made to throw more light on this

important question. An appropriate device for the investigation of this problem is the thermal gradient tube, the main characteristics of which have been described in Section 6.2.1.1. Out of the early experiments performed in this field, those of Castleman and Tang (1967; 1970) deserve to be mentioned, in which irradiated uranium metal was heated in a laboratory facility to temperatures of 1200 to 2500 °C (1500 to 2800 K). In a pure helium atmosphere, fission product iodine was plated out in the thermal gradient tube at a temperature of about 280 °C, whereas in the presence of air it condensed at about 100 °C, indicating its transport as elemental iodine I_2. The deposition maximum of fission product cesium in both atmospheres occurred at about 450 °C, that is, it did not coincide with that of iodine, which rules out the existence of a compound CsI under such conditions. When heating trace-irradiated UO_2 in steam to temperatures of 1000 to 1300 °C (1300 to 1600 K), about 80% of the released iodine was detected as I_2 in the condensed steam; from these results, it was concluded that the concentrations of both iodine and cesium in the steam were too low to render feasible the formation of an appreciable fraction of CsI. When, however, the steam contained hydrogen, the I_2 fraction decreased to about 10%, whereas the I^- fraction increased to about 60%, indicating an I_2-H_2 reaction in the steam phase (Castleman et al., 1968), consistent with the results of kinetic calculations which will be discussed below. In the above-mentioned experiments it was observed that a 10 to 20% fraction of iodine (depending on the experimental conditions) was present in the steam flow as an organoiodine compound (CH_3I). Since this compound was not detected in the heating experiments carried out by other investigators (see below) and since the mechanism of its formation under the prevailing conditions is highly obscure, it cannot be ruled out that its appearance was the result of the experimental conditions applied, in particular in the course of the separation of the volatilized individual iodine species by a liquid-liquid extraction procedure.

When interpreting the results of analyses of fission product chemical species released from fuel in heating experiments, there is always the question as to what extent secondary reactions occurring in the experimental facility during the performance of the investigations might have changed their original states. To clarify this question, various investigations have been performed (e. g. Collins et al., 1985), in which small amounts of the fission product compounds under consideration were volatilized in an appropriate device and the resulting species analyzed in a thermal gradient tube. In these studies CsI showed little decomposition; however, small proportions of elemental iodine I_2 observed in some of the experiments were probably formed by secondary reactions (see below). CsOH was observed to be very reactive with the ZrO_2 material of the furnace liner in the temperature range 800 to 1000 °C (1100 to 1300 K). In the presence of elemental tellurium, a CsOH–Te reaction with formation of CsTe was also observed. These results suggested that the chemical species detected are in general representative for those released from the fuel, provided that appropriate precautions have been taken in the design of the experimental device. Earlier experiments (Lorenz et al., 1976) had demonstrated that organoiodide compounds (in particular CH_3I) are readily decomposed in a steam–argon atmosphere at temperatures beyond 800 °C (1100 K); organoiodides detected in the containment in the course of a reactor accident, therefore,

can be assumed to be exclusively the product of reactions occurring there and do not originate from the overheated fuel.

In the heating experiments reported by Peehs et al. (1983), small specimens of irradiated LWR fuels from power reactors were treated in a Knudsen cell under high-vacuum conditions. These tests, which have been discussed in Section 3.2.3.3., and the results of which were summarized in Fig. 3.18. and 3.19., show a steep increase in the release rates of iodine and cesium for increasing temperatures beyond about 1200 °C (1500 K), with both elements exhibiting a virtually identical behavior. They also showed that higher fuel burnup considerably facilitates the release of both fission products from the fuel. This effect was explained by the limited solubility of these fission products in the UO_2 lattice, the consequence of which would be migration of a fraction of them out to the grain boundaries, increasing with increasing element concentration; from the grain boundaries a faster release is possible than out of the UO_2 crystallites.

Johnson and Johnson (1989) analyzed by mass spectrometry the substances released from highly irradiated fuel when it was heated to temperatures in the range 800 to 1900 °C (1100 to 2200 K). Their results showed that in a reducing environment the xenon release rates at temperatures exceeding 1200 °C exhibit an exponential dependence on temperature, whereas at lower temperatures they show a different activation energy. To explain this deviating behavior, it was assumed that at low temperatures pore diffusion in the fuel is the rate-controlling step for release, while at higher temperatures it is solid state diffusion. It was possible to correlate deviations in the xenon release rates between different fuel specimens with the degree of their open porosity. In an oxidizing atmosphere, the xenon release rates at temperatures beyond 1200 °C were higher by a factor of about 80 than in a reducing environment; this difference was assumed to be partly caused by oxidation of the fuel specimen, leading to an increased diffusion rate of the noble gases, and partly due to the formation of cracks in the sample under the experimental conditions. The cesium release rate in a reducing environment was about 6% of the xenon value; in contrast, in an oxidizing environment the cesium release rates were below the detection limit of the experiment. Only at high test temperatures were low release rates of atomic iodine species detected. A similar behavior was observed for tellurium: in contact with Zircaloy the compound SnTe was found, quite in agreement with the results of other investigators (see below).

7.3.1.1.2 Out-of-pile experimental programs

Laboratory investigations like those described exemplarily above (as well as numerous others conducted in many laboratories) have provided valuable information on the basic mechanisms of the release of fission products from overheated nuclear fuel. Insight has been gained into the vaporization behavior of volatile and less volatile fission products, into the chemical forms of the released species, into the impact of environmental conditions (e. g. redox potential), etc. However, these experiments were often carried out under experimental conditions which are not

representative of severe accidents (ambient atmosphere, bare fuel specimens without cladding etc.), partly due to differences in the objectives of the work. Moreover, in the early years of nuclear technology there were limitations in the definition of the boundary conditions to be expected in the course of a severe reactor accident. As a result, the release rates of fission products measured in these experiments cannot be directly applied for the calculation of the release rates to be expected in the course of a degraded core accident. In order to obtain realistic data on the release behavior of fission products from overheated fuels, several experimental programs have been initiated, out-of-pile as well as in-pile, in which the conditions of different anticipated accident sequences were simulated as close to reality as possible. In this section the most important out-of-pile programs, the SASCHA experiments and the ORNL experiments, will be discussed; the in-pile tests will be addressed in the following section.

In the framework of the severe reactor accident research program conducted in the laboratories of the Kernforschungszentrum Karlsruhe (KfK), the SASCHA experiments dealt with the study of release characteristics of fission products from overheated fuel; a summary description of these experiments and the results obtained was given by Albrecht (1987 a). In these experiments, non-irradiated UO_2 doped with simulant fission products was used (so-called fissium). As regards the preparation of these specimens, the simulant fission products were first labelled by neutron irradiation and then they were added as metals or oxides to the UO_2 powder. This mixture, with a mass of 100 to 200 g and a composition corresponding to a fuel burnup of about 44 MWd/kg U, was pressed to pellets and then encapsulated in Zircaloy tubes. In some cases, the highly volatile elements were omitted and the pellets were additionally sintered at a temperature of 1500 °C prior to encapsulation. As can be seen from Fig. 7.5., the specimens were heated in a crucible; depending on the required conditions, the atmosphere in the experimental facility was composed of argon and steam in varying ratios. The substances volatilized from the specimen during the experiment were transported by the gas flow to a filter system allowing separate collection of the fractions, which were consecutively volatilized from the fuel specimen at different sample temperature intervals.

As can be seen from Fig. 7.6. (according to Albrecht, 1987 a), iodine and cesium show a similar volatilization behavior, which is not changed when both elements are simultaneously present in the sample. The volatilized iodine was mainly attached to aerosol particles and collected on the glass fibre filters of the analytical duct; another fraction of it was retained on the steel walls of the experimental setup; and only a small fraction was able to pass through the aerosol filters and was retained on a special iodine filter. When CsI was added to the sample instead of separate cesium and iodine compounds, the release proceeded significantly more slowly; the volatilized fission product compound was also almost completely transported to the aerosol filters; on the iodine filters downstream from the aerosol filters only very small fractions of the volatilized iodine of less than 1% were detected. If the specimen was in contact during heating with control rod alloy (Ag-In-Cd alloy), a significant fraction of the volatilized iodine (originally present in the sample as CsI) was detected on the aerosol filters as a compound which was not soluble in water, but could be dissolved in $Na_2S_2O_3$ solution. Obviously, a

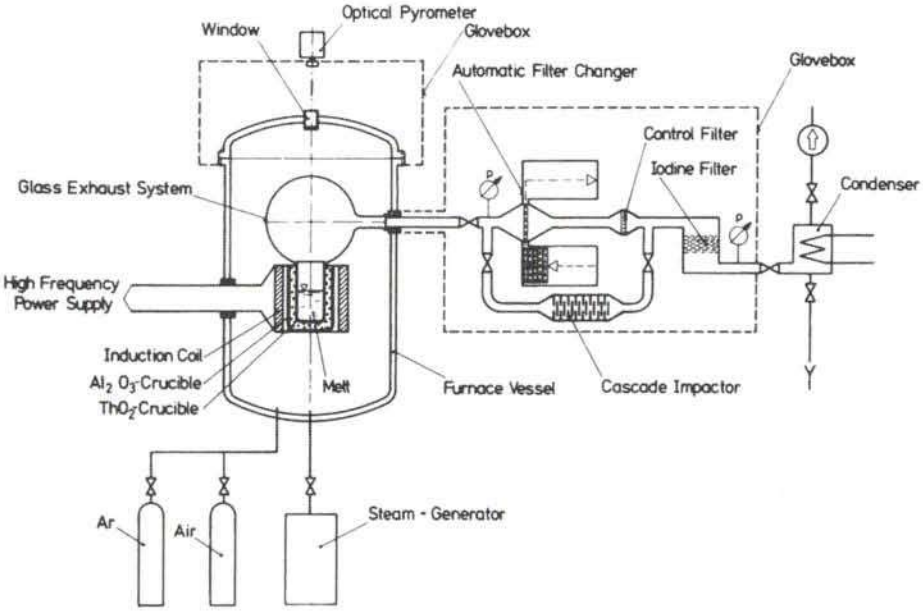

Figure 7.5. SASCHA facility for core melt release studies (Albrecht, 1987 a)

fraction of iodine was converted in the gaseous phase to AgI as a thermodynamically stable compound, in agreement with the thermodynamic calculations of Hahn and Ache (1984).

Similar experimental conditions to those in the SASCHA experiments, that is a flowing steam–hydrogen atmosphere at atmospheric pressure, were used in the ORNL high temperature tests, the principal aim of which was to determine the impact of specific accident conditions on the behavior of fuel and fission products. In the early ORNL high-temperature experiments (HT series), fuel rod segments fabricated of power-reactor irradiated fuel and encapsulated in Zircaloy cladding were heated for a short time (a few minutes) to temperatures up to 1900 K in atmospheres of various composition. The results obtained in these tests were the main basis for the assessment of fission product release from overheated fuels made in the NUREG-0772 report (US NRC, 1981).

In the more recent high-temperature test series (HI, HS, VI) an improved induction furnace design was employed that allowed heating to much higher temperatures and for longer periods of time, independent of the extent of cladding oxidation by steam. While in the HI and HS tests a horizontal furnace arrangement was used (similar to that shown in Fig. 6.1.), in the VI series a vertical orientation was employed (see Fig. 7.7.). In the HI and VI experiments, high-burnup fuel specimens were investigated (burnup levels ranging from 10 to 47 MWd/kg U), each of them as a fuel rod segment 15 to 20 cm long, containing 100 to 200 g fuel, encapsulated in a highly irradiated Zircaloy cladding. In contrast, in the HS tests non-irradiated

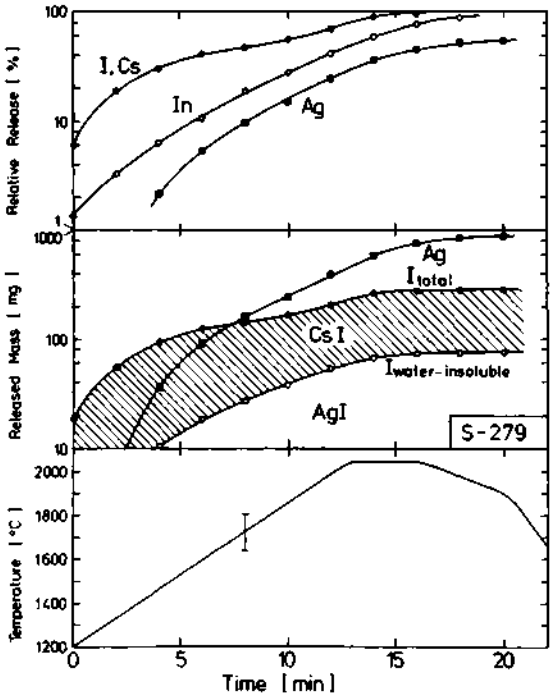

Figure 7.6. Release of I, Cs, Ag, and In in steam; formation of AgI from initially present CsI
(Albrecht, 1987 a)

UO_2 specimens containing fission product simulants were subjected to heating similar to that used in the SASCHA experiments discussed above. All tests were carried out at atmospheric pressure for 2 to 60 minutes at the test temperature; different atmospheres (in particular different ratios of $H_2 : H_2O$) have been used in different tests of the series.

In the VI tests, the substances volatilized from the furnace (which is located inside a hot cell) were collected on three sequentially operated collection trains (see Fig. 7.8., according to Osborne and Lorenz, 1992), each of which consisted of a thermal gradient tube (TGT) to collect condensing vapors, a package of graduated filters and impregnated charcoal cartridges to collect particulate material and gaseous iodine species, respectively; further, they contained a cold charcoal trap to collect and measure fission gases, in particular ^{85}Kr. Radiation detectors were positioned to monitor continuously the location of the fuel specimen, which tended to move downward in those tests where melting of the cladding took place. Other radiation detectors provided on-line information on the progress of collection of ^{134}Cs and ^{137}Cs on the walls of the TGTs and on the filters and of ^{85}Kr in the gas traps. Since all the fuel specimens used in the experiments had experienced long decay times (6 to 10 years) prior to the tests, the possibilities of direct gamma spectrometry measurement of the volatilized fission products were limited to a few

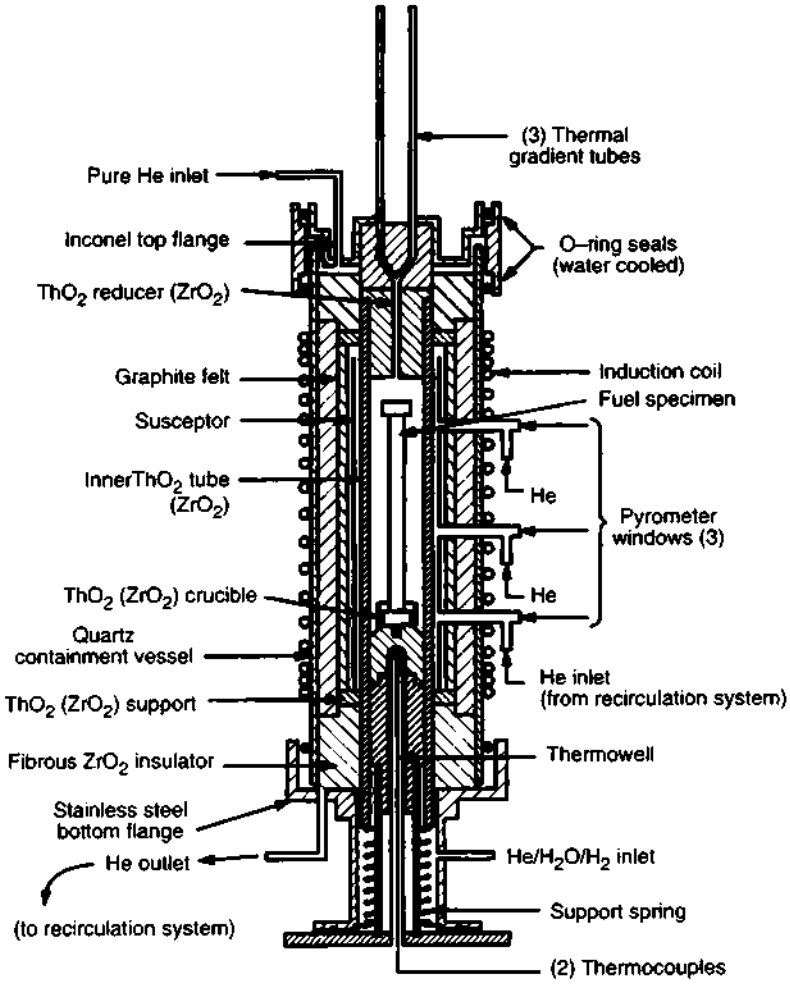

Figure 7.7. ORNL vertical furnace device for high-temperature fission product release studies
(Osborne and Lorenz, 1992)

radionuclides only. Therefore, additional analytical techniques were applied for the determination of the various elements, such as neutron activation analysis for iodine and bromine, spark source mass spectrometry for all elements heavier than neon, and emission spectrometry for molybdenum, tellurium, barium and uranium.

The execution and the results of the HI experiments which were conducted over the temperature range 1400 to 2000 °C (1700 to 2300 K) were published in a number of reports and, as far as the question of release kinetics from the fuel is concerned, summarized by Osborne et al. (1987). These tests mainly aimed at the study of the release behavior of the volatile fission products krypton, iodine and

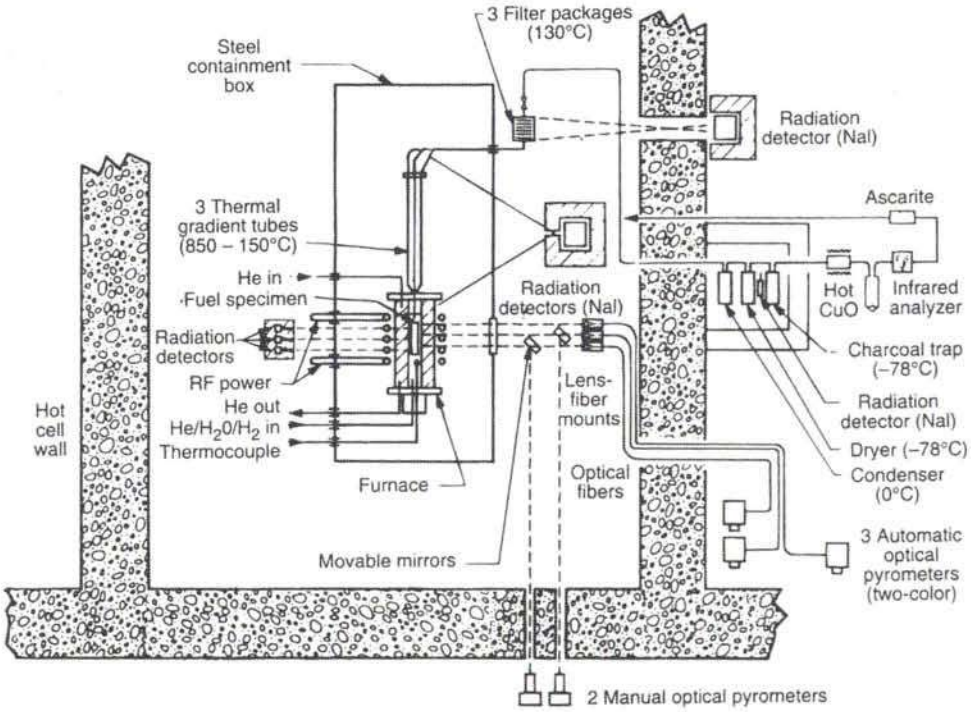

Figure 7.8. ORNL vertical-furnace fission product release facility (Osborne and Lorenz, 1992)

cesium from the fuel specimen; their results showed that the fractional releases of these three elements were similar to each other in all the tests, ranging from about 2% in 30 minutes at 1700 K to a maximum value of about 60% in 20 minutes at 2300 K. The release rates shown in Fig. 7.9. were calculated from the cumulative release fractions and the effective times the specimens were held at the test temperatures. According to these results, the dependence of the release rates of the three elements on the test temperature is quite similar; with the exception of two data sets (HI-2 and HI-6) the release rates were distinctly lower than those obtained in the former short-term experiments (HT series), from which the temperature-dependence mentioned in the NUREG-0772 report (US NRC, 1981, in Fig. 7.9. designated as Ref. 1) was calculated. The two higher results could be explained by specific differences in the test conditions: In test HI-2, an unusually large cladding rupture led to significant UO_2 oxidation, an effect which is known to result in an accelerated and enhanced fission product release, whereas test HI-6 lasted only for a short time, so that the release rate obtained here represents mainly the initial stage of heating, which generally shows faster release. For this reason, the four lower release rate results seem to be more representative of the conditions prevailing in an overheated reactor fuel; their deviations from the NUREG-0772 data can be attributed to the fact that, as was mentioned above, the latter data had

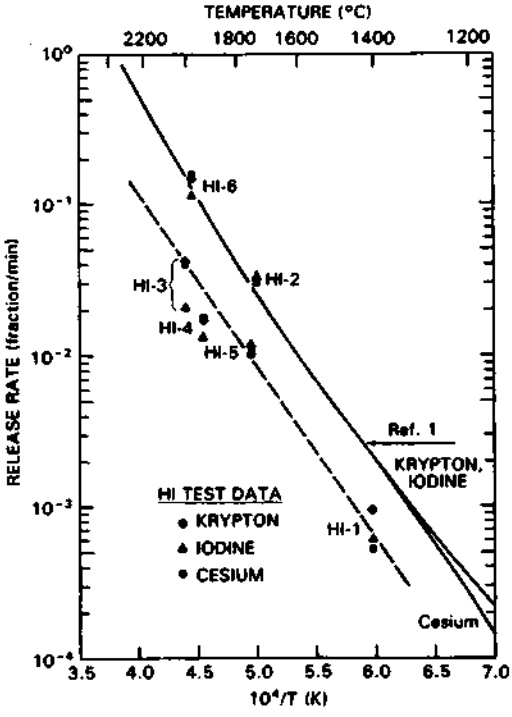

Figure 7.9. Inverse temperature dependence of ORNL HI test data, compared with the NUREG-0772 data
(Osborne et al., 1987; Copyright 1987 by the American Nuclear Society, La Grange Park, Illinois)

been calculated from heating tests in which only comparatively short experimental periods were used.

The release rates of the volatile fission products measured in the VI test series were consistent with those obtained in the HI tests. As is exemplarily shown in Fig. 7.10., enhanced volatilization of krypton and cesium from the fuel specimen starts when the temperature exceeds values of about 1400 °C (the same applies to iodine), suggesting that at these temperatures the release of the fission products from the grain boundary inventories increases in importance, as well as their diffusion out of the UO_2 crystallites. At temperatures beyond 1600 °C a considerable fraction of the inventory of the volatile fission products is vaporized from the fuel specimen within a comparatively short time. Grain growth in the fuel at higher temperatures and an associated grain boundary sweeping mechanism are major contributors to the extensive fission product release in this temperature range. Likewise, the degree of fuel porosity is assumed to be an important parameter in the release of the volatile substances.

At temperatures beyond about 1800 °C (2100 K), fuel liquefaction begins to play an important role in the vaporization of volatile fission products. The next step is

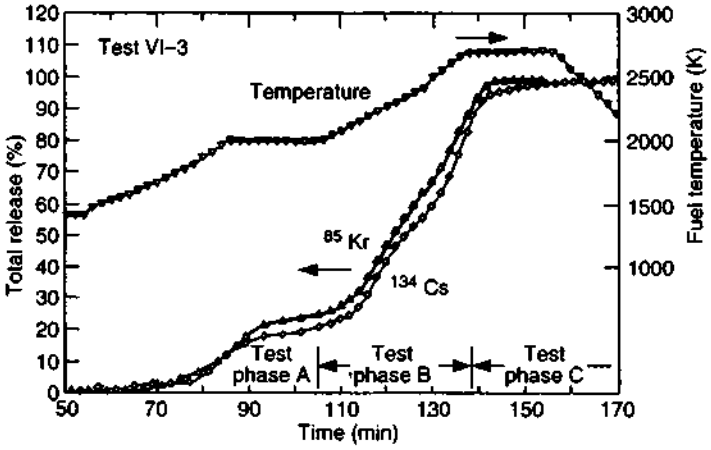

Figure 7.10. Fission product release from irradiated UO_2 fuel as a function of temperature (ORNL test VI-3)
(Osborne and Lorenz, 1992)

the formation of a eutectic melt in which the fuel grains are dissolved. Another phenomenon which can support the release of volatile fission products is the breakup of the fuel, if it is rapidly quenched from high temperature, as will happen as a result of core reflooding when core cooling is restored again. This causes the fuel to fracture along the grain boundaries, increasing the effective surface area. The impact of fuel liquefaction on fission product release is particularly pronounced with low-burnup fuels (< 5 MWd/kg U); in such a material, interlinking of bubbles present at the grain boundaries is not yet fully developed and, thus, liquefaction can lead to a burst release. In contrast, in high-burnup fuels diffusion of the volatile fission products along the grain boundaries and bubble channels and out of the fuel, resulting in a depletion of the grain boundary and pore inventories, already proceeds as the temperature increases to liquefaction values; as a result, with such fuels no significant burst release of volatile fission products will occur upon liquefaction or sudden quenching of the core. This mechanism was confirmed by release data obtained from both out-of-pile and in-pile experiments (Cronenberg et al., 1983).

Tellurium exhibits a particularly complicated release behavior from overheated nuclear fuels. As a result, for a rather long time contradictory statements were made in this field. In the early years of nuclear technology, Parker and Lorenz (1963) reported on heating experiments of low-irradiated UO_2 that under otherwise identical conditions tellurium release from Zircaloy-cladded fuel appeared to be lower by about a factor of 40 than from steel-cladded or non-cladded UO_2. From this behavior they concluded that tellurium release from LWR fuel rods would not be identical to that from the UO_2 fuel itself, but was controlled by some additional mechanism. In order to find out the reasons for these differences in behavior, the experimental results reported by different authors were systematically evaluated by Lorenz et al. (1983). It is well known from basic studies that metallic tellurium

reacts with zirconium at temperatures above 673 K. Under reactor accident conditions, this reaction leads to the formation of compounds whose composition depends on the temperature; below about 1273 K it varies between $ZrTe_2$ and ZrTe, at higher temperatures Zr_5Te_4 is stable, with all these compounds being plated out on the inner surface of the fuel rod cladding. The vapor pressure of Te_2 above these compounds is lower by about 5 orders of magnitude than that above $NiTe_2$ or other tellurides of constituents of stainless steel. $ZrTe_2$ can be decomposed by oxygen at 1500 K as well as in systems showing oxygen potentials more positive than −171 kJ/mol; the tellurium liberated by this reaction can react with Ziracaloy not yet oxidized, it can remain as a metallic tellurium melt or it can be volatilized, depending on the ambient conditions. In addtition, with tin the compound SnTe is formed, which melts without decomposition at 1077 K.

On the basis of the results of a larger number of experiments, two different types of tellurium behavior during core meltdown can be distinguished:

- High tellurium release, identical with that of iodine within a factor of 2, was observed in all heating experiments of bare fuel specimens without Zircaloy cladding in inert and reducing atmospheres, as well as in various experiments with Zircaloy cladding showing extensive Zircaloy oxidation.
- Low tellurium release, lower by a factor of 10 or more than that of iodine, was measured in virtually all experiments using Zircaloy-cladded fuel specimens.

Thus, it can be concluded that the temperature-dependence and kinetics of tellurium volatilization from the oxide fuel itself is comparable to that of iodine and cesium, but that this element is retained in the reactor core by reaction with metallic Zircaloy; as a result, the extent of tellurium release from the fuel rod depends strongly on the degree of Zircaloy oxidation. If this oxidation starts exclusively from the outside of the cladding, then tellurium retention would be terminated not earlier than after almost complete oxidation of the cladding material; if, however, the oxidation proceeds on both cladding surfaces (inner and outer surface), then an oxide layer of a minimum thickness would be sufficient to prevent or to retard the progress of the Zr−Te reaction. From this behavior as a starting point for the calculation of tellurium release in the course of an accident it can be assumed that

- at a local Zircaloy oxidation (i. e. in the respective control volume) of less than about 90%, release of tellurium would be low, on the order of 2.5% of that of iodine;
- at a local Zircaloy oxidation of more than 90%, one has to expect a tellurium release on the same level as that of iodine and cesium.

These assumptions are consistent with the findings of the corresponding SASCHA experiments (Albrecht, 1987 a), which showed that tellurium release is highest in a steam atmosphere, higher by about a factor of 5 than in an Ar + 5% H_2 atmosphere under otherwise identical conditions.

Additional studies (Collins et al., 1987) have, on the whole, confirmed the results mentioned above. According to these experimental investigations (which were performed in the ORNL heating device), tellurium is transported from the fuel pellet to the pellet − cladding gap most probably as the tellurides of cesium and rubidium

and/or as elemental tellurium. Here, the tellurium vapor species react with the inner surface of the cladding to form zirconium telluride, which effectively retains the tellurium from volatilization as long as metallic zirconium is available. The parameters that most affect tellurium release from the fuel rods are temperature, availability of steam, cladding damage due to oxide and/or hydride embrittlement cracking, and eutectic melting and runoff.

Consequently, in a high-steam, slow-heatup environment, the release of tellurium from the fuel rods would initially be very slow. Following oxidation of the zirconium metal, the release rate from the fuel rod would increase strongly due to the simultaneous volatilization from the cladding metal and from the pellet itself; experiments have shown that at the time of complete Zircaloy oxidation, 30 to 40% of the tellurium inventory of the fuel was held by the cladding, with the remainder still present in the fuel. After this phase, the tellurium release rate decreases again and becomes comparable with the release rates of the other volatile fission products. From the results of the TGT analyses it can be concluded that the chemical forms of tellurium initially released are primarily SnTe, CsTe, and RbTe until the tin supply from the cladding is exhausted; afterwards, the remainder of tellurium being released from the pellets would be CsTe and RbTe. In contrast, in a steam-starved, slow-heatup environment, there would be the opportunity for eutectic melting and runoff of cladding Zircaloy in contact with the fuel pellets. This melt can carry a significant fraction of the tellurium down to lower regions of the core to form larger masses of melt with structural materials, keeping this tellurium from being volatilized. The degree of tellurium retained in this melt depends largely on the timing of the runoff; it can be assumed that a slow runoff retains a greater fraction of tellurium than a faster one, which would accelerate complete oxidation of the cladding material.

The results of the laboratory studies mentioned above have been clearly supported by the TMI-2 post-accident investigations (Vinjamuri et al., 1984 a), which will be discussed in more detail in Section 7.4.2.

When an analytical duct as shown in Fig. 7.8. is used, the different chemical forms of the volatilized fission products can be identified. Substances which are plated out on the walls of the thermal gradient tube can be assumed to have been deposited there from the vapor phase, whereas the substances collected on the aerosol filters presumably were transported from the furnace through the thermal gradient tube as aerosols. In order to rule out interfering secondary reactions of the fission products with the materials of the thermal gradient tube, in the ORNL high-temperature tests the inner surface of the tube was lined with platinum or gold. Iodine species collected in the charcoal trap (impregnated with triethylendiamine) can be assumed to consist of the gaseous forms I_2, HI, and/or organoiodides; in the experiments no further separation of these species was carried out because of the small amounts detected.

As can be seen from the summary paper of Collins et al. (1988), in the ORNL high-temperature experiments about 40% of the iodine released from the fuel specimen was plated out in the thermal gradient tube, with a condensation maximum at about 500 °C when a steam–helium–hydrogen atmosphere was used. Since cesium showed a quite similar distribution in the thermal gradient tube (see the example

shown in Fig. 6.3.), it was concluded that iodine had been mainly transported in the form of CsI, i. e. as the compound that under such conditions is favored for thermodynamic reasons. Another essential iodine fraction was detected on the aerosol filters, where it was also accompanied by cesium. Only very small fractions of iodine, on the order of 0.4% and less, were transported to the charcoal filters located at the end of the analytical duct.

In all the ORNL tests with iodine releases greater than about 1% of the inventory of the fuel specimen, virtually all the volatilized iodine behaved like CsI. In general, no more than about 1% of the released iodine was in volatile forms that can penetrate glass-fiber filters (i. e. I_2, HI and organic iodides). Furthermore, the total mass of iodine appearing in these penetrating forms has proved to be relatively constant in all the tests, which suggests the action of a small but relatively constant reaction mechanism which might convert iodide originally present to more volatile species, such as by reaction with impurities present in the collection system (Osborne and Lorenz, 1992). In steam atmospheres, about 10% of the cesium released from the fuel specimen behaved like CsI and the remaining 90% like highly reactive CsOH. Concentrations of cesium detected on the ZrO_2 ceramics in a narrow temperature band at the furnace outlet suggested a reaction to form Cs_2ZrO_3. In the tests with steam, about 70% of the cesium collected outside the furnace was associated with aerosols (i. e. collected on the filters) with the smaller fraction deposited from the vapor phase onto the TGT surfaces. In contrast, in a hydrogen atmosphere this ratio of cesium vapor and cesium aerosol was approximately reversed, which indicated that under such conditions the major fraction of the cesium was transported in vapor form. From this behavior it can be concluded that in an accident sequence (or in a certain period of an accident sequence) accompanied with abundant steam supply, a smaller fraction of the cesium released from the reactor core would condense on cool surfaces than would occur under reducing conditions in a steam-starved environment. As a result, in such a sequence the larger cesium fraction (aerosol-associated) would be more transportable.

As was mentioned above, there is always the question of whether the chemical forms of fission products identified in the thermal gradient tube and in the analytical duct are identical with those released from the fuel specimen or whether they have been generated during transport in the prevailing atmosphere. The chemical form in which fission product iodine is originally released from the fuel apparently depends on the fuel burnup. From high-burnup fuel, CsI seems to be the predominant chemical form released to a steam–hydrogen atmosphere, while in dry air atmosphere elemental iodine accounts for almost all the iodine released (Collins et al., 1988). On the other hand, from the measurements performed in the first Severe Fuel Damage Tests it was concluded that from low-burnup fuel cesium and iodine are released from the fuel in atomic form rather than as CsI (Cronenberg et al., 1986). These differences in the chemical form of iodine released from low-burnup and high-burnup fuels are consistent with the differences in the chemical states of cesium and iodine in the fuel, with low-burnup fuels showing mainly atomic-dispersed fission products in the fuel grains, while in high-burnup fuels a considerable fraction of both elements is precipitated as CsI on the fuel grain boundaries (see Section 3.2.2.3.). In every case, it is very difficult to distinguish incontestably be-

tween the primary chemical forms of fission products released from the fuel specimen and those forms that arise very quickly under the influence of the ambient atmosphere.

Cesium and iodine atoms which are released from fuel specimens into a high-temperature steam–hydrogen environment are thermodynamically unstable and will be rapidly converted into species that are stable under these conditions. Since the chemical form of iodine in particular will considerably influence its transport and retention behavior within the reactor pressure vessel and the primary system, it is important to know the kinetics of these conversion reactions. A kinetics assessment of the most essential reactions (Cronenberg and Osetek, 1988) has shown that for extremely low concentrations of iodine and cesium in steam (e. g. mole ratio $I : H_2O < 10^{-8}$), the predominant form of iodine is HI and that of cesium is CsOH. This is due to the fact that because the concentrations of iodine and cesium are so dilute, the elements are much more likely to collide and react with H_2O and H_2 than with each other. Low concentrations of iodine and cesium increase the time for thermochemical equilibrium to be established for their reaction products. For mixtures which are so dilute in fission products, the reaction times may approach tens of seconds or longer, so that for high effluent rates the environmental conditions may change (e. g. by transport into the next control volume showing other conditions) before thermochemical equilibrium has been achieved. Under such conditions, certain limitations caused by reaction kinetics may exist.

With fission product iodine-to-steam mole ratios on the order of 10^{-5}, the collision probability between iodine and cesium is sufficiently high for rapid formation of CsI. (For example, for the TMI-2 accident during the main release phases of iodine and cesium, i. e. during liquefaction of the fuel and relocation as well as during the reflood transient, an $I : H_2O$ ratio in the gas–steam effluent from the core of about $3 \cdot 10^{-5}$ was calculated.) However, even at this concentration level the kinetics of the reactions are complex, with iodine and hydrogen first reacting to form HI, which in turn reacts in the presence of cesium to form CsI over a time period of about 0.1 seconds. Finally, at high fission product concentrations (i. e. $I : H_2O > 10^{-4}$), the collision frequency between iodine and cesium is sufficiently high to establish CsI equilibrium in about 10^{-3} seconds, with CsI being the predominant form for iodine. The ultimate partitioning of the species and the time required to reach the equilibrium state are not only affected by the concentrations of the reactive species, but also by the temperature of the gas mixture (the data mentioned above were calculated for 1500 K). A decrease in temperature will increase the time to reach equilibrium but, on the other hand, will push iodine equilibrium further in the direction of CsI formation. Additional chemical reactions may occur in the gas mixture escaping from the reactor core (e. g. with boric acid); these will be treated in Section 7.3.2.

The calculations of Cronenberg and Osetek (1988) additionally suggested that formation of HOI and organic iodides does not occur to a noticeable extent under such conditions.

Summarizing the results obtained from the theoretical studies as well as from the experimental investigations, it can be expected that, in the course of a severe core damage accident, fission product iodine released from the fuel is converted to

iodide compounds already within the reactor pressure vessel, and that the fraction of elemental iodine which reaches the containment is well below 1% of the amount of iodine released from the fuel. This fraction is distinctly smaller than that discussed in the context of the loss-of-coolant design basis accident (see Section 6.2.1.1.). Obviously, this decrease in the residual concentration of elemental iodine is caused by the much higher concentrations of both iodine and cesium in the gaseous phase due to the higher fuel temperatures prevailing in a severe accident. However, as will be discussed later on, the primary chemical form of fission product iodine released from the fuel is of minor significance for its final behavior in the containment. In the presence of silver volatilized from the control rod alloys, the formation of AgI in the gaseous phase cannot be ruled out, as was indicated by the SASCHA results (see Fig. 7.6.).

Based on the experiments mentioned before, as well as on thermodynamic considerations, fission product cesium is generally assumed to be present in the gaseous phase above the reactor core mainly as CsOH with a fraction of about 10% as CsI. The formation of minor amounts of other cesium species, however, cannot be ruled out as has been shown e. g. by Gomme et al. (1986), who applied the techniques of matrix isolation infrared absorption spectrometry as well as of mass spectrometry to identify the chemical compounds present in the gas phase above a mixture of Cs_2CO_3 and TeO_2 when it was heated to 1200 K. The results showed that cesium appeared as Cs_2TeO_3 when the Cs : Te ratio was in the range of 2; at lower ratios, polymer species such as $Cs_2Te_2O_3$ were also observed. The formation of such low-volatility, water-soluble compounds can, in principle, influence the behavior of a part of the released cesium in the subsequent stages of the accident.

The release behavior of the less volatile fission products from overheated fuels was studied in detail in the SASCHA experiments (Albrecht, 1987 a). These results demonstrated that the low-volatility elements (e. g. barium, ruthenium, cerium) were essentially released at the highest temperatures realized in the tests, i. e. from the liquid melt. In Fig. 7.11. some of the measured release rates for low-volatility elements are shown and compared with the assumptions made in the NUREG-0772 report. With the exception of barium (and potentially strontium), the release rates of these elements apparently depend only little on the amount of steam supplied. Barium release rates in a pure steam atmosphere have proved to be lower by a factor of nearly 100 than in an Ar + 5% steam atmosphere or in an Ar + 5% H_2 atmosphere. This behavior was assumed to be due to a reduction of the BaO initially present by still non-oxidized Zircaloy, which converted it into the more volatile elemental form.

The ORNL VI tests, the realization and results of which were described in special reports and summarized by Osborne and Lorenz (1992), were carried out at temperatures ranging from 2300 to 2700 K. They yielded extensive information on the release behavior of the less volatile elements in particular. Similar to tellurium, but quite different from the other volatiles, the release behavior of some of these elements proved to be highly dependent on the test atmosphere. As can be seen from Table 7.2., antimony shows high release in an oxidizing (steam) environment, but much lower volatilization in a reducing (hydrogen) atmosphere. Apparently, antimony is readily released from the oxide fuel but is retained in the same

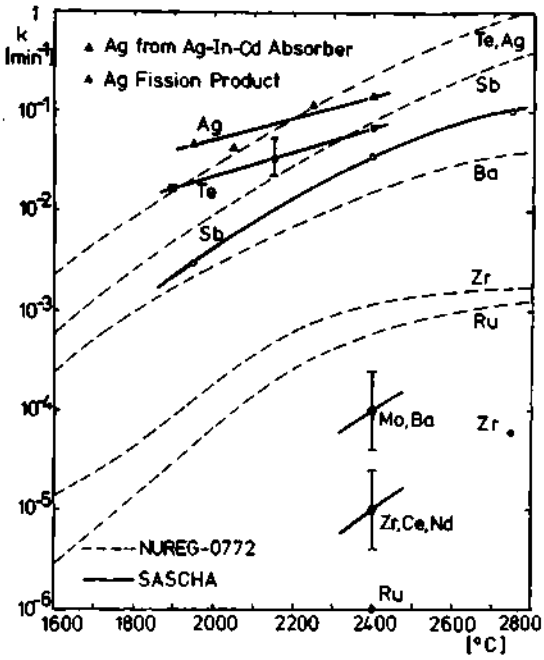

Figure 7.11. Release rates of less volatile fission products measured in the SASCHA experiments
(Albrecht, 1987 a)

manner as tellurium by the Zircaloy cladding that has not yet been oxidized. On the other hand, europium is not released from the fuel in a steam atmosphere, but significantly volatilized under hydrogen; apparently, the extremely low-volatile Eu_2O_3, which is the probable chemical state of this element in the UO_2 fuel, is reduced to a lower, more volatile oxide or even to the element. Maximum europium release was found to take place during the period of cladding melting and rundown, i. e. in an extremely reducing environment. Enhanced volatilization of lower oxides in a strongly reducing environment may also apply to other rare earth elements (such as lanthanum). Since elemental barium and strontium are also more volatile than their oxides, a similar dependence of the release behavior on the nature of the environment can be expected; however, significant barium release was only observed in test VI-3 at 2700 K. Fundamentally, BaO as well as probably SrO can be converted by steam into the more volatile hydroxides.

As to the refractory elements molybdenum and ruthenium, the oxides RuO_4 and MoO_2 are much more volatile than the elements, so that significant release was only observed at 2700 K in a steam atmosphere. The measured releases of the actinide elements were low and primarily in the form of aerosols. At 2300 K in steam, 0.026% of the uranium was collected outside the furnace; at 2700 K in steam the release from the furnace amounted to 0.69%. Fractional releases of pluto-

Table 7.2. Release data as function of temperature and atmosphere (Osborne and Lorenz, 1992)

Test No.	Maximum temperature, K	Effective time, min	Reactive atmosphere	Fission product released (% of inventory)		
				Cs (Kr, I)	Sb (Te)	Eu (Ba, Sr)
VI-3A	2000	34	Steam	22	0	0
VI-5A	2000	33	Hydrogen	31	0	1
VI-2AB	2300	25	Steam	57	49	0
VI-4ABC	2440	31	Hydrogen	96	6.4	19
VI-3ABC	2700	46	Steam	100	99	0.01
VI-5ABC	2700	31	Hydrogen	100	18	57

nium were at least one order of magnitude lower in these two tests than those of uranium.

Despite obvious differences in the experimental techniques between the SASCHA experiments and the ORNL high-temperature tests, mainly with regard to the nature of the analytical specimens (simulant fuel vs. irradiated fuel, melt composition and geometry of the specimens), the results showed general consistencies in the behavior, in particular, of the less volatile fission products (Osborne and Lorenz, 1992).

Immediately after having left the hot region of the melting reactor core, the low-volatility fission products condense to form aerosols. The chemical state of the individual elements in the freshly formed aerosols may be either metallic or oxides, depending on the prevailing oxidation potential of the system. Thermodynamic calculations (Wichner and Spence, 1985) yielded the data given in Table 7.3., together with those for the volatilized core structural materials (see Section 7.3.1.2.).

Table 7.3. Chemical forms of aerosols in the reactor pressure vessel prior to failure (Wichner and Spence, 1985; Copyright 1985 by the American Nuclear Society, La Grange Park, Illinois)

Oxidic	Metallic	Indefinite[a)]
ZrO_2	Silver	$Fe/FeO/Fe_2O_3$
Al_2O_3	Tellurium	Sn/SnO_2
RE_2O_3[b)]	Nickel	In/In_2O_3
UO_2	Cadmium	Mo/MoO_2
BaO	Rhodium	
SrO	Palladium	
B_2O_3	Ruthenium	

[a)] Could be either oxidic or metallic
[b)] Rare earth oxides

While in a number of cases the chemical state of the elements is not significantly affected by variations in the ambient conditions within a broad range, some of these elements are very sensitive to such changes; they were, therefore, listed under "Indefinite" in the table.

7.3.1.1.3 In-pile experimental programs

The experiments discussed before are characterized by the fact that they have been performed on a laboratory scale using comparatively small fuel specimens. Although these experiments have greatly contributed to the current state of knowledge in this field, it should not be overlooked that their results reflect various differences in conditions as compared with those that would be encountered in a degrading reactor core. In this respect, the main features are the mode of heating (fission product decay heated vs. inductively heated), the magnitude of the prevailing radiation field and the size of the specimens, with the impact of these parameters on the release behavior of the fission products being a priori unknown. In order to cover this gap, severe damage tests have also been conducted in-pile using fuel rods or even complete fuel bundles. A comprehensive review of these in-pile tests, their performance and their results has been given by Harman and Clough (1992). Some of these experiments will be treated shortly in the following; the LOFT FP-2 experiment as well as the Phebus-FP test series, both of which aim at a simulation of the entire accident sequence, will be discussed in Section 7.3.5.

The objective of the Source Term (ST) experiments performed in the Annular Core Research Reactor (ACRR) was to investigate fission product release behavior under the conditions of high pressure, high radiation field and high hydrogen concentrations. They were intended to supplement out-of-pile experiments, in particular the ORNL VI test series (see the preceding section). Consequently, comparatively small specimes (about 300 g) of high burnup fuel (about 45 MWd/kg U) were used and inserted into a closed recirculated gas flow system in which the atmosphere was hydrogen and argon; the maximum fuel temperatures during the experiment were 2300 to 2400 K and were maintained for about 16 minutes. The sampling system used consisted of 7 sequentially operated collection trains, each containing a thermal gradient tube (900 to 400 K) equipped with metallic deposition wires, followed by a high-temperature aerosol filter and a charcoal filter.

The results of the post-test measurements of the low-pressure test ST-1 (Allen et al., 1990) showed, besides extensive volatilization of cesium, a high release of europium (~ 20%), the overwhelming fraction of which redeposited in the upper fuel region. In contrast, only very low tellurium volatilization was observed. This unusual behavior, which was qualitatively confirmed by the results of the high-pressure test ST-2, is clearly due to the strongly reducing environment and, thus, is only of limited relevance for LWR accident conditions.

Fuel bundles were used in the Severe Fuel Damage (SFD) tests which were conducted in the US Power Burst Facility (PBF), a reactor which consists of a driver core and a pressurized water loop into which the test assembly was inserted.

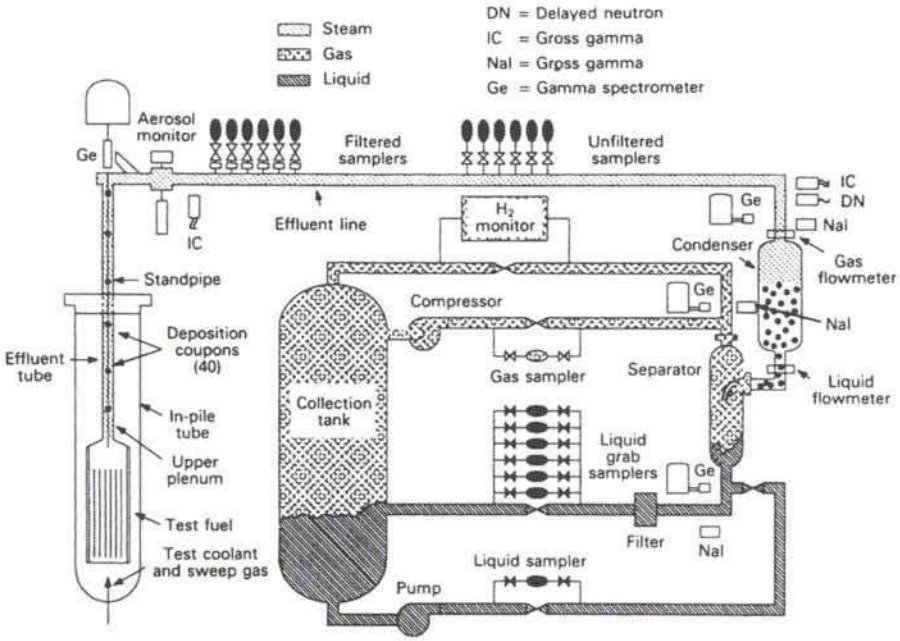

Figure 7.12. SFD 1−4 effluent sampling and monitoring system
(Petti et al., 1991; Copyright 1991 by the American Nuclear Society, La Grange Park, Illinois)

In addition to the determination of fission product release and transport effects as well as of details of hydrogen production, a main objective of these experiments was to characterize the nature of core damage that will occur during a severe degraded core accident. Each of the test assemblies used consisted of a bundle 1 meter in length containing 32 fuel rod positions. In the first two tests (SFD ST and SFD 1−1), trace-irradiated fuel was used, while the other two tests were carried out using a fuel which had been pre-irradiated in a commercial power reactor to a burnup of about 36 MWd/kg U. The SFD 1−4 bundle additionally contained 4 Ag-In-Cd control rods encapsulated in stainless steel guide tubes; thus, this experiment was the most representative one for a PWR degraded core situation. Each of the tests was initiated by a transient in which the coolant flow to the loop was reduced and nuclear power was increased, until the high temperature typical of severe accidents was reached in the bundle. As can be seen from Fig. 7.12., the test SFD 1−4 was highly instrumented, in particular with respect to the effluent sampling and monitoring system, in order to acquire as much data as possible.

The measurements performed during the first two SFD tests (in which trace-irradiated fuels were used) up to about 2000 K showed release rates for the noble gases, iodine, cesium and tellurium which were quite low compared with the out-of-pile data (Vinjamuri et al., 1984 b; Osetek et al., 1984). At temperatures higher than about 2200 K, at which fuel liquefaction due to molten Zircaloy started, the release rates of the noble gas were in good agreement with the out-of-pile data,

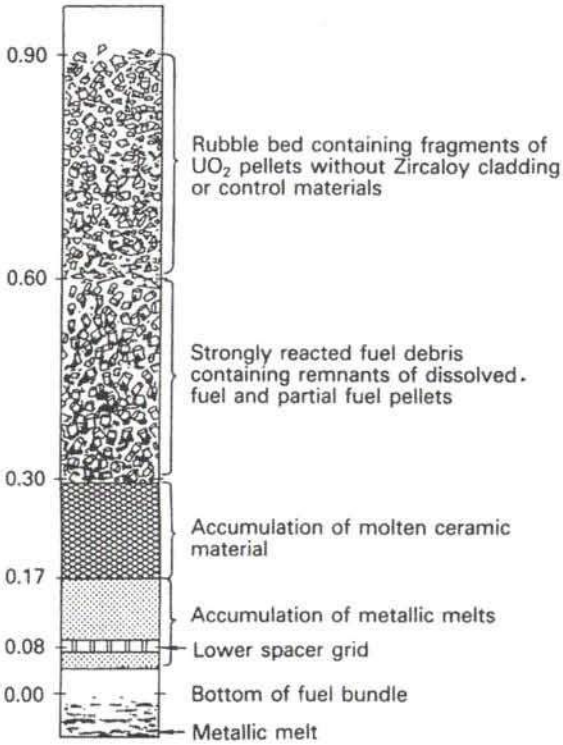

Figure 7.13. Schematic of the different regions of bundle damage produced during test SFD 1−4
(Petti et al., 1991; Copyright 1991 by the American Nuclear Society, La Grange Park, Illinois)

while the measured release data of the other fission products were distinctly lower. At the low element concentrations present in the trace-irradiated fuel and at an H : O ratio of only 2.06 in the steam phase of one test showing high steam flow-rate conditions, predominantly free iodine and CsOH were detected; in contrast, in another test with much higher H : O ratios and low steam flow-rate conditions, CsI appeared to be the predominant iodine species.

The particular conditions and the results of the SFD 1−4 test have been described in detail by Petti et al. (1991). In this test, in which a small-break initiating event with limited steam supply to the fuel bundle was simulated (corresponding to the S_2D sequence of WASH-1400), the temperatures in the bundle increased rapidly to about 2400 K; about one-third of the bundle experienced peak temperatures of 2800 K during the test. The post-test damage state of the bundle, which is schematically shown in Fig. 7.13., appeared to be quite analogous to that of the damaged TMI-2 core (in which, however, the accident was brought under control at a later point than the test was terminated), and showed a debris bed of fuel fragments in the upper region. The high-temperature U-Zr-O material in the lower region represents a precursor to the molten pool in TMI-2, while the accumulation

of metallic melts near the bottom of the bundle is a precursor to the metallic crust formed in the TMI-2 core. Measurements of the amount of hydrogen that evolved from the test loop in the course of the test showed that, even with the limited steam supply during the experiment, about 32% of the Zircaloy material of the test bundle was oxidized, with more than 90% of this oxidation apparently occurring after the onset of Zircaloy melting. Most of the Ag-In-Cd control rod material relocated downward, where it formed a metallic melt; only very little of this material was vaporized, possibly because of the high pressure prevailing in the system during the test.

The radionuclide releases from the damaged bundle in the course of the test are shown in Table 7.4. With regard to the behavior over time, it was observed that releases increased dramatically during rapid oxidation of the Zircaloy and remained relatively constant during the high-temperature phase of the experiment, when fuel dissolution and changes of bundle geometry were occurring. Elevated releases were also measured during cooldown of the damaged bundle. Detailed study of the results suggested that fission product release apparently is a function of both fuel morphology and the halflife of the respective fission product. The observed differences in release behavior between short-lived and long-lived isotopes are believed to be related to the morphology of the high-burnup fuel and to the location of fission products within the UO_2 microstructure. The preferential release of longer-lived fission gases (compared to the shorter-lived isotopes) can be explained by the fact that the longer-lived isotopes can migrate during normal fuel operation to the grain boundaries where they accumulate and from which release at elevated temperatures is relatively rapid, whereas shorter-lived isotopes reside primarily within the fuel grains (because they do not live long enough to migrate to the grain boundaries) from which release is more difficult, even at higher temperatures.

Under the conditions of the SFD 1–4 test, i. e. high-burnup fuel heated to high temperatures in a steam-starved environment, the dominant chemical forms of the volatilized cesium and iodine were calculated to be CsI and CsOH, with some elemental cesium at very high temperatures. The dominant form of tellurium released was probably SnTe; the calculations showed that silver, cadmium and tin would be released in their elemental forms.

During the high-temperature transient of the test, aerosols were generated continuously as a result of vaporization of Ag-In-Cd control rod material, of tin volatilization favored by Zircaloy oxidation, of volatile fission product release and, finally, of relocation of ceramic melts and their interaction with control rod material. The collected aerosols predominantly consisted of cadmium, tin and cesium. Detailed investigations of aerosol transport behavior indicated that aerosols provide a mobile surface onto which fission products may condense. Below 700 K, >95% of the volatile fission products in the effluent would be transported as aerosols. This condensation of volatile substances onto already existing primary aerosols can change their transport behavior considerably. Aerosols are able to transport this condensible matter farther than if the material were in a pure vapor state. On the other hand, aerosols are subjected to processes like agglomeration, gravitational settling and inertial impaction, resulting in a reduction of the aerosol

Table 7.4. Best-estimate release fractions for fission products in SFD test 1–4 (Petti et al., 1991; Copyright 1991 by the American Nuclear Society, La Grange Park, Illinois)

Isotope	Release fraction
Noble gas	
^{85}Kr	$4.2 \cdot 10^{-1} \pm 11\%$
^{85m}Kr[a]	$3.6 \cdot 10^{-1} \pm \sim 25\%$
^{87}Kr[a]	$4.1 \cdot 10^{-1} \pm \sim 25\%$
^{88}Kr[a]	$3.4 \cdot 10^{-1} \pm \sim 25\%$
^{133}Xe	$2.3 \cdot 10^{-1} \pm 18\%$
^{135}Xe[a]	$4.1 \cdot 10^{-1} \pm \sim 25\%$
^{137}Xe[a]	$2.3 \cdot 10^{-1} \pm \sim 25\%$
^{138}Xe[a]	$4.2 \cdot 10^{-1} \pm \sim 25\%$
stable krypton	$5.2 \cdot 10^{-1} \pm 100\%$
stable xenon	$5.1 \cdot 10^{-1} \pm 42\%$
High volatility[b]	
^{129}I	$2.42 \cdot 10^{-1} \pm 19\%$
^{131}I[c]	$2.43 \cdot 10^{-1} \pm 19\%$
^{134}Cs	$3.93 \cdot 10^{-1} \pm 14\%$
^{137}Cs	$5.11 \cdot 10^{-1} \pm 15\%$
^{127m}Te	$3.16 \cdot 10^{-2} \pm 37\%$
^{129m}Te	$3.16 \cdot 10^{-2} \pm 37\%$
^{129}Te	$1.10 \cdot 10^{-2} \pm 50\%$
Medium and low volatility[b]	
^{103}Ru	$6.83 \cdot 10^{-5} \pm 56\%$
^{125}Sb	$1.32 \cdot 10^{-3} \pm 35\%$
^{90}Sr	$8.83 \cdot 10^{-3} \pm 28\%$
^{154}Eu	$7.60 \cdot 10^{-4} \pm 40\%$
^{140}Ba[d]	$7.34 \cdot 10^{-3} \pm 46\%$
^{144}Ce	$1.28 \cdot 10^{-4} \pm 70\%$
Actinides[b]	
^{241}Am	$4.21 \cdot 10^{-6} \pm 47\%$
^{242}Cm	$2.89 \cdot 10^{-7} \pm 39\%$
^{244}Cm	$9.22 \cdot 10^{-7} \pm 49\%$
^{239}Pu	$1.79 \cdot 10^{-6} \pm 44\%$
^{235}U	$3.14 \cdot 10^{-5} \pm 42\%$

[a] Based on average release fraction from integration of the on-line γ spectrometer results
[b] Represents release from the bundle following flushing of the system with water
[c] Based partially on ^{129}I results
[d] Based on activity of ^{140}La daughter

concentration and increasing fission product deposition. Which of these two types of influence, enhanced transport or increased deposition, is the dominant one depends on the particular conditions (see Section 7.3.2.).

Summarizing the results from the in-pile tests, Harman and Clough (1992) concluded that the qualitative features of fission product release were fully consistent

with the patterns established by the out-of-pile experiments. However, the release rates measured in the in-pile tests were generally lower than those of the out-of-pile data. With respect to the chemical forms of the released fission products, the in-pile tests yielded little direct information mainly because of the problems associated with sampling and post-test analyses. However, the conclusions which could be drawn from the measurements essentially confirmed the results of the out-of-pile experiments and were not contradictory to the theoretical calculations.

7.3.1.1.4 Conclusions regarding fission product release behavior in an actual severe accident

As was mentioned above, results from in-pile and out-of-pile tests, as well as from the post-accident investigations at TMI-2, suggest that, in addition to the effects of temperature and time at temperature, the effects of fuel morphology such as restructuring of the UO_2 microstructure, fuel liquefaction, molten pool formation, debris bed formation, as well as the effect of fuel chemistry can strongly influence the release behavior of fission products from the reactor core under severe accident conditions. Hobbins et al. (1993) have summarized the current state of knowledge with respect to the significance of these parameters, the consideration of which is an important prerequisite for the development of complete models of fission product release from the reactor core during such events. Several important examples (a part of which have been shortly discussed above) will be summarized in the following.

The burnup state of the fuel influences the release behavior of the volatile fission products as a consequence of the restructuring of the fuel, resulting in the collection of fission gas bubbles at grain boundaries and in the interlinkage of bubbles to form tunnels along the grain edges. Bubbles containing fission gases and vapors migrate to grain boundaries during irradiation, and if tunnels have developed, the gases and vapors can be released fairly easily to the gap of the rod outside the fuel pellets during core heatup under accident conditions. On the other hand, the formation of fission product compounds in high-burnup fuels may lower the partial pressures of these elements and, consequently, decrease their volatility. Moreover, the increased fission product inventory can affect the chemical form of iodine in the gas phase above the core following release from the fuel, leading in low-burnup fuel mainly to the formation of HI, while in high-burnup fuel CsI will be the predominant form of released iodine.

Another potential feature of the structure of highly irradiated fuel is fragment size resulting from fuel pellet cracking. However, this difference in particle size to that of trace-irradiated fuel is not expected to be large enough to cause significant differences in the release behavior of fission products, since the particle size in either case is much larger than the grain size of the fuel.

The release of volatile fission products from the still-solid fuel matrix is primarily controlled by diffusion processes, i. e. intragranular diffusion from the interior

of the fuel grains and subsequent diffusion along the grain boundaries. For these processes, fuel morphology (grain size, porosity etc.) is an important parameter and calculations of release rates also have to take the fuel grain sizes into account in order to obtain data that agree satisfactorily with experimental results; such calculations were reported on by Suh and Hammersly (1991) in re-analyzing the measurements from the Severe Fuel Damage (SFD) tests. To improve the techniques for calculating the release of the volatile fission products from still-solid fuel particles, the ORNL Diffusion Release Model was developed (Osborne and Lorenz, 1992).

The release of volatile fission products from the solid particles of the debris bed (average particle size around 1 mm, compared to fuel grain sizes of about 10 μm) can be assumed to be quite similar to that from fuel fragments within the fuel rods under identical temperature conditions. It is determined by migration first to grain boundaries and then through an interconnected network of pores.

In addition, diffusion of fission products may also be strongly influenced by the prevailing ambient conditions. Experiments performed in the temperature range from 1200 to 1800 °C (~1500 to 2100 K) (Lewis et al., 1992) demonstrated that normal diffusion is the rate-controlling process for the release of fission products from the fuel matrix in a reducing/inert atmosphere, which may exist in the upper regions of a LWR core under steam-starved conditions. In a pure steam atmosphere, on the other hand, the slower diffusion component is superimposed on by a first-order burst process which is caused by the purging of fission products from the UO_{2+x} matrix (for x in the range of 0.07 to 0.1). Based on these results, a physically-based release model was developed which is claimed to describe these processes with good accuracy.

The dissolution of fuel by molten Zircaloy at about 2200 K and to some extent even at lower temperatures by eutectic melts of iron and nickel in zirconium, liquefies the fuel and facilitates the release of bubbles of fission gases and volatile fission products. Relocating fuel- and fission product-containing liquid streams and drops with a large surface-to-volume ratio will solidify again at lower, cooler elevations in the core on top of a metallic blockage which was formed earlier at lower elevations. In the further progress of the core damage process, this debris can reheat to form once again a molten pool with a small surface-to-volume ratio that reduces both heat removal and fission product volatilization. Bubbles of fission gases and volatile fission products are swept out of the pool as a result of natural circulation, but can be trapped again at the interface between the pool and the crust that surrounds the pool. At the top of the core, debris consisting of UO_2 fragments may be formed; following core reflood, cracks can form within these fragments, which intersect grain boundaries and enhance fission product release at this stage of a recovered accident.

The extent of fission product release during relocation of larger masses of the core down to the water volume still present in the lower plenum of the pressure vessel is assumed not to be large, since the time for coherent relocation is short, the fission gases and the volatile fission products have largely been released from the fuel earlier and a part of the relocated debris is quenched in water.

The oxygen potential in the degrading core, represented by the $H_2 : H_2O$ ratio in the gas phase above it, is another important parameter, which influences in particular the volatilization of the less volatile fission products. This effect applies to the rare earth elements as well as to barium and strontium, which all show higher volatility under strongly reducing conditions. In contrast, ruthenium is only volatilized in a strongly oxidizing environment, tellurium after extensive oxidation of the Zircaloy cladding. Antimony released from the fuel can alloy with other metals present in the core such as nickel and silver. In reality, the prevailing oxygen potential will depend strongly on the specific characteristics of the respective accident sequence; therefore, no generally valid numbers can be given. (As an example, in the TMI-2 accident there was evidence from the nature of the oxide layer in the upper plenum (Fe_3O_4) that the $H_2 : H_2O$ ratio was ≤ 1 for most of the time during which high-temperature effluent was leaving the core.)

Although iodine and cesium are readily released from the fuel during core heatup and are expected to be removed by bubble dynamics in molten pools, frequently small fractions (3 to 10%) of these fission products remain in the molten and re-solidified fuel debris. The reason for this presence of volatile fission products in molten fuel debris is not yet fully understood, but the small surface-to-volume ratio of large pools and the possibility of chemical forms of cesium that are relatively stable at high temperatures may be contributing factors. This retention of smaller amounts of iodine and cesium in the molten material might be favored by rapid local heat-up, as would occur if the oxidation of Zircaloy by steam were a significant heat source.

The common aim of all the experiments and theoretical considerations discussed above is the calculation of the degree and timing of fission product release from the melting core of a large power reactor, using the experimental results previously mentioned, in particular the release rate coefficients as a function of fuel temperature. From the results of the SASCHA experiments, Albrecht (1987 a) has calculated the release fractions to be expected in a low-pressure accident sequence until the moment of failure of the reactor pressure vessel; the values shown in Table 7.5. have been obtained using a simplified temperature-time diagram. According to these data, one has to assume complete vaporization of the fission product noble gases, halogens and alkali elements from the reactor core. Tellurium and antimony are largely vaporized in this sequence, whereas the other fission products, as well as the actinides, show release fractions that are well below 1% of their core inventories. When this method is used, the total release of fission products will be overestimated rather than underestimated, in particular since in this calculation the time – temperature diagram was related to the whole core mass.

Such approaches, which aim at the establishment of a single quantity to represent the fraction of the core inventory that would be released in the event of a severe reactor accident, have now been widely abandoned. As has been summarily described by Malinauskas and Kress (1991), currently fission product release is recognized to be both scenario- and plant-specific, and it has become necessary to replace simple release fractions by computer codes that couple release and transport with thermal-hydraulic aspects. In particular it has been realized that the timing of fission product release can be of great importance and that the releases

Table 7.5. Activity release from the fuel until failure of the reactor pressure vessel (German low-pressure sequence)
(according to Albrecht, 1987 a)

Element	Core inventory, GBq	Release fraction,%
Kr, Xe	$1.47 \cdot 10^{10}$	100
Br, I	$2.58 \cdot 10^{10}$	100
Rb, Cs	$3.61 \cdot 10^{9}$	100
Te	$9.40 \cdot 10^{9}$	80
Sb	$1.63 \cdot 10^{9}$	53
Sr, Ba	$2.06 \cdot 10^{10}$	0.2
Mo, Tc	$1.27 \cdot 10^{10}$	0.2
Ru, Rh, Pd	$2.02 \cdot 10^{10}$	0.002
Y, Zr, Nb	$4.77 \cdot 10^{10}$	0.02
La, Ce, Pr	$5.22 \cdot 10^{10}$	0.02
U, Np, Pu, Am	$2.09 \cdot 10^{9}$	0.02

over the period just after cladding failure and prior to fuel melting are of special interest in those accidents which it was possible to stop by re-establishing core cooling before extensive core melting. To calculate the rates of fission product release (in particular that of the volatile elements) during the core damage process, several special computer codes have been developed in recent years. One of the most frequently used codes, the CORSOR code, which empirically correlates experimental data, originally was developed on the basis of experiments performed at ORNL. During the following years, mechanistic codes have been developed, taking into account basic phenomena such as solid-state diffusion, bubble nucleation and redissolution, bubble migration along pores and microcracks (e. g. the FASTGRASS code, Rest, 1984). Fission product chemistry effects were also included in this code. The results of FASTGRASS calculations haved proved to be in good agreement with the experimental results of both the out-of-pile ORNL heating tests and the in-pile SFD tests (Rest and Cronenberg, 1987).

As has been mentioned above, when one calculates fission product release rates from an overheated reactor core, it has to be taken into account that over a long period of time the core is not at a uniform temperature. Thus, as a prerequisite for applying the experimentally determined release rates the spatial temperature distribution in the core as a function of time has to be calculated. To this end, in the modern computer codes the core is subdivided into a great number of nodes, for each of which the temperature as a function of time is calculated. The amount of release of a given species from a particular node is assumed to be equal to the product of the amount remaining of the species, the release rate coefficient, and the time interval; the total mass release for each species is then obtained by summing over all nodes for the time interval. The accurate calculation of temperature is of particular importance for estimating the release of the less volatile fission products, since the possible uncertainties in their calculated release rates depend to a great deal on uncertainties in evaluating the temperature distribution in the core.

In particular accident sequences with high-pressure, low-flow conditions the buildup of a significant vapor pressure of volatilized fission products in the reactor pressure vessel over the surface of the overheated core may limit the release rates (e. g. Taig, 1984). Since the release rates used in the codes have mostly been determined in experiments in which vapor pressures did not limit the release, this effect has to be taken into account in order not to overestimate the fission product volatilization rates to be expected in such accidents.

In their review paper, Malinauskas and Kress (1991) compared the current understanding of fission product release behavior with the assumptions made in the US Reactor Safety Study (US NRC, 1975). With regard to the gap release, it can be concluded from current knowledge of the magnitude of the gap inventories that the amount of fission products released in this phase of the accident is rather insignificant when compared with the subsequent meltdown release, though it occurs at a rather early moment in the accident sequence. In the core meltdown phase, the newer approaches using computer codes such as those mentioned above predict markedly higher releases of most of the fission products earlier in an accident which develops gradually, than would be predicted using the WASH-1400 methodology for severe core damage accidents. In contrast, under conditions of rapid local heatup (as occurs when the steam–Zircaloy reaction is a significant heat source), the diffusion-based models indicate that substantial amounts of cesium and iodine would be retained in the molten fuel pool. Tellurium release, finally, depends strongly on the extent of cladding oxidation, as was discussed above.

In the US Reactor Safety Study (US NRC, 1975), an additional release step was specified, the so-called oxidation release, which would occur if a steam explosion took place as the molten material escaped from the reactor pressure vessel, resulting in the dispersion of finely divided fuel particles into the steam–air atmosphere in the containment. In such an environment, oxidation of the UO_2 fuel material and of some of the fission products contained within the particles would result, leading to high release fractions of various elements such as ruthenium, molybdenum etc., the oxides of which show a considerably higher volatility than the virtually non-volatile metals. According to Malinauskas and Kress (1991), this type of release is also to be expected during the ejection of the molten core through a leak in the reactor pressure vessel at high primary system pressure. Little research has since been conducted with regard to the release behavior of fission products from fuel under such conditions.

7.3.1.2 Radionuclides from core components and structural materials

The melting down of the reactor core does not only affect the nuclear fuel, but also the core internals, i. e. the core support structures, control rods, BWR fuel assembly shrouds etc. (see Chapters 1 and 2). At the very high temperatures which are experienced during the meltdown process, radionuclides as well as non-radioac-

Table 7.6. Element masses in the core structural materials of a typical US PWR and estimated vaporized fractions
(according to Wichner and Spence, 1985; Copyright 1985 by the American Nuclear Society, La Grange Park, Illinois)

Material/ Element	Mass (kg)	Percent vaporized	Condensing form	Mass vaporized (kg)
Zircaloy-4				
Zirconium	16,200	$2.6 \cdot 10^{-5}$	ZrO_2	0.006
Tin	240	0.55	SnO_2	1.6
Stainless steel				
Iron	1360	0.36	FeO	6.4
Chromium	380	2.3	Cr_2O_3	12.4
Manganese	40	28.2	MnO	14.6
Nickel	200	0.51	$Ni^{o*)}$	1.0
Control rods				
Silver	2260	24	Ag^o	532
Indium	425	47	In_2O_3	242
Cadmium	142	100	Cd^o	142

*) indicates elemental form

tive elements are also volatilized from these materials and are transported by the steam–hydrogen flow in the direction of the primary circuit. The amount of radioactivity volatilized from the core internals is not of significance when compared with the radioactivity of the volatilized fission products; the mass of material volatilized, however, may act as a carrier for gaseous fission products and, thus, may considerably influence their transport behavior.

The materials present inside the reactor pressure vessel and, in particular, their masses depend highly on the type of plant and its particular design. The numbers given in Tables 7.6, 7.7., and 7.9., therefore, are only examples to give an idea of the materials and elements to be considered in this context.

Because of the presence of different alloys in the reactor core, calculations of the vaporized amounts of the individual elements contained therein cannot be performed by using the vapor pressures of the respective pure elements. Two different effects have to be taken into account when calculating the effective vapor pressures. The first is the dilution effect, which can be corrected for by applying Raoult's law for the phase containing the element in question. In addition to the dilution effect, interatomic forces between the minor constituent and the host material may also influence the resulting vapor pressure. These forces can be expressed by activity coefficients which, according to present knowledge, can vary by orders of magnitude for different combinations of elements, and can include positive values (i. e. Raoult's law underpredicts the resulting vapor pressure) as well as negative values (i. e. the actual vapor pressure is lower than that calculated according to Raoult's law). However, current knowledge of these activity coefficients at very high temperatures, e. g. 2700 K, is still limited.

Table 7.7. Element masses in the core structural materials of a typical US BWR (according to Wichner and Spence, 1985)

Material/Element	Mass (kg)
Zircaloy-4	
Zirconium	59,300
Tin	875
Stainless steel	
Iron	7700
Chromium	2160
Nickel	1140
Inconel X	
Nickel	15,300
Chromium	3160
Iron	1470
B_4C Control rods	
Boron	793

In their calculations of the volatilized amounts of materials from an overheated reactor core, Wichner and Spence (1985) have assumed the existence of six different phases, four of which consist of structural/control-rod materials (Zircaloy-4, stainless steel, control rod alloy, Inconel X) and two of which consist of fuel (UO_2–rich phase and noble metals). They have stated that during core heatup new, additional phases may be formed (e. g. Ag-Zr alloy), with the possible effect of reduction of the vapor pressure of the more volatile constituent. Such new phases, however, were not taken into consideration in their calculations; likewise, only the dilution effect was taken into account, activity coefficients having been assumed to be unity. With regard to the reaction system, vaporization of the individual elements from the phases was calculated using idealized assumptions, such as a constant temperature of 2700 K uniform over the entire reactor core, and a static system bounded by the reactor pressure vessel, with vaporization limited by the developed partial pressure of the volatilized elements. As a result of these assumptions, the absolute values of the vaporized masses do not show a high degree of accuracy; however, they give some idea of the relative significance of the different core materials with regard to the aerosols formed during the core meltdown process.

Some results of these calculations are shown in Tables 7.6. and 7.8. Under the assumption of a static system in which the vaporization takes place, in both PWR and BWR cores the control rod materials are the main contributors to the total mass of aerosols formed during core meltdown, followed by fission product cesium and rubidium (not included in the tables), while vaporized constituents originating from the other structural materials represent only a small fraction. In total, about 1% of the PWR core mass is vaporized (including silver from the control rods); in a BWR, the corresponding value is 1.4% (including the contents of the B_4C control rods). If the volatilized materials from the control rods are not considered, the

Table 7.8. Estimated vaporized fractions for BWR core (according to Wichner and Spence, 1985)

Element	Percent vaporized	Condensing form	Mass vaporized (kg)
Structure			
Zirconium	$7.2 \cdot 10^{-6}$	ZrO_2	0.006
Tin	0.15	SnO_2	1.7
Iron	0.053	FeO	6.4
Chromium	0.16	Cr_2O_3	24.8
Manganese	3.0	MnO	14.8
Nickel	0.047	Ni^o	7.7
B_4C control rods			
Boron	97	B_2O_3	2258

volatilized fraction decreases to 0.1% of the core mass (PWR) or to 0.2% (BWR), with CsOH and CsI as the main constituents of the aerosols formed in cooler regions of the primary circuit (76 to 79%). When boron is included in the calculations, these numbers increase to 0.3 and 0.9% of the PWR and BWR core masses, respectively; in this case, B_2O_3 and $CsBO_2$ are the main components of the aerosols, amounting to 42 and 33%, respectively, with CsI not being thermodynamically stable under such conditions. The calculated amounts of volatilized constituents of the structural materials (Fe, Zr, Sn, Mo, Cr, Ni) are comparatively low: 36 kg in the PWR case and 57 kg in the BWR case. The PWR numbers agree reasonably well with the prediction of < 17 kg, which has been calculated from a model developed by Lorenz (1982).

Experimental studies of the vaporization behavior of the constituents of structural and control rod materials at temperatures of 2300 to 2400 °C in a flowing steam atmosphere have been conducted within the SASCHA test series (Albrecht, 1987 b). From heated steel specimens chromium, iron and cobalt showed quite similar volatilization characteristics, while the release of manganese proved to be higher by at least an order of magnitude. Apparently, the release rates of iron and cobalt under the conditions of abundant steam supply are higher than under steam-starved conditions, probably since the boiling points of the respective oxides (FeO, CoO) are lower than those of the elements; this means that the vaporization behavior of these elements is influenced by the prevailing redox potential. The release behavior of tin from a synthetic Zircaloy melt proved to be quite similar to that of manganese from steel specimens. As for the PWR control rod material, the measurements showed that at temperatures above 2000 °C more than 50% of all three constituents of the alloy are volatilized. The release rates of silver apparently depend on the extent of steam supply; under steam-starved conditions a considerable fraction of the initially volatilized silver was retained on the surfaces of still non-oxidized Zircaloy.

The amounts of volatilized elements summarized in Table 7.9. have been calculated on the basis of the SASCHA results, under the assumption that the entire core is at 2400 °C for 15 minutes. According to these data, the total mass of aerosol

Table 7.9. Element inventory of the structural and control rod materials of a 1300 MWe PWR and fractions vaporized prior to reactor pressure vessel failure (linear extrapolation of measured SASCHA results) (according to Albrecht, 1987 b)

Element	Core inventory (kg)	Percent vaporized	Aerosol mass formed (kg)*)
Iron	21,300	1.5	411
Chromium	5750	1.5	126
Nickel	4000	1.5	60
Manganese	450	14	87
Zirconium	30,350	0.015	6
Tin	350	19	84
Silver	1850	88	1628
Indium	350	95	332
Cadmium	115	100	131

*) Assumed oxide forms: FeO, Cr_2O_3, Mn_3O_4, ZrO_2, SnO_2, CdO

originating from the structural and control rod materials amounts to about 2800 kg (plus 345 kg UO_2, plus 256 kg of volatile fission products), which is considerably higher than the data of Wichner and Spence (1985) given above. Albrecht (1987 b) has admitted that the values given in Table 7.9. are upper limits of release and that the lower limit may amount to about 20% of these values. The assumption of an entire core temperature of 2400 °C for 15 minutes is mentioned by the author as the main reason for the high values, which represents a highly conservative assumption regarding an actual core melt process. The calculations of Wichner and Spence (1985), assuming equilibrium partial pressures of the volatilized elements in a static system with limited volume, are potentially more representative of a high-pressure, low-flow accident sequence with the vaporization limited by the established vapor pressure of the volatilized elements, while the data of Albrecht (1987 b) are more representative of a low-pressure sequence with high effluent flow rates.

As for the chemical form of the structural materials during the vaporization process, it has to be assumed that for a number of constituents (e. g. zirconium, tin) the metal is vaporized, due to its higher volatility; the volatilized metal can be expected, however, to react in the steam–hydrogen environment to form the oxide. Thus, the mass of zirconium aerosol formed would be related to the volatility of elemental zirconium in the Zircaloy phase, but its nucleation and condensation behavior is assumed to be more a function of the properties of the oxide.

Virtually all the substances which are volatilized from the core structural materials have low vapor pressures and, therefore, will condense immediately after having left the high-temperature region to form aerosols. The chemical nature of the aerosols depends on the redox conditions in the gas flow escaping from the reactor pressure vessel, i. e. on the H_2 : H_2O molar ratio which in most of the accident sequences will increase from about 0.1 at the moment of cladding failure to about 0.8 at the time of failure of the reactor pressure vessel. In particular accident se-

quences showing low steam production (steam-starved conditions), ratios of up to 10 can be reached over short intervals. According to calculations, the thermodynamically stable forms of the aerosols under such conditions are either oxides (or oxidic compounds) or metals (see Table 7.3.). In general, one has to take into account that the thermodynamic calculations can give a true picture only if all the components present in the mixture are considered, a condition difficult to satisfy if there are a great number of different species present in widely differing concentrations. Modern thermodynamic codes are able to cope with such problems, but in many cases experimental investigations are needed to validate the results obtained.

As was mentioned above, the masses of the vaporized materials presented in Tables 7.6. and 7.8. were calculated under the assumption of a static equilibrium system. The situation prevailing during core meltdown, however, usually does not fulfil this requirement, with the possible consequence of considerable deviation in the vaporized amounts of some of the components. Such deviations are of particular interest in the case of the control rod materials, which may represent the greatest fraction of the aerosols formed. The behavior of the PWR control rod materials under simulated core melt conditions was analyzed in detail by Bowsher et al. (1986). The melting point of this alloy, consisting of 80% Ag, 15% In and 5% Cd, is about 1100±10 K; this means that during core heatup a molten phase of the alloy exists for a certain period of time inside the still intact steel cladding. Upon cladding failure, which is caused by the melting of steel at about 1700 K or by the formation of a steel–Zircaloy eutecticum melting at about 1500 K, the molten absorber material partly flows down to lower regions of the core. The production of cadmium/indium aerosols depends strongly on the accident sequence. In a low-pressure sequence, the high cadmium vapor pressure within the control rod will cause a high release of cadmium and indium oxide/hydroxide vapor upon cladding failure, with the resulting high level of supersaturation leading to an extensive aerosol formation in the cooler regions of the reactor pressure vessel. Conversely, in high-pressure sequences there are no significant pressure gradients and no violent expulsions of vapor which would lead to supersaturation; the vapors formed may condense on bulk surfaces or may form aerosols. Another parameter influencing the early formation of control rod aerosols is the prevailing steam-to-hydrogen ratio. Extensive Zircaloy oxidation will produce a hydrogen-rich environment which inhibits the formation of indium oxide/hydroxide, and will result in cadmium dominating the airborne release. Heating experiments at ORNL reported by Parker (1986) using 1 kg and 10 kg fuel rod bundles showed that upon failure of the control rod cladding, silver is completely retained by the cladding, where it forms a low-melting alloy and candles down to the bottom of the fuel rods. Therefore, no or only very little silver is vaporized by the ultimately higher temperatures reached in the center of the fuel bundle during meltdown. The larger fuel bundle applied in these tests had a significant geometric effect in suppressing the silver release through increased condensation on still unoxidized Zircaloy surfaces.

The vaporization rates of the different components of the control rod alloy depend strongly on the type and the size of the cladding failure as well as on the environmental conditions. In an argon atmosphere, cadmium represents the predominant fraction of the volatilized material (up to 99%); these experimental

results agree well with data calculated according to Raoult's law, yielding vaporization ratios of 100 Cd : 3 In : 0.25 Ag. In contrast, in an argon–steam atmosphere an enhanced vaporization of indium was observed, yielding up to 70% of the total volatilized mass, the reason for which was probably the formation of the less stable suboxide In_2O and/or hydroxide InOH; the compound finally appearing in the condensed aerosols is In_2O_3. The aerosols produced during heating of the control rod materials consisted of two different collectives: comparatively large (~1 μm) cadmium particles which showed rapid sedimentation, and smaller particles rich in indium which remained airborne for a longer period of time (Bowsher et al., 1986).

The vaporization kinetics of the silver component of the control rod alloy is of particular interest for iodine chemistry in the reactor pressure vessel and in the primary circuit as regards the possible formation of the compound AgI in the gaseous phase. Even when the disputed question of the thermodynamic stability of this compound in the high temperature environment containing CsOH, H_2 and H_2O is ignored, one has to take into consideration that in the course of the progressive heating-up of the reactor core from the top to the bottom, the control rod cladding will start to fail in the top region; as a consequence, the molten silver (the vapor pressure of which is still comparatively low at these temperatures) can be assumed to flow down to the residual water volume where it would solidify again. For this reason, only a small fraction of the silver inventory of the reactor core is probably volatilized in this phase of the accident and, consequently, formation of a significant amount of AgI in the gaseous phase in this stage of the accident cannot be assumed to occur. Following complete evaporation of the residual water and penetration of the reactor pressure vessel, the silver inventory of the molten core is completely vaporized and transported as an aerosol to the containment atmosphere, together with the other aerosols, i. e. at a moment when the largest fraction of iodine has already been plated out into the containment sump water (see Section 7.3.1.3.).

B_4C is the effective constituent of the BWR control rods; this material reacts upon contact with high-temperature water or steam to form B_2O_3 and/or H_3BO_3 and CH_4. Details of these decomposition reactions have been studied by Elrick et al. (1987). According to these results, at 1270 K the reaction proceeds in two steps, with the first one being the formation of B_2O_3, followed then by the formation of boric acid. After a transient phase in which a B_2O_3 layer is produced at the B_4C surface with a high reaction rate, an equilibrium state of the reaction is reached during which the reaction rates depend on temperature, H_2O partial pressure, boric acid partial pressure in the steam and the surface-to-volume ratio of the B_4C. Under the experimental conditions applied, production rates for boron oxide and boric acid on the order of 10^{-4} g B/cm^2·min for non-compacted B_4C geometries and one to two orders of magnitude lower for B_4C particle beds were measured; the reaction rates are somewhat reduced by increasing boric acid partial pressures in the steam phase. However, it has to be mentioned that these decomposition reactions will only be significant in case B_4C is not incorporated into a eutectic melt with its stainless steel cladding, which would then flow down to the residual water volume, removing it from the reaction zone (see Section 7.2.2.). The boric acid produced is mainly volatilized with the steam, making possible reactions be-

tween boric acid and fission product compounds in the primary circuit (see Section 7.3.2.); at temperatures around 100 °C, the steamborne boric acid condenses on the walls of the systems or under formation of aerosol particles. CH_4 produced as the second reaction product will enter the gaseous phase directly and completely. Under reducing conditions (i. e. limited steam supply), small amounts of diborane B_2H_6 were formed instead of B_2O_3 (Parker, 1986).

In PWR cores equipped with burnable poison rods containing borosilicate glass, this B_2O_3 may also contribute significantly to the aerosol mass formed, and may be capable of changing the chemical nature of the condensing species. The same applies to the boric acid present in the primary coolant and in the emergency coolant solutions. The volatilization rates of B_2O_3 and/or of H_3BO_3 from these sources in the reactor pressure vessel depend strongly on the particular accident sequence, so that no generally valid numbers can be given; in each case it can be assumed that the amount of boron oxides present in the reactor pressure vessel of both PWRs and BWRs is large enough to tie up all the fission product cesium present in the fuel and, thus, to influence the chemical state of iodine (see Section 7.3.2.3.), provided that boron oxides and cesium appear simultaneously in the gas phase.

7.3.1.3 Radionuclides from the core melt – concrete interaction

Following failure of the reactor pressure vessel, the molten core will fall down to the basemat below. In the case of a 1300 MWe PWR, the mass of this material amounts to about 230 Mg, with an initial temperature of about 2400 °C; about 70 Mg of this mass are in the metallic state, with the remainder consisting of oxides.

In every accident scenario, this running down of the molten material will give rise to the formation of aerosols, which now will not be transported to the primary circuit, but will be dispersed about the reactor cavity; a fraction of the aerosols will reach the containment free volume, while another fraction will be plated out along the way on the walls and structures. In the high-pressure accident sequence, in particular, forced ejection of the core melt from the failed reactor pressure vessel will act as a significant aerosol source. Experiments with melts generated by a thermite reaction and pressurized with N_2 or CO_2 to values ranging from 1.3 to 17 MPa and then ejected into an air atmosphere showed an aerosol production on the same order of magnitude as the in-vessel aerosol generation (Brockmann and Tarbell, 1984). These aerosol particles may be formed by condensation of vapor escaping from the melt and also by physical breakup of the melt; the effervescence of gases dissolved in the melt may support the disruption of the melt jet. In addition, fission products may be volatilized from the molten material due to the changed environment (oxidation release, see Section 7.3.1.1.4.). As a result of these mechanisms, the concentration of low-volatility radionuclides in the atmosphere is increased at least for a certain time until the aerosols have settled.

Upon contact, the molten core material (the so-called "corium") starts to react with the material of the basemat concrete, with the details of this reaction depending on the particular conditions. During the first hours of the molten core – concrete interaction, the temperature of the melt decreases from 2400 to about 1500 °C. Due to the radial progress of the melt in the reactor cavity, in the KWU plant design sump water is expected to pour down onto the melt about 6 to 7 hours after the beginning of the core – concrete interaction. When the reaction zone is flooded by sump water, an exothermal reaction between the metallic constituents of the melt which have not yet been oxidized inside the reactor pressure vessel (in particular Zircaloy) and the water may start. The consequence of this reaction is a considerable increase in temperature, so that it is assumed that in this phase of the accident the highest temperatures might be reached.

The first step of the molten core – concrete interaction is high-temperature decomposition of the concrete accompanied by the production of gases, mainly H_2O and CO_2, followed by melting of the concrete materials and their incorporation into the melt. As a consequence, an erosion of the concrete will start with the formation of a cavern, in which the melt separates into two phases, a lower metallic one which is covered by a lighter oxidic phase, with the former containing metallic fission products like ruthenium, technetium, palladium, and the latter containing barium, strontium and other oxides. The gases produced during the attack on the concrete in the lower regions of the cavern will rise and penetrate through the molten phases where a part of them will be reduced to CO and H_2 by metallic zirconium and iron present in the melt. These reactions will continue for as long as the heat production of the melt is high enough to compensate for the endothermal concrete decomposition reactions and for the heat losses by heat conductivity and radiation. The heat production in the oxidic phase of the melt is mainly due to fission product decay heat, whereas in the metallic phase the exothermal metal –water reaction is the main contributor.

Due to the very high temperatures prevailing during this stage of the accident, the molten core – concrete interaction is the principal source of the release of low-volatility fission products to the containment. The volatilization of these elements, such as barium, strontium, lanthanum and cerium, is strongly supported by the gas bubbles which penetrate through the molten zone. This vaporization results in a comparatively late aerosol source, arising at a time when the initial concentration of aerosols (which had been generated by in-vessel vaporization) in the containment atmosphere has already been largely reduced by deposition reactions. In addition to the comparatively high temperatures, the changed chemical conditions are also responsible for this enhanced aerosol production.

When source terms for a complete core melt accident (in which the melt progress could not be stopped within the reactor pressure vessel) have to be calculated, the aerosol production during the core – concrete interaction phase also has to be taken into consideration. In the Reactor Safety Study (US NRC, 1975), an empiric approach was used with respect to the fission product release during this phase, in recognition of the fact that during this stage the environment is chemically oxidizing and that a metallic iron phase is present. From this approach, it was concluded that the remainder of the volatile fission products still present in the molten corium

Table 7.10. Calculated release fractions of different elements during molten core – concrete interaction
(Cubicciotti and Sehgal, 1984)

Element	Release fraction	volatilized as
Cs	100%	CsOH
I	100%	CsI
La	<0.1%	
Mo	2%	MoO_3
Nb	<0.1%	
Sb	100%	Sb_2
Sn	0.2%	Sn
Sr	<0.1%	
Ag	3%	Ag
Te	79%	Te
Ru	<0.1%	

would now be completely volatilized, together with 5% of the inventory of the noble metals and 1% of that of the refractory oxides.

More detailed calculations performed during the following years yielded substantial differences in the fractions of the more refractory fission products that were expected to be vaporized from the interaction zone under such conditions. Release fractions of barium and strontium fission products as high as 40 to 60% and of lanthanum in the range 6 to 8% have been reported. These values were orders of magnitude greater than those estimated in the Reactor Safety Study, and their acceptance would increase the calculated source term significantly. In contrast, much lower release fractions were reported by Cubicciotti and Sehgal (1984) as a result of calculations of the vaporization behavior of fission products performed on the basis of the accident propagation defined in the CORCON code, which assumes thermodynamic equilibrium and application of the principle of minimum free energies. According to these calculations, the oxidic phase consists of UO_2 and ZrO_2 and fission product oxides, mainly of lanthanum, strontium, antimony, tin, niobium and molybdenum, whereas the metallic phase contains iron, chromium, nickel, manganese, silver, ruthenium as well as the non-oxidized remainder of Zircaloy and tellurium which is still chemically tied up by this material. It is from these calculations that the vaporized fractions of fission products initially present in the core – concrete interaction zone shown in Table 7.10. were obtained. Cesium, iodine and antimony are completely released during a short interval immediately after the onset of the core – concrete interaction; tellurium is vaporized corresponding to the progress of decomposition of the ZrTe compound. As for strontium and lanthanum, various chemical compounds were assumed, including the formation of silicates. The non-radioactive alkali elements originating from the concrete material will also be vaporized, resulting in a considerable consumption of the heat produced in the interaction.

In order to throw more light onto these questions, Roche et al. (1991) carried out small-scale experiments in which mixtures of UO_2, ZrO_2, steel and concrete of

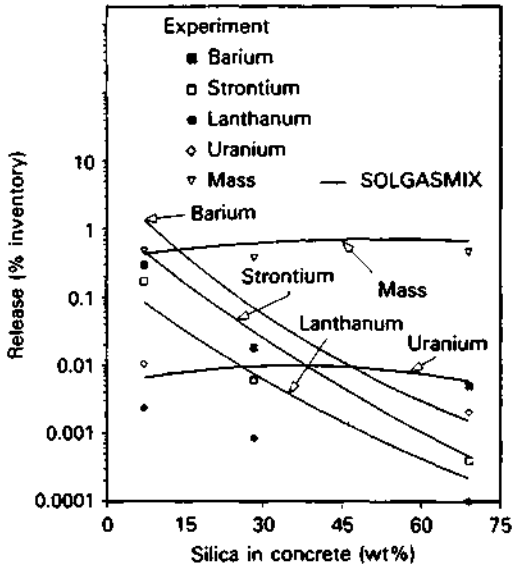

Figure 7.14. Release of fission products, uranium and total mass from mixtures of urania, zirconia and three concretes at 2400 K
(Roche et al., 1991; Copyright 1991 by the American Nuclear Society, La Grange Park, Illinois)

various compositions (to which adequate concentrations of the fission product simulants strontium, barium, lanthanum had been added) were heated to temperatures between 2150 and 2400 K in a flowing H_2 or He−6% H_2 atmosphere, which had been previously adjusted by addition of H_2O vapor to partial free molar oxygen energies of −550 kJ/mol and −420 kJ/mol, respectively. The results obtained from these experiments, which were also used to validate thermodynamic calculations (SOLGASMIX code), indicated that the gas mixture escaping from the molten core − concrete material is in equilibrium with the oxidic phase. The release fractions of strontium, barium, lanthanum from these specimens depend strongly on the chemical composition of the concrete material, ranging for barium and strontium from <1% with a basemat concrete of low silica content to <0.01% with a concrete of high silica content; lanthanum release fractions are considerably smaller and decrease with increasing silica content from $\sim 10^{-3}$% to $\sim 10^{-4}$% (see Fig. 7.14.). In contrast, the total mass release as well as the uranium release fraction was observed to be almost independent of the chemical composition of the concrete applied.

According to the qualitative results obtained from informal SASCHA experiments (Albrecht, 1987 b), silver is largely vaporized under the conditions of the molten core − concrete interaction. This means that any silver not volatilized during the in-vessel phase would become airborne in this late stage of the accident and be transported to the containment sump water phase, i. e. at a moment when volatilized iodine would have been largely plated out in the containment sump water.

Several large-scale experiments have been initiated in recent years to measure the rates of concrete ablation during the molten core – concrete interaction phase – for example the BETA program (Alsmeyer, 1988). In addition, the Advanced Containment Experiments (ACE) Phase C tests were designed to measure the release of low-volatility fission products (Wall and Sehgal, 1993). In each of these seven tests, approximately 300 kg of molten corium material (consisting of UO_2, ZrO_2, Zircaloy and control rod materials) were brought to interact with different types of concrete, reaching temperatures of up to 2500 K. The corium mixture contained inactive fission product simulants; all the aerosols released were collected and analyzed for their characteristic data, such as size distribution, morphology and chemical composition.

The results of these experiments showed that the aerosols released from the interaction mixture were primarily composed of elements originating from the concrete materials. Silicon species made up at least 50% of the aerosol mass in the tests with siliceous or limestone/sand concrete in which appropriate amounts of metal had been present. With the exception of tellurium, fission product elements contributed less than about 1% to the total aerosol mass. The release fractions of several low-volatility fission products during the first seven minutes of the tests (in order to compare the different experimental conditions such as type of concrete, type of corium etc.) are shown in Table 7.11. In general, the release fractions of the fission product elements and uranium were about an order of magnitude or more higher for limestone concrete than for siliceous or limestone/sand concretes. These release fractions were greatest when the metal content of the melt was largest, and decreased as metal content decreased and more concrete became incorporated into the melt.

A major task of the ACE Phase C experiments was validation of data obtained from code calculations. Measured concrete ablation rates agreed to within about 35% with the predictions obtained with various codes such as CORCON, WECHSL etc. Agreement of the fission product release data between the experiments and model predictions, however, was considerably worse, demonstrating that chemical models in which the formation of silicates and zirconates during the core – concrete interaction phase is not taken into account predict release fractions that are one to two orders of magnitude higher than the measured values.

Thus, the measurements made in different experiments agree in that the release fractions of the low-volatility fission product elements during the molten core – concrete interaction phase are comparatively small, and that only small amounts of radiologically hazardous aerosols will be transported to the containment atmosphere in this stage of the accident, together with larger amounts of volatilized non-radioactive constituents of the concrete material. The amount of airborne aerosols is even more reduced when a sump water layer covers the reaction zone. Preliminary measurements have been reported from experiments with about 46 kg of molten steel which showed that a water layer of 50 cm thickness on top of the interaction zone results in a retention factor for aerosols of 10 to 30 (Blose et al., 1987). In these experiments, however, the water pool was continuously replaced by fresh water, which kept the temperature of the water well below the boiling point and the concentration of trapped aerosols low. Calculations using a simplified model of aerosol scrubbing from bubbles rising through water (Powers and

Table 7.11. Fractions of fission product elements released during first seven minutes of basemat ablation (Wall and Sehgal, 1993)

Test	L5	L2	L1	L6	L4	L7	L8
Concrete type[a)]	L/S	S	L/S	S	Serp/S	L/S	L/L
Corium type	PWR	PWR	PWR	PWR	BWR	BWR	PWR
Temp.[b)]	2200 K	2420 K	2625 K	2425 K	2300 K	2536 K	2480 K
Ba	$1.4 \cdot 10^{-5}$	$2.0 \cdot 10^{-5}$	$7.6 \cdot 10^{-4}$	$2.2 \cdot 10^{-4}$	$4.0 \cdot 10^{-4}$	$1.7 \cdot 10^{-4}$	$3.9 \cdot 10^{-3}$
Ce	$5.7 \cdot 10^{-6}$	$3.4 \cdot 10^{-6}$	$4.3 \cdot 10^{-5}$	$1.2 \cdot 10^{-5}$	$4.5 \cdot 10^{-6}$	$9.7 \cdot 10^{-6}$	$2.1 \cdot 10^{-4}$
La	$2.0 \cdot 10^{-6}$	$2.0 \cdot 10^{-6}$	$5.4 \cdot 10^{-5}$	$1.1 \cdot 10^{-5}$	$3.1 \cdot 10^{-6}$	$8.5 \cdot 10^{-6}$	$1.3 \cdot 10^{-4}$
Mo		$3.6 \cdot 10^{-3}$	$< 5.3 \cdot 10^{-4}$	$1.4 \cdot 10^{-3}$	$1.1 \cdot 10^{-3}$	$1.2 \cdot 10^{-3}$	$3.0 \cdot 10^{-3}$
Ru				$1.8 \cdot 10^{-5}$			
Sr	$5.6 \cdot 10^{-6}$	$1.3 \cdot 10^{-5}$	$9.8 \cdot 10^{-4}$	$1.7 \cdot 10^{-4}$	$2.6 \cdot 10^{-4}$	$9.3 \cdot 10^{-5}$	$5.6 \cdot 10^{-3}$
Te		$1.0 \cdot 10^{-1}$	$5.6 \cdot 10^{-2}$	$8.0 \cdot 10^{-2}$	$3.5 \cdot 10^{-1}$	$4.3 \cdot 10^{-2}$	$2.6 \cdot 10^{-1}$
U	$4.6 \cdot 10^{-6}$	$1.1 \cdot 10^{-5}$	$1.1 \cdot 10^{-4}$	$2.0 \cdot 10^{-5}$	$8.9 \cdot 10^{-6}$	$4.2 \cdot 10^{-5}$	$1.9 \cdot 10^{-4}$
Zr	$3.6 \cdot 10^{-6}$	$9.4 \cdot 10^{-7}$	$2.6 \cdot 10^{-5}$	$2.3 \cdot 10^{-5}$	$2.6 \cdot 10^{-6}$	$2.0 \cdot 10^{-5}$	$3.9 \cdot 10^{-5}$

[a)] Concrete type: L/S Limestone/common sand
S Siliceous
L/L Limestone/limestone
Serp/S Serpentine/siliceous

[b)] Temperature during basemat ablation

Sprung, 1992) have shown that the aerosol decontamination factors caused by an overlying water pool depend both on the depth of the layer and on the degree of subcooling of the pool water, increasing sharply (compared with values obtained for saturation conditions) as subcooling increases from 2 to about 10 K; the effect of subcooling by more than about 10 K was found to be less striking.

References Section 7.3.1

Albrecht, H. (a): Results of the SASCHA program on fission product release under core melting conditions. Radiochim. Acta **41**, 133–140 (1987)

Albrecht, H. (b): Freisetzung von Spalt- und Aktivierungsprodukten beim LWR-Kernschmelzen. Abschlußbericht des SASCHA-Programmes. Bericht KfK 4264 (1987)

Allen, M. D., Stockman, H. W., Reil, K. O., Grimley, A. J.: Fission product release and fuel behavior in irradiated light water reactor fuel under severe accident conditions: The ST-I experiment. Nucl. Technology **92**, 214–228 (1990)

Alsmeyer, H.: Melt-concrete interaction during severe light water reactor accidents. Kerntechnik **53**, 30–38 (1988)

Blose, R. E., Gronager, J. E., Suo-Antilla, A. J., Brockmann, J. E.: Swiss: Sustained heated metallic melt/concrete interactions with overlying water pools. Report NUREG/CR-4727 (1987)

Bowsher, B. R., Jenkins, R. A., Nichols, A. L., Simpson, J. A. H.: Silver-indium-cadmium control rod behaviour during a severe reactor accident. Report AEEW-R 1991 (1986)

Brockmann, J. E., Tarbell, W. W.: Aerosol source term in high pressure melt ejection. Nucl. Sci. Engng. **88**, 342–356 (1984)

Browning, W. E. jr., Miller, C. E. jr., Shields, R. P., Roberts, B. F.: Release of fission products during in-pile melting of UO_2. Nucl. Sci. Engng. **18**, 151–162 (1964)

Castleman, A. W. jr., Tang, I. N.: Vaporization of fission products from irradiated fuel. I. Experimental method and general fission product behavior. Nucl. Sci. Engng. **29**, 159–164 (1967)

Castleman, A. W. jr., Tang, I. N.: Vaporization of fission products from irradiated uranium. II. Some observations on the chemical behavior of fission products iodine and cesium. J. Inorg. Nucl. Chem. **32**, 1057–1064 (1970)

Castleman, A. W. jr., Tang, I. N., Munkelwitz, H. R.: The chemical states of fission-product iodine emanating into a high temperature aqueous environment. J. Inorg. Nucl. Chem. **30**, 5–13 (1968)

Collins, J. L., Osborne, M. F., Lorenz, R. A., Norwood, K. S., Travis, J. R., Webster, C. S.: Observed behavior of cesium, iodine, and tellurium in the ORNL fission product release program. Report NUREG/CR-3930 (1985)

Collins, J. L., Osborne, M. F., Lorenz, R. A.: Fission product tellurium release behavior under severe light water reactor accident conditions. Nucl. Technology **77**, 18–31 (1987)

Collins, J. L., Osborne, M. F., Lorenz, R. A., Malinauskas, A. P.: Fission product iodine and cesium behavior under light water reactor accident conditions. Nucl. Technology **81**, 78–94 (1988)

Cordfunke, E. H. P., Konings, R. J. M.: The release of fission products from degraded UO_2 fuel: Thermochemical aspects. J. Nucl. Materials **201**, 57–69 (1993)

Cronenberg, A. W., Appelhans, A. D., MacDonald, P. E., Rest, J., Lorenz, R. A.: An assessment of liquefaction-induced I, Cs, and Te release from low and high burnup fuel. Proc. Internat. Meeting on Light Water Reactor Severe Accident Evaluation, Cambridge, Mass., USA, 1983, Paper 4.5

Cronenberg, A. W., Osetek, D. J., Reed, P. R.: Analysis of iodine chemical form for the Severe Fuel Damage Scoping Test and 1–1 Test. Proc. Symp. on Chemical Phenomena Associated with Radioactivity Release During Severe Nuclear Plant Accidents. Anaheim, Calif. USA, 1986; Report NUREG/CP-0078 (1987), p. 6/59–6/72

Cronenberg, A. W., Osetek, D. J.: Reaction kinetics of iodine and cesium in steam/hydrogen mixtures. Nucl. Technology **81**, 347–359 (1988)

Cubicciotti, D., Sehgal, B. R.: Fission product and material transport during molten core-concrete interactions. Proc. 5. Internat. Meeting on Thermal Nuclear Reactor Safety, Karlsruhe 1984, Report KfK 3880/3, p. 1535–1553

Elrick, R. M., Sallach, R. A., Ouelette, A. L., Douglas, S. C.: Boron carbide–steam reactions with cesium hydroxide and with cesium iodide at 1270 K in an Inconel-600 system. Report NUREG/CR-4963 (1987)

Eriksson, G., Hack, K.: ChemSage – A computer program for the calculation of complex chemical equilibria. Metallurgical Transactions B **21B**, 1013–1023 (1990)

Gomme, R. A., Ogden, J. S., Bowsher, B. R.: The characterisation of vapour-phase alkali metal–tellurium–oxygen species. Report AEEW-R 2204 (1986)

Hahn, R., Ache, H. J.: Thermodynamic calculations on the behavior of gaseous iodine species following a hypothetical severe LWR accident. Nucl. Technology **67**, 407–410 (1984)

Harman, N. F., Clough, P. N.: A review of radionuclide release and transport in recent in-pile experiments. Report EUR 14230 EN (1992)

Hobbins, R. R., Petti, D. A., Hagrman, D. L.: Fission product release from fuel under severe accident conditions. Nucl. Technology **101**, 270–280 (1993)

Hobbins, R. R., Petti, D. A., Osetek, D. J., Hagrman, D. L.: Review of experimental results on light water reactor core melt progression. Nucl. Technology **95**, 287–306 (1991)

Johnson, I., Johnson, C. E.: Release of volatile fission products from irradiated LWR fuel. Mass spectrometry studies. Report EPRI NP-6328 (1989)

Lewis, B. J., Iglesias, F. C., Laurence Hunt, C. E., Cox, D. S.: Release kinetics of volatile fission products under severe accident conditions. Nucl. Technology **99**, 330–342 (1992)

Lorenz, R. A.: The vaporization of structural materials in severe accidents. Proc. Internat. Meeting on Thermal Nuclear Reactor Safety. Chicago, USA, 1982; Report NUREG/CP-0027 (1983), Vol. 1, p. 1090

Lorenz, R. A., Beahm, E. C., Wichner, R. P.: Review of tellurium release rates from LWR fuel elements under accident conditions. Proc. Internat. Meeting on Light Water Reactor Severe Accident Evaluation, Cambridge, Mass., 1983, Paper 4.4.

Lorenz, R. A., Osborne, M. F., Collins, J. L., Manning, S. R., Malinauskas, A. P.: Behavior of iodine, methyl iodide, cesium oxide, and cesium iodide in steam and argon. Report ORNL/NUREG/TM-25 (1976)

Malinauskas, A. P., Kress, T. S.: Effects of chemical phenomena on LWR severe accident fission product behavior. Nucl. Safety **32**, 56–64 (1991)

Osborne, M. F., Collins, J. L., Lorenz, R. A.: Experimental studies of fission product release from commercial light water reactor fuel under accident conditions. Nucl. Technology **78**, 157–169 (1987)

Osborne, M. F., Lorenz, R. A.: ORNL studies on fission product release under LWR severe accident conditions. Nucl. Safety **33**, 344–365 (1992)

Osetek, D. J., Cronenberg, A. W., Hagrman, D. L., Broughton, J. M., Rest, J.: Behavior of fission products released from severely damaged fuel during the PBF Severe Fuel Damage Tests. Proc. 5. Internat. Meeting on Thermal Nuclear Reactor Safety, Karlsruhe 1984, Report KfK 3880/3, p. 1367–1376

Parker, G. W.: The chemistry of nuclear reactor accidents: Problems and progress. Proc. Symp. on Chemical Phenomena Associated with Radioactivity Releases During Severe Nuclear Plant Accidents. Anaheim, Calif., USA, 1986; Report NUREG/CP-0078 (1987), p. 2/1–18

Parker, G. W., Lorenz, R. A.: Melting of UO_2 fuel pins by a centered tungsten resistor. Report ORNL-3401 (1963), p. 11–26

Peehs, M., Kaspar, G., Neeb, K. H.: Cs and I release source terms from irradiated LWR fuel. J. Nucl. Materials **119**, 284–290 (1983)

Petti, D. A., Martinson, Z. R., Hobbins, R. R., Osetek, D. J.: Results from the Power Burst Facility Severe Fuel Damage Test 1–4: A simulated severe fuel damage accident with irradiated fuel rods and control rods. Nucl. Technology **94**, 313–335 (1991)

Powers, D. A., Sprung, J. I.: A simplified model of aerosol scrubbing by a water pool overlying core debris interacting with concrete. Report NUREG/CR-5901 (1992)

Rest, J.: An improved model for fission product behavior in nuclear fuel under normal and accident conditions (FASTGRASS code). J. Nucl. Materials **120**, 195–212 (1984)

Rest, J., Cronenberg, A. W.: Modeling the behavior of Xe, I, Cs, Te, Ba, and Sr in solid and liquefied fuel during severe accidents. J. Nucl. Materials **150**, 203–225 (1987)

Roche, M. F., Leibowitz, L., Settle, J. L., Johnson, C. E., Vogel, R. C., Ritzman, R. L.: Vaporization of strontium, barium, lanthanum, and uranium from mixtures of urania, zirconia, steel, and concretes at 2150 and 2400 K. Nucl. Technology **96**, 96–116 (1991)

Suh, K. Y., Hammersly, R. J.: Modeling of fission product release and transport for severe fuel damage analyses. Nucl. Sci. Engng. **109**, 26–38 (1991)

Taig, A. R.: Release and retention phenomena in LWR degraded cores. Proc. Am. Nucl. Soc. Meeting on Fission Product Behavior and Source Term Research. Snowbird, Utah, USA, 1984; Report EPRI NP-4113-SR (1985), p. 5/1–14

US Nuclear Regulatory Commission (NRC): Reactor Safety Study: An Assessment of Accident Risks in US Commercial Nuclear Power Plants, Appendix VII. Report WASH-1400, 1975

US Nuclear Regulatory Commission (NRC): Technical bases for estimating fission product behavior during LWR accidents. Report NUREG-0772 (1981)

Vinjamuri, K., Osetek, D. J., Hobbins, R. R. (a): Tellurium behavior during and after the TMI-2 accident. Proc. 5. Internat. Meeting on Thermal Nuclear Reactor Safety, Karlsruhe 1984, Report KfK 3880/3, p. 1583–1592

Vinjamuri, K., Osetek, D. J., Hobbins, R. R. (b): Fission product release rates measured during in-pile fuel damage tests. Trans. Am. Nucl. Soc. **46**, 480–482 (1984)

Wall, I. B., Sehgal, B. R.: Molten corium concrete interactions. Advanced Containment Experiments (ACE) Project: Summary report.Report EPRI TR-103483s (1993)

Wichner, R. P., Spence, R. D.: A chemical equilibrium estimate of the aerosols produced in an overheated light water reactor core. Nucl. Technology **70**, 376–393 (1985)

7.3.2 Chemical reactions and behavior of the radionuclides in the primary system

7.3.2.1 General aspects

Depending on the accident sequence in question, the substances released from the overheated reactor core have to travel over paths of different length through the primary circuit, until they reach the location of the break from where they can pass over into the containment free volume. These differences in pathway mean that there are different temperature regions, residence times, flow characteristics etc., which are able to influence chemical reactions and transport behavior and

which have to be taken into account when analyzing fission product behavior. In general terms, in a severe accident initiated by a large break in the primary system, e. g. resulting from a guillotine break of the main coolant pipe in the immediate vicinity of the reactor pressure vessel, the volatilized fission products will experience only a very short residence time in the reactor vessel upper plenum and in the primary system before being released to the containment, which will limit the possibilities of physical and chemical reactions. In contrast, in a severe accident initiated by a small leak or a transient, the gas flow escaping from the region of the reactor core has to pass over longer distances, partly in pipes of smaller diameter, perhaps through vessels as well, before reaching the containment free volume, resulting in a comparatively long residence time in the primary circuit. In the course of such a transport, aerosols and volatile substances may be deposited onto the walls or, possibly, resuspended from there; fission product vapors may be deposited onto the surfaces of primary aerosols formed from refractory substances and, thus, will be transported with them. Chemical reactions, homogeneous gas phase reactions as well as heterogeneous gas–solid reactions, may occur during this transport which can change considerably the properties of the fission products and, thus, influence their further behavior. Such reactions may also take place in the upper plenum of the reactor pressure vessel, with their extent depending on the particular accident sequence (residence time, temperature gradient, availability of reaction partners, etc.). Therefore, the region "primary system" discussed in the following sections usually will also include the upper vessel plenum.

The gas–steam mixture escaping from the degrading core shows a complex chemical composition; besides H_2O and hydrogen in varying proportions (see below), a number of chemical elements – vaporized fission products as well as constituents of structural and control rod materials – will be present. The situation is even more complicated by the fact that a part of these elements is in aerosol form while the other part is in vapor form.

Besides the gas composition, the temperature and the temperature gradient within the primary system are important parameters for establishing the chemical species and physical forms of the fission products and other materials released from the overheated core. The temperatures prevailing on the way through the pipes to the break are a function of the location of the leak, but they depend also on the gas-flow rate and on the composition of the gas mixture; therefore, they are strongly influenced by the details of the particular accident sequence. Very roughly spoken, values in the range of 1000 to 1200 °C (1300 to 1500 K) are to be assumed at the entry to the main coolant pipe; in the event of a small break at a greater distance from the reactor pressure vessel, the temperature decreases to values of several hundred degrees Celsius along the path to the exit of the pipes to the containment. During the progress of core degradation the temperatures may change considerably, in most cases towards a higher temperature level. To be able to assess the retention effectiveness of the primary system, the temperatures and temperature profiles the fission products will be exposed to, have to be calculated for each particular accident sequence.

When evaluating possible chemical reactions which may occur in the primary system, one has to take into consideration that, in general, the different release

rates of the individual fission products as a function of the fuel temperature are only of minor relevance for the chemical composition of the gas phase which enters the primary system. The progress of the melt front from the top of the core downward and in radial direction from the core center to its periphery has as a result that a large fraction of the volatile fission product isotopes of the noble gases, iodine and cesium is vaporized from the overheated fuel just in front of the melting zone, while from the hotter molten zone the less volatile substances are volatilized. Since the released substances are transported upwards in the reactor pressure vessel, i. e. in the opposite direction to the progress of the melt zone, an effective mixing of the different volatilized elements already within the reactor pressure vessel can be assumed. Thus, in the initial stage of a core degrading process the volatile fission products will dominate the composition of the gas phase. With progressive degradation of the core, the contribution of less volatile elements will increase until a nearly constant equilibrium composition is achieved which can be expected to last over a certain period of time. The time schedule of the vaporization, however, depends strongly on the accident sequence in question; this is especially true for non-fission product elements such as silver and boric acid, which are possible reaction partners for specific fission products. This results in a highly complex chemical system whose composition could change significantly during the course of an accident.

The hydrogen content in the gas flow is of great significance for the chemical reactions that will occur in the primary circuit. As was mentioned earlier, the $H_2 : H_2O$ ratio may vary over a wide range depending on the accident sequence, but may also change with time within a given sequence. Generally, with increasing temperatures in the reactor core and an increasing rate of Zircaloy oxidation, the conditions will become more steam-starved and, consequently, the oxygen potential in the gas–steam atmosphere will decrease.

Most of the analyses performed in severe reactor accident research have been devoted to PWR plants, where the substances released from the core directly enter the primary coolant piping after having passed the upper core structure and the upper plenum of the reactor pressure vessel. In the BWR severe accident sequences, the gas–steam mixture escaping from the reactor core and carrying fission products and aerosols has to travel through the steam moisture separator and the steam dryer before reaching the steam line. In these components a certain retention of fission products may take place, aerosols by mechanical filtering and gaseous iodine species by chemical reactions at the large steel surfaces. Likewise, the BWR pressure suppression pool can be considered as a part of the primary system in which a considerable fraction of the gaseous and particulate substances is retained from the gas–steam mixture by being trapped in the water phase.

In WASH-1400 (US NRC, 1975), no retention of the fission products during their transport through the primary system of a PWR was assumed, since it was argued that such an attenuation was already taken into account in the estimated release fractions. Likewise, it was assumed that the fission products released from the core were transported to the containment building without changing their nature, irrespective of what might have occurred in between. These assumptions were made since the thermal-hydraulic and structural conditions in the primary circuit

of a PWR were so complex and, at that time, poorly understood that no trustworthy calculations could be made. Both the American Nuclear Society and the American Physical Society studies (see Section 7.1.) emphasized the role of chemical phenomena that may occur in the primary circuit as a significant uncertainty in the evaluation of fission product source terms to the reactor containment building. The experimental and theoretical investigations which have been performed in the meantime, although still not perfect, have yielded the basis for a much better understanding of the behavior of the fission products in the primary system, including the chemical reactions they are subjected to there.

The three different groups of radioactive substances, the fission product noble gases, the volatile fission products and the low-volatility radionuclides, which have already been distinguished in the preceding sections, also show considerable differences from each other in their transport behavior in the reactor primary system. The noble gases are transported without any delay through the systems, they do not participate in chemical reactions and they do not influence the chemical reactions of other fission products. Since they are only subjected to radioactive decay, they will not be discussed in the following. In contrast, the low-volatility substances already condense at a short distance from the melting zone to form aerosol particles, a part of which may be deposited inside the reactor pressure vessel while the remainder enters the primary system. The transport behavior of these substances in the primary system is mainly controlled by physical mechanisms, with chemical reactions being of significance in particular cases only; they may, however, act as a carrier for condensed volatile fission products. Finally, the volatile fission products cesium (and rubidium), iodine (and bromine) and tellurium are transported in vapor form over a certain distance before condensing in regions of lower temperature, either on structural surfaces or on pre-existing aerosols; their chemical states may be strongly influenced by chemical reactions.

According to the review paper by Bowsher (1987) on chemical reactions occurring in the primary system under severe accident conditions, the following types of interactions have to be considered:

a) vapor – vapor
b) vapor – aerosol
c) vapor – surface (either clean, oxidized or with surface deposit)
d) aerosol – aerosol
e) aerosol – surface

The extent of these interactions will be determined not only by the chemical and physical forms of the volatilized materials and by the prevailing ambient conditions, but also by the availability of the required reaction partners. Obviously, it is "unreasonable to suppose that the chemical forms of any element would necessarily remain unaffected by the numerous changes in bulk physical and chemical conditions, or by interaction with other fission products and inactive materials" (Bowsher, 1987). The products of chemical reactions of volatile fission products with aerosols or with structural surfaces often show reduced volatility; on the other hand, highly volatile species may be formed, for example as a result of the decomposition of CsI induced by such reactions. Upon deposition onto the surfaces of

the primary system or of less volatile aerosol particles previously formed in regions of higher temperature, volatile fission product species may be converted into less volatile ones; however, revaporization of deposited radionuclides as a consequence of an increase in temperature at the locations of deposition may result in a late source feeding fission products into the containment. Finally, the transport behavior of fission products deposited on primary aerosols will be governed by that of the aerosols and, thus, may show significant differences to the transport and deposition behavior of pure volatile substances.

In the following sections, the behavior of the aerosols and the volatile substances (in particular of iodine) will be discussed with special emphasis on the chemical reactions that can affect the transport behavior of the radionuclides and, thus, their supply to the reactor containment building.

7.3.2.2 Low-volatility substances

A large fraction by mass of the substances vaporized from the overheated reactor core can nucleate to form aerosols or can condense on cooler surfaces inside the reactor pressure vessel. Two different mechanisms may effect this aerosol formation: In a gas flow showing low concentrations of pre-existing particles, homogeneous nucleation from supersaturated vapors is the primary mechanism; a special case of this type is aerosol generation as a result of chemical reaction between two volatile species to form a less volatile product (e. g. formation of Cs_2BO_3 from CsOH and boric acid). In contrast, in an atmosphere with a high concentration of particles, supersaturated vapors are mainly precipitated by heterogeneous nucleation; this means that initially small particles will grow by vapor condensation, with the rate being a function of the concentration and the particle size of the initial aerosol. In the primary circuit, the two mechanisms of aerosol formation are in competition with each other and with vapor deposition onto structural surfaces, with the distribution between aerosol formation and deposition being strongly dependent on the temperature gradient in the system, in the sense that a steep gradient will favor aerosol formation.

The transport and the deposition of the condensation aerosols in the reactor coolant system depend on a number of parameters such as heat and mass transfer, chemical reactions and aerosol kinetics. With respect to their transport behavior, all the substances volatilized from the reactor core do not directly enter the primary circuit. First, they have to pass through the upper plenum of the reactor pressure vessel; their residence time here depends on the specific accident sequence. The masses deposited here on the walls and structures will differ and, consequently, the fraction which, after having passed through the upper plenum, enters the actual primary circuit will depend on the details of the accident.

The aerosols of the low-volatility substances which enter the primary system of the reactor consist mainly of refractory oxides of the less volatile fission products, as well as of those of the core structural and component materials; metals such as silver and cadmium from the PWR control rod materials are also present. In addi-

tion, a very small proportion of fuel dust particles may be carried by the gas–steam flow; this material can be released mechanically in particular when the fuel rod claddings burst, as well as during core slumping. The primary aerosol particles nucleating from the gaseous phase initially have very small dimensions. On their way through the primary circuit they are subjected to reactions such as agglomeration and co-condensation of other substances onto their surfaces, effects which will change substantially the dimensions of the aerosol particles. The mechanisms determining aerosol nucleation and particle growth are very complex and depend on different parameters; the nature of the resulting particle is of importance not only for its transport and retention behavior in the primary system – the size and the properties of its surface are an important parameter with respect to the condensation (or chemisorption) of volatile fission products (see below). Fundamentally, the chemical forms of the aerosol particles during their stay in the primary circuit depend on the prevailing conditions; nonetheless, it can be generally assumed that the chemical nature of the refractory species which were produced inside the reactor pressure vessel is not changed to an extent worth mentioning in regions of lower temperature. For this reason, the chemical forms described by Wichner and Spence (1985) and summarized in Table 7.3. are to be expected within the primary system as well, since chemical reactions that would significantly change the chemical forms of these primary aerosols are not believed to proceed at the lower temperatures prevailing in the primary system. Little is known today about the chemical nature of some of the fission products which are usually included in the less volatile category, such as molybdenum. Besides the extremely low volatile molybdenum metal, more volatile species may exist, such as the oxide MoO_2, as well as mixed oxides/hydroxides. Cesium molybdate Cs_2MoO_4 is another potential compound showing a certain volatility (Bowsher, 1987); however, it is not clear whether or not this compound can be formed in the steam–hydrogen mixture emanating from the reactor core.

In the cooler regions of the primary circuit volatile fission product species such as CsOH and CsI deposit onto the surfaces of the primary aerosols, due to sorption, condensation or chemical reaction (see Section 7.3.2.3.). Not only is the mass of the aerosol particles increased by this deposition, the nature of the surface is simultaneously changed by the precipitation of hygroscopic compounds, and the deposition and resuspension behavior of the particles may be influenced. In the surrounding steam–water atmosphere, this effect can change considerably the nature and effectiveness of retention mechanisms. In addition, particles with hygroscopic constituents on their surfaces may grow when they are exposed to a high-steam atmosphere, due to transfer of steam to the particle. Usually, the gas-phase mass transport of vapor species to aerosols is calculated on the basis of diffusion in a quiescent medium. Despite the fact that the gas flow in the primary system is turbulent it has been mentioned that turbulent enhancement of the gas-phase mass transfer coefficients for aerosols under such conditions is not significant, i. e. that it can be ignored for most purposes (Kress et al., 1993).

In the primary system, physical mechanisms such as diffusion, gravitational settling, inertial impact and thermophoresis will effect a deposition of the aerosol

particles onto the walls. The effectiveness of the retention depends strongly on specific parameters such as the aerosol concentration, the mean particle size of the aerosols, the residence time in the respective volume and the wall temperature. Roberts et al. (1984) have summarized the different mechanisms which contribute to aerosol retention in the components of a primary circuit. When the results of experiments are applied to the real dimensions of the reactor components, thermophoresis proves to be the most important mechanism in particle deposition onto the structural surfaces. The extent of its contribution to aerosol deposition from a turbulent flow depends on a number of parameters such as the Reynolds number and Prandtl number, as well as on the temperature gradient and the length of the piping; in very general terms, a retention effectiveness of >10% is obtained even in rather short pipes, with the maximum value for very long pipes being in the range of 75%. At very low flow rates sedimentation also contributes significantly; the same is true for inertial impact from a turbulent flow, in particular when the ratio of the pipe length to its diameter exceeds values which are between 10 and 100. Inertial impact may be the dominant deposition mechanism in tube bends, valves and at other flow barriers. When applying the results of experiments to the conditions of the so-called S_2D sequence (see WASH-1400), up to 20% retention due to thermophoresis is obtained in the steam generator tubes even when a conservative manner of calculation is used. A similar retention effectiveness in the same accident sequence was calculated for inertial impact at higher gas flow rates in the bends of the main steam line. Brownian movement generally is of less significance in particle deposition. These calculations suggest an effective aerosol retention by deposition even in simple geometries; the application of the calculations to original plant dimensions, however, is of a complicated nature and has to be confirmed experimentally (see below). In particular the behavior of particles larger than 1 μm is an important question, since smaller particles will grow rather quickly to that size. With larger particles, the significance of sedimentation and inertial impact will increase, whereas thermophoresis does not depend very much on particle size. Gieseke et al. (1984) have calculated that up to 65% of the volatile fission products (excluding the noble gases) and over 99% of the aerosols can be retained within a PWR primary circuit. Several computer codes have been developed such as RAFT, RETAIN, TRAPMELT in order to quantify fission product transport and retention in PWR primary systems. The TRAPMELT code has been validated for a wide range of parameters in the Aerosol Transport Tests (ATT) which were performed at ORNL; these tests and their results have been shortly summarized by Rahn et al. (1988). However, none of the codes mentioned above takes account of chemical reactions nor of revolatilization of chemisorbed fission product vapors.

Once an aerosol particle is deposited on a structural surface it is subjected, on the one hand, to gravitational and electrostatic (Van der Waals) adhesive forces, which tend to hold the particle to the surface and, on the other hand, to forces that tend to effect resuspension of the particle. Resuspension in the reactor primary system may reduce the retention effectiveness and, consequently, enhance the source term to the containment. According to Benson and Bowsher (1988), resuspension of deposited aerosols can be caused by one of three processes:

- physical resuspension caused by a change in gas-flow characteristics,
- revaporization of aerosol caused by a local increase in temperature,
- chemical resuspension of fission products and aerosols due to changes in their chemical states (e. g. by a change in the oxygen potential of the system).

Physical resuspension occurs exclusively under turbulent flow conditions, i. e. at Reynolds numbers of more than about 1500, although any obstacles in the flow may reduce this limit. Significant changes in the aerodynamic conditions in the primary circuit, potentially resulting in particle resuspension, may occur as a consequence of reactor core quenching due to delayed action of the emergency core cooling systems, of core slumping into the pool of water still present in the lower regions of the reactor pressure vessel, or of fast depressurization of the primary circuit caused by failure of the reactor pressure vessel or of primary circuit pipework. The resuspension behavior of deposited aerosols is controlled by a number of parameters, such as the physical and chemical properties of the aerosol, the time of contact, the roughness of the surface and its thermal conditions and humidity, and, finally, the characteristics of the gas flow and its variations.

Resuspension experiments with deposited control rod aerosols carried out at room temperature using argon as a carrier gas, yielded a drastic reduction in the loading for deposits with an initially high loading, but a much smaller reduction for initially low loadings (Benson and Bowsher, 1988). The final loadings after exposure to turbulent flow did not significantly depend on the initial loading, suggesting that the aerosol deposits consist of two types of material, a layer which is only loosely bound to the substrate and a layer which is more adherent. The rate of resupension usually decreases exponentially with time; a mathematical model which describes physical resuspension in good agreement with the experimental results has been developed by these authors.

In a steam-containing gas flow, the presence of a significant fraction of soluble substances (e. g. CsOH) on the surfaces of the deposited aerosols will result in a drastic decrease in the degree of resuspension, even at very high gas velocities. In the LACE experiments, the measured resuspension fluxes were two to three orders of magnitude lower with mixed aersosols (MnO and CsOH) than those obtained for pure insoluble deposits (Rahn, 1988). Similarly, it was observed in these experiments that chemical effects could not be ignored.

Thermal revaporization mainly concerns the most volatile component of the deposited aerosol. Thus, in the experiments of Benson and Bowsher (1988), cadmium was primarily volatilized from a deposited control rod aerosol, with the residue enriched in silver and indium. Similarly, deposited volatile fission products may be revaporized when the temperature at a given location tends to increase over the course of an accident. Finally, as an example of chemical resuspension, when such a deposit of control rod aerosols is heated in steam, indium will show an enhanced volatilization due to the formation of volatile indium monohydroxide InOH. In contrast, revolatilization of deposited cadmium is not significantly reduced in the presence of steam, in spite of the possible formation of low-volatility CdO.

Because of the pronounced dependence of the transport behavior of aerosols on the flow characteristics of the carrier gas and on the geometric configuration of

the system, the results of small-scale experiments have to be validated in large-scale tests. The two most important test programs in this area have been the Marviken Large-Scale Aerosol Transport Tests (LSATT) and the Aerosol Containment Experiments (LACE), the results of which, insofar as they are related to the aerosol transport in the primary system, have been summarized by Rahn et al. (1988).

The LSATT experiments were performed in a full-scale LWR primary circuit (without steam generator) and have focused on the impact of a wide range of parameters such as aerosol mass concentration, temperature, superheated steam and water environment. In the so-called fissium-only tests CsOH, CsI and tellurium aerosols were injected into the system, while in the combined corium–fissium test MnO generated in a plasma torch was added. The results of the tests showed gravitational settling and inertial impaction to be the dominant deposition mechanisms, in part due to the flow conditions and residence times in the various parts of the system. The extent of retention depended strongly on the specific conditions of the tests, going as high as 70%. This demonstrated the importance of the primary system for the extent of aerosol transport from the reactor pressure vessel to the containment. There was evidence in the combined corium–fissium test of differing transport behavior of the different species.

The large-scale LACE experiments focused on aerosol transport behavior in a postulated containment bypass accident (V sequence of WASH-1400), but their results can be applied to the general problem of aerosol deposition and resuspension in pipes. In order to approach realistic conditions, aerosols of two species were introduced in these experiments, water-insoluble MnO and water-soluble CsOH. The two species were separately generated by vaporizing manganese metal in a plasma torch (which is the most frequently used technique to produce aerosols of refractory oxides showing very small particle sizes) and by evaporating cesium metal in a vaporization system. Both vapors were then introduced into an aerosol-mixing chamber that contained superheated steam in a nitrogen atmosphere, which oxidized the vapors to MnO and CsOH. According to the summary of the results given by Rahn (1988) as well as by Rahn et al. (1988), the amount of aerosol material retained in a pipe is strongly influenced by the physical nature of the aerosol. Resuspension processes, which may strongly influence the amount of material retained, are different for liquid, liquid-solid and dry-solid aerosol materials after they are deposited on the pipe wall. The passage of aerosol material through the pipe changes the aerosol characteristics in such a manner as to promote inherent retention processes in larger volumes downstream from the pipe (e. g. in vessels or the containment building). The material exiting the test pipes into volumes with lower gas velocities was no longer a well-defined suspended aerosol since large uncharacterized particles were detected in the aerosol samples.

An important property of the primary condensation aerosols which is of high importance for the behavior of the volatile fission products is their large surface area. The surface area of the aerosols within the primary system of a severely damaged PWR can be approximately 500 times greater than that of the primary system structural surfaces (Beard et al., 1988 b). An aerosol mass of 1000 kg formed in a core melting process and having a specific surface area of 1 m^2/g has a total surface area of about $10^6 m^2$. If one assumes that the space needed for one fission

product atom is about 20 $Å^2$, then the surface area mentioned above would be able to trap about 150 moles of vapor by adsorption to form a monolayer; this corresponds to 5 to 100% of the core inventory of a given fission product element, so that the transport behavior of the deposited fission products would be no longer dictated by the vapor properties but by the aerosol transport characteristics (Spence and Wright, 1987). Other authors have estimated that physisorption would only remove approximately 10 moles of vapor, and that this process would only have a secondary impact on the fission product transport, compared with the condensation of fission products onto pre-existing aerosols and chemical reactions between the two species (Beard et al., 1988 b). As for physisorption, under isothermal conditions a reversible adsorption–desorption equilibrium would be established, with the amount of mass deposited being controlled by the partial pressure of the respective species in the gas phase above. If, however, the aerosol with adsorbed fission products is transported quickly into a region with lower temperatures, the fission product deposition would be frozen and desorption could not take place. Chemisorption would be a stronger interaction than physical adsorption, but unlike physisorption it is restricted to the formation of only one monolayer of the adsorbed species; substances which are fixed by chemisorption are not subject to a reversible desorption. At temperatures beyond 800 K, chemisorption is usually of greater importance; physisorption does not occur at temperatures higher than the critical value of a given species, so that it would be of no relevance for most of the permanent gases. Compared to the sorption processes, considerably larger amounts of volatile fission products can be deposited onto the surfaces of the primary aerosols by bulk condensation (induced by heterogeneous nucleation) as well as by chemical reactions. The purely physical parameters of condensation are rather well known and, therefore, this effect is taken into account in different transport codes such as the TRAPMELT-2 code. Chemical reactions occurring under such conditions between aerosols and vapor species will be discussed in Section 7.3.2.3.

Such interactions can only occur, however, when the volatile fission products and the primary aerosols appear simultaneously in the primary system, in spite of the large differences in their volatilization behavior. As was discussed above, uniform thermal-hydraulic conditions do not prevail within the reactor core during a severe accident (for example, the peripheral fuel rods may fail relatively late in the accident sequence, at a point when a large part of the central rods may already be molten) and it can be assumed that the broad time-envelope of significant release of structural aerosols will encompass the release of the volatile fission products. However, as was mentioned in Section 7.3.1.2., the amount of primary aerosols formed and the timing of their formation depend highly on the specific accident sequence; this is particularly true for the control rod materials.

In a BWR, the substances volatilized from the overheated reactor core have to pass through the moisture separator and the steam dryer before reaching the main steam line. These components can be assumed to retain aerosols effectively. Since a theoretical evaluation of their retention effectiveness is only possible with large uncertainties, corresponding experiments have been performed in order to answer this question. In the tests reported by Gieseke and Jordan (1988), different kinds

of aerosols were investigated with regard to their behavior in dry air using original-sized components. The results showed that small particles (< 1 μm) are only retained to a small extent in the moisture separator; for medium-sized particles (~5 μm), the retention effectiveness increases with increasing flow rate from 6 to 32%. For larger particles and a medium flow rate, a retention of up to 80% was measured, whereas at higher flow rates resuspension effects play an increasing role, decreasing the retention effectiveness. While this behavior in the moisture separator corresponds approximately to the expectations based on existing models, the experiments at a steam dryer yielded results which were markedly different from the models based on gravitational settling or on deposition from turbulent flow. Charged particles exhibited a higher retention than neutral ones; the retention effectiveness increased with increasing flow rate, corresponding to a deposition caused by inertial impact. From a heated carrier gas that has a temperature gradient to the structural surfaces, the particle deposition is considerably higher than under isothermal conditions, in particular with larger particles. However, since these experiments were conducted in a dry air atmosphere, it is a question to what extent their results can be applied to a real accident atmosphere which contains high steam concentrations.

7.3.2.3 Volatile fission products

Cesium, iodine and tellurium are commonly classified as volatile fission products. This means that they are present in the vapor state at the temperatures prevailing inside the reactor pressure vessel, but that, in contrast with the noble gases, they will condense at least in part in the cooler regions of the primary system. In addition, these elements may undergo chemical reactions during their transport through the primary system, which can change their initial chemical states, either towards compounds of lower volatility or towards those of higher volatility.

In regions of lower temperatures in the primary circuit, volatile fission product species can condense either on the walls or on the surfaces of already existing aerosols. The relative rates of condensation on both types of surfaces depend on the relative mass transfer rates to these very different geometric structures, the relative values of the thermodynamic driving forces, and the relative surface areas of the walls to the aerosol particles. Since the surface of an aerosol particle can be expected to be at the temperature of the gas in which it is carried (which usually is markedly hotter than adjacent structural surfaces, at least during the early heatup phase of a severe accident sequence), the driving force for condensation onto structural surfaces would significantly exceed that for condensation onto aerosol particles. On the other hand, mass transfer coefficients for small particles generally exceed considerably those estimated for larger structures, which may tend to compensate for the comparatively low driving force for condensation on the aerosols. As for the surface areas, that of the aerosols is expected to be much greater than that of the walls (see Section 7.3.2.2.); on the other hand, the surface area of the walls can be expected to remain constant during the whole core melt-

down period, while the surface area of the aerosol may change, depending on nucleation rate and growth rate. Model studies (Johnson et al., 1989) showed that, similar to the condensation behavior of the low-volatility substances, the rate of temperature decrease in the transport of the volatile fission products is an important parameter in the competition between vapor condensation on the structural surfaces and aerosol formation. If this rate is small, then vapor condensation is more likely to be the major process for the removal of fission product compounds from the gas phase. When, however, this gradient is steep, supersaturation of the gas will occur and aerosols will be formed. The deposition of vapors onto the surfaces of primary aerosols present in the gas flow was not evaluated in this model.

In any case, deposition of volatile fission products onto the surfaces of other aerosols will influence significantly their transport behavior and, consequently, their source term to the containment. Because of their great importance, such vapor–aerosol interactions in the primary system have been extensively studied at many institutions. However, investigations on a laboratory scale are very difficult to perform in such a way that their results can be meaningfully transferred to a full-scale facility.

The main processes of vapor–aerosol interaction are physical and chemical adsorption, condensation and chemical reaction. In spite of the large sorption capacity of the primary aerosols (see Section 7.3.2.2.), in practice the simple sorption processes seem to be of secondary importance. Condensation and chemical reactions apparently dominate what happens in the system vapor–aerosol.

The kinetics of chemical interactions between fission product vapor and aerosols is mainly controlled by gas phase mass transport, by the kinetics of the chemical reaction, and by mass transport in the condensed phase. Another factor potentially influencing the kinetics of vapor deposition is that the heat liberated by condensation or by chemical reaction of vapor with aerosol must be disposed of. Because of their small masses, aerosol particles have only limited capacity for conducting away this heat, compared with the structures within the reactor coolant system. This problem may arise particularly in the deposition of water vapor onto aerosol particles which have been previously covered by hygroscopic or water-soluble compounds such as CsOH.

Substances which have been plated out from the vapor phase by condensation onto structural surfaces may be revaporized again when the temperature at the location of the deposit increases during the further progress of the accident; besides thermal-hydraulic heatup, decay heat from the deposited fission products is a possible contributor to such an increase in local temperature. If, however, the chemical state of the fission product has changed upon deposition, revolatilization would be delayed or even completely suppressed. Depending on the prevailing conditions, resuspension (or revolatilization) of deposited fission products may lead either to a simple relocation of the material in the primary circuit or to an effective reentrainment in airborne form, resulting in a late aerosol source which is of potential significance in the event of late containment failure at a time when the aerosols directly transported into the containment have been largely removed from the atmosphere by deposition and plate-out (Malinauskas and Kress, 1991).

An overview of the chemical reactions of the volatile fission products in the primary system was given by Bowsher (1987), who summarized the state of knowledge at that time. Calculations of their possible chemical states were performed by different authors, e. g. by Cubicciotti and Sehgal (1984) and, more recently, by Cordfunke and Konings (1993) and by Ball et al. (1993). It has to be emphasized, however, that such a thermochemical treatment refers to the equilibrium state of the system, but that in practice reaction kinetic limitations may exist. As was mentioned in Section 7.3.1.1., the time needed to reach the equilibrium state for some of the important fission product reactions varies over a broad range, from about 10^{-4} seconds to tens of seconds, depending on the concentrations of the reaction partners and on the prevailing temperature. Thus, at comparatively low concentrations, high gas flow rates and steep temperature gradients, high-temperature equilibria may be frozen and the chemical composition established at high temperatures will be conserved even in regions of lower temperature. Such kinetic limitations can be assumed to be of significance only in special cases so that, in general, thermochemical treatment can be expected to yield reasonable results. It has to be noted, however, that kinetic studies that have been performed in chemically simple systems, without consideration of the possible action of a greater number of possible reaction partners, are not directly applicable to the analysis of vapor behavior in the reactor coolant system.

7.3.2.3.1 Cesium

As was stated in the previous sections, cesium is released from the overheated reactor core mainly as CsOH and, in part, as CsI or is rapidly converted into these species in the iodine-containing steam atmosphere surrounding the reactor core. Taking into account the mass ratios of iodine and cesium in an equilibrium burnup reactor core, it can be estimated that about 90% of the fission product cesium released from the reactor core (including the stable and the very long-lived isotopes) are present as CsOH in the primary system and about 10% as CsI. Since both species can be classified as medium-volatile, it can be expected that a fraction of them will deposit onto the surfaces of the already-suspended aerosol particles, whereas another fraction will be deposited onto the structural surfaces of the primary system. CsI may be subjected to decomposition reactions in the primary system; these processes will be discussed in Section 7.3.2.3.2. According to thermochemical calculations, at high temperatures and high hydrogen concentrations a minor proportion of elemental cesium would be stable in the equilibrium (Cordfunke and Konings, 1993). In addition, there are other cesium compounds which may be formed under specific circumstances in the primary system. For example, cesium molybdate Cs_2MoO_4 is sufficiently stable at high temperatures; the formation of this compound would lower the volatility of cesium (as compared with CsOH and CsI), but would increase the volatility of molybdenum as compared with elemental molybdenum. However, since contact with steam at high temperature would favor the decomposition of this compound to MoO_3 and CsOH, ce-

sium molybdate is not expected to be of significance in cesium transport in the primary system. The same applies to various cesium–tellurium compounds such as Cs_2Te which, in principle, may be formed under the conditions prevailing during a severe reactor accident (Bowsher, 1987).

Thus, CsOH is the predominant cesium species during transport through the primary system. When the temperature of the gas flow decreases below a certain level, deposition of gaseous CsOH onto the surfaces of the primary aerosols will start. This deposition may include pure condensation, but also reactions such as physisorption, chemisorption and formation of chemical compounds; for this reason, the extent of deposition can be expected to depend on the nature of the already-suspended aerosol particles. In order to obtain basic data for cesium transport calculations, Spence and Wright (1987) have investigated the sorption of CsOH and CsI onto silver and Cr_2O_3 aerosols in the temperature range 600 to 1000 °C. The results showed that the measured sorption isotherms can be represented by modified Freundlich isotherm expressions. CsOH sorption onto silver (0.7 to 3 mg/g) proved to be considerably smaller than onto Cr_2O_3 (15 to 35 mg/g); the latter value, in turn, was higher than CsI sorption onto Cr_2O_3 (14 to 26 mg/g). An even stronger interaction was observed between CsOH and both metallic iron and iron oxide aerosols. At 700 °C in a helium atmosphere and at a CsOH partial pressure of 30 Pa, the adsorbed mass amounted to 1900 mg of CsOH/g iron oxide and 2400 mg/g of metallic iron. The addition of hydrogen (0.5%) to the atmosphere resulted in a virtually complete suppression of the adsorption of CsOH onto metallic iron aerosols and in a reduction of the adsorption onto iron oxide aerosols to values of about 850 mg/g; once adsorbed, however, CsOH was not desorbed upon the addition of H_2 to the gas flow. It is known from other investigations that at $H_2 : H_2O$ ratios < 1 an interaction between CsOH and Fe may occur which has been interpreted as the result of a bulk chemical reaction. On the other hand, Bowsher and Dickinson (1985) reported that CsOH physisorbs (with no chemical reaction) onto Fe_2O_3 powder in an inert atmosphere, whereas in an Ar–5% H_2 atmosphere Fe_2O_3 would be reduced with no significant reaction observed between CsOH and the resulting iron powder. Since the $H_2 : H_2O$ ratios inside the reactor pressure vessel in the course of core melt accidents are expected to range from 0.1 to 10 (depending on the accident sequence), sorption of CsOH and CsI onto the surfaces of metallic and oxidic aerosols cannot be ruled out, so that their transport behavior would be dictated by that of the aerosols. To be sure, it seems questionable whether there would be sufficiently large sources of such metal oxide aerosols during the course of a severe reactor accident; on the other hand, these results may also be of significance with respect to the possible adsorption of these fission products onto structural surfaces.

Only physisorption is expected between CsOH vapor and cadmium aerosols (which in many accident sequences are a major constituent of the aerosols during the period of cesium evolution from the fuel and of formation of cesium hydroxide) with no chemical interactions predicted (Bowsher, 1987). Beard et al. (19988 b) reported condensation to be the dominant mechanism in this system.

The influence of sorption reactions on the transport behavior of fission products was calculated by Spence and Wright (1987) exemplarily for two severe accident

sequences. In the AB sequence (terminology of WASH-1400), representing a medium- to large-sized break, the residence time of the fission products and the aerosols in the high-temperature region and in the primary circuit will be comparatively short (<1 min); therefore, while sorption of vapors onto the surfaces of aerosols can occur, no equilibrium state will be reached, and the fraction of adsorbed vapors is determined by mass transfer kinetics and by the residence time. Under such conditions, sorption can be assumed to affect the transport behavior of CsOH and CsI only insignificantly, since condensation of the volatile substances predominates due to their comparatively high concentrations. In the so-called TMLB sequence, which is characterized by a comparatively long residence time of the aerosols and vapors inside the reactor pressure vessel, a considerable fraction of the primary aerosols will be deposited onto the core structural components. Since the temperature here is too high for condensation of volatile fission products, earlier calculations (according to TRAPMELT-2) assumed that these substances would stay in the vapor phase and would be transported slowly out of the primary circuit. In contrast, when sorption effects are included the calculations show retention of significant fractions of CsOH and CsI attached to the refractory aerosols remaining in the reactor pressure vessel. However, the deposited aerosols and the associated fission products are not necessarily immobile; they may be resuspended, for example, by the steam jet which is caused by core slumping. The impact of such a mobilization of volatile fission products (now attached to aerosols) on the transport behavior of cesium to the containment has not yet been clarified, in particular in comparison to the retention by condensation of the volatile substances in the piping of the primary system. The same applies for questions involving the reaction of liquid water with adsorbed fission products.

CsOH can also be plated out onto stainless steel surfaces, resulting in a very tightly adherent deposit. Experimental investigations of the deposition of CsOH onto stainless steel at high temperatures in steam and hydrogen showed that a significant fraction of the deposited cesium is deeply embedded into the superficial oxide layer and that it cannot be removed by water leaching. Similar results were obtained in the post-accident investigations of stainless steel components from the core and the upper vessel plenum of the TMI-2 reactor where the deposited cesium could not be dissolved by immersion into warm water, even when the immersion lasted for years. There are strong indications that this cesium fraction is bound as cesium silicate, most likely $Cs_2Si_4O_9$, to the silica impurities of the steel oxide layer (Elrick et al., 1984; Elrick and Sallach, 1986). This would mean that the amount of cesium retained on the stainless steel surfaces depends on the availability of SiO_2, formed by steel corrosion either during plant normal operation prior to the accident or concurrently with the volatilization of fission product cesium from the reactor core. Under steam-starved conditions, i. e. when H_2 is the predominant constituent of the gas flow, the oxidation of stainless steel is largely inhibited, limiting the production of SiO_2 which can react with CsOH. The rate of cesium silicate formation is controlled both by the rate of the $CsOH-SiO_2$ reaction and by the rate at which CsOH from the gas phase reaches the reaction site. From experiments, a value of $5 \cdot 10^{-4}$ m/s was calculated for the rate at which the cesium

species travel through the outer stainless steel oxide layer at 1270 K and react with the silica (Elrick and Sallach, 1986).

According to Bowsher (1987), the reaction between CsOH vapor and stainless steel surfaces is characterized by the formation of both water-soluble and insoluble cesium-based reaction products; it proceeds via a fast physisorption process which is followed by a slower diffusion of cesium into the metal oxide. The cesium is predominantly associated with the inner chromite layer of the duplex oxide which covers the stainless steel surface; the results of these studies imply that cesium is present as isolated cations in the chromia layer. Beard et al. (1989) reported that the water-soluble fraction of deposited CsOH is progressively converted upon heating to the insoluble form. At temperatures above 1150 K a significant vaporization of cesium took place, identified tentatively as cesium chromate vapor (Cs_2CrO_4); however, a substantial fraction was retained in the oxide layer on the metal surface and was not vaporized until the steel began to melt.

Experiments (Johnson et al., 1989) in which CsOH in a steam–hydrogen flow was conducted through a stainless steel duct with a temperature gradient from 1000° down to 200 °C showed that significant amounts of cesium deposited well above the condensation temperature of CsOH. Moreover, the observed revaporization behavior of cesium required that the vapor pressure of CsOH from these deposits would have to be significantly less than the vapor pressure of pure CsOH. Both effects suggest a chemical reaction between gaseous CsOH and oxidized stainless steel surfaces at high temperatures. In these experiments, $CsOH \cdot H_2O$ deposits were found in the cooler regions of the duct, indicating a "hydration" of the CsOH deposits by steam.

A comparatively slow reaction between CsOH vapor and Inconel has been reported by Elrick et al. (1984), with the formation of a cesium silicate or aluminate as a reaction product being assumed. CsOH can also react with various other metals and metal oxides at high temperature, for example with zirconia at 1900 K to form cesium zirconate Cs_2ZrO_3. These reactions indicate that significant retention of cesium can be expected to occur in the primary circuit during a severe reactor accident, since the compounds formed are generally less volatile than CsOH.

CsOH initially formed in the overheated core region may react in the primary circuit, either in a homogeneous gas-phase reaction or in a heterogeneous gas–solid reaction, with boron oxide or boric acid originating from the PWR coolants or from the decomposition of BWR B_4C control rod material. This reaction proceeds over a wide range of ambient conditions, with its products depending on the proportions of the reactants and on the environmental conditions. Calculations based on thermodynamic data have shown that $CsBO_2$ and Cs_2BO_3 species will be preferentially generated (Powers and Bieniarz, 1986). More recent calculations, based on newer thermodynamic data, yielded $CsBO_2$ as the most stable compound in gaseous as well as in liquid form, depending on the temperature of the system; variations in pressure and mole ratios of the reactants are reported not to be of major significance (Minato, 1991). The cesium borates show only low reactivity, they are water-soluble and relatively non-volatile (as compared with CsOH), and they may undergo significant attenuation in the primary system by rapid condensa-

tion and deposition. On the other hand, the reaction of CsOH with boron oxide or boric acid will limit or even prevent the reaction of CsOH with I_2 or HI; moreover, CsI once formed can be decomposed under the influence of these boron compounds, potentially enhancing the volatility of iodine (see Section 7.3.2.3.2.).

There is, however, the question of whether or not sufficiently large amounts of boron compounds will be available in the primary system during cesium and iodine transport to influence significantly the nature of the chemical compounds formed. As was mentioned in Section 7.3.1.2., the boron originates from various sources and, therefore, both the volatilized amounts and the timing of vaporization depend on the type of reactor, its operation history and the availability of the emergency systems, as well as on details of the accident sequence. The amount of boron which will be in contact with the degrading core may range between a few tens of kilograms and a few megagrams; with the exception of the lower mass range, this amount would, in principle, be sufficient to tie up the whole cesium inventory of the degrading core.

Carry-over of boron from the liquid to the steam phase can be effected by various mechanisms: flashing of the coolant during early stages of the accident, during injection of emergency coolant solution onto the overheated core and during core slumping into the lower plenum will result in the formation of boric acid aerosols. Boric acid is volatilized during evaporation of the primary coolant and of emergency coolant, with the extent of carry-over depending on temperature and pressure; in cooler regions and in dried-out regions boric acid or boron oxide will crystallize. The volatility of boric acid is little affected by other coolant additives, such as LiOH, because of their comparatively small concentrations. However, the availability of boron in the vapor phase is limited by reactions with core materials or by deposition onto the structures; in the further progress of the accident these deposits can be volatilized again as a result of increasing temperatures at these locations. Thus, in spite of remarkable retention in the primary system, considerable amounts of boron will be transported to the containment and, moreover, large parts of the leak path will be covered with boron-containing deposits before fission products are released from the core.

As for the boron concentration in the gas phase, it can be expected to be comparatively high during core uncovery (in many cases on the order of 1000 ppm), i. e. during the time when a considerable fraction of the volatile fission products is released. In the presence of steam the vapor-phase boron will be orthoboric acid H_3BO_3 or metaboric acid HBO_2, with boron oxide as aerosol.

7.3.2.3.2 Iodine

The iodine species which are released from the overheated fuel (mainly CsI and iodine atoms, depending on the burnup state of the fuel) are subject in the primary circuit to various chemical reactions, the most important of which are shown sche-

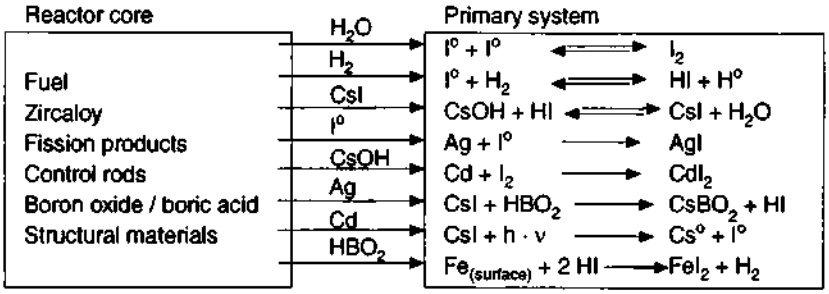

Figure 7.15. Chemical reactions of fission product iodine in the primary system (schem.)

matically in Fig. 7.15. Most of the elements able to react with iodine to form iodide compounds are present in the primary system in clear or even great excess; thus, from basic considerations, it can be concluded that no elemental iodine can be stable under the prevailing conditions. However, in order to evaluate final iodine chemical states, besides the potential reaction partners, additional parameters also have to be considered such as the temperature, which ranges from very high values (>1000 °C) at the entry to the primary system down to a few hundred degrees Celsius at the location of the primary circuit break or leak. The precise temperature distribution along the pathway of the fission products through the primary system depends largely on the details of the accident sequence. In addition, as has been mentioned above, the residence time of the reaction mixture in any given temperature zone is an important parameter for assessing whether or not reaction equilibria will be established.

Some of the iodine species (e. g. CsI) will condense on surfaces or will form aerosols in the reactor pressure vessel or during their residence time in the pipes and components of the primary system; they can be transported together with the primary aerosols or deposited within the primary system, but in each case they may undergo further chemical reactions potentially leading to other, more volatile products. Other species such as elemental iodine I_2 are transported in gaseous form inside the primary circuit; after having reached the containment free volume, they may enter into a partition equilibrium between sump water and containment atmosphere. For this reason, it is of considerable interest to know the chemical forms of fission product iodine that can be generated within the primary circuit.

First, some short remarks on the basic chemistry of iodine in a high-temperature steam environment shall be made. In such a steam phase as is present in the reactor pressure vessel above the core melt zone, as well as in wide regions of the primary system, ionic iodine species such as I^- and IO_3^- (which are the dominant products in aqueous solution at higher pH) are not stable. As a result, the disproportionation reaction of I_2 caused by H_2O is not expected to proceed inside the primary system to any significant extent (perhaps with the exception of liquid water pools which may be formed in regions of lower temperature), quite in contrast to the sump water of the containment, where it is one of the essential mechanisms controlling

iodine volatility. Only neutral species will appear in such a steam environment, mainly elemental iodine I_2. However, in pure steam at higher temperatures I_2 will be decomposed to form neutral iodine atoms according to the equilibrium reaction

$$I_2 \rightleftharpoons 2\ I^\circ$$

The degree of decomposition here depends mainly on the parameters concentration, temperature and pressure. At an $I_2 : H_2O$ ratio of $2 \cdot 10^{-3}$, an H_2O pressure of 0.1 MPa and a temperature of 600 °C, about 50% of the elemental iodine will be present as neutral atoms I°. According to the law of mass action, the degree of decomposition of a molecule to atoms increases with decreasing iodine concentration, and decreases with increasing system pressure and decreasing temperature, so that a 50% ratio will also be attained at 10 MPa and 1000 °C at the concentration mentioned above. As a consequence, in a severe accident there are significant differences to be expected between the high-pressure and the low-pressure sequences with regard to the relative yields of these two iodine species under equilibrium conditions.

The formation of non-dissociated HOI in the vapor phase was claimed to be possible only if the steam contained liquid water, i. e. in saturated steam (Lemire et al., 1981). On the other hand, from measurements of iodine partition coefficients it was concluded that HOI is the predominant neutral iodine species in steam at low concentrations and high temperatures (see Section 4.3.4.2.). In any case, the possible appearance of HOI under the prevailing conditions is of little significance for the chemical and transport behavior of fission product iodine, because of the low I_2 fractions present and of the large excess of possible reaction partners.

In case the steam contains significant amounts of hydrogen (which applies to all LWR accident sequences), this element will rapidly react with elemental iodine to form hydrogen iodide HI. According to Sullivan (1967), in the iodine concentration range from 10^{-4} to 10^{-5} g-atom/l, the reaction mainly follows the equation

$$2\ I^\circ + H_2 \rightleftharpoons 2\ HI$$

whereas at lower concentrations (10^{-5} to 10^{-10} g-atom/l) the reaction

$$I^\circ + H_2 \rightleftharpoons HI + H^\circ$$

is primarily responsible for the conversion (Castleman et al., 1968). The status of both equilibria depends primarily on the H_2 partial pressure. According to the results of Castleman et al. (1968), which are shown in Fig. 7.16., at an H_2 partial pressure of 0.01 MPa and at temperatures below 1000 °C, the equilibrium state is almost quantitatively shifted to the HI side. Higher temperatures as well as lower H_2 partial pressures will favor HI decomposition, resulting in the appearance of increasing proportions of I° in the mixture of the iodine species. The experimental data suggest that the above-mentioned equilibria are established within a few seconds at the latest. The HI formed is volatile with steam; after partial condensation of the steam, this strong acid enters the liquid phase where it dissociates instantaneously and completely to H^+ and I^- ions. The capacity of liquid water for HI depends on various parameters such as temperature and pressure; the high degree of dissociation means that in virtually all situations which may occur in an LWR

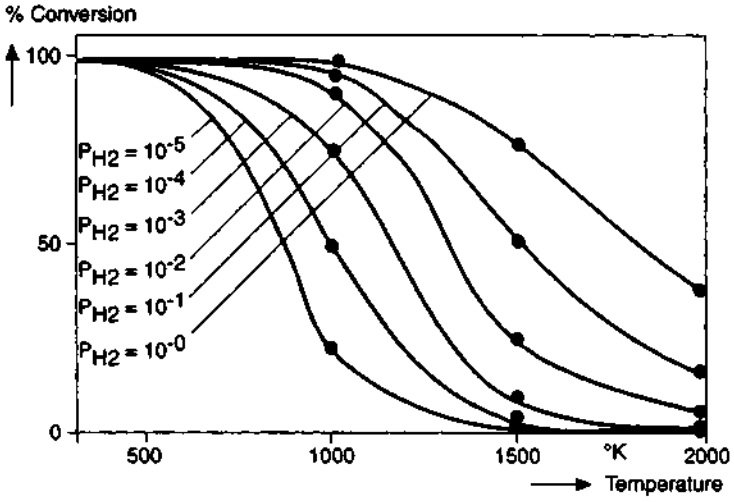

Figure 7.16. Calculated conversion equilibrium $I^{\circ} \rightleftharpoons HI$ as a function of temperature and H_2 partial pressure
(Castleman et al., 1968; Copyright 1968, with kind permission from Elsevier Science Ltd, The Boulevard, Langford Lane, Kidlington OX5 1GB, UK)

accident, HI is completely trapped in the water phase and that its volatility from the resulting dilute solutions is extremely low, resulting in a very high partition coefficient (see Section 6.2.2.).

In the presence of cesium in the steam, this alkali metal which, under such conditions, exists predominantly in the form of CsOH, will react with I_2, I°, and HI to form CsI. According to the results of thermodynamic calculations, the reaction equilibria are shifted to the CsI side by increasing iodine concentrations, provided that the H : O ratio in the steam is greater than 2 (i. e. that elemental hydrogen is present in the steam). At an iodine concentration of $2 \cdot 10^{-5}$ g-atom/l, an H : O ratio of 3, a Cs : I ratio of 10 and temperatures below 1000 °C, the iodine present will be virtually completely converted to CsI. According to the results of Paquette et al (1983) on thermodynamic and kinetic calculations for three different temperature regions, under the conditions to be expected in an LWR accident within the primary circuit of a PWR ($5 \cdot 10^{15}$ atoms I/ml, Cs : I ratio 10, steam atmosphere 1.2 MPa), CsOH and CsI are the predominant species after the very short time interval of 10^{-3} to 10^{-2} seconds at 750 °C (see Fig. 7.17.). These numbers are consistent with the results reported by Cronenberg and Osetek (1988), which have been discussed in Section 7.3.1.1. At very high temperatures, iodine atoms will be present at the lower percent level, whereas they are without significance in the lower temperature regions; I_2 and HI exhibit a similar behavior.

These results have been essentially confirmed by more recent calculations in which the currently available basic data were applied to specific accident sequences at four US PWR and BWR plants (Kress et al., 1993). In most of the sequences studied, the total amount of iodine released from the primary system into the

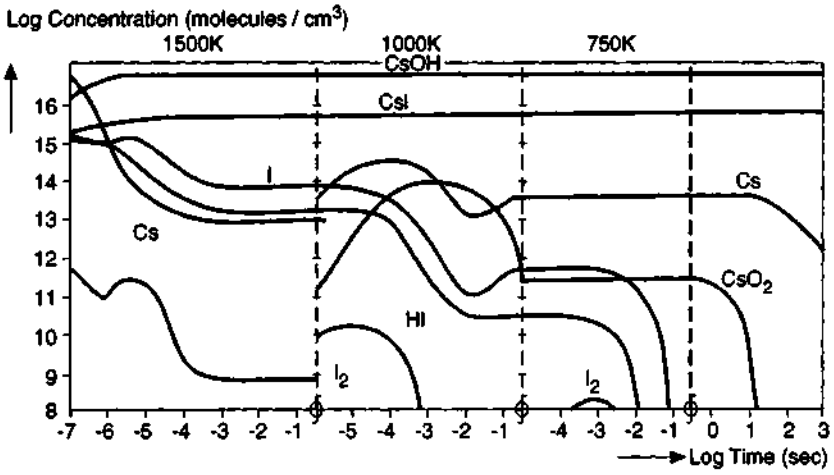

Figure 7.17. Calculated time-dependent formation of iodine and cesium compounds in steam in three temperature regions
(Paquette et al., 1983; by courtesy of Thomas Telford Ltd., London)

containment was found to be almost entirely in the form of CsI with very small contributions of I_2 or HI, amounting to <0.1% in total. However, in a particular accident sequence (large break loss-of-coolant accident, low-pressure sequence) in which the temperatures in the core region were calculated to be in excess of 2000 K, calculations showed that the upper grid plate located immediately downstream from the core would be relatively cold for a short period of time, so that equilibrium compositions would be frozen in the core region at a relatively high temperature. For this sequence, the overall iodine species distribution was 2.8% for I_2 and 0.4% for HI, with the balance as CsI. However, there are also other influences than the pure gas-phase chemistry; as will be discussed below, additional amounts of highly volatile iodine species may be formed as a result of CsI chemical reactions occurring in the primary system.

CsI shows a certain volatility at higher temperatures; its vapor pressure in a steam atmosphere is about 1 mbar at 700 °C, and about 10^{-2} mbar at 500 °C, which is comparable to that of CsOH (Cummings et al., 1982). Since the temperatures of the steam flow decrease with increasing distance from the overheated reactor core, CsI will start to condense along this way, resulting in a corresponding decrease of the residual CsI concentration in the gas phase. Calculations performed by Cubicciotti and Sehgal (1984) on the progress of this condensation from the steam flow showed that in the low-pressure sequence (0.3 MPa) no CsI condensation is to be expected down to temperatures of about 750 °C; when the temperature decreases further to 350 °C, the concentration of gaseous CsI is reduced by a factor of about 1000. In the high-pressure scenario (17 MPa), however, CsI condensation already starts at about 1500 °C; at 500 °C the fraction which is still in gaseous form is lower by about 4 orders of magnitude than at the higher temperature. In addition to the primary system inner surfaces, the surfaces of the primary aerosols may also repre-

sent a condensation area for CsI (see Section 7.3.2.3.). Because of the very high surface area of the primary aerosols (see Section 7.3.2.2.) it can be expected that a large fraction of the CsI will deposit onto the aerosols and will be transported together with them. Such a behavior seems reasonable to assume, at least when the gas and the aerosol temperature are not greatly in excess of that of the pipe walls, a situation which can be expected after a certain time interval following the onset of the fission product release from the reactor pressure vessel.

Experiments in which simulated fission product compounds were introduced into a superheated steam–hydrogen flow and passed down a stainless steel duct onto which a temperature gradient was imposed (1000 to 200 °C) showed that gaseous CsI exhibited a normal deposition behavior, i. e. that it did not significantly react with the oxidized steel surface. In the simultaneous presence of gaseous CsOH, the temperature at the onset of CsI condensation was lowered by as much as 100 K; this effect was shown to be due to the formation of the complex gaseous species CsI · CsOH. On the other hand, due to the low proportion of CsI in the CsI–CsOH mixture, the deposition behavior of cesium associated with CsOH was not significantly affected. The observed revaporization behavior indicated that the vapor pressure of CsI–CsOH deposits during revaporization corresponded approximately to the vapor pressure of pure CsI at the temperature of the deposit (Johnson et al., 1989).

In spite of its high thermodynamic stability, CsI transported in the steam flow can be decomposed by the action of third partners. Several reactions can effect this decomposition, which results in the formation of highly volatile iodine species. In general, according to the overall equilibrium equation

$$CsI + H_2O \rightleftharpoons CsOH + HI$$

any process that reduces the concentration of CsOH in the equilibrium will tend to drive the reaction to the right side, i. e. towards higher concentrations of more volatile iodine species. In particular, the reaction

$$H_3BO_3 + CsOH \longrightarrow CsBO_2 + 2\,H_2O$$

is able to reduce the CsOH partial pressure considerably, shifting the equilibrium above to the right. In addition, the direct high-temperature reaction (i. e. at temperatures >1000 °C) of CsI with boric acid or boron oxide can lead to its decomposition according to

$$HBO_2 + CsI \longrightarrow CsBO_2 + HI$$

In severe accidents in PWR's, the availability of boric acid vapor and aerosols for reactions with CsOH and CsI depends on the particular accident sequence (see Section 7.3.2.3.1.). These reactions are of greater significance in the high-pressure accident sequence, since in this case the boric acid inventory of the primary coolant and the emergency coolant solutions becomes concentrated in the residual water volume inside the reactor pressure vessel; because of the considerable volatility of boric acid at a pressure of 16 MPa, this compound will be partly volatilized with the steam. In contrast, in low-pressure accident sequences most of the primary coolant boric acid inventory will be ejected during blowdown and, thus, not be

available. In addition, at ambient pressure the co-evaporation of boric acid with water is comparatively low. In BWR severe accidents, the possible decomposition of B_4C control rod material by steam may also provide considerable amounts of boric acid, a part of which will be transported with the steam.

Calculations performed by Cubicciotti and Sehgal (1984) suggested that HI is the predominant iodine species formed in the CsI–boric acid reaction, and that this reaction does not lead to the production of significant amounts of elemental iodine. More recent calculations confirmed HI and CsI as the main iodine species over a broad range of temperature and pressure, as well as concentration ratios of the different chemical elements present in the gas–steam flow (Minato, 1991). As was mentioned above, HI produced by this reaction will be readily dissolved upon appearance of liquid water to form I^- ions; thus, its behavior later on in the containment will not be significantly different from that of CsI which is transported to the containment sump water. Several investigations concerning the decomposition of CsI by boric acid have been performed. According to Elrick et al. (1987), steamborne CsI reacts in the same manner as does CsOH with boron-containing deposits on steel surfaces, however at a considerably slower rate. The homogeneous gas-phase reaction between CsI and boron compounds which has been reported by other investigators (see below) was not observed in these experiments, probably due to their specific design.

Detailed investigations of the reaction of CsI with boric acid in the condensed phase over the temperature range 400–1000 °C under Ar, Ar–H_2, and Ar–H_2–steam atmospheres were performed by Bowsher and Nichols (1985). The results showed that CsI decomposition in these reactions starts at temperatures above 400 °C and increases considerably beyond 700 °C, with the HI produced being partly converted to I_2 (and/or iodine atoms) by thermal dissociation. Under such conditions, HI as well as I_2 may react with the iron and nickel content of stainless steels under formation of the corresponding iodides (see below). Up to 960 °C, CsI and molten boric acid or boron oxide react in a diffusion-controlled reaction the rate of which is determined by the diffusion of the partners to the reaction zone. The reaction data measured in these experiments were consistent with Arrhenius' law, showing an activation energy of 190 ± 30 kJ/mol.

Bowsher and Dickinson (1986) analyzed both the gas-phase reaction between CsI and boric acid and this reaction in the heterogeneous system steam–condensed phase. In the homogeneous gas-phase reaction, CsI is largely decomposed at 800 °C in the presence of steam with HI as the reaction product. The same applies to the reaction of volatile boric acid with condensed CsI; in contrast, gaseous CsI and condensed boric acid reacted only after condensation of the CsI. In the presence of an excess CsOH, the formation of HI proved to be greatly reduced, but not decreased to zero; the reason for this behavior seems to be the preferential formation of $CsBO_2$ from CsOH, as well as the recombination of HI produced with excess CsOH. Since the volatility of boric acid is enhanced in the presence of steam, it will prevent the co-condensation of boric acid and CsI; thus, reactions of both partners in the condensed phase seem in practice to be of little significance.

From these experiments it was concluded that the yield of HI in the CsI–boric acid reaction will strongly depend on the prevailing conditions, i. e. on the accident

sequence under consideration. Whereas in the low-pressure sequences this reaction seems to be of little significance, it can prove to be an important feature in the high-pressure sequences where the homogeneous gas-phase reaction inside the reactor pressure vessel is assumed to be the predominant mechanism during core meltdown. In the later stages of the accident, the reaction between boric acid vapor and condensed CsI may be of importance; the reaction of CsI vapor with condensed boric acid finally seems to be of significance only under steam-starved conditions, i. e. when co-condensation of both reaction partners is possible.

As was previously discussed, there is still the question of whether or not the steam escaping from the reactor pressure vessel carries enough boric acid to initiate reaction with CsOH and/or CsI to an extent worth mentioning. Calculations (Kress et al., 1993) have indicated that in low-pressure sequences the boric acid is almost completely boiled away from the reactor pressure vessel before fission product release from the fuel begins and, therefore, is probably not present in airborne form to influence the chemistry of iodine (boron could, however, still be present as a surface oxide deposit in the primary system). In contrast, in the high-pressure sequence, the boric acid will concentrate in the residual water in the reactor pressure vessel. In principle then, boric acid would be available in the steam at a concentration that should be approximately given by the product of its equilibrium partition coefficient and its current concentration in the liquid phase. In these calculations, however, whether or not the boric acid can remain airborne in the presence of other core materials was not taken into consideration. Given the results of two simulated core melt tests which were run to assess the behavior of boric acid under such conditions, it is highly likely that boric acid co-vaporized from residual water in the reactor pressure vessel will be tied up by the hot Zircaloy still present in the uncovered regions of the core and, therefore, will not become sufficiently airborne to affect significantly the chemical form of the released iodine.

CsI, although very stable against reactive surfaces, may also be decomposed upon contact with steel surfaces at high temperatures, but at a rate which is much slower than CsOH reaction with such surfaces (see Section 7.3.2.3.1.). According to Elrick et al. (1989), this decomposition is a complex process which starts from the CsOH being present in the above-mentioned equilibrium between steam and CsI. Their calculations showed that the fraction of CsOH present in this equilibrium mixture increases with increasing temperature, as well as with decreasing H_2 concentration in the steam atmosphere. In the range $1000\ K < T < 1600\ K$, at $H_2 : H_2O$ ratios between 0.1 and 10 and at CsI partial pressures of 10^{-3} to 10^{-5} atm, up to 25% of the CsI will be converted to CsOH. As was previously discussed, the CsOH produced will move towards the steel surface (e. g. the pipe walls), and will react there with the silica content in the oxide layer to form cesium silicate. The experiments described by Elrick et al. (1989) were carried out at 1180 K using steel SS 304 with a silicon content of $< 1\%$; different flow rates as well as $H_2 : H_2O$ and $CsI : H_2O$ ratios were studied, with some of these conditions yielding considerable excess iodine in the effluent as compared with the CsI composition, due to cesium retention on the steel surfaces. An essential parameter in cesium retention is the contact time between the steam flow and the steel surface; besides this, the

CsI decomposition shows a dependence on the parameters similar to that of the calculated CsOH formation.

These results, however, cannot be directly applied to a real accident situation since the impact of an approximately tenfold surplus of CsOH simultaneously present in the gas phase on the decomposition of CsI was not investigated in the studies; according to the law of mass action, such an excess of one reactant will shift the equilibrium state of the decomposition reaction cited above towards regions of higher CsI stability. Moreover, in the presence of a large excess of CsOH (as compared with CsI), the probability is high that the HI once formed will be immediately trapped again by CsOH under back-formation of CsI, reducing the final extent of CsI decomposition. Taking into account this back-reaction, one can assume that total HI formation is governed by the rate of CsOH depletion in the gas flow (caused by retention on the surfaces or by cesium borate formation) during the transport through the pipes of the primary system. Calculations of the progress of CsOH deposition on oxidized stainless steel surfaces and the resulting extent of CsI decomposition under the conditions of a severe accident (Johnson et al., 1989) showed that the final amount of HI formed in the primary system will be small in both high-pressure and low-pressure accident sequences.

Once CsI (as well as CsOH) is deposited on the surfaces of the primary system under high-pressure accident conditions it can potentially revaporize as a consequence of heatup from its radioactive decay and from the system thermohydraulics, which means it would be released to the containment. Usually, it is assumed that the re-released material remains in the form of CsI; however, the question arises of whether or not a fraction of the revaporized CsI is converted to HI. Calculations performed by Kress et al. (1993) showed that at 1000 K even in the absence of H_2 and excess CsOH, only $<3.8\%$ of the CsI was converted to HI under the conditions of different accident sequences. This result demonstrates that revaporization is not likely to produce significant amounts of volatile forms of iodine under such conditions.

Besides the chemical reactions mentioned above, CsI potentially can also be decomposed by radiation-induced reactions, and some earlier investigations indicated significant CsI decomposition in a radiation field under the temperature and environmental conditions to be expected in the primary system during a severe reactor accident. The starting reaction in this context is always the radiolysis of H_2O molecules, leading to oxidizing intermediate products such as the $OH\cdot$ radical which can react subsequently with iodides to form elemental iodine I_2. Calculations have shown that the concentration of such intermediate radiolysis products in the steam flow is small compared with the iodine concentration and, on the other hand, that the major fraction of these products will be scavenged prior to their reaction with iodides by the comparatively high hydrogen concentration in the steam. For these reasons, a significant impact of radiation-induced reactions on the chemical state of the fission product iodine in the primary system is not to be expected. These theoretical conclusions have been confirmed by experimental investigations reported by Wren et al. (1988; 1989). In these tests, CsI in a steam atmosphere at 900 °C was passed through a steel pipe under irradiation by a ^{60}Co source. By analyzing the Cs : I ratio appearing in the effluent, a certain CsI decom-

position was measured; however, the extent of decomposition obviously depended on the contact time in the steel tube rather than on the dose rate in the radiation field applied (up to 0.5 Mrad/h). From these results it was concluded that the observed decomposition was caused by the chemical reactions mentioned above and that the influence of radiation would play a negligible role. Even if radiation-induced reactions were to lead to some decomposition in experiments performed in a steam environment containing CsI exclusively, the excess CsOH present simultaneously in the gas–steam flow during real reactor accidents would compensate for the consequences of radiation-induced decomposition, resulting in a shift of the gas-phase equilibria towards higher CsI stability. It was reported (Torgerson et al., 1986) that under conditions where pure CsI is decomposed by radiation to 15% (1200 K, steam), a tenfold excess of CsOH simultaneously present in the reaction system would reduce radiolytic CsI decomposition to only about 0.3%.

Hydrogen iodide and elemental iodine are both very reactive species which interact readily with a wide variety of materials. In particular, gaseous I_2 as well as HI may react with steel surfaces under formation of non-volatile FeI_2 and, under certain circumstances, of CrI_2, CrI_3, and NiI_2 as well; therefore, the large Inconel/Incoloy surfaces in a PWR steam generator or the large steel surfaces in the upper region of the BWR reactor pressure vessel (moisture separator, steam dryer) may act as an efficient trap for volatile iodine species. The results of these reactions are influenced by a number of parameters such as temperature, iodine concentration, steam and hydrogen content of the gaseous phase, as well as types of steel and the chemical conditions on the steel surface. A review and critical evaluation of the chemical reactions occurring in the system iodine–iron has been recently published by Funke and Hellmann (1994).

Extensive investigations on iodine deposition from the gas phase onto steel surfaces were carried out in the past in the high-temperature reactor (HTR) field; however, since the gas phase in this type of reactor is a dry noble gas atmosphere, these results cannot be applied at all or only in a restricted sense to LWR accident conditions with a flowing gas phase mainly consisting of steam and hydrogen. They will, therefore, not be discussed here. Conditions representative of LWR accidents can be found in the early investigations reported by Genco et al. (1968; 1969); in these experiments the deposition behavior of I_2 and of HI onto stainless steel SS 304 was studied in the temperature ranges 375 K to 820 K and 420 K to 1020 K, respectively, with variation of the steam content in the gas flow between 0 and 95%. The results obtained showed that the oxide layer on the steel surfaces does not prevent iodine reaction with the steel surface; obviously, the volatile iodine species are able to penetrate the oxide layers. Since hydrogen, which is always present in the gas flow, will effect a reduction of I_2 to HI, the HI deposition results are of greater significance for the evaluation of iodine behavior in LWR severe accidents.

These experiments yielded deposition velocities which are of first order with respect to the iodine concentration in the gas phase. Presence of steam in the gas phase resulted in an enhancement of the deposition velocities, in particular in the HI–steel interaction; with increasing temperature the deposition velocity decreased in accordance with an Arrhenius' relationship. The numeric values obtained in

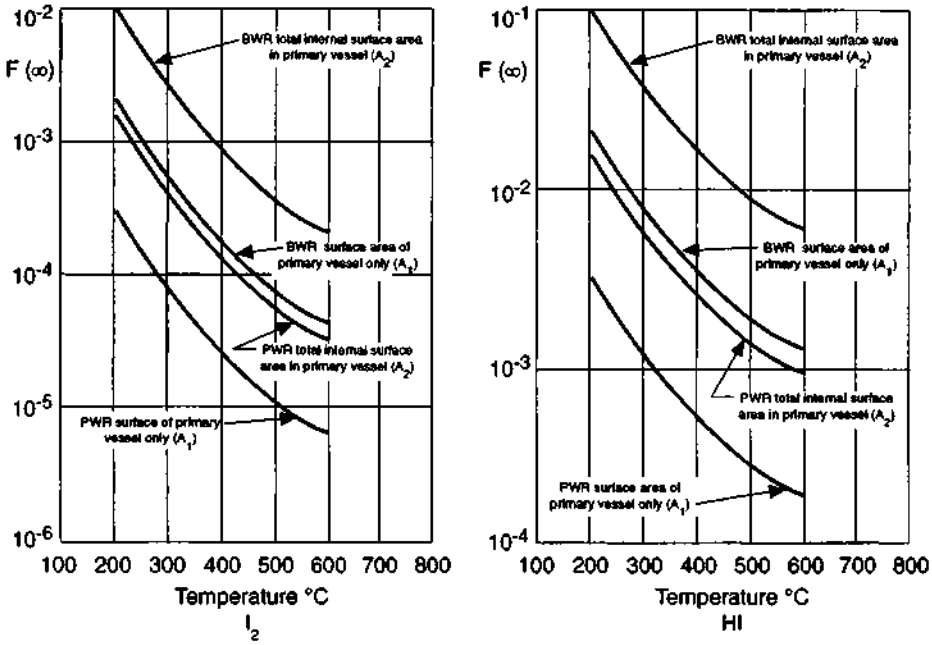

Figure 7.18. Maximum I_2 and HI retention by reaction with steel surfaces in the primary circuit, calculated for different surface areas
(Genco et al., 1969)

these experiments were used by Genco et al. (1969) to calculate iodine retention in the reactor primary system; the retention fractions shown in Fig. 7.18. were obtained using the experimentally obtained values of the deposition velocity as a function of temperature. According to these data, even at the comparatively low temperature of 200 °C only about 1% of the I_2 carried in the gas flow and about 10% of the HI are retained on the surfaces. More recent experiments reported by Abrefah et al. (1994) showed irreversible deposition of I_2 from steam–hydrogen flows onto preoxidized stainless steel surfaces, in particular in the temperature range 200 to 300 °C. The reaction rate proved to be controlled by a surface reaction which proceeds considerably more slowly than the gas-phase mass transfer. The deposited iodine formed islands of iodine-containing compounds, principally associated with iron; no formation of HI was observed in the gas mixture. When the surfaces were covered with aerosols originating from the reactor core (e. g. volatilized control rod material), retention was enhanced by about a factor of 10 (Beard et al., 1988 a). Since the oxides of iron, chromium and nickel are thermodynamically more stable than their iodides, under high-temperature steam conditions the metal oxides would be preferentially formed, leading to revolatilization of the iodine from the initially formed iodides (according to Bowsher, 1987). Thus, reactions of I_2 and HI with the structural surfaces are not expected to result in a significant retention of fission product iodine in the primary system. However,

since the revolatilized iodine is in the form of HI, the small fraction of I_2 potentially entering the primary system would be further reduced by this reaction.

As was discussed in the preceding sections, volatile fission product species such as CsOH may be trapped by aerosols, so that their transport behavior in the primary system is dictated by that of the aerosols. Likewise, gaseous I_2 as well as HI and CsI can react with aerosols present in the steam flow. Different experiments have been carried out to study these effects, since the amount of gaseous iodine species which would be present later on in the containment atmosphere may be significantly affected by such reactions. In this context, the aerosols formed from the volatilized constituents of the control rod materials are of particular interest due to their relatively large mass and since silver as well as indium and cadmium are able to form stable iodides. In the experiments reported by Beard et al. (1988 a), control rod segments (alloy 80% Ag, 15% In, 5% Cd encapsulated in stainless steel SS 304 cladding) were heated to 1670 K to produce aerosols which deposited onto steel coupons at temperatures below 310 K. These coupons then were exposed to I_2 vapor in Ar or Ar–H_2O (10 to 30%) atmospheres at temperatures in the range 370 to 670 K. The results of these experiments showed that the I_2 deposition rate constant is significantly increased by the presence of steam in the gas flow, which is consistent with the results reported by Genco et al. (1969) on I_2 deposition onto steel surfaces. However, the total deposition rate of I_2 onto surfaces coated with control rod aerosol (about 1 g/m^2) proved to be higher by about a factor of 10 than on pure preoxidized steel surfaces, due to the greater specific surface area but also due to additional chemical reactions (e. g. with deposited silver and cadmium). In H_2O–Ar atmospheres at temperatures in excess of 470 K, CdO is formed; in the presence of I_2, however, CdI is preferentially formed, due to its formation energy, which is more negative than that of CdO. On pure steel surfaces, iodides of iron and nickel are formed but at a considerably lower rate (about an order of magnitude) than the reaction with the cadmium aerosol.

In a dynamic system, one has to take into account that the concentration of aerosols originating from the control rod materials in the gas–steam flow is not constant over time. Experiments reported by Beard et al. (1988 b) showed that the initial burst release upon failure of the claddings at about 1700 K produced an aerosol density (mainly cadmium) higher by about two orders of magnitude than the subsequent diffusional release.

Vapor–aerosol interactions which are assumed to take place in the primary system were studied in detail in the British FALCON test facility. This facility, which is schematically shown in Fig. 7.19. (according to Beard et al., 1991), has been specifically designed to investigate the transport and deposition behavior of fission products under severe accident conditions. To produce representative aerosols, fuel pellets containing simulant fission products as well as trace-irradiated fuel pellets, both cladded in Zircaloy, were heated up to 2000 K in a steam–helium atmosphere in the presence of bulk-core materials. Fission product transport could be studied along a pathway which was designed to represent the upper plenum, hot-leg structures and containment. Considerable efforts were made to ensure that, as far as possible, the thermal-hydraulic conditions represented those of a selected accident.

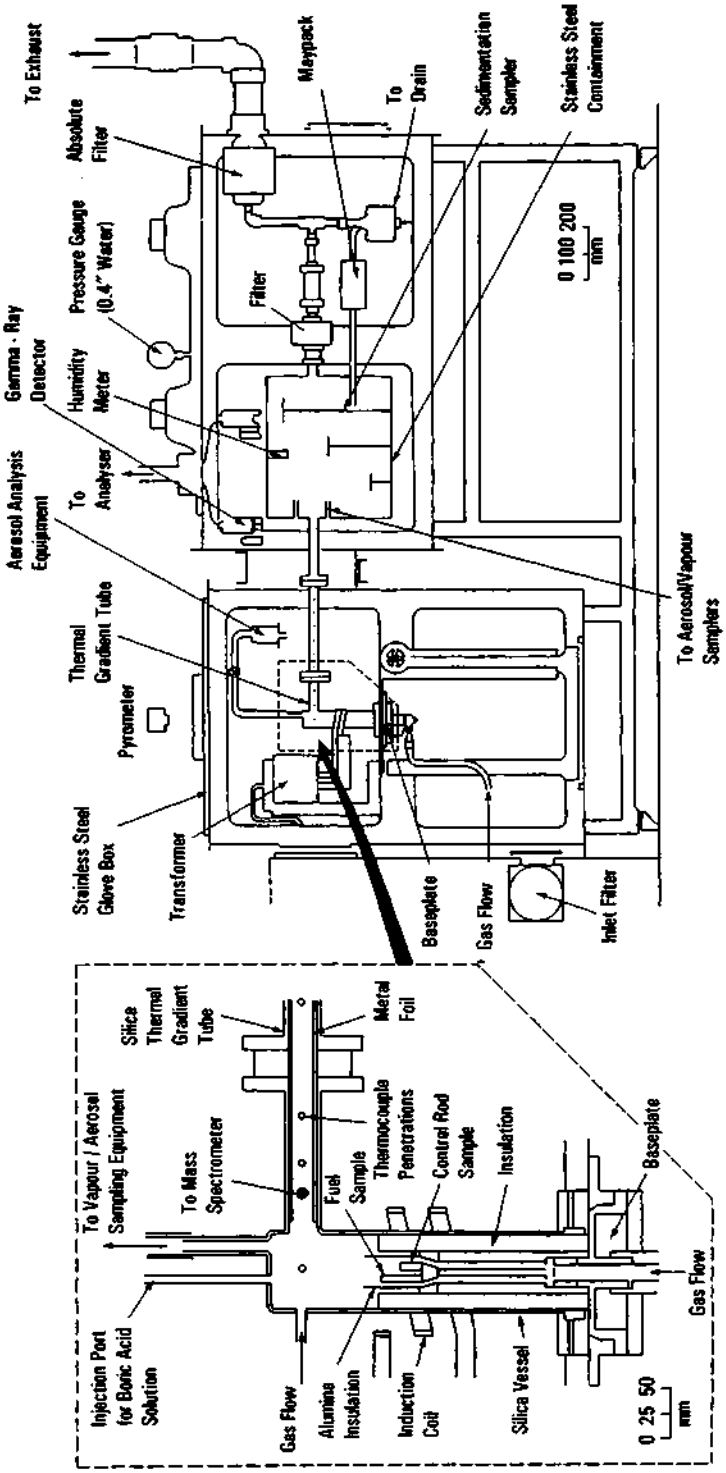

Figure 7.19. FALCON test facility for investigation of fission product aerosol interactions (schematic) (Beard et al., 1991)

A broad variety of analytical techniques was applied to characterize the different chemical species and to quantify the vapors and aerosols released from the UO_2 fuel and other sources.

In general, the results of these tests showed that significant interaction occurred between the fission product vapors and bulk material aerosols. The aerosol particles released from the fuel rod specimens as well as from the control rod specimens acted as centers for nucleation of the fission product vapors and induced sorption of fission products as well. Likewise, chemical reactions were observed between control rod aerosols and fission product vapors (e. g. formation of CdTe and CdI_2). In addition, the results demonstrated that the concentration of fission products in the vapor is the determining parameter as regards the dominant interaction mechanism. At high concentrations (represented by simulant fuel specimens), chemical reaction and vapor condensation are the dominant mechanisms, whereas at low concentrations (represented by trace-irradiated fuel specimens) sorption phenomena predominate.

According to Beard and Benson (1989), in experiments in which trace-irradiated UO_2 was heated to about 2000 K, the vaporized ^{131}I showed another deposition behavior in the presence of PWR control rod material than in the absence of this material; whereas in the latter case iodine was plated out in the temperature range below 400 K, in the presence of the control rod material its deposition range was virtually identical with that of indium and cadmium (500 to 600 K). This behavior probably is not the consequence of chemical reactions between iodine and the aerosols; it can be assumed that sorption of the very small iodine concentrations volatilized from the trace-irradiated fuel (which are by far below the adsorption capacity of the surfaces of the aerosols present) is the responsible mechanism.

Experiments performed by Henshaw et al. (1991) as well as the results reported by Bowsher et al. (1991) on the reactions of gaseous I_2 with aerosols of MnO, Ag and Cd demonstrated the generally valid fact that formation of a compound can only be expected in the case of a negative Gibbs' energy; thus, no chemical reaction will take place between I_2 and MnO. In the I_2–metal systems, two different mechanisms were observed, showing a linear rate when gas phase mass transfer was the controlling parameter, and a parabolic rate when diffusion through the newly formed product layer controlled the progress of the reaction. In simple cases, the rate constants show an Arrhenius' dependence on temperature, but more often a complex behavior is observed. For example, in the system I_2–Ag an increase of the reaction rate with temperature starts at temperatures above 140 °C, probably caused by variations in the charge-carrier species, as well as in the concentration of lattice defects. In the systems I_2–Cd and I_2–Ag, linear reaction kinetics was only observed when the experimental temperature was higher than the melting point either of the substrate (Cd 321 °C) or of the reaction product (AgI 552 °C), i. e. when the rate-limiting mechanisms were mass transfer of iodine molecules from the gas phase. The same applies in the case of slow gas-phase mass transfer due to low flow rates or to low concentrations of the gaseous species; in all other cases parabolic rates were observed. In general, the mechanism of interaction between gaseous species and aerosols is assumed to be quite similar to that of the oxidation of metals. With thicknesses of the layers of the reaction products of more

than about 100 Å, a linear or parabolic dependence of the reaction rates on time was observed (i. e. in these cases the reaction rate is limited by a diffusion process through the reaction product), whereas at thinner layers a logarithmic function was occasionally found, especially at low temperatures. In particular, the AgI formation shows a steep increase of the rate constant at temperatures beyond the $\alpha-\beta$ transition point of AgI.

The possible condensation of CsI onto cadmium aerosols may be an important mechanism for transport and/or attenuation, but no chemical reaction between these two partners is to be expected; Beard et al. (1988 b) found only evidence at a microscopic level for a limited chemical reaction at the Cd–CsI interface.

Under accident conditions one has to take into account possible competition in the formation of the iodides of hydrogen, cesium, silver, indium and cadmium. According to thermochemical calculations which were performed by Cordfunke and Konings (1993) for both CsI and HI as iodine-bearing species in the multicomponent/multiphase system Cs–I–Te–Ag–In–Cd–O–H, CsI is stable up to 1000 K, above which temperature its proportion decreases in favor of the stability of InI which becomes the predominant vapor species at temperatures up to 1700 K; likewise, at temperatures above 1500 K the proportions of HI, AgI and CdI in the mixture increase. However, if HI is the initial species by which iodine is being transported, the speciation is quite different below 1000 K, where the formation of gaseous CdI_2 would predominate. Above this temperature the stability of this compound rapidly decreases in favor of gaseous InI, and the same equilibrium will be approached as in the case of CsI. These calculations show that the speciation of iodine is quite different below 1000 K, depending upon whether iodine is transported as CsI or as HI in the steam–hydrogen gas flow. In this respect, the availability of boron in the primary system is of great significance since the decomposition of CsI to form cesium borate may lead to the formation of HI.

It has been widely discussed whether or not in a steam atmosphere at high temperature and in the additional presence of an excess of cesium hydroxide, iodine can react with gaseous silver to form AgI. This question is of considerable interest since AgI is highly insoluble in water and the fraction of iodine which is tied up in this compound would be able to participate neither in the iodine partition equilibrium between sump water and containment atmosphere nor in the iodine reactions with the wall materials. According to the thermodynamic calculations of Hahn and Ache (1984), AgI is the most stable compound in a mixture with an Ag : Cs : I ratio of 100 : 10 : 1 (all components in gaseous form) at temperatures below 1500 °C. When the concentration ratios change towards a smaller excess of silver, the stability region of CsI increases and the region of thermodynamic stability of AgI is shifted towards lower temperatures. Beyond about 1700 °C, only HI and I° are the stable species in a mixture containing H_2O, H_2, I, Cs, and Ag. The SASCHA experiments (Albrecht, 1987) confirmed that during heating of UO_2 doped with CsI and metallic silver to 1500–2000 °C in a steam atmosphere, a part of the volatilized iodine was recovered as a water-insoluble compound which it was possible to dissolve in $Na_2S_2O_3$ solution, suggesting the presence of AgI. Thus, although systematic investigations are still lacking, there is at least a qualitative agreement between thermodynamic calculations and experimental results. On the

other hand, the results obtained in this field by different investigators are apparently not consistent. Sallach et al. (1986) found cesium iodide vapor to be stable in the presence of silver at temperatures below 1220 K. Cordfunke and Konings (1993) have mentioned that simple thermodynamic calculations concerning the reactions between the iodine compounds and silver would show that CsI is thermodynamically stable, but that HI would react with silver to form AgI. According to the results reported by Moers (1986), gaseous I_2 is adsorbed onto a clean metallic silver surface at a linear deposition rate up to about one half of an AgI monolayer, with chemisorption being the responsible mechanism. With larger deposited amounts, iodine atoms are chemically bound after dissociation of the primary I_2 molecules, resulting in an AgI lattice being formed on the metallic substrate as a homogeneous and dense surface layer. Further growth of this layer satisfies a parabolic law depending on the square root of the I_2 partial pressure. Apparently, cation (Ag^+) diffusion through the AgI layer is the rate-controlling step.

In general, it can be assumed that the reaction between silver and iodine species in the gas phase, as well as the reaction of iodine vapor with silver aerosol or with silver deposited on the primary circuit surfaces, is only of minor significance for iodine behavior in the course of a severe accident. The main reasons are the rather short residence time of the silver aerosols in the gas phase, the fact that iodine and silver volatilization from the reactor core may differ considerably over time and, finally, the small proportion of elemental I_2 and of HI (compared with the CsI fraction) assumed to be present in the gas phase during transport through the primary circuit. In contrast, AgI formation is expected to proceed to a significant extent later on in the containment sump water (see Section 7.3.3.3.3.).

Summarizing the results just discussed, it can be concluded that chemical reactions occurring in the primary system do not act as a significant additional source of elemental I_2 or HI in the gas flow. On the contrary, when small fractions of these highly volatile species escape from the reactor pressure vessel or are generated by secondary reactions, they will be largely converted to less volatile iodides, either by reaction with the primary circuit surfaces or by reactions with the aerosols. In the high-pressure sequences with long pathways in the primary system, a fraction of the iodides can be assumed to be retained in the pipes due to condensation in regions showing temperatures below 500 °C; the magnitude of this fraction depends greatly on the particular accident sequence in question.

7.3.2.3.3 Tellurium

Tellurium exhibits a chemical behavior which is nearly as complex as that of iodine, but only little is known about its reactions under the conditions prevailing in the primary system during the course of a severe reactor accident. As was discussed in Section 7.3.1.1., the formation of temperature-stable Zr-Te compounds retains tellurium for a certain period of time and results in a significant release from the reactor core only after extensive oxidation of the Zircaloy cladding. According to

Collins et al. (1987), the main tellurium compound volatilized from the oxidized Zircaloy is SnTe; another potential species is elemental Te_2.

Thermodynamic analyses of the I–Cs–Te system in the PWR primary circuit under severe accident conditions suggest that Te and Te_2 are the most important tellurium species for neutral and reducing steam conditions (Garisto, 1986). Beyond 1400 K, Te_2 decomposes partially in steam, and TeO and Te can become the predominant species for neutral and reducing steam conditions, respectively; under typical severe accident conditions (i. e. a steam–hydrogen atmosphere), the monoxide TeO was calculated to account for less than 0.1% of the tellurium species at 1700 K (Bowsher et al., 1986; Bowsher, 1987). Beahm (1987) obtained similar results by thermodynamic calculations, according to which the conditions inside the primary circuit, in particular the $H_2 : H_2O$ ratios, would be unfavorable for the formation of tellurium oxide and hydroxide species. Thus, with a high degree of probability, one has to assume the presence of Te_2 in the gaseous phase, although under certain circumstances the formation of CsTe may also take place. In laboratory experiments in which tellurium was injected into a superheated steam–hydrogen flow and passed through a stainless steel duct on which a temperature gradient was imposed (1000 to 200 °C), it was partly deposited well above its condensation temperature, indicating that gaseous tellurium (probably Te_2) chemically reacts with the surface at a rate which is limited by the rate of mass transfer. When CsOH was simultaneously present in the steam flow, a Cs–Te compound was formed (probably Cs_2TeO_3) as a result of a gas-phase reaction between tellurium and CsOH in the steam (Johnson et al., 1986; 1989). This tellurite is less volatile than TeO_2, Te or CsOH and, hence, its formation would be able to reduce the rate of revolatilization of tellurium and cesium from the surfaces of the primary system, as these would heat up in the further course of the accident.

Under reducing steam conditions, particularly at temperatures above 770 K with large H_2 : Te ratios, hydrogen telluride H_2Te may become an important tellurium species (Garisto, 1986). This highly volatile compound is very soluble in water, giving HTe^- and Te^{2-} ions. It would, therefore, be plated out into liquid water if the gas phase contacted water on its way. H_2Te (similar to tellurium vapor) reacts rapidly with stainless steel surfaces; the reaction is not significantly affected by competing oxidation effects up to 1470 K. Iron tellurides are the dominant initial product because iron is the major component of stainless steels; on a longer time-scale, however, the formation of the thermodynamically more stable chromium and nickel tellurides would be favored. These metal tellurides are thermally stable, but on exposure to high-temperature and high-pressure steam they may decompose to form hydrogen telluride and the corresponding metal oxides (Bowsher, 1987).

In principle, tellurium deposition on stainless steel in the primary system would largely prevent this element from being released to the containment. However, tellurium vapor could react chemically with a variety of metallic aerosols to form tellurides; in particular it has a high affinity for silver and cadmium, as well as for tin volatilized from the Zircaloy claddings. Thus, tellurium transport through the primary system would be primarily controlled by aerosol transport characteristics. Spence and Wright (1987) have calculated that inclusion of these processes of depo-

sition onto aerosols into the transport models would increase considerably the tellurium source term from the primary circuit to the containment for the so-called AB sequence (according to WASH-1400). However, according to Beard et al. (1988 b), cadmium telluride is unstable in the vapor phase and decomposes to release elemental cadmium and tellurium. Simple sorption processes of tellurium onto the metal aerosols are believed to be of secondary importance; condensation and chemical reaction will dominate the interactions between the aerosols and vapor species. Between tellurium vapor and boric acid aerosols only physisorption processes are expected. According to Harman and Clough (1992), the deposition of tellurium onto aerosol particles should play a minor role compared with its deposition onto the surfaces of the structural materials of the primary system. Nonetheless, it can be expected that the distribution of tellurium between aerosols and structural surfaces will strongly depend on the conditions prevailing in the specific accident sequence.

The radioactive tellurium isotopes decay to their isobaric iodine daughter products. This means that from each location where tellurium deposits have formed, radioactive iodine isotopes will be released to the steam flow. However, the magnitude of these iodine sources can be assumed to be small compared to the direct volatilization of iodine from the fuel. Thus, they can usually be ignored when evaluating iodine input into the containment, with the only exception possibly being the short-lived ^{132}I.

7.3.2.4 Radionuclide retention in BWR pressure suppression pools

In almost all accident sequences, fission products originating from a degrading reactor core and then released from a BWR primary system must pass through the pressure suppression pool before reaching the containment (drywell). Originally, the pressure suppression pool was designed to condense the steam entering the drywell in the course of a loss-of-coolant accident and, thus, to reduce the thermal and pressure loadings to the containment. Although this pool is not especially designed to remove fission products from the gas–steam flow, some scrubbing of contaminants from the gas–steam mixture entering the pool can be expected, supported by the large gas–liquid interface provided by the bubbles before they reach the surface of the pool. For a number of years the retention effectiveness of such a pool was inadequately taken into account in source term calculations; thus, in WASH-1400 a decontamination factor of 100 for aerosols injected into subcooled water pools was assumed, but no credit was given to the retention of fission products in the pressure suppression pool when it was thermally saturated. Since then, efforts have been undertaken to study in more detail the processes occurring in the pressure suppression pool, to determine its retention effectiveness under the conditions of an accident and to develop computer codes which quantitatively describe the processes taking place in the pool (see the review paper of Ramsdale

et al., 1992). These studies suggest that the scrubbing process might be significantly more effective for attenuating aerosols than was originally assumed; they also demonstrate, however, that the decontamination factors are highly sensitive to prevailing conditions.

The retention of fission products by scrubbing the steam flow in a BWR pressure suppression pool is based on the exchange of matter between gas and liquid phases. Similar scrubbing processes are also at work in other accident situations, such as in a PWR steam generator tube rupture event (see Section 6.2.3.), as well as in the Venturi scrubbing process during controlled depressurization of the containment after a core melt accident (see Section 7.3.4.4.).

A pressure suppression pool is a passive engineered safety feature. Such a pool essentially consists of a large chamber which is partly filled with water; in some designs it contains about 4000 m^3 of water. Fission products volatilized from the degrading reactor core are carried by a gas–steam mixture into the suppression pool through pipes that are submerged in the water, ending in spargers of different designs depending on the manufacturer of the plant. The thermal-hydraulic phenomena occurring in the water pool can be shortly described as follows (Paul et al., 1984): In the injection zone, significant scrubbing of the radioactive aerosols takes place during the impaction of the gas stream against the relatively stagnant liquid in the pool, resulting in a vigorous gas jet action with the water. This injection zone is characterized by the formation of large, hydrodynamically unstable vapor globules. In the subsequent vapor globule breakup zone, the initially unstable globules break up into smaller bubbles; typically, this complete breakup occurs within about 10 initial globule diameters from the injector outlet. Finally, in the bubble rise zone, the size distribution of the bubbles remains nearly constant as they rise in the water pool. Bubble growth in the water pool, occurring as a consequence of changes in hydrostatic pressure with pool depth, is compensated for by continued break up of larger bubbles. The bubble swarm rises to the pool surface in several seconds depending on the inlet flow rate of non-condensible gases and the pool depth. In the initial stage of the accident, when the pool water is markedly cooler than the incoming steam–gas mixture, most of the steam is condensed before the vapor globule has completely broken up into small bubbles. Later on, when the pool is thermally saturated, no further massive steam condensation will occur, although exchange of matter between the two phases will continue to take place. Even in a thermally saturated deep pool, some steam condensation may occur near the injector orifice, as a consequence of the subcooled condition of the pool water at the injection depth due to hydrostatic pressure.

While a typical steam sparger may contain hundreds of holes for gas injection, most of the basic investigations were conducted using single-hole devices. Such a procedure seems to be justified since in the bubble rise zone the bubble size distribution is well represented by a log-normal frequency function and, consequently, the gas–liquid hydrodynamics may be represented using a single average bubble model. Out of the number of experiments performed on pool scrubbing, only a few will be discussed below. Because of the strong dependence of the resulting decontamination factor on different parameters, the quantitative results obtained

in the individual experiments strictly apply only for the configuration used in a specific experiment.

Aerosol particles which are transported by the gas–steam flow will be trapped in the water phase when the particle strikes the gas–liquid interface. The mechanisms which contribute to the removal of aerosol particles from the gas bubbles scrubbed in a water pool include gravitational settling, inertia of particle motion, and Brownian diffusion. Inertial impaction occurs because the gases circulate within the rising bubbles and large aerosol particles (> 0.5 μm) cannot follow the stream lines of the gas flow; in addition, particles larger than about 1 μm will be affected by gravitational settling. Diffusion significantly affects only very small particles of a size < 0.1 μm; in the case of submicron particles present in condensible gas bubbles, thermophoresis and diffusiophoresis may also contribute to the scrubbing effect. Thus, the combined effect of all the possible phenomena on the decontamination effectiveness in the pool is a complicated function of several parameters including temperature, the non-condensible fraction in the gas–steam mixture, fluid dynamic parameters and the sizes of the bubble and the aerosol particles.

The decontamination factor of the aerosol particles in the pool depends strongly on the particle size, decreasing with decreasing size until it reaches a minimum at about 0.2 μm diameter, when it increases again with further decreasing particle size. At larger sizes, inertia and sedimentation are the dominant mechanisms, the efficiency of which decreases with decreasing particle size; for very small particles sizes, Brownian diffusion acquires increasing significance, resulting in increasing decontamination factors with further decreasing particle sizes (Marble et al., 1982, according to Ramsdale et al., 1992). Condensation of steam onto aerosol particles during the time they are enclosed in the bubbles will enhance their removal from the bubbles by sedimentation and inertial processes. This effect is especially important for water-soluble aerosols such as CsI and CsOH. When the carrier gas contains both steam and non-condensible gas, discharge into a water pool can cause particle removal by rapid steam condensation. This phenomenon is independent of the subsequent scrubbing mechanisms and may yield an enhancement factor of considerable magnitude.

In addition to the particle size, several other parameters may influence the decontamination factors of aerosol particles in the pool. An important parameter is the submergence depth of the vents in the water pool. For a constant rise velocity, the bubble residence time in a water pool is directly proportional to the submergence depth; a longer residence time means a higher probability that particles in the bubble will come into contact with the gas–liquid interface. As a result, the decontamination factor can be expected to show an exponential dependence on the submergence depth, indicating a first-order rate process. The GE experiments performed with Eu_2O_3 (particle diameter in the range 0.1 to 1 μm) as an insoluble test substance and CsI (particle diameter 0.3 μm) as a soluble aerosol (Marble, 1983) have demonstrated this relationship very clearly. Higher gas and water temperatures or larger temperature differences between the gas and the water phase may promote particle scrubbing because of enhanced diffusion velocities or of thermophoresis effects. On the other hand, the bubble size shows but little effect

on the decontamination factor. A possible explanation is that the bubble shape for the larger bubbles (> 0.5 cm) is elliptical rather than spherical; this means that the distance between particles in the bubble and the gas–liquid interface increases much slower than linearily with increasing bubble size. Likewise, the concentration of the particles in the bubbles is of only minor relevance for the decontamination factor.

In the EPRI experiments CsI, TeO_2 (0.4 μm diameter) and Sn aerosols (~3 μm diameter) were injected into the water phase of a scrubbing tank of 1.8 meters in diameter and 2.6 meters in height through a horizontally oriented 1.27 cm orifice (Cunnane et al., 1984). The results confirmed that the parameters which dominate the behavior of an ambient temperature pool are aerosol particle size and the steam mass fraction in the carrier gas, with the effect of the latter on the decontamination factor being particularly evident for the CsI and TeO_2 aerosols; it proved to be less pronounced for the Sn aerosol because, owing to its large particle size, the decontamination factors are already very large without the presence of steam fractions in the carrier gas. The decontamination factors in a hot pool were also high, although the effect of the steam mass fraction at higher temperatures was less pronounced than that observed in the ambient temperature pool tests. Generally, small decontamination factors only occur when the steam mass fraction is low and the particle size is in the 0.4 μm range.

From the Marviken large-scale aerosol tests (see Section 7.3.2.2.) it was reported that the aerosols remaining after passage of the simulated primary system were retained to at least 99% in the water-filled scrubber located at the back end of the test facility at a submergence depth of about 1 meter (Rahn et al., 1988).

In the framework of the Advanced Containment Experiments (ACE) program, several tests on the retention of radionuclides in a pressure suppression pool were also conducted (McCormack et al., 1989). These experiments were carried out in a comparatively large vessel (diameter 1.5 meters, height 6.1 meters); the aerosols consisting of MnO, CsOH and CsI carried in a 140 to 150 °C gas flow with varying steam fractions (0.012 to 0.41) were injected into the water volume by means of a multi-orifice sparger. The particle sizes of the aerosols were on the order of 2 μm, while in additional tests the retention behavior of DOP (di-octyl phthalate) aerosols with a particle size of about 0.6 μm was investigated. The aerosol concentration in the gas flow was typically on the order of 5 to 10 g/m^3; about one-half of the aerosol mass consisted of MnO, the other half of CsOH; the CsI fraction in the aerosol mixture was adjusted to a concentration corresponding to a Cs : I ratio of 10 : 1 in the total aerosol. The results measured in these tests are summarized in Table 7.12. (according to Ramsdale et al., 1992). In general, a marked reduction in the average size of the aerosol particles was observed when they passed through the pool, an effect which is expected since the scrubber removes larger aerosol particles more efficiently than smaller ones. As can be seen from Table 7.12., the measured decontamination factors were higher in the tests with a higher steam fraction and a deeper submergence of the sparger. The higher temperature of the pool water used in some of the tests obviously did not adversely affect the retention of the aerosols, though firm conclusions were difficult to draw due to the simultaneous variation of other parameters. The decontamination factors for the water-

Table 7.12. Results of the ACE pool scrubbing tests (according to Ramsdale et al., 1992; by courtesy of the European Communities)

Test	Temperature pool, °C	Submergence sparger, m	Substance	Decontamination factor
1	26	1.38	Cs	145–160
steam fraction			Mn	11–33
0.012*			I	47–80
2	24	4.52	Cs	840–2000
steam fraction			Mn	260–high
0.185*			I	1500–high
3	82	2.62	Cs	320–330
steam fraction			Mn	75–140
0.013*			I	180–220
4	83	4.61	Cs	3000
steam fraction			Mn	180–220
0.41*			I	1300–2600

*) by volume

soluble elements cesium and iodine were considerably higher than for the non-soluble MnO, probably due to a better wetting of their compounds. On the other hand, these differences in the decontamination factors indicate that the three materials were present, at least in part, as separate particles. Special tests have confirmed that re-entrainment of aerosols from the pool was insignificant and would not significantly affect the decontamination factors cited in Table 7.12. Additional tests using DOP as a test medium showed significantly lower decontamination factors for these very fine aerosol particles than for the larger mixed aerosol particles mentioned above. Decontamination factors calculated with the SPARC code (Owczarski and Burk, 1991) showed satisfying agreement with the results of the large-scale experiments performed in the context of the Advanced Containment Experiments (ACE).

From these results it can be concluded that fission product iodine reaching the pressure suppression pool in the chemical form of CsI will be retained in the water phase to an extent which is virtually identical with that of the aerosols. Small fractions of HI and I_2 potentially entering the pool in gaseous form are also readily absorbed; at higher water temperatures in particular, diffusion of these molecules to the bubble–liquid interface is very fast so that similar scrubbing efficiencies as for the aerosols can be assumed for these gases. While HI dissociates readily in the water phase to non-volatile I^-, the I_2 molecule undergoes hydrolysis, initially forming I^- and HOI. Organic iodides, as far as they are present at all in the gas–steam flow, are only weakly retained in the pool water volume, provided they are not decomposed by hydrolytic or radiation-induced reactions upon contact with the pool water phase.

The behavior of elemental iodine in the scrubbing process has been studied in the POSEIDON experiments (Güntay, 1990) where I_2 vapor in N_2 as a carrier gas was introduced into a water pool in which it was possible to vary the submergence of the orifice assembly between 1 and 4 meters and the pool temperature was varied between 21 and 60 °C. The results showed that smaller orifices yielded higher decontamination factors (e. g. 10^5 for 0.5 mm and 3 m submergence; 10^3 for 9 mm and the same submergence), because of the larger surface-to-volume ratio. The decontamination factor also increased with increasing submergence (e. g. 10^2 for 1 mm orifice and 1 m submergence; $\sim 10^5$ for the same orifice and 3 m submergence), demonstrating the effect of longer contact time of the bubbles with the water at greater submergences and the resulting enhanced diffusion of the I_2 molecules to the gas–liquid interface. At 60 °C pool temperature, the decontamination factor was determined to be higher by about one order of magnitude than at 40 °C. However, as in other experiments, it was not possible to determine with a high degree of certainty whether the increases in the decontamination factors were due to the increase in pool temperature.

The decontamination factors mentioned above may be affected over time by mechanisms which lead to a revolatilization of fission products from the pool water. When the bubbles break up at the pool surface, they produce new aerosol droplets by which non-volatile fission products can be carried to the containment atmosphere. Calculations using the SPARC code (Owczarski and Burk, 1991), however, showed that radionuclide entrainment caused by this mechanism is very small and, thus, can be ignored in source term analyses. Iodine, on the other hand, can be revolatilized if the pH of the aqueous phase is decreased as a consequence of water radiolysis. In the presence of alkalizing substances such as CsOH, such a decrease in pH leading to a lower I_2 partition coefficient is not to be expected. The existing codes (such as SPARC, SUPRA, BUSCA) do not take chemical reactions into consideration and, thus, do not provide any information on chemical iodine revolatilization from the pool.

According to calculations with the SUPRA code (Wassel et al., 1984), condensation of steam in the compartment above the pool can additionally result in high system decontamination factors. Calculations showed that for hot pools the system decontamination factor would be higher by about a factor of 10 than that of the pool itself.

References Section 7.3.2

Abrefah, J., de Abreu, H. F. G., Tehranian, F., Kim, Y. S., Olander, D. R.: Interaction of iodine with preoxidized stainless steel. Nucl. Technology **105**, 137–144 (1994)

Albrecht, H.: Results of the SASCHA program on fission product release under core melting conditions. Radiochim. Acta **41**, 133–140 (1987)

Ball, R. G. J., Bowsher, B. R., Cordfunke, E. H. P., Dickinson, S., Konings, R. J. M.: Thermochemistry of selected fission product compounds. J. Nucl. Materials **201**, 81–91 (1993)

Beahm, E. C.: Tellurium behavior in containment under light water reactor accident conditions. Nucl. Technology **78**, 295–302 (1987)

Beard, A. M., Bennett, P. J., Bowsher, B. R., Nichols, A. L., Sabathier, F.: Iodine chemistry in FALCON. in: Ishigure, K., Saeki, M., Soda, K., Sugimoto, J. (editors): Proc. 3. CSNI Workshop on Iodine Chemistry in Reactor Safety, Tokai-mura, Japan, 1991; Report JAERI–M 92–012 (1992), p. 311–324

Beard, A. M., Benson, C. G.: Fission product vapour – aerosol interactions in the containment: Trace-irradiated fuel studies. Report AEEW-R 2472 (1989)

Beard, A. M., Benson, C. G., Bowsher, B. R., Dickinson, S., Nichols, A. L.: Fission product and aerosol behaviour within the containment. Report AEEW-R 2474 (1989)

Beard, A. M., Bowsher, B. R., Nichols, A. L. (a): Interaction of molecular iodine vapour with silver–indium–cadmium control rod aerosol. Proc. Internat. Symposium Severe Accidents in Nuclear Power Plants, Sorrento, Ital., 1988; IAEA-SM-298/108, Vol. 2, p. 201–213

Beard, A. M., Benson, C. G., Bowsher, B. R. (b): The interaction of simulant fission product vapours with control rod aerosols in a flowing system. Report AEEW-R 2470 (1988)

Benson, C. G., Bowsher, B. R.: Physical resuspension and revaporisation phenomena in control rod aerosols. Report AEEW-R 2427 (1988)

Bowsher, B. R.: Fission-product chemistry and aerosol behaviour in the primary circuit of a pressurized water reactor under severe accident conditions. Progress in Nuclear Energy **20**, 199–233 (1987)

Bowsher, B. R., Dickinson, S.: The interaction of caesium hydroxide vapour with iron and ferric oxide (Fe_2O_3) powders at 760 °C. Report AEEW-M 2262 (1985)

Bowsher, B. R., Dickinson, S.: The interaction of caesium iodide with boric acid: Vapour phase and vapour–condensed phase reactions. Report AEEW-R 2102 (1986)

Bowsher, B. R., Dickinson, S., Nichols, A. L., Gomme, R. A., Ogden, J. S., Young, N. A.: Chemical forms of fission product tellurium in a severe reactor accident. Proc. Symposium on Chemical Phenomena Associated with Radioactivity Releases During Severe Nuclear Plant Accidents, Anaheim, Calif., 1986; Report NUREG/CP-0078 (1987), p. 3/93–105

Bowsher, B. R., Henshaw, J. G., Newland, M. S.: The kinetics of reaction between iodine vapour and bulk-material aerosols. Proc. 3. CSNI Workshop on Iodine Chemistry in Reactor Safety, Tokai-mura, Japan, 1991; Report JAERI–M 92–012 (1992), p. 165–180

Bowsher, B. R., Nichols, A. L.: High-temperature studies of simulant fission products. Part IV: Interaction of caesium iodide with boric acid over the temperature range 400 to 1000 °C. Report AEEW-R 1973 (1985)

Castleman, A. W. jr., Tang, I. N., Munkelwitz, H. R.: The chemical states of fission product iodine emanating into a high temperature aqueous environment. J. Inorg. Nucl. Chemistry **30**, 5–13 (1968)

Collins, J. L., Osborne, M. F., Lorenz, R. A.: Fission product tellurium release behavior under severe light water reactor accident conditions. Nucl. Technology **77**, 18–31 (1987)

Cordfunke, E. H. P., Konings, R. J. M.: The release of fission products from degraded UO_2 fuel: Thermochemical aspects. J. Nucl. Materials **201**, 57–69 (1993)

Cronenberg, A. W., Osetek, D. J.: Reaction kinetics of iodine and cesium in steam/hydrogen mixtures. Nucl. Technology **81**, 347–359 (1988)

Cubicciotti, D., Sehgal, B. R.: Vapor transport of fission products in postulated severe light water reactor accidents. Nucl. Technology **65**, 266–291 (1984)

Cummings, J. C., Elrick, R. M., Sallach, R. A.: Status report on the fission product research program. Report NUREG/CR-1820 (1982)

Cunnane, J. C., Kuhlman, M. R., Oehlberg, R. N.: The scrubbing of fission product aerosols in LWR water pools under severe accident conditions – Experimental results. Proc. American Nuclear Society Meeting on Fission Product Behavior and Source Term Research, Snowbird, Utah, USA, 1984; Report EPRI NP-4113-SR (1985), p. 31/1–16

Elrick, R. M., Merill, R. M., Ouellette, A. L.: The thermal instability of cesium iodide. Report NUREG/CR-5155 (1989)

Elrick, R. M., Sallach, R. A.: Importance of environment on high temperature reactor accident chemistry. Proc. Symposium on Chemical Phenomena Associated with Radioactivity Releases During Severe Nuclear Plant Accidents, Anaheim, Calif., 1986; Report NUREG/CP-0078 (1987), p. 3/19–36

Elrick, R. M., Sallach, R. A., Ouellette, A. L., Douglas, S. C.: Reaction between cesium iodine compounds and the reactor materials 304 stainless steel, Inconel-600, and silver. Vol. 1: Cesium hydroxide reactions. Report NUREG/CR-3179, Vol. 1, (1984)

Elrick, R. M., Sallach, R. A., Ouellette, A. L., Douglas, S. C.: Boron carbide–steam reactions with cesium hydroxide and cesium iodide at 1270 K in an Inconel-600 system. Report NUREG/CR- 4963 (1987)

Funke, F., Hellmann, S.: Reaction of iodine with steel surfaces. Final Report–Part 1: Literature study. Report EUR 15668/1 EN (1994)

Garisto, F.: Thermodynamic behaviour of fission products at high temperatures: Ruthenium and tellurium. Proc. Symposium on Chemical Phenomena Associated with Radioactivity Releases During Severe Nuclear Plant Accidents. Anaheim, Calif., USA, 1986; Report NUREG/CP-0078, p. 3/107–118

Genco, J. M., Berry, W. E., Rosenberg, H. S., Morrison, D. L.: Fission product deposition and its enhancement under reactor accident conditions: Deposition on primary systems surfaces. Report BMI-1863 (1969)

Genco, J. M., Rosenberg, H. S., Morrison, D. L.: Iodine deposition and its enhancement under reactor accident conditions. Nucl. Safety **9**, 226–238 (1968)

Gieseke, J. A., Cybulskis, P., Denning, R. S., Kuhlmann, M. R., Lee, K. W., Chen, H.: Radionuclide release under specific LWR accident conditions. Report BMI-2104 (1984)

Gieseke, J. A., Jordan, H.: Aerosol deposition in BWR steam separators and dryers. Report EPRI NP-5597 (1988)

Güntay, S.: Experiment Poseidon: Pool scrubbing effect on iodine decontamination. Paper presented at the ENC '90, ENS/ANS – Foratom Conf. Lyon, Sept. 1990

Hahn, R., Ache, H. J.: Thermodynamic calculations on the behavior of gaseous iodine species following a hypothetical severe LWR accident. Nucl. Technology **67**, 407–410 (1984)

Harman, N. F., Clough, P. N.: A review of radionuclide release and transport in recent in-pile experiments. Report EUR 14230 EN (1992)

Henshaw, J. G., Newland, M. S., Wood, S. J.: Thermogravimetric studies of vapour–aerosol interactions. Report AEA TRS 5074 (1991)

Johnson, I., Farahat, M. K., Settle, J. L., Johnson, C. E., Ritzman, R.: Downstream behavior of fission products. Proc. Symposium on Chemical Phenomena Associated with Radioactivity Releases During Severe Nuclear Plant Accidents, Anaheim, Calif. 1986; Report NUREG/CP- 0078 (1987), p. 3/53–65

Johnson, I., Farahat, M. K., Settle, J. L., Arntzen, J. D., Johnson, C. E.: Downstream behavior of volatile iodine, cesium and tellurium fission products. Report EPRI NP-6182 (1989)

Kress, T. S., Beahm, E. C., Weber, C. F., Parker, G. W.: Fission product transport behavior. Nucl. Technology **101**, 262–269 (1993)

Lemire, R. J., Paquette, J., Torgerson, D. F., Wren, D. J., Fletcher, J. W.: Assessment of iodine behaviour in reactor containment buildings from a chemical perspective. Report AECL-6812 (1981)

Malinauskas, A. P., Kress, T. S.: Effects of chemical phenomena on LWR severe accident fission product behavior. Nucl. Safety **32**, 56–64 (1991)

Marble, W. J. (comp.): Preliminary report on the fission product scrubbing program. GE Report NEDO-30017 (1983)

Marble, W. J., Wong, T. L., Moody, F. J., Hankins, D. A.: Retention of fission products by BWR suppression pools during severe reactor accidents. Proc. Internat. Nuclear Reactor Safety Conf., Chicago, Sept. 1982 (cited according to Ramsdale et al., 1992)

McCormack, J. D., Dickinson, D. R., Alleman, R. T.: Experimental results of ACE vent filtration, pool scrubber tests. Report ACE-TR-A1 (1989)

Minato, K.: Thermodynamic analysis of cesium and iodine behavior in severe light water reactor accidents. J. Nucl. Materials **185**, 154–158 (1991)

Moers, H.: Oberflächenanalytische Untersuchungen zum Freisetzungsverhalten flüchtiger Spaltprodukte bei simulierten Kernschmelzunfällen und zum Reaktionsverhalten von Iod mit Silberoberflächen. Bericht KfK-4073 (1986)

Neeb, K. H.: Auswirkungen chemischer Reaktionen auf das Verhalten des Spaltiods bei hypothetischen Ereignissen im Leichtwasserreaktor. VGB Kraftwerkstechnik **66**, 389–394 (1986)

Owczarski, P. C., Burk, K. W.: SPARC-90: A code for calculating fission product capture in suppression pools. Report NUREG/CR-5765 (1991)

Paquette, J., Sunder, S., Torgerson, D. F., Wren, C. J., Wren, D. J.: The chemistry of iodine and cesium under reactor accident conditions. Proc. 3. BNES Conf. Water Chemistry of Nuclear Reactor Systems, Bournemouth, UK, 1983, Vol. 1, p. 71–79

Paul, D. D., Flanigan, L. J., Cunnane, J. C., Cudnik, R. A., Collier, R. P., Oehlberg, R. N.: Radionuclide scrubbing in water pools – Gas–liquid hydrodynamics. Proc. American Nuclear Society Meeting on Fission Product Behavior and Source Term Research. Snowbird, Utah, USA, 1984; Report EPRI NP-4113-SR (1985), p. 30/1–15

Powers, D. A., Bieniarz, P. P.: Influence of chemical form on cesium revaporization from the reactor coolant system. Proc. Symposium on Chemical Phenomena Associated with Radioactivity Releases During Severe Nuclear Plant Accidents, Anaheim, Calif., 1986; Report NUREG/CP-0078 (1987), p. 3/67–78

Rahn, F.: The LWR Aerosol Containment Experiments (LACE) project: Summary report. Report EPRI NP-6094-D (1988)

Rahn, F. J., Collèn, J., Wright, A. L.: Aerosol behavior experiments on light water reactor primary systems. Nucl. Technology **81**, 158–182 (1988)

Ramsdale, S. A., Bamford, G. J., Fishwick, S., Starkie, H. C.: Status of research and modelling of water-pool scrubbing. Report EUR 14566 EN (1992)

Roberts, D. L., Kiang, R. L., Witham, C. L.: Aerosol retention in nuclear reactor components. Report EPRI NP-3705 (1984)

Sallach, R. A., Elrick, R. M., Douglas, S. C., Ouellette, A. L.: Reaction between some cesium-iodine compounds and the reactor materials 304 stainless steel, Inconel-600 and silver. Vol. 2. Cesium iodide reactions. Report NUREG/CR-3197, Vol. 2 (1986)

Spence, R. D., Wright, A. L.: The importance of fission product–aerosol interactions in reactor accident calculations. Nucl. Technology **77**, 150–160 (1987)

Sullivan, J. H.: Mechanism of the "bimolecular" hydrogen–iodine reaction. J. Chem. Physics **46**, 73–78 (1967)

Torgerson, D. F., Vikis, A. C., Wren, D. J.: Reactor coolant system and containment aqueous chemistry. Proc. Symposium on Chemical Phenomena Associated with Radioactivity Releases During Severe Nuclear Plant Accidents, Anaheim, Calif., 1986; Report NUREG/CP-0078 (1987), p. 3/1–17

US Nuclear Regulatory Commission: Reactor Safety Study: An Assessment of Accident Risks in US Commercial Nuclear Power Plants. Report WASH-1400 (1975)

Wassel, A. T., Hoseyni, J. L., Farr, J. L.jr., Oehlberg, R. N.: Scrubbing of radionuclide aerosols in water pools. Proc. American Nuclear Society Meeting on Fission Product Behavior and Source Term Research. Snowbird, Utah, USA, 1984; Report EPRI NP-4113-SR (1985), p. 34/1–19

Wichner, R. P., Spence, R. D.: A chemical equilibrium estimate of the aerosols produced in an overheated light water reactor core. Nucl. Technology **70**, 376–393 (1985)
Wren, D. J., Rondeau, R. K., Pellow, M. C.: The influence of radiation on the stability of CsI in flowing steam. Proc. 2. CSNI Workshop on Iodine Chemistry in Reactor Safety, Toronto, Can., 1988; Report AECL-9923 (1989), p. 114–130
Wren, D. J., Rondeau, R. K., Pellow, M. D.: Studies on the radiation stability of cesium iodide. Report EPRI NP-6344 (1989)

7.3.3 Chemical reactions and behavior of the radionuclides within the containment

7.3.3.1 General aspects

The mixture consisting of steam and hydrogen and containing vaporized fission products as well as fuel assembly and core structural materials, the composition of which was established within the reactor pressure vessel and, to a certain extent, was changed by chemical reactions and deposition during transport through the primary system, expands through the primary system break into the containment. Within the containment the behavior of the fission products, in particular of fission product iodine, can be regarded as part of a dynamic system in which the species entering from the primary system interact with a complex gas mixture including transport to and from surfaces and aqueous solution (Beahm et al., 1986). Usually, in most fission product transport models it is anticipated that the radionuclides are released from the leak in the primary system directly to the containment free volume, forming a system in which the liquid of the sump water is in direct contact with the atmosphere of the containment free volume. In reality, however, in almost all cases the break will be located inside an equipment compartment which is separated from the containment free space by massive walls and doors. In these compartments, a fraction of the volatilized fission products may be plated out permanently or at least temporarily, as a result of physical and chemical reactions which will be discussed in the following sections. A quantitative treatment of the extent of retention in these compartments is very difficult, since it depends highly on the design of the plant, the specific characteristics of the accident sequence and the physico-chemical properties of the radionuclide species. Several attempts have been undertaken to model the behavior of radionuclides in such a multi-compartment system; however, since deposition and revolatilization are very sensitive to the specific conditions (gas flow rate, geometry, surface area etc.) prevailing in the individual compartment, no generally valid conclusions can be drawn from such considerations. For this reason, in most of the source term calculations the reactions and the behavior of the radionuclides in the equipment compartments are not taken into account; it should be kept in mind, however, that neglecting the effects which occur in these compartments will result in an overestimation of fission product release to the containment and, finally, from the plant. Only the fission product noble gases are not significantly subject to retention or delay in the equipment compartments.

The comparatively low temperature in the containment during the early stages of a severe accident will effect an extensive condensation of the incoming steam onto the surfaces (the surface area in a KWU 1300 MWe containment is about 60,000 m^2, including 30,000 m^2 surface area of internals, 3500 m^2 of steel in the containment sphere and 14,000 m^2 of concrete structures) and an accompanying effective plate-out of aerosols and iodine introduced into the containment. A part of the deposited substances will be washed down into the sump water volume which forms in the lower regions of the reactor building, the volume of which is 1000–1500 m^3, depending on the design of the plant and on the accident sequence under consideration. The remainder of the aerosols and volatile substances will be transported to the containment free space, which in a KWU 1300 MWe plant has a volume of about 70,000 m^3; this airborne fraction is of particular interest, since in the event of a failure of the reactor building confinement a fraction of it may be transported out of the plant to the environment. As was mentioned above, the containment is subdivided into numerous compartments. For reasons of simplicity these details of the structure will be largely ignored in the following; thus, in most considerations a direct contact between the entire sump water volume and the whole containment atmosphere is postulated, which is a highly conservative assumption compared to the situation in an actual severe accident.

As a result of retention effects in the primary system, the proportion of vaporized fission products that can escape into the containment depends on the specific sequence of a degraded core accident. Whereas in an accident initiated by a large break only a limited retention in the primary system has to be assumed, the high-pressure accident sequences are expected to result in appreciable retention of substances in the piping and components of the primary system. As a consequence, smaller fractions of the fission product core inventory will reach the containment. In Table 7.13. (according to Soffer, 1991), calculated values of the fractions entering the containment are shown for both types of sequences, with the accident sequence subdivided into four stages. These newer results demonstrate that the formerly used simplified version of one cumulative release phase to the containment with time-constant concentrations of fission products in the steam–hydrogen flow and constant element ratios has to be replaced by a more sophisticated model. In the gap release phase of the accident, identical fractions of the fission products are assumed to be released in both accident sequences; in contrast, in the early in-vessel release phase, which covers melting and slumping of the core material, the release fractions which are to be expected in the high-pressure sequence are significantly affected by retention in the primary system, quite in contrast with the low-pressure sequence. In the ex-vessel phase, i. e. in the core – concrete interaction phase after failure of the reactor pressure vessel, the release process is strongly influenced by the type of concrete used for the reactor cavity. The data given in Table 7.13. are typical for limestone concrete; due to the greater production of CO and CO_2, higher fractions of the less-volatile elements (Sr, Ba, La) are sparged to the atmosphere than in the case of siliceous concrete (see Section 7.3.1.3.). The magnitude of transport of radionuclides to the containment free volume during this phase will be significantly reduced if the interaction zone is covered by water, either as a result of cooling of the core debris or by scrubbing of the releases and

Table 7.13. Core fractions released into containment
a) under high RCS pressure, b) under low RCS pressure
(according to Soffer, 1991)

Nuclide	Gap Release 0.1–0.5 hours	Early In-Vessel 0.7–3.0 hours	Ex-Vessel 2–5 hours	Late In-Vessel 10 hours
a)				
Xe, Kr	0.05	0.95	0	0
Iodine	0.05	0.14	0.22	0.12
Cesium	0.05	0.11	0.30	0.08
Tellurium	10^{-4}	0.05	0.23	0.04
Strontium	10^{-6}	0.01	0.11	0
Barium	10^{-6}	0.02	0.09	0
Ruthenium	0	$3 \cdot 10^{-3}$	0.027	0
Cerium	0	$4 \cdot 10^{-3}$	0.018	0
Lanthanum	0	$1 \cdot 10^{-3}$	0.015	0
b)				
Xe, Kr	0.05	0.95	0	0
Iodine	0.05	0.40	0.21	0.12
Cesium	0.05	0.30	0.34	0.08
Tellurium	10^{-4}	0.15	0.30	0.04
Strontium	10^{-6}	0.03	0.14	0
Barium	10^{-6}	0.04	0.11	0
Ruthenium	0	$8 \cdot 10^{-3}$	$1 \cdot 10^{-3}$	0
Cerium	0	0.01	0.017	0
Lanthanum	0	$2 \cdot 10^{-3}$	0.017	0

retention of a fraction of them in the water. Finally, in the late in-vessel phase some of the volatile nuclides not volatilized during the previous early in-vessel phase will be transported to the containment.

Not only does the fraction of the fission product core inventory reaching the containment depend on the particular accident sequence, the same is true for the chemical forms of the fission products, which result in part from reactions within the primary system, as has been discussed in Section 7.3.2. However, when fission products are transported from the high-temperature reducing conditions of the primary system to the lower-temperature, predominantly oxidizing and condensing steam conditions of the containment, their chemical forms may change again; simultaneously, fission products deposited on the surfaces of bulk material aerosols could be resuspended due to the formation of more volatile species.

The behavior of the radionuclides within the containment depends strongly on its postulated state during the accident. According to the Deutsche Risikostudie Kernkraftwerke DRS (GRS, 1989), two fundamentally different situations have to be distinguished:

- If all the penetrations through the containment steel shell are closed according to design, the containment can be regarded as a closed physical and chemical system; the operational leakages of the steel shell (which are very small) can be

ignored for the considerations of fission product behavior inside the containment, although they have to be taken into account when considering leakage of radionuclides from the closed containment (see Section 7.3.4.1.). As a consequence of the continuing decay heat of the core melt which is now flooded by sump water, there will be a continuous evaporation of water from the sump which condenses again at the surfaces of the containment, resulting in a heating-up of all the containment structures. Due to this water evaporation, temperature and pressure inside the containment will increase steadily, reaching the design pressure of the steel shell after 5 to 6 days at about 0.8 MPa and an associated saturation temperature of the steam of about 170 °C. A failure of the containment will only occur if no countermeasures such as a controlled depressurization via filters are undertaken (see Section 7.3.4.4.).

- In the low-probability event of a failure of the containment safety isolation, one has to assume that steam will escape via an open penetration in the steel shell (e. g. belonging to the ventilation system) to the annuli or to the reactor auxiliary building. Inside the containment, therefore, a lower overpressure will be built up and the temperature will rise more slowly, with both figures depending on the size of the opening. In the DRS, the worst case was defined as an open penetration with a size of about 300 cm^2. Under such conditions, the average residence time of a volume element of steam with the radionuclides it contains inside the containment will be on the order of 5 to 10 hours. In practice it can be assumed that such an opening will be locked within a comparatively short time, so that the condition of a closed containment will be established. In the risk analyses, an additional release category is postulated which is characterized by a steam explosion as a consequence of the falling down of a large amount of molten corium material into the residual water inside the reactor pressure vessel. The possible consequence of this event would be a disruptive failure of the reactor pressure vessel, generating missiles which would be able to penetrate the containment steel shell and to effect large-area damage of the shell, opening a direct path to the environment. Since detailed analyses of the possible energy releases in such a situation which have since been performed have demonstrated that such a large-sized containment failure is not a realistic event, it will not be considered in what follows.

The effectiveness of the natural processes leading to a plate-out of the radionuclides inside the containment depends on the type of reactor, the accident sequence and the prevailing thermohydraulic and chemistry conditions. As a general rule, the longer the containment remains intact, the more effective the natural plate-out processes will be. Included under the concept basic natural processes are both chemical reactions and phase transitions, transport of gases and aerosols to the walls caused by diffusion or convection, sedimentation, thermophoresis, diffusiophoresis and, finally, growth of the aerosol particles by agglomeration. In practice, these effects are supported by engineered measures such as spray systems, filters, ice condensers, scrubbers or suppression water pools, as far as the respective installations are part of the individual plant design. In WASH-1400, several natural and engineered removal mechanisms were considered to be effective in radionuclide

retention, such as deposition onto surfaces, removal by containment sprays and, for BWRs, by pool scrubbing; likewise, partition equilibria between the atmosphere and aqueous media were taken into account for retention of elemental iodine. Modelling has since been considerably improved by the use of more sophisticated computer codes and, above all, by taking into consideration a multitude of chemical reactions.

For the treatment of the behavior of the radionuclides in the containment, it seems reasonable to divide them into three groups: aerosols, tellurium, and iodine. The fission product noble gases as the fourth group of elements are distributed homogeneously over the entire free volume of the containment after a short time interval and they are only subject to radioactive decay; thus, their behavior will not be discussed in detail in the following. In spite of the considerable differences between PWR and BWR plants, the environmental conditions within the containment are in most cases not so different as to influence fundamentally the chemical reactions of the fission products. Therefore, the discussions in the following sections will apply to both types of LWR plants; where there are significant differences they will be mentioned in the respective section.

7.3.3.2 Aerosols

The largest fraction of radionuclides by far enters the containment attached to aerosol particles which are carried by the steam flow. As was shown in Table 7.3., according to thermodynamic calculations oxides and metals are the predominant species of the refractory aerosols generated in the reactor pressure vessel, and one has to assume that at the lower temperatures prevailing in the containment no significant changes in the chemical nature of these primary aerosols will occur. The primary aerosol particles will be coated by layers of more volatile substances such as CsOH and CsI which are deposited in regions of lower temperatures in the primary system; other fission product species may also be attached to the aerosol surfaces by condensation, chemical reactions and, probably to a lesser extent, by physi- and chemisorption.

In the gas–steam flow which enters the containment in the low-pressure accident sequence, maximum aerosol densities in the range of 20 g/m^3 may occur. When the core – concrete interaction begins, about 1 to 3 Mg of aerosols in total are assumed to be present in the containment atmosphere, according to corresponding calculations.

Within the containment, the aerosols undergo physical reactions and deposition, resulting in a reduction of their airborne concentration. The very small primary aerosol particles which did not experience particle growth in the primary system can be assumed to agglomerate very rapidly in the steam–hydrogen–air environment inside the containment. The resulting particles are then transported to the walls or plated out into the sump water, with the most important mechanisms here being sedimentation, diffusion, diffusiophoresis and thermomigration. The rate and

effectiveness of these natural deposition processes depend highly on the particle size of the aerosols and on the concentration of the particles in the atmosphere. At particle diameters of about 0.1 μm and concentrations below about 0.5 g/m^3 the aerosols are stable; the main deposition mechanisms are then diffusion and thermophoresis. At higher concentrations the tendency for agglomeration increases, with the diameters of the resulting particles growing proportionally to the cube root of the concentration, and the main deposition mechanism changing to sedimentation. Under the conditions prevailing in the containment, condensation of water from the supersaturated steam onto the particles will also take place and will influence the rate of deposition of the aerosols. The two-phase mixture, steam plus water droplets, escaping from the primary system leak to the containment atmosphere will also effect a reduction in the airborne aerosol concentration caused by the water droplets. The hygroscopic properties of some aerosol species (e. g. CsOH) can influence the rates and the amounts of moisture adsorbed while the aerosols are still airborne in the containment. Moreover, the condensation of large amounts of steam in the containment in the very first stages of a severe accident will lead to an enhanced deposition of the aerosols caused by diffusiophoresis.

The influence of the different processes contributing to aerosol deposition within the containment is difficult to evaluate theoretically by calculations based solely on the results of laboratory experiments, mainly because of the importance of dimensional parameters. Therefore, in order to obtain reliable data on the fraction of aerosols which is still airborne in the containment at a given moment, large-scale experiments have been performed at different institutions. Already in the 1960's, the Containment Systems Experiments (CSE) formed a basis for predicting the behavior of the aerosols and other fission products in reactor containment buildings. By the early 1980's, it had become evident that the CSE provided only partial results, in that the experiments were performed under quasi-static thermal-hydraulic conditions, while in the course of a real reactor accident the conditions may vary rapidly as a result of a broad variety of influencing effects. To close this gap and to validate the results of aerosol transport and behavior codes that had since been established, several large-scale experimental programs have been carried out in the recent years, with the most important ones being the NSPP program, the DEMONA program and the LACE containment experiments. The special features of these tests and their main results have been summarized by Schöck et al. (1988).

In the NSPP experiments the behavior of U_3O_8, Fe_2O_3 and concrete material aerosols in a 38 m^3 single-volume vessel has been studied in dry-air as well as in steam environments. In a dry-air atmosphere the rates of removal of the three aerosol materials showed only slight differences; in contrast, in the presence of steam (relative humidity 100% at about 100 °C) the rates of removal of U_3O_8 and Fe_2O_3 increased significantly while the behavior of the concrete aerosol was virtually unaffected. These differences in behavior proved to be caused by the nature of the aerosol particles. The particle shape of U_3O_8 and Fe_2O_3 (as well as of U_3O_8 $-Fe_2O_3$ mixed aerosol particles) changed upon addition of steam from chain agglomerates to generally spherical clumps, followed by condensation of steam on the particles, increasing the effect of gravitational settling. The shape of the con-

crete aerosol particles was considerably less influenced by steam, probably due to differing physical and chemical responses of the surfaces to condensing steam.

The main objectives of the DEMONA program were to demonstrate the validity of calculations made with the NAUA aerosol behavior code. These experiments were carried out in a 640 m^3 concrete model containment with structured geometry; the aerosol materials used were SnO_2 and Fe_2O_3 (in one test Ag + MgO). The results clearly showed the considerable impact of the condensing-steam environment on the removal rates of the aerosols from the atmosphere, resulting in a decrease of the initial airborne concentration of 10 g/m^3 by about four orders of magnitude within 6 to 8 hours, compared to about 2 days in a dry atmosphere. The effect of the aerosol material on the overall removal behavior proved to be small.

In addition to these test series, it was felt that a further series of experiments was necessary which would provide data under more dynamic conditions for bypassed or leaking containments. On the basis of these requirements, the experimental containment aerosol retention test program LACE was defined, which was carried out in the Containment Systems Test Facility (CSTF), using a 850 m^3 single-volume vessel. The goal of this program, besides investigation of aerosol behavior in the primary system (see Section 7.3.2.), was investigation of aerosol behavior in the containment, including the conditions prevailing during failure of containment isolation as well as in the event of delayed containment failure sequences, with the latter being studied to cover the case when aerosol resuspension is significant. A summary of these experiments and of their results was given by Rahn (1988).

In contrast with the experimental programs mentioned above, the aerosols introduced in these experiments consisted of two different species, i. e. water-insoluble MnO and water-soluble CsOH. These two species were generated separately by vaporizing manganese metal in a plasma torch and by evaporating cesium metal in a vaporization system. Both vapors then were introduced into an aerosol-mixing vessel that contained superheated steam in a nitrogen atmosphere, oxidizing the metal vapors to MnO and CsOH. The results of the experiments demonstrated that the rapid growth in size of the particles containing hygroscopic substances due to water attraction resulted in a considerably faster deposition of the aerosols than under so-called "dry" conditions. As an example, in one of these experiments less than 2% of liquid or liquid-solid aerosol was vented, while substantially more was vented from the containment in an experiment performed under otherwise identical conditions where 100% solid aerosol was used. Few, if any, accident scenarios are thought to involve only solid aerosols. Therefore, attenuation of such partly water-soluble aerosols will be enhanced, particularly during periods when the containment atmosphere is at or below saturation temperature or when steam is rapidly condensing on surfaces.

The experiments in the CSTF vessel showed that for most accident scenarios the assumption of a homogeneous distribution of the aerosols in the free volume is justified, in particular during periods when steam and/or other hot gases rise from the lower levels of the containment. Such a situation induces natural convection forces which are strong enough to keep the aerosol concentration reasonably uniform. In addition, the experiments demonstrated that the steam condensation

flux to the wall of the containment vessel was essentially identical at all the elevations in the experimental vessel where it was measured. However, the two species of aerosol behaved somewhat differently. The measured particle size distribution showed that, in general, large particles were slightly richer in MnO than were smaller particles, with the opposite being true for CsOH; despite this difference in distribution, the average removal rate from the containment atmosphere was about 40% faster for CsOH than for MnO. Moreover, the condensate film on the vertical walls which, on the average, was about 0.5 mm thick effected a separation of both aerosol species after their deposition. Approximately 99% of the CsOH mass that plated out onto the walls and other heat sink surfaces was washed down by condensate to the sump of the vessel, while for MnO most of the plated mass remained near the location where it was deposited.

After being plated out into the sump water, the volatile fission product species (such as CsOH, CsI, $CsBO_2$) which had been carried on the surfaces of the low-volatility aerosol materials, will be readily dissolved in the water to form the respective ions. The same is true for the iodides of cadmium and indium, which might have been formed within the primary system. Dissolved iodide can undergo different chemical reactions which are able to change its valency state; these reactions will be discussed in Section 7.3.3.3. The refractory-oxide and metallic components of the aerosol particles are mainly water-insoluble and, as far as they are transported to the sump water, remain as suspended solids in the water phase.

Even relatively simple leak paths from a reactor containment building to the environment in real accidents may retain a large fraction of suspended fission products. The dominant removal mechanism for aerosols in these leaks appears to be turbulent deposition (see Section 7.4.).

Resuspension potentially effects a renewed transport of deposited material to the containment atmosphere, an effect that can be initiated by different mechanisms. As was mentioned above, when aerosols containing condensed volatile fission products are transported from a high-temperature region in a reducing environment to a low-temperature region with oxidizing conditions and condensing steam, then fission products may be revolatilized because of the formation of a new chemical species. Besides this chemical reaction, physical resuspension can be induced by a change in the thermal-hydraulic conditions; events which potentially lead to resuspension of deposited aerosols are hydrogen deflagration, steam explosion and rapid depressurization due to failure of the containment. As in the primary system (see Section 7.3.2.2.) the extent of physical resuspension depends on the properties of the deposited aerosols, among other parameters; the presence of a significant fraction of soluble substances (e. g. CsOH) in the deposits decreases the resuspension effect considerably. Finally, the boiling sump water will transport liquid droplets carrying dissolved or suspended radionuclides into the atmosphere. However, the experiments reported by Bleier et al. (1988 a) have shown that this effect does not contribute significantly to the airborne concentration of radionuclides. In these experiments, a simulant sump water solution containing Li^+ as a tracer representing non-volatile fission products was evaporated, using area-related heat ratings ranging from about 4 to about 15 W/cm^2. At different elevations above

the boiling surface, samples were taken of the steam–droplet mixture; in addition, the droplet concentration in this mixture was measured by means of a light-scattering probe. The results showed a tracer carry-over factor (i. e. ratio of mass-related concentrations in the steam and the liquid phases) on the order of 10^{-5}, virtually independent of the heat rating applied and slightly decreasing with increasing elevation between 40 and 150 cm. The light-scattering measurements yielded approximately the same results; in addition, they showed volume-averaged droplet diameters of about 5 μm. It can be assumed that a fraction of the droplets will be plated out upon contact with surfaces. As was demonstrated in the LACE experiments (Rahn, 1988), the change in flow conditions which may be caused by rapid depressurization events appears to have only a relatively small potential for carrying large quantities of fission products out of the reactor containment building. Fractional releases below 10^{-5} were observed for aerosol materials that had been previously dissolved in water pools, and below 10^{-3} for aerosols that had been suspended in the containment atmosphere.

As in a LOCA design basis accident (see Section 6.2.1.2.), the aerosol concentration in the containment atmosphere will also be reduced by the action of the containment spray system. Since larger aerosol particles are removed more readily by the spray droplets than are small particles, the removal efficiency to be expected in a severe accident is higher than in a design basis accident which has much lower aerosol concentrations in the containment atmosphere and, consequently, smaller dimensions of the aerosol particles (Pasedag et al., 1981).

Experiments on aerosol retention in an ice-condenser system (see Section 1.1.4.) during the course of severe accidents were reported on by Ligotke et al. (1991); these tests were performed in a full-scale height and reduced-scale cross section test facility based on the design of the ice compartment of a Westinghouse PWR ice-condenser containment system. The results showed that particle retention in the test section is greatly influenced by thermal-hydraulic and aerosol test parameters. Generally, the presence of ice in the baskets results in a significant increase in the decontamination factors as compared to tests without ice, but with identical conditions in the other parameters. In the order of apparent importance, parameters that cause particle retention in the test section in the presence of ice were:

- the steam molar fraction in the gas flow, with higher steam fractions resulting in considerably higher decontamination factors;
- the flow rate of non-condensible gases, which affects the retention of particles in the test section by influencing the residence time;
- particle solubility: soluble particles (KCl) in the presence of ice and steam show decontamination factors higher by a factor of 2 to 7 than insoluble ones (ZnS);
- inlet particle size: at aerodynamic mass median diameters of less than about 10 μm, the effect of inlet particle size is apparently only weakly pronounced.

Depending on the test conditions, the decontamination factors measured ranged between 2.4 and 36 (tests with ice). The deposition mechanisms identified as being important for the trapping of aerosol particles include settling on upward-facing horizontal basket surfaces, impaction and interception by basket surfaces, diffusiophoresis, thermophoresis, and particle growth.

7.3.3.3 Tellurium

Tellurium is also probably transported in aerosol form into the containment, at least in part. Among the fission products introduced as aerosols into the containment, only tellurium (besides iodide and cesium) is subjected to further chemical reactions; however, as can be seen from the survey paper of Beahm (1987), current knowledge about these reactions is still limited. A significant fraction of the Te_2 species introduced into the containment will be plated out onto the surfaces and, because of their extremely low vapor pressure under the conditions prevailing in the containment, will remain there, as can be concluded from older CSE investigations. The only tellurium compounds which are readily soluble in water are H_2Te and Cs_2Te; these species, however, will be decomposed in the containment sump water under precipitation of elemental tellurium which, in turn, is oxidized by dissolved oxygen to TeO_2, an amphoteric compound having a solubility minimum in water at about pH 5. The distribution of tellurium radiosiotopes between suspended solids (about 93%) and water phase (about 7%), as measured in the TMI-2 post-accident investigations, corresponds approximately to the data obtained from solubility measurements of TeO_2. The vapor pressures of the inorganic tellurium compounds which are stable under containment conditions are very low, so that no detectable radiotellurium concentration in the atmosphere will be caused by them. However, there is a basic possibility that volatile organo-tellurium compounds will be formed by reaction of finely dispersed metallic tellurium with organic radicals. The resulting compounds $(CH_3)_2Te$ and $(C_2H_5)_2Te$ have boiling points of 92 and 138 °C, respectively. If they are produced, they will be quantitatively transported to the containment gaseous phase; detailed information on their formation and behavior under accident conditions, in particular with regard to their stability in the presence of steam and of ionizing radiation, is still lacking.

7.3.3.4 Iodine

7.3.3.4.1 Iodine chemical species entering the containment

In the evaluation of the potential consequences of degraded core reactor accidents, fission product iodine, in particular its isotope ^{131}I, deserves special interest because of its specific properties:

- high activity inventory in the fuel, on the order of 10^6 TBq in the equilibrium burnup core of a 1300 MWe reactor
- fast and nearly complete volatilization from the fuel at higher temperatures
- possible formation of volatile species under specific conditions, even in the environment of a light water reactor accident
- comparatively long halflife of ^{131}I of 8.05 days
- after release to the environment, possibility of enrichment of ^{131}I in the human food chain and the human thyroid.

The possible extent of ^{131}I release to the environment is strongly influenced by the progress and the products of the chemical reactions occurring within the containment. For this reason, iodine chemistry in the containment has been (and still is) the subject of numerous investigations in many laboratories in different countries, in particular as regards its most important chemical reactions.

The relative concentrations of the individual iodine chemical species entering the containment from the reactor coolant system depend highly on the specific accident sequence, in particular on the temperatures, the residence times at a given temperature and on the presence of possible reaction partners in the steam–hydrogen environment. As was discussed in Section 7.3.2.3., fission products and other substances that are released from the reactor core will be subjected to changes in temperature and concentration as they pass through the different regions of the reactor primary system. In each region, a specific equilibrium in the system iodine –cesium–other elements–hydrogen–steam tends to be established; however, in a very steep temperature gradient an equilibrium once attained can become frozen. This means that the temperatures and the concentrations of species in subsequent control volumes are not able to induce a new, appropriate equilibrium composition during the available residence time. In such a case, the frozen equilibrium will be the species distribution entering the containment. As an example, calculations of the iodine species distribution (Beahm et al., 1992; Kress et al., 1993) have shown that in most accident sequences fission product iodine entering the containment from the reactor primary system is almost entirely in the form of CsI; however, it was calculated that in one specific sequence with high steam flow rates and steep temperature gradients in the reactor pressure vessel, comparatively high proportions of elemental iodine and of HI would enter the containment, with the balance as CsI (see Section 7.3.2.3.2.). Organoiodides are not assumed to be introduced into the containment, since the conditions prevailing in the reactor primary system will prevent the formation of these species.

In a highly simplified view (see Fig. 7.20.) it can be assumed that the steam flow escaping from the primary system and entering the containment will partly condense there, in the course of which a fraction of the aerosols (CsI included) and of the I_2 and HI being carried by the gas–steam flow is directly washed down to the liquid sump water. After being dissolved in the water phase, CsI is immediately and quantitatively dissociated to Cs^+ and I^- ions. HI transported into the containment is also readily dissolved in water to form H^+ and I^- ions; consequently, whether iodine enters the containment as CsI or as HI probably does not make much of a difference with respect to its subsequent chemical and transport behavior. I_2, on the other hand, will be distributed between the liquid and the gas phase; the degree of instantaneous partitioning depends mainly on the magnitude of the condensed steam fraction, with the precipitated I_2 fraction increasing almost linearily with an increasing degree of steam condensation (see the results of laboratory measurements in Fig. 7.28.). Since the details of steam condensation probably depend highly on the special characteristics of the escape process, quantitative figures on the degree of instantaneous partitioning of iodine between the atmosphere and the condensed water phase are difficult to obtain. Some conclusions may be drawn

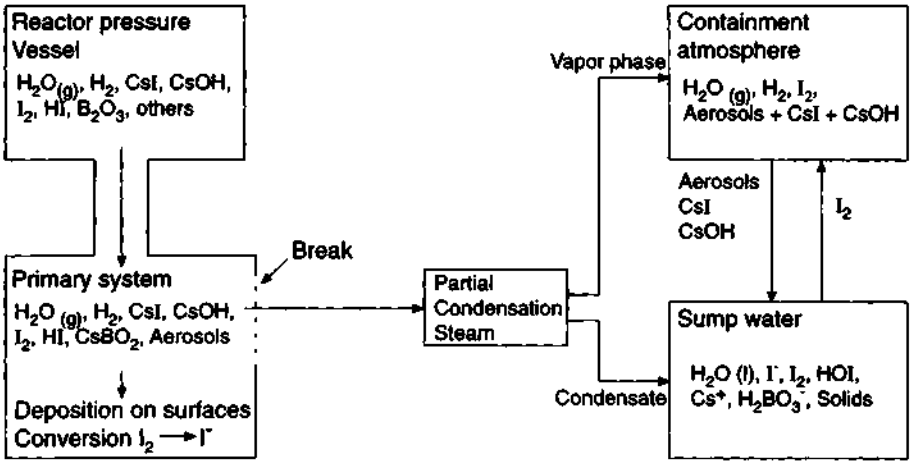

Figure 7.20. Transport of fission product iodine from the primary system to the containment

from the results of other experiments, such as the coolant flashing tests reported by Hellmann et al. (1991), which demonstrated that even after addition of I_2 to the solution to be flashed, the bulk of iodine is instantaneously washed down to the liquid phase, with less than 1% remaining in the atmosphere, predominantly as liquid aerosol particles (see Section 6.2.2.). To be sure, these experiments were related to the coolant flashing process and not to the steam escape mechanism characteristic for this stage of a severe accident, but it is likely that relevant conclusions can be drawn from them. Additional fractions of I_2 carried by the steam can be plated out into the liquid phase upon contact of the gas flow with water films at the structural surfaces.

Within the containment a multitude of reactions may affect the chemical state of iodine; a selection of potential reaction partners and of interconnections among the three compartments sump water (dissolved phase and solid ingredients), atmosphere and walls is schematically shown in Fig. 7.21. The overwhelming fraction of iodine is transported into the containment as aerosol CsI with minor fractions of I_2 and/or HI. Under the influence of ionizing radiation, dissolved I^- can be oxidized to volatile I_2 and further to non-volatile iodine oxides; alternatively, I_2 can be reduced by thermal or radiolytic processes to non-volatile I^-. Organoiodine compounds may be formed and decomposed again. Iodine species may be deposited onto structural surfaces and converted there to another chemical state; in the sump water I_2 may react with metallic silver to form insoluble AgI. Thus, the iodine species distribution entering the containment can be considerably altered, with the yields of the different products depending highly on the ambient conditions, such as iodine concentration, sump water pH, redox potential, temperature, radiation dose rates, presence of reaction partners etc. These conditions do not only depend on the type of reactor and on the accident sequence in question, they may also change in the course of an accident. As a result, the behavior of fission product

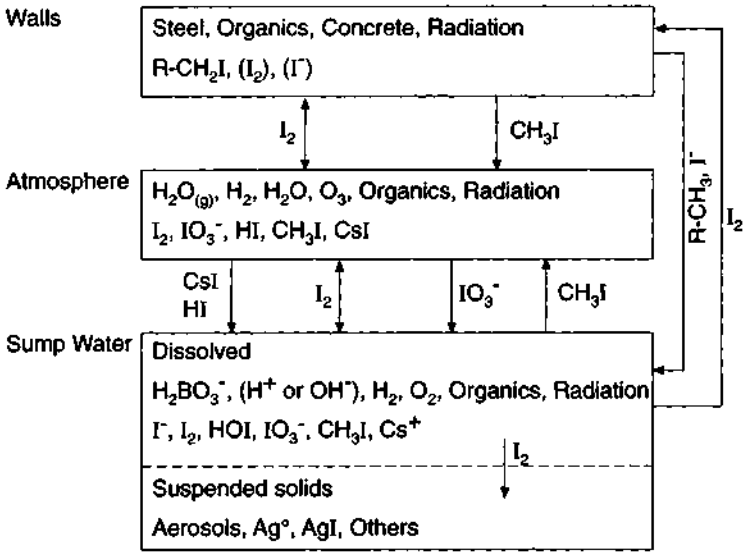

Figure 7.21. Iodine reactions and behavior in the containment

iodine in the containment is much more complex than that of the aerosols, with chemical reactions being the dominating parameters; the most important of these processes will be discussed in the following sections.

7.3.3.4.2 Basic iodine chemistry in aqueous solution and iodine volatility

During the course of a core melt accident, a large fraction of the total core inventory of fission product iodine is volatilized from the overheated nuclear fuel and transported to the containment building where the bulk of it is dissolved in the sump water. In the case of a 3900 MWth reactor core (i. e. 1300 MWe plant), this inventory in the burnup equilibrium state near the end of a fuel cycle amounts to about 18 kg iodine, the overwhelming fraction of which is stable ^{127}I and very long-lived ^{129}I. This iodine inventory results in a total iodine concentration in the containment sump water on the order of 10 to 20 mg/l or of a few 10^{-4} mol/l (depending on the degree of retention in the primary system and on the sump water volume and, therefore, on the accident sequence and on the design of the plant). This iodine concentration is by far higher than that appearing in the primary coolant during plant normal operation phases or in the sump water solution after a loss-of-coolant design basis accident, and it approaches a concentration level which is common in aqueous macrochemistry. Moreover, the temperatures of the aqueous solutions prevailing in such a situation are markedly different from those of the

primary coolant during steady-state operation or of the sump water in a design basis accident. For these reasons, it is to be expected that the progress of iodine chemical reactions and the yields of their products show significant differences from the values given in Chapters 4 and 6. Therefore, a short discussion of the basic features of aqueous iodine chemistry would seem to be advisable in this context.

Since the early days of modern inorganic chemistry, the hydrolysis reaction of elemental iodine I_2 with water has been a frequently analyzed standard reaction:

$$I_2 + H_2O \rightleftharpoons I^- + HOI + H^+. \tag{1}$$

The disproportionation of hypoiodous acid HOI has also been often studied:

$$3\ HOI \rightleftharpoons 2\ I^- + IO_3^- + 3\ H^+ \tag{2}$$

with the two reactions yielding the resulting summary reaction:

$$3\ I_2 + 3\ H_2O \rightleftharpoons 5\ I^- + IO_3^- + 6\ H^+ \tag{3}$$

Further, the impact of the pH of the aqueous solution, as well as of the temperature and the iodine concentration, on the yields of the different iodine species in the equilibrium state have been widely investigated. However, the results of these "classic" chemical investigations proved to be not sufficiently detailed with regard to the range of ambient conditions that have to be taken into consideration in the course of a severe reactor accident.

Systematic studies of the iodine hydrolysis and disproportionation equilibria were, therefore, undertaken in past years in several laboratories, including both thermodynamic and kinetic calculations as well as experimental investigations (e. g. Bell et al., 1982 a; Palmer and Lietzke, 1982). These studies showed that in order to completely describe the iodine reaction equilibria, additional reactions have to be taken into account; among them, the most important are:

$$I_2 + I^- \rightleftharpoons I_3^- \tag{4}$$

$$I_2 + H_2O \rightleftharpoons H_2OI^+ + I^- \tag{5}$$

$$HOI + H_2O \rightleftharpoons H_3O^+ + OI^- \tag{6}$$

$$OI^- + I^- + H_2O \rightleftharpoons I_2OH^- + OH^- \tag{7}$$

$$OI^- + I^- \rightleftharpoons I_2O^{2-} \tag{8}$$

These reactions are of different importance for the fractional concentrations of the individual iodine species formed from initial I_2 in the aqueous solution. In the development of mechanistic models describing iodine chemistry in a severe reactor accident, these reactions also have to be considered; in spite of some gaps in knowledge, the currently available thermodynamic database is considered to be sufficiently accurate. However, because of the action of third partners, in particular of radiation-induced phenomena (see the following sections), the pure I_2 hydrolysis and disproportion reactions frequently are only of limited significance.

HOI is the product of the first I_2 hydrolysis step (reaction 1) and is, therefore, an important intermediate in all iodine chemistry codes (see Section 7.3.3.4.9.). For reasons of charge conservation in I_2 hydrolysis, I^+ has to be produced in the same

amount as I^- and should be stable in the solution until formation of IO_3^-, which is a fast reaction at higher solution pH but which proceeds slowly at low pH. Therefore, intensive efforts have been undertaken in different laboratories to measure directly the presence of HOI in aqueous solutions, e. g. by absorption spectrometry. Haimovich and Treinin (1965) detected the OI^- ion in a strongly alkaline solution, showing a molar absorption distinctly lower what would be expected from analogy with OCl^- and OBr^-; thus, frequently the existence of the anion even in neutral solutions was assumed, despite the severe doubts confirmed by the investigations of Toth et al. (1984). Their results demonstrated that the decay kinetics of the intermediate species in neutral solutions is not influenced by the ionic strength of the solution; consequently, the existence of ionic species such as OI^- and HOI_2^- under such conditions has been ruled out. From investigations involving the presence and the decay kinetics of the I^+ species, it was concluded that at pH levels near the neutral point HOI does exist, but that it shows such a low molar absorption that it cannot be measured directly, quite in contrast to the corresponding chlorine and bromine compounds. According to Palmer and van Eldick (1986), the dominating presence of the I_3^- ion interferes with direct spectrometric identification of HOI in an untreated aqueous I_2 solution. By treating the solution with mercuric carbide perchlorate polymer, I^- ions are completely removed by exchange for perchlorate ions; it was possible to measure the HOI spectrum in the resulting solution, which showed an absorption maximum at 278 nm.

Because of the pronounced differences in the reaction kinetics between reactions (1) and (2), in particular at low solution pH, it seems advisable to look separately at the relative concentrations of the different iodine species present in the equilibrium solution for the cases "with iodate formation" and "without iodate formation". The results of both Bell et al. (1982 a) and of Palmer and Lietzke (1982) on the equilibrium state of the main hydrolysis reactions can be summarized as follows:

- With increasing pH of the solution, the equilibrium state in both the reactions (1) and (2) is shifted to the right side, i. e. the concentration of I_2 decreases steadily. For reaction (1), elemental I_2 is the dominating component up to a pH of about 5; in the pH range 5 to 10, hypoiodous acid HOI gains in importance, while beyond pH 10 the hypoiodite anion OI^- is the main component. Taking into account the additional reactions (2) and (3), the I_2 fraction already decreases strongly at a pH above 4; at a higher pH, I^- and IO_3^- are the main components; they are present in the molar concentration ratio 5:1, as determined by the hydrolysis equilibrium.
- With increasing temperature of the solution, the equilibrium state of both reactions is also shifted to the right side. When all other conditions are kept constant, the I_2 fraction in the equilibrium mixture decreases by about two orders of magnitude when the temperature is raised from 25 to 100 °C. This tendency applies over a broad range of pH values and iodine concentrations (see Fig. 7.22.). More recent measurements (Burns et al., 1988) have yielded the equilibrium constants of reaction (1) shown in Fig. 7.23. as a function of temperature in the range 25 to 100 °C. These data deviate to a certain extent from those presented in some former publications.

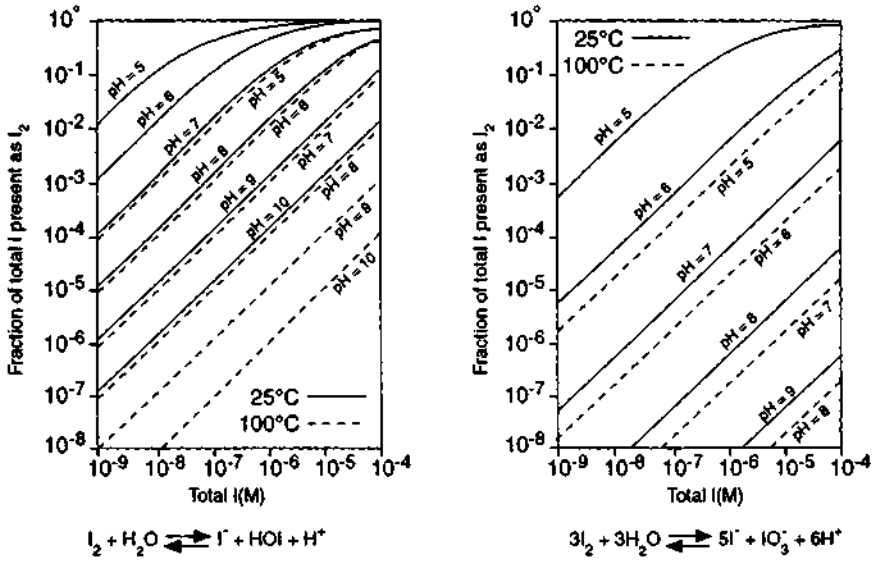

Figure 7.22. I_2 as a fraction of total iodine in the equilibirum state of the hydrolysis reactions, with and without iodate formation
(Bell, 1981)

- A decrease in the concentration of total iodine in the solution results in a parallel decrease of the relative I_2 fraction. Therefore, at low concentrations I^- + HOI or I^- + IO_3^- are the predominant species, even at lower solution pH; I_2 is of little significance, quite in contrast to the situation at high total iodine concentrations.

These results, which have only been summarized very shortly here, are valid for solutions containing I_2 and water exclusively, with variation of pH, temperature and iodine concentration. The presence of additional substances in the solution may effect a considerable change in the relative concentrations of the individual components; the influence of some of these substances will be discussed in the following section. An example which is of particular significance for iodine behavior in a severe accident involves solutions which, from the very beginning, contain an excess of I^- besides I_2; as has been discussed above, the largest fraction of iodine by far is transported to the containment in form of CsI with only small proportions of I_2. Since the I^- concentration in the solution influences the state of both equilibria, the consequence of an initial I^- excess will be a shift in the stability ranges of the individual species. Calculations have shown that in solutions containing 10^{-4} g-atom I^-/l beside 10^{-6} g-atom I_2/l (temperature 140 °C), the stability range of I_2 and of IO_3^- is shifted towards a higher pH. As a consequence, in the pH range 5 to 8 (which is the sump water pH assumed for severe accidents), the proportion of volatile I_2 will be higher than in a pure I_2 solution with 10^{-6} g-atom/l, but significantly lower than in such a solution having 10^{-4} g-atom I_2/l. The impact of this shift in the equilibrium state on the I_2 partition coefficient will be discussed below.

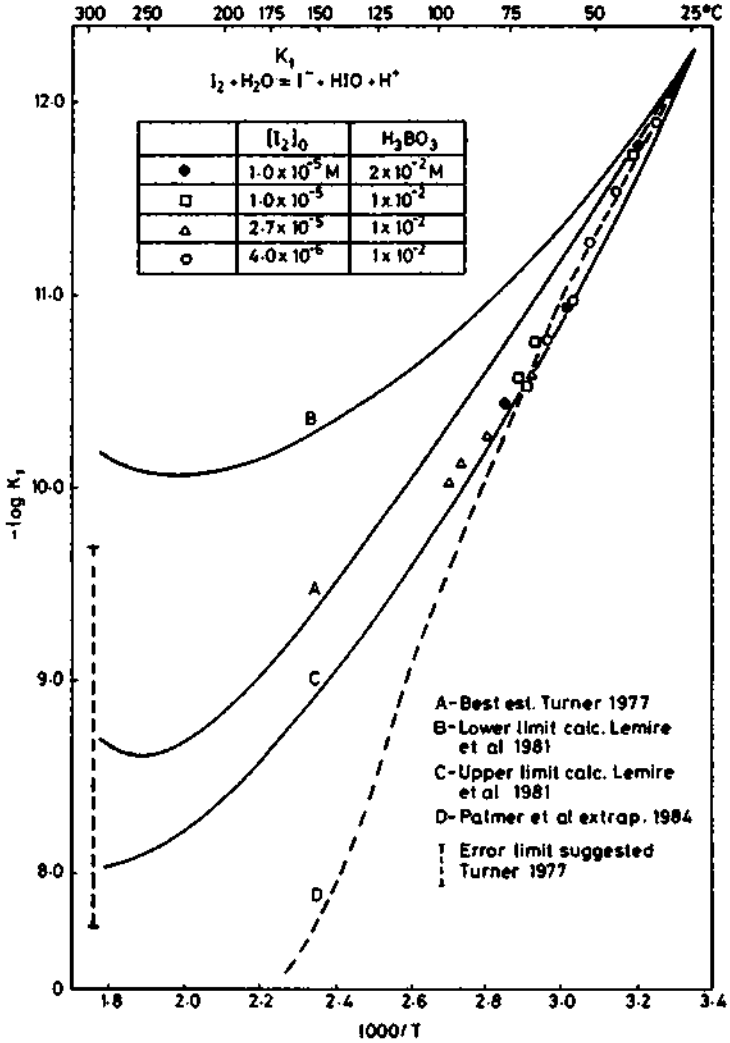

Figure 7.23. Temperature dependence of the I_2 hydrolysis constant (Burns et al., 1988; by courtesy of Atomic Energy of Canada Limited)

The data on the relative concentrations of the different iodine species in the hydrolysis solution which were given above apply only when the equilibrium state has been completely established. However, if important reactions proceed only slowly, compared to the time scale of the accident, the distribution of species will be different from that to be expected for the equilibrium state. Thus, for the evaluation of fission product iodine behavior, the rates of the reactions leading to the equilibrium state also have to be taken into account.

The kinetics of the first stage of iodine hydrolysis, i. e. reaction (1), was studied very early on by Eigen and Kustin (1962). According to these investigations, this

reaction is of first order with respect to the I_2 concentration and proceeds very rapidly; at an I_2 concentration in the solution on the order of 10^{-4} g-atom/l and a temperature of 25 °C, the equilibrium state is established within 1 second. Since under accident conditions the temperatures are usually considerably higher, for practical applications one can assume an instantaneous establishment of the equilibrium state. Palmer and van Eldick (1986) observed no dependence of the reaction rate on pH in the range 3 to 7, indicating that decay of the intermediate I_2OH^- is the rate-controlling step.

The kinetics of HOI disproportionation (reaction 2) has been analyzed by different investigators (e. g. Thomas et al., 1980; Palmer and Lyons, 1988), with somewhat conflicting results. Measurements of Wren et al. (1986) have shown that the rate of disproportionation in alkaline solutions can be expressed as a function of the concentrations $[I_2 + I_3^- + IO^- + I_2OH^-]$, with the iodine +1 oxidation state species IO^- being the primary component, and the reaction proceeding through the +3 species IO_2^-. In addition, the rate of disproportionation is catalyzed by both phosphate and borate buffers.

Three typical examples of the results of these calculations which are of interest in reactor accident considerations are shown in Fig. 7.24. The tendency of these results can be summarized as follows: At pH 5, 100 °C and an initial I_2 concentration of 10^{-4} g-atom/l, iodate formation proceeds very slowly, reaching the same concentration as I_2 after about 1 day; the equilibrium state of the reaction would only be established after about 100 days. This means that over a comparatively long period of time one has to deal with rather high fractions of the molecular species I_2 and HOI. Raising pH to about 7 at the same temperature results in a much faster IO_3^- formation, with the equilibrium state already being established after about 10 minutes. At lower temperatures, the reaction rates are correspondingly lower. In solutions with very low total iodine concentrations, the I_2 fraction decreases very quickly at pH 7; however, HOI disproportionation proceeds rather slowly with the consequence that the equilibrium state of reaction (3) is attained only after several days.

There is comparatively little detailed information on the kinetics of the backreaction (3), i. e. on the formation of I_2 in solutions containing I^- and IO_3^- (the so-called Dushman reaction) in the pH range under consideration. This question is of interest with regard to the evaluation of I_2 supply from the disproportionation products in the event that the I_2 fraction in the solution is diminished by volatilization. As far as is known, reaction (1) proceeds very rapidly also from the right to the left side, whereas the rate of the backreaction (3) seems to be too slow (Palmer and Lyons, 1988) to be of significance as a determinant of iodine volatility, compared to the effect of radiolytic oxidation of I^-. Only in the case of low radiation doses would the Dushman reaction be the controlling parameter for iodine volatilization rates from aqueous solutions.

The kinetic data obtained from most of the laboratory measurements as well as from theoretical calculations are fully valid only for the pure system $I_2 + H_2O$, as is the case for the thermodynamic data mentioned above; the presence of third partners in the solution may result in deviating reaction rates. In this context as well, the presence of a large excess of initial I^- besides the I_2 hydrolysis products

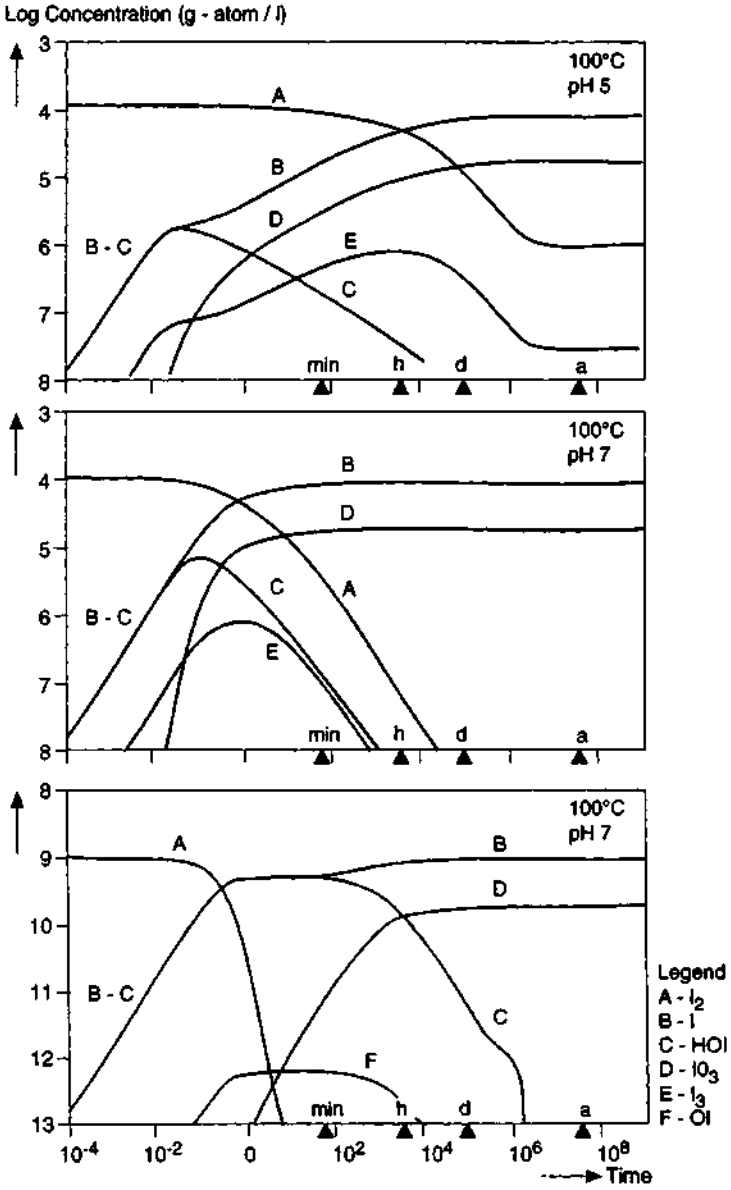

Figure 7.24. Kinetics of iodate formation
(according to Bell et al., 1982 b)

is of particular interest. According to Thomas et al. (1980), the rate of HOI disproportionation does not depend on the I^- concentration present in the solution, suggesting that an excess I^- will not (or not significantly) influence the reaction kinetics; an experimental verification of this theoretical statement, however, is still pending.

With regard to their partitioning between sump water and containment atmosphere, the different iodine chemical species produced in the I_2 hydrolysis and disporportionation reactions can be divided into two groups

- the molecular species I_2, HOI (and eventually HI) which may be volatile under the conditions prevailing in the containment; and
- the non-volatile ionic species I^- and IO_3^- (and possibly I_3^- and OI^-).

As a consequence of the volatility of the first group of species, a certain iodine concentration will be established in the gas phase above an aqueous solution containing iodine, the magnitude of which is determined by the parameters affecting the chemical equilibrium and, in addition, by the temperature. The characteristic term for the iodine concentration in the gas phase as a function of the iodine concentration in the solution is the partition coefficient K_d which is defined according to

$$K_D = \frac{[\text{iodine}]_{aq}}{[\text{iodine}]_g} \tag{9}$$

where [ ] denotes the relevant concentrations of iodine species present in the aqueous and the gas phases, respectively. Usually, volume-related concentrations are used; when mass-related concentrations are used, the different densities of liquid water and steam under the prevailing conditions of temperature and pressure have to be taken into account. In reactor accident chemistry, the equation in the form (9) is commonly used, in contrast with "classic" values in fossile power plant water chemistry where frequently the reciprocal value is employed. Equation (9) therefore means that lower iodine fractions in the gas phase are expressed by a higher partition coefficient and vice versa. When the behavior of radioactive iodine is to be evaluated, the so-called integral iodine partition coefficient is of particular importance, i. e. the ratio of the concentrations of total iodine (irrespective of its chemical form) in the liquid and gas phases. On the other hand, in order to understand the fundamentals of iodine volatility, the specific partition coefficients of the individual iodine species also have to be known.

The specific partition coefficient of the I_2 species and its dependence on temperature is well known. Experimental measurements performed by Toth et al. (1984) yielded results which are in satisfying agreement with the calculations made according to Henry's law (see Table 7.14.). The deviations between the theoretical data and the measured values, in particular at low temperatures, are assumed to be due to a solvatization of the I_2 molecule in water, leading to a decrease in the I_2 vapor pressure and, consequently, to an increase in the partition coefficient compared with the calculated values.

Considerably larger uncertainties have to be noted regarding the specific partition coefficient of hypoiodous acid HOI; in this respect, several contradictory mea-

Table 7.14. Specific I_2 partition coefficients (according to Toth et al., 1984)

Temperature	measured K_d	calculated K_d
19 °C	108	97.1
52 °C	29.7	27.2
86 °C	11.6	11.4
92 °C	10.9	10.3
151 °C	5.1	5.2

surements have been reported, which shall be discussed shortly. While Styrikovich et al. (1964) have claimed HOI to be the dominant iodine species at low concentrations in high-temperature steam, no HOI volatility was assumed by Eggleton (1967) in his calculations of the integral iodine partition coefficient at 100 °C. The identification of HOI in the gas phase above an aqueous iodine solution performed by mass spectrometry measurements was reported by Kabat (1980) and from these data an HOI partition coefficient of about 400 at 25 °C and of about 300 at 60 °C was derived. In contrast, Paquette et al. (1983) reported that mass spectrometry measurements in the gas phase above solutions showing total iodine concentrations in the range of 10^{-4} M did not give any indication on the presence of HOI; a small HOI^+ peak the intensity of which depended on the I_2 concentration in the gas phase was interpreted to belong to a secondary iodine species which was produced by reactions between I_2 and H_2O in the mass spectrometer ion source. Mass spectrometric studies of Wren and Sanipelli (1984) indicated very low or even essentially zero volatility of HOI. Experiments reported by Toth et al.(1984) on solutions with iodine concentrations on the order of 10^{-4} M showed that no HOI could be detected in the gas phase by absorption spectrometry; from these findings, an HOI partition coefficient significantly higher than 10^4 at 20 °C was estimated.

The problems involved with the direct measurement of HOI in the gas phase have favored the determination of the partition coefficient of this species by indirect methods. Investigations carried out by Lin (1981) on iodine volatility from dilute aqueous solutions showed that, depending on the iodine concentration present, the iodine species seems to be the determining parameter for the integral iodine partition coefficient. With concentrations in the aqueous phase greater than 10^{-6} g-atom I/l, the partition coefficient is controlled by the behavior of I_2 (according to the results of selective filter measurements), whereas at lower concentrations a different iodine species is the dominant contributor to the total iodine concentration in the gas phase – this compound was identified as HOI, according to its behavior on selective filter devices. From these measurements, HOI partition coefficients were calculated ranging from about 7000 at 20 °C to about 240 at 100 °C. From these results the data shown in Fig. 4.13. can be explained; in this curve, the experimentally determined partition coefficient down to total iodine concentrations in the solution of about 10^{-6} g-atom/l increases in agreement with the values which can be calculated taking into account the decreasing I_2 fraction in the solution. As can be seen from the figure, at lower concentrations the partition

coefficient obviously does not depend on the iodine concentration; this horizontal branch of the curve would correspond to an HOI partition coefficient on the order of 8000 at 21 °C and of 1650 at 72 °C. Harrell et al. (1988) reported an HOI partition coefficient of about 930 at 20 °C which was determined through measurement of the integral iodine partition coefficient at pH 9 and subsequent correction for I_2 volatility by using data which had been calculated according to Henry's law. Such an indirect method of determination might be susceptible to error, so the results should be viewed with some reserve.

Recently Barnes et al. (1992) have reported on spectroscopic measurements of gaseous HOI using Fourier transform infrared spectrometry (FTIR). The compound was generated by UV irradiation of $I_2-H_2O_2$, $CH_3I-H_2O_2$ and $CH_2I_2-H_2O_2$ mixtures and showed two absorption features at wavenumbers 1070 and 3620 cm^{-1}. In the dark, HOI was observed to decay with a first-order rate constant on the order of 10^{-2} s^{-1} at 298 K (corresponding to a lifetime of 1 to 2 minutes). This reaction rate indicates that heterogeneous reaction with the walls of the reaction chamber is not the responsible mechanism for decomposition, since this effect would result in a considerably smaller rate constant (10^{-4} s^{-1}).

According to current knowledge, the specific partition coefficient of HOI seems to be significantly higher than that of I_2. Consequently, it can be assumed that iodine volatility under the conditions prevailing in the containment in the course of a severe reactor accident is governed by the partition coefficient of I_2 (besides that of organoidide compounds) and that HOI volatility is only of minor importance. At much lower total iodine concentrations in the water phase and at temperatures well above 200 °C, however, HOI volatility may be of significance with respect to iodine volatilization.

As was mentioned above, for the evaluation of radioiodine behavior in light water reactor accidents, the specific partition coefficient of a particular iodine chemical species is usually of minor interest as compared with the integral partition coefficient including all iodine chemical species. The results of calculations of the integral iodine partition coefficient above an initially pure I_2 solution at 100 °C which were carried out by Eggleton (1967) are shown as an example in Fig. 7.25. and they clearly demonstrate the impact of solution pH and of the total iodine concentration. In these calculations no HOI volatility has been considered and complete attainment of the equilibrium state of equation (2) has been assumed. The differences in the partition coefficients which are frequently found in the literature are often the result of differing assumptions concerning the progress of this reaction. These differences in the assumptions as to the establishment of the equilibrium state of iodate formation can result in differences in the partition coefficient amounting to several orders of magnitude.

Hence, the most important parameter for the magnitude of the integral iodine partition coefficient is iodate formation and, consequently, as a result of the rather slow rate of HOI disproportionation in the pH range 5 to 7, a time-dependent value of the partition coefficient can be expected. This effect, quantitatively predicted by the kinetic calculations e. g., of Bell et al. (1982 b), has been confirmed by numerous measurements. As an example, the experimental investigations of Beahm and Shockley (1983) shall be mentioned, which show that at a total iodine concentra-

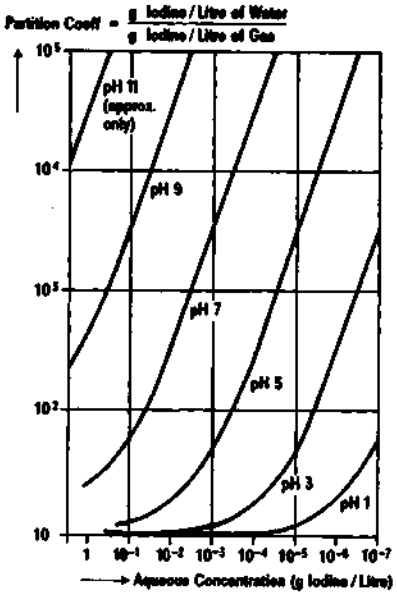

Figure 7.25. Iodine partition coefficient as function of solution pH and total iodine concentration (no HOI volatility assumed)
(Eggleton, 1967; by courtesy of AEA Technology plc)

tion of 10^{-4} g-atom/l (pure I_2 solution) at pH 7 the partition coefficient at 25 °C increases markedly with time, from an initial value (22 minutes after start of the experiment) of 190 to about 1200 after 310 hours. Due to the faster progress of HOI disproportionation (reaction 2) at higher temperatures, the rate at which partition equilibrium is reached increases significantly with increasing temperature.

Due to the increasing vapor pressure of I_2 the integral iodine partition coefficient decreases with increasing temperature. At temperatures above 100 °C, however, a further increase in temperature does not influence significantly the partition coefficient. This behavior is the result of two competing effects: the higher vapor pressure of I_2, on the one hand, and the decreasing specific I_2 concentration in the solution due to a higher degree of hydrolysis and iodate formation on the other.

The equilibrium partition state is not established instantaneously, not only because of its dependence on the disproportionation of HOI, but also because of the mechanisms of iodine transport in the liquid and gas phases. Under isothermal conditions, i. e. when both phases are at the same temperature, I_2 molecules present in the water phase have to be transported by diffusion to the gas–liquid boundary layer from where they can pass over to the gas phase. When, however, the liquid phase shows a higher temperature than the atmosphere, diffusion transport will be supported by convection in the water phase. In the case of a boiling iodine solution the rate of I_2 carry-over to the gas phase is greatly enhanced as a consequence of the vigorous convection within the solution. Usually, the time taken to reach the equilibrium state of iodine partitioning is not of significance for the situation inside

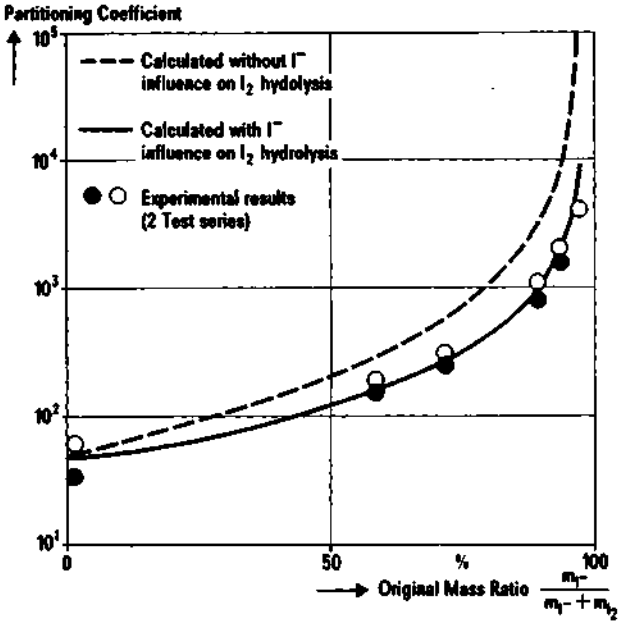

Figure 7.26. Iodine partition coefficient of I_2 – I^- mixtures (Richter and Neeb, 1985; by courtesy of AEA Technology plc)

the closed containment. In transient situations, however, the concept of equilibrium partition coefficients cannot be applied; instead, volatilization rates have to be used in such a case (see Section 7.3.4.3.).

All the results discussed above were relative to the pure system starting from $I_2 + H_2O$. As has been mentioned, in the situation of a core melt accident one has to deal with solutions containing a mixture of I^- and I_2, usually showing a large excess of initial I^-. At the containment temperatures to be considered, no measurable volatility is to be expected for I^- from aqueous solutions. Alm et al. (1979) have derived from measurements made on pure iodide solutions in dilute boric acid, an I^- partition coefficient of about 10^5 (pH 5, 100 °C, 10^{-2} gI/l) and have explained this value by the volatility of hydrated I^- ions. However, possible alternative explanations such as I^- carry-over by droplets (entrainment), volatility of HI or the presence of trace amounts of I_2 in the iodide solution due to air oxidation may be more probable; according to a rough estimate, the apparent I^- partition coefficient mentioned above could be caused by an I_2 fraction in the test solution of about 0.05%.

Systematic investigations of integral iodine partition coefficients in $I^- - I_2$ mixtures at pH 5.3 and 100 °C were reported on by Richter et al. (1985 a) as well as by Richter and Neeb (1985). These results demonstrated that, as expected, the partition coefficient increases with decreasing I_2 fraction in the solution; as can be seen from Fig. 7.26., at high excess I^- a pronounced increase in the partition coefficient is observed, reaching a value of about 10^4 at a mixture of 98% I^- + 2% I_2 (total iodine concentration 10^{-2} g/l). These data, which were obtained after short

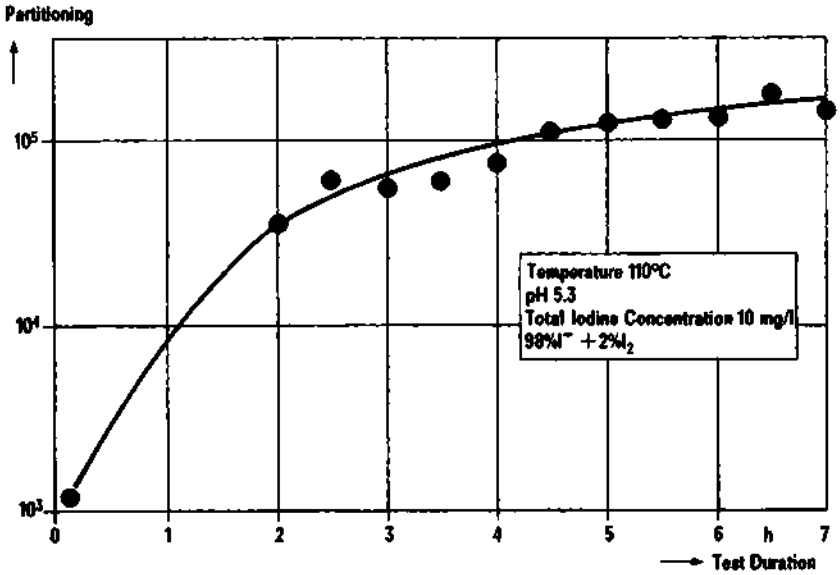

Figure 7.27. Iodine partition coefficient of an $I_2 - I^-$ mixture as a function of time (Richter and Neeb, 1985; by courtesy of AEA Technology plc)

experimental periods (i. e. which were not significantly affected by iodate formation), are in good agreement with the results of calculations of the influence of an excess of I^- on the I_2 hydrolysis equilibrium (1), resulting in a shift towards higher equilibrium concentrations of volatile iodine species (when compared to a pure I_2 solution). Due to increasing iodate formation, the partition coefficient of I_2-I^- mixtures increases considerably within a rather short time even in a boric acid solution at 110 °C, from an initial value of about 10^3 to more than 10^5 after 7 hours (Figure 7.27.). Experiments in a $2\,m^3$ pressure vessel at 170 °C with I^-–2% I_2 solutions yielded partition coefficients of 10^5 to 10^6 after a few hours (Richter and Neeb, 1985).

The comparatively high values of the integral iodine partition coefficient measured in the large-scale CSE tests (see Section 7.3.3.4.8.) at temperatures between 80 and 120 °C, which were about $2 \cdot 10^4$, are presumably due to the presence of considerable fractions of iodide in the solution, which had been formed in the feed line from the I_2 originally added. The influence on the partition coefficient of reducing constituents in the solution will be treated in more detail in Section 7.3.3.4.3.

The discussion of iodine partition coefficients in this section relates solely to a gas phase consisting of saturated steam which is in thermal equilibrium with liquid water. With increasing steam temperatures and pressures, dissociated compounds such as CsI also exhibit an increasing volatility with steam; according to the measurements reported by Styrikovich and Martynova (1963), NaCl shows a partition coefficient of 10^5 to 10^6 at a steam pressure of 7 MPa. Beyond the critical temper-

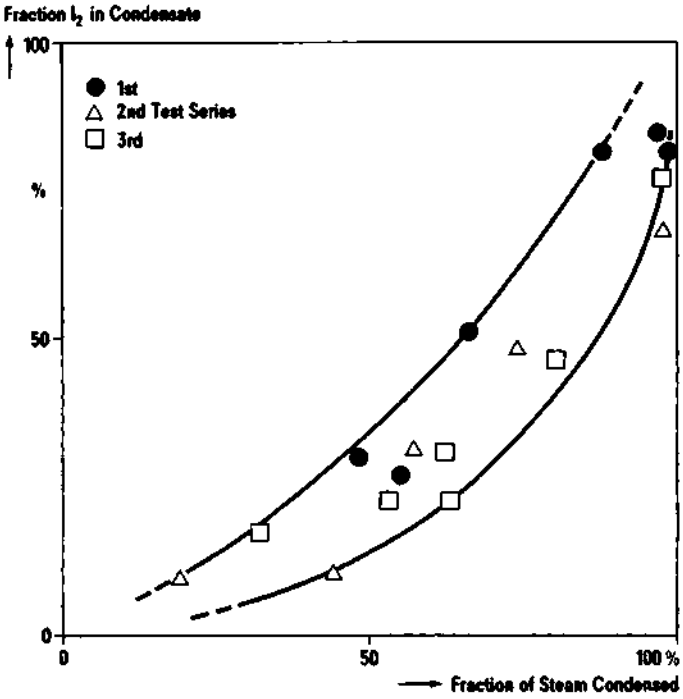

Figure 7.28. Plate-out of steamborne I_2 during partial condensation of steam (Richter and Neeb, 1985; by courtesy of AEA Technology plc)

ature of water (374 °C), the partition coefficient of all these compounds, including the iodides, reaches a value of 1. This type of volatility, however, is of no relevance whatsoever for severe reactor accidents; the only possible exception is the direct vicinity of the overheated reactor core where the steam temperature may be higher than the critical temperature of water.

In the course of a complete or partial condensation of I_2–containing steam, a fraction of the I_2 is simultaneously plated out into the liquid phase. Relevant investigations have indicated that a close correlation exists between the condensed fraction of the steam and the co-condensed I_2 fraction (Richter and Neeb, 1985). As can be seen from Fig. 7.28., the exact trend of the I_2 plate-out, which is somewhat smaller than the degree of steam condensation, depends on the particular condensation conditions, explaining the relatively broad range of scatter of the individual measurement points. The measured values shown in Fig. 7.28. correspond to iodine partition coefficients between 650 and 1400, depending on the particular condensation flows and iodine concentrations. According to Weber et al. (1992), diffusiophoresis is the essential mechanism controlling I_2 plate-out with the condensing steam.

It has to be pointed out that most of the partition coefficient values obtained in laboratory experiments are representative only of "clean conditions" and do not

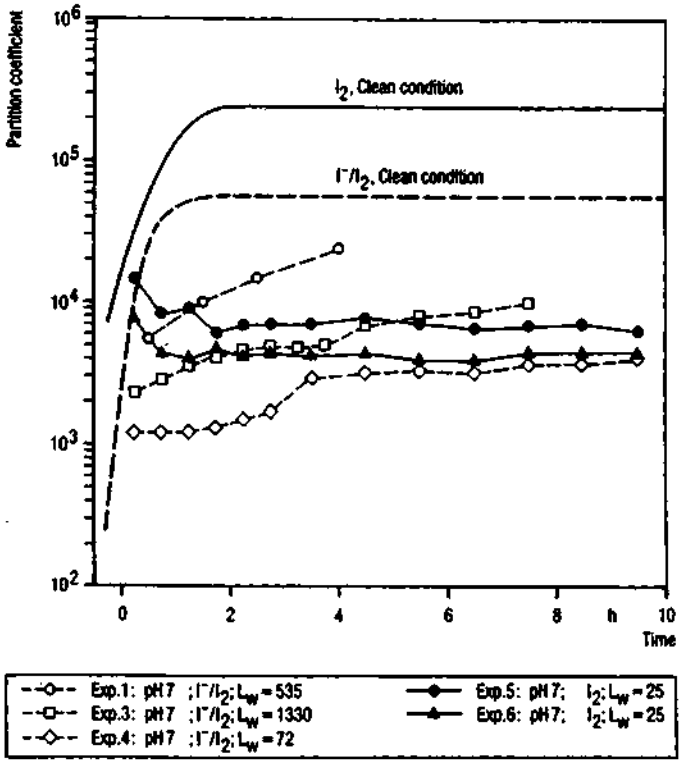

Figure 7.29. Clean-condition I_2 partition coefficients compared to effective I_2 partition coefficients measured in a technical-scale apparatus
(Bleier et al., 1988)

take into account side reactions that can take place under real accident conditions. As an example, attention is drawn to the data shown in Fig. 7.29., which were obtained in experiments performed in a 2 m^3 vessel, the inner surface of which was provided with an organic coating (Bleier et al., 1988 b). These technical-scale values are markedly lower than those obtained in the corresponding clean-condition experiments and they tend to long-term values which are virtually independent of the initial composition of chemical iodine species. The reason for this behavior is probably the formation of organoiodine compounds under these experimental conditions, even in the absence of ionizing radiation. When organic iodine compounds are present (e. g. CH_3I), their concentration in the gas phase has to be added to that of the equilibrium species in order to obtain the total iodine concentration and, thus, the value which determines the behavior of radioiodine in severe accidents. As an example, when about 10^{-11} g-atom CH_3I/l are present in the gas phase (which corresponds roughly to the TMI-2 situation) above a solution with 10^{-6} M total iodine at 25 °C and pH 8, then the partition coefficient of radioiodine will decrease from $1.8 \cdot 10^7$ to about 10^5.

When the data on iodine partition coefficients are applied to the conditions prevailing in accident sequences where an early failure of containment isolation is postulated, the kinetics of establishing the partition equilibrium are of great interest. But, because of the very large dimensions of the containment and the complicated structures within it, it is very difficult to deduce such results from measurements carried out under laboratory conditions. An additional question which may significantly influence the time behavior of the iodine concentration in the containment atmosphere is whether all the fission product iodine escaping from the break in the primary circuit is at first transported to the atmosphere or whether a significant fraction of it is directly plated out to the sump water by condensing steam (see Fig. 7.28.). The time-dependent concentration of iodine in the atmosphere can be assumed to be greatly influenced by the extent of spontaneous I_2 condensation; however, quantitative data on the situation in the containment are still lacking. Despite these uncertainties, it can be postulated that, in the most unfavorable case, the fission product iodine concentration in the containment atmosphere during the first hours after the release of the fission products from the reactor core will be on the same order of magnitude as the equilibrium concentration.

In the very unlikely event that the steam losses caused by a containment failure cannot be replaced and, in addition, when it is not possible to cool the sump water down below its boiling point, the sump water will boil off. Under extreme conditions it will reach dryness in the course of about 10 days (depending on the design of the plant). In the first stage of this process, the I_2 still present in the aqueous phase will be transported to the steam at a rate controlled by the water evaporation rate and the respective iodine partition coefficient, as was concluded by Richter et al. (1985 b) from measurements performed with vigorously boiling solutions (heating power $3\,W/cm^2$ surface area). Moreover, additional I_2 will be generated by radiolytic oxidation of I^- (see Section 7.3.3.4.4.), and will subsequently be volatilized, but now according to its production rate. This can be assumed to be comparatively low in the absence of dissolved oxygen, which, for the most part, has already escaped from the solution during depressurization of the containment volume. On the other hand, Beahm et al. (1992) calculated that the iodine fraction which is volatilized during evaporation of a water pool to dryness will depend highly on the initial pH of the sump water solution. According to these results, radiation enhances I_2 production considerably by oxidation of I^-, in particular in solutions with an initial pH that is markedly below the neutral point. By contrast, I_2 production in the solution from I^- and IO_3^- according to the Dushman reaction can be assumed to be quite low under the conditions prevailing in the sump water and, thus, not to contribute significantly to iodine volatilization.

In large volumes of sump water, HI does not contribute significantly to iodine volatility, due to its virtually complete dissociation in the solution. However, it cannot be ruled out that in the final stage of the boiling down of the sump water, non-dissociated HI will be produced in the now concentrated solution and that this compound can be volatilized with steam. Preliminary experiments reported by Furrer and Bühler-Gloor (1988) showed that during evaporation of a CsI solution to dryness, the volatilized proportion of iodide depended highly on the initial solution pH. In the presence of boric acid in the solution, up to about 15% of the

iodide present was volatilized; addition of metallic silver, of core structural materials (simulated aerosols) and of concrete decomposition products did not influence the volatilization behavior. When the solution pH was kept constant by addition of a phosphate buffer, iodine volatilization decreased to a few percent. Since iodide was the only species detected in the condensate, it was concluded that HI was the volatile iodine compound. Generally, the conditions in the highly concentrated sludge which is present during the final stage of evaporation of sump water in a real reactor accident are very difficult to evaluate; on the other hand, it can be assumed that this stage does not significantly contribute to the total fission product iodine release from the containment and, moreover, that in reality such an evaporation to dryness can be ruled out by the different measures which will be taken to counter the effects of the accident.

7.3.3.4.3 Influence of solution partners on iodine chemistry in the sump water

In the preceding section, iodine chemistry and the iodine partition coefficient in a pure iodine solution have been discussed. The containment sump water which is to be expected in a severe reactor accident, however, may contain a number of other substances that have a potential impact on the chemical reactions and on the resulting reaction products. It is not possible to give detailed and trustworthy information on the nature and the concentrations of all these substances, which in addition might be different in different accident sequences and in different plants; therefore, only some of them can be treated here exemplarily. The particular case of the presence of an excess of I^- in the I_2-H_2O system and its implications for the iodine species distribution and for the partition coefficient have been discussed in the preceding section.

One of the parameters determining the fractional concentrations of the different iodine oxidation states in the solution is the redox potential of the sump water. Under severe accident conditions its value is governed not only by the concentration of dissolved oxygen in equilibrium with the oxygen content of the containment atmosphere. Radiolysis of water (see Section 7.3.3.4.4.), through the formation of oxidizing as well as of reducing products, significantly influences the redox potential. In addition, dissolved hydrogen will be present in the sump water in equilibrium with the hydrogen content of the containment atmosphere, originating in the hydrogen production caused by the metal–steam reactions occurring in the reactor core. Likewise, coupled redox systems (such as Fe^{2+}/Fe^{3+}) may influence the resulting redox potential. Because of the multitude of influencing parameters, calculation of the redox potential to be expected in real sump water is very difficult or even impossible. Further, it will highly depend on the details of the particular accident sequence.

According to the calculations of Lemire et al. (1981), in a neutral solution with a total iodine concentration of 10^{-9} g-atom/l the partition coefficient shows a mini-

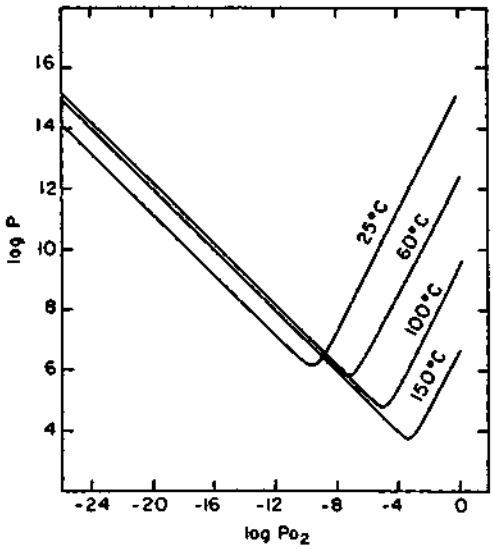

Figure 7.30. Iodine partition coefficient as a function of the redox potential in terms of O_2 concentration of the solution
(Lemire et al., 1981; by courtesy of Atomic Energy of Canada Limited)

mum at an oxygen partial pressure of about 10^{-8} bar at 25 °C, with this value increasing to about 10^{-4} bar at 150 °C (see Fig. 7.30.). At lower oxygen partial pressures, I_2 will be reduced to I^-, at higher partial pressures it will be oxidized to IO_3^-, with both reactions resulting in a decrease in the concentrations of volatile iodine species and, consequently, in an increase of the partition coefficient. Paquette et al. (1983) reported that the direct oxidation of I^- by dissolved oxygen at low iodine concentrations and at a solution pH near the neutral point proceeds at a rather slow rate. The rate might be enhanced by UV light and is increased in the presence of trace impurities such as Fe^{3+} and Cu^{2+}. As yet, no detailed information has been published on the direct oxidation of HOI by dissolved oxygen.

At room temperature, only a small fraction of dissolved iodide will be oxidized to form volatile iodine species (Evans et al., 1993). In dilute solutions the rate of iodide oxidation was found to be proportional to the square root of the iodide concentration; under acidic conditions the rate increases with decreasing pH while in basic solutions it is virtually unaffected by changes in pH. The progress of oxidation of I^- by dissolved oxygen at elevated temperatures was studied by Burns and Marsh (1986) and was found to proceed at 100 °C in the presence of boric acid at a higher rate than in the absence of this substance. The rate of I^- oxidation to I_2 depends on the solution temperature: it increases with increasing temperature and, at higher temperatures, reaches an almost constant value after a certain time (see Fig. 7.31.). At 300 °C, iodate was formed at a rate which was not influenced by the presence of boric acid and which did not depend on the concentration of dissolved oxygen, if oxygen was present at all; by contrast, at 100 °C no iodate formation was observed. The I_2 formed is subjected to hydrolysis and disproportionation at

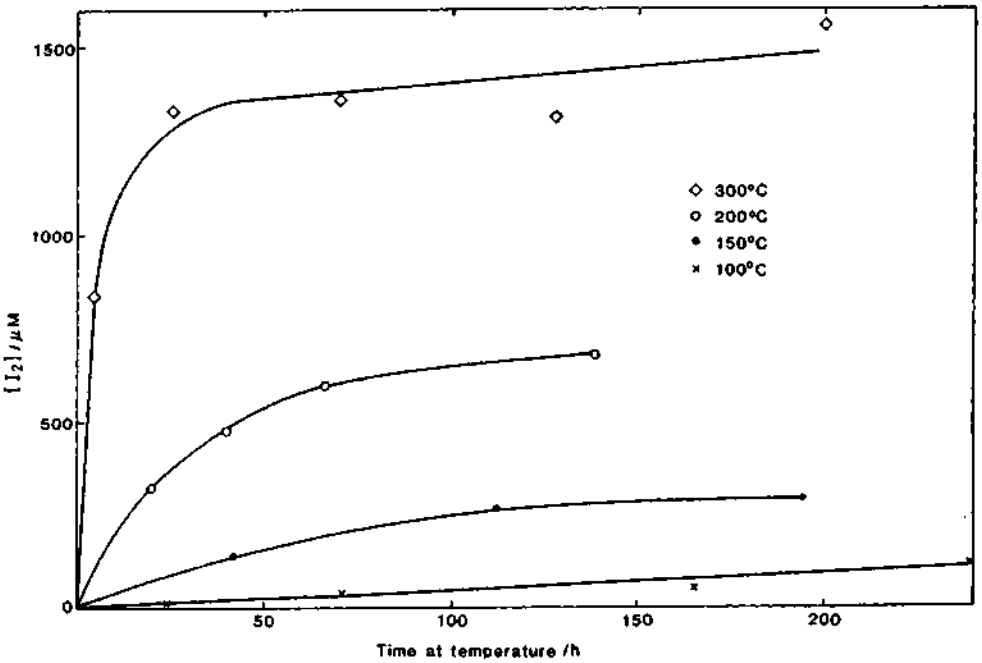

Figure 7.31. Thermal oxidation of aqueous iodide solution at 100 to 300 °C (CsI 0.1 M; H_3BO_3 0.2 M; aerated)
(Burns and Marsh, 1986; by courtesy of AEA Technology plc)

a rate and with an equilibrium state depending both on temperature and solution pH. In total, thermal oxidation of iodide is assumed to be of minor significance under accident conditions, since the radiation-induced oxidation proceeds much faster.

I_2 and HOI present in the sump water can be reduced rather quickly by reducing substances such as organic impurities, hydrazine and metallic trace impurities like Fe^{2+} and Cu^{+}. Dissolved iodate is only slowly reduced by these substances. Addition of 100 ppm $Na_2S_2O_3$ to a solution containing 0.05 g I_2/l rises the partition coefficient from 900 to $3 \cdot 10^5$; addition of 100 ppm hydrazine results in a partition coefficient of about $3 \cdot 10^4$ (Postma, 1980). On the other hand, it was concluded from comparative measurements in pure water and in spent fuel pool water at comparatively low temperatures that hydrazine concentrations up to 60 ppm do not significantly affect the iodine partition coefficient (Pelletier and Hemphill, 1979).

The role of ionizing radiation as an oxidizing or reducing agent for iodine will be discussed in the following section.

Sump water pH is the most important parameter for controlling the iodine partition coefficient, as was discussed in the preceding section. When the sump water is merely composed of the primary coolant and the emergency core coolant solutions (boric acid solution), a pH on the order of 5.5 has to be expected. Addi-

tion of pH correctives, such as sodium triphosphate or the alkaline containment spray solution, leads to an increase in pH to values in the range 7 to 8. Under the influence of a strong radiation field, nitric acid may be generated from the nitrogen present in the moist containment atmosphere, the consequence of which would be a decrease in sump water pH. Finally, the fission products dissolved in the sump water, as well as leached concrete constituents, are also able to influence pH to a certain extent. Due to these different influencing parameters, calculation of the sump water pH to be expected in the course of a severe reactor accident is quite difficult. A model for pH calculation which takes into account all these parameters was recently given by Weber et al. (1992).

The sump water pH can also be influenced by CO_2 and organic acids which are produced by the interaction of organic paints and coatings with the radiolysis products of water. Irradiation of these organic materials in aqueous solution gives rise to the formation of a variety of organic degradation products, among which aliphatic ketones, alcohols and aldehydes are assumed to have the most pronounced effect on the solution pH; these compounds are soluble in water and decompose rapidly to form CO_2 and organic acids. Experiments conducted in the Canadian Radioiodine Test Facility (RTF) have shown that there is a rapid decrease in pH over the first 15 hours of irradiation, after which a steady-state level is reached; the gas-phase iodine concentration proved to increase parallel to the decrease in pH. With vinyl paints the decrease in pH was considerably more pronounced than with other organic materials such as epoxy paints. The results indicated that methyl isobutyl ketone, a thinner used in vinyl paints, was the main source of organic products, with acetone, formaldehyd and acetaldehyd being the main radiolysis products (Ball et al., 1994).

Other redox-inert impurities present in the sump water are not expected to affect significantly the fractional concentrations of the individual iodine species (e. g. Pelletier and Hemphill, 1979). An exception which might be of relevance in a severe accident environment is the presence of metallic silver in the boric acid solution. This silver originates in the PWR control rod materials: a 1300 MWe PWR core contains a silver mass inventory which is higher by about a factor of 100 than the fission product iodine inventory in the equilibrium fuel burnup state. However, there is currently no detailed knowledge of the nature, the particle size and the specific surface area of the silver-containing particles which will be present in the sump water. In the absence of ionizing radiation and of other oxidizing agents, iodide reacts only to a negligible extent with metallic silver, whereas I_2 in the solution at 100 °C undergoes a rather fast reaction under formation of AgI layers on the silver particles. The progress of this reaction is controlled by kinetics: after a relatively fast formation of 10 to 50 monolayers, the further reaction proceeds rather slowly, with the reaction rate then being controlled by diffusion in the solid Ag/AgI. The rate of AgI formation on the silver surface also depends on the I_2 supply to the surface and, therefore, is supported by convective movement of the solution (Richter et al., 1985 b; Moers, 1986). As yet, a generally valid theoretical treatment of the rate of buildup of the AgI layer has not been worked out. A comprehensive experimental parameter study is currently being carried out at the Siemens/KWU radiochemical laboratory (Hellmann, personal communication).

In the absence of a radiation field, iodide present in the solution is only able to form a very thin deposit on the silver surface of up to one half of a monolayer, while under irradiation this species reacts to an extent comparable to that of original I_2, with the first step probably being the oxidation of dissolved I^- to an intermediate atomic iodine species. In the presence of dissolved air or oxygen in the solution, the reaction of I^- and metallic silver proceeds at a rate on the same order of magnitude as that induced by a radiation field of about 5 kGy/h (Furrer and Gloor, 1985), suggesting that intermediately generated iodine atoms are the reaction partner. Similar results were reported by Beahm et al. (1986), showing that under irradiation (10 kGy) I_2, I^-, and CH_3I present in the solution are readily and almost completely converted to AgI. The first step in the CH_3I reaction probably is radiolytic decomposition of this compound to form iodine atoms, which then react with the silver metal. The specific surface area of the silver metal strongly affects the reaction rate, with a silver-containing aerosol agglomerate being much more effective in iodine conversion than commercially available silver powder of the same mass. These results indicate that AgI formation under such conditions is a pure surface reaction.

The formation of water-insoluble AgI removes a fraction of the iodine from the solution equilibria, resulting in a reduction of the dissolved I_2 concentration and, consequently, in an increase of the partition coefficient. However, similar to its sensitiveness to UV light, AgI is not completely stable against ionizing radiation, but will tend to be decomposed again to form I_2. Measurements originally performed regarding the long-term storage of radioactive waste from reprocessing plant iodine retention filters showed a quite low decomposition rate, amounting to about 10^{-3}% decomposition after an exposure of 10 MGy in a water environment (Lieser et al., 1985). On the other hand, Furrer and Gloor (1985) in their studies on the $Ag-I_2$ reaction in the presence of radiation observed a residual steady-state fraction of about 0.2% I_2, which probably was the result of radiation-induced decomposition of AgI.

Another feature potentially affecting iodine behavior under severe accident conditions is solubility of AgI in the sump water solution. The solubility data in the literature (see Gmelin, 1972) cover neither the temperature range nor the solution composition of interest. In order to determine whether or not the mass of AgI potentially formed will exceed the solubility product of this compound, studies of the solubility of AgI in boric acid solution (2000 ppm B) at 160 °C have been performed in the Siemens Radiochemical Laboratory (Funke, to be published). From Fig. 7.32., where the measured solubility value is shown together with the data from the literature, it can be seen that AgI solubility increases with increasing temperature, reaching a value of about $1 \cdot 10^{-5}$ mol/l at 160 °C. This value means that, when one assumes that the entire mass of iodine is ready for reaction with silver to form AgI, insoluble AgI is stable in the solution and is able to tie up the largest fraction of iodine to form a solid compound. Taking into account additionally the large excess of metallic silver to be expected in the sump water solution, it can be concluded that this reaction is an efficient trap for dissolved iodine and would be able to reduce iodine volatility considerably in a real accident environment.

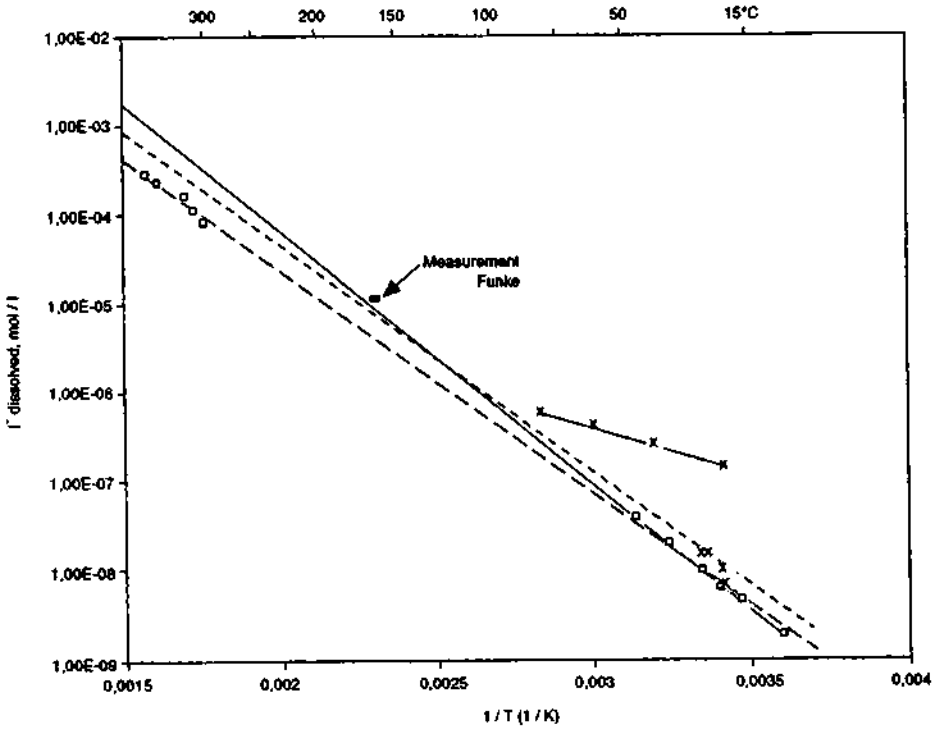

Figure 7.32. Solubility of AgI in water
(By courtesy of Dr. Funke)

The presence of Cu^+ ions in the sump water potentially results in the formation of insoluble CuI; it is questionable, however, whether the concentrations of both partners are high enough to allow formation of a solid compound and, thus, to influence the iodine partition coefficient.

7.3.3.4.4. Effects of ionizing radiation on iodine chemistry in the containment

In the preceding sections, iodine chemical reactions within the containment were discussed exclusively from the perspective of classic chemistry. However, following a severe reactor accident, the sump water as well as the containment atmosphere are affected by strong radiation fields which may give rise in particular to changes in the chemical states of fission product iodine, resulting either in a conversion of non-volatile iodide to volatile I_2 and/or organoiodide or in a decomposition of the volatile species to non-volatile dissolved ones. As will be shown in the following

Table 7.15. Radiation dose rates in the containment atmosphere following core melt (By courtesy of Siemens/KWU)

Time (hours)	β dose rate (Gy/h)	γ dose rate (Gy/h)
1	46900	3000
4	23000	1500
6	18500	1200
48	4310	400
84	3130	320
132	2060	250

section, besides sump water pH the radiation-induced reactions are probably the dominating parameters in establishing the final chemical states of iodine.

As a consequence of the release of radionuclides from the nuclear fuel in the course of a severe core damage accident and of their transport to the closed containment, the gaseous and the liquid phases there are exposed to a considerable radiation dose rate. The dose rate in the containment atmosphere is essentially caused by the fission product noble gases; the contribution of other radionuclides present in the containment atmosphere is negligible. Under the assumption of a complete volatilization of the noble gases from the reactor core, the values shown in Table 7.15. were calculated for the containment atmosphere of a 1300 MWe reactor as a function of time after core meltdown. In the sump water liquid phase, the non-volatile radionuclides plated out there also give rise to considerable dose rates. In the low-pressure sequence of a 1300 MWe PWR core melt accident with a sump water volume of 500 Mg and assuming a quantitative transport of the cesium and iodine core inventories to the sump water, the β dose rate 6 hours after core meltdown amounts to 3800 Gy/h and the γ dose rate to 25,400 Gy/h, totalling about 29,000 Gy/h (Siemens/KWU, unpublished).

The radiolysis of water leads to the appearance of a large number of oxidizing and reducing radical and molecular primary products; in pure water, absorption of 100 eV γ radiation results in the decomposition of water according to the generally accepted equation

$$4.9\ H_2O \rightleftharpoons 2.7\ e_{aq} + 2.7\ OH\cdot + 3.4\ H^+ + 0.7\ OH^- + 0.45\ H_2 + 0.75\ H_2O_2 + 0.6\ H\cdot \qquad (10)$$

In non-aerated solutions water radiolysis does not change the pH of the solution, while in aerated solutions it lowers the pH. The most important radiolysis products with respect to iodine chemistry are the radicals $OH\cdot$, e_{aq}^-, $H\cdot$ and the molecules H_2O_2 and H_2. Some of these primary products are highly reactive, leading to secondary reactions and resulting in a final composition which depends on the radiation dose rate as well as on the nature of the constituents of the solution. As an example, an increase in the radiation dose rate results in an increased formation of H_2O_2, which in turn may react with e_{aq}^- to form the $OH\cdot$ radical and the OH^- ion; on the other hand, formation of the oxidizing $OH\cdot$ radical may be suppressed

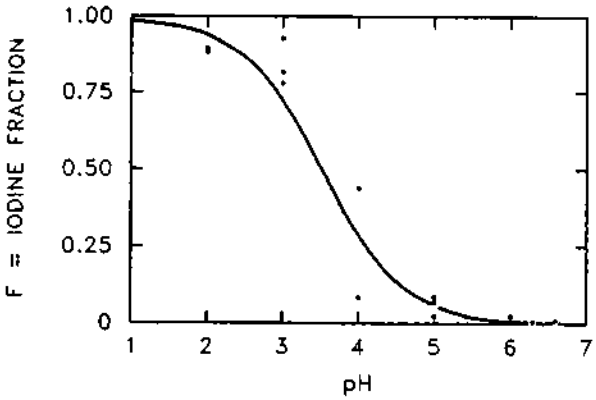

Figure 7.33. Effect of the solution pH on the radiolytic oxidation of iodide to I_2 (Lin, 1980; Copyright 1980, with kind permission from Elsevier Science Ltd, The Boulevard, Langford Lane, Kidlington OX5 1GB, UK)

by dissolved oxygen under formation of the reducing O_2^-. At higher solution pH the continued existence of the reducing radiolysis products is generally favored.

Iodine dissolved in the sump water, with its ability to readily change oxidation states, may be affected by the radiolytic primary products, with the hydroxyl radical OH· being the main oxidant. The aquated electron as well as the hydrogen atom (through reactions with oxygen to form the superoxide radical) and, in neutral and alkaline solutions, H_2O_2 are the reductants. As a result of such reactions, non-volatile iodide initially present in the sump water solution can be oxidized to form volatile species such as I_2, potentially increasing the concentration of iodine present in the containment atmosphere. On the other hand, I_2 can be reduced by radiation-induced reactions to non-volatile soluble species. The fundamentals of the radiation-induced iodine reactions in aqueous solution have been summarized by Sellers (1977); according to this review, the main reactions can be described as follows (the impact of ionizing radiation on the formation and decomposition of organoiodine compounds will be treated in the following section):

In the radiation-induced reactions, the yields of the different iodine species depend on the solution pH. With increasing pH, the radiolytic I_2 yield generally decreases, reaching very low values at pH 6 to 7 (see Fig. 7.33., according to Lin, 1980; Weber et al., 1991). In acid solutions, I^- will be oxidized by radiolytically produced OH· and H· radicals, as well as by H_2O_2, to form I_2 according to the summary reactions

$$2\,I^- + 2\,OH\cdot \rightleftharpoons I_2 + 2\,OH^- \tag{11}$$

$$2\,I^- + 2\,H\cdot + 2\,H^+ \rightleftharpoons I_2 + 2\,H_2 \tag{12}$$

$$2\,I^- + H_2O_2 + 2\,H^+ \rightleftharpoons I_2 + 2\,H_2O \tag{13}$$

with iodine atoms as an intermediate species. The yields of the reactions of iodide with H· and H_2O_2 increase strongly with decreasing solution pH, reaching virtually complete oxidation of I^- to I_2 at pH <3. The I_2 formed by all these reactions will

be subjected to the hydrolysis and disproportionation reactions mentioned in Section 7.3.3.4.2. On the other hand, the steady-state concentration of OH· in the irradiated solution decreases with increasing pH. In neutral solutions, I_2 is reduced by aquated electrons as well as by hydrogen atoms

$$I_2 + e_{aq}^- \longrightarrow I_2^- \tag{14}$$

$$I_2 + H\cdot \longrightarrow I_2^- + H^+ \tag{15}$$

The I_2^- ion is decomposed via the intermediate product I_3^- to form $I_2 + I^-$ again. At pH >7, the I_2 yield is below the detection limit due to both the rapid thermal disproportionation reactions and the reduction of I_2, as well as of HOI, by H_2O_2

$$I_2 + H_2O_2 \longrightarrow 2\,I^- + 2\,H^+ + O_2 \tag{16}$$

Since radiolytically formed H_2O_2 will accumulate in the aqueous solution, this reaction may have a significant impact on the final amount of volatile I_2 formed.

In order to rule out potentially interfering effects of secondary reactions on the extent of radiation-induced I_2 formation, Ashmore et al. (1994) have carried out experiments in which the I_2 produced was continuously removed from the irradiation vessel by an air flow and trapped in a solution for continuous measurement. These results confirmed that the rate of radiation-induced oxidation of I^- at ambient temperature depends strongly on the solution pH, decreasing by a factor of about 100 between pH 4.6 and pH 8. This strong effect within a comparatively narrow pH region underlines the importance of maintaining the solution pH, which can be affected by various mechanisms such as absorption of atmospheric CO_2 and of nitric acid produced by radiolysis of moist air, as well as by the formation of carboxylic acids by radiolytic or thermal decomposition of organic materials (see Section 7.3.3.4.3.). Thus, both in experimental solutions and in real sump water the use of solution buffers is highly advisable.

In addition, the radiolytic I_2 yield depends on the radiation dose applied. As can be seen from Fig. 7.34. (Burns et al., 1990), the I_2 yield increases with increasing radiation dose until it reaches an equilibrium value, at which I^- oxidation by the OH· radical is compensated for by I_2 reduction due to the action of e_{aq}, H·and H_2O_2. With increasing temperature of the solution, the I_2 equilibrium level decreases considerably, presumably due to accelerated I_2 hydrolysis and disproportionation. At still higher radiation doses (which, however, will be reached in the containment sump water within a rather short time) the I_2 equilibrium level decreases again, due to the reduction of the oxidizing OH· radical by H_2 to the reducing H· radical (see Fig. 7.35.).

According to these studies, the radiation dose rates seem to have little, if any, influence on the I_2 equilibrium concentration.

The influence of the solution temperature on the radiolytic I_2 yield is shown in Fig. 7.36. (Burns et al., 1990). Besides the higher rates of I_2 hydrolysis and disproportionation at elevated temperatures, the accelerated consumption of H_2O_2 by the IO^- ion to form $I^- + O_2$ is assumed to be responsible for this pronounced dependence. As was pointed out by Burns et al. (1988), at elevated temperatures (likely to be the case in accident conditions) hydrolysis of I_2 to form HOI becomes more important and the subsequent ionization to form OI^- and reaction with

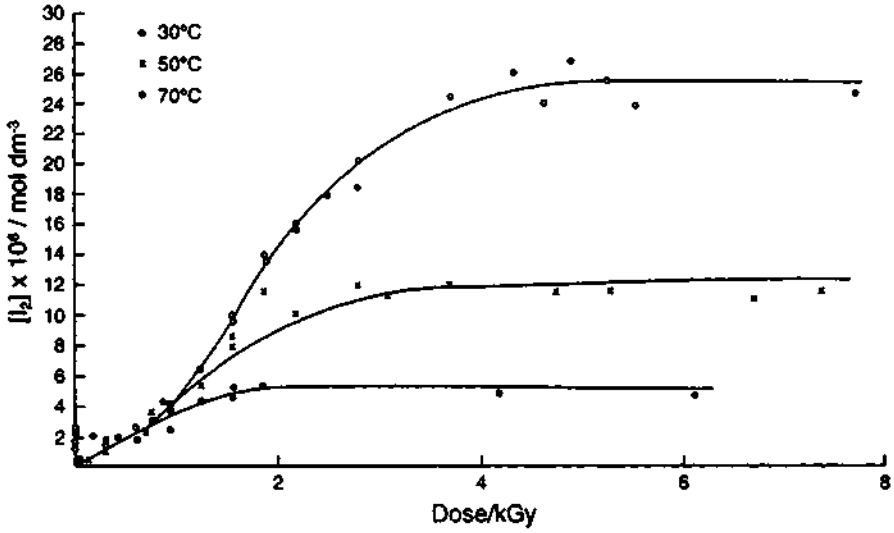

Figure 7.34. Formation of I_2 as a function of the radiation dose (medium dose levels) (Burns et al., 1990; by courtesy of AEA Technology plc)

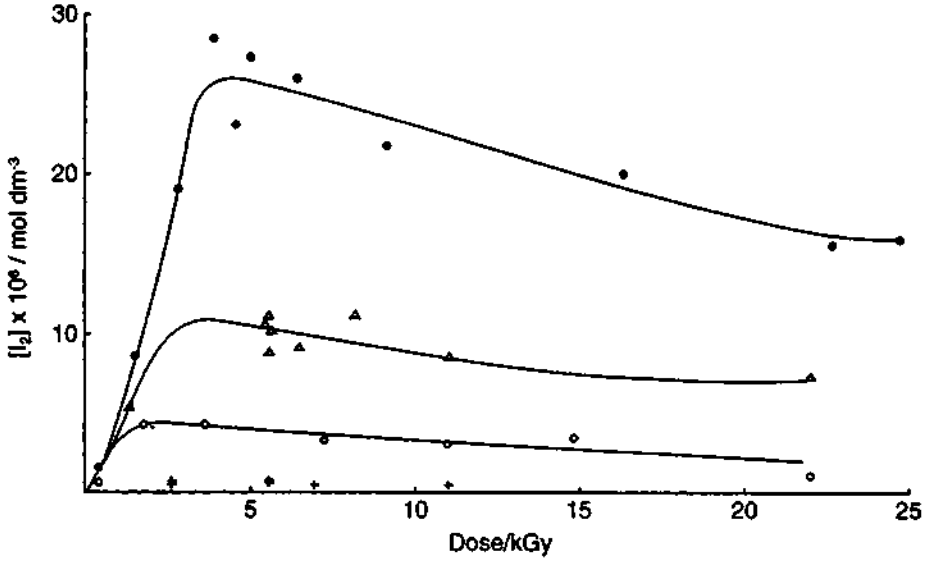

Figure 7.35. Formation of I_2 as a function of the radiation dose (high dose levels) (Burns et al., 1990; by courtesy of AEA Technology plc)

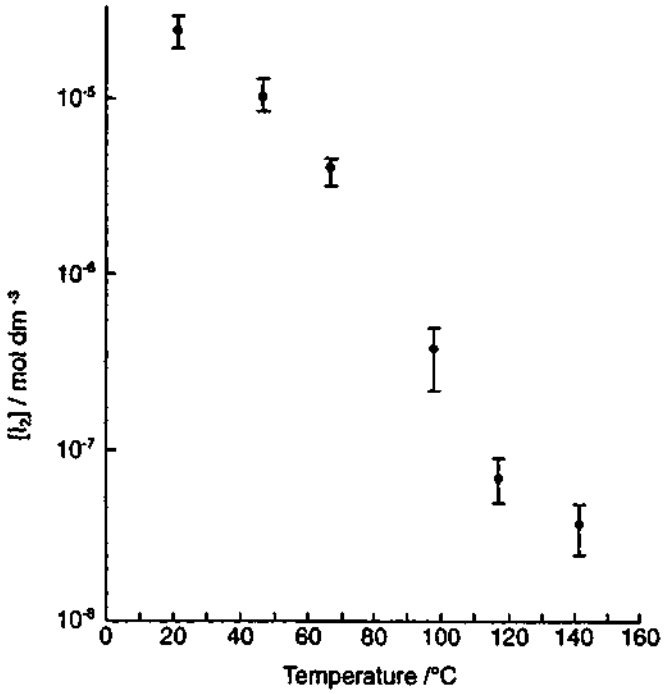

Figure 7.36. Radiolytic I_2 yield as a function of temperature (10 kGy; $1 \cdot 10^{-4}$ M I^-; 0.2 M H_3BO_3)
(Burns et al., 1990; by courtesy of AEA Technology plc)

peroxide to I^- are more efficient. The result of these reactions is less peroxide and less net oxidation; the steady-state level is reached at a lower concentration of these two species. These experiments showed that the steady-state I_2 concentration in a boric acid solution at 140 °C is about two orders of magnitude lower than at 30 °C. Boiling of the solution favors the oxidation of I^- to IO_3^-, in particular in dilute solutions ($< 10^{-5}$ mol/l). As a consequence of void formation during boiling, the H_2 and O_2 produced by radiolysis are rapidly removed from the solution so that the concentration of OH· radicals is not decreased due to reduction by H_2 (Karasawa et al., 1991).

According to the results reported on by Ashmore et al. (1994), the rate of radiation-induced I_2 formation in the solution does not strongly depend on the initial I^- concentration in the range 10^{-6} to 10^{-4} M; there are indications that this rate decreases with decreasing iodide concentration. Possible reasons for this fall of the rates at lower concentrations are side reactions with impurities present in the solution. In addition, the possible decrease in the concentrations of iodine-containing intermediates and even of I^- down to the same order of magnitude as that of some of the water radiolysis products, in particular of reducing O_2^-, would limit the extent of I_2 formation.

At low initial I^- concentrations ($<10^{-5}$ M), high radiation dose rates and a solution pH of less than 8, radiation-induced oxidation may also lead to the formation of iodate. However, different yields of iodate formation have been reported, ranging from almost complete I^- conversion (Lin, 1980) down to iodate yields of only about 10% of the initial I^- amount (Burns et al., 1988). Under the conditions mentioned above, iodate formation will be favored by high concentration of OH· radicals in the solution (due to the high radiation dose rate) as well as by low initial iodide concentration, reducing the probability of reactions among the iodine species initially formed. If, for example, HOI originating from I_2 hydrolysis reacted with radiolytically formed IO, the formation of iodate would be markedly reduced. According to Kent and Sims (1991), at the iodine concentrations to be expected in the sump water, iodate does not seem to be a significant radiolysis product, while at lower total iodine concentrations it could be a major product.

In addition, hypoiodous acid HOI can be formed by radiolytic oxidation of iodide in aqueous solution saturated with nitrous oxide or by radiolytic reduction of iodate in hydrogen-saturated aqueous solution (Fletcher and Miller, 1985).

Laboratory experiments performed by Marimuthu et al. (1989) on the radiolytic oxidation of CsI solutions (10^{-2} M I^-) at ambient temperature in the dose range 2 to $11 \cdot 10^4$ Gy (^{60}Co γ radiation) yielded G values for I_3^- and IO_3^- formation on the order of 10^{-3} to 10^{-4} at a solution pH of 5.5 to 7.2. At the highest radiation dose applied, about 2.6% of the I^- initially present was volatilized from the solution; the G values were not significantly changed by the addition of boric acid (up to 200 ppm B) to the solution.

In the experiments reported by Lucas (1985) the influence of additives to the solution and the gas phase on radiolytic oxidation of I^- was studied. At a composition of the test solution which was claimed to be quite similar to that assumed for the containment sump water, irradiation was carried out using a dose rate of 4 kGy/h. The results showed that in a closed vessel an I_2 saturation concentration is reached at an integrated radiation dose of about 60 kGy; the presence of CO_2 in the gas phase resulted in an increase of the saturation level to about 20% I_2 formation, while the presence of H_2 did not significantly affect the results. By contrast, in an open system where I_2 evolved from the test solution was trapped in a $NaHCO_3$ solution, no saturation I_2 yield was obtained; under such conditions, the I_2 yield increased linearily with the dose rate, reaching about 55% at an integrated radiation dose of 0.24 MGy.

I_2 volatility from irradiated solutions can be considerably influenced by the presence of third partners in the solution. Investigations performed by Beahm et al. (1986) showed that under irradiation in boric acid (pH 6) I_2-I^- solutions the I_2 partition coefficient is lower by about one order of magnitude than without irradiation. In the presence of metallic silver in the solution, however, the partition coefficient is not noticeably affected by irradiation, presumably because of the reaction of the I_2 generated to form insoluble AgI. Ionizing radiation promotes the reaction between dissolved I^- and metallic silver present in the solution which, if at all, proceeds at a very slow rate in the absence of radiation (see Section 7.3.3.4.3.). The residual I^- concentration in the solution proved to decrease steadily according to a pseudo-first order reaction with increasing integrated radiation

dose. The rate constants of I^- consumption (corresponding to AgI formation) depended on several parameters; in the presence of air or oxygen they were observed to be significantly higher than under inert conditions.

Trace contaminants present in the solution may also intensify or reduce the extent of I_2 production considerably by reaction with the intermediate products of water radiolysis. Such traces of metals (e. g. iron, copper) may be unintentionally present in the test solutions of laboratory experiments as well as, at even higher concentrations, in real containment sump water. The widely unknown nature and concentration of trace ingredients in the sump water is one of the main problems in the application of the laboratory results on radiation-induced iodine reactions to the situation prevailing in a severe reactor accident.

Probably as a result of the dependence of the yields of the radiolysis products on the specific characteristics of the experiments, in particular the composition of the test solution, results obtained from different experimental runs frequently show considerable scatter and also may differ from the results of calculations. A critical evaluation of relevant experiments and a recommendation of currently "best" results has been given by Weber et al. (1992).

From the topics discussed above it can be concluded that most of the iodine chemical reactions which proceed within the containment are affected by ionizing radiation. While the experimental investigations mentioned above mostly focused on specific effects, a systematic study of the synergistic effects of radiation and other parameters was started in the Canadian Radioiodine Test Facility (RTF), built at the AECL Whiteshell Laboratories. The central component of this facility (see Fig. 7.37.) is the shielded main vessel which is designed to represent the reactor containment building. This vessel has a volume of 400 l and can be heated up to 80 °C; ^{60}Co irradiation sources are installed in the main vessel, providing average γ radiation dose rates of up to 2 kGy/h. Numerous peripheral installations render possible the selection of a broad range of operating conditions (Kupferschmidt et al., 1991 c). To obtain as much information as possible from the test runs, the RTF is equipped with a sophisticated analytical instrumentation, in particular for radiochemical determinations (see Evans et al., 1994 a).

The tests performed in the RTF have revealed that, in high radiation fields, the long-term volatility of iodine is virtually independent of the initial iodine speciation (I^-, I_2, CH_3I). The reason for this behavior is that radiolytic reactions interconvert the aqueous iodine species, primarily by aqueous phase radiolysis. In the absence of radiation, interconversion of I^-, I_2, and organic iodides is relatively slow; ionizing radiation results in a hydrolytic decomposition of CH_3I as well as in an oxidation of I^- and a reduction of I_2, with the progress of all these reactions depending on the prevailing conditions. Tests at pH 9 and at pH 5.5 demonstrated that iodine volatility from an initial I^- solution increased significantly with decreasing pH, mainly caused by the respective yields of the essential primary radiolysis products of H_2O. At pH 9, I_2 is effectively reduced by O_2^- formed in irradiated aerated solution; at pH 5.5, however, the quantity of O_2^- is reduced through protonation to form $HO_2\cdot$, which is a less effective reductant for elemental iodine, while it readily oxidizes I_2^-. Changing the solution pH from acidic to alkaline conditions in the course of a running experiment did not result in rapid decreases in iodine

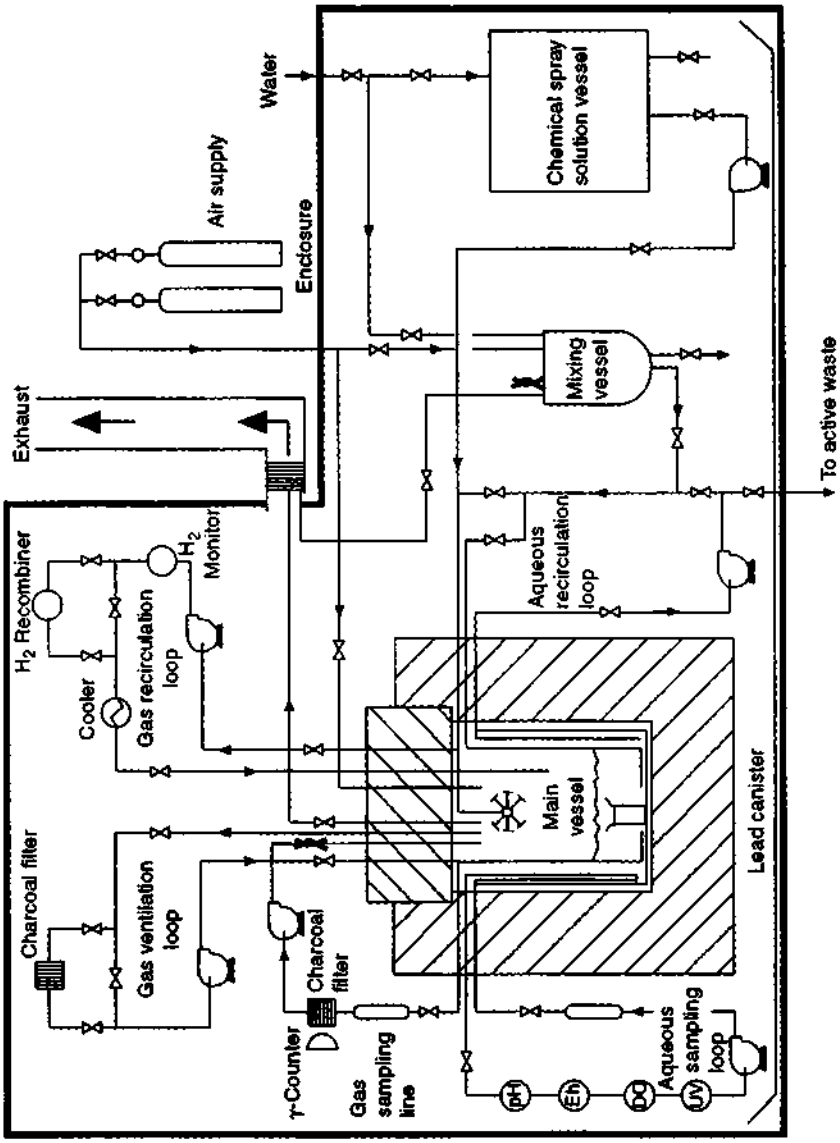

Figure 7.37. Schematic diagram of the Radioiodine Test Facility (RTF) (Ritzman, 1991)

volatility. This effect is assumed to be due to desorption of volatile iodine species from surfaces (stainless steel) and competing radiolytic processes for the formation and destruction of organic iodides, in particular in tests carried out with epoxy-coated surfaces. The studies demonstrated that containment surfaces can play an important role in determining iodine volatility, gas and aqueous phase iodine speciation, and surface adsorption (Kupferschmidt et al., 1991 c); these reactions will be discussed in the following sections.

Tests with an alkaline system (pH 8 to 9) yielded low overall volatility of iodine, giving partition coefficients in the range of 10^4 to 10^6. Simultaneously, low levels of organic iodine species were formed (on the order of 0.1%), even when relatively large amounts of epoxy paint materials were present; further, low iodine deposition onto the surfaces of the vessel took place. Under acidic conditions (pH 4 to 6), the total iodine partition coefficient was lower by a factor of about 100 and the organic iodide level was higher by about a factor of 10 (but still remained a small fraction of the total iodine) than under alkaline conditions. Moreover, under acidic conditions an appreciable iodine buildup on vessel surfaces is to be expected which may constitute a significant delayed source of volatile iodine if the system equilibrium is disturbed (Ritzman et al., 1991).

Elemental iodine present in the containment atmosphere can be oxidized by radiolytically generated ozone (Vikis and Torgerson, 1985). Conservative calculations using a $G(O_3)$ value of 2 yielded a production rate of 0.1 µl O_3/l air·min at a dose rate of 1 kGy/h; taking into account the calculated dose rates in the containment atmosphere cited in Table 7.15., even considerably higher production rates may be possible in the course of a core melt accident. Gas phase O_3 is thermally stable below 400 K and does not react with H_2O and H_2; the main reactions which are expected to consume O_3 are surface-catalyzed decomposition as well as reaction with nitrogen oxides, which are also produced by the radiolysis of air. From the production rate mentioned above, a steady-state O_3 concentration on the order of 1 µl O_3/l air was calculated. The main product of the reaction between I_2 and O_3 is solid I_4O_9 which, upon deposition onto liquid aerosols or wet surfaces, is dissolved to form IO_3^-. The oxidation reaction is of first order with respect to the I_2 concentration, as well as to the O_3 concentration. The removal rates of I_2 from the atmosphere shown in Fig. 7.38. were calculated on the basis of experimentally determined reaction rates, assuming O_3 steady-state concentrations of 0.1, 1 and 10 µl/l and temperatures of 300 and 350 K (Vikis and Torgerson, 1985). Thus, this reaction may be a chemical sink for I_2 in the atmosphere which is much more effective than ^{131}I radioactive decay. Even higher rates have to be expected for the reaction of O_3 with iodine atoms generated from I_2 photolytically by visible light. In addition, the decrease in airborne I_2 concentration will indirectly result in a reduced production of organoiodides.

According to calculations performed by Sagert (1988), I_2 in moist air can also be converted by radiation into oxygenated species such as IO_2 and I_2O_3, with reaction of $OH^\cdot$ radicals with I_2 molecules being the chief mechanism. Although this reaction is assumed to proceed very fast, its kinetics has not yet been determined; the reaction products may be converted into soluble species such as I_4O_9 and IO_3^-.

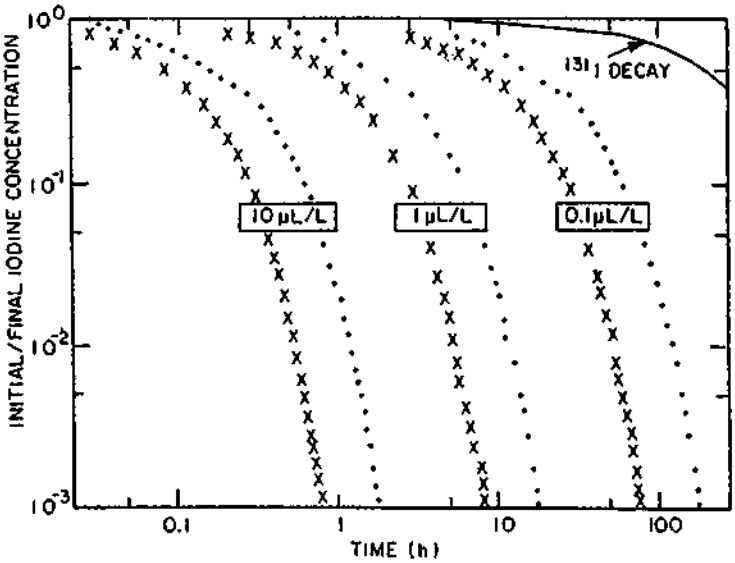

Figure 7.38. Removal of iodine (I_2) by reaction with ozone at different ozone concentrations (····· 300 K; xxxxx 350 K)
(Vikis and Torgerson, 1985; by courtesy of AEA Technology plc)

The two above-mentioned gas-phase reactions, oxidation of I_2 by radiolytically generated O_3 and $OH^{\cdot}$, are expected to influence substantially the amount of volatile iodine as well as iodine speciation in the containment atmosphere. However, a validated data base on their progress in steam-containing atmospheres is still lacking.

7.3.3.4.5 Formation and behavior of organoiodine compounds

The preceding sections on iodine chemistry in the containment under accident conditions have been limited to inorganic iodine species. However, in addition to these species considerable fractions of organic iodine compounds may also be formed under such conditions; this was clearly demonstrated by the analyses of the TMI-2 containment atmosphere, where several months after the accident the major fraction of the airborne iodine was found to be in the form of organic iodides. These "filter-penetrating iodine species" (as they were called in early years) are often summarized under the term methyl iodide, CH_3I, which usually amounts to 80–90% of the sum of organic iodine compounds volatilized under such conditions. Besides this species, higher molecular-weight organic iodides (e. g. ethyl iodide C_2H_5I) have also been observed, as well as products of reactions of I_2 or HI with other organic compounds such as alcohols, ethers etc. Since CH_3I is the most volatile of these compounds, using this compound to represent all volatile organic

iodides will not result in an underprediction of the impact of such species, unless one of the other compounds is produced in significantly larger quantities than CH_3I (Weber et al., 1992).

The formation of volatile organoiodides in the containment building in the course of a degraded core reactor accident is a crucial topic, since every I_2 molecule originally present in the atmosphere which is converted to an organic iodide compound is removed from the I_2 partition equilibrium. As a consequence, a corresponding amount of I_2 would be delivered from the sump water to the containment atmosphere in order to maintain the appropriate gas–liquid equilibrium, thus increasing the total amount of airborne radioactive iodine. Because of the obviously great importance of these reactions, organic iodide formation was already considered in WASH-1400. Based on the data presented by Postma and Zavadoski (1972), two different cases were distinguished, one that applied to accidents in which containment sprays were operable and a second one that applied to compartments in which sprays would not be expected to deplete the concentration of airborne molecular iodine. For the PWR case in which sprays were not operable, 0.7% of the iodine was estimated to appear as methyl iodide, whereas only 0.4% conversion was estimated for situations involving sprays. For BWR accidents, 0.7% conversion was assumed for all accident sequences. It is of interest to note that in developing the conversion estimates a distinction was made between the formation of methyl iodide by radiolytic reactions and that by non-radiolytic reactions; this was the only situation in which radiolytic effects were taken into consideration in this basic investigation.

Because of the formation of organoiodine compounds in the containment during plant normal operation as well and because of the difficulties that exist in removing these compounds from the plant off-gas by means of filters, numerous investigations have been dedicated to the organoiodide complex. Already at the beginning of the 1970's, Parsly (1971) as well as Postma and Zavadosky (1972) summarized the state of knowledge at that time; a more recent review and evaluation has been given by Deane (1988). According to the data contained in these review papers, formation and decomposition of organic iodine compounds can proceed in the liquid as well as in the gaseous phase; in both cases, reaction with organic coatings on the surfaces will substantially contribute to the total organoiodide production. Besides the numerous chemical reactions that can lead to organoiodide compounds, their formation as well as their decomposition can be greatly promoted by ionizing radiation. The first step of interaction of ionizing radiation with organic molecules is the formation of free radicals, atoms or groups of atoms, which are quite reactive due to an unpaired electron; iodine is a very effective scavenger of such free radicals.

With regard to the formation of organoiodine compounds by homogeneous reaction in the liquid phase of the sump water, I_2 (and potentially HOI) seems to be the most important iodine species. As was discussed in Section 7.3.3.4.2., the fractional concentration of I_2 in the solution strongly depends, because of hydrolysis and disproportionation, on the sump water pH. The organoiodide production reactions are, therefore, primarily affected by the prevailing pH, but also by the available dissolved organic substances, the nature and concentration of which are

widely unknown and which probably depend heavily on the particular situation. When methane is taken as an example, the direct production reaction

$$CH_4 + I_2 \longrightarrow CH_3I + HI \tag{17}$$

(I_2 either being originally present or being formed by radiation-induced oxidation of I^-) proceeds only slowly in the absence of ionizing radiation (halftime of the reaction about 20 days). According to the investigations of Beahm et al. (1987), CH_3I formation in the aqueous phase in the presence of radiation even proceeds when methane is introduced into the gas phase above the surface of the iodine-containing liquid. In this case, however, conversion to CH_3I is less than when methane is bubbled through the mixture, probably due to the smaller concentration of organic substances present in the solution. It was assumed that the initial reactions involve the radiolytically-formed OH· radical

$$OH\cdot + I^- \longrightarrow I\cdot + OH^- \tag{18}$$

$$OH\cdot + CH_4 \longrightarrow CH_3\cdot + H_2O \tag{19}$$

with newly formed radicals combining

$$I\cdot + CH_3\cdot \longrightarrow CH_3I \tag{20}$$

Alternatively, the reaction

$$CH_3\cdot + I_2 \longrightarrow CH_3I + I\cdot \tag{21}$$

may take place, demonstrating the significance of the specific I_2 concentration in the solution which, in turn, depends on the solution pH. However, the CH_3I yields measured in these experiments can be assumed to be comparatively high, since the CH_3I formed during the course of the experiment was continuously removed from the solution so that radiolytic decomposition could not proceed to a significant extent, and only the CH_3I formation step could be measured.

Paquette and Ford (1988), using solutions saturated with methane and containing dissolved iodine concentrations on the order of 10^{-4} mol/l, observed that after absorption of a γ radiation dose of 4 kGy, nearly all the initial iodine was transformed into iodoalkanes, virtually independent of its initial chemical form (iodide, iodine, iodate, periodate). Although only CH_4 was used as a reactant, the formation of higher alkyliodides was also observed, probably due to more complex radiation-induced reactions. Elemental iodine reacts directly according to the equations above, iodide probably after oxidation to the elemental state. In the case of iodate and periodate, these reactions were assumed to be preceded by those involving the methyl radical and oxyiodine species. The formation of iodoalkanes was found to be inhibited by the presence of air and hydrazine, due to a scavenging effect of methyl radicals by oxygen in the case of air and to reduction of I_2 and HOI in the case of hydrazine. The G value of organoiodide formation proved to depend on the methane concentration in the solution and to decrease strongly with decreasing concentration. This means that at the extremely low CH_4 concentrations to be expected in the hot sump water in the course of a reactor accident, formation of organoiodide by means of this reaction is not assumed to proceed to any significant degree.

Basically, CH_3I formation may also proceed according to

$$CH_3OH + I_2 \longrightarrow CH_3I + HOI \tag{22}$$

This reaction is assumed to be of little importance since the intermediately produced radicals $CH_3\cdot$ and $I\cdot$ are preferentially trapped by O_2, as well as by H_2O radiolysis products. Methanol in an irradiated iodide solution of low pH was found to suppress radiation-induced iodide oxidation and, thus, to keep the iodine partition coefficient high, with the responsible mechanism probably being the effective scavenging of the primary $OH\cdot$ radicals by CH_3OH (Lutz and Kelly, 1988).

Addition of organic impurities such as methyl ethyl keton (MEK), a common paint solvent, to an aqueous I^- solution in the absence of radiation proved not to result in a measurable organoiodide formation. Under the influence of radiation, however, addition of MEK leads to an increase in the total airborne iodine concentration by more than an order of magnitude over a period of several hours, corresponding to a decrease of the steady-state iodine partition coefficient from 10^5 to 10^6 in the absence of MEK to about 10^4 after addition of this compound (Fluke et al., 1991).

CH_3I once formed can be decomposed again by several reactions occurring in the aqueous phase

$$2\,CH_3I + \gamma \longrightarrow 2\,CH_3\cdot + I_2 \tag{23}$$

$$CH_3I + H_2O \longrightarrow I^- + CH_3OH + H^+ \tag{24}$$

$$CH_3I + OH^- \longrightarrow I^- + CH_3OH \tag{25}$$

$$CH_3I + O_2/O_3 \longrightarrow IO_3^- + \ldots \tag{26}$$

$$CH_3I + A^- \longrightarrow CH_3A + I^- \tag{27}$$

Radiolytic decomposition (reaction 23) of iodoalkanes in aqueous solution proceeds via the $OH\cdot$ radical, the solvated electron, the hydrogen atom, and the perhydroxyl radical. The perhydroxyl radical, which appears in air-saturated solutions, seems to be the most effective reagent (Paquette and Ford, 1988). By contrast, Beahm et al. (1987) supposed the aqueous electron e_{aq}^- to be the most effective agent for CH_3I decomposition. The $CH_3\cdot$ radical formed in reaction (23) is preferentially trapped by other radiolysis products such as O_2; therefore, this reaction can be considered to be an effective CH_3I sink in the aqueous phase. Reactions (24) and (25) proceed at a comparatively fast rate, with their halftime at 150 °C being on the order of 30 to 50 seconds. Reaction 26, i. e. CH_3I decomposition in aqueous solution by O_2 and/or radiolytically generated O_3, is as yet only incompletely known; therefore, no reliable data on yields and reaction rates are available. Finally, as is indicated in reaction (27), CH_3I can be subjected to an anion exchange reaction where A^- may be any anion such as Cl^-, $H_2BO_3^-$, PO_4^{3-}, CO_3^{2-}; at 150 °C the halftimes of these reactions are on the order of several minutes. Organoiodide decomposition in the aqueous phase can also be enhanced in the presence of metallic impurities, in particular of heavy metals.

CH_3I formation under irradiation in aqueous solutions can be largely suppressed by the addition of soluble silver salt (e. g. $AgNO_3$) to the solution; likewise, CH_3I which has been dissolved in the water is decomposed by irradiation in the presence of silver salt. The AgI compound formed is stable up to high radiation

doses (Ishiwatari, 1991). As was reported in Section 7.3.3.4.3., CH_3I in aqueous solution is rapidly decomposed by ionizing radiation in the presence of metallic silver (Beahm et al., 1986).

In the results on the formation of organoiodine compounds in homogeneous phases as reported by various authors (e. g. Beahm et al., 1987; Paquette and Ford, 1988), there are indications that surface reactions may play an important role. In these reaction chains, the first steps are assumed to be represented by the reaction of adsorbed organic material and iodine species at reactive surface (hydroxyl) sites to form surface compounds (Deane, 1991). These surface compounds react to form adsorbed organoiodide which can then equilibrate with the gas phase. By such a desorption, the de-activated sites are re-activated again; the organic iodine produced can partly be decomposed again, resulting in an equilibrium atmospheric concentration in a closed system.

However, a significant fraction of the iodine, once it is deposited onto the paint, will not be volatilized as a low-molecular-weight organoiodide compound, but will be converted to a low-volatility higher-molecular-weight organoiodide which is permanently fixed to the organic surface. The early investigations of Genco et al. (1968) as well as of Rosenberg et al. (1969) showed that the reaction mechanisms are greatly influenced by the type of paint used and by the ambient conditions; re-evaluation of these experimental results by Weber et al. (1992) yielded differences in the kinetic parameters at different paints by more than a factor of 2. Because paints occasionally are porous, iodine may diffuse and react in the interior and not just on the surface. In addition, ageing effects of the paint can be assumed to change the state of the surface, the number and nature of reactive sites etc., and thus to influence the progress of the surface reactions. For this reason, direct application of experimental results usually obtained with comparatively fresh paint specimens to containment surfaces which, prior to the accident, had been exposed for several years to the containment atmosphere, is thought to be somewhat problematic. These effects are assumed to be important in iodine reactions on the surfaces exposed to the sump water as well as to the containment atmosphere.

Experiments on I_2 deposition from aqueous solutions onto immersed epoxyphenolic paint surfaces showed deposition velocities increasing from about $1 \cdot 10^{-3}$ cm/s at 30 °C to about $3 \cdot 10^{-2}$ cm/s at 100 °C (Burns et al., 1988). After the termination of the experiment, approximately 50% of the original amount of elemental iodine was present in the solution as iodide ions. The remainder of the iodine was either adsorbed onto the surfaces or was present in the solution as an organic species of unknown nature; purging of the solution with N_2 after the experiment showed that the material was not volatile. CsI solution in contact with the epoxyphenolic paint under irradiation also reacted with the organic material, with about 10% of the amount of iodine being adsorbed onto the paint, while dissolved organoiodine compounds were at or below the detection limit, indicating that such compounds would be readily decomposed by irradiation.

Under the influence of ionizing radiation (0.6 kGy/h), iodide ions which are adsorbed from aqueous solutions onto organic-painted surfaces are to a part converted to volatile organoiodide compounds, with the degree of conversion as well

as the nature of the newly formed organoiodine compound depending strongly on the specific type of paint used. The extent of iodine adsorption proved to decrease strongly with increasing solution pH. Comparable, or even larger, quantities of elemental I_2 as a second volatile iodine species were also detected (Deane, 1991).

Under irradiation, different organic substances influence the volatility of iodine from solutions in a different manner. Comparative studies performed by Quan and Evans (1994), using a 10^{-5} M CsI solution with an initial pH of 9 irradiated in the presence of 20 different organic compounds and polymers, showed that most of the organic compounds influence iodine volatility primarily through their impact on the pH of the solution. The organic substances investigated were divided into three groups, depending on their impact on iodine volatility. The members of the first group tended to produce, under irradiation, both a low solution pH and a low iodine partition coefficient. This group included compounds containing the carbonyl group, with irradiation probably resulting in the formation of carboxylic acids, as well as chloroalkanes from which Cl^- ions are released. Other members of this group were ethylene glycol, methanol and ethyl ether. By contrast, in the presence of the substances of the second group (n-hexane, polyethylene, polypropylene, polystyrene, teflon, toluene and xylene) the solution pH remained close to neutral and the iodine partition coefficient was high. Finally, the members of the third group (cyclohexamine, formaldehyde, glycerin, phenol and styrene oxide) effected a reduction in solution pH to values below 6, but had virtually no impact on the iodine partition coefficient. Phenol as an antioxidant can be assumed to suppress iodide oxidation by peroxy radicals, while only little information is available on the mechanisms of reaction of the other compounds in this group, in particular with regard to the differences in behavior of glycerine, on the one hand, and the alcohols of the first group, on the other.

Experiments in the absence of radiation with vinyl surfaces using I^- solutions (Kupferschmidt et al., 1991 b) yielded low gas-phase iodine concentrations and little deposition of iodine onto the surfaces. By contrast, under irradiation (2 kGy/h) gas-phase iodine concentrations higher by more than two orders of magnitude were observed, coinciding with pronounced decreases in pH and dissolved oxygen concentration. In addition, at least two-thirds of the iodine inventory of the experimental system was retained on surfaces, primarily on those which were exposed to the gas phase. These studies suggested that the behavior of pH, dissolved oxygen and iodine volatility can be attributed to the radiolytic decomposition of organic compounds originating from the organic-based coating. Iodine volatility can be minimized, even in the presence of vinyl surfaces and aqueous phase organics, if alkaline pH conditions are maintained. The vinyl coating (which is a vinyl chloride −vinyl acetate copolymer) is decomposed by radiation under production of HCl and consumption of oxygen. On the other hand, the plastic solvent methyl isobutyl keton and its degradation product methyl ethyl keton are decomposed to peroxy radicals and to carboxylic acids, resulting in a decrease in the solution pH (see Section 7.3.3.4.3.). Under such conditions, I^- ions are oxidized to elemental iodine by radiolytically produced $OH^\cdot$ radicals, resulting in a steady-state I_2 concentration

in the solution which, in turn, leads to a corresponding concentration of I_2 in the gas phase. Interaction of this I_2 with vinyl surfaces leads to iodine deposition. However, since zinc primer was used in the experiment to coat the specimens, it cannot be ruled out that this material also contributed to iodine deposition (see Section 7.3.3.4.8.), by means of iodine penetration through the vinyl layer.

Interaction of I_2 with organic materials can be enhanced by conditions which support corrosive attack of the solution on the organic surfaces. Evans and Palson (1991) reported strong iodine conversion on epoxy-coated surfaces at 80 °C, in particular at a solution pH of 8 to 9, considerably higher than from acidic solutions or from solutions at 25 °C; this conversion was substantially enhanced when the solution had been in contact with the epoxy surface for a certain period of time before addition of I_2. From these results it was concluded that the high rate of conversion might be due to a reaction in the homogeneous aqueous phase with dissolved or suspended degradation products of the organic material and that alkaline pH and increased temperatures would accelerate the formation of such degradation products. Under irradiation, the rate of I_2 adsorption onto submerged epoxy surfaces depended but little on the nature of the initial iodine species (I_2 or I^-), although it was strongly affected by the solution pH, being higher in acidic solutions by about two orders of magnitude than in alkaline solutions.

Once CH_3I is formed in the aqueous phase, it is largely volatilized to the containment atmosphere, with the specific partition coefficient of this compound in the temperature range 100 to 150 °C lying between 0.5 and 1.0. The fraction of this organic iodine species present in the gas phase is not significantly affected by an increase in the temperature of the system from 25 to 80 °C. This behavior is believed to be due to a competition between volatility and hydrolysis of the organoiodide compound: whereas CH_3I volatility in this temperature range increases by about a factor of 4, the rate of CH_3I hydrolysis increases by about a factor of 3, which results in a decrease in its amount in the solution (Deane, 1988).

According to the results presented above, formation of organoiodide compounds in aqueous solution depends on the solution pH, generally being considerably higher in acidic solutions than in alkaline ones and showing a particularly pronounced dependence in the pH range 5 to 6 (Evans and Palson, 1991). Ionizing radiation enhances organoiodide formation with I^- solutions, while it results in a reduction of organoiodide formation in I_2 solutions; as a whole, organoiodide formation in the aqueous phase under irradiation does not significantly depend on the iodine species initially present. From these results it was concluded that I_2 would be the reactive species and that the dependence on pH was a consequence of the influence of pH on the hydrolysis equilibrium between I_2, on the one hand, and HOI and I^- (and IO_3^-) on the other.

Organoiodine compounds can also be formed in the containment atmosphere by homogeneous gas-phase reactions, with the reaction partners being volatile organic compounds originating from paints, lubricants etc., as well as the degradation products of such materials. Depending on the particular situation, the concentrations of volatile organics in the atmosphere can vary over a wide range and can considerably exceed the concentration of gas-phase I_2. The formation reactions are influ-

enced both by ionizing radiation and by water vapor present in the atmosphere. The main formation reactions are assumed to be

$$CH_4 + I_2 \longrightarrow CH_3I + HI \tag{28}$$

$$CH_3{-}R + I_2/HI + \gamma \longrightarrow CH_3I + RI/H_2 \tag{29}$$

$$CH_3OH + HI \longrightarrow CH_3I + H_2O \tag{31}$$

As in a homogeneous aqueous solution, the gas-phase reaction (28) can be ignored because of its low reaction rate of $4 \cdot 10^{-7}\ s^{-1}$, leading to a halftime of the reaction of about 20 days. Calculations (Sagert, 1988) have shown that in the containment atmosphere CH_3I cannot be formed by abstraction of iodine atoms from I_2 by radiolytically generated methyl radicals, since the oxygen present in the atmosphere would compete too efficiently for the methyl radicals. According to the experimental results of Lutz and Kelly (1988), significant formation of CH_3I under irradiation takes place only at high methane concentrations in the atmosphere. Reaction (29) also suffers from effective competing reactions, mainly with O_2 and H_2O. Only reaction (31) may proceed in a humid atmosphere at the comparatively high rate of about $6 \cdot 10^{-4}\ s^{-1}$ and a resulting halftime of about 20 minutes (Borkowski, 1985). The question has been raised, however, whether (31) is in reality a heterogeneous gas – surface reaction (Deane, 1988).

Further, radioactive CH_3I may also be generated by isotope exchange between radioactive I_2 and natural, non-radioactive CH_3I. Methyl iodide is a ubiquitous halocarbon which is present in normal air at concentrations that vary somewhat with the distance from the ocean. Measurements at different locations in the United States yielded values between 10^{-12} and 10^{-10} mol CH_3I/l air. It is of interest to note that this concentration is on the same order of magnitude as the long-term ^{129}I mass concentration in the TMI-2 containment atmosphere, which was measured to be about $3 \cdot 10^{-12}$ mol/l. From these data it was concluded that during a severe core damage accident a minimum concentration of radioactive organoiodide compounds of about $2 \cdot 10^{-12}$ mol/l will be reached in the containment atmosphere within a time span of about 14 days, caused by isotope exchange of inorganic radioactive iodine species with atmospheric non-radioactive methyl iodide (Weber et al., 1992).

The possible CH_3I formation reactions in the gas phase also face several decomposition reactions such as

$$CH_3I + H_2O \longrightarrow CH_3OH + HI \tag{32}$$

$$CH_3I + O_2 \longrightarrow CH_3O_2 + I\cdot \tag{33}$$

$$CH_3I + \gamma \longrightarrow CH_3\cdot + I\cdot \tag{34}$$

$$CH_3I + HI \longrightarrow CH_4 + I_2 \tag{35}$$

Reactions (32) and (33) proceed very slowly, their reaction rates are on the order of $1.3 \cdot 10^{-7}\ s^{-1}$ and $5 \cdot 10^{-7}\ s^{-1}$ at 150 °C, respectively, with corresponding halftimes of 60 days and 15 days. The progress of reactions (34) and (35) depends strongly on the ambient conditions: at high γ dose rates, reaction (34) can act as a significant CH_3I sink; however, the G value of this reaction decreases with decreasing CH_3I concentration in the gas phase, and H_2O vapor present in the atmosphere

is reported to act as an inhibitor. Radiolytic CH_3I decomposition may be additionally induced by β^- radiation (mainly originating from the fission product noble gases present in the atmosphere), probably according to

$$CH_3I + e^- \longrightarrow CH_3\cdot + I^- \text{ (or } I_2) \tag{36}$$

Until now, this reaction has not yet been studied in detail.

At higher temperatures, which are potentially attained in some containment volumes, organic iodide is expected to decompose thermally back into I_2; however, this reaction does not seem to be of great significance in organic iodide chemistry during a severe reactor accident.

From these considerations it may be concluded that no significant net production of organoiodide by homogeneous reactions in the containment atmosphere (as in the homogeneous aqueous phase) is to be expected; on the contrary, at high radiation dose rates a net decomposition can be assumed. On the other hand, on the basis of experiments on the buildup of the organoiodide concentration in the containment atmosphere, Beahm et al. (1985) established the following relationship

$$dC / dt = \alpha \cdot (C^* - C) - Q \cdot C \tag{37}$$

where C = concentration of organic iodide at time t
C^* = equilibrium concentration of organic iodide
Q = constant for removal of organic iodide (e. g. by radiolysis)
α = organic iodide formation rate constant

From the results of these experiments, a comparatively rapid organoiodide formation in the presence of radiation was derived and α values in the range from $1 \cdot 10^{-3}$ to $8 \cdot 10^{-2}\ s^{-1}$ were calculated; this result would seem to contradict the assumption mentioned as to the net consumption of organoiodides in the atmosphere, although it proves to be consistent when all possible sources of organoiodide are considered (see below).

The most important source of CH_3I formation seems to be the reaction of I_2 (and possibly of HI) present in the gas phase with organic materials present on surfaces, primarily organic coatings and paints. In this reaction mechanism, I_2 from the atmosphere is deposited onto the surface where a part of it is converted to organoiodide and is subsequently released to the atmosphere again according to

$$I_{2\,(gas)} \xrightarrow{\text{deposition}} \text{Iodine}_{(surface)} \xrightarrow{\text{resuspension}} \begin{cases} I_{2\,(gas)} \\ CH_3I_{(gas)} \end{cases}$$

In order to calculate the resulting CH_3I concentration in the gas phase, the rate of I_2 deposition on the surfaces and the rates of I_2 and CH_3I resuspension from the surfaces are required. The deposition velocity of I_2 onto the containment surfaces is assumed to be on the order of $5 \cdot 10^{-3}$ cm/s, which means that 50% of the gas volume in the containment will have had contact with the surfaces within 5 hours (Hellmann, personal communication); turbulent gas movement in the containment free volume significantly increases the deposition rate. The progress of chemical reactions between I_2 and the surface material will be affected by various parameters, in the first place by the chemical nature of the organic coatings, but also by the moisture content of the atmosphere. When evaluating these reactions one has

to consider that freshly applied organic paints may react differently than paints aged for several years, due to the volatilization of reactive constituents of the material with time or to a saturation of reactive surface centers by air or dust components. The resuspension rates of I_2 and CH_3I also depend on the nature of the organic materials and on the H_2O content of the atmosphere. For painted surfaces at 30 °C, I_2 resuspension rate constants between $3 \cdot 10^{-7}$ and $2 \cdot 10^{-6}\ s^{-1}$ and CH_3I resuspension rate constants between $2 \cdot 10^{-8}$ and $7 \cdot 10^{-8}\ s^{-1}$ have been reported, depending on the relative humidity of the air (Hemphill and Pelletier, 1978).

Laboratory experiments have confirmed that at 80 °C epoxy paints on surfaces can act as a significant sink for gas-phase iodine (Evans and Palson, 1991). Iodine loadings on the paint ranging from 0.14 to 0.65 mg/cm^2 were measured, depending on the I_2 concentration in the gas phase. This loading is equivalent to a coverage of hundreds of monolayers, although the majority of the iodine on the surface was found to be irreversibly bound to the substrate. The initial deposition velocity proved to be relatively independent of the I_2 concentration, amounting to about 0.2 cm/s. A similar value was obtained for a silver coupon, indicating that the rate of deposition was governed by the rate of gas-phase mass transfer rather than by the nature of the surfaces. Thus, when one considers the different results on deposition velocities reported by other authors (e. g. Rosenberg et al., 1969), these values seem to reflect more a property of the apparatus used in the experiments than of the nature of the surface. The highest loading mentioned above appeared to be a saturation value. In the tests involving high gaseous I_2 concentrations, the initially white epoxy paint developed an orange/yellow discoloration which was limited to the surface of the paint; there was no evidence to indicate that iodine reached the carbon steel substrate below. The adsorbed iodine was found to desorb from the paint at a very slow rate; less than 20% of the iodine was removed during 600 hours of exposure at 80 °C to dry air flowing at 800 ml/min, which demonstrated that the bulk of iodine was tightly bound to the paint, probably by a chemical reaction with some component of the paint. It has to be pointed out, however, that these deposition experiments were conducted in the absence of steam and of ionizing radiation.

From these results a model of iodine adsorption onto organic paints was developed (Evans and Palson, 1991). In this model it was assumed that gaseous I_2 deposits on the painted surface at a rate which is limited by the gas-phase mass transfer coefficient and the number of available sites. The balance between the rates of deposition and of desorption of the reversibly bound I_2 results in a constant distribution between airborne and surface I_2. However, while on the surface, the I_2 can react with the paint to become chemically bound. The rate of this reaction is proportional to the concentration of I_2 on the surface and its extent is limited by the number of available reactive sites. After reacting, the chemically bound iodine can be desorbed from the surface only at a very slow rate. From this model it can be concluded that, once the ratio of the surface loading to the gas phase concentration approaches the partition coefficient, the deposition velocity will decrease substantially as the rate of loading now becomes governed by the rate of chemical reaction. When all the sites for deposition are filled, the loading achieves a maximum value. At the very small gaseous I_2 concentrations which are

to be expected in the containment atmosphere in the course of a severe accident, saturation will never be achieved, although a steady-state balance between the rates of the forward and reverse chemical reactions can be assumed to take place.

I_2 carried in a gas flow can also be adsorbed onto vinyl-coated surfaces, with the steady-state loadings obviously depending on the gas-phase iodine concentration (Evans and Bekeris, 1994); the rate of deposition apparently is not affected by the humidity of the gas flow. Desorption of iodine from the vinyl material increases with both the surface iodine loading and the temperature.

Summarizing these and other results, one can conclude that the question of the relative significance of the different mechanisms for organoiodide formation in the containment has not yet been entirely clarified. Based on the results of experiments in which CH_4 was sparged through an iodine-containing solution, Beahm et al. (1987) concluded that formation in the aqueous phase would be the most important contributor, whereas other results seem to indicate that this mechanism does not play a significant role in the buildup of the total organoiodide amount. On the contrary, there are strong indications that organoiodides will be decomposed in the liquid phase sufficiently fast to create an organoiodide sink that will be of importance in medium- and long-term considerations. This applies both in the presence of γ radiation and in its absence. In the containment atmosphere, all possible chemical paths to organoiodide formation or decomposition are of little effect because of the comparatively slow reaction rates and of the very low concentrations of the possible reaction partners. In contrast, radiation-induced reactions are of significance in the containment atmosphere, probably resulting primarily in CH_3I decomposition; however, as yet this has only been confirmed for a dry environment. Thus, as long as there are high dose rates in the atmosphere it can be regarded as a CH_3I sink. On the other hand, Postma and Zavadoski (1972) assumed gas-phase reactions under the influence of radiation as the principal source of organic iodides.

The heterogeneous reaction between airborne I_2 (and probably HI as well) and organic paints and coatings on surfaces seems to be the predominant organoiodide source, with the first stage of the reaction being the addition of I_2 to reactive groups on the surface of the coating, which is then followed by the formation of organoiodine compounds. Low-molecular-weight organoiodide compounds (e. g. CH_3I) are then released to the atmosphere, while higher-molecular-weight compounds will remain on the surface. In summary, it is not possible as yet to assign responsibility to a single source for the amount of organoiodide formed; rather, one has to expect a dynamic interaction between the different sources, on the one hand, and different decomposition mechanisms on the other.

In the early stages of a severe reactor accident, the very high β/γ dose rates and the resulting radiolytic decomposition reactions can be assumed to compensate almost completely for the CH_3I formation, resulting in a low equilibrium concentration of this species in the containment atmosphere. In the later phases (weeks to months after the onset of the accident) the radiation dose rate decreases drastically and, consequently, the organoiodide equilibrium concentration increases steadily. Therefore, the data obtained from the TMI-2 containment atmosphere several months after the onset of the accident cannot be taken to be representative of the situation to be considered in a short-term accident analysis.

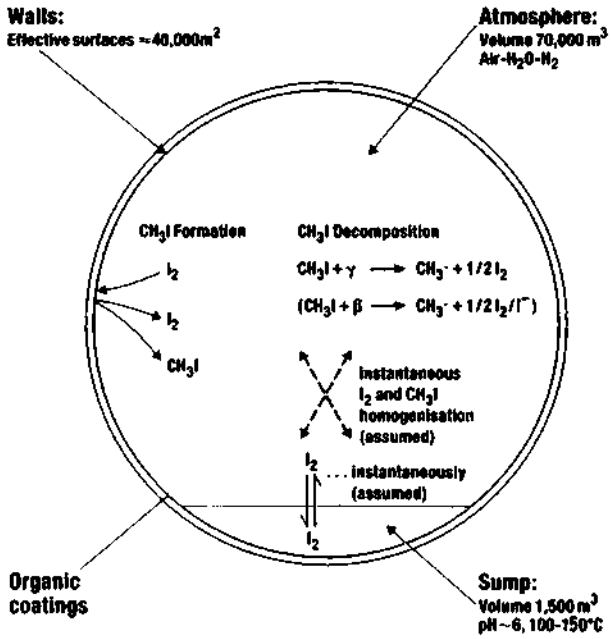

Figure 7.39. Organoiodide formation and decomposition; main reactions inside the containment
(By courtesy of Dr. Hellmann)

On the basis of the data mentioned above, Hellmann and Bleier (1989) have calculated the extent of organoiodide formation in the containment atmosphere in the first days after the onset of the accident; the reactions considered by them are schematically shown in Fig. 7.39. The results obtained demonstrate that, without taking into account radiolytic decomposition, an organoiodide fraction of about 85% (related to total airborne iodine) would be reached within 5 days (see Fig. 7.40.). Taking into account γ-induced radiolytic decomposition, the organoiodide fraction would be stabilized at a value of about 25%. When, in addition, β-induced decomposition is included in the calculations with the same G values, then the equilibrium organoiodide fraction is reduced to about 3%; note that the β^- dose rate in the containment atmosphere in the time period under consideration is higher by about a factor of 10 than the γ dose rate. In order to correct for the uncertainties in the individual reaction data, several calculations using different sets of data were performed; the most conservative results, i. e. those leading to the highest organoiodide concentrations, are shown in Fig. 7.40.

Due to the uncertainties that still exist both in the reaction data and in the assumptions regarding the available concentrations of the different reaction partners, all the predictions of organoiodide formation and decomposition in the early stages of a degraded core accident still suffer from considerable unclarity. The main reason for this is the strong dependence of the essential reactions on a large number of parameters; however, it can be expected that investigations currently being per-

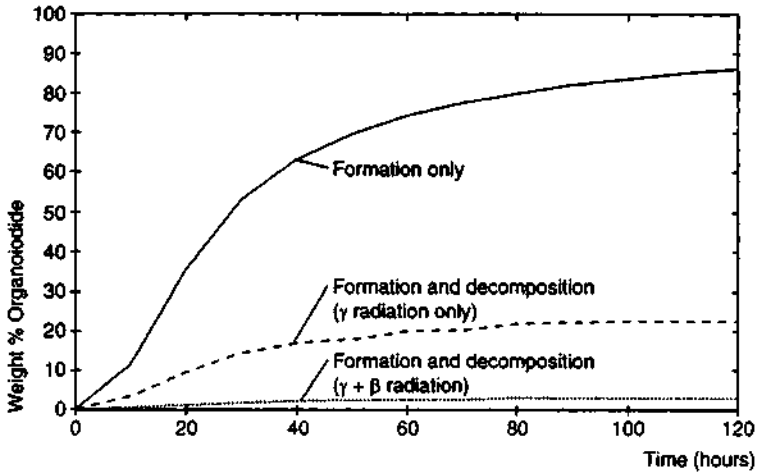

Figure 7.40. Buildup of organoiodide concentration in the containment atmosphere (By courtesy of Dr. Hellmann)

formed will reduce this unclarity considerably. In addition, the reliability of the analytical methods usually applied in experiments for the discrimination of the different iodine species has to be regarded with some reserve. CH_3I identification is almost exclusively performed by means of specific iodine filters, on the selectivity of which differing and partly contradicting statements have been made. Confirmation of these results by independent analytical methods such as radio-gaschromatography, mass spectrometry or laser-induced fluorescence spectrometry would often be desirable; because of the very low concentrations of the substances under interest, however, such analyses are extremely difficult to perform.

7.3.3.4.6 Further reactions of iodine in the containment atmosphere

As a result of the reactions discussed in the preceding sections, in the short-term period following core meltdown fission product iodine will be present in the atmosphere of the containment in different chemical forms. The by far largest fraction will exist in particulate form, with most of this fraction being chemically bound as CsI or other inorganic iodides and the remainder being adsorbed onto the surfaces of the aerosols. Besides the particulates, a small fraction of iodine is expected to be present in the gaseous state, including the species I_2, organoiodide and perhaps HI. In addition to the formation and decomposition of organoiodine compounds and the radiolytic reactions (which were treated in the preceding sections), further reactions may proceed in the containment atmosphere, resulting either in an enhancement or in a reduction of the concentrations of volatile iodine species.

In principle, CsI aerosol can be oxidized by oxygen still present in the containment atmosphere. Ionizing radiation will promote this reaction, particularly when supersaturated steam and/or liquid water are in contact with the aerosol particles; thus, this oxidation reaction follows the mechanisms of the radiation-induced oxidation of dissolved iodide discussed in Section 7.3.3.4.4. The degree of oxidation depends, among others, on the CsI concentration in the water droplets, on the integrated radiation dose and on the pH value in the liquid phase. However, since CsOH is simultaneously present in these aerosol particles, the pH of the droplets can be expected to be in the alkaline region (unless the aerosol particles contain significant amounts of condensed boron oxide/boric acid), so that radiation-induced reactions will produce only small amounts of I_2. These I_2 traces will be able to react again with excess CsOH to form CsI, given the comparatively long residence times of these small-sized aerosol particles in the containment atmosphere. Investigations of the irradiation behavior of concentrated HI solutions ($3.7 \cdot 10^3$ Gy/h) to obtain information on the formation of volatile I_2 under such conditions showed that only an insignificant fraction of the HI present was converted into I_3^- or I_2. Upon contact with the wet walls and structures, the aerosols as well as the water droplets will be readily removed from the atmosphere and transported to the sump water.

Another possible reaction is CsI decomposition as a result of a postulated hydrogen burn in the containment atmosphere (see Section 7.1.), in the course of which the aerosol particles can be heated over a short time interval to high temperatures in the presence of residual air. As was described by Brown et al. (1990), laboratory experiments showed that in a continuously burning hydrogen flame dry CsI is partly oxidized to I_2 and/or IO_3^-. In a more detailed investigation which was performed in a 6.6 m^3 vessel, Kupferschmidt et al. (1991 d) observed different reaction mechanisms, depending on the prevailing ambient conditions. In a dry air $-H_2$ combustion, up to 15% of the CsI suspended in the vessel atmosphere was oxidized to I_2; besides this oxidation, increased concentrations of organic iodides were produced, probably due to a reaction between traces of organic compounds present in the vessel and I_2 formed in the combustion process. By contrast, hydrogen combustion in an atmosphere containing 10% steam did not lead to the formation of detectable amounts of I_2.

The reason for these differences in the results was assumed to be the presence of a condensate film on the surfaces of the CsI particles which, during the short interaction period of the hydrogen burn, was not completely vaporized, protecting the CsI from being oxidized. Since CsI conversion is believed to involve a homogeneous gas-phase reaction, it would be necessary that the CsI boiling point (1280 °C) be exceeded; otherwise, no CsI oxidation would occur (Weber et al., 1992). Under the conditions prevailing in real reactor accident environments, it is a question whether the surfaces of the aerosol particles will be covered by a condensate film or not and, thus, whether or not a significant amount of I_2 would be generated by this reaction. Independent of the results of CsI oxidation in hydrogen burns, the impact of this reaction on the longer-term I_2 concentration in the containment atmosphere seems to be small. I_2 potentially produced in the hydrogen flame will have the opportunity to react with the excess CsOH present in the atmo-

sphere to form CsI again. Therefore, a permanent increase in the concentrations of volatile iodine species as a consequence of a hydrogen burn is not to be expected.

Similar to the situation in the reactor primary system (see Section 7.3.2.), interactions between iodine vapor and bulk material aerosols may occur in the containment atmosphere, although at a lower temperature level, and may have significant influence on iodine speciation and transport. CsI usually appears in the condensed form in the containment and is transported as aerosol particles. In rare cases, conditions may occur (e. g. in a BWR drywell) in which a significant fraction of the CsI present would exist in gaseous form, which can then migrate to cooler regions to condense on structural surfaces or on aerosols. However, in such a case normal condensation without additional chemical reactions is to be expected.

Greater significance has to be attributed to the deposition of I_2 vapor onto aerosol surfaces. This kind of reaction of gaseous iodine species with aerosols in the containment atmosphere will mainly result in a reduction in the concentrations of volatile species. These processes may be written as

$$\text{gas} + \text{solid} \longrightarrow \text{solid}$$

Deposition of volatile species onto aerosol surfaces includes mass transport to the surface, resulting in adsorption; this step will be followed either by revaporization from the surface or by chemical reaction of the adsorbed species with the surface material. These mechanisms can be written as

$$c_g \underset{k_2}{\overset{k_1}{\rightleftharpoons}} c_p \underset{k_4}{\overset{k_3}{\rightleftharpoons}} c_c$$

where c_g = gas-phase concentration
c_p = intermediately or physisorbed iodine
c_c = chemisorbed iodine (reaction with surface material).

The constants k_1 and k_2 represent mass transfer coefficients to and from the surface; k_3 and k_4 denote chemical reaction rate constants (Weber et al., 1992). In most cases, the chemical reaction step is essentially irreversible, resulting in $k_4 = 0$. Since mass transfer, among others, depends on the geometry and the dimensions of the system, care has to be taken in extrapolating results which were obtained in laboratory facilities to the situation of real reactor containments. Adsorption reactions will depend on the concentrations and the composition of the aerosols and, finally, chemical interactions between the two species are highly dependent on the chemical nature of both the volatiles and the aerosols, in particular of their surfaces.

The aerosols present in the containment atmosphere can be roughly divided into two groups, the water-solubles and the water-insolubles (Wichner and Spence, 1985); in the evaluation of the interactions of gaseous substances with aerosols in the containment atmosphere, their bulk composition obviously is of less significance than the nature of the aerosols' surface. In general, it is assumed that the inner region of the aerosol particles consists of refractory oxides which condensed immediately after having left the core melt zone; this central part is covered by a layer of more volatile compounds, in particular CsOH and/or boron oxide, both of which are readily soluble in water. Within the containment, chemical changes

can proceed on the surfaces of the aerosols, with one of the reasons being the change in environmental conditions from a reducing atmosphere in the primary circuit to oxidizing and steam-condensing conditions in the containment atmosphere. In addition, varying degrees of hydration may be expected, as well as reactions of CsOH to form carbonates, borates, and nitrates. Other aerosol oxides and metals may also react with gaseous HNO_3 produced by the interaction of radiation with humid air. Aerosols that contain liquid H_2O are a special case, since the iodine adsorption behavior of an insoluble aerosol in an aqueous aerosol droplet is that of the aqueous phase, and iodine phenomena to be expected in aqueous solutions such as mass transport, hydrolysis, and radiolysis effects would predominate. With water-soluble aerosols in H_2O-containing particles the same phenomena would occur, along with additional pH and ionic strength effects of the dissolved aerosol material.

Beahm et al. (1990) reported on investigations concerning the interaction between different aerosol materials and gaseous iodine compounds. These experiments were carried out in a quartz tube where I_2, HI and CH_3I in air (concentrations between $5 \cdot 10^{-8}$ and $5 \cdot 10^{-5}$ mol/l) were passed over the aerosol materials kept at temperatures of 30, 60 and 100 °C. The results showed that I_2 reacts very rapidly and irreversibly with basic materials such as CsOH, Cs_2O and even Cs_2CO_3 at 100 °C, with the reaction products being I^- and IO_3^- at a ratio of about 5:1; with Cs_2O rapid reaction was observed even at temperatures as low as 30 °C. At 100 °C, the deposition rate constants of I_2 onto these three solids were on the order of 0.1 cm/s; calculations indicated that the rates were controlled only by gas-phase mass transport. $Cs_2B_4O_7$ powder reacted with I_2 at 100 °C at a rate slower than the other reactive powders; the deposition velocity measured with $1 \cdot 10^{-7}$ g-atom I/l was $1 \cdot 10^{-3}$ cm/s at 100 °C. No reaction between I_2 and $CsNO_3$ was observed.

As the experiments showed, iodide and iodate were formed in a ratio of about 5:1 upon contact of I_2 with the basic aerosol materials. Apparently, it is easier for I_2 to disproportionate on the surface than it is for it to undergo a redox reaction with ions in the crystal to form CsI alone. Thermochemical data show that the formation of iodide and iodate would result in a lower free energy of reaction than formation of iodide alone. Formation of iodate alone would give a lower iodine potential than formation of iodide and iodate; however, iodate formation seems to be limited by reaction kinetics. The extent of I_2 reaction with anhydrous Cs_2O and Cs_2CO_3 is probably limited only by the surface concentration of iodide and iodate which prevents or delays further interaction between I_2 and the host crystal. In tests in which saturated aqueous solutions of these compounds were present, no such limitation was observed, nor had it been expected.

Qualitative tests of I_2 reaction with other aerosol materials at 100 °C showed that BaO reacts very similarly to Cs_2O and Cs_2CO_3. The reaction with cadmium aerosol produced a combination of I^- and I_2 with about 30% of the surface iodine as I_2; this result is different from that reported by Beard et al. (1988) where CdI_2 was observed as the reaction product while adsorption of I_2 was not mentioned. Other substances such as Ni, CaO, In_2O_3, ZrO_2, SnO_2, Cr_2O_3 showed no or only very little reaction with I_2 at temperatures around 100 °C. Physical adsorption of I_2 without chemical reaction seems not to be a very important process. Further-

more, I_2 did not react to a significant extent with most structural components or with boric acid.

CH_3I also reacted with the basic aerosol materials Cs_2O, CsOH, Cs_2CO_3 and BaO under formation of iodide; unlike I_2, no iodate was formed in these reactions. The deposition velocities of CH_3I were considerably lower than in the I_2 reactions, being on the order of 10^{-4} to 10^{-5} cm/s at 100 °C. The most probable mechanism in this reaction is that the organic iodide undergoes a nucleophilic substitution reaction to form iodide and alcohol. Gaseous HI proved to be quite reactive with all the test substances but also with the test equipment materials. The reaction product was iodide on the surface of the simulated aerosol materials with a small fraction (1–2%) in the form of iodate. While the rates of reaction of HI with HBO_2, $CsNO_3$, MnO and Cs_2CO_3 amounted to values between 10^{-5} and 10^{-2} times the concentration of HI [g-atom I/m^2·s], its reaction with CsOH-saturated solutions was limited only by the rate of transport to the surface.

As a special case of gas–aerosol interaction, the uptake of I_2 and/or CH_3I by the water droplets of the containment spray system has to be mentioned. This reaction was discussed in greater detail in Section 6.2.1.2. in the context of the LOCA design basis accident. The beneficial impact of spray systems on the longer-term iodine concentration in the containment atmosphere in severe core damage accidents seems to be questionable, because of the comparatively high concentrations of fission products in the sump water which is used as a spray solution at an advanced stage of the accident. Spray washout of CsI in the first stages of a severe core damage accident is assumed to proceed more efficiently than in a LOCA design basis accident, since the higher aerosol concentrations in the containment will result in larger aerosol particles, which are removed by the spray droplets more readily than smaller ones. Frequently the question has been raised of whether or not chemical additives to the spray solution will enhance iodine removal from the containment atmosphere (see, e. g., Pasedag et al., 1981). It has been argued that in the early stage of an accident sequence, when CsI is the dominant iodine species in the atmosphere, they would be of limited benefit; in the longer-term, however, when elemental iodine is the dominant iodine species they have been claimed to be necessary, in particular because of their contribution to the establishment of a higher pH in the containment sump water.

7.3.3.4.7 Reactions of iodine with structural surfaces in the containment

At the comparatively low temperatures prevailing in the containment, CsI (as well as the dissolved I^- ion) is not expected to react with surfaces, either with those immersed in the sump water or with the surfaces exposed to the containment atmosphere. However, elemental I_2 may undergo reactions resulting in a conversion of this volatile species to non-volatile I^-. Since the fraction of iodine which originally enters the containment from the primary system as I_2 is very small, such reactions

are not assumed to be of high significance during the very first stages of the accident; on the other hand, they are of potential importance in the later stages since they are able to reduce the amount of I_2 formed by radiation-induced reactions.

In the construction of reactor containments a variety of materials are used resulting in surfaces that iodine can interact with. These materials are, most notably, steel, concrete, and organic coatings and paints. The first step in such reactions is deposition of the iodine species onto the surfaces; this adsorption step can be followed by a desorption step or by a chemical reaction step, the product of which can either be tightly fixed to the surface or can be resuspended in the liquid or gaseous phase. This means that the basic situation is similar to that in the reaction of volatile iodine species with aerosols, as discussed in the preceding section. The main parameter affecting kinetics and products of these reactions is the type of the surface material, with the most important ones being metals and organics. The reactions of iodine with organic paints and coatings have been already treated in the context of organoiodide formation and behavior in Section 7.3.3.4.5.

Reaction of iodine with steel surfaces, both those exposed to the sump water and to the containment atmosphere, may lead to deposition or to conversion of I_2 to non-volatile I^-, with both effects decreasing the amount of gaseous iodine species. In aqueous solution, I_2 is partly reduced to I^- upon contact with stainless steel surfaces (see the review paper of Funke and Hellmann, 1994), as was qualitatively indicated by an enhancement of the partition coefficient at 110 °C under such conditions (see Fig. 7.41.). Similarly, the results of the detailed investigations reported by Deane and Marsh (1990) yielded complete conversion of I_2 to I^- within a few hours; this effect is not caused by iodine hydrolysis but is the result of redox reactions. Since the iodide formed in this reaction is immediately dissolved in the water phase, no information is available on the nature of the intermediately formed compound; however, this question is of subordinate importance for modelling the process of I_2 reduction on steel surfaces in the containment. As a result of the immediate dissolution of the reaction product, the surface remains clean and no saturation effects of the reactive sites will occur. The kinetics of this process has been investigated by Funke et al. (1994) using steel 1.4541 (main steel material of KWU PWRs) in the as-received state, immersed in an I_2 solution with a concentration of $1 \cdot 10^{-4}$ g-atom/l at pH 2.4 (to avoid I_2 hydrolysis in water). At test temperatures of 50, 90 and 140 °C the rate constants of I_2 conversion shown in Fig. 7.42. were obtained. From these data an activation energy of the conversion of 80 kJ/mole was calculated. On the other hand, experiments using steel AISI 316 L surfaces in the electropolished state and I_2 concentrations of $5 \cdot 10^{-5}$ mol/l in slightly acidic solution yielded rate constants of about $7 \cdot 10^{-9}$ m/s at 50 °C and of about $4 \cdot 10^{-7}$ m/s at 90 °C, resulting in an activation energy of the reaction of 94 kJ/mole (Funke, 1994).

Deposition of I_2 from the gas phase onto steel surfaces resulting in physisorption occurs in any environment, although it is greatly enhanced by condensing water vapor. By contrast, irreversible sorption takes place only in the presence of water vapor; apparently, the relative humidity of the gas phase does not significantly affect the progress of the surface reactions, provided the moisture content exceeds some threshold value. A liquid water film on the surface greatly reduces

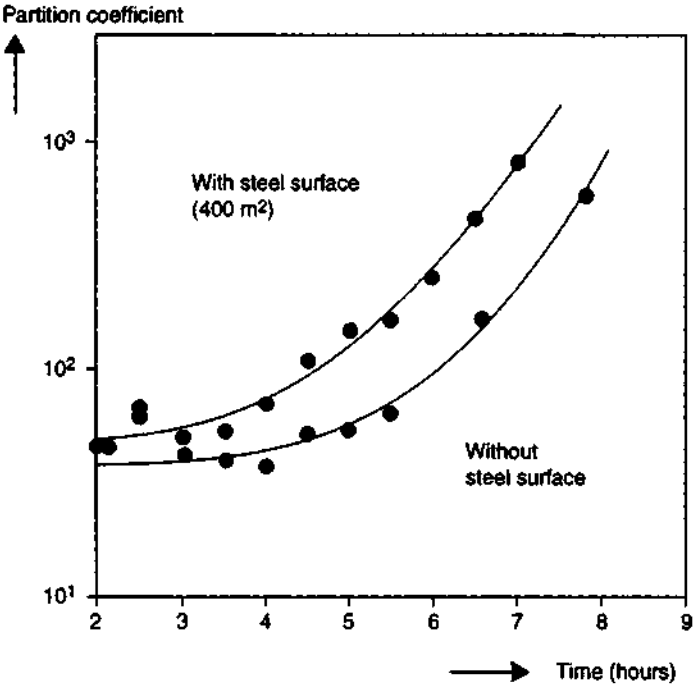

Figure 7.41. Iodine partition coefficient with and without contact with steel surface (Total iodine concentration 10 mg/ml, mass ratio I^- to total iodine 0.58, boric acid solution pH 5.3, 110 °C)
(Richter and Neeb, unpublished)

the I_2–steel interaction; condensation of liquid water after I_2 reaction with steel leads to the dissolution of the metal iodides to form I^- ions in the resulting solution.

Upon contact of gas-phase I_2 with stainless steel surfaces, a deposited amount of iodine on the order of 0.1 mg /cm^2 was measured, whereas comparable experiments with liquid I_2 solution did not result in a measurable deposition of iodine, apparently due to the rapid dissolution of the metal iodides formed (Deane and Marsh, 1990). From the earlier desorption experiments performed by Rosenberg et al. (1969) it was assumed that FeI_2 is the main primary product of this reaction, but that parallel formation of NiI_2 and/or CrI_3 cannot be ruled out; all these compounds are readily soluble in water. Experiments using tubes made of steel 1.4541 (Funke et al., 1994) showed an I_2 deposition rate constant in dry air at 120 °C of about $6 \cdot 10^{-5}$ m/s. Under condensing steam conditions at the same temperature a considerably higher value of $1.4 \cdot 10^{-3}$ m/s was measured, indicating that under such conditions the I_2–I^- conversion on steel surfaces is a fast process. Analysis of the surfaces after completion of the test yielded only a small iodine retention; in the condensed steam no iodate could be detected, indicating that no unreacted I_2 had passed through the reaction tube and that only metal iodides had been

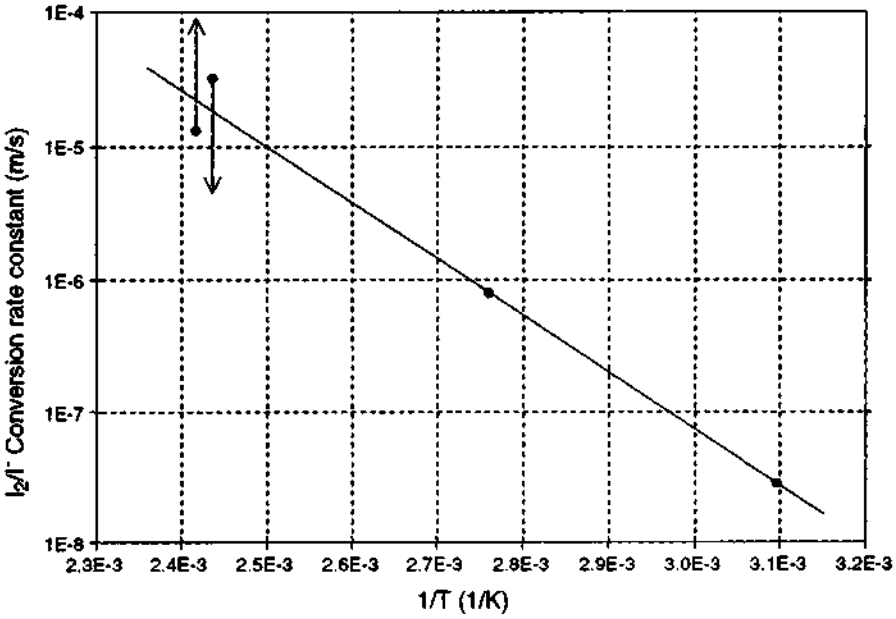

Figure 7.42. Temperature dependence of the I_2-I^- conversion rate constant in the aqueous phase
(Funke et al., 1994)

transported to the condensate vessel. At 160 °C in steam, virtually the same rate constant was measured, indicating an activation energy of nearly zero in this temperature range. The pronounced differences in the I_2-I^- conversion rate constant between aqueous-phase experiments (see above) and gas-phase experiments point to different reaction mechanisms.

The question of I_2 deposition onto stainless steel walls is also of great significance with regard to iodine transport in the sampling lines which are installed to obtain representative samples from the containment atmosphere in the period following a severe accident. Because of the unfavorable surface-to-volume ratio of these small-diameter lines and their considerable length (up to 100 meters), even comparatively small retention effects could lead to erroneous results for the radionuclide content in the gas phase of the containment. This problem is well-known from plant normal operation analyses and has been studied in detail; however, the conditions and the requirements in an accident sampling system are quite different. In order to get an idea of the extent of retention under the prevailing conditions (temperature, steam content etc.) and on the possibility of obtaining appropriate pipe factors, several investigations have been carried out in this field. Of these investigations, the experiments performed by Evans et al. (1994 b) shall be mentioned, according to which adsorption of gas-phase iodine onto stainless steel type 316 surfaces increases with increasing relative humidity of the gas flow (experimental range 20 to 90% relative humidity), in particular at low relative humidities.

With increasing temperature (experimental range 25 to 90 °C), iodine deposition decreased, suggesting that water traces present on the steel surface may play a role in the deposition process. In addition, adsorption at low gas-phase iodine concentrations (10^{-10} mol/l) differed considerably from that at higher concentrations (10^{-6} mol/l); in general, however, the rate of deposition proved to be proportional to the gas-phase iodine concentration, indicating a first-order deposition process. Depending on the experimental conditions, physisorption as well as chemical reactions were observed. Iodine desorbed again from the steel surface to air was predominantly in an inorganic form, probably I_2, rather than being present as organic iodide. On the other hand, in the water used to wash the exposed steel specimens iron, manganese and iodide were found, suggesting that the deposited iodine reacted to form iodides. The chemisorbed iodine was found to be primarily located in areas of corrosion, indicating that water traces and iodine effect a type of corrosion reaction on the steel surfaces. From these results it was concluded that it is difficult at this time to establish reliable corrections for the iodine losses in such a sampling line, due to the considerable complexity of the phenomena involved in the retention of elemental iodine.

Gas phase I_2 also reacts with copper surfaces under formation of an iodide layer with measured iodine loadings of about 1.8 mg/cm^2. Since the calculated iodine amount of a monolayer of I_2 is only on the order of 0.1 to 0.3 mg/cm^2, the measured amount either indicates a deposition in several layers or is due to the fact that the surface roughness of the experimental material was extremely high. When the system liquid water–metallic copper is investigated, it has to be taken into account that the CuI formed is poorly soluble in water (Deane and Marsh, 1990).

In order to protect carbon steel surfaces against corrosion, these are usually coated by an inorganic zinc primer, a zinc silicate matrix in which unreacted zinc particles are embedded. Investigations have shown that steady-state gas-phase iodine concentrations are drastically reduced in the presence of such zinc primer coatings, both in the presence and in the absence of ionizing radiation (Kupferschmidt et al., 1991 a). This effect is assumed to be due to the strong reducing nature of this material, which favors I^- formation; its comparatively low content of organic material results in decreased organic iodide formation. Besides their reducing effect, zinc primer surfaces have a significant affinity for iodine, in particular those surfaces which are in contact with the aqueous phase. Experiments showed that up to two-thirds of the I^- initially added to the solution was retained on the zinc primer surfaces; rinsing with water or aqueous solutions of hydrazine removed only a small fraction of the adsorbed iodide. This surface retention proceeds exclusively under oxidizing conditions, suggesting that zinc oxidation is a prerequisite for this behavior; the degree of adsorption is not significantly affected by radiation. It is assumed that iodine retention is effected by incorporation of I^- into oxidized zinc(II) products, such as hydroxides, oxides and basic carbonates, which exhibit minimal solubility in the pH range 9 to10.

Adsorption/desorption experiments (Evans and Bekeris, 1994) showed that the rate of I_2 deposition from the gas phase onto surfaces coated with a zinc primer increases with decreasing temperature (deposition velocity 0.8 cm/s at 23 °C and 0.06 cm/s at 90 °C) and with increasing humidity of the gas flow (at 90% it is higher

by a factor of 4 than at 5%). The rate of adsorption proved to be directly proportional to the iodine concentration in the gas phase, indicating a first-order process. The highest loadings attained in these experiments were on the order of 10^{-5} mol I_2/cm^2, but they did not appear to have reached the saturation value; thus, zinc primer coatings show a high affinity for I_2 from the gas phase, much higher for example than that of vinyl-based coatings. Desorption appears to increase with increasing temperature; preliminary results indicated that the desorbed iodine is mainly in the form of I_2.

Summing up, it can be expected that chemical reactions of elemental iodine I_2 with the surfaces in the containment, in particular those occurring in the liquid phase, will effect a conversion to non-volatile I^-, thus effectively counteracting the radiolytic oxidation of I^- to form I_2.

The retention effectiveness of the ice compartments installed in some PWR designs to condense steam can also be classified as based on a surface reaction. In a 1000 MWe PWR outfitted with ice compartments more than 10^6 kg of ice is held in an annular compartment through which the steam which escapes from the primary circuit is forced to pass in an upward direction. CsI aerosol particles which are transported to the surface of the ice baskets will be dissolved in the melt water to form Cs^+ and I^- ions. Two mechanisms are assumed to be effective in removing elemental I_2 from the gas flow, the first one being deposition onto the cold surfaces of the ice grains and of the steel baskets in which the ice is stored. The efficiency of this step obviously depends on the contact time and, thus, on the flow patterns of the gas phase and of the liquid formed by the melting of the ice and the condensation of steam. Absorption of I_2 by this liquid is the second mechanism; in order to enhance the absorption capacity, the ice is usually made from alkaline borax solution; when molten, the pH of the aqueous solution has a design value of 9.3. Model calculations (Winegardner et al., 1983) have yielded removal efficiencies for I_2 in the ice compartments of >98%, without considering specific accident sequences. The assumptions used in this model were compared with results from earlier laboratory studies (Malinowski, 1970), and showed satisfying agreement. Calculations with the special ice condenser code ICEDF (Owczarski and Winegardner, 1986) showed that the decontamination factors for particles are fairly high when the inlet steam concentration is high. I_2 is scrubbed very effectively if the ice meltwater is alkaline; for a transient accident sequence in a large PWR, retention factors on the order of 10^9 have been calculated. After complete melting of the ice inventory the decontamination factors for I_2 decrease drastically to values near 1 to 2. For CH_3I, the decontamination factors are usually near 1.0, unless the inlet steam mole fraction is very high.

7.3.3.4.8 Large-scale containment experiments

Knowledge about the chemical reactions of the fission products as discussed in the preceding sections and about their resulting behavior in the course of a severe reactor accident is mainly based on the results of laboratory experiments. These

special-effect results are characterized by an accurate determination of the impact of all relevant parameters and are trustworthy from a scientific point of view. Their application to the actual situation of an accident, however, suffers from the large differences between the dimensions of the experimental systems and the real reactor containment; for this reason, the transferability of the laboratory results to the plant conditions has to be verified. To be sure, chemical equilibria (e. g. the ratios of individual species in the equilibrium state, partition coefficients) do not depend on the dimensions of the reaction system, but all the kinetic effects (e. g. rate of buildup of the equilibria) as well as side effects originating from the walls of the system are affected by dimensional parameters. In particular, the surface-to-volume ratio of the reaction system may have a crucial impact on the progress and the results of the processes. Low concentrations of fission products may be affected by surface reactions as well as by reactions with unknown trace impurities present in the large volumes, which are usually carefully excluded in "clean-conditions" laboratory experiments. Therefore, experiments in large-scale test facilities are indispensable for validation of laboratory results. Quite in contrast to all the data collected on fission product behavior during plant normal operation periods, the probability of verifying data on fission product behavior in a real reactor accident situation is extremely low. The only event until now in which it was possible to study fission product behavior in a severe LWR accident was at TMI-2; the experience gained here will be discussed in detail in Section 7.4.2.

A series of large-scale containment systems experiments (CSE) was conducted in the second half of the 1960's using the Containment Systems Test Facility (CSTF) at the BNWL Hanford site; the results concerning the behavior of iodine in these tests have been summarized by Hilliard and Postma (1981). This facility represents the containment of a US 1000 MWe PWR, scaled down linearily by a factor of 5 and enclosing a free volume of about 850 m^3. After having established a 120 °C saturated steam atmosphere in the vessel, simulated fission products, which had been generated by volatilization of I_2 and Cs_2O and bringing these vapors into contact with molten UO_2, were introduced by an air flow. In the course of each of the tests, samples were taken in short time intervals from the sump water as well as from the containment atmosphere, in the latter case by using selective iodine filter samplers.

The experiments demonstrated that the condensation of water droplets in the originally transparent saturated steam atmosphere started a few minutes after the introduction of the simulant fission products. Simultaneously, a rapid decrease in the concentration of airborne fission products started, as can be seen from the results of a typical experiment shown in Fig. 7.43. From the data obtained in the measurements, an initial halftime of the iodine concentration in the gas phase of about 15 minutes was calculated; after having reached values below 1% of the initial concentration, further reduction of the gas-phase iodine concentration proceeded more slowly, with a halftime of about 2 hours. Typical values for the distribution of iodine and cesium in the experimental system at the end of a test (about 24 hours after the introduction of the simulant fission products) are shown in Table 7.16. A considerable fraction of iodine as well as of cesium was retained in the feed line, Cs_2O by condensation in the lower temperature region of the line, I_2 probably

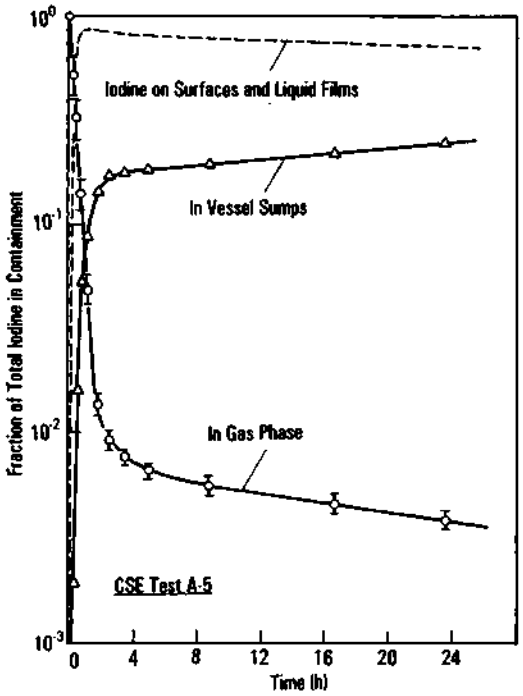

Figure 7.43. Iodine partitioning in the CSE vessel as a function of time (Hilliard and Postma, 1981; Copyright 1981 by the American Nuclear Society, La Grange Park, Illinois)

by chemical reactions with the surfaces in the air atmosphere that contained only small fractions of steam.

After termination of the experiment, the containment atmosphere contained only a comparatively small fraction of the fission products iodine and cesium. From these data, iodine partition coefficients between sump water and gas phase in the range 10^4 to 10^5 were calculated, which are comparatively high values when one considers that the sump water consisted solely of condensed steam and, consequently, had a pH of about 7. Obviously, a large fraction of the initial I_2 was

Table 7.16. Iodine and cesium distribution in the natural transport CSE tests (according to Hilliard and Postma, 1981)

	Iodine	Cesium
Generation Equipment and Line	28%	67%
Airborne	0.16%	0.02%
Condensate Pool	31%	22%
Condensate Film	7%	6%
Paint	33%	5%

converted to iodide in the course of the experiment. Moreover, the partition coefficients did not depend strongly on the iodine concentration in the sump water or on the prevailing temperature. A surprisingly high fraction of the iodine inventory of the test system was found to be attached to the organic coatings of the vessel walls, confirming the trapping effect of these materials; in the time interval considered in these experiments, revolatilization of iodine from these surfaces, either as I_2 or as organic iodine compound, apparently played only a minor role.

Regarding the initial rate of fission product plate-out from the atmosphere, the results of the CSE tests can be assumed to be conservative, since the radionuclides were fed into a preheated containment. Thus, the extent of initial steam condensation in these experiments was considerably smaller than is to be expected in an actual reactor accident when the gas–steam mixture escaping from the primary circuit will enter a containment which is nearly at ambient temperature; there is no doubt that stronger steam condensation favors fission product plate-out in the early stages of a severe accident. Moreover, the aerosol concentrations applied in these CSE tests were significantly lower than those to be expected in a real accident, resulting in a lower aerosol deposition rate.

The washout of gas-phase iodine by containment sprays (alkaline borate solutions) was also studied in the CSE tests. As was mentioned in Section 6.2.1.2., the action of the spray in the initial period of a test greatly exceeded the natural removal processes. However, in the later stage of the test, when recirculated sump water was used as a spray solution, the effect on the now low gas-phase iodine concentration was weak.

The CSTF facility was also employed within the framework of the Advanced Containment Experiments (ACE). This experimental program also included, besides laboratory experiments in which separate-effects tests and intermediate-scale multi-effects tests (a part of which were cited in the preceding sections) were performed, a large-scale combined-effects experiment devoted to the investigation of iodine and cesium behavior in the containment (Ritzman, 1991; Ritzman et al., 1991), in particular to the interaction of HI and I_2 with bulk aerosol materials, to the reactions of iodine with organic paintings, and to the retention of iodine in the sump water. In this test, a combined CsOH/MnO aerosol was used; CsOH generated by reaction of cesium vapor with steam and MnO produced in a plasma torch were mixed in a mixing chamber and transported by a steam-nitrogen flow to the containment free volume. Simultaneously, HI vapor and, in a second test section, I_2 vapor were injected into the containment atmosphere. The vessel had been preheated to about 100 °C and had been brought before to an internal pressure of 0.24 MPa by the addition of steam; during the experiment, heat losses were made up for by the further addition of steam, resulting in a continuous condensation of water on the walls which flowed down to the sump. Prior to the experiment, the lower part of the vessel had been provided with a water sump adjusted to pH 5.2 and heated to reach thermal equilibrium within the vessel. During the 24 to 40-hour test period, samples were collected from the gas phase as well as from the sump water; aerosol sampling was carried out using a cascade impactor and iodine sampling by a selective filter device which was somewhat modified compared to those normally applied. The inner walls of the facility had been previously coated

by an epoxy resin; a number of deposition coupons which were coated with different organic materials had also been inserted.

After feeding the aerosols into the containment vessel, the CsOH and MnO concentrations in the atmosphere decreased exponentially with a halftime of 40 to 45 minutes. In the test section with HI addition, the iodine and the cesium aerosols displayed similar removal rates; up to 400 minutes the dominant iodine chemical form was particulate. In the test section with I_2 addition, the early removal of iodine was similar to that in the HI test and was dominated by particulate forms up to 200 minutes. This behavior indicates that the injected species I_2 and HI reacted very quickly with the aerosol material to form non-volatile compounds. From 200 to 2000 minutes, elemental iodine was the predominant species of the now strongly diminished iodine concentration in the atmosphere of the vessel. From 2000 minutes on, organic iodide was the main chemical form and had a higher concentration in the I_2 test section than in the HI section of the experiment (by about a factor of 10); about 0.2% of the initially added I_2 finally remained as an organic iodine compound in the vessel atmosphere. The measured halftimes of I_2 and CH_3I plate-out from the containment atmosphere amounted to 11 hours and to 30–50 hours, respectively. The long-term airborne iodine in the experiment involved less than 2% of the initial mass charged and was almost completely due to the I_2 addition. The comparatively long halftime of I_2 removal suggests that it was not simply caused by irreversible wall deposition (the halftime of this process was estimated to be about 16 minutes), but represented the net effect of a probably more complicated kinetics, potentially involving a source–sink competition.

The total iodine partition coefficient between sump water and atmosphere 24 hours after addition of HI amounted to about $1.5 \cdot 10^5$; at the same time interval after I_2 addition a value of about $2.5 \cdot 10^4$ was measured which increased to about $5.2 \cdot 10^4$ by the end of the experiment. The lower value after I_2 addition is assumed to be due to the stronger CH_3I formation in this case. The increase in sump water pH from the initial value of 5.6 to a value of 8.4 (which was performed at an advanced stage of the test) did not result in significant changes in the concentrations or the chemical forms of the airborne species, indicating that in the absence of ionizing radiation a change in sump water pH once the equilibrium state has been reached does not noticeably influence the existing partitioning of the iodine species.

Final material balances from the liquid and the gas phases exhibited a recovery rate of 95% of the cesium and 88% of the manganese fed to the facility, which is within the expected range of analytical accuracy (including sampling). On the other hand, only 59% of the iodine added during the test was recovered, which may be the result of iodine adsorption from the water pool by the painted walls of the vessel. Iodine retention on the painted vessel surfaces was highest for surfaces exposed to non-condensing air, lowest for the surfaces of the wall under condensing steam conditions and intermediate for submerged pool surfaces.

Comparing these results with those of the earlier CSE tests, one finds a quite similar behavior of cesium, but pronounced differences in iodine removal from the vessel atmosphere. While in the ACE experiment the major part of the iodine was transported together with the aerosols to the vessel sump, in the corresponding

CSE experiment a large iodine fraction had been deposited onto the vertical surfaces of the vessel. The reason for this difference in iodine behavior is assumed to be the comparatively small input of cesium in the CSE test (1.1 g cesium and 85.5 g iodine), compared to the ACE test (266 g cesium and 101 g iodine). As a consequence, there was insufficient cesium aerosol in the CSE test to adsorb most of the I_2 vapor and iodine removal in this test was controlled by boundary-layer vapor diffusion and sorption onto internal surfaces. In the ACE experiment, the vapor – aerosol interaction process probably was complete within the time scale of the atmosphere mixing process (a few minutes). The estimated rate constants for I_2 wall deposition were about 2.7 times those for aerosol settling; this difference is consistent with the measured differences in the early-stage halftimes of iodine removal in the CSE and ACE experiments.

When the results of the large-scale containment experiments are to be applied to the conditions of a real reactor accident, one cannot ignore the absence of ionizing radiation in these experiments, an effect which is able to influence significantly iodine chemistry and behavior, as was discussed in detail in Section 7.3.3.4.4.

7.3.3.4.9 Evaluation of overall iodine behavior in the containment

In the preceding sections it was demonstrated that, following a severe reactor accident, the chemical state of fission product iodine in the containment will be determined by a number of chemical reactions. In order to evaluate the iodine fraction which will be present in the containment atmosphere, as well as the chemical forms it is composed of, all the significant reactions have to be considered and their product yields under the prevailing conditions have to be estimated. Today, there is a well-founded basis for evaluations, since the extensive research work conducted in recent years has elucidated not only the reactions of the fission products, but the progress of these reactions and their products as well. In general terms, the ability to predict iodine behavior in the containment is limited more by lack of knowledge of what environment actually exists under given conditions, than by deficiencies in our understanding of what iodine will do under given environmental conditions (Beahm et al., 1992). This means that, with but a few exceptions, prediction of the chemical forms or the magnitude of iodine which would be ready for release from the containment is limited by lack of information about the substances and environments involved in iodine reactions in the containment.

In the early US Regulatory Guides 1.3. and 1.4. it was assumed that in the course of a "maximum credible reactor accident" 50% of the maximum iodine inventory of the reactor core would be released to the containment. Of this amount, 25% would be available for leakage, i. e. present in airborne form in the containment atmosphere; as for the chemical states, 91% of the airborne iodine was assumed to be elemental I_2, 5% to be in the form of particulate iodide and 4% in the form of organic iodide. Subsequent investigations, both experiments and

Table 7.17. Substances that affect pH in containment water pools (according to Beahm et al., 1992)

Substance	Effect
Boron oxides	acidic
Basic fission product compounds (e. g. CsOH, Cs borates)	basic
Iodine as HI	acidic
pH additives	basic
Atmospheric species (e. g. CO_2, HNO_3)	acidic
Core – concrete aerosols	basic
Pyrolysis and radiolysis products from organic materials	acidic

theoretical studies, have demonstrated that iodine behavior within the closed containment is considerably more complex. From the original mixture of particulate CsI and gaseous HI and I_2, with the by far largest proportion being particulates, a re-release of molecular iodine has to be anticipated due to revolatilization from water repositories, accompanied by small contributions of organic iodide. As was described in the preceding sections, a number of chemical reactions and physical transport mechanisms can influence these processes.

In recent years, several attempts have been made to estimate the magnitude of the airborne iodine fraction in the containment in a highly simplified manner, mostly based on the results of laboratory experiments. But because of the multitude of potentially influencing parameters, no well-founded results can be expected from such a procedure. On the contrary, the relative significance of the individual parameters for the specific conditions of the accident sequence under consideration has to be evaluated in detail.

One of the most important parameters controlling iodine volatility is sump water pH; not only will the I_2 hydrolysis equilibrium and the iodine partition coefficient be affected by this parameter, but the product yields of radiolytic reactions and the extent of formation of organoiodine compounds as well. Because of the lack of practical experience, the sump water pH to be expected under severe accident conditions has to be calculated on the basis of assumed concentrations of potential sump water ingredients. In Table 7.17. (according to Beahm et al., 1992) an overview of substances to be expected in the sump water, which would effect a shift in solution pH either to lower or to higher values, is given. Besides these chemical substances, radiation may also affect sump water pH; irradiation of trisodium phosphate solution (5.3 kGy/h) was reported to decrease the pH from an initial value of 9.0 to about 4.0 after 60 hours of irradiation (Beahm et al., 1992). It is obvious that in such a complicated system definition of the sump water pH to be expected in a real severe reactor accident is a difficult task. Nonetheless, a model for calculation has been developed by Weber et al. (1992).

When modelling the various chemical reactions occurring within the containment, it has to be considered that, because of the comparatively low temperatures, complete attainment of an equilibrium state cannot be postulated in all cases; this means that the kinetics of the chemical reactions, i. e. the reaction rates, are impor-

tant parameters. Weber et al. (1992) have critically evaluated experimental results concerning the reactions in the gas phase and the liquid phase, as well as the gas –liquid interface transport, and have compiled data on reaction rates, which can be directly applied in modelling and calculation.

According to Beahm et al. (1992), the iodine behavior in the containment can be divided up, timewise, into three categories:

1. In the first time interval, lasting from initial release from the primary system to the containment to about 1000 to 1200 minutes after the onset of the accident, the predominant uncertainty concerns the amount and chemical forms of fission product iodine entering the containment. The upper time limit for this category is the moment when the airborne aerosol concentrations have been substantially reduced from their peak values. All of the chemical and physical interactions of HI are expected to occur during this time interval. Reactions leading to the formation of I_2 by radiolysis would also occur in this, as well as in the next, time interval. Thus, during this period, all substances of importance for iodine reactions are expected to deposit in water pools or onto surfaces, all essential interactions between gaseous iodine and aerosols are expected to take place, and all HI effects, except for those related to pH, are expected to occur.
2. In the following time interval, lasting from 1000 minutes to about 2 to 3 weeks, vapor-phase iodine will essentially consist of the species I_2 produced by radiolysis and be partitioned between aqueous solution and the gas phase; there will also be minor amounts of organic iodide in the vapor phase. Iodine will be present in aqueous solution in forms that are determined both by radiolysis and by pH; in addition, a fraction of iodine will be deposited onto structural surfaces. During this time interval, the chemical forms of iodine are not expected to be closely related to the chemical forms that entered the containment from the reactor primary system, because of the iodine reactions that have occurred in the meantime.
3. Long after the onset of a severe accident (more than about 3 weeks), gas-phase iodine is expected to be dominated by organic iodide, with a small contribution from I_2; the conclusions drawn from the TMI-2 accident are highly consistent with these results of model calculations. Iodine behavior and distribution, in the long run, are expected to have little relationship to the chemical forms or amounts released into the containment, because the iodine will have had enough time to deposit onto surfaces or in water pools, so that the environmental conditions in the containment will prevail in determining the chemical forms.

Calculations of the behavior of fission product iodine in the course of different accident sequences in different plants yielded considerable differences in the iodine fraction expected to be present in the containment atmosphere (Beahm et al., 1992; Kress et al., 1993). In each case, sump water pH is the major parameter controlling radiation-induced I_2 formation and volatility. Whereas at a pH at or above 7 the amount of volatile I_2 is quite small (on the order of 1% of the sump water iodine inventory), failure to control pH at this value would lead to extensive I_2 volatilization which, in extreme cases, was calculated to increase to almost complete I_2 release from the aqueous phase. It was assumed that the reason for this behavior

is an increasing acidification of the unbuffered solution due to the radiolytic formation of nitric acid. According to these calculations, I_2 volatilization in small containments with large water volumes will be less pronounced. Generally, in PWR containments it will be higher than in BWRs, due to the larger water volumes present in BWRs, resulting in lower radiation concentrations as well as in higher I_2 retention. These calculations also showed that formation of organic iodides depends strongly on sump water pH; the fractions formed after 15 hours range from 0.6 to 0.01% of the total iodine at an uncontrolled pH (depending on the plant and the accident sequence investigated), but only from <0.001 to 0.03% when sump water pH is maintained at 7. However, as there is no clearly defined impurity composition of the sump water, the significance of these results (in which calculation of pH was performed taking into account the substances mentioned in Table 7.17.) for real accident situations has to be looked upon with some reserve. This applies particularly for PWR sump water, which probably contains appreciable amounts of metallic silver.

The calculations reported by Beahm et al. (1992) also showed a pronounced influence of the temperature on the I_2 volatile fraction in the containment atmosphere, in particular in BWR sequences. According to these calculations, an increase in containment temperature (at the gas–liquid interface) from 60 to 115 °C produces nearly an order of magnitude increase in the airborne fraction of iodine. The short- to medium-term fraction of organic iodides was calculated to be quite low, about 0.5% of the iodine core inventory in PWRs and close to 0.1% in BWRs.

Iodine volatilization behavior during postulated evaporation of the sump water to dryness is subject to considerable uncertainty. According to the calculations of Beahm et al. (1992), from 2 to 20% of the iodine in such pools could be converted to a volatile form, most likely to I_2. The presence of boric acid in the evaporating water volume is assumed to enhance iodine volatility markedly, likely due to the lower pH values that develop late in the evaporation process under the influence of the prevailing strong radiation field. On the other hand, silver which is present in the evaporating solution is very effective in decreasing iodine volatility; even in a borate solution at pH 4.4, a tenfold excess of Ag (related to the I^- content) resulted in an almost complete suppression of iodine volatility (Beahm et al., 1986).

Calculations of iodine behavior and transport in such complex systems can only be performed with the aid of computer codes based on appropriate iodine chemistry models. When compared to containment aerosol codes such as the NAUA code, iodine models are much more complicated, since they have to include chemical reactions, the progress of which depends on a large number of parameters – not only temperature and pressure, but concentrations, pH values, radiation dose rates, redox conditions, nature of the surfaces, etc. It is evident that determining the essential parameters and deriving their impact on the chemical reactions of interest from basic physico-chemical data (in most cases determined under "clean" laboratory conditions) is difficult to carry out. As Burns et al. said (1988): "Although large-scale integral experiments will provide much useful information for the prediction of iodine behavior under accident conditions, computer models present the only practical means of correlating a wide range of possible scenarios".

Table 7.18. Inorganic iodine species modelled in the three European codes (according to Sims et al., 1995; by courtesy of the European Communities)

Oxidation state	INSPECT	IMPAIR/IODE
−2	HI^-	
−1	I^-	I^-
−0.5	I_2^-	
−0.33	I_3^-	
0	I, I_2, $H_2I_3O_3^-$, HOI^-, I_2OH^-	I_2
+1	OI^-, HOI	OI^-, HOI
+2	IO, I_2O_2	
+3	IO_2^-, HIO_2	
+4	IO_2, IO_3^-, HIO_3^-	
+5	IO_3^-	IO_3^-
+6	IO_3	

Consequently, in recent years considerable effort has been dedicated to the elaboration of iodine chemistry codes. In Europe, three different codes describing the behavior of iodine in the containment during a severe reactor accident have been developed: INSPECT (AEA Harwell, UK), IODE (CEA/IPSN, France) and IMPAIR (PSI, Switzerland, and Siemens/KWU, Germany). The characteristic features of these codes have recently been outlined and compared by Sims et al. (1995). While INSPECT is a mechanistic code, IMPAIR as well as IODE are basically empirical codes. Because of this difference, the number of iodine species required by each code is different; as can be seen from Table 7.18., the empirical codes need fewer species than the mechanistic code because the latter has to have mechanisms and intermediate reaction products to cover the whole range of oxidation states from I^- to IO_3^-. Each of these approaches has its specific advantages and disadvantages; empirical models are simpler, but they require correlations for a wide range of conditions; further, the experimental data base must be good and has to be used with care outside the range the correlations are based on. On the other hand, mechanistic models are complicated and obtaining adequate knowledge of the reaction mechanisms that have to be included may not be practical; however, they do not rely on correlations and can in principle be used for any scenario. Because of the low temperatures prevailing in the containment (compared to the reactor pressure vessel and to the primary circuit), attainment of the equilibrium state for any given reaction often cannot be assumed. For this reason it is essential that the computer model to be used be able to simulate the chemical kinetics of the reactions to be considered.

The code IMPAIR is based on a compromise between a mechanistic and a phenomenological approach; this means that a minimum of "classical" mechanistic reactions are employed, but a phenomenological approach is used where the mechanistic one is deemed less suitable for modelling complex reactions (Cripps et al., 1992). For example: the radiolytical models are based on global equations intended to replace a large number of mechanistic reactions formulated from clean-condition data. This phenomenological approach is dependent on a set of parameters chosen

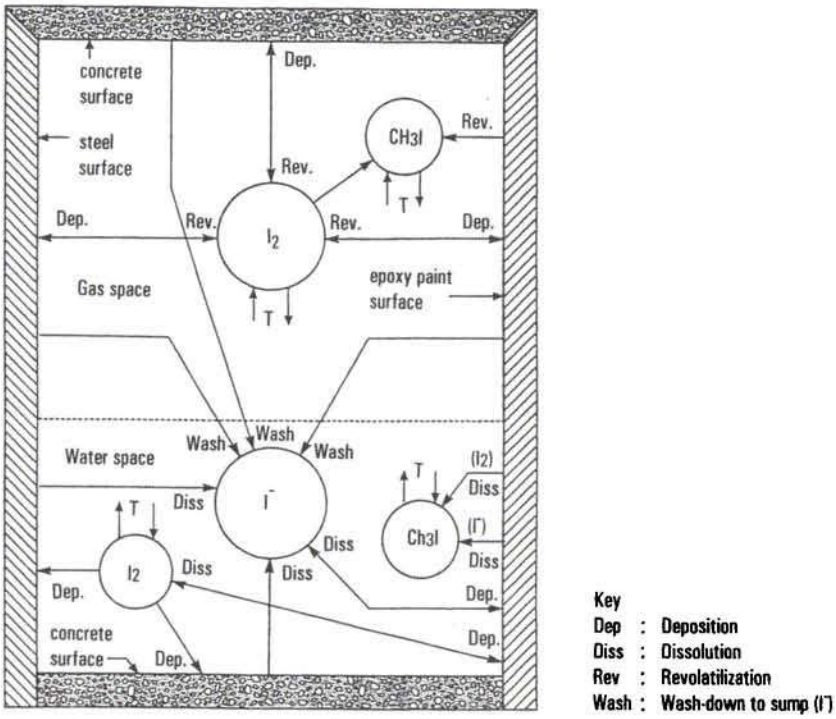

Figure 7.44. Overview of the reactions modelled in the IMPAIR code (according to Sims et al., 1995; by courtesy of the European Communities)

within boundary conditions derived from data obtained from experiments in the RTF facility (Furrer and Cripps, 1991). The IMPAIR code models postulated conditions of iodine chemistry present in a containment (sump, deposition and atmosphere) by using 28 differential equations and 69 rate constants; the basic mechanisms for the iodine chemistry that may take place in the containment are shown in Fig. 7.44. An advanced version, IMPAIR 3, also simulates iodine behavior in multiple compartments of any type of reactor containment, starting with release from the reactor core until the postulated end of accident (Güntay and Cripps, 1992).

The code IODE has been developed to calculate iodine behavior in a reactor containment and the auxiliary building; it is part of the French computer system ESCADRE which, similar to the US Source Term Code Package, describes the whole sequence of a severe reactor accident. The general philosophy of IODE is to model the main phenomena which may influence the behavior of iodine in the reactor containment; 15 chemical reactions are modelled, concerning both the water phase and the gas phase (Gauvain et al., 1991). Similar to IMPAIR, radiolysis is not described in detail but is taken into account over its global effect on iodine species. The kinetic data of the reactions were taken from the literature as far as inorganic iodine thermal reactions are concerned; other kinetic data were compiled from the elaboration of the IMPAIR 2 code.

Table 7.19. Iodine chemical forms used in the ORNL model (Beahm et al., 1988; by courtesy of Atomic Energy of Canada Limited)

Species	Phases considered
I_2	Gas, aerosol, liquid, surfaces (paint, steel, concrete), deposited aerosol
CH_3I	Gas, liquid, surface (paint)
CsI or I^-	Gas, aerosol, liquid, surfaces, deposited aerosol
HI	Gas, aerosol, surface (steel), deposited aerosol
AgI	Precipitate

The full INSPECT code, originally developed for a design basis loss-of-coolant accident, is a multi-compartment model dealing with chemistry and mass transport in the reactor pressure vessel, as well as in the different regions of the containment such as sump, aerosols, spray, gas phase and surfaces. This code may be considered as a data set for the numerical integration package FACSIMILE; it is a mechanistic code, which means that as far as possible all important chemical reactions are included within the model (Burns and Sims, 1988). Concerning the aqueous solution, the model includes about 150 reactions of which about 70 are required to describe most of the important features of iodine chemistry. The INSPECT reaction set has been used successfully to make predictions concerning the results of both small-scale laboratory experiments (Barton and Sims, 1991) and the intermediate-scale ACE-RTF tests.

Besides differences in the reaction data, there are differences in the reactions which are considered in the three codes. Only INSPECT deals with the reaction of iodine with silver aerosols in the gas phase while IODE is the only code that models iodine transport under steam condensing conditions. Concerning homogeneous reactions in the gas phase, IODE and IMPAIR include the oxidation of I_2 by radiolytically formed ozone and methyl iodide formation; in addition, IMPAIR contains the radiolytic decomposition of methyl iodide. INSPECT does not have the above reactions but the production of nitric acid is modelled. As to the water phase, reaction between iodine and silver particles is only modelled in IODE and IMPAIR. The current version of INSPECT does not include the modelling of organic iodide formation and hydrolysis, since it was considered that the mechanisms are not yet sufficiently understood for these processes to be included in a mechanistic model. Semi-empirical models such as those considered in IMPAIR and IODE have been added to the model for specific applications. The homogeneous reactions of organic iodides in the water phase (formation, hydrolysis, radiolysis) are treated in a comparable way in both IMPAIR and IODE. IODE presently takes one species into account (CH_3I), while IMPAIR can take into account other organic iodides with chemical properties different from those of CH_3I.

The ORNL containment iodine behavior model TRENDS (Beahm et al., 1988) lies somewhere in-between the empirical and mechanistic models; it includes five different iodine species, each of them existing in different phases (see Table 7.19.). Subsequent interconversions between different species are modelled, which transfer $I^-_{(aq)}$ to $CH_3I_{(aq)}$ and $I_{2(aq)}$ as well as $I_{2(g)}$ to $CH_3I_{(g)}$, also taking the associated

backreactions into account. The formation of AgI precipitate from aqueous iodine species is also considered, as well as aqueous–gas partitioning of I_2 and CH_3I. The calculation of sump water pH under the conditions of different accident sequences plays an important role and the radiation levels for the sump water are calculated for different plant conditions. With regard to mass transfer, convection between volumes or leakages, removal via condensing steam, convective transport to and from surfaces (containment walls as well as aerosol surfaces) are also considered, using data from various other transport codes. As a basis for the calculations, data obtained from basic calculations are used, as well as data obtained from laboratory and intermediate-scale experiments.

In Canada, the LIRIC model was developed (Wren et al., 1991) and is still undergoing improvement. LIRIC is a comprehensive model of an essentially mechanistic nature, showing similarities in the reaction sets used for the INSPECT code described above. LIRIC was developed to predict the time-dependent behavior of iodine in the containment under a variety of reactor accident conditions. Out of the large number of reactions involving physical and chemical processes, aqueous thermal reactions of iodine are considered, as well as water radiolysis processes and the interaction of the radiolysis products with aqueous iodine species. In addition, radiolytic decomposition of organic substances in the aqueous phase, formation and decomposition of organoiodine compounds, iodine reactions with aqueous impurities such as buffers and metal ions, mass transfer between the aqueous and gas phases and, finally, adsorption of gaseous I_2 onto surfaces and its desorption from them are included in the model. The LIRIC model has been developed in close cooperation with the experimental work carried out in the Radioiodine Test Facility.

References Section 7.3.3

Alm, M., Johannsen, K.-H., Dreyer, R.: Untersuchungen zum Verhalten der anorganischen Formen des Radioiods in den Kreisläufen von Druckwasserreaktoren. Isotopenpraxis **15**, 85–89 (1979)

Ashmore, C. B., Gwyther, J. R., Sims, H. E.: Some effects of pH on iodine volatility in containment. Proc. 3. Internat. Conf. on Containment Design and Operation, Toronto, Ontario, Can., 1994, Vol. 1

Ball, J. M., Wren, J. C., Portman, R., Sanipelli, G. S.: Iodine volatility in containment: The role of organic surfaces. Proc. 3. Internat. Conf. on Containment Design and Operation, Toronto, Ontario, Can., 1994, Vol. 1

Barnes, I., Becker, K. H., Starcke, J.: FTIR spectroscopic observation of gaseous HOI. Chemical Physics Letters **196**, 578–582 (1992)

Barton, R. A., Sims, H. E.: A comparison of the predictions of the INSPECT reaction set with experimental data. Proc. 3. CSNI Workshop on Iodine Chemistry in Reactor Safety, Tokai-mura, Japan, 1991; Report JAERI–M 92–012 (1992), p. 346–361

Beahm, E. C.: Tellurium behavior in containment under light water reactor accident conditions. Nucl. Technology **78**, 295–302 (1987)

Beahm, E. C., Brown, M. L., Shockley, W. E.: Adsorption of iodine on aerosols. Report ACE-TR-B 5 (1990)

Beahm, E. C., Shockley,W. E.: Trans. Am. Nucl. Soc. **45**, 482 (1983)

Beahm, E. C., Shockley, W. E., Culberson, O. L.: Organic iodide formation following nuclear reactor accidents. Report NUREG/CR-4327 (1985)

Beahm, E. C., Shockley, W. E., Weber, C. F., Wisbey, S. J., Wang, Y.-M.: Chemistry and transport of iodine in containment. Report NUREG/CR-4697 (1986)

Beahm, E. C., Wang, Y.-M., Wisbey, S. J., Shockley, W. E.: Organic iodide formation during severe accidents in light water nuclear reactors. Nucl. Technology **78**, 34–42 (1987)

Beahm, E. C., Weber, C. F., Kress, T. S., Parker, G. W.: Iodine chemical forms in LWR severe accidents. Report NUREG/CR-5732 (1992)

Beahm, E. C., Weber, C. F., Kress, T. S., Shockley, W. E., Daish, S. R.: Chemistry and mass transport of iodine in containment. Proc. 2. CSNI Workshop on Iodine Chemistry in Reactor Safety, Toronto, Can., 1988; Report AECL-9923 (1989), p. 251–266

Beard, A. M., Bowsher, B. R., Nichols, A. L.: Interaction of molecular iodine vapour with silver–indium–cadmium aerosol. Proc. International Symposium Severe Accidents in Nuclear Power Plants, Sorrento, Italy, 1988: IAEA-SM-298/108, Vol. 2, p. 201–213

Bell, J. T.: Chemistry of iodine and cesium. in: M. Silberberg (Report Coordinator) Technical Bases for Estimating Fission Product Behavior during LWR Accidents. Report NUREG-0772 (1981), Chapter 5

Bell, J. T., Campbell, D. O., Lietzke, M. H., Palmer, D. A., Toth, L. M. (a): Aqueous iodine chemistry in LWR accidents: Review and assessment. Report NUREG/CR-2493 (1982)

Bell, J. T., Lietzke, M. H., Palmer, D. A. (b): Predicted rates of formation of iodine hydrolysis species at pH levels, concentrations and temperature anticipated in LWR accidents. Report NURG/CR-2900 (1982)

Bleier, A., Greger, G.-U., Gropp, Ch.(b): Experimentelle Untersuchungen zum Verhalten des Iods bei hypothetischen Störfällen – Iodverteilungsquotienten. Abschlußbericht Förderungsvorhaben BMFT 1500 709/A 2; Siemens/KWU U 9414/88/022 (1988)

Bleier, A., Richter, F., Fernholz, O., Rippel, R., Pröbstle, G., Neeb, K. H.(a): Carry-over of fission products by droplets during sump water evaporation in severe reactor accidents. Paper presented at the Nuclear Reactor Severe Accident Chemistry Symposium, 3. North American Chemical Congress, Toronto, Can., 1988

Borkowski, R.: Untersuchungen zum chemischen Verhalten des Methyliodids bei schweren Störfällen im Druckwasserreaktor. Report KfK-3968 (1985)

Bowsher, B. R., Nichols, A. L.: High-temperature studies of simulant fission products. Part IV. Interaction of cesium iodide with boric acid over the temperature range 400 to 1000 °C. Report AEEW-R 1973 (1985)

Brown, M. L., Beahm, E. C., Shockley, W. E.: The oxidation of cesium iodide in stationary, premixed hydrogen flames. Report ACE-TR-B 6 (1990)

Burns, W. G., Davies, C. P., Deane, A. M., Kent, M. C., Marsh, W. R., Matsuda, M., Saunders, S. F., Sims, H. E.: Iodine chemistry in nuclear reactor environments. Proc. 5. BNES Conf. Water Chemistry of Nuclear Reactor Systems, Bournemouth 1989, Vol. 1., p. 281–287

Burns, W. G., Kent, M. C., Marsh, W. R., Potter, P. E., Sims, H. E.: Radiolytic and surface reactions of dilute iodine solutions. Proc. 2. CSNI Workshop on Iodine Chemistry in Reactor Safety, Toronto, Can., 1988; Report AECL-9923 (1989), p. 19–38

Burns, W. G., Kent, M. C., Marsh, W. R., Sims, H. E.: The radiolysis of aqueous solutions of caesium iodide and caesium iodate. Report AERE-R-13520 (1990)

Burns, W. G., Marsh, W. R.: The decomposition of aqueous iodide solution induced by γ-radiolysis and exposure to temperatures up to 300 °C. Proc. 3. BNES Conf. Water Chemistry in Nuclear Reactor Systems, Bournemouth 1983, Vol. 1, p. 89–101

Burns, W. G., Marsh, W. R.: The thermal and radiolytic oxidation of aqueous I^- and the hydrolysis and disproportionation of aqueous I_2. Report AERE-R-10767 (1986)

Burns, W. G., Sims, H. E.: The use of the FACSIMILE program in the speciation of iodine in a PWR reactor containment following a loss of coolant accident. Proc. 2. CSNI Workshop on Iodine Chemistry in Reactor Safety, Toronto, Can., 1988; Report AECL-9923 (1989), p. 197–214

Cripps, R., Furrer, M., Hellmann, S., Funke, F.: User's handbook for the iodine severe accident behaviour code IMPAIR 2.2. Report PSI Nr. 114 (1992)

Deane, A. M.: Organic iodide chemistry relevant to nuclear reactors: A review. Report AERE-R-12359 (1988)

Deane, A. M.: Volatile organic iodine formation by surface processes. Proc. 3. CSNI Workshop on Iodine Chemistry in Reactor Safety, Tokai-mura, Japan, 1991; Report JAERI–M 92–012 (1992) p. 181–194

Deane, A. M., Marsh, W. R.: The reaction of iodine (I_2) with surfaces. Report AEA-TRS-2015 (1990)

Eggleton, A. E. J.: A theoretical examination of iodine–water partition coefficients. Report AERE-R-4887 (1967)

Eigen, M., Kustin, K.: The kinetics of halogen hydrolysis. J. Am. Chem. Soc. **84**, 1355–1361 (1962)

Elrick, R. M., Merill, R. M., Ouelette, A. L.: The thermal instability of cesium iodide. Report NUREG/CR-5155 (1989)

Evans, G. J., Bekeris, P. A.: The sorption of iodine onto containment paints. Proc. 3. Internat. Conf. on Containment Design and Operation, Toronto, Ontario, Can., 1994, Vol. 1

Evans, G. J., Deir, C., Ball, J. M. (b): The retention of iodine in stainless steel sample lines. Paper presented at the 23. DOE/NRC Air Cleaning and Treatment Conf., Buffalo, N. Y., USA, 1994

Evans, G. J., Kupferschmidt, W. C. H., Portman, R., Palson, A. S., Sanipelli, G. G. (a): Radiochemical analysis of iodine behaviour in the Radioiodine Test Facility. J. Radioanal. Nucl. Chemistry Articles **180**, 225–235 (1994)

Evans, G. J., Mirbod, S. M., Jervis, R. E.: The volatilization of iodine species over dilute iodide solutions. Canadian J. of Chemical Engineering **71**, 761–765 (1993)

Evans, G. J., Palson, A. S.: ACE bench-scale studies of iodine volatility and interaction with epoxy painted surfaces. Proc. 3. CSNI Workshop on Iodine Chemistry in Reactor Safety, Tokai-mura, Japan, 1991; Report JAERI–M 92–012 (1992), p. 230–245

Fletcher, J. W., Miller, O. A.: Radiolytic formation and reactivity of aqueous hypoiodous acid. Proc. Specialists Workshop on Iodine Chemistry in Reactor Safety, Harwell, UK, 1985; Report AERE-R-11974 (1986), p. 107–120

Fluke, R. J., Frescura, G. M., Sagert, N. H., Tennankore, K. N., Vikis, A. C.: The Canadian program on iodine chemistry in reactor safety. Proc. 3. CSNI Workshop on Iodine Chemistry in Reactor Safety, Tokai-mura, Japan, 1991; Report JAERI–M 92–012 (1992), p. 49–61

Funke, F.: Reaction of iodine with steel surfaces. Final Report–Part 2: Assessment of iodine/steel interactions and experimental study. Report EUR 15668/2 EN (1994)

Funke, F., Greger, G.-U., Hellmann, S., Bleier, A., Morell, W.: Iodine/steel reactions under severe accident conditions in LWRs. Proc. 3. Internat. Conf. on Containment Design and Operation, Toronto, Ontario, Can, 1994, Vol.1

Funke, F., Hellmann, S.: Reaction of iodine with steel surfaces. Final Report–Part 1: Literature study. Report EUR 15668/1 EN (1994)

Furrer, M., Bühler-Gloor, T.: Revolatilisation of fission products, especially iodine, from water phases during evaporation to dryness. Proc. 2. CSNI Workshop on Iodine Chemistry in Reactor Safety, Toronto, Can., 1988; Report AECL-9923 (1989), p. 185–193

Furrer, M., Cripps, R.: Validation of IMPAIR 2 code using ACE test results from the Radioiodine Test Facility (RTF). Proc. 3. CSNI Workshop on Iodine Chemistry in Reactor Safety, Tokai-mura, Japan, 1991; Report JAERI-M 92-012 (1992), p. 329-344

Furrer, M., Gloor, T.: Effects of β^-, γ radiolysis on cesium iodide solutions in contact with simulated silver metal aerosol. Proc. Specialists Workshop on Iodine Chemistry in Reactor Safety, Harwell, England, 1985; Report AERE R 11974 (1986), p. 193-199

Gauvain, J., et al.: IODE 2.0 User manual. Report SEAC/91/04 (1991)

Genco, J. M., Rosenberg, H. S., Morrison, D. L.: Iodine deposition and its enhancement under reactor accident conditions. Nucl. Safety **9**, 226-238 (1968)

Gesellschaft für Reaktorsicherheit (GRS): Deutsche Risikostudie Kernkraftwerke Phase B. GRS-72 (1989)

Gmelins Handbuch der anorganischen Chemie, 8. Auflage Silber Teil 2B, 289-305 (1972)

Güntay, S., Cripps, R.: IMPAIR 3: A computer program to analyze the iodine behaviour in multi-compartments of a LWR containment. Report PSI Nr. 128 (1992)

Haimovich, O., Treinin, A.: Nature **207**, 185 (1965)

Harrell, J. R., Lutz, J. B., Kelly, J. L.: On the volatility and disproportionation of hypoiodous acid. J. Radioanal. Nucl. Chemistry Letters **127**, 13-20 (1988)

Hellmann, S., Bleier, A.: unpublished (1989)

Hellmann, S., Bleier, A., Rippel, R., Funke, J., Morell, W.: Large-scale experiments on iodine release associated with coolant flashing due to ruptured high-pressure tubes. Proc. 3. CSNI Workshop on Iodine Chemistry in Reactor Safety, Tokai-mura, Japan, 1991; Report JAERI-M 92-012 (1992), p. 280-297

Hemphill, R. T., Pelletier, C. A.: Surface effects in the transport of airborne radioiodine at light water nuclear power plants. Report EPRI NP-876 (1978)

Hilliard, R. K., Postma, A. K.: Large-scale fission product containment tests. Nucl. Technology **53**, 163-175 (1981)

Ishiwatari, N.: Aqueous solution of iodide under gamma ray irradiation. – Fixation of iodide by adding soluble silver salt. Proc. 3. CSNI Workshop on Iodine Chemistry in Reactor Safety, Tokai-mura, Japan, 1991; Report JAERI-M 92-012 (1992) p. 81-96

Kabat, M. J.: Chemical behaviour of radioiodine under loss-of-coolant accident conditions. Proc. 16. DOE Nuclear Air Cleaning Conf., San Diego, USA, 1980, p. 867-890

Karasawa, H., Endo, M., Tagawa, H., Takahashi, M, Ibe, E.: Effect of boiling upon radiolysis of iodide solution. Proc. 3. CSNI Workshop on Iodine Chemistry in Reactor Safety, Tokai-mura, Japan, 1991; Report JAERI-M 92-012 (1992) p. 137-151

Kent, M. C., Sims, H. E.: The radiolytic formation and destruction of the aqueous iodate anion. Report AEA TRS 2019 (1991)

Kress, T. S., Beahm, E. C., Weber, C. F., Parker, G. W.: Fission product transport behavior. Nucl. Technology **101**, 262-269 (1993)

Kupferschmidt, W. C. H., Buttazoni, J. B., Evans, G. J., Ford, B. L., Palson, A. S., Portman, R., Sanipelli, G. G. (b): Iodine chemistry in the presence of vinyl surfaces. Proc. 3. CSNI Workshop on Iodine Chemistry in Reactor Safety, Tokai-mura, Japan, 1991; Report JAERI-M 92-012 (1992) p. 213-229

Kupferschmidt, W. C. H., Buttazoni, J. B., Evans, G. J., Harris, D. R., Greig, D. R., Koroll, G. W., Sanipelli, G. G. (d): The oxidation of cesium iodide aerosols during hydrogen combustion. Proc. 3. CSNI Workshop on Iodine Chemistry in Reactor Safety, Tokai-mura, Japan, 1991; Report JAERI-M 92-012 (1992), p. 298-310

Kupferschmidt, W. C. H., Buttazoni, J. B., Melnyk, A. J., Portman, R., Sanipelli, G. G. (a): The effects of zinc primer surfaces on iodine behaviour within containment. Proc. 3. CSNI Workshop on Iodine Chemistry in Reactor Safety, Tokai-mura, Japan, 1991; Report JAERI-M 92-012 (1992) p. 195-212

Kupferschmidt, W. C. H., Evans, G. J., Jobe, D. J., Melnyk, A. J., Portman, R., Palson, A., Sanipelli, G. G. (c): The Advanced Containment Experiments (ACE) Radioiodine Test Facility experimental program. Proc. 3. CSNI Workshop on Iodine Chemistry in Reactor Safety, Tokai-mura, Japan, 1991; Report JAERI–M 92–012 (1992), p. 249–263

Lemire, R. J., Paquette, J., Torgerson, D. F., Wren, D. J., Fletcher, J. W.: Assessment of iodine behaviour in reactor containment buildings from a chemical perspective. Report AECL-6812 (1981)

Lieser, K. H., Coetzee, P. P., Förster, M.: Liberation of iodine from AgI during radiolysis. Radiochim. Acta **38**, 33–35 (1985)

Ligotke, M. W., Eschbach, E. J., Winegardner, W. K.: Ice-condenser aerosol tests. Report NUREG/CR-5768 (1991)

Lin, C. C.: Chemical effects of gamma radiation on iodine in aqueous solution. J. Inorg. Nucl. Chemistry **42**, 1101–1107 (1980)

Lin, C. C.: Volatility of iodine in dilute aqueous solutions. J. Inorg. Nucl. Chemistry **43**, 3229–3238 (1981)

Lucas, M.: Radiolysis of cesium iodide solutions in conditions related to those prevailing in a pressurized water reactor after severe core damage. Proc. OECD Specialists Workshop on Iodine Chemistry in Reactor Safety, Harwell, 1985; Report AERE-R-11974 (1986), p. 167–184

Lutz, J. B., Kelly, J. L.: The effects of organic impurities on the partitioning of iodine. Nucl. Technology **80**, 431–442 (1988)

Malinowski, D. D.: Iodine removal in the ice condenser system. Report WCAP-7426 (1970)

Marimuthu, K., Mitragori, D. S., Sundararajan, A. R.: Radiolysis of aqueous cesium iodide. J. Radioanal. Nucl. Chemistry Articles **131**, 253–259 (1989)

Moers, H.: Oberflächenanalytische Untersuchungen zum Freisetzungsverhalten flüchtiger Spaltprodukte bei simulierten Kernschmelzunfällen und zum Reaktionsverhalten von Iod mit Silberoberflächen. Bericht KfK-4073 (1986)

Neeb, K. H.: Auswirkungen chemischer Reaktionen auf das Verhalten des Spaltiods bei hypothetischen Ereignissen im Leichtwasserreaktor. VGB Kraftwerkstechnik **66**, 389–394 (1986)

Owczarski, P. C., Winegardner, W. K.: Capture of iodine in pressurized water reactor ice condensers. Proc. Symp. on Chemical Phenomena Associated with Radioactivity Releases During Severe Nuclear Plant Accidents. Anaheim, Calif., USA, 1986; Report NUREG/CP-0078 (1987), p. 6/87–6/94

Palmer, D. A., van Eldick, R.: Spectral characterization and kinetics of formation of hypoiodous acid in aqueous solution. Inorganic Chemistry **25**, 928–931 (1986)

Palmer, D. A., Lietzke, M. H.: The equilibria and kinetics of iodine hydrolysis. Radiochim. Acta **31**, 37–44 (1982)

Palmer, D. A., Lyons, L. J.: Kinetics of iodine hydrolysis in unbuffered solutions. Proc. 2. CSNI Workshop on Iodine Chemistry in Reactor Safety, Toronto, Ontario, Can., 1988; Report AECL-9923 (1989), p. 7–16

Paquette, J., Ford, B. L.: The radiation-induced formation of iodoalkanes and the radiolysis of iodomethane. Proc. 2. CSNI Workshop on Iodine Chemistry in Reactor Safety, Toronto, Can., 1988; Report AECL-9923 (1989), p. 48–73

Paquette, J., Sunder, S., Torgerson, D. F., Wren, C. J., Wren, D. J.: The chemistry of iodine and cesium under reactor accident conditions. Proc. 3. BNES Conf. Water Chemistry in Nuclear Reactor Systems, Bournemouth 1983, Vol. 1, p. 71–79

Parsly, L. F.: Chemical and physical properties of methyl iodide and its occurrence under reactor accident conditions. Report ORNL-NSIC-82 (1971)

Pasedag, W. F., Blond, R. M., Jankowski, M. W.: Regulatory impact of nuclear reactor accident source term assumptions. Report NUREG-0771 (1981)

Pelletier, C. A., Hemphill, R. T.: Nuclear power plant related iodine partition coefficients. Report EPRI NP-1271 (1979)

Postma, A. K.: Aqueous-gas partitioning. Proc. NSAC Workshop on Iodine Releases in Reactor accidents. Report NSAC-14 (1980)

Postma, A. K., Zavadoski, R. W.: Review of organic iodide formation under accident conditions in water-cooled reactors. Report WASH-1233 (1972)

Quan, R. C., Evans, G. J.: The impact of organic compounds on pH and iodine volatility in nuclear reactor containment structures. J. Radioanal. Nucl. Chemistry Articles **180**, 237–243 (1994)

Rahn, F.: The LWR Containment Systems Experiments (LACE) Project. Summary Report. Report EPRI NP-6094-D (1988)

Richter, F., Fischer, P., Morell, W., Neeb, K. H. (a): Experimentelle Daten zur Iod-Verteilung unter den Bedingungen hypothetischer Kernschmelz-Unfälle. Proc. Jahrestagung Kerntechnik Deutsches Atomforum, München, FRG, 1985, p. 247–250

Richter, F., Neeb, K. H., Rippel, R. (b): Experimentelle Untersuchungen zum Verhalten des Iods bei hypothetischen Störfällen. Abschlußbericht Förderungsvorhaben BMFT 1500 634/5, KWU R 917/85/007, 1985

Richter, R., Neeb, K. H.: Laboratory-scale and technical-scale investigations concerning iodine water–vapour phase partitioning under severe accident conditions. Proc. OECD Specialists Workshop on Iodine Chemistry in Reactor Safety, Harwell, UK, 1985; Report AERE-R-11974 (1986), p. 209–223

Ritzman, R. L.: Overview of the ACE iodine project. Proc. 3. CSNI Workshop on Iodine Chemistry in Reactor Safety, Tokai-mura, Japan, 1991; Report JAERI–M 92–012 (1992), p. 23–34

Ritzman, R. L., McCormack, J. D., Dickinson, D. R., Alleman, R. T.: The ACE large-scale iodine experiment at the Containment Systems Test Facility (CSTF). Proc. 3. CSNI Workshop on Iodine Chemistry in Reactor Safety, Tokai-mura, Japan, 1991; Report JAERI–M 92–012 (1992), p. 264–278

Rosenberg, H. S., Genco, J. M., Morrison, D. L.: Fission product deposition and its enhancement under reactor accident conditions: Deposition on containment surfaces. Report BMI-1865 (1969)

Sagert, N. H.: Radiolysis of iodine in moist air: A computer study. Proc. 2. CSNI Workshop on Iodine Chemistry in Reactor Safety, Toronto, Can., 1988; Report AECL-9923 (1989), p. 235–250

Schöck, W., Bunz, H., Adams, R. E., Tobias, M. L., Rahn, F. J.: Large-scale experiments on aerosol behavior in light water reactor containments. Nucl. Technology **81**, 139–157 (1988)

Sellers, R. M.: A review of the radiation chemistry of iodine compounds in aqueous solutions. CEGB Report RD/B/N 4009 (1977)

Sims, H., Dickinson, S., Henshaw, J., Hueber, C., Funke, F., Greger, G.-U., Hellmann, S.: Iodine code comparison. Report EUR 16507 EN (1995)

Soffer, L.: Iodine chemical form in LWR reactor accidents: Regulatory perspectives in the United States. Proc. 3. CSNI Workshop on Iodine Chemistry in Reactor Safety, Tokai-mura, Japan, 1991; Report JAERI–M 92–012, p. 35–48 (1992)

Styrikovich, M. A., Martynova, O. I.: Contamination of the steam in boiling reactors from solution of water impurities. Atomnaya Energiya **15**, 214–218 (1963)

Styrikovich, M. A., Martynova, O. I., Katkovskaya, K. Ya., Dubrovskii, I. Ya., Smirnova, I. N.: Transfer of iodine from aqueous solutions to saturated vapour. Atomnaya Energiya **17**, 45–49 (1964)

Thomas, T. R., Pence, D. T., Hasty, R. A.: The disproportionation of hypoiodous acid. J. Inorg. Nucl. Chemistry **42**, 183–186 (1980)
Toth, L. M., Pannell, K. D., Kirkland, O. L.: The chemical behavior of iodine in aqueous solutions up to 150 °C. I. An experimental study of non-redox conditions. Report NUREG/CR-3514, Vol.1 (1984)
Vikis, A. C., Torgerson, D. F.: Gas-phase radiation chemistry of iodine in post-accident environments. Proc. Specialists Workshop on Iodine Chemistry in Reactor Safety, Harwell, England, 1985; Report AERE R 11974 (1986), p. 185–192
Weber, C. F., Beahm, E. C., Kress, T. S.: Iodine chemical forms in LWR severe accidents. Proc. 3. CSNI Workshop on Iodine Chemistry in Reactor Safety, Tokai-mura, Japan, 1991; Report JAERI–M 92–012 (1992), p. 414–430
Weber, C. F., Beahm, E. C., Kress, T. S.: Models of iodine behavior in reactor containments. Report ORNL/TM-12202 (1992)
Wichner, R. P., Spence, R. D.: A chemical equilibrium estimate of the aerosols produced in an overheated light water reactor core. Nucl. Technology **70**, 376–393 (1985)
Winegardner, W. K., Postma, A. K., Jankowski, M. W.: Studies of fission product scrubbing within ice compartments. Report NUREG/CR-3248 (1983)
Wren, J. C., Paquette, J., Sunders, S., Ford, B. L.: Iodine chemistry in the +1 oxidation state. II. A Raman and uv-visible spectroscopic study of the disproportionation of hypoiodite in basic solutions. Canadian J. of Chemistry **64**, 2284–2296 (1986)
Wren, J. C., Sagert, N. H., Sims, H. E.: Modelling of iodine chemistry: The LIRIC database. Proc. 3. CSNI Workshop on Iodine Chemistry in Reactor Safety. Tokai-mura, Japan, 1991; Report JAERI–M 92–012 (1992), p. 381–394
Wren, D. J., Sanipelli, G.: The volatility of HOI. Proc. American Nucl. Soc. Meeting on Fission Product Behavior and Source Term Research, Snowbird, Utah, USA, 1984; Report EPRI NP-4113-SR (1985), p. 42/1–13

7.3.4 Release of radionuclides from the containment to adjacent areas

As has been discussed in the preceding sections, the containment of a nuclear power plant represents a very effective passive barrier, at least for a certain period of time, for confining the radionuclides released from the reactor core and from the primary system in a severe accident. This renders possible their plate-out from the containment atmosphere by natural processes such as deposition of aerosols or, as regards iodine, formation of non-volatile compounds, as well as by the action of engineered safety features (e. g. sprays). Nevertheless, in safety considerations it has to be assumed that the containment is not a permanent and absolutly tight confinement, but that there would be several fundamental mechanisms by which a certain fraction of the radionuclides could escape from the containment. The most important of these mechanisms are

- penetration through operational leaks in the steel shell;
- release through piping in the event of an incomplete containment isolation;
- late overpressure failure of the containment steel shell;
- controlled depressurization of the containment.

The fundamental possibility that one or more of these release paths might open up, however, does not result in a direct transport of radionuclides to the environment. In such a case, natural as well as engineered retention mechanisms come into play; these mechanisms will be discussed shortly in the following sections.

7.3.4.1 Penetration through operational leaks in the containment steel shell

The containment steel shells or liners of pressurized and boiling water reactors may contain small leaks originating in the manufacturing process. For example, in German PWR plants the leak rates through such leaks are allowed to amount to 0.25% of the containment free volume per day, at the maximum; these figures have to be verified by appropriate leak tests which have to be performed in the course of commissioning of the plant, as well as at regular intervals during its operational phase. As a consequence of the presence of such leaks, radionuclides may escape from the containment in the post-accident phase and may reach the adjacent areas of the plant.

In safety analyses it is frequently assumed that the rate of penetration of fission products through the usually very narrow slits would be identical to the leak rate that would be measured using air as a penetrating medium. To be sure, this assumption is true for the fission product noble gases; for airborne aerosols, however, narrow slits can act as a trap, so that under otherwise identical conditions aerosol leak rates will usually be lower by some orders of magnitude than the air leak rate. Early observations in this field showed that the presence of steam in a heated vessel atmosphere results in a drastic decrease of the leak rate to values that are well below those measured with dry air at ambient temperature (Witherspoon, 1970). Likewise, quick plugging of natural leak paths was observed when higher steam contents were introduced into the containment atmosphere; under such conditions, even artificially made leaks in the vessel effected an appreciable retention of both airborne iodine and particles (Witherspoon and Postma, 1971).

These early results were confirmed by numerous observations and experiments, a selection of which was summarized by Morewitz (1982), and were compared with a simple model established by Vaughan (1978), describing the plugging of ducts by aerosol flows. This model predicts that the mass of aerosol entering the duct before plugging is proportional to the cube of the duct diameter with a proportionality constant apparently being a function of the effective density of the deposited aerosol. According to this model, capillary tubes with 1 mm diameter will already be plugged after the passage of about 10 mg of aerosol, tubes with 1 cm diameter after the passage of about 10 g of aerosol. The amount of aerosols that has passed through the tubes until blockade does not significantly depend on the aerosol concentration, on the flow rate or on the particle size of the aerosols. The impact of steam or moisture on the deposition of the aerosols was not considered in this model. Other experiments indicated that the size distribution of the aerosols after

having passed through the duct is shifted to larger sizes by agglomeration of particles within the capillary; some of the agglomerates may break off and be resuspended in the air stream. Summarizing the experimental findings, Morewitz (1982) concluded that less than 1 mg of respirable aerosol may penetrate even through a short-length 1 mm diameter tube.

Under the conditions prevailing in the containment in the course of a severe reactor accident, there are two effects which may enhance the retention efficiency of the leak paths. First, both the models and most of the experiments mentioned above did not consider the impact of steam on the transport of aerosols; as was mentioned above, condensing steam can further narrow or even plug a narrow gap. Second, real leak paths through steel shells and concrete walls usually are irregularly shaped cracks which show rough surfaces so that additional aerosol removal phenomena, such as impaction at bends, may occur, reducing the penetrating mass of aerosol even more. Taking into account the second effect in particular, it was estimated that the mass of respirable aerosol escaping from an intact reactor containment building at an air leak rate of 0.1% per day would be less than 1 mg per day, i. e. lower by a factor of 10^4 to 10^6 than the gas leak rate (Morewitz, 1982).

Similarly, elemental iodine I_2 as well as HI can be expected to be retained during passage through narrow slits. With steel materials, the mechanisms discussed in Section 7.3.3.4.7. will be effective, and revolatilization of deposited iodine can be assumed to be small at the comparatively low temperature of the containment shell; with concrete materials, reaction of I_2 and HI with the alkaline constituents of the concrete will result in iodine retention. However, detailed investigations in this field are still lacking.

The retention of airborne fission products in narrow gaps was verified in the CSE tests, where the containment showed a leak rate of about 0.1% per day in the dry state, i. e. the same order of magnitude as that of a real LWR containment (Hilliard and Postma, 1981). Since in these experiments the natural leaks in the steel shell of the vessel plugged very quickly under the influence of steam, artificial leaks were created to measure the extent of penetration of iodine and cesium. The results showed that the magnitude of retention in these leak paths corresponded to a decontamination factor of about 15 for iodine and 100 for cesium. Iodine and cesium released with the steam through the leaks proved to be almost quantitatively plated out with the steam condensing outside the containment. Similar results have been obtained in the LACE experiments, which showed that even simple leak paths may retain a large fraction of suspended fission products, with turbulent deposition being the dominant removal mechanism (Rahn et al., 1988).

These results mean that penetration of fission products (except the fission product noble gases) through operational leaks in the containment shell in the course of a severe reactor accident will be very small. The largest fraction of the penetrating fission products will be plated out in the adjacent rooms and compartments with the condensing steam, while the still airborne fraction will be transported to the filters of the annulus air extraction system. Fission product iodine plated out into the water pools formed in the annuli will be subjected to the reactions to be discussed in Section 7.3.4.3.

7.3.4.2 Release of radionuclides in the event of a failure of containment isolation

The piping which penetrates the containment steel shell (e. g. fresh air and exhaust air ducts) is automatically locked in the very early stages of an accident. Despite these measures, in risk studies it has to be assumed that one of these penetrations will fail to be closed, thus permitting the transport of radionuclides out of the containment. The TMI-2 accident demonstrated that such a situation may occur in reality: in this event an open connection to the auxiliary building was the main pathway for the escape of fission product radionuclides from the containment to the environment.

Concerning the transport of fission products out of the containment, the relative locations of the break in the primary system and of the open penetration in the containment steel shell are of great importance. It can always be assumed that these two positions are in different compartments so that the fission products have to travel a certain distance over which deposition may occur; moreover, the time required to cover this distance provides an opportunity for chemical reactions to occur, in particular with respect to iodine. This time delay depends highly on the specific accident sequence, in particular on the rate of pressure increase within the containment and, thus, on the steam mass flow from the primary system to the containment. With a high degree of probability it can be assumed that the open penetration can be locked (e. g. by manual action) within a comparatively short time.

The steamborne fission products which can pass through the open penetration will reach a region of lower temperature, either in the annuli or in the auxiliary building. There, the largest fraction will be plated out by condensing steam, and their subsequent behavior, in particular that of iodine, will be dictated by the reactions which are discussed in the following section.

7.3.4.3 Late overpressure failure of the containment steel shell

The heat transport from the core melt into the sump water, as well as the production of permanent gases in the core melt – concrete interaction, will result in a pressure increase inside the closed containment. Provided that no measures for controlled depressurization are undertaken (see next section), then, according to the results of thermodynamic calculations, the steam–gas pressure within the containment would reach the postulated failure value of the containment steel shell of about 0.9 MPa after 5 to 10 days, depending on the accident sequence. Such an overpressure failure will not be a catastrophic burst of the shell, but rather the enlargement of the operational leaks to a size permitting the escape of gas and steam at a rate high enough to keep the pressure inside the containment at a

constant level. Another fundamental possibility is the sudden opening of a larger leak area on the order of some hundred cm^2.

The failure of the containment steel shell may be associated with a rapid depressurization, leading to an effervescence of the hot sump water and to an enhanced transport of radionuclides from the liquid to the steam phase. In order to study this effect, depressurization experiments were performed in a $2\,m^3$ pressure vessel starting from 170 °C, 0.8 MPa, which showed that the magnitude of entrainment of non-volatile elements with the steam phase depends on the size of the opening (Richter and Neeb, 1985). The diameters of the orifices used in these experiments ranged from 4 to 10 mm, corresponding to openings beteween 150 and $900\,cm^2$ in a real containment steel shell; during the depressurization periods, which lasted for 10 to 30 minutes, approximately 20 to 30% of the sump water volume originally present was evaporated. From the amounts of substances transported to the condensate during this period, apparent partition coefficients (apparent, since they did not represent an equilibrium situation) between $2 \cdot 10^7$ and $3 \cdot 10^6$ were measured using a non-volatile tracer (Li^+). For $I^- - 2\%\ I_2$ solutions, apparent partition coefficients of about $5 \cdot 10^5$ were obtained using a 6 mm diameter orifice, while a partition coefficient of about $7 \cdot 10^6$ was measured for a pure iodide solution. Hence, taking into account the assumed difference in the concentrations of both iodine species in the sump water, carry-over of I^- seems to be smaller by about an order of magnitude than that of volatile I_2.

After opening of the leak in the containment shell, the gas-steam atmosphere present in the containment, together with the gaseous and aerosol radionuclides carried by it, will enter the annuli between the steel shell and the concrete secondary shielding. Here, the temperatures of the walls and structures are well below 100 °C, resulting in a partial condensation of steam, in the course of which a large fraction of the aerosols will be washed down to the newly formed sumps. In addition, deposition of aerosols will take place during their residence time in the annuli and in the auxiliary building; modelling of such processes, however, is very difficult and, until now, has only been performed in a simplified manner.

Due to its different chemical forms present in the containment atmosphere, fission product iodine shows a complex behavior in these areas as well. CsI carried by water droplets or by aerosol particles will behave in the same manner as do the other aerosols. The volatile iodine species I_2 and CH_3I will be distributed between the newly formed sump water and the atmosphere of the annuli, as is schematically shown in Fig. 7.45. Experiments have demonstrated that the extent of I_2 plate-out depends on the degree of steam condensation, amounting to about 90% at a condensation temperature of about 40 °C (see Section 7.3.3.4.2.). The newly formed sumps in the annuli and in the auxiliary building show a pH of about 7 (since they consist solely of condensed steam), and temperatures between 50 and 80 °C; this means that I_2 plated out into these liquid phases is not only instantaneously hydrolyzed to I^- and HOI, but will also disproportionate rather quickly under formation of IO_3^-. As can be seen from Fig. 7.24., under such conditions the disproportionation equilibrium will be reached within a comparatively short time. If one assumes very conservatively an initial I_2 concentration in the sump water of about 1 mg/l and a temperature of 100 °C, then it can be derived from Fig. 7.24. that the

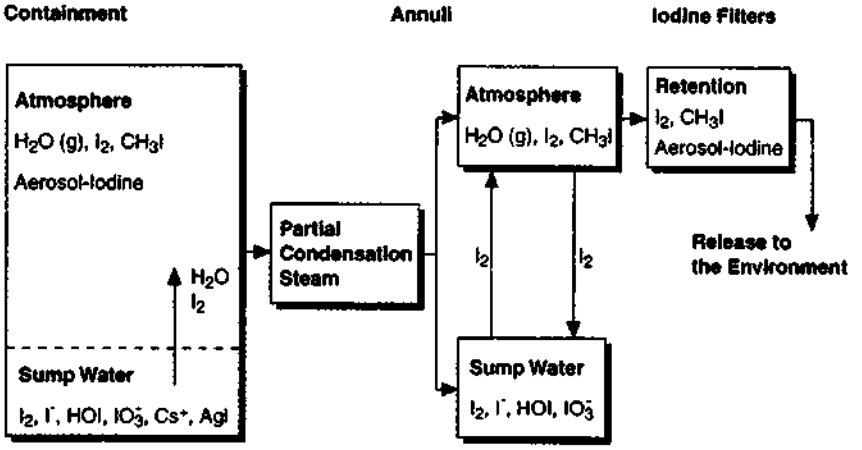

Figure 7.45. Iodine release from the containment; behavior in the annuli

I_2 partition coefficient will increase rapidly with time and will reach values of about 10^5 after 3 hours.

Unlike the containment, the annuli do not represent a closed system. This means that equilibrium considerations cannot be applied here, since the buildup of a partition equilibrium is continuously disturbed by the flowing atmosphere which consists of steam and permanent gases and contains traces of I_2. Consequently, the processes which take place inside the annuli are very complex, and a simple calculation of the extent and the rate of iodine revolatilization from the liquid phases is not possible. Assuming an instantaneous establishment of the equilibrium state in each volume element of the flowing atmosphere would result in an overconservative approach, leading to the result that iodine would be only temporarily retained in the annuli. Therefore, the thermodynamic approach has to be complemented by kinetic considerations which include the rate of formation of I_2 from I^- and IO_3^- by the Dushman reaction, as well as the kinetics of the diffusion-controlled transport of I_2 from the liquid to the gas phase. In addition, revolatilized I_2 can be temporarily or even permanently trapped by the paint on the walls of the annuli and the auxiliary building, which would additionally diminish or at least delay iodine release from the plant.

In an open system with a gas phase moving parallel to the surface of the shallow water pool formed, the attainment of an equilibrium characterized by the I_2 partition coefficient R applies only for a boundary layer that is limited by the flow characteristics, and not for the whole moving gas phase. This means, then, that there is a greatly reduced transport of I_2 from the liquid to the gas phase, as compared to the assumption of an instantaneous attainment of equilibrium for the entire gas phase. It can be theoretically derived that the fraction of I_2 released (X) in time t is given by

$$X = 1 - e^{-k \cdot t / R}$$

where R is constant or can be reasonably averaged. k comprises both the diffusion constant for I_2 in the gas phase and the flow characteristics, including the thickness of the boundary layer; it is $1 \cdot 10^{-3}$ to $5 \cdot 10^{-3}$ for the experimental conditions applied in the revolatilization studies cited below. An analogous theoretical treatment was described by Yuill et al. (1970), as well as by Pelletier and Hemphill (1979). Experimental studies of I_2 revolatilization from pH 7 water pools at temperatures to be expected in the PWR annuli (about 75 °C) were conducted by Bleier et al. (1988). The results demonstrated very clearly that I_2 revolatilization is considerably smaller (factor 5 to 20) than that calculated under the assumption of an instantaneous equilibrium in the whole gas phase with a partition coefficient of 5000.

Low-molecular-weight organoiodine compounds (e. g. CH_3I), which are released from the containment together with the gas-steam flow, remain virtually unaffected by the steam condensation in the annuli, which means that they will remain almost completely in the gaseous phase. Moreover, it has to be expected that additional organoiodide will be formed in the annuli by reaction of I_2 with the painted and coated surfaces. As yet there is no detailed knowledge on the kinetics and the equilibrium state of organoiodide formation under these conditions, which are characterized by low temperature and a very low radiation field; it can be expected to be highly dependent on the specific conditions of the particular accident sequence. Experiments in a $2\,m^3$ vessel at temperatures around 75 °C (Bleier et al., 1988) showed an effective partition coefficient which was considerably smaller than that measured in clean-condition experiments conducted in parallel (see Fig. 7.29.). This decrease in the partition coefficient proved to be partly caused by a noticeable formation of organoiodides in these experiments, with the extent depending on experimental parameters and ranging from 3 to 60% of the total iodine emission from the water phase. This conversion was caused by the organic coating on the inner surface of the vessel (epoxy-resin base coating). The by far highest organoiodide formation occurred in the first of the experiments, indicating that fresh organic paintings are much more reactive than older ones. An additional contribution to the low partition coefficient came from an enhanced I_2 volatilization, which probably resulted from the formation of I_2 deposits on the surfaces of the experimental vessel above and near the water surface very early on in the experiment, from which I_2 would have been desorbed afterwards to the gas phase in addition to the I_2 directly volatilized from the water phase.

It is probably not very far from reality to assume that under steady-state conditions the volatile iodine in the annuli atmosphere would consist of 50% each of I_2 and CH_3I, and that this ratio would be established within about 10 hours. It is important to note that errors in these estimates do not seriously affect the evaluation of the accident consequences, since, on the one hand, I_2 is retained in the emergency filters with high efficiency, whereas, on the other, the radiotoxicity attributed to organoiodine compounds (which are retained in the filters to a lesser degree) is significantly lower than that of I_2. In addition, calculations have shown that the consequences of a severe accident in the environment will be determined by the released aerosol iodide.

If no appropriate countermeasures are taken, one has to assume that after failure of the containment steel shell the containment sump water will slowly boil down; according to very conservative assumptions it will evaporate to dryness after a longer period of time (on the order of 10 days), depending on several parameters. The chemical reactions which take place during this period have been discussed in Section 7.3.3.4.2. I_2 still present or newly formed in the water phase (e. g. by radiation-induced reactions) will be volatilized at a rate which is proportional to the rate of water evaporation, and will be transported to the annuli, presumably undergoing along the way one or more deposition and revolatilization steps. Due to the boiling containment sump water, an almost instantaneous attainment of the I_2 partition equilibrium has to be assumed, quite in contrast to the situation in the non-boiling annuli sumps mentioned above.

Iodide as well as iodate present in the containment sump water show an extremely high partition coefficient under the prevailing conditions (an initial temperature of about 150 °C at a system pressure of about 0.8 MPa, with the temperature decreasing to about 100 °C at ambient pressure in the event of a larger defect size); therefore, no true volatility of these species can be assumed at this stage. On the other hand, traces of dissolved or suspended fission products can be carried by fine water droplets out of the containment. Corresponding experiments have shown that under realistic boiling conditions the concentration of droplets (related to the total mass of H_2O in the steam flow) at a short distance above the boiling surface was only on the order of 10^{-4} to 10^{-5} (see Section 7.3.3.2.). This means that the amount of non-volatile iodine carried by these droplets would be negligibly small compared with the amount of volatilized I_2 and CH_3I. On the other hand, droplet carry-over is a possible mechanism by which non-volatile fission products such as cesium isotopes could be transported out of the containment. During steam condensation in the annuli, the bulk of these aerosols is expected to be washed down to the newly formed sumps.

In the final stage of the evaporation of containment sump water the formation of a certain amount of undissociated HI cannot be ruled out in a sump water that has not been treated with alkalizing agents (see Section 7.3.3.4.2.). The limited knowledge we have about the process of evaporation of the residual amounts of water in the presence of large amounts of suspended solids does not permit an estimate of the magnitude of HI volatilization, although it is probably quite small and of no significance for radioiodine release from the containment.

Non-volatile radionuclides transported as aerosols out of the containment are partly washed down during steam condensation in the annuli, as was already mentioned above. The temperatures of the sumps here are well below the boiling point, so that a noticeable resuspension of radionuclides by droplet carry-over is not to be assumed. However, a small resuspension of non-volatile radionuclides cannot be ruled out under these conditions, with the mechanism for this being the formation of small droplets by the action of the air flow. As was discussed in Section 6.2.2., experimental studies have yielded a very small carry-over of non-volatiles to the air flow. Due to the differences in the conditions, the results of these investigations cannot be directly applied to the release from sumps in the annuli or in the auxiliary building, but it can be assumed that the experimental values obtained in

these experiments represent an upper limit for the release rates of non-volatile radionuclides from unperturbated sump solutions.

Finally, the standby filters of the annulus air extraction system will act as an additional barrier, preventing the release of radionuclides from the annuli to the environment. The comparatively high humidity of the off-gas under accident conditions does not adversely affect the function of the aerosol filters, but potentially reduces the efficiency of the iodine filters. Nonetheless, a retention efficiency of >99% for I_2 and of >90% for CH_3I can be assumed, even under such unfavorable conditions.

7.3.4.4 Controlled depressurization of the containment

The late overpressure failure of the containment steel shell can be prevented by a controlled depressurization, in the course of which the gas–steam mixture escaping from the containment is directed to an additional system in which the radionuclides are retained. The purpose here is to further reduce the possibility of release of radionuclides to the environment as a consequence of a severe reactor accident. Practical application of this idea can be based on various principles; an overview of the design of different systems was given by Schlueter and Schmitz (1990).

In the Swedish BWR plant Barsebäck, a so-called "vented containment" was employed for the first time, consisting of a 10,000 m^3 gravel bed filter to which the gas–steam mixture from the containment would be directed in the event of a severe accident. The steam will condense on the initially cold pebble surfaces, resulting in an effective retention of aerosols and iodine. However, for various reasons this solution proved not to be optimal.

Significant progress in this field was represented by the development of mechanical filters consisting of steel filaments which can be operated up to temperatures of 500 °C, which easily enables them to withstand the heat introduced by the steam as well as the radiation and the decay heat caused by the radionuclides trapped in the filter (Dillmann et al., 1988). This deep-bed filter consists of several layers of steel fibers, starting with a fiber thickness of 30 μm in the first layer down to 8 μm in the final layer; by such a design, a rapid plugging of the fine filter section is prevented and the load capacity of the filter is enhanced. Downstream from this filter, a moisture separator is installed, followed by a final fine filter with 2 μm fibers by which a retention factor for typical core melt aerosols of 10^3 to 10^4 is obtained at steam flow velocities of 40 cm/s. These results were verified in tests using the uranine technique which yields particles with an average diameter of about 0.2 μm, thus resulting in test conditions that are more stringent than the DOP (dioctylphosphate) technique usually applied. In the range from 100 to 140 °C, the retention factor increases with temperature due to the increasing importance of diffusion.

Volatile iodine species are not efficiently retained by the steel fiber filter. For this reason, an additional filter was proposed containing a silver-impregnated

molecular sieve as an active matrix, which is to be installed downstream from the steel fiber filter. Since the retention efficiency of this material, in particular with respect to organoiodine compounds, is adversely affected by condensing steam, the filter must be heated to temperatures beyond the dew point of the venting gas. If these requirements are fulfilled, a CH_3I decontamination factor of up to 2000 can be obtained using a filter thickness of 7.5 cm (Dillmann et al., 1990).

The retention systems which are installed in the Canadian CANDU plants show a similar design (McArthur and Salaff, 1988). They consist of a combination of an aerosol filter with different pore sizes and an impregnated charcoal filter with an iodine retention efficiency of better than 99.9%.

When compared to the solid state filters, liquid-phase retention systems prove to have several advantages. The heat introduced by the venting flow as well as by the decay of the absorbed radionuclides is passively removed by boiling of the water phase, the load capacity for aerosols is virtually unlimited, and the retention of volatile iodine compounds can be guaranteed by appropriate chemical conditioning of the water phase. An important prerequisite for high retention efficiency, besides the thermal and radiation stability of the chemicals applied, is a very intimate contact between the gas–steam flow and the liquid phase of the retention system, in order to obtain a fast and effective exchange of matter.

In general, the extent of exchange of matter between a gas flow and a water pool depends on several parameters, in particular for short contact times (see Section 7.3.2.4., where particle retention in a BWR pressure suppression pool is discussed). Particle size is one of them; experiments using Eu_2O_3 aerosol showed that the decontamination factor exhibits a minimum value at particle diameters of about 0.2 to 0.5 μm. For submicron size particles, particle diffusion is the mechanism which controls retention in the water phase; the same mechanism is responsible for the retention of ionic dissolved species. By contrast, for particles in the several micron range, sedimentation and inertia are the dominant retention mechanisms. As a result, the scrubbing efficiency as a function of particle size passes through a minimum at a certain particle size where neither diffusion nor sedimentation and inertia contribute significantly. Another important parameter is the submergence height, which is equivalent to the residence time of the bubbles in the water. A longer residence time means a higher probability that particles in the bubble will come into contact with the liquid interface; therefore, the decontamination factor is expected to depend exponentially on the residence time, i. e. on the submergence height. When the bubble size exceeds a certain limit it seems to have little influence on the retention efficiency. Enhanced temperature and steam fraction of the gas flow positively affect the retention efficiency, in the former case by accelerated diffusion and reduced surface tension, in the latter by steam condensation resulting in an intensified mixing of both phases and an increased plate-out of the particles and ions being carried in the bubbles.

One possible design for a liquid-phase retention system is a submerged gravel bed into which the venting flow is introduced. Due to the flow barriers represented by the gravel particles in the bed, the venting flow has to take a long pathway through the liquid, resulting in a comparatively long contact time. An even better

contact between steam and liquid is obtained by using a Venturi-type scrubber in which the liquid is injected into the gas flow which is accelerated to very high speeds (50 to 150 m/s) by the drag effect of a specially designed nozzle. Due to the dispersion of the liquid into very fine droplets or lamellas, a large interface area is formed, resulting in a virtually instantaneous absorption of gases or aerosols. For this reason, the absorption efficiency of the scrubber increases with increasing pressure drop. Venturi scrubbers are widely used in the industry for the retention of gases and particles from gas flows. The application of this type of retention system in the controlled venting of the containment is favored by the fact that a rather high driving pressure (0.4 to 0.6 MPa) automatically results from the containment inner pressure. Due to the special design of the nozzles, a highly intimate mixing of steam and liquid is achieved. About 800 nozzles are installed in the retention system of a multi-Venturi scrubber (Espefält and Persson, 1988).

The sliding-pressure Venturi scrubber developed by Siemens/KWU and described by Eckardt (1988) allows operation at the pressure level prevailing inside the containment down to an overpressure of about 0.1 MPa, without need of a throttle valve in the venting line; the water droplets generated in the liquid phase of the scrubber during operation of the system are retained by a steel fiber filter located inside the scrubber tank. The scrubber can be designed in a manner to reduce water losses due to evaporation caused by the decay heat of the absorbed radionuclides to an insignificant level.

In order to achieve an effective retention of fission product iodine, the water volume in the scrubber is alkalized by addition of NaOH. During normal operation of the plant the liquid in the scrubber is covered by an inert gas, preventing NaOH consumption by the CO_2 content of the air. In addition, $Na_2S_2O_3$ solution is stored in a separate vessel; caused by the pressure increase which is associated with the beginning of the venting procedure, a rupture diaphragm will fail so that the thiosulphate solution is fed passively into the scrubber. Because of the high stability of thiosulphate in alkaline solution, it is also possible to use one scrubber solution containing both chemicals. Moreover, when the water volume of the scrubber is permanently heated to about 90 °C, a condensation of steam in the first stages of the venting action and, as a consequence, the possible formation of a burnable H_2–air mixture is prevented. Experiments in a real-size test unit yielded retention factors on the order of 10^4 for aerosols, of 10^2 for I_2 and of about 5 for organoiodine compounds.

In the retention of volatile radioiodine species in a Venturi scrubber unit, two different stages have to be distinguished. The first one is the transfer from the venting flow to the liquid phase, the second one the prevention of revolatilization from the liquid phase even in the case of a continuing and long-lasting (up to 36 hours) venting flow.

In the first stage of the process, a very rapid exchange of matter between the two phases is of great importance. This is achieved by the very intimate phase contact in the Venturi nozzles, on the one hand, and by the comparatively high temperature in the system, on the other, resulting in enhanced Brownian movement of the radionuclides to be trapped. Upon contact with the liquid water phase, a

steam-borne I_2 molecule is immediately hydrolyzed to I^- and HOI; in the solution, which is alkalized by NaOH to a pH of about 10 to 11, a rapid disproportionation of HOI to I^- and IO_3^- will take place. The additional presence of thiosulphate in the scrubber solution favors the reduction of I_2 and HOI to non-volatile I^-. Experiments in a real-size test facility proved that more than 99% of the I_2 activity in the venting flow was retained in the scrubber, even when the working pressure dropped from the design value of 0.4 to 0.6 MPa to values of about 0.15 MPa (Eckardt, 1988).

The largest fraction of the activity that is airborne in the containment atmosphere (which, with the exception of the fission product noble gases, is only a small fraction of the total activity inventory of the containment) is transported to the scrubber during the first venting phase. Due to the continuing heat input from the molten core – concrete interaction zone, steam production persists over a longer period of time, making repeated venting phases necessary in order to prevent containment overpressure failure. Therefore, appropriate measures have to be taken to ensure that no significant revolatilization of iodine activity already plated out in the scrubber solution will take place during these phases. The experiments mentioned above showed that a renewed production of volatile I_2 in the scrubber solution from its hydrolysis, disproportionation and reduction products is almost completely prevented by the combined action of the NaOH and $Na_2S_2O_3$ additives; even over a longer time period (tens of hours), the fraction of revolatilized iodine activity amounted to less than 1% of the iodine inventory in the scrubber solution.

As the consequence of the molten core – concrete interaction, the venting gas will contain huge amounts of CO_2. However, due to the presence of NaOH in the scrubber solution, its pH is stabilized at a value of about 9 by a $CO_3^{2-}-HCO_3^--CO_2$ equilibrium; as a result, the retention efficiency of the scrubber solution for elemental iodine is not adversely affected by the continuing CO_2 flow. Other substances which are potentially transported to the scrubber solution (such as boric acid, aerosols, decomposition products of organic compounds etc.) do not lead to a pH decrease down to values at which significant decomposition of thiosulphate is to be expected.

As was discussed in Section 7.3.3.4.9., only a small fraction of the airborne I_2 in the containment atmosphere will be converted to organiodine compounds within the first days following the accident; for this reason, as well as because of the rather low radiological significance of these compounds, their retention in the course of containment venting is not necessary. In the Venturi scrubber experiments mentioned above, it was observed that CH_3I unintentionally formed in the test facility was also retained in the scrubber solution with an efficiency of about 90%; only at high air contents in the venting gas flow (up to 70%, which is unrealistically high under severe accident conditions), did the retention efficiency decrease to about 50%. Calculations showed that the reaction

$$CH_3I + S_2O_3^{2-} \longrightarrow CH_3S_2O_3^- + I^-$$

is sufficiently fast to effect a far-reaching decomposition of this organoiodine compound, even in the very short contact time between gas flow and liquid phase. Other decomposition reactions such as hydrolysis of the organoiodide compounds

by H_2O and/or NaOH proved to be not fast enough to account for an appreciable decomposition (Siemens/KWU, unpublished).

The question was raised whether thiosulphate would be sufficiently stable under the rigid conditions prevailing in the scrubber solution during containment venting. According to the results reported by Row et al. (1969), an alkaline $S_2O_3^{2-}$ solution is far more stable against thermal load and radiation than an acidic one; 50 hours at 140 °C resulted in a 20% decomposition, and after a gamma irradiation dose of 10^6 Gy at 140 °C about 15% of the original $S_2O_3^{2-}$ concentration was still effective. Since the starting concentration of thiosulphate in the scrubber solution represents a stoichiometric excess of about 400-fold compared to the total I_2 input and the integrated β/γ dose during 48 hours of venting amounts to only about $5 \cdot 10^4$ Gy, there is no danger of a significant decrease in thiosulphate effectiveness.

Within the framework of the Advanced Containment Experiments (ACE) program, various retention-system designs were tested in the technical-scale CSTF facility. In most of these experiments a mixed aerosol was used as test substance, consisting of water-insoluble MnO (prepared in a plasma torch) and water-soluble CsOH and CsI (generated by reaction of cesium vapor with steam or of CsOH with HI gas in a mixing chamber, respectively), and with an average particle size of about 2 μm; as a carrier gas a mixture of steam and nitrogen was used. Using a simple water-pool scrubber, the measured decontamination factors increased, as was expected, with increasing steam fraction in the venting gas and with increasing immersion depth of the vent line into the liquid. Retention of aerosols in the water pool was favored by higher temperature of the liquid due to a faster exchange of matter as a consequence of an accelerated Brownian movement and to the reduced surface tension of the liquid phase. Cesium decontamination factors between 145 and 3000 were measured, compared to manganese decontamination factors between 11 and 260 (McCormack et al., 1989). The question still remains of whether these differences in the retention factors were caused by the fact that MnO and CsOH were present in the gas-steam flow as separate aerosol particles or whether they resulted from the rapid dissolution of the cesium compound in the mixed-aerosol particles in the liquid phase. The revolatilization of aerosol particles by the action of an aerosol-free venting flow was reported to be small enough to be neglected.

The steel fiber filter and the Venturi scrubber were tested under similar conditions (Dickinson et al., 1990; McCormack et al., 1990). The decontamination factors for manganese and cesium with the steel fiber filter were on the order of 10^6; for particle iodide, a retention on the same order of magnitude was measured, whereas the decontamination factor for total iodine was only on the order of 10^5, probably due to a partial decomposition of CsI or to an incomplete consumption of HI during the generation of the CsI aerosol. The tests performed with the Venturi scrubber showed aerosol decontamination factors of more than 10^6; here also, the iodine decontamination factor was lower by a factor of about 10. More than 99% of the retained matter remained in the scrubber solution, less than 1% in the steel fiber filter, which is installed downstream. In contrast with the solid-state filters, in the Venturi scrubber no problems resulted from the aerosol load of the retention system.

References Section 7.3.4

Bleier, A., Greger, G.-U., Neeb, K. H.: Iodine revolatilisation from sumps in annuli and auxiliary buildings formed after a severe accident. Paper presented at the Nuclear Reactor Severe Accident Chemistry Symposium, 3. North American Chemical Congress, Toronto, Can, 1988

Dickinson, D. R., McCormack, J. D., Allemann, R. T.: Experimental results of ACE venting filtration: KfK metal fiber filter tests. Report ACE-TR-A 14 (1990)

Dillmann, H. G., Pasler, H., Wilhelm, J. G.: Containment venting filter designs incorporating stainless-steel fiber filter. Kerntechnik **53**, 75–80 (1988)

Dillmann, H.-G., Pasler, H., Wilhelm, J. G.: Filtered venting for German power reactors. Nucl. Technology **92**, 40–49 (1990)

Eckardt, B.: Containment venting for light water reactor plants. Kerntechnik **53**, 81–82 (1988)

Espefält, R., Persson, I.: Water scrubbers as new mitigating devices in Swedish reactors. Nuclear Europe **1988**, (10), 19–20

Hilliard, R. K., Postma, A. K.: Large-scale fission product containment tests. Nucl. Technology **53**, 163–175 (1981)

McArthur, D., Salaff, S.: Canadas EFADS emergency filtered venting system. Nuclear Europe **1988**, (10), 21–22

McCormack, J. D., Dickinson, D. R., Allemann, R. T.: Experimental results of ACE vent filtration, pool scrubber tests. Report ACE-TR-A 1 (1989)

McCormack, J. D., Dickinson, D. R., Allemann, R. T.: Experimental results of ACE venting filtration: Siemens combined Venturi scrubber tests. Report ACE-TR-A 12 (1990)

Morewitz, H. A.: Leakage of aerosols from containment buildings. Health Physics **42**, 195–207 (1982)

Pelletier, C. A., Hemphill, R. T.: Nuclear power plant related iodine partition coefficients. Report EPRI NP-1271 (1979)

Rahn, F. J., Collén, J., Wright, A. L.: Aerosol behavior experiments on light water reactor primary systems. Nucl. Technology **81**, 158–182 (1988)

Richter, F., Neeb, K. H.: Laboratory-scale and technical-scale investigations concerning iodine water–vapour phase partitioning under severe reactor accident conditions. Proc. OECD Specialists Workshop on Iodine Chemistry in Reactor Safety, Harwell, UK, 1985; Report AERE-R-11974 (1986), p. 209–223

Row, T. H., Parsly, L. F., Zittel, H. E.: Design considerations of reactor containment spray systems. – Part I. Report ORNL-TM-2412 (1969)

Schlueter, R. O., Schmitz, R. P.: Filtered vented containments. Nucl. Engng. and Design **120**, 93–103 (1990)

Vaughan, E. U.: Simple model for plugging of ducts by aerosol deposits. Trans. Am. Nucl. Soc. **28**, 507–508 (1978)

Witherspoon, M. E.: Leakage rate tests on the CSE containment vessel with heated air and steam–air atmosphere. Report BNWL-1475 (1970)

Witherspoon, M. E., Postma, A. K.: Leakage of fission products from artificial leaks in the Containment Systems Experiments. Report BNWL-1582 (1971)

Yuill, W. A., Bastor, V. F., Cordes, O. L.: Release of radioiodine from open pools. Report TID-4500 (1970)

7.3.5 Integral experiments dealing with severe core damage

All the investigations cited in the preceding sections have concentrated on separate stages of an accident sequence; this is also true for the in-pile tests, as well as for the large-scale containment experiments. In order to obtain a complete overview of the behavior of the fission products over an entire accident sequence, the results of these experiments have to be joined together, using computerized models some of which were shortly described in the corresponding sections. A verification of the reliability of the results of such model calculations can be performed by conducting integral experiments in which a whole accident is reproduced experimentally, starting from the volatilization of fission products from an overheated real reactor core and covering the whole transport pathway to the final stage of the behavior of the released fission products in the reactor containment. The performance of such an integral experiment is similar to the LOFT FP-1 test described in Section 6.2.1.3. which was designed to simulate a loss-of-coolant design basis accident. Integral experiments are very costly and time-consuming and, therefore, only a very limited number can be conducted.

In the early years of nuclear power development, the cores of several research reactors in the US were deliberatedly damaged by experimental power excursions in order to study the behavior of the fission products under such conditions. To be sure, the characteristic data of these reactors, such as the nature of the nuclear fuel, the design of the safety installations, the construction of the buildings etc., showed great differences from that of modern power reactors so that the results are of only limited value for the assessment of severe accidents. However, certain qualitative impressions can be derived from these results, as can be seen from the summary paper of Smith (1981).

In all these experiments, the reactor core was severely damaged by the power excursion produced, in some of the accidents parts of the core were molten; in one experiment which was performed in the absence of water (SNAPTRAN-2), the metallic fuel showed ignition. Release of fission product iodine to the environment was very small in all the experiments which were conducted in the presence of water, although the reactor buildings were normal industry buildings whose tightness was far lower than that of a commercial power reactor containment. Only in the "dry" SNAPTRAN-2 test did significant amounts of the fission products escape to the environment: 75% of the fission product noble gas inventory, 70% of the iodine, 45% of the tellurium and 4% of the solid fission products. These results clearly demonstrated the effect of the ambient conditions and of the resulting chemical reactions on fission product release and transport behavior.

One of the most important integral experiments including severe core damage was the LOFT FP-2 test, conducted in 1985 in the US Loss of Fluid Test Facility (which was shortly described in Section 6.2.1.3. and schematically shown in Fig. 6.4.). In this experiment, the performance and the results of which were summarized by Carboneau (1990), a pipe break in the low-pressure injection system was simulated, representing an accident initiated by a small break event. The cold-leg line of the intact loop served as the primary blowdown pathway prior to fission product release. During the period of fission product release, only the "broken line" of the low-pressure injection system was open; consequently, fission products

released from the reactor core were transported and deposited in the upper plenum of the reactor pressure vessel, the broken line of the low-pressure injection system and the blowdown suppression tank. Prior to the subsequent reflood phase, the blowdown suppression tank was separated from the primary coolant system, so that only fission products released during the transient phase were transported there. Due to the design of the facility, fission product behavior could be followed in the reactor pressure vessel and in the primary system, whereas the situation to be expected in the containment of a commercial power plant was not properly reflected by the blowdown suppression tank, because of the comparatively small dimensions of this component.

For this experiment, the reactor core had been equipped with a central fuel module containing 100 pre-pressurized fuel rods, the UO_2 fuel of which had been enriched to 9.7% ^{235}U and which had been pre-irradiated to a burnup of about 450 MWd/t U. The transient phase started with the reactor scram and was terminated about 30 minutes later when the external temperature on the surface of the shroud of the central fuel module reached 1517 K; at this time, the highest measured cladding temperature reached 2100 K. When reflooding of the reactor core with emergency coolant was started, a rapid temperature excursion occurred within the central fuel module which was caused by the enhanced metal–water reaction. The transient was followed by a post-transient period of 44 days during which the reactor core was cooled by recirculating coolant and the concentrations of fission products deposited in the primary coolant system as well as their behavior in the blowdown suppression tank were measured.

In order to follow the transport of the fission products, the test facility was equipped with a number of analytical devices. In addition to direct-reading gamma spectrometers and gross-gamma monitors, stainless steel deposition coupons (protected coupons which were sealed before start of reflood, thus providing information on the total deposition of fission products and control rod aerosol material before reflood, and unprotected ones providing information on the irreversible deposition) and aerosol samplers were installed at several positions. Despite some problems associated with the detection limits of direct-reading gamma spectrometers for noble gases, which were caused by an unexpectedly high deposition of iodine and cesium at the measurement positions, the analytical installations worked satisfactorily.

Post-irradiation examination of the fuel bundle (Jensen and Akers, 1990) revealed that it had been seriously affected by the transient and the reflood phases, resulting in the formation of low-melting-point metallic melts near the bottom of the bundle, a high-temperature $(U,Zr)O_2$ ceramic melt region above, and a debris bed of fuel pellets near the top of the bundle. In the vicinity of the metallic melts, consisting of liquefied Zr eutectica, fuel grain separations were observed indicating that reduction of UO_2 might have occurred, resulting in the formation of liquid uranium phases; by contrast, this effect was not observed in regions where high-temperature ceramic melts had been in contact with the fuel. About 63% of the Zircaloy material of the cladding and the shroud inner layer had been liquefied, compared to approximately 15% of the fuel. Most of the molten material was contained in the ceramic melt region, where zirconium was the most abundant element. Large amounts of zirconium were also present in various metallic melts.

The best estimate of the extent of hydrogen generation from the Zircaloy–H_2O reaction corresponded to an oxidation of about 50% of the cladding and shroud inner liner. Additional hydrogen was estimated to have been produced from the oxidation of stainless steel and Inconel components. The data obtained from the hydrogen measurements agreed well with the results obtained in the post-irradiation examinations of the test bundle.

Fission product cesium was generally retained within intact and fragmented fuel pellets. Likewise, iodine was almost completely retained in the intact fuel pellets, while significant iodine losses from fragmented fuel at temperatures of approximately 2200 to 2600 K were calculated from the results of the measurements. Both cesium and iodine were significantly volatilized from partially liquefied fuel as well as from the ceramic melt region, in the latter case ranging from essentially complete release to about 50% retention. Fission product release in these melt regions proved to be correlated not only to the peak temperatures to which the materials were exposed, but to other parameters as well (such as time at the temperature and the nature of the surrounding material). In general, the final state of the fuel as well as the extent of release of fission products were quite similar to that experienced in the TMI-2 damaged reactor core, as well as to that observed in the small-scale PBF-SFD tests, despite large differences in scale, fuel burnup and numerous other parameters (Hobbins and McPherson, 1990).

The measured temperatures of the gas–steam flow in the upper plenum above the central fuel module generally ranged from 500 to 900 K, with an average temperature of about 730 K; the temperatures of the structural surfaces were somewhat lower. These temperatures suggest that during the experiment the majority of the fission product chemical species in the upper plenum would exist either in a liquid or a solid form, not in the gaseous state. However, because of the limited dimensions of the central fuel module (compared to a real reactor core) it seems highly questionable whether these results can be directly applied to the situation to be expected in a commercial power reactor during degraded core accidents.

The data obtained in the measurements showed that about 1% of the iodine inventory of the central fuel module reached the blowdown suppression tank, while only 0.23% of the cesium inventory appeared there. These data and those taken from the simulated broken line indicated that cesium deposited in this line more readily than iodine; the reverse situation occurred in the upper plenum of the reactor pressure vessel. Here, almost no cesium was detected on the deposition coupons while iodine was present in amounts similar to those in the line of the low-pressure injection system. Besides iodine, silver was found on the upper plenum coupons in equivalent amounts; in addition, the iodine deposited on these coupons could not be leached by water, indicating that it was present there as an insoluble compound. From these data it was concluded that fission product iodine was transported out of the reactor core as AgI, rather than as CsI. Formation of AgI as the main iodine compound deposited in the upper plenum of the reactor pressure vessel is a behavior markedly different from that observed in other in-pile experiments and in the TMI-2 post-accident investigations. The reason for this behavior was assumed to be the low concentrations of both cesium and iodine present in the low-burnup fuel, which resulted in a very high stoichiometric excess

of silver originating from the control rod materials in the regions above the reactor core. This effect underlines the influence of specific plant parameters, such as fuel burnup, on the chemistry of the fission products during their transport in the primary system.

With respect to cesium, the measured data suggested that this element was transported as a highly volatile compound, most likely as CsOH, so that only negligible deposition took place in the upper plenum of the reactor pressure vessel.

The fraction of fission product noble gases released during the transient amounted to 1.7% of the xenon and 2.0% of the krypton inventories of the central fuel module (according to the measurements performed in the blowdown suppression tank). This comparatively small release fraction was probably caused by the initially large grain structure of the fuel (about 14 μm) and the low maximum fuel temperature of < 2700 K during the transient. However, about 9% of the krypton inventory was detected in the primary coolant system following reflood (xenon was not measured here); apparently, the greatest fraction of the noble gases was released from the fuel during reflood, presumably because of the higher temperatures prevailing during this period which were a result of the metal–water reaction. The same effect was observed with the iodine and cesium isotopes; likewise, most of the hydrogen gas generated during the experiment was not produced during the transient, but was generated following start of reflood. These facts indicate that a thermal excursion within the central fuel module might have occurred in the first stage of reflood, leading to local fuel melting with peak temperatures of about 3100 K; similar effects have been observed in the in-pile PBF experiments (see Section 7.3.1.1.).

The amounts of fission products measured in the reactor coolant system after termination of the experiment proved to be significantly greater than those transported during the transient (prior to the start of reflood) to the primary system and to the blowdown suppression tank. These discrepancies might have been caused by various effects such as leaching of the fuel by the liquid reflood water, wash-off of fission products previously released from the reactor core during the transient but deposited on upper plenum structures or, finally, enhanced fission product release from the fuel during the reflood period. The last-mentioned effect which is caused by the thermal excursion in the central fuel module due to the enhanced metal–water reaction in the first phases of reflood, seems to be the main mechanism for fission product release from the fuel, according to the results of the post-test calculations (Modro and Carboneau, 1990).

The most comprehensive program of integral experiments is being conducted over the period 1993 through 2003 in the French PHEBUS reactor (Benson et al., 1991; von der Hardt and Tattegrain, 1992; von der Hardt et al., 1994). In this experimental system, the fuel bundle to be tested is located in the driver core of the reactor. The system includes a simulant primary circuit with steam generator and a containment vessel of 10 m^3 volume. Transport and deposition of the fission products is monitored by on-line instrumentation (such as gamma spectrometers), as well as by sampling instruments (inertial impactors, selective iodine species samplers, gas and liquid sampling instrumentation). An overview of the analytical instrumentation used in the test FPT1 is shown in Fig. 7.46. (according to Zeyen et al., 1996), demonstrating the efforts that have to be undertaken to obtain a com-

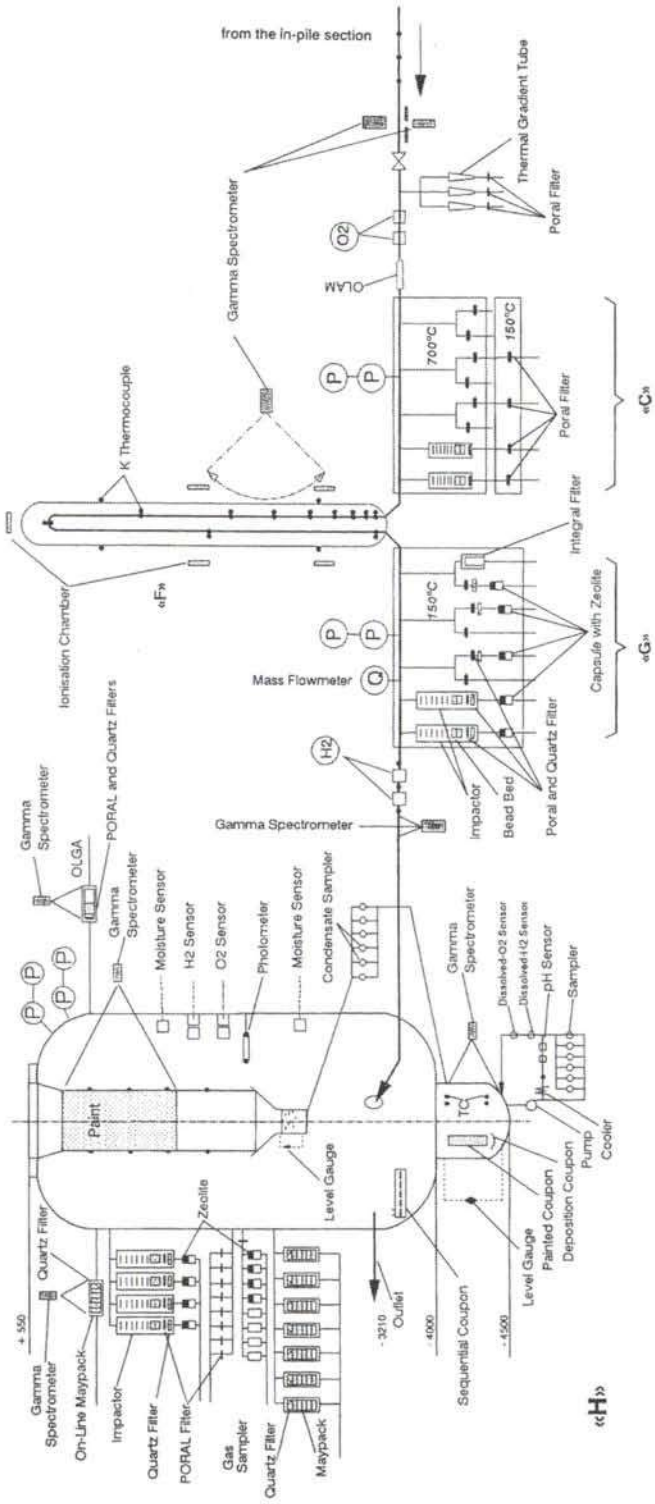

Figure 7.46. PHEBUS FPT1 analytical instrumentation plan (Zeyen et al., 1996)

plete picture of the transport and behavior of the fission products released from the overheated fuel.

The test matrix includes 6 in-pile experiments in which different features will be studied, making this program the most comprehensive project in this field. The main objectives of these experiments are to improve our understanding of fission product behavior during severe reactor accidents and, in particular, to obtain experimental data for the validation of the code systems used in source term evaluation. In these tests, trace-irradiated as well as high-burnup fuel bundles pre-irradiated to 25 to 30 MWd/kg U are to be overheated to fuel melting. Fission products which are released from the core region will be transported through a system representing the primary coolant piping and the steam generator to the containment vessel. The study of iodine behavior in the containment is an important objective of the PHEBUS-FP project. Therefore, the experimental sequence includes a fission product release phase of one to two hours, followed by a containment test phase of two to four days for measurements of aerosol depletion and fission product chemistry. Four main criteria will be used to analyse variations in iodine behavior: the impact of radiolysis, sump water pH, organic paints and temperature. Thus, the results of special-effects investigations obtained in laboratory-scale and intermediate-scale studies (e. g. RTF, FALCON) will be checked here on a scale more in accordance with reality.

The first of the PHEBUS in-pile tests was successfully conducted in December 1993, using a trace-irradiated fuel assembly. In the course of the transient which was performed at low system pressure and under oxidizing conditions, peak temperatures as high as 2700 K were reached, resulting in extensive degradation of the test fuel bundle. Preliminary results (Schwarz and Jones, 1995) indicated the release of a large fraction (> 50%) of the volatile fission products from the fuel. Most of the volatilized fission products proved to be in condensed form at the inlet of the steam generator, i. e. at 700 °C, although iodine was mostly in vapor form at this temperature level; further, a significant fraction of the iodine was still in a volatile form at the outlet of the steam generator, i. e. at low temperature. Due to the low concentrations of fission products released from the trace-irradiated fuel and the short residence time in the primary system, the chemical equilibria in the gas phase probably were not fully established. Detailed results of this experiment have not yet been published. The next test in which fuel pre-irradiated to a burnup of about 35 MWd/kg U is used will be conducted in April 1996.

References Section 7.3.5

Benson, C. G., Drossinos, Y., van Rijn, H. M.: Activities of the Commission of the European Communities in the area of iodine chemistry in severe reactor accidents. Proc. 3. CSNI Workshop on Iodine Chemistry in Reactor Safety, Tokai-mura, Japan, 1991; Report JAERI–M 92–012 (1992), p. 62–78

Carboneau, M. L.: Highlights of the OECD LOFT LP-FP-2 experiment including hydrogen generation, fission product chemistry, and transient fission product release fractions. Proc. Open Forum The OECD LOFT Project: Achievements and Significant Results. Madrid, Spain, 1990, p. 261–284

Hobbins, R. R., McPherson, G. D.: A summary of results from the LOFT LP-FP-2 test and their relationships to other studies at the Power Burst Facility and of the Three Mile Island Unit 2 accident. Proc. Open Forum The OECD LOFT Project: Achievements and Significant Results. Madrid, Spain, 1990, p. 404–413

Jensen, S. M., Akers, D. W.: Postirradiation examination results from the LP-FP-2 center fuel module. Proc. Open Forum The OECD LOFT Project: Achievements and Significant Results. Madrid, Spain, 1990, p. 330–387

Modro, S. M., Carboneau, M. L.: The LP-FP-2 severe fuel damage scenario; Discussion of the relative influence of the transient and reflood phase in affecting the final condition. Proc. Open Forum The OECD LOFT Project: Achievements and Significant Results. Madrid, Spain, 1990, p. 388–402

Schwarz, M., Jones, A. V.: Analytical interpretation of FPT0 and preparation of future Phebus FP tests. Paper presented at the Internat. ENS Topical Meeting Safety of Operating Nuclear Power Plants "ENS TOPSAFE 95", Budapest, Hungary, 1995

Smith, R. R.: Radiological consequences of the BORAX/SPERT/SNAPTRAN experiments. Nucl. Technology **53**, 120–134 (1981)

von der Hardt, P., Tattegrain, A.: The Phebus fission product project. J. Nucl. Materials **188**, 115–130 (1992)

von der Hardt, P., Jones, A. V., Lecomte, C., Tattegrain, A.: Nuclear safety research: The Phebus FP severe accident experimental program. Nucl. Safety **35**, 187–205 (1994)

Zeyen, R., Poss, G., Clément, B.: A spectral light extinction photometer for the characterisation of nuclear aerosols in the containement of the PHEBUS FP integral severe accident simulating experiment. Paper presented at the AAAR '96 (American Association for Aerosol Research), Orlando, 1996

7.4 Fission product behavior in actual severe reactor accidents

7.4.1 General remarks

In the past decades several reactor accidents have occurred with consequences significantly exceeding the dimensions of a design basis accident. Only one of these accidents affected a light-water cooled and moderated power reactor of Western design, namely that at the TMI-2 plant near Harrisburg in 1979, whereas the others took place in reactor plants of considerably different design. Consequently, the initiating events in these accidents as well as the accident sequences are not representative for light-water reactors; moreover, there are large differences in the conditions prevailing within the plant during the progress of the accidents. In spite of these fundamental differences, some of these accidents will be described shortly here, since they can still be used to show the impact of ambient conditions on the chemical reactions and on the behavior of the fission products. A short survey of severe reactor accidents was published, among others, by Wolters (1987); the behavior of fission products in a number of such accidents was reviewed and evaluated by Morewitz (1981).

For obvious reasons, the measurements of fission product behavior inside and outside the affected plants which were performed during and after the accidents show considerable shortcomings and are by far are not as complete and reliable as measurements performed in the course of planned experiments. For this reason, the results reported have to be critically evaluated prior to their application in fission product transport and behavior models; moreover, most of these data can only be used in very limited areas. But they are the only results which have been obtained in full-scale reactor accidents and, therefore, they may be able to contribute to our understanding of the processes in question and of relevant countermeasures.

One of the first severe reactor accidents happened at the British plant Windscale-1, an air-cooled, graphite-moderated reactor for plutonium production which, in contrast to light-water reactors, was not surrounded by a tight and pressure-resistant containment. Due to the low operating temperature of this type of reactor, the graphite moderator material whose carbon atoms are knocked out of their regular lattice positions by the impact of fast neutrons is not annealed during plant normal operation; in order to prevent deterioration of the graphite material, the stored energy (Wigner energy) has to be annealed at regular intervals by slow heating-up of the reactor core to higher than operating temperatures. In one such action performed in October 1957, overheating of the metallic fuel occurred, causing a fire which was only able to be extinguished after two days. The consequence of the resulting high temperatures in the core was failure of a large number of fuel rods, associated with a considerable release of fission products from the fuel. As a consequence of the lack of water in the reactor system and in the reactor building, the behavior of the fission products in this accident was dictated by the ambient conditions "dry and oxidizing".

A short summary of the fission product release to the environment in the course of this accident is shown in Table 7.20. Particle iodide (700 to 2000 TBq) was largely retained in the off-gas filters of the plant; however, about 700 TBq of gaseous iodine penetrated these filters and were dispersed to the environment; this amount of iodine released represented about 12% of the fission product iodine inventory of the reactor core at the time of the accident. Since the inventory of radioactive fission product noble gases in the fuel during reactor operation is higher by about a factor of 10 than the iodine activity inventory, the release data indicated that the fractional releases of noble gases and iodine were almost identical. The stack filter of the plant retained additional 30 to 40 TBq of cesium; hence, 25 to 43% of the iodine and 17 to 18% of the cesium inventories appear to have escaped from the reactor core. Besides fission product noble gases and fission product iodine, considerable fractions of other radionuclides were also released to the environment (see Table 7.20.). In the time before the annealing operation, the reactor was used to simultaneously produce ^{210}Po and tritium by irradiation of bismuth and lithium, respectively, and a considerable fraction of these radionuclides also escaped to the environment; the total ^{210}Po release from the plant during the accident was estimated to be in the range 7 to 10 TBq.

From general chemistry considerations it can be assumed that under the prevailing conditions, i. e. access of sufficiently large amounts of air to the overheated

Table 7.20. Fission product releases during severe reactor accidents (according to Morewitz, 1981)

	Windscale-1	SL-1	TMI-2
Thermal reactor power	~250MW	3 MW	2720 MW
Accident conditions	dry	wet	wet
Release to the environment			
* Iodine	700 TBq (12%)	3.4 TBq (<0.5%)	0.6 TBq ($\sim 10^{-5}$%)
* Noble gases	10^4 TBq	370 TBq	$4 \cdot 10^5$ TBq
* Others	60 TBq Te 20 TBq ^{137}Cs 3 TBq ^{89}Sr 0.3 TBq ^{90}Sr	~20 GBq ^{137}Cs ~4 GBq ^{90}Sr	not detected
Contaminated area	500 km^2	0.3 km^2	Reactor building Auxiliary building

reactor core, the released fission product iodine was present as elemental I_2, tellurium as volatile TeO_2, with cesium in metallic form in areas of high temperature, and as Cs_2O_2 at lower temperatures. Because of the absence of water, there were no efficient plate-out mechanisms that would have been able to prevent or at least to minimize the release of these radionuclides to the environment.

Among the reactor accidents which have occurred up to the present, Windscale-1 and Chernobyl-4 (see Section 7.4.3.) represent by far the most serious ones with respect to the thyroid burdens to the public as well as to the field contamination of the surrounding areas. In the days and weeks after the Windscale-1 accident, it was possible to measure the released radionuclides in low concentrations even in Norway and in Germany. As was pointed out before, accidents of this type cannot happen in light-water reactors; on the other hand, such release values are not to be expected from gas-cooled reactors of modern design, since the fission products in their fuels are confined in graphite-coated fuel elements which are stable even under very high temperatures.

First impressions of the significance of water-induced chemical reactions were obtained from the SL-1 accident. This small boiling water reactor, which was operated by the US Army at the National Reactor Testing Station, Idaho, was designed as a prototype plant for electricity generation and district heating in remote areas. During a startup of the reactor in January 1961, a nuclear power excursion occurred, leading to a sudden very strong steam production, by which a part of the reactor was destroyed and three persons in the vicinity were killed. The release and behavior of radionuclides in the course of this accident was summarized by Mendoza et al. (1981); however, it has to be pointed out that only a small number of measurements were carried out after the accident, and that the released amounts of radioactivity had to be calculated from contamination measurements performed subsequently in the area surrounding the reactor plant.

As the result of the power excursion, about 20% of the U-Al alloy fuel was liquefied and a part of it was vaporized. It was calculated (Mendoza et al., 1981) that about 20% of the iodine and cesium inventory was released from the fuel, i. e. about 200 TBq ^{131}I and approximately 25 TBq ^{137}Cs. Out of these radioactivities, only about 400 GBq ^{131}I and 20 GBq ^{137}Cs were transported out of the reactor building within 12 hours after the onset of the accident (see Table 7.20.). This means that the reactor building, a normal industrial building without a gas-tight containment, had a retention factor of about 500 for iodine and of about 1000 for cesium. In the days following the accident, an additional 3 TBq ^{131}I were released to the environment, mainly caused by leakage of contaminated water from the building and volatilization of iodine from this water volume to the environmental air.

The effective retention of iodine in the building obviously was the result of chemical reactions occurring between I_2 and water, leading to non-volatile iodine species generated by hydrolysis and disproportionation reactions. However, when analyzing fission product release during this accident, it has to be taken into account that almost all the energy released in the accident was produced during the short nuclear transient. The reactor system was not pressurized and the fission product decay heat was not sufficiently high to cause the core to remain molten after the accident or to cause further core melting when the coolant was lost. There was, therefore, little driving force for the transport of radionuclides out of the reactor system and out of the reactor building.

Because of these differences in the conditions compared with an LWR severe accident, and because of the limited number of measurements performed, the data obtained here have not been introduced into the evaluations of the consequences of severe light water reactor accidents, so that the high degree of retention of fission product iodine within the plant which was observed in the TMI-2 accident turned out to be an unexpected and surprising fact for the accident analysts.

7.4.2 TMI-2

As was stated above, the TMI-2 accident which occurred on March 28, 1979 has been the only one in a commercial light-water reactor of Western design showing severe damage to the reactor core and excessive release of fission products from the fuel. This accident has greatly influenced the public attitude towards nuclear energy; on the other hand, the observations which were made during and after the accident initiated a new phase in considerations of fission product behavior. Shortly after the accident it became evident that the release of iodine isotopes to the environment was considerably smaller than had been generally expected in prior estimates, and the idea was brought into the discussion that this behavior was the consequence of chemical reactions which were able to convert volatile I_2 into non-volatile I^-. From there, extensive studies of the fundamentals of such reactions were initiated in numerous countries and institutions, resulting in considerable progress in the understanding of the mechanisms which control fission

product release and transport, as well as chemical forms produced during a severe accident in a light water reactor. Extensive post-accident examination of the degraded fuel as well as of the reactor primary system and the containment have contributed substantially to our understanding of fission product behavior under the conditions prevailing in a real reactor accident.

The initiation and the progress of the accident have been described in numerous publications; therefore, only the aspects which are of significance for fission product behavior will be summarized here. The initiating event was a failure of the feedwater supply to the secondary side of the steam generator so that the water inventory of the steam generator boiled off within several minutes, leading to a temporary loss of the primary coolant heat sink. The resulting increase in temperature and pressure of the primary coolant caused an opening of the pressurizer relief valve and, a few minutes later, a reactor trip. As a consequence of these events, the primary coolant pressure decreased again below the design value, but the open relief valve failed to close again. Initiated by the continuing drop in coolant pressure, the high-pressure safety injection pumps started to operate; however, as a result of an erroneous interpretation of the instrument reading of the coolant level indicator of the reactor pressure vessel, they were turned off manually after a few minutes. Due to the still open relief valve, coolant loss from the primary circuit continued and formation of steam in the reactor pressure vessel started. One to two hours after accident initiation the main coolant pumps were switched off in order to avoid damage by cavitation, but no natural convection of the coolant could be achieved. Due to the coolant loss, the reactor core was insufficiently cooled to remove the decay heat, and the fuel rods overheated, causing severe damage to the reactor core, the results of which will be described below in greater detail. After various attempts to restore the coolant flow, natural convection in one primary loop was achieved after 11 hours, and 5 hours later one main coolant pump was put into operation again, so that only from this moment on was the reactor core cooled sufficiently to remove the decay heat. Several days more were needed to remove non-condensible gases (mainly hydrogen) from the reactor pressure vessel and the primary circuit.

Caused by the increasing pressure in the pressurizer relief tank, about 15 minutes after the onset of the accident a rupture disk failed, and primary coolant flowed into the reactor building for about two hours. Later on, hydrogen from the reactor pressure vessel escaped to the containment, causing there a local hydrogen burn. Containment isolation was achieved only 4 hours after the onset of the accident; in the meantime, a part of the liquid which had escaped from the primary system to the containment floor was transported to the auxiliary building by the containment sump drain system. From this coolant volume, which overflooded large areas of the auxiliary building, volatile radionuclides were released to the environment via the off-gas system. This pathway was the main source of radioactivity release to the environment during the accident.

Very soon it became evident that the reactor core had been severely damaged by the accident. Detailed investigations were conducted over the following months and years to get a clear idea of the state of the reactor core, starting with non-destructive means prior to the unloading of the fuel and the core structural materi-

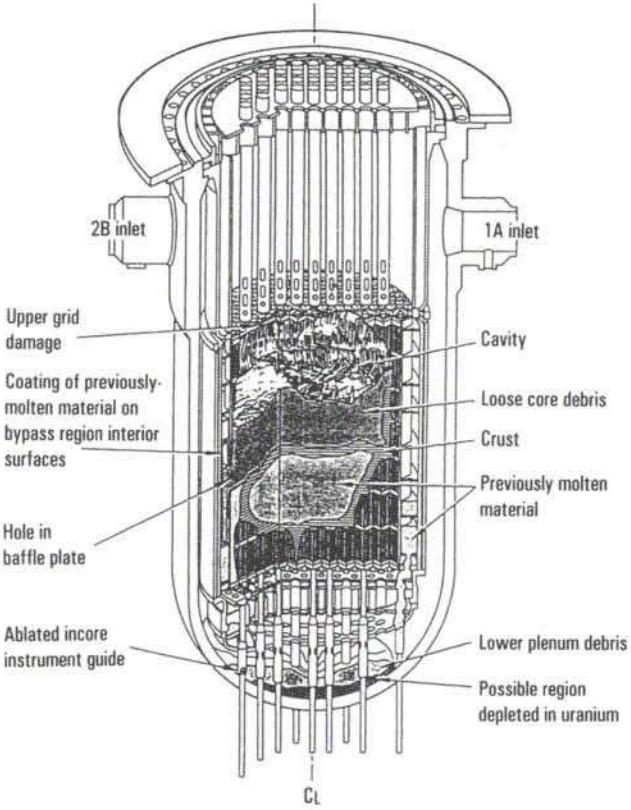

Figure 7.47. TMI-2 reactor accident; end-state core configuration (McCardell et al., 1990; with kind permission from Elsevier Science S.A., P.O. Box 564, 1001 Lausanne, Switzerland)

als from the reactor pressure vessel, continuing during this action and terminating by detailed destructive examination of the discharged materials. These efforts, summarized among others by McCardell et al. (1990), yielded the findings which are schematically shown in Fig. 7.47. After the accident, the core region consisted of an upper void region which was almost entirely surrounded by damaged but still standing peripheral fuel assemblies. The void region was approximately 1.5 m deep with an overall volume of 9.3 m^3. Directly below the void region there was a region of loose debris resting on a hard crust; this crust completely surrounded a centrally located, consolidated region that had previously become molten. A region of still-intact, standing fuel rods extended upwards from the bottom of the core to the bottom of the crust surrounding this molten region. About 19 Mg of molten core material had relocated to the lower plenum region of the reactor pressure vessel. The post-accident distribution of the core materials is schematically shown in Fig. 7.48. (according to Akers et al., 1990). From all these regions, samples were taken and were subjected to extensive metallurgical, chemical and radiochemical examinations.

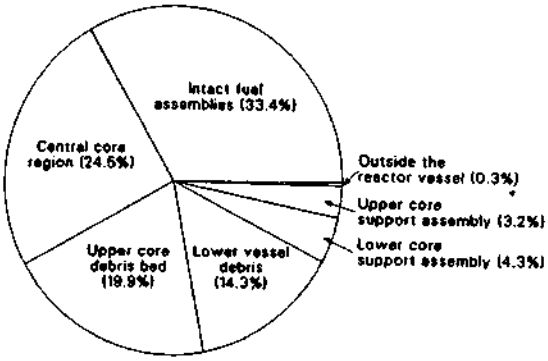

Figure 7.48. TMI-2 core; end-state core materials distribution
(Akers et al., 1990; with kind permission from Elsevier Science S.A., P.O. Box 564, 1001 Lausanne, Switzerland)

This accident sequence demonstrated that a core melt can be stopped even in an advanced stage (in this case after the destruction of about one-third of the reactor core) by renewed supply of coolant, without any deterioration of the reactor pressure vessel. From this result it can be concluded that penetration of the pressure vessel by the molten core, as is assumed to occur in the final stages of the accident scenarios discussed in Section 7.2., will only be possible if no measures at all can be taken to successfully re-establish coolant flow.

The bed of loose debris below the core void ranged in depth from 0.6 to 1 m and consisted of whole and fractured fuel pellets, control rod spiders, end fittings and resolidified material. The debris bed exhibited a broad range of oxidation and material interactions. Most of it consisted of shattered and resolidified material that contained regions of previously molten $(U,Zr)O_2$, indicating temperatures in excess of 2700 K; a few samples of previously molten, almost pure UO_2 indicated temperatures up to 3100 K. However, until reflooding of the core most of the debris bed had remained at temperatures below 2000 K or had been exposed to higher temperatures for only a short period of time. The bulk elemental composition of the loose debris bed was primarily uranium, zirconium and oxygen with an unexpected significant depletion of silver, indium and cadmium control rod material, Zircaloy cladding and structural material. In addition to these components, comparatively high concentrations of boric acid were present in the upper pebble bed which probably had been concentrated there during the core melt process.

The large, crust-enclosed, previously molten and then resolidified region below the loose debris was approximately 3 m in diameter, 1.5 m thick at its center and 0.25 m thick at its periphery. It consisted of a mixture of structural, control rod and fuel material which reached temperatures of 2700 K and possibly 3100 K during the accident. The bulk of the previously molten region was a mixture of both ceramic and metallic phases, with the ceramic phases being primarily oxides of uranium and zirconium with small amounts of iron and nickel oxides, and the metallic phases being principally Fe-Ni and Ag-In phases. Thus, the central region

contained much more metal than the upper debris bed, where no pure metallic phases were found.

The upper crust consisted of two phases, a ceramic phase mainly composed of fuel material components, and a metallic phase containing predominantly structural and control rod material components; its peak temperature during the accident was estimated to have been at least 2700 K. Whereas the elemental composition of the ceramic material was similar to that of the central region, the metallic phases exhibited significant differences in that they were primarily composed of Fe-Ni, Ag-In-U, and Ni-Sn phases; they contained considerably more metallic uranium than the central region and considerably less cadmium. With respect to its composition, the peripheral crust was similar to the upper crust, except that there were remnants of intact fuel pellets that might have fallen into the peripheral crust from the upper debris bed. The high percentage of zirconium present in the peripheral crust implied that this crust was formed at a time in the accident when the molten zirconium as well as control rod and structural materials were flowing downward and solidifying. The lower crust, finally, consisted of vertical fuel pellet stack columns surrounded by previously molten material. Apparently, during the early stage of the accident, structural and control rod material flowed down the coolant channels, dissolved the Zircaloy cladding and flowed into the pellet–pellet interfaces as well as into cracks in the pellets, freezing to form the lower crust. Detailed investigations showed that this material reached at least 1400 K and partially approached 2200 K.

The standing fuel assembly stubs below the previously molten region varied in length from about 0.2 to 1.5 m, with the longer ones located at the core periphery. According to the post-accident investigations, they reached only relatively low temperatures (below 1100 K) during the accident. It has been assumed that empty instrument guide tubes provided an escape path for the relocating metallic material and that some of this material may have reached the lower plenum of the reactor pressure vessel by this means.

The debris resting on the lower vessel head amounted to about 20 Mg of material which flowed down in the molten state without destroying larger regions of the core support structure; they showed a depth of 0.75 to 1 m above the lowest head elevation and a diameter of 4 m. The particles showed large differences in size and were mostly previously molten $(U,Zr)O_2$ ceramic material with a very porous structure. In addition, resolidified silver, indium and nickel from the control rods, as well as tin from the Zircaloy, was found in this debris. According to the results of the post-accident examinations, the peak temperatures of the lower plenum debris varied between 2800 and 3100 K. It is of considerable interest to note that the interaction of the molten fuel running downward with the residual water in the lower region of the reactor pressure vessel did not cause an energetic steam explosion (Hobbins et al., 1989).

In general, the temperatures and elemental compositions of the various regions of the degraded reactor core were consistent with the materials interactions that had been determined in both in-pile and out-of-pile experiments.

From the measured amount of hydrogen produced during the accident (459 kg), it was calulated that about 43% of the Zircaloy present in the reactor core had

been oxidized. Taking into account that some structural metallic material (e. g. Fe, Cr) may also have been oxidized by steam under production of hydrogen, this number can be considered to be a conservative one.

Some attempts were made to obtain more detailed information on the chemical conditions prevailing inside the reactor pressure vessel during the core meltdown phase, in particular on the redox conditions. Post-accident examinations showed that the oxide layers on the steel structural surfaces consisted exclusively of Fe_3O_4, with neither FeO nor Fe_2O_3 being detected. From these and other results it was concluded that over long periods of the accident sequence the ratio $H_2 : H_2O$ had been somewhat below 1.0.

The fuel rod materials (i. e. uranium dioxide, zirconium and zirconium dioxide, tin) essentially remained inside the reactor pressure vessel. According to the results of laboratory experiments cited in the preceding sections, the behavior of the control rod materials in a degraded core accident is of great significance for the transport characteristics of the volatile fission products, not only with respect to the potential formation of insoluble AgI but also to the uptake of volatile fission products by aerosols in the primary system. The TMI-2 post-accident analyses indicated that during the accident the control rod materials melted and, since the system was nearly at operating pressure, the molten material did not spray into the upper region of the core, but that it relocated downward into the core, probably dissolving Zircaloy during its relocation. The amount of silver detected in the upper pebble bed corresponded to about 9% of the total mass originally present in the control rods; it was assumed that during the progress of the core melt the bulk of silver from the destroyed control rods flowed down in liquid form to the residual water volume in the lower part of the pressure vessel where it resolidified. Small amounts of silver (about 1% of the core inventory) were detected on the surfaces of the upper vessel plenum where they were deposited as small spheres of an Ag-In-Cd alloy of various composition. Only a small fraction of silver, well below 1%, was released from the reactor pressure vessel, as was concluded from the results of examinations of samples collected from outside the core. Indium also remained in the lower core region; likewise, much of the relatively volatile cadmium was not released from the core but was retained in the central molten part. As a consequence of the inhomogeneous composition of the damaged core, collecting representative samples was very difficult, and the accuracy of the analyses performed during the post-accident examinations is comparatively poor; moreover, additional repositories may have been present that have not yet been examined (e. g. in the lower plenum debris).

The structural materials of the damaged core region (i. e. Fe, Cr, Ni) were mainly relocated to the central and lower regions of the reactor core; there was virtually no release of such elements or their radionuclides from the reactor pressure vessel.

Numerous analyses were carried out concerning the fractions of the radionuclides vaporized from the fuel during the course of the accident. One of the early material balances which were conducted prior to the detailed examinations of the core materials is shown in Fig. 7.49. (according to Morewitz, 1981). With respect to the release of fission products from the reactor core, these data were essentially

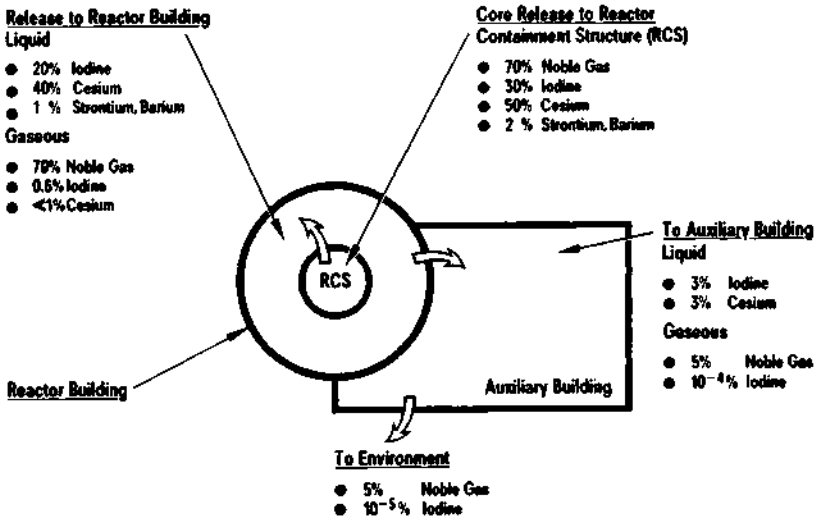

Figure 7.49. Fission product transport and distribution in the TMI-2 reactor accident (Morewitz, 1981; Copyright 1981 by the American Nuclear Society, La Grange Park, Illinois)

confirmed by the detailed examinations performed over the following years, the results of which have been shortly summarized by Akers et al. (1990). The low-volatility fission products (e. g. rare earth radioisotopes) were not volatilized from the fuel and only a small part of them was physically transported (i. e. as dust fuel particles) from intact or molten fuel to the reactor coolant system. Out of the medium-volatility fission products, ^{90}Sr was essentially retained in the reactor vessel; about 93% of the original strontium inventory remained in the molten material, showing there a distribution similar to that of the fuel material. Less than 3.5% of the ^{90}Sr core inventory was transported to the reactor building, with only about 0.1% being released to the auxiliary building. ^{125}Sb and ^{106}Ru showed only insignificant release from the reactor pressure vessel (< 1%); in the degraded reactor core they were predominantly retained in the metallic phases.

In the course of the accident, about 54% of the ^{85}Kr inventory was released from the reactor core; about 6% was retained in the upper core debris bed, and about 30% in the intact fuel rods. These data agree well with those shown in Fig. 7.49., which were based on early measurements of the ^{133}Xe concentration in the containment atmosphere. The distributions of the volatile radionuclides ^{129}I (the short-lived ^{131}I had completely decayed by the time of the post-accident fuel examinations) and ^{137}Cs are schematically shown in Fig. 7.50. In general, the release behavior of both radionuclides from the fuel proved to be quite similar, as was their distribution in the reactor vessel. The release fractions of these radionuclides and their distribution outside the reactor pressure vessel show several differences when compared to the early data in Fig. 7.49.

The degree of retention of some of the fission products in the debris bed from the upper and lower plenum of the reactor pressure vessel is shown in Table 7.21.

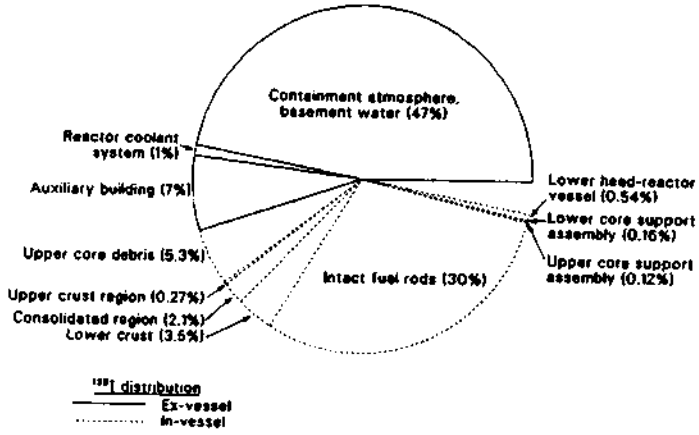

^{129}I

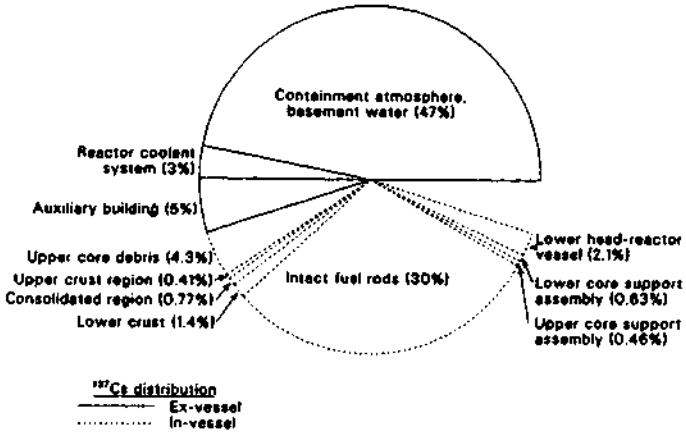

^{137}Cs

Figure 7.50. TMI-2 reactor accident; end-state ^{129}I and ^{137}Cs distribution (Akers et al., with kind permission from Elsevier Science S.A., P.O. Box 564, 1001 Lausanne, Switzerland)

(Petti et al., 1989). Besides a comparatively broad scatter of the data, which is probably caused by the heterogeneous nature of the material in the reactor core, retention of the fission products in the upper and the lower debris shows considerable differences, reflecting the differences in temperatures and time at a given temperature the materials underwent. However, in some regions of the lower debris an unexpectedly high retention in the previously molten and then resolidified material was detected, possibly indicating that relatively large zones with an unfavorable surface-to-volume ratio were in the molten state for only a rather short period of time. In addition, the unexpectedly high retained fraction of cesium suggests that it may be present in a low-volatility chemical form that is stable even at very high temperatures. Results of elemental analyses of samples which were collected from this debris indicated that cesium may be combined with chromium and iron oxides

Table 7.21. Fission product retention in the TMI-2 upper and lower core debris (Petti et al., 1989; Copyright 1989 by the American Nuclear Society, La Grange Park, Illinois)

Radionuclide	Inventory retained %[a]			
	Lower debris		Upper debris	
	Average	Range	Average	Range
^{129}I	3	0 to 25	23	10 to 39
^{137}Cs	3	0 to 34	19	5 to 29
^{106}Ru	6	0 to 17	49	31 to 77
^{125}Sb	6	0 to 35	47	37 to 78
^{90}Sr	107	68 to 178	87	74 to 96
^{154}Eu	113	96 to 250	118	79 to 143
^{144}Ce	96	78 to 142	99	78 to 113

[a]) Compared with inventory from center region of the core that participated in the accident

at the grain boundaries of the solidified ceramics in forms such as Cs_2CrO_4 and $CsFeO_2$. Other possible cesium compounds which are stable at high temperatures with low vapor pressures include Cs_2MoO_4, Cs_2ZrO_3 and $CsBO_2$, with all of the required reaction partners present in the molten material. The virtually complete retention of strontium, europium and cerium is in agreement with the low vapor pressures of the oxides and their solubility in oxide phases. The very low concentrations of antimony and ruthenium in the lower plenum debris, on the other hand, cannot be explained by a significant volatility of these elements but is assumed to be due to an inclusion of these elements into metallic phases (mainly iron and nickel) present in the melt (Hobbins et al., 1989).

In order to analyze fission product release from the reactor core during the accident by using fission product release and transport models, Petti et al. (1989) have divided the accident sequence into different phases. In phase 1, lasting from the onset of the accident until the last main coolant pump was turned off at 100 minutes, no core uncovery and heatup and, consequently, no fission product release occurred. In the following phase 2 (until the "B-pump transient" at 174 minutes) core heatup started, reaching about 2400 K at the end of this phase. Using a series of sensitivity calculations which were based on basic fission product release models, the authors concluded that during this phase the release of volatile fission products was dominated by diffusion up to the point that significant liquefaction of the fuel occurred. Depending on the location within the reactor core and on the basic data assumed, the release of the volatile fission products at the end of phase 2 was calculated to amount to values between 0 and 43% of the initial inventory, while individual locations within the core might have undergone complete release.

During phase 3A (the "B-pump transient") when one main coolant pump was operated again for about 19 minutes, the hot reactor core was quenched, resulting in the formation of macrocracks and in intergranular fracturing of the upper debris bed. From the results of corresponding in-pile experiments and from the results of metallurgical post-accident examinations of the debris bed it was concluded that

considerable additional release of fission gases and volatile fission products could have taken place following reflood. However, quantitative comparisons of the results of the calculations with those of the analyses of the upper debris bed were not possible, due to variations in diffusional and quenching releases, which have to be expected for different positions of the core.

In the following phase 3B (180 to 224 minutes), the molten U-Zr-O material and a part of the debris bed continued to heat up to produce a large molten mass surrounded by a crust. Fission product release during this phase could have originated in three separate regions, i. e. from fuel still with a rod-like geometry, from the debris bed and from the molten pool; however, since the rods and the debris bed were relatively cool, the molten pool presumably was the predominant source. Since the volatile fission products are in the gaseous state at the high temperatures of the molten pool (>2850 K), their release will be dominated by bubble dynamics. Model calculations indicated that they should be released very quickly from the melt, due to the sweeping of small gas bubbles by larger ones to the surface of the melt. However, the gas would probably be trapped inside the crust until the crust failed in phase 4 (at 224 to 230 minutes) when major relocation of the core material down to the lower plenum occurred. The breakup of the molten fuel and macrocracking can be expected to result in the release of any trapped volatile fission products. The magnitude of the potential release depends on the extent of debris breakup when the molten material enters the lower plenum of the reactor pressure vessel. These results are in agreement with the data on iodine retention measured in the lower plenum samples.

In the upper plenum of the reactor pressure vessel and in the primary circuit, only comparatively small amounts of fission products were detected in the post-accident investigations; probably, the deposits which initially were formed here have been dissolved during the following reflood and recirculation phases. In the upper plenum about 2% of the tellurium inventory was still deposited; small amounts of cesium present here were always accompanied by silicon so that the existence of the chemical compound $Cs_2Si_4O_9$ was assumed.

Already the first measurements performed in the containment about one day after the onset of the accident showed that the major fraction of fission product iodine was plated out in the sump water, while only a very small fraction was airborne in the containment atmosphere. Taking the different volumes of both phases into account, an integral iodine partition coefficient of about $2 \cdot 10^5$ was calculated from these data (Pelletier, 1980). The pH of the sump water was about 8.6 (due to sodium hydroxide solution which was automatically injected into the containment sump to improve iodine retention in the liquid phase); the value of the partition coefficient is consistent with the data obtained in the CSE experiments, when the lower pH of the sump water in these experiments is taken into account. This high value indicates that in the TMI-2 accident the bulk of the fission product iodine was released from the primary circuit to the containment in the form of an iodide compound and not as elemental I_2. This assumption is consistent with the observation made later on that only about 1% of the iodine present in the sump water was in the form of iodate; it is also consistent with the redox conditions in the reactor pressure vessel which were mentioned above: For such an $H_2 : H_2O$

ratio the iodine species CsI and HI are thermodynamically stable. Moreover, it has to be noted that, right from the first measurements carried out one day after the onset of the accident, the iodine partition coefficient remained virtually constant over a longer period of time, indicating that long-term processes such as radiation-induced reactions did not significantly affect the resulting overall iodine partition coefficient. Another indication of the rapid establishment of the iodine partition equilibrium even in the complex geometry of the TMI-2 containment is that in the days after the accident the airborne ^{131}I concentration decayed with an effective halflife of 8.05 days, i. e. corresponding to its physical halflife; this means that virtually no changes occurred in the spatial distribution of this radionuclide. Basically, such a time-constant iodine partition coefficient seems to contradict the results mentioned in the preceding sections on the influence of radiation on iodine chemistry in aqueous solution, which, in the absence of silver, would lead to an oxidation of I^- to I_2 and, then, potentially to IO_3^-. It can be assumed that the pH of 8.6 and additional effects resulting from reducing impurities present in the sump water effectively compensated for the effect of the radiolytic oxidation reactions.

The first iodine species analyses in the containment atmosphere were carried out about 3 months after the accident. Their results:

8–9% I_2
6–13% HOI
75–86% organoiodine compounds

showed a pronounced predominance of organoiodine compounds which was confirmed by measurements performed in the course of the containment venting in July-August 1980 (see below). However, because of the great differences in the conditions prevailing in the containment (temperature, steam content in the atmosphere, radiation level) between the days immediately following the accident and the situation more than one year later, it seems highly questionable that conclusions can be drawn from these results as to the relative concentrations of the iodine species present in the containment atmosphere during the period immediately following the accident. The comparatively high fractions of airborne HOI detected in these measurements are not consistent with the results of laboratory experiments which have yielded a low volatility of this compound. Since the TMI-2 analyses were performed using iodine-selective filter packs, systematic errors in the results caused by other iodine species penetrating into the iodophenol fraction of the filter pack or erroneously retained by it cannot be ruled out.

As was discussed previously, high fractions of airborne organoiodine compounds are typical for mixtures of iodine species which are aged by deposition and resuspension. Inside the containment, this deposition would mainly occur on the large surface areas which are covered with organic coatings and paints, where considerable fractions of the original I_2 probably had been fixed in the first stages of the accident. In the resuspension phase, volatile organoiodides of low molecular weight will be split off from these surfaces. The resuspension rate, on the one hand, and hydrolytic and radiolytic decomposition of airborne organoiodides, on the other, are the important parameters controlling the equilibrium organoiodide concentration in the atmosphere. These reactions, which are well known from the

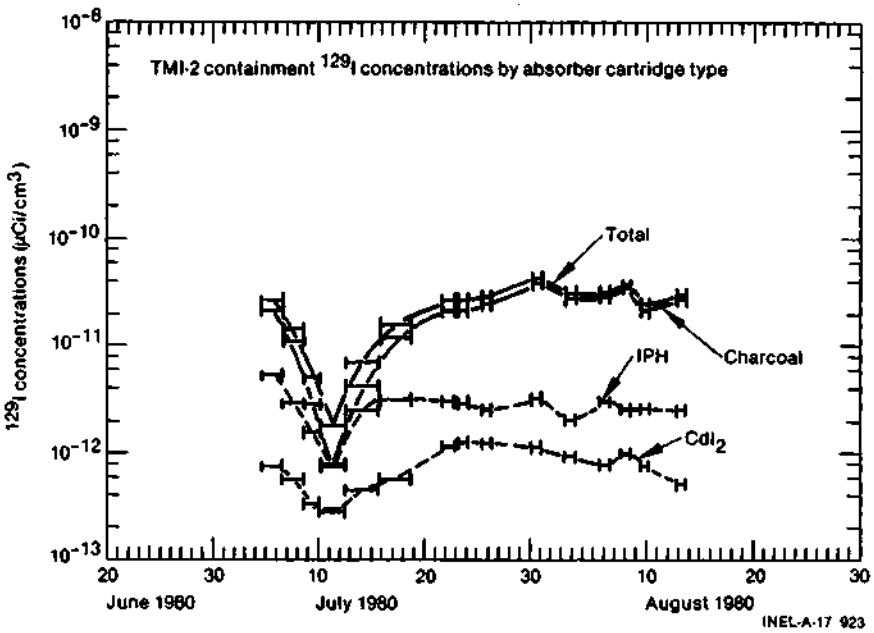

Figure 7.51. ^{129}I activity concentrations in the TMI-2 containment atmosphere during and after krypton venting
(Cline et al., 1981)

experimental studies discussed in the preceding sections, are an additional indicator that the high organoiodide fractions measured in the TMI-2 containment in a rather late stage of the accident are not representative of the conditions prevailing during the first days after the onset of the accident. Consequently, such high organoiodine fractions cannot be applied to describe the short-term iodine behavior in a degraded core accident.

Some information on the progress of such resuspension reactions can be obtained from the results of the measurements performed before, during and after the venting of the TMI-2 containment, which was carried out in order to reduce the ^{85}Kr concentration in the containment atmosphere. The results of these iodine measurements are shown schematically in Fig. 7.51. (Cline et al., 1981). Starting from a total ^{129}I concentration in the containment atmosphere of about $7 \cdot 10^{-11}$ µCi/cm^3, the venting effected a reduction to about $1 \cdot 10^{-12}$ µCi/cm^3, in parallel with the reduction of the ^{85}Kr activity concentration from about 1 down to $4 \cdot 10^{-5}$ µCi/cm^3. Following termination of the action, the ^{85}Kr concentration in the re-closed containment increased once again to a long-term constant value of about $2 \cdot 10^{-3}$ µCi/cm^3, i. e. to about 0.2% of its original value; by contrast, the concentrations of the different ^{129}I species in the atmosphere increased again within 10 to 20 days nearly to those concentration values which were already present before the venting procedure. Predominant iodine species were again the organoiodine compounds (adsorbed on the charcoal section of the filters), indicating that

the volatile compounds were rapidly generated from their precursor compounds, which presumably had been deposited on the surfaces as low-volatility organoiodine species. The measurements of the CdI_2 and iodophenol (IPH) sections of the filters showed that the increase in the airborne I_2 and HOI (see the remarks on this compound made above) concentrations in the containment atmosphere after the venting procedure was of minor significance as compared with that of the organoiodine compounds. From the measured data of the increase in the airborne iodine concentrations, a halftime of about 7 days for reaching a new equilibrium state can be calculated. This time period is considerably longer than that of the observations reported above, that about 3 days after the accident the original iodine partitioning equilibrium between sump water and containment atmosphere had been attained. A possible explanation for this discrepancy may be that in the turbulent atmosphere immediately after the accident the partitioning process proceeds at a faster rate than at the lower temperatures and the virtually quiet atmosphere 15 months later. In addition, it can be assumed that the release of deposited iodine species to the containment atmosphere proceeds at a slower rate than the initial partitioning of I_2 between the sump water and the gas phase.

Little data is available on the concentrations of the cesium isotopes in the atmosphere of the containment. Measurements carried out about one year after the accident yielded the result that about $4 \cdot 10^{-9}$ % of the ^{134}Cs and ^{137}Cs core inventories were present as airborne species; the apparent cesium partition coefficient calculated from these data would amount to about $3 \cdot 10^{11}$, confirming its essentially zero volatility under such conditions. In reality, the true value of the partition coefficient can be assumed to be considerably higher, since the major part, if not all, of the airborne cesium is in the form of aerosols. This assumption is supported by the observations made during the krypton venting which showed that, in contrast to the krypton and iodine values, the airborne cesium activity concentrations as well as the ^{90}Sr data increased during the venting procedure and decreased slowly again after the end of this operation. Obviously, physical resuspension of deposited material under formation of an aerosol of small particle sizes took place during the venting.

Investigations of the behavior of fission product tellurium in the TMI-2 accident showed that only about 4% of the tellurium inventory of the reactor core was released from the reactor pressure vessel (Vinjamuri et al., 1984), i. e. an amount which is very small compared to the iodine release. About 2.4% of the tellurium inventory was detected in the sump water as dissolved species, 0.88% attached to the solid material suspended in the sump water, 0.42% on the ion exchangers of the purification systems, 0.17% on the surfaces in the containment and 0.086% in the primary coolant. An essential fraction of the tellurium released from the reactor core was retained in the upper plenum of the reactor pressure vessel. This low tellurium release strongly supports the results of laboratory experiments concerning tellurium retention on non-oxidized Zircaloy and steel surfaces.

Due to the failure of containment isolation during the first hours after the onset of the accident, large volumes of water containing high concentrations of fission products were transported to the auxiliary building, where large areas were overflooded. Here, a new iodine partition equilibrium was established with about 3%

of the original ^{131}I core inventory in the water phase and 10^{-4} % in the atmosphere. Because of the unknown volume ratios of both phases in the auxiliary building, an accurate calculation of the resulting iodine partition coefficient was not possible; it was estimated to be in the range 10^4 to 10^5. Measurements performed in the auxiliary building in the weeks after the accident showed that the magnitude of the airborne ^{131}I concentration depended on the prevailing temperature (Daniel et al., 1987). In these flowing-air areas where no equilibrium state could be established, the airborne ^{131}I concentration increased by about 65% when the temperature increased by 10 K. Due to the complicated air flow in the building, no reliable statement could be made on this iodine source, i. e. whether it was volatilized from liquids or resuspended from surfaces. About 10% of the airborne ^{131}I present in the atmosphere of the auxiliary building was released to the environment, i. e. about 10^{-5} % of the original iodine core inventory. Virtually the entire fission product iodine release to the environment took this path, with the direct release from the containment being negligibly small.

Summarizing the data given in this section, it can be stated that the results and the experience gained during and after the TMI-2 accident do not contradict the results obtained in laboratory and pilot-plant experiments.

7.4.3 Chernobyl-4

The reactor of the nuclear power plant Chernobyl-4, which was destroyed by a severe accident in the morning of April 26, 1986, belonged to the Soviet RBMK-1000 series, the basic design of which was described in Section 2.2. This type is a graphite-moderated boiling water reactor the core of which consists of a large number of cooling channels, each of them containing one fuel assembly. Another essential difference of these nuclear power plants from those of Western design is that RBMK reactors do not have a gas-tight and robust containment to confine the entire reactor building, but only pressure-resistant compartments designed to withstand the pressure increase caused by a break of a main steam line, in which case the escaping steam is directed to a water-filled condensation chamber. Since both features contributed essentially to the initiation and to the consequences of the accident, the statement is justified that such a severe accident cannot happen in a nuclear power plant of Western design.

The initiating event, the progress and the consequences of this accident have been described several times, in detail in the relevant INSAG-1 report of the IAEA Safety Series No 75 (1986) and, more recently, in INSAG-7 (1992). In this section, therefore, only those aspects will be treated which are of significance with respect to the radiochemical aspects of fission product release; the question of the long-distance transport of the radionuclides released from the plant will not be discussed.

The day before the accident occurred, the reactor was operated for about 10 hours at a reduced load, so that a comparatively high inventory of the strongly neutron-absorbing fission product ^{135}Xe was built up in the fuel. In preparation

for various turbine-related experiments, the reactor load was then further reduced; in the course of this action difficulties in the reactor operation occurred. In order to avoid subcriticality of the reactor, the control rods were completely drawn out of the core; a short time later, as a consequence of the positive void coefficient of this reactor type, a prompt supercriticality of the reactor core took place, leading to a nuclear excursion with a peak value which was higher by about a factor of 400 than the rated power. According to calculations which were conducted after the accident, the temperature in some regions of the fuel at the climax of the excursion reached values of about 3000 °C, resulting in a rapid destruction of the fuel rod claddings as well as in a disintegration of the fuel pellets into very fine particles when they contacted water. The high heat transfer of this configuration led to a steam explosion in the cooling channels which destroyed a large number of these channels and lifted the upper cover plate of the reactor. As additional effects leading to fuel pellet disintegration, the very fast release of volatile fission products from the pellets and the oxidation of UO_2 by steam, with both effects being strongly pronounced at the extremely high temperatures, have been mentioned. The reaction of molten zirconium from the claddings and from the liners of the cooling channels with water caused large amounts of hydrogen to be produced which escaped through the lifted upper core plate to the building above the reactor. In this space, a hydrogen–air detonation occurred which completely destroyed the reactor building and killed two operators who were in the reactor building. Burning core debris was thrown out onto the roofs of the turbine building, where they caused additional fires; moreover, the refuelling machine crashed down to the reactor top. Right from the moment of the explosion, the reactor core was virtually open without any barrier to restrain the dissemination of radionuclides to the environment. The fuel still present in the destroyed core then overheated, resulting in further fission product volatilization and, due to the access of air to large regions of the core, caused a longer-lasting graphite burn. In the final state, about 135 Mg of nuclear fuel had accumulated on the lower floors of the reactor building. This material was primarily in the form of lava-like masses of varying chemical composition, with UO_2 concentrations ranging from 1 to 20 weight%.

More recent evaluations have shown that an essential contribution to the nuclear power excursion was due to the particular design of the RBMK control rods. Under certain circumstances, insertion of these rods into the reactor core (in order to initiate a reactor scram) will result in an increase in power rather than in a reduction, i. e. the nuclear chain reaction will not be terminated, but accelerated (so-called positive scram effect).

The "lavas" on the lower floors of the reactor building were solidified silicate melts that contained inclusions of various discrete phases in which uranium was present in different forms. Besides uranium impurity (1.5 to 4.5%) in the matrix glass, particles of dispersed and chemically unchanged UO_x fuel were detected, as well as crystals of UO_x with zirconium impurity, globules of a Zr-U-O phase of variable chemical composition containing up to 14–20% U and, finally, crystals of a compound $(Zr,U)SiO_4$ with high uranium content. These reaction products are assumed to be the result of processes that changed during the course of the acci-

dent. The Zr-U-O phase apparently was formed at temperatures of 1850 to 1900 °C, while the formation of the UO_x phase with the zirconium impurity requires temperatures of more than 2500–2600 °C. From the relative amounts of both compounds it was concluded that the interaction of fuel and zirconium proceeded in an extremely short time interval prior to the explosion of the reactor core, and that the highest temperature occurred in a local section of the core, while the lower temperatures of formation of the Zr-U-O phase affected essentially larger volumes of the core (Burakov et al., 1994).

In the days after the accident, the reactor debris was covered with approximately 4000 Mg of a mixture of dolomite, sand, clay, B_4C, lead, etc.; this action was the only way of extinguishing the graphite fire which continued to burn inside the core debris, to stop chemical reactions leading to hydrogen production and to stop radionuclide release to the environment. In the course of these activities, about 30 persons suffered lethal radiation doses; the fate of other workers who were exposed to high radiation doses over the course of the following liquidation operations is not exactly known. The destroyed reactor building is now enclosed in a confinement system, the so-called sarcophagus.

The original reactor core contained about 190 Mg UO_2 and, at the time of the accident, showed an average burnup of 11 MWd/kg U. The total radionuclide inventory of the reactor core at the time of the accident was calculated to be about $4 \cdot 10^7$ TBq, the core inventories of some selected radionculides are shown in Table 7.22. (INSAG, 1986). Because of the ill-defined state of the destroyed reactor core, balance measurements of the fission products retained in the fuel could not be made to an degree comparable to the detailed analyses performed on the damaged TMI-2 core. It was only possible to calculate the release fractions of the radionuclides from the destroyed reactor core to the environment from the results of immission measurements performed in the areas surrounding the plant, in more remote regions of the former USSR, as well as in many other countries, e. g. Sweden (Liljenzin et al., 1988) and Germany (SSK, 1987). It is obvious that data gained in this way can only yield results with very wide margins of error, since all the uncertainties in transport and deposition of the fission products are included here. One data set of release fractions which was published rather shortly after the accident is shown in Table 7.22., based on the results of early measurements of the contamination analyses in areas close to and farther away from the plant. These data summarize the integral release of fission product and transuranium isotopes over the whole period until the covering of the reactor debris had been completed, i. e. over about 10 days. From these data, it can be concluded that the radionuclide releases from the destroyed reactor contained two main components: fuel in the form of fine-grained dust, on the one hand, and volatile radioactive products in the form of gases and aerosols, on the other. Nearly the total core inventory of the fission product noble gases was released from the plant, as well as a significant fraction of the iodine, cesium and tellurium inventories. The less volatile fission products, as well as the transuranium elements showed release fractions of a few percent; at least a fraction of these radionuclides is assumed to have been transported mechanically out of the plant during the nuclear power excursion in the first stage of the accident. When assuming that an

Table 7.22. Fission product and transuranium element fractions released in the Chernobyl-4 accident
(INSAG, 1986; by courtesy of IAEA)

Nuclide	Halflife (days)	Inventory[a)] (Bq)	Percentage released
^{85}Kr	3930	$3.3 \cdot 10^{16}$	~100
^{133}Xe	5.27	$1.7 \cdot 10^{18}$	~100
^{131}I	8.05	$1.3 \cdot 10^{18}$	20
^{132}Te	3.25	$3.2 \cdot 10^{17}$	15
^{134}Cs	750	$1.9 \cdot 10^{17}$	10
^{137}Cs	11000	$2.9 \cdot 10^{17}$	13
^{99}Mo	2.8	$4.8 \cdot 10^{18}$	2.3
^{95}Zr	65.5	$4.4 \cdot 10^{18}$	3.2
^{103}Ru	39.5	$4.1 \cdot 10^{18}$	2.9
^{106}Ru	368	$2.0 \cdot 10^{18}$	2.9
^{140}Ba	12.8	$2.9 \cdot 10^{18}$	5.6
^{141}Ce	32.5	$4.4 \cdot 10^{18}$	2.3
^{144}Ce	284	$3.2 \cdot 10^{18}$	2.8
^{89}Sr	53	$2.0 \cdot 10^{18}$	4.0
^{90}Sr	10200	$2.0 \cdot 10^{17}$	4.0
^{239}Np	2.35	$1.4 \cdot 10^{17}$	3
^{238}Pu	$3.15 \cdot 10^{4}$	$1.0 \cdot 10^{15}$	3
^{239}Pu	$8.9 \cdot 10^{6}$	$8.5 \cdot 10^{14}$	3
^{240}Pu	$2.4 \cdot 10^{6}$	$1.2 \cdot 10^{15}$	3
^{241}Pu	4800	$1.7 \cdot 10^{17}$	3
^{242}Cm	164	$2.6 \cdot 10^{16}$	3

[a)] decay corrected to 6.5.1986 and calculated as prescribed by the Soviet experts

identical fraction of the uranium inventory was released from the core, it can be calculated that about 8 Mg of the fuel were disseminated into the environment, with the bulk of this material being deposited in the immediate vicinity of the plant.

The release of radionuclides from the reactor core showed pronounced differences with time; from the data given in Fig. 7.52., four different phases can be distinguished:

(1) Very high releases on the first day, caused by the nuclear power excursion and its direct consequences.
(2) A period of about 5 days during which the release rate decreased to a minimum lower by about a factor of 6 than the value of the first day.
(3) Another period of about 4 days in the course of which the release rate increased again to a maximum higher by about a factor of 4 than the preceding minimum.
(4) Nine days after the onset of the accident a sharp decrease in the release rate occurred down to values of less than 1% of the initial rate, with a further decrease in the following days.

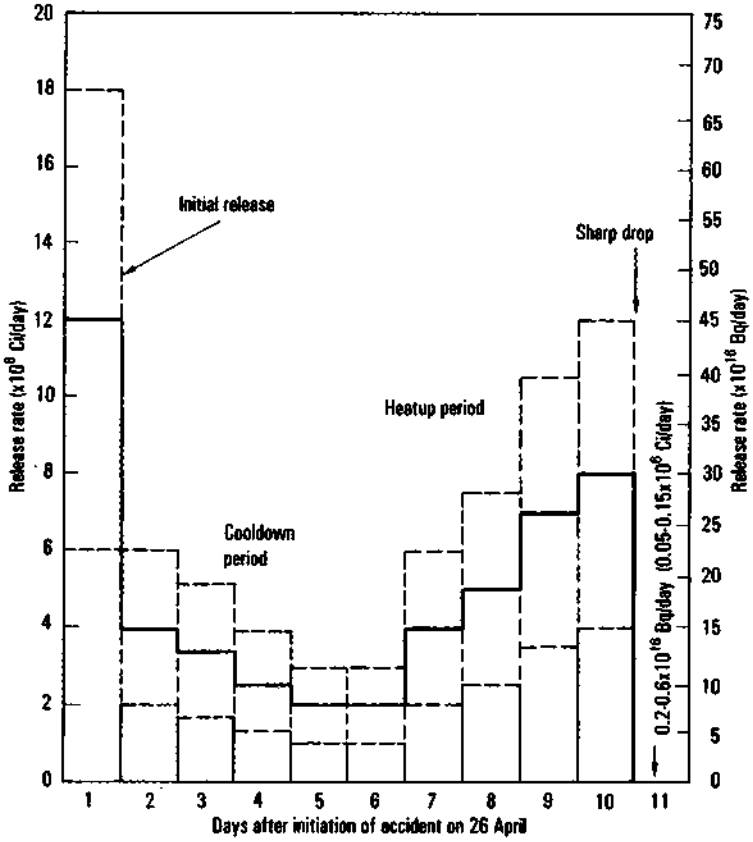

Figure 7.52. Time-dependent release of radionuclides to the atmosphere in the course of the Chernobyl-4 accident
(INSAG, 1986; by courtesy of IAEA)

Table 7.23. Parameters affecting fission product release in the Chernobyl-4 accident and in LWR core melt accidents
(Albrecht, 1987)

Parameter	Chernobyl accident	Core melt accident
Initiating event	Reactivity excursion + loss of coolant	Loss of coolant
Fuel behavior	Dispersion	Melting
Temperature	a) ~3000 °C (<3s) b) <2000 °C	2000–2500 °C
Atmosphere	Air, steam, CO, CO_2, H_2, CH_4	Steam/H_2

During the first two phases, the relative ratios of the different radionuclides released remained essentially constant, whereas in the early stage of phase (3) the increase in the release rates was restricted to iodine and cesium isotopes, with the other fission products following after a certain delay.

Since the release fractions shown in Table 7.22., as well as in Fig. 7.52., suffered from a broad range of uncertainties, attempts were made to re-evaluate these data on the basis of all the then currently existing results of measurements. According to Khan (1990), the best estimates of the release fractions are:

essentially all of the noble gases
40 to 68% of the halogens
10 to 43% of alkali metals
7 to 15% of tellurium
0.4 to 6.0% of alkaline earths
0.5 to 6.5% of noble metals
0.02 to 3.0% of rare earths
0.02 to 4.0% of refractory elements.

As to iodine and cesium, these numbers are distinctly higher than the data given in Table 7.22., whereas the range of release fractions of the other fission products includes the early figures. The higher iodine and cesium release fractions have been confirmed by more recent evaluations (e. g. Krüger et al., 1996). Concerning the release of fuel from the reactor, calculations on the basis of numerous measurements in the vicinity of the plant yielded a value of 3.5±0.5%. Measurements of the gamma spectra of samples taken from the destroyed reactor delivered a cesium release of 33±10% of its original inventory (Belayew et al., 1991). However, taking into account the large dimensions of the reactor core and the probable differences in temperature and redox conditions in the individual regions, it is unknown to what extent these samples are representative of the entire destroyed core.

A detailed evaluation of the mechanisms of release of the radionuclides from the reactor core is extremely difficult since the accident sequence and the prevailing conditions differ fundamentally from those which were theoretically and experimentally investigated in the framework of the LWR core melt analyses (see Table 7.23.). In addition, due to the large dimensions of the RBMK core (compared to that of a Western light water reactor), different regions of the core may have experienced substantial differences in temperature and other conditions during the accident. When one compares the data published by INSAG (1986) with the results of the SASCHA experiments (Albrecht, 1987; Feuerstein, 1987), it can be seen that in the Chernobyl accident the differences between the released amounts of volatile and of less volatile radionuclides amounted to a factor of 3 to 6 only, whereas in the SASCHA high-temperature heating experiments factors of more than 100 were measured. The only explanation for these discrepancies is the existence of different release mechanisms occurring in the course of the accident:

- In the phases (1) and (2) mentioned above, a mechanical release of very finely dispersed fuel particles took place, supported by a hot air flow, together with ignition products of the graphite moderator; it is also possible that during and

immediately after the nuclear excursion a congruent vaporization of fuel and fission products at very high temperatures occurred. From adjacent core regions at lower temperatures, predominantly volatile fission products were emitted during these phases so that the volatiles are overrepresented to a certain extent (compared with their inventory in the whole reactor core) when the total release is considered. Since a large fraction of the less volatile substances was deposited near the plant, the substances which travelled over longer distances showed a ratio of volatile to less volatile radionuclides of about 10.

- In phase (3), the radionuclide release was essentially governed by vaporization of volatile fission products from the core debris at temperatures of around 2000 °C. The increase in release noticed during this phase was apparently caused by a hindrance of heat removal due to the cover of dolomite, sand, clay, B_4C etc., which resulted in a renewed increase in the temperature of the debris, but not in an absolute confinement of the degraded core against the atmosphere. When tightness of the cover was reached on May 6, 1986, the release was drastically reduced. No detailed knowledge exists of the mechanisms of retention of iodine, cesium and tellurium in the covering materials (e. g. whether chemical compounds were formed and, if so, which ones).

Some attempts were made to obtain information on the mechanisms of radionuclide release from immission measurements performed in the first days after the accident. However, when evaluating the significance of immission measurements of radionuclides (which, to a part, were transported by the chimney effect of the burning reactor core to about 1500 m height and then carried over long distances) for conclusions on the release processes, some limitations cannot be ignored. From the data measured at a great distance from the source no direct information on the released amounts can be obtained since all the uncertainties occurring during transport will affect the results (dispersion parameter, dry and wet deposition etc.). The relative composition of the aerosol particles can only be assumed to remain unchanged during transport when their initial main constituents are low-volatility and water-insoluble substances, since otherwise a part of them would be removed by volatilization or by leaching during transport. In addition, the chemical state of fission product iodine can be affected by interconversions of the chemical species particle iodide–elemental I_2–organoiodide; for this reason, no reliable conclusions can be drawn from the measured immission species on the species originally released.

Likewise, it is hardly possible to draw conclusions as to the chemical conditions prevailing in the reactor core during the progress of the accident. From the observation that the ratio $^{131}I : {}^{137}Cs$ in the immission samples was significantly higher than that calculated for the core inventory, it can be derived that a fraction of the iodine was released from the core as I_2, thus indicating oxidizing conditions. Another indication of this is the comparatively high tellurium release. Oxidizing conditions can be caused by H_2O as well as by air ingress into the disintegrated reactor core. Other chemical reactions between fuel, fission products and other materials in the reactor core, e. g. with graphite, may have resulted in reducing conditions and, possibly, in the formation of carbides and their subsequent decomposition by

steam or oxygen. Reducing chemistry conditions may have been caused by the presence of CO and H_2 in certain parts of the reactor as a result of high-temperature graphite–water reactions. Thus, it can be assumed that significant differences in the chemistry conditions prevailed in different regions of the core.

In many of the immission samples so-called hot particles were detected. This term denotes small-sized radioactive fragments which can be distinguished and separated from the continuous fallout background due to their comparatively large specific activities. In the areas surrounding the plant the hot particles were mostly represented by dispersed UO_x fuel. Further, particles composed of the Zr-U-O phase, as well as small quantities of the UO_x phase with zirconium impurity were detected; these two phases were also observed in the lava-like masses on the lower floors of the reactor building (Burakov et al., 1994). The hot particles detected at a greater distance from the plant can, with respect to their radionuclide composition, be classified into two main categories

- monoelemental, predominantly containing ruthenium radioisotopes
- fuel fragments containing non-volatile fission products with highly depleted volatile elements and varying amounts of ruthenium.

The frequency of occurrence of such particles obviously depended on where samples were taken, but also on the sensitivity of detection during the search, since the ruthenium particles on the average showed a radioactivity level which was as much as an order of magnitude higher than the fuel fragment particles. Along the radioactive cloud trajectory, the rapid decrease in the number of hot particles per unit area was immediately apparent, indicating a comparatively fast deposition rate. The reported sizes of the particles varied considerably (Devell, 1987) and were often not correlated with the magnitude of their radioactivity, indicating the simultaneous presence of other core materials such as carbon, zirconium or silica. Typical activities of ruthenium particles detected in Sweden were on the order of 10–20 kBq, while most of the hot particles detected in Southern Germany contained about 100 Bq per particle with inhomogeneous radionuclide composition, mainly radioisotopes of ruthenium, barium, lanthanum and of other elements of low volatility.

The hot particles collected in Poland showed different shapes, with sizes varying between 20 and 600 μm (Broda et al., 1989). Structurally, the larger fuel-like particles were often thin regular plates, but some of them looked very similar to monoelemental ruthenium particles being porous conglomerates of irregular crystals. The surprising fact that such large objects could travel by air for many hundreds of kilometers suggests that the bulk part of them consisted of non-radioactive fragments of the graphite moderator. As to the formation of the ruthenium particles, the absence of other fission products in these particles led to the assumption that they did not originate from the metallic inclusions which are usually present in irradiated reactor fuel. A possible means of formation of such particles is release of volatile ruthenium oxides from the fuel, followed by their reduction when they contact the burning graphite moderator and by immediate condensation of metallic ruthenium. The $^{106}Ru : ^{103}Ru$ activity ratios of different particles showed a scatter which was distinctly smaller than that of the fuel-like particles, possibly indicating

a partial mixing of ruthenium activity originating from different fuel rods of various burnup prior to the formation of monoelemental particles; this property of the particles would be compatible with the formation mechanism assumed above. The size and activity of the particles were found not to correlate with the ruthenium isotope ratio. On the other hand, the ruthenium clusters which were contained in fuel-like particles undoubtedly represented inclusions formed in the operating fuel.

The analysis of α-active components in hot particles showed a quantitative relationship which allowed the calculation of the integral α activity from the measured ^{144}Ce γ-ray intensity; about 80% of the measured α activity was caused by ^{242}Cm. In the release and transport behavior, the actinides proved to behave similar to cerium. A comparative evaluation of the results of analyses of different particles leads to the conclusion that the composition of the fuel of various fuel rods differed considerably. Likewise, comparison with the results reported from Scandinavia led to the suggestion that hot particles deposited in Poland probably originated from a different region of the Chernobyl reactor.

References Section 7.4

Akers, D. W., McCardell, R. K., Russell, M. L., Worku, G.: TMI-2 core materials and fission product inventory. Nucl. Engng. and Design **118**, 451–461 (1990)

Albrecht, H.: Radioactivity emission from the Chernobyl accident in comparison with the results of the SASCHA program. Radiochim. Acta **41**, 141–143 (1987)

Belayew, S., Borovoi, A., Volkov, V., Gagarinski, A.: Chernobyl five years after. Nuclear Europe Worldscan **1991**, (3–4), 22–24

Broda, R., Kubica, B., Szeglowski, Z., Zuber, K.: Alpha emitters in Chernobyl hot particles. Radiochim. Acta **48**, 89–96 (1989)

Burakov, B. E., Anderson, E. B., Galkin, B. Ya., Pazukhin, E. M., Shabalev, S. I.: Study of Chernobyl "hot" particles and fuel containing masses: Implications for reconstructing the initial phase of the accident. Radiochim. Acta **65**, 199–202 (1994)

Cline, J. E., Roy, P. A., Hollcroft, J. W., Houbaugh, J., McVey, T. L., Thomas, C. D., Pelletier, C. A., Voillequé, P. G.: Measurements of ^{129}I and radioactive particulate concentrations in the TMI-2 containment atmosphere during and after the venting. Report GEND-009 (1981)

Daniel, J. A., Daniel, E. A., Seth, E. L., jr.: Correlation of radioiodine resuspension with temperature at TMI-2. Report NUREG/CR-4953 (1987)

Devell, L.: Nuclide composition of Chernobyl hot particles. Proc. Internat. Workshop Hot Particles from the Chernobyl Fallout, Theuern, Germany, 1987, p. 23–34

Feuerstein, H.: Conditions during the release of radionuclides during the Chernobyl reactor accident. Kerntechnik **51**, 55–59 (1987)

Hobbins, R. R., Russell, M. L., Olsen, Ch.S., McCardell, R. K.: Molten material behavior in the Three Mile Island Unit 2 accident. Nucl. Technology **87**, 1005–1012 (1989)

International Nuclear Safety Advisory Group (INSAG): Summary Report on the Post-Accident Review Meeting on the Chernobyl Accident. IAEA Safety Series No. 75-INSAG-1 (1986)

International Nuclear Safety Advisory Group (INSAG): The Chernobyl accident: Updating of INSAG-1. IAEA Safety Series No. 75-INSAG-7 (1992)

Khan, S. A.: The Chernobyl source term: A critical review. Nucl. Safety **31**, 353–374 (1990)

Krüger, F. W., Albrecht, L., Spoden, E., Weiss, W.: Der Ablauf des Reaktorunfalls Tschernobyl 4 und die weiträumige Verfrachtung des freigesetzten Materials: Neuere Erkenntnisse und ihre Bewertung. Paper presented at the Chernobyl Seminar of the Bundesamt für Strahlenschutz (BfS) and the Strahlenschutzkommission (SSK), München, FRG, 1996

Liljenzin, J. O., Skalberg, M., Persson, G., Ingemansson, T., Aronsson, P. O.: Analysis of the fallout in Sweden from Chernobyl. Radiochim. Acta **43**, 1–25 (1988)

McCardell, R. K., Russell, M. L., Akers, D. W., Olsen, Ch.S.: Summary of TMI-2 core sample examinations. Nucl. Engng. and Design **118**, 441–449 (1990)

Mendoza, Z. T., Stevens, C. A., Ritzman, R. L.: Radiation releases from the SL-1 accident. Nucl. Technology **53**, 155–162 (1981)

Morewitz, H. A.: Fission product and aerosol behavior following degraded core accidents. Nucl. Technology **53**, 120–134 (1981)

Pelletier, C. A.: TMI-2 evaluations and modeling. Workshop on Iodine Releases in Reactor Accidents. Report NSAC 14 (1980)

Petti, D. A., Adams, J. P., Anderson, J. L., Hobbins, R. R.: Analysis of fission product release behavior from the Three Mile Island unit 2 core. Nucl. Technology **87**, 243–263 (1989)

Strahlenschutzkommission (SSK): Auswirkungen des Reaktorunfalles in Tschernobyl auf die Bundesrepublik Deutschland. Veröffentlichungen der Strahlenschutzkommission, Band 7 (1987)

Vinjamuri, K., Osetek, D. J., Hobbins, R. R.: Tellurium behavior during and after the TMI-2 accident. Proc. 5. Internat. Meeting on Thermal Nuclear Reactor Safety, Karlsruhe, Germany, 1984; Report KfK 3880/3, p. 1583–1592

Wolters, J.: Thermische Reaktoren. Aufgetretene Unfälle mit Kernschäden. Ursachen, Ablauf und Konsequenzen. Atomwirtschaft **1987**, 285–293

Subject Index

Actinide elements, irradiated fuel 124
Actinide isotopes,
– behavior in PWR primary coolant 224
– incorporation into primary circuit contamination layers 225
– release from failed fuel rods 195
Actinides,
– activity concentrations in irradiated fuel 76
– buildup in irradiated fuel 75
– mass concentrations in irradiated fuel 76
Activated corrosion products,
– contamination buildup 241
– deposition on surfaces 302
– generation in PWR primary circuit 264
Activation period, corrosion products, determination 260
Actranf code, PWR contamination buildup 330
Advanced Containment Experiments (ACE) large-scale tests, iodine behavior 649
Aerosol behavior in containment, large-scale tests 587
Aerosol deposition in containment,
– effect of ambient atmosphere 587
– mechanisms 586
Aerosol formation,
– core–concrete interaction 533
– reactor pressure vessel failure 532
Aerosol–vapor interactions, primary system, severe accident 545
Aerosols,
– behavior in containment, severe accidents 586
– behavior in primary system during severe accident 544
– chemical nature, primary system, severe accident 544
– effect of chemical composition on deposition velocity 589
– effect of surface composition on resuspension 548
– formation in core melt accidents 497
– resuspension in containment 589
– resuspension in primary system, severe accident 546
– retention in BWR pressure suppression pool 575
– retention in BWR steam dryers 549
– retention in ice-condenser systems 590
– retention in primary system, severe accident 546
– retention in small leaks 665
– severe accidents, surface area 548
– washdown by containment sprays 590
^{110m}Ag, contribution to PWR contamination buildup 330, 333
AgI,
– formation in containment sump water, severe accident 613
– formation in primary system, severe accident 570
– solubility under sump water conditions 614
AgI formation, Loft FP-2 degraded core test 680
Alara principles 376
Amda mobile decontamination equipment 391
Annulus air extraction system 27
Antimony isotopes,
– contribution to PWR contamination buildup 330
– removal from PWR primary circuit 332
Apac decontamination process 384
Autoradiography, irradiated nuclear fuel 80
AVT chemistry treatment, PWR secondary-side water 41

B_4C control rod material, high-temperature interactions 531
Beyond design basis accidents 477
Blowdown phase, large-break design basis accident 422
Blowdown process, large-break design basis accident 438
Boric acid,
– ^{10}B-enriched 38

– behavior in core melt accidents 556
Boric acid control system, PWR 24
Boron, concentration in PWR primary coolant 36
Boron carbide, BWR control rod material 50
Boron oxide, behavior in core melt accidents 556
Borosilicate burnable poison rods, behavior during core meltdown 532
Borosilicate glass, tritium production 148
Burnable poison gadolinium 14
Burnable poison rods,
– PWR core 21
– tritium production 148
Burnup monitors, basic requirements 92
Burst release,
– fission products from fuel rods, large-break design basis accident 423
– fission products, severe accidents 496
BWR fuel rods,
– corrosion product loadings 345
– mechanism of formation of corrosion product deposits 345
BWR reactor water, radiation dose rates 229

^{14}C,
– chemical species discharged from LWR plants 172
– chemical state in fuel 132
– chemical state in irradiated fuel 132
– chemical state in primary coolant 174
– formation reactions in Zircaloy cladding 143
– inventory in irradiated fuel 132
– production in primary coolant 172
^{14}C in coolant, analytical determination 173
^{14}C in fuel,
– analytical determination 126, 132
– production reactions 131
^{14}C in Zircaloy cladding, analytical determination 139
^{14}C inventory, fuel rod cladding 143
Can-Decon decontamination process 382
Can-Derem decontamination process 383
Capa decontamination process 382
Catalytic recombiner, BWR 50
Ceramic phases in irradiated fuel 86
Cesium, chemical state in primary system, severe accident 552
Cesium behavior, Loft FP-2 experiment 680
Cesium chemical reactions, high-temperature environment 511
Cesium isotopes in PWR coolant, purification effectiveness 221
Cesium spiking, reactor transients 202, 206
CH_3I, partition coefficient 631
Chemical control system, PWR 24
Chernobyl-4 reactor accident,
– fission product release fractions 702
– fission product release mechanisms 705
– general aspects 700
– reactor core, chemical conditions 706
– release of hot particles 707
Citrox decontamination process 383
^{58}Co contamination in PWR primary circuit, influencing parameters 317
^{58}Co, main sources in PWR primary circuit 285
^{60}Co,
– incorporation into BWR oxide layers 357, 361, 362
– main sources in PWR primary circuit 282
– release from BWR contamination layers 364
^{60}Co deposition rate, BWR primary system, influencing parameters 360
^{60}Co in BWR reactor water, chemical state 351
Co^{2+} ions, role in contamination buildup 309
Cobalt,
– change in chemical state during PWR shutdown spiking 299
– mechanism of deposition onto primary circuit surfaces 308
– neutral atoms in PWR contamination layers 310
– transport in BWR systems 354
Cobalt deposition,
– effect of oxidizing coolant conditions 310
– effect of pipe bends 311
Cobalt deposition onto surfaces, influencing parameters 305
Cobalt ferrites, stability in PWR primary coolant 293
Cobalt in PWR primary coolant, chemical state 291
Cobalt incorporation, PWR contamination layers, effect of coolant chemistry 312

Cobalt monitor, neutron fluence measurement 153
Cobalt release rates, PWR primary circuit conditions 271
Cobalt sources,
– BWR primary system 342
– PWR primary circuit 274
– PWR primary system 280
Cobalt traces,
– adsorption on iron oxides 291
– precipitation on fuel rod surfaces 281
Colloids, role in contamination buildup 308
Computer codes, severe accident consequences 481
Concrete secondary shielding, Siemens/KWU PWR reactor building 31
Containment,
– conditions during severe accidents 584
– controlled depressurization following severe accident 672
– failure of isolation in severe accidents, release of radionuclides 667
– late overpressure failure in severe accidents 667
Containment BWR 46
Containment depressurization, use of Venturi scrubber 674
Containment PWR, volume and surface area 583
Containment spray system 30
Containment sprays,
– chemical composition 443
– modelling of radionuclide washout 444
– washout of iodine 443
Containment steel shell,
– leaks, escape of fission products 452
– PWR 31
Containment sump water,
– chemical composition, severe accident 612
– pH 652
Containment Systems Experiments (CSE) large-scale tests, iodine behavior 647
Containment Systems Test Facility (CSTF) 452
Containment venting,
– ACE experiments 676
– liquid-phase retention systems 673
– mechanical filters 672
– TMI-2 accident 698
Contaminated metallic scrap, melting 408
Contamination buildup,
– countermeasures 312
– effect of plant shutdown procedures 323
– general 241
– influencing parameters 247
– saturation levels 245
– time behavior 245
Contamination buildup BWR,
– effect of iron concentration in reactor water 366
– effect of reactor water purification flow 366
– effect of zinc addition 368
– general aspects 339
– minimization of shutdown spiking 368
– modelling 372
Contamination buildup PWR,
– effect of coolant purification 322
– effect of primary coolant chemistry 319
– mechanisms 262
– modelling 325
Contamination layers,
– BWR systems, chemical composition 357
– BWR systems, structure 357, 360
– PWR, radionuclide loadings 303
Control rod materials BWR, vaporization behavior during severe accidents 531
Control rod materials PWR, vaporization behavior during severe accidents 529
Control rods,
– BWR 50
– BWR, tritium inventories 149
– PWR 20
– PWR, radionuclide inventories 147
CoO, solubility in high-temperature water 291
Coolant chemistry, PWR 33
Coolant degasification system, PWR 25
Coolant pumps, BWR 45
Coolant purification system, PWR 24
Coolant sampling system 26
Coolant storage system 26
"Coordinated" Li/B coolant chemistry, PWR 37
Cora code, PWR contamination buildup 328
Cord decontamination process 386
Core–concrete interaction,
– ACE tests 536
– core melt accidents 532

– fission product retention in overlying water 538
– fission product volatilization 533
– fission product volatilization, effect of concrete composition 534
– gas production 533
Core components, vaporization behavior during severe accidents 525
Core configuration, PWR 20
Core damage,
– Chernobyl-4 reactor accident 701
– TMI-2 reactor accident 688
Core melt accident,
– aerosol formation 497
– containment radiation dose rates 616
– fission product retention in primary system 542
Core melt process,
– chemical reactions 487
– severe accidents 487
Core neutron sources, radionuclide inventories 146
Core slumping, severe accidents 489
Corium 533
Corrosion process,
– BWR reactor water conditions, influence of radiation 344
– BWR reactor water conditions, influence of zinc 343
Corrosion product deposits,
– chemical composition 278
– dependence on coolant pH 277
– sampling 256
Corrosion product layers PWR, buildup 269
Corrosion product radionuclides,
– activity concentrations in BWR reactor water 352
– activity concentrations in PWR primary coolant 286
– BWR primary system, formation 339
– chemical state in PWR primary coolant 287
– release to coolant 285
Corrosion product release rates, BWR primary system conditions 342
Corrosion products,
– BWR, origin 342
– BWR reactor water, chemical composition 351
– carry-over with BWR main steam 355
– chemical and radiochemical analysis 252, 261
– chemical state in BWR reactor water 350
– colloidal matter in PWR primary coolant 289
– concentrations in PWR primary coolant 286
– deposition onto PWR fuel rods 275
– dissolved species in PWR primary coolant 287
– formation of suspended matter in PWR primary coolant 288
– neutron activation 275
– PWR primary circuit, sources 266
– PWR primary coolant, deposition velocities 297
– residence time in neutron field 283
– retention in sampling lines 255
– retention on primary circuit purification system 297
– sampling from primary coolant 251
– shutdown spiking 297
– shutdown spiking in BWR reactor water 355
– solid-suspended species in PWR primary coolant 288
– solubility data 289
– solubility in PWR primary coolant 276
– startup spiking 301
– volatility with BWR main steam 355
Corrosion product solubility, dependence on temperature 277
Corrosion rates, PWR primary circuit materials 270
Cracks in fuel pellets 88
Crud 267
Crudsim code, PWR contamination buildup 329
CsI,
– behavior in primary system, severe accident 560
– decomposition in a hydrogen burn in containment 638
– decomposition in primary system, severe accident 561
– formation in primary system, severe accident 559
– formation kinetics in steam–hydrogen atmospheres 512
– high-temperature reaction with aerosols 567

– radiation-induced decomposition in the primary system, severe accident 564
– reaction with boric acid in the primary system, severe accident 562
– reaction with steel in the primary system, severe accident 563
– reactions under loss-of-coolant accident conditions 433
– revaporization from hot steel surfaces in the primary system 563
CsOH,
– behavior in primary system, severe accident 553
– deposition onto primary system stainless steel, severe accident 554
– reaction with boric acid in primary system, severe accident 556
– reactions under loss-of-coolant accident conditions 433
CsOH–aerosol interactions in primary system, severe accident 553
Curium isotopes, appearance in PWR primary coolant 224

DCD decontamination process 383
Decay chains, uranium isotopes 60
Decommissioning,
– decontamination of primary systems 406
– melting of contaminated materials 408
Decommissioning nuclear power plants, general strategy 406
Decontaminated materials, activity measurement before release 410
Decontamination,
– Amda mobile equipment 391
– basic requirements 376
– cost–benefit analysis 380
– electrochemical procedures 387
– $HMnO_4$ oxidizing agent 386
– in-service, PWR primary circuit 324
– non-chemical procedures 381
– plants to be decommissioned 405
– resulting radioactive waste 378
– treatment of spent ion exchangers 403
– treatment of waste 402
Decontamination for unrestricted use 408
Decontamination process,
– pre-oxidation step 385
– technical feasibility requirements 378
Decontamination solutions,
– evaporation 402
– materials compatibility 377
Demona aerosol experiments 588
Design basis accidents, radiologically representative accidents 419
Diffusion release, fission products, severe accidents 497
Discrete radioactive particles, PWR primary coolant 227, 284
Dissolved cobalt ions, role in contamination buildup 308
Dose rates, primary system PWR and BWR 246
Droplet entrainment, fission products 228
Dushman reaction 599

EdF-Emma decontamination process 385
Electrochemical decontamination,
– bath technique 389
– electrolytes 388
– in-situ technique 389
– treatment of spent electrolyte 404
Electromagnetic filtration, removal of corrosion products from primary coolant 322
Electropolishing, pretreatment of primary circuit surfaces 318
Element-specific activities, corrosion product radionuclides 260
"Elevated" Li/B coolant chemistry, PWR 37
Emergency coolant, mode of injection 30
Emergency core cooling systems 30
Emergency installations, PWR 29
Engineered safety features 29
Eutectic materials interaction, core melt process 487

^{18}F, chemical state in primary coolant 67
Failed fuel rods,
– evaluation of failure type and size 189
– evaluation of the number 188
– identification 207
– influence of steam on iodine mobility 185
Falcon test facility, fission product behavior in primary system, severe accident 568
Fast neutrons, impact on core materials ductility 151
Fission fragment recoil 68, 86
Fission fragments 67
Fission gas delay system PWR 26
Fission monitors, neutron fluence measurement 158

Fission product barium, behavior in fuel 123
Fission product bromine, appearance in PWR primary coolant 216
Fission product carry-over, BWR reactor water to steam 237
Fission product ceramic phases, irradiated fuel 86
Fission product cesium,
– behavior in PWR primary coolant 221
– chemical state in fuel 112, 116
– chemical state in the pellet–cladding gap 136
– mobility in fuel 119
– release fractions in large-break design basis accident 430
– release from failed fuel rods 195
– release from fuel 113
Fission product decay chains 59
Fission product distribution, large-break design basis accident, assumed numbers 424
Fission product distribution in irradiated fuel, analytical methods 79
Fission product 3H, production by ternary fission 70
Fission product iodine,
– behavior in PWR primary coolant 215
– behavior in PWR water–steam circuit 228
– chemical forms upon release from fuel 510
– chemical species in fuel, thermodynamic stability 112
– chemical species volatilized from fuel 116
– chemical state in BWR reactor water 230
– chemical state in fuel 112
– chemical state in fuel, determination 112
– chemical state in PWR primary coolant 216
– chemical state in the pellet–cladding gap 135
– mobility in fuel 118
– radiation-induced reactions in BWR reactor water 233
– radiation-induced reactions in PWR primary coolant 218
– release fractions in large-break design basis accident 430
– release from failed fuel rods 185
– release from fuel 113
– transport behavior in BWR water–steam circuit 235
Fission product isotopes, R : B ratios 184
Fission product metallic phases, irradiated fuel 86
Fission product noble gases,
– adsorption on charcoal 213
– behavior in BWR reactor water 228
– behavior in PWR primary coolant 210
– bubble formation in fuel 107
– bubble migration in fuel 107
– diffusion in fuel 106, 111
– distribution in fuel 107
– effect of coolant degasification 212
– release from failed fuel rods 186
– release from fuel 107, 111
– release from fuel during transients 110
– retention in plant 212
Fission product oxides,
– free enthalpy of formation 99
– solubilities 105
Fission product penetration, containment leaks 452
Fission product phases in irradiated fuel 86
Fission product phases, irradiated fuel 123
Fission product release,
– chemical state, design basis accident 432
– design basis accident, experimental results 424
– leaching phase, large-break design basis accident 436
– overheated fuel, effect of radionuclide halflife 519
– severe accident, influence of oxygen potential 523
– severe accidents, computer codes 524
– severe accidents, influencing parameters 521
Fission product release experiments, design basis accident conditions 424
Fission product release fractions, dependence on ambient atmosphere 431
Fission product release from failed fuel rods, modelling 188
Fission product release mechanism, design basis accients 430
Fission product release model, large-break design basis accident 430
Fission product release rates, ORNL high-temperature tests 507
Fission product retention,

– filters 453
– primary circuit, large-break design basis accident 435
Fission product rubidium, appearance in PWR primary coolant 221
Fission product simulants 112, 499
Fission product spiking, reactor transients 197
Fission product technetium,
– behavior in fuel 124
– behavior in PWR primary coolant 223
– release from failed fuel rods 195
Fission product tellurium,
– behavior in fuel 123
– release from failed fuel rods 197
Fission product transport behavior, large-break design basis accident 434
Fission product tritium, mobility in fuel 119
Fission product vapors,
– behavior in primary system, severe accident 550
– deposition onto aerosols 550
Fission product volatilization,
– change in chemical state 500
– overheated fuel, small-scale experiments 499
Fission product washdown, hot-leg injection 435
Fission product yields 67
Fission product zirconium, behavior in fuel 123
Fission products,
– activity concentrations in irradiated fuel 74
– axial distribution in fuel rod 78
– chemical forms upon release from overheated fuel 510
– chemical state in nuclear fuel 96
– chemical state in the gap 135
– chemical state, leaching phase, design basis accident 438
– distribution in irradiated fuel 103
– electro-neutrality requirement 97
– escape rate coefficients from operationally defective fuel rods 186
– gap inventory 133
– mass concentrations in irradiated fuel 71
– neutron capture 70
– neutron emission 68
– partitioning in containment, design basis accident 440
– polyvalent elements, behavior in fuel 122
– positions in UO_2 lattice 95
– radial migration in the fuel pellet 85
– redistribution in fuel 119
– release characteristics from fuel 105
– release fractions into containment, severe accidents 583
– release from fuel, impact of fuel stoichiometry 116
– release from molten fuel 522
– retention in BWR pressure suppression pool 573
– retention in narrow slits 452
– retention in primary system 542
– source to the coolant 182
– space requirements in fuel lattice 103
– thermochemistry codes 498
– valency states in irradiated fuel 98
– vaporization experiments 499
Fission products in reactor coolant, origin 177
Fissium, simulated irradiated fuel 502
Flash evaporation,
– coolant, radionuclide behavior 458
– steam generator tube rupture 465
– transducer line break 458
Forward-pumped plants, BWR 46
Fuel assembly channel, BWR 48
Fuel assembly damage, design basis accident 471
Fuel assembly end pieces, radionuclide inventories 146
Fuel assembly spacer grids 19
Fuel assembly spacer grids, radionuclide inventories 144
Fuel assembly,
– BWR 48
– PWR 19
Fuel burnup, effect on fission product release behavior in core melt accidents 521
Fuel liquefaction, severe accidents 487
Fuel liquefaction release, fission products, severe accidents 497
Fuel microchemistry 103
Fuel morphology, effect on fission product release behavior in core melt accidents 521
Fuel pellet,
– BWR 48
– dishing 15
– grain size 16
– PWR, dimensions 15

– UO_2 14
Fuel pellet–cladding gap, oxygen potential 135
Fuel pellets,
– crack formation 88
– grain size, change during reactor operation 89
– irradiated, annular zones 89
– irradiated, density 90
– irradiated, porosity 89
– irradiated, structure 89
– irradiated, swelling 90
Fuel rod,
– BWR 16
– PWR 16
Fuel rod cladding 16
Fuel rod cladding,
– fission product inventories 138
– 3H inventory 139
– oxide layers 137
– radionuclide inventories 138
– transuranium radionuclides 138
Fuel rod damage, release of fission products to pool water 471
Fuel rod defect types, influence on fission product release 190
Fuel rod deposits,
– BWR, radiochemical composition 348
– BWR, radionuclide release to the reactor water 349
– BWR, residence time in the neutron field 349
– effect of shutdown spiking 280
– influence of coolant pH 278
– sampling 259
Fuel rod failure, large-break design basis accident 423
Fuel rod failures,
– causes 177
– differentiation from uranium contamination 193
– fission product escape rates 187
– fuel losses 178
– impact of UO_2 stoichiometry on fission product source strength 180
– iodine gap inventory 180
– iodine release from fuel 181
– iodine transport to the coolant 185
– UO_2 oxidation 179
Fuel rods,
– PWR, linear heat rating 21
– failure rates 17
– failure types 177
– non-destructive burnup determination 92
– surface contamination with fuel 179
Fuel temperature profile, PWR fuel rod 21

Gadolinium, distribution in irradiated fuel 84
Gamma scanning 79
Gap chemistry conditions 135
Gap inventories, fission products, intact fuel rods 427
Gap inventory,
– failed fuel rod 203
– fission products, magnitude in intact LWR fuel rods 134
Gap purge experiments, ORNL 428
Gas delay line, noble gas retention 212
Gas plenum, fuel rod 16
GE model, BWR contamination buildup 372
Graphite moderator, RBMK reactors 51

^3H,
– activity concentration in primary coolant 170
– chemical state in borosilicate glass and B_4C 150
– chemical state in primary coolant 170
– isotope fractionation during distillation 128
– penetration through stainless steel cladding 141
– permeation through intact fuel rod claddings 169
– production by ternary fission 70
– production in primary coolant 168
– release from fuel 130
^3H in Zircaloy cladding, analytical determination 139
H_2O, radiation-induced decomposition 616
H_2O_2, application for in-service decontamination PWR primary circuit 324
HI,
– formation in high-temperature steam environment 558
– high-temperature reaction with aerosols 567
– reaction with steel in the primary system, severe accident 564

HI volatilization, evaporating sump water 609
High-pressure scenario, severe accidents PWR 486
HOI,
– disproportionation equilibrium 599
– existence in aqueous solutions 595
– volatility from BWR reactor water 230
HOI partition coefficient 601
HOI partition coefficient, large-break design basis accident conditions 440
Hot particles, release from Chernobyl-4 reactor core 707
Hugh-pressure safety injection system 30
Hydrogen burn, effect on iodine chemistry in containment 638
Hydrogen production,
– large-break design basis accident 425
– severe accidents 490
Hydrogen water chemistry,
– BWR 55
– BWR, effect on contamination buildup 361

^{129}I,
– analytical determination in irradiated fuel 118
– appearance in PWR primary coolant 215
I_2,
– deposition onto organic surfaces, severe accident conditions 633
– gas-phase oxidation by ozone 624
– plate-out by condensing steam 607
– reaction with aerosols in the primary system, severe accident 567
– reaction with containment surfaces, design basis accident conditions 443
– reaction with steel in the primary system, severe accident 565
– reaction with zinc primer in containment 645
– reduction on steel surfaces in containment 642
I_2 hydrolysis equilibria, influencing parameters 596
I_2 partition coefficient 601
Ice condenser system 31
Impair iodine chemistry code, severe accidents 656
Impregnated charcoal, testing iodine retention efficiency 457
Impregnated charcoal filters 454
Incoloy 800 steam generator tube material 11
Inconel 600, 690 steam generator tube material 11
Inconel fuel assembly spacer grids, replacement by Zircaloy 317
Inherent safety aspects, light water PWR 27
In-service decontamination, PWR primary circuit 324
Inspect iodine chemistry code, severe accidents 657
Internal axial pumps, BWR 45
Iode iodine chemistry code, severe accidents 655
Iodide,
– oxidation in design basis accident sump water 441
– radiation-induced oxidation, effect of radiation dose 618
– radiation-induced oxidation, effect of temperature 618
– radiation-induced oxidation, influence of third partners 621
– thermal oxidation in aqueous solutions 611
Iodide partition coefficient, severe accident conditions 604
Iodine,
– basic chemistry in aqueous solutions 594
– behavior in containment sampling lines, severe accident 644
– behavior in coolant flash evaporation 459
– behavior in the annuli after containment failure 668
– chemical forms entering containment, severe accident 591
– chemical state in containment sump water, influence of solution partners 610
– chemical state in primary system, severe accident 556
– chemistry in high-temperature steam environment 557
– effect of sump water pH on chemical state 612
– formation of AgI in sump water 613
– influence of radiation-induced reactions on chemical state 617
– interaction with aerosols in containment atmosphere 639

– non-equilibrium partitioning between aqueous and gas phases 669
– radiation-induced reactions, effect of solution pH 617
– reaction with silver in the primary system, severe accident 570
– reactions in containment atmosphere during severe accidents 638
– reactions with containment surfaces during severe accidents 641
– retention in BWR pressure suppression pool 577
– retention in ice-condenser systems, severe accidents 646
– retention in small leaks 666
– retention in Venturi scrubber 674
– time-dependent behavior in containment, severe accidents 653
– transport from primary system to containment, severe accident 592
– volatilization from evaporating sump water 671
– volatilization from open pools 463
– volatilization from spent fuel pool 471
– volatilization in auxiliary building accidents 472
Iodine behavior,
– Advanced Containment Experiments (ACE) 649
– Containment Systems Experiments (CSE) 647
– Loft FP-2 experiment 680
– steam generator tube rupture accident 467
Iodine carry-over,
– BWR reactor water to steam 234
– effect of BWR hydrogen water chemistry 235
– PWR steam generator 228
Iodine chemical species, analytical determination in dilute solutions 230
Iodine chemistry models, severe accidents 654
Iodine disproportionation reactions 595
Iodine filters,
– degradation effects 456
– in-plant efficiency testing 457
Iodine hydrolysis equilibrium 230
Iodine hydrolysis reactions,
– equilibria 595
– kinetics 599
Iodine isotopes,
– effectiveness of primary circuit purification system 219
– inventory on PWR purification resin bed 220
Iodine partition coefficient,
– basic features 601
– BWR reactor water 231
– condensing-steam conditions 607
– effect of redox potential 610
– I_2–I^- mixtures 605
– kinetics of establishment 605
– large-break design basis accident 440
– severe accident conditions 602
– steam generator tube rupture accident 467
Iodine partition equilibrium, large-break design basis accident conditions 440
Iodine partitioning, evaporating sump water 609
Iodine retention, filters 453
Iodine revolatilization, TMI-2 accident 698
Iodine spiking,
– mechanism 201
– modelling 205
– reactor transients BWR 201
– reactor transients PWR 198
– significance in steam generator tube rupture accident 466
Ion exchanger filter beds 24
Ionizing radiation,
– effect on decomposition of organoiodine compounds 628
– effect on iodine chemistry in containment 617
– effect on production of organoiodine compounds 627
Iron–manganese monitor, neutron fluence measurement 154
Isolde in-core fission product release experiments 428

Knock-out release, radionuclides from fuel 134
Konvoi PWR plants, Siemens/KWU design, characteristic data 6

Lace containment aerosol experiments 587
Lace experiments, aerosol transport in primary system 548
Large-break design basis accident,

– accident sequence 422
– hydrogen production 425
Leaching phase, large-break design basis accident 423
Leaks in containment, fission product retention 452, 665
Less-volatile fission products, release from overheated fuel 513
^{7}LiOH alkalizing agent, PWR primary coolant 36
Li/B primary coolant chemistry, PWR 36
Liquid waste processing system 26
Liric iodine chemistry code, severe accidents 658
Loft experiment FP1,
– fission product behavior 450
– test conditions 449
Loft facility, general description 447
Loft FP-2 reactor core damage test 678
Lomi decontamination process 383
Loss-of-coolant accident (Loca), design basis accident 419
Loss-of-coolant accident PWR, accident sequence 419
Low-pressure safety injection system 30
Low-pressure scenario, severe accidents PWR 486
Lsatt experiments, aerosol transport in primary system 548

Maximum credible accident 478
Metal release rates, PWR primary circuit conditions 270
Metallic inclusions (ε phase) in irradiated fuel 86
Mixed-oxide (Mox) fuel,
– chemical composition, analysis 14
– fabrication 14
– stoichiometry 15
Mixed-oxide fuel, isotopic composition 62
Mixed-oxide fuels, pellet structure 86
"Modified" Li/B coolant chemistry, PWR 36
Moisture separator, BWR 45
Molten core–concrete interaction, severe accidents 490
Mopac decontamination process 386

^{16}N, ^{13}N, chemical state in primary coolant 164
^{146}Nd burnup monitor 92
Neptunium isotopes, behavior in PWR primary coolant 224
Neutron fluence monitors, basic requirements 152
Neutron source, PWR 22
Nickel–cobalt monitor, neutron fluence measurement 155
Niobium monitor, neutron fluence measurement 156
NS-1 decontamination process 383
Nuclear auxiliary building, design basis accidents 472
Nuclear auxiliary systems 23
Nuclear fission,
– basic features 66
– energy release 67
– fission product mass distribution 67
Nuclear fuel,
– burnup determination 91
– radiation effects on fission product chemistry 103
– redox potential 101
– redox potential, analysis methods 98

Occupational radiation exposure, LWR plants 251
On-line g spectrometry,
– corrosion product deposits 257
– primary coolant 256
Open pools,
– iodine volatilization, non-equilibrium conditions 463
– radionuclide volatilization behavior 462
Optimi code, PWR contamination buildup 329
Organic compounds, effect on iodine volatility from irradiated solutions 630
Organoiodide retention,
– filters 454
– impregnated charcoal, influencing parameters 454
Organoiodine compounds,
– behavior in PWR primary coolant 218
– behavior in the annuli after containment failure 670
– decomposition in containment atmosphere 632
– decomposition in containment sump water 628
– decomposition reactions, severe accidents 628, 632

– formation by surface reactions 629, 633
– formation in the aqueous phase, severe accident conditions 626
– formation in the containment atmosphere 631
– formation, design basis accident 442
– fractions formed in severe accidents 636
– isotope exchange with natural CH_3I 632
– main sources in severe accidents 635
– production reactions, severe accidents 626
– radiation-induced reactions in spray solutions 445
– stability in irradiated fuel 117
– TMI-2 accident 697
ORNL fission product release tests, experimental setup 505
ORNL heating experiments, design basis accident conditions 426
ORNL high-temperature fission product volatilization tests 503
Oxidation release, fission products, severe accidents 525
Oxide layers, PWR primary circuit, chemical composition 303
Ozone, oxidation of gas-phase I_2 624

^{32}P, production in primary coolant 174
Pactole code, PWR contamination buildup 327
Passive safety barriers, PWR 28
Pellet–cladding gap, fuel rod 16
Phebus FP reactor core damage test program 681
Phosphoric acid, treatment of spent decontamination solutions 404
Plutonium,
– enhanced production at fuel pellet rim 83
– incorporation into PWR contamination layers 224
– inventory on PWR primary ion exchanger 225
Plutonium-containing fuel 14
Plutonium isotopes,
– behavior in PWR primary coolant 224
– irradiated fuel 76
Polyvalent fission products,
– behavior in BWR reactor water 237
– behavior in fuel 122
– behavior in PWR primary coolant 223
Pool scrubbing,
– ACE experiments 576
– aerosol retention 575
Pressure suppression pool, BWR 51
Pressure suppression pool BWR,
– fission product retention 573
– gas-liquid hydrodynamics 574
Pressurized water reactor (PWR), general description 6
Pretreatment, decontaminated surfaces 400
Primary circuit, PWR 10
Primary circuit materials,
– effect of pretreatment on cobalt deposition 305
– PWR, pretreatment to reduce contamination buildup 318
Primary coolant, sampling problems 251
Primary coolant chemistry PWR, impact on contamination buildup 319
Primary coolant chemistry specifications, PWR 34
Primary coolant PWR 10
Primary coolant PWR,
– chemical analysis 39
– hydrogen addition 39
– $KOH-NH_3$ chemistry, VVER reactors 40
– LiOH alkalizing agent 36
– pH 34
– radiation-induced reactions 38
Primary neutron source, PWR 22
Primary system,
– fission product behavior during severe accidents 541
– gas-phase composition during severe accidents 541
Primary system materials BWR, pretreatment to reduce contamination buildup 371
PWR primary coolant, radiation dose rates 216
PWR water–steam circuit, iodine partitioning 228

R : B ratios,
– dependence on fuel rod defect type 190
– fission product isotopes 184
Radiation-induced corrosion effects, BWR reactor water conditions 344
Radioiodine Test Facility (RTF) 622
Radionuclides, penetration through leaks in containment shell 665
RBMK reactor, basic design 51

Reactor accidents, general 415
Reactor components, decontamination 393
Reactor core, PWR 13
Reactor full systems, decontamination 394
Reactor pressure vessel,
– BWR 44
– PWR 7
Reactor pressure vessel failure, severe accidents 489
Reactor pressure vessel internals, PWR 7
Reactor safety studies 479
Reactor subsystems, decontamination 391
Reactor water BWR,
– hydrogen chemistry 55
– normal chemistry 54
– radiation-induced reactions 55
Reactor water chemistry BWR, zinc addition 56
Reactor water cleanup system, BWR 50
Recirculation lines, BWR 45
Recirculation phase, large-break design basis accident 423
Recoil release, fission products from fuel 133
Recontamination, decontaminated surfaces 399
Recontamination rates, influence of surface pretreatment 400
Refill phase, large-break design basis accident 422
Reflood phase, large-break design basis accident 422
Reprocessed uranium fuel,
– isotopic composition 64
– residual fission products 64
Residual heat removal system 26
Revaporization, deposited fission products 551

^{35}S, production in primary coolant 174
Safety installations,
– BWR 51
– PWR 28
Safety measures, defense-in-depth concept 415
Sampling,
– corrosion product deposits 256
– corrosion products in coolant 251
Sascha tests, fission product vaporization experiments 502
Secondary neutron source, PWR 22
Severe accidents,
– accident sequences BWR 494
– accident sequences PWR 485
– core melt process 487
– in-plant chemistry environments 480
– modelling 481
– reactor pressure vessel failure 489
Severe core damage accidents 478
Severe Fuel Damage Tests (SFD), release of fission products from overheated fuel 516
Severe reactor accidents, pressure buildup in containment 492
Shutdown spiking,
– corrosion products 297
– fission products 198
Simulant fuels, use in vaporization experiments 499
Sipping technique, failed fuel assembly identification 208
SL-1 reactor accident 686
Snaptran reactor core damage tests 678
Source strength, fission products from failed fuel rod 181
Source strengths, dependence on fuel rod heat rating 186
Source term,
– radionuclides to the environment 416
– severe reactor accidents 479
Source Term Code Package 482
Source Term Experiments, release of fission products from overheated fuel 516
Spent fuel pool 22, 471
Spent fuel pool, iodine volatilization 471
Spray solutions,
– methyl iodide chemical reactions 445
– radiation-induced iodine chemical reactions 445
– radiation-induced reactions 444
Steam dryer, BWR 46
Steam generator, PWR 11
Steam generator heating tubes, leak detection 228
Steam generator tube failure, detection 466
Steam generator tube rupture,
– accident sequence 465
– droplet transport 467
Steam generator tube rupture accident, effect of break location on radionuclide behavior 469
Steam generator water PWR, chemical treatment 41

Stellite replacement,
– effect on BWR radiation levels 364
– effect on primary circuit dose rates 314
– effect on primary coolant ^{60}Co concentration 314
Stellites in BWR primary system, replacement 364
Stellites in PWR primary circuit, replacement 313
Sump water,
– chemical composition, large-break design basis accident 438
– chemical composition, severe accidents 652
Suspended corrosion products, behavior in PWR primary coolant 295

Tellurium,
– behavior in primary system, severe accident 571
– chemical state in containment, severe accident 591
– high-temperature reactions 572
– release from overheated fuel rods 508
Ternary fission 71
Thermal gradient tube 117, 504, 510
Thermal gradient tube,
– fission product deposition behavior 432
– identification of fission product chemical species 432
Thermochemistry codes, fission products 498
Thiosulphate, radiation stability 676
TMI-2 reactor accident,
– behavior of control rod materials 692
– cesium behavior 699
– containment venting, effect on airborne iodine concentration 698
– core end state 689
– end-state ^{129}I and ^{137}Cs distribution 694
– fission product release from the core 693
– general aspects 687
– hydrogen production 692
– iodine behavior in containment 696
– iodine behavior in the auxiliary building 700
– iodine chemical species in containment 697
– mechanisms of fission product release from core 695
– redox conditions inside reactor pressure vessel 692
– tellurium behavior 699
Toshiba model, BWR contamination buildup 373
Tramp uranium 179
Tramp uranium,
– distribution in PWR primary circuit 226
Transducer line, break, accident sequence 458
Transuranium isotopes, buildup in irradiated fuel 76
Trends iodine chemistry code, severe accidents 657
Tritium,
– chemical state in fuel 128
– diffusion in Zircaloy 142
– distribution in fuel rod 129
– inventory in irradiated fuel 129
– migration in fuel 129
– pellet–cladding gap 136
– production in burnable poison rods 148
– production in BWR control rods 149
– release from Zircaloy 142
– retention in B_4C 149
– retention in borosilicate glass 149
– retention in Zircaloy cladding 141
Tritium in fuel, analytical determination 126

UO_2, solid-state physics aspects 101
UO_2 crystal lattice structure 94
UO_2–fission products, thermodynamics 99
UO_2 fuel,
– chemical composition, analysis 15
– fabrication 13
– Gd_2O_3 burnable poison 14
– impurities 15
– stoichiometry 15
Uranium contamination, fission product release to coolant 193
Uranium decay products, behavior during uranium processing 60
Uranium isotopes, decay chains 60
Uranium nuclear fuel, isotopic composition 60
Uranium oxide fuel, chemical system 94

Vapor–aerosol interactions, primary system, severe accident 551
Ventilation system, PWR 26

Venturi scrubber, retention of radionuclides 675
Volume control system, PWR 24
VS decontamination process 387
VVER reactors, basic design 31

Windscale-1 reactor accident 685

Xenon isotopes, generation in the PWR primary system 210
Xenon poisoning 70

Zinc,
– effect on ^{60}Co incorporation into BWR oxide layers 360
– effect on ^{60}Co incorporation onto PWR oxide layers 321
– effect on BWR corrosion rates 360
Zinc addition, BWR reactor water, reduction of contamination buildup 369
Zircaloy–hydrogen system, basic features 141
Zircaloy–steam reaction,
– large-break design basis accident 425
– severe accidents 490
Zircaloy cladding,
– activation products 138
– ^{3}H retention 141
Zircaloy-2 fuel rod cladding material 16, 48
Zircaloy-4 fuel rod cladding material 16
Zirconium hydrides 141